ISSN 0021-9673

VOL. 706 NOS. 1 + 2 7 JULY 1995

COMPLETE IN ONE ISSUE

International Ion Chromatography Symp. 1994
Turin, 19–22 September 1994

JOURNAL OF CHROMATOGRAPHY A

INCLUDING ELECTROPHORESIS AND OTHER SEPARATION METHODS

ELSEVIER

JOURNAL OF CHROMATOGRAPHY A

INCLUDING ELECTROPHORESIS AND OTHER SEPARATION METHODS

Scope. The *Journal of Chromatography A* publishes papers on all aspects of **chromatography, electrophoresis** and related methods. Contributions consist mainly of research papers dealing with chromatographic theory, instrumental developments and their applications. In the *Symposium volumes*, which are under separate editorship, proceedings of symposia on chromatography, electrophoresis and related methods are published. *Journal of Chromatography B: Biomedical Applications* —This journal, which is under separate editorship, deals with the following aspects: developments in and applications of chromatographic and electrophoretic techniques related to clinical diagnosis or alterations during medical treatment; screening and profiling of body fluids or tissues related to the analysis of active substances and to metabolic disorders; drug level monitoring and pharmacokinetic studies; clinical toxicology; forensic medicine; veterinary medicine; occupational medicine; results from basic medical research with direct consequences in clinical practice.

Submission of Papers. The preferred medium of submission is on disk with accompanying manuscript (see *Electronic manuscripts* in the Instructions to Authors, which can be obtained from the publisher, Elsevier Science B.V., P.O. Box 330, 1000 AH Amsterdam, Netherlands). Manuscripts (in English; *four* copies are required) should be submitted to: Editorial Office of *Journal of Chromatography A*, P.O. Box 681, 1000 AR Amsterdam, Netherlands, Telefax (+31-20) 485 2304, or to: The Editor of *Journal of Chromatography B: Biomedical Applications*, P.O. Box 681, 1000 AR Amsterdam, Netherlands. Review articles are invited or proposed in writing to the Editors who welcome suggestions for subjects. An outline of the proposed review should first be forwarded to the Editors for preliminary discussion prior to preparation. Submission of an article is understood to imply that the article is original and unpublished and is not being considered for publication elsewhere. For copyright regulations, see below.

Publication information. *Journal of Chromatography A* (ISSN 0021-9673): for 1995 Vols. 683–714 are scheduled for publication. *Journal of Chromatography B: Biomedical Applications* (ISSN 0378-4347): for 1995 Vols. 663–674 are scheduled for publication. Subscription prices for *Journal of Chromatography A*, *Journal of Chromatography B: Biomedical Applications* or a combined subscription are available upon request from the publisher. Subscriptions are accepted on a prepaid basis only and are entered on a calendar year basis. Issues are sent by surface mail except to the following countries where air delivery via SAL is ensured: Argentina, Australia, Brazil, Canada, China, Hong Kong, India, Israel, Japan, Malaysia, Mexico, New Zealand, Pakistan, Singapore, South Africa, South Korea, Taiwan, Thailand, USA. For all other countries airmail rates are available upon request. Claims for missing issues must be made within six months of our publication (mailing) date. Please address all your requests regarding orders and subscription queries to: Elsevier Science B.V., Journal Department, P.O. Box 211, 1000 AE Amsterdam, Netherlands. Tel.: (+31-20) 485 3642; Fax: (+31-20) 485 3598. Customers in the USA and Canada wishing information on this and other Elsevier journals, please contact Journal Information Center, Elsevier Science Inc., 655 Avenue of the Americas, New York, NY 10010, USA, Tel. (+1-212) 633 3750, Telefax (+1-212) 633 3764.

Abstracts/Contents Lists published in Analytical Abstracts, Biochemical Abstracts, Biological Abstracts, Chemical Abstracts, Chemical Titles, Chromatography Abstracts, Current Awareness in Biological Sciences (CABS), Current Contents/Life Sciences, Current Contents/Physical, Chemical & Earth Sciences, Deep-Sea Research/Part B: Oceanographic Literature Review, Excerpta Medica, Index Medicus, Mass Spectrometry Bulletin, PASCAL-CNRS, Referativnyi Zhurnal, Research Alert and Science Citation Index.

US Mailing Notice. *Journal of Chromatography A* (ISSN 0021-9673) is published weekly (total 52 issues) by Elsevier Science B.V., (Sara Burgerhartstraat 25, P.O. Box 211, 1000 AE Amsterdam, Netherlands). Annual subscription price in the USA US$ 5389.00 (US$ price valid in North, Central and South America only) including air speed delivery. Second class postage paid at Jamaica, NY 11431. **USA POSTMASTERS**: Send address changes to *Journal of Chromatography A*, Publications Expediting, Inc., 200 Meacham Avenue, Elmont, NY 11003. Airfreight and mailing in the USA by Publications Expediting.

See inside back cover for Publication Schedule, Information for Authors and information on Advertisements.

0021-9673/95/$09.50

Printed in the Netherlands

For Contents see p. VII.

JOURNAL OF CHROMATOGRAPHY A

VOL. 706 (1995)

JOURNAL OF CHROMATOGRAPHY A

INCLUDING ELECTROPHORESIS AND OTHER SEPARATION METHODS

ELSEVIER

Amsterdam – Lausanne – New York – Oxford – Shannon – Tokyo

Piazza San Carlo, the first stone of which was laid in 1619, was completed in 1638; it is 186 yards long and 82 yards wide, and is considered one of the most beautiful squares in Italy. Designed by Castellamonte with a theatrical sense that is quite eighteenth century, it has recently been restored after the destruction caused by the last war. In the centre is the monument to Emanuele Filiberto, the work of Marochetti, in the act of reining in his horse and sheathing his sword after his victory at St. Quentin. A singular effect is produced by the two beautiful matching churches, San Carlo, with its façade of pink granite, erected in 1639 and the work of Castellamonte, and Santa Cristina, which was built in 1639 to the orders of Madama Reale by Juvarra, who decorated it with marble statues and candelabra.

Also by Castellamonte are the palaces which surround the square. In that of the Solari del Borgo family, on the right-hand side, are the premises of the ancient society of the Philharmonic Academy which recently amalgamated with the Whist Club founded by Cavour. In its rooms, which are an example of eighteenth-century Piedmontese taste, splendid ceremonies, concerts and memorable celebrations took place such as those for the marriage of Vittorio Emanuele II with the Grand Duchess Maria Teresa of Austria and of Umberto I with Margherita of Savoy.

0021-9673/95/$09.50

SYMPOSIUM VOLUME

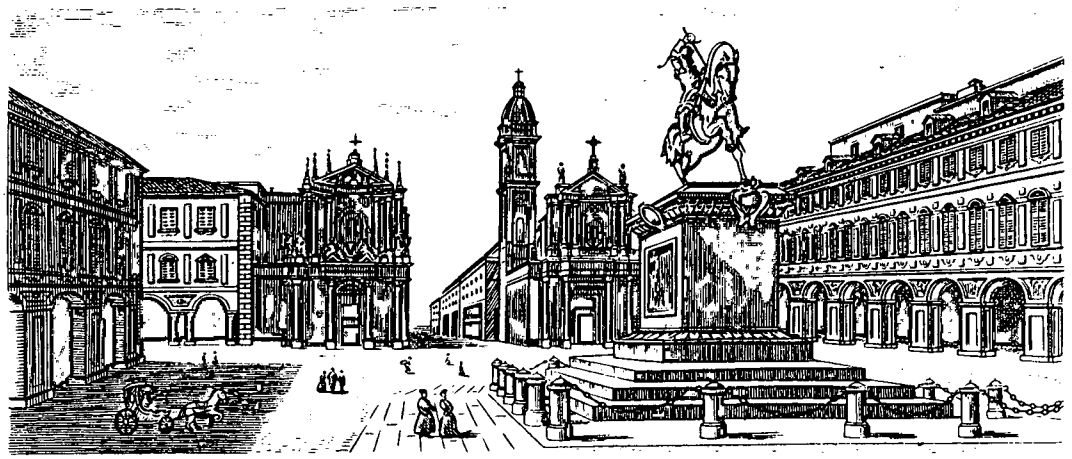

Torino – Piazza S. Carlo

INTERNATIONAL ION CHROMATOGRAPHY SYMPOSIUM 1994

Turin (Italy), 19–22 September 1994

Guest Editor

C. SARZANINI
(Turin, Italy)

VOL. 706, NOS. 1 + 2 JOURNAL OF CHROMATOGRAPHY A 7 JULY 1995

CONTENTS

(Abstracts/Contents Lists published in Analytical Abstracts, Biochemical Abstracts, Biological Abstracts, Chemical Abstracts, Chemical Titles, Chromatography Abstracts, Current Awareness in Biological Sciences (CABS), Current Contents/Life Sciences, Current Contents/Physical, Chemical & Earth Sciences, Deep-Sea Research/Part B: Oceanographic Literature Review, Excerpta Medica, Index Medicus, Mass Spectrometry Bulletin, PASCAL-CNRS, Referativnyi Zhurnal, Research Alert and Science Citation Index)

INTERNATIONAL ION CHROMATOGRAPHY SYMPOSIUM 1994, TURIN, 19–22 SEPTEMBER 1994

GENERAL PRINCIPLES

TECHNICAL ASPECTS

ELSEVIER

Journal of Chromatography A, 706 (1995) 1

JOURNAL OF CHROMATOGRAPHY A

Foreword

The 7th International Ion Chromatography Symposium (IICS'94) was held at Torino Incontra, the Congress Centre of the Chamber of Commerce in Turin, Italy, 19–22 September, 1994. Over 230 scientists from 23 countries attended and more than 160 technical presentations were given. Theoretical aspects and the more recent applications of ion chromatography (IC) and capillary electrophoresis (CE) were the main subjects developed. The symposium was opened with a welcome from Professor M.U. Dianzani, Rector of the University of Turin, and included four invited plenary lectures: "Chemical Suppressors: IC and Beyond" (J. Stillian, Dionex, Sunnyvale, CA, USA), "What Happens in IC Columns and What We See Through Bulk-Property Detectors" (H. Sato, Yokohama National University, Japan), "Recent Trends in Capillary Zone Electrophoresis" (P.G. Righetti, University of Milan, Italy) and "Modelling and Prediction of Retention Behaviour in Ion Chromatography" (P. Hajos, University of Veszprem, Hungary). John Stillian was the 1994 recipient of the Ion Chromatography Achievement Award, which is given annually to recognize significant contributions to the field of IC. To stimulate the presence of young researchers, four student awards were also given, the IICS'94 winners being B. Edwards (Brigham Young University, Provo, UT, USA), P. Fagan (University of Tasmania, Hobart, Australia), P. Dumont (Iowa State University, Ames, IA, USA) and I. Haumann (Technische Hochschule, Darmstadt, Germany). Both oral and poster sessions featured IC and CE developments in the following fields: process monitoring and control, separation of metal ions, separation selectivity and column technology, developments in separation methodology, special sample treatment procedures, standard methods and data processing, clinical and pharmaceutical applications, environmental and general applications and advances in detection.

Thanks are due to the members of the Scientific Committee (R.M. Cassidy, P.K. Dasgupta, J.S. Fritz, P.R. Haddad, P. Hajos, J.D. Lamb, D.J. Pietrzyk, H. Small, J. Stillian and K. Tanaka) and the Organizing Committee (R. Ardizoia, S. Cavalli, E. Mentasti, G. Sacchero, M. Valcarcel and O. Zerbinati) for their valuable contributions. Special appreciation is due to Janet Strimaitis of Century International and to O. Abollino, M.C. Bruzzoniti and A.M. Fogliz-zo for their fine organization and valuable contributions to solving any problems that arose. Recognition of the efforts of Dr. Erich Heftmann of the *Journal of Chromatography*, the Editor of this Proceedings Volume, must also be made.

For the success of the meeting, due to high-quality scientific papers, the joint financial support from the Turin Chamber of Commerce, the Chemical Laboratory of the Chamber of Commerce, Dionex Corporation and the University of Turin is gratefully acknowledged.

We look forward to seeing you in Dallas, TX, USA on 1–4 October, 1995, where IICS'95 will be held under the chairmanship of Professor Donald J. Pietrzyk of the University of Iowa.

Turin, Italy C. Sarzanini

SSDI 0021-9673(95)00176-X

ELSEVIER

Journal of Chromatography A, 706 (1995) 3–12

JOURNAL OF CHROMATOGRAPHY A

Studies on system performance and sensitivity in ion chromatography

P.E. Jackson[a,*], J.P. Romano[b], B.J. Wildman[b]

[a]*Waters Australia Pty. Ltd., Private Bag 18, Lane Cove, N.S.W. 2066, Australia*

[b]*Waters Corporation, 34 Maple Street, Milford, MA 01757, USA*

Abstract

Improvements in HPLC instrumentation, suppressor technology and ion-exchange columns have occurred over the past several years to the point where an ion chromatograph can now be configured for anion analysis using a considerable variety of hardware, suppressor and column combinations. A number of parameters, including hardware configuration, effect of temperature, column type and suppressor device, were studied with a view toward optimizing the performance of an ion chromatographic (IC) system. It was found that dual-piston, reciprocating pumps used with low-pressure pulse dampeners significantly reduced baseline noise for both suppressed and non-suppressed conductivity detector combinations, while column temperature control proved essential in order to achieve routine sub-ppb detectability in non-suppressed IC. In general, the use of suppressed IC resulted in lower detection limits than non-suppressed IC when using the same columns and hardware. Of the columns studied, the methacrylate-based HR column was found to give the best overall separation selectivity when using a carbonate–bicarbonate eluent and suppressed conductivity detection. The majority of column and suppressor combinations evaluated gave acceptable performance, although some gave less than satisfactory results. Also, some combinations resulted in lower than expected analytical results, particularly for chloride, when quantitated using single-point calibration. In addition to the use of commercially available suppressor devices, there is also a large number of high-capacity cation exchangers which can be used as suppressors and these columns, in some instances, may offer equivalent (or superior) performance compared to the commercial devices.

1. Introduction

Ion chromatography (IC) is now the preferred (and regulatory approved) methodology for the determinations of anions in aqueous samples [1]. While the original scope of IC was limited to the determination of inorganic (and organic) anions and cations using an ion-exchange separation with conductivity detection [2], the growth of IC has seen the technique employed with a much wider range of separation and detection methods [3]. Improvements in chromatographic hardware, column and suppressor technology have increased the range of solutes which can be analyzed, and also lowered the levels at which they can be detected.

Despite its widespread use, by far the most significant application of IC is the routine determination of the common inorganic anions, e.g. fluoride, chloride, nitrite, bromide, nitrate, phosphate and sulfate, in fresh water and wastewater samples [3]. A number of recent developments, including the expiration of the original packed-bed suppressor patent [4], has allowed

* Corresponding author.

0021-9673/95/$09.50
SSDI 0021-9673(95)00131-X

further possibilities for anion analysis, in terms of hardware, column and suppressor combinations. The objective of this paper was to evaluate a number of possible combinations in order to determine an optimal IC system configuration. Parameters investigated include hardware configuration, the effect of temperature, column type and suppressor device. Results presented include sample quantitation, linearity, peak-area repeatability, efficiency, baseline noise data and detection limits for a variety of column and suppressor combinations.

2. Experimental

2.1. Instrumentation

The ion chromatograph consisted of Waters (Milford, MA, USA) 600 solvent delivery system, 717+ autosampler, 431 conductivity detector and a Millennium 2010 chromatography management system. Data were collected at 1 point/s. Three analytical columns were used: a Waters IC Pak Anion HR (75 × 4.6 mm I.D.), a Sarasep (Alltech, Sydney, Australia) AN 300 (100 × 7.8 mm I.D.) and a Dionex (Sunnyvale, CA, USA) AS4A-SC (250 × 4.0 mm I.D.). The Waters column was used with a borate–gluconate eluent at a flow-rate of 1.0 ml/min and also with an eluent of 1.2 m*M* bicarbonate–1.2 m*M* carbonate at 1.0 ml/min. Both the AN 300 and Dionex columns were used with an eluent of 1.7 m*M* bicarbonate–1.8 m*M* carbonate at 2.0 ml/min. The borate–gluconate eluent consisted of 1.6 m*M* sodium tetraborate, 7.3 m*M* boric acid, 1.6 m*M* sodium gluconate, 5 g/l glycerin, 120 ml/l acetonitrile and 20 ml/l *n*-butanol at pH 8.5. Two commercially available suppressor devices were used: an Alltech (Sydney, Australia) Model 335 solid-phase chemical suppressor (SPCS) and a Dionex anion micromembrane suppressor (AMMS). A regenerant of 25 m*M* sulfuric acid at 3.0 ml/min was used with the Dionex AMMS [5]. Two high-capacity cation-exchange columns were also used as suppressor devices: a Waters IC Pak C Cation-Guard (50 × 4.6 mm I.D.) and Waters Fast Fruit Juice column (150 × 7.8 mm I.D.).

2.2. Reagents and procedures

Millipore (Bedford, MA, USA) Milli-Q 18-MΩ water was used for all eluent, sample and standard preparation. Sodium tetraborate, sodium carbonate, sodium bicarbonate, boric acid (all analytical-reagent grade) and glycerin (laboratory-reagent grade) were obtained from Ajax (Sydney, Australia), as were the analytical-reagent grade sodium salts used for the preparation of the anion standards. HPLC grade acetonitrile and *n*-butanol were also obtained from Ajax. Sodium gluconate (laboratory-reagent grade) was obtained from Fluka (Buchs, Switzerland). Eluents were prepared daily, filtered through a Millipore 0.45-μm HV filter and degassed in an ultrasonic bath before use. High- and low-level anion standard mixtures were prepared containing fluoride, chloride, nitrite, bromide, nitrate, phosphate and sulfate at 1, 2, 4, 4, 4, 6, and 4 ppm, respectively, for the high-level standard. This high-level standard was diluted 10 × to prepare the low-level standard. Tap water samples were directly injected and the wastewater sample was diluted 1:10 and filtered through a 0.45-μm Millex HV filter before injection.

3. Results and discussion

3.1. Column and suppressor combinations

Three conventional anion-exchange columns, Waters IC Pak Anion HR, Sarasep AN 300 and Dionex AS4A-SC, were used in conjunction with an Alltech SPCS and Dionex AMMS. The HR column was used in both the non-suppressed and suppressed conductivity detection modes, while the AN 300 and AS4A columns were only used in the suppressed conductivity mode, as it has been previously established that such columns do not typically perform well in the non-suppressed mode [6]. Each column and suppressor combination was used to chromatograph a series of

injections of the high-level (1–6 ppm) standard, the low-level (0.1–0.6 ppm) standard, a tap water and a diluted wastewater sample. The linearity of each of the combinations was determined and the peak area repeatability was calculated from six replicate injections of the high-level anion standard. The 'sensitivity' of the various column, suppressor and hardware combinations was evaluated in terms of individual peak detection limits, rather than calculating sensitivity according to the correct definition of the term; that is as analyte response/concentration, e.g. in units of μV ml μg^{-1} [7]. This approach was strictly a practical one, as the majority of analytical chromatographers use detection limits, rather than the slope of the analyte response/concentration curve, when considering system sensitivity. The detection limits were calculated (at a signal-to-noise of 3) from the chromatogram of the low-level anion standard for each of the column and suppressor combinations.

3.2. Non-suppressed ion chromatography

A borate–gluconate eluent was used with the HR column in the non-suppressed mode as this eluent has been shown to give the best overall separation selectivity for the common inorganic anions with methacrylate-based columns [6]. The background conductivity of the eluent was 283 $\mu S\ cm^{-1}$ and low-pressure pulse dampeners were used with the pump, as specified by Waters [8]. Fig. 1a shows a chromatogram of a 100-μl injection of the low-level anion standard obtained using the borate–gluconate eluent with the HR column and conductivity detection. A poor baseline was obtained, which proved to be the result of the column not being placed in a temperature controlled environment. Fig. 1b shows the chromatogram of the low-level standard with the HR column maintained at 35°C in a column oven. The use of temperature control significantly improved the baseline and was crucial when performing non-suppressed IC analyses at sub-ppm levels. Heating the column at 35°C also affected the separation selectivity somewhat, i.e. retention times generally increased and the retention of sulfate and phosphate increased relative to the other peaks.

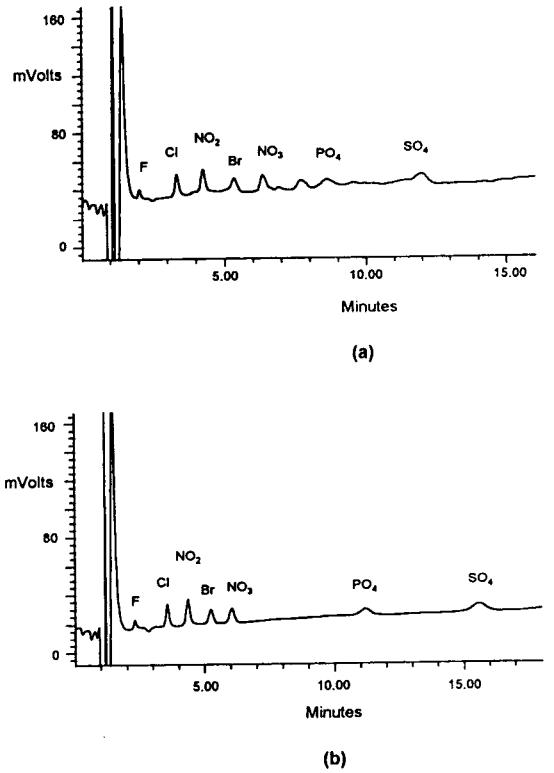

Fig. 1. Chromatogram of a low-level anion standard obtained using the HR column with non-suppressed conductivity detection. Conditions: column, Waters IC Pak Anion HR; eluent, borate–gluconate at 1.0 ml/min; injection volume, 100 μl; detection, non-suppressed conductivity; column temperature, (a) ambient and (b) 35°C; solutes, 0.1–0.6 ppm as detailed in Experimental.

The tap water and $10\times$ diluted wastewater samples were chromatographed using injection volumes of 100 and 50 μl, respectively. The results calculated for these two samples were generated using single-point calibration with the high-level anion standard, as was the case for all the other column and suppressor combinations. Both sample chromatograms showed the typical baseline disturbance which is characteristic of borate–gluconate eluents. This disturbance, or system peak, occurs from the presence of calcium and magnesium in the injected sample forming anionic complexes with the borate–gluconate diester [9] and elutes near the nitrate

Table 1
Tap water and wastewater sample results (ppm) obtained using each of the column and suppressor combinations

	HR	HR-S	HR-A	AN 300-S	AN 300-A	AS4A-S	AS4A-A
Tap water							
F	1.05	1.00	1.02	0.98	1.13	1.32	1.04
Cl	21.4	18.5	16.9	22.5	14.4	21.2	17.2
NO_3	1.40	1.19	1.15	1.74	1.77	1.74	1.78
SO_4	7.09	7.49	7.45	7.39	7.34	7.57	7.40
Wastewater							
F	12.8	9.78	11.7	9.18	11.1	12.32	8.55
Cl	17.3	13.3	14.4	16.4	11.8	21.4	13.7
NO_3	3.97	4.73	6.84	4.07	4.23	4.73	4.12
SO_4	796	893	801	823	787	846	785

HR = Waters HR column, AN 300 = Sarasep AN 300 column, AS4A = Dionex AS4A column, -S = Alltech SPCS, -A = Dionex AMMS.

peak. The presence of the system peak is a significant limitation of this mobile phase, as detection limits in real samples are typically not as good as for standards. This problem can be overcome by using a cation-exchange, hydrogen ion-donating device [10]; however, this adds additional sample preparation time (and expense) to the analysis. The sample results obtained using the HR column, and also those for each of the column and suppressor combinations, are given in Table 1.

Calibration curves were prepared for the HR column using a series of standards containing chloride, nitrate, phosphate and sulfate. The curves were prepared for each column and suppressor combination over as wide a concentration range as possible. Non-suppressed IC intrinsically gives linear calibration curves with conductivity detection [11] and the regression constants (r^2) were >0.9999 for all four solutes with the HR column. The linearity data for the HR column, and for each of the column and suppressor combinations, is given in Table 2. Peak-area repeatability data were calculated for the HR column from six replicate injections of the high-level standard, with any obvious outliers being statistically rejected [12]. Table 3 summarises the peak-area repeatability data for the HR column, and for each of the column and suppressor combinations, while Table 4 shows the peak efficiency data, calculated using the half-height method, for the HR column and each of the other column and suppressor combinations. Method detection limits (signal-to-noise ratio of 3) were calculated from the chromatogram of low-level standard shown in Fig. 1b. Table 5 shows the detection limit (and baseline noise data) for each solute with the HR column, and also for each of the other column and suppressor combinations.

Table 2
Linearity data (regression constant, r^2) for each of the column and suppressor combinations

	HR	HR-S	HR-A	AN 300-S	AN 300-A	AS4A-S	AS4A-A
Cl	0.999975	0.999608	0.999798	0.999510	0.993370	0.999830	0.994999
NO_3	0.999987	0.999263	0.999929	0.998778	0.998582	0.998856	0.998201
PO_4	0.999974	0.999026	0.999955	0.999054	0.997979	0.998891	0.998827
SO_4	0.999960	0.999568	0.999542	0.999677	0.999531	0.999656	0.999744

Column and suppressor identities as in Table 1.

Table 3
Peak-area repeatability data (% R.S.D.) for six replicate injections of the high-level anion standard for each of the column and suppressor combinations

	HR	HR-S	HR-A	AN 300-S	AN 300-A	AS4A-S	AS4A-A
F	1.167	1.010	2.151	3.250	1.672	28.559	2.725
Cl	0.588	0.553	2.302	1.795	0.520	1.782	0.204
NO_2	0.553	1.929	0.729	3.573	0.974	2.270	0.429
Br	0.543	0.102	0.607	2.241	0.565	2.808	1.378
NO_3	0.660	0.340	0.514	3.291	0.293	3.814	2.038
PO_4	1.022	0.882	0.796	0.635	0.363	0.581	0.404
SO_4	2.318	0.137	1.549	1.112	0.129	0.860	0.245

Column and suppressor identities as in Table 1.

Table 4
Peak efficiency (theoretical plates) data, averaged for six replicate injections of the high-level standard for each of the column and suppressor combinations, calculated using the half-height method

	HR	HR-S	HR-A	AN 300-S	AN 300-A	AS4A-S	AS4A-A
F	2618	1141	1114	2653	2489	944	712
Cl	2910	1872	1923	3074	3356	1656	1689
NO_2	3029	1855	1737	3525	3381	1926	2158
Br	3377	2532	2578	4027	3595	3439	3428
NO_3	3151	2613	2672	3402	3087	3012	2962
PO_4	2475	2707	2660	4666	4394	3938	3898
SO_4	3123	2882	2880	5262	5057	4888	4832

Column and suppressor identities as in Table 1.

3.3. Suppressed ion chromatography

All three columns, i.e. the HR, AN 300 and the AS4A, were then used in the suppressed mode with carbonate–bicarbonate eluents and both the SPCS and AMMS devices. Fig. 2a shows a chromatogram of a 100-μl injection of the low-level standard obtained using an eluent of 1.2 m*M* bicarbonate–1.2 m*M* carbonate at 1.0 ml/min with the HR column and the SPCS

Table 5
Detection limits (ppb) at a signal-to-noise ratio of 3 and baseline noise data (μV) for each of the column and suppressor combinations

	HR (183 μV)	HR-S (93 μV)	HR-A (508 μV)	AN 300-S (46 μV)	AN 300-A (66 μV)	AS4A-S (44 μV)	AS4A-A (40 μV)	HR-CatEx (33 μV)
F	9.8	0.7	2.4	0.4	0.4	0.5	0.2	0.2
Cl	7.4	1.0	3.3	0.6	0.4	0.4	0.2	0.2
NO_2	12.5	2.6	9.5	1.2	1.1	1.0	0.5	0.8
Br	23.2	4.5	16.4	2.1	2.1	1.5	0.9	1.4
NO_3	22.7	4.3	15.6	2.0	2.0	1.3	0.8	1.3
PO_4	75.2	10.5	37.4	4.3	3.9	4.0	2.6	2.6
SO_4	40.4	4.2	17.5	1.8	1.7	1.7	1.2	1.4

Column and suppressor identities as in Table 1, except CatEx = cation-exchange suppressor.

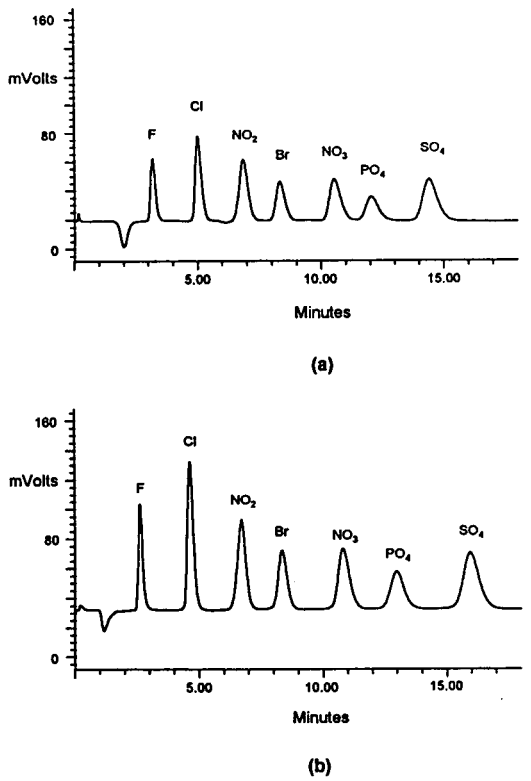

Fig. 2. Chromatogram of a low-level anion standard obtained using the HR column with suppressed conductivity detection. Conditions: column, Waters IC Pak Anion HR; eluent, 1.2 m*M* bicarbonate–1.2 m*M* carbonate at 1.0 ml/min; injection volume, 100 μl; detection, suppressed conductivity using (a) SPCS and (b) AMMS suppressors; solutes, 0.1–0.6 ppm.

suppressor, while Fig. 2b shows the low-level standard chromatogram obtained using the same column and eluent with the AMMS suppressor. All the chromatograms for the low-level anion standards are shown using the same millivolt scale to allow direct comparison of the relative response for each column, eluent and suppressor combination. The overall selectivity of the methacrylate-based HR column was particularly good with the carbonate–bicarbonate eluent, i.e. the peaks were evenly resolved and fluoride was well separated from the column void.

The background conductivity of the 1.2 m*M* bicarbonate–1.2 m*M* carbonate eluent after suppression by the SPCS device was 17 and 25 μS cm^{-1} after passing through the AMMS device. The use of the low-pressure pulse dampeners proved crucial to obtaining a 'pulseless' baseline with both suppressor devices, as conductivity detectors are sensitive to even very minor pump pressure fluctuations, particularly at lower flow-rates. The addition of the pulse dampeners decreased the height of the baseline noise, from 1322 to 93 μV for the SPSC device and from 1566 to 508 μV for the AMMS device. A similar, although less drastic, effect was also seen with the HR column in the non-suppressed mode.

The AMMS device produced increased peak response relative to the SPCS device with the HR column; however, detection limits were lower with the latter combination due to the significantly lower (~5 ×) baseline noise. The greater peak response of the AMMS device was due to a combination of slightly lower dead volume and more efficient suppression in the micromembrane device. Perhaps surprisingly, both suppressor devices reduced peak efficiencies by approximately the same amount (~40%) for the early-eluting solute ions, as compared to the HR column in the non-suppressed mode. The use of the carbonate–bicarbonate eluent and suppressed conductivity detection resulted in calibration curves being somewhat less than linear with the HR column, although this eluent has an advantage over the borate–gluconate eluent for tap water and wastewater analysis in that no system peaks were observed. Also, bicarbonate present in the sample is not typically detected when using this mobile phase. The sample results, linearity, peak-area repeatability, peak efficiency and detection limit data for the HR column and both suppressor devices are shown in Tables 1–5, respectively.

Fig. 3a shows a chromatogram of a 100-μl injection of the low-level anion standard obtained using an eluent of 1.7 m*M* bicarbonate–1.8 m*M* carbonate at 2.0 ml/min with the AN 300 column and the SPCS suppressor, while Fig. 3b shows the low-level standard chromatogram obtained using the same column and eluent with the AMMS suppressor. The background conductivity of the 1.7 m*M* bicarbonate–1.8 m*M* carbonate eluent after suppression by either the SPCS or the AMMS devices was 21 μS cm^{-1}.

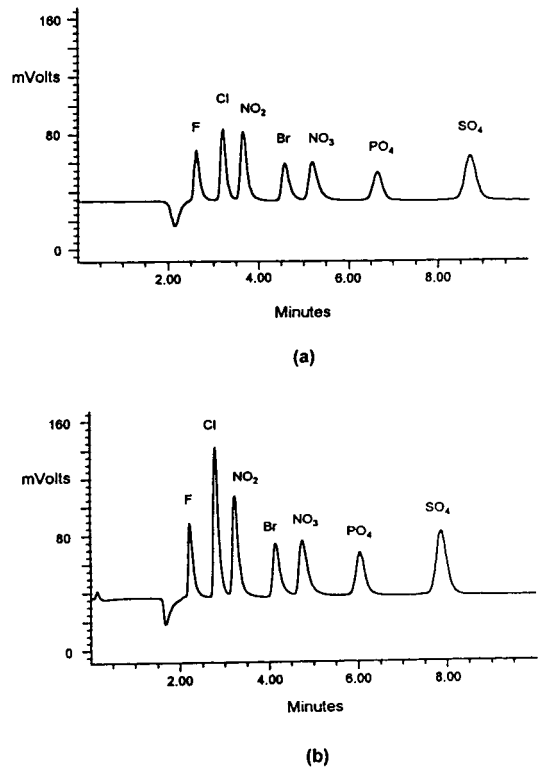

Fig. 3. Chromatogram of a low-level anion standard obtained using the AN 300 column with suppressed conductivity detection. Conditions: column, Sarasep AN 300; eluent, 1.7 m*M* bicarbonate–1.8 m*M* carbonate at 2.0 ml/min; injection volume, 100 μl; detection, suppressed conductivity using (a) SPCS and (b) AMMS suppressors; solutes, 0.1–0.6 ppm.

The overall selectivity of the AN 300 column was not as good as the HR column and fluoride was not particularly well separated from the column void, however, the total run times were shorter. The addition of the pump pulse dampeners decreased the height of the baseline noise, by approximately 3 × for both suppressor devices, when using the AN 300 column. Both devices gave less baseline noise at a flow-rate of 2.0 rather than 1.0 ml/min, particularly the AMMS suppressor. Very similar detection limits resulted with the AN 300 column and either suppressor device. The higher efficiency of the AN 300 column, combined with the better operation of either suppressor device at 2.0 ml/min, resulted in detection limits being approximately 2 × lower than with the HR column and the SPCS device combination.

Despite its proximity to the column void volume, the fluoride peak appeared sufficiently resolved from the void to allow quantitative determination in the tap water and wastewater samples. Generally, the results obtained for both samples using the AN 300 column were similar to those previously obtained with the HR column, except for chloride with the AMMS device. The AN-300 and the AMMS combination resulted in a calibration curve for chloride which significantly deviated from being linear, resulting in lower than expected sample results for chloride when quantitating using single-point calibration, as shown in Table 1. The sample results, linearity, peak-area repeatability, peak efficiency and detection limit data for the AN 300 column and both suppressor devices are shown in Tables 1–5, respectively.

Fig. 4a shows a chromatogram of a 100-μl injection of the low-level anion standard obtained using an eluent of 1.7 m*M* bicarbonate–1.8 m*M* carbonate at 2.0 ml/min with the AS4A column and the SPCS suppressor, while Fig. 4b shows the low-level standard chromatogram obtained using the same column and eluent with the AMMS suppressor. Once again, the background conductivity of the 1.7 m*M* bicarbonate–1.8 m*M* carbonate eluent after suppression by either the SPCS or the AMMS devices was 21 μS cm^{-1}. The overall selectivity of the AS4A column was very similar to that of the AN 300 column, although fluoride was not as well resolved from the column void. Once again, the addition of the pump pulse dampeners decreased the height of the baseline noise by approximately 3 × for both suppressor devices with the AS4A column. As was previously the case with the HR and AN 300 columns, the peak response with the AMMS device was greater than the SPCS device, due perhaps to more efficient suppression in the micromembrane device. Despite being slightly less efficient than the AN 300 column, the detection limits obtained with the AS4A were approximately 2 × lower than with the AN 300 column, due to the difference in column dimensions. The use of the 4.0 mm I.D. AS4A

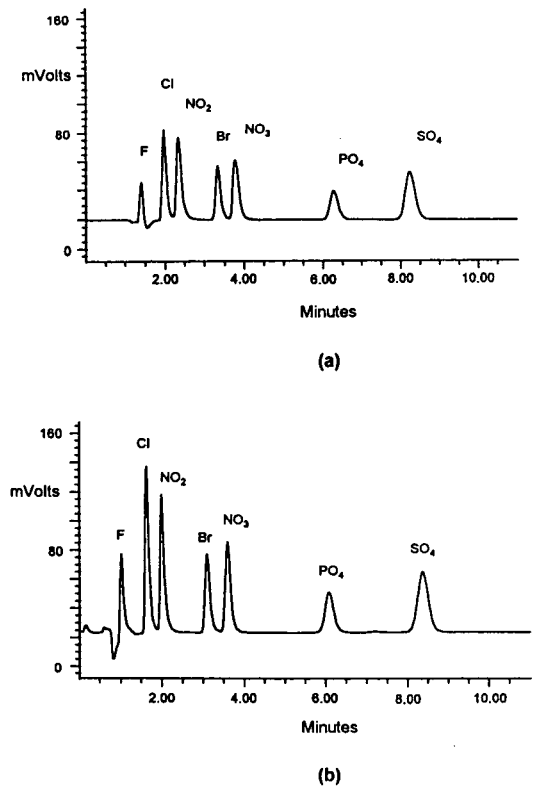

Fig. 4. Chromatogram of a low-level anion standard obtained using the AS4A column with suppressed conductivity detection. Conditions as for Fig. 3, except the column (Dionex AS4A-SC).

column resulted in less peak dilution than the 7.8 mm I.D. AN 300 column, leading to greater peak response.

The combination of the AS4A column with the SPCS device did produce significant differences in fluoride results for both the tap water and wastewater samples. The peak area repeatability, shown in Table 3, for fluoride was also very poor as a result of the lack of resolution from the column void and the fact that the retention time of the void varied as a result of ion-exclusion effects within the packed-bed SPCS device [3]. However, the fluoride results obtained using the AS4A column and AMMS combination were similar to the those obtained previously, indicating that ion-exclusion effects within the SPCS device were leading to the poor fluoride results when it coupled with the AS4A column. As was also the case with the AN 300 column, the use of the AS4A column and the AMMS device resulted in a calibration curve for chloride which significantly deviated from being linear, leading to lower than expected sample results for chloride when quantitating using single point calibration, as shown in Table 1. The sample results, linearity, peak-area repeatability, peak efficiency and detection limit data for the AS4A column and both suppressor devices are shown in Tables 1–5, respectively.

3.4. Alternative suppressor devices

Both the commercially available suppressor devices used in this work have their relative advantages and disadvantages. The SPCP utilises disposable cartridges which only have a finite lifetime. The cartridges are coated with an inert dye which provided a visible indication of the cartridge condition and gave a lifetime of only about 4 h with the 1.7 m*M* bicarbonate–1.8 m*M* carbonate eluent at 2.0 ml/min, although they had a lifetime of about 8 h when used with the 1.2 m*M* bicarbonate–1.2 m*M* carbonate eluent at 1.0 ml/min. Alternatively, the AMMS is continually regenerated, however, it required a large volume of dilute sulfuric acid along with a pneumatic reservoir and a gas supply. These problems were overcome with the recent introduction of a self-regenerating suppressor device, which requires no regenerant as it uses the electrolytic breakdown of water as a source of hydronium ions [13]. Despite the elegant advantage of continual regeneration, a disadvantage exists in that the membrane-based suppressors need to be replaced periodically as the membranes only have a finite lifetime. However, a much greater disadvantage is that it only takes one inappropriate sample or eluent to permanently damage a membrane-based device, while this is obviously of minimal concern when using disposable cartridges.

In principle, there is no need to use a specialised suppressor device for IC, as virtually any high-capacity cation exchanger can function as a suppressor. Fig. 5 shows a chromatogram of the

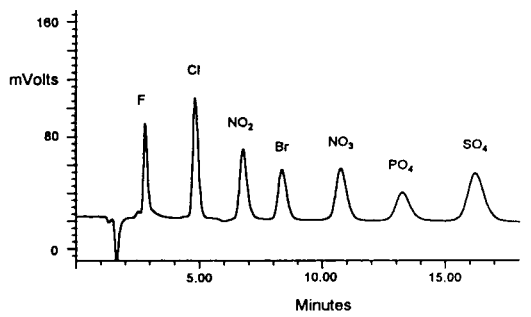

Fig. 5. Chromatogram of a low-level anion standard obtained using the HR column with a cation-exchange suppressor and conductivity detection. Conditions as for Fig. 2, except the detection method (suppressed conductivity using cation-exchange suppressor).

low-level anion standard obtained using a 1.2 m*M* bicarbonate–1.2 m*M* carbonate eluent at 1.0 ml/min with the HR column, conductivity detection and a 50×4.6 mm I.D. 'suppressor' column packed with sulfonated (2.0 mequiv./ml) polystyrene gel. The background conductivity of the eluent after suppression was 21 μS cm^{-1}. In terms of peak response, this cation-exchange column was superior to the SPCS suppressor and very similar to the AMMS device. The combination of the less efficient HR column with the cation-exchange suppressor gave virtually identical detection limits to the combination of the more efficient AS4A column and AMMS, as shown in Table 5. The column could be used for approximately 8 h with the above eluent before regeneration (with 25 m*M* sulfuric acid) was required. An attempt to use a still higher-capacity (5.0 mequiv./g) cation-exchange column (Waters Fast Fruit Juice) as a suppressor met with mixed success. This column was the best of all the suppressor devices investigated, in terms of peak response, however, ion-exclusion effects resulted in nitrite being eluted as a negative peak. As this column was specifically intended for use as an ion-exclusion column, it was hardly surprising that exclusion effects were prominent. Therefore, selecting an appropriate cation exchanger to function as a suppressor for anion analysis should simply be a matter of choosing a column with good chromatographic efficiency, high cation-exchange capacity and minimum exclusion effects.

In terms of an optimal system configuration for the IC analysis of anions in water and wastewater samples, a dual-piston pump equipped with low-pressure pulse dampeners should be used to minimise baseline fluctuations. The use of a methacrylate-based anion-exchange column permits the best overall separation selectivity with a carbonate–bicarbonate eluent, while a solid-phase cation-exchange suppressor and conductivity detector offer the best detection compromise in terms of sensitivity, linearity and analytical sample performance.

4. Conclusions

A number of conclusions relating to optimising system performance and sensitivity in IC are evident from this study. The use of a dual-piston pump equipped with low-pressure pulse dampeners will minimise baseline noise when using conductivity detection. Column temperature control was essential in order to achieve routine sub-ppb detectability in non-suppressed IC, although temperature control appeared to make little difference for suppressed IC.

In general, the use of suppressed IC resulted in significantly lower ($5–10\times$) detection limits than non-suppressed IC when using the same columns and hardware, with the methacrylate-based HR column giving the best overall separation selectivity when using a carbonate–bicarbonate eluent and suppressed conductivity detection. Both the SPCS and the AMMS suppressor devices gave similar performance in terms of band broadening, with the latter resulting in slightly improved peak response. Not all the column and suppressor combinations studied gave satisfactory results; the AMMS device resulted in excessive baseline noise when used at the flow-rates required for the HR column, while the combination of the AS4A column and SPCS resulted in unacceptable results for fluoride. The use of the AMMS device with the AN-300 and AS4A columns gave the least linear calibration curves, particularly for chloride, resulting in

lower than expected analytical results for chloride when quantitating using single point calibration.

In addition to the use of commercially available suppressor devices, there is also a large number of high-capacity cation exchangers which can be used as suppressors. These columns may, in some instances, offer equivalent (or superior) performance when compared to the commercial devices and it appears that an appropriate solid-phase cation-exchange suppressor may well offer the best compromise for suppressed conductivity detection in terms of sensitivity, linearity and analytical performance.

References

[1] J.P. Romano and J. Krol, *J. Chromatogr.*, 602 (1992) 205.
[2] H. Small, T.S. Stevens and W.C. Bauman, *Anal. Chem.*, 47 (1975) 1801.
[3] P.R. Haddad and P.E. Jackson, *Ion Chromatography: Principles and Applications* (*J. Chromatogr. Library Series*, Vol. 46), Elsevier, Amsterdam, 1990.
[4] H. Small and T.S. Stevens, *U.S. Pat.*, 3,925,019.
[5] *Dionex Ion Chromatography Cookbook, Issue I*, Dionex, Sunnyvale, CA, 1987.
[6] P.E. Jackson and T. Bowser, *J. Chromatogr.*, 602 (1992) 33.
[7] K. Robards, P.R. Haddad and P.E. Jackson, *Principles and Practice of Modern Chromatographic Methods*, Academic Press, New York, 1994, Ch. 9.
[8] A.L. Heckenberg, P.G. Alden, B.J. Wildman, J. Krol, J.P. Romano, P.E. Jackson, P. Jandik and W.R. Jones, *Waters Innovative Methods for Ion Analysis*, Millipore, Milford, MA, 1989.
[9] C. Erkelens, H.A.H. Billiet, L. De Galan and E.W.B. De Leer, *J. Chromatogr.*, 404 (1987) 67.
[10] W.R. Jones and P. Jandik, *J. Chromatogr. Sci.*, 27 (1989) 449.
[11] M. Doury-Berthod, P. Giampaoli, H. Pitsch, C. Stella and C. Pointrenaud, *Anal. Chem.*, 57 (1985) 2257.
[12] R.B. Dean and W.J. Dixon, *Anal. Chem.*, 23 (1951) 636.
[13] S. Rabin, J. Stillian, V. Barreto, K. Friedman and M. Toofan, *J. Chromatogr.*, 640 (1993) 97.

ELSEVIER

Journal of Chromatography A, 706 (1995) 13–19

JOURNAL OF CHROMATOGRAPHY A

Precision of ion chromatographic analyses compared with that of other analytical techniques through intercomparison exercises

Aldo Marchetto[a], Rosario Mosello[a,*] Gabriele A. Tartari[a], Herbert Muntau[b], Michele Bianchi[b], Helga Geiss[b], Giorgio Serrini[b], Gianna Serrini Lanza[b]

[a]*CNR Istituto Italiano di Idrobiologia, I-28048 Verbania Pallanza, Italy*
[b]*JRC Environmental Institute, Ispra (VA), Italy*

Abstract

Three intercomparison exercises on simulated rainwater were held in 1991–1993 involving 72–98 laboratories in Europe and South America. Ion chromatography was used for the determination of anions (chloride, nitrate and sulphate) by 59–72% of the participating laboratories and for the determination of cations (Na, K, Mg and Ca) by 14–22% of them. The concentration of the single ions ranged between 5 and 150 μmol l^{-1}. The results were used to evaluate the precision of the method, and showed that it was comparable to that of spectrophotometric methods. For ammonium ion, ion chromatography was used by only 4–14% of the laboratories and the results depended on the calibration technique adopted. A general improvement in precision was observed in the course of the exercises.

1. Introduction

The authors have been involved since 1984 in intercomparison exercises for inorganic ions, in the framework of limnological research in Italy [1] and the Italian network for the study of atmospheric deposition chemistry (RIDEP) [2]. Since 1991, intercomparison exercises have been carried out every year, involving laboratories participating in, besides RIDEP, also the EEC projects "AQUACON–MedBas" and "AL:PE, acidification of mountain lakes: paleolimnology and ecology", or working with the International Commission for the Protection of Lake Leman, or requesting participation, such as laboratories in South America and in the former Eastern Europe. The number of participating laboratories was 72 in 1991, 78 in 1992 and 99 in 1993. Full data and the list of participating laboratories have been published elsewhere [3–5].

The aim of the work described in this paper was to obtain general information on the precision of ion chromatography (IC), one of the methods most widely used by the participating laboratories for the determination of inorganic ions (Table 1). The exercises and the range of application of the results are aimed at the analysis of freshwater and atmospheric deposition.

2. Experimental

For each exercise, two solutions were prepared starting from water of the highest quality

* Corresponding author.

0021-9673/95/$09.50
SSDI 0021-9673(95)00039-9

Table 1
Number of laboratories participating in the three intercomparison exercises and percentage of laboratories using ion chromatography for the determination of each ion

Exercise	1991	1992	1993
No. of participating laboratories	72	77	99
Ion	**Laboratories using IC (%)**		
Anions			
Cl^-	72	68	64
NO_3^-	69	66	59
SO_4^{2-}	72	73	65
Cations			
Na^+	14	23	22
NH_4^+	4	14	14
K^+	15	22	21
Mg^{2+}	15	21	21
Ca^{2+}	15	21	21

(Nanopure UWS, Barnstead) and the purest chemicals available. The carefully weighed chemicals were dissolved and water was added to prepare a stock standard solution (1 l), which was then checked analytically for correctness of the envisaged analyte concentrations. The stock standard solution was added to approximately 20 l of Nanopure water in a 50-l polyethylene container, previously conditioned with the same quality of water for 2 weeks. The calculated amount of Suprapur HCl required to reach the previously fixed pH value of the final solution was added and the solution was made up to a total of 50 l. The solution was mixed by rolling the container. Bottling was performed by hand, rinsing the previously conditioned 0.5-l polypropylene bottles (2 weeks with Nanopure water) with the samples and then filling them up to the top.

Samples were sent to the participating laboratories by mail, and the stability of the samples was checked by analysing samples kept in the dark at room temperature over the period allowed for the exercise [3–5]. Participating laboratories were only requested to perform a single analysis for each sample.

Target values were calculated as the mean of the values obtained by the organizing laboratories, using IC for anions, the salicylate spectrophotometric method for ammonium and atomic absorption spectrometry for the other cations.

3. Data analysis

3.1. Sample homogeneity

The total variance measured at the JRC laboratory on ten randomly selected samples (representing about 3% of the whole population) is assumed to be equal to the sum of the variances resulting from the analytical method used, the non-homogeneity of the samples and other random errors:

$$(S.D._{tot})^2 = (S.D._{method})^2 + (S.D._{heterog.})^2 + (S.D._{random})^2$$

The variance due to the analytical method for each ion was estimated by repeating the measurement ten times on the same bottle of each sample. All the measurements were performed in one laboratory by the same analyst using the same analytical method for each variable. Heterogeneity of the variables in the solutions was then estimated as the square root of the difference of the squares of the standard deviations of samples and methods.

3.2. Outlier detection

In intercomparison exercises it often happens that some laboratories obtain results which stand out from the rest, either because of some error in calibration, or unreliable laboratory practice, mistakes in recording the results, contamination of the samples or of the standard solutions used for calibration, and so on. The effect of these outliers is to increase the estimate of the variance of the results, which would then show a wide deviation from the normal distribution. For these reasons, it is common practice to discard outliers before statistical treatment of the data. In this paper, outlier rejection was performed by excluding data out of the range of ±50% of the

Table 2
Selected statistical parameters of the values obtained using ion chromatography for each ion and sample

Ion	Parameter	Sample					
		1991A	1992A	1993A	1991B	1992B	1993B
Sulphate	No. of data	52	56	64	52	57	66
	Target concentration (μM)	24.6	27.1	36.1	121.3	124.9	150.9
	Heterogeneity (%)	0.4	0.5	0.8	0.6	0.5	0.4
	Parametric estimate of R.S.D. (%)	8.6	6.9	12.2	8.3	8.4	10.7
	Robust estimate of R.S.D. (%)	6.5	6.1	5.0	6.4	6.2	4.3
	No. of outliers	1	1	3	1	1	3
	R.S.D. after outliers rejection (%)	7.6	6.0	6.6	6.6	7.1	4.9
Nitrate	No. of data	50	51	58	50	52	61
	Target concentration (μM)	7.9	9.3	8.6	56.4	74.3	69.3
	Heterogeneity (%)	0.5	0.3	0.5	0.6	0.1	0.7
	Parametric estimate of R.S.D. (%)	67.6	42.8	11.2	63.4	17.5	36.6
	Robust estimate of R.S.D. (%)	17.5	16.7	9.7	7.7	4.2	4.0
	No. of outliers	7	4	0	5	4	2
	R.S.D. after outliers rejection (%)	14.2	14.9	11.2	7.7	4.4	5.7
Chloride	No. of data	52	52	63	52	56	65
	Target concentration (μM)	5.1	4.5	24.5	57.5	33.6	53.9
	Heterogeneity (%)	1.4	1.4	0.3	1.1	0.6	0.2
	Parametric estimate of R.S.D. (%)	221.8	59.5	21.0	53.9	18.8	12.6
	Robust estimate of R.S.D. (%)	45.9	16.7	12.3	11.3	10.3	8.9
	No. of outliers	16	11	2	3	2	1
	R.S.D. after outliers rejection (%)	21.7	21.5	15.3	15.2	11.2	11.2
Sodium	No. of data	10	18	22	10	18	24
	Target concentration (μM)	7.4	8.7	7.4	52.2	64.3	30.4
	Heterogeneity (%)	1.4	1.5	1.4	0.5	0.2	0.6
	Parametric estimate of R.S.D. (%)	65.0	114.1	22.5	25.4	18.6	28.0
	Robust estimate of R.S.D. (%)	38.5	26.2	16.3	25.4	6.8	13.8
	No. of outliers	2	2	2	0	0	1
	R.S.D. after outliers rejection (%)	24.0	21.9	14.9	25.4	18.6	13.6
Ammonium	No. of data	3	11	14	3	11	15
	Target concentration (μM)	22.9	27.1	27.1	90.0	83.6	100.0
	Heterogeneity (%)	1.3	1.1	0.8	0.6	0.4	0.1
	Parametric estimate of R.S.D. (%)	103.5	55.5	50.3	69.2	24.8	18.3
	Robust estimate of R.S.D. (%)	103.3	48.2	16.8	69.1	12.7	14.5
	No. of outliers	2	4	1	1	1	0
	R.S.D. after outliers rejection (%)		15.5	14.8	4.6	14.4	18.3
Potassium	No. of data	11	17	21	10	17	24
	Target concentration (μM)	5.9	7.4	5.1	8.2	11.0	11.5
	Heterogeneity (%)	1.5	1.2	1.3	1.4	0.6	0.5
	Parametric estimate of R.S.D. (%)	187.2	31.8	81.0	40.1	43.5	29.6
	Robust estimate of R.S.D. (%)	69.6	31.5	8.2	35.2	19.0	10.8
	No. of outliers	4	2	1	3	3	1
	R.S.D. after outliers rejection (%)	15.0	22.7	7.2	12.9	12.7	11.3

(*Continued on page 16*)

Table 2 (*continued*)

Ion	Parameter	Sample					
		1991A	1992A	1993A	1991B	1992B	1993B
Magnesium	No. of data	11	16	21	11	17	23
	Target concentration (μM)	4.1	4.1	5.8	8.6	13.2	14.0
	Heterogeneity (%)	0.4	0.4	0.4	0.5	0.5	0.4
	Parametric estimate of R.S.D. (%)	56.0	27.0	32.8	38.1	137.8	36.6
	Robust estimate of R.S.D. (%)	23.8	17.1	10.6	18.4	13.9	8.9
	No. of outliers	2	1	1	2	1	1
	R.S.D. after outliers rejection (%)	15.6	17.0	12.7	12.6	13.3	13.9
Calcium	No. of data	11	16	21	11	17	23
	Target concentration (μM)	5.2	5.0	9.0	20.2	31.4	26.9
	Heterogeneity (%)	1.0	1.1	1.1	0.6	0.1	0.3
	Parametric estimate of R.S.D. (%)	68.0	32.1	15.3	38.4	14.4	20.4
	Robust estimate of R.S.D. (%)	49.8	26.3	10.6	30.5	9.6	11.7
	No. of outliers	5	1	0	1	0	1
	R.S.D. after outliers rejection (%)	29.2	22.7	15.3	25.1	14.4	13.6

expected values. The mean and standard deviation of the remaining results were then calculated and values out of the range of ± 3 S.D. iteratively excluded [6].

3.3. Robust estimate of the S.D.

Outlier rejection is not correct practice when included in the evaluation and comparison of the

Table 3
Summary of the results of the *F*-test to compare the variance obtained using ion chromatography and that obtained using more common concurrent methods

Ion	Method[a]	Sample[b]					
		1991A	1991B	1992A	1992B	1993A	1993B
Chloride	MAS	n.s.	n.s.	n.s.	n.s.	n.s.	n.s.
Nitrate	MAS	n.s.	n.s.	n.s.	n.s.	S	S
Sulphate	Turb.	S	S	S	S	S	S
Sodium	AAS	L	n.s.	n.s.	n.s.	n.s.	n.s.
	AES	L	n.s.	n.s.	S	S	n.s.
Ammonium	MAS: Nessler	n.s.	n.s.	n.s.	S	n.s.	n.s.
	MAS: indophenol	L	L	L	L	L	L
Potassium	AAS	L	n.s.	n.s.	L	n.s.	n.s.
	ICP	n.s.	n.s.	n.s.	L	S	n.s.
Magnesium	AAS	L	L	L	L	n.s.	n.s.
	ICP	L	L	L	L	n.s.	n.s.
Calcium	AAS	L	n.s.	n.s.	n.s.	S	n.s.
	ICP	L	n.s.	n.s.	n.s.	n.s.	n.s.

[a] AAS = atomic absorption spectrometry; AES = atomic emission spectrometry; ICP = inductively coupled plasma spectrometry; MAS = molecular absorption spectrometry; Turb = turbidimetry.

[b] L, variance of ion chromatography significantly ($p < 0.01$) larger than that of concurrent method; S, variance of ion chromatography significantly ($p < 0.01$) smaller than that of concurrent method; n.s., no significant difference.

precision of analytical methods, as it can produce a smaller S.D. for methods producing a larger number of outliers. An alternative approach is robust statistics (e.g., Ref. [7]), which shifts from outliers rejection to outlier accommodation: extreme values are downweighted and that downweighting is compensated for. In this paper we used the iterative technique known as H15, assuming a value of 1.5 for the constant c [8].

The procedure begins by assigning to the estimated robust mean (m_0) the median of the sample values (x_i) and to the estimated robust S.D. (s_0) the median absolute deviation (MAD), that is the median of the quantities $(|x_i - m_0|)/0.6745$. Then, at each nth iteration, all values higher than $m_{n-1} + cs_{n-1}$ or lower than $m_{n-1} - cs_{n-1}$ are replaced by the pseudo-values $m_{n-1} + cs_{n-1}$ and $m_{n-1} - cs_{n-1}$, respectively, while the pseudo-values for the remaining values are the values themselves. The new estimate of the robust mean m_n will be the mean of the pseudo-values, while the new estimate of the robust S.D. (s_n) will be their S.D. divided by the square root of the constant β, which compensates for the downweighting of the extreme values. At $c = 1.5$, $\beta = 0.736$ [8]. The estimated parameters rapidly converge to the robust mean and S.D.

4. Results

The results for the three intercomparison exercises are summarized in Table 2. For all the ions, the number of laboratories using IC increased during the period of the exercises.

As expected, for more dilute solutions, higher RSDs were observed. The contribution of sample heterogeneity to the final data dispersion was not significant in all instances.

As the first exercises contributed to stimulating the analysts to solve technical problems and improve laboratory practice, the dispersion of the values and the number of outliers generally decreased from the first to the last exercise. Apart from ammonium, the robust S.D. obtained for the last exercise can be considered to be a good estimate of the precision of the method. However, in the case of ammonium, the number of laboratories using IC was too small for such an estimate.

5. Discussion

The relative performance of IC compared with the more widely used concurrent methods was evaluated by comparing the robust estimates of the averages and variances by means of Student's t- and the F-tests. No significant difference was obtained for the means, whereas for the vari-

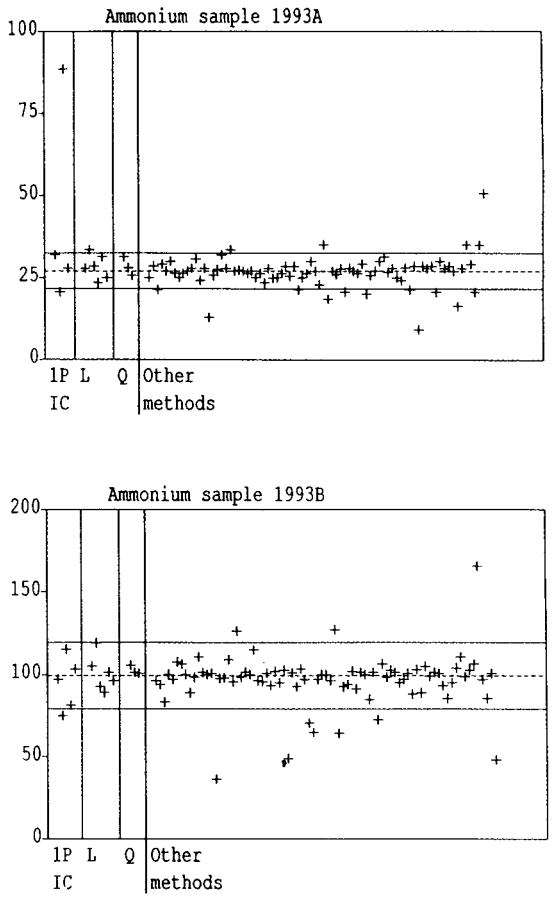

Fig. 1. Distribution plot of the values obtained for ammonium using ion chromatography and other methods in the third intercomparison exercise. Note the different dispersion of the values obtained using different calibration techniques (1P = single point; L = multi-point linear; Q = multi-point quadratic). Units: μmol l^{-1}.

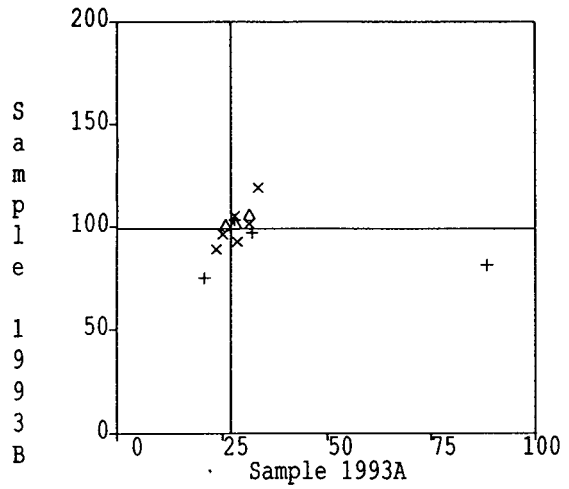

Fig. 2. Youden plot of the values obtained in the third intercomparison exercise for ammonium using ion chromatography and different calibration techniques (+ = single point; × = multi-point linear; △ = multi-point quadratic). Units: μmol l^{-1}.

ances the results of the tests were as summarized in Table 3.

From the first to the last exercise, as the analysts' practice improved, the precision of the chromatographic method increased. In the last exercise, IC performed better than turbidimetric and spectrophotometric methods for sulphate and chloride, respectively, whereas for metals, the differences with respect to the common spectrophotometric methods were not generally significant. It seems that, at low levels, IC would perform better than atomic emission spectrometry for Na and K and than atomic absorption spectrometry for Ca. For ammonium, the dispersion of the values obtained by IC is significantly higher than that of values obtained by molecular absorption spectrometry. As the detector did not show a linear response for ammonium in this range of concentration (e.g., [9]), the results were divided on the basis of the calibration technique used (Fig. 1). The exercise for ammonium focused on such low concentration levels as are typically encountered during monitoring. Although the number of the data is too small for a statistical comparison, it is evident that values obtained using multi-point quadratic calibration have a smaller dispersion around the target values.

The Youden plot [10] presented in Fig. 2 shows the scatter of the data relative to both samples, analysed by each laboratory using IC. It allows for the distinction between random and systematic errors: if analyses were only affected by random errors, the results would be spread over the whole diagram. In this case, the results obtained by multi-point linear calibration are mainly located along the line passing through the origin and the expected values. This clearly shows the presence of systematic errors which underestimate or overestimate the concentration in both samples. Values obtained with single-point calibration generally stand out from the rest, and the better performance of multi-point quadratic calibration is also evident.

6. Conclusions

The importance of repeated intercomparison exercises for rainwater analysis, aimed at better performance from an analytical method, finds further confirmation in the case of IC. From the first to the third exercise the dispersion of the data decreased. The values obtained in the last exercise, apart from those for ammonium, can be used to estimate the precision of the method: the R.S.D. ranges from 4–5% for sulphate (24–151 μmol l^{-1}) to 13–16% for sodium (7.4–64 μmol l^{-1}), depending on the sample concentration. For ammonium (23–100 μmol^{-1}), the number of laboratories using IC was too small for such an estimate, but it was clear that the tendency for systematic errors is related to an unreliable calibration technique; multi-point non-linear calibration at very low concentration is required.

References

[1] R. Mosello, R. Baudo, G. Tartari, M. Camusso, G. Marengo, H. Muntau, A. Barbieri and G. Righetti, *Doc. Ist. Ital. Idrobiol.*, 18 (1989) 1.

[2] G. Serrini, M. Bianchi, H. Geiss, A. Marchetto, R. Mosello, H. Muntau, G. Serrini Lanza and G.A. Tartari, *Doc. Ist. Ital. Idrobiol.*, 27 (1990) 1.
[3] R. Mosello, M. Bianchi, H. Geiss, A. Marchetto, L. Morselli, H. Muntau, G.A. Tartari, G. Serrini and G. Serrini Lanza, *Doc. Ist. Ital. Idrobiol.*, 35 (1992) 1.
[4] R. Mosello, M. Bianchi, H. Geiss, A. Marchetto, L. Morselli, H. Muntau, G.A. Tartari, G. Serrini and G. Serrini Lanza, *Doc. Ist. Ital. Idrobiol.*, 39 (1993) 1.
[5] R. Mosello, M. Bianchi, H. Geiss, A. Marchetto, L. Morselli, H. Muntau, G.A. Tartari, G. Serrini and G. Serrini Lanza, *Doc. Ist. Ital. Idrobiol.*, 47 (1994) 1.
[6] H. Hovind, *Intercalibration 8903. Dissolved Organic Carbon and Aluminium Fractions*, Niva, Oslo, 1990.
[7] P.J. Huber, *Outliers in Statistical Data*, Wiley, Chichester, 2nd ed., 1984.
[8] Analytical Methods Committee, *Analyst*, 114 (1989) 1693.
[9] G.A. Tartari, A. Marchetto and R. Mosello, *J. Chromatogr. A*, 706 (1995) 21.
[10] W.J. Youden and E.H. Steiner, *Statistical Manual of the Association of Official Chemists*, AOAC, Arlington, VA, 1975.

ELSEVIER

Journal of Chromatography A, 706 (1995) 21–29

JOURNAL OF CHROMATOGRAPHY A

Precision and linearity of inorganic analyses by ion chromatography

Gabriele A. Tartari*, Aldo Marchetto, Rosario Mosello

Consiglio Nazionale delle Ricerche, Istituto Italiano di Idrobiologia, I-28048 Verbania Pallanza, Italy

Abstract

The repeatability of the measurements of peak areas for calibration solutions and the precision of anion and cation determinations (3–600 μM) in freshwater are discussed on the basis of 2 years of measurements on calibration solutions and stabilized internal standards. Anion measurements show higher repeatability of the measurements of peak areas for calibration solutions (R.S.D. 2–5%) and precision (R.S.D. 2–8%) than those of cations (R.S.D. 2–10% and 2–15%, respectively). Results for the calibration technique show that multi-point (6–8 concentrations), quadratic or cubic regressions permit a correct quantification over a wide range (1.5–2 orders of magnitude) of concentrations. Thanks to the repeatability of the measurements of peak areas for calibration solutions, only two calibrations, at the beginning and end of a batch of 20–30 samples, are adequate. These conditions give better results than calibrations performed with 2–3 points and repeated every 8–10 samples.

1. Introduction

In the last decade, ion chromatography (IC) has become one of the most frequently used techniques for the determination of anions and, more recently, cations at low levels. Long-term quantitative reports of the performance of the method are required to estimate its precision and to allow method optimization.

In this work we used long-term (months or years) records of the peak areas for calibration solution and control charts to estimate the precision of the IC determination of inorganic ions. One of the major problems arising from routine analytical activity is the evaluation of the precision of chemical data, defined following the APHA as the measurement of the degree of agreement among replicate analyses of a sample with concentrations stable in time [1]. Leaving aside the problems related to sample representativeness, there are several manual and instrumental factors that contribute to precision, such as sample pretreatments, standard preparation and conservation, repeatability of the measurements of peak areas for calibration solutions and type of calibration [1–3].

This paper also aims to define an efficient calibration procedure, to assist those whose work involves routine analyses. In 5 years' operation as a reference laboratory in intercomparison exercises [4], we have found that most of the participating laboratories use one-point or multi-point linear calibration, repeated every batch of 5–20 samples. A different calibration function is

* Corresponding author.

0021-9673/95/$09.50
SSDI 0021-9673(94)01222-9

generally required if the concentration of any sample lies out of the calibration range. To simplify this procedure, we investigated the reliability of a single calibration function over large ranges of concentration (1.5–2 order of magnitude, depending on the specific ion).

As our laboratory deals mainly with atmospheric deposition and surface water analysis (an average of 2000 samples per year), the application of our results to different media is not recommended.

2. Definitions

Response Factor (R.F.): ratio between the amount of the analyte (μmol) in the calibration solution and the detector signal (nS cm^{-1} s), expressed in μmol cm S^{-1} s^{-1}.

Repeatability of the measurements of peak areas for calibration solutions: relative standard deviation [R.S.D. (%)] of the peak areas of calibration solutions at different levels of concentrations, measured in 24–150 calibrations during 1 year. Of these, only complete multipoint calibrations (24–29 depending on the specific ion) were used to evaluate the reproducibility of whole calibration functions. It is assumed to be dependent on (a) preparation of standards (weighing, dissolution, volumetric dilution), (b) equipment repeatability of the measurements of peak areas for calibration solutions and (c) random, non-identifiable errors.

Precision: R.S.D. (%) of the measured concentrations of natural or artificial samples, stabilized with chloroform (control charts), analysed 1–2 times every batch of analyses. It is assumed to be dependent on (1) factors (a), (b) and (c) of repeatability of the measurements of peak areas for calibration solutions, (2) calibration (incorrect regression between concentration and instrument signals), (3) interferences among the ions present in the sample and (4) contamination or unrepeatability of the measurements of peak areas for calibration solutions of the natural or artificial samples used.

3. Experimental

3.1. Equipment for anions

A Dionex (Sunnyvale, CA, USA) Model 2010i ion chromatograph including analytical pump and CDM-1 conductivity detector, Spectra-Physics (San Jose, CA, USA) SP8780 autosampler with a Rheodyne Model 7010 injection valve and a 50-μl sample loop was used. The Dionex anion column consisted of an Ion Pac AG4A guard column, Ion Pac AS4A separation column and chemical suppression by an anion self-regenerating suppressor used in the autosuppression recycle mode. The eluent was 1.8 m*M* sodium carbonate–1.7 m*M* sodium hydrogencarbonate at a flow-rate of 2.0 ml min^{-1}, the system pressure was 650–750 p.s.i (1 p.s.i. = 6894.76 Pa) and the background conductivity was 14–15 μS cm^{-1}.

3.2. Equipment for cations

A Dionex Model 4000 ion chromatograph including an analytical gradient pump and CDM-2 conductivity detector, Spectra-Physics AS3500 autosampler with a Rheodyne Model 9010 injection valve and a 100-μl sample loop was used. The Dionex cation column consisted of an Ion Pac CG12 guard column, Ion Pac CS12 separation column and chemical suppression by a cation self-regenerating suppressor used in the autosuppression recycle mode. The eluent was 20 m*M* methansulfonic acid at a flow-rate of 1.0 ml min^{-1}, the system pressure was 1000–1100 p.s.i. and the background conductivity was 0.6–1.0 μS cm^{-1}.

Both the cation and anion columns were changed during the study period, without any noticeable effect on the response factors.

3.3. Integration

A Dionex Model III advanced computer interface with AI-450 program release 3.31 was used. Peak-area integration using external standards was applied.

3.4. Reagents

Eluents and combined standards were prepared fresh weekly using ultra-pure water (resistivity 18 MΩ cm, filtered through a 0.2-μm membrane filter), analytical-reagent grade chemicals for chloride, nitrate, sulphate and ammonium and ready-for-use standard solutions (1 mg ml^{-1}) for sodium, potassium, calcium and magnesium. Standards were kept at room temperature, stored in polycarbonate bottles.

3.5. Analyses

The equipment was equilibrated for at least 1 h before starting the analyses. All the analyses were performed as a single measurement. Up to now calibration was performed using three external standards, with concentrations including those of the samples, and it was repeated every 8–12 sample measurements. Calibration was done on the basis of peak areas, using linear regressions in the case of cations and linear or quadratic regressions, depending on the range of concentrations, in the case of anions. All the area signals of the calibration solutions in the period August 1993–July 1994 were recorded and are used in this paper to evaluate the repeatability of the measurements of peak areas for calibration solutions and mean response factor.

Control charts [1] were obtained from the analyses of natural and artificial samples of 2-l volume, filtered and stabilized with chloroform (0.2% v/v), with 2–4 concentration levels for each ion in the range of those normally used. Two different types of stabilized, multi-variable samples were used: the first analysed routinely 3–5 times per week, covering the whole range of concentrations, preserved for 6 months–1 year, the second analysed monthly, with a narrow range of variation in the concentrations, and preserved for 2–3 years. Precision values presented in this paper were obtained from both types of stabilized samples, while the examples of control charts refer to the second type.

4. Results and discussion

The repeatability of the measurements of peak areas for calibration solution values for all anions (Fig. 1a), obtained from the signals of the calibration solutions, is between 2 and 3% for concentrations higher than 10 μM, increasing to 5% for the lowest concentration of 3 μM. The repeatability of the measurements of peak areas for calibration solution values for cations (Fig. 1c) is 2–5% for concentrations lower than 100 μM, slightly higher than those for anions; the highest values of 5–10% were calculated for concentrations lower than 10 μM.

For every batch of analyses, natural and artificial stabilized samples were analysed as internal quality controls. Chloroform (0.2%, v/v) was sufficient to stabilize the solutions for a period of years in the case of calcium, magnesium, potassium, sulphate and nitrate. Examples of the control charts obtained are shown in Fig. 2. Magnesium is an example of a stable analyte, whereas in the case of ammonium a statistically significant decrease in concentration was observed after 3 years, probably due to the evaporation of chloroform and the consequent bacterial oxidation of the ammonium. A slight increase in the concentrations of chloride and sodium was observed, probably because of contamination during manipulation.

As in the case of repeatability of the measurements of peak areas for calibration solutions, precision values, obtained from the R.S.D.s for stabilized samples used for the control charts, are lower for anions then for cations (Fig. 1b and d, respectively). Sodium, potassium and magnesium show the highest R.S.D.s for concentrations lower than 10 μM; several factors may contribute, including sample contamination and release from the glass vials used for the autosampler. As expected, the precisions are worse than the repeatability of the measurements of peak areas for calibration solution values.

As regards the signal response to different analyte concentrations, apart from ammonium, it was apparently linear up to 0.6–2 μM (Fig. 3). However, a more accurate evaluation (restricted

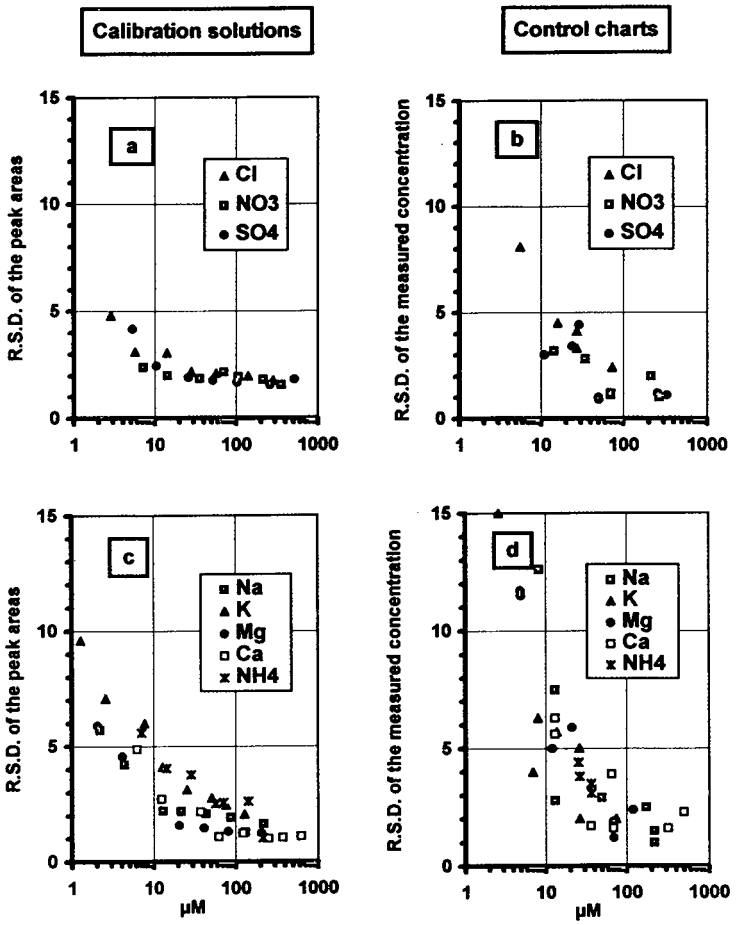

Fig. 1. Repeatability of the measurements of peak areas for calibration solutions and precision on control charts of anions and cations.

to the most common calibration ranges) showed that anions, base cations and ammonium have different patterns: in the case of anions, linear regression overestimates the lowest and highest concentrations and underestimates the values in the central part of the calibration range (Table 1). The residual of the regression is very large, up to 150–300%, in the case of the lowest concentrations of the anions, whereas in the central part the underestimation may account for 10%. The residuals decrease using the quadratic regression, and are least with the cubic regression. It must be stressed that in all cases the correlation coefficient was very close to unity. In the case of cations, excluding ammonium, the signal response is more linear, but even in this case the residual is large in the lowest range of concentrations. In the case of ammonium the signal response is the opposite of that of anions: linear regression greatly underestimates the lowest and highest concentrations and overestimates concentrations in the middle of the calibration range. The use of quadratic or cubic regressions significantly improves the results (Table 1).

The goodness of fit of the calibration models was compared by the analysis of variance. The F-test was used to evaluate the significance of the cubic versus the quadratic, the quadratic versus the linear, and the linear versus the constant-response model. The linear model was

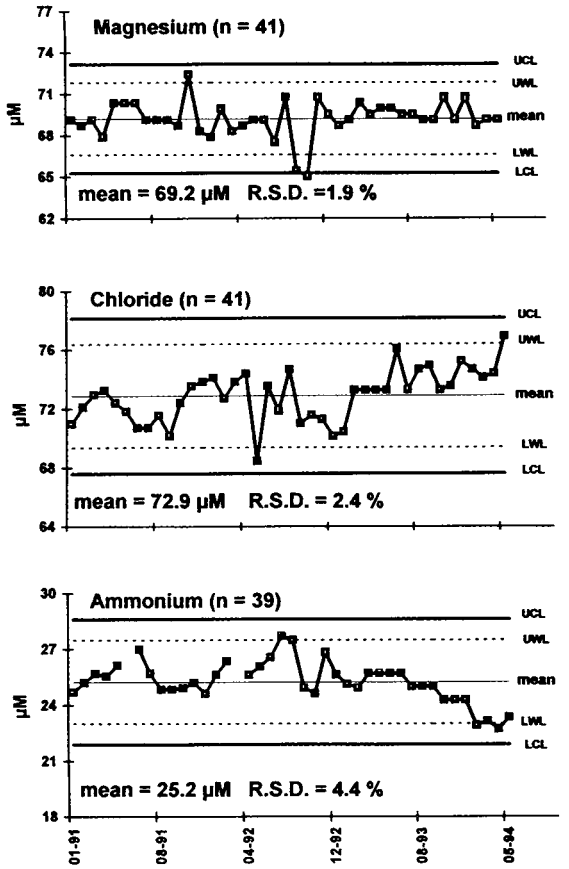

Fig. 2. Examples of control charts. UCL and LCL = upper and lower control limits (±3 S.D.); UWL and LWL = upper and lower warning limits (±2 S.D.).

obviously significantly different from the null model in all cases. The quadratic model was significantly better than the linear model for ammonium, sodium and all the anions. Only for sulphate did the introduction of the cubic term lead to a significant improvement in the goodness of fit of the model.

These different patterns may be due to the type of signal response (R.F.) of the conductivity detector to different concentrations of anions, cations and ammonium (Fig. 4). In the case of anions there is evident overlapping of chloride and nitrate, both monovalent ions, and roughly halved values for sulphate, a bivalent ion. All three anions show a decrease in R.F. with increasing concentration. The standard deviations relative to each concentration, calculated from 24–150 measurements on calibration solutions over about 1 year, are very low, if compared with the variations in R.F. as a function of concentration. In the case of cations (ammonium excluded), the R.F. values show no significant variations with concentration; further, there is a clear difference between mono- and bivalent ions. The ammonium R.F. increases with increasing concentration, even in the absence of sodium and potassium, whose peaks are close to that of ammonium. Also for cations and ammonium, the standard deviations are small compared with the variations of R.F. with concentration (Fig. 4).

The reasons for these differences are not known; however, we can assess that the background signal is 14–15 $\mu S\ cm^{-1}$ for anions (suppressed eluent, carbon dioxide and water), whereas it is only 0.6–1.0 $\mu S\ cm^{-1}$ for cations (suppressed eluent, water after the exchange of methanesulphonate). Finally, for ammonium, a partial conversion into non-ionized ammonia as a function of pH must be expected. In the absence of other buffering ions, as is the case with the ammonium solution after suppression, the pH of solutions in the range 7–215 μM ammonia solution, is between 8.73 and 9.72. At these pH values, at a temperature of about 25°C, the percentage of non-ionized ammonia is 24 and 75% [5] of the total ammonium, respectively, with a corresponding decrease in conductivity.

5. Conclusions

Ion chromatography is one of the most widely used techniques for inorganic analyses of natural waters. The equipment gives very good repeatability of the measurements of peak areas for calibration solutions, permitting a high analytical precision. A strict program of both internal and external quality controls is essential, however, to ensure accuracy. In particular, critical aspects are the preparation of calibration solutions and the use of control charts for every analyte, at different levels of concentration. Of

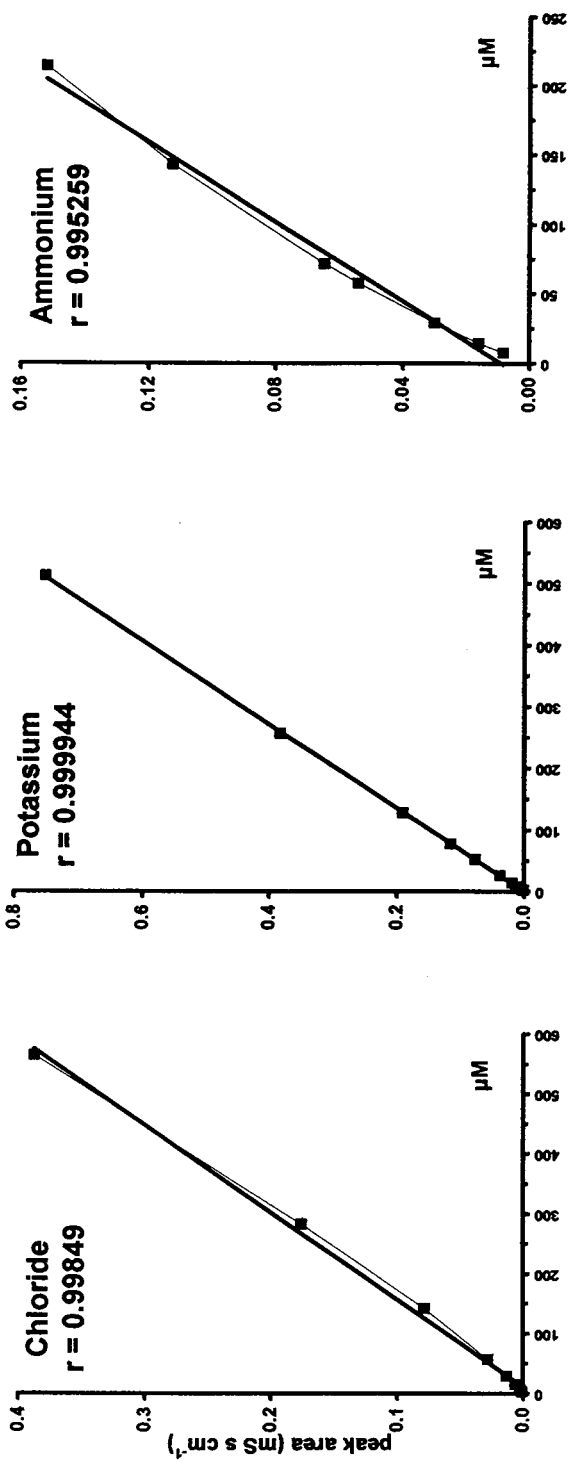

Fig. 3. Examples of calibration graphs for anions, cations and ammonium. ■ = Measured values; straight lines = linear regression.

Table 1
Mean and S.D. of the expected concentrations for the calibration concentrations (Cal.) obtained by repeating the application of different calibration functions 24–28 times

Sodium (μM) ($n = 24$)			
Cal.	Linear	Quadratic	Cubic
2.2	2.6 ± 0.4	2.1 ± 0.3	2.1 ± 0.3
4.3	4.8 ± 0.4	4.3 ± 0.2	4.3 ± 0.2
13.0	13.3 ± 0.4	13.3 ± 0.2	13.0 ± 0.3
21.7	21.9 ± 0.4	21.9 ± 0.4	21.9 ± 0.5
43.5	43.1 ± 0.6	43.5 ± 0.6	43.5 ± 0.4
87.0	86.0 ± 1.2	86.8 ± 0.8	86.8 ± 0.7
130.5	129.9 ± 1.5	130.6 ± 0.9	130.6 ± 0.4
217.5	218.3 ± 1.0	217.5 ± 0.2	217.47 ± 0.04
r^2	0.99978 ± 0.00033	0.999937 ± 0.000049	0.999963 ± 0.000025
s_y	1.01 ± 0.54	0.61 ± 0.23	0.51 ± 0.19
m_0	0.33 ± 0.42	-0.21 ± 0.27	-0.25 ± 0.35
m_1	$6.82 \cdot 10^{-4} \pm 9.39 \cdot 10^{-6}$	$7.00 \cdot 10^{-4} \pm 1.71 \cdot 10^{-5}$	$7.03 \cdot 10^{-4} \pm 3.44 \cdot 10^{-5}$
m_2		$-5.85 \cdot 10^{-11} \pm 6.51 \cdot 10^{-11}$	$-8.55 \cdot 10^{-11} \pm 2.78 \cdot 10^{-10}$
m_3			$6.25 \cdot 10^{-17} \pm 6.25 \cdot 10^{-16}$
F	92819 $p < 0.001$	144.6 $p < 0.001$	0.049 n.s.

Potassium (μM) ($n = 27$)			
Cal.	Linear	Quadratic	Cubic
1.3	1.3 ± 0.3	1.5 ± 0.3	1.1 ± 0.3
2.6	2.7 ± 0.3	2.9 ± 0.2	2.6 ± 0.3
7.7	7.6 ± 0.4	7.7 ± 0.4	7.8 ± 0.4
12.8	12.6 ± 0.4	12.6 ± 0.4	12.9 ± 0.6
25.6	25.2 ± 0.7	25.1 ± 0.8	25.6 ± 0.8
51.1	51.1 ± 1.3	50.8 ± 1.4	51.0 ± 1.2
76.7	77.8 ± 1.8	77.5 ± 1.3	76.8 ± 0.6
127.9	127.3 ± 1.0	127.6 ± 0.3	127.85 ± 0.07
r^2	0.99938 ± 0.00061	0.99954 ± 0.00054	0.99975 ± 0.00028
s_y	1.02 ± 0.48	0.90 ± 0.54	0.73 ± 0.41
m_0	0.06 ± 0.29	0.27 ± 0.30	-0.21 ± 0.40
m_1	$6.59 \cdot 10^{-4} \pm 1.15 \cdot 10^{-5}$	$6.47 \cdot 10^{-4} \pm 2.51 \cdot 10^{-5}$	$7.01 \cdot 10^{-4} \pm 4.89 \cdot 10^{-5}$
m_2		$6.88 \cdot 10^{-11} \pm 1.52 \cdot 10^{-10}$	$-7.43 \cdot 10^{-10} \pm 8.45 \cdot 10^{-10}$
m_3			$2.86 \cdot 10^{-15} \pm 3.33 \cdot 10^{-15}$
F	54328 $p < 0.001$	1.58 n.s.	1.76 n.s.

Magnesium (μM) ($n = 29$)			
Cal.	Linear	Quadratic	Cubic
2.1	2.3 ± 0.3	2.2 ± 0.2	2.0 ± 0.2
4.1	4.4 ± 0.3	4.3 ± 0.2	4.1 ± 0.1
12.3	12.4 ± 0.3	12.3 ± 0.2	12.3 ± 0.2
20.6	20.4 ± 0.2	20.4 ± 0.2	20.6 ± 0.3
41.1	40.8 ± 0.4	40.9 ± 0.4	41.2 ± 0.4
82.3	81.9 ± 0.8	82.1 ± 0.7	82.2 ± 0.6
123.4	123.7 ± 1.2	123.9 ± 0.7	123.5 ± 0.3
205.7	205.8 ± 0.8	205.6 ± 0.2	205.71 ± 0.04
r^2	0.99988 ± 0.00015	0.999947 ± 0.000064	0.999970 ± 0.000042
s_y	0.67 ± 0.41	0.49 ± 0.29	0.39 ± 0.26
m_0	0.13 ± 0.33	0.02 ± 0.23	-0.24 ± 0.26
m_1	$3.44 \cdot 10^{-4} \pm 3.62 \cdot 10^{-6}$	$3.46 \cdot 10^{-4} \pm 7.48 \cdot 10^{-6}$	$3.56 \cdot 10^{-4} \pm 8.83 \cdot 10^{-6}$
m_2		$-3.09 \cdot 10^{-12} \pm 1.50 \cdot 10^{-11}$	$-5.04 \cdot 10^{-11} \pm 5.08 \cdot 10^{-11}$
m_3			$5.37 \cdot 10^{-17} \pm 6.90 \cdot 10^{-17}$
F	476889 $p < 0.001$	0.31 n.s.	0.57 n.s.

Calcium (μM) ($n = 28$)			
Cal.	Linear	Quadratic	Cubic
6.2	6.8 ± 0.6	6.9 ± 0.5	6.2 ± 0.5
12.5	12.7 ± 0.7	12.8 ± 0.4	12.3 ± 0.3
37.4	37.4 ± 0.8	37.5 ± 0.5	37.6 ± 0.6
62.4	61.9 ± 0.5	61.9 ± 0.5	62.4 ± 0.6
124.8	124.0 ± 1.1	123.9 ± 1.2	125.0 ± 1.1
249.5	249.0 ± 2.2	248.8 ± 1.9	249.1 ± 1.6
374.3	375.8 ± 2.8	375.7 ± 1.8	374.4 ± 0.8
623.8	623.2 ± 1.9	623.4 ± 0.4	623.73 ± 0.09
r^2	0.999926 ± 0.000072	0.999957 ± 0.000046	0.999979 ± 0.000027
s_y	1.70 ± 0.81	1.38 ± 0.72	1.05 ± 0.59
m_0	0.12 ± 0.63	0.25 ± 0.60	-0.63 ± 0.65
m_1	$3.37 \cdot 10^{-4} \pm 3.40 \cdot 10^{-6}$	$3.37 \cdot 10^{-4} \pm 5.59 \cdot 10^{-6}$	$3.47 \cdot 10^{-4} \pm 7.10 \cdot 10^{-6}$
m_2		$4.63 \cdot 10^{-13} \pm 3.61 \cdot 10^{-12}$	$-1.59 \cdot 10^{-11} \pm 1.38 \cdot 10^{-11}$
m_3			$5.99 \cdot 10^{-18} \pm 5.78 \cdot 10^{-18}$
F	474455 $p < 0.001$	0.18 n.s.	0.29 n.s.

(Continued on page 28)

Table 1 (*continued*)

Chloride (μM) ($n = 28$)

Cal.	Linear	Quadratic	Cubic
2.8	7.5 ± 1.1	4.0 ± 0.4	2.9 ± 0.2
5.6	9.6 ± 0.9	6.5 ± 0.4	5.6 ± 0.2
14.1	16.0 ± 0.6	14.2 ± 0.3	14.1 ± 0.4
28.2	27.1 ± 0.5	27.2 ± 0.5	28.2 ± 0.5
56.4	50.6 ± 1.3	54.1 ± 1.2	56.4 ± 0.3
141.0	132.9 ± 3.4	142.5 ± 0.7	141.03 ± 0.03
282.1	286.5 ± 1.5	281.8 ± 0.1	282.064 ± 0.002
r^2	0.9950 ± 0.0015	0.9996 ± 0.0003	0.999986 ± 0.000009
s_y	7.22 ± 1.10	2.10 ± 0.69	0.45 ± 0.16
m_0	5.64 ± 0.63	1.84 ± 0.49	−0.38 ± 0.26
m_1	$1.62 \cdot 10^{-3} \pm 3.66 \cdot 10^{-5}$	$1.93 \cdot 10^{-3} \pm 6.41 \cdot 10^{-5}$	$2.18 \cdot 10^{-3} \pm 6.49 \cdot 10^{-5}$
m_2		$-1.83 \cdot 10^{-9} \pm 4.52 \cdot 10^{-10}$	$-6.46 \cdot 10^{-9} \pm 1.55 \cdot 10^{-9}$
m_3			$1.88 \cdot 10^{-14} \pm 7.82 \cdot 10^{-15}$
F	1956 $p < 0.001$	57.2 $p < 0.01$	270 $p < 0.01$

Sulphate (μM) ($n = 26$)

Cal.	Linear	Quadratic	Cubic
5.2	13.4 ± 1.9	7.3 ± 0.6	5.3 ± 0.3
10.4	17.3 ± 1.6	11.9 ± 0.5	10.4 ± 0.2
26.0	29.3 ± 0.9	26.0 ± 0.3	25.9 ± 0.3
52.1	50.0 ± 0.8	50.1 ± 0.8	51.9 ± 0.8
104.1	94.1 ± 2.3	100.4 ± 1.4	104.2 ± 0.5
260.3	245.8 ± 4.8	262.7 ± 0.8	260.24 ± 0.06
520.5	528.5 ± 2.2	520.1 ± 0.1	520.520 ± 0.004
r^2	0.9954 ± 0.0013	0.99969 ± 0.00012	0.999988 ± 0.000017
s_y	12.69 ± 1.81	3.60 ± 0.68	0.72 ± 0.37
m_0	10.02 ± 1.05	3.26 ± 0.48	0.82 ± 0.37
m_1	$8.11 \cdot 10^{-4} \pm 2.11 \cdot 10^{-5}$	$9.62 \cdot 10^{-4} \pm 1.77 \cdot 10^{-5}$	$1.07 \cdot 10^{-3} \pm 2.49 \cdot 10^{-5}$
m_2		$-2.39 \cdot 10^{-10} \pm 4.02 \cdot 10^{-11}$	$-8.07 \cdot 10^{-10} \pm 1.31 \cdot 10^{-10}$
m_3			$6.26 \cdot 10^{-16} \pm 1.78 \cdot 10^{-16}$
F	2127 $p < 0.001$	64.6 $p < 0.01$	0.57 n.s.

Nitrate (μM) ($n = 26$)

Cal.	Linear	Quadratic	Cubic
7.1	12.2 ± 1.4	8.3 ± 0.8	7.3 ± 0.3
14.3	18.1 ± 1.2	14.9 ± 0.6	14.3 ± 0.3
35.7	36.3 ± 0.6	35.2 ± 0.4	35.6 ± 0.6
71.4	67.9 ± 1.3	69.9 ± 1.5	71.2 ± 1.2
107.1	101.4 ± 2.2	105.9 ± 1.9	107.3 ± 1.1
214.2	209.2 ± 3.6	216.0 ± 1.7	214.13 ± 0.22
357.0	361.6 ± 2.1	356.5 ± 0.4	356.978 ± 0.024
r^2	0.9967 ± 0.0014	0.99970 ± 0.00024	0.999958 ± 0.000035
s_y	7.23 ± 1.50	2.23 ± 0.96	0.93 ± 0.41
m_0	6.63 ± 1.08	1.99 ± 0.89	0.47 ± 0.61
m_1	$1.79 \cdot 10^{-3} \pm 3.79 \cdot 10^{-5}$	$2.02 \cdot 10^{-3} \pm 5.92 \cdot 10^{-5}$	$2.17 \cdot 10^{-3} \pm 9.72 \cdot 10^{-5}$
m_2		$-1.19 \cdot 10^{-9} \pm 3.63 \cdot 10^{-10}$	$-3.38 \cdot 10^{-9} \pm 1.70 \cdot 10^{-9}$
m_3			$7.49 \cdot 10^{-15} \pm 6.50 \cdot 10^{-15}$
F	3705 $p < 0.001$	56.4 $p < 0.01$	248 n.s.

Ammonium (μM) ($n = 27$)

Cal.	Linear	Quadratic	Cubic
7.1	−0.7 ± 0.6	6.5 ± 1.1	7.1 ± 0.7
14.3	10.3 ± 0.8	14.4 ± 0.5	14.4 ± 0.4
28.6	29.7 ± 1.1	29.0 ± 0.9	28.5 ± 1.4
57.1	64.5 ± 1.5	58.2 ± 2.2	57.6 ± 1.4
71.4	78.8 ± 1.9	71.3 ± 2.0	71.0 ± 1.7
142.8	146.6 ± 3.8	141.7 ± 3.7	142.8 ± 0.6
214.2	206.2 ± 2.6	214.5 ± 1.4	214.16 ± 0.15
r^2	0.9791 ± 0.0031	0.9990 ± 0.0012	0.99967 ± 0.00029
s_y	10.97 ± 0.83	2.26 ± 1.48	1.51 ± 0.77
m_0	−12.65 ± 1.03	−1.62 ± 1.94	−0.05 ± 2.45
m_1	$1.43 \cdot 10^{-3} \pm 1.62 \cdot 10^{-5}$	$9.43 \cdot 10^{-4} \pm 9.42 \cdot 10^{-5}$	$8.18 \cdot 10^{-4} \pm 2.50 \cdot 10^{-4}$
m_2		$3.07 \cdot 10^{-9} \pm 5.62 \cdot 10^{-10}$	$5.11 \cdot 10^{-9} \pm 5.03 \cdot 10^{-9}$
m_3			$-8.46 \cdot 10^{-15} \pm 2.32 \cdot 10^{-14}$
F	645 $p < 0.001$	312 $p < 0.01$	0.61 n.s.

r^2 = Correlation coefficient squared; s_y = standard error; m_i = regression coefficient of ith order; F = F-ratio and significance level (p) for the introduction into the model of the higher degree term (see text); n.s. = Not significant.

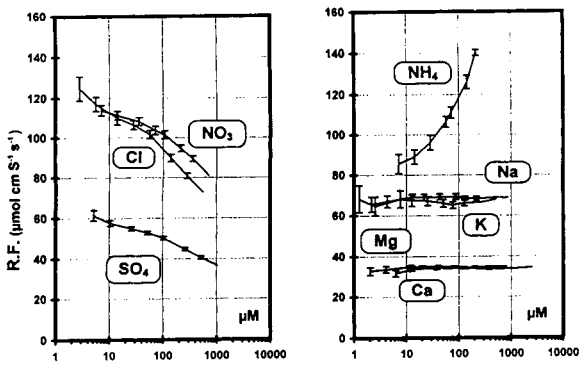

Fig. 4. Response factors in relation to concentrations. Bars indicate S.D.s obtained from 24–150 measurements.

the many aspects related to instrument calibration, this paper highlights the importance of the type of regression and frequency of calibration used. The results show that multi-point (6–8 concentrations), non-linear regression permits a correct quantification over a wide range of concentrations of anions and cations. Because of the repeatability of the measurements of peak areas for calibration solutions, two calibrations, at the beginning and end of the batch of 20–30 samples, are adequate. These conditions give better results than calibrations performed with 2–3 points and repeated every 8–10 samples.

References

[1] APHA, AWWA and WEF, *Standard Methods for the Examination of Water and Wastewater*, American Public Health Association, New York, 1992.

[2] R.A. Durst, W. Davison, K. Toth, J.E. Rothert, M.E. Peden and B. Griepink, *Pure Appl. Chem.*, 63 (1991) 908.

[3] L.N. Polite, H.M. McNair and R.D. Rocklin, *J. Liq. Chromatogr.*, 10 (1987) 829.

[4] A. Marchetto, R. Mosello, G.A. Tartari, H. Muntau, M. Bianchi, H. Geiss, G. Serrini and G. Serrini Lanza, *J. Chromatogr.*, (1995) in press.

[5] K. Emerson, R.C. Russo, R.E. Lund and R.V. Thurston, *J. Fish. Res. Board Can.*, 32 (1975) 2379.

ELSEVIER

Journal of Chromatography A, 706 (1995) 31–36

JOURNAL OF CHROMATOGRAPHY A

"Chromatogram generator" chromatogram modelling software

A.V. Pirogov*, O.N. Obrezkov, O.A. Shpigun

Chemistry Department, M.V. Lomonosov Moscow State University, Lenin Hills, GSP-3, 119899 Moscow, Russian Federation

Abstract

Software called "Chromatogram Generator" was developed for IBM-compatible computers. This software allows the approximation of chromatographic peaks with several mathematical functions and their superposition, the construction of series of chromatograms with various parameters (or with smooth variations of single or several parameters), the construction of the graphical image of a chromatogram with minimum size and the ability to be added to a chromatographic database.

1. Introduction

Recently, much attention has been paid to the development of computerized expert systems, which aid analysts in the choice of the analytical method for a particular application and the search for the optimum conditions. For this purpose, the computer should have an option of quantitative estimation of the quality of chromatograms and effect their comparison. This can be performed using various optimization criteria. A number of papers have discussed these criteria [1–5]. However, the estimation of the quality of a chromatogram made by a specialist in the field of chromatography still appears to be the most reasonable method. Commercially available expert systems for chromatographic analysis pay most attention to the data acquisition and handling and to the choice of the optimum analytical conditions. These systems do not have the option of chromatogram modelling for expert estimation of their quality. At present, widely used chromatographic expert system software such as DryLab (LC Resources) does not provide for these important options. The best way to solve the task of peak estimation is to build a system that is able to learn about the shape of the chromatogram according to human experience.

To evaluate such chromatographic modelling software, a lot of chromatograms should be available, and the number of peaks, their shape, resolution, analysis time and a number of other parameters should vary over wide ranges to provide representative and reliable estimates. One of the ways to solve this problem is to create special software that can generate the chromatographic peaks, use them to build chromatograms and treat the resulting information.

2. Software specifications and hardware requirements

The software developed is called "Chromatogram Generator". It is written in C++ programming language (Borland International, Scotts Valley, CA, USA). The following external libraries were used: Borland Graphics Interface

* Corresponding author.

0021-9673/95/$09.50
SSDI 0021-9673(94)01243-1

(BGI) graphical library (EGAVGA.BGI) and IMPLODE compression library (PkWare, version 1.02). "Chromatogram Generator" requires an IBM PC/AT or higher computer equipped with an EGA or VGA display adapter and MS-DOS 3.00 or above operational system. The chromatogram printout can be performed on any Epson-compatible dot matrix printer. In this work, Epson FX-1050 and FX-800 nine-pin matrix printers were used to test the printing facilities. The software requires at least 300 K of RAM and about 200 K of free disk space; it can be installed on a hard disk or a floppy disk. A co-processor is preferable, but the software can emulate its work to accelerate floating point operations for the systems without a mathematical co-processor. The graphical image of a chromatogram can be stored on the disk or loaded for the future use with "Chromatogram Generator" or with other software programs. The size of the stored file is minimal (not more than 300 bytes), which allows the storage of large amount of data on the disk (approximately 2000 files per double-sided high-density floppy disk).

3. Peak shapes

In this software, we applied the approach of chromatogram creation from a certain set of various predefined function templates. The user can visually determine the parameters of each peak, and the chromatogram is treated as the superposition of the user-defined functions. Theoretically, symmetrical, well resolved peaks can be described with sufficient accuracy by the approximation with a Gaussian distribution curve [6]:

$$h(t) = h_{max} \exp\left[-\frac{1}{2}\left(\frac{t-t_0}{\sigma}\right)^2\right] \quad (1)$$

where h_{max} is the maximum height of the peak, t_0 is the time corresponding to the peak minimum and σ is the standard deviation.

However, usually real peaks are asymmetric owing to non-linear sorption isotherms or other causes. Hence it is convenient to treat each peak as the combination of two separate (front and tail) parts and to consider two separate equations for each part:

$$h(t) = \begin{cases} \frac{h_{max}}{\sigma_1\sqrt{2\pi}} \cdot \exp\left[-\frac{(t-t_0)^2}{2\sigma_1^2}\right] & -\infty < t \leq t_0 \\ \frac{h_{max}}{\sigma_2\sqrt{2\pi}} \cdot \exp\left[-\frac{(t-t_0)^2}{2\sigma_2^2}\right] & t_0 \leq t < +\infty \end{cases} \quad (2)$$

In the above equations the peak is described by the curve of a Gaussian distribution with half-widths (σ_1 and σ_2) defined independently for the front and tail parts. This distribution is called bi-Gaussian [7]. Peaks with a strongly diffuse front are poorly approximated with Eq. 2, and a more accurate description is reached with the approximation

$$h(t) = \frac{h_{max}}{\tau} \int_{-\infty}^{t} dt_1 \cdot \exp\left[-\frac{(t_1-t_0)^2}{2\omega^2}\right] \cdot \exp\left[-\frac{(t-t_1+t_0)}{\tau}\right] \quad (3)$$

A tailed peak can also be described by an exponentially modified Gaussian function [8]:

$$h(t) = \frac{h_{max}}{\tau} \cdot \exp\left[\frac{1}{2}\left(\frac{\tau}{\sigma}\right)^2 - \frac{(t-t_0)}{\tau}\right] \cdot \int_{-\infty}^{z} \exp\left[\frac{\left(-\frac{x^2}{2}\right)dx}{\sqrt{2\pi}}\right]$$
$$z = \frac{1}{\sqrt{2}} \cdot \left(\frac{t}{\sigma} - \frac{\sigma}{\tau}\right) \quad (4)$$

where $x = (t-t_0)/\sigma$, h_{max} is the maximum height of the peak, t_0 is the time corresponding to the peak maximum and τ and σ are the parameters corresponding to the curvature and the width of the peak. In this case, varying the ratio of τ to σ can result in peaks with predefined overlapping (S) and resolution (R_S). This problem was described in detail by Sekulic and Haddad [9] and Crubner [10,11].

In addition to modified Gaussian curves, the chromatographic peaks can be described with a first-order Poisson distribution function (Eq. 5) and a Cauchi function (Eq. 6) [7,12]:

$$h(t) = h_{max} \cdot \exp[\lambda(e^{u} - 1)] \quad \lambda > 0 \tag{5}$$

$$h(t) = \frac{h_{max}}{1 + \left[\frac{2(t - t_0)}{\sigma}\right]^2} \tag{6}$$

In some cases (e.g., gas chromatographic determination of alcohols), the peaks can be treated with good accuracy as triangles. Strenberg [13] proposed the following equation to describe these peaks:

$$h(t) = \begin{cases} h_{max} \cdot \left[1 - \frac{|t - t_0|}{\sigma}\right] & |t - t_0| < \sigma \\ 0 & |t - t_0| \geq \sigma \end{cases} \tag{7}$$

This approach does not always provide the required accuracy of the approximation, but it is suitable for the purpose of the software discussed. The parabolic shape of the peaks is, of course, very peculiar in the "pure form", but it may be useful for modelling shouldered peaks.

4. Chromatogram modelling process

The program interface is shown in Fig. 1. To model the real chromatogram the user defines the peak shape, half-widths (separately for the left and right parts), peak height and retention time using the icons at the top of the screen. The ranges over which these parameters vary are presented in Table 1. This determines the "skeleton" of the chromatogram.

The user has an option to fine tune further to generate a chromatographic peak by choosing and editing any peak to obtain maximum agree-

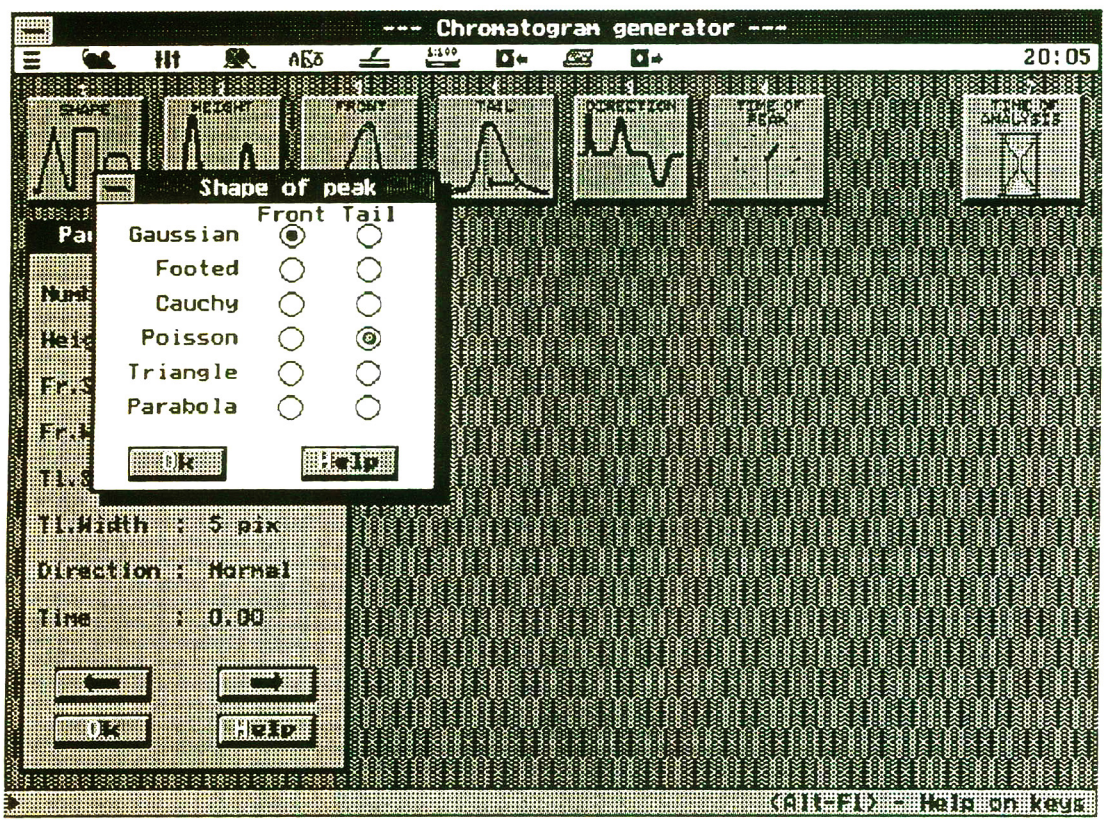

Fig. 1. The main window of the "Chromatogram Generator" program.

Table 1
Variables in the "Chromatogram Generator" software used to approximate chromatographic peaks

Varying parameter	Range of variation
Time of analysis	From 2 to 120 min
Retention time of peaks	With precision of 0.01 min
Height of peaks[a]	From 0 to 400 mm
Width of front or tail of peaks	From 0 to 200 mm
Direction of peaks	"Positive" or "negative"
Shape of peaks[b]	Six functions

[a] Height and width of peak can be defined in screen pixels also.
[b] Front and tail of peak can be approximated with different functions.

ment between the model and the real chromatograms (Fig. 2). The baseline drift can be emulated in most instances by the superposition of "pseudo-peaks", e.g., with very large widths. Usually, the process of modelling of a real chromatogram takes 2–3 min.

It was found that "Chromatogram Generator" provided a good approximation of real chromatograms (Figs. 3 and 4). The process of the construction of a series of model chromatograms for expert estimation is simplified by using a template stored on the disk. Users have the option to edit the files with chromatogram images using a simple additional utility program. This allows subsequent variation of a single parameter (e.g., peak width) to produce a series of chromatograms with various peak resolutions for subsequent expert estimation.

The approximation of chromatograms with the use of a number of functions leads to a considerable increase in the compression ratio of the

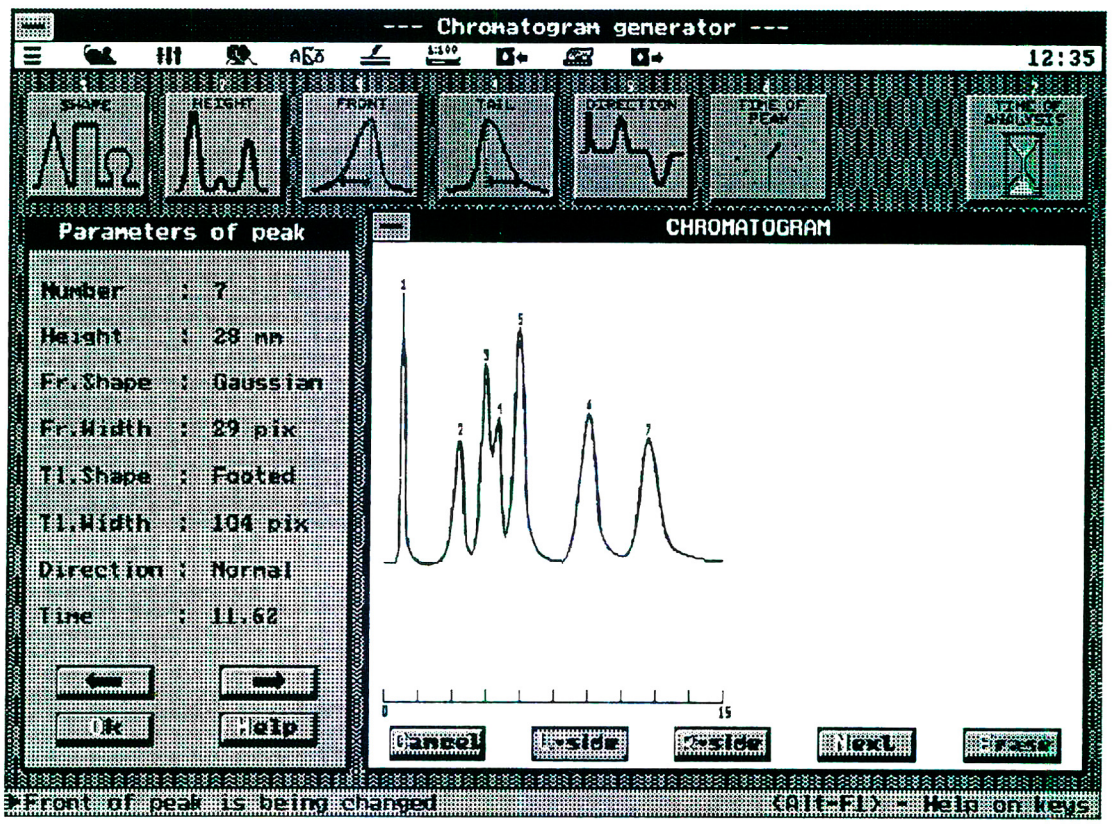

Fig. 2. Process of modelling real chromatograms.

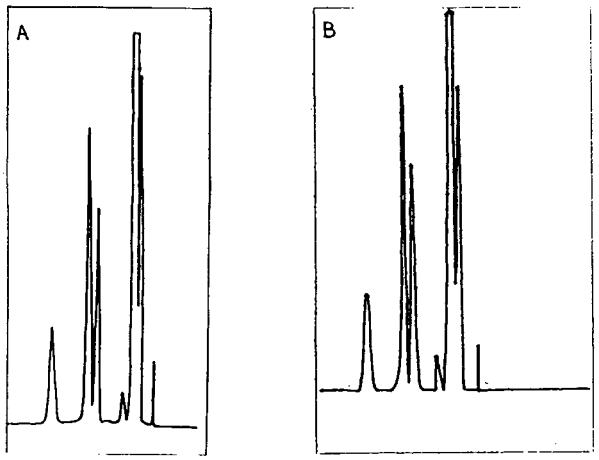

Fig. 3. (A) Real and (B) modelled chromatograms.

information. This decrease in the file size results from the approximation of chromatographic peaks by superposition of mathematical functions. Thus, "pixel-by-pixel" storage of a chromatographic image is not necessary. The size of the file of a chromatogram is 100–300 bytes. It can be added to a database, which allows one to keep the graphical image of the chromatogram. The file sizes for graphical images of chromatograms produced with some popular image-editing software packages and "Chromatogram Generator" are presented in Table 2. It should be noted that the file size generated by "Chromatogram Generator" is only about 168 bytes.

Table 2
File sizes with image of the chromatograms (Fig. 2) built by different graphic image editors and the "Chromatogram Generator" program

Graphic image editor	Size of file (bytes)
Ventura Publisher V.2.0	48 952
MS-Paintbrush V.4.0	42 537
Microsoft Word V.2.0c	23 582
Pizza V.1.12	5376
Chromatogram Generator	168

5. Conclusions

The developed software allows the solution of the following tasks: (i) approximation of chromatographic peaks with several mathematical functions and their superposition, which is of interest for several chromatographic methods; (ii) construction of series of chromatograms with various parameters (or with a smooth variation of a single or several parameters) to obtain a

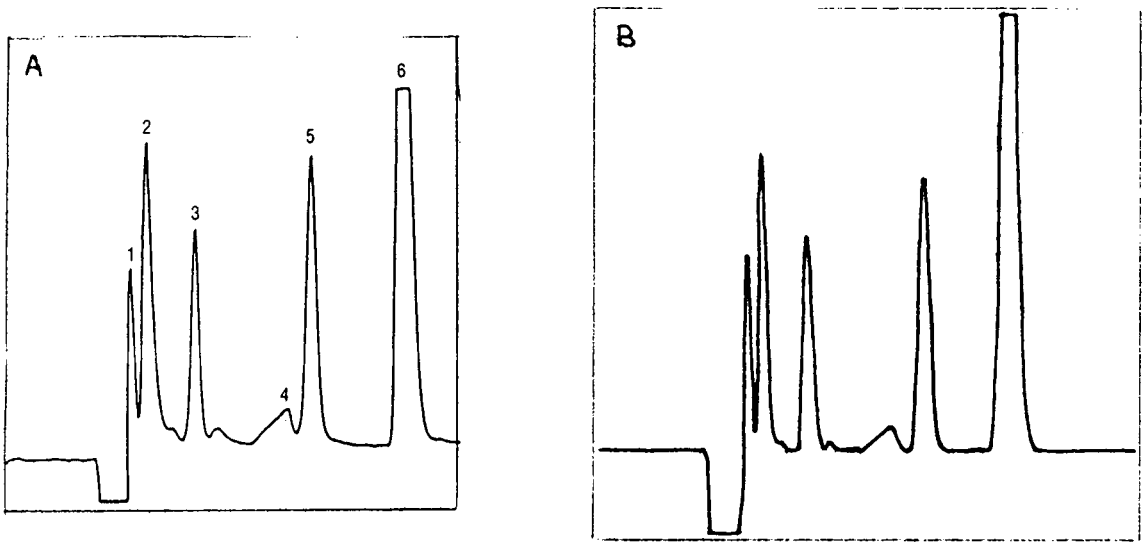

Fig. 4. (A) Real and (B) modelled chromatograms with different shapes and direction of peaks.

representative set for expert estimation of chromatogram quality, which is necessary for the choice of the weight factors of the equations of optimization criteria; and (iii) the construction of a graphical image of a chromatogram with minimal size and the ability to be added to a chromatographic database.

References

[1] M.W. Watson and P.W. Carr, *Anal. Chem.*, 51 (1979) 1835.
[2] J.L. Glajch, J.J. Kirkland, K.M. Squire and J.M. Minor, *J. Chromatogr.*, 199 (1980) 57.
[3] A.C.J.H. Drouen, H.A.H. Billiet, P.J. Schoenmakers and L. Galan, *Chromatographia*, 16 (1982) 48.
[4] J.C. Berridge and E.G. Morrisey, *J. Chromatogr.*, 316 (1984) 69.
[5] O.N. Obrezkov, A.V. Pirogov, I.V. Pletnev and O.A. Shpigun, *Mikrochim. Acta*, 1 (1991) 293.
[6] W.E. Barber and P.W. Carr, *Anal. Chem.*, 53 (1981) 1939.
[7] T.S. Buyeand and K. De Clerk, *Anal. Chem.*, 44 (1972) 1273.
[8] J.P. Foley and J.G. Dorsey, *Anal. Chem.*, 55 (1983) 730.
[9] S. Sekulic and P.R. Haddad, *J. Chromatogr.*, 459 (1988) 65.
[10] O. Crubner, *Adv. Chromatogr.*, 6 (1968) 173.
[11] O. Crubner, *Anal. Chem.*, 43 (1971) 1934.
[12] R.D.B. Fraser and E. Suzuki, *Anal. Chem.*, 38 (1966) 1770.
[13] J.C. Strenberg, *Adv. Chromatogr.*, 2 (1966) 205.

ELSEVIER

Journal of Chromatography A, 706 (1995) 37–42

JOURNAL OF CHROMATOGRAPHY A

Retention mechanism of anions in micellar chromatography: Interpretation of retention data on the basis of an ion-exchange model

Tetsuo Okada* Hidetomo Shimizu

Faculty of Liberal Arts, Shizuoka University, Shizuoka 422, Japan

Abstract

Micellar chromatography is an effective method not only for organic separations but also for inorganic separations because of its unique selectivity. Although a pseudo-phase model is widely utilized in the interpretation of the retention of neutral organic compounds, there is some ambiguity in applying this model to the quantitative description of the micellar chromatographic behaviour of inorganic ions. In this paper, a novel retention model based on a stoichiometric ion-exchange model is developed to elucidate the retention behaviour of anions in cationic micellar chromatography. The developed model involves the dissociation constant of a counter ion from a micelle and two ion-exchange equilibrium constants at the interfaces between the solution and micelles and between the solution and stationary phase.

1. Introduction

Secondary equilibria have promised effectiveness in varying and enhancing liquid chromatographic selectivity [1]. Partition to a micellar phase, which has been successfully utilized in organic liquid chromatography [1,2], is one of the representatives of secondary equilibria. It is well known that, in micellar chromatographic separations of organic compounds, a pseudo-phase retention model describes the experimental results well, where the hydrophobic or lipophilic partitioning of electroneutral analytes into a micellar pseudo-phase is though to be an important factor in determining retention [2,3]. If both an analyte and a micelle are ionic, electrostatic interactions rather than hydrophobic partitioning will be dominant in the retention mechanisms.

Although the use of micellar mobile phases has rarely been applied in inorganic chromatography, it is known that even in this application micellar mobile phases enhance the selectivity of separation [4–7]. Fig. 1 shows chromatograms of some inorganic anions. The elution order of ions can be altered not only by varying the micellar concentration but also by changing the concentration of added salts.

The aim of this paper is to explain quantitatively the behaviour of inorganic anions in cationic micellar chromatography. The partition of ions to oppositely charged micelles can be represented by an ion-exchange model, although micelles are not static but dynamic [8,9]. Various ion-exchange models have been reported [10–15], of which a stoichiometric ion-exchange model [13] is the most common. Although it has

* Corresponding author.

0021-9673/95/$09.50
SSDI 0021-9673(94)01133-8

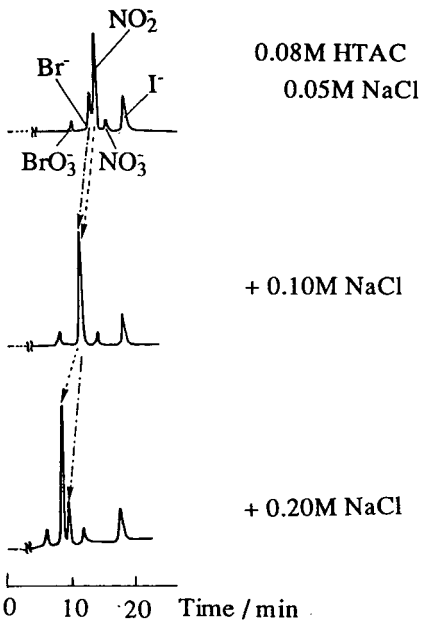

Fig. 1. Micellar chromatograms of some inorganic anions. Detection at 215 nm. Mobile phases are given on the right of each chromatogram.

recently been indicated that a stoichiometric ion-exchange model does not describe ion-exchange processes in a strict sense [10–12], this model has been extensively used and successfully explains not only the retention mechanisms of ions in ion-exchange chromatography [13] but also the behaviour of counterions of micelles [8,9]. In a previous paper [6], we succeeded in developing a model capable of describing the retention behaviour of cations in sodium dodecylsulfate (SDS) micellar chromatography. As the separation of transition metal ions by SDS micellar chromatography required the addition of a suitable ligand to the mobile phase, the mobile phase necessarily contained salts at concentrations high enough to neglect the dissociation of counter ions from SDS micelles. In this paper, we attempt to interpret the retention behaviour of anions in cationic micellar chromatography using a stoichiometric ion-exchange model. Not only does this model elucidate the applicability of a stoichiometric ion-exchange model but also it allows the evaluation of the dissociation of counter ions from micelles.

2. Experimental

The chromatographic system was composed of a Tosoh computer-controlled CCPD pump, a Rheodyne injection valve equipped with a 100-μl sample loop, a JASCO Model 875-UV, UV–visible detector and a recorder. A Wakosil 5C8 stainless-steel column (150 mm × 4.6 mm I.D.) packed with 5-μm octylsilanized silica gel, with specific surface area 300 $m^2\ g^{-1}$, carbon content 12% and carbon coverage 1.29 μmol m^{-2}, was used. Data were processed on a NEC PC-9801 personal computer.

Hexadecyltrimethylammonium chloride (HTAC) was recrystalized from acetone–methanol and dried over P_2O_5 under vacuum after rinsing with diethyl ether. Distilled, deionized water was used. Other reagents were of analytical-reagent grade.

The amounts of HTAC adsorbed on the column were determined by ion-pair extraction as follows: the column was equilibrated with a solution containing HTAC and in some instances NaCl; after adsorption equilibrium had been established, the column was rinsed well with methanol; after evaporation of the methanol, acetate buffer and Orange II solution were added to the residue; the ion pair of HTAC and Orange II was extracted into chloroform and the absorbance of the chloroform phase was measured spectrometrically. After correcting for the moles of HTAC existing in the dead volume of the column, the amount of adsorbed HTAC was calculated. Column dead volumes were determined by a method described by Shibukawa and Ohta [16].

3. Results and discussion

3.1. Retention model

Assuming monovalent anions as analytes for simplicity, we took the following ion-exchange equilibria into account to derive the equation describing of the retention of anions:

$$A^-(aq) + C^-(s) \overset{K_{IE}^{s}}{\rightleftharpoons} A^-(s) + C^-(aq) \qquad (1)$$

$$A^-(aq) + C^-(m) \overset{K^m_{IE}}{\rightleftharpoons} A^-(m) + C^-(aq) \quad (2)$$

where A^- and C^- are an analyte and a counter anion, respectively, s, aq and m in parentheses denote stationary, solution and micellar phase, respectively, and K^s_{IE} and K^m_{IE} are the ion-exchange equilibrium constants at the solution–resin and solution–micelle interface, respectively. Counter ions are not fully bound to micelles, but are partly dissociated; this causes mass action in ion-exchange equilibria even in the absence of added salts. The dissociation of counter ions is given by

$$\text{Surf C(m)} \overset{K_d}{\rightleftharpoons} \text{Surf}^+ \text{(m)} + C^-(aq) \quad (3)$$

$$K_d = [\text{Surf}^+ \text{(m)}][C^-(aq)]/[\text{Surf C(m)}]$$

where Surf C(m) and Surf^+ (m) denote a surfactant forming an ion pair with a counter ion and that existing as a cation in the micelles, respectively.

The capacity factor of an analyte is represented by

$$k' = \phi[A^-(s)]/([A^-(aq)] + [A^-(m)]\bar{v}C_M) \quad (4)$$

where ϕ is the phase ratio, $\bar{v}$ is the molal volume of micelles and C_M is the micellar concentration; these are introduced to convert the micellar phase concentration of an analyte into the solution phase concentration. Substitution of equilibrium constants in Eq. 4 gives

$$\frac{\phi}{k'} = \frac{[C^-(aq)]}{K^s_{IE}[C^-(s)]}\left\{1 + \frac{K^m_{IE}C_M}{[C^-(aq)] + K_d}\right\} \quad (5)$$

Free counter ions in solution come from (1) the dissociation of micelles (C^-_{dis}), (2) the counter ions of monomeric surfactants [equal to the critical micellar concentration (cmc) of a micelle] (C^-_{cmc}), and (3) added salts (C^-_{add}):

$$[C^-(aq)] = [C^-_{dis}] + [C^-_{cmc}] + [C^-_{add}] \quad (6)$$

The second and third terms in Eq. 6 are known, and $[C^-_{dis}]$ can be calculated if K_d is known. Eq. 5 can therefore represent the retention of anions in any case.

3.2. Calculation of equilibrium constants involved in the above retention model

The validity of the above model was verified both in the presence and in the absence of an added salt. A single anion system was assumed for simplicity; NaCl was used as an added salt. In the presence of a large amount of added salts, $[C^-(aq)]$ can be regarded as equal to $[C^-_{add}]$, because $[C^-_{cmc}]$ is not more than 1.3 mM (equal to cmc of HTAC; usually the cmc is lowered by the addition of salts), and $[C^-_{dis}]$ is also neglected as K_d is very small, as shown below. If $K_d \ll [C^-(aq)]$, plots of $\phi/k'[C^-(aq)]$ vs. $1/[C^-(aq)]$ will be linear at any constant C_M. Fig. 2 shows example plots obtained at $C_M = 0.08$ M. In order to facilitate the determination of K^s_{IE}, Eq. 5 was changed into the following form in the plots depicted in Fig. 2:

$$\frac{n_{C(s)}}{(V_r - V_0)[C^-(aq)]} = \frac{1}{K^s_{IE}}\left\{1 + \frac{K^m_{IE}C_M}{[C^-(aq)]}\right\} \quad (5')$$

where $n_{C(s)}$ is the moles of a counter ion in the stationary phase, which is equal to the moles of adsorbed HTAC on the stationary phase, and V_r

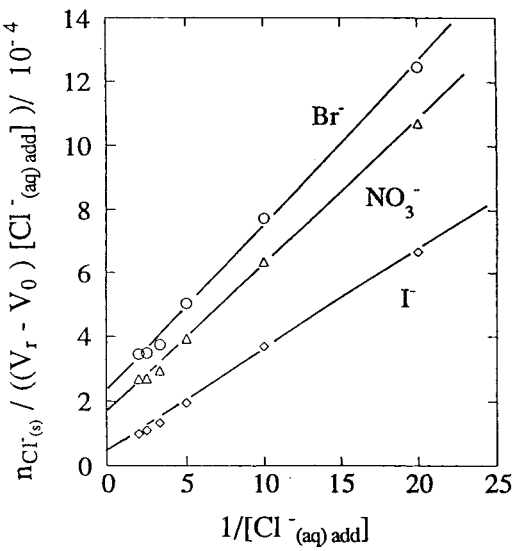

Fig. 2. Examples of linear plots based on Eq. 5. Details are given in the text.

and V_0 denote the retention volume of an analyte and the void volume of the column, respectively. The constancy of $n_{C(s)}$ was confirmed by the determination of the amount of HTAC adsorbed on the column as follows: 0.66 mmol with 0.1 *M* NaCl, 0.67 mmol with 0.2 *M* NaCl, 0.68 mmol with 0.3 *M* NaCl and 0.66 mmol with 0.5 *M* NaCl. Table 1 lists ion-exchange constants obtained at $C_M = 0.06$ and 0.08 M. Similar values were obtained for both micellar concentrations, indicating the validity of the model developed.

On the other hand, in the absence of an added salt, $[C^-(aq)] = [C^-_{dis}] + [C^-_{cmc}]$. As CMC is constant (1.3 m*M*) regardless of C_M, $[C^-(aq)]$ is a function of C_M alone. We can therefore determine K_d and the ion-exchange equilibrium constants by applying non-linear regression based on the reciprocal form of Eq. 5 to experimental data set of k' and C_M. Fig. 3 shows example plots of $V_r - V_0$ vs C_M, and Table 2 lists equilibrium constants obtained with non-linear regression.

K_d is almost constant, and the ion-exchange equilibrium constants agree well with values listed in Table 1.

3.3. Relationship between the retention model developed and a pseudo-phase model

The equilibrium constants listed in Tables 1 and 2 permit the calculation of partition coefficients, which are used in a pseudo-phase retention model:

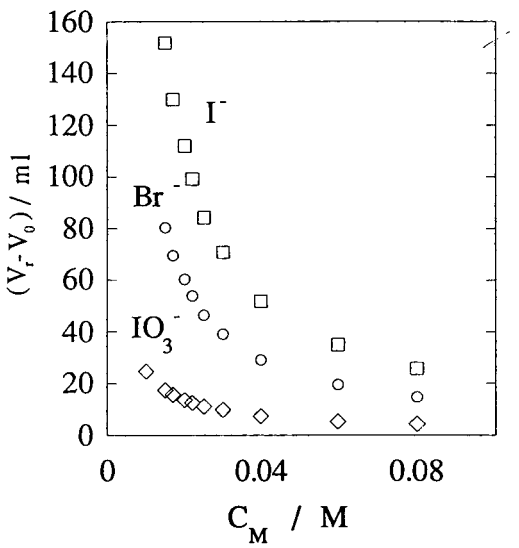

Fig. 3. Relationships between $(V_r - V_0)$ and C_M. Non-linear regression was applied to these relationships to determine K^m_{IE}, K^s_{IE} and K_d. Details are given in the text.

$$K_{SW} = [A^-(s)]/[A^-(aq)] = K^s_{IE}[C^-(s)]/[C^-(aq)] \quad (7)$$

$$K_{MW} = [A^-(m)]/[A^-(aq)] = K^m_{IE}[C^-(m)]/[C^-(aq)] = K^m_{IE}/\bar{v}([C^-(aq)] + K_d) \quad (8)$$

where K_{SW} and K_{MW} are partition coefficients of an analyte between the solution and stationary phase and between the solution and micellar phase, respectively. According to our model, both partition coefficients are not constant but

Table 1
Ion-exchange equilibrium constants obtained on the basis of Eq. 5

Ion	$C_M = 0.06$ *M*		$C_M = 0.08$ *M*	
	K^m_{IE}	K^s_{IE}	K^m_{IE}	K^s_{IE}
BrO_3^-	1.44	1.79	1.37	1.77
Br^-	3.09	4.63	2.77	4.32
I^-	13.2	33.2	12.1	30.1
NO_2^-	1.71	2.05	1.74	2.16
NO_3^-	3.55	6.21	3.53	6.17

$[Cl^-_{add}]$ was changed from 0.05 to 0.5 *M*.

Table 2
Ion-exchange equilibrium constants and the dissociation constant of Cl^- from HTAC micelles

Ion	K^m_{IE}	K^s_{IE}	K_d
BrO_3^-	1.4	2.0	$6.9 \cdot 10^{-4}$
Br^-	2.8	4.8	$6.5 \cdot 10^{-4}$
I^-	13	36	$6.1 \cdot 10^{-4}$
NO_2^-	1.7	2.2	$6.7 \cdot 10^{-4}$
NO_3^-	3.4	6.4	$6.8 \cdot 10^{-4}$

functions of $[C^-(aq)]$. If a large amount of salts is added, $[C^-(aq)]$ becomes constant and hence the partition coefficients also become constant. This situation is clearly shown in Figs. 4 and 5. Fig. 4 shows the changes in K_{MW}, K_{SW} and $(K_{MW}-1)/K_{SW}$ with C_M in the absence of added salts. $(K_{MW}-1)/K_{SW}$ is the slope of a plot based on a pseudo-phase model represented by [2]

$$1/(V_r - V_0) = (K_{MW} - 1)\bar{v}C_M/V_s K_{SW} \quad (9)$$

where V_s is the volume of the stationary phase. Both partition coefficients increase with decreasing C_M, because $[C^-(aq)]$ decreases with decreasing C_M. $(K_{MW}-1)/K_{SW}$, in contrast, decreases with decreasing C_M; the change in this value is much smaller than those in the partition coefficients. This indicates that a plot based on Eq. 9 seems linear at high micellar concentrations, but that it is actually concave rather than linear.

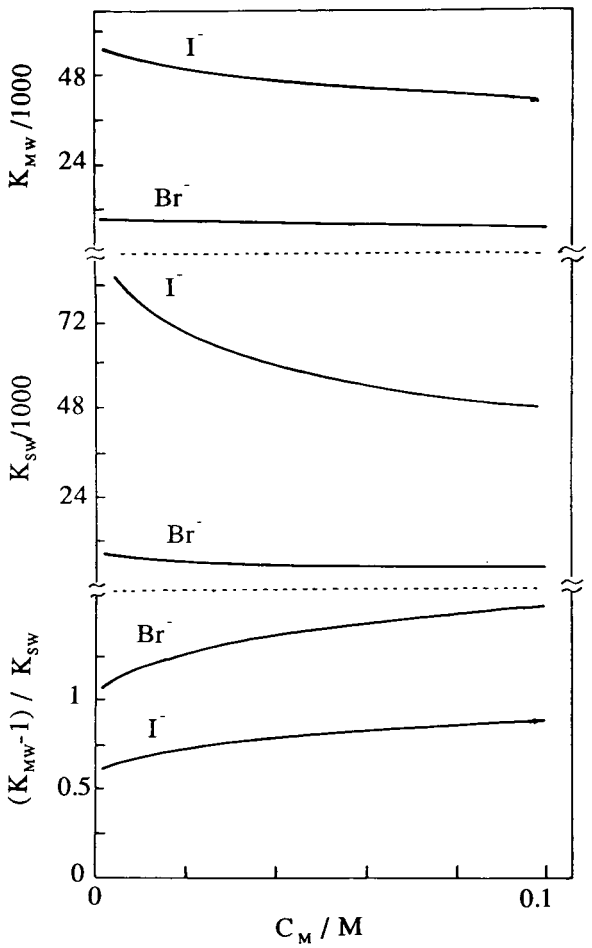

Fig. 4. Changes in K_{MW}, K_{SW} and $(K_{MW}-1)/K_{SW}$ with C_M in the absence of an added salts. These values were calculated according to Eqs. 7 and 8.

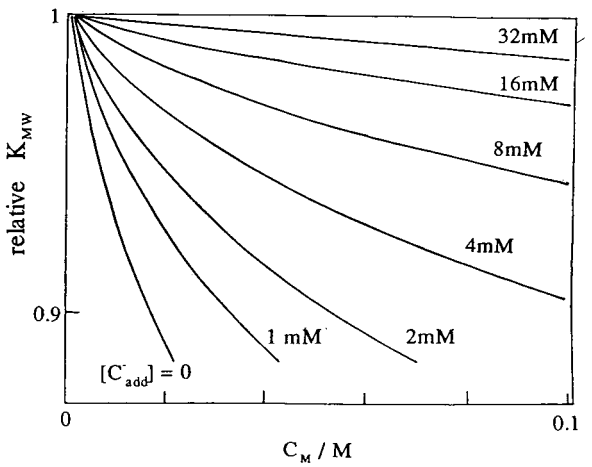

Fig. 5. Changes in K_{MW} for I^- with $[C^-_{add}]$. Relative K_{MW} with respect to that at $C_M \rightarrow 0$ is plotted against C_M. Eq. 7 was used for calculation.

Fig. 5 shows the effect of added salts on the partition coefficients, where K_{MW} for I^- is taken as an example and relative K_{MW} is plotted against C_M. It is obvious that K_{MW} becomes constant as the salt concentration increases.

In conclusion, the developed model implies that the retention of ions in ionic micellar chromatography can be described by a stoichiometric ion-exchange model, and formally obeys a pseudo-phase model when the concentration of an added counter-ion is high enough to neglect the concentration of the counter-ion coming from the dissociation of micelles.

References

[1] J.G. Dorsey, W.T. Cooper, J.F. Wheeler, H.G. Barth and J.P. Foley, *Anal. Chem.*, 66 (1994) 500R.
[2] D.W. Armstrong, *Sep. Purif. Methods*, 14 (1984) 213.

[3] D.W. Armstrong and F. Nome, *Anal. Chem.*, 53 (1981) 1662.
[4] T. Okada, *Anal. Chem.*, 60 (1988) 1511.
[5] T. Okada, *J. Chromatogr.*, 538 (1991) 348.
[6] T. Okada, *Anal. Chem.*, 64 (1992) 589.
[7] F.G.P. Mullins and G.F. Kirkbright, *Analyst*, 112 (1987) 701.
[8] F.H. Quina and H. Chaimovich, *J. Phys. Chem.*, 83 (1979) 1844.
[9] E. Lissi, E. Abuin, G. Ribot, E. Valenzuela, H. Chaimovich, P. Araujo, R.M.V. Aleixo and I.M. Cuccovia, *J. Colloid Interface Sci.*, 1985 (103) 139.
[10] J. Ståhlberg, B. Jonsson and Cs. Horváth, *Anal. Chem.*, 63 (1991) 1867.
[11] J. Ståhlberg, B. Jonsson and Cs. Horváth, *Anal. Chem.*, 64 (1992) 3118.
[12] J. Ståhlberg, *Anal. Chem.*, 66 (1994) 440.
[13] P.R. Haddad and P. Jackson, *Ion Chromatography*, Elsevier, Amsterdam, 1990.
[14] J. Horst, W.H. Höll and S.H. Eberle, *React. Polym.*, 14 (1990) 209.
[15] J. Horst, W.H. Höll and M. Wernet, *React. Polym.*, 15 (1991) 251.
[16] M. Shibukawa and N. Ohta, *Chromatographic*, 25 (1988) 288.

ELSEVIER

Journal of Chromatography A, 706 (1995) 43–54

JOURNAL OF CHROMATOGRAPHY A

Preliminary tests to select operating conditions for the accurate determination of stability constants by cation-exchange chromatography: the Cd^{2+}–Cl^- and Cd^{2+}–NO_3^- systems

P. Papoff*, A. Ceccarini, P. Carnevali

Dipartimento di Chimica e Chimica Industriale, Università di Pisa, via Risorgimento 35, 56126 Pisa, Italy

Abstract

Ion chromatography (IC) has been demonstrated to be a powerful tool for equilibrium constant determination, related to various cation–ligand systems. Nevertheless, no systematic research has been carried out to develop preliminary checks in order to verify whether the variation in ligand concentration in the eluent at constant ionic strength affects the exchange mechanism for the system of interest in the selected chromatographic column. In this paper, tests are proposed which allow one to determine beforehand the experimental conditions to be used in cation-exchange chromatography, whereby parallel mechanisms of elution (mainly in the reversed-phase mode) are avoided. In this way IC becomes an independent rather than an auxiliary means to obtain accurate β_i values. Cd(II)–Cl^- and Cd(II)–NO_3^- systems were considered and are discussed.

1. Introduction

Haddad and Foley [1] described a chromatographic retention model for metal ions that simultaneously participate in heterogeneous cation exchange and in homogeneous phase complex-forming equilibria. A retention model, based on chromatographic separation by an anion-exchange mechanism of metal ions present in the eluent solution as negatively charged complexes, was described by Hajos et al. [2]. Of the above two exchange mechanisms, cation exchange seems to present a wider field of application in the study of association equilibria, starting with positively charged and/or neutral complexes. On the other hand, success in the determination of stability constants via cation-exchange chromatography depends on the following conditions: (1) the concentration of the complex-forming agents may be varied in as wide a range as possible at constant concentration of the counter ion (competing cation) E^{n+} and constant ionic strength I; (2) this variation must have no effect on the characteristics of the chromatographic column mainly in terms of its capacity Q and its path length; (3) the solute elution is controlled by ion-exchange mechanisms only, regardless of the actual concentration of the complex-forming agent; and (4) departures from the above conditions must meet experimental evidence.

As far as we know, no mention has been made in the literature about any side-effects on the determination of association constants by ion chromatography (IC), most of the papers published on this topic being concerned with mea-

* Corresponding author.

0021-9673/95/$09.50
SSDI 0021-9673(95)00205-7

surements in a short range of concentrations of ligand, C_L, at $I < 0.1$. In these cases, only the first equilibrium step was predominant and data were treated for β_1 calculation only [3–6], sometimes according to a semi-quantitative approach.

The aim of this paper is to show that (i) the nature of both the counter ion and of the co-ion (anion) may affect under some experimental conditions the elution mechanism as a result of one or more of the first three conditions above not being fulfilled and (ii) once some preliminary proof has been obtained for the system of interest, these conditions can be experimentally highlighted so that accurate values of β_i can be obtained, for well defined eluent electrolyte compositions, thus avoiding misleading contributions.

Systematic errors were also considered, which may affect the experimental determination of the capacity factor k' and, in turn, the calculated β_i values, as a function of the concentration C_L in the range from zero up to the maximum allowable value.

The potential of IC in the determination of reliable β_i values, and its peculiar feature of giving auto-consistent information on mileading side mechanisms, were tested for the systems Cd(II)–Cl^- and Cd(II)–NO_3^-, which are used as examples.

2. Theoretical

2.1. Cation-exchange mechanisms in the absence or presence of ligands

For the sake of clarity, the most significant equations related to the above mechanisms are reported here with some comments. Detailed information on this topic is available in the literature [7]. Throughout this paper the analyte cation will be considered as being bivalent and the counter ion monovalent.

In the absence of ligands, the chromatographic exchange process involves the free hydrated species M^{2+} and the counter ion E^+ of the eluent, according to

$$M_m^{2+} + 2E_r^+ = M_r^{2+} + 2E_m^+ \quad (1)$$

$$K_{M,E} = \frac{[M^{2+}]_r[E^+]_m^2}{[M^{2+}]_m[E^+]_r^2} \cdot \left(\frac{\gamma_M}{\gamma_E^2}\right)_r \left(\frac{\gamma_E^2}{\gamma_M}\right)_m \quad (2)$$

where the subscripts r and m refer to the stationary and mobile phases, respectively, and the other terms have the usual meanings. It is implicitly assumed that the nature of the co-ions of the eluent does not affect the exchange equilibria. This assumption becomes increasingly valid the more the surface of the stationary phase is only occupied by the negatively charged groups, so that adsorption of electrolyte co-ions as the primary step on the resin bed is electrostatically hindered. This is not the case, for example, in gel chromatography, where the distribution of ionic species is taken to be a combined effect of size exclusion and partition, and where the partitioning depends very much on the type of both the counter ion and its co-ion [8].

Apart from the extreme case above, once the distribution and capacity factor have been defined by Eqs. 3 and 4, the experimentally measurable capacity factor depends, in the absence of ligands, on the characteristics of the column and on the eluent according to Eq. 5.

$$D_{M,E} = \frac{[M^{2+}]_r}{[M^{2+}]_m} \quad (3)$$

$$k'_s = D_{M,E} \cdot \frac{V_r}{V_m} \quad (4)$$

$$k'_s = K_{M,E} \cdot \frac{V_r}{V_m} \left(\frac{[E^+]_r}{[E^+]_m}\right)^2 \left(\frac{\gamma_E^2}{\gamma_M}\right)_r \left(\frac{\gamma_M}{\gamma_E^2}\right)_m = \frac{V_R - V_0}{V_0} \quad (5)$$

where V_R is the solute retention volume and V_0 is the void volume ($V_0 = V_m$).

According to Eq. 5, k'_s depends on both I and $[E^+]$. It will be shown later that, in pure cation exchange, the activity coefficient ratio in Eq. 5 may be considered as being independent of I. If a ligand is present in the eluent, Eq. 5 takes the form

$$k'_L(I, [E^+]_m, [L^-]) = \alpha(I, [L^-])k'_S([E^+]_m) \quad (6)$$

where, in addition to the dependence on counter ions, k'_L depends on I, $[L]_m$ and α:

$$\alpha = \frac{[M^{2+}]}{C_M} = \frac{1}{1 + \beta_1[L^-] + \beta_2[L^-]^2 + \cdots} \quad (7)$$

For a given column, at a constant concentration of E^+ and constant I, Eq. 6 becomes

$$\frac{1}{(k'_L)_{I,[E]}} = \frac{1}{(k'_S)_{[E]}} \cdot (1 + \beta_1[L^-] + \beta_2[L^-]^2 + \cdots) \quad (8)$$

Eq. 8 shows that the intercept of the $1/k'_L$ vs. $[L^-]$ plot gives the value of the term $1/k'_s$. Otherwise, as the k'_s value can also be experimentally obtained for $\alpha = 1$, Eq. 8 can be rewritten as

$$\left(\frac{k'_S}{k'_L}\right)_{I,[E]} = 1 + \beta_1[L^-] + \beta_2[L^-]^2 + \cdots \quad (9)$$

If both the theoretical and experimental conditions hold, Eqs. 8 and 9 show that the capacity factor, obtained at various ligand concentrations and constant I and $[E^+]$, is related to the β_i values of the system without any non-specific contribution. This is a distinguishing feature of IC, for example, compared with potentiometry and calorimetry. In the first case allowance must be made for the non-specific contribution of junction potential on ΔE and in the second case for the non-specific contribution of mixing or dilution heat on ΔQ.

If the metal-containing species (e.g., ML^+ and ML_2) undergo an exchange with the stationary phase, Eq. 6 becomes

$$k'_{mix} = \alpha_{M^{2+}}k'_{M^{2+}} + \alpha_{ML^+}k'_{ML^+} + \alpha_{ML_2}k'_{ML_2} \quad (10)$$

where k'_{mix}, the experimental capacity factor, is the sum of the various capacity factors concerning each metal-containing species multiplied by the respective ionic fraction. In terms of β_i and of the ligand concentration:

$$k'_{mix} = \frac{k'_{M^{2+}} + \beta_1[L^-]k'_{ML^+} + \beta_2[L^-]^2k'_{ML_2}}{1 + \beta_1[L^-] + \beta_2[L^-]^2} \quad (11)$$

Eq. 11 is non-linear in both the β_i and the k'_{ML_i} parameters. In principle, working at constant ionic strength and variable ligand concentrations, fitting of the data will improve by increasing the number of parameters regardless of their physical meaning.

To ascertain the validity of the model assumed, sets of data obtained at different ionic strengths and various concentrations of L are required. Only when all the values of k'_{ML_i}, multiplied by the actual counter-ion concentration ($k'_{ML_i}[E^+]^{2-i}$), are found be the same is the validity of the model confirmed. If not, one or more of the k'_{ML_i} values initially assumed must be set to zero and the data reprocessed until consistent values of k'_{ML_i} are obtained regardless of I.

Eq. 11 has been derived only on thermodynamic grounds; however, steric effects may play a very important role in the exchange process. The higher the charge and the larger the size of the complex size, the more important these effects are.

It will be shown later that in the Cd^{2+}–Cl^- system, only the Cd^{2+} species undergoes exchange.

3. Experimental

3.1. Equipment

Two Dionex Series 4000i high-pressure pumps, totally computer controlled, were used for pumping the eluent and the postcolumn derivatization solution. A Dionex UV spectrophotometer was used in both V_0 and V_R detection. The eluent was mixed with the postcolumn derivatization solution in a three-way tee and the mixture was passed to the detector through a bead-packed reaction coil (the total postcolumn dead volume was 450 μl). Eluents, column and postcolumn derivatization systems were thermostated at 25 ± 0.1°C.

3.2. Columns

The following Dionex columns were used: a 250 × 4 mm I.D. and a 50 × 4 mm I.D. Omnipac PCX 100 IC-cation analytical column, manufactured using microporous substrate beads functionalized with sulphonic groups as cation-exchange sites (surface area 1 m^2/g, pore size 60 Å, capacity 120 μequiv. per column); a 250 × 4 mm I.D. Omnipac PCX-500 IC-cation analytical column, manufactured using macroporous substrate beads functionalized with sulphonic groups as cation-exchange sites (surface area 300 m^2/g, pore size 60 Å, capacity 120 μequiv. per column) was also used in some preliminary experiments.

3.3. Chemicals

Carlo Erba RPE doubly distilled water, Baker Instra-Analyzed perchloric acid, Merck Suprapur hydrochloric acid, Baker Analyzed sodium chloride, Baker Analyzed sodium perchlorate monohydrate and Baker Analyzed acetonitrile were used in the eluent preparation. Aldrich 2-(5-bromo-2-pyridylazo)-5-diethylamino)phenol, Baker Analyzed Triton X-100, Baker Analyzed boric acid and Baker Analyzed sodium hydroxide were used for the derivatization solution.

3.4. Eluents

For each ionic strength (0.05, 0.10, 0.22, 0.30, 0.50), stock standard solutions of $HClO_4$ and HCl were prepared from the corresponding commercial concentrated solutions. The correct molarities of the stock standard solutions were determined by titration with Na_2CO_3. In addition, stock standard solutions of $NaClO_4$ and NaCl, for each ionic strength, were prepared from the corresponding sodium salts; these stock standard solutions contained 0.01 *M* H^+. Working standard solutions were prepared by diluting appropriate volumes of the stock standard solutions. All the eluents contained 1% of acetonitrile to ensure that the column packing was wetted properly.

3.5. Procedures

In all experiments concerning cadmium elution, 25 μl of a 5 ppm Cd in 0.01 in 0.01 *M* HNO_3 solution were injected. Cd detection was performed by using a postcolumn derivatization system: a solution of 2-(5-bromo-2-pyridylazo)-5-diethylamino)phenol (0.4 mmol at pH 10, adjusted with 0.5 *M* sodium borate–boric acid buffer) was mixed with the eluent at the column end (the UV detector was set at 565 nm).

When using the postcolumn derivatization device, the mobile phase volume of the column (V_0) was determined at 300 nm from the positive peak of NO_3^-; otherwise, V_0 was determined by detecting the peak elution of nitrate at 230 nm and/or the negative elution peak of the solvent at 205 nm.

A flow-rate of 1 ml/min was used for all the eluent compositions with the exception of I = 0.5, where 0.5 ml/min was used to improve the measurements of both T_R and T_0. A flow-rate of 0.2 ml/min was used for the derivatization solution.

4. Results and discussion

4.1. Experimental evidence (in perchloric acid medium) for the type of dependence of the activity coefficient ratio on the ionic strength and on the type of chromatographic column

Eq. 2 predicts that when the concentration of a uni–univalent electrolyte, containing E^+ as a counter ion, is changed, the product $k'[E^+]^n$ will vary as the activity coefficient ratio, R, does:

$$k'_s[H^+]^n_m = a\left(\frac{\gamma^n_H}{\gamma_M}\right)_r\left(\frac{\gamma_M}{\gamma^n_H}\right)_m = aR \qquad (12)$$

where n is the charge of the solute ($n = 2$ in our example) and $a = K_{ME}(V_r/V_m)[H^+]^n_r$. Expressed in logarithmic form, Eq. 12 becomes

$$\log(k'_s[H^+]^n_m) = \log a + \log R \qquad (13)$$

Haddad and Foley [1] reported the slopes of log k' vs. log(mean activity of perchloric acid)

for bi- and trivalent solutes as obtained according to Refs. [9,10]. Depending on the nature of the solute, the relevant value of the slope was found to vary from the theoretical value $(-n)$, sometimes significantly. For instance, the experimental values of the slope were −1.66 for Mg^{2+}, −1.87 for Ni^{2+} and −2.08 for Cd^{2+}, instead of −2.

Apart from the questionable use of the activity of perchloric acid instead of I (the activity coefficient of the counter ion H^+ is included in R), these behaviours appeared to be due more to different partition mechanisms than to a different (and even counter) effect of the solutes on the activity coefficient ratio. Specifically, depending on the column features, we expected that the adsorption of solute and counter ions on the resin bed might give rise to an inverse phase elution mechanism, in parallel with the exchange mechanism. Since the specific adsorption of both solute and counter ions was also considered by Stählberg [11] in his double-layer model, we decided to carry out additional experiments whereby values of k'_s for the above solutes Cd^{2+} and Ni^{2+} were obtained, using different columns, both at various counter-ion concentrations and I (perchloric acid). If experimental conditions had been found where R does not depend (or only very slightly) on I, one could confidently expect, when studying association equilibria, that changes in the nature of the salt composition in the eluent, at constant I, would be made without significant misleading effects. It was found that:

(i) When using a micropore substrate bed column (surface area 1 m^2/g) the slope of log aR vs. log I plot can be considered constant and near to zero in the range of I used (0.06–0.5): the maximum variation in aR between the limit concentrations of $HClO_4$ was 4% and 7% for Cd^{2+} and Ni^{2+}, respectively (see Fig. 1, curves a and b); the shape of the chromatograms for both Cd^{2+} and Ni^{2+} is regular regardless of I.

(ii) When using a macropore substrate bed column (surface area 300 m^2/g) with the same fixed charge equivalents Q as before, the dependence of log aR on log I is clearly outside the experimental uncertainty (see Fig. 1, curve c), while the shape of the chromatogram is distorted

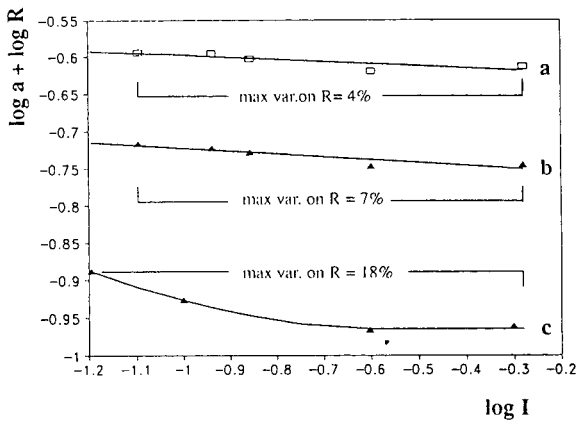

Fig. 1. Effect of ionic strength ($HClO_4$ medium) on the activity coefficient ratio (see Eq. 12). Solutes considered: Cd (curve a) and Ni (curves b and c). Curves a and b refer to a micropore column (Dionex PCX100) and curve c to a macropore column (Dionex PCX500).

as shown in Fig. 2b for Ni^{2+}: the lower the $HClO_4$ concentration, the greater is the distortion.

The above experiments, performed at various

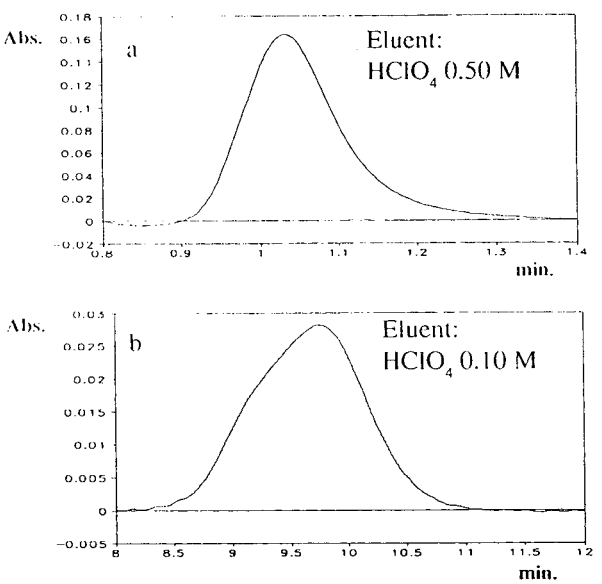

Fig. 2. Evidence of parallel mechanisms of elution from the dependence of the shape of the chromatogram (Ni^{2+}) on the counter-ion concentration at variable I ($HClO_4$ medium). Dionex PCX500 macropore column.

I ($HClO_4$ medium) and in the absence of ligands, show that parallel mechanisms of elution are possible. They should be minimized by using columns where only the ionic functional groups are active at the surface of the stationary phase, as the free sites on the surface of the resin bed, if any, are preferentially occupied by protons so that the elution of solute is controlled by the ion-exchange mechanism. Under these conditions, the activity coefficient ratios of the species involved in the exchange equilibrium are fairly independent of I.

4.2. Effects of the nature of the counter ion on the Cd^{2+} capacity factor

Once it had been ascertained that hydrogen ions may hinder the specific adsorption of solute ions such as Cd^{2+} and Ni^{2+} on the surface of the resin bed, other monovalent species were tested, such as sodium, to verify whether they play the same role as H^+ and under what experimental conditions. This is an important issue whenever the ligand to be considered in equilibrium studies is a weak acid or base, so that pH is not an independent variable.

These experiments were performed using the micropore resin bed column, Cd^{2+} as a solute and a mixture of $HClO_4$ and $NaClO_4$ at constant I (0.1 or 0.3) in the eluent. It was found that:

(i) At $I = 0.1$ the equivalent fraction of H^+ (N_{H^+}) added to the mixture can be lowered to zero (pH 7); the shape of k' vs. N_{H^+} plot assumes the form shown in Fig. 3, which is different from that predicted by the replacement of H^+ with Na^+ as a counter ion according to the equation

$$k'_s = \frac{V_r}{V_m} \cdot Q^2 K_{M,H} \left([H^+] + [Na^+] \sqrt{\frac{K_{M,H}}{K_{M,Na}}} \right)^{-2} \quad (14)$$

where the term $(V_r/V_m)Q^2K_{M,H}$ can be obtained

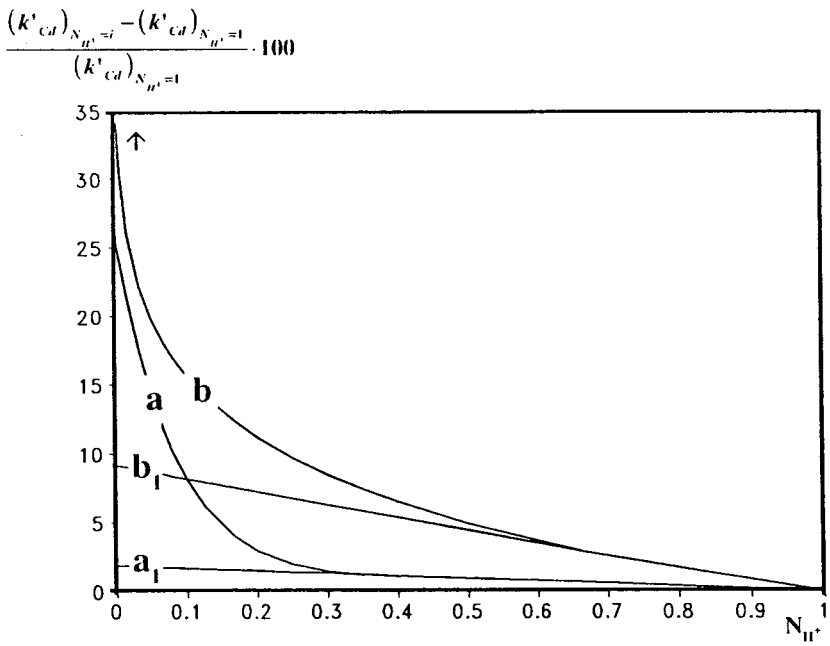

Fig. 3. Effect of the nature of the counter ion (Na^+ or H^+) on Cd(II) capacity factor in perchlorate medium at constant ionic strength. I = (a) 0.10 and (b) 0.30; curves a_1 and b_1 refer to the theoretical shapes calculated at the respective ionic strength according to Eq. 14.

from the experimental values of k'_s at $N_{H^+} = 1$, and $K_{M,Na}$ is an unknown parameter. The $K_{M,Na}$ value can be estimated by using the k'_s values in the N_{H^+} region where k' is a nearly linear function of N_{H^+}.

(ii) At $I = 0.3$, a minimum value of $N_{H^+} = 1.7 \cdot 10^{-3}$ ($C_{H^+} = 5 \cdot 10^{-4}$ M) is required to avoid irreversible adsorption of Cd^{2+}.

4.3. Effect of the nature of the co-ion in the eluent

In cation-exchange chromatography, the nature of the anions present in the eluent should have no effect on the performance of the chromatographic column, at least when the functional fixed charges are close together [8,12]. It will be shown that, when measuring V_0 by using nitrate solute, the plot of V_0 vs. N_{Cl^-} shows a slope variation in the region of N_{Cl^-} 0.9–1. In the same interval the $k'_{Cd^{2+}}$ vs. N_{Cl^-} plot shows anomalous behaviour. Table 1 summarizes the results obtained by using both the solvent and nitrate peaks in measuring V_0. Each value is the mean of nine replicates; the sample relative standard deviation was typically 0.1% and the repeatability of mean V_0 among days was 0.2% so that differences between V_0 mean values higher than 0.1% ($\alpha = 0.5$) were statistically highly significant. It was found that:

(i) With $HClO_4$ solutions, V_0 decreases when the acid concentration is increased from 0.05 to 0.5 M, regardless of the criteria used to measure it. The variation in V_0, ΔV, using the solvent and nitrate peaks, was found to be positive and increased from 0.05 M (0.018 ml) to 0.3 M (0.025 ml).

(ii) With HCl solutions, V_0 increases up to 0.3 M when the solvent peak is used, and continuously decreases with decreasing acid concentration when the NO_3^- peak is used. The greatest variation between the V_0 values obtained by the two methods of measurements was found at 0.05 M ($\Delta V = 0.118$) and the smallest at 1 M ($\Delta V = 0.009$).

As shown in Fig. 4, where V_0 and k'_s/k'_L vs. N_{Cl^-} plots are compared, both V_0 [measured in the absence of Cd(II)] and k'_s/k'_L for Cd(II) present consistent variations in slope within almost the same N_{Cl^-} interval. Thus, whenever V_0 vs. N_{X^-} presents a shape comparable to that shown in Fig. 4 for Cl^-, sound information is obtained about the useful range of N_{X^-} in measuring equilibrium constants.

From all the above experimental findings, including those on the effect of the nature of the counter ion on the capacity factor, a model can

Table 1
Measurements of V_0 at various ionic strengths (Dionex PCX100 microporous substrate bed column)

Ionic strength	Eluent	Peak elution considered		Δ
		H_2O	NO_3^-	
1.00	HCl	1.105	1.114	−0.009
	$HClO_4$	1.110	1.085	0.025
	Δ	−0.005	0.029	
0.50	HCl	1.106	1.136	−0.030
	$HClO_4$	1.127	1.102	0.025
	Δ	−0.021	0.034	
0.30	HCl	1.123	1.145	−0.022
	$HClO_4$	1.125	1.100	0.025
	Δ	−0.002	0.045	
0.10	HCl	1.096	1.158	−0.062
	$HClO_4$	1.104	1.084	0.020
	Δ	−0.008	0.074	
0.05	HCl	1.076	1.193	−0.117
	$HClO_4$	1.080	1.062	0.018
	Δ	−0.004	0.131	

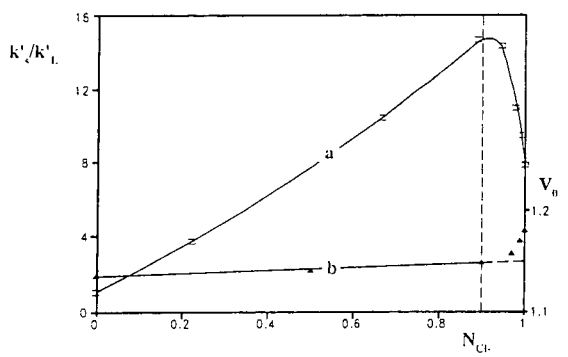

Fig. 4. Effect of substitution of ClO_4^- by Cl^-: (a) on k'_s/k'_L and (b) on V_0 (nitrate as solute). Cd^{2+}–Cl^- system, $I = 0.50$ M, Dionex PCX100 microporous column.

be proposed, however rough, to interpret and correlate the data, as follows.

(i) The resin matrix cannot be exactly considered as a plane sheet to which a surface area corresponds. Pores or some surface points, where functional groups are lacking, are possible depending on the resin's peculiar characteristics, i.e., area per gram or equivalents per square metre. Whenever any interaction by the reversed-phase mode of solute with pores or with free surface points is (or is made) not significant, all the assumptions concerning the surface complexation model [10,13,14] hold. In particular, the electrical charge of the fixed sites is neutralized by the different types of counter ions which are arranged in characteristic individual Stern layers [11]. The Stern layers contain most of the counter ions; further counter ions are distributed in the adjacent layer with a diffuse distribution of counter and co-ions.

(ii) In micropore substrate resins, whenever the number of resin equivalents per unit area is very large and charges are very close, direct specific adsorption (on free resin bed sites) of anions as a primary step is hindered, while some cation adsorption is still possible, owing to the synergic effects of the electrostatic field due to the negative fixed charges, and the hydrophilic-like bed surface–solute interaction. Once the cation has been specifically adsorbed, the anionic co-ion can be bound on the same surface plane forming ion pairs, or arranged in an outer layer, inside the double layer. It is likely that relatively hydrophobic co-ions, such as perchlorate, may enhance and stabilize the direct cation adsorption. In principle, the charges of the specifically adsorbed cation can be in part neutralized by the negative charges of the functional groups.

(iii) When pores and free surface sites are effective in promoting solute-specific adsorption on a micropore porous resin surface, they affect the solute elution mechanism the greater is the equivalent free surface area on the resin bed and the weaker is the competitivity of counter ions of the eluent in counteracting the solute adsorption. This may explain the elution behaviour of Cd ion in perchlorate medium, at variable equivalent fraction of protons and sodium ion, found at two different I (0.1 and 0.3). When N_{H^+} goes below 0.3 ($I = 0.1$) or 0.7 ($I = 0.3$) to zero (see Fig. 3, curves a and b, respectively), the cadmium elution increasingly departs from the cation-exchange mechanism as its adsorption competes with the proton or sodium adsorption at their respective concentrations in the eluent. Specifically, at $I = 0.3$ the antagonistic effect of sodium alone in reducing cadmium adsorption is no longer sufficient (salting-out effect?) with N_{H^+} decreasing to zero. A finite concentration of protons is required to avoid complete irreversible adsorption of cadmium ions (see Fig. 3, curve b).

When the microporous substrate is replaced by a macroporous substrate, owing to the very large increase in the surface area, sites are possible where the charge effect of the functional groups is too weak to repel surface adsorption of anions. As a second step, ion-pair formation with multicharged cations is favoured. This accounts for the need to use very high concentrations of protons (>0.1 M) to counteract Cd ion adsorption, when macropore resins are used.

(iv) In an eluent containing ClO_4^- and Cl^- at constant I, when the equivalent fraction of Cl^- becomes higher than 0.8, the specific adsorption of the $H^+ClO_4^-$ ion pairs decreases. This decrease is in part compensated by the formation of ion pairs between protons and chloride ions. Unlike ClO_4^-, chloride ions are not specifically adsorbed as co-ions but are located in the double layer. The amount of Cl^- sorbed decreases, at constant N_{Cl^-}, as I increases (because of the desorption of the univalent cation). When Cl^- is sorbed in the double layer, the resin acts as both a cation and anion exchanger. This infers that, at increasing N_{Cl^-}, V_0 will present a higher variation the lower is I and k'_s/k'_L a lower variation the lower is I.

The equivalent capacity of the anion exchanger depends on the amounts of sorbed Cl^-, that is, it depends on N_{Cl^-} and I. This accounts for the following findings: when nitrate is used as a solute in measuring V_0 at different N_{Cl^-} values and these values are compared with that obtained at $N_{Cl^-} = 0$ at the same ionic strength, the relevant ΔV is always higher than zero in all the

situations considered because the capacity factor of nitrate is no longer zero under these conditions, but tends to zero as N_{Cl^-} decreases or I increases; when Cd^{2+} is used as a solute, since the proton specific adsorption (which is much larger than sodium ion adsorption) decreases as N_{Cl^-} or I increases, the reversed-phase mode exchange becomes more significant in the elution of Cd^{2+} the higher is N_{Cl^-} or I, with a consequent anomalous increase in the observed capacity factor k'_{Cd} (Fig. 4). All the above considerations are based on the stoichiometric model for data interpretation, the only one that is available as far as we know for solutes distributed among several different metal-containing forms. Further, the electrostatic retention model in developing the surface complex formation with each counter-ion species arranged in the double layer specifically excludes the presence of free sites, so differences in behaviour between macro- and microporous resin beds cannot be explained.

It is interesting to compare our findings on the dependence of the cadmium capacity factor on N_{H^+} at constant I, with those of Günter, discussed by Höll et al. [14,15] on the distribution of calcium ion and protons on a strong acid resins. Günter's experiments were performed under true equilibrium conditions by pouring increasing amounts of resin, in the calcium form, into a hydrochloric acid solution of a given concentration, and after some days measuring the concentrations of the solutes in both phases. It was found that for small resin loadings, the proton concentration in the resin phase is higher than expected with a consequent desorption of some bivalent ions. This agrees with our findings about preferential adsorption of protons with respect to cadmium ion.

4.4. *Conclusions about preliminary tests in IC investigations of complex equilibria*

In order to minimize the effects due to parallel mechanisms of elution (reversed-phase interaction), from the above findings the following conclusions and recommendations are proposed:

(1) In the stationary phase the number of equivalents of fixed groups per square metre has to be as high as possible.

(2) At constant total concentrations of competing cations, a minimum concentration of hydrogen ion is suggested in the eluent, whenever possible, to prevent adsorption phenomena on the stationary phase bed. If not, the value of k'_s, at zero ligand concentration, may be affected by error, the higher is the ionic strength.

(3) When the ligand is anionic and the ionic strength is kept constant with perchlorate, the maximum ligand concentration in the eluent must not reach 100% of the total anionic concentration.

Point (1) can be verified by plotting log $k'_s[E^+]^n$ vs. I and from the shape of the solute chromatographic curves. Point (2) can be verified from the plot of k'_s vs. $[H^+]$ with $[H^+] + [E^+] =$ constant and $[H^+]$ varying from 0 to 100%. Point (3) can be verified from the plot of k'_s/k'_L vs. $[A^-]$ (or $[ClO_4^-]$) at constant total concentration of counter ions at varying $[ClO_4^-]$ and/or from the plot of V_0 vs. $[L^-]$ at $[L^-] + [ClO_4^-] =$ constant.

4.5. *Cadmium–chloride and cadmium–nitrate ionic complexes*

Once the experimental conditions for the cadmium–chloride system had been defined, whereby the chromatographic ion elution is purely controlled by the ion-exchange mechanism, measurements were made at 0.50, 0.30, 0.22, 0.10, and 0.05I. The ionic fraction of ligand was varied from 0 to 0.8. When a mixture of sodium and hydrogen ions in the eluent was used, the concentration of proton was kept constant and equal to 0.01 equiv./l. Table 2 shows the most significant values. The thermodynamic ${}_T\beta_i$ values were roughly estimated by using the activity coefficient values calculated by Kielland [23] at the operating ionic strength (0.05, 0.10). The agreement with literature data is fairly good. The same holds for β_1 at $I = 0.1$ and 0.5, for which literature data are available. For β_2 at $I = 0.5$, good agreement was found

Table 2
Comparison of IC results with literature data for the Cd(II)–Cl^- system

I	${}_T\beta_1$	β_1	β_2	Method[a]	Ref.
0	95.5 ± 7.2%				[16]
0	93.54			Pot.	[17]
0	93.5			Pot.	[18]
0.05[b]	97.0[d]	44.3		IC	TW[e]
0.05[b]	92.9[d]	42.4		IC	TW[e]
0.10		38.9 ± 9.6%		Kin.	[19]
0.10[b]	95.4[d]	35.3 ± 1.4%	77.4 ± 8.5%	IC	TW[e]
0.22[b]		27.8 ± 1.3%	66.5 ± 4.1%	IC	TW[e]
0.22[b]		27.6 ± 1.2%	61.1 ± 3.9%	IC	TW[e]
0.30[b]		26.1 ± 1.0%	46.0 ± 1.3%	IC	TW[e]
0.30[c]		26.1 ± 0.3%	40.7 ± 0.6%	IC	TW[e]
0.50[c]		23.4 ± 1.5%	34.2 ± 4.2%	IC	TW[e]
0.50[c]		21.9 ± 0.5%	33.8 ± 6.1%	IC	TW[e]
0.5		22 ± 4	33 ± 6	Pot.	[20]
0.5		23.5	57	Pot.	[21]
0.5		23.5 ± 0.2	63 ± 2	Cal.	[22]
0.5		22.39 ± 4.7%	50.12 ± 26%		[14]

[a] Pot. = potentiometry; IC = ion chromatography; Kin. = kinetic; Cal. = calorimetry.
[b] The eluent composition is a proper mixture of solutions 1 and 2 at the given ionic strength (I): (1) HCl; (2) $HClO_4$.
[c] The eluent composition is a proper mixture of solutions 1 and 2: (1) NaCl ($I - 0.01$ M) + $HClO_4$ (0.01 M); (2) $NaClO_4$ ($I - 0.01$ M) + $HClO_4$ (0.01 M).
[d] As a rough estimate, assuming that the activity of coefficient values of Kielland [23] at the operating I are correct.
[e] This work. These data include the confidence interval percentage ($\alpha = 0.05$); data from literature include the percentage of uncertainty.

with the data from Ref. [18]. Note that the β_2 data from Refs. [18] and [19], which differ by a factor of about two, were both obtained from potentiometric measurements using a transport-type cell. In the former case a calomel electrode was used in $LiCl$–$LiClO_4$ medium and in the latter case a cadmium amalgam in $HClO_4$–$NaClO_4$ medium was used as a reference electrode; clearly, the wide difference in β_2 values arises, at least in one case, from ineffective elimination of the junction potential contribution. The relative confidence interval at the 0.05 significance level and the repeatability among different sets of data are particularly good. This is confirmed by the data relating to the cadmium–nitrate complexes. In this case, as the stability constant is low ($\beta_1 = 0.60$ at $I = 0.5$) and the set of k'_s/k'_L data are in the range 1–1.15, one would expect a wider relative confidence interval for β_1 than in chloride; in fact, as Table 3 shows, the confidence interval found was 2%. This is further proof that very low stability constants can be accurately measured by IC without non-specific contributions.

Table 3
Comparison of IC results with literature data for the Cd(II)–NO_3^- system

I	β_1	Method[a]	Ref.
0.05	0.31	Pot.	24
0.10	1.56 ± 2.0%	IC	TW[b]
0.1	1.86 ± 14.8%	Kin.	17
0.1	1.25	Extraction	25
0.30	0.78 ± 1.2%	IC	TW[b]
0.45	0.62 ± 1.5%	IC	TW[b]
0.5	0.60 ± 1.6%	IC	TW[b]
0.5	0.77 ± 0.02	Pot.	18
0.5	0.776		14
1	1.17 ± 17.5%	Kin.	24

[a] See Table 2.
[b] This work.

4.6. Sources and sizes of systematic errors affecting calculated k' values

The accuracy of k' calculated from chromatographic experiments depends both on the accuracy of all the variables considered in Eq. 6 and on the accuracy of the V_R and V_0 measurement from the chromatogram:

$$k' = \frac{V_R - V_0}{V_0} = \frac{T_R - T_0}{T_0} \quad (15)$$

From Eqs. 6 and 15, it is possible to obtain an equation for the error affecting the capacity factor k', expressed as $\Delta k'$.

The $\Delta k'$ dependence on all the variables is expressed by the following equation:

$$\Delta k' = \frac{\delta k'}{\delta V_R} \cdot \Delta V_R + \frac{\delta k'}{\delta V_0} \cdot \Delta V_0 + \frac{\delta k'}{\delta [L^-]} \cdot \Delta [L^-] + \frac{\delta k'}{\delta [E^-]} \cdot \Delta [E^-] \quad (16)$$

Considering the partial derivatives for the different terms in Eq. 16:

$$\frac{\delta k'}{\delta V_R} = \frac{1}{V_0}; \quad \frac{\delta k'}{\delta V_0} = -\frac{V_r}{V_0^2};$$
$$\frac{\delta k'}{\delta [L^-]} = -\frac{k'_s(\beta_1 + 2\beta_2[L^-])}{(1 + \beta_1[L^-] + \beta_2[L^-]^2)^2}; \quad (17)$$
$$\frac{\delta k'}{\delta [E^+]} = -2 \cdot \text{constant} \cdot \frac{1}{[E^+]^3}$$

one has for the relative bias

$$\frac{\Delta k'}{k'} = \frac{V_R}{V_R - V_0}\left(\frac{\Delta V_R}{V_R}\right) - \frac{V_R}{V_R - V_0}\left(\frac{\Delta V_0}{V_0}\right) - \frac{\beta_1 + 2\beta_2[L^-]}{1 + \beta_1[L^-] + \beta_2[L^-]^2} \cdot \Delta [L^-] - 2 \cdot \frac{\Delta [E^-]}{[E^-]} \quad (18)$$

As we found experimental evidence that the flow-rate of the eluent v' does not change during a chromatographic run, the value of k' calculated by Eq. 15 is independent of the flow-rate reproducibility while the values of V_R and V_0 (or T_R and T_0) may change among days. Assuming for $|\Delta V_R|$ and $|\Delta V_0|$ an uncertainty equal to

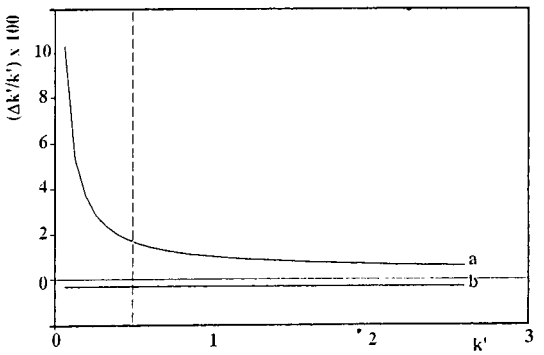

Fig. 5. Effect of errors in V_R and V_0 estimation on k' values. $|\Delta V_R| = |\Delta V_0| = 5 \cdot 10^{-3}$ ml from experimental evidence: (a) $\Delta V_R = -\Delta V_0$; (b) $\Delta V_R = \Delta V_0$.

$5 \cdot 10^{-3}$ ml for the same set of data when using the postcolumn derivatization device, according to whether they have the same sign or not, the $\Delta k'/k'$ (%) values assume the shape in Fig. 5 (curve a or b). It follows that values of k'_L lower than 0.5 and consequently values of α lower than $0.5/k'_s$ (see Eq. 9) are imprecise.

The other terms that affect the size of $\Delta k'$ are due to systematic errors in the preparation of the individual solutions at constant $[E^+]$ and variable $[L^-]$. Eq. 18 shows that the bias of k' due to systematic error in C_L determination depends not only on the size of ΔC_L but also on the particular association equilibria considered. Further, the ΔC_L and ΔC_E values depend on the different ways in which stock and working standard solutions are prepared; for this reason, no examples are considered here.

5. Conclusions

As has been demonstrated for the cadmium–chloride and cadmium–nitrate systems, accurate values of equilibrium constants can be achieved by cation-exchange chromatography, provided that non-specific contributions on the capacity factor of the solute are nullified. These non-specific contributions may originate from the nature of the competing and or co-ions in the

eluent and/or the presence of free sites in the exchange resin surface. Several preliminary tests have been proposed that enable the correct experimental conditions to be identified with confidence.

Acknowledgements

The financial support of CNR and MURS is gratefully acknowledged.

References

[1] P.R. Haddad and R.C. Foley, *J. Chromatogr.*, 500 (1990) 301.
[2] P.H. Hajos, G. Revesz, C. Sarzanini, G. Sacchero and E. Mentasti, *J. Chromatogr.*, 640 (1993) 15.
[3] R.G. Seys and C.B. Monk, *J. Chem. Soc.*, (1965) 2452.
[4] F.H. Lin and C. Horváth, *J. Chromatogr.*, 589 (1992) 185.
[5] P. Janoš, *J. Chromatogr.*, 641 (1993) 229.
[6] P. Janoš, *J. Chromatogr. A*, 657 (1993) 435.
[7] P.R. Haddad and P.E. Jackson, *Ion Chromatography, Principles and Applications (Journal of Chromatography Library*, Vol. 46), Elsevier, Amsterdam, 1990, p. 133.
[8] M. Shibukawa and N. Ohta, *Anal. Chem.*, 53 (1981) 1620.
[9] G.J. Sevenich and J.S. Fritz, *J. Chromatogr.*, 371 (1986) 361.
[10] D.T. Gjerde, *J. Chromatogr.*, 439 (1988) 49.
[11] J. Ståhlberg, *Anal. Chem.*, 66 (1994) 440.
[12] J. Horst and W.H. Höll, *React. Polym.*, 13 (1990) 209.
[13] W.H. Höll, J. Horst and M. Wernet, *React. Polym.*, 14 (1991) 251.
[14] W.H. Höll, J. Horst and M. Franzreb, *React. Polym.*, in press.
[15] J.A. Marinsky and Y. Marcus, *Ion Exchange and Solvent Extraction*, Vol. 11, Marcel Dekker, New York, 1993, p. 151.
[16] A.E. Martell and R.M. Smith, *Critical Stability Constants*, Vol. 4, Plenum Press, New York, 1977, p. 108.
[17] G. Sahu and B. Prasad, *J. Indian Chem. Soc.*, 46 (1969) 233.
[18] B. Prasad, *J. Indian. Chem. Soc.*, 45 (1968) 1037.
[19] M.H. Hutchinson and W.C.E. Higginson, *J. Chem. Soc., Dalton Trans.*, (1973) 1247.
[20] V.A. Fedorov, A.M. Robov, V.P. Plekhanov, V.V. Kudruk, M.A. Kuznechikhina and G.E. Chernikova, *Russ. J. Inorg. Chem.*, 19 (1974) 666.
[21] C.E. Vanderzee and H.J. Dawson, *J. Am. Chem. Soc.*, 75 (1953) 5659.
[22] P. Gerding and I. Jönsson, *Acta Chem. Scand.*, 22 (1968) 2247.
[23] J. Kielland, *J. Am. Chem. Soc.*, 59 (1937) 1675.
[24] V.P. Vasil'ev, *Izv. Vyssh. Uchebn. Zaved. Khim. Khim. Tekhnol.*, 4 (1961) 936.
[25] H.E. Hellwege and G.K. Schweitzer, *J. Inorg. Nucl. Chem.*, 27 (1965) 99.

ELSEVIER

Journal of Chromatography A, 706 (1995) 55–57

JOURNAL OF CHROMATOGRAPHY A

Short communication

Colour-indication suppressor for anion chromatography

Hideki Watanabe*, Hisakuni Sato

Laboratory of Analytical Chemistry, Faculty of Engineering, Yokohama National University, Tokiwadai 156, Hodogaya-ku, Yokohama 240, Japan

Abstract

A background suppressor used for anion chromatography was coloured to indicate the consumption and state of regenerating of the cation exchanger. Methyl yellow and methyl red are strongly adsorbed on Dowex 50W-X8 resin. Methyl yellow is not desorbed in alkaline medium. When 0.1–0.5 ml of a 0.1% (w/w) solution of methyl yellow in methanol is added to an aqueous slurry of the resin (H^+ form, 1 g) and stirred, the indicator is adsorbed quickly. The colour of the cation exchanger containing methyl yellow changes to yellow when the resin is converted from the H^+ to the Na^+ form with 1 m*M* $NaHCO_3$ or more basic eluents. Regeneration of the suppressor column can easily be done with a 0.1–0.5 *M* mineral acid solution, such as HCl or HNO_3. The colour change (yellow to red-purple) indicates the completion of regeneration. One column of size 70 × 6 mm I.D. has a capacity of about 3.2 mequiv., and is sufficient for 1 day of operation under the usual ion chromatographic conditions.

1. Introduction

Conventional ion exchangers, commercially available for preparative use, can be used as packings for suppressor columns in ion chromatography [1]. Today, membrane-type suppressors are used widely because they can be used continuously. However, column suppressors are convenient for occasional use. The most significant defect of the column suppressor is that it has a limited exchange capacity and it may become exhausted during an analysis. Therefore, it is very convenient if the remaining capacity for suppression can be established from a colour change. Miller [2] reported the use of solid indicators that involved an anion-exchange resin adsorbing pH indicators such as phenolphthalein or thymol blue. Such indicator resins can be used as the suppressor for cation chromatography. A suppressor is thought to be more valuable for anion chromatography, in which a cation exchanger is necessary. Although a commercial coloured suppressor became available recently, the preparation method was not given [3]. In this paper, the preparation of a cation-exchange resin loaded with adsorbing pH indicators is described and its applicability is discussed.

2. Experimental

A pump (Tosoh, CCPM), a UV absorbance detector (Tosoh, UV-8000), a conductivity detector (Tosoh, CM-8) and a data processor (SIC Chromatocorder 11) were used. An IC anion PW separation column (50 mm × 4.6 mm I.D.) from Tosoh was used. The cation exchanger used as the suppressor was Dowex 50W-X8 (200–400 mesh). Glass columns (Omni, 70 × 6 mm I.D.) were used as the container of the coloured cation

* Corresponding author.

0021-9673/95/$09.50
SSDI 0021-9673(94)01159-1

exchanger. The Dowex resin was first washed with water, converted into the H^+ form with 0.5 *M* HCl and then washed again with water.

The indicators studied were *p*-dimethylaminoazobenzene (methyl yellow), 4′-dimethylaminoazobenzene-2-carboxylic acid (methyl red) and *p*-ethoxychrysoidine hydrochloride. An aliquot of a 0.1% (w/w) solution of indicators in methanol was added to an aqueous slurry of the H^+ form of cation exchanger and stirred. The coloured cation exchanger was packed into glass columns by using a glass syringe and a vacuum pump. All reagents used were of analytical-reagent grade. Water was purified with a mixed-bed ion-exchange column and with a Milli-Q system (Millipore).

3. Results and discussion

Relatively hydrophobic azo compounds are adsorbed very well on the H^+ form of cation exchangers. Among several azo compounds, methyl yellow and *p*-ethoxychrysoidine are strongly adsorbed even in alkaline medium. Methyl red is probably desorbed in alkaline medium. The colour change of methyl yellow adsorbed on a cation exchanger takes place between pH 5 (red-purple) and 7 (yellow) and that of *p*-ethoxychrysoidine at pH 7–9. These pH values are higher than the colour change region of these indicators in aqueous solution. The colour of the cation exchanger containing methyl yellow (**A**) changes to yellow when the H^+ ions on the exchange sites are converted into Na^+ with 1 m*M* $NaHCO_3$, whereas the colour of the cation exchanger containing *p*-ethoxychrysoidine (**B**) does not change under the same conditions. A 1 m*M* borax solution changes the colour of **B**. As a suppressor for anion chromatography, **A** seems superior to **B**. A suitable amount of methyl yellow is about 1 μmol/g resin. When 0.1–0.5 ml of a 0.1% solution of methyl yellow in methanol is added to an aqueous slurry of the resin (H^+ form, 1 g) and stirred, all of the indicators are adsorbed quickly. A dilute solution of Na_2CO_3 slowly dissolves the adsorbed methyl yellow. In a column, however, the desorbed indicators are adsorbed again on the remaining H^+ form of the resin. Therefore, the distribution of methyl yellow in the suppressor column shifts slowly down the column during use. If the flow direction is reversed on every regeneration with an acidic solution, the indicators do not leave the column. The boundary of the two parts, H^+ form and Na^+ form, can be seen clearly similarly to plug flow. Although the boundary diffuses slowly with time on storage, it soon becomes distinctive again when an alkaline eluent is passed.

Fig. 1 shows two chromatograms of a mixture of Br^- and NO_3^-. That on the left side was obtained without the suppressor and that on the right with the suppressor. Because the CO_3^{2-} and HCO_3^- in the eluent were changed to H_2CO_3 by the suppressor, the background absorbance was lowered about 0.1 absorbance in the right-hand chromatogram. This effect is reflected in the intensity of the first system peaks. Baseline stability, or flatness, indicates no elution of adsorbed, coloured materials. The peaks in the right-hand chromatogram are slightly distorted by the suppressor column. If the suppressor is prepared under a higher pressure with a more pressure-safe container, the peak distortion may become smaller. The back-pressure of the present suppressor was only about 1 kg/cm^2. The conductivity of the suppressed effluent was about 10 μS/cm for the same eluent as in Fig. 1.

With the present suppressor, the detection sensitivity for nitrite ion varies depending on the

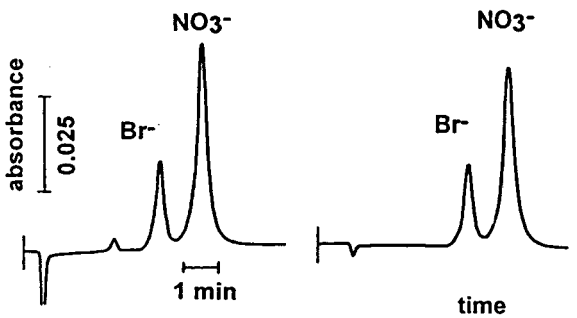

Fig. 1. Chromatograms of Br^- and NO_3^- ions without (left) and with (right) a suppressor column. Eluent, 1 m*M* $NaHCO_3$–1 m*M* Na_2CO_3 (1 ml/min); detection, UV absorbance; sample, KBr and KNO_3, 0.1 m*M* each, 50 μl.

remaining amount of the H^+ form of the resin in the column, as reported [4]. To determine nitrite ion, UV absorbance detection is recommended. Because of the low back-pressure with the present suppressor column, series connection of a UV absorbance detector, a coloured suppressor column and a conductivity detector is possible. Regeneration of the suppressor column can easily be done with 0.1–0.5 *M* mineral acid solution, such as HCl or HNO_3. The colour change (yellow to red-purple) indicates the completion of the regeneration. The above-mentioned commercial product [3] is generally considered to be disposable.

A column of size 70×6 mm I.D. has a capacity of about 3.2 mequiv. and is sufficient for 1 day of operation under the usual ion chromatographic conditions. The effective time period for the continuous suppression can easily be estimated from the ion-exchange capacity, the equivalent concentration of the eluent used and the flow-rate. Although the indicator–adsorbed cation exchanger presented here is useful as a suppressor, it is considered more convenient for the indicator to be bound covalently to the cation exchanger. Such a modification of the ion exchanger should not be difficult, and coloured exchangers may be useful in various schemes of chemical analyses for preventing erroneous operations.

References

[1] H. Small, T.S. Stevens and W.C. Bauman, *Anal. Chem.*, 47 (1975) 1801.
[2] W.E. Miller, *Anal. Chem.*, 30 (1985) 1462.
[3] R. Saari-Nordhaus and J.M. Anderson, Jr., *Am. Lab.*, 26 (1994).
[4] W.F. Koch, *Anal. Chem.*, 51 (1979) 1571.

ELSEVIER

Journal of Chromatography A, 706 (1995) 59–68

JOURNAL OF CHROMATOGRAPHY A

Selectivity of chemically bonded zwitterion-exchange stationary phases in ion chromatography

Pavel N. Nesterenko*, Alexandr I. Elefterov, Dmitry A. Tarasenko, Oleg A. Shpigun

Department of Analytical Chemistry, Lomonosov State University, Leninskie Gory, GSP-3, 119899 Moscow, Russian Federation

Abstract

A number of zwitterion-exchange stationary phases were prepared by immobilization of amino acids of different structure (Asp, Glu, Val, Tyr, Pro, Hypro, Arg and Lys) on a silica surface. The occurrence of oppositely charged groups in a single ion-exchange site provided cation-, anion- and zwitterion-exchange properties. The chromatographic behaviour of these stationary phases was evaluated by the retention of a series of test organic compounds of different ionogenic nature. The role of the type and structure of the ion-exchange site was considered. The structure of the bonded molecules and the pH of the eluent were shown to be key parameters influencing the ion-exchange properties of amino acid-bonded silicas. The cation-exchange selectivity of phases containing primary or secondary amino groups was investigated for alkali and alkaline earth metal ions. The application of amino acid-bonded silicas to the ion chromatographic separation of anions and cations is described.

1. Introduction

There are two basic advantages of zwitterionic stationary phases (ZSP) which attract the attention of chromatographers. First, the existence of oppositely charged layers on the surface of these ion exchangers provides short diffusion paths and excellent mass transfer characteristics. As a result, more efficient separations were achieved for ZSP. Second, the use of these phases with fixed concentrations of ligands and varying pH and ionic strength of mobile phases provides a wide range of selectivity changes. Most recently the zwitterionic phases proved to be very useful for the efficient and selective separations of inorganic anions [1,2], cations [3] and ampholyte molecules [4–6] and for the simultaneous separation of both anions and cations [7–9].

There are several types of zwitterionic stationary phases used in high-performance liquid chromatography (HPLC) and ion chromatography (IC). The zwitterionic properties of ion exchangers have been realized on different varieties of delocalization of positive and negative charges in stationary phases. First, there are agglomerated ion exchangers [10] and "centrally localized" ion exchangers [11] in which two oppositely charged layers occur at the surface. The distance between the oppositely charged layers on the surface of agglomerated ion exchangers depends on the diameter of the latex microbeads. The thickness of the negatively charged layer at the surface of the "centrally localized" anion exchangers is defined by the

* Corresponding author.

0021-9673/95/$09.50
SSDI 0021-9673(95)00300-2

time of the treatment of the polymeric anion-exchange resin with sulphuric acid. Second, the oppositely charged sites can be distributed in a random order on the surface of inorganic oxides such as amphoteric alumina [12]. The distance between the positive and negative charges is determined by the structure of the oxide. Lastly, the permanently bonded matrix zwitterionic molecules [1–3] and corresponding dynamically modified ion exchangers [7,8] form a third group of ZSP in which the oppositely charged groups are very close together in one molecule. Amino acid-bonded silicas are widely used in ligand-exchange [13], metal chelate [13] and affinity chromatography [14]. However, their ion-exchange properties have not been systematically investigated.

The main purpose of this study was to characterize the ion-exchange properties of amino acid-bonded silicas and to study the selectivity of these types of ZSP for the separation of organic and inorganic anions and cations.

2. Experimental

2.1. Chromatographic system

The chromatographic system consisted of a Model 114M high-pressure pump (Beckman, Palo Alto, CA, USA), a Model 7125 injection valve (Rheodyne, Cotati, CA, USA) equipped with a 50-μl loop and Conductolyzer 5300 and Uvicord 2238 conductivity detectors (both from LKB, Bromma, Sweden). A Spectra-Physics (San Jose, CA, USA) DP-700 chromatographic data system was used for data collection and processing.

2.2. Eluents

Solutions of perchloric, nitric and citric acids (Reakhim, Moscow, Russian Federation) were used as eluents. Deionized, distilled water was used for the preparation of eluents. Solutions of 1 *M* LiOH and 1 *M* NaOH were used to adjust pH of the eluent. The pH values of eluents were measured with a pH-340 pH meter (ZIP, Moscow, Russian Federation) with a glass electrode.

2.3. Columns and sorbents

KSK-1 silica with a specific surface of 350 m^2/g and particle size 5 or 7.5 μm (Reakhim), Polyol-100 of 5 μm, Silasorb 600 of 7.5 μm and Silasorb 300 of 5, 7.5 or 10 μm particle size (Lachema, Brno, Czech Republic) were used as a matrix for synthesis. All amino acid-bonded phases were prepared by the initial reaction of amino acids with 3-glycidoxypropyltriethoxysilane (Reakhim) followed by surface treatment of the silica with the amino acid (Scheme 1) according to a slightly modified method [15]. A weak acid cation exchanger containing propionic acid residues bonded to silica was purchased from JV BioChemMack. Stainless-steel or PEEK chromatographic columns were slurry packed. The values of the ion-exchange capacity were calculated from CHN elemental analysis data.

2.4. Chemicals

All chemicals were of analytical-reagent grade. Stock standard solutions of inorganic cations were prepared by dissolving appropriate amounts of alkali and alkaline earth nitrates in deionized, distilled water. Aqueous solutions of aniline sulphate, benzoic acid, benzenesulphonic acid, *p*-aminobenzoic acid, *p*-sulphanilic acid (all purchased from Reakhim) and N,N,N-trimethylphenylammonium bromide (Fluka, Buchs, Switzerland) were used for the characterization of the ion-exchange properties of bonded phases.

3. Results and discussion

3.1. Selection of amino acid-bonded silicas

α-Amino acids are the simplest available zwitterionic molecules which can be easily attached to a silica surface. In accordance with their structure and presumably ion-exchange proper-

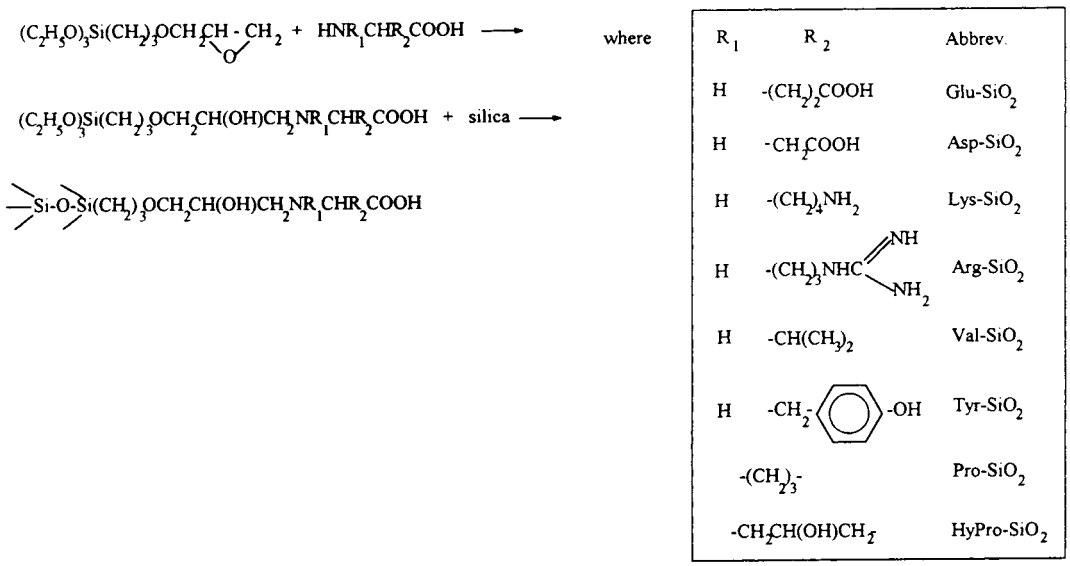

Scheme 1

ties, all naturally occurring amino acids can be subdivided into four groups:

(1) monoaminocarboxylic acids containing one primary amino group and one carboxylic group;

(2) diaminocarboxylic acids such as lysine and arginine; it should be noted that the guanidino group containing several nitrogen atoms is considered as one basic group;

(3) monoaminodicarboxylic acids such as aspartic acid and glutamic acid;

(4) heterocyclic amino acids containing a secondary amino group and one carboxylic group, e.g., proline and hydroxyproline.

In aqueous solutions, amino acids behave as inner salts and are generally both weak acids and weak bases. At low pH the conjugated acid is the predominant form. At intermediate pH, amino acids exist in an equilibrium between the neutral molecules and the appropriate zwitterion form.

The attachment of amino acids to the surface of silica leads to a change in their ion-exchange properties owing to the interactions of the amino groups of the bonded molecules with residual silanols and an increase in the basicity of amino groups after linkage with a 3-glycidoxypropyl spacer [1]. Taking these and multiple acid–base equilibrium in bonded molecules into consideration, it is possible a priori to provide only an approximate evaluation of the relative affinities of amino acid-bonded phases for different ions. In previous work the anion-exchange properties of L-hydroxyproline-bonded silica and L-proline-bonded silica were carefully studied [1,2]. The cation-exchange properties were mentioned for silicas with attached arginine, valine and tyrosine.

For the investigation of the effect of the structure of the amino acid attached to silica on the ion-exchange properties, new sorbents with bonded lysine, aspartic acid and glutamic acid were synthesized. Hence each of the above-mentioned structural groups of amino acids were studied using two sorbents.

3.2. Selection of eluent

Evidently the main factor influencing the ionic state of bonded amino acids will be the pH and the concentration of eluent. Thus, citric acid ($pK_1 = 3.14$; $pK_2 = 4.66$; $pK_3 = 6.40$ [16]) providing a suitable buffer capacity over a wide range of pH was chosen for the investigation of

the chromatographic behaviour of these sorbents. For the study of the affinity of sorbents to cations of alkali and alkaline earth metals, aqueous solutions of perchloric and nitric acids were used as eluents to avoid possible complexation of alkaline earth metals with citric acid.

3.3. Ion-exchange properties of amino acid-bonded silicas

The retention of ionogenic solutes depends on both the ion-exchange capacity of the sorbents and the nature of bonded functional groups. The direct characterization of the ion-exchange properties of ZSP is difficult owing to the constant change in ionic state of bonded amino acids with changes in pH and ionic strength. The pH dependence of the retention of a set of test solutes of different acidity–basicity in an eluent of constant concentration would be more informative for the characterization of the different zwitterion exchangers. The difference in the surface concentrations of bonded molecules (Table 1) and the influence of residual silanol groups should be taken into consideration to explain the results obtained.

Six benzene derivatives were chosen for the characterization of the ion-exchange properties of sorbents. These were primary amine (aniline), quaternary amine (trimethylphenylammonium), two acids (benzoic and benzenesulphonic acid) and two ampholytes (sulfanilic acid and *p*-aminobenzoic acid). Fig. 1 shows the dependence of the capacity factors for test solutes on the pH of the eluent for different columns, illustrating the ion-exchange properties of the studied ZSP supports.

The retention of the strongly acidic benzenesulphonic acid and weakly acidic benzoic acid decreased as the pH of eluent increased from 2.85 to 7.0 for all sorbents. This is in accordance with the increase in negative charge of bonded zwitterionic molecules owing to the dissociation of carboxylic groups and the increase in the eluting power of citric acid. Pro-SiO_2 and Hypro-SiO_2 exhibit a stronger anion-exchange ability at acidic pH. Evidently, this is connected with the presence of a more basic tertiary amino group in the ion-exchange sites of these sorbents. The application of these ion exchangers for the separation of inorganic anions was shown earlier [1,2].

The retention of zwitterionic solutes sulphanilic acid and *p*-aminobenzoic acid on Pro-SiO_2 and Hypro-SiO_2 showed a maximum corresponding to the isoelectric point for both bonded molecules (Fig. 1). At the respective isoelectric points of zwitterionic solutes, both the anionic and cationic groups are charged and these bipolar molecules are mainly retained via a quadruple interaction with doubly charged ion-exchange sites of sorbents [5,6]. Of course, the maximum of retention for sulfanilic acid, having a lower pK_a value of 3.20 for the sulpho group, would

Table 1
Characterization of the stationary phases investigated

Sorbent	Specific surface area (m^2/g)	Particle size (μm)	Capacity[a] ($\mu mol/g$)
Glu-SiO_2	300	5	140
Asp-SiO_2	300	7.5	60
Lys-SiO_2	600	7.5	130
Arg-SiO_2	300	7.5	160
Pro-SiO_2	100	5	150
Hypro-SiO_2	350	5	120
Tyr-SiO_2	300	7.5	750
Val-SiO_2	100	5	180
COOH-SiO_2	350	10	980

[a] Calculated from elemental analysis data.

correspond to a lower value of the pH of the eluent than is the case for *p*-aminobenzoic acid, having a carboxylic group with $pK_a = 4.89$ [16]. The above property of silica-bonded proline and hydroxyproline allows their use for the simultaneous separation of anions and cations with a single eluent [9]. It is also interesting that this bell-shaped dependence was not observed for the other sorbents investigated in which bonded amino acids had a free proton in amino group and hence gave the possibility of interaction with residual silanol groups.

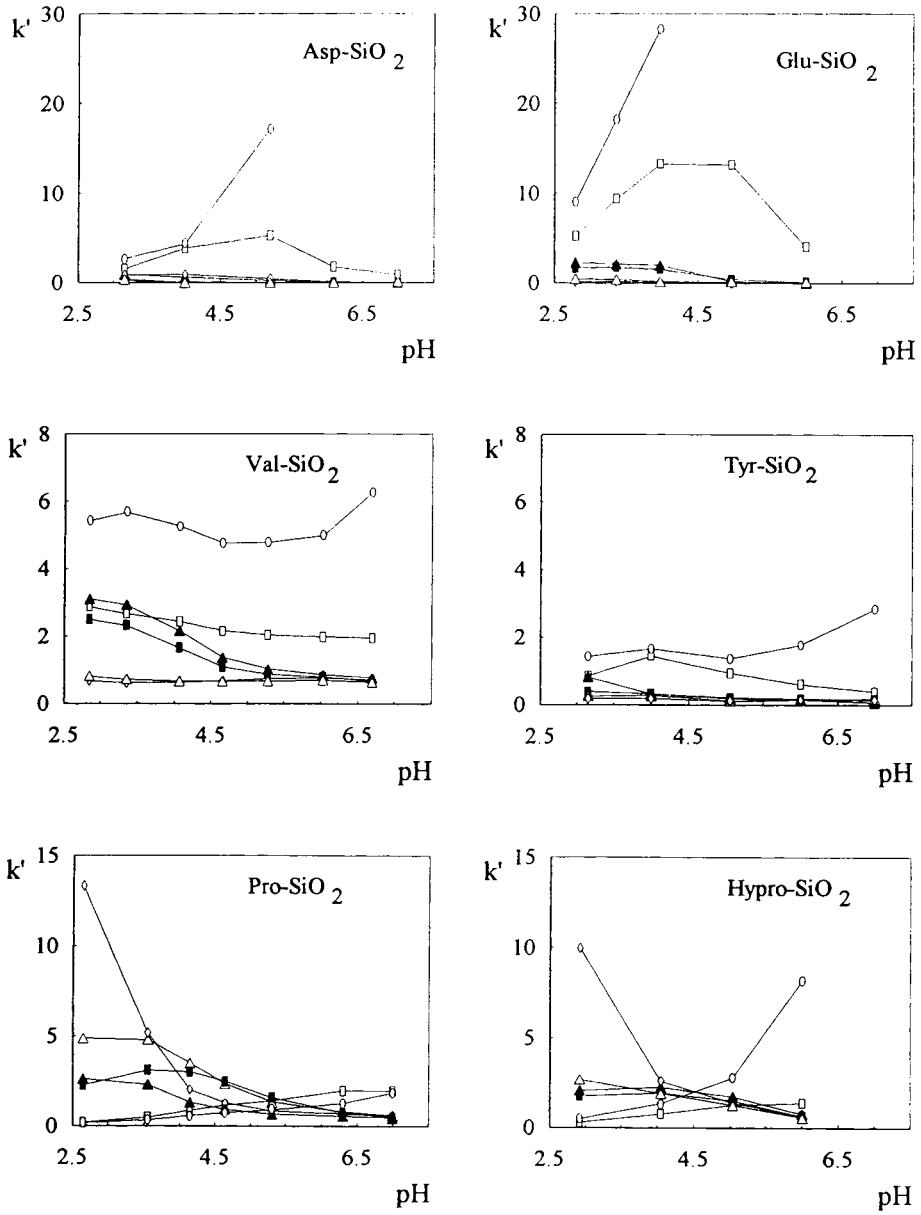

Fig. 1.

(*Continued on p. 64*)

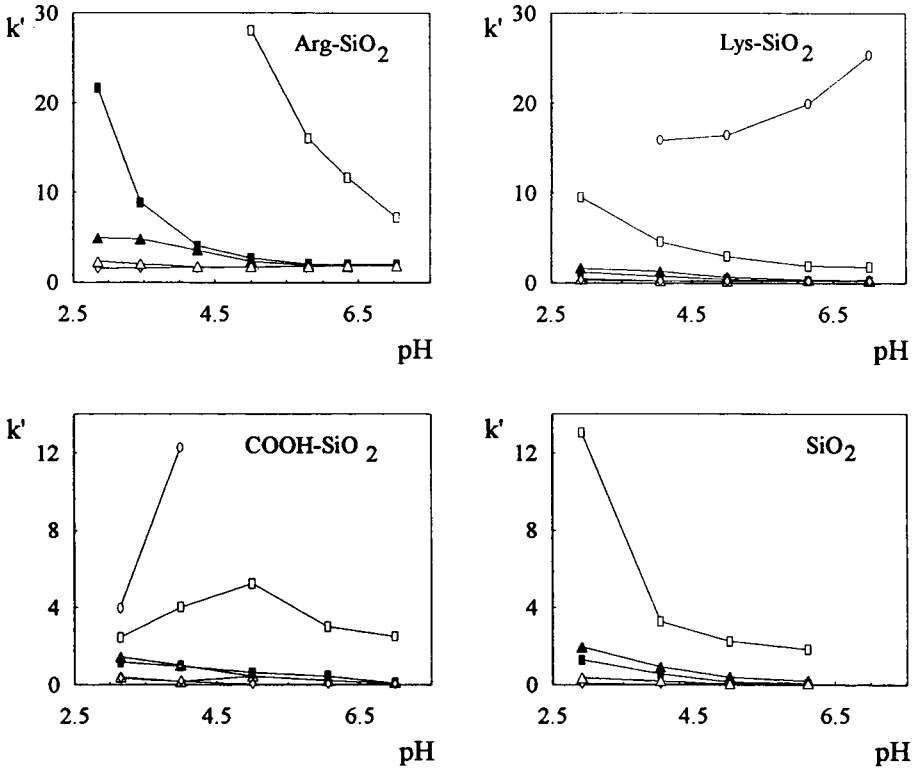

Fig. 1. Effect of eluent pH on capacity factor (log k') of some ionogenic organic compounds for different amino acid-bonded silicas. Eluent: 5 mM citric acid. △ = Sulfanilic acid; ◇ = benzenesulphonic acid; ■ = p-aminobenzoic acid; ▲ = benzoic acid; □ = aniline; ○ = trimethylphenylammonium.

The retention of positively charged trimethylphenylammonium increased dramatically with increase in the pH of citric acid eluent for both ZSP having bonded monoaminodicarboxylic acids and for a cation exchanger having only carboxylic functional groups. This corresponds to the growing dissociation of carboxylic groups at the surface of the ion exchanger. The retention of aniline shows an inversion point at pH 4.8–5.0 for the above sorbents. Such behaviour is a sum of two processes taking place in the column: the dissociation of carboxylic functional groups of the ion exchanger, which increases the retention, and the deprotonation of anilinium ion, which reduces its retention.

Unexpectedly, the most notable cation-exchange properties were observed for the silica-bonded arginine and lysine. The isoelectric points of these amino acids are higher than those for other amino acids and are 10.76 and 9.74, respectively (Table 2), so one can consider the related sorbents as stronger anion exchangers in acidic media. In contrast, the observed ion-exchange affinity to the organic cations was found to be higher than that for silica-bound aspartic and glutamic acid. This may be connected with the self-organization of the three oppositely charged layers at the silica surface. The inner layer is formed by negatively charged residual silanol groups, the middle positively charged layer is formed by protonated amino groups of bonded amino acids and the last, external layer consists of the negatively charged carboxylic groups. The localization of the positively charged layer between two negatively charged layers causes repulsion of protons from carboxylic functional groups of bonded amino acids and leads to their acidification. It should be noted that the number of carboxylic groups is double that of the amino groups in the case of aspartic

Table 2
Acid–base and complexing properties of amino acids [16]

Amino acid	pK_1	pK_2	pK_3	pI	Log K_1			
					Mg^{2+}	Ca^{2+}	Sr^{2+}	Ba^{2+}
Asp	1.88	3.65	9.66	2.77	2.43	1.60	1.48	1.14
Glu	2.16	4.32	9.96	3.24	3.44	1.43	1.37	1.28
Lys	2.18	9.12	10.53	9.82				
Arg	2.17	9.04	12.84	10.76	1.30			
Val	2.32	9.62	–	5.96				
Tyr	2.20	9.11	10.07	5.66	2.0	1.48		
Pro	1.99	10.6	–	6.30				
Hypro	1.92	9.73	–	5.83		0.48	0.04	

and glutamic acid, so there is no similar phenomenon for simple amino acids such as valine or tyrosine. As a result, strong cation-exchange properties were observed for the ion exchanger with carboxylic functionality.

Bare silica shows a marked affinity only to aniline. This is in accordance with known specific interactions of aniline with residual silanol groups. Obviously, the degree of functionalization of the surface of silica should not be of great value for the resulting ion-exchange selectivity of the prepared stationary phases.

Therefore, the above results show that only cyclic amino acids bonded to silica can be considered as zwitterion exchangers. The sorbents containing bonded amino acids of other types behave as weak or strong cation exchangers.

3.4. Ion-exchange selectivity for cations

The other interesting property of amino acid-bonded silicas to be used in ion chromatography is the ion-exchange selectivity to alkali and alkaline earth metal cations. It is known that silica-based carboxylic cation exchangers having a functional groups with $pK_a < 3$ have the ability to separate effectively monovalent and divalent classes in an isocratic elution mode with a dilute strong acid or mildly acidic complexing eluents [17,18]. According to a previous report [19], the acidity of the carboxylic group in the molecules is not changed after their attachment to the silica surface. Hence one could hope that attachment to silica of an amino acid having a carboxylic group with relatively low pK_a value (Table 1) would produce such a kind of ion exchanger. However, this is not completely correct for the molecules having an α-amino group. Owing to specific interactions with residual silanol groups, the basicity of amino groups is changed, which induces uncertain alterations in the acidity of the carboxylic group and in the selectivity of ion exchange. The sorbents with bonded arginine, lysine, aspartic acid and glutamic acid show relatively strong retention of organic cations such as aniline and trimethylphenylammonium and were chosen for further study of cation-exchange selectivity. Fig. 2 shows the retention of alkali and alkaline earth cations by the above sorbents as a function of concentration of the perchloric acid used as the eluent. The log k'–log C dependences are nearly linear for all the cations studied. The slopes for monovalent and divalent ions are 0.8–0.85 and 1.7–1.75, respectively.

The data on the selectivity of chromatographic separation ($\alpha = k'_2/k'_1$) of pairs of cations are presented in Table 3. The ion exchanger with a functionality incorporating two carboxylic groups shows a group selectivity to monovalent and divalent cations (Fig. 2). It is interesting that the potential complexing ability of aspartic and glutamic residues (Table 2) for alkaline earth metals has a poor effect on the selectivity of separation of the above cations and is similar to the selectivity observed for ion exchangers with

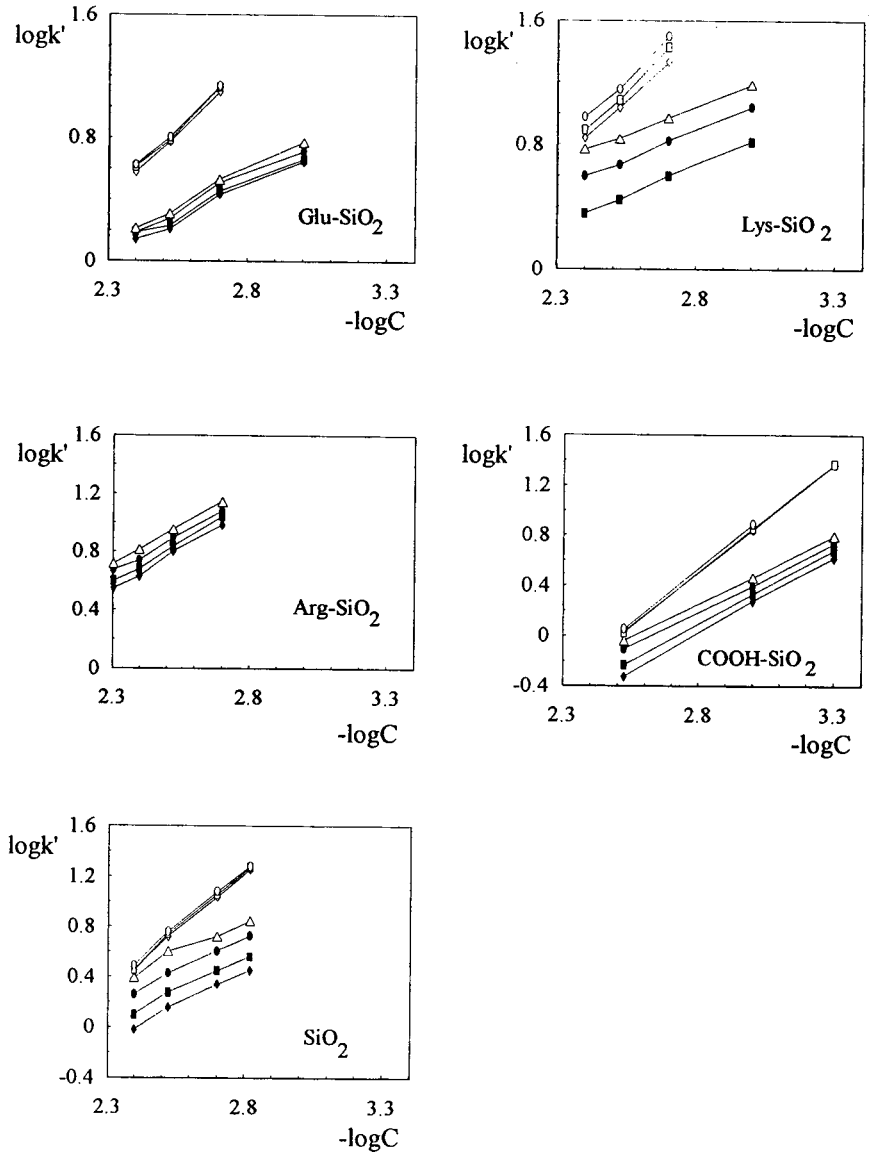

Fig. 2. Relationship between logarithm of capacity factor (log k') of alkali and alkaline earth metal cations and logarithm of eluent concentration (log C). Eluent: perchloric acid. ◆ = Li^+; ■ = Na^+; ● = NH_4^+; △ = K^+; ◇ = Mg^{2+}; □ = Ca^{2+}; ○ = Ba^{2+}.

propionic residues. At the same time, the ion exchangers bearing two or more amino groups at the ion-exchange site show good selectivity both for alkali and alkaline earth metal cations.

Bare silica shows a higher affinity to the divalent cations than was observed for propionic acid-bonded silica. At the same time, the selectivity of separation of alkaline earth metals is very poor.

There are two possible explanations for the results obtained. The first is an increase in acidity of the carboxylic group in the presence of two or more protonated amino groups. This improves the selectivity of carboxylic ion ex-

Table 3
Selectivity of separation for alkali and alkaline earth metal ions: $\alpha = k'_2/k'_1$ (3 m*M* perchloric acid)

Sorbent	NH_4–Na	K–NH_4	Mg–K	Ca–Mg	Ba–Ca
Asp-SiO_2	1.91	1.03	0.80	1.02	1.04
Glu-SiO_2	1.38	1.57	1.34	1.02	1.07
Lys-SiO_2	1.67	1.36	1.72	1.12	1.17
Arg-SiO_2[a]	1.15	1.18	–	–	–
COOH-SiO_2	1.34	1.17	1.17	1.01	1.05
Silasorb 600	1.42	1.56	1.27	1.04	1.03

[a] Alkaline earth metals are not eluted.

changers, as shown by Jensen et al. [17] and Kolla et al. [18]. Evidently, the presence of a single protonated amino group in the attached molecule of amino acid cannot provide an effective repulsion of protons in a carboxylic functionality and hence does not produce a marked change in acidity and selectivity. Second, as the radius of the separated cations increases, their repulsion from protonated amino groups also increases. In this case the repulsive interactions between amino groups and cations are responsible for the changes in ion-exchange selectivity.

The simultaneous separation of a mixture of alkali and alkaline earth metal ions on column packed with Lys-SiO_2 is shown in Fig. 3. It should be noted the peak corresponding to potassium is broad, which restricted the application of this column. A column packed with silica-bonded arginine having a similar concentration of bonded molecules as Lys-SiO_2 (Table 1) and hence having an identical concentration of carboxylic functional groups shows strong cation-exchange properties. The alkaline earth metals were not eluted from this column under the optimum conditions for the separation of monovalent cations (Fig. 4).

4. Conclusions

The ion-exchange properties of eight sorbents prepared by attachment of different amino acids to a silica surface were studied and compared with those for bare silica and propionic acid bound to silica. A strong cation-exchange ability was demonstrated for bonded monoaminodicar-

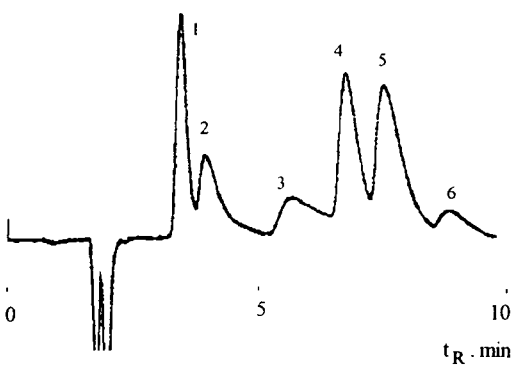

Fig. 3. Separation of a mixture of alkali and alkaline earth metal ions. Column, Lys-SiO_2 (150 mm × 4 mm I.D.); injection volume, 20 μl; eluent, 5 m*M* HNO_3; flow-rate, 1.5 ml/min. 1 = Li^+; 2 = Na^+; 3 = K^+; 4 = Ca^{2+}; 5 = Sr^{2+}; 6 = Ba^{2+}.

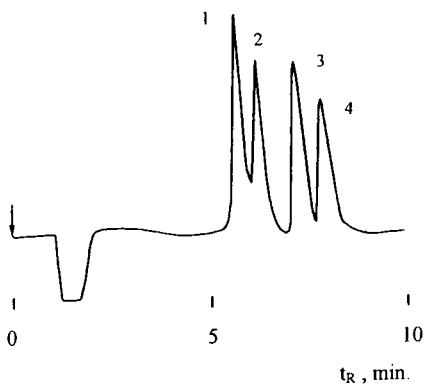

Fig. 4. Separation of a mixture of alkali metal ions and ammonium. Column, Arg-SiO_2 (250 × 4 mm I.D.); eluent, 5 m*M* $HClO_4$; flow-rate, 1 ml/min; injection volume, 20 μl. 1 = Li^+; 2 = Na^+; 3 = NH_4^+; 4 = K^+.

boxylic acids (Asp, Glu) and, curiously, for bonded amino acids containing at least two basic groups (Lys, Arg). Evidently, the latter is connected with the formation of a multi-layer structure at the surface of silica, which causes a localization of charges in ion-exchange sites in a particular arrangement. Only bonded lysine and arginine show a reasonable selectivity for the separation of monovalent and divalent cations. The ability of bonded glutamic and aspartic acids for the group separation of alkali and alkaline earth metal cations was demonstrated. The data obtained from this study could be of special interest in those modes of HPLC using amino acid-bonded silica as a stationary phase.

Acknowledgement

The authors thank Dr. P. Jones (University of Plymouth, UK) for fruitful discussions on the mechanisms of separation and help with the preparation of the paper.

References

[1] P.N. Nesterenko, *J. Chromatogr.*, 605 (1992) 199.
[2] P.N. Nesterenko, *J. High Resolut. Chromatogr.*, 14 (1991) 767.
[3] P.N. Nesterenko, O.A. Shpigun and Yu.A. Zolotov, *Dokl. Akad. Nauk*, 324 (1992) 107.
[4] W. Hu and H. Haraguchi, *Anal. Chim. Acta*, 285 (1994) 335.
[5] L.W. Yu and R.A. Hartwick, *J. Chromatogr. Sci.*, 27 (1989) 176.
[6] L.W. Yu, T.R. Floyd and R.A. Hartwick, *J. Chromatogr. Sci.*, 24 (1986) 177.
[7] W. Hu, T. Takeuchi and H. Haraguchi, *Anal. Chem.*, 65 (1993) 2204.
[8] W. Hu, H. Tao and H. Haraguchi, *Anal. Chem.*, 66 (1994) 2514.
[9] P.N. Nesterenko, R.V. Kopylov, D.A. Tarasenko, O.A. Shpigun and Yu.A. Zolotov, *Dokl. Akad. Nauk*, 326 (1992) 838.
[10] P.R. Haddad and P.E. Jackson, *Ion Chromatography—Principles and Application* (*Journal of Chromatography Library*, Vol. 46), Elsevier, Amsterdam, 1990, Ch. 3.
[11] A.M. Dolgonosov, *J. Chromatogr.*, 671 (1994) 33.
[12] T. Takeuchi, E. Suzuki and D. Ishii, *Chromatographia*, 25 (1988) 480.
[13] V.A. Davankov, J.D. Navratil and H.F. Walton, *Ligand Exchange Chromatography*, CRC Press, Boca Raton, FL, 1988, Ch. 5.
[14] A.V. Gaida, V.A. Monastyrskii, Yu.V. Magerovskii, S.M. Staroverov and G.V. Lisichkin, *J. Chromatogr.*, 424 (1988) 385.
[15] M. Gimpel and K. Unger, *Chromatographia*, 17 (1983) 200.
[16] L.G. Sillen and A.E. Martell, *Stability Constants of Metal-Ion Complexes* (*Special Publications* 17 and 25), Chemical Society, London, 1964 and 1971.
[17] D. Jensen, J. Weiss, M. Rey and C.A. Pohl, *J. Chromatogr.*, 640 (1993) 65.
[18] P. Kolla, J. Kohler and G. Schomburg, *Chromatographia*, 23 (1987) 465.
[19] D.V. Miltchenko, G.V. Kudryavtsev and G.V. Lisichkin, *Teor. Eksp. Khim.*, 27 (1986) 243.

ELSEVIER

Journal of Chromatography A, 706 (1995) 69–79

JOURNAL OF CHROMATOGRAPHY A

Macrocycle-based column for the separation of inorganic cations by ion chromatography

Brad R. Edwards, Anthony P. Giauque, John D. Lamb*

Department of Chemistry and Biochemistry, Brigham Young University, Provo, UT 84602, USA

Abstract

A tetradecyl-18-crown-6 (TD18C6) column previously used exclusively for anion separations, has been successfully applied to the separation of mono- and divalent cations. The separation is dependent on the selectivity of the macrocycle for inorganic cations. Because of the unusual selectivity exhibited by TD18C6, this macrocycle-based stationary phase is suitable for the simultaneous separation of three alkaline earth metal cations, five alkali metal cations and the ammonium ion. Due to the similar selectivity of TD18C6 for Mg^{2+} and Ca^{2+}, these ions coelute. The affinity of this column for the hydronium ion is great enough that the cations of interest can be eluted by mildly acidic eluents which are amenable to chemical suppression. The innovations of the macrocycle-based cation chromatographic separation system described herein are fourfold. First, due to the high capacity of the columns, an acidic eluent is employed resulting in a different selectivity than previously seen. The selectivity is unique among macrocycle-based columns because there is no variability in retention times resulting from different counter-anions associated with the analytes. Second, the stationary phase is composed of macrocycle adsorbed onto a non-polar polymer resin, rather than to a silica-based column. This allows for the use of basic eluents for the separation of anions without fear of destroying the polymeric substrate. Third, tetradecyl-substituted 18-crown-6 has not been used in other reported separation schemes of this type. Fourth, this system allows for a greater sensitivity for Cs^{+} because it elutes early in the analysis without coelution. Gradient separations employing organic modifiers, temperature, and pH provided improvements in separation over isocratic analyses.

1. Introduction

Macrocyclic ligands have been used as effective components of both the stationary and mobile phases in ion chromatography (IC) as described in a recent review [1] and in other publications [2–6]. These ligands provide novel IC separations due to the unusual specificity with which they selectively bind cations of various sizes to create charged complexes on the column [1]. This selectivity can be exploited to manipulate the separations of an assortment of analytes.

With its long hydrocarbon tail, the tetradecyl-18-crown-6 macrocycle utilized in this study is sufficiently hydrophobic to adsorb strongly onto a non-polar polystyrene–divinylbenzene substrate. When such adsorbed resins are packed into separatory columns and used with aqueous eluents, the macrocycle remains adsorbed to the resin. In the past, macrocycle-based columns using silica gel substrates have been employed as a separation system for the alkali and alkaline earth metal cations [7–11]. However, the TD18C6 column used in this work has a distinct advantage over its predecessors in that the polymer substrate is stable to basic eluent systems.

* Corresponding author.

0021-9673/95/$09.50
SSDI 0021-9673(94)01241-5

This stability makes it possible to use the same column for separating both inorganic cations and inorganic anions [1,3]. The separation mechanism for both types of analyses is based on the selectivity of the macrocycle among cations. Cation separations result from complexation of sample cations by the column macrocycle, while anion separations result from an interaction between the sample anions and the positively charged macrocycle–cation complex exchange sites.

Macrocycle-based ion chromatographic cation separations result from the formation of complexes between analytes and stationary phase macrocyclic ligands. Much research has been directed at obtaining thermodynamic binding constants and related selectivities of macrocycle–metal cation complexes. Table 1 shows log K values for the interaction between inorganic cations and 18-crown-6 in water [12,13].

The cryptands decyl-2.2.1 (D221) and decyl-2.2.2 (D222), which were suitable for chromatographic anion separations [1–6], are not adapted to the separation of cations as they are easily protonated in acidic environments. Consequently, when acidic eluent is used, cryptands are unable to bind metal cations due to competition from hydronium ion. Unlike the cryptands, crown ethers interact only weakly with H_3O^+. Therefore, the resulting competition for macrocyclic binding sites by the H_3O^+ is just sufficient to provide eluent strength. All cation separations reported herein were performed at low pH, using the hydronium ion as eluent.

The log K values in Table 1 predicted that the elution order of the cations on a TD18C6 column would be Li^+, Na^+, Cs^+, NH_4^+, Rb^+, and K^+ among the monovalent cations and Ca^{2+}, Sr^{2+}, and Ba^{2+} among the alkaline earth cations. This selectivity is attributed to the different cationic sizes and their related hydration energies. For example, the size of K^+ corresponds more closely to that of the TD18C6 cavity than for any of the other alkali metal ions. Therefore, the binding constant is significantly higher for K^+ than for the other alkali metal cations.

2. Experimental

2.1. Materials

All columns used in this work were prepared in our laboratory by the following method: the macrocycle-based resin used in packing columns was prepared by dissolving ~0.8 g of TD18C6 in methanol. The dissolved ligand was added to a slurry of ~2.5 g of underivatized MPIC resin (Dionex Corp., Sunnyvale, CA, USA) in methanol–water (60:40) and the resulting mixture was evaporated to dryness. The resin-macrocycle mixture was subsequently resuspended in NaOH and a small amount of methanol and packed into a 28 cm × 4 mm I.D. column using a Dionex column packing system.

The TD18C6 was synthesized specifically for this research by Dr. Jacek Jagodzinsky (Dionex Corporation) using a procedure reported by Ikeda et al. [14]. The 10-μm MPIC resin was also supplied by Dionex and it is an ethylvinyl benzene particle crosslinked with 55% divinylbenzene. Reagent-grade compounds were used in making all standards and eluents. Water used in making eluents and standards was purified to 18 MΩ resistivity with a Milli-Q water purification system (Millipore) and all eluents were degassed by sparging with helium.

Table 1
Log K[a] binding for monovalent and divalent cations to 18-crown-6 in water at 25°C

Cation	Li^+	Na^+	Cs^+	NH_4^+	Rb^+	K^+	Ca^{2+}	Sr^{2+}	Ba^{2+}
Log K	0	0.8	0.99	1.23	1.56	2.03	1.26	2.72	3.87

[a] Refs. [12,13].

2.2. Instrumentation

A Dionex 4000i series ion chromatograph with conductivity detection was used for all chromatography. A Dionex cation micromembrane suppressor (CSRS-I) was employed in all separations–using the autosuppression mode for all separations not involving organic additives to the eluent, and the external water mode of suppression when an organic species was added. Column temperature was controlled as needed by a Dionex column heater. The instrument was controlled by a personal computer and data collected using Dionex AI-450 software.

3. Results and discussion

3.1. Isocratic separations–the effect of eluent concentration

The separation of five alkali metal cations and NH_4^+ was accomplished using a single TD18C6-MPIC column. A typical chromatogram of the separation using a methanesulfonic acid (MSA) eluent is presented in Fig. 1B. As predicted from thermodynamic data in Table 1, the monovalent cations eluted in the order $Li^+ < Na^+ < Cs^+ < NH_4^+ < Rb^+ < K^+$.

Experiments were designed to determine the effect of eluent concentration on the macrocycle-based separation of these cations. The acid concentration was varied from 0.1 m*M* MSA to 5.0 m*M* MSA in a series of isocratic analyses (Fig. 1A–D). As the pH of the eluent was lowered, sample cations eluted more rapidly due to the increased H_3O^+ concentration. More rapid elution resulted in poor resolution of Li^+ and Na^+ as well as Cs^+ and NH_4^+, with resolution between these analytes almost completely disappearing when 5.0 m*M* MSA eluent was used (Fig. 1D). This loss of resolution was accompanied by a large decrease in overall analysis time, with retention times for both Rb^+ and K^+ reduced by a factor of ten. The two alkali metal ions with the greatest affinities for TD18C6, Rb^+ and K^+, eluted in under six min with the increased H_3O^+ concentration (Fig. 1C,D).

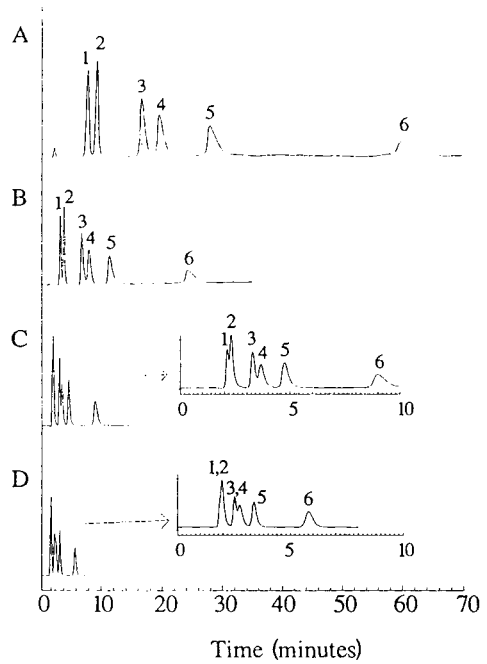

Fig. 1. Isocratic separation of 5 alkali metal cations and NH_4^+ on a TD18C6 column. The eluent concentrations are (A) 0.1 m*M* MSA (methanesulfonic acid); (B) 0.25 m*M* MSA; (C) 1.0 m*M* MSA; and (D) 5.0 m*M* MSA. The injection volume is 50 μl and all analyte concentrations are 0.1 m*M*. The peak identities are as follows: 1 = Li^+, 2 = Na^+, 3 = Cs^+, 4 = NH_4^+, 5 = Rb^+, 6 = K^+. Suppressed conductimetric detection was used.

The effect of eluent strength on the alkaline earth metals was similar to that seen with the alkali metals. As eluent strength increased, the increased H_3O^+ concentration resulted in a dramatic change in elution times. Fig. 2 exhibits the relationship between eluent concentration and retention time for all nine cations examined in this study. A dramatic change in retention time was observed as eluent concentrations approached 1.0 m*M* MSA. However, after the 1.0 m*M* MSA concentration was reached, little further change occurred. This trend is made even more obvious by comparing the alkaline earth separations under acidic conditions from 0.25

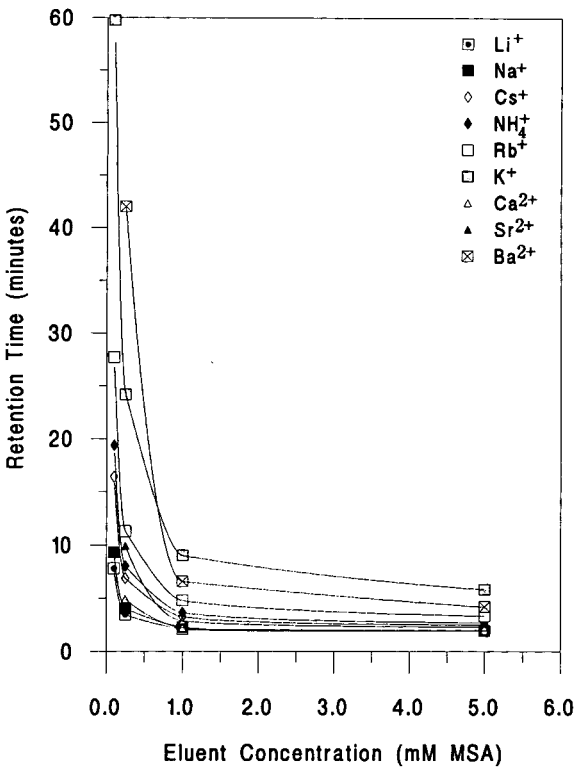

Fig. 2. Plot of eluent concentration vs. retention time for the 9 cations explored in this study.

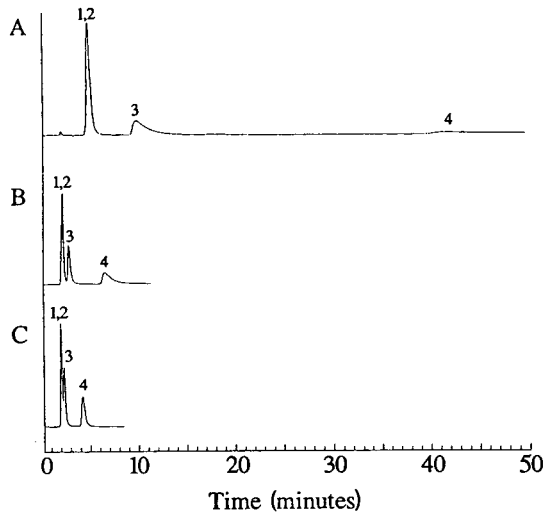

Fig. 3. Chromatograms showing the separation of 4 alkaline earth metal cations on a TD18C6/MPIC column. The eluent concentrations are (A) 0.25 m*M* MSA; (B) 1.0 m*M* MSA; and (C) 5.0 m*M* MSA. The injection volume is 50 μl and all analyte concentrations are 0.1 m*M*. The peak identities are as follows: 1, 2 = Ca^{2+} and Mg^{2+}, 3 = Sr^{2+}, 4 = Ba^{2+}. Suppressed conductimetric detection was used.

m*M* to 5.0 m*M* MSA (Fig. 3). The analysis times are more than halved as the mobile phase is changed to more acidic eluents.

A drawback to alkaline earth cation separations using the TD18C6 column results from the lack of selectivity of TD18C6 between Mg^{2+} and Ca^{2+}. This is evidenced by their coelution at all eluent concentrations in Fig. 3A-C.

A composite standard of the nine alkali, alkaline earth, and NH_4^+ cations was prepared and chromatographed. Isocratic separation conditions were used at eluent concentrations ranging from 0.1 m*M* MSA to 5.0 m*M* MSA. The separations are illustrated in Fig. 4. The best isocratic separations achieved were at low H_3O^+ concentrations (0.1, 0.25 m*M*), where the early eluting peaks were resolved (Fig. 4A,B). However, the total analysis time on such a separations was ~2 h. Nine peaks were observed when an eluent of 0.5 m*M* MSA was used but a number of peaks were unresolved (Fig. 4C).

The most noteworthy result of this experiment is the greater effect of eluent pH on divalent cations than on monovalent ions. This is likely due to the distribution coefficients for divalent cations. In an ion-exchange system the K_D, and therefore k', is inversely proportional to the square of the hydronium activity for divalent cations. For monovalent cations, a simple inverse relationship applies. Therefore, the change in retention of divalent species decreases more rapidly than for monovalent species [15]. While the system we used is not a sulfonated stationary phase, this inverse relationship for divalent cations clearly applies. As the divalent species partitions between the mobile and stationary phases a charge balance is maintained resulting in this relationship. Although the alkali metals retain the same elution order among themselves at all eluent concentrations, the retention relationship between the alkali and alkaline earth

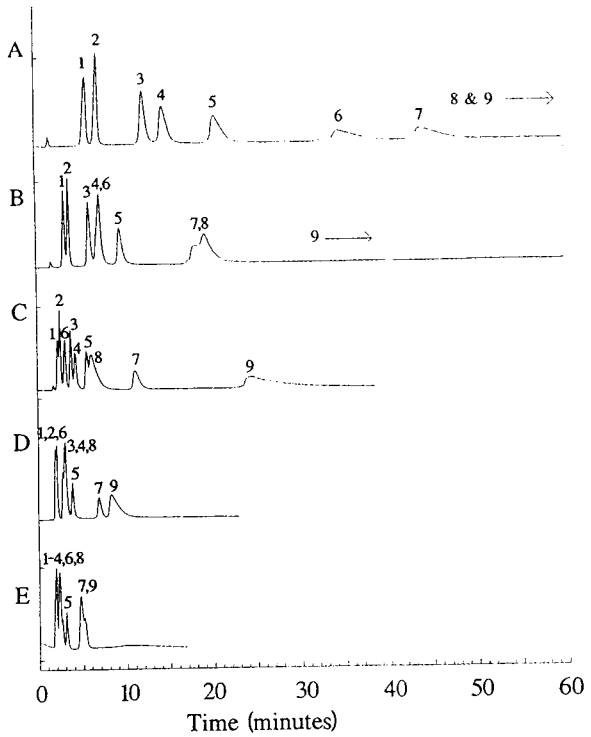

Fig. 4. Chromatograms showing the effect of eluent concentration on the 9 cations explored in this study. All separations were performed on a TD18C6/MPIC column. The eluent concentrations are (A) 0.1 m*M* MSA; (B) 0.25 m*M* MSA; (C) 0.5 m*M* MSA; (D) 1.0 m*M* MSA; and (E) 5.0 m*M* MSA. The injection volume is 50 μl and all analyte concentrations are 0.1 m*M*. The peak identities are as follows: 1 = Li^+, 2 = Na^+, 3 = Cs^+, 4 = NH_4^+, 5 = Rb^+, 6 = Ca^{2+}, 7 = K^+, 8 = Sr^{2+} and 9 = Ba^{2+}. Suppressed conductimetric detection was used.

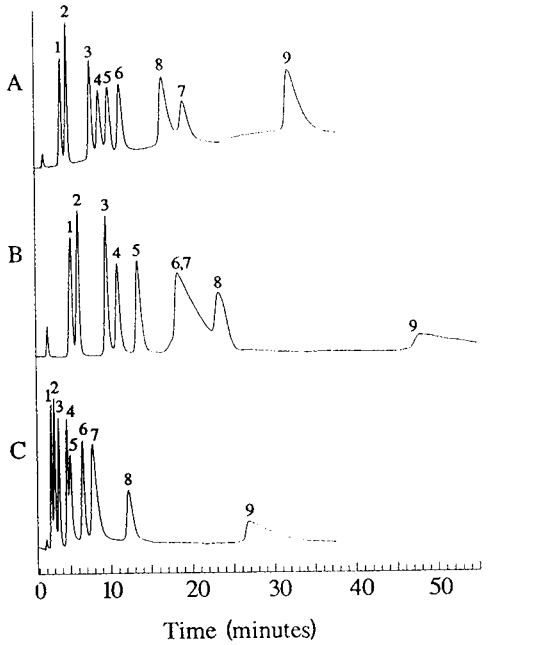

Fig. 5. Three chromatograms showing three different gradient separations of the 9 cations explored in this study. The injection volume is 50 μl, all separations are performed on a TD18C6/MPIC column and all analyte concentrations are 0.1 m*M*. The gradients were as follows: (A) Linear concentration gradient of 0.2 m*M* MSA eluent to 0.5 m*M* MSA from 0 to 15 min followed by a second gradient of 0.5 m*M* MSA to 1.0 m*M* MSA from 15–20 min. The peak identities are as follows: 1 = Li^+, 2 = Na^+, 3 = Cs^+, 4 = NH_4^+, 5 = Ca^{2+}, 6 = Rb^+, 7 = Sr^{2+}, 8 = K^+ and 9 = Ba^{2+}. (B) Temperature gradient from 25°C to 99°C at the time of injection. The eluent was 0.15 m*M* MSA and the peak identities are as follows: 1 = Li^+, 2 = Na^+, 3 = Cs^+, 4 = NH_4^+, 5 = Rb^+, 6 = Ca^{2+}, 7 = K^+, 8 = Sr^{2+} and 9 = Ba^{2+}. (C) Organic modifier gradient from 0.5 m*M* MSA + 5% methanol to 0.5 m*M* MSA at the time of injection. The peak identities are as follows: 1 = Li^+, 2 = Na^+, 3 = Ca^{2+}, 4 = Cs^+, 5 = NH_4^+, 6 = Rb^+, 7 = Sr^{2+}, 8 = K^+ and 9 = Ba^{2+}. Suppressed conductimetric detection was used.

metals changed dramatically. The higher H_3O^+ concentration altered the overall elution order and resulted in poor resolution between the alkaline earth metals and some of the alkali metal ions (Fig. 4D,E).

3.2. Gradient separations–the effect of eluent concentration

Gradients are commonly used in chromatographic separations to decrease the overall analysis time, as well as to enhance the efficiency of later eluting peaks, while retaining resolution between early peaks. Due to the poor affinity of the TD18C6 column for Li^+ and Na^+, it was necessary to keep eluent [H_3O^+] low until after the elution of these two peaks. A variety of step gradients were studied. However, step gradients were always accompanied by a corresponding baseline shift, a result of the suppressor's inability to immediately adjust to large changes in

$[H_3O^+]$. It was therefore necessary to attempt linear gradients involving more gradual changes in $[H_3O^+]$. A linear gradient was performed in which the eluent was changed from 0.2 m*M* MSA to 0.5 m*M* MSA over a 15-min period, then from 0.5 m*M* MSA to 1.0 m*M* MSA over a 5-min period. This gradient produced the best separation of nine cations in terms of total analysis time (Fig. 5. Not only were all peaks resolved, but the efficiency improved from that of an isocratic run in which the eluent was 0.2 m*M* MSA. As expected, the efficiencies of later eluting peaks were improved considerably using the linear gradient over the isocratic run, as indicated in Table 2. While there was a gradual rise in baseline accompanying this separation, the abrupt shifts in the baseline seen with step gradients were not evident.

3.3. Isocratic separations–the effect of temperature

In the past, chromatographic separations involving the use of macrocyclic ligands at variable temperatures were effective in removing longer-retained anionic species from macrocycle-based columns [2]. The binding of ions to macrocyclic ligands is an exothermic process; therefore, at higher temperatures binding decreases. This concept was exploited in our cation separations system by raising the eluent temperature in an effort to decrease overall analysis time via reduced binding of K^+, Sr^{2+}, and Ba^{2+}. Fig. 6 shows a plot of the retention times for all nine cations as isocratic temperature analyses were performed at intervals from 25°C to 80°C. With the exception of Ca^{2+}, the increased temperature resulted in the decrease in retention times as thermodynamically predicted. As can be seen by the slope of the lines, the general trend was a greater change in retention time for longer retained species.

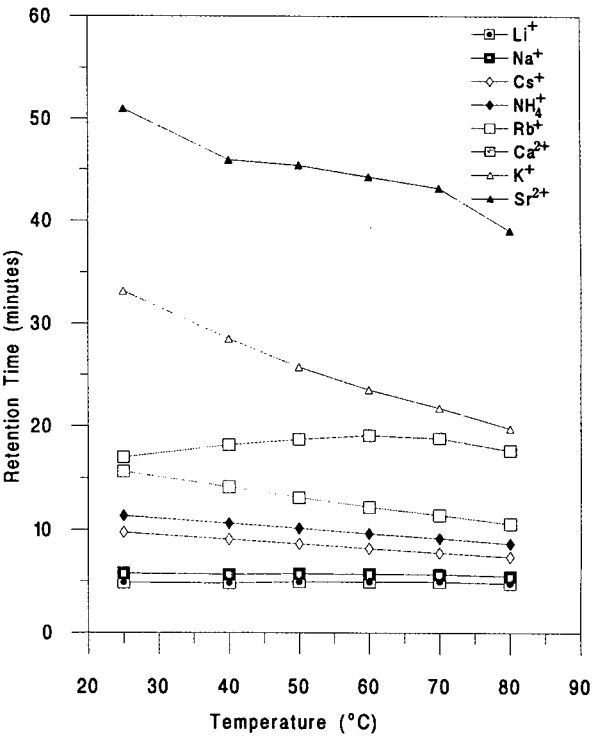

Fig. 6. Plot of temperature vs. retention time for each of the 9 cations studied.

The chromatograms illustrating the irregular behavior of Ca^{2+}, as well as the effect of tem-

Table 2
Efficiency: linear gradient vs. isocratic separation

Analysis	Li^+	Na^+	Cs^+	NH_4^+	Rb^+	Ca^{2+}	Sr^{2+}	K^+	Ba^{2+}
Isocratic[a]	1086	1711	1726	1594	836	1757	1498	1662	not eluted
Linear[a]	1105	1755	2280	2094	2122	2259	1507	2429	1918

[a] Theoretical plates.

Conditions: Separations were performed on a TD18C6/MPIC column, the injection volume was 50 μl and all analyte concentrations were 0.1 m*M*; 0.2 m*M* MSA eluent was used for the isocratic analysis and a changing eluent of 0.2 m*M* MSA eluent to 0.5 m*M* MSA from 0 to 15 min followed by 0.5 m*M* MSA to 1.0 m*M* MSA from 15 to 20 min was employed for the linear gradient. Suppressed conductimetric detection was used for both types of analyses.

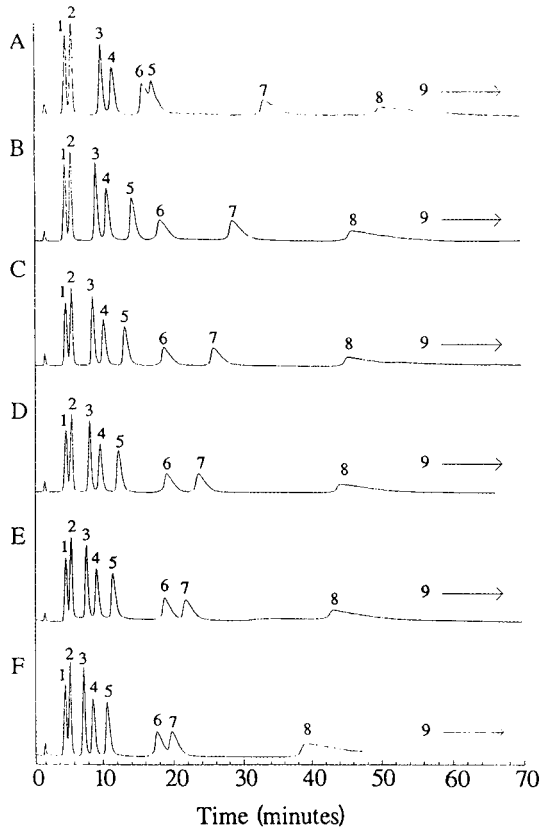

Fig. 7. Chromatograms showing the effect of increasing temperature on the 9 cations explored in this study. All separations were performed on a TD18C6/MPIC column. The eluent concentration was 0.15 m*M* MSA and the temperatures were (A) 25°C; (B) 40°C; (C) 50°C; (D) 60°C; (E) 70°C and (F) 80°C. The injection volume is 50 μl and all analyte concentrations are 0.1 m*M*. The peak identities are as follows: 1 = Li^+, 2 = Na^+, 3 = Cs^+, 4 = NH_4^+, 5 = Rb^+, 6 = Ca^{2+}, 7 = K^+, 8 = Sr^{2+} and 9 = Ba^{2+}. Suppressed conductimetric detection was used.

perature on resolution, are shown in Fig. 7. Initially, Ca^{2+} and Rb^+ are unresolved. However, as temperature increases, the retention of Ca^{2+} increases, then decreases. At the upper end of the temperature scale (80°C), the retention time of Ca^{2+} is still relatively unchanged, causing it to coelute with K^+. This may be due to its small ΔH value of complexation (Table 3) [12]. The ΔH values shown in Table 3 are for reactions in a homogeneous solution. Indeed, the ΔH values for the extraction reaction may be endothermic. The alkaline earth metal ions exhibit strong retention even at higher temperatures, for example at the highest temperatures, Ba^{2+} is retained longer than 70 min.

As separations were performed at higher temperatures, the ions Li^+ and Na^+ as well as Cs^+ and Rb^+ began to lose resolution. The resolution between these analytes can be seen in Table 4. However, the minor effect of the increase in temperature on resolution is a distinct advantage over experiments in which concentration gradients are used. With differences in concentration, the resolution between early eluting species disappears (Fig. 1), whereas the loss of resolution between these early peaks is minor when temperature is increased.

3.4. Gradient separations–the effect of temperature

Temperature gradients were attempted as a means to avoid the baseline shift which generally accompanies concentration gradient separations. Fig. 5B shows a chromatogram which employed a step gradient from 25°C to 99°C at the time of

Table 3
ΔH Values for complexation–homogeneous solution

Analyte	Li^+	Na^+	K^+	Rb^+	Cs^+	NH_4^+	Ca^{2+}	Sr^{2+}	Ba^{2+}
ΔH Values (kJ/mol)	–	−9.41	−26.0	−16.0	−15.85	−9.79	−2.91	−15.1	−31.7

Conditions: ΔH values were obtained from the literature [12,13].

Table 4
The effect of temperature on resolution

Analytes	25°C	40°C	50°C	60°C	70°C	80°C
Li^+/Na^+ resolution	1.52	1.44	1.37	1.37	1.32	1.29
Cs^+/NH_4^+ resolution	1.62	1.72	1.83	1.84	1.83	1.84

Conditions: Separations were performed on a TD18C6/MPIC column and all analyte concentrations were 0.1 m*M*. The eluent concentration was 0.15 m*M* MSA and suppressed conductimetric detection was used.

injection. This procedure dramatically improved the overall analysis time, as eight of the nine cations eluted in under 25 min with only one coelution. In addition, there was no baseline rise like that seen in the concentration gradient separation in Fig. 5A. This enhanced baseline stability is due to the nature of the separation. Instead of an increase in eluting power of the eluent, the ability of the stationary phase to bind cations is decreased and column capacity decreases. Therefore the inability of the suppressor to compensate for an increase in eluent concentration is not a factor in temperature gradient separations. In addition, the heated mobile phase is cooled by the regenerant in the suppressor before being detected. This eliminates any increase in conductivity due to the increase in temperature.

3.5. Isocratic separations–the effect of adding an organic modifier to the eluent

To aid in the simultaneous separation of all cations, addition of an organic modifier to the eluent was tested. It was anticipated that by adding an organic solvent, such as methanol, the effective capacity of the column would increase. Methanol increases the binding constants of cations with macrocyclic ligands by reducing competition of solvent molecules for the cations. Thus, when methanol is present in the eluent, the cations are retained longer on the column than when an aqueous eluent is used. This would allow use of higher eluent concentrations, resulting in a more rapid analysis. In previous studies, it was shown that high percentages of organic solvent strip the macrocycle from the column [1]. Fig. 8A shows a separation without methanol in the eluent. It is compared to eluents containing 1% (Fig. 8B), 5% (Fig. 8C) and 10% (Fig. 8D) methanol. As expected, the increasing percentage of organic modifier in the eluent increased retention times and thus yielded better resolution for the early eluting Li^+ and Na^+ peaks (see Table 5).

3.6. Gradient separations–the effect of adding an organic modifier to the eluent

It was desirable to develop a gradient system that not only eliminated baseline shifts (e.g. temperature gradient Fig. 5B) but also resulted in short analysis times (e.g. concentration gradient Fig. 5A). One experiment aimed at achieving this goal was a gradient which switched, at the time of injection, from a 0.5 m*M* MSA eluent that contained methanol to an eluent without methanol. The switch allowed residual methanol to aid in the resolution of early eluting peaks, while the acidic eluent decreased the analysis time. Fig. 5C shows the effect of such a methanol gradient on a 9 cation separation. As predicted, the first peaks were better resolved with the gradient than with an isocratic separation using 0.5 m*M* MSA (Fig. 4C), and the overall analysis time was decreased from analyses in which methanol was ever present in the eluent (Fig. 8B–D). In addition, altering the concentration of methanol had no significant effect on the performance of the suppressor, and therefore, baseline shifts did not occur.

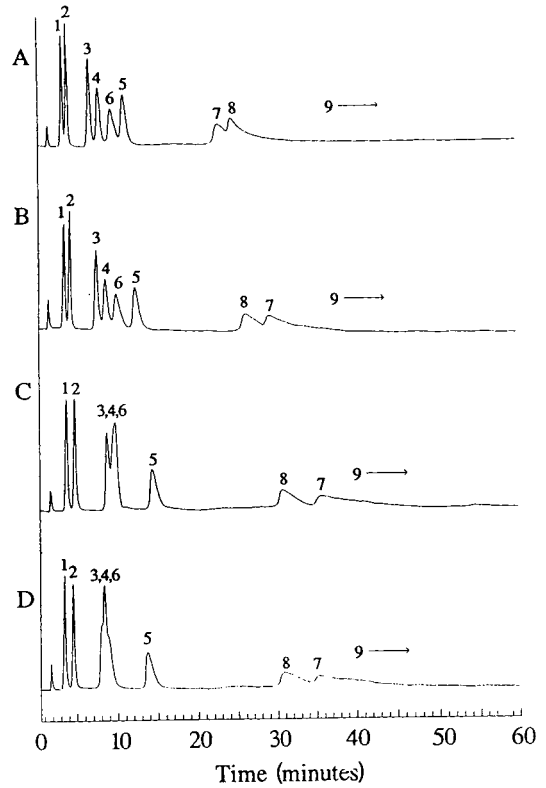

Fig. 8. Chromatograms showing the effect of the addition of an organic modifier on the 9 cations explored in this study. All separations were performed on a TD18C6/MPIC column. The eluent concentration was 0.2 m*M* MSA and the % methanol was (A) 0%; (B) 1%; (C) 5%; and (D) 10%. The injection volume is 50 μl and all analyte concentrations are 0.1 m*M*. The peak identities are as follows: 1 = Li^+, 2 = Na^+, 3 = Cs^+, 4 = NH_4^+, 5 = Rb^+, 6 = Ca^{2+}, 7 = K^+, 8 = Sr^{2+} and 9 = Ba^{2+}. Suppressed conductimetric detection was used.

3.7. Quantitative aspects

Linearity of calibration curves

Calibration curves were generated for each species studied and detection limits were determined at 3σ baseline noise. The correlation coefficients for each sample's calibration curve as well as detection limits can be seen in Table 6. In generating the calibration curves, each concentration was measured three times and a standard deviation calculated. As the retention time increased, band broadening occurred and detection limits decreased. NH_4^+ was the only exception to this trend. Its detection limit was as low as that of Li^+. This result may be due to the higher conductivity of the NH_4^+ ion over the other cations examined in this study.

It is significant to note that the detection limit for Cs^+ is 100 ppb using this macrocycle-based IC system. Other analytical methods such as inductively coupled plasma (ICP) [16], exhibits a poor sensitivity for Cs^+. In addition, other methods of analysis by IC elute Cs^+ very late, and only then after changing eluent strength considerably. Consequently, loss of efficiency, band broadening, and decreased detection occur.

While the correlation coefficients indicate linearity for all analytes over a wide range of concentrations, there were a few unusual results. For instance, at concentrations greater than 10 ppm, NH_4^+ exhibited a significant flattening in the calibration curve. This may be due to the equilibrium expression NH_4^+&rjhar2;NH_3 and H^+. Indeed, all cations show deviations from linearity at high concentrations.

Another oddity we noticed concerned K^+ and column capacity. The column capacity was determined to be 1670 μmol assuming 100% adsorption of the macrocycle. At concentrations greater than 100 ppm, results for K^+ were not reproducible. Perhaps the concentration of K^+ had exceeded the capacity of the column and therefore behaved unpredictably. Other species would likely behave similarly at high concentrations, however this behavior was seen by K^+ at this relatively low concentration because it binds TD18C6 to a greater degree.

3.8. Effect of the counter-anion

Experiments were performed to determine whether the presence of a sample counter-anion played any significant role in the separation and detection of alkali metal cations. Individual samples of various K^+ and Na^+ salts were separated on a TD18C6 column to determine the average retention time of these alkali metal cations with different counter-anions. Specifically, four analyses of potassium acetate, dichromate, bromate, thiocyanate, fluoride, nitrate, nitrite, and iodide were performed. The overall

Table 5
The effect of methanol on the resolution of Li^+ and Na^+

Analyte	No (0%) Methanol	1.0% Methanol	5.0% Methanol	10.0% Methanol
Li^+/Na^+	1.50	1.69	2.08	2.39

Conditions: Separations were performed on a TD18C6/MPIC column and all analyte concentrations were 0.1 m*M*. The eluent concentration was 0.2 m*M* MSA and HPLC grade methanol was used in all analyses. Suppressed conductimetric detection was used.

Table 6
Quantitative results

Analyte	Li^+	Na^+	K^+	Rb^+	Cs^+	NH_4^+	Ca^{2+}	Sr^{2+}	Ba^{2+}
Detection limit	10 ppb	50 ppb	500 ppb	100 ppb	100 ppb	100 ppb	10 ppb	100 ppb	1 ppm
Correlation coefficient	0.9985	0.9993	0.9989	0.9999	0.9999	0.9971	0.9993	0.9999	0.9999

Conditions: Analyses were performed on a TD18C6/MPIC column with varying analyte concentrations. The eluent concentration was 1.0 m*M* MSA and suppressed conductimetric detection was used.

Table 7
Counter-anion effect

Analyte	Number of runs	Deviation (%)
KCH_3COOH	4	0.6
$K_2Cr_2O_7$	4	0.3
KBr	4	0.8
KSCN	4	0.8
KF	4	0.5
KNO_3	4	0.7
KNO_2	4	1.7
KI	4	0.1
$NaNO_3$	3	0.2
NaI	3	0.3
NaH_2PO_4	3	0.2
Na_2CO_3	3	0.3
NaBr	3	1.0
NaCl	2	0.3
Na_2SO_4	3	0.3
NaF	3	1.0
$NaCH_3COOH$	3	0.3
All K-salts	32	3.4
All Na-salts	26	1.2

Conditions: All experiments were performed on a TD18C6/MPIC column and all analyte concentrations were 10 ppm. Dilute concentrations of MSA were used in analyzing both sodium salts and potassium salts. For the potassium analysis, the eluent pH 1.6, and for the sodium analysis, the eluent pH 3.6. Suppressed conductimetric detection was used.

retention time for these runs was 6.20 ± 0.21 when eluted at pH 1.6. In addition, 3 runs each of sodium nitrite, iodide, biphosphate, carbonate, bromide, chloride, sulfate, fluoride, and acetate were performed and the overall retention time for these runs was 3.11 ± 0.04 when eluted at a pH 3.6. Table 7 shows the relative standard deviation of each potassium and sodium salt elution. It is important to note that the larger overall standard deviations for each set of alkali salts is due to a baseline drift which occurs throughout each day, possibly due to environmental temperature changes.

It is noteworthy that the different counter-anions play no significant role in the retention of the alkali metals when an acidic eluent is employed. This is because unlike H_2O–methanol systems studied in the past [7,8,10,11], the acidic eluent system allows the sample counter-anions to be uniformly replaced by the eluent counter-anion, methylsulfonate. The literature demonstrates that when pure water is used as the eluent, the counter-ions associated with the sample cations are not displaced and therefore a different retention time is observed for each cation-anion pair [8–11]. In contrast, we observe no effect of sample counter-anions on cation

retention in the presence of an acidic mobile phase.

4. Conclusions

The TD18C6-based IC system reliably separates and quantitates both anions and cations. The shifting retention times due to matrix anions or analyte concentration seen previously using water eluents is effectively eliminated by the use of acidic eluents. In addition, the polymer stationary phase substrate makes it possible to use this column with basic eluents for the separation of anions.

Acknowledgements

We express appreciation to Dionex Corporation, who has generously funded this research. In addition, we acknowledge the assistance of Dr. Robert G. Smith (Morton International, Brigham City, UT, USA) and undergraduate research assistants Max Mortensen, Nolan Polson, and Tyler Crawford.

References

[1] J.D. Lamb and R.G. Smith, *J. Chromatogr.*, 546 (1991) 73.
[2] J.D. Lamb and R.G. Smith, *J. Chromatogr.*, 640 (1993) 33.
[3] J.D. Lamb, P.A. Drake and R.G. Smith, *J. Chromatogr.*, 546 (1991) 139.
[4] J.D. Lamb and R.G. Smith, *Talanta*, 39 (1992) 923.
[5] R.G. Smith and J.D. Lamb, *J. Chromatogr. A*, 671 (1994) 89.
[6] J.D. Lamb, R.G. Smith, R.C. Anderson and M.K. Mortensen, *J. Chromatogr. A*, 671 (1994) 55.
[7] K. Kimura, E. Hayata and T. Shono, *J. Chem. Soc., Chem. Commun.*, (1984) 271.
[8] M. Takagi and H. Nakamura, *J. Coord. Chem.*, 15 (1986) 53.
[9] M. Igawa, K. Saito, J. Tsukamoto and M. Tanaka, *Anal. Chem.*, 53 (1981) 1942.
[10] K. Kimura, H. Harino, E. Hayata and T. Shono, *Anal. Chem.*, 58 (1986) 2233.
[11] M. Nakajima, K. Kimura and T. Shono, *Bull. Chem. Soc. Jpn.*, 56 (1983) 3052.
[12] R.M. Izatt, J.S. Bradshaw, S.A. Nielsen, J.D. Lamb and J.J. Christensen, *Chem Rev.*, 85 (1985) 271.
[13] J.S. Bradshaw, R.L. Bruening, K.E. Krakowiak, J.B. Tarbet, M.L. Bruening, R.M. Izatt and J.J. Christensen, *J. Chem. Soc., Chem. Commun.*, (1988) 812.
[14] I. Ikeda, S. Yamamura, Y. Nakatsuji and M. Okahara, *J. Org. Chem.*, 45 (1980) 5355.
[15] H. Small, T.S. Stevens and W.C. Bauman, *Anal. Chem.*, 47 (1975) 1801.
[16] P.W.J.M. Boumans, *Line Coincidences Tables for Inductively Coupled Plasma Atomic Emission Spectroscopy*, 2nd edn., Pergamon Press, New York, NY, 1984.

ELSEVIER

Journal of Chromatography A, 706 (1995) 81–92

JOURNAL OF CHROMATOGRAPHY A

Stationary phase for the determination of fluoride and other inorganic anions

Joachim Weiss[a,*], Sabine Reinhard[a], Christopher Pohl[b], Charanjit Saini[b], Latha Narayaran[b]

[a]*Dionex GmbH, Am Wörtzgarten 10, D-65510 Idstein, Germany*
[b]*Dionex Corporation, 1228 Titan Way, Sunnyvale, CA 94086, USA*

Abstract

A pellicular anion-exchange column was developed for the determination of inorganic anions including fluoride and oxyhalides such as chlorite, chlorate and bromate. Compared with conventional latex-agglomerated resins, the new anion exchanger allows the retention of fluoride well out of the water dip with elution of sulfate in less than 15 min using a carbonate–hydrogencarbonate eluent under isocratic conditions. Because the ethylvinylbenzene–divinylbenzene substrate is highly cross-linked, the new separator is solvent compatible, thus allowing the use of organic solvents to alter the selectivity of the separation, and also to remove organic contaminants from the column. The separation characteristics of this column are presented and various applications are discussed.

1. Introduction

Since the introduction of ion chromatography for the determination of inorganic anions in 1975 [1], the determination of fluoride has been a problem owing to its low affinity towards strongly basic anion exchangers [2–4]. To elute fluoride together with other common inorganic anions such as chloride, nitrate and sulfate within an acceptable time frame of less than 15 min, mixtures of sodium carbonate and sodium hydrogencarbonate are the most widely used eluents [5]. Another advantage of carbonate–hydrogencarbonate-based eluents is their compatibility with membrane-based suppressor systems, which are essential for the sensitive conductimetric detection of sample analytes. However, under these chromatographic conditions fluoride elutes very close to the system void volume, making determination at concentration levels of less than 100 μg/l difficult if not impossible owing to interference from the negative water dip. The water dip occurs when the injected water passes the conductivity cell, decreasing the background conductivity of carbonic acid formed in the suppressor by exchanging the eluent cations with hydronium ions.

There have been numerous attempts to circumvent this problem by sample pretreatment, by changing the eluent conditions or by tailoring the stationary phase design. An easy way to compensate for the negative dip is to add carbonate to the sample, matching the carbonate concentration in the mobile phase, thus making the negative dip invisible. However, this approach does not work with real samples such as mineral waters. If the carbonate concentration in the sample is higher than the total carbonate

* Corresponding author.

0021-9673/95/$09.50
SSDI 0021-9673(94)01162-1

concentration in the mobile phase, a positive signal that is almost indistinguishable from the fluoride peak is obtained within the void volume of the separator column. Diluting the sample with deionized water does not solve this problem because even small amounts of carbonate in the sample lead to a significant decrease in the fluoride peak height [6]. Another problem for the verification of fluoride, especially in environmental samples, is monocarboxylic acids. As many of these acids co-elute with or are only partly resolved from fluoride, interpretation of the signals near the void volume is extremely difficult.

The exact determination of fluoride is possible if the advantage of the simultaneous determination of other mineral acids is eliminated and if the chromatographic conditions are changed so that fluoride is separated from the carbonate–hydrogencarbonate travelling with the mobile phase. An increase in fluoride retention can be achieved by using an eluent of lower eluting power such as sodium tetraborate. This method has only limited applicability because sulfate has a much longer retention time under these conditions, interfering with subsequent analyses. Alternatively, a gradient technique with sodium hydroxide as the eluent can be employed. Starting with very dilute NaOH solution, fluoride and various other monocarboxylic acids can be separated, while the final NaOH concentration suffices to elute other inorganic and organic anions of higher valencies.

IonPac AS10 was the first anion exchanger effectively to address the resolution of fluoride from the system void volume by combining a high ion-exchange capacity with a relatively weak eluent. The main drawback to the use of this column for general ion chromatographic applications is that the elution times for bromide and nitrate exceed 40 min under standard conditions. These analysis times are significantly longer than what is required of ion chromatography in a water analysis laboratory. We also evaluated a commercially available polymeric quaternary ammonium compound (quat)-coated resin from another source as it allows the resolution of fluoride from the system void volume with a standard carbonate eluent. As shown in Fig. 1, the separation of fluoride compares well with that obtained with ion-pair chromatography with the advantage of a much shorter analysis time. However, during the evaluation of this column we discovered that the polymeric quat-coated resin permanently loses its capacity following treatment with organic solvents (Fig. 2). Solvent levels as low as 10% caused significant decreases in column capacity. Recognizing the importance of solvents in cleaning contaminated ion-exchange materials and in altering ion-exchange selectivity, we began a project to develop a new solvent-compatible ion-exchange material with which fluoride is resolved from the system void volume and oxyhalides are separated from other mineral acids in the same run under isocratic conditions.

Because of the high degree of hydration of the

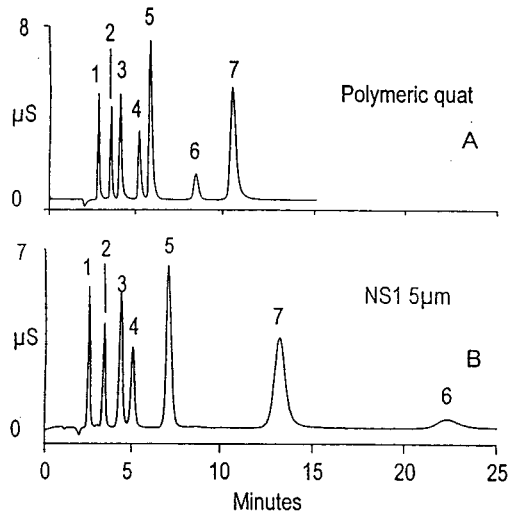

Fig. 1. Comparison of anion separations using ion-exchange chromatography on a polymeric quat-coated resin and ion-pair chromatography on highly cross-linked divinylbenzene. (A) Separator, polymeric quat-coated resin; eluent, 1.7 mmol/l sodium hydrogencarbonate–1.8 mmol/l sodium carbonate; flow-rate, 1.5 ml/min; detection, suppressed conductivity; injection volume, 25 µl. (B) Separator column, IonPac NS1 (5 µm); eluent, 2 mmol/l TBAOH + 1 mmol/l sodium carbonate–acetonitrile (90:10, v/v); flow-rate, 1 ml/min; detection, suppressed conductivity; injection volume, 25 µl. Solute concentrations: (1) 3 mg/l fluoride; (2) 4 mg/l chloride; (3) 10 mg/l nitrite; (4) 10 mg/l bromide; (5) 20 mg/l nitrate; (6) 10 mg/l orthophosphate; (7) 20 mg/l sulfate.

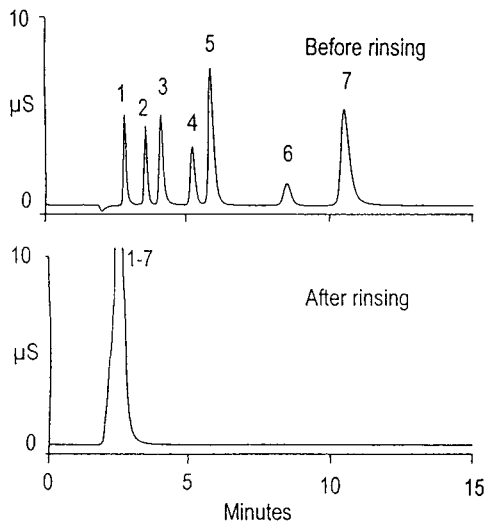

Fig. 2. Evaluation of a polymeric quat-coated resin for solvent resistance. Eluent, 1.7 mmol/l sodium hydrogencarbonate–1.8 mmol/l sodium carbonate; flow-rate, 1.5 ml/min; detection, suppressed conductivity; injection volume, 25 µl; solute concentrations as in Fig. 1. (A) Before rinsing with acetonitrile–water (90:10, v/v); (B) after a 30-min rinse with acetonitrile–water (90:10 v/v).

fluoride ion, it was necessary to generate a stationary phase with an extremely high water content. This can be accomplished by using very hydrophilic quaternary ion-exchange sites. However, fluoride is so highly hydrated that the only viable method of obtaining a reasonable fluoride retention is to produce an extremely low cross-linked latex. Using a cross-link level significantly under 1% allows the generation of polymers of very high water content needed for the effective retention of fluoride.

A key point in successful trace fluoride determination is that the eluent conductivity needs to be moderate. The higher the eluent conductivity, the greater is the void dip for any given column. Given the proximity of fluoride to the void dip, its absolute size needs to be minimized to allow maximum resolution of fluoride from the void dip. We therefore tried to develop a column that would work with as dilute an eluent as possible. We also determined that the higher the flow-rate, the faster the system void peak recovers to the baseline. Therefore, the column of choice should work at flow-rates above 1 ml/min. In order to obtain an acceptable capacity, given that a very low cross-linked latex had to be employed, we had to use a superporous substrate such as that used in the IonPac AS10 column mentioned earlier. The surface area of standard microporous packing materials is inadequate to provide sufficient capacity with these low cross-linked latexes.

The work presented in this paper was focused on the chromatographic properties and the applicability of such a packing material. In order to study this new separation material, chromatographic parameters such as eluent composition, eluent concentration and flow-rate were varied.

2. Experimental

2.1. Apparatus

All experiments were carried out with a DX 500 ion chromatographic system (Dionex, Sunnyvale, CA, USA) consisting of a quaternary gradient pump (GP40), a chromatography module (LC20) and a conductivity detector (CD20). Eluents were degassed by using the built-in vacuum solvent degassing device.

Separations were performed on an IonPac AS12A anion exchanger. A guard column (IonPac AG12A) was used all times. Conductivity detection was carried out using an Anion Self Regenerating Suppressor (ASRS-1) in the recycle mode.

A PeakNet chromatography data system (Dionex) was used for instrument control and for data collection and processing.

2.2. Reagents

Ultrapure water (18 MΩ/cm resistivity at 25°C) used for the preparation of the eluents was obtained from a water purification system (SERAL, Ransbach-Baumbach, Germany). Sodium hydrogencarbonate and sodium carbonate (Fluka, Ulm, Germany) and sodium tetraborate (Merck, Darmstadt, Germany) were of analyti-

Table 1
Structural and physical properties of the IonPac AS12A separator

Parameter	Value
Column dimensions	200 mm × 4 mm I.D.
Particle diameter	9 μm
Substrate material	Macroporous polyethylvinylbenzene cross-linked with 55% divinylbenzene
Pore size	200 nm
Column capacity	52 μequiv.
Latex polymer	Vinylbenzyl chloride
Latex cross-linking	Very low (0.15%)
Latex diameter	140 nm
Functional group	Quaternary ammonium group
pH stability	0–14
Solvent compatibility	0–100%

cal-reagent grade. Acetonitrile (Chrom AR grade) was purchased from Promochem (Wesel, Germany).

Dilute working standards of all inorganic anions and organic acids under investigation were prepared daily from 1000 ppm stock standard solutions. All standard solutions were stored in polyethylene containers.

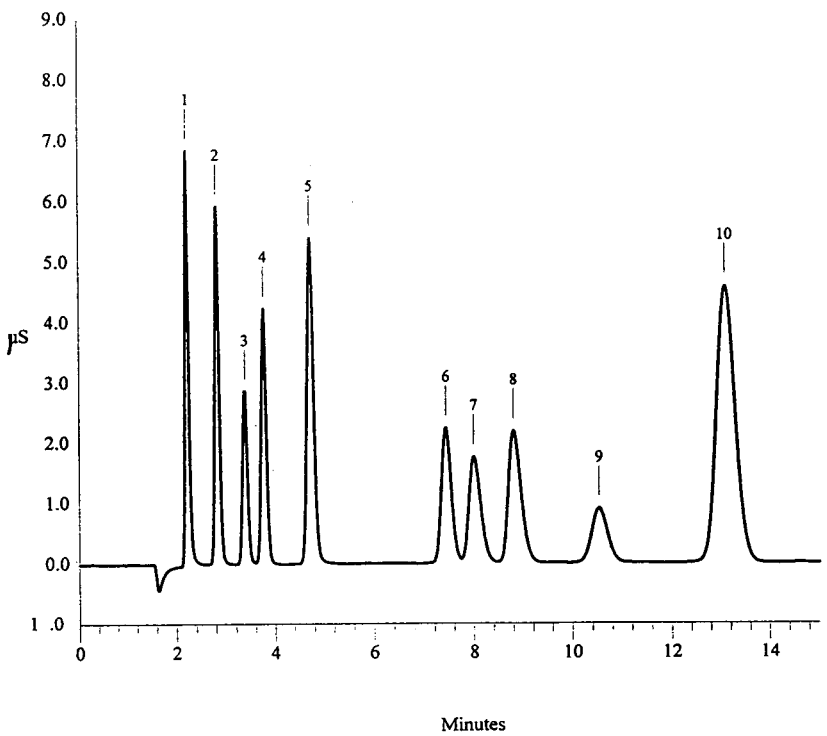

Fig. 3. Separation of common anions on IonPac AS12A. Eluent, 0.3 mmol/l sodium hydrogencarbonate–2.7 mmol/l sodium carbonate; flow-rate, 1.5 ml/min; detection, suppressed conductivity; injection volume, 25 μl. Solute concentrations: (1) 3 mg/l fluoride; (2) 10 mg/l chlorite; (3) 10 mg/l bromate; (4) 4 mg/l chloride; (5) 10 mg/l nitrite; (6) 10 mg/l bromide; (7) 10 mg/l chlorate; (8) 10 mg/l nitrate; (9) 10 mg/l orthophosphate; (10) 20 mg/l sulfate.

3. Results and discussion

The new anion exchanger for use as a stationary phase for the determination of fluoride and other inorganic anions has been commercialized under the trade-name IonPac AS12A. Its structural and physical properties are summarized in Table 1.

To accomplish all the objectives, we used a 0.15% cross-linked latex derived from vinylbenzyl chloride. The agglomeration of the latex was carried out on a superporous ethylvinylbenzene–divinylbenzene resin with a bead diameter of 9 μm, an average pore size of 200 nm and a specific surface area of approximately 15 m^2/g. The substrate was sulfonated under vigorous conditions to ensure that no unsulfonated surface existed on the substrate. This was necessary to avoid problems with the reversed-phase behaviour of anions such as bromide and nitrate. The ion-exchange capacity of this column is 52 μequiv. per column, or roughly double that of a conventional anion exchanger such as IonPac AS4A-SC. This doubling of capacity is remarkable considering that the water content of this latex is far higher than that of AS4A-SC. In latex-based ion-exchange materials, the ion-exchange capacity is inversely proportional to the latex water content because the water in the ion-exchange phase is essentially a diluent, occupying volume that would otherwise contain the ion-exchange polymer. Hence the superporous resin was necessary to compensate for the capacity by making use of a latex of high water content.

3.1. Water analysis

As with conventional latex-agglomerated anion exchangers such as the IonPac AS4A-SC and AS9-SC, generally used for water analysis applications, very simple eluents based on carbonate–hydrogencarbonate can be used to elute standard inorganic anions rapidly and efficiently

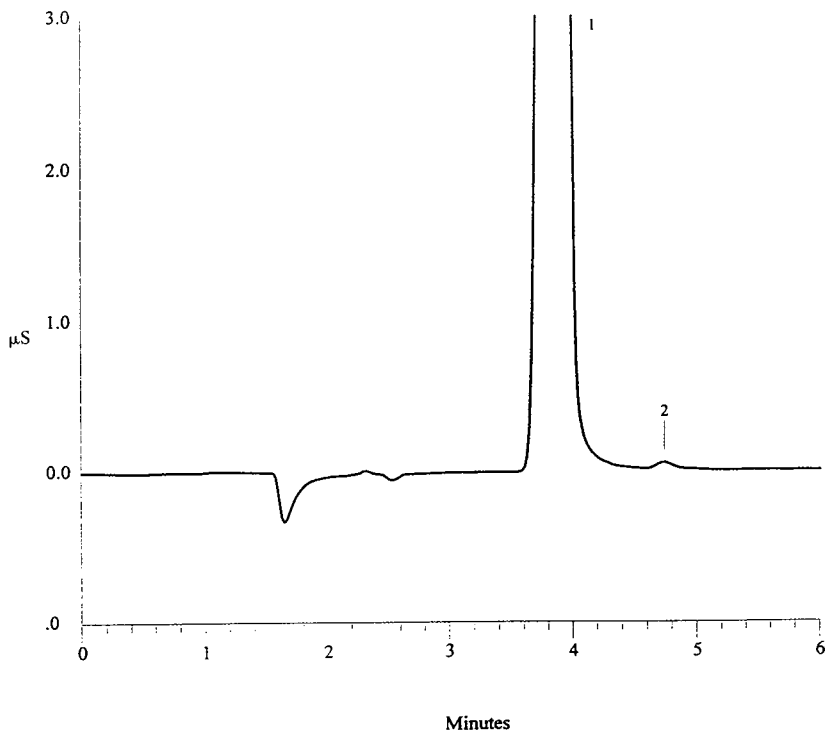

Fig. 4. Determination of nitrite in the presence of high chloride concentration. Separator, IonPac AS12A; chromatographic conditions as in Fig. 3. Solute concentrations: (1) 100 mg/l chloride; (2) 0.1 mg/l nitrite.

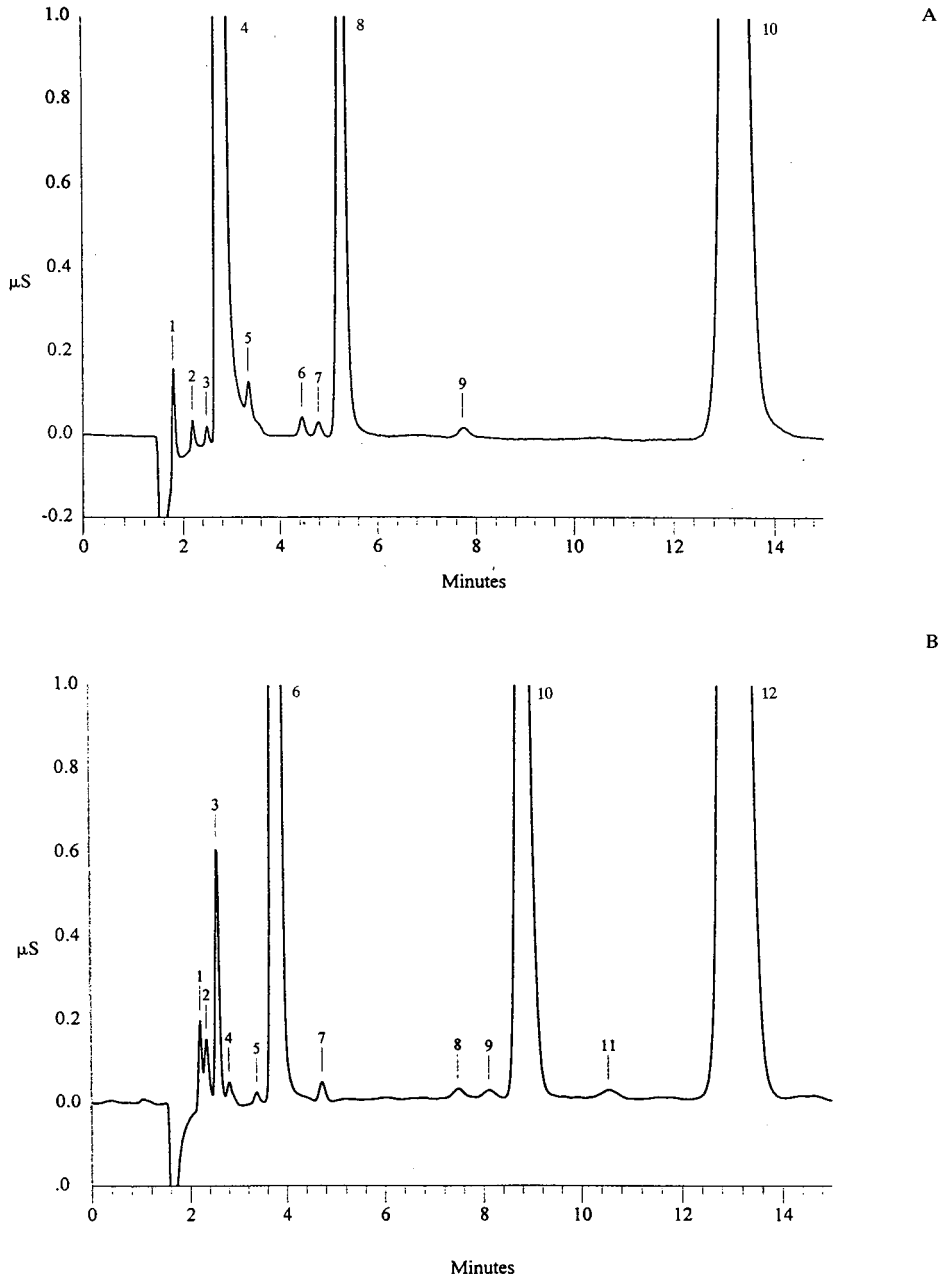

Fig. 5. Selectivity comparison of IonPac AS12A with the IonPac AS9-SC for the determination of common anions and disinfectant by-products in simulated drinking water. Separator column, (A) IonPac AS9-SC and (B) IonPac AS12A; eluent, (A) 1.7 mmol/l sodium hydrogencarbonate–1.8 mmol/l sodium carbonate and (B) 0.3 mmol/l sodium hydrogen-carbonate–2.7 mmol/l sodium carbonate; flow-rate, (A) 1 ml/min and (B) 1.5 ml/min; detection, suppressed conductivity; injection volume, 25 µl. Solute concentrations: (A) (1) 0.1 mg/l fluoride; (2) 0.1 mg/l chorite, (3) 0.1 mg/l bromate; (4) 20 mg/l chloride; (5) 0.1 mg/l nitrite; (6) 0.1 mg/l bromide; (7) 0.1 mg/l chlorate; (8) 5 mg/l nitrate; (9) 0.2 mg/l orthophosphate; (10) 20 mg/l sulfate; (B) (1) 0.1 mg/l fluoride; (2) 1 mg/l acetate; (3) 1 mg/l formate; (4) 0.1 mg/l chlorite; (5) 0.1 mg/l bromate; (6) 30 mg/l chloride; (7) 0.1 mg/l nitrite; (8) 0.1 mg/l bromide; (9) 0.1 mg/l chlorate; (10) 10 mg/l nitrate; (11) 0.2 mg/l orthophosphate; (12) 30 mg/l sulfate.

under isocratic conditions. Fig. 3 shows that fluoride is well resolved from the system void volume and separated to the baseline from other mineral acids and oxyhalides in less than 15 min, using a flow-rate of 1.5 ml/min and an eluent consisting of 2.7 mmol/l sodium carbonate and 0.3 mmol/l sodium hydrogencarbonate. Both the eluent composition and flow-rate were optimized for maximum resolution between all the analyte anions. It is remarkable that the large resolution between chloride and nitrite cannot be achieved by any other existing anion exchanger. This allows the separation of chloride and nitrite at large concentration differences, which previously was possible only with UV detection at 215 nm. Fig. 4 shows the separation of nitrite in presence of a 1000-fold excess of chloride employing suppressed conductivity detection.

Because of the increasing popularity of disinfecting water with ozone and chlorine dioxide, modern anion-exchange materials used for water analysis have to be capable of separating the most important disinfectant by-products such as chlorite, chlorate and bromate from other inorganic anions. Fig. 5 contrasts the new IonPac AS12A with the conventional acrylate-based IonPac AS9-SC anion exchanger, using simulated drinking water with more realistic concentrations of the disinfectant by-products as an example. As can be seen from these chromatograms, more than adequate resolution of both bromide and chlorate from nitrate can be achieved with both separators. However, the separation between fluoride, chlorite, bromate, chloride and nitrite on AS12A is clearly superior

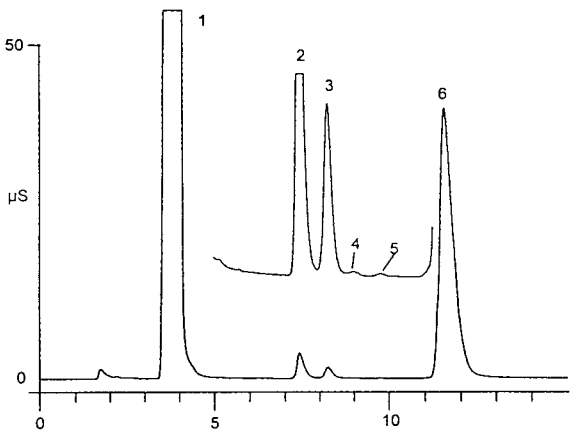

Fig. 7. Bath water analysis on an IonPac AS12A column. Chromatographic conditions as in Fig. 3; injection, 50 μl of a bath water sample with (1) 635 mg/l chloride, (2) 8.4 mg/l bromide, (3) 10 mg/l chlorate, (4) 0.04 mg/l nitrate, (5) 0.14 mg/l orthophosphate and (6) 105 mg/l sulfate.

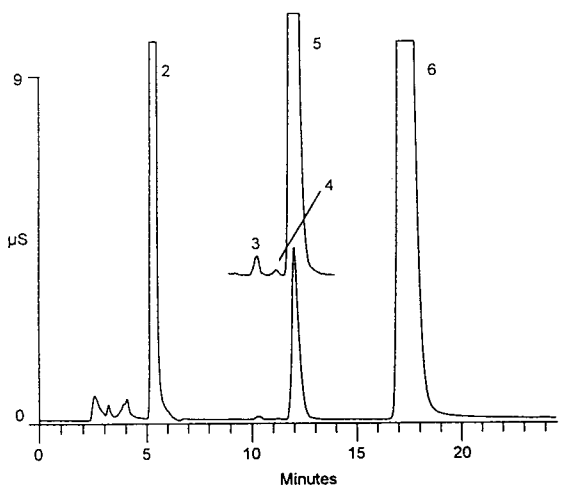

Fig. 6. Tap water analysis on an IonPac AS12A column. Chromatographic conditions as in Fig. 3; injection, 50 μl of a tap water sample with (1) 0.07 mg/l fluoride, (2) 58 mg/l chloride, (3) 0.17 mg/l bromide, (4) <0.10 mg/l chlorate, (5) 7.9 mg/l nitrate and (6) 75 mg/l sulfate.

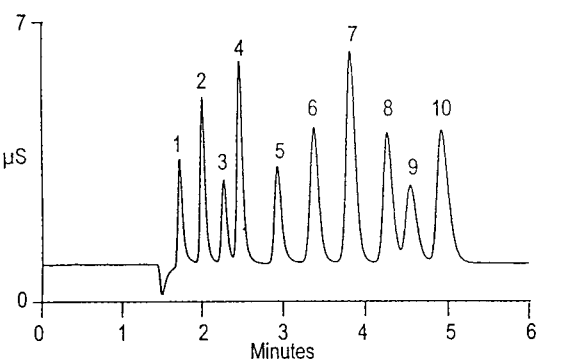

Fig. 8. Rapid separation of inorganic anions on an IonPac AS12A column. Eluent, 0.5 mmol/l sodium hydrogencarbonate–10.5 mmol/l sodium carbonate; flow-rate, 1.5 ml/min; detection, suppressed conductivity; injection volume, 10 μl. Solute concentrations: (1) 3 mg/l fluoride; (2) 20 mg/l chlorite; (3) 20 mg/l bromate; (4) 5 mg/l chloride; (5) 10 mg/l nitrite; (6) 30 mg/l orthophosphate; (7) 20 mg/l sulfate; (8) 20 mg/l bromide; (9) 20 mg/l chlorate; (10) 20 mg/l nitrate.

to that obtained with AS9-SC. Even short-chain fatty acids such as acetic acid, which co-elutes with fluoride on an AS9-SC column, can be partly separated from fluoride on an AS12A column under the given chromatographic conditions. In contrast, a polymeric quat-coated resin cannot be used for this purpose, as chlorite and chloride, nitrite and bromate and orthophosphate and chlorate co-elute, even under optimized chromatographic conditions. The only disadvantage of the AS12A column compared with the acrylate-based AS9-SC column is that polarizable anions such as iodide, thiocyanate and thiosulfate cannot be separated in the same run with mineral acids because they are highly retained.

Compared with the simulated drinking water shown in Fig. 5, the analysis of a real tap water sample renders more problems for determining anions with low affinities towards the stationary phase because of interferences in and around the system void volume. As shown in Fig. 6, fluoride can be separated from these interferences. However, the determination of chlorite, especially at trace levels, is interfered with by hydrogencarbonate present in this particular sample, thus displacing carbonate at the stationary phase. The displaced carbonate appears as a positive peak with a retention time similar to that of chlorite. The low chlorite concentration does not allow further dilution of the sample with deionized water, although this would remove the interference. Traces of chlorate, however, could be identified without any problems in this sample.

Because of its toxicity, chlorate is also a critical parameter in determining the water quality in swimming pools. The co-elution of nitrate and chlorate on conventional pellicular anion exchangers has often caused chlorate peaks to be misinterpretated as nitrate peaks. Fig. 7 shows a typical example of this kind of misinterpretation in the chromatogram of a sample that was

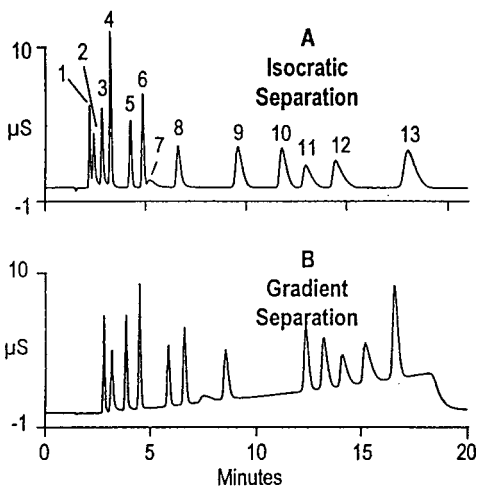

Fig. 9. Comparison of isocratic and gradient separation of anions on an IonPac AS12A column using a borate eluent. Isocratic separation: eluent, 20 mmol/l sodium borate–18 mmol/l sodium hydroxide. Gradient separation: eluent A, water; eluent B, 50 mmol/l sodium borate–37.5 mmol/l sodium hydroxide; gradient, linear from 22% to 73% B in 16 min. Flow-rate, 1.5 ml/min; detection, suppressed conductivity; injection volume, 25 μl. Solutes: (1) 5 mg/l fluoride; (2) 10 mg/l acetate; (3) 5 mg/l formate; (4) 5 mg/l chlorite; (5) 5 mg/l bromate; (6) 1 mg/l chloride; (7) 1 mg/l carbonate; (8) 2 mg/l nitrite; (9) 5 mg/l bromide; (10) 5 mg/l chlorate; (11) 5 mg/l nitrate; (12) 10 mg/l orthophosphate; (13) 5 mg/l sulfate.

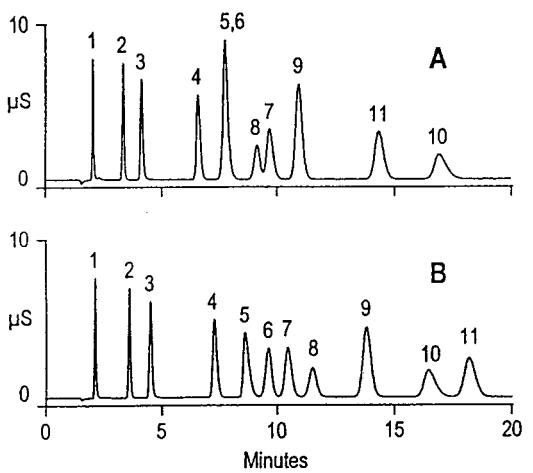

Fig. 10. Separation of common anions, sulfite, selenite, selenate, and arsenate on an IonPac AS12A column. Eluent A, 0.3 mmol/l sodium hydrogencarbonate–2.7 mmol/l sodium carbonate; eluent B, 0.8 mmol/l sodium hydrogencarbonate–2.1 mmol/l sodium carbonate; flow-rate, 1.5 ml/min; detection, suppressed conductivity; injection volume, 10 μl. Solute concentrations: (1) 3 mg/l fluoride; (2) 5 mg/l chloride; (3) 10 mg/l nitrite; (4) 20 mg/l bromide; (5) 20 mg/l nitrate; (6) 20 mg/l selenite; (7) 30 mg/l orthophosphate; (8) 20 mg/l sulfite; (9) 20 mg/l sulfate; (10) 40 mg/l arsenate; and (11) 20 mg/l selenate.

analysed using a conventional AS4A-SC anion exchanger. The signal appearing shortly after the bromide peak has erroneously been attributed to nitrate. With the baseline-resolved separation between bromide, chlorate and nitrate on IonPac AS12A, the unequivocal identification of this signal is possible. As can be seen from Fig. 7, nitrate is only present in this sample at a low ppb level, while the signal following bromide represents about 10 ppm of chlorate.

By modifying the carbonate-to-hydrogencarbonate ratio in the mobile phase, the analysis speed can be significantly increased. As can be seen from Fig. 8, the rapid elution of anions is accomplished with a mixture of 10.5 mmol/l sodium carbonate and 0.5 mmol/l sodium hydrogencarbonate at a flow-rate of 1.5 ml/min, allowing an analysis time of ca. 5 min. The ionic strength was adjusted so that orthophosphate and sulfate elute before bromide and nitrate. The chromatogram in Fig. 8 clearly demonstrates that under less demanding conditions the AS12A column is capable of the rapid determination of common anions with good resolution.

The chromatograms in Fig. 9 show the use of a borate eluent on the AS12A column for the separation of the common disinfectant by-products. The main advantage of this system is the ability to move the carbonate interference to a location in the chromatogram well away from chlorite and bromate where it does not interfere. Because of the high pH and the different elution properties of the borate eluent, carbonate elutes after chloride, being out of the way of the trace anions found in drinking water. However, as can be seen from the upper chromatogram in Fig. 9, the analysis is lengthy when employing a borate eluent on the AS12A column. Alternatively, a gradient technique can be applied in place of an

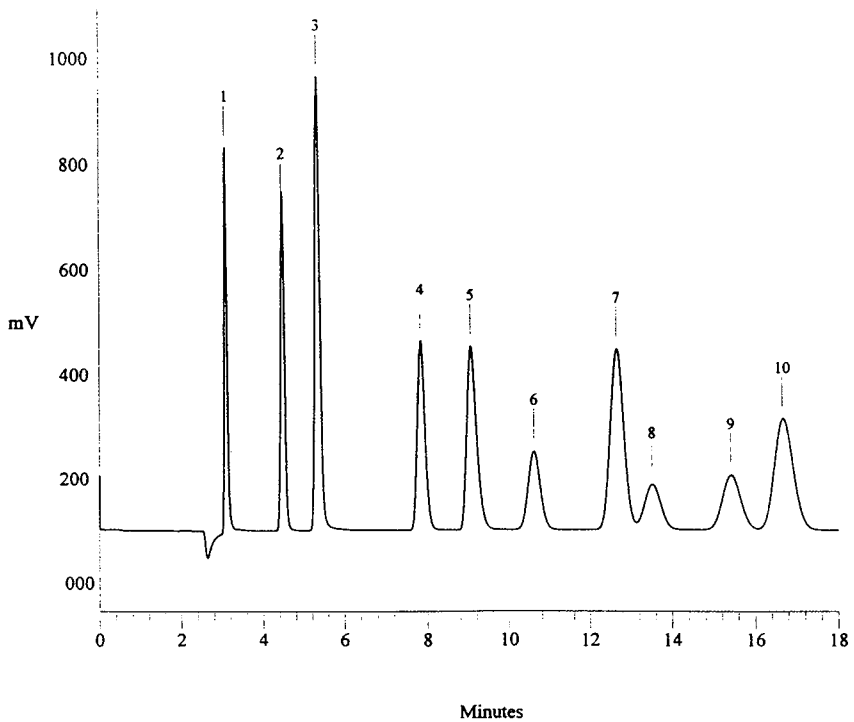

Fig. 11. Separation of common anions and aliphatic dicarboxylic acids on an IonPac AS12A column. Chromatographic conditions as in Fig. 3. Solute concentrations: (1) 3 mg/l fluoride; (2) 4 mg/l chloride; (3) 10 mg/l nitrite; (4) 10 mg/l bromide; (5) 10 mg/l nitrate; (6) 10 mg/l orthophosphate; (7) 10 mg/l sulfate; (8) 10 mg/l malate; (9) 10 mg/l tartrate; and (10) 10 mg/l oxalate.

isocratic eluent system for samples that are not trace in nature. For comparison, the bottom chromatogram in Fig. 9 shows the gradient separation of the same standard. As the baseline shift is modest, borate gradients on the AS12A column are suitable for a number of sample types.

In addition to disinfectant by-product separations, common anions and also sulfite, selenite, selenate and arsenate can be separated on the AS12A column. Under the chromatographic conditions in Fig. 3, resolution problems between nitrate and selenite and between orthophosphate and sulfite are observed (upper chromatogram in Fig. 10). This can be solved by modifying the carbonate-to-hydrogencarbonate ratio. As illustrated in Fig. 10 (bottom chromatogram), a mixture of 2.1 mmol/l sodium carbonate and 0.8 mmol/l sodium hydrogencarbonate results in a baseline-resolved separation of all analytes.

3.2. Organic acid analysis

A common problem with conventional polymer-based anion exchangers such as AS4A-SC and AS9-SC is that the retention behaviour of aliphatic dicarboxylic acids is very similar to that of inorganic anions such as bromide, nitrate, orthophosphate and sulfate. While orthophosphate can be moved out of the way by changing the pH of the mobile phase, the determination of the other three inorganic anions can be interfered with by organic acids, especially in food and beverage samples. Therefore, the retention

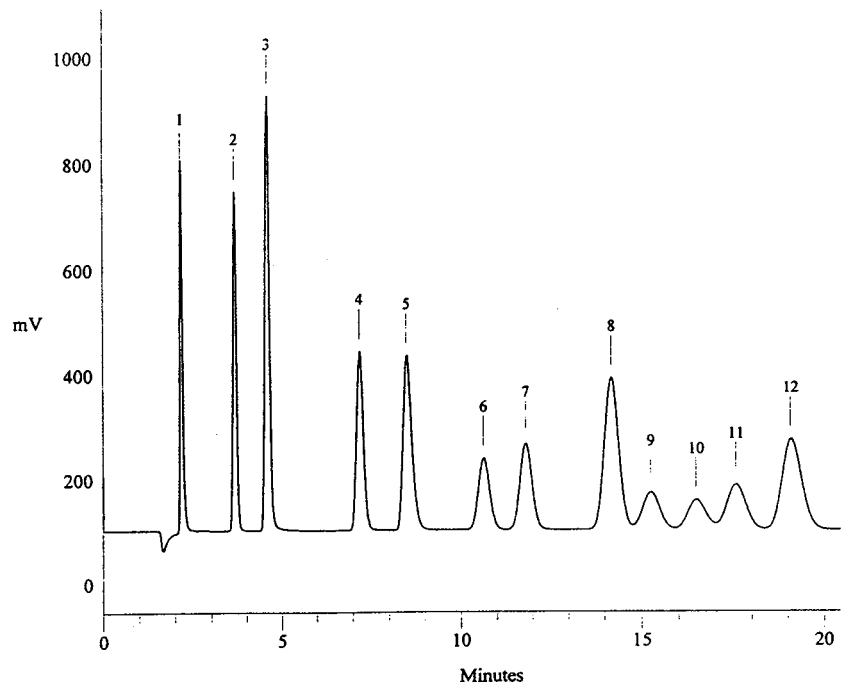

Fig. 12. Separation of common anions, oxy non-metal anions and aliphatic carboxylic acids on an IonPac AS12A column. Chromatographic conditions as in Fig. 10 (bottom chromatogram). Solute concentrations: (1) 3 mg/l fluoride; (2) 4 mg/l chloride; (3) 10 mg/l nitrite; (4) 10 mg/l bromide; (5) 10 mg/l nitrate; (6) 10 mg/l orthophosphate; (7) 10 mg/l sulfite; (8) 10 mg/l sulfate; (9) 10 mg/l malate; (10) 10 mg/l arsenate; (11) 10 mg/l tartrate; (12) 10 mg/l oxalate.

behaviour of malic, tartaric and oxalic acid was investigated under standard chromatographic conditions. The chromatogram in Fig. 11 shows that all three organic acids elute behind sulfate and therefore do not represent an interference in the determination of common inorganic anions.

The modified eluent system described in Fig. 10 (2.1 mmol/l sodium carbonate–0.8 mmol/l sodium hydrogencarbonate) enables all common inorganic anions, and also sulfite, arsenate and the organic acids mentioned above, to be determined in the same isocratic run (Fig. 12).

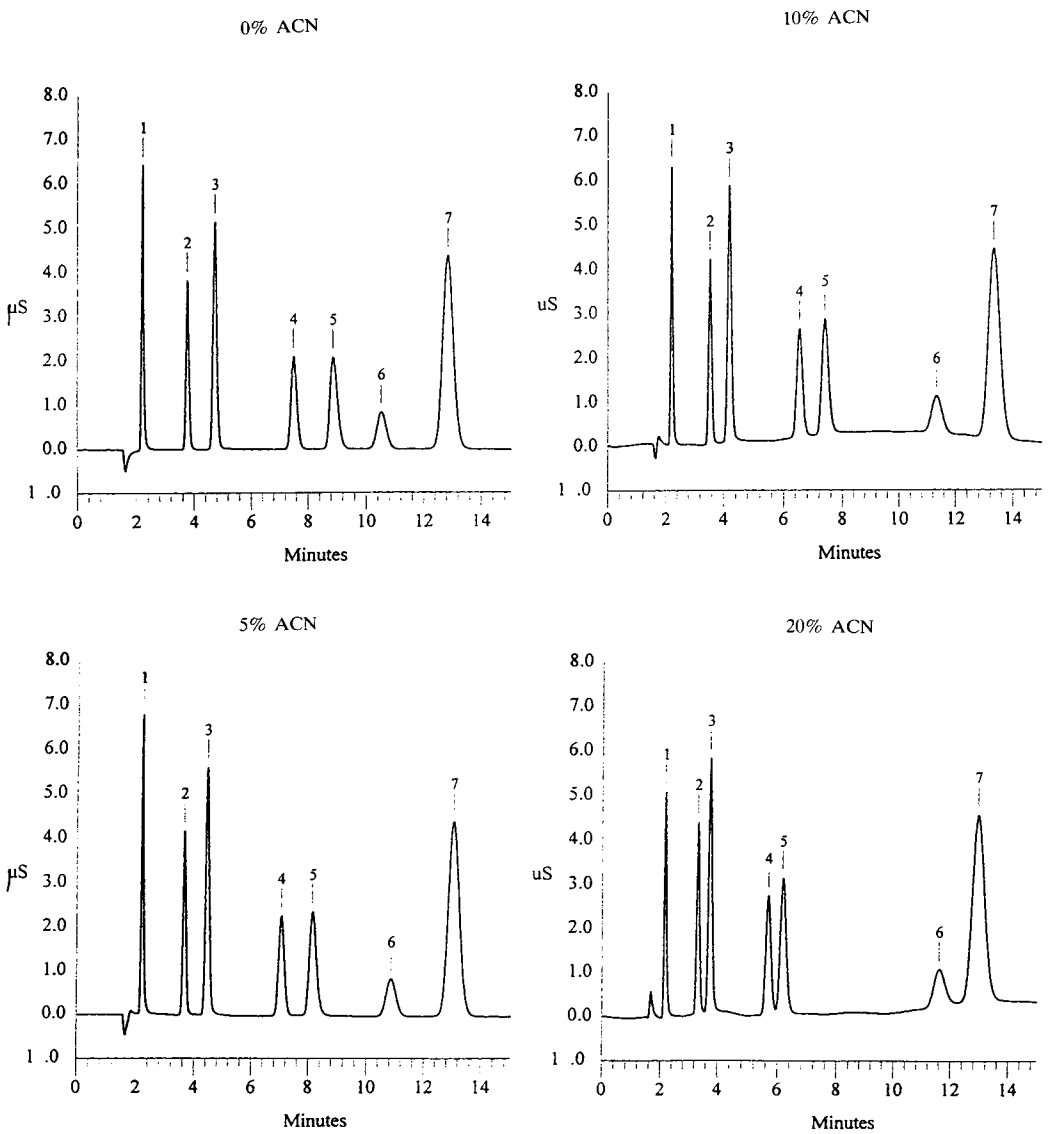

Fig. 13. Influence of organic solvents on the retention of common anions on an IonPac AS12A column. Eluent, 0.3 mmol/l sodium hydrogencarbonate–2.7 mmol/l sodium carbonate–acetonitrile; flow-rate, 1.5 ml/min; detection, suppressed conductivity; injection, 25 μl anion standard. Solute concentrations: (1) 3 mg/l fluoride; (2) 4 mg/l chloride; (3) 10 mg/l nitrite; (4) 10 mg/l bromide; (5) 10 mg/l nitrate; (6) 10 mg/l orthophosphate; (7) 20 mg/l sulfate.

3.3. Influence of organic solvents

As the AS12A column is solvent-compatible, organic solvents can be used to remove organic contaminants. In this respect, the resistance to humic acids was investigated. We consider this parameter to be important because most real water samples contain humic acids at various concentration levels. Also, the molecular mass distribution can differ considerably, ranging from 2000 to 500 000. The test was carried out with a humic acid standard with a molecular mass distribution between 600 and 1000. A 300 mg/l aqueous alkaline solution was prepared and injected twenty times. A significant deviation of the retention times of common inorganic anions was not observed. Column degradation was then simulated by injecting a concentrated liquid detergent formula without any sample preparation other than filtration. As expected, a decrease in capacity was observed with every injection. The original separation performance could be restored by rinsing the column with dilute HCl–acetonitrile (20:80, v/v) for 30 min.

Organic solvents can also be used to affect the selectivity of the anion exchanger. The influence of organic solvents on retention was investigated by injecting a standard solution of common inorganic anions under optimized chromatographic conditions (2.7 mmol/l sodium carbonate–0.3 mmol/l sodium hydrogencarbonate), adding different amounts of acetonitrile to the mobile phase. Fig. 13 shows the resulting chromatograms with solvent additions of 5, 10 and 20% (v/v). The effect is remarkable: whereas the retention of fluoride, chloride and sulfate does not change, orthophosphate moves slowly towards the sulfate peak, co-eluting with it at about 40% (v/v) acetonitrile in the mobile phase. As expected, anions undergoing adsorption in addition to the ion-exchange process, such as nitrite (to a certain extent), bromide and nitrate, are less retained with increasing solvent content in the eluent. Thus, polarizable anions strongly retained on an AS12A column can be decreased in retention by adding solvents to the mobile phase. On the other hand, with more than 20% (v/v) acetonitrile in the mobile phase, bromide and nitrate are no longer resolved.

References

[1] H. Small, T.S. Stevens, and W.C. Bauman, *Anal. Chem.*, 47 (1975) 1801.
[2] D.T. Gjerde and J. Fritz, *Ion Chromatography*, Hüthig, Heidelberg, 2nd ed., 1987.
[3] H. Small, *Ion Chromatography*, Plenum Press, New York, 1989.
[4] J. Weiss, *Ionenchromatographie*, VCH, Weinheim, 2nd ed., 1991.
[5] J. Weiss, *Ionenchromatographie*, VCH, Weinheim, 1991, pp. 67ff.
[6] J. Weiss, *Ionenchromatographie*, VCH, Weinheim, 1991, pp. 93ff.

ELSEVIER

Journal of Chromatography A, 706 (1995) 93–98

JOURNAL OF CHROMATOGRAPHY A

Modified silica as a stationary phase for ion chromatography

O.V. Krokhin, A.D. Smolenkov, N.V. Svintsova, O.N. Obrezkov*, O.A. Shpigun

Chemistry Department, M.V. Lomonosov Moscow State University, Lenin Hills, GSP-3, 119899 Moscow, Russian Federation

Abstract

The possibility of the rapid preparation of agglomerated anion exchangers was demonstrated on a reversed-phase silica support with the polymeric agents poly(N-ethyl-4-vinylpyridinium bromide), poly(dimethyldiallylammonium chloride), poly(hexamethyleneguanidinium hydrochloride) and 2,5-ionene as modifiers. A 90-min sorbent preparation and column packing allowed an efficiency of more than 10000 theoretical plates per metre to be obtained for 10-μm spherical beads. The polymeric agents showed different selectivity, stability and capacity for the resulting anion exchangers (owing to changes in the structure and the density of functional groups in the polymer chain). The sorbents were used for the simultaneous determination of weakly and strongly retained anions and some heavy metals with EDTA solutions as eluent.

1. Introduction

Many packing materials are available for the separation of anions by ion chromatography (IC) and polymer-based and silica-based sorbents are very common [1]. Silica-based sorbents have the advantage of high mechanical strength and performance. However, eluents of high pH will damage the columns. Vydac IC 302 is one example of a surface-bonded silica packing [2].

Polymer-based materials are more popular for the suppressed ion chromatography of anions as they are stable in alkaline media. Surface-agglomerated resins were prepared by Small et al. [3] in which fine particles of anion-exchange latex are attracted to the superficial sulfonated beads of polymers.

A simple way to prepare anion exchangers for IC is to coat commercially available reversed-phase material with quaternary ammonium salts [4,5]. Coated anion-exchange resins with various capacities have been produced by static and dynamic procedures.

The aim of this study was the production of new sorbents with different selectivities and to study the factors that influence selectivity. An attempt was made to prepare sorbents for anion IC using the interaction of polymeric anion exchangers with dynamically coated reversed-phase silica.

2. Experimental

A SIC-800 ion chromatograph (Biotronik, Maintal, Germany) with UV and conductivity detectors and a Shimadzu CR-3A integrator was

* Corresponding author.

0021-9673/95/$09.50
SSDI 0021-9673(94)01244-X

used. The separation column used was made of stainless steel (100 × 3 mm I.D.).

The eluents were prepared by dissolving analytical-reagent grade potassium hydrogenphthalate or EDTA (or their mixtures) in deionized water and adjusting the pH value with potassium hydroxide. Stock standard solutions of inorganic anions and heavy metals were prepared from the salts and diluted to the desired concentrations. On-column and precolumn (with potassium hydrogenphthalate as eluent) formation of the metal–EDTA complexes was used.

For sorbent preparation, the required amount of 10-μm spherical Silasorb C_8 (Lachema, Brno, Czech Republic) was shaken with an excess of dodecylbenzenesulfonic acid (DBSA) solution (Johnson Matthey, Karlsruhe, Germany). Polymer solution (from the High-Molecular-Mass Compounds Division of Lomonosov Moscow State University) in deionized water was added to modified Silasorb C_8 immediately after centrifugation and removal of excess DBSA. The columns were filled using common packing procedures and washed with the eluent for 60 min. The polymer structures are summarized in Table 1.

3. Results and discussion

Dynamically coated cation-exchangers with a low capacity (0.1–0.2 mmol/g) were obtained in the first stage of modification with DBSA. The final capacity of anion exchangers (Table 1) depends on the functional group density of the polymer chain. Thus, PEVP produced a higher capacity than Ionene, because PEVP has one quaternary ammonium group per two atoms in the chain and Ionene has two groups per nine atoms.

Table 1
Polymer structures and capacities of agglomerated anion exchangers

Polymer	Structure	Capacity (mmol/g)
Poly(N-ethyl-4-vinyl Pyridinium bromide) (PEVP)	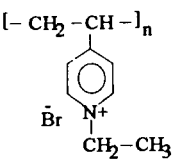	0.032
Poly(dimethyldiallyl ammonium chloride) (PDMDAA)	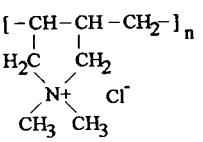	0.031
Poly(hexamethylene guanidinium hydrochloride)(PHMG)	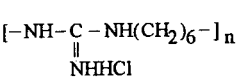	0.012
2,5-Ionene (Ionene)	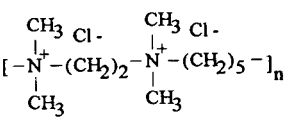	0.010

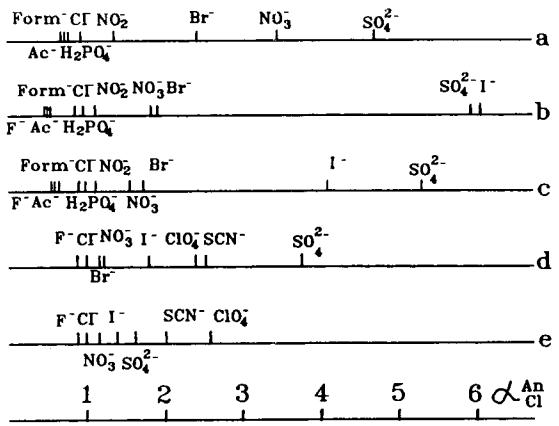

Fig. 1. Scales of selectivity for Silasorb C_8 (a) coated with CTMA and agglomerated with (b) PEVP, (c) PDMDAA, (d) PHMG, and (e) Ionene to some anions. α_{Cl}^{An} = Selectivity factor. Eluent, 1.0 mmol/l potassium hydrogenphthalate (pH 6.0).

The selectivities of the different exchangers were investigated using 1 mmol/l potassium hydrogenphthalate (pH 6.0), as the eluent. The retention times of several anions and the selectivity scales are shown in Table 1 and Fig. 1, respectively. The polymer-coated stationary phases are compared with Silasorb C_8 that was dynamically coated with cetyltrimethylammonium bromide (Silasorb C_8-CTMA), which is commonly used for coating reversed-phase silica in IC. The anion retentions decreased with decreasing column capacity, as shown by comparing Tables 1 and Table 2. The behaviour of anions, with the exception of SCN- and ClO_4^-, does not depend on the type of polymer. It is interesting that an increase in the distance between the silica surface and the exchange layer leads to a decrease in the affinity to the N-containing anions (compare Fig. 1a and c). A linear relationship between log k' and log C_{el} was observed for all packing materials and anions.

The simultaneous determination of strongly and weakly retained anions could be performed using Silasorb C_8–PHMG and Silasorb C_8–Ionene (Figs. 2 and 3). Strongly retained anions were not eluted from Silasorb C_8–PEVP with 1 mmol/l potassium hydrogenphthalate (pH 6.0) as eluent. However, it was demonstrated that the concentration and pH of the mobile phase affected the separation of complex mixtures (Fig. 4).

The possibility of a decrease in capacity for this system should be taken into account. This decrease may be caused by two effects. The first is the desorption of DBSA. Thus, attempts to obtain reproducible results using Silasorb C_2 support were unsuccessful. A tenfold decrease in capacity was observed after 100 ml of the eluent

Table 2
Retention times of some anions on the agglomerated anion exchangers

Anion	Retention time (min)				
	Silasorb C_8–CTMA	Silasorb C_8–PEVP	Silasorb C_8–PDMDAA	Silasorb C_8–PHMG	Silasorb C_8–Ionene[a]
F^-	–	0.81	0.93	0.59	0.78
Acetate	1.00	0.83	0.94	–	0.77
Formate	1.05	0.98	1.09	–	0.79
$H_2PO_4^{2-}$	1.17	1.59	1.67	–	0.82
Cl^-	1.44	1.78	1.77	0.71	0.84
NO_2^-	2.20	2.05	1.84	–	0.86
NO_3^-	4.90	3.37	2.60	0.91	0.90
Br^-	3.60	3.49	3.01	0.81	0.92
I^-	–	10.97	7.50	1.25	1.18
SO_4^{2-}	7.05	10.87	9.60	2.65	1.34
SCN^-	>30	>30	>30	1.85	1.69
ClO_4^-	>30	>30	>30	1.75	2.18

Conditions: column, 100 × 3 mm I.D.; eluent, 1 mmol/l potassium hydrogenphthalate (pH 6.0); flow-rate, 1.5 ml/min; indirect UV detection (λ = 260 nm).
[a]Flow-rate 1.0 ml/min.

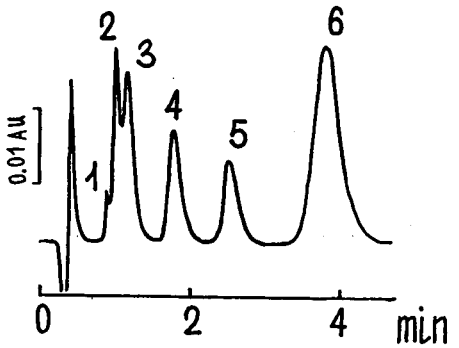

Fig. 2. Rapid separation of strongly and weakly retained anions. Column, Silasorb C_8–PHMG; eluent, 1 mmol/l potassium hydrogenphthalate (pH 6.0); flow-rate, 1.0 ml/min; indirect UV detection ($\lambda = 260$ nm). Peaks: 1 = F^-; 2 = Cl^-; 3 = Br^-; 4 = I^-; 5 = ClO_4^-; 6 = SO_4^{2-}.

(pH 4) had passed through the Silasorb C_2–PEVP column. The second effect is the weak electrostatic attraction of the PHMG chain to the sulfonated surface, which led to a twofold decrease in the capacity of Silasorb C_8 matrix after 4 l of the eluent had passed through the column.

The highest stability was obtained for the Silasorb C_8–PEVP system; the retention times and column efficiencies were constant during 2 months of continuous work. An efficiency of more than 10000 theoretical plates per metre was

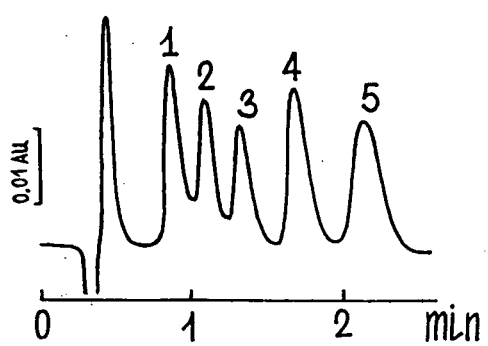

Fig. 3. Rapid separation of strongly and weakly retained anions. Column, Silasorb C_8–Ionene; eluent, 1 mmol/l potassium hydrogenphthalate (pH 6.0); flow-rate, 1.0 ml/min; indirect UV detection ($\lambda = 260$ nm). Peaks: 1 = Cl^-; 2 = I^-; 3 = SO_4^{2-}; 4 = SCN^-; 5 = ClO_4^-.

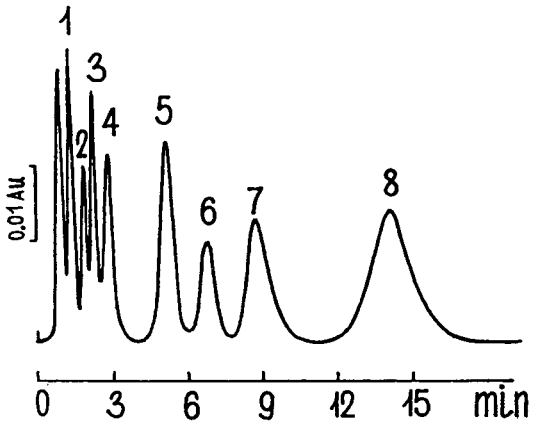

Fig. 4. Chromatographic separation of some anions. Column, Silasorb C_8–Ionene; eluent, 2.6 mmol/l potassium hydrogenphthalate (pH 7.0); flow-rate, 1.3 ml/min; indirect UV detection ($\lambda = 260$ nm). Peaks: 1 = IO_3^-; 2 = Cl^-; 3 = $H_2PO_4^-$; 4 = NO_3^-; 5 = SO_4^{2-}; 6 = I^-; 7 = SCN^-; 8 = ClO_4^-.

observed for all the packing materials, with the exception of systems showing a large decrease in capacity (Silasorb C_2–PEVP and Silasorb C_8–PHMG).

Because of the good stability of the Silasorb C_8–PEVP column, it was used for the simultaneous determination of inorganic anions and heavy metals. First, retention times of the anions and metal–EDTA complexes were obtained with potassium hydrogenphthalate–EDTA (pH 7) eluent (Fig. 5). Various detection parameters for UV detection ($\lambda = 210$–260 nm) or conductivity detection were used for peak identification. Indirect UV ($\lambda = 260$ nm) and direct UV ($\lambda = 210$ nm) or conductivity detection was used for the eluents with predominant potassium phthalate and EDTA, respectively. Thus, the addition of triply charged EDTA to the phthalate eluent led to a decrease in the retention for all of the analytes. The selectivity did not change for the equally charged anions. However, the retention of I^- and SCN^- increased with an EDTA-only eluent, which indicates that the phthalate anions are characterized by strong hydrophobic interactions with the sorbent. Figs. 6 and 7 illustrate the ability of the Silasorb C_8–PEVP packing for the simultaneous determination of anions and heavy

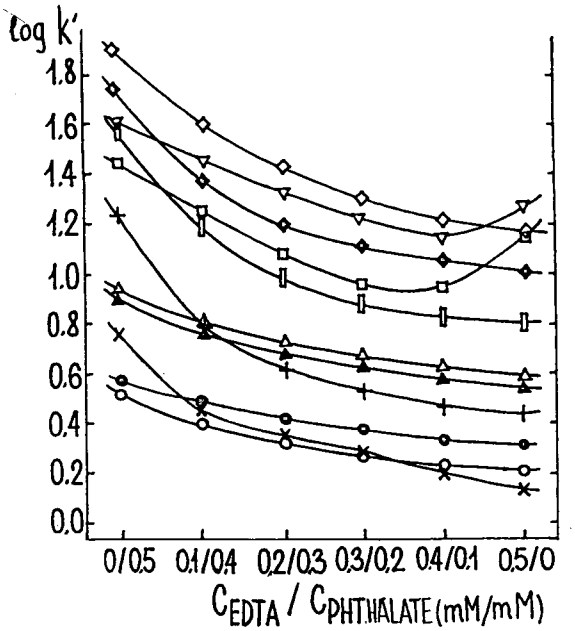

Fig. 5. Influence of the ratio of EDTA to potassium hydrogenphthalate concentration in the eluent (pH 7.0). Column, Silasorb C_8–PEVP; UV and conductivity detection. ○ = Cl^-; ◉ ≙ NO_2^-; × = $H_2PO_4^-$; △ = Br^-; ▲ = NO_3^-; + = Pb(II), Mn(II); = SO_4^{2-}, Co(II), Cd(II), Zn(II); ◆ = Ni(II); ◇ = Cu(II); □ = I^-; ▽ = SCN^-.

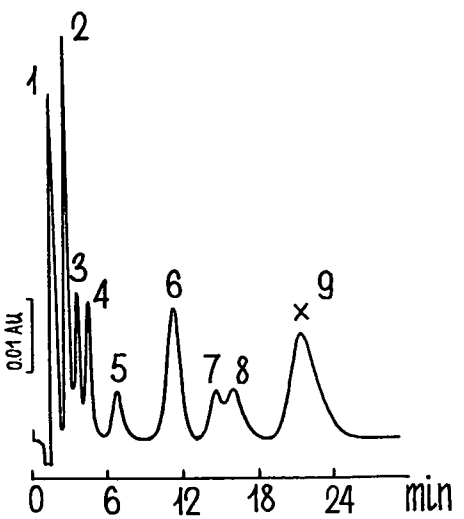

Fig. 6. Simultaneous IC of some anions and metal–EDTA complexes. Column, Silasorb C_8–PEVP; eluent, 1.5 mmol/l potassium hydrogenphthalate (pH 6.9); flow-rate, 1.0 ml/min, indirect UV detection (λ = 260 nm). Peaks: 1 = acetate; 2 = Cl^-; 3 = $H_2PO_4^-$; 4 = Br^-; 5 = Mn(II); 6 = SO_4^{2-}; 7 = SCN^-; 8 = Ni(II); 9 = Cu(II); × = reversed negative signal.

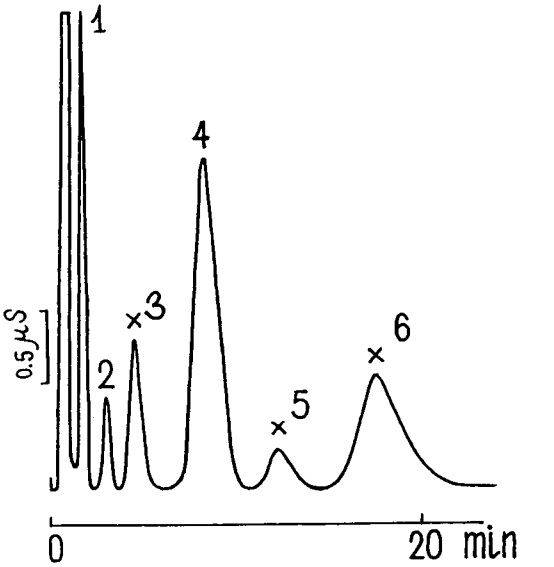

Fig. 7. Simultaneous IC of some anions and metal–EDTA complexes with EDTA as eluent. Column, Silasorb C_8–PEVP; eluent, 0.2 mmol/l EDTA (pH 7.0); flow-rate, 0.75 ml/min; conductivity detection. Peaks: 1 = Cl^-; 2 = NO_3^-; 3 = Mn(II); 4 = SO_4^{2-}; 5 = Ni(II); 6 = Cu(II); × = reversed negative signal.

metals. Fig. 5 also shows that the separation of Pb(II) and Mn(II) or SO_4^{2-}, Co(II), Cd(II) and Zn(II) could not be achieved by changing the concentration of the eluent components in the range shown in Fig. 5. Moreover, it is possible to alter the selectivity of this sorbent for non-resolvable analytes, e.g., by simultaneously varying the pH and the eluent concentration of potassium hydrogenphthalate and EDTA (Fig. 8). Under these conditions the peaks of SO_4^{2-}, Co(II), Cd(II), and Zn(II) are successfully resolved. Unfortunately, a complicated composition of the eluent leads to the formation of a system peak and changes in the direction of some peaks.

Acknowledgement

This work was supported by Eppendorf-Biotronik (Maintal, Germany).

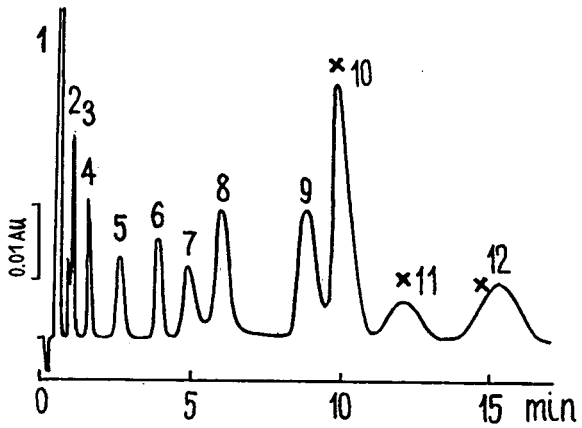

Fig. 8. Simultaneous IC of some anions and metal–EDTA complexes with potassium hydrogen phthalate–EDTA mixture as eluent. Column, Silasorb C_8–PEVP; eluent: 1.0 mmol/1 potassium hydrogenphthalate–0.5 mmol/1 EDTA (pH 6.0); flow-rate, 1.0 ml/min; indirect UV detection (λ = 260 nm). Peaks: 1 = acetate; 2 = Cl^-; 3 = NO_2^-; 4 = NO_3^-; 5 = Mn(II); 6 = SO_4^{2-}; 7 = Zn(II); 8 = Co(II); 9 = Cd(II); 10 = system peak; 11 = Ni(II); 12 = Cu(II); × = reversed negative signal.

References

[1] P.R. Haddad and P.E. Jackson, *Ion Chromatography: Principles and Applications* (*Journal of Chromatography Library*, Vol. 46), Elsevier, Amsterdam, 1990, Ch. 3, p. 29.
[2] P.R. Haddad, P.E. Jackson and A.L. Heckenberg, *J. Chromatogr.*, 346 (1985) 139.
[3] H. Small, T.S. Stevens and W.W. Bauman, *Anal. Chem.*, 47 (1975) 1801.
[4] R.M. Cassidy and S. Elchuk, *Anal. Chem.*, 54 (1982) 1558.
[5] R.M. Cassidy and S. Elchuk, *J. Chromatogr. Sci.*, 21 (1983) 454.

ELSEVIER

Journal of Chromatography A, 706 (1995) 99–102

JOURNAL OF CHROMATOGRAPHY A

Short communication

Cation analysis on a new poly(butadiene–maleic acid)-based column

Markus W. Läubli*, Barbara Kampus

Metrohm Ltd., CH-9101 Herisau, Switzerland

Abstract

The use of poly(butadiene–maleic acid)-coated silica for the determination of monovalent and divalent cations is well accepted in ion chromatography. The new Metrosep Cation 1-2 column based on this type of material extends the use of such materials to a broad range of amines due to its improved stability against organic solvents. Sample preparation was performed by diluting the sample in eluent or at least millimolar nitric acid.

1. Introduction

Since its introduction in 1989 by Schomburg [1] the poly(butadiene–maleic acid)-coated silica found a wide range of applications in ion chromatography (IC) [2,3]. This material showed a relatively poor stability against organic solvents. The use of eluents containing more than 5% organic solvents led to a loss of capacity and resolution within a short time. Therefore, the use of eluents containing such organics has been limited. The new Metrosep Cation 1-2 column (Metrohm, Herisau, Switzerland) is based on the same type of ion exchanger, but with much improved stability against organics. This improvement could be reached by using a different manufacturing procedure. This type of material may be washed with pure acetone without any change in separation performance. Due to the carboxylic groups alcohols should be avoided as eluent modifiers. Therefore, the direct determination of different basic components (amines, ethanolamines, etc.) is possible by using eluents with organic modifier.

2. Experimental

All measurements were performed on an IC instrument comprising a 709 IC pump, 690 ion chromatograph (both Metrohm). Data acquisition took place on a 714 IC Metrodata integration system (Metrohm). All chemicals used were purchased from Fluka (Buchs, Switzerland) or Merck (Darmstadt, Germany) and used without further purification.

Eluents were prepared with freshly deionized water and the respective amounts of components as mentioned in the figure legends. Eluents were degassed for about 2 min under vacuum.

Sample solutions were prepared in 2 mmol/l nitric acid or eluent except in case of the pH dependence measurements.

* Corresponding author.

0021-9673/95/$09.50
SSDI 0021-9673(95)00235-9

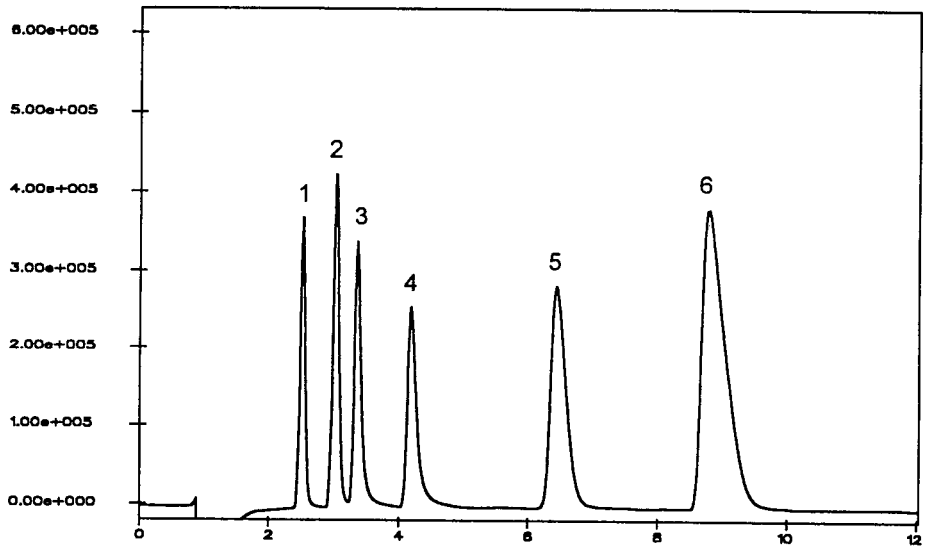

Fig. 1. Determination of alkali and alkaline earth metal cations. Eluent: 4 mmol/l tartaric acid–1 mmol/l dipicolinic acid. Peaks: 1 = lithium (1 ppm); 2 = sodium (5 ppm); 3 = ammonium (5 ppm); 4 = potassium (10 ppm); 5 = calcium (10 ppm); 6 = magnesium (10 ppm).

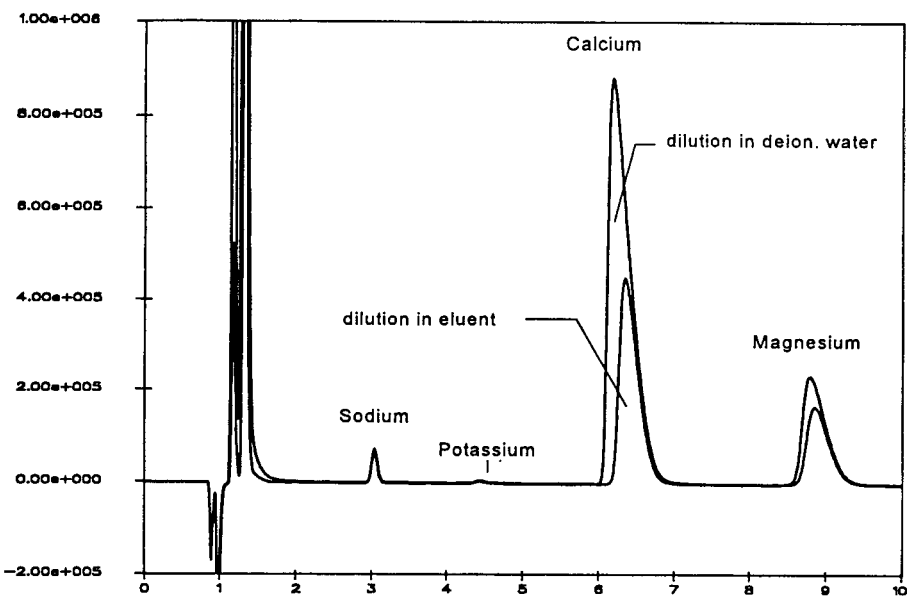

Fig. 2. Influence of sample acidification of drinking water. Drinking water was 1:10 diluted with deionized water or eluent, respectively. Eluent: 4 mmol/l tartaric acid–1 mmol/l dipicolinic acid.

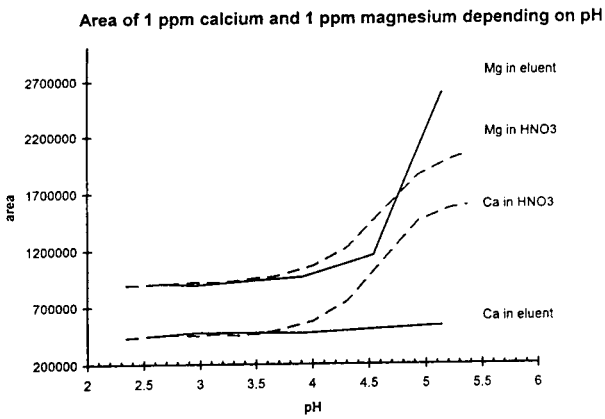

Fig. 3. Influence of sample pH on peak area and height. Ca^{2+} and Mg^{2+} in HNO_3: the standard solutions were prepared in the appropriate concentration of HNO_3 to reach the respective pH value. Ca^{2+} and Mg^{2+} in eluent: the standard solutions were prepared in eluent and adjusted to the respective pH with 2 *M* NaOH.

3. Results and discussion

3.1. Alkali and alkaline earth metal

The Metrosep Cation 1-2 column is packed with a weak cation exchanger that was based on spherical silica gel coated with poly(butadiene–maleic) acid groups. The main application is the determination of alkali and alkaline earth metal within a single isocratic run.

Fig. 1 presents the separation of lithium, sodium, ammonium, potassium, calcium and magnesium within 10 min, using 4 mmol/l tartaric acid–1 mmol/l dipicolinic acid as eluent.

Dipicolinic acid acts as complexing agent for heavy metals and calcium. As a result, the heavy metals are eluted with the front peak and calcium is moved in front of the magnesium peak thus improving the separation of the divalent cations.

3.2. Sample pretreatment

Cation analysis requires a correct sample pretreatment to get reproducible results. Fig. 2 presents two injections of drinking water diluted with either deionized water or eluent. The area of the divalent cation depends on the sample pH.

As Fig. 2 shows, the calcium peak is 2.3 and the magnesium peak 1.5 times larger than the peaks of the acidified sample.

Reproducible results were obtained when stan-

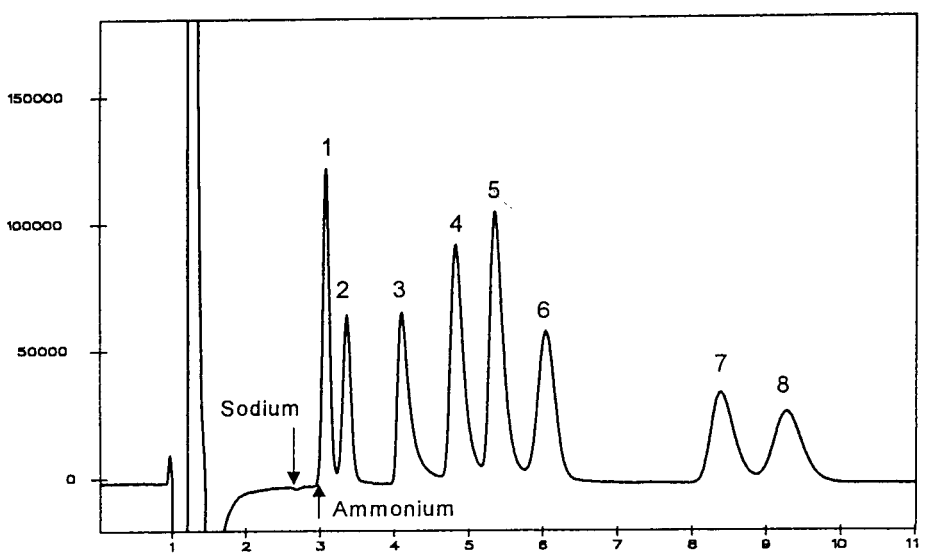

Fig. 4. Separation of organic amino compounds. Eluent: 8 mmol/l tartaric acid–10% acetone. Peaks: 1 = ethanolamine (5 ppm); 2 = diethanolamine (5 ppm); 3 = dimethylamine (5 ppm); 4 = diethylamine (10 ppm); 5 = trimethylamine (10 ppm); 6 = cyclohexylamine (10 ppm); 7 = triethylamine (10 ppm); 8 = dibutylamine (10 ppm).

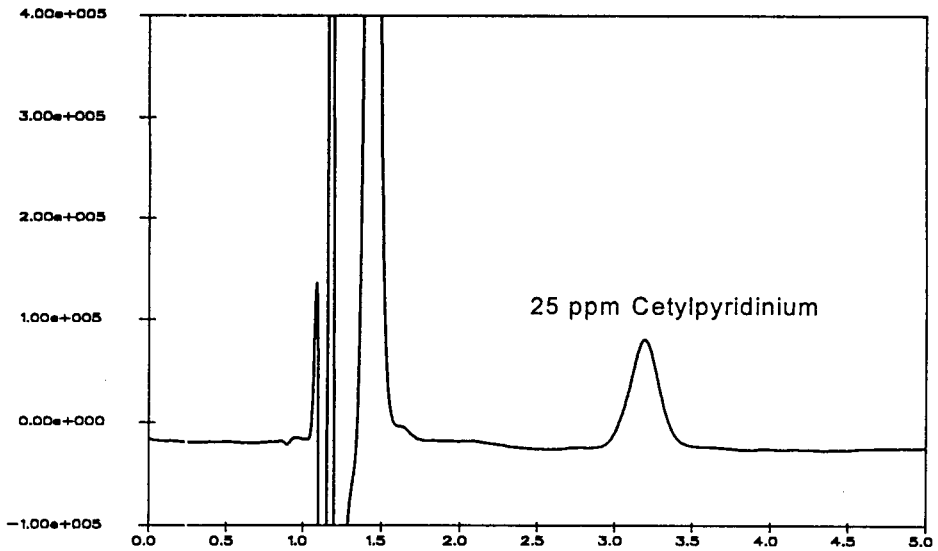

Fig. 5. Determination of cetylpyridinium chloride in throat tablets. Eluent: 10 mmol/l tartaric acid–1 mmol/l dipicolinic acid–2 mmol/l HNO_3–60% acetone.

dard and sample were prepared in eluent or nitric acid; thereby the pH should reach a value between 2.5 and 3.5 (see Fig. 3).

The influence of this pretreatment on area and height of the monovalent cations is very small. The reason for this pH dependence is not yet clear and has to be investigated further. The same effect can be recognized on other types of cation exchangers (e.g. silica-based strong acid cation exchangers) [4].

3.3. Organic modifiers

The Metrosep Cation 1-2 column can be used with a variety of eluents; especially the wide range of organic modifier concentrations makes it possible to analyse organic amines by direct conductivity detection.

Fig. 4 presents the separation of ethanolamines, alkylamines and cyclohexylamine.

Fig. 5 presents the determination of cetylpyridinium chloride (hexadecylpyridinium chloride) in throat tablets. After dissolving the tablet in eluent followed by filtration (0.25 μm), the solution could be injected directly without further sample preparation.

Under these conditions, the component can be analyzed without interference of other organic compounds.

References

[1] G. Schomburg, P. Kolla and M.W. Läubli, *Int. Lab.*, 4 (1989) 40–48.
[2] M.W. Läubli, in P.A. Williams (Editor), *Recent Development in Ion Exchange*, 1990, pp. 31–39.
[3] L.M. Nair, R. Saari-Nordhaus and J.M. Anderson, Jr., *J. Chromatogr.*, 640 (1993) 41–48.
[4] M.W. Läubli, unpublished results.

ELSEVIER

Journal of Chromatography A, 706 (1995) 103–107

JOURNAL OF CHROMATOGRAPHY A

Selectivity enhancement on a poly(butadiene–maleic acid)-coated cation phase induced by ethylene oxide-based complexing agents

Markus W. Läubli*, Barbara Kampus

Metrohm, CH-9101 Herisau, Switzerland

Abstract

Crown ethers as well as acyclic compounds bearing ethylene oxide units are well-known as complexing agents for different cations. They are mainly used as ionophores in ion selective electrodes. In ion chromatography some studies have been preformed using crown ether stationary phases.

Using crown ethers as eluent components for the separation of alkali and alkaline earth metal cations on a poly(butadiene–maleic acid)-coated phase, it is possible to tune the selectivity to the special needs of the sample. An eluent with addition of 18-crown-6 elutes potassium after magnesium and calcium with an improved separation of sodium and ammonium compared to the same eluent without addition of 18-crown-6. In contrast, the addition of a polyethylene glycol improves the sodium ammonium separation without changing the elution order.

1. Introduction

The simultaneous and isocratic separation of alkali and alkaline earth metal cations with poly(butadiene–maleic acid)-coated silica has been introduced by Schomburg et al. [1]. The Metrosep Cation 1-2 (Metrohm, Herisau, Switzerland) is based on the same type of material, but with improved stability against organic solvents which especially allows also the determination of different amines [2]. The usage of dipicolinic acid as eluent additive enables the determination of the above-mentioned cations within 10 min [3].

Sodium and ammonium are separated to baseline on this type of material but selectivity is poor compared to e.g. strong acid silica-based materials. Particularly the determination of low amounts of ammonium in an excess of sodium is difficult. Ivask et al. [4] used polyethylene glycols (PEG) to improve this selectivity on methacrylate-based strong acid ion exchangers. We tested the addition of polyethylene glycols to the weak acid ion exchanger Metrosep Cation 1-2 and found the same effect, but the rather large contamination with sodium in commercially available products minimizes the use of these types of eluents.

Crown ethers are well-known as complexing agents for monovalent cations and are used in ion chromatography [5,6]. We tested the use of crown ethers as eluent additives on the Metrosep Cation 1-2 ion exchanger.

* Corresponding author.

0021-9673/95/$09.50
SSDI 0021-9673(95)00262-6

2. Experimental

All measurements have been performed on an ion chromatograph consisting of a 709 IC-pump, 690 ion chromatograph (both from Metrohm, Herisau, Switzerland). Data acquisition was performed with a 714 IC-Metrodata integration system (Metrohm). All chemicals used were purchased from Fluka (Buchs, Switzerland) or Merck (Darmstadt, Germany) and were used without further purification.

Eluents were prepared with freshly deionized water. The composition of the eluents is given in the legends to the figures. Eluents were degassed for about 5 min under vacuum. The eluents were used without any further pH adjustments.

Sample solutions were prepared in 2 m*M* nitric acid [2].

3. Results and discussion

3.1. Polyethylene glycols

In preliminary tests on a Super-Sep cation column, which is the original material introduced by Schomburg et al. [1], three different polyethylene glycols have been tested (PEG 400, PEG 1000 and PEG 3000). Due to contamination with sodium and baseline disturbances in the chromatograms, PEG 1000 and PEG 3000 have not been used further.

With the standard eluent the new Metrosep Cation 1-2 [2] shows almost baseline separation between sodium and ammonium (Fig. 1).

The addition of 5% of PEG 400 to this eluent leads to shorter retention times and a better separation between ammonium and sodium. Fig.

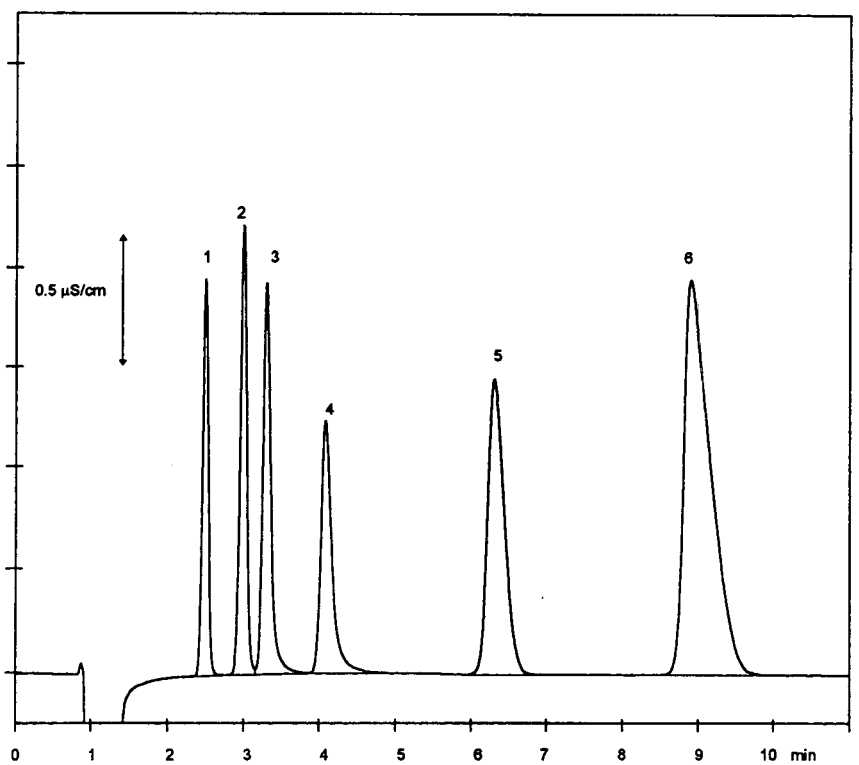

Fig. 1. Separation of Li^+ (1 = 1 mg/l), Na^+ (2 = 5 mg/l), NH_4^+ (3 = 5 mg/l), K^+ (4 = 10 mg/l), Ca^{2+} (5 = 10 mg/l) and Mg^{2+} (6 = 10 mg/l) on Metrosep Cation 1-2. Eluent: 4 mmol/l tartaric acid, 1 mmol/l dipicolinic acid. Flow-rate 1 ml/min. Injection volume 10 µl.

2a shows a standard chromatogram with this eluent. The separation of the peak apexes is now 0.4 min compared to 0.3 min without PEG (Fig. 2b).

The eluent contains about 0.2 mg/l sodium as well as traces of ammonium due to contamination of the PEG 400. The fairly small improvement in selectivity and the contamination of the eluent limits the use of such an eluent.

3.2. Crown ethers

Three crown ethers (15-crown-5, 18-crown-6 and dibenzo-18-crown-6) have been used in the present study. 15-Crown-5 contains five oxygen atoms which may act as coordination sites. The cavity built by this compound is small and only lithium can be complexed. The two other compounds contain six oxygen atoms and their cavity fits well to potassium.

The influence of these crown ethers is analyzed by adding different amounts of the respective compound to the standard eluent. Table 1 summarizes the results for the six cations lithium, sodium, ammonium, potassium, calcium and magnesium.

There is virtually no influence of 15-crown-5 on the retention times. Both 18-crown-6 and dibenzo-18-crown-6 show a large influence on potassium elution. With increasing concentrations of this crown ether potassium elutes later. At ca. 0.5 mmol/l potassium elutes at the same time as magnesium. With 1 mmol/l potassium elutes well separated after magnesium. Here it is very important to use dipicolinic acid in the eluent to avoid coelution of potassium and calcium. Dibenzo-18-crown-6 is even more powerful in changing the elution of potassium.

Another important difference between the two 18-crown-6 types is primarily seen in the be-

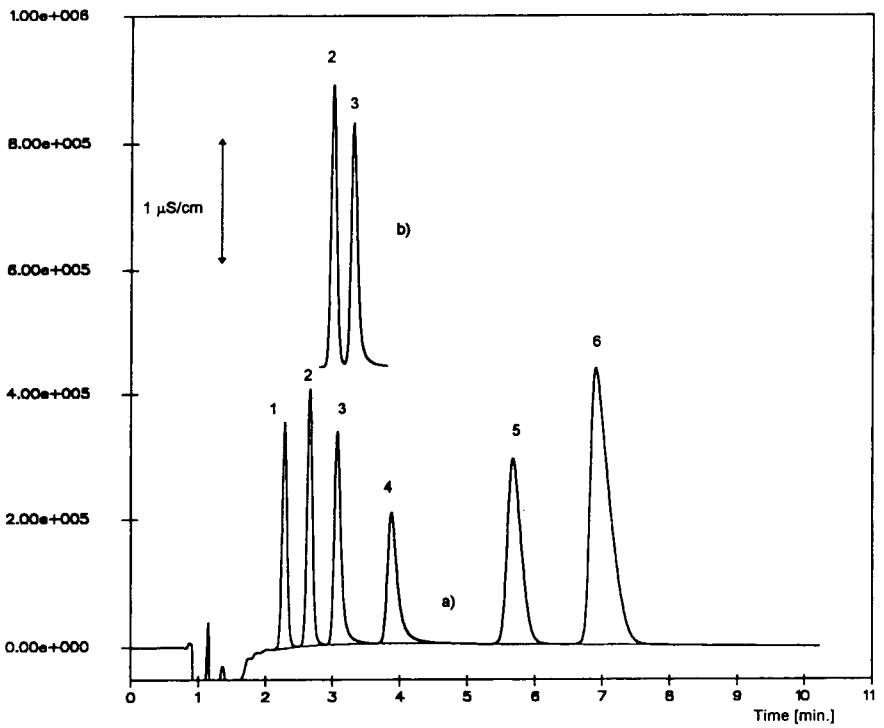

Fig. 2. Standard cations with addition of 5% PEG 400 to the eluent (same conditions and numbering as in Fig. 1): (a) chromatogram with PEG 400; (b) sodium and ammonium part of chromatogram without PEG 400.

Table 1
Influence of crown ethers on the selectivity of Metrosep Cation 1-2[a]

Crown ether (mmol/l)	Retention time (min)					
	Lithium	Sodium	Ammonium	Potassium	Calcium	Magnesium
15-Crown-5						
0.00	2.52	3.02	3.33	4.18	6.40	9.09
0.50	2.52	3.09	3.35	4.26	6.45	9.10
1.00	2.50	3.09	3.31	4.26	6.33	8.86
1.50	2.50	3.12	3.32	4.31	6.36	8.84
18-Crown-6						
0.00	2.50	2.99	3.29	4.08	6.30	8.89
0.10	2.51	3.08	3.49	5.68	6.47	9.09
0.25	2.51	3.13	3.64	7.09	6.51	9.01
0.50	2.48	3.19	3.82	9.25	6.56	8.77
1.00	2.49	3.32	4.17	12.0	6.87	8.84
Benzo-18-Crown-6						
0.00	2.52	3.02	3.32	4.11	6.42	9.06
0.10	2.50	3.19	3.43	5.83	6.45	8.99
0.25	2.50	3.39	3.57	7.82	6.59	8.98
0.50	2.49	3.67	3.67	10.2	6.71	8.81
1.00	2.47	4.08	4.08	15.5	6.93	8.62

[a] Reproducibility is about 1% of the respective retention time. Eluent: 4 mmol/l tartaric acid; 1 mmol/l dipicolinic acid; x mmol/l of the respective crown ether.

haviour of ammonium and sodium. While the influence on ammonium is the same for both compounds, dibenzo-18-crown-6 leads to a higher retention of sodium. Thus the separation of ammonium from sodium with 18-crown-6 increases with increasing concentration in the eluent. With dibenzo-18-crown-6 the peaks of these cations tend to coelute.

Fig. 3 shows chromatograms of six cations with the standard eluent (tartaric acid–dipicolinic acid) as well as with 1 mmol/l 18-crown-6 added to the same eluent.

In contrast to dipicolinic acid the cation complexed with crown ether elutes later than the uncomplexed cation. Since the complexes of dipicolinic acid with e.g. calcium are neutral (or even negatively charged for 1:2 complexes), they are not retarded on the cation column. The crown ether complexes on the other hand have the same charge as the cation itself, but they are much larger. Thus the potassium complex shows a larger retention on the stationary phase than free potassium. The net retention is higher as long as the crown ether is present in the eluent.

We also tested whether it would be possible to analyze the 18-crown-6–potassium complex directly. The sample contained 10 mg/l potassium in 1 mmol/l 18-crown-6. On a Metrosep Cation 1-2 column with the tartaric acid–dipicolinic acid eluent the sample peak eluted at the retention time expected for uncomplexed potassium. This proves that the complex is not stable on column. Thus, addition of crown ether to the eluent is necessary to produce this type of change in selectivity.

4. Conclusions

Ethylene oxide-based compounds may be used to change the selectivity of the poly(butadiene–maleic acid)-based ion exchangers. Of the used crown ethers addition of 18-crown-6 to the eluent is the most promising since it moves

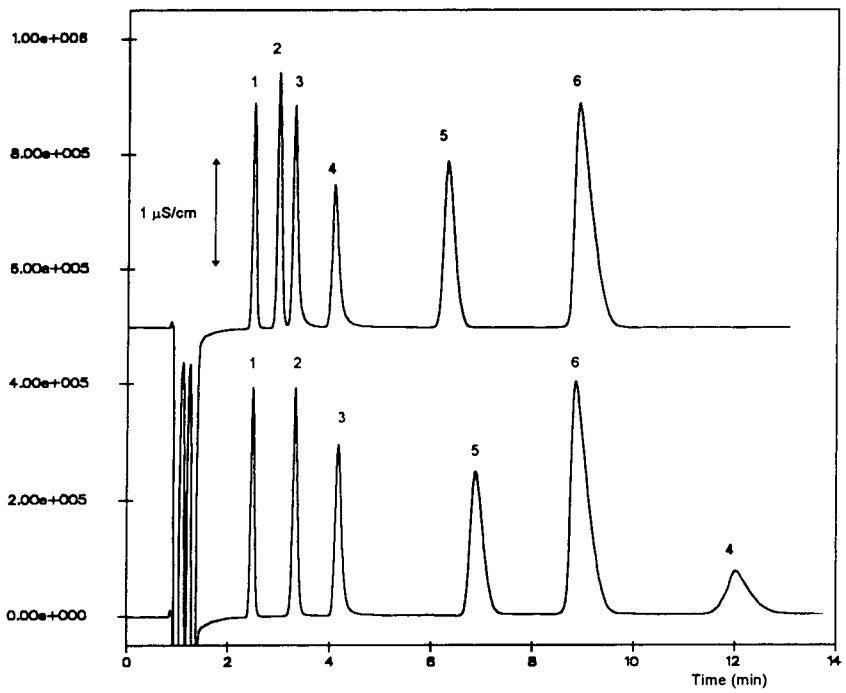

Fig. 3. Standard cations (same peak numbering as in Fig. 1). (a) Eluent: 4 mmol/l tartaric acid, 1 mmol/l dipicolinic acid. (b) Eluent: 4 mmol/l tartaric acid, 1 mmol/l dipicolinic acid, 1 mmol/l 18-crown-6.

potassium to longer retention times and improves the sodium–ammonium separation. Addition of polyethylene glycols to the eluent improves this separation without changing the selectivity for potassium. Overall, eluents with 18-crown-6 are preferred for use in routine work because they give the best separation between ammonium and sodium and because of their high purity.

References

[1] G. Schomburg, P. Kolla and M.W. Läubli, *Int. Lab.*, 4 (1989) 40–48.

[2] M.W. Läubli and B. Kampus, *J. Chromatogr. A*, 706 (1995) 99–102.

[3] M.W. Läubli, in P.A. Williams (Editor), *Recent Developments in Ion Exchange*, Vol. 2, Elsevier, Amsterdam, 1990.

[4] J. Ivask et al., *Eesti Tead. Akad. Toim.*, 41 (1992) 94–96 (cit.: Chem. Abstr. 119: 173154g).

[5] P.R. Haddad and P.E. Jackson, *Ion Chromatography* (*J. Chromatogr. Library*, Vol. 46), 1990, 233–238.

[6] J.D. Lamb, R.G. Smith and J. Jagodzinski, *J. Chromatogr.*, 640 (1993) 33–40.

ELSEVIER

Journal of Chromatography A, 706 (1995) 109–114

JOURNAL OF CHROMATOGRAPHY A

Cation-exchange chromatography in non-aqueous solvents

Philip J. Dumont, James S. Fritz*, Luther W. Schmidt

Ames Laboratory, US Department of Energy and Department of Chemistry, Iowa State University, Ames, IA 50011, USA

Abstract

Much of the selectivity of organic ions in conventional ion chromatography comes from hydrophobic interaction between the carbon chain of the analyte ions and the polymer matrix of the ion exchanger. By operating in organic solvents containing little, if any, water, the true ion-exchange selectivity of various organic ions can be measured. Retention factors (capacity factors, k') for a series of protonated amine cations were measured in methanol, ethanol, 2-propanol and acetonitrile using a polymeric cation-exchange resin, conductivity detection, and eluents of methanesulfonic acid in the same organic solvent. Plots of log t'_R vs. log methanesulfonic acid concentration were linear with slopes close to the theoretical slope of -1.0 except for acetonitrile where the slopes averaged -0.82. The retention factor showed little change with increasing carbon chain length in *n*-alkylamine cations, but increased substantially at fixed eluent concentration in going from methanol, to ethanol, to 2-propanol and especially to acetonitrile.

Several practical separations of organic amine cations were demonstrated in non-aqueous media. One advantage of this technique is that neutral organic analytes elute very quickly in non-aqueous media and thus do not interfere with chromatographic separations of the ions.

1. Introduction

Organic solvents have been used extensively in classical ion-exchange chromatography to aid in the separation of metal cations [1–3]. Formation of metal complexes with chloride and other anions was found to occur much more readily in organic solvents than in water alone. Organic solvents have also been added to aqueous eluents in modern ion chromatography to modify the behavior of various ionic analytes. However, the percentage of organic solvent in the eluent has generally been $<20\%$. Rabin and Stillian [4] recently discussed practical aspects on the use of organic solvents in ion chromatography (IC). The solvents were used primarily for selectivity mediation of the ion-exchange process for separation of various anions.

In the IC separation of organic cations it has long been known, or at least suspected, that the mechanism involved more than simple ion exchange. Hoffman and co-workers [5,6] have shown that two mechanisms occur in such cases: ion exchange and hydrophobic interaction between the sample cations and the resin matrix. For example, these authors showed that the slopes of the linear plot of log k' vs. carbon number for protonated amine cations decrease going from 30% acetonitrile (70% water) to 70% acetonitrile in the eluent. This is due to lower hydrophobic interaction in the 70% acetonitrile.

The purpose of the present investigation was to study IC in organic solvents containing little if any water. Under these conditions solvation of

* Corresponding author.

0021-9673/95/$09.50
SSDI 0021-9673(94)01150-8

the lipophilic part of the cation should be sufficient to virtually eliminate the hydrophobic interaction between the sample cations and the resin. In this way the true ion-exchange selectivity can be measured. This paper deals with ion-exchange chromatography of organic cations in non-aqueous solvents. A companion paper is concerned with alkali-metal cations in organic solvents [7].

2. Experimental

2.1. Chromatographic system

The chromatographic system consisted of several components. An Alltech (Deerfield, IL, USA) 425 HPLC pump was used to deliver a flow of 1 ml/min. A 7125 Rheodyne (Berkeley, CA, USA) injector delivered a 10-μl sample which was detected with a Alltech 320 conductivity detector. A Hitachi D-2000 integrator (EM Science, Cherry Hill, NJ, USA) was used to measure retention times. Separations were recorded by a Servogor 120 chart recorder (Abb Goerz Instruments, Vienna, Austria), and a Keithley Chrom 1-AT data acquisition board (Keithley MetraByte Corp., Taunton, MA, USA) with Labtech Notebook software (Laboratory Technologies Corp., Wilmington, MA, USA). Columns were packed with a Shandon Southern (Sewichley, PA, USA) HPLC packing pump at 3000 p.s.i. (1 p.s.i. = 6894.76 Pa).

2.2. Reagents and chemicals

The cation-exchange resin was prepared in our laboratory from 5-μm macroporous polystyrene–divinylbenzene (Sarasep, Santa Clara, CA, USA). A 2-g amount of resin was slurried with a few milliliters glacial acetic acid. An excess of concentrated sulfuric acid was then added to the resin slurry and placed in an ice bath. This reaction mixture was stirred for 0.5 to 4 min to produce the desired exchange capacity of 0.15 or 0.65 mequiv./g. Methanol, acetonitrile and 2-propanol were of HPLC grade and used as obtained from Fisher Scientific (Pittsburgh, PA, USA). Punctilious absolute ethanol was used as obtained from Quantum Chemicals (Newark, NJ, USA). All eluents were prepared daily. The analytes and methanesulfonic acid eluent were all of reagent grade and used as obtained from Lancaster Synthesis (Windham, NH, USA), Aldrich (Milwaukee, WI, USA), and Fisher Scientific. Stock solutions of 1000 ppm were used to prepare all samples.

3. Results and conclusions

3.1. Types of resin

One common resin used for separation of cations in modern IC is a sulfonated microporous resin of low exchange capacity [8,9] or a resin coated with a latex of low cross-linking. These materials tend to swell somewhat in water to form a gel. In the present study a sulfonated macroporous resin of high cross-linking was used. This resin is compatible with a wide variety of organic solvents and appears to undergo little if any swelling in going from one solvent to another.

3.2. Effect of eluent cation concentration

After trying several different inorganic acids, methanesulfonic acid was selected as the eluting acid for the separation of protonated amine cations. In IC of cations with H^+ as the eluting cation, k' should vary according to the following equation:

$$\log k' = -m \log H^+ + b$$

where m is the slope of a linear plot and b is a constant. Linear plots were obtained for the C_1–C_{10} n-alkylamines in methanol, ethanol, 2-propanol and acetonitrile. The slopes (m) were very close to the theoretical slope of -1 in the three alcohols and only a little less than -1 in acetonitrile (Table 1).

3.3. Effect of solvent on k'

A plot of log k' vs. the number of carbon atoms is linear for members of a homologous

Table 1
Slopes of log t'_R–log $[H^+]$ lines for several solvents

	Methanol	Ethanol	2-Propanol	Acetonitrile
Methylamine	−0.95	−1.02	−0.92	−0.85
Ethylamine	−0.94	−1.00	−0.92	−0.85
Propylamine	−0.93	−1.01	−0.93	−0.84
Butylamine	−0.93	−1.01	−0.92	−0.83
Pentylamine	−0.92	−1.00	−0.93	−0.81
Hexylamine	−0.90	−1.00	−0.93	−0.80
Heptylamine	−0.92	−1.00	−0.93	−0.78
Octylamine	−0.92	−1.01	−0.92	−0.79
Nonylamine	−0.90	−1.00	−0.92	−0.82
Decylamine	−0.89	−1.01	−0.92	−0.81

The resin contained 0.65 mmol/g of $-SO_3^-H^+$. Eluents contained 75, 50, 25 and 10 m*M* methanesulfonic acid.

series in HPLC [10]. The slope of such a plot is an indication of the extent of the hydrophobic effect of the carbon chain on the retention factor, k'.

The retention factors of C_1–C_{10} *n*-alkylamine cations were measured under identical chromatographic conditions in each of four organic solvents. The results are shown graphically in Fig. 1. The values of k' are very similar for the various amines in any given solvent except in methanol, where a gradual increase is noted for k' with increasing carbon chain length. This could be interpreted as some residual hydrophobic attraction in methanol of the amine cations for the resin. The k' values for the homologous series increases in the order methanol < ethanol < propanol ≪ acetonitrile.

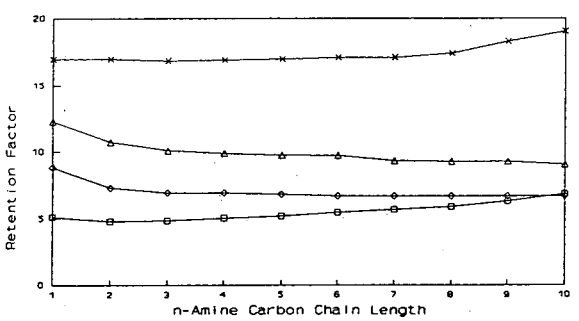

Fig. 1. Effect of solvent on retention of *n*-alkylamines. Eluent contained 25 m*M* methanesulfonic acid. The resin contained 0.65 mmol/g of $-SO_3^-H^+$. □ = Methanol; ◇ = ethanol; △ = 2-propanol; × = acetonitrile.

These results might be explained by a lower degree of solvation of the RNH_3^+ in acetonitrile than in the alcohols where hydrogen bonding through the–OH is a possibility. A higher degree of solvation would attract the RNH_3^+ more strongly to the liquid mobile phase and could impede the approach of a highly solvated ion to the ion-exchange sites on the resin.

The retention factors of a number of amine cations are given in Table 2. Elution is strongly dependent on solvation of the amine cation and the dielectric of the eluent. The effect of dielectric is seen by the 2-propanol k' values in Table 2. Although 2-propanol should be a stronger eluent for the amines, retention times are longer. This is due to the low dielectric constant of 2-propanol which favors the amine cation remaining paired to the resin exchange sites. Methanol and ethanol have more moderate dielectric constants but have different efficiencies for solvating straight-chain and aromatic amines as can be seen by the retention factors of the octyl and aniline cations.

3.4. Separation of protonated amine cations

The data in Fig. 2 indicate that none of the solvents studied would be a suitable choice for separation of the *n*-alkylamine ions. However, an excellent separation was obtained for the protonated cations of aniline, N-methylaniline and N,N-dimethylaniline (Fig. 2). These ions

Table 2
Retention factors of protonated amine cations in alcohol solvents

Amine	Methanol	Ethanol	2-Propanol
Aniline	1.98	1.62	5.78
N-Methylaniline	3.18	4.10	13.64
N,N-Dimethylaniline	4.37	7.68	27.6
Octylamine	2.39	1.82	4.83
Dioctylamine	4.57	3.26	9.43
Trioctylamine	7.54	4.61	17.6

Conditions. 1 m*M* methanesulfonic acid, 5 cm column with 0.15 mmol/g of $-SO_3^-H^+$.

differ only by one or two methyl groups. Good separations were also obtained in methanol for a sample containing ethylamine, diethylamine and triethylamine and for another sample containing *n*-octylamine, di-*n*-octylamine and tri-*n*-octylamine (Fig. 3) A mixture of pyridine, quinoline and benzoquinoline could be separated in methanol or in mixed solvents containing 65% methanol and 35% of ethanol, propanol (Fig. 4) or butanol.

Conductivity detection can be used in any of the solvents studied but the sensitivity is better in eluents with higher dielectric constants (methanol and acetonitrile). Elution of an amine cation reduces the concentration of the more mobile H^+ and thereby gives a peak of decreased conductance for the alcohol solvents. Conversely, H^+ has a lower conductivity than the amine cations in acetonitrile and a positive signal was measured. For convenience, the chromatograph-

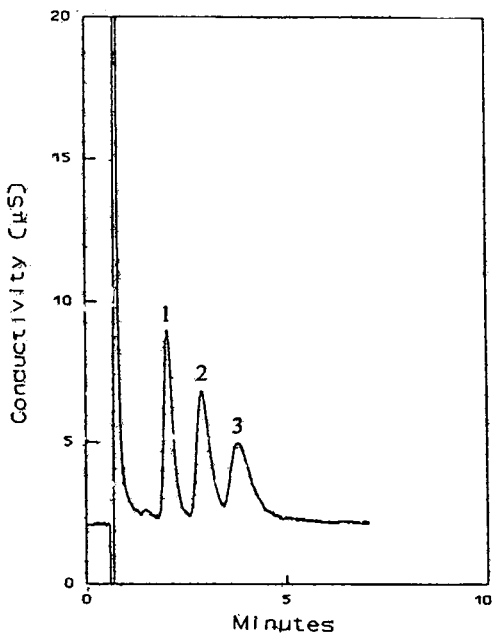

Fig. 2. Separation of 12.5 ppm aniline (1), N-methylaniline (2) and N,N-dimethylaniline (3) on a 5-cm sulfonated resin column (0.15 mmol/g) The eluent was 1 m*M* methanesulfonic acid in methanol at a flow-rate of 1 ml/min.

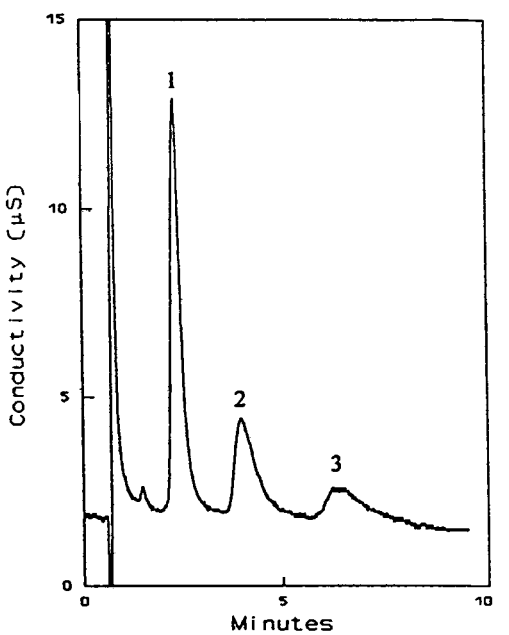

Fig. 3. Separation of 50 ppm *n*-octylamine (1), di-*n*-octylamine (2) and tri-*n*-octylamine (3) in methanol. Conditions as in Fig. 2.

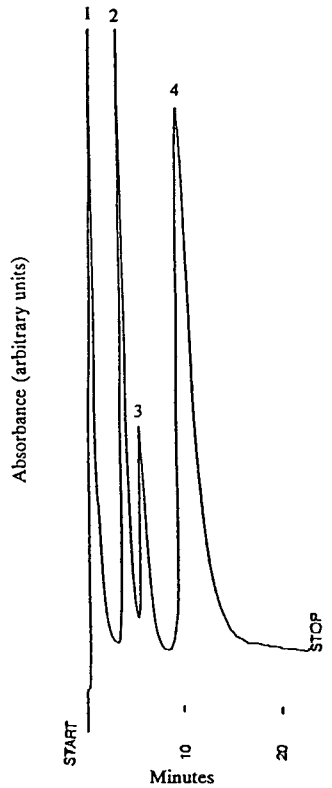

Fig. 4. Separation of 0.4 ppm pyridine, 40 ppm quinoline and 60 ppm 5,6-benzoquinoline in a sample also containing 2000 ppm each of benzonitrile, nitrobenzene, octane and isophorone. The solvent was methanol–*n*-propanol (65:35). Peaks: 1 = 2000 ppm each of benzonitrile, octane, nitrobenzene, isophorone (collect fraction and GC: 100, 95, 92 and 100% recoveries, respectively); 2 = pyridine; 3 = quinoline; 4 = 5,6-benzoquinoline.

ic peaks are displayed graphically on a conventional *y*-axis of increasing signal.

The retention factors of most neutral organic compounds are very low in the solvents studied. This means that neutral organic compounds will be eluted quickly enough not to interfere with chromatographic separation of the amine cations. Fig. 4 shows a successful separation of 0.4 ppm pyridine, 40 ppm quinoline and 60 ppm of 5,6-benzoquinoline in a sample that also contained 2000 ppm each of benzonitrile, *n*-octane, nitrobenzene and isophorone. The neutral fraction was collected and analyzed by gas chromatography giving recoveries of 100, 95, 92 and 100%, respectively for the four neutral compounds.

Separation of 50 ppm each of aniline, N-methylaniline and N,N-dimethylaniline in a sample spiked with 10 000 ppm of toluene is shown in Fig. 5. The toluene elutes in a very compact, early peak.

3.5. Determination of trace amines in organic solvents

With the use of organic eluents, it should be possible to detect very small amounts of organic bases in solvents. A large volume of organic solvent may be injected. The amine will be retained by electrostatic attraction while the solvent passes through the column with the injection peak. In Fig. 6, 50 ppb aniline in toluene (with 0.75 m*M* methanesulfonic acid) is determined. The detection limit of this system was determined by analyzing the baseline noise after the elution of the aniline peak. Using three times the standard deviation of the signal noise

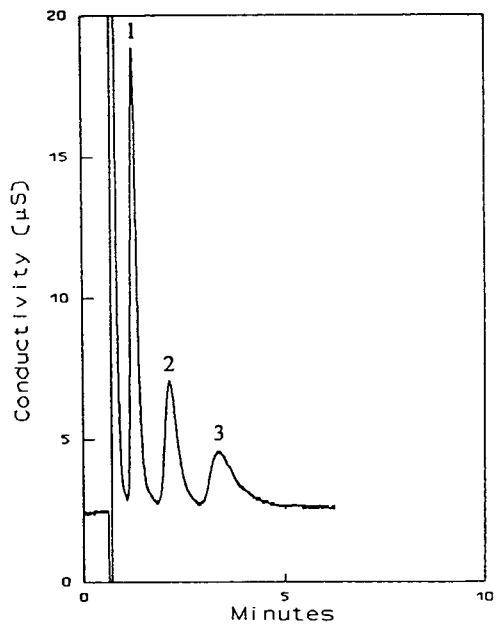

Fig. 5. Separation of 50 ppm aniline (1), N-methylaniline (2) and N,N-dimethylaniline (3) in a sample spiked with 10 000 ppm toluene. The eluent was 2.5 m*M* methanesulfonic acid in ethanol. Other conditions as in Fig. 2.

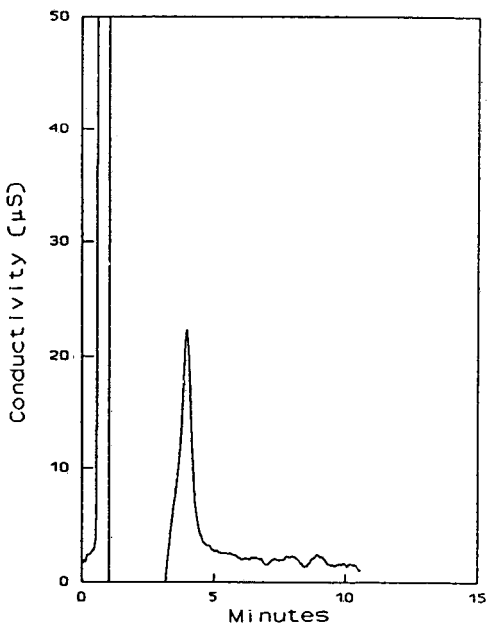

Fig. 6. Injection of 200 μl of toluene with 50 ppb aniline and 0.75 m*M* methanesulfonic acid. The eluent is 0.75 m*M* methanesulfonic acid in methanol at 1.5 ml/min.

as the criteria, a detection limit of 5 ppb was determined. This type of trace analysis should be applicable to many bases in organic solvents.

4. Conclusions

A plot of log t'_R vs. log H^+ (from methanesulfonic acid) is linear with a slope close to −1 in each of the four solvents studied. This is an indication that the separation mechanism is pure ion exchange and not partition based on hydrophobic attraction. The retention factors of C_1–C_9 alkylamine cations show very little change with regard to the number of carbon atoms. However, amine cations, such as aniline, N-methylaniline and N,N-dimethylaniline, are easily separated. These results indicate that the size and shape of the cation may affect the ion-exchange selectivity.

Practical separations of amine cations can be obtained in methanol or ethanol with indirect conductivity detection. Large concentrations of neutral organic compounds in the sample do not interfere with the chromatographic separation and determination of cations.

Acknowledgements

We wish to thank Alltech Associates, Inc., Deerfield, IL, USA for a gift of the chromatographic pump and 320 conductivity detector used in this work. We also thank Doug Gjerde of Sarasep Inc. (Santa Clara, CA, USA) for the resin used in this work. This research was supported by a grant from the 3M Co., St. Paul, MN, USA. The work was performed in the Ames Laboratory of Iowa State University. Ames Laboratory is operated for the US Department of Energy under contract No. W-7405-Eng-82.

References

[1] J.S. Fritz and T.A. Rettig, *Anal. Chem.*, 34 (1962) 1562.
[2] F.W.E. Strelow, A.H. Victor, C.R. van Zyl and C. Eloff, *Anal. Chem.*, 43 (1971) 870.
[3] J. Korkisch and I. Hazan, *Talanta*, 11 (1964) 1157.
[4] S. Rabin and J. Stillian, *J. Chromatogr. A*, 671 (1994) 63.
[5] A. Rahman and N. Hoffman, *J. Chromatogr. Sci.*, 28 (1990) 157.
[6] N. Hoffman and J. Liao, *J. Chromatogr. Sci.*, 28 (1990) 428.
[7] P.J. Dumont and J.S. Fritz, *J. Chromatogr.*, 706 (1995) 149.
[8] G J Sevenich and J.S. Fritz, *React. Polym.*, 4 (1986) 195.
[9] G.J. Sevenich and J.S. Fritz, *J. Chromatogr.*, 371 (1986) 361.
[10] G.E. Berendsen, P.J. Schoenmakers and L. de Galan, *J. Liq. Chromatogr.*, 3 (1980) 1669.

ELSEVIER

Journal of Chromatography A, 706 (1995) 115–119

JOURNAL OF CHROMATOGRAPHY A

Evaluation of 1,2-diaminocyclohexanetetraacetic acid as eluent in the determination of inorganic anions and cations by ion chromatography

Eduardo A. Gautier*, Raquel T. Gettar, Roberto E. Servant, Daniel A. Batistoni

Dto. Química Analítica, Div. Espectrometría de Masas, Comisión Nacional de Energía Atómica, Av. Libertador 8250, 1429 Buenos Aires, Argentina

Abstract

The chelating agent 1,2-diaminocyclohexanetetraacetic acid (DCTA) was tested as an eluent for the separation and determination of inorganic anions (Cl^-, NO_3^-, SO_4^{2-}) and some selected metals using single-column ion chromatography with ultraviolet detection. The effects of pH and eluent concentration on retention times for the system were studied to overview the possibilities of attaining optimum separations. The metals studied included Fe(III), Cr(III), Y(III), La(III), Nd(III), Gd(III), Ba(II), Ca(II), Cd(II), Co(II), Cu(II), Hg(II), Mg(II), Ni(II), Pb(II), Sr(II), Zn(II) and Mo(VI). The detection limits were generally below 0.5 $\mu g\ ml^{-1}$. Results for the analysis of synthetic samples and drinking water are presented.

1. Introduction

The possibility of using a complexing agent in the mobile phase for the determination of metals in the form of ligand complexes has become a widely used technique in the field of ion chromatography, with metal species being separated using either cation, anion or combined anion/cation exchangers [1–15]. Highly charged, strongly complexing anions such as aminopolycarboxylic acids react with most metals producing singly or doubly charged anions, allowing the simultaneous determination of metal cations and inorganic anions.

1,2-Diaminocyclohexanetetraacetic acid (DCTA), acting as a multidentate chelating ligand, forms strong complexes with most divalent and trivalent metals. The combination ratio of DCTA with metals ions is 1:1, the chelate being negatively charged. These complexes have chemical structures similar to those formed with EDTA but have higher stability constants for most metals. EDTA complexes have been widely studied [1,3–15], but few reports about DCTA complexes have been published [1,2,7].

The purpose of this work was to investigate the ion chromatographic behaviour of some inorganic anions and of several di- and trivalent metals using DCTA as eluent. The ultimate goal of the study was to separate and determine these ionic species.

* Corresponding author.

0021-9673/95/$09.50
SSDI 0021-9673(95)00028-3

2. Experimental

2.1. Apparatus

A Konik (Barcelona, Spain) KNK-500A liquid chromatograph with a Rheodyne Model 7125 injector and equipped with a 100-μl sample loop and a Vydac 302 IC 4.6 silica-based anion-exchange column (25 cm × 4.6 mm I.D.) was used for all separations. A Linear (Reno, NV, USA) UVis 204 variable-wavelength UV–Vis detector was employed. Data were transferred to a personal computer via an A/D interface and processed by means of integration software (Konikrom Chromatography Data System V.5). Molecular absorptions spectra of the complexes were obtained with a Perkin-Elmer (Norwalk, CT, USA) Model 559A UV–Vis spectrophotometer.

2.2. Reagents

Water used for the preparation of all solutions and eluents was obtained by passing distilled water through a Nanopure water-purification unit (Sybron/Barnstead, Boston, MA, USA). Stock standard solutions of the different cations were prepared from analytical-reagent grade chemicals. All metal ion solutions (except chromium) were injected directly into the instrument. The metal ion complexes were formed within the chromatographic system, which was operated in the isocratic mode at 30°C. Cr(III) required the addition of the complexing agent before injection. Formation of the chromium complex was attained by heating the mixture at 80°C for 20 min.

Eluents were prepared by dissolving DCTA (Merck, Darmstadt, Germany) in water, followed by pH adjustment with 1 *M* sodium hydroxide solution. All eluents were passed through a 0.22-μm membrane filter and deaerated with helium.

3. Results and discussion

To establish the optimum conditions for chromatography, factors that affect the retention behaviour and the detection, such as pH and concentration of the eluent and UV wavelength, were studied. The solution pH and the DCTA concentration are considered to be the most important factors in the chelation reaction.

Trivalent metal ions such as Fe(III), Cr(III), Y(III), La(III), Nd(III) and Gd(III) form monovalent complexes with DCTA, while the divalent metal ions form divalent complexes. For that reason, the trivalent metal ions are eluted earlier than the divalent species Ca(II), Cd(II), Co(II), Cu(II), Hg(II), Mg(II), Ni(II), Pb(II), Sr(II) and Zn(II)).

An exception was Ba(II), which showed a short retention time. This behaviour could arise from the lower formation constant ($\log K = 7.99$) [16] of the Ba–DCTA complex when compared with other divalent ion constants and the larger ionic radius of the metal ion.

3.1. Effect of eluent concentration

The retention times of metals were studied at four different eluent concentrations, 0.75, 1.2, 1.5 and 2 m*M*, at pH 5.8. The variation of the logarithm of the capacity factors ($\log k'$) as a function of the logarithm of DCTA concentration is shown in Fig. 1. In each instance a peak from an unretained compound was employed as reference for t_0 estimation.

The retention time decreases for high concentrations of the eluent because once the complex is formed, an increase in DCTA concentration will increase the concentration of the non-complexed anions of DCTA which compete with the metal complex ions for the ion-exchange sites.

Straight lines were obtained. The negative slope of the lines is considered to be equal to x/y, where x is the charge of the complexed metal anion and y the charge of the eluent anion [1,17].

Experimental values of the slope ranged from −0.48 to −0.56 for trivalent cations and from −0.57 to −0.62 for divalent cations. These results agree with an effective charge of about −2 and −3.3, respectively, for the eluent. However, equilibrium calculations for the distribution

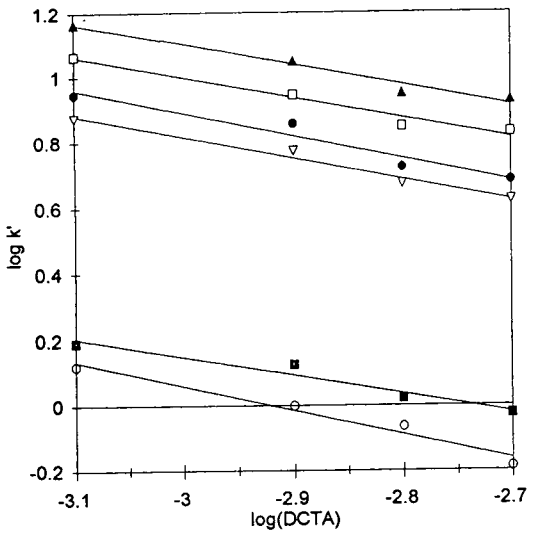

Fig. 1. Log(capacity factor) vs. log(DCTA concentration). ○ = $BaDCTA^{2-}$; ◘ = $FeDCTA^{-}$; ▽ = $SrDCTA^{2-}$; □ = $CuDCTA^{2-}$; ▲ = $ZnDCTA^{2-}$; ● = $HgDCTA^{2-}$.

of DCTA species show that 67% of [$HDCTA^{2-}$] and 33% of [$HDCTA^{3-}$] are present at pH 5.8, giving an "effective charge" of −2.33. These results suggest that mechanisms other than pure ion exchange could be active during the separation process. Haddad and Jackson [17] discussed several examples in which steric and activity effects and/or ion-pair formation could explain the observed behaviour.

3.2. Effect of pH

Changes in the pH range produce variations in the proportions of the anionic species in the eluent, as expected from the DCTA acid dissociation constants ($pK_1 = 2.43$, $pK_2 = 3.52$, $pK_3 = 6.12$ and $pK_4 = 11.70$) [16]. In addition, the conditional stability constants of metal chelates are often strongly dependent on pH owing to the acid–base equilibrium of the chelating agent.

Separations were performed at four different pH values, 4.5, 5.0, 5.5 and 5.8, with the eluent concentration fixed at 1.2 m*M*. At pH values lower than 4.5 broader peaks with longer retention times were observed; pH values higher than 6.0 were not tested because this is the upper recommended pH limit for column operation.

Fig. 2a and b show that an increase in the pH of the mobile phase decreases the retention time of some complexed metal anions. The "effective

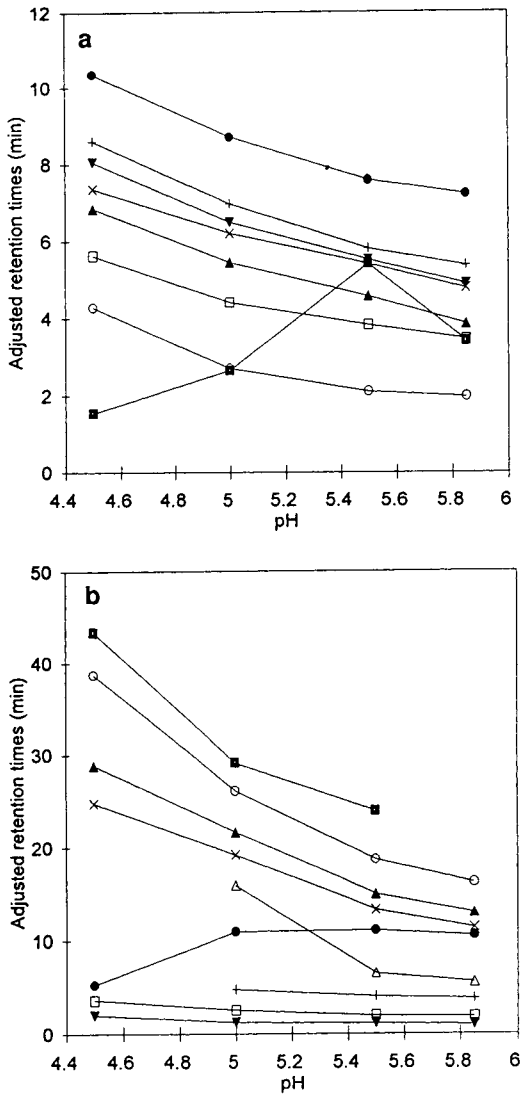

Fig. 2. Adjusted retention time vs. pH of 1.2 m*M* DCTA eluent. (a) Flow-rate, 0.8 ml min^{-1}. ◘ = $BaDCTA^{2-}$; × = $FeDCTA^{-}$; ▲ = $YDCTA^{-}$; + = $NdDCTA^{-}$; ▼ = $LaDCTA^{-}$; ● = $CrDCTA^{-}$; ○ = Cl^{-}; □ = NO_3^{-}. (b) Flow-rate, 1.5 ml min^{-1}. × = $CaDCTA^{2-}$; ● = $SrDCTA^{2-}$; + = $CrDCTA^{2-}$; ◘ = $MnDCTA^{2-}$; ○ = $CoDCTA^{2-}$; △ = MoO_4^{2-}; ▲ = $CuDCTA^{2-}$; ▼ = Cl^{-}; □ = NO_3^{-}.

charge" of the eluent should increase with increase in pH.

Ba and Sr complexes exhibit lower than expected retention times at pH <5.5. This result means that a considerable dissociation of the complexes occurred at pH <5.5.

3.3. Wavelength selection

In order to investigate the location of the relative absorption maxima, plots of absorbance vs. wavelength for divalent metal complexes were obtained. Some results are depicted in Fig. 3. Other divalent metals not included in Fig. 3 showed a continuous increase in absorbance from 300 to 210 nm, similar to that in the spectrum of the Co(II) complex. An operating wavelength of 210 nm was chosen for divalent cations. However, it is worth mentioning that other wavelengths can be employed to improve the selectivity in particular cases.

A wavelength of 195 nm was selected for trivalent metals because Y(III), La(III), Nd(III) and Gd(III) only produced positive chromatographic peaks below 200 nm. Cr(III) and Fe(III) could be measured at either 210 or 195 nm without significative losses in sensitivity.

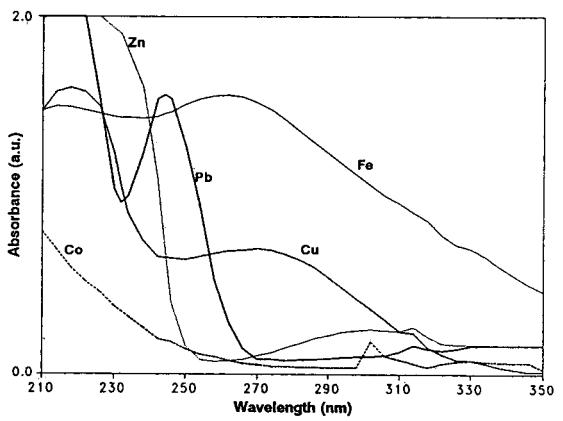

Fig. 3. Absorbance vs. wavelength for some complex anions. Metal concentration, 0.2 m*M*; DCTA/metal molar ratio, 1:1.

3.4. Applications

To establish the elution order of the elements studied, individual retention times were measured at a flow-rate of 0.8 ml min^{-1}. The values obtained and the corresponding detection limits, defined as three times the standard deviation of the baseline noise, are given in Table 1. A detection wavelength of 210 nm was employed for all metals except Y, La, Nd and Gd, for which a 195 nm was utilized.

Chromatograms depicting the behaviour of different metal and anion mixtures are included in Figs. 4 and 5.

The method was also applied to the determination of Ca(II), Mg(II), Cl^-, NO_3^- and SO_4^{2-} in drinking water, as shown in Fig. 6. Chloride and sulfate gave negative peaks because these ions do not absorb UV radiation.

Table 1
Retention times (t_R) and detection limits (D.L.)

Cation complex	t_R (min)	D.L. ($\mu g\ ml^{-1}$)
Ba–DCTA	7.1	0.1
Y–DCTA	7.5	0.3
Fe–DCTA	8.5	0.05
La–DCTA	9.6	0.05
Gd–DCTA	8.7	0.2
Nd–DCTA	9.1	0.04
Cr–DCTA	10.9	0.01
MoO_4^{2-}	12.9	0.02
Mn–DCTA	16.7	0.2
Ca–DCTA	24.6	0.3
Sr–DCTA	24.6	0.3
Hg–DCTA	27.2	0.03
Pb–DCTA	28.8	0.03
Cu–DCTA	32.1	0.03
Cd–DCTA	32.6	0.8
Mg–DCTA	32.7	0.2
Zn–DCTA	35.5	0.4
Ni–DCTA	37.2	0.03
Co–DCTA	38.0	0.03

Mobile phase: 1.2 m*M* DCTA, pH 5.8, flow-rate 0.8 ml min^{-1}

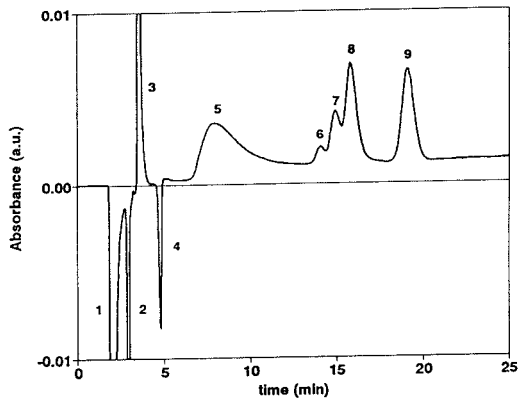

Fig. 4. Chromatogram for some selected metal ions and anions. Observed peaks: 1 = injection; 2 = Cl^-; 3 = NO_3^-; 4 = SO_4^{2-}; 5 = MoO_4^{2-}; 6 = $CaDCTA^{2-}$; 7 = $HgDCTA^{2-}$; 8 = $CuDCTA^{2-}$; 9 = $CoDCTA^{2-}$. [DCTA] = 1.2 m*M* at pH 5.8; flow-rate, 1.5 ml min^{-1}; concentration of each metal ion, 2.5 μg ml^{-1}; detection wavelength, 210 nm.

4. Conclusions

This work has shown the potential of DCTA as a chelating agent for measuring a variety of metals and inorganic anions using ion-exchange chromatography. The concentration of DCTA, the pH of the mobile phase and the detection wavelength can be changed to optimize the conditions for any given application in order to obtain reasonable retention times.

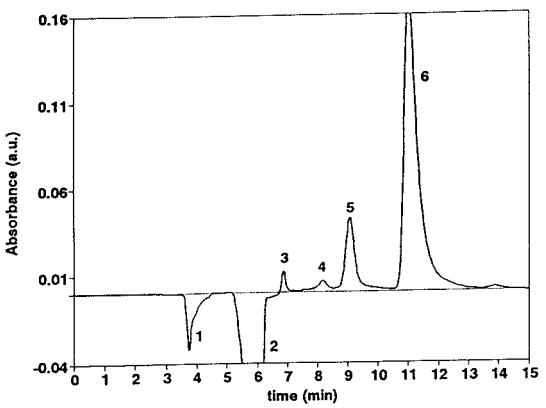

Fig. 5. Chromatogram for some selected metal ions and anions. Observed peaks: 1 = injection; 2 = Cl^-; 3 = $BaDCTA^{2-}$; 4 = $YDCTA^-$; 5 = $FeDCTA^-$; 6 = $CrDCTA^-$. [DCTA] = 1.2 m*M* at pH 5.8; flow-rate, 0.8 ml min^{-1}; concentration of each metal ion, 10 μg ml^{-1}; detection wavelength, 195 nm.

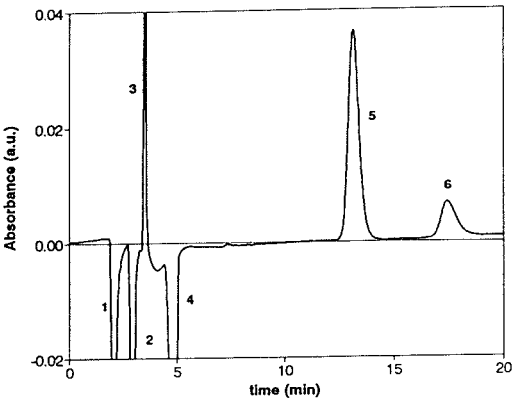

Fig. 6. Chromatogram of drinking water. Observed peaks: 1 = injection; 2 = Cl^-; 3 = NO_3^-; 4 = SO_4^{2-}; 5 = $CaDCTA^{2-}$; 6 = $MgDCTA^{2-}$. Concentrations: Cl^- = 33.0 μg ml^{-1}; NO_3^- = 1.3 μg ml^{-1}, SO_4^{2-} = 58.0 μg ml^{-1}; Ca^{2+} = 20.9 μg ml^{-1}; Mg^{2+} = 4.4 μg ml^{-1}. Other conditions as in Fig. 4.

References

[1] S. Matsushita, *J. Chromatogr.*, 312 (1984) 327.
[2] A.I. Valle, M.J. González and M.L. Marina, *J. Chromatogr.*, 607 (1992) 207.
[3] M. Yamamoto, H. Yamamoto, Y. Yamamoto, S. Matsushita, N. Baba and T. Ikushige, *Anal. Chem.*, 56 (1984) 832.
[4] T. Tanaka, *Fresenius' Z. Anal. Chem.*, 320 (1985) 125.
[5] W.-F. Lien, B.K. Boerner and J.G. Tarter, *J. Liq. Chromatogr.*, 10 (1987) 3213.
[6] A.F. Geddes and J.G. Tarter, *Anal. Lett.*, 21 (1988) 857.
[7] G. Schwedt and B. Kondratjonok, *Fresenius' Z. Anal. Chem.*, 332 (1989) 855.
[8] O.N. Obrezkov, V.I. Slyamin and O.A. Shpigun, *Anal. Sci.*, 6 (1990) 617.
[9] C. Sarzanini, O. Abollino, E. Mentasti and V. Porta, *Chromatographia*, 30 (1990) 293.
[10] A. Nitsch, K. Kalcher and U. Posch, *Fresenius' J. Anal. Chem.*, 338 (1990) 618.
[11] T.V. Komarova, O.N. Obrezkov and O.A. Shpigun, *Anal. Chim. Acta*, 254 (1991) 61.
[12] J.-F. Jen and C.-S. Chen, *Anal. Chim. Acta*, 270 (1992) 55.
[13] E.A. Gautier, R.T. Gettar and R.E. Servant, *Anal. Chim. Acta*, 283 (1993) 350.
[14] M.L. Marina, P. Andrés and J.C. Díez-Masa, *Chromatographia*, 35 (1993) 621.
[15] P. Hajos, G. Revesz, C. Sarzanini, G. Sacchero and E. Mentasti, *J. Chromatogr.*, 640 (1993) 15.
[16] L.G. Sillen and A.E. Martell, *Stability Constants of Metal-Ion Complexes*, Chemical Soc. London, 1964, p. 690.
[17] P. Haddad and P. Jackson, *Ion Chromatography*, Elsevier, Amsterdam, 1990, Ch. 5, p. 133.

ELSEVIER

Journal of Chromatography A, 706 (1995) 121–126

JOURNAL OF CHROMATOGRAPHY A

On-line thermal lens spectrometric detection of Cr(III) and Cr(VI) after separation by ion chromatography

Mateja Šikovec[a], Milko Novič[b], Vida Hudnik[b], Mladen Franko[a,*]

[a]*Jožef Stefan Institute, P.O. Box 100, 61111 Ljubljana, Slovenia*

[b]*National Institute of Chemistry, P.O. Box 30, 61115 Ljubljana, Slovenia*

Abstract

The applicability of thermal lens spectrometry for the on-line detection of trivalent and hexavalent chromium species after high-performance ion chromatographic (HPIC) separation was investigated. A collinear dual-beam thermal lens spectrometer was utilized to detect Cr species separated as anions on a Dionex HPIC CS5 column. Precolumn derivatization of Cr(III) by pyridine-2,6-dicarboxylic acid and postcolumn derivatization of Cr(VI) by diphenylcarbazide were necessary for the efficient separation and on-line detection of both Cr species. Under the proposed experimental conditions, i.e. 200-μl sample loop and an argon ion laser operating at 514.5 nm, providing 160 mW power at the sample site, detection limits of 30 and 0.3 ng/ml for Cr(III) and Cr(VI), respectively, were achieved.

1. Introduction

Some industries, such as leather tanning and chromium plating, produce wastewaters containing significant concentrations of Cr(III) and/or Cr(VI). Because of the high toxicity of dichromate species, a sensitive, precise and accurate procedure for its determination is necessary. On the other hand, Cr(III) is an essential element, and no toxic effects of Cr(III) to humans are known [1,2]. However, cytogenetic effects on fish were observed at Cr(III) concentrations below 50 ng/ml [3], which is lower than the proposed drinking water standard or threshold limit level for natural waters of the first category (100 ng/ml) [4]. Therefore, levels of Cr(III) in water must also be carefully monitored.

Cr in water can be determined by a number of standard analytical methods [5], including atomic absorption (AAS) and emission spectrometry (AES), and spectrophotometry. While graphite furnace AAS and inductively coupled plasma (ICP) AES are very sensitive and useful tools for the determination of total chromium concentration, spectrophotometry is better suited for the detection of individual Cr species. The spectrophotometric determination of Cr(VI) or Cr(III) after its oxidation and reaction with 1,5-diphenylcarbohydrazide (DPC) [6–8] is highly selective and simple. Other chromogenic reagents, such as pyridine-2,6-dicarboxylic acid (PDCA) for Cr(III), can also be applied to avoid time-consuming oxidation of Cr(III) and to permit the simultaneous measurement of Cr(III) and Cr(VI) species [8]. However, matrix effects (e.g., colour of wastewater) and some interfering ions [e.g., Fe^{3+}, V^{5+} and Hg^{2+} in the case of Cr(VI)] frequently demand prior separation of

* Corresponding author.

0021-9673/95/$09.50
SSDI 0021-9673(95)00139-5

Cr(III) and Cr(VI) from other species. This can be achieved by different separation techniques, including high-performance ion chromatography (HPIC) [8]. In the case of HPIC, on-line spectrophotometric detection of separated chromium species is most convenient and therefore most frequently applied. However, spectrophotometry is not sensitive enough for the simultaneous and accurate on-line detection of minute amounts of Cr species, which can still be toxic {below 50 ng/ml for Cr(III) [3]}.

Spectroscopic techniques such as direct current plasma (DCP) AES, ICP-AES and ICP–MS have been reported as sensitive and selective detectors in chromatographic separations of chromium species [9–11]. Nevertheless, these techniques are not yet widely accepted for routine chromatographic analysis. Partly this can be attributed to the high cost of ICP-AES and particularly ICP–MS instruments. Relatively cheaper photothermal techniques, including thermal lens spectrometry (TLS), have been attracting attention recently. TLS is also known for its extreme sensitivity and ability to measure absorbances as low as 10^{-7} cm^{-1} [12]. Therefore, the measurement of absorbance through the thermal lens effect should, in principle provide better sensitivity and lower limits of detection (LOD) than spectrophotometry. This was also confirmed by our preliminary investigations [13], which resulted in LOD lower than 0.1 ng/ml for Cr(VI) in non-flowing systems. This LOD is comparable to or better than those obtained by coupled systems including DCP-AES and ICP-AES (5–10 ng/ml) [9,10] or ICP–MS (0.3 ng/ml) [11]. However, in contrast to ICP-AES and ICP–MS, which in principle provide better selectivity, TLS is a non-specific detection technique and therefore requires prior separation of analyte species. However, as with TLS, the selectivity of coupled ICP–AES and ICP–MS techniques when used for speciation studies also depends strongly on the separation efficiency.

TLS has already been applied for the detection of different compounds in HPLC but, to the best of our knowledge, not yet in ion chromatography. It was therefore the main objective of this work to investigate the applicability of TLS for the simultaneous on-line detection of Cr(III) and Cr(VI) species after HPIC separation.

2. Experimental

2.1. Reagents

The eluent stock solution consisted of 20 m*M* PDCA, 20 m*M* Na_2HPO_4, 10 m*M* NaI, 50 m*M* CH_3COONH_4 and 28 m*M* LiOH in 18 MΩ deionized water, Cr(III) stock solution of 1 mg/ml was prepared by dissolving 4.577 g of $Cr(NO_3)_3$ (dried at 105°C for 1 h) in 1 l of distilled water and Cr(VI) stock solution of 1 mg/ml was prepared by dissolving 2.828 g of $K_2Cr_2O_7$ in 1 l of distilled water.

2.2. Chromatographic conditions

An HPIC CG5 guard column (4 mm I.D.) and an HPIC CS5 separation column (4 mm I.D.), both from Dionex, were used. The sample volume was 200 μl. The eluent was 2 m*M* PDCA–2 m*M* $NaHPO_4$–1 m*M* NaI–5 m*M* CH_3COONH_4–2.8 m*M* LiOH in 18 MΩ deionized water at a flow-rate of 1.0 ml/min. The postcolumn reagent was 2 m*M* DPC–10% CH_3OH–0.45 *M* H_2SO_4 at a flow-rate of 0.5 ml/min.

2.3. Detection system

A dual-beam (pump–probe configuration) thermal lens spectrometer with non-focused probe beam was constructed to perform the measurements (Fig. 1). A Spectra-Physics Model 2025-05 argon ion laser or an air-cooled Omnichrome argon ion laser operating at 514.5 nm were used as an excitation source. The pump beam from the argon ion laser was modulated by a variable-speed mechanical chopper (Scientific Instruments Model 300) and focused on to the flow-through sample cell by a 100-mm focal length lens. The optimum signal-to-noise ratio was obtained at 75 Hz modulation frequency. A Uniphase helium–neon laser (Model 1103P) was used to provide the probe beam. Lens L2 was

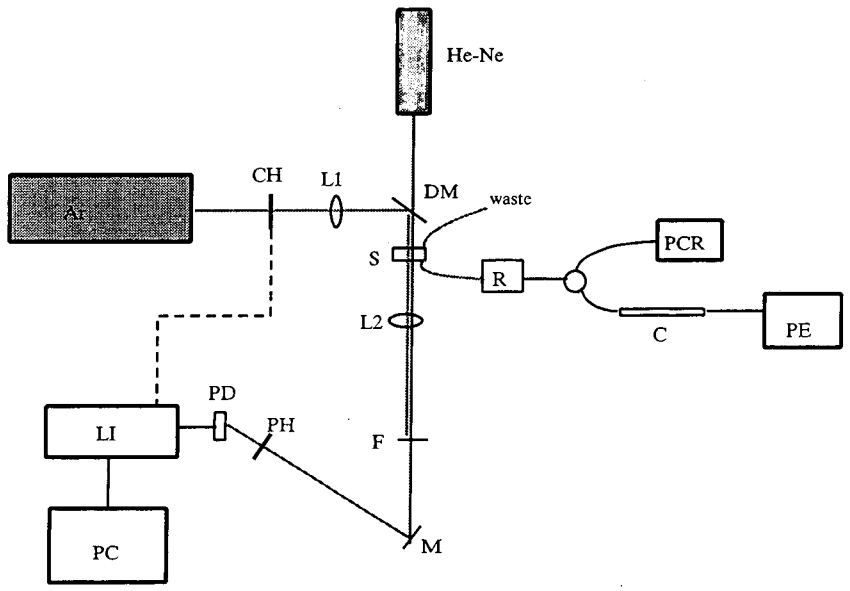

Fig. 1. Schematic diagram of the chromatographic system used in this work. PE = HPLC pump; C = column; R = postcolumn reactor; PCR = postcolumn reagent; Ar = argon ion laser; He–Ne = helium–neon laser; CH = chopper; L1 and L2 = lenses; DM = dichroic mirror; S = sample cell; F = filter; M = mirror; PH = pinhole; PD = photodiode; LI = lock-in amplifier; PC = personal computer.

used to increase the beam radius at the detector site and to facilitate sampling of the beam centre intensity. The fluctuation of the probe beam intensity was measured by a silicon photodiode (Laser Components OSD 5-E) placed 1.4 m from the sample and behind a red filter and a horizontal slit. The output of the photodiode was fed into a Stanford Research lock-in amplifier (Model SR510), which was connected to a personal computer for data processing and recording of chromatograms.

2.4. Chromatographic procedure

Cr(III) was converted into $Cr(PDCA)_2^-$ complex after adjusting the pH of the Cr(III) solution to 4 (at higher pH the precipitation of chromium oxide hydroxide occurs). Subsequently 5 ml of the Cr(III) stock solution were added to 10 ml of eluent stock solution and the mixture was heated and boiled for 1 min. After cooling, the pH was adjusted to 6.8 and the solution was diluted to 100 ml with distilled water and used as a stock solution of $Cr(PDCA)_2^-$. Samples containing known concentrations of Cr(VI) and $Cr(PDCA)_2^-$ were prepared by mixing and diluting appropriate volumes of corresponding stock solutions.

The chromatographic system depicted in Fig. 1 consisted of a Hitachi Model L-6200 HPLC pump, Rheodyne injection valve with a 200-μl sample loop, Dionex HPIC CG5 guard column and Dionex HPIC CS5 separation column attached to the on-line postcolumn reactor and further to the flow-through cell (Helma, volume 15 μl, path length 1 cm). The DPC reagent was delivered into the system at 0.5 ml/min by using a Dionex pneumatic postcolumn reagent-delivery device.

3. Results and discussion

Initial verification of the efficiency of the HPIC separation procedure [8] was performed with an air-cooled argon ion laser providing 10

mW power at the location of the flow-through cell. Retention times of about 180 and 280 s for $Cr(PDCA)_2^-$ and Cr(VI), respectively, were observed, as shown in Fig. 2. Based on a signal-to-noise ratio (S/N) of 3, the LOD was estimated to be 5 μg/ml for Cr(III) and 20 ng/ml for Cr(VI).

It is known from the theory of the thermal lens effect [12] that the relative change in the probe beam intensity ($\Delta I/I$) is proportional to the absorbance (A) and parameters such as temperature coefficient of refractive index (dn/dT), thermal conductivity (k) and probe beam wavelength (λ):

$$\frac{\Delta I}{I} = \frac{1.21A(-dn/dT)P}{\lambda k} \quad (1)$$

In addition, the thermal lens signal increases linearly with increasing laser power (P). For this reason, a more powerful laser, providing 160 mW at the location of the detection cell, was used in further experiments.

Differently from TLS measurements in non-flowing samples, the fluctuations in eluent flow strongly affect the signal stability in HPIC. Therefore, the TLS parameters such as modulation frequency and lock-in amplifier time constant must be carefully selected to maximize S/N. By selecting longer lock-in time constants, the signal was averaged over longer time intervals and the signal noise was reduced. Owing to the longer averaging periods, the chromatographic peaks were also shifted and appeared at longer retention times. These effects can be observed by comparing the chromatograms in Fig. 2 (time constant = 1 s) and Figs. 3 and 4 (time constant = 10 s).

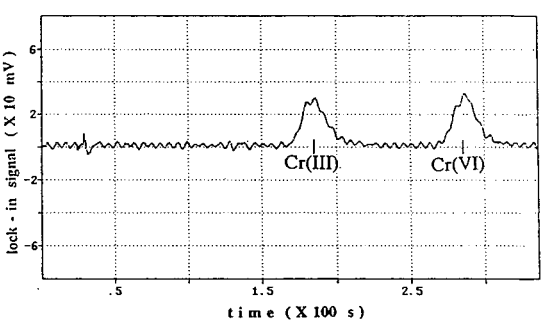

Fig. 2. Chromatogram of $Cr(PDCA)_2^-$–Cr(VI) mixture [10 μg/ml Cr(III) + 50 ng/ml Cr(VI)]. f = 8 Hz; P = 10 mW; time constant = 1 s.

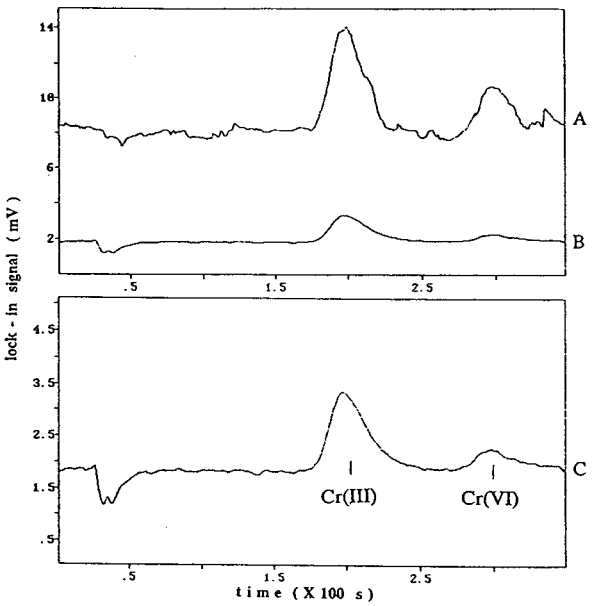

Fig. 3. Effect of chopping frequency on thermal lens signal and signal-to-noise ratio. Sample, 500 ng/ml Cr(III) + 5 ng/ml Cr(VI); P = 160 mW; time constant = 10 s; f = (A) 15, (B) 60 and (C) 60 Hz with expanded y-axis.

Additional improvements in S/N were obtained by optimizing the modulation frequency of the pump beam. A clear increase in S/N was evident when the modulation frequency was changed from 15 to 60 Hz. This is shown in Fig. 3, where a decrease of peak height can also be observed owing to the shorter excitation periods at higher modulation frequencies. However, for the same reason, the background thermal lens signal from the eluent is also reduced. Further, owing to the lock-in detection, which allows discrimination between the thermal lens signals appearing at the frequency of modulation and signals appearing at other frequencies, S/N is improved. For the experimental conditions used in this work (HPLC pump type, flow-rate), the optimum modulation frequency was found to be 75 Hz (Figs. 4 and 5).

The performance of the chromatographic sys-

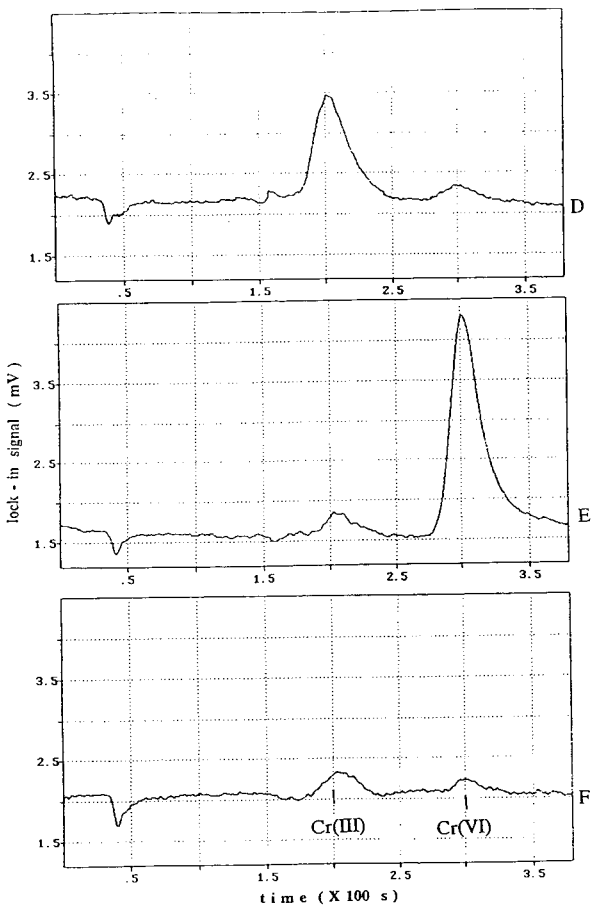

Fig. 4. Chromatograms of different $Cr(PCDA)_2^-$–Cr(VI) mixtures. $P = 160$ mW; $f = 75$ Hz; time constant = 10 s. (D) 500 ng/ml Cr(III) + 1 ng/ml Cr(VI); (E) 100 ng/ml Cr(III) + 20 ng/ml Cr(VI); (F) 100 ng/ml Cr(III) + 1 ng/ml Cr(VI).

tem with TLS detection under optimum conditions is evident from Fig. 4, which shows chromatograms obtained with samples containing different amounts of $Cr(PDCA)_2^-$ and Cr(VI). At present, the LOD ($S/N = 3$ basis), as calculated from chromatogram F (Fig. 4), is 30 and 0.3 ng/ml for Cr(III) and Cr(VI), respectively. These LODs equal the best LOD for the simultaneous determination of Cr(III) and Cr(VI) by HPIC with conventional UV–Vis detection as given in the literature [8]. It must be mentioned, however, that a detailed comparison between the results presented here and those in

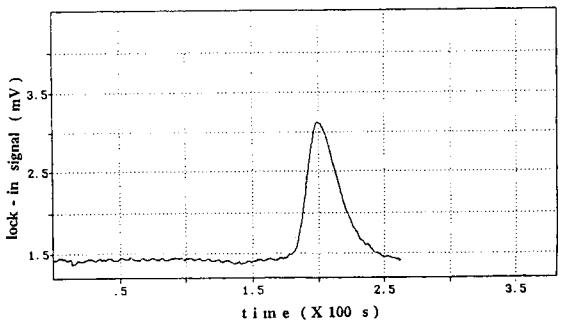

Fig. 5. Thermal lens signal in the absence of postcolumn reagent flow. Sample, 500 ng/ml Cr(III); $P = 160$ mW; $f = 75$ Hz; time constant = 10 s.

the literature is impossible, because the S/N used for the calculation of LOD is not given in Ref. [8] and the lowest concentration of Cr(VI) used to obtain a chromatogram was 3.8 ng/ml. Nevertheless, in terms of the minimum mass of Cr(III) and Cr(VI) that can still be detected, i.e., 6 ng and 60 pg, respectively, the LODs obtained by TLS are superior because of the smaller sample loop used in this work.

In addition to the use of a larger sample loop, the most significant improvement in the LOD of TLS detection in HPIC of Cr(III) and Cr(VI) is expected from stabilization of the eluent flow, which contributes to the thermal lens signal noise. To reveal the source of this signal noise, a chromatogram of Cr(III)–PDCA complex was recorded without the addition of postcolumn DPC reagent (Fig. 5). This experiment confirmed that signal instability arises primarily from periodic changes in eluent flow caused by the pulsed operation of the HPLC pump and not from the addition of DPC reagent. It is expected that better stability of the eluent flow and consequently lower baseline noise could be obtained by the use of a pulseless HPLC pump. As a result, lower LODs are expected.

The added postcolumn DPC reagent, which is needed for the detection of Cr(VI), actually dilutes the eluent and reduces the concentrations of eluted $Cr(PDCA)_2^-$ and Cr(VI) anions. The resulting decrease in peak height is clearly evident when chromatogram D in Fig. 4 is compared with the chromatogram in Fig. 5 (no DPC

added). The $Cr(PDCA)_2^-$ peak in Fig. 5 is about 30% higher, which is in good agreement with the eluent dilution factor in the case of added DPC (eluent flow-rate 1.0 ml/min, postcolumn reagent flow-rate 0.5 ml/min). This implies the possibility of obtaining an improved LOD for Cr(III) in the absence of postcolumn reagent and an improved LOD for both species by optimizing the postcolumn reagent concentration and/or flow-rate. Further improvements, which are currently under investigation, are possible by an additional increase in laser power or by application of lasers (krypton, excimer-pumped dye lasers) that better match the absorption maximum of the Cr(III) and Cr(VI) complex.

By fully exploring the potential of TLS, the LOD for the simultaneous determination of Cr(III) and Cr(VI) after HPLC separation should approach the LOD obtained for Cr(VI) in non-flowing samples, i.e., 0.1 ng/ml [13] and correspondingly 10 ng/ml for Cr(III).

4. Conclusions

It has been demonstrated that thermal lens spectrometry is a simple, rapid and sensitive method for the on-line detection of Cr(III) and Cr(VI) after HPIC separation. The LOD of 30 ng/ml for Cr(III) and 0.3 ng/ml for Cr(VI) permits the determination of Cr(III) concentrations lower than 100 ng/ml and Cr(VI) concentrations lower than 1 ng/ml in solutions containing both chromium species. Considering the smaller injection loop (200 μl), the LODs obtained are superior to those obtained with spectrophotometric detection at 520 nm [8].

Acknowledgement

Financial support for this work was provided by Slovenian Ministry of Science and Technology.

References

[1] P.S.J. Lees, *Environ. Health Perspect.*, 92 (1991) 93.
[2] S.A. Katz, *Environ. Health Perspect.*, 92 (1991) 13.
[3] K. Al-Sabti, M. Franko, B. Andrijanič and S. Knez, *J. Appl. Toxicol.*, 14 (1994) 333.
[4] *Official Gazette of SFR Yugoslavia (Uradni List SFRJ)*, No. 8, 1978, pp. 185–187.
[5] L.S. Clesceri, A.E. Greenberg and R.R. Trussell (Editors), *Standard Methods for the Examination of Water and Wastewaters*, Port City Press, Baltimore, 1989.
[6] T.L. Allen, *Anal. Chem.*, 30 (1958) 447.
[7] Z. Marczenko, *Separation and Spectroscopic Determination of Elements*, Ellis Horwood, New York, 1986.
[8] *Dionex Ion Chromatography Cook Book, a Practical Guide to Quantitative Analysis by Ion Chromatography*, Issue 1, Dionex, Sunnyvale, CA, 1987.
[9] I.S. Krull, K.W. Panaro and L.L. Gershman, *J. Chromatogr. Sci.*, 21 (1983) 460.
[10] I.S. Krull, D. Bushee, R.N. Savage, R.G. Schleider and S.B. Smith, *Anal. Lett.*, 15 (1982) 267.
[11] J. Lintschinger, K. Kalcher, W. Gössler, G. Kölbl and M. Novič, *Fresenius J. Anal. Chem.*, in press.
[12] N.J. Dovichi, *CRC Crit. Rev. Anal. Chem.*, 17 (1987) 357.
[13] M. Franko, *12th International Symposium on Microchemical Techniques—Book of Abstracts, Cordoba, September 1992*, p. 159.

ELSEVIER

Journal of Chromatography A, 706 (1995) 127–136

JOURNAL OF CHROMATOGRAPHY A

Simultaneous determination of chromium(III) and chromium(VI) by ion chromatography with inductively coupled plasma mass spectrometry

Yoshinori Inoue*, Tetsushi Sakai, Hiroki Kumagai

Division of R&D, Yokogawa Analytical Systems, 11–19 Nakacho 2-chome, Musashino-shi, Tokyo 180, Japan

Abstract

A combined system of inductively coupled plasma mass spectrometry (ICP-MS) with ion chromatography (IC) was used for the speciation of the chromium (Cr) species. After chelation with ethylenediaminetetraacetic acid (EDTA), Cr(III) and Cr(VI) were separated by anion-exchange chromatography. Subsequently, eluates from a separation column were directly introduced into the ICP-MS and detected at m/z 52 and 53. Separation parameters were optimized for the chromium species. Excelpak ICS-A23 (75 × 4.6 mm I.D.) packed with hydrophilic polymer based anion-exchange resin (ion-exchange capacity: 0.05 mequiv. g^{-1} dry weight) was used as separation column and $1.0 \cdot 10^{-3}$ *M* EDTA-2NH_4–0.01 *M* oxalic acid (pH 7.0) was used as a mobile phase. Cr(III) and Cr(VI) were completely separated within 8 min without any interference of ArC^+ and ClO^+. Detection limits ($S/N = 3$) for Cr(III) and Cr(VI) were $8.1 \cdot 10^{-5}$ and $8.8 \cdot 10^{-5}$ mg Cr/l, respectively. The linear range was 4 orders of magnitude, from $0.5 \cdot 10^{-3}$ to 5 mg Cr/l. With regard to reproducibility, R.S.D. ($n = 5$) was better than 2.5%. The developed IC–ICP-MS method was applied to the determination of the chromium species and metal elements in water.

1. Introduction

Chromium (Cr) can occur in at least three different valences, viz., Cr(VI), Cr(III) and Cr(II). In general, most of the chromium species are either Cr(III) or Cr(VI), with far fewer existing as Cr(II). In water samples, chromium exists as chromic [Cr^{3+}] or chromate [CrO_4^{2-} = Cr(VI)]. Cr(III) is an essential element for humans and animals and plays an important role as the glucose-tolerance factor (GTF) in insulin metabolism [1,2]. On the other hand, Cr(VI) is very toxic for humans and causes chronic adverse effects [1]. Therefore, to evaluate the toxicity of chromium in environmental and biological samples, speciation of the chromium species is required.

High-performance liquid chromatography (HPLC) and ion chromatography (IC) are good separation methods for such a speciation study. Separation procedures utilizing chelating reagents have been described for the speciation of the chromium species [3–13]. When using the chelation technique, both chromium species are

* Corresponding author.

0021-9673/95/$09.50
SSDI 0021-9673(95)00125-5

retained on the separation column and not affected by a solvent front peak (water dip). Dithizone [3], β-diketones [4], 8-quinolinol [5] and dithiocarbamate derivatives [6,7] were applied to the speciation of the chromium species by reversed-phase HPLC. Ethylenediaminetetraacetic acid (EDTA) [8–13] has also been used for the speciation chromium. The EDTA chelates are retained on anion-exchange resins because EDTA easily forms stable negatively charged chelates with many metal elements, regardless of the metal ion charge. Although the EDTA chelating method is an effective separation procedure for metal elements, lack of sensitivity and selectivity causes a problem in the determination of trace amounts of elements in samples containing complicated matrices.

In order to improve its sensitivity and selectivity, an atomic emission spectrometric method, such as direct current plasma emission spectrometry (DCP) or inductively coupled plasma atomic emission spectrometry (ICP-AES), has been combined with HPLC or IC as an element-selective detector [14–18]. However, these methods cannot perform simultaneous multi-elemental detection. Inductively coupled plasma mass spectrometry (ICP-MS) is a sensitive, accurate and precise analytical tool for ultra-trace multi-elemental and isotopic analysis. Although ICP-MS cannot give any information on speciation, several researchers have applied ICP-MS as an element-selective and multi-elemental detector because it combines well with HPLC or IC [19–26].

In this paper, simultaneous determination of the chromium species by IC with ICP-MS as the element-selective and multi-elemental detector is described. The chromium species were separated by an anion-exchange chromatograph after chelating with EDTA. The eluate was directly introduced into the ICP-MS system for the detection of the chromium species. The conditions for separation and complex formation were optimized for the chromium species. The developed IC–ICP-MS method was applied to the determination of chromium species and metal elements in water.

2. Experimental

2.1. Reagents

Chromium nitrate and potassium chromate used in this study were purchased from Wako Pure Chemical Industries (Osaka, Japan). Pure water was obtained from a Milli-Q/SP system (Nihon Millipore, Tokyo, Japan). Stock solutions (0.01 mol Cr/l) of both chromium species were prepared by dissolving each reagent in pure water and were stored in a refrigerator. Analytical solutions were prepared by diluting the stock solutions to obtain an adequate chromium concentration.

Analytical reagent grade oxalic acid, ultrapure acetic acid and ammonium hydroxide (25%) were purchased from Wako Pure Chemical Industries (Osaka, Japan). Ethylenediaminetetraacetic acid diammonium salt (EDTA-2NH_4) and metal–EDTA chelates were purchased from Dojindo Laboratories (Kumamoto, Japan).

2.2. Ion chromatography

The ion chromatograph used in this experiment was a Model IC7000S (Yokogawa Analytical Systems, Tokyo, Japan). Excelpak ICS-A23 and Excelpak ICS-A2G (Yokogawa Analytical Systems, Tokyo, Japan) were chosen as separation columns. The ICS-A23 column is 75 × 4.6 mm I.D., packed with hydrophilic polymer-based anion-exchange resin (particle diameter, 6 μm) with 0.05 mequiv./g dry weight. ICS-A2G (25 × 2.7 mm I.D., packed with the same packing) is used as a guard column for the ICS-A23. For separation of the chromium species, EDTA-2NH_4 and oxalic acid were used as the mobile phase, the pH being adjusted with 25% ammonium hydroxide. Ammonium salt was selected as the mobile phase in this study, because sodium salt might clog the ICP torch and decrease the sensitivity of the ICP-MS [25].

Poly[ethylenetetrafluoroethylene] (ETFE) tubing (800 × 0.3 mm I.D.) was used for the connection between the column and the nebulizer of the ICP-MS system. Unless otherwise

stated, the ion chromatograph was operated under the following conditions: mobile phase flow-rate, 1.0 ml/min; column temperature, 40°C; and injection volume, 0.05 ml.

2.3. ICP-MS

The ICP-MS instrument used in this experiment was a Model HP 4500 (Hewlett-Packard, Wilmington, DE, USA). The operating parameters are described in Table 1. A Scott-type spray chamber, maintained at 0°C by means of a Peltier-type thermoelectric module, a Fassel-type torch and a concentric glass nebulizer (Precision Glassblowing, CO, USA) were used in the experiments. For data acquisition of the IC–ICP-MS, a selected-ion monitoring (SIM) mode was used. A quantitative analysis mode (QTM) was used for data acquisition of the conventional introduction system. For the QTM, an atomic mass unit (amu) was divided into 20 points and the middle three points were used for data acquisition. An adequate dwell time of the amu was chosen for each metal element and the scan was repeated three times. A pulse-counting mode was used. For data acquisition of calcium (Ca), an analog detection mode was used, because a large amount of Ca was generally present in the water samples, i.e. tap water, ground water and river water. For tuning of the ICP-MS system, a standard solution of 0.01 mg/l yttrium (Y) was analyzed. The system was tuned to get a maximum signal for Y by monitoring m/z 89 and changing a bias of lenses.

Table 1
ICP-MS operating conditions

Instrument	Model HP 4500
Radiofrequency forward power	1.3 kW
Radiofrequency reflected power	<5 W
Plasma gas flow	Ar, 16 l/min
Auxiliary gas flow	Ar, 1.0 l/min
Carrier gas flow	Ar, 1.03 l/min
Sampling depth	5 mm from load coil
Monitoring mass	m/z 52 and 53
Dwell time	0.1 s
Number of scans	1

2.4. Other procedures

In order to determine the water hardness, the concentrations of magnesium and calcium were determined by both a titration method and by IC with conductometric detection. The titration method was operated according to the JIS (Japanese Industrial Standard) K0102-1993, "The Testing Method for Industrial Waste Water". The IC operating parameters were as follows: Excelpak ICS-C25 column (Yokogawa Analytical Systems, Tokyo, Japan) packed with silica-based weak cation-exchange resin; mobile phase, $1 \cdot 10^{-3}$ M 2,6-pyridinedicalcoxylic acid–$5 \cdot 10^{-3}$ M tartaric acid; flow-rate, 1.0 ml/min; column temperature, 40°C; injection volume, 0.05 ml.

3. Results and discussions

3.1. Formation of complex

The formation rate of the complex between Cr(III) and EDTA is very slow [27]. With regard to the toxic compound analysis, it is essential to increase the complex formation rate to shorten the analysis time. The formation rate of the complex is affected by reaction temperature and pH. Complex formation was performed according to previous reports [11–13] with slight modifications. In the present study, the effects of temperature and pH on the complex-forming reaction were confirmed.

A mixed solution of Cr(III) and EDTA (molar ratio 1:50) was incubated at 20, 40 and 60°C. A 0.05-ml volume of the reactant solution was analyzed by IC–ICP-MS, using 0.01 M of EDTA-2NH_4 (pH 7.0) as the mobile phase. The time required for complete complex formation at 20, 40 and 60°C was 350, 30 and 15 min, respectively. Complex formation was favoured by higher temperatures. It should be noted that higher temperatures might also provoke oxidation of Cr(III) by chromate, because the oxidation ability of chromate is enhanced at higher temperatures. As a consequence of this result

and the results of previous reports [11–13], a reaction temperature of 40°C was chosen.

The rate of complex formation is also affected by the pH of the reaction medium. The pH was varied from 3 to 10. pH adjustment was made by adding acetic acid or ammonium hydroxide. Fig. 1a shows the relationship between pH and the peak area of the Cr(III)–EDTA complex formed in a mixed solution of $1 \cdot 10^{-5}$ *M* of Cr(III) and EDTA (molar ratio 1:100) during an incubation time of 30 min at 40°C. While the peak area of Cr(III)–EDTA remained constant at pH 3–6, it decreased above pH 6, due to ionization of EDTA above pH 6, resulting in less complex formation. At pH 10, the peak of free Cr(III) (chromic ion, Cr^{3+}) was observed at the solvent front and the sum of both peak areas was the same as that of the Cr(III)–EDTA peak at pH 6.

The oxidation ability of chromate is enhanced at higher pH. Fig. 1b shows that the relationship between the reaction pH and the peak area of the Cr(III)–EDTA complex formed in the mixed solution was correlated with the chromate peak (chromate concentration was $1 \cdot 10^{-5}$ *M*) under the same conditions. The peak area of Cr(III)–EDTA decreased above pH 6 as shown in Fig. 1a, but that of Cr(VI) increased above pH 6. The sum of the peak areas of both chromium species at pH 10 was the same as that at pH 6, which means that part of the Cr(III) was oxidized to Cr(VI) by chromate during the complex-forming reaction at higher pH.

As a consequence of these results, the following reaction conditions were chosen for the complex formation: pH for the complex-forming reaction, 6.0; reaction temperature, 40°C; incubation time, 30 min. These optimized conditions were almost the same as those described in previous reports [11–13].

3.2. Optimization of separation conditions

The effect of the mobile-phase pH was examined in order to optimize the IC operating conditions. EDTA-2NH_4 was used as the mobile phase and the mobile-phase pH was varied from 6 to 10 at a fixed EDTA-2NH_4 concentration of $3 \cdot 10^{-3}$ *M*. A sample of Cr(III)–EDTA and Cr(VI) ($1 \cdot 10^{-5}$ *M*) was used of which 0.05 ml was injected. Detection on the ICP-MS system was performed at *m/z* 52 and 53.

Fig. 2 shows the relationship between the retention time of the chromium species and the

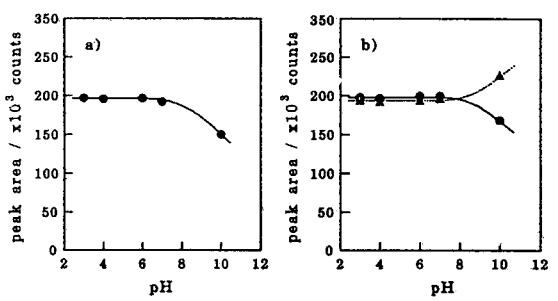

Fig. 1. Relationship between the pH used for the complex forming reaction and the peak areas of the Cr(III)–EDTA complex and Cr(VI). (a) The peak area of the Cr(III)–EDTA complex formed in a mixed solution of Cr(III) and EDTA. (b) The peak area of the Cr(III)–EDTA complex formed in the mixed solution coexisting with chromate. Column, Excelpak ICS-A2G/ICS-A23, mobile phase, 0.01 *M* EDTA-2NH_4 (pH 7.0); flow-rate, 1.0 ml/min; column temperature, 40°C. Detection is performed at *m/z* 53. Sample is $1 \cdot 10^{-5}$ mol Cr/l each and the injection volume is 0.05 ml. (●) Cr(III), (▲) Cr(VI).

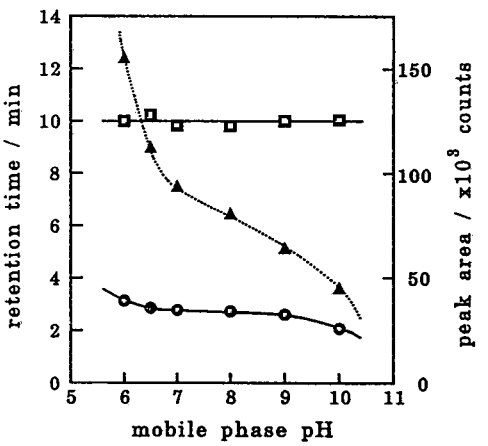

Fig. 2 Relationship between the retention times of the chromium species, the Cr(III)–EDTA peak area and the mobile phase pH. Conditions and sample as in Fig. 1 except for the mobile phase. The mobile phase is $3 \cdot 10^{-3}$ *M* EDTA-2NH_4. (●) Cr(III), (▲) Cr(VI), (□) peak area of Cr(III)–EDTA.

mobile-phase pH. In the range of this experiment, Cr(III)–EDTA and Cr(VI) were clearly retained and Cr(III)–EDTA was completely separated from the solvent front. Below pH 6, the peak of Cr(VI) was not eluted within 30 min. Although the retention time of Cr(VI) decreased as the mobile-phase pH increased, a peculiar elution behaviour was observed, as shown in Fig. 2. This behaviour was due to ionization of EDTA and chromate. Because EDTA has four acidic dissociation constants (p*K*a), viz., 1.99, 2.67, 6.16 and 10.26, and chromate has two, viz., 0.74 and 6.49, two inflection points were observed in the vicinity of pH 6.5 and 10. It should be noted that a higher pH of the mobile phase might provoke oxidation of Cr(III) by chromate and decomposition of the Cr(III)–EDTA complex, as well as complex-forming reaction. As indicated by the constant Cr(III)–EDTA peak area, no oxidation and no degradation were observed at pH 6–10 (Fig. 2).

However, the peak shape of Cr(VI) showed severe tailing and the peak height was about one-half that of Cr(III)–EDTA under these elution conditions. This means that the ionic strength of EDTA was essentially low at neutral pH. Furthermore, the background counts of the ICP-MS detection were very high at m/z 52. Therefore, the mobile phase was changed from EDTA to oxalic acid which is a strongly ionic and low-carbon compound. The effect of the oxalic acid concentration in the mobile phase was examined. The oxalic acid concentration was varied from 0.005 to 0.012 *M* at a fixed mobile-phase pH of 7.0 and an EDTA-2NH$_4$ concentration of $2 \cdot 10^{-3}$ *M*. EDTA-2NH$_4$ was added to the mobile phase to stabilize the complex. In order to determine the void volume (V_0), a sample containing 1 mg Li/l (Li) was analyzed at m/z 7 under the same conditions. Fig. 3 shows the relationship between the capacity factors (k') of the chromium species and the concentration of oxalic acid. The capacity factors of both chromium species decreased as the oxalic acid concentration increased. A linear relationship was obtained between the k' values of the chromium species and the oxalic acid concentration. When using oxalic acid as the mobile

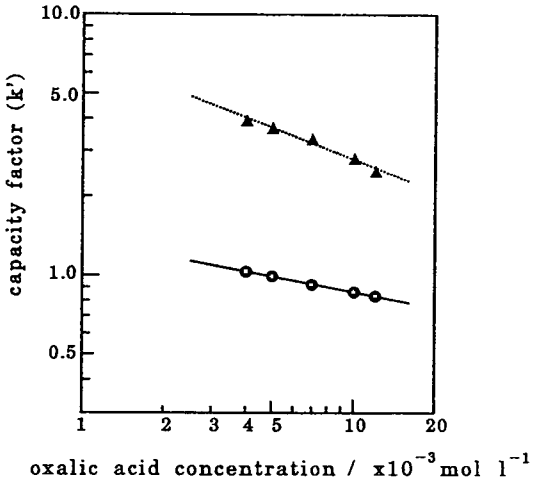

Fig. 3. Relationship between the capacity factors of the chromium species and the concentration of oxalic acid. Conditions and sample as in Fig. 1 except for the mobile phase. The mobile phase is $2 \cdot 10^{-3}$ *M* EDTA-2NH$_4$–oxalic acid (pH 7.0). (●) Cr(III), (▲) Cr(VI).

phase, symmetrical peaks of the chromium species were observed and the peak height of Cr(VI) was higher than when EDTA was used as the mobile phase.

An adequate addition of EDTA to the mobile phase is required to stabilize the EDTA complex. Since the background counts and the baseline noise of the ICP-MS detection depended on the EDTA concentration, the effect of the concentration of EDTA added to the mobile phase was examined. The EDTA-2NH$_4$ concentration was varied from 0 to $3 \cdot 10^{-3}$ *M* at a fixed mobile-phase pH of 7.0 and a fixed oxalic acid concentration of 0.01 *M*. Fig. 4 shows the relationship between the k' values of the chromium species and the EDTA-2NH$_4$ concentration. The capacity factors of the chromium species decreased as the EDTA-2NH$_4$ concentration increased. Fig. 5 shows the effect of the EDTA-2NH$_4$ concentration on the background counts, the baseline noise and S/N ratio of the ICP-MS system. The background counts and the baseline noise at both m/z 52 and 53 increased with increasing EDTA-2NH$_4$ concentration. Although the S/N ratio at m/z 52 decreased with increasing EDTA-2NH$_4$ concentration, m/z 53 revealed a maximum at $1 \cdot 10^{-3}$ *M* EDTA-2NH$_4$.

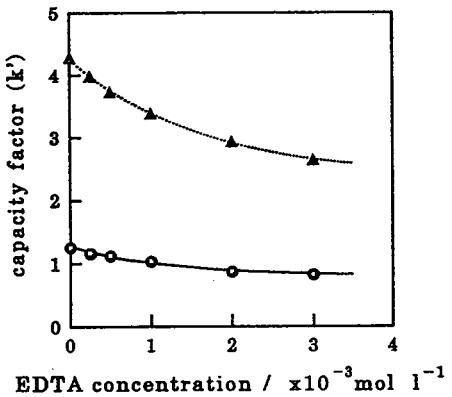

Fig. 4. Relationship between the capacity factors of the chromium species and the EDTA-2NH_4 concentration. Conditions and sample as in Fig. 1 except for the mobile phase. The mobile phase is EDTA-2NH_4–0.01 *M* oxalic acid (pH 7.0). (●) Cr(III), (▲) Cr(VI).

The reason of the conflicting *S/N* ratio has still to be solved.

The optimized operational conditions are described in Table 2. To determine low-level concentrations of the chromium species, the injection volume was increased from 0.05 ml to 0.5 ml and the dwell time was increased from 0.1 to 1.0 s. A chromatogram of Cr(III) and Cr(VI) is shown in Fig. 6. The chromium species were completely separated and detected within 8 min without interference of the water dip.

In this study two buffer modifiers (EDTA and oxalic acid) were used as the mobile phase. These modifiers may form a complex with Cr(III). At pH 7.0, EDTA can form a very stable complex with Cr(III), whereas oxalic acid can not because of its acidity. With EDTA as modifier Cr(III) mainly exists as the complex Cr(III)–EDTA (though the existence of a hydroxo complex should be considered because the logarithm of the stability constant of the hydroxo complex is very low compared with that of the complex Cr(III)–EDTA). Of the two buffer modifiers, oxalic acid only functions as an eluent of the Cr species, while EDTA functions both as

Table 2
Optimized operating conditions

Instrument	Model IC7000S
Column	Excelpak ICS-A2G/ICS-A23 (25 × 2.7 mm I.D./75 × 4.6 mm I.D.)
Mobile phase	$1.0 \cdot 10^{-3}$ *M* EDTA-2NH_4–0.01 *M* oxalic acid (pH 7.0)
Flow-rate	1.0 ml/min
Column temperature	40°C
Detector	ICP-MS
Monitoring mass	*m/z* 52
Dwell time	1.0 s
Injection volume	0.5 ml

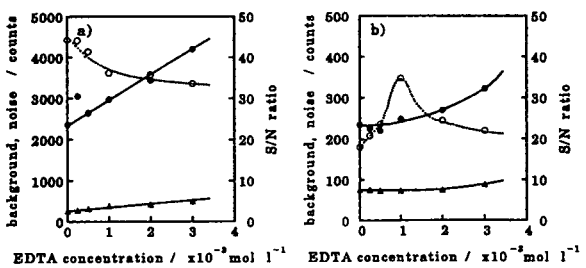

Fig. 5. Effect of the EDTA-2NH_4 concentration on background counts, baseline noise and *S/N* ratio of ICP-MS at *m/z* 52 (a) and 53 (b). Conditions and sample as in Fig. 4. (●) Background counts, (▲) baseline noise, (○) *S/N* ratio.

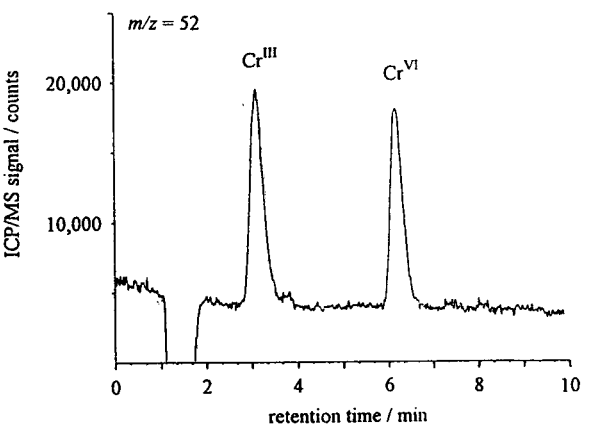

Fig. 6. Chromatogram of chromium species obtained by IC–ICP-MS. Conditions as in Table 2. Sample is $0.5 \cdot 10^{-3}$ mg Cr/l each. Injection volume is 0.5 ml.

an eluent of the Cr species and as a stabilizer of the Cr(III) complex.

3.3. Linearity, detection limits, reproducibility and interferences

Linearity, detection limits and reproducibility were determined for both chromium species. The linear range was 4 orders of magnitude, from $0.5 \cdot 10^{-3}$ to 5 mg Cr/l. The detection limits and the reproducibility were calculated for a $1 \cdot 10^{-3}$ mg Cr/l solution by injection of a 0.5-ml sample. The detection limits ($S/N = 3$) for Cr(III) and Cr(VI) at m/z 52 were $8.1 \cdot 10^{-5}$ and $8.8 \cdot 10^{-5}$ mg Cr/l, respectively. The relative standard deviations ($n = 5$) for $1 \cdot 10^{-3}$ mg Cr/l of both chromium species were 2.35% and 1.79%, respectively. Furthermore, the recoveries of added chromium species were examined. An amount of $1 \cdot 10^{-3}$ mg Cr/l of both chromium species was added to ground water and analyzed under the same conditions. The recoveries of Cr(III) and Cr(VI) by IC–ICP-MS ranged from 102 to 115% with averages of about 103.9 and 110.4%, respectively ($n = 5$).

Since the chromium species are decomposed and turned into Cr, O, H and C ions in plasma, the sensitivity of the determination of the chromium species as chromium does not depend on its structure. When the concentration as chromium is the same, each species must give the same peak area on the chromatogram. In this study, good agreement was obtained for the different chromium species.

It must be taken into consideration that polyatomic ion (molecular ion) interference may occur in ICP-MS [28,29]. The $^{40}Ar^{12}C^+$ ion can be generated from carbon in the mobile phase and the argon gas used as the plasma gas. This ion interferes with the determination of chromium at m/z 52, which is the most abundant chromium isotope. Interference by the $^{37}Cl^{16}O^+$ ion at m/z 53, due to high contents of chlorine in the sample ion, also occurred. Although the background count at m/z 52 was relatively high due to the use of organic acid as the mobile phase, interference from carbon in the sample was not observed. When a 100 mg/l chloride solution was analyzed under the same conditions, the ClO^+ ion at m/z 53 was detected before and separated from the Cr(III)–EDTA complex.

3.4. Simultaneous separation of other metal elements

As described above, EDTA can form stable chelates with many metal elements. The IC–ICP-MS system with EDTA as the chelating compound was applied to the determination of metal elements. Several metal EDTA chelates were determined by the IC–ICP-MS system under the same conditions. The retention times of the metal–EDTA chelates and their detection limits as metal element are given in Table 3. Although metal–EDTA chelates could not be completely separated with the IC column, qualitative and quantitative analysis of metal elements can easily be carried out by using ICP-MS because of its element selectivity (Fig. 7).

3.5. Determination of the chromium species and metal elements in water

The developed IC–ICP-MS method was applied to the determination of chromium species and metal elements in water. Each sample was analyzed by both IC–ICP-MS and ICP-MS with the conventional introduction system. For the determination of magnesium and calcium, the same samples were also analyzed by the titration method and IC with conductometric detection. Hardness, as calcium carbonate ($CaCO_3$), was calculated from the concentrations of magnesium and calcium. The concentrations of the metal elements as determined by each procedure are given in Table 4.

Although 2 μg Cr/l (total Cr) or less was determined in each sample, Cr(VI) was not detected in samples A and B. The concentration of Cr as determined by IC–ICP-MS agreed with the ICP-MS results which were relatively higher than those obtained with IC–ICP-MS. This means that the ICP-MS results obtained with the conventional introduction method suffered from

Table 3
Retention times and detection limits of the chromium species and metal elements

Element	m/z	Dwell time (s)	Counting mode	Retention time (min)	Detection limit (μg/l)[a]
Cr(III)	52	0.50	pulse	3.08	0.14
Cr(VI)	52	0.50	pulse	6.13	0.16
Mg	24	0.01	pulse	3.17	0.16
Ca	44	0.01	analog	2.78	27.78
Mn	55	0.20	pulse	3.05	0.02
Fe	57	0.20	pulse	2.62	1.82
Co	59	0.10	pulse	3.46	0.007
Ni	60	0.10	pulse	3.43	0.18
Cu	63	0.10	pulse	3.60	0.01
Zn	66	0.10	pulse	3.50	0.27
Pb	208	0.10	pulse	3.17	0.05

[a] As metal element.

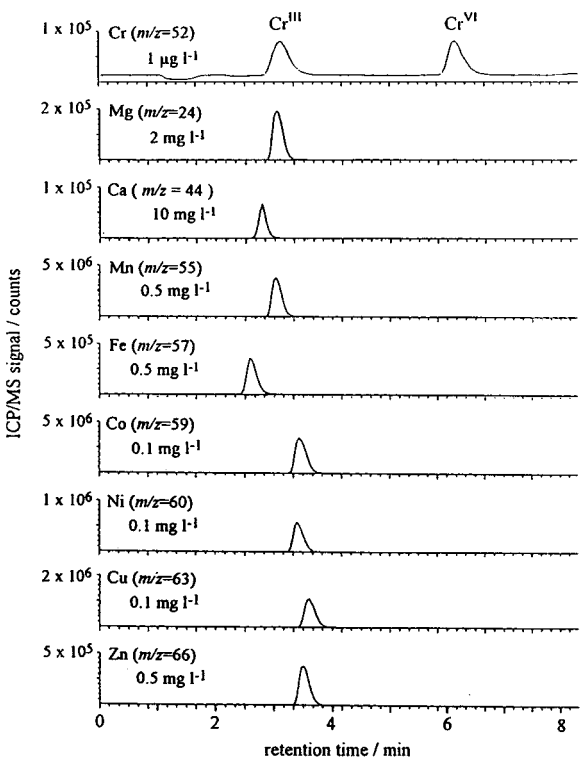

Fig. 7. Chromatograms of chromium species and metal elements by IC–ICP-MS. Conditions as in Tables 2 and 3.

interference by some matrices components, such as carbon and chlorine. The concentrations of the metal elements as determined by both methods correlated rather well, except for Fe. The concentration of Fe as determined by ICP-MS may appear higher than that determined by IC–ICP-MS, because m/z 57 shows interference from the ions $^{40}Ar^{16}O^{1}H$ and $^{40}Ca^{16}O^{1}H$. With respect to hardness, good agreement was observed for all methods.

4. Conclusions

An analytical method for the speciation of chromium species utilizing chelation is presented. Cr(III) and Cr(VI) were completely separated and detected within 8 min by the IC–ICP-MS method without any interference by ArC^{+} and ClO^{+}. The IC–ICP-MS chelation method not only presents a useful procedure for the speciation of chromium species, but can also be used for a multi-element analysis. Moreover, the IC–ICP-MS system facilitates the sample preparation process. The combination of IC–ICP-MS and chelation will be very useful for environmental monitoring of chromium species and many other metal elements in water. Further experiments will be required on the precision

Table 4
Determination of the chromium species and metal elements in water

Element	Procedures	m/z	Dwell time (s)	Concentration (μg/l)[a]				
				A	B	C	D	E
Cr^{III}	IC–ICP-MS	52	0.50	0.81	1.01	0.17	0.41	0.75
Cr^{VI}	IC–ICP-MS	52	0.50	N.D.	N.D.	0.23	0.13	1.19
Total Cr	IC–ICP-MS	–	–	0.81	1.01	0.40	0.54	1.94
	ICP-MS	52	1.00	0.71	0.75	0.68	0.93	2.21
Mn	IC–ICP-MS	55	0.20	2.53	1.97	0.37	0.09	0.01
	ICP-MS	55	0.50	2.79	2.78	0.25	0.09	0.01
Fe	IC–ICP-MS	57	0.20	57.70	60.53	88.02	126.80	45.86
	ICP-MS	57	0.10	84.32	106.90	114.70	156.00	77.42
Ni	IC–ICP-MS	60	0.10	1.53	8.02	1.10	0.42	0.91
	ICP-MS	60	0.50	1.47	11.00	1.57	0.57	0.92
Cu	IC–ICP-MS	63	0.10	3.39	7.81	1.78	0.48	0.88
	ICP-MS	63	0.10	2.84	12.69	3.14	0.32	1.04
Mg (mg/l)	IC–ICP-MS	24	0.01	3.75	3.64	4.80	3.52	3.77
	ICP-MS	24	0.10	4.71	4.71	6.64	3.57	4.39
	IC	–	–	4.00	3.80	5.90	3.50	4.00
	Titration	–	–	4.20	4.20	5.60	4.30	1.90
Ca (mg/l)	IC–ICP-MS	44	0.01	24.22	25.86	37.31	48.89	23.48
	ICP-MS	44	0.10	20.65	22.70	31.90	39.57	20.09
	IC	–	–	18.20	19.70	28.90	38.50	18.80
	Titration	–	–	18.80	20.40	30.80	38.60	19.50
Hardness as $CaCO_3$[b] (mg/l)	IC–ICP-MS	–	–	76	79	112	136	74
	ICP-MS	–	–	70	76	107	114	68
	IC	–	–	62	65	96	110	52
	Titration	–	–	64	68	100	112	57

The conditions of IC–ICP-MS were the same as those given in Table 2 except for the dwell times of ICP-MS.
[a] Unit is μg/l except for the concentrations of Mg, Ca and hardness.
[b] Calculated from the concentration of Mg and Ca.
N.D. = not detected. A–C = tap-water samples; D, E = ground-water samples.

and the accuracy of the determination of metal elements by IC–ICP-MS.

References

[1] S. Langård and T. Norseth, in L. Friberg, G.F. Nordberg and V.B. Vouk (Editors), Handbook on the Toxicology of Metals, Vol. II, Specific Metals, Elsevier, Amsterdam, 2nd ed., 1990, pp. 185–210.
[2] T.M. Florence and G.E. Batley, *CRC Crit. Rev. Anal. Chem.*, 9 (1980) 219–267.
[3] B.R. Willeford and V. Hans, *J. Chromatogr.*, 251 (1982) 61.
[4] R.C. Gurira and P.W. Carr, *J. Chromatogr. Sci.*, 20 (1982) 461.
[5] L.H.J. Lajunen, E. Eijrvi and T. Kenakkala, *Analyst*, 109 (1984) 699.
[6] A.M. Bond and G.G. Wallace, *Anal. Chem.*, 54 (1982) 1706.
[7] T. Tande, J.E. Pettersen and T. Torgrimsen, *Chromatographia*, 13 (1980) 607.

[8] Y. Suzuki and F. Serita, *Ind. Health*, 23 (1985) 207.
[9] J.-F. Jen and C.-S. Chen, *Anal. Chim. Acta*, 270 (1992) 55.
[10] M.L. Marina, P. Andés and J.C. Díez-Masa, *Chromatographia*, 35 (1993) 621.
[11] Y. Suzuki, *Ind. Health*, 24 (1986) 23.
[12] J.-F. Jen, G.-L. Ou-Yang, C.-S. Chen and S.-M. Yang, *Analyst*, 118 (1993) 1281.
[13] G.-L. Ou-Yang and J.-F. Jen, *Anal. Chim. Acta*, 279 (1993) 329.
[14] D. Bushee, I.S. Krull, R.N. Savage and S.B. Smith Jr., *J. Liq. Chromatogr.*, 5 (1982) 463.
[15] I.S. Krull, K.W. Panaro and L.L. Gershman, *J. Chromatogr. Sci.*, 21 (1983) 460.
[16] I.T. Urasa and S.H. Nam, *J. Chromatogr. Sci.*, 27 (1989) 30.
[17] I.S. Krull, D. Bushee, R.N. Savage, R.G. Schleicher and S.B. Smith Jr., *Anal. Lett.*, 15 (1982) 267.
[18] S. Ahmed, R.C. Murthy and S.V. Chandra, *Analyst*, 115 (1990) 287.
[19] D.S. Bushee, *Analyst*, 113 (1988) 1167.
[20] D. Heikemper, J. Creed and J. Caruso, *J. Anal. Atom. Spectrom.*, 4 (1989) 279.
[21] H. Suyani, J. Creed, T. Davodson and J. Caruso, *J. Chromatogr. Sci.*, 27 (1989) 139.
[22] H. Suyani, D. Heikemper, J. Creed and J. Caruso, *Appl. Spectrosc.*, 43 (1989) 962.
[24] Y. Shibata and M. Morita, *Anal. Chem.*, 61 (1989) 2116.
[25] K. Kawabata, Y. Kishi, O. Kawaguchi, Y. Watanabe and Y. Inoue, *Anal. Chem.*, 63 (1991) 2137.
[26] Y. Inoue, K. Kawabata, H. Takahashi and G. Endo, *J. Chromatogr. A*, 675 (1994) 149.
[27] W.R. Seitz, W.W. Suydam and D.M. Hercules, *Anal. Chem.*, 44 (1972) 957.
[28] M. Vaughan and G. Horlick, *Appl. Spectrosc.*, 40 (1986) 434.
[29] S.H. Tan and G. Horlick, *Appl. Spectrosc.*, 40 (1986) 445.

ELSEVIER

Journal of Chromatography A, 706 (1995) 137–140

JOURNAL OF CHROMATOGRAPHY A

Clean-up procedure for the determination of inorganic anions by ion chromatography

Orfeo Zerbinati

Department of Analytical Chemistry, University of Turin, Via Giuria 5, I-10125 Turin, Italy

Abstract

Many organic anions can be strongly absorbed on ion chromatographic (IC) stationary phases, thus compromising analyses for inorganic anions. Selective removal of these organic anions from aqueous samples before IC was tried with four different types of SPE cartridges. An octadecylsilica cartridge loaded with cetyltrimethylammonium *p*-hydroxybenzoate was found to be effective in removing the tested organic anions without reducing the precision of analysis for common inorganic anions.

1. Introduction

Organic sulphonates are widely used as detergents, dyes and intermediates of dyes synthesis. Difficulties can arise when inorganic anions have to be determined in samples that also contain organic sulphonates. Although some application of ion chromatographic (IC) columns to the separation of mixtures organic anions have been reported [1], the eluents usually employed for the IC of common inorganic anions are not strong enough to elute organic anions, especially if multiply charged.

Fluctuations of the baseline, ghost peaks and rapid decreases in the column resolving power were encountered when common inorganic anions had to be routinely determined in samples of river water that was polluted by a dye factory. Regeneration of columns by washing with alkaline solutions or organic solvents was not successful, as the dark colour of the stationary phase resulted when a deteriorated column was examined. Guard columns were also tried, but organic pollutants quickly saturated them, probably because of the low ion-exchange capacity of the usual IC stationary phases.

Considering that similar difficulties can be met also when analyses of synthetic detergents or soft drinks have to be performed, a clean-up procedure capable of eliminating substances undesirable in IC could be of interest. Octadecylsilica coated with a cetyltrimethylammonium (CTMA) compound has already been employed as a stationary phase for IC [2,3]; a similar stationary phase was also used for the trace enrichment of organic anions in environment water samples [4]. Therefore, it seemed worthwhile to investigate whether such a stationary phase, or similar ones, would be suitable for the clean-up procedure needed. The results obtained by employing either silica or polymer-based C_{18} stationary

0021-9673/95/$09.50
SSDI 0021-9673(95)00042-9

phases, Quaternary Amine and Amino, are reported in this paper.

2. Experimental

2.1. Apparatus and reagents

A Metrohm (Herisau, Switzerland) Model 690 ion chromatograph equipped with a Hamilton PRP-X 100 column (150 × 4.1 mm I.D.) (Alltech, Deerfield, IL, USA) was used with 5 m*M* *p*-hydroxybenzoate (pH 8.6) as the eluent at a flow-rate of 1.8 ml min^{-1}. Both types of 100-mg C_{18} SPE cartridges used for this work were obtained from Alltech. Quaternary Amine and Amino cartridges were supplied by Baker (Deventer, Netherlands). Chemicals were obtained from Aldrich Italy (Milan, Italy).

2.2. Procedure

The following SPE cartridges were examined: Quaternary Amine, 500 mg; Amino, 500 mg; C_{18} silica, 100 mg loaded with CTMA; and C_{18} HEMA, 100 mg loaded with CTMA.

CTMA is absorbed on reversed-phase materials as an ion pair. To accomplish the purpose of this investigation, the counter anion of the absorbed CTMA should not be one of those sought by IC; *p*-hydroxybenzoate, which was adopted as a component of the IC eluent, was judged suitable. CTMA hydroxide and various CTMA salts are commercially available; considering their cost, a convenient procedure employing CTMA bromide was adopted. CTMA was deposited on C_{18} materials as its *p*-hydroxybenzoate salt by passing four times the following series of eluents: 5 ml of methanol; 10 ml of water; 10 ml of 1 m*M* CTMA bromide containing 10 m*M* sodium *p*-hydroxybenzoate; and 10 ml of 10 m*M* sodium *p*-hydroxybenzoate. After completing the CTMA loading procedure, the cartridges were dried by flushing them with air. Sodium *p*-hydroxybenzoate was prepared by neutralizing *p*-hydroxybenzoic acid solution with sodium hydroxide.

The test analytes were F^-, Cl^-, NO_2^-, Br^-, NO_3^-, HPO_4^{2-} and SO_4^{2-}, and the following organic anionic substances were chosen to test the effectiveness of the clean-up procedure: (A) 2-amino-1-naphthalenesulphonic acid, (B) 2-hydroxy-3,6-naphthalenesulphonic acid, (C) 2-anthraquinonesulphonic acid, (D) 2,7-naphthalenedisulphonic acid, (E) tartrazine (CI 19140), (F) Patent Blue V (CI 42051), (G) octylbenzenesulphonic acid, (H) dodecylbenzenesulphonic acid and (I) dodecyl sulphate.

Mixtures of compounds A–D, E–F and G–I were separately dissolved in ultra-pure water and added to solutions of inorganic anions in order to prepare three solutions containing 5 mg l^{-1} of each organic anion, while the concentrations of the seven inorganic anions ranged from 2 to 25 mg l^{-1}, in order to obtain chromatograms with uniform peak heights. Volumes of 10 ml of each of these three solutions were eluted on SPE cartridges to test the effectiveness of the clean-up procedure.

To test the dependence of organic removal on pH, the pH of the three standard solutions was adjusted with sodium hydroxide or *p*-hydroxybenzoic acid.

After clean-up, residual concentrations of organics were determined by appropriate techniques (HPLC for A–D [5], visible spectrophotometry for E and F and methylene blue extraction for G–I [6]).

3. Results

3.1. Removal of organic anions

Quaternary Amine and Amino cartridges removed organics quantitatively from solutions whose pH ranged from 3.5 to 12. Elution on both types of C_{18} cartridges produced complete removal in the pH range 4–8.

3.2. Recovery of inorganic analytes

Quaternary Amine silica proved not to be suitable for the purpose of this work, as it retained completely all anions other than chloride, and replaced them with the latter.

Table 1
Recoveries (%) of inorganic analytes ± standard deviations ($n = 4$)

Stationary phase	F^-	Cl^-	NO_2^-	Br^-	NO_3^-	PO_4^{2-}	SO_4^{2-}
Octadecylsilica	100 ± 1	100 ± 3	100 ± 1	98 ± 2	102 ± 1	97 ± 1	96 ± 1
C_{18} HEMA	100 ± 2	96 ± 6	98 ± 2	95 ± 2	98 ± 3	86 ± 6	83 ± 5
Amino	91 ± 4	106 ± 3	95 ± 3	91 ± 1	101 ± 3	16 ± 8	78 ± 9

The recoveries and their standard deviations ($n = 4$) for the remaining stationary phases are reported in Table 1. Singly charged anions were quantitatively recovered with C_{18} silica cartridges, while the concentration of multiply charged anions decreased slightly and reproducibly. C_{18} HEMA gave lower recoveries, with larger fluctuations, than C_{18} silica for all anions except fluoride. Amino cartridges retained considerable amounts of fluoride, phosphate and sulphate, and released chloride into test solutions.

Considering these results, octadecylsilica loaded with *p*-hydroxybenzoate was judged to be the most suitable for the purpose of this work among the stationary phases examined, and further experiments were carried out to test its performances.

3.3. Release of bromide ion from octadecylsilica cartridges

Considering that the bromide salt of CTMA was employed for loading the octadecylsilica stationary phases, an experiment was conducted to ascertain if bromide ion could have been released into eluted solutions. A 10-ml volume of a 25 mg l^{-1} solution of 2,7-naphthalenedisulphonic acid was passed through a treated cartridge and the eluted solution was analysed for bromide ion (detection limit 0.3 mg l^{-1}, signal-to-noise ratio = 3). Bromide ion was not detected.

3.4. Ion-exchange capacity

The maximum amount of organic substance that could have been absorbed was measured by eluting a 60 mg l^{-1} solution of Patent Blue V at pH 6.0. Up to 2.7 mg (4.7 μmol) of substance was retained by a C_{18} 100-mg silica cartridge, loaded with CTMA. For this anion, the breakthrough volume was larger than 50 ml.

3.5. Recycling of octadecylsilica cartridges

The CTMA loading and clean-up procedure employing C_{18} cartridges has been already employed for the trace enrichment of some aromatic sulphonic acids in water samples [4]. Good recoveries of those organic analytes have been obtained by washing the cartridges with methanol. Considering this, an experiment was carried out in order to ascertain if cartridges used once could have been employed for some further clean-up steps. CTMA loading and clean-up of standard solutions were repeated five times on the same group of C_{18} silica cartridges. It was found that, although the removal of organic substances was complete for all five clean-ups, the recoveries of inorganic analytes were reduced by about 5–10% if the cartridges were used more than twice.

3.6. Analysis of aqueous samples

Fig. 1 shows the chromatograms obtained for the analysis of two aqueous solutions after cleaning-up. Chromatogram A was obtained from a waste from the dye industry, which contained about 120 g l^{-1} of a mixture of aromatic sulphonic acids. A 5-ml volume of waste diluted 1:1000 was cleaned up and analysed. Chromatogram B refers to a 0.01% solution of a laundry detergent powder, containing sodium dodecylbenzene sulphonate, which was neutralized with *p*-hydroxybenzoic acid prior to analysis. As can be seen, in both chromatograms no

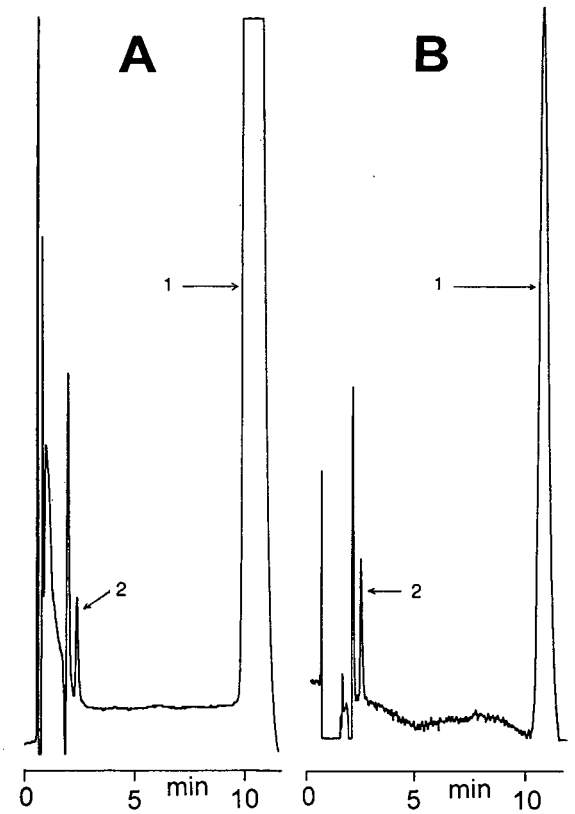

Fig. 1. Chromatograms of two cleaned-up aqueous samples. (A) Liquid industrial waste containing 120 g l^{-1} of a mixture of aromatic sulphonic acids (diluted 1000-fold); peaks: 1 = SO_4^{2-}, 300 mg l^{-1}; 2 = Cl^-, 0.87 mg l^{-1}. (B) 0.01% Solution of a laundry detergent powder (neutralized with *p*-hydroxybenzoic acid prior to clean-up); peaks: 1 = SO_4^{2-}, 13.5 mg l^{-1}; 2 = Cl^-, 0.17 mg l^{-1}.

peak is visible at 4.13 min, corresponding to the retention time of bromide ion under the conditions adopted. Quantitative calculations were based on peak height and an absolute calibration graph was employed. The 96% recovery of clean-up was taken into account for calculating the sulphate ion concentration in the original sample.

Acknowledgements

The author is indebted to Miss S. Pittavino and Mr. M. Cicottino for their careful assistance and to Dr. M. Ginepro for having stimulated interest in this work.

References

[1] I.S. Kim, F.I. Sasinos, D.K. Rishi, R.D. Stephens and M.A. Brown, *J. Chromatogr.*, 589 (1991) 177–183.
[2] K. Ito, Y. Ariyoshi, F. Tanabiki and H. Suhanara, *Anal. Chem.*, 63 (1991) 273–276.
[3] K. Ito, Y. Ariyoshi and H. Sunahara, *J. Chromatogr.*, 598 (1992) 237–241.
[4] O. Zerbinati, G. Ostacoli, D. Gastaldi and V. Zelano, *J. Chromatogr.*, 640 (1993) 231–240.
[5] O. Zerbinati and G. Ostacoli, *J. Chromatogr. A*, 671 (1994) 217–223.
[6] *Standard Methods for the Examination of Water and Wastewater*, APHA, AWWA and WPCF, Washington, DC, 13th ed., 1971.

ELSEVIER

Journal of Chromatography A, 706 (1995) 141–147

JOURNAL OF CHROMATOGRAPHY A

Studies on the retention behaviour of metal–EDTA complexes in cation chromatography

Corrado Sarzanini[a,*], Giovanni Sacchero[a], Edoardo Mentasti[a], Peter Hajós[b]

[a]*Department of Analytical Chemistry, University of Turin, Via P. Giuria 5, 10125 Torino, Italy*

[b]*Department of Analytical Chemistry, University of Veszprém, P.O. Box 158, 8201 Veszprém, Hungary*

Abstract

Separation of metal–EDTA complexes (e.g. with Cu^{2+}, Ni^{2+} and Pb^{2+}) has been carried out with a cation-exchange polymer based column. Two mobile-phase systems, containing either nitric or perchloric acid, have been studied and the metal complexes with EDTA have been detected by UV spectrophotometry. A retention model has been developed. It takes into account both ion-exchange and adsorption phenomena of all positive, neutral and, as an attempt, negative metal–EDTA species. The ion-exchange behaviour of the metal–EDTA complexes and the adsorption effects due to neutral species have been applied for an on-line preconcentration procedure.

1. Introduction

The ion chromatographic determination of metal–EDTA complexes (MY) can be performed with anion-exchange columns [1–8]; in this way anions and metals can be separated as anionic complexes in the same run. Alternatively the separation of MY can be carried out with a cation-exchange column [9]. The retention mechanism of analytes involves the cation exchange of free metal ions (e.g. Cu, Fe, Zn, Ni, Pb, Mn, alkali metals and alkali-earth metals) which are present at low pH values.

Theoretical approaches to the retention behaviour of anionic metal complexes, taking into account only negatively charged species, have been developed for anion exchange [8,10], for cation exchange [11–15] and for dynamic ion exchange [15,16]. In fact at slightly basic or acid pH values, the negatively charged species generally represent the total molar fraction. Nevertheless, if cation exchange is selected as separation method, not only the free metal but also the neutral, positive and negative species must be considered.

In this work the cation-exchange behaviour of some MY complexes has been investigated. Factors affecting retention have been examined and the trends observed have been related to the nature of the complexes which exist under the chromatographic conditions used. The use of a cationic system for the separation of metal complexes broadens the scope of cation chromatography. In this system elution may be effected by progressively varying the mobile phase in an acid pH range. Negatively and positively charged species have been considered in a retention theory and some adsorption effects have been discussed. The behaviour of neutral species has

* Corresponding author.

0021-9673/95/$09.50
SSDI 0021-9673(95)00194-8

been utilized to develop an on-line preconcentration procedure.

2. Theory

The theory for ion-exchange of metal cations (M^{n+}) in the presence of complexing ligands has been investigated by Haddad and Foley [15] and Sevenich and Fritz [12]. But, if cationic complexes are present, e.g. in the case of copper–EDTA chelates, more than one positively charged species exists. The chromatographic system contains several ionic species, such as Na^+, H^+, EDTA in the eluent and different complex forms in the sample. Furthermore, the eluted metal ions are partly complexed and partly exist in solution as free metal cations. In order to have a reliable retention model all forms of cationic species in the system must be considered in the same run:

$$Cu^{2+} + 2R\text{-}SO_3H \overset{K_{Cu^{2+}/H^+}}{\rightleftharpoons} (R\text{-}SO_3)_2Cu + 2H^+ \quad (1)$$

$$CuH_3Y^+ + R\text{-}SO_3H \overset{K_{CuH_3Y^+/H^+}}{\rightleftharpoons} R\text{-}SO_3CuH_3Y + H^+ \quad (2)$$

where $R\text{-}SO_3H$ represents the resin exchange site.

By considering the related ion-exchange selectivity coefficients $K_{Cu/H}$ and $K_{CuH_3Y/H}$ the distribution ratio is:

$$D_{Cu} = \frac{(Cu^{2+}) + (CuH_3Y^+)}{C_{Cu}} = \frac{K_{Cu/H}[Cu^{2+}](H^+)^2}{C_{Cu}[H^+]^2} + \frac{K_{CuH_3Y/H}[CuH_3Y^+](H^+)}{C_{Cu}[H^+]} = \frac{K_{Cu/H}[Cu^{2+}](H^+)^2 + K_{CuH_3Y/H}[CuH_3Y^+][H^+](H^+)}{C_{Cu}[H^+]^2} \quad (3)$$

where round and square brackets refer to stationary and mobile-phase concentrations, respectively.

As there may be more than one eluent ion, e.g. H^+ and Na^+, an intereluent ion-exchange equilibrium must be considered:

$$Na^+ + R\text{-}SO_3H \overset{K_{Na/H}}{\rightleftharpoons} R\text{-}SO_3Na + H^+ \quad (4)$$

The column capacity Q (expressed as mol/l) is:

$$Q = (Na^+) + (H^+) \quad (5)$$

and by substituting (Na^+) obtained from the equilibrium constant

$$(Na^+) = \frac{K_{Na/H}[Na^+](H^+)}{[H^+]} \quad (6)$$

Eq. 5 results in:

$$Q = \frac{K_{Na/H}[Na^+](H^+)}{[H^+]} + (H^+) = \frac{K_{Na/H}[Na^+] + [H^+]}{[H^+]}(H^+) \quad (7)$$

From Eq. 7 one can obtain:

$$(H^+) = \frac{Q[H^+]}{K_{Na/H}[Na^+] + [H^+]} \quad (8)$$

and by substituting Eq. 8 into Eq. 3, Eq. 9 derives:

$$D_{Cu} = K_{Cu/H}Q^2(K_{Na/H}[Na^+] + [H^+])^{-2}\Phi_{Cu^{2+}} + K_{CuH_3Y/H}Q(K_{Na/H}[Na^+] + [H^+])^{-1}\Phi_{CuH_3Y^+} \quad (9)$$

where Φ is the molar fraction of the cationic species with respect to the total metal concentration C_{Cu}. Values of Φ were calculated according to our previous work [8], which was developed for elution of anionic metal complexes when a carbonate buffer was present in the eluent.

$$\Phi_{Cu^{2+}} = \frac{[Cu^{2+}]}{C_{Cu}} \quad (10)$$

$$\Phi_{CuH_3Y^+} = \frac{[CuH_3Y^+]}{C_{Cu}} \quad (11)$$

On a cation-exchange column the general expression for the capacity factor, k', of a metal ion in the presence of ligands and considering all the interacting species is:

$$k' = \frac{V_s}{V_m} \Sigma_i K_i Q^{n_i} [E^+]^{-n_i} \Phi_i \quad (12)$$

where V_s and V_m are the stationary and mobile-phase volumes, K_i are the ion-exchange constants for the different species, n_i are the absolute values of their charge and E^+ represents the eluent ions (e.g., if Na^+ and H^+ are the eluent ions, $[E^+] = K_{Na/H}[Na^+] + [H^+]$ as described in Eq. 9).

The adsorption effects due to the neutral species are defined for $n = 0$ and therefore $Q^{n_i} [E^+]^{-n_i} = 1$. If at a selected pH only the neutral species exists, its molar fraction is 1 and Eq. 12 becomes:

$$k' = \frac{V_s}{V_m} K$$

where K is the partition constant of the neutral species considered.

The negatively charged species are involved in a way similar to that of the positive ones (see Section 4).

3. Experimental

3.1. Reagents and solutions

The eluents were prepared by dissolving analytical reagent grade chemicals in high-purity water obtained using a Milli-Q system (Millipore, Bedford, MA, USA) and filtering through a 0.45-μm filter. The reagents were perchloric acid (65%) and EDTA (Carlo Erba, Milan, Italy), nitric acid (65%) and sodium hydroxide (Merck, Darmstadt, Germany). Working solutions of metal ions, namely Cu(II), Ni(II) and Pb(II), were prepared by dilution of concentrated standard stock solutions (Merck).

3.2. Instrumentation

A Dionex Series 4000i ion chromatograph was used with an UV–Vis variable-wavelength detector (Dionex, Sunnyvale, CA, USA). The chromatograms were recorded with an SP 4270 data module integrator (Carlo Erba). Curve fittings and regressions, based on the Marquandt–Levemberg algorithm, and graphic elaborations have been performed by Sigma Plot software (Jandel Scientific) on a PS/2 56 486SLC2 IBM personal computer. The sample loading for the preconcentration procedure has been performed with a Model DQP-1 pump (Dionex).

The separation column (Dionex CS 10, 250 × 4 mm I.D.) and the preconcentration column (Dionex CG 10, 50 × 4 mm I.D.) were cation-exchange polymer based, functionalized with sulphonic groups and having a medium hydrophobicity. The void volume V_m has been obtained experimentally as the water dead volume, therefore stationary-phase volume V_s was defined by $V_{column} - V_m$, were V_{column} is the geometric volume of the column (computed). The column capacity Q has been given by the producer.

All chromatograms were obtained at room temperature. The flow-rate was 1.0 ml/min unless otherwise stated. Retention times were the mean of triplicate injections of single samples containing a single metal at $1.0 \cdot 10^{-5}$ M prepared using the eluent solution.

4. Results and discussion

Studies were performed in order to verify the effectiveness of the cation-exchange column, Dionex CS10, for metal–EDTA complex separation. Not only the sample but also the mobile phase was $5.00 \cdot 10^{-4}$ M EDTA (ligand to metal ratio 50:1) in order to avoid complex dissociation owing to inadequate ligand concentration. To evaluate the influence of pH and ionic strength (i.s.), two different procedures were adopted. In the first case eluents were prepared by dissolving Na_2EDTA salt ($5.00 \cdot 10^{-4}$ M) which gives a solution of pH 5.0. Then the pH was adjusted to the proper value by adding either concentrated acid or sodium hydroxide. In the second case $HClO_4$ was added to $5.00 \cdot 10^{-4}$ M EDTA solution to obtain pH 0.80; this eluent was used as such or by varying the pH in the range 0.80–6.00 by addition of concentrated NaOH. The first eluent enabled us to study the influence of pH on k' by working at the lowest i.s. consistent with

ligand concentration, the second furnished an i.s. value constant for all experiments, $[H^+] + [Na^+]$ being constant at all pH values. During the preliminary studies HNO_3 was used to modify the eluent pH values; in this case Cu(II)–EDTA and Pb(II)–EDTA complexes were detected at 242 nm, but the detection of other complexes, e.g. those with Ni(II), which have a lower molar absorptivity with a behaviour similar to nitrate, required the use of eluents with a higher transmittance. For this reason perchloric acid has been adopted.

Figs. 1–3 compare the k' behaviour obtained for MY at the different eluent compositions investigated, the k' computed by Eq. 12 for the above systems and the molar fractions of MY species as a function of pH for copper, lead and nickel. The molar fractions of the MY species have been computed on the basis of the formation constants reported in the literature for these metals [17,18]; the eluents were obtained according to the first procedure and the terms of Eq. 12, referring to the MHY^- and MY^{2-} species, have been calculated by considering the modulus of the charge values. Taking copper as an example for the computation, the equation results in a summation of 5 terms: 2 terms due to the cationic species, 1 term due to the neutral species and 2 terms due to the anionic species.

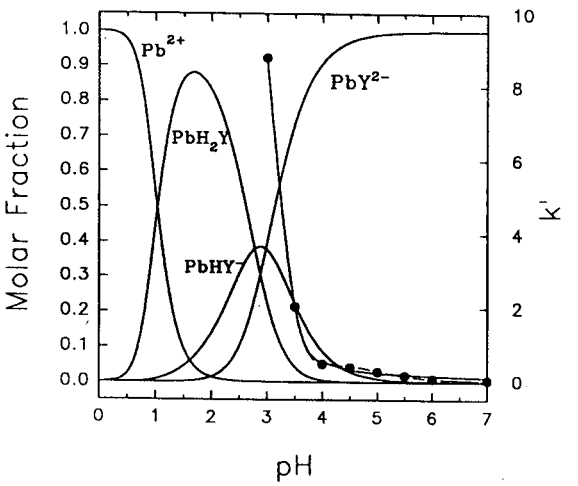

Fig. 2. Molar fraction of Pb–EDTA species, experimental k' (dots) and the respective calculated curve (dashed line overlapping the experimental curve) as a function of pH. Experimental conditions as Fig. 1.

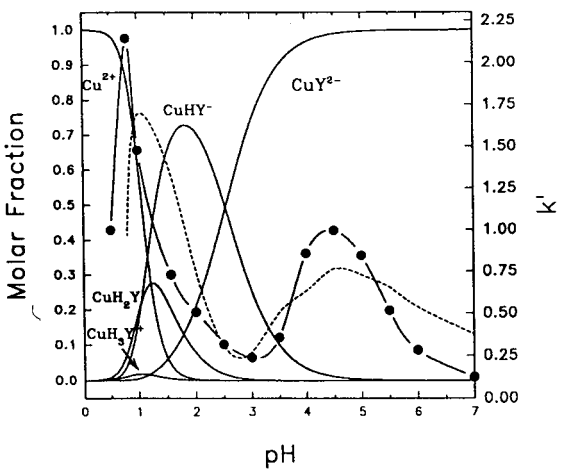

Fig. 1. Molar fractions of Cu–EDTA species, experimental k' (dots) and the respective calculated curve (dashed line) as a function of pH. Experimental conditions: eluent $5.00 \cdot 10^{-4}$ M Na_2EDTA, pH adjusted with either $HClO_4$ or NaOH, flow-rate 1.0 ml/min; 100-μl samples prepared in eluent and containing $1.0 \cdot 10^{-5}$ M Cu^{2+}; UV detection at 242 nm.

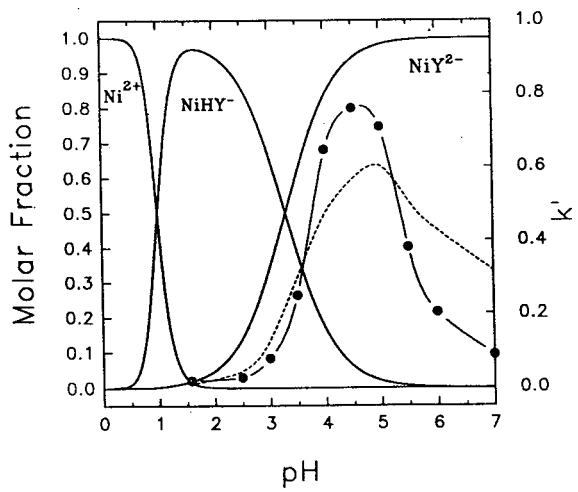

Fig. 3. Molar fraction of Ni–EDTA species, experimental k' (dots) and the respective calculated curve (dashed line) as a function of pH. Experimental conditions: eluent $5.00 \cdot 10^{-4}$ M Na_2EDTA, pH adjusted with either $HClO_4$ or NaOH, flow-rate 1.0 ml/min; 100-μl samples prepared in eluent and containing $1.0 \cdot 10^{-5}$ M Ni^{2+}; UV detection at 240 nm.

The molar fraction, Φ, of each species and the eluent ion concentrations have been calculated for each pH value. At this point Φ_i and E^+ are known and theoretical plots are obtained by regression of this equation with the experimental data.

The k' values for copper (Fig. 1) show a maximum due to the high molar fraction value of Cu^{2+} species at pH 0.8. Nevertheless, for pH < 0.8 the very high ionic strength results in a k' decrease. At pH values greater than 1.00, one and two negatively charged Cu–EDTA species appear and, in agreement with the nature of the stationary phase, are repelled, lowering the k' values. An anomalous behaviour is evidenced around pH 4–5 where a relative maximum of k' occurs. This fact, as regards the ion-exchange mechanism, disagrees with the molar fraction distribution of copper and nickel (see below), because only negative species are predicted for pH > 4. Since small variations of ionic strength, obtained by increasing or reducing the pH 5.0 value, have a strong effect on k', one may assume that retention and interaction with the stationary phase are caused by the anionic secondary layer. Two opposite effects are predicted from the ionization model at a pH range 3–7. Increasing the pH of the eluent ($3 < pH < 4.5$) will increase the capacity factors, because the analyte is converted from the MHY^- to the MY^{2-} form. Increasing the pH of the eluent to $4.5 < pH < 7$, the capacity factors decrease progressively because the predominant form of the eluent becomes HY^{3-} ($\log K_{H_2Y^{2-}/HY^{3-}} = 6.18$) and the molar fraction of the analyte is constant. The modelling, by introducing the anionic species, shows a good agreement between the experimental and computed behaviour of the k' values for Cu and Ni; however, it does not explain the absence of the same peak for Pb. A second consideration regarding the similar behaviour of Ni and Cu could be based on the similar structure of the complexes PbY^{2-} and CuY^{2-}, and their ability to be protonated at the pH values considered. In this case neutral species should be formed and retained; on the other hand a comparison of the k' values of the Cu species at pH 4.5 and at pH 1.25, where the neutral species CuH_2Y is active, agrees with this supposition.

Table 1
Ion-exchange selectivity coefficients calculated according to Eq. 12 for metal–EDTA species

Species	$K_{species/H^+}$ low i.s. (see Fig. 3)	$K_{species/H^+}$ high i.s. (see Fig. 4)
Cu^{2+}	16	28
CuH_3Y^+	$4.6 \cdot 10^{-5}$	$8.0 \cdot 10^{-6}$
CuH_2Y	$2.8 \cdot 10^{-6}$	$1.6 \cdot 10^{-7}$
Pb^{2+}	$2.4 \cdot 10^{-8}$	700
PbH_2Y	32	$5.0 \cdot 10^{-9}$

Experimental conditions as for Fig. 1.

Table 1 shows the values of ion-exchange selectivity coefficients for metal ions and their species calculated from the experimental data. The values have been obtained as the result of the regression mentioned above. The intereluent Na^+/H^+ ion-exchange equilibrium constant, $K_s = 1.5$, has been selected according to the literature values [19]. By comparing the behaviour of k' (Figs. 1–3), species distribution and computed ion-exchange selectivity coefficients, the relative contribution to the retention mechanisms (ion exchange and adsorption) are evidenced. While in the case of copper the free metal cation exchange and the double-charged species interactions prove to be the main active retention mechanisms, in the case of lead neutral species adsorption is dominant (see Fig. 2). Lead (PbH_2Y) proves to be totally retained between pH 0.5 and 3.0; on the other hand below pH 0.5 i.s. competition hinders the cation-exchange mechanism. The behaviour of nickel is similar to that of copper for pH > 2.5 but due to detection problems the nickel peak was not visible at low pH and high i.s.

The experiments performed with eluents at high i.s. (0.16 *M* $HClO_4$) are compared in terms of k' as a function of pH for copper and lead (see Fig. 4). For pH values lower than 2.0 the free cation (Pb^{2+}) and neutral species (PbH_2Y) are totally retained. At increasing pH values, according to the previous experiments, k' values decrease both for copper and lead; however, for

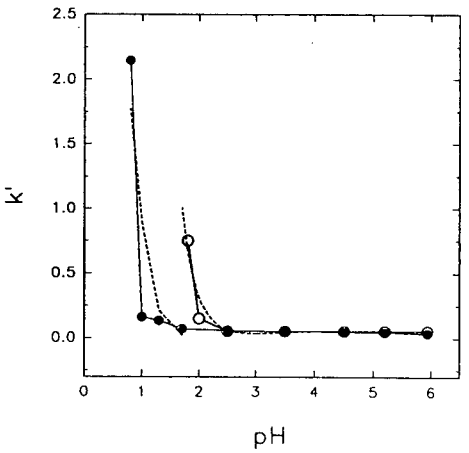

Fig. 4. k' Behaviour of copper (dots) and lead (circles) as a function of pH and for high ionic strength (dashed line = calculated curve). Experimental conditions: eluent, $5.00 \cdot 10^{-4}$ *M* Na_2EDTA, 0.158 *M* $HClO_4$, pH adjusted with NaOH, 1.0 ml/min flow-rate; 100-μl samples prepared in eluent and containing $1.0 \cdot 10^{-5}$ *M* of every metal; UV detection at 225 nm.

the latter at pH 2.0, owing to the maximum value for the molar fraction of the neutral species, the k' value is still consistent. The two different behaviours give further information on the retention mechanisms involved.

Fig. 5 shows a chromatogram of the metals investigated, obtained after eluent and procedure optimization.

Furthermore, from an experimental point of view, the behaviour of Pb–EDTA complexes as a function of pH and ionic strength provides data that can be used to develop a selective method for preconcentrating and determining Pb at trace levels. The above results suggested the possibility to retain and preconcentrate lead species on a cation microcolumn (CG 10) by working at pH values between 1.0 and 2.0. Measurements of preconcentration recoveries at pH 1.5 (optimal value), performed by loading 100.0-ml samples at 5.0 μg/l Pb onto the CG 10 which replaced the injection valve loop, gave 70%

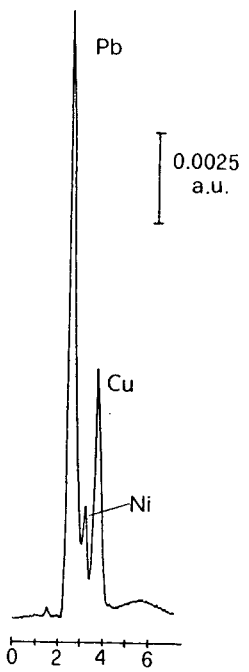

Fig. 5. Chromatogram of Pb(II)–, Ni(II)– and Cu(II)–EDTA complexes. Experimental conditions: eluent, $5.0 \cdot 10^{-4}$ *M* Na_2EDTA, $HClO_4$ up to pH 4.30, 1.0 ml/min flow-rate; 100-μl sample, metals $1.0 \cdot 10^{-5}$ *M* each in eluent; UV detection at 240 nm.

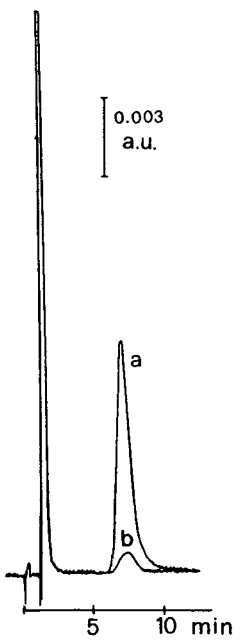

Fig. 6. Preconcentration of lead: 5.0 μg/l standard solution (a) and blank (b). Experimental conditions: eluent $5.0 \cdot 10^{-4}$ *M* Na_2EDTA, 0.100 *M* $HClO_4$; NaOH up to pH 1.7, flow-rate 1.5 ml/min; 100-ml sample containing $5.0 \cdot 10^{-4}$ *M* Na_2EDTA and $HClO_4$ up to pH 1.5, flow-rate of preconcentration 4.0 ml/min; UV detection at 242 nm.

recovery and 0.5 μg/l as the Pb detection limit. One has to consider that this pH does not allow retention of the ionic species and only the neutral complex (about 80% of total species) contributes to the retention mechanism.

A chromatogram showing the preconcentration of lead in comparison with the blank is shown in Fig. 6.

Acknowledgement

We acknowledge financial support from Consiglio Nazionale delle Ricerche (CNR, Italy) and OTKA-2562 (Hungary).

References

[1] M. Yamamoto, H. Yamamoto, Y. Yamamoto, S. Matsushita, N. Baba and T. Ikushige, *Anal. Chem.*, 56 (1984) 832.
[2] S. Matsushita, *J. Chromatogr.*, 312 (1984) 327.
[3] K. Hayakawa, T. Sawada, K. Shimbo and M. Miyazaki, *Anal. Chem.*, 59 (1987) 2241.
[4] W. Buchberger, P.R. Haddad and P.W. Alexander, *J. Chromatogr.*, 558 (1991) 181
[5] W. Zhou, W. Liu and D. An, *J. Chromatogr.*, 589 (1992) 358.
[6] C.A.A. leGras, *Analyst*, 118 (1993) 1035.
[7] C. Sarzanini, O. Abollino, E. Mentasti and V. Porta, *Chromatographia*, 30 (1990) 293.
[8] P. Hajos, G. Revesz, C. Sarzanini, G. Sacchero and E. Mentasti, *J. Chromatogr.*, 640 (1993) 15.
[9] D. Yan and G. Schwedt, *Fresenius Z. Anal. Chem.*, 338 (1990) 149.
[10] A. Yamamoto, K. Hayakawa, A. Matsunaga, E. Mizukami and M. Miyazaki, *J. Chromatogr.*, 627 (1992) 17.
[11] R.D. Rocklin, M.A. Rey, J.R. Stillian and D.L. Campbell, *J. Chromatogr. Sci.*, 27 (1989) 474.
[12] G.J. Sevenich and J.S. Fritz, *Anal. Chem.*, 55 (1983) 12.
[13] D.T. Gjerde, *J. Chromatogr.*, 439 (1988) 49.
[14] P. Alumaa and J. Pentšuk, *Chromatographia*, 38 (1994) 566.
[15] P.R. Haddad and R.C. Foley, *J. Chromatogr.*, 500 (1990) 301.
[16] P. Janos and M. Broul, *Fresenius Z. Anal. Chem.*, 344 (1992) 545.
[17] J. Inczedy, *Analytical Application of Complex Equilibria*, Ellis Horwood, Chichester, and Akadémiai Kiadó, Budapest, 1976.
[18] L.G. Sillen, *Stability Constants of Metal Complexes*, Chemical Society, London, 1971.
[19] M. Marhol, in G. Svehla (Editor), *Wilson and Wilson's Comprehensive Analytical Chemistry, Vol. XIV, Ion Exchangers in Analytical Chemistry. Their Properties and Use in Inorganic Chemistry*, Elsevier, New York, 1982, Ch. 2, p. 54.

ELSEVIER

Journal of Chromatography A, 706 (1995) 149–158

JOURNAL OF CHROMATOGRAPHY A

Ion chromatographic separation of alkali metals in organic solvents

Philip J. Dumont*, James S. Fritz

Ames Laboratory, US Department of Energy and Department of Chemistry, Iowa State University, Ames, IA 50011, USA

Abstract

Ion-exchange chromatography is a common method for the separation and determination of metal cations. Although much research has been done on improving various aspects of this technique, the use of non-aqueous eluents has received little attention. The effect of organic solvents on the retention of alkali-metal cations on a macroporous polystyrene–divinylbenzene resin was studied. The retention of alkali cations increases as the organic content in the eluent increases for most organic solvents. Methanol was an exception with a maximum retention occurring at an eluent composition of methanol–water (75:25). Since organic solvents do not solvate these cations in the same manner as water, increases in the separation factors and changes in elution order are observed. Several separations that are not possible with aqueous eluents will be shown.

The effect of crown ethers in the mobile phase was also investigated. In most solvents 18-crown-6 (18C6) altered the retention of all cations. In some cases 18C6 changed elution order or improved peak shape. Separations with an organic eluent and 18C6 modifier will also be shown.

1. Introduction

Factors that influence the aqueous selectivity of cation-exchange resins for various 1+ metal cations have been studied extensively over many years. Diamond and co-workers [1,2] proposed a theory of water-enforced ion pairing to explain selectivity toward various cations. Electrostatic attraction of the sulfonate groups within the ion-exchange resin for alkali-metal cations suggests that cations with the smallest ionic radii would be the most strongly retained. The Pauling radii in Table 1 [3] would predict a chromatographic elution order of Cs^+, Rb^+, K^+, Na^+, Li^+, which is exactly the opposite of that observed in ion-exchange chromatography. However, hydrated ionic radii and approximate hydration number (Table 1) are in the opposite order to the Pauling radii, with Li^+ being the most highly hydrated. The cation-exchange resins used in classical ion-exchange chromatography are highly sulfonated and take up a great deal of water inside the microporous resin. The hydration of the alkali-metal ions thus would remain much the same inside the resin as in the aqueous mobile phase.

The effects of performing ion-exchange separations in aqueous–organic or in organic solvents have been studied by a number of investigators. A recent review concludes that ion exchange in non-aqueous solvents is very complicated from a theoretical point of view [4]. Organic solvents

* Corresponding author.

0021-9673/95/$09.50
SSDI 0021-9673(94)01119-2

Table 1
Ionic radii of alkali metal cations

	Li^+	Na^+	K^+	Rb^+	Cs^+
Pauling radii (Å)	0.60	0.96	1.33	1.48	1.69
Hydrated radii (Å)	3.40	2.76	2.32	2.28	2.28
Approximate hydration number	25.3	16.6	10.5	10.0	9.90

are obviously going to affect the solvation of alkali-metal cations compared to the situation in water alone. The dielectric constant, viscosity, and other effects will also be different in organic solvents.

In the present work the ion chromatographic separation of alkali-metal ions and the ammonium ion was studied in aqueous–organic mixtures of four different organic solvents and in the organic solvents which contain little, if any, water. Some major changes in selectivity were observed and several practical separations were obtained.

2. Experimental

2.1. Chromatographic system

The chromatographic system consisted of several components. An Alltech (Deerfield, IL, USA) 425 HPLC pump was used to deliver a flow of 1 ml/min. A 7125 Rheodyne (Berkeley, CA, USA) injector delivered a 10-μl sample which was detected with an Alltech 320 conductivity detector. A Hitachi D-2000 integrator (EM Science, Cherry Hill, NJ, USA) was used to measure retention times. Separations were recorded by a Servogor 120 chart recorder (Abb Goerz Instruments, Vienna, Austria), and a Keithley Chrom 1-AT data acquisition board (Keithley MetraByte, Taunton, MA, USA) with Labtech Notebook software (Laboratory Technologies, Wilmington, MA, USA). Columns were packed with a Shandon Southern (Sewichley, PA, USA) HPLC packing pump at 3000 p.s.i. (1 p.s.i. = 6894.76 Pa).

2.2. Reagents and chemicals

The cation-exchange resin was prepared in our laboratory from 5-μm macroporous polystyrene–divinylbenzene (Sarasep, Santa Clara, CA, USA). A 2-g amount of resin was slurried with a few milliliters of glacial acetic acid and placed in an ice bath. A 5-ml volume of concentrated sulfuric acid was added to the resin with stirring. The resin mixture was reacted for 30 s then poured into ice water to quench the reaction. This procedure produced a sulfonic acid cation-exchange resin with a capacity of approximately 0.15 mequiv./g. Absolute ethanol was punctilious grade and used as obtained from Quantum Chemicals (Newark, NJ, USA). All other organic eluents used were of HPLC grade and used as obtained from Fisher Scientific (Pittsburgh, PA, USA) and Sigma (St. Louis, MO, USA). The salts and methanesulfonic acid eluent were all of reagent grade and used as obtained from Aldrich (Milwaukee, WI, USA) and Fisher Scientific. Either halide or acetate salts were dissolved in organic solvents to prepare 1000 ppm stock solutions which were then diluted with eluent to produce samples of desired concentrations.

3. Results and discussion

3.1. Type of resin

Ion chromatographic separations of alkali-metal cations are generally performed with sulfonated microporous polymeric resins [5,6] or with resins coated with a sulfonated latex. A

lightly sulfonated macroporous resin with a very high degree of cross-linking was selected for the present study. Such a resin would be less likely to undergo volume changes due to swelling and should be more compatible with organic solvents.

A separation of alkali-metal ions was first attempted in water alone using the lightly sulfonated macroporous cation exchanger with aqueous 3 m*M* methanesulfonic acid as the eluent. Under these conditions the sample cations exhibited very similar retention times (Fig. 1). A much better separation would be obtained with a microporous cation exchanger [5]. The selectivity of the macroporous resin for alkali-metal ions was improved considerably by chemically introducing hydroxymethyl groups [7] prior to sulfonation.

These results seem to indicate that solvation of the resin plays a role in imparting selectivity for the various sample ions. Microporous cation-exchange resins form a gel and are highly hydrated within. With sulfonated macroporous resins the hydrated alkali-metal ions may be repelled somewhat by the hydrophobic resin matrix. The presence of hydroxymethyl groups on the macroporous resin makes it less hydrophobic and improves selectivity for the hydrated alkali ions.

When the macroporous resin column in Fig. 1 was used with the same acidic eluent in 100% methanol, the chromatographic separation was improved considerably (Fig. 2). Now the alkali-metal ions are solvated with methanol and the resin matrix is probably coated with a thin layer of methanol, which makes the ions and the resin surface more compatible with one another.

3.2. Ion chromatography in organic solvents

Ion-exchange selectivity in organic solvents and in mixed solvents involves a complex series of effects. The dielectric effect and ionic solvation seem to play the major roles, but interactions involving the solvent, resin exchange sites, analyte ion, and eluting ion also affect retention [8].

Capacity factors for the alkali-metal cations were measured in eluents containing 0–100% organic solvent (Table 2). The retention factors (capacity factor), k', of the cations generally increase with greater organic content of the

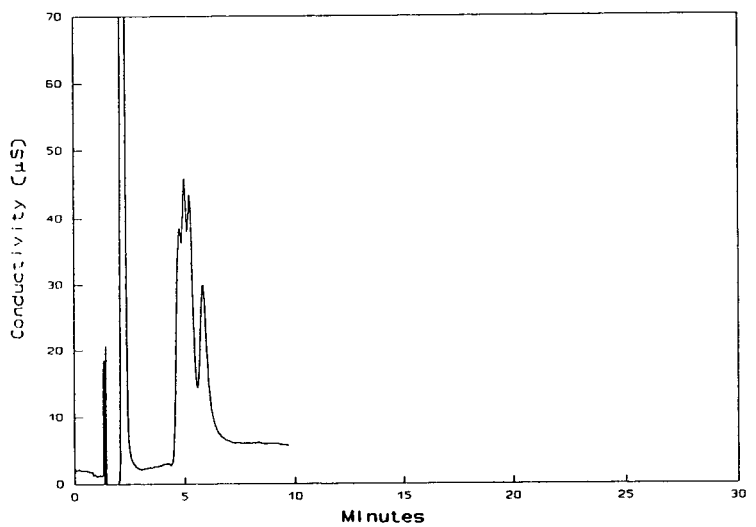

Fig 1. Separation of Li^+ (2 ppm), Na^+ (5 ppm), K^+ (16 ppm), Rb^+ (24 ppm) and Cs^+ (48 ppm) on a 15-cm cation-exchange column with 3 m*M* methanesulfonic acid in water as the eluent.

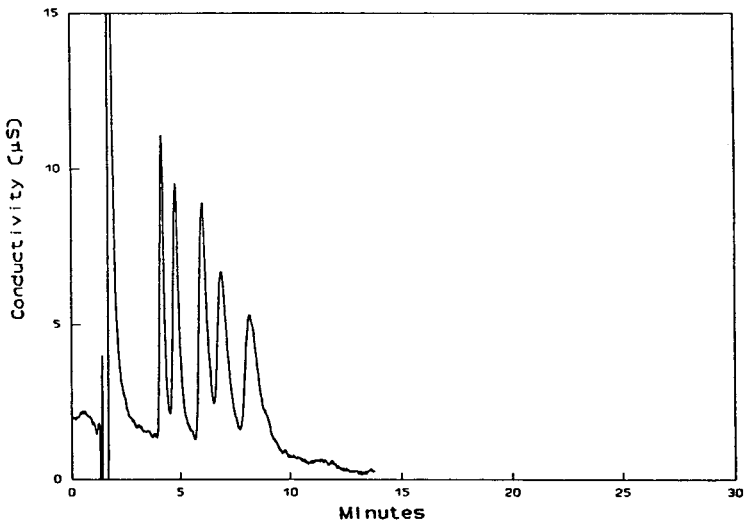

Fig. 2. Same separation as in Fig. 1 with 3 m*M* methanesulfonic acid in methanol as the eluent.

Table 2
Capacity factors in organic and mixed solvents with 0.5 m*M* methanesulfonic acid as the eluent

Solvent	*k'*					
	Li^+	Na^+	K^+	Rb^+	Cs^+	NH_4^+
Water, 100%	2.27	2.27	2.71	2.74	2.96	3.04
Methanol						
25%	2.66	2.47	2.77	2.80	2.98	3.13
50%	3.10	3.07	3.31	3.39	3.80	3.70
75%	4.43	5.07	6.32	7.30	8.33	5.82
100%	2.08	2.82	3.73	4.33	5.15	3.09
Ethanol						
25%	2.75	2.57	2.78	2.78	2.96	3.13
50%	3.25	3.09	3.37	3.48	3.76	3.78
75%	4.61	5.14	6.90	7.62	8.76	5.98
100%	1.86	3.84	7.24	8.84	9.87	2.12
2-Propanol						
25%	2.20	1.98	2.11	2.05	2.17	2.45
50%	2.26	2.14	2.35	2.41	2.62	2.88
75%	3.41	3.52	4.42	4.81	5.66	4.69
100%	8.84	12.3	19.5	>20	>20	4.54
Acetonitrile						
25%	2.10	2.10	2.37	2.38	2.54	2.51
50%	2.50	2.38	2.89	2.98	3.35	3.10
75%	3.00	3.12	3.79	3.95	4.45	3.98
100%	4.46	2.11	1.75	1.59	1.54	2.40

solvent. This trend was observed for all eluents up to a composition of organic–water (75:25). Retention decreased when the organic content was increased to 100% for all cations in methanol and several cations in acetonitrile and ethanol. Increased retention of sample cations may be explained at least partly by the lower dielectric of organic solvents. This favors ion-pair formation with the result that analyte cations will be electrostatically attracted more strongly to the resin sulfonate anion. Solvation also appears to be a major force. As the organic content is increased toward 100%, analyte cations must become less solvated by water and more solvated by the organic solvent molecules which are all larger than water molecules [8]. The larger radii should inhibit the approach of the cation to the resin and therefore cause a decrease the retention times. At about 75% methanol this effect becomes more important than the continued decrease in dielectric. The data for ethanol also support this. Maxima are observed for Li^+ and Na^+ which are the most highly solvated ions. Replacing water with ethanol in the hydration sphere should have a larger effect on the solvated radii of these ions than the other less solvated alkali ions. The change in solvated radii is therefore more important for Li^+ and Na^+ than the decrease in dielectric. No maxima is observed for 2-propanol, indicating that the decrease in dielectric is more important than the change in solvation radii. The maxima in methanol are represented graphically in Fig. 3. A similar maximum has been observed by others [9–12].

Linear plots were obtained in 100% methanol for log k' vs. log H^+ (methanesulfonic acid), as shown in Fig. 4. Slopes of all the cations were very close to the theoretical slope of -1.0 (± 0.02).

The separation factor for potassium/ammonium on most chromatographic systems is usually fairly small. However, the ratio of retention times is quite large in 100% ethanol: $t(K^+)/t(NH_4^+) = 7.24/2.12 = 3.4$. The chromatogram in Fig. 5 shows that an ammonium peak of only 10 ppm can easily be separated from a 1000 ppm K^+ peak. An even larger ratio of $t(K^+)/t(NH_4^+)$ is found in 2-propanol. However, the peaks in 2-propanol were much broader than in methanol and ethanol, and the sensitivity of the conductivity detector was appreciably lower.

Retention in acetonitrile followed the same general trend as with the alcohol eluents. In 100% acetonitrile a unique elution order was observed; Cs^+ eluted first and Li^+ eluted last.

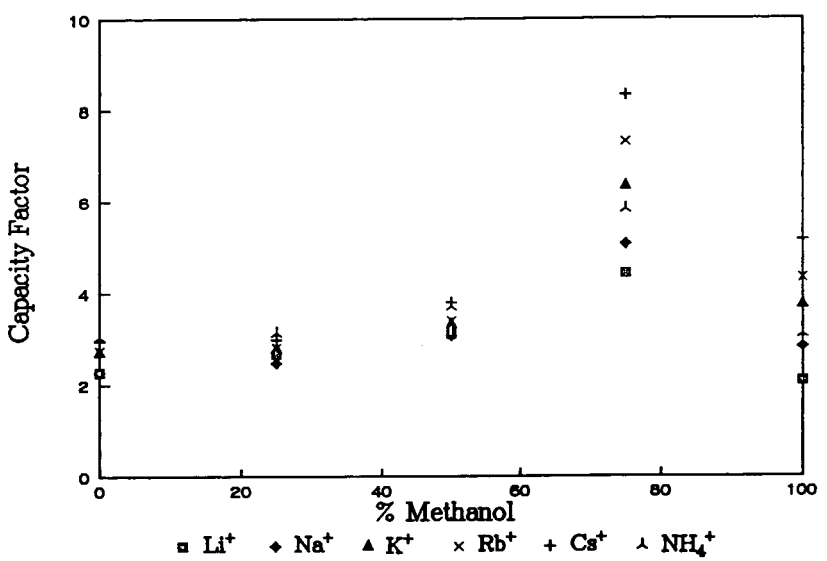

Fig. 3. Effect of methanol on the retention of alkali-metal ions. The eluent contains 0.5 m*M* methanesulfonic acid.

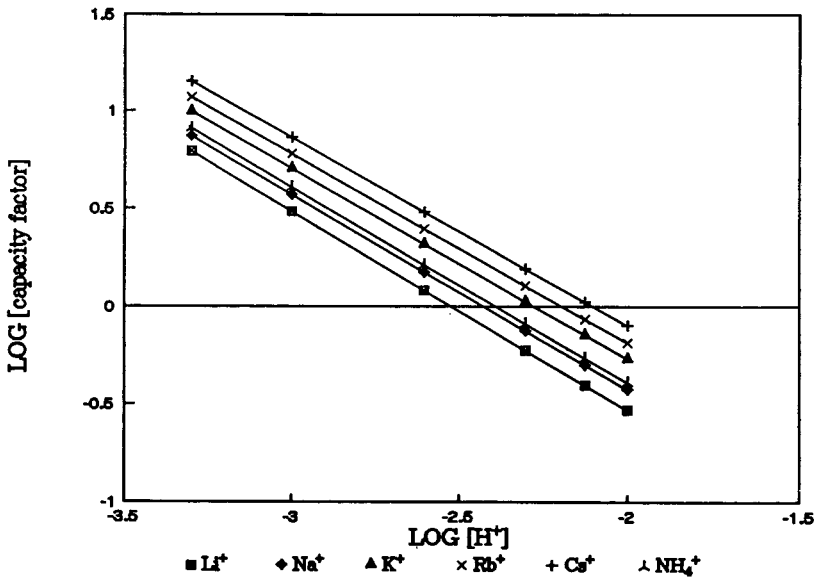

Fig. 4. Effect of methanesulfonic acid concentration on retention of alkali metals in 100% methanol.

This is the reverse of the normal elution order for the alkali metals. Unfortunately, the chromatographic peaks obtained in 100% acetonitrile were generally quite broad.

3.3. Effect of 18-crown-6

Crown ethers have been known for many years to complex alkali-metal cations [13]. In

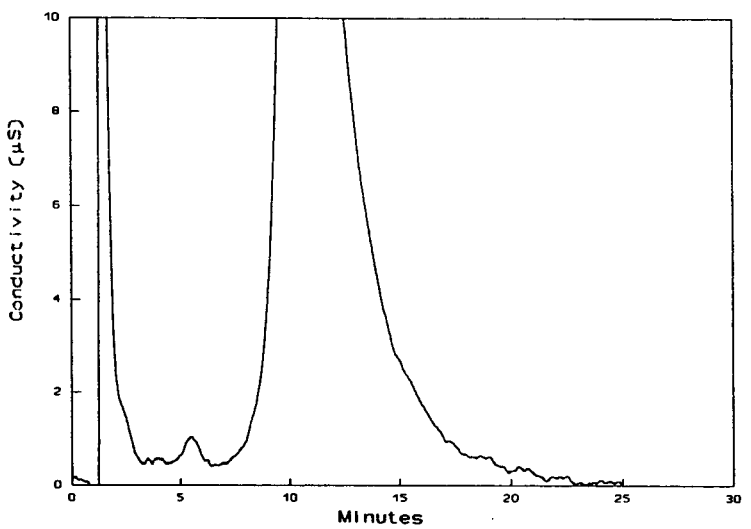

Fig. 5. Separation of 1000 ppm K^+ and 10 ppm NH_4^+ on a 10-cm column with 1 m*M* methanesulfonic acid in 100% ethanol as the eluent.

recent years they have been used to manipulate selectivity in ion-exchange chromatography [14–16]. Often they are used in a water–organic mobile phase to dynamically coat a silica C_{18} or polymeric resin column. The retention mechanism involves ligand exchange rather than ion exchange.

In this research a crown ether was added the methanesulfonic acid eluent in an organic solvent. The crown ether was sufficiently soluble that no dynamic coating of the stationary phase took place [14]. This was verified by plotting log k' vs. log H^+ for Li^+ and K^+ in organic eluents containing 10 m*M* 18-crown-6 (18C6); 100% acetonitrile and 75% methanol were tested. In both eluents, slopes of the Li^+ and K^+ lines were very close to −1.0. If 18C6 were coating the resin, a second retention mechanism of ligand exchange would affect the K^+ ion significantly more than the Li^+ ion and a difference in slopes would be expected. Since the slopes were nearly identical in both eluent it was concluded that no coating was taking place and the retention mechanism was purely ion exchange.

The alkali-metal ions have larger formation constants with 18C6 in organic solvents than in water [17]. It was expected that 18C6 would increase retention due to formation of a larger cationic complex. This was found to be generally true but not necessarily because of the formation of larger cations.

The effect of 18C6 on the ion-exchange behavior of alkali metals in non-aqueous solvents is shown in Table 3. Although increasing concentrations of 18C6 in acetonitrile increase the retention factors of all of the ions studied, the large increase in the k' of lithium was the most striking. The separation factor $[k'(Li^+)/k'(Na^+)]$ was 3.8 compared with 2.6 with no crown ether. The presence of the crown ether also sharpens the chromatographic peaks. This effect permitted the separation of 1 ppm Li^+ from 500 ppm Na^+ (Fig. 6). Data in Table 3 suggests small amounts of Li^+ can be separated from much larger amounts of all other alkali-metal ions as well.

H^+ does not complex 18C6 in water or methanol, but it does have a large formation constant in acetonitrile ($K_f = 10^{6.5}$) [17]. The longer retention times in acetonitrile may be a consequence of the strong complex between H^+ and the crown ether. This complex is stronger than the 18C6 complexes with any of the alkali-metal ions. A large H^+ complex would be a weaker eluting species than H^+ alone and the retention times of the alkali metals would increase. The alkali-metal formation constants with 18C6 are generally higher in methanol than in acetonitrile except for Li^+, which is not complexed. Addition of 0.1 m*M* 18C6 increases k', but increasing the concentration further has little effect. H^+ is scarcely complexed in methanol, so the changes in retention are due to the interaction of the crown ether with the metal cations. It is unclear why K^+ is affected so little since it has the largest K_f with 18C6. The other cations generally elute in order of decreasing K_f. The metals with higher K_f values spend more time as a larger, complexed ion. The larger ions have the largest k' values in methanol.

Including NH_4^+ in a separation with the alkali

Table 3
Effect or 18C6 on k' of alkali metal ions in organic solvents

	m*M* 18C6			
	0	0.1	1.0	10
10-cm column with 2 mM methanesulfonic acid in methanol as the eluent				
Li^+	1.45	1.31	1.32	1.34
Na^+	1.80	2.06	2.21	2.20
K^+	2.55	2.67	2.63	2.59
Rb^+	3.05	4.08	4.05	4.01
Cs^+	3.77	4.17	4.21	4.23
NH_4^+	1.93	2.71	3.34	3.36
10-cm column with 1 mM methanesulfonic acid in acetonitrile as the eluent				
Li^+	3.57	4.59	7.17	8.97
Na^+	1.39	1.33	1.64	2.34
K^+	1.34	1.26	1.65	2.48
Rb^+	1.26	1.26	1.73	2.45
Cs^+	1.24	1.27	1.71	2.74
NH_4^+	1.50	1.39	2.18	3.35

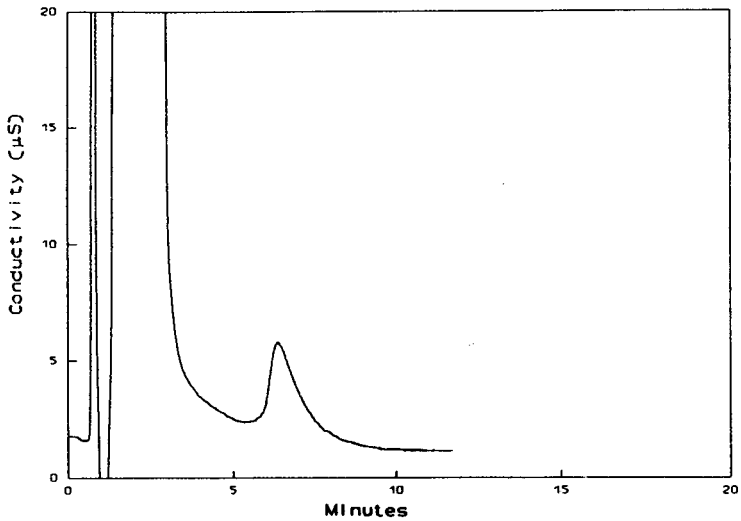

Fig. 6. Separation of 500 ppm Na^+ and 1 ppm Li^+ on a 10-cm column with 1 m*M* methanesulfonic acid and 1 m*M* 18C6 in 100% acetonitrile as the eluent.

metals was not possible in 100% methanol. It eluted very closely to Na^+ and could not be separated. The addition of 18C6 did adjust the retention times but not in a manner to allow a separation. An eluent of 75% methanol was found to increase separation factors of several cations. Adding 18C6 to this eluent further increased the resolution and improved peak shapes. A separation of four ions in 75% methanol, 1.5 m*M* methanesulfonic acid and 1 m*M*

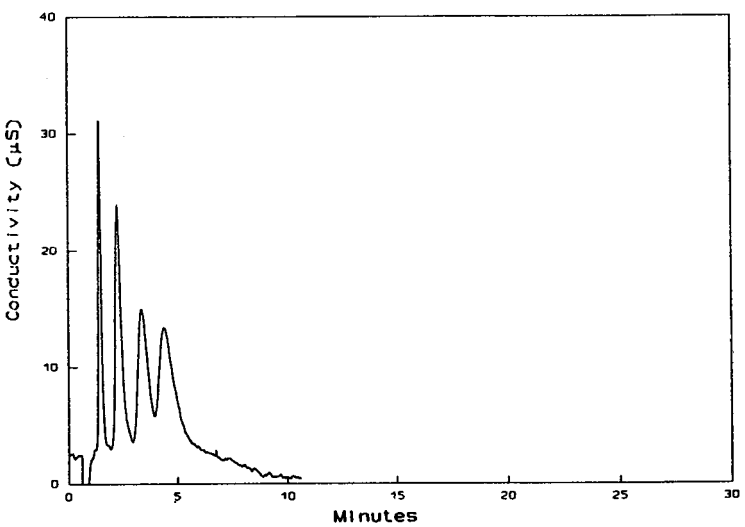

Fig. 7. Separation of Li^+ (1 ppm), Na^+ (3 ppm), NH_4^+ (3 ppm) and K^+ (9 ppm) on a 5-cm column with 1.5 m*M* methanesulfonic acid and 1 m*M* 18C6 in a 75% methanol as the eluent.

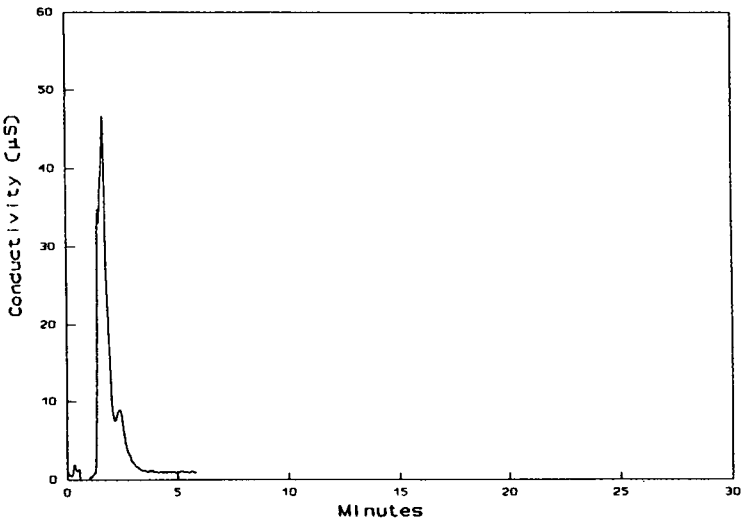

Fig. 8. Same separation as in Fig. 7 but without 18C6.

18C6 is shown in Fig. 7. The effect of 18C6 is easily seen when comparing this to a similar separation without 18C6 (Fig. 8).

4. Conclusions

The use of non-aqueous solvents with macroporous cation-exchange resin permit several separations that are very difficult with aqueous eluents. Methanol was found to be the most favorable solvent due to the best combination of resolution and peak shape. Acetonitrile and ethanol, although producing broader peaks, are useful for separating ions that usually elute close together, Li^+/Na^+ and K^+/NH_4^+ respectively. Elution order in acetonitrile is reversed from that found with aqueous eluents: $Cs^+ < Rb^+ < K^+ < Na^+ < Li^+$. Addition of 18C6 to the mobile phase improves both peak shape the resolution of several ions.

Acknowledgements

We wish to thank Alltech Associates, Inc. (Deerfield, IL, USA) for a gift of the 425 HPLC pump and 320 conductivity detector used in this work. We also thank Doug Gjerde of Sarasep Inc. (Santa Clara, CA, USA) and Jim Benson of Sierra Separations Inc. (Reno, NV, USA) for the resin used in this work. This research was supported by a grant from the 3M Co., St. Paul, MN, USA. The work was performed in the Ames Laboratory of Iowa State University. Ames Laboratory is operated for the US Department of Energy under contract No. W-7405-Eng-82.

References

[1] R.M. Diamond and C.H. Jensen, *J. Phys. Chem.*, 75 (1971) 79.
[2] R.M. Diamond, C.H. Jensen, A. Partridge and T. Kenjo, *J. Phys. Chem.*, 76 (1972) 1040.
[3] F.A. Cotton, G. Wilkinson and P.L. Gaus, *Basic Inorganic Chemistry*, Wiley, New York, 1987, p. 271.
[4] S. Rabin and J. Stillian, *J. Chromatogr. A*, 671 (1994) 63.
[5] J.S. Fritz, D.T. Gjerde and R.M. Becher, *Anal. Chem.*, 52 (1980) 1519.
[6] G.J. Sevenich and J.S. Fritz, *J. Chromatogr.* 371 (1986) 361.
[7] J.J. Sun and J.S. Fritz, *J. Chromatogr.*, 522 (1990) 95.
[8] W.R. Heumann, *Crit. Rev. Anal. Chem.*, 2 (1971) 425.

[9] R.G. Fessler and H.A. Strobel, *J. Phys. Chem.*, 67 (1963) 2562.
[10] R.W. Gable and H.A. Strobel, *J. Phys. Chem.*, 60 (1956) 513.
[11] A. Ghodstinat, J.L. Pauley, T. Chen and M. Quirk, *J. Phys. Chem.*, 70 (1966) 512.
[12] J.L. Pauley, D.D. Vietti, C.C. Ou-Yang, D.A. Wood and R.D. Sherrill, *Anal. Chem.*, 41 (1969) 2047.
[13] C.J. Pederson, *J. Am. Chem. Soc.*, 89 (1967) 7017.
[14] K. Kimura, H. Harino, E. Hayata and T. Shono, *Anal. Chem.*, 58 (1986) 2333.
[15] T. Iwachido, H. Naitor, F. Samukawa and K. Ishimaru, *Bull. Chem. Soc. Jpn.*, 59 (1986) 1475.
[16] J.D. Lamb and R.G. Smith, *J. Chromatogr.*, 546 (1991) 73.
[17] R.M. Izatt, J.S. Bradshaw, S.A. Nielsen, J.D. Lamb and J.J. Christensen, *Chem. Rev.*, 85 (1985) 271.
[18] J. Burgess, *Metal Ions in Solution*, Wiley, New York, 1978.

ELSEVIER

Journal of Chromatography A, 706 (1995) 159–166

JOURNAL OF CHROMATOGRAPHY A

Separation of Pd(II) and Cu(II) in chloride solutions on a glycol methacrylate gel derivatized with 8-hydroxyquinoline

E. Anticó[a], A. Masana[a], V. Salvadó[a], M. Hidalgo[a], M. Valiente[b,*]

[a]*Química Analítica, Dept. de Química, Universitat de Girona, Pl. Hospital 6, 17071 Girona, Spain*

[b]*Química Analítica, Dept. de Química, Universitat Autònoma de Barcelona, 08193 Bellaterra, Spain*

Abstract

The adsorption of Pd(II) ions on Spheron Oxine 1000, a hydrophilic glycol methacrylate gel bearing 8-hydroxyquinoline groups, was investigated. The work was undertaken in flow conditions, using columns with different inner diameters packed with 1 g of the dry polymer. The adsorption and desorption isoplanes were determined under different hydrodynamic and chemical conditions. The breakthrough volume (95% removal efficiency) and the corresponding capacities were calculated from the isoplanes at different flow-rates and compared with batch results. The dynamic capacity obtained under saturation conditions was 57 ± 1 mg Pd(II)/g resin, at a flow-rate of 1.0 ml/min. High concentration and almost complete elution of Pd(II) were achieved using acidified thiourea solution, which also allowed the recycling of the chromatographic material. The separation of mixtures of Pd(II) and Cu(II) was achieved by appropriate adjustment of the pH of the feed solution to ensure selective sorption. Separation via appropriate acidic elution did not accomplish good selectivity.

1. Introduction

The use of chelating sorbents has been successfully applied as an alternative to liquid–liquid extraction for the concentration and selective separation of noble metals [1–3]. Functional groups capable of interacting selectively with metal ions have been introduced into different polymeric matrices. The organic matrices most extensively used are based on styrene–divinylbenzene copolymers [4]. However, supports obtained by addition of methacrylates are distinguished by their hydrophilicity and a high degree of porosity, which provide a rapid attainment of equilibrium. This is useful with platinum group of metals (PGM) because of the slow kinetics of their coordinating reactions. For this reason, methacrylate-based polymers bearing chelating groups have appropriate characteristics to be used for sorption–desorption processes under dynamic conditions.

A chelating molecule that has received much attention is 8-hydroxyquinoline (8-HQ), used extensively in solvent extraction [5,6]. 8-HQ has been immobilized on different supports in order to be used in ion-exchange or chromatographic applications [7–9].

Spheron Oxine 1000 is a chelating ion exchanger containing 8-HQ moieties bonded via azo groups in the side-chains of the modified hydroxyethyl methacrylate gel. This resin was developed by Slovák et al. [10] and has been shown to be suitable for the chromatographic separation of base metals.

* Corresponding author.

0021-9673/95/$09.50
SSDI 0021-9673(94)01176-1

This work was undertaken to study the processes of both sorption and elution of Pd(II) in chloride media using Spheron Oxine 1000. The influence of different parameters on the achievement of the selective separation of metal ions from solutions containing Pd(II) and base metals, mainly Cu(II), was investigated. The study was carried out under flow conditions with a chromatographic column and took advantage of previous batch sorption results to determine the optimum operating conditions [11].

2. Experimental

2.1. Reagents and solutions

A $9.4 \cdot 10^{-3}$ *M* stock standard solution of Pd(II) was prepared from solid $PdCl_2$ (for synthesis; Merck, Darmstadt, Germany). Working standard solutions with metal concentrations ranging from $1.0 \cdot 10^{-3}$ to $2.3 \cdot 10^{-3}$ *M* were prepared by dilution and then standardized gravimetrically with dimethylglyoxime [12]. A $1.57 \cdot 10^{-2}$ *M* stock standard solution of Cu(II) was obtained from solid $CuCl_2$ (analytical-reagent grade; Panreac, Spain) and was standardized volumetrically [12]. From this, working standard solutions with Cu(II) concentrations in the same range as for Pd(II) were obtained by dilution. Sodium chloride (analytical-reagent grade; Panreac) was purified as described elsewhere [13] and was employed to adjust the ionic strength of the metal solution to 0.1 *M*. The pH was varied between 0.0 and 2.0 using standarized HCl solution. For solutions with pH < 1.0 no sodium chloride was added, the ionic strength being determined by the HCl present. Solutions of thiourea (analytical-reagent grade; Pancreac), 0.5 *M* at pH 2.0, and hydrochloric acid, 0.5–2.0 *M*, were used in metal elution processes.

Spheron Oxine 1000, a glycol methacrylate support functionalized with 8-HQ moieties, was kindly supplied by Lachema (Brno, Czech Republic). The particle size and the pore diameter of the supported polymer were 40–63 μm and 37–50 nm, respectively.

2.2. Apparatus

A Varian SpectrAA-300 atomic absorption spectrometer (Varian Australia, Mulgrave, Victoria, Australia) was used to determine metal concentrations.

A Gilson Minipuls 2 peristaltic pump [Gilson Medical Electronics (France), Villiers-le-Bel, France] was employed to propel the solutions through the column. A Gilson FC 203 fraction collector (Gilson Medical Electronics, Middleton, WI, USA) was used to collect effluent samples at the outlet of the column.

All pH measurements were made with a Micro pH 2000 pH meter (Crison Instruments, Alella, Barcelona, Spain) and a Crison Model 50-02 combined glass electrode.

2.3. Column preparation

Glass columns were gravity packed with weighed samples of 1 g of air-dried resin (about 3 ml). The polymer was placed in the column in a suspension with a 0.1 *M* solution of sodium chloride or hydrochloric acid and allowed to settle. Two columns of different diameter (1.5 and 0.5 cm I.D.) were used.

2.4. Procedure for breakthrough studies

After column preparation, solution volumes of 250 ml containing Pd(II) or mixtures of Pd(II) and Cu(II) were processed through the column at a given flow-rate. In some instances, 350 ml of metal solution were necessary to achieve a higher degree of saturation. Effluent samples of 2.5 ml, for feed solutions containing only Pd(II), or 5 ml, when loading with both metals was studied, were periodically collected for analysis. Breakthrough curves were obtained from these analyses.

The adsorbed metal was eluted at a constant flow-rate (2.0 ml/min). The elution process was monitored as described for the loading process. In some instances, all the eluting solution was collected in several volumetric flasks until no metal was detected in the outlet of the column,

in order to determine the percentage of metal eluted at a given time.

The influence of the chemical and physical conditions on the palladium loading and its separation from copper was studied. Also, the behaviour of the eluting reagent, thiourea or HCl at different concentrations, was checked.

Experiments were carried out at a controlled room temperature of 22 ± 2°C and their reproducibility was verified in duplicate, which also indicated the uncertainty of the experimental data to be ±1 mg palladium/g resin.

3. Results and discussion

The reaction between 8-HQ and Pd(II) is on the basis of the palladium adsorption process described here. Such a reaction can be expressed by the equation [5]

$$M^{n+} + (n + r)(HOx)_{org} \rightleftharpoons [MOx_n(HOx)_r]_{org} + nH^+ \quad (1)$$

This process depends strongly on the acidity of the medium and the nature of the metal ion (i.e., the variation of the related stability constant is considerable). For palladium, the stability constant is high enough to allow the formation of the corresponding complex in very highly acidic media [5].

The adsorption of palladium by Spheron Oxine 1000 follows the mentioned pattern, as described previously [11]. The total amount of counter ions extracted per unit mass of solid chelating material is commonly called the apparent capacity [14]. The theoretical value of the metal adsorption capacity of Spheron Oxine 1000 (calculated from its nitrogen content and assuming a stoichiometry of 1:1 of the complex formed) was found to be 0.68 mmol/g resin. When the sorption of Pd(II) was determined in batch experiments, this theoretical value was only reached under specific chemical conditions, i.e., ionic strength, as described previously [11]. At pH 2.0 and ionic strength 0.1 *M* and after 24 h of contact between the resin and Pd(II) solution, a value of 0.536 mmol Pd(II)/g resin [57.03 mg Pd(II)/g resin] was found. Sorption of Pd(II) was not affected at pH values above 1.5.

The breakthrough capacity was determined to characterize Spheron Oxine 1000 under dynamic column operation. The breakthrough capacity is defined as the amount of metal ion that can be adsorbed per unit mass of solid before being detected in the outlet of the column. Different levels of metal in the effluent have been reported to be used to evaluate the breakthrough capacity [15]. In this work, the breakthrough capacity was determined from the volume of metal solution where the sorbent gives a removal efficiency higher than 95% under specified conditions. Breakthrough volumes were determined directly from the curves where $(C/C_0) \cdot 100 = 5$ (C_0 and C are the metal concentrations in the solution at the inlet and outlet of the column, respectively).

Factors that directly affect the breakthrough capacity, i.e., flow-rate, concentration of metal solution and column dimensions, were studied. Breakthrough curves were obtained for Pd(II) solutions at pH 2.0, ionic strength 0.1 *M* and flow-rates of 1.0, 2.0 and 3.0 ml/min using a column of 1.5 cm I.D. In Fig. 1, the percentage of metal in the effluent outlet is plotted against the bed volume (*BV*), defined as the ratio of the volume of effluent to the volume of resin. From the isoplanes, breakthrough capacities can be

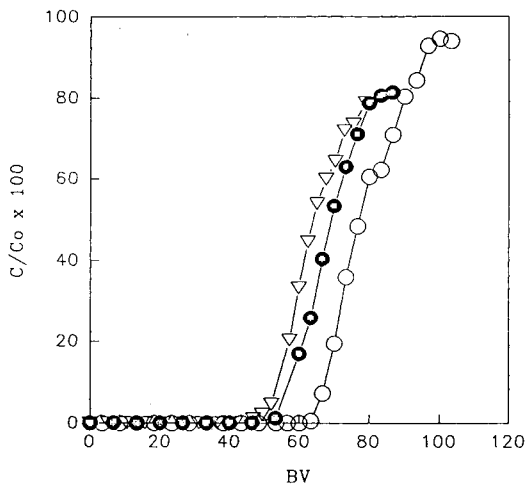

Fig. 1. Breakthrough curves for Pd(II) sorption at different flow-rates: ○ = 1.0; ● = 2.0; ▽ = 3.0 ml/min. Feed solutions as reported in Table 1. Column of 1.5 cm I.D.

Table 1
Breakthrough and dynamic capacities obtained at different flow-rates in a column of 1.5 cm I.D. with feed solutions at pH 2.0 and ionic strength 0.1 *M*

Flow-rate (ml/min)	Initial metal concentration (10^{-3} *M*)	Breakthrough capacity (mg/g resin)[a]	Dynamic capacity (mg/g resin)[a]
1.0	1.9	40 ± 1	48 ± 1
2.0	2.0	35 ± 1	44 ± 1
3.0	2.1	36 ± 1	45 ± 1

[a] Mean ± S.D. ($n = 2$).

determined. On the other hand, a better measure of capacity can be expressed as the total amount of metal loaded under flow conditions. This value, termed the dynamic capacity, can be calculated from the experimental points when $(C/C_0) \cdot 100 = 100$. As the achievement of this value occurs very slowly for the uptake of Pd(II) by Spheron Oxine 1000, an approximate dynamic capacity was calculated graphically from the point where $(C/C_0) \cdot 100 = 80$. Different numerical integration methods, i.e., Simpson and trapezium methods, were used in these calculations [16]. Both values are summarized in Table 1. As expected, an increase in the flow-rate reduces both the breakthrough and dynamic capacities, in spite of this effect being more obvious at lower flow-rates [17]. Such a decrease can be ascribed to a lower residence time. As seen in Table 1, the dynamic capacities calculated as mentioned before are lower than the theoretical adsorption capacity. Saturation conditions were reached at a flow-rate of 1.0 ml/min and with 350 ml of feed solution. In this manner, a total amount of Pd(II) loaded of 57 ± 1 mg/g resin was obtained, which is similar to the corresponding batch capacity value.

The sorption and desorption isoplanes of Pd(II) at pH 2.0, flow-rate 2.0 ml/min and initial metal concentration $1.2 \cdot 10^{-3}$ *M* are shown in Fig. 2. The breakthrough capacity determined from the data obtained was 40 ± 1 mg/g resin. It was also determined that the capacity obtained depends on the metal concentration in the feed

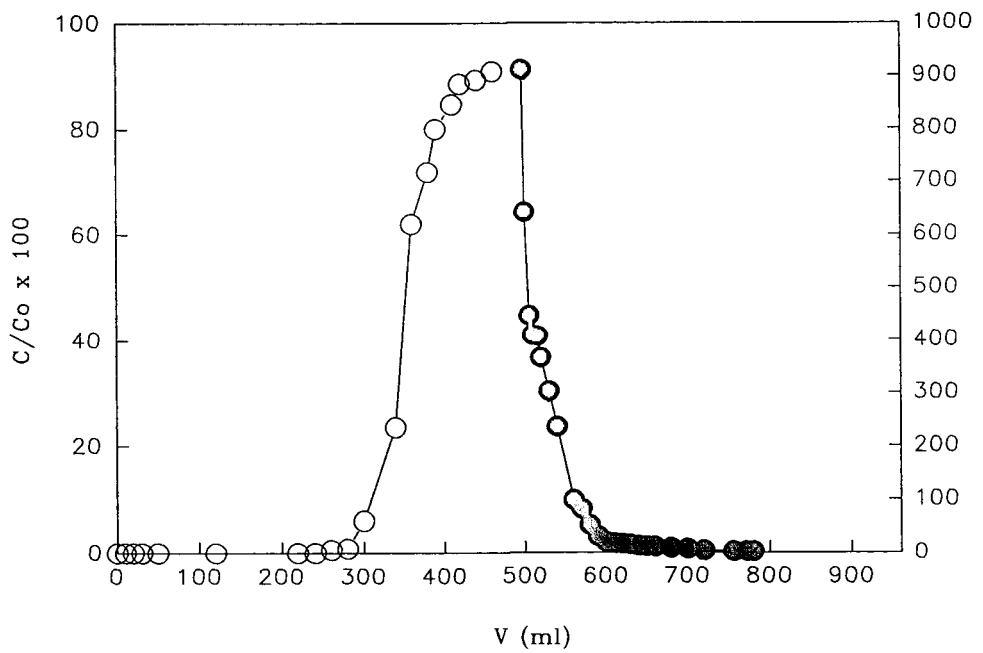

Fig. 2. (○) Sorption and (●) desorption isoplanes for $1.2 \cdot 10^{-3}$ *M* Pd(II), pH 2.0, ionic strength 0.1 *M*. Column of 1.5 cm I.D. Elution carried out with 0.5 *M* thiourea at pH 2.0. Flow-rate, 2.0 ml/min in both processes.

solution. As expected, the capacity increases when the metal concentration decreases. The elution data with 0.5 *M* thiourea at pH 2.0 show high efficiency.

A comparison of the elution efficiencies with 0.5 *M* thiourea at pH 2.0 and 2.0 *M* HCl as eluents is illustrated in Fig. 3. Loading was carried out at a flow-rate of 1.0 ml/min, initial metal concentration $1.9 \cdot 10^{-3}$ *M*, pH 2.0 and ionic strength 0.1 *M* in both experiments. Data are expressed as percentage of metal eluted calculated with respect to the total metal loaded [57 ± 1 mg Pd(II)/g resin]. As seen, the elution efficiency obtained with acidified thiourea was 81% and a considerable concentration of initial palladium solution is easily obtained. On the other hand, the efficiency of HCl elution was found to be much lower (only 36% was eluted in this instance).

The following experiments deal with the influence of the column diameter. The results obtained with a 1.5 cm I.D. column were compared with those with a 0.5 cm I.D. column packed with the same mass of resin. Under the same experimental conditions, an increase in column efficiency was obtained when a narrow column was used. Breakthrough capacities were calculated and are given in Table 2. The effect of

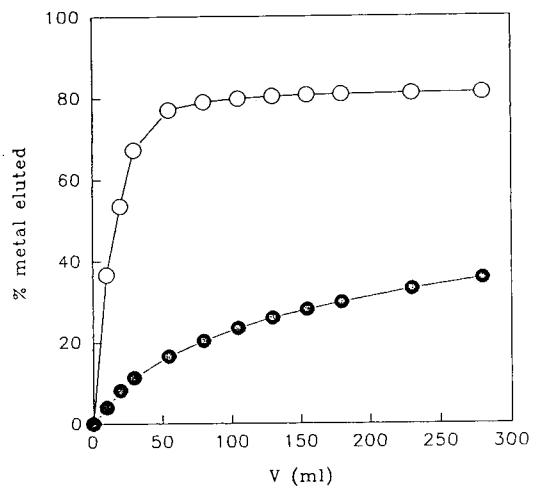

Fig. 3. Elution efficiency: percentage of metal eluted as a function of eluent volume. Flow-rate, 2.0 ml/min. ○ = 0.5 *M* thiourea, pH 2.0; ● = 2.0 *M* HCl.

Table 2
Breakthrough capacities as a function of inner diameter of the column

I.D. (cm)	Initial metal concentration (10^{-3} *M*)	Breakthrough capacity[a] (mg/g resin)
1.5	2.0	35 ± 1
0.5	2.2	50 ± 1

Flow-rate, 2.0 ml/min; feed solutions at pH 2.0 and ionic strength 0.1 *M*.
[a] Mean ± S.D. ($n = 2$).

column dimensions on breakthrough capacities can be interpreted as a diffusional effect, because for a large column diameter the diffusion within the column does not occur quickly enough to utilize as many of the available complexation sites [17].

The reuse of the chromatographic material was determined to be efficient. For this purpose, a loaded resin was washed with 300 ml of 0.5 *M* thiourea solution of pH 2.0, rinsed with 0.1 *M* NaCl solution of pH 2.0, allowed to dry in air and then loaded again with palladium solution. No relevant differences were observed in the breakthrough capacities between the new and the reused resin [35 ± 1 mg Pd(II)/g resin for both new and reused materials].

Under dynamic conditions, sorption studies of precious metals and selected base metals were carried out with regard to potential applications of the chelating resins in hydrometallurgy. In this sense, results reported previously indicate that Spheron Oxine 1000 could be used for the separation of Pd(II) and Cu(II) taking into account the different apparent capacities obtained for these ions at pH 2.0, where the adsorption of palladium is much higher [11].

In a chromatographic column, separation can be obtained by either selective sorption or elution. Both factors were studied following the same procedure as described for the adsorption of palladium. Breakthrough curves were obtained under the following experimental conditions: initial concentration of Pd(II) $2.3 \cdot 10^{-3}$ *M*, initial concentration of Cu(II) $2.2 \cdot 10^{-3}$ *M*

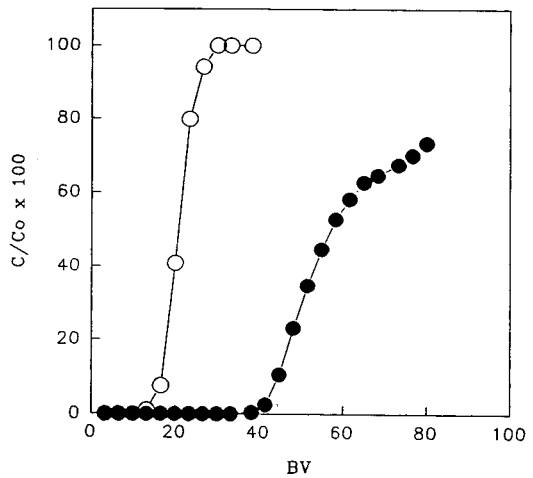

Fig. 4. Breakthrough curves for a solution containing $2.3 \cdot 10^{-3}$ *M* Pd(II) and $2.2 \cdot 10^{-3}$ *M* Cu(II), pH 1.4. Flow-rate, 2.0 ml/min. ○ = Cu(II); ● = Pd(II).

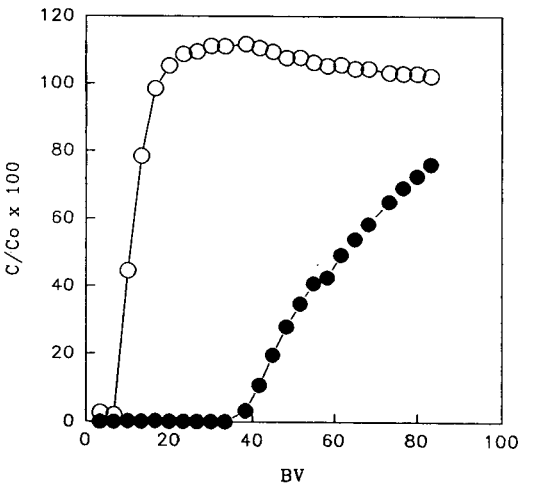

Fig. 6. Breakthrough curves for a solution containing $2.3 \cdot 10^{-3}$ *M* Pd(II) and $2.2 \cdot 10^{-3}$ *M* Cu(II), pH 0.3. Flow-rate, 2.0 ml/min. ○ = Cu(II); ● = Pd(II).

and flow-rate 2.0 ml/min. As the most important parameter affecting the loading of base metals on Spheron Oxine 1000 was found to be the pH of the initial metal solution [10], the pH was varied systematically in order to obtain a selective loading. Experiments at pH 1.4, 0.8, 0.3 and 0.0 were performed and the breakthrough curves obtained are shown in Figs. 4–7. As expected, an improvement in the separation is observed when the pH of the solution is decreased. Nevertheless, for high acidity (pH < 0.3) the loading of palladium is also affected: copper is not adsorbed at all and palladium appears in the effluent in a shorter time. The breakthrough curves at pH 0.8 or 0.3 show that the sorption of palladium in the resin displaces the adsorbed

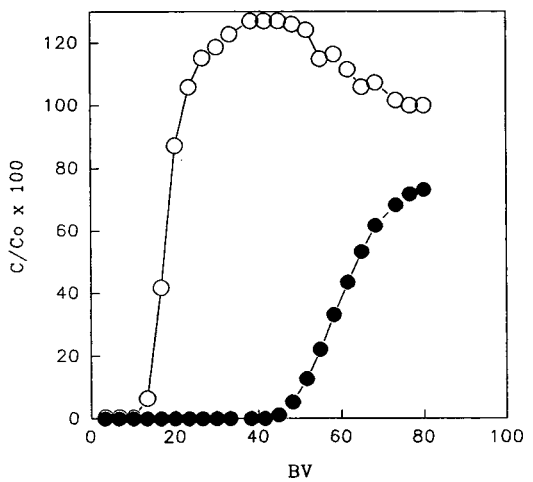

Fig. 5. Breakthrough curves for a solution containing $2.3 \cdot 10^{-3}$ *M* Pd(II) and $2.2 \cdot 10^{-3}$ *M* Cu(II), pH 0.8. Flow-rate, 2.0 ml/min. ○ = Cu(II); ● = Pd(II).

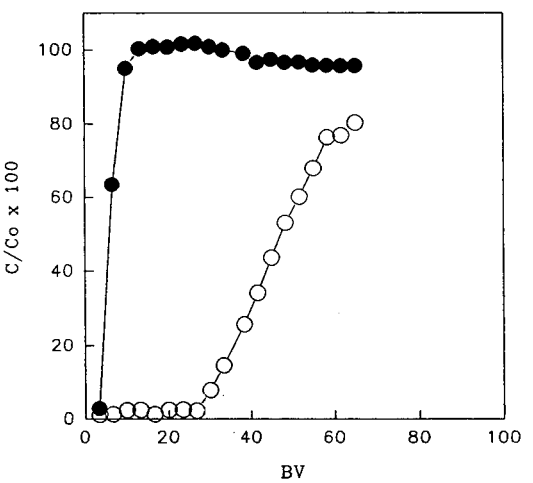

Fig. 7. Breakthrough curves for a solution containing $2.3 \cdot 10^{-3}$ *M* Pd(II) and $2.2 \cdot 10^{-3}$ *M* Cu(II), pH 0.0. Flow-rate, 2.0 ml/min. ○ = Pd(II); ● = Cu(II).

copper, producing the values of the ratio $(C/C_0) \cdot 100$ greater than 100.

Dynamic capacities for loading of palladium and copper at pH 0.3 were determined as the difference between the total metal concentration and the concentration in the effluent after a certain volume of solution has circulated through the column. In this instance, the volume corresponds to an efficiency of 20% with respect to palladium. The values obtained are summarized in Table 3. The breakthrough and dynamic capacities obtained for Cu(II) are similar whereas for Pd(II) a considerable difference in these values can be observed, in agreement with the shape of the isoplanes in Fig. 6. The value of the dynamic capacity obtained experimentally agrees with the value calculated by means of numerical integration methods, which was found to be 46 mg Pd(II)/g resin. At pH 0.3, complete separation of the two metals is not obtained, but the copper sorbed in the resin is only 6% of the initial value. Only at pH 0.0 is Pd(II) selectively adsorbed, according to the results shown in Fig. 7.

Results of elution experiments are shown in Figs. 8 and 9. In Fig. 8 the elution profiles were obtained using 2.0 *M* HCl as eluent (loading at pH 1.4). As can be seen, this stripping is very effective for Cu(II), even though a small amount of Pd(II) is eluted simultaneously. It must be taken into account that the resin contains much more palladium than copper (see Fig. 4). Lower concentrations of hydrochloric acid did not improve the palladium–copper separation. However, a high efficiency of separation was achieved by loading the mixture under very acidic conditions (pH < 0.3). Under these conditions copper is virtually unadsorbed. Elution in this in-

Table 3
Breakthrough and dynamic capacities obtained for a mixture of Pd(II) and Cu(II)

Metal	Breakthrough capacity[a] (mg/g resin)	Dynamic capacity (mg/g resin)[a]
Pd(II)	28 ± 1	45 ± 1
Cu(II)	3 ± 1	2 ± 1

$[Pd(II)] = 2.3 \cdot 10^{-3}$ *M*; $[Cu(II)] = 2.2 \cdot 10^{-3}$ *M*; pH = 0.3; flow-rate, 2.0 ml/min.
[a] Mean ± S.D. ($n = 2$).

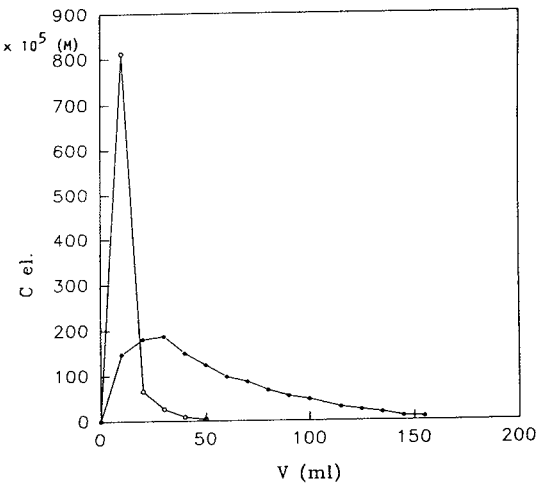

Fig. 8. Elution profiles of loaded Pd(II) and Cu(II) from the experiment shown in Fig. 4 using 2.0 *M* HCl as eluent at 2.0 ml/min. Results expressed as concentration of metal [Pd(II) or Cu(II)] in the elution outlet as a function of volume of eluent. ○ = Cu(II); ● = Pd(II).

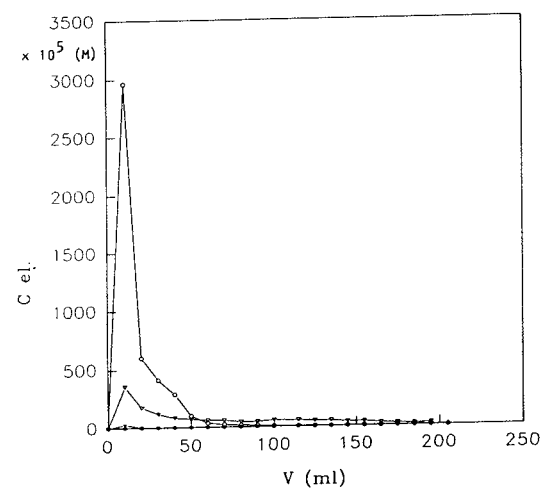

Fig. 9. Elution profiles of loaded Pd(II) and Cu(II) from the experiment shown in Fig. 6 using either 2.0 *M* HCl or 0.5 *M* thiourea at pH 2.0 as eluent at 2.0 ml/min. Results expressed as concentration of metal [Pd(II) or Cu(II)] in the elution outlet as a function of volume of eluent. ○ = Pd(II) and ● = Cu(II) with 0.5 *M* thiourea at pH 2.0; ▽ = Pd(II) and ▼ = Cu(II) with 2.0 *M* HCl.

stance (see Fig. 9), both with 0.5 *M* thiourea of pH 2.0 and 2.0 *M* HCl, verifies the separation by the loading process. The experiments also reveal the higher efficiency of thiourea than hydrochloric acid solutions.

Acknowledgement

This work was carried out under CICYT (Spanish Commission for Research and Development) Project No. MAT93-0621.

References

[1] G.V. Myasoedova, I.I. Antokol'skaya and S.B. Savvin, *Talanta*, 32 (1985) 1105.
[2] S.B. Savvin, I.I. Antokol'skaya, G.V. Myasoedova, L.I. Bolshakova and O.P. Shvoeva, *J. Chromatogr.*, 102 (1974) 287.
[3] F. Švec and A. Jehličková, *Angew. Makromol. Chem.*, 121 (1984) 127.
[4] P.M.M. Jonas, D.J. Eve and J.R. Parrish, *Talanta*, 36 (1989) 1021.
[5] J. Starý, *Anal. Chim. Acta*, 28 (1963) 132.
[6] E. Ma and H. Freiser, *Inorg. Chem.*, 23 (1984) 3344.
[7] J.R. Parrish and R. Stevenson, *Anal. Chim. Acta*, 70 (1974) 189.
[8] F. Vernon and K.M. Nyo, *J. Inorg. Nucl. Chem.*, 40 (1978) 887.
[9] J.R. Jezorek and H. Freiser, *Anal. Chem.*, 51 (1979) 366.
[10] Z. Slovák, S. Slováková and M. Smrž, *Anal. Chim. Acta*, 75 (1975) 127.
[11] E. Anticó, A. Masana, V. Salvadó, M. Hidalgo and M. Valiente, *Anal. Chim. Acta*, 296 (1994) 325.
[12] A.I. Vogel, *Vogel's Textbook of Quantitative Inorganic Analysis*, Longman, London, 1978.
[13] *Some Laboratory Methods*, Inorganic Chemistry, Royal Institute of Technology (KTH), Stockholm, 1959.
[14] F. Helfferich, *Ion Exchange*, McGraw-Hill, New York, 1962.
[15] D. Lindsay, D.C. Sherrington, J.A. Greig and R.H. Hancock, *React. Polym.*, 12 (1990) 75.
[16] S.C. Chapra and R.P. Canale, *Métodos Numéricos para Ingenieros con Aplicaciones en Computadoras Personales*, McGraw-Hill, Méjico, 1991.
[17] M.A. Marshall and H.A. Mottola, *Anal. Chem.*, 57 (1985) 729.

ELSEVIER

Journal of Chromatography A, 706 (1995) 167–173

JOURNAL OF CHROMATOGRAPHY A

Determination of Cd, Co, Cu, Fe, Mn, Ni and Zn in coral skeletons by chelation ion chromatography

William Shotyk*, Ina Immenhauser-Potthast

Geological Institute, University of Berne, Baltzerstrasse 1, CH-3012 Berne, Switzerland

Abstract

Cadmium, Co, Cu, Fe, Mn, Ni and Zn incorporated in the aragonitic skeletons of corals (*Porites*) were analyzed by chelation ion chromatography (CIC). A 500-mg amount of bleached, oven-dried coral powder was dissolved in 1 ml of 14.4 *M* HNO_3 and buffered at pH 5.4 ± 0.1 using 50 ml of 2 *M* ammonium acetate. A 30-g amount of sample was concentrated on-line by pumping the solution through a Dionex MetPac CC-1 chelating concentrator column at a rate of 3 ml/min, and the MetPac was rinsed with 2 *M* ammonium acetate to elute alkaline earth metals to waste. The transition metals were eluted on a second concentrator column (Dionex TMC-1) using 2 *M* HNO_3, and the TMC-1 was then converted to a salt form using 0.1 *M* NH_4NO_3 and switched on-line with the analytical column, the Dionex IonPac CS-5. The metals were then eluted from the separator column using 6 m*M* pyridine–2,6-dicarboxylic acid–0.4 *M* NaOH; the pH of this eluent was 4.4. The separated metals were, after they had left the column, complexed by 0.5 m*M* 4-(2-pyridylazo)resorcinol, and the absorbance was measured in a Dionex ultraviolet–visible detector at 520 nm. The use of two separator columns in series improved the metal separation. This is especially important for Ni and Co because coral samples typically contained an order of magnitude more Zn than Ni or Co. With two columns in series, Ni, Co and Zn were baseline-separated even when a 30-g sample containing 5 ppb Ni, 5 ppb Co and 100 ppb Zn was concentrated. The absolute sensitivity of the instrument was approximately 10 ng Cd. Although Cd was successfully determined in several corals using CIC, most coral samples contain on the order 1 ng/g Cd or less and, thus, the quantitative measurement of Cd in most corals by CIC would require tens of grams of coral powder. Unfortunately, it is not possible to obtain such large quantities of coral material from annual bands. The chelation system may be useful, however, to pre-concentrate coral digests for Cd analyses using more sensitive methods of detection (e.g. graphite furnace atomic absorption spectrometry or inductively coupled plasma mass spectrometry).

1. Introduction

Man-made pollution is an increasing problem in tropical marine environments. Heavy loads of sediments may be lethal to corals and lesser quantities may inhibit coral growth, cause changes in growth forms or alter the species composition of reef-building organisms [1]. The fringing reef ecosystem of Mauritius (Indian Ocean) is degenerating because of coral diseases, widespread eutrophication and algal growth in some parts of the reef and degradation of lagoons. An increase in the number of sea urchins, a reduction in coral vitality and a decrease in specimen variation can be observed [2]. A geochemical study was undertaken using the widespread recent scleractinian coral genus

* Corresponding author.

0021-9673/95/$09.50
SSDI 0021-9673(95)00104-2

Porites to find possible reasons for reef degradation.

Anthropogenic inputs of sewage could be responsible for the degradation of the corals, caused by nutrients or toxic heavy metals [3,4]. There are several possible sources of pollution that could affect the coastal environment of Mauritius, e.g., waste dump sites, sugar cane industry and sewage from towns, hotels and private houses on the beach. In addition there is an industrial region in Port Louis Harbour. Nutrients, pesticides and heavy metals may be washed out during the rainy season and transported into the lagoon by rivers, canals and ground water.

A wide range of trace metals have been determined in the calcium carbonate (aragonite) skeletons of reef-corals [5]. Pb and Cd in corals, for example, are well known indicators of anthropogenic activity [6,7]. In contrast, Mn is an indicator of detrital inputs [8,9]. There have been reports of Pb measurements in acid digests of coral skeletons directly, without preconcentrating the solutions, using anodic stripping voltammetry [10]. However, in most cases, especially with respect to ultratrace metals such as Cd and Pb, some kind of preconcentration step is required before the coral digests can be analyzed. For example, St. John [11] concentrated Cd, Co, Cu, Fe, Ni, Pb and Zn using ammonium pyrrolidine dithiocarbamate (APDC) followed by extraction into methyl isobutyl ketone (MIBK). Other investigators [7–9,12] used a very similar approach.

To evaluate the possible role of heavy metals in degrading the reef ecosystem at Mauritius, an effort was made to measure the concentrations of Cd, Co, Cu, Fe, Mn, Ni and Zn in acid-dissolved skeletons of massive colonial corals of the genus *Porites*. The principle objective of this report is to evaluate the chelation ion chromatography (CIC) method for measuring these metals in the aragonitic coral skeletons. The CIC system combines an on-line chelation preconcentration step with the analytical chromatography for the simultaneous determination of these metals [13,14].

2. Experimental

2.1. Sampling and preparation of corals

Massive, hermatypic, colonial coralla of the scleractinian coral genus *Porites* LINK were used in this study. *Porites solida* and *Porites lutea*, both recent species, were chosen because of their widespread occurrence in all parts and all depths of the reef complex. Samples were taken in the autumn of 1990 and the summer of 1991 from the lagoon and the outer reef slope in relation to various possible sources of pollution. Samples from unaffected areas were taken as control samples to determine background concentrations.

After sampling, the corals were washed and cleaned several times in water and a desinfectant (Sagrotan) and dried in the sun. For transport they were well wrapped in clean paper. Longitudinal cuts of the central part of the colonies were made parallel to the growth of the coral using a rock cutting saw (type Cutler-Hammer). These cuts were X-rayed to examine growth rate and structure. Parts of these coral slices were cut into small pieces with a fretsaw. For each sample a new saw blade was used to avoid metal contamination by abrasion. After sawing, the skeleton pieces were washed in 18 MΩ deionized water, blown dry with compressed air and cleaned ultrasonically in PTFE beakers containing deionized water. The corals were bleached in 30% H_2O_2 (Merck Suprapur) to remove tissues and organic substances. Finally, the corals were leached in deionized H_2O and dried at 90–105°C. Special care was taken to use clean preparation procedures and appropriate materials for labware [12,15]. All plastic ware was cleaned with soap and hot water, rinsed in deionized water, put in a 10% HNO_3 bath (made from Merck Suprapur HNO_3) for several days and finally washed four times with deionized water before use. The clean coral pieces were powdered using an agate mortar and pestle in a laminar air flow cabinet and stored in clean plastic jars.

2.2. Preparation of acid digests

Samples (500 mg) of oven-dried coral powder were placed in clean, acid-washed PTFE bottles and dissolved in 1 ml of 14.4 *M* HNO_3 (Merck Suprapur). The solutions were buffered at pH 5.4 ± 0.1 using 52.5 g of 2 *M* ammonium acetate to give a final volume of sample solution of 50 ml. All of the reagents used were trace-metal grade (Merck Suprapur HNO_3, CH_3COOH, NH_4OH) and all solutions were made up in 18 MΩ deionized water. Ammonium acetate was made from Merck Suprapur CH_3COOH and NH_4OH, and ammonium nitrate was made from Merck Suprapur NH_4OH and HNO_3.

2.3. Chelation ion chromatography

CIC was performed using a Dionex 4500i IC system. The recommended configuration, preparation, operation and applications of this system are described in detail elsewhere [16]. We evaluated two configurations: a single CS-5 separator column and two CS-5 separator columns in series to improve peak separation (see below).

Samples were concentrated on-line by pumping the solution through a MetPac CC-1 chelating concentrator column. This column contains a macroporous iminodiacetate chelating resin; the capacity, selectivity and retention characteristics of this column are described elsewhere [16]. The sample solutions were pumped through this column at a rate of 3 ml/min. The coefficient of variation of the mass of solution concentrated by the sample pump was approximately 1%. The MetPac was then rinsed with high-purity 2 *M* ammonium acetate to remove alkaline earth metals (which were eluted to waste). The transition metals were then eluted to a second concentrator column (TMC-1) using 2 *M* Suprapur HNO_3. The TMC-1 contains a fully sulfonated cation-exchange resin as interface between the high-capacity chelation concentrator column (MetPac CC-1) and the low-capacity analytical column (IonPac CS-5). Before the TMC-1 could be switched on-line with the analytical stream, it had to be converted from the H^+ form to the NH_4^+ form; this was accomplished using 0.1 *M* NH_4NO_3 (pH 3.5). Following this step, the TMC-1 was switched on-line with the analytical column, the IonPac CS-5. The concentrated metals were then eluted with 6 m*M* pyridine–2,6-dicarboxylic acid (PDCA) in 0.4 *M* NaOH; the pH of this eluent was 4.4. After the separated metals left the column they were complexed by 0.5 m*M* 4-(2-pyridylazo)resorcinol (PAR), a metallochromic indicator. Absorbance was measured in a Dionex UV–VIS detector at 520 nm.

3. Results

3.1. Metal analyses of corals

Single separator column

Using a single separator column, Fe, Cu, Zn and Mn could be readily quantified by concentrating a 15-g digest (Fig. 1a). Using this approach, Ni could also be determined in most of the samples. However, in some samples Ni was below the limit of detection. Concentrating more sample to increase the Ni signal did not solve this problem because the Zn peak eventually overlapped that of Ni. A second disadvantage of this arrangement was that Co could not be quantified because it was masked by Zn (Fig. 1a). The Zn-to-Co ratio in corals was typically 10:1 at least; thus, Co could not be determined using a single separator column, especially in contaminated samples containing elevated concentrations of Zn. A third problem with this configuration was that Cd could not clearly be separated from Co [17]. Cadmium concentrations in these materials were much lower than those of Co; thus, it was not possible to measure Cd under these conditions.

Two separator columns in series

Using two separator columns in series with the same eluent improved the metal separation (Fig. 1b). The main advantage of using two columns was the clear separation of Ni, Zn and Co. Coral samples typically contain an order of magnitude

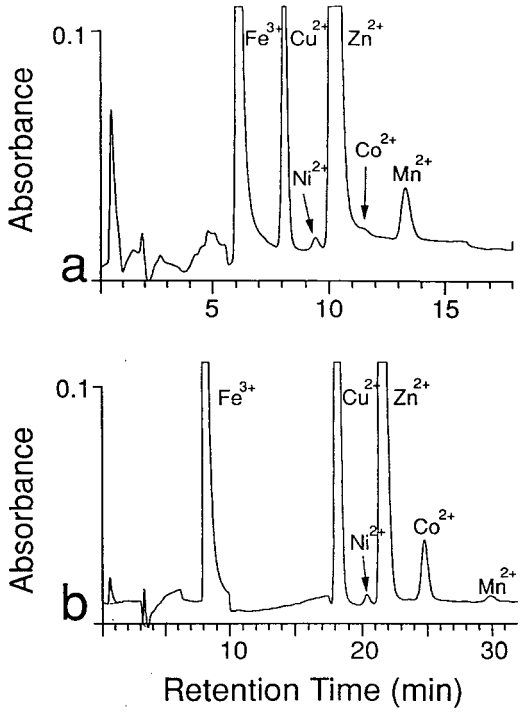

Fig. 1. (a) 6 m*M* PDCA eluent with one CS-5 separator column, 15 g of coral digest (sample No. 9005) concentrated. Notice that Co appears as a shoulder on Zn. Concentrations (ng/g) are as follows: 14.9 Fe, 2.8 Cu, 0.5 Ni, 12.1 Zn and 1.5 Mn. (b) 6 m*M* PDCA eluent with two CS-5 separator columns in series, 30 g of coral digest (sample No. 9187) concentrated. Notice that Co is now clearly separated from Zn. Concentrations (ng/g) are as follows: 24.4 Fe, 21.8 Cu, 1.5 Ni, 19.5 Zn, 2.2 Co and 0.9 Mn.

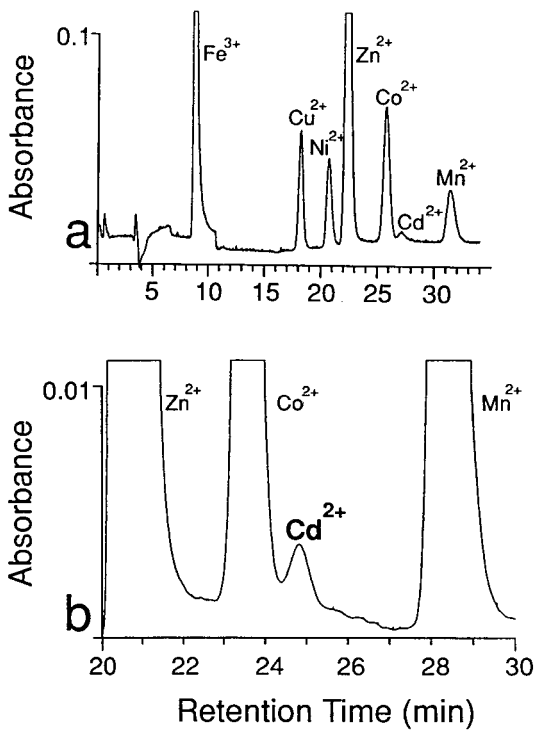

Fig. 2. (a) Chromatogram of National Institute of Science and Technology Standard Reference Material 1643c "Trace Metals in Water". Again, 6 m*M* PDCA eluent was used with two CS-5 separator columns in series, 30 g concentrated. Note the Cd peak with a retention time of approximately 27 min. Concentrations (ng/g) are as follows: 16.2 Fe, 3.3 Cu, 9.9 Ni, 10.3 Zn, 3.3 Co, 1.7 Cd and 4.3 Mn. (b) Expanded view of part of the chromatogram of an acid digest of a coral sample (9127) showing a Cd peak (1.1 ng/g Cd); this corresponds to 110 ng/g in the solid coral.

more Zn than Ni or Co. While concentrating 15 g of sample was sufficient for measuring Ni in many samples, it was not for measuring Co. With two columns in series, however, even when 30-g samples were concentrated, Ni and Co were still clearly separated from Zn (Fig. 1b). Nickel, Co, and Zn were baseline-separated even when a 30-g sample containing 5 ng/g Ni, 5 ng/g Co and 100 ng/g Zn was concentrated. The principle disadvantage of using two separator columns is the increased time required per analysis.

Determination of Cd

Using two separator columns in series, Cd was clearly separated from Co and Zn (Fig. 2a and b). To identify a Cd peak readily, a peak area of approximately 3000 counts · s (30 mAU · s) was required. A plot of the absolute quantity of Cd concentrated versus measured peak area (Fig. 3) yielded the response function which could be used to calculate the amount of Cd needed to produce a peak of this size. The linear regression equation indicates that 10 ng of Cd must be concentrated in order to obtain a measurable peak: this quantity of Cd is the absolute detection limit of the method. Thus, when a 30-g digest (obtained by dissolving a 500-mg sample) is concentrated, a minimum detection limit of approximately 0.3 ng/g Cd can be achieved. Using the CIC method described here, Cd was measured in two coral samples. However, Cd

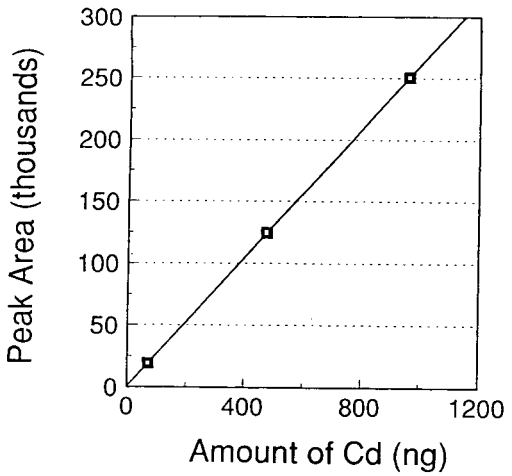

Fig. 3. Measured area of Cd peaks as a function of absolute quantity of Cd concentrated from water samples. For a Cd peak to be readily identifiable, a peak area of approximately 3000 counts · s (30 mAU · s) is required. The linear regression ($y = 263x + 261$, $r^2 = 0.9999$) indicates that approximately 10 ng of Cd must be concentrated in order to obtain a peak area of this magnitude: this quantity of Cd is the absolute detection limit of the method.

was not detected in the majority of the corals. In other words, it was not possible to determine the 'background' Cd concentrations in the corals. While it may be possible to improve the detection limit by concentrating more sample, some tens of grams of solid material would probably be needed. Not only is it impossible to obtain such large quantities of coral material from annual bands, but concentrating such large quantities of material would also concentrate Zn and Co which might eventually mask the Cd peak. The detection limit for Cd is, therefore, generally inadequate for measuring Cd in coral samples from annual bands. The chelation concentration system may be useful, however, to preconcentrate coral digests and eliminate the matrix for Cd analyses by graphite furnace atomic absorption spectrometry (GFAAS) or inductively coupled plasma mass spectrometry (ICP-MS) [18,19].

Effect of $CaCO_3$ matrix

In order to evaluate the effect of the $CaCO_3$ matrix on the metal measurements, solid $CaCO_3$ powder (Merck Suprapur) was used to prepare a series of calibration standards. A 100-mg quantity of $CaCO_3$ was dissolved in 2 ml of HNO_3. Appropriate volumes of individual 1000-ppm metal standards and 2 ml of HNO_3 were added to ensure stability, and the standards were diluted to 50 ml. Prior to analysis, these standards were buffered to pH 5.4 ± 0.1 by adding 52.5 g of 2 *M* ammonium acetate which diluted them to 100 ml.

The influence of the $CaCO_3$ matrix is seen in the extreme example given in Fig. 4 which shows a calibration curve for Mn in pure water compared with Mn in a $CaCO_3$ background. The effect of matrix suppression on measured peak area for the other metals ranges from approximately 5 to 20%.

Determination of Pb

Using an eluent consisting of 4 m*M* PDCA, 0.4 *M* NaOH, 2 m*M* Na_2SO_4 and 15 m*M* NaCl (also pH 4.4), Pb was clearly separated from the other peaks (Fig. 5). However, the CIC method was not sufficiently sensitive to determine Pb at the low concentrations present in these corals. If unlimited amounts of sample material were available, Pb could have been measured in the coral digests by concentrating for a sufficiently long time. However, as noted above, the amount of material available from annual bands was

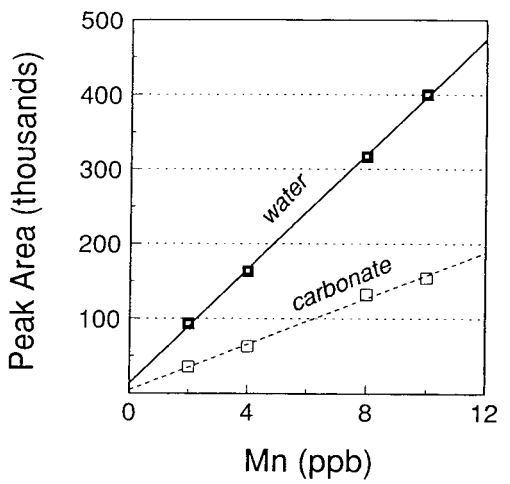

Fig. 4. Measured area of Mn peaks as a function of Mn concentration in solution. Solid squares correspond to Mn concentrations in a water matrix, open squares to Mn concentrations in a $CaCO_3$ matrix.

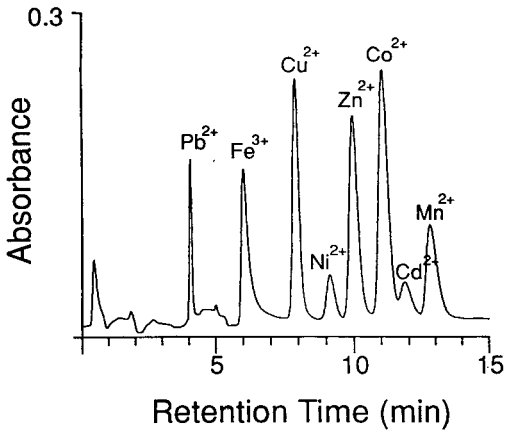

Fig. 5. Chromatogram of trace metals in water. A 10-g amount of solution containing 36 ng/g of each metal was concentrated. Eluent used was 4 m*M* PDCA, 0.4 *M* NaOH, 2 m*M* Na_2SO_4 and 15 m*M* NaCl (also pH 4.4). Note the Pb peak at approximately 4 min.

limited. Again, the CIC method may be useful to preconcentrate the coral digests and eliminate the matrix for Pb analyses using more sensitive detection methods (GFAAS or ICP-MS).

4. Conclusions

CIC was used for the simultaneous determination of Cd, Co, Cu, Fe, Mn, Ni and Zn in acid digests of coral samples. With a single separator column the method was suitable for the quantitative measurement of Fe, Cu, Zn and Mn. The use of two separator columns in series greatly improved peak separation and allowed the quantitative determination of Ni and Co, in addition to the other metals. Even in samples containing Zn/Ni and Zn/Co ratios greater than 20 or more, Ni and Co were clearly separated from Zn. Although the method is relatively slow (10 min for concentrating the sample and almost 40 min for analytical chromatography), the sensitivity is comparable to that of GFAAS for Cu, Fe, and Zn and better than GFAAS for Co, Ni and Mn.

For 30-g digests made up using 500-mg samples of coral powder, the detection limit for Cd was approximately 0.3 ng/g. Using the CIC method, however, Cd was measured only in two samples. While it may be possible to measure lower Cd concentrations by concentrating more sample, some tens of grams of solid material might be needed. It is not possible to obtain such large quantities of coral material from annual bands. The detection limit for Cd, therefore, is generally inadequate for measuring Cd in such samples. The chelation concentration system may be useful, however, to preconcentrate coral digests and eliminate the matrix for Cd analyses by GFAAS or ICP-MS.

Acknowledgements

This work is a summary of part of the Ph.D. Thesis by I.I.-P., supervised by Dr. J. Geister. We are indebted to Prof. A. Matter of this institute for generously providing all of the required laboratory facilities. Additional financial support from the Canton of Berne (SEVA Lottofonds) and the Swiss National Science Foundation (Grants 21-30207.90 and 21-30207.92) is also sincerely appreciated. René Trost (now at Dionex Switzerland) and Stefan Brand of Henry A. Sarasin (Basel, Switzerland) provided expert technical support with all aspects of ion chromatography.

References

[1] R.A. Pastorok and G.R. Bilyard, *Mar. Ecol. Prog. Ser.*, 21 (1985) 175.
[2] L. Hottinger, N. Muller, J. Muller and P. Vasseur, *Etude des Ecosystemes Littoraux de Maurice*, Rapport No. 1, Université d'Aix-Marseille I et III, Université de Maurice, 1990, 56 pp.
[3] J. Muller et al., *Etude des Ecosystemes Littoraux de Maurice*, Rapport No. 5, Université d'Aix-Marseille I et III, Université de Maurice, 1991.
[4] F. Gendre, *Thèse*, Faculté de Sciences, Institut de Géologie, Neuchâtel, 1992.
[5] L.S. Howard and B.E. Brown, *Oceanogr. Mar. Biol. Ann. Rev.*, 22 (1984) 195.
[6] G.T. Shen, *Ph.D. Thesis*, Massachusetts Institute of Technology, Cambridge, MA, 1986.

[7] G.T. Shen, E.A. Boyle and D.W. Lea, *Nature*, 328 (1987) 794.
[8] L.J. Linn, M.L. Delayney and E.R.M. Druffel, *Geochim. Cosmochim. Acta*, 54 (1990) 387.
[9] G.T. Shen, T.M. Campbell, R.B. Dunbar, G.M. Wellington, M.W. Colgan and P.W. Glynn, *Coral Reefs*, 10 (1991) 91.
[10] R.E. Dodge and T.R. Gilbert, *Mar. Biol.*, 82 (1984) 9.
[11] B.E. St. John, *Proc. 2nd Int. Coral Reef Symp.*, 2 (1974) 461.
[12] G.T. Shen and E.A. Boyle, *Chem. Geol.*, 67 (1988) 47.
[13] A. Siriraks, H.M. Kingston and J.M. Riviello, *Anal. Chem.*, 62 (1990) 1185.
[14] N. Cardellicchio, S. Cavalli and J.M. Riviello, *J. Chromatogr.*, 640 (1993) 207.
[15] C.F. Boutron, *Fresenius J. Anal. Chem.*, 337 (1990) 482.
[16] Dionex, *Technical Note* No. 25, 1992, 20 pp.
[17] W. Shotyk, I. Potthast and J. Geister, *Proc. 9th Int. Conf. Heavy Metals Environ.*, 2 (1993) 37.
[18] D.W. Boomer, M.J. Powell and J. Hipfner, *Talanta*, 37 (1990) 127.
[19] L.W. McLaren, J.W.H. Lam, S.S. Berman, K. Akatsuka and M.A. Azeredo, *J. Anal. Atom. Spectrom.*, 8 (1993) 279.

ELSEVIER

Journal of Chromatography A, 706 (1995) 175–181

JOURNAL OF CHROMATOGRAPHY A

Determination of thorium and uranium in nitrophosphate fertilizer solution by ion chromatography

Abdulla W. Al-Shawi*, Roger Dahl

Norsk Hydro AS, Research Centre, N-3901 Porsgrunn, Norway

Abstract

Different phosphate rocks contain various concentrations of thorium and uranium and the range of these concentrations can be significant. Digestion of phosphate rocks with concentrated nitric acid in a fertilizer production process leads to the dissolution of these metals in the resulting nitrophosphate solution. A direct method with a total analysis time of 10 min is described for the determination of thorium and uranium in nitrophosphate fertilizer solution. The method is based on cation-exchange chromatography coupled with spectrophotometric postcolumn detection with Arsenazo III at 660 nm. Elution is performed with a gradient concentration of hydrochloric acid or nitric acid and ammonium sulphate, utilizing a strong cation-exchange analytical column to perform the separation.

1. Introduction

Thorium and uranium are present in phosphate rocks at concentrations that can vary widely in different rocks depending on the mining location. Table 1 illustrates the concentrations of thorium and uranium in various phosphate rocks.

Dynamic ion-interaction chromatography has been used as a powerful tool in the determination of thorium and uranium [2] and in the presence of rare earths and/or transition metals [3,4]. A C_{18} column is usually used to perform the separation [5], with elution using hydroxyisobutyric acid (HIBA) with or without a sodium *n*-octanesulphonate (OSA) coating as the ion-interacting reagent (IIR). Usually postcolumn spectrophotometric detection with Arsenazo III is applied. Detailed investigations on the retention behaviour of both cations have been carried out and it was concluded that a retention mechanism based on hydrophobic adsorption rather than cation exchange was operating [6,7].

Table 1
Typical concentrations of thorium and uranium in phosphate rocks [1].

Phosphate rock	Th (ppm)	U (ppm)
Kola, Russia	22	2.8
North Carolina, USA	5	90
Florida, USA	40	120
Western region, USA	–	660
Palabora rock, S. Africa	90	9
BouCraa, Morocco	4	60
Khourigba, Morocco	8	100
Senegalese, Africa	–	190
Togolese, Africa	220	85
Tunisian, Africa	–	90
Israeli, Middle East	23	106
Jordanian, Middle East	4	60

* Corresponding author.

0021-9673/95/$09.50
SSDI 0021-9673(95)00006-2

The ion interaction method of analysis offered excellent separations of the rare earths, thorium and uranium, where the anion ligand in the sample matrix is nitrate or chloride, but was less effective in the analysis of nitrophosphate fertilizer solutions. The main factor contributing to this decrease in efficiency was the phosphate ligand affinity for the thorium ion at the ion interaction method pH of ca. 4.0. In addition, the ion interaction method was unable to handle a large ratio of rare earths (RE) to thorium or uranium concentration. This ratio varies in the original phosphate rock used in the digestion stage of the fertilizer production process. A typical RE/Th and Re/U ratios are 350 and 2770, respectively. Moreover, the sample pH would have to be between 2.4 and 4.5 in order to achieve a quantitative recovery of both metals in the chromatographic run [8]. This pH range is unacceptable for samples containing phosphate and thorium owing to the very low solubility product values.

The determination of thorium and uranium by ion-exchange chromatography has also been reported, the elution of uranium being carried out first with hydrochloric acid, followed by thorium with the introduction of sulphate ligand. This method seems to involve an initial on-column removal of calcium ions, with uranium and thorium then being concentrated on the same column and subsequently injected separately. It also employs an analytical column which is no longer commercially available [9]. Moreover, another version of this method seems to have a different gradient programme, which was confusing [10].

The aim of this investigation was to develop a rapid and reliable method for the determination of thorium and uranium in nitrophosphate fertilizer solution. This investigation is connected with Norsk Hydro's continuous monitoring of the environmental aspects of nitrophosphate fertilizer production.

2. Theory

Uranium forms weaker cationic species than thorium with hydrochloric and nitric acids, in the form of UO_2Cl^+ and $UO_2NO_3^+$. When the chloride concentration of the eluent is increased, the concentration of the cationic species retained on the stationary phase decreases because the solution equilibrium is displaced to higher complex species [11]. In sulphuric acid media, uranium can form retainable complexes on a strong cation-exchange resin in the form of $[UO_2(HSO_4)]^+$. This hydrogensulphato complex of the uranyl ion cannot be formed from a neutral sulphate solution such as ammonium sulphate [12]. Uranium, in fact, is eluted very close to solvent front when the concentration of the sulphate ion is more than 0.1 *M* in the initial gradient programme.

The combination of high charge and low hydrolysis makes thorium ion particularly retainable on cation-exchange resins from HCl and HNO_3 at concentrations below about 1 *M*. Separations from other cations is thus facilitated, and trace amounts of thorium may be concentrated. Complexing agents such as citric acid, oxalic acid, hydrofluoric acid, carbonate and sulphate are necessary for its elution from the column [13]. This implies, that thorium forms weak cationic species with a sulphate ligand in the form of $ThSO_4^{2+}$ [9]. The retention times of thorium decrease with increasing concentration of sulphate ion in the initial gradient programme.

3. Experimental

3.1. Instrumentation

A Dionex (Sunnyvale, CA, USA) 4000i eluent pump system with a 0.05-ml injection loop, a Gilson (Villiers-le-Bel, France) Model 221 autosampler and a Spectra-Physics (Santa Clara, CA, USA) were used. Data handling was performed with a Multichrom system (VG Instruments, UK). The analytical column was a dionex IonPac CS10 with strong cation-exchange functionality.

The postcolumn reagent was introduced (0.7 ml/min) via a low-volume T-mixer with a helium-pressurized delivery system. The length of the reaction coil between the mixing tee and the detector was 10 cm.

3.2. Reagents

The eluent and standard and sample solutions were prepared with pretreated water obtained via ion exchange and double distillation, followed by passage through Milli-Q water-purification system (Millipore, Waters Chromatography Division, Oslo, Norway).

Hydrochloric acid (2 *M*) or nitric acid (2 *M*), ammonium sulphate solution (2 *M*) and water were the separate eluents required for the analysis. The detection reagent Arsenazo III was 0.3 m*M* in 0.5 *M* glacial acetic acid. Detection was carried out at 660 nm. A reagent flow-rate of 0.7 ml/min was maintained.

Standard solutions (1 mg/ml) of thorium and uranium were obtained from Teknolab (Drøbak, Norway).

3.3. Sample preparation

Nitrophosphate fertilizer solution samples were diluted with water and made 0.25 *M* in hydrochloric acid or 0.25 *M* in nitric acid to prevent the precipitation of thorium phosphate. Typical mother liquor samples were diluted 1:25 or 1:50 depending on the concentration of the analytes.

4. Results and discussion

It was understood that an ideal method for the determination of thorium and uranium in nitrophosphate fertilizer solution would involve the detection of both metals at a relatively high acidity range (0.25–1.0 *M*) in order to minimize the complication of thorium phosphate precipitation. Arsenazo III offers this advantage, and is capable of forming coloured complexes with thorium and uranium at acid concentrations between 0.01 and 10 *M* HCl. In this high acid concentration range, the interferences from other metals are minimal, except those of zirconium, hafnium and the rare earths [14].

Therefore, a cation-exchange method that took advantage of the detection power of Arsenazo III was developed. The method also relies on the mass distribution ratios of both metals between a strong cation-exchange polymer and strong minerals acids. The potential interference in the determination of thorium and uranium in a nitrophosphate fertilizer solution arises from calcium, iron and, in some instances, rare earths, depending on the origin of the phosphate rock. The method developed can be applied with two different elution systems, as follows.

4.1. HCl–$(NH_4)_2SO_4$ system

The mass distribution ratios for thorium, uranium and other potential interfering metals at different HCl concentrations are given in Table 2. Table 2 implies that an initial elution with HCl would separate uranium from thorium and would resolve uranium from calcium and iron(III). When the uranium ion has been totally eluted, the thorium ion can be eluted by the introduction of a sulphate ligand, as thorium has a much lower mass distribution ratio with sulphate [16].

Fig. 1 illustrates the selectivity of thorium and uranium for two different ligand systems. As seen from Table 2, thorium has a strong affinity for the sulphonated stationary phase when elution is carried out with 0.4 *M* HCl, while uranium has a much weaker affinity for the same stationary phase. Thorium, however, would lose this strong affinity when the sulphate ligand was introduced and therefore was eluted after the uranium ion.

Linear calibration graphs were obtained for

Table 2
Distribution ratio of metal ions between strong cation-exchange resin polymer and hydrochloric acid [15]

Cation	Concentration (*M*)			
	0.1	0.2	0.5	1.0
UO_2^{2+}	5420	860	102	19.2
ZrO^{2+}	$>10^5$	$>10^5$	10^5	7250
Th^{4+}	$>10^5$	$>10^5$	10^5	2049
La^{3+}–Y^{3+}	$>10^5$	10^5	2480–1460	264–144
Ca^{2+}	3200	790	151	42.29
Fe^{3+}	9000	4300	225	35.45

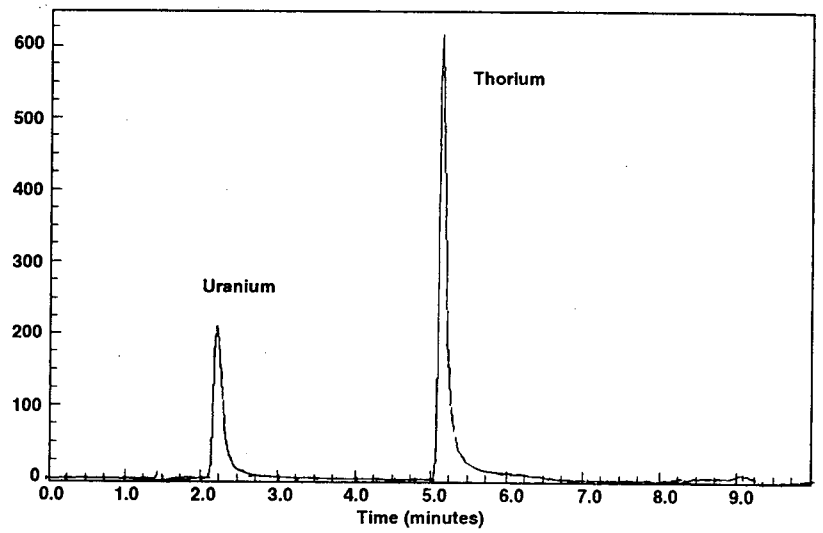

Fig. 1. Chromatogram of standard solution of thorium and uranium. Chromatographic conditions: Analytical column Ion Pac CS10. (Dionex Cop.). From 0.4 *M* HCl, 0.1 *M* $(NH_4)_2SO_4$ to 0.4 *M* HCl, 1 *M* $(NH_4)_2SO_4$ in 5 min; 2 ppm of each thorium and uranium; 0.05 ml injection volume; 0.1 μVs (10 ↑ 4) intensity. Eluent flow-rate 1 ml/min. Detection with Arsenazo III 0.2 m*M* in 0.5 *M* acetic acid at a flow-rate of 0.7 ml/min.

thorium and uranium in the concentration range 0.2–2.0 mg/l. The relative standard deviation with multiple injections ($n = 10$) was calculated and found to be ca. 1% for uranium and 1.5% for thorium. These repeatability experiments were conducted on samples with uranium and thorium concentrations more than ten times the detection limits. Detection limits at three times the baseline noise for a 0.05-ml injection volume were 0.02 mg/l for uranium and 0.005 mg/l for thorium.

Two different mother liquor solutions [17] obtained directly from a fertilizer production line were investigated in detail. These solutions differed in the origin of the phosphate rock, namely 100% Kola from Russia and 100% BouCraa from Morocco. Fig. 2 shows the chromatograms of each mother liquor solution investigated.

The proposed method gave an excellent separation of calcium ion from uranium ion in the initial part of the analysis, which enabled the direct analytical procedure to be applied and made sample preconcentration and prior calcium removal unnecessary.

4.2. HNO_3–$(NH_4)_2SO_4$ system

Similar chromatograms were obtained from the substitution of the initial HCl with HNO_3, as the mass distribution ratio in nitric acid medium is comparable to that in hydrochloric acid (Table 3). The application of this elution system on the same production line samples gave similar chromatograms (Fig. 3).

To demonstrate the accuracy of the method, two international standard samples, viz., different phosphate rocks obtained from different locations in the USA, were analysed and the results for uranium and thorium were compared. These standard samples were digested in hot concentrated nitric acid and analysed using the HNO_3–$(NH_4)_2SO_4$ elution system. Moreover, the analytical data obtained from this method were compared with data obtained by inductively coupled plasma mass spectrometry (ICP-MS). It can be seen from Table 4 that the results are in good agreement. The slightly lower results for thorium in the Western rock standard material may be due to incomplete dissolution of the

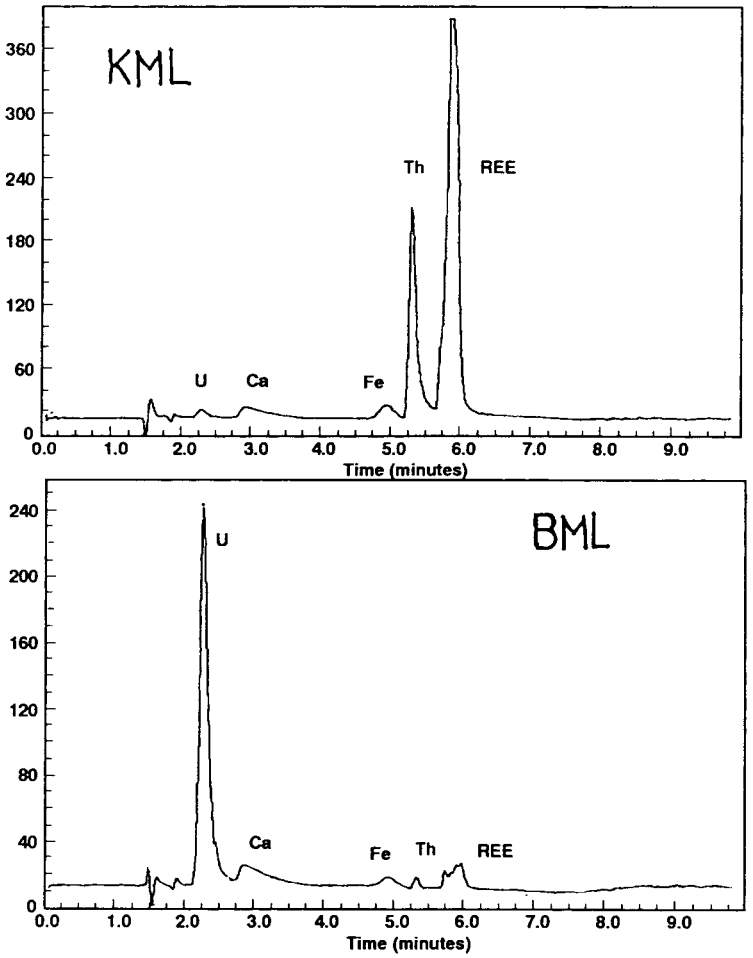

Fig. 2. Chromatograms of two different fertilizer solutions from production lines. KML = Kola Motherliquor, BML = BouCraa Motherliquor. Chromatographic conditions: 1/25 dilution factor with 0.25 *M* HCl; Other conditions as in Fig. 1.

Table 3
Mass distribution ratio of cations between strong cation-exchange polymer and nitric acid [18]

Cation	Concentration (*M*)			
	0.1	0.2	0.5	1.0
ZrO^{2+}	$>10^4$	$>10^4$	$>10^4$	6500
Th^{4+}	$>10^4$	$>10^4$	$>10^4$	1180
$(Rare\ earths)^{3+}$	$>10^4$	$>10^4$	1870–1000	267–167
Ca^{2+}	1450	480	113	35.3
Fe^{3+}	>10	4100	362	74
UO_2^{2+}	659	262	69	24.4

apatite in hot nitric acid, owing to the presence of thorium fluoride, which is difficult to digest.

The ion chromatographic method offers accurate analytical results and a simple sample preparation procedure compared with other instrumental methods.

5. Conclusion

Thorium and uranium can be determined directly and accurately in nitrophosphate sam-

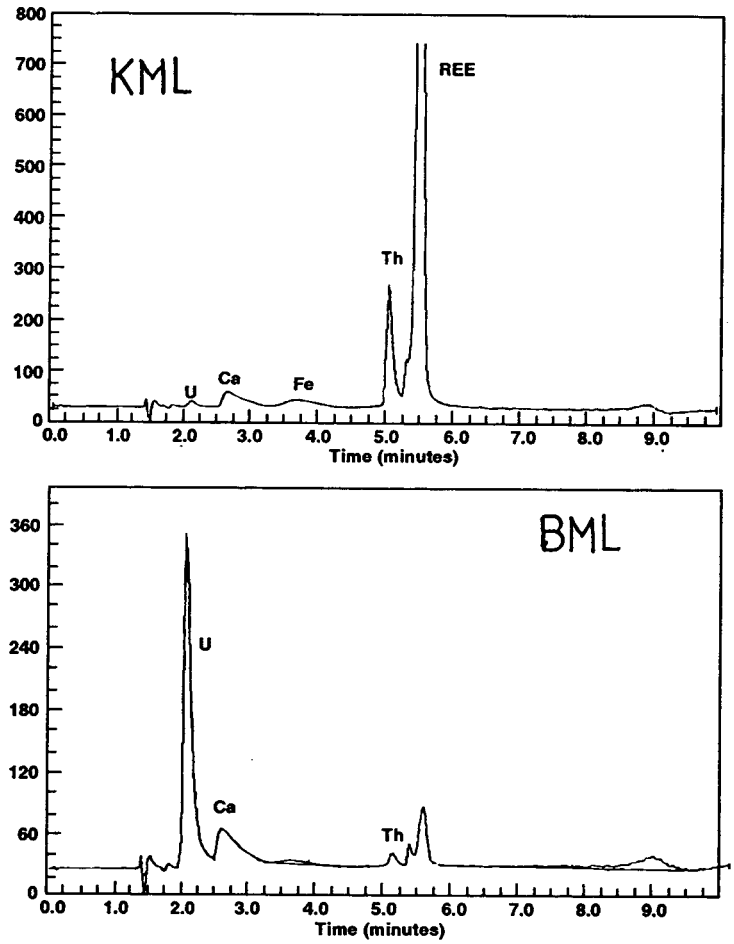

Fig. 3. Chromatograms of two different fertilizer solutions from production line. KML = Kola Motherliquor, BML = BouCraa Motherliquor. Chromatographic conditions: from 0.25 *M* HNO_3, 0.1 *M* $(NH_4)_2SO_4$ to 0.25 *M* HNO_3, 1 *M* $(NH_4)_2SO_4$ in 5 min. 1/25 dilution factor with 0.25 *M* HNO_3. Other conditions as in Fig. 1.

Table 4
Uranium and thorium concentrations in international standard materials

Standard material	Certified values	Found values	
		IC	ICP-MS
Florida rock 120b	U, 114.48 ppm	U, 113.8 ppm	
	Th, unavailable	Th, 9.2 ppm	
Western rock 694 NB	U, 141.4 ppm	U, 135.7 ppm	
	Th, unavailable	Th, 3.9 ppm	
Kola fertilizer solution		U, 2.44 mg/l	U, 2.57 mg/l
		Th, 17.1 mg/l	Th, 16.5 mg/l
BouCraa fertilizer solution		U, 74.6 mg/l	U, 73.5 mg/l
		Th, 0.84 mg/l	Th, 0.81 mg/l

ples obtained from a fertilizer process production line. Analysis can be carried out without sample preconcentration or calcium ion removal prior to the analytical procedure. The two different elution systems were described that resulted in similar chromatograms. The method takes advantage of the complexing power of Arsenazo III at high acidity and of the difference in selectivity of thorium and uranium ions with different ligand systems.

References

[1] G. Kongshaug, O.C. Bøckman, O. Kaarstad and H. Morka, presented at the *International Symposium for Chemical Climatology and Geomedical Problems, 21–22 May 1992, Oslo, Norway*.
[2] R.M. Cassidy and M. Frarer, *Chromatographia*, 18 (1984) 370.
[3] C.A. Lucy, L. Gureli and S. Elchuk, *Anal. Chem.*, 65 (1993) 3320.
[4] C.H. Knight, R.M. Cassidy, B.M. Recoskie and L.W. Green, *Anal. Chem.*, 56 (1984) 474.
[5] D. Barkley, L.A. Bennett, J.R. Charbonneau and L.A. Pokrajac, *J. Chromatogr.*, 606 (1992) 195.
[6] P.E. Jackson, J. Carnevale, H. Fuping and P.R. Haddad, *J. Chromatogr. A*, 671 (1994) 181.
[7] H. Fuping, P.R. Haddad, P.E. Jackson and J. Carnevale, *J. Chromatogr.*, 640 (1993) 187.
[8] D.J. Barkley, M. Blanchette, R.M. Cassidy and S. Elchuk, *Anal. Chem.*, 58 (1986) 2222.
[9] M.P. Harrold, A. Siriraks and J. Riviello, *J. Chromatogr.*, 602 (1992) 119.
[10] *Application Note 79*, Dionex, Sunnyvale, CA, 1992.
[11] F.T. Bunus, *J. Inorg. Nucl. Chem.*, 36 (1974) 917.
[12] C. Heitner-Wirguin and M. Gantz, *J. Inorg. Nucl. Chem.*, 35 (1973) 3341.
[13] J. Korkisch and F. Tera, *Anal. Chem.*, 33 (1961) 1264.
[14] S.B. Savvin, *Talanta*, 8 (1961) 673.
[15] F.W.E. Strelow, *Anal. Chem.*, 32 (1960) 1185.
[16] K. Kawabuchi, T. Ito and R. Kuroda, *J. Chromatogr.*, 39 (1969) 61.
[17] A.W. Al-Shawi and R. Dahl, *J. Chromatogr. A*, 671 (1994) 173.
[18] F.W.E. Strelow, R. Rethemeyer and C.J.C. Bothma, *Anal. Chem.*, 37 (1965) 106.

ELSEVIER

Journal of Chromatography A, 706 (1995) 183–189

JOURNAL OF CHROMATOGRAPHY A

Determination of anions in human and animal tear fluid and blood serum by ion chromatography

R. Salas-Auvert[a,*], J. Colmenarez[a], H. de Ledo M[b], M. Colina[b], E. Gutierrez[b], A. Bravo[a], L. Soto[a], S. Azuero[a]

[a]*Laboratorio de Ecología Microbiana y Biotecnología, Universidad del Zulia, Facultad de Ciencias, P.O. Box 526, Maracaibo, Venezuela*

[b]*Laboratorio de Química Ambiental, Universidad del Zulia, Facultad de Ciencias, P.O. Box 526, Maracaibo, Venezuela*

Abstract

An important factor contributing to the development of ion chromatography (IC) has been the need for repetitive analyses of samples with high ionic contents and samples available in microvolumes. IC was selected for the determination of Cl^-, NO_3^-, SO_4^{2-} and PO_4^{3-} anions in tear fluid and serum from ten human volunteers of both sexes, seven young-adult black vultures (*Coragyps atratus*) and three young-adult chickens (*Gallus gallus domesticus*). The samples were analysed on a Dionex Model 2000i/SP ion-exchange chromatograph equipped with an anion guard column (*Dionex* IonPac AG4A), anion separator column (*Dionex* IonPac AS4A), suppressor column (*Dionex* AMMS-II) and a conductivity detector. The flow-rate of the mobile phase, 1.7 m*M* $NaHCO_3$–1.8 m*M* Na_2CO_3 was set at 2.0 ml/min. The R.S.D. was calculated to be less than 1.5% for all anions. In the human, black vulture and chicken serum samples, the NO_3^-, PO_4^{3-} and SO_4^{2-} anion contents were higher than in tears; for Cl^- the reverse was found. No correlation was found amongst the anion concentrations present in the tear fluid and blood serum in all samples ($p > 0.05$). With no sample treatment, column maintenance was required.

1. Introduction

Chemical equilibrium in the animal body is achieved through fluid, electrolyte and acid–base balance, all responsible for its dynamic condition. Extracellular fluids are continuously mixed by the circulatory system and fluid interchange takes place between capillaries and interstitial space. This chemical exchange reflect the normal volume, distribution, composition and pH of body fluids. These fluids constitute both the external and internal environments of the cell, serving various important functions. They are composed of water and numerous solutes, comprising electrolytes and non-electrolytes.

Fluid and electrolytes contained in the intracellular and extracellular space have distinct electrolyte patterns. In the intracellular fluid [1], potassium is the major cation and phosphate and proteins are the major anions. In the extracellular fluid, sodium is the major cation and chloride the major anion. An important difference amongst the components in the intravascular and interstitial fluid is the greater concentration of negatively charged proteins in the intravascular fluid. Blood serum serves as an essential electrolyte source for other body fluids, reflecting its general composition in all extracellular fluids.

* Corresponding author.

0021-9673/95/$09.50
SSDI 0021-9673(95)00083-6

As body fluids are regulated by the same mechanism, balance disruption in one of the compartments induces a corresponding alteration in the electrolyte concentration in other body spaces and fluids, including serum and lachrymal secretions [2]. Tear fluid may serve as a biological source of reference electrolyte levels, when available. The ionic content of lachrymal fluid, amongst other elements, is significantly responsible for tear osmolarity. The cornea, conjunctiva and the integrity of other ocular tissues depend on this biological lubricant. Additionally, a number of tear constituents bear a relationship to elements present in blood serum. Its composition includes proteins, lipids, metabolites, ions and excretable drugs [3]. Potassium, sodium and chloride ions have been reported to be present in higher concentrations than in plasma. No studies on the anion content of tear fluid could be found in the literature. The average tear pH is 7.35 and the osmolarity of tear films varies between 295 and 309 mOsm/l [4].

In plasma, the chloride concentration has been reported to be between 97 and 103 mmol/l [5] and in tear fluid between 100 and 138 mmol/l [6–8]. The levels of phosphorus and calcium are internally related as both metabolisms are regulated by the same mechanisms.

Higher animals, such as bovines, may utilize ammonia as a nitrogen source for the synthesis of non-essential amino acids, but are unable to use nitrate [9], nitrite or gaseous nitrogen. The presence of nitrate in serum and tear fluid may be considered as an indicator of blood urea-nitrogen linked to homeostatic balance [10].

The sulfate anion present in plasma, tears and other body fluids may be difficult to associate with particular metabolic functions or homeostatic balance. Its presence may be related to sulfur amino acids and their metabolic pathway.

Vultures exhibit particular feeding habits where severe chemical and biological contamination may be present, without apparently affecting their overall healthy status. Eye involvement during their feeding process does not result in the development of ocular diseases. Lachrymal secretion may play an important role in a non-specific protective mechanism and amongst the tear constituents, the anion content has not been reported.

The study of certain serum cations by ion chromatography (IC) [11] and capillary zone electrophoresis [12] has been reported. In this work, the basal chloride, nitrate, phosphate and sulfate anion contents in tears and serum samples from humans, black vultures and chickens were determined by IC. The values obtained were analysed and general relationships were determined. Chickens were included in this study to establish comparable anion values in samples from a well documented source.

2. Experimental

2.1. Sample collection

Tears

Tear samples were obtained from the lower parpebral sac and internal canthus of seven adult black vultures (*Coragyps atratus*) with an average mass of 1.5 kg ± 300 g. Tear samples from individual specimens ranged from 10 to 100 μl and were pooled until a working volume of at least 150 μl was obtained. A similar procedure was applied for the collection of the human and chicken samples. The black vulture specimens were captured in a nearby rural area (Palmarejo, Estado Zulia, Venezuela) between June 1993 and February 1994. For comparison purposes, three domestic chickens (*Gallus gallus domesticus*) were included in the study, with an average mass of 2.15 kg ± 200 g. The specimens were acquired locally.

Ten human adults (five males and five females, all volunteers) participated in the investigation. Their mean age was 20 ± 3 years. Tear samples were collected as indicated previously.

Tear volumes of up to 150 μl per individual (animal and human) were collected with a blood dilution pipette (Thomas Type, 120 mm). Prior to use, the pipettes were washed with non-ionic soap and rinsed with doubly distilled water, 95% (v/v) ethanol, acetone, distilled water and finally deionized water.

Serum

Blood samples were obtained from the brachial or marginal wing vein of seven healthy adult black vultures and three healthy chickens, using a venous infusion set with a 22 XG needle. A maximum of 2.0 ml of whole blood was collected from each bird and dispensed into glass test-tubes. Each sample was allowed to coagulate for 20 min at room temperature and was then centrifuged in a Hettich Model EBA 35 centrifuge at 2000 rpm for 20 min. The serum aliquots were kept refrigerated at 4°C until needed. The serum samples were processed within ten consecutive days.

Human blood samples were obtained by venipuncture of the anticubital vein from healthy young adult volunteers (five males and five females) aged 20 ± 3 years. Whole blood was collected with a 6-ml syringe, coupled to a 22 XG needle. The volume collected ranged from 4 to 5 ml. The serum was processed as indicated previously.

2.2. Sample preparation

Tears

During collection, tear aliquots were maintained at 4°C and they were subsequently refrigerated at −70°C in 1.5-ml Eppendorff capped vials until processed. Prior to analysis, the samples were allowed to thaw and maintained under refrigeration at 4°C. Then they were centrifuged at 13500 rpm for 10 min in an Eppendorff Model 5412 centrifuge. The samples were diluted 100-fold in deionized water and filtered immediately before chromatography.

Serum

Serum samples were allowed to reach room temperature (28°C), before analysis. A 100-fold dilution was prepared with deionized water and filtered before chromatography.

2.3. Reagents, apparatus and conditions

Reagents

All reagents were filtered at least twice through a 0.22-μm Millipore membrane filter and were of the highest purity. Deionized water was used for dilution. Calibration standards were prepared by serial dilutions of stock solutions containing 28.2 mmol/l Cl^-, 71.4 mmol/l N-NO_3^-, 32.3 mmol/l P-PO_4^{3-} and 10.4 mmol/l SO_4^{2-}.

Apparatus

Samples were analysed on a Dionex Model 2000i/SP ion chromatograph equipped with a (Dionex AG4A) anionic pre-column, a (Dionex AS4A) anionic column separator, a (Dionex AMMs-II) suppressor column, a Dionex Conductivity Detector II CDM conductivity detector and a (Dionex 4400) integrator.

Chromatographic conditions

Standards and samples were membrane filtered before injection into the chromatograph. The analytical run time was 10 min, which allowed resolution of the peaks. External standardization was used, with recalibration following every ten samples and column washing with deionized water. Tetrabutylammonium hydroxide was used occasionally to prevent column poisoning. The mobile phase (flow-rate 2.0 ml/min) was 1.7 m*M* $NaHCO_3$–1.8 m*M* Na_2CO_3 and the regenerating solution was 12.5 m*M* H_2SO_4. The injection volume, conductivity sensitivity and chart speed were 100 μl, 30 μs and 0.5 cm/s, respectively. The integrator attenuation range was from 0.5 to 4096.

3. Results and discussion

3.1. Ion chromatography

Typical human, vulture and chicken serum anion chromatograms are illustrated in Fig. 1. The corresponding tear chromatograms are represented in Fig. 2. The detection limits were $Cl^- = 2.7$ μg/l, $NO_3^- = 5.6$ μg/l, $PO_4^{3-} = 5.0$ μg/l and $SO_4^{2-} = 3.318$ μg/l. The R.S.D. for all anions was less than 1.5% ($n = 18$).

IC has previously been compared with potentiometric methods in a reference laboratory

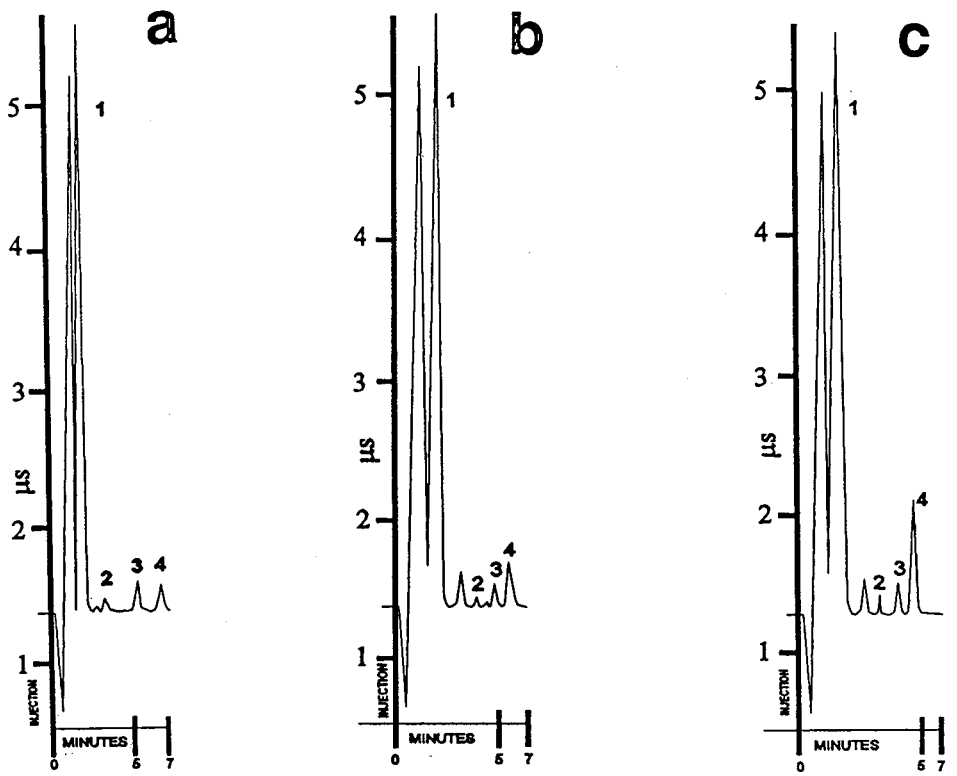

Fig. 1. (a) Chromatogram of human serum sample. Peaks: 1 = Cl^- (44.86 mmol/l); 2 = NO_3^- (0.17 mmol/l); 3 = PO_4^{3-} (2.04 mmol/l); 4 = SO_4^{2-} (0.54 mmol/l). Chart range: 65 μs FS. (b) Chromatogram of black vulture serum sample. Peaks: 1 = Cl^- (42.96 mmol/l); 2 = NO_3^- (0.40 mmol/l); 3 = PO_4^{2-} (1.37 mmol/l); 4 = SO_4^2 (0.66 mmol/l). Chart range: 65 μs FS. (c) Chromatogram of chicken serum sample. Peaks: 1 = Cl^- (40.35 mmol/l); 2 = NO_3^- (0.20 mmol/l); 3 = PO_4^{3-} (1.88 mmol/l); 4 = SO_4^{2-} (2.00 mmol/l). Chart range: 65 μs FS.

using an ion-selective electrode [13]. The results obtained in that study were in good agreement with those obtained by IC.

3.2. Mean anion concentrations in human serum and tear samples

The mean nitrate (0.14 mmol/l), phosphate (0.22 mmol/l) and sulfate (0.39 mmol/l) anion concentrations obtained were 26, 85 and 26% lower, respectively, in the human tear samples than in serum (0.19, 1.42 and 0.53 mmol/l, respectively). The opposite effect was observed for chloride ion (Tables 1 and 2). The high levels of chloride ion in the tear fluid, with a maximum value of 104.81 mmol/l, were in agreement with the mean reported concentration of 100 mmol/l [14].

3.3. Mean anion concentrations in vulture serum and tear samples

Nitrate (0.29 mmol/l), phosphate (1.27 mmol/l) and sulfate (0.75 mmol/l) concentrations determined in black vulture serum (Table 1) were 62, 9 and 11%, higher, respectively, than in tear samples (Table 2). The overall mean chloride ion concentration determined in the tear samples (82.59 mmol/l) was 47% higher than in serum (43.71 mmol/l). This chloride concentration pattern was constant throughout the values obtained, from all samples studied except for chicken.

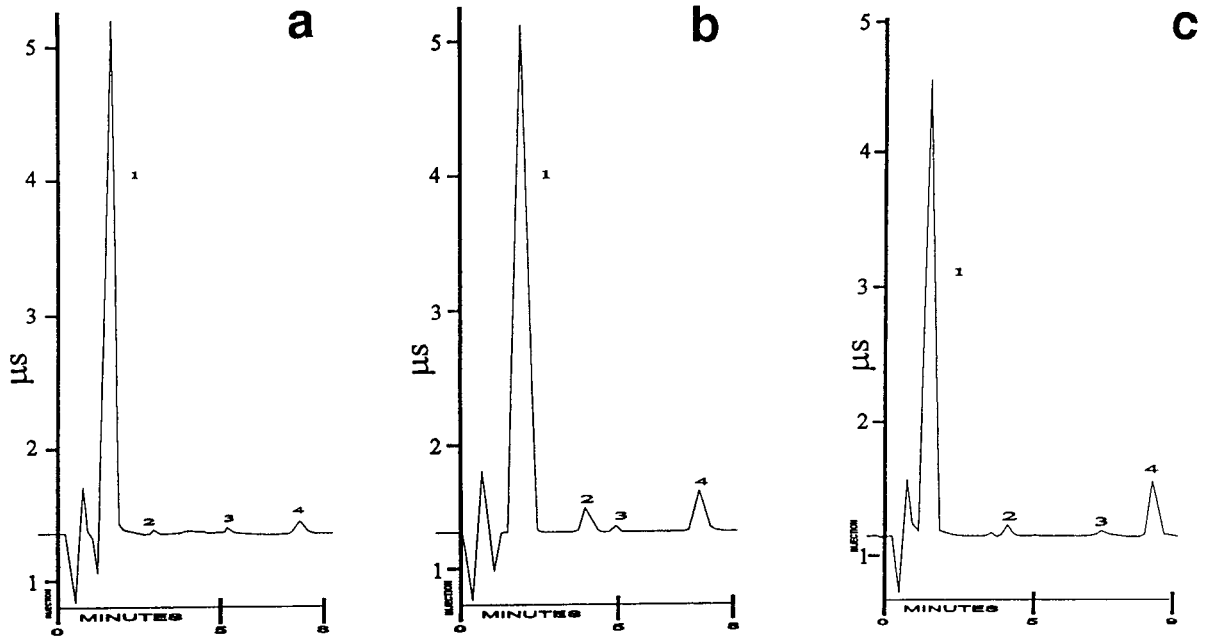

Fig. 2. (a) Chromatogram of human tear sample. Peaks: 1 = Cl^- (104.81 mmol/l); 2 = NO_3^- (0.13 mmol/l); 3 = PO_4^{3-} (0.52 mmol/l); 4 = SO_4^{2-} (0.17 mmol/l). Chart range: 65 µs FS. (b) Chromatogram of black vulture tear sample. Peaks: 1 = Cl^- (107.01 mmol/l); 2 = NO_3^- (0.16 mmol/l); 3 = PO_4^{3-} (0.84 mmol/l); 4 = SO_4^{2-} (0.45 mmol/l). Chart range: 65 µs FS. (c) Chromatogram of chicken tear sample. Peaks: 1 = Cl^- (186.30 mmol/l); 2 = NO_3^- (0.67 mmol/l); 3 = PO_4^{3-} (1.08 mmol/l); 4 = SO_4^{2-} (3.15 mmol/l). Chart range: 65 µs FS.

3.4. Mean anion concentrations in chicken serum and tear samples

Nitrate (0.20 mmol/l), phosphate (1.88 mmol/l) and sulfate (2.00 mmol/l) concentrations determined in chicken serum (Table 1) were 41, 2 and 61% lower, respectively, than in tear samples (Table 2). The overall mean chloride ion concentration determined in the tear samples (33.69 mmol/l) was 17% lower than in serum

Table 1
Comparative anion concentrations (mmol/l) present in human, black vulture and chicken serum samples

Anion	N	Nature	Mean ± S.D.	Maximum value	Minimum value
Cl^-	10	Human	37.75 × 6.20	47.48	25.53
	7	Vulture	43.71 ± 4.27	50.16	35.07
	3	Chicken	40.35 ± 2.61	42.57	36.62
NO_3^-	10	Human	0.19 ± 0.07	0.29	0.11
	7	Vulture	0.29 ± 0.16	0.45	0.00
	3	Chicken	0.20 ± 0.02	0.21	0.16
PO_4^{3-}	10	Human	1.42 ± 0.46	2.27	0.63
	7	Vulture	1.27 ± 0.36	1.84	0.49
	3	Chicken	1.88 ± 0.25	2.20	1.50
SO_4^{2-}	10	Human	0.53 ± 0.16	0.78	0.14
	7	Vulture	0.75 ± 0.38	1.39	0.21
	3	Chicken	2.00 ± 0.28	2.18	1.89

Table 2
Comparative anion concentrations (mmol/l) present in human, black vulture and chicken lachrymal secretion samples

Anion	N	Nature	Mean ± S.D.	Maximum value	Minimum value
Cl^-	10	Human	68.71 ± 17.93	104.81	50.22
	7	Vulture	82.59 ± 19.85	108.76	55.45
	3	Chicken	33.69 ± 2.91	37.91	30.35
NO_3^-	10	Human	0.14 ± 0.13	0.40	0.01
	7	Vulture	0.11 ± 0.08	0.27	0.00
	3	Chicken	0.34 ± 0.09	0.45	0.19
PO_4^{3-}	10	Human	0.22 ± 0.37	1.17	ND[a]
	7	Vulture	1.15 ± 0.61	2.72	0.77
	3	Chicken	1.91 ± 0.76	2.63	0.71
SO_4^{2-}	10	Human	0.39 ± 0.30	1.18	0.06
	7	Vulture	0.67 ± 0.41	1.37	0.25
	3	Chicken	0.79 ± 0.32	1.07	0.36

[a]Not detectable.

(40.35 mmol/l). This chloride concentration value pattern was the opposite to that for the other samples studied.

3.5. Comparative anion concentrations among human, vulture and chicken serum samples

Vulture blood serum chloride (43.71 mmol/l) and nitrate (0.29 mmol/l) concentrations were 14 and 34% higher, respectively, than the human values and 8 and 31% higher, respectively, than the chicken values. Direct comparison of mean phosphate concentrations in the chicken serum samples yielded a 24% higher value than the human value and 32% higher than the vulture value (Table 1). The sulfate anion concentration in chicken serum (2.00 mmol/l) was 63% than that in vulture serum and 74% higher than that in human serum.

3.6. Comparative anion concentrations among human, vulture and chicken tear samples

The mean chloride content determined in the vulture tear samples (82.59 mmol/l) was 17% higher than the human value (68.71 mmol/l) and 59% higher than the chicken value. Nitrate (0.34 mmol/l) and phosphate (1.91 mmol/l) values in the chicken sample were 59 and 90% higher, respectively, than the human values and 68 and 40% higher, respectively, than the vulture values (Table 2). Comparative analysis of sulfate mean values among the tear samples analysed yielded differences of 51% (0.79 mmol/l) higher for chicken than for human (0.39 mmol/l) and 15% higher than for vulture (0.67 mmol/l).

3.7. Correlations

No correlation was found ($p > 0.05$) amongst the anion concentrations present in the tear fluid and those in blood serum for all the samples analysed under the present conditions. The chloride and nitrite values in vulture samples were higher than in the other samples analysed. The chicken phosphate and sulfate values were higher than those in the other samples studied. High chloride levels present in human serum corresponded to high levels of phosphate ($r = 0.795$; $p < 0.01$) and high concentrations of nitrate corresponded to high contents of sulfate ($r = 0.726$; $p < 0.05$). No correlation was obtained amongst the individual values obtained for human, vulture and chicken tear fluid and serum ($p > 0.05$). It must be stated that the anion contents of the samples analysed in this investigation are pertinent to the population studied. Further generalization of these data should include a larger population sample and particular pathophysiological variables if reference concentrations are to be considered. The higher chloride anion concentration obtained in all the tear

samples studied than in serum samples may be due to its relevant function in maintaining tear osmolarity.

4. Conclusions

Ion chromatography was used for the quantitative study of the anion contents of two important biological extracellular fluids in humans and birds. Analysis of the data obtained indicate a high level of all anions studied in the bird specimens when compared with the human values. The chloride content considerably higher in tear fluid than in serum for all samples. For all samples, no correlation was found amongst anion concentrations present in the tear fluid and in serum samples. High chloride contents present in human serum corresponded to high levels of phosphate and high concentrations of nitrate corresponded to high levels of sulfate. No correlation was obtained amongst the studied ions in human and vulture tear fluid.

Ion chromatography is a relatively simple and reproducible procedure allowing repetitive ion analyses of large numbers of samples. Ion concentrations in biological samples, available only in critical volumes, can be readily studied. Column washing was required after repetitive substance analyses. Sample membrane filtration was a critical factor for keeping column fouling to the minimum.

References

[1] E. Goldberg, *A Primer of Water, Electrolyte and Acid Base Syndrome*, Lea and Febiger, Philadelphia, 4th ed., 1970, p. 256.
[2] M.G. Reed and V.F. Sheppard, *Regulation of Fluid and Electrolyte Balance*, W.B. Saunders, Philadelphia, 1977, pp. 9–11.
[3] B. Weil and B. Milder, *Sistema Lagrimal*, Editorial Médica Panamericana, Buenos Aires, 3rd ed., 1985, p. 178.
[4] J.E. Terry and R.M. Hill, *Arch. Ophthalmol.*, 96 (1978) 120.
[5] D. Rose, *Clinical Physiology of Acid–Base and Electrolyte Disorders*, McGraw-Hill, New York, 1977, p. 154.
[6] G.E. Lowther, R.B. Miller and R.M. Hill, *Am. J. Ophthalmol.*, 47 (1970) 266.
[7] P.D. Schmidt, P. Schoessler and R.M. Hill, *Am. J. Ophthalmol.*, 51 (1974) 84.
[8] J.H. Thaysen and N.A. Thorn, *Am. J. Physiol.*, 178 (1954) 160.
[9] A. Meister, *Biochemistry of the Amino Acids*, Vols. I and II, Academic Press, New York, 5th ed., 1993, p. 203.
[10] F. Llach, *Drug Ther. Bull.*, 3, No. 2 (1978) 25.
[11] C. Sarzanini, E. Metnasi and M. Nerva, *J. Chromatogr. A* 671 (1994) 259.
[12] W. Buchberger, K. Winna and M. Turner, *J. Chromatogr. A* 671 (1994), 375.
[13] H. Ledo, J. Morales and M. Colina, presented at the *14th International Ion Chromatography Symposium*, 1993.
[14] F.J. Holly and M.A. Lemp, *Surv. Ophthalmol.*, 22 (1977) 69.

ELSEVIER

Journal of Chromatography A, 706 (1995) 191–198

JOURNAL OF CHROMATOGRAPHY A

Determinations of trace anions in hydrogen peroxide

Jutta Kerth, Detlef Jensen*

Dionex GmbH, Am Wörtzgarten 10, 65510 Idstein, Germany

Abstract

Hydrogen peroxide plays an important role in the semiconductor industry and needs to be analyzed for anionic impurities. In the past, the sample was pretreated with Pt to avoid reactions of H_2O_2 with the resin material of the respective anion exchanger. However, this pretreatment with Pt is time-consuming, may cause contaminations and leads to degradation of stabilizers because of the heat generated during the treatment. An ion chromatographic technique has been developed allowing the direct injection of the sample. Within this paper chromatograms of different types of H_2O_2 were analyzed, the observed method detection limits and the reproducibility of this method are shown.

1. Introduction

Hydrogen peroxide is a chemical having a variety of uses. One of its common applications is the use as a reactant in the synthesis of inorganic and organic peroxides, such as perborates, percarbonates and peroxoacetic acid. Furthermore, H_2O_2 is used during the formation of softening compounds in polymers by the epoxidation of oils, fatty acids and for the technical production of diphenols and hydrazine [1]. It is used for bleaching of cellulose, paper, natural and synthetic fibres, and a variety of other materials, e.g. oils, waxes, starch, sulfuric acid, feathers, furs, sponges, etc. In the treatment of waste water, hydrogen peroxide plays an important role in the removal of cyanide, phenols and sulfur compounds. It can also be used for the desodoration of waste water and sludges by oxidation of H_2S. It can be applied as an antiseptic for medical purposes, for the disinfection of surfaces, and for the sterilisation of food packaging [2].

Since hydrogen peroxide is one of the most important chemicals for etching and cleaning processes in the semiconductor industry, the interest in an automated determination technique is increasing [3]. Since ionic impurities may cause defects and malfunction of the final micro chips, H_2O_2 has to be analyzed for ions. Due to the special purity requirements (e.g. anion concentrations in the low μg/l range) it is necessary to eliminate sources for contamination during the sample preparation and the subsequent analytical determination. For hydrogen peroxide samples, it is known that repeated injections of solutions containing higher concentrations of H_2O_2 than 3% can irreversibly degrade the analytical anion exchanger column used for ion chromatographic determinations [4,5]. The high eluent pH (>10) seems to support the oxidation reactions of hydrogen peroxide with the resin due to the formation of the peroxohydroxide anion (HO_2^-) [2,6].

0021-9673/95/$09.50
SSDI 0021-9673(94)01277-6

The most commonly applied sample preparation for H_2O_2 solutions is treatment with metals such as Pt to decompose hydrogen peroxide catalytically to H_2O and O_2 [7]. This pretreatment, however, is time-consuming, may cause contaminations and leads to the degradation of stabilizers because of the heat generated during the treatment.

We have developed an ion chromatographic (IC) technique allowing the direct injection of hydrogen peroxide samples. This technique includes an on-line matrix elimination and an enrichment step followed by an analytical separation. Due to the commonly used industrial formation process of hydrogen peroxide (autoxidation of anthrahydrochinone, extraction with organic solvents, distillation, etc.) mono- and divalent organic acids are present in the final product [7]. Therefore, a gradient elution is appropriate for the separation of the inorganic ions from these organic acids.

This paper presents the analysis of different types of H_2O_2, the observed method detection limits (MDLs) and the reproducibility.

2. Experimental

2.1. Apparatus

All experiments were carried out with a DX-300 IC system (Dionex, Sunnyvale, CA, USA) consisting of a quaternary gradient pump (AGP), a chromatographic module and a conductivity detector. Eluents were degassed by purging them with helium using the eluent degas module. The DX-300 system was modified as shown in Fig. 1. An additional inert double stack four-way slider valve (5000 p.s.i.; 1 p.s.i. = 6894.76 Pa) was placed between a rotary injection valve (Rheodyne 9126) and the analytical column. Both valves were controlled by controls 5 and 6 on the AGP. Separations were performed on an IonPac AS11 anion exchanger. The respective guard column (IonPac AG11) was used as a concentrator column. Conductivity detection was carried out using an anion self-regenerating suppressor (ASRS-1) in the recycle mode. To remove anionic contaminants from the eluent an anion trap column (ATC-1, Dionex)

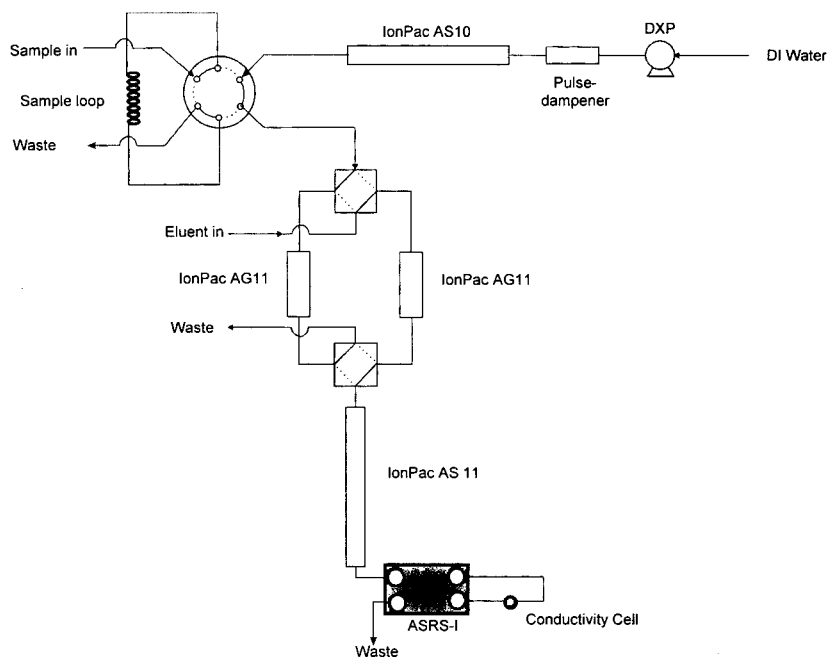

Fig. 1. Schematic flow diagram of the IC system used for the determination of anions in hydrogen peroxide. For experimental details see Table 1. DI = Deionized.

was placed in line with the gradient pump and the concentrator column. An external pump (DXP, Dionex) was used for sample delivery to the concentrator column via the injection valve, and for the subsequent rinsing step with water. The DXP flow-rate was set to 1.5 ml/min. In order to remove anionic traces from the water used, an additional column (IonPac AS10) was placed between the DXP and the metal free injection device. Instrument control, data collection and processing were performed with a chromatographic data system (AI-450, Dionex).

2.2. Reagents

Deionized water (18 MΩ cm resistivity at 25°C, used for eluent preparation) was obtained from a water-purification system (Seral, Ransbach-Baumbach, Germany). Sodium hydroxide (50%) was purchased from Baker (Gross Gerau, Germany).

Diluted working standards of all anions under investigation were prepared freshly from 1000 mg/l stock solutions. All stock solutions were stored in polyethylene containers, the working standards were prepared in polypropylene flasks.

2.3. System preparation

After installation of the IC system all parts including DXP and IonPac AS10 column were rinsed with 200 m*M* NaOH for about 12 h. During this cleaning procedure, the valves 5 and 6 were switched periodically ON and OFF to remove contaminants from interior valve parts. After this rinsing procedure, the DXP and the IonPac AS10 were flushed with deionized water for about 1 h. Before starting the analytical examinations, the "system blank" was tested by running the method (Table 1) without flushing the injection loop. Since metals are known to induce the decomposition of hydrogen peroxide, it is necessary to reconfigure the injector by using a rotor seal, which is normally used for the

Table 1
Ion chromatographic conditions

Columns	Dionex IonPac AG11 / AS11
Trap columns	ATC-1
	IonPac AS10
Eluents	E1: 50 m*M* NaOH
	E2: deionized water
	E3: 200 m*M* NaOH

AGP Program (linear gradient)

Time (min)	Curve	E1 (%)	E2 (%)	E3 (%)	5 INJ	6 AUX
0.0 start rinsing step	5			100	0	0
2.0 end rinsing step	5			100	0	0
2.1 start equilibration	5	3	97		0	0
10.5 end equilibration	5	3	97		1	0
12.1 start sampling	5	3	97		1	1
15	5	3	97		1	1
28	5	80	20		1	1
30	5	80	20		1	1

Eluent flow-rate	1 ml/min
Detection	Dionex CDM-3 conductivity detector
Suppressor	ASRS-1 (auto-recycle mode; range 3)
Sample injection volume	750 μl
DXP Flow-rate	1.5 ml/min

automation with autosamplers, to avoid metallic injection needles (Fig. 1).

2.4. System operation

The chromatographic conditions are listed in Table 1. After the rinsing and equilibrating step the DXP was started to deliver water with a flow-rate of 1.5 ml/min. At 10.5 min the injection valve was switched on, while valve 6 was kept off. Concurrently, the DI water flushed the sample loop and passed through the IonPac AG11 column. At this point, the dissolved anions were retained, while the hydrogen peroxide was eluted off the concentrator column to the waste. At 12.1 min, the IonPac AG11 concentrator was switched in-line with the IonPac AS11 (valve 6 ON) at which point the retained anions were eluted to the analytical column. At the same time, the DXP was stopped.

2.5. Samples

The samples were obtained from different suppliers. Sample B was not stabilized, whereas phosphate and pyrophosphate were added to the samples W1 and W2 to prevent catalytic decomposition of H_2O_2 by formation of phosphate or pyrophosphate complexes. However, sample F was stabilized with an unidentified compound. The chemical properties are shown in Table 2. These samples represent a collection of the different types of commercially available hydrogen peroxide.

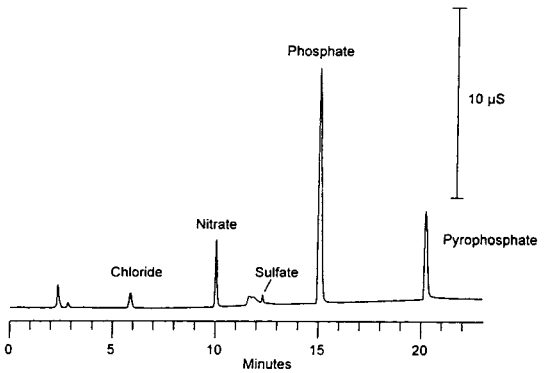

Fig. 2. Standard separation of five anions using the chromatographic conditions mentioned in Table 1. Sample concentrations: chloride (10 µg/l), nitrate (100 µg/l), sulfate (5 µg/l), phosphate (1 mg/l), pyrophosphate (500 µg/l).

3. Results and discussion

As hydrogen peroxide is one of the most important chemicals in the semiconductor industry, it must be analyzed for low concentrations of anionic impurities. Therefore, a new sample preparation technique, combining a matrix elimination and a concentrating step, was developed.

To ensure the applicability of the described method for both stabilized and non-stabilized H_2O_2, a guard column was used as the concentrator. A combination of both an IonPac AG11 as a concentrator column and an IonPac AS11 analytical column allows simplified gradient work [8] due to their common selectivity.

Fig. 2 shows that the ions of interest elute within 20 min. For hydrogen peroxide containing

Table 2
Chemical properties of the H_2O_2 samples investigated

Sample	Supplier	Content of H_2O_2 (%)	Stabilizer	Used for
B	A	35	None	Semiconductor purposes, "electronic grade"
W1	B	60	Phosphate, pyrophosphate	Oxidation reactions, "reagent grade"
W2	B	60	Phosphate, pyrophosphate	Oxidation reactions, "reagent grade"
F	Fluka	30	?	Oxidation reactions, "reagent grade"

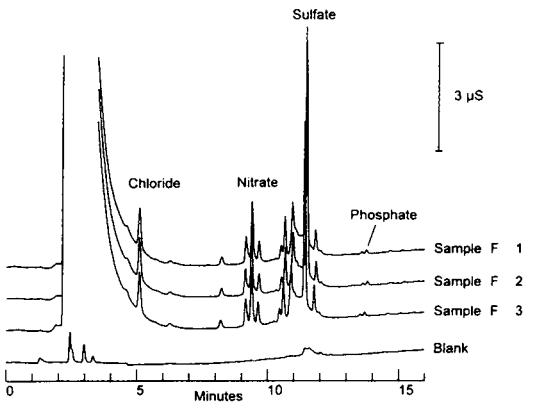

Fig. 3. Determination of anions in 30% H_2O_2 ("reagent" grade). For quantitative details see Table 3 (sample F).

no pyrophosphate, separation time can be reduced to 15 min.

Fig. 3 shows a summary of chromatograms, obtained by multiple injections of sample F. Using the described chromatographic conditions, it is possible to separate chloride from the predominant peak in the beginning of the chromatogram. Due to the NaOH eluent, phosphate elutes as a trivalent anion at about 13.5 min. A blank chromatogram is included in this figure to demonstrate the good baseline performance. The small peaks, which can be seen in the blank chromatogram can be attributed to compounds that are not totally removed from the deionized water. Short-chain organic acids such as formic and acetic acid elute between 2 and 4 min. The little hump at 11.5 min can be assigned to carbonate. These peaks do not interfere with the ions of interest. The upper three chromatograms represent typical chromatographic results for sample F. The respective amounts for the inorganic ions are summarized in Table 3. Close to the retention time of sulfate various unknown peaks are detected. Due to their retention, these peaks can probably be assigned to the group of divalent organic acids, or to organic acids with a stronger adsorptive behaviour towards the resin of the analytical column.

Fig. 4 shows the analysis of the electronic-grade sample B. Here, much lower amounts of anions (Table 3) are present with a different content of organic acids. In contrast to sample F, where two peaks elute close to nitrate, no

Table 3
Concentrations and standard deviations (S.D.) observed for the anions in the investigated hydrogen peroxide samples

Sample	Concentration				
	Chloride	Nitrate	Sulfate	Phosphate	Pyrophosphate
W1	422 µg/l	21.5 mg/l	0.74 mg/l	172 mg/l	32.9 mg/l
S.D.	29 µg/l	0.34 mg/l	0.03 mg/L	3.7 mg/l	0.6 mg/l
W2	4.42 mg/l	115 mg/l	3.04 mg/l	32.9 mg/l	97.9 mg/l
S.D.	0.5 mg/l	4 mg/l	1.1 mg/l	1.7 mg/l	3.8 mg/l
F	13.67 µg/l	44.3 µg/l	97.2 µg/l	9.79 µg/l	–
S.D.	0.12 µg/l	1.54 µg/l	2.09 µg/l	0.13 µg/l	–
B	2.47 µg/l	1.44 µg/l	<3.4 µg/l	–	–
S.D.	0.12 µg/l	0.20 µg/l	0.62 µg/l	–	–

All values are averages of three replicates.

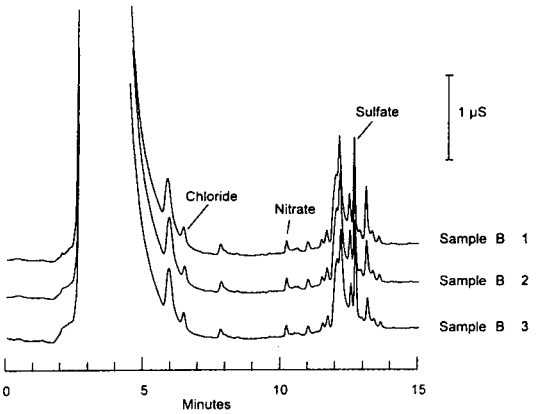

Fig. 4. Anion analysis in electronic grade H_2O_2 (35%). The observed concentrations and standard deviations are summarized in Table 3 (sample B).

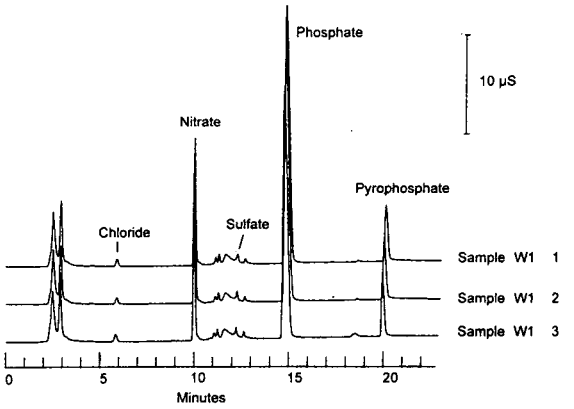

Fig. 5. Replicate chromatograms for the determination of anions in stabilized 60% hydrogen peroxide. For experimental conditions see Table 1. The sample was diluted with freshly prepared deionized water (1:50). The contents for the determined anions are summarized in Table 3 (sample W1).

significant signals are observed in this sample within this time frame. Despite the lower content of ionic contaminants in sample B, the composition of organic acids seems to be more complicated than in sample F. A significant difference between these samples can be found in the retention region around sulfate. While sample F harbors only four major peaks within this region, the chromatograms (Fig. 4) for the electronic-grade H_2O_2 show at least nine different compounds eluting close to sulfate. Both experiments show that sulfate is resolved from these impurities, allowing a reproducible quantitation (Table 3).

For the analysis of sample W1 a dilution of the original sample with deionized water was necessary to prevent an overloading of the concentrator column due to the higher concentrations of all ions of interest (Table 3). Fig. 5 shows chromatograms obtained by replicate injections of this sample, demonstrating the repeatability of this technique. Due to the resulting lower concentrations of the expected organic acids eluting in front of chloride, at least two peaks were obtained within the time frame of 2 to 4 min.

To shorten the overall analysis time, as shown in Fig. 6, a step gradient allows the determination of the major components within 12 min, in comparison to about 21 min with a linear gradient (Fig. 5) [9]. Sample W2 is hydrogen peroxide stabilized with a different content of phosphate and pyrophosphate (Table 3) compared to sample W1. To avoid overloading of the concentrator column with the ions of interest it was necessary to dilute sample W2 with deionized water, too.

All chromatograms of the examined samples

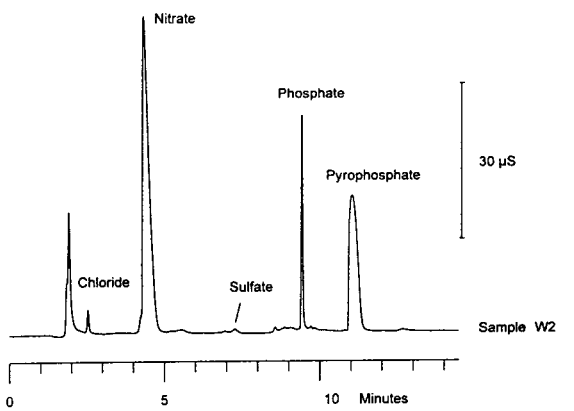

Fig. 6. Anion determination in stabilized 60% hydrogen peroxide (sample W2) using a step gradient [9]. Sample loop: 250 µl; gradient: 10 m*M* NaOH for 6 min, then change to 44 m*M* NaOH. Further experimental details see Table 1. The sample was diluted with freshly prepared water (1:10). Concentrations and standard deviations are summarized in Table 3.

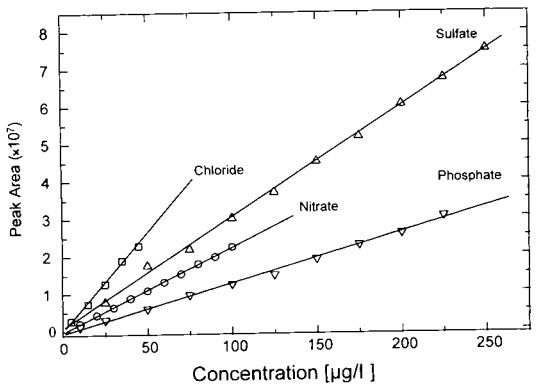

Fig. 7. Calibration curves for the determined trace anions in hydrogen peroxide.

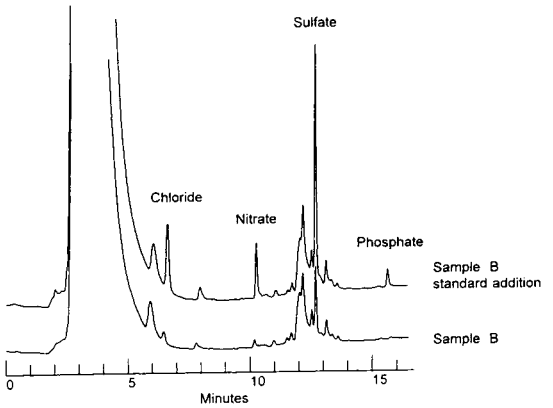

Fig. 8. Standard addition of anions to sample B. Bottom: original sample; top: sample B after spiking with 20 µg/l of chloride, nitrate, sulfate and phosphate.

show a predominant peak during the first minutes of the separation. The identification of the compounds responsible for this peak was carried out using capillary electrophoresis. Using a buffer solution consisting of 5 m*M* potassium hydrogenphthalate with 3.25 m*M* NaOH, and 1.6 m*M* triethanolamine with 0.75 m*M* hexamethonium hydroxide, adjusted to pH 6.3 with HCl (1 *M*), it is possible to detect acetate and formate via indirect UV detection at 250 nm. The voltage applied for the separation was 15 kV and was kept constant during the run. The chosen capillary had an inner diameter of 50 µm and a length of 50 cm. Gravity injection was used for 10 s at an altitude of 100 mm. Preliminary investigations indicate concentrations of about 33 mg/l acetate and 4 mg/l formate in sample B, and 27 mg/l acetate and 4 mg/l formate in sample F.

Sample W1 was also investigated but due to the high concentrations of nitrate, phosphate and pyrophosphate, no peaks were detected, even after a dilution of the sample.

The quantification for the ions of interest was carried out using external standard calibration utilizing mixed standard solutions with at least five different calibration levels (Fig. 7). The results are listed in Table 4. As can be seen, most of the linear calibration plots result in *r* values around 0.999. For concentrations lower than 5 µg/l the relative standard deviations (R.S.D.s) increased (Table 3), therefore standard addition should be used to more accurately determine the respective anions (Fig. 8).

The detection limits —based on three times

Table 4
Calibration parameters for anion determinations in hydrogen peroxide

Ion	Range (µg/l)	Linear correlation coefficient	Within-run precision (µg/l), $n = 3$[a]	MDL (µg/l)	R.S.D. (retention time)[a]
Chloride	5–45	>0.998	0.47	1.5	0.2
Nitrate	10–100	>0.999	0.14	0.4	0.1
Sulfate	25–250	>0.999	1.14	3.4	0.2
Phosphate	10–225	>0.999	0.82	2.5	0.1

[a]For the lowest calibration level.

standard deviation of the lowest respective standard— are between 0.4 to 3.4 μg/l (Table 4).

4. Conclusions

An improved method for the determination of trace anions in concentrated hydrogen peroxide solutions has been developed. This method involves elimination of the hydrogen peroxide matrix while the anions of interest are concentrated. The retained anions (chloride, nitrate, sulfate, phosphate and pyrophosphate) can be eluted using a sodium hydroxide gradient, and can be determined in low μg/l concentration ranges using suppressed conductivity detection, without further sample pretreatment. Due to the matrix-elimination step, it is possible to inject hydrogen peroxide solutions up to an H_2O_2 content of 35% directly, without damaging the anion exchange column. The detection limits for most anions are 0.4 to 3.4 μg/l.

References

[1] *Brockhaus der Chemie*, Vol. 2, Brockhaus Verlag, Leipzig, 1971, p. 1521.
[2] *Ullmanns Encyklopädie der technischen Chemie*, Vol. 24, VCH, Weinheim, 1983, 4th ed., p. 97.
[3] H. Schäfer and K. Budde, presented at the *4th International Symposium on Ion Chromatography, Baltimore, MD, 1993.*
[4] R.E. Smith, *Ion Chromatography Applications*, CRC Press, Boca Raton, FL, 1990.
[5] C.D. Chriswell, D.R. Mroch and R. Markuszewski, *Anal. Chem.*, 58 (1986) 319.
[6] J. Weiss, *Ionenchromatographie*, VCH, Weinheim, 2nd ed., 1991.
[7] F.A. Cotton and G. Wilkinson, *Anorganische Chemie*, VCH, Weinheim, 1974.
[8] C.A. Pohl and C. Saini, presented at the *3rd International Symposium on Ion Chromatography, Linz, 1992.*
[9] *Application Report No. 02/94/05*, Dionex, Idstein, 1994.

ELSEVIER

Journal of Chromatography A, 706 (1995) 199–207

JOURNAL OF CHROMATOGRAPHY A

Determination of phosphorus by sample combustion followed by non-suppressed ion chromatography

Joselyn C. Umali[a], Grainne M. Moran[a], Paul R. Haddad[b,*]

[a]*Department of Analytical Chemistry, University of New South Wales, Sydney, NSW 2052, Australia*
[b]*Department of Chemistry, University of Tasmania, G.P.O. Box 252C, Hobart, Tasmania 7001, Australia*

Abstract

The determination of phosphorus using sample combustion in oxygen followed by quantification of orthophosphate using non-suppressed ion chromatography (IC) was studied using phenylphosphonic acid as a model sample compound. Even under optimal conditions, the recovery of phosphorus (measured as orthophosphate) was <70% when dilute aqueous hydrogen peroxide was used as the absorbing solution employed to collect the combustion products. However, use of inductively coupled plasma atomic emission spectroscopy and spectrophotometry using heteropoly blue formation showed that all of the phosphorus in the original sample was in fact also present in the absorbing solution, but suggested that some of this phosphorus was present as forms other than orthophosphate. ^{31}P Nuclear magnetic resonance was used to study the composition of the combustion solution and confirmed the presence of orthophosphate, pyrophosphate and trimetaphosphate. Hydrolysis of the combustion sample solution by boiling for at least 20 min at pH < 3 was shown to convert all of these forms of phosphorus to orthophosphate, thereby enabling their determination by IC. Quantitative recoveries of phosphorus were achieved when this post-combustion hydrolysis step was incorporated into the analytical procedure.

1. Introduction

Combustion by the oxygen flask technique has been used extensively for the detemination of species such as halogens, sulfur, nitrogen and phosphorus. In this technique, the sample is combusted in oxygen and the desired species are released from the sample matrix in the form of oxides which are then absorbed in an appropriate absorbing solution. This procedure has greatly simplified the sample treatment required for the analysis of phosphorus in organophosphorus compounds, and the combustion solution thus produced contains phosphates in their inorganic form. A number of analytical techniques for the analysis of inorganic phosphates have been reported. These methods include both gravimetric and titrimetric analyses [1,2], electrochemical methods such as polarography [3], and other instrumental methods such as atomic absorption spectrometry [4], UV spectrophotometry [5], inductively coupled plasma atomic emission spectroscopy (ICP-AES) [6], ^{31}P nuclear magnetic resonance (NMR) [7] and ion chromatography (IC) [8,9].

Gravimetric and titrimetric methods are often unsuitable for ultramicro analysis due to losses during sample manipulation, and these methods are subject to interferences from other elements produced during combustion. UV spectropho-

* Corresponding author.

0021-9673/95/$09.50
SSDI 0021-9673(94)01160-5

tometry involving reaction of oxidised phosphates with a molybdate reagent, Mo(V)–Mo(VI), with subsequent formation of a phosphomolybdate complex (commonly known as heteropolyblue) is used widely. This technique is relatively free from interferences but requires a lengthy sample preparation time and takes at least 1 h for the reaction to be complete [10]. ^{31}P NMR may be employed in the analysis of phosphates [7] and has the advantage of specificity of defined chemical shifts of phosphorus nuclei. Its limitations, however, include inherent low sensitivity, which necessitates the use of a large amount of sample, and the complexity of spectra for polyphosphates higher than tripolyphosphate [11]. ICP-AES provides the total phosphorus content without structural information but has the advantage of detection of numerous other elements in a simultaneous determination. IC is used routinely for the determination of orthophosphate in the presence of other anions by both the suppressed and non-suppressed approaches. When orthophosphate is present together with the other lower oxides of P such as phosphite ($H_3PO_2^-$) and hypophosphite ($H_2PO_2^-$) speciation may be achieved using conductivity detection in suppressed IC [12].

Anomalous chromatographic behaviour of pyrophosphate in classical ion-exchange chromatography was observed by Fukuda et al. [13] who found that hydrolysis of pyrophosphate occurred during the chromatographic run causing the appearance of an orthophosphate peak in the elution chromatogram. They attributed this observation to the action of multivalent metals which promoted the hydrolysis of pyrophosphate at pH values above 4. Addition of ethylenediaminetetraacetic acid (EDTA) secured the normal chromatographic behaviour of pyrophosphate by masking the heavy metals present in the solution. Nakamura et al. [14] applied the same approach in the separation of linear oligophosphates.

The problem of low recovery of phosphorus (as orthophosphate) following the combustion of an organophosphorus compound has been encountered by several workers. Binkowski and Rutkowski [15] attributed this difficulty to the use of platinum wire as the sample holder because this wire absorbed too much heat and therefore the combustion temperature was insufficient to cause complete combustion of the organic compound. For a high combustion temperature to be attained, they used a very thin fused-silica hook and in so doing obtained quantitative recoveries for phosphorus by titrating the absorbed orthophosphate with standard lanthanum solution. Busman et al. [16] encountered the same difficulty in suppressed IC and associated the problem with the formation during combustion of either some polyphosphates that were not detectable by IC or some insoluble metal phosphates. Senior [17,18] also suggested the formation of some polyphosphates, such as pyrophosphate and cyclic metaphosphate, but did not report the methods employed.

The chemical instability of polyphosphates is well known, and under appropriate conditions all P–O–P linkages in a structure can be ruptured [19]. The ultimate products of hydrolysis are discrete orthophosphate ions, although the route and rate of hydrolysis are characteristic of the particular polyphosphate anion and of the conditions employed. The principal factors influencing the rate of hydrolysis of a polyphosphate solution are the number of corners shared by the PO_4 tetrahedra in the structure, the temperature, the pH and the concentration of the polyphosphates. The hydrolysis rate is accelerated by either raising or lowering the pH from neutral and by increasing the temperature. The hydrolysis rate may also be influenced to some degree by the type of cations present. Watanabe et al. [20] demonstrated the effect of cations on the rate of hydrolysis of pyro- and tripolyphosphates. They found that alkali metal, alkaline earth metal, aluminium and some transition metals such as Mn(II), Co(II), Ni(II), Cu(II) and Zn(II) cations retard the hydrolysis of the phosphates in acidic media. Pyrophosphates are almost completely stable in alkaline or neutral solutions at normal temperatures. They are hydrolysed under acid conditions although over the whole pH range they are the most stable of the polyphosphates.

In this paper we examine in detail the nature

of the combustion products formed when an organophosphorus test compound, phenylphosphonic acid, is combusted in oxygen. The aim of this work was to develop a sample treatment procedure which would permit the reliable determination of phosphorus in organophosphorus compounds by non-suppressed IC.

2. Experimental

2.1. Combustion apparatus and procedure

The oxygen combustion flask used throughout the work is shown in Fig. 1 and consisted of a modified 500-ml Erlenmeyer flask, fitted with inlet and outlet tubes. Inserted into this tube and held in place by elastic bands affixed to glass hooks was a glass stopper assembly, through which were passed two platinum wires. These wires were supported mechanically by a PTFE disc inside the stopper and by encasing them in glass extensions attached to the underside of the stopper. One of the platinum wires was coiled to form a sample basket. The two platinum wires were then joined with a short length of nichrome wire using stainless-steel connectors. The above design gave sufficient rigidity to the electrode assembly to enable the flask to be swirled during operation without risk of breakage.

Phenylphosphonic acid, $C_6H_5P(O)(OH)_2$ (Aldrich, Milwaukee, WI, USA) was used as the model phosphorus-containing compound. The purity of this reagent was determined by microanalysis. The required amount of the sample was weighed in an ashless filter paper (Whatman No. 41) and folded in such a way to provide a paper protrusion which served as a wick. Absorbing solution (usually 10 ml) was added to the flask. The sample was positioned in the sample holder which was then placed inside the flask, sealed with silicone grease and held securely by two elastic bands wrapped around the hooks provided. After passing a suitable amount of oxygen (CIG, Grade 020) into the flask, the oxygen inlet and outlet were both closed simultaneously. Ignition of the sample was initiated inside the flask using an electrical igniter connected to a variable-voltage regulator. After the combustion of the sample was complete, the flask was shaken to allow rapid absorption of gaseous products. The solution was allowed to stand for a few minutes, after which it was transferred quantitatively to a 25-ml volumetric flask and diluted to the mark with distilled water. After each combustion, the sample holder was removed from the flask and heated on a Bunsen burner to eliminate any uncombusted residues.

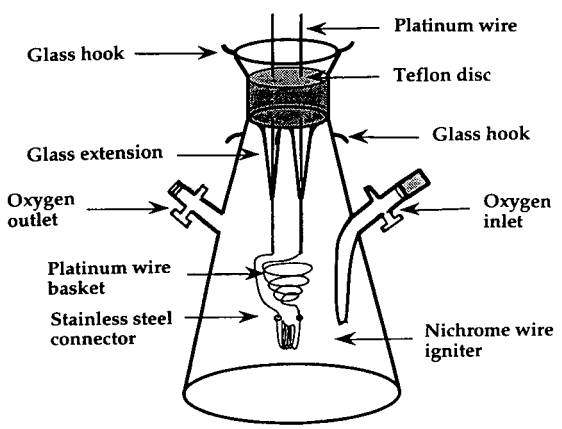

Fig. 1. Construction of the oxygen combustion flask.

2.2. Analysis of combustion solutions

IC was performed using a Waters (Milford, MA, USA) Model 510 pump, U6K injector and Model 430 conductivity detector interfaced to an Omniscribe (Houston, TX, USA) Model 5000 dual-pen strip-chart recorder. The chromatographic column was a Waters IC-PAK A anion column, 50 × 4.6 mm I.D., packed with polymethacrylate-based resin of 10 μm particle size and an exchange capacity of 30 μequiv./g. A stock gluconate–borate eluent solution was prepared by mixing 12.5 g of sodium tetraborate decahydrate, 9.0 g of boric acid and 8.0 g of sodium D-gluconate in 1 l of Milli-Q (Millipore, Bedford, MA, USA) water. A 20-ml aliquot of this stock solution was mixed with 120 ml of acetonitrile and 10 ml of 25% glycerol and diluted to 1 l with Milli-Q water. The resulting eluent was then filtered through a 0.45-μm filter and degassed in an ultrasonic bath prior to use.

Analysis by ICP-AES was performed using a Plasmalab instrument manufactured by Labtam International (Melbourne, Australia), which employed a 27.12-MHz plasma operating at a power of 1.4 kW. Spectrophotometric determinations of phosphorus as orthophosphate were performed using the procedure of Yoza and Ohashi [10] by reacting the sample solution with a mixture of 1 ml of 1 *M* sodium hydrogensulphite solution and 2 ml of the Mo(V)–Mo(VI) reagent for 1 h at 98–100°C.

^{31}P NMR spectra were acquired on a Bruker AC300P spectrometer with a multinuclear probe tuned to 121.49 MHz for ^{31}P. Free induction decays were routinely acquired with a spectral width of 12 kHz (100 ppm), ~45° pulse width (10 μs), using 8K data points and a relaxation delay of 2 s. Chemical shifts, δ_P, were reported with respect to 85% H_3PO_4 ($\delta_P = 0$ ppm) as an external reference. Positive shifts were downfield to higher frequency. No ^{1}H decoupling was used. Between 400 and 1600 scans were collected for each sample and spectra were acquired at 300 K.

3. Results and discussion

3.1. Optimisation of the combustion–absorption process

Using the chromatographic conditions described in the experimental section, non-suppressed IC was used to determine the recovery of phosphorus (as orthophosphate) from combusted phenylphosphonic acid. The effects on recovery of varying the composition and volume of the absorbing solution, the time and conditions used for absorption of the combustion gases, and the sample size were studied. Changes to the volume of the absorbing solution and the conditions used for absorption produced only minor alterations in recovery and it is worth noting that the water produced as a by-product of combustion plays an important role in the absorption of the combustion gases. A number of different absorbing solutions were examined, including water, dilute hydrogen peroxide and gluconate–borate eluent. The results obtained showed that solutions containing hydrogen peroxide at or above a concentration of 0.15% (v/v) gave the best results. Some problems were encountered with the use of the gluconate–borate eluent as the absorbing solution in that a nitrate peak was produced, presumably from oxidation of the acetonitrile which forms part of this eluent. It should also be noted that all chromatograms showed a large carbonate peak resulting from absorption of the carbon dioxide produced in the combustion and a chloride peak resulting from the residual chloride in the filter paper used to contain the sample. A dilute solution of hydrogen peroxide (0.15%, v/v) was selected as the optimal absorbing solution and was used to study the effect of sample size on recovery (Fig. 2a). It can be seen that recovery decreased steadily as the sample size increased.

In all of the above experiments, the recovery fell in the range 40–70%. The precision of combustion, as determined by eight successive replicates performed under uniform conditions and with careful attention to the performance of the flask, was found to be 6.56% R.S.D. These analytical performance values are unsatisfactory and suggested that the combustion process and/

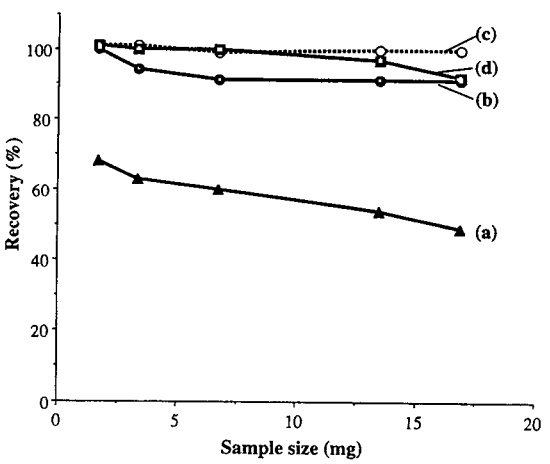

Fig. 2. Recovery of phosphorus from combusted samples of phenylphosphonic acid under optimal combustion conditions (see text) and with 0.15% (v/v) H_2O_2 as absorbing solution, as determined using (a) IC without post-combustion hydrolysis, (b) ICPAES, (c) spectrophotometry and (d) ion chromatography with post-combustion hydrolysis.

or the absorption process was incomplete and variable, or that the chromatographic analysis method used was not measuring all of the phosphorus species present in the absorbing solution.

3.2. Analysis of combustion solutions by ICP-AES and spectrophotometry

The second of the above possibilities was examined using ICP-AES to determine the recovery values under the same combustion conditions used for the IC determinations. These results, plotted in Fig. 2b, show that recovery was >90% for all sample sizes, despite the fact that the IC results showed decreasing recoveries.

ICP-AES provides a measure of total phosphorus and does not give information about the identity of the species present. One method which has been frequently used in the identification of polyphosphates is the formation of the heteropolyblue complex followed by UV spectrophotometric determination. Yoza and Ohashi [10] used this method to investigate the oxidation products of thirteen P-acids and showed that the absorption spectrum of the heteropolyblue reaction product could be used to indicate the type of phosphate species that had reacted.

Application of the derivatization procedure of Yoza and Ohashi (summarized under Experimental) gave the results shown in Fig. 2c. It can be seen that quantitative recoveries of phosphorus were obtained. Moreover, the visible spectrum of the heteropolyblue product gave only a single maximum at 810 nm, which suggested only the presence of the heteropolyblue complex of orthophosphate. Such a complex can be produced from reaction of those phosphate species that contain either a single P atom or multiple P atoms that are not adjacent to each other. Phosphate species of this type which can be expected to show resistance to hydrolysis include hypophosphite, phosphite, orthophosphate and trimetaphosphate (Fig. 3). A further phosphate species that was not included in the study of Yoza and Ohashi [10] and which was possibly formed during combustion is pyrophosphate (Fig. 3). The reaction of pyrophosphate with Mo(V)–Mo(VI) was investigated by treating a standard solution of this species according to the procedure described in the Experimental section. The product of this reaction exhibited an absorption spectrum with a single λ_{max} at 810 nm which again indicated the sole formation of orthophosphate in the heteropolyblue complex.

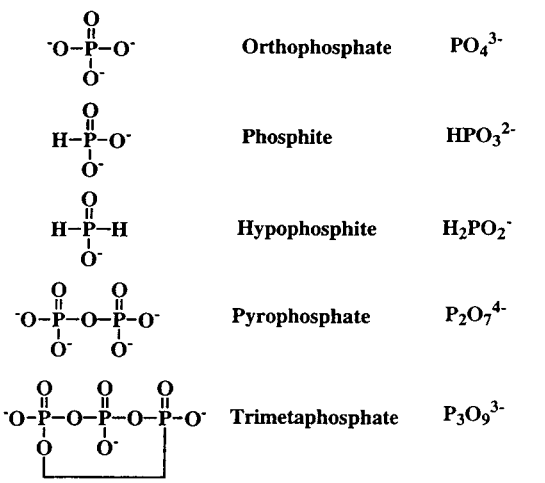

Fig. 3. Structures of inorganic phosphates likely to be present in the combustion solution.

3.3. Identification of combustion products by IC and NMR

The results obtained above suggested that the phosphate species likely to be present in the solution would include hypophosphite, phosphite, orthophosphate and pyrophosphate. The formation of the first two of these species was indicated in the early work of Belcher and MacDonald [21] and Gedansky et al. [22]. Non-suppressed IC using a tartrate eluent at pH 3.2 has been used previously to separate orthophosphate, hypophosphite and phosphite, all of which were weakly retained on a strong-base anion-exchange material [23]. However, we have found it necessary to raise the eluent pH to a value in excess of pK_{a2} for tartaric acid (4.91) in order to eliminate interference from system peaks produced by the presence of undissociated tartaric acid [24–26]. At a pH of approximately 5, there should be no non-ionised tartaric acid present. Using an eluent comprising 2 m*M*

sodium tartrate at pH 4.98, hypophosphite could be resolved from orthophosphate, but no peaks attributable to phosphite or pyrophosphate could be identified, perhaps due to hydrolysis of these species at the eluent pH used. These chromatographic conditions were then employed to analyse the combustion products from phenylphosphonic acid, absorbed in aqueous hydrogen peroxide. No peak for hypophosphite was detected.

^{31}P NMR has been used to identify different forms of phosphorus in mixtures of inorganic phosphates [27,28]. Gard et al. [29] employed this method in the simultaneous determination of lower oxo acids of phosphates including orthophosphate, pyrophosphate, trimetaphosphate and tripolyphosphate in a commercial tripolyphosphate sample. In their work, samples were maintained at pH near 9 in order to optimise the signal separation. Yoza et al. [30] showed the effect of pH changes on chemical shifts for a series of eleven inorganic phosphates. ^{31}P Chemical shifts of the phosphates in the combustion solution were obtained at pH 8.56 and the chemical shifts were reported relative to the signal of 85% orthophosphoric acid as an external reference. A small amount of EDTA was used, the purpose of which was to sequester any trace of multiply charged metal ions that may be present in solution.

The ^{31}P NMR spectrum of the combustion solution is shown in Fig. 4. The peak identities, assigned using published chemical shift data [29,30], were a singlet at $\delta_P = 3.2$ ppm due to orthophosphate and a singlet at $\delta_P = -6.9$ ppm due to pyrophosphate. The absence of a doublet at $\delta_P = 5.5$ ppm ruled out the presence of tripolyphosphate in the solution, but the presence of a small peak at $\delta_P = -20.74$ ppm suggested the presence of trimetaphosphate. The formation of a cyclic metaphosphate during combustion of an organophosphorus compound was mentioned in the early work of Cohen and Chezch [31] and more recently by Senior [17]. However, no positive identification of the type of cyclic metaphosphate has been given. The sole product

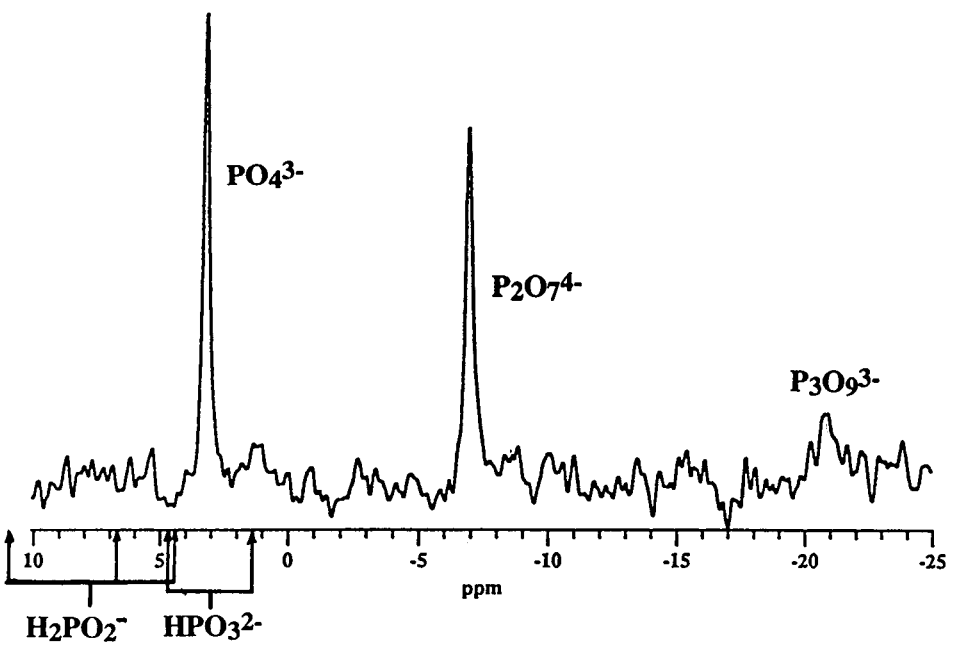

Fig. 4. ^{31}P NMR spectrum of a combustion solution obtained from phenylphosphonic acid. The chemical shifts for hypophosphite (triplet) and phosphite (doublet) are indicated.

of the reaction of trimetaphosphate with Mo(V)–Mo(VI) can be expected to be the orthophosphate heteropolyblue complex. The spectrophotometric results described earlier are therefore consistent with the presence of trimetaphosphate in the combustion solution.

The influence of pH on the chemical shifts of phosphate species was studied and downfield shifts were observed on going from acidic to alkaline pH, in accordance with similar findings in the literature [32]. The third weak peak, which was present in all solutions analysed and which was assigned as trimetaphosphate, also shifted downfield at alkaline pH. This change in chemical shift toward the deshielded portion of the spectrum with increasing pH has been attributed to a decreasing degree of protonation of the phosphate tetrahedra as the solution becomes alkaline [33].

3.4. Post-combustion hydrolysis

Having identified the higher phosphates present in the combustion solution, a post-combustion reaction which would convert these species to orthophosphate was sought in order to simplify the use of the combustion–IC analysis approach. Methods published for the hydrolysis of phosphates usually require the use of a high concentration of acid, such as sulfuric, hydrochloric, nitric or perchloric acid, because polyphosphates are rather stable under alkaline conditions but are more easily hydrolysed in an acidic medium. The use of these acids, however, must be avoided where possible in IC due to the probable interference of large amounts of the acid anion in the detection of orthophophosphate. This is, of course, aside from the fact that the very low pH of the hydrolysis solution is not suitable for use with chromatographic columns having limited tolerance to low pH values. While this limitation can be overcome by neutralising the solution to an appropriate pH this is not recommended since interferences and contamination are easily introduced by further sample manipulation. Based on the above-mentioned limitations, the best alternative was to use an oxidising agent which will not introduce any anion in the determination. In this case H_2O_2 was again the best choice. Since it was essential that the reaction take place at a low pH, tartaric acid was used and attention was focussed on the hydrolysis of pyrophosphate because it was present at much higher concentrations than trimetaphosphate in the combustion solutions.

The optimal conditions for hydrolysis of pyrophosphate were determined by performing the hydrolysis using a range of concentrations of H_2O_2 at varying pH, and by adjusting the boiling time. Best results were obtained using 0.6% (w/v) H_2O_2 at pH < 3 (using tartaric acid for pH adjustment) and boiling for at least 20 min. The presence of alkali metal cations in the solution should be avoided since these are known to retard the hydrolysis of pyrophosphate [34]. Fig. 2d shows the phosphorus recovery (as orthophosphate) obtained when this hydrolysis procedure was applied to a series of combustion solutions prepared using varying weights of phenylphosphonic acid as sample. Quantitative recovery was obtained for sample sizes less than 10 mg.

3.5. Analysis of a vegetation sample

The developed method was applied to the analysis of a vegetation sample. Two combustions of 0.06 g each were performed using water as the absorbing solution. The solution from the first combustion was injected directly onto the ion chromatograph after filtration, while into the second ten drops of 30% H_2O_2 were added. The introduction of tartaric acid was not necessary because the pH was measured to be 2.75 which was sufficiently acidic to allow the hydrolysis to take place. Hydrolysis was performed by boiling the solution for 45 min to ensure complete conversion of pyrophosphate to orthophosphate.

The chromatograms produced by the two combustion solutions are shown in Fig. 5. Important features of the chromatogram for the unhydrolysed sample (Fig. 5a) are a large peak for nitrite and a very small peak for orthophosphate. After hydrolysis (Fig. 5b), increased peak areas for nitrate, orthophosphate and sulfate are evident as a result of hydrolysis of

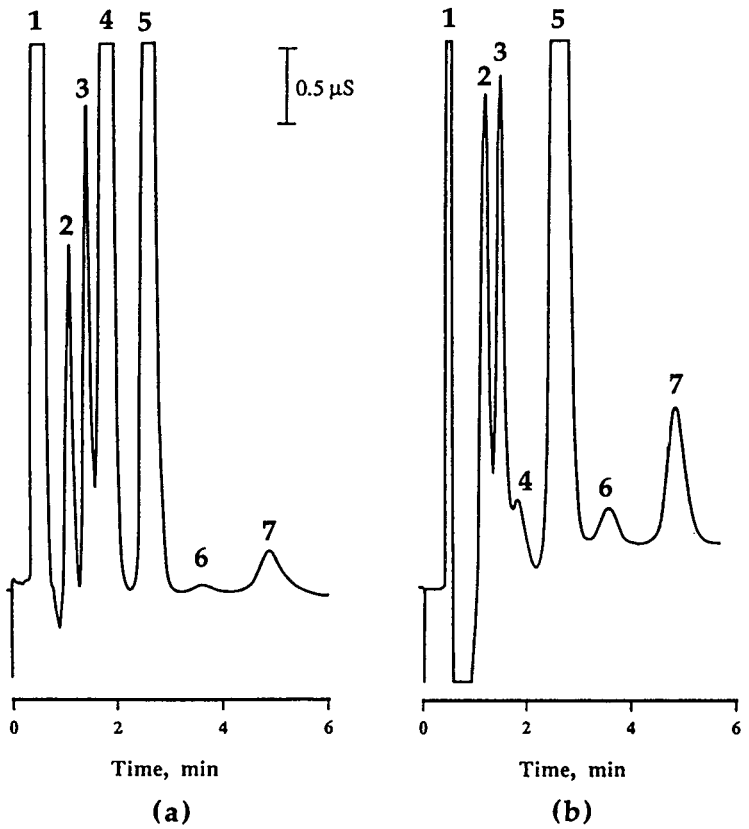

Fig. 5. Chromatograms of the combustion solution obtained from a vegetation sample (a) before hydrolysis and (b) after hydrolysis by boiling for 45 min. A gluconate–borate eluent was used with an IC-PAK A anion-exchange column. Peaks: 1 = injection peak; 2 = HCO_3^-; 3 = Cl^-; 4 = NO_2^-; 5 = NO_3^-; 6 = HPO_4^{2-}; 7 = SO_4^{2-}.

polyphosphates and the oxidation of nitrite and sulfite to nitrate and sulfate, respectively.

4. Conclusions

It has been shown that more than one phosphorus species is produced upon combustion of an organophosphorus compound. The presence (as well as the confirmed absence) of several P species was demonstrated by IC in combination with ICP-AES, spectrophotometry and ^{31}P NMR measurements performed on combustion samples. The latter technique identified the phosphates as orthophosphate, pyrophosphate and trimetaphosphate. Post-combustion hydrolysis using tartaric acid and H_2O_2 converted the pyrophosphate and trimetaphosphate to orthophosphate. Application of the hydrolysis method to a combusted vegetation sample illustrated the utility of the technique.

Acknowledgements

We thank Dr. Jim Hook for performing the NMR measurements and Mr. Richard Finlayson for performing the ICP-AES measurements.

References

[1] G.F. Anisimova and V.A. Kilmova, *Zh. Anal. Khim.*, 37 (1982) 1100.

[2] R.L. Grob and M.E.P. McNally, *Anal. Lett. A*, 13 (1980) 219.
[3] S.W. Rishara and F.M. El-Samman, *Microchem. J.*, 27 (1982) 44.
[4] F.J. Langmyr and I.M. Dahl, *Anal. Chim. Acta*, 131 (1981) 303.
[5] W.A. Dick and M.A. Tabaitabai, *Agron. J.*, 74 (1982) 59.
[6] M. Siroki, G. Vujicic, V. Milun, Z. Hudovsky and L. Marie, *Anal. Chim. Acta*, 192 (1987) 175.
[7] T.W. Gurley and W.M. Ritchey, *Anal. Chem.*, 47 (1975) 1444.
[8] A Quinn, K.W.M. Sui, G.J. Gardner and S.S. Berman, *J. Chromatogr.*, 370 (1986) 203.
[9] J.F. Colaroutolo, *Anal. Chem.*, 49 (1977) 884.
[10] N. Yoza and S. Ohashi, *Chem. Soc. Jpn.*, 37 (1964) 37.
[11] D.R. Gard, J.C. Burquin and J.K. Gard, *Anal. Chem.*, 64 (1992) 557.
[12] T. Tanaka, K. Hiiro, A. Kawahara and S. Wakida, *Bunseki Kagaku*, 32 (1983) 771.
[13] F. Fukuda, T. Nakamura and S. Ohashi, *J. Chromatogr.*, 128 (1976) 212.
[14] T. Nakamura, T. Yano, A. Fujita and S. Ohashi, *J. Chromatogr.*, 130 (1977) 384.
[15] J. Binkowski and P. Rutkowski, *Mikrochim. Acta (Wien)*, 1 (1986) 245.
[16] L.M. Busman, R.P. Dick and M.A. Tabatabai, *Soil Sci. Soc. Am. J.*, 47 (1983) 1167.
[17] J.P. Senior, *Anal. Proc.*, 27 (1990) 116.
[18] J. Senior, in P.A. Anthony, M.J. Hudson (Editors), *Proc. Int. Conf. Ion Exchange Processes*, 2 (1990) 17.
[19] N.W. Alcock and K.A. Raspin, *J. Chem. Soc. A*, (1968) 2108.
[20] M. Watanabe, M. Matsuura and T. Yamada, *Bull. Chem. Soc. Jpn.*, 54 (1981) 738.
[21] R. Belcher and A.M.G. Macdonald, *Talanta*, 1 (1958) 408.
[22] S.J. Gedansky, J.E. Bowen and O.I. Milner, *Anal. Chem.*, 32 (1960) 1447.
[23] *Waters IC Lab.*, Report No. 354.
[24] P.E. Jackson and P.R. Haddad, *J. Chromatogr.*, 346 (1985) 125.
[25] P.E. Jackson and P.R. Haddad, *J. Chromatogr.*, 355 (1986) 87.
[26] P.R. Haddad and P.E. Jackson, *Ion Chromatography: Principles and Applications*, Elsevier, Amsterdam, 1990, p. 124.
[27] S.A. Sojka and R.A. Wolfe, *Anal. Chem.*, 50 (1978) 585.
[28] D.A. Stanislawski and J.R. Van Wazer, *Anal. Chem.*, 52 (1980) 96.
[29] J.K. Gard, D.R. Gard and C.F. Callis, *Am. Chem. Soc. Symp. Series*, 486 (1992) 41.
[30] N. Yoza, N. Ueda and S. Nakashima, *Fresenius J. Anal. Chem.*, 348 (1994) 633.
[31] L.E. Cohen and F.W. Chezch., *Chem. Anal.*, 47 (1958) 86.
[32] I.B. Rubin, *Anal. Lett.*, 17 (1984) 1259.
[33] R.K. Osterheld, in E.J. Griffith and M. Grayson (eds), *Topics in Phosphorus Chemistry*, Vol. 7, Interscience, New York, 1972, p. 103.
[34] P.S. Belton, K.J. Packer and T.E. Southon, *J. Sci. Food Agric.*, 40 (1987) 283.

ELSEVIER

Journal of Chromatography A, 706 (1995) 209–213

JOURNAL OF CHROMATOGRAPHY A

Determination of nitrate, phosphate and organically bound phosphorus in coral skeletons by ion chromatography

William Shotyk*, Ina Immenhauser-Potthast, Hubert A. Vogel

Geological Institute, University of Berne, Baltzerstrasse 1, CH-3012 Berne, Switzerland

Abstract

Nitrate, phosphate and sulphate incorporated in the aragonitic skeletons of corals (*Porites*) were analyzed by ion chromatography (IC). All anion analyses were performed using a Dionex 4500i IC system with Dionex columns, conductivity detector and computer interface. The anions were separated on an AS4A separator column behind an AG4 guard column, and the background conductivity of the eluent was suppressed using an AMMSII membrane suppressor. The suppressor was continually regenerated using an anion membrane suppressor regenerant cartridge and H_2SO_4. The eluent used was 1.8 m*M* Na_2CO_3–1.7 m*M* $NaHCO_3$. Bleached, oven-dried coral powder (200 mg) was dissolved in 0.5 ml of 30% HCl (Merck Suprapur) and diluted to 100 ml. Standards were also prepared in HCl, and the linearity was excellent for each anion ($r^2 > 0.999$) over the range 20–100 ng/g (ppb) for nitrate, 100–500 ng/g for phosphate and 0.5–12.0 μg/g (ppm) for sulphate. All samples and standards were passed through a chloride-removal cartridge (Dionex OnGuard AG) prior to injection. This cartridge consisted of silver and its sole purpose was to remove Cl^- which might otherwise overwhelm the separator column. Using a 250-μl injection loop, the detection limits were approximately 5 ng/g for nitrate and 10 ng/g for phosphate. The analytical procedure variability was 9% for nitrate, 2% for phosphate and 0.5% for sulphate. The concentrations of these species in the corals varied from 0.2 to 18 ppm, 8 to 118 ppm and 560 to 590 ppm, respectively. Coral samples taken from three coral heads at the Grande Rivière Noire Bay (slabs 1Ks, 5Ks, 6Ks) averaged 4.5 ± 0.5 ppm nitrate and 55 ± 1 ppm phosphate, compared with 2.2 ± 0.5 ppm nitrate and 16 ± 1 ppm phosphate for the samples taken further out in the lagoon (slabs 7Ks and 11Ks). Thus, the nitrate and phosphate concentrations clearly distinguish between corals taken from the bay, which are closer to anthropogenic N and P inputs, from samples collected from the lagoon, which are further from such N and P sources. To estimate the possible importance of organically bound phosphorus, samples were also treated with H_2O_2. Following dissolution in HCl, 1 ml of 30% H_2O_2 (Merck Suprapur) was added, and the samples were heated at 50°C for 3 h. The instrument was calibrated using standards prepared in HCl–H_2O_2. The phosphate concentrations measured in the samples dissolved in HCl–H_2O_2 were up to 100% higher than those dissolved in HCl alone, suggesting that organically bound phosphorus contributes significantly to the total phosphorus concentrations of the corals.

1. Introduction

The fringing reef ecosystem on the Island of Mauritius in the Indian Ocean is degenerating because of algal growth, coral diseases and degradation of lagoons. A reduction in coral vitality and a decrease in specimen variation is now well documented [1]. The ultimate cause of

* Corresponding author.

0021-9673/95/$09.50
SSDI 0021-9673(94)01153-2

these problems may be the extensive eutrophication which arises from marine sewage disposal.

Anthropogenic inputs of sewage from towns, hotels and private houses on the beach could be responsible for the degradation of the corals either because of nutrients, toxic heavy metals or both [2,3]. These contaminants are transported directly into the lagoon by rivers, canals and groundwater, or may be washed out during the rainy season [4]. Once they have reached the reef ecosystem, there are a number of possible mechanisms by which the corals may be affected [5].

Phosphate is normally a trace constituent in seawater (of the order of 10 ng/g or less in uncontaminated waters), but elevated concentrations of this species can decrease calcification rates (i.e. coral growth rates) by as much as 50% [6]. Phosphate can also affect coral vitality indirectly by stimulating the growth of nuisance algae which reduce light intensity and promote sediment accumulation [7]. Bacterial infection of coral mucus may increase, causing localized tissue death and allowing algal growth to become established [8]. Thick algal mats have been known to form and may smother all underlying reef organisms [5].

To identify possible reasons for reef degradation, a geochemical study was undertaken using the widespread recent coral genus *Porites*. One goal of the project was to measure nitrate and phosphate concentrations in the coral skeletons and to use these as indicators of marine pollution. A second goal was to reconstruct the chronology of these types of marine pollution using the annual growth bands of the corals.

Previous investigations have used a colorimetric method (reaction with molybdenum blue) for measuring phosphate in acid digests of coral skeletons [9]. Because our interest included nitrate, we sought to measure nitrate and phosphate *simultaneously* in acid digests of coral skeletons using ion chromatography (IC). The main purpose of the present report is to summarize an evaluation of the IC method for measuring nitrate and phosphate in corals.

2. Experimental

2.1. Preparation of coral samples

Individual samples (approximately 5–7 g) of annual growth bands were removed from coral head slabs using a jig saw. The samples were placed in clean 100-ml polypropylene bottles, rinsed three times and left for two days in 18 MΩ deionized water. Following this, the samples were dried at 50°C. The bottles were then filled with 30% H_2O_2 (Merck Suprapur) and left for three days in order to remove any organic material from the sample surface. Next, the samples were rinsed and soaked in deionized water for another three days before drying at 50°C overnight. The dry samples were then powdered with an agate mortar and pestle and stored in small sample bottles.

2.2. Preparation of acid digests of coral powders

Dissolution in hydrochloric acid

About 200 mg of the powdered samples were weighed into 100-ml glass flasks. Samples were weighed out in duplicate in order to allow measurements both in HCl alone and in HCl–H_2O_2. Samples were dissolved in 0.5 ml of 30% HCl (Merck Suprapur). Dissolution was carried out at room temperature for 3 h. The digests were then diluted to 100 ml with deionized water.

Dissolution in hydrochloric acid and hydrogen peroxide

To evaluate the possible importance of organically bound phosphorus, the set of duplicate samples was dissolved in HCl as described above. In a second step, 1 ml of 30% H_2O_2 (Merck Suprapur) was added to destroy organic matter. The samples treated with H_2O_2 were warmed in a water bath at 50°C for 3 h in order to accelerate the oxidation process. Following this, the solutions were heated to 90°C to decompose any unreacted H_2O_2. This ensured that no further oxidation could take place. Trials

were made with H_2O_2 ranging from 1 to 5 ml, but 1 ml was found to be optimal. These digests were also diluted to 100 ml with deionized water.

2.3. Calibration of the ion chromatograph

Standards prepared in hydrochloric acid

Stock solutions were made up in 200 ml of deionized water from 1000 mg/l nitrate, phosphate and sulphate standards (Merck). From the stock solutions, the following working standards were prepared: 20, 40, 60, 80 and 100 ng/g (ppb) nitrate, 100, 200, 300, 400 and 500 ng/g phosphate and 0.5, 2.5, 5.0, 7.5 and 12.5 μg/g (ppm) sulphate. Suprapur HCl was used in the standards at the same concentration as in the samples to reduce the error of the analysis (i.e. matrix effect and/or blank values). The standards and samples were passed through a chloride-removal cartridge (Dionex OnGuard AG) to eliminate Cl^- prior to injection (Fig. 1). One cartridge was used per sample. Previous studies have shown that this cartridge has no significant effect on the measurement of HPO_4^{2-} even at concentrations of 20 ng/g [10]. The linearity of the standards was excellent in each case ($r^2 > 0.999$).

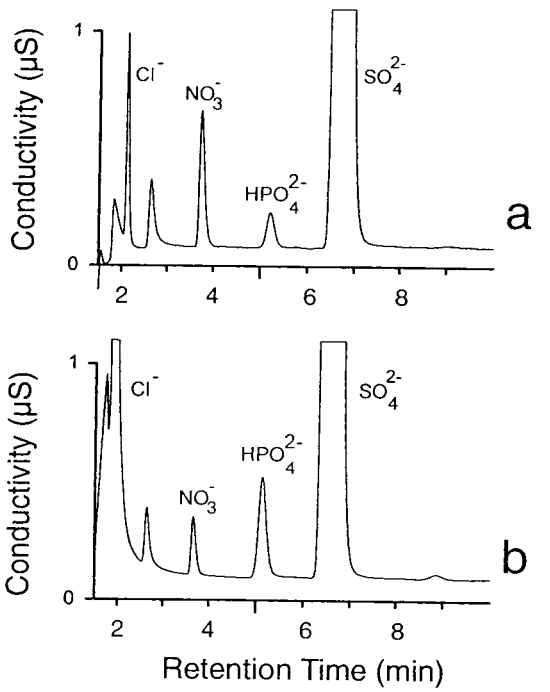

Fig. 1. (a) Chromatogram showing nitrate (150 ng/g), phosphate (150 ng/g) and sulphate (7.5 μg/g) in a working standard (HCl matrix), following injection through an AG chloride-removal cartridge. (b) Chromatogram showing nitrate (67 ng/g), phosphate (449 ng/g) and sulphate (10.9 μg/g) in an HCl digest of a coral skeleton, following injection through an AG chloride-removal cartridge.

Standards prepared in hydrochloric acid and hydrogen peroxide

The contribution of H_2O_2 to the blank values was evaluated by preparing three anion working standards in HCl and analyzing them with and without the addition of H_2O_2. After calibrating the IC system with standards made up only in HCl, the same standards were analyzed in duplicate after adding H_2O_2. Blanks containing only HCl and H_2O_2 were also measured. After correcting for blank values (phosphate in the blanks was below the limit of detection), nitrate and sulphate concentrations in the standards consisting of HCl plus H_2O_2 were 5–10% below the concentrations in the standards containing only HCl. At this time no explanation is given for this difference.

2.4. Accuracy, precision and quality control

There is no calcite or aragonite standard reference material certified for either nitrogen or phosphorus. Thus, a quantitative evaluation of the accuracy of the analyses was not possible. Using blind standards after every sixth sample injection, the analytical procedure variability was estimated to be 9% for nitrate, 2% for phosphate and 0.5% for sulphate. The precision of the analyses diminished in the order sulphate > phosphate > nitrate because the concentrations of the anions in the digests also decreased in that order. Relative to the detection limits, the concentration ranges for these anions in the sample digests were: nitrate, 1–2 × ; phosphate, 3–10 × ; sulphate, 100 × . The precision of the nitrate

analyses could probably be improved simply by analyzing more concentrated solutions (e.g. by diluting the digest to 25 ml instead of 100 ml).

3. Results

3.1. Nitrate

Dissolution in hydrochloric acid

Corals from the Grande Rivière Noire Bay (slabs 1Ks, 5Ks, 6Ks) average 4.5 ± 0.5 ppm nitrate, compared with 2.2 ± 0.5 ppm nitrate for the samples taken from the lagoon (7Ks and 11Ks). Thus, the nitrate concentrations clearly distinguish coral specimens taken in the bay, which are closer to anthropogenic N inputs (primarily from fertilizers used in the sugar cane industry and from livestock), from samples collected in the lagoon, which are further from such N sources.

Dissolution in hydrochloric acid and hydrogen peroxide

The nitrate concentrations in the samples dissolved in HCl versus those dissolved in HCl–H_2O_2 were not significantly different. It appears, therefore, that organically bound nitrogen is not a quantitatively significant N pool in the corals.

3.2. Phosphate

Dissolution in hydrochloric acid

Samples from the bay average 55 ± 1 ppm phosphate, compared with 16 ± 1 ppm phosphate for the samples taken from the lagoon. Again, therefore, the measured phosphate concentrations clearly distinguish coral specimens taken in the bay, which are closer to anthropogenic P inputs (primarily from municipal sewage inputs and livestock), from samples collected in the lagoon, which are further from such P sources.

Dissolution in hydrochloric acid and hydrogen peroxide

Samples treated with HCl–H_2O_2 yielded phosphate concentrations that were up to 100% higher than the phosphate concentrations measured in HCl alone. With respect to core 11Ks from the lagoon, however, in some cases there was no significant difference between the two treatments. In most cases, samples treated with HCl–H_2O_2 yielded phosphate concentrations that were 50% higher than the phosphate concentrations measured in HCl alone.

The difference between these two kinds of digests is attributed to organically bound phosphorus, with the following *caveat*. It has recently been shown that H_2O_2 does not completely destroy the organic components present in calcium carbonate minerals. Full-strength Clorox (5% NaOCl) is more effective, and more or less completely destroys all types of organic materials [11]. Until measurements of phosphate concentrations are also performed using samples treated with NaOCl, the phosphate concentrations measured in HCl–H_2O_2 should probably be interpreted as an estimate of the lower limit of organically bound phosphorus in these samples.

3.3. Sulphate

The sulphate concentrations in the corals ranged from 516 to 596 ppm, about twenty times higher than phosphate. The much higher concentrations of sulphate reflect the relatively high concentrations of sulphate in seawater (approximately 2700 mg/l). Despite the high background concentrations of sulphate in seawater, specimens collected from the bay show on average significantly higher sulphate values in the HCl digests (567 ± 3 ppm) than those from the lagoon (540 ± 3 ppm). This may be an indication of anthropogenic sulphur inputs to the Grande Rivière Noire Bay and warrants further study.

4. Conclusions

Nitrate, phosphate and sulphate in the skeletons of the scleractinian coral *Porites lutea* can be measured with sufficient sensitivity and precision using IC. The samples are simply dissolved in high-purity, concentrated HCl, diluted to volume, and passed through a chloride-removal cartridge prior to injection. Nitrate and

phosphate concentrations were found to be significantly higher in the samples collected from the Grande Rivière Noire Bay compared to the lagoon. Thus, both nitrate and phosphate concentrations in the coral skeletons are useful environmental indicators of reef eutrophication. Despite the high background concentration of sulphate in seawater, measured sulphate concentrations were also higher in the corals from the Grande Rivière Noire Bay than from the lagoon. Thus, even sulphate may also function as an indicator of coastal marine pollution.

Adding H_2O_2 to these digests significantly increased the measured phosphate concentrations in the majority of cases; in some samples, the difference was as large as a factor of 2. The difference in measured phosphate concentrations between the HCl versus HCl–H_2O_2 treatments was attributed to organically bound phosphorus which is incorporated within the skeletal fine structure of the coral specimens. Further studies are needed to determine how much of the total concentration of organically bound phosphorus was liberated by treatment with H_2O_2.

Acknowledgements

This work is a summary of the Diploma Thesis by H.A.V., supervised by Dr. J. Geister. We are grateful to Prof. A. Matter of this Institute for providing all of the required laboratory facilities. Financial support from the Swiss National Science Foundation (Grants 21-30207.90 and 21-30207.92) is sincerely appreciated. René Trost (now at Dionex Switzerland) and Stefan Brand of Henry A. Sarasin AG (Basel, Switzerland) provided expert technical support with all aspects of IC.

References

[1] L. Hottinger, N. Muller, J. Muller and P. Vasseur, *Etude des Ecosystemes Littoraux de Maurice*, Rapport No. 1, Université d'Aix-Marseille I et III, Université de Maurice, 1990, 56 pp.
[2] F. Gendre, *Thèse Faculté de Sciences*, Institut de Géologie, Neuchâtel, 1992.
[3] J. Muller, *Etude des Ecosystemes Littoraux de Maurice*, Rapport No 5, Université d'Aix-Marseille I et III, Université de Maurice, 1991, pp. 255 and 257–294.
[4] I. Immenhauser-Potthast, *Ph.D. Thesis*, University of Berne, Berne, 1994.
[5] R.A. Pastorok and G.R. Bilyard, *Mar. Ecol. Prog. Ser.*, 21 (1985) 175.
[6] D.W. Kinsey and P.J. Davies, *Limnol. Oceanogr.*, 24 (1979) 935.
[7] D.I. Walker and R.F.G. Ormond, *Mar. Poll. Bull.*, 13 (1982) 21.
[8] R. Mitchell and I. Chet, *Microb. Ecol.*, 2 (1975) 227.
[9] R.E. Dodge, T.D. Jickells, A.H. Knap, S. Boyd and R.P.M. Bak, *Mar. Poll. Bull.*, 15 (1984) 178.
[10] W. Shotyk, *J. Chromatogr.*, 640 (1993) 309.
[11] S.J. Gaffey and C.E. Bronnimann, *J. Sed. Petrol.*, 63 (1993) 752.

ELSEVIER

Journal of Chromatography A, 706 (1995) 215–220

JOURNAL OF CHROMATOGRAPHY A

Detection of iodide in geologic materials by high-performance liquid chromatography

Jean E. Moran*, Ray T.D. Teng, Usha Rao, Udo Fehn

Department of Earth and Environmental Sciences, University of Rochester, Rochester, NY 14627, USA

Abstract

A method for the detection of iodide in geologic materials including surface and ground waters, brines, and extracts from sediment, plants, soil and crude oil is presented. The detection limit of the HPLC system under ideal conditions is 0.45 ng. Applications of the method are related to the use of the ^{129}I isotope system in environmental science and geology. Ion chromatography is used to monitor extraction of I and to determine total I concentrations from samples prepared for measurement of $^{129}I/I$ ratios by accelerator mass spectrometry. Methods of extraction and sample preparation are described.

1. Introduction

Geologic sample materials such as ground water, saline formation water, meteoric and surface water, and aqueous derivatives of soil, sediment, crude oil and vegetation may have iodine concentrations ranging from a few ppb to thousands of ppm (mass/mass). Methods of sample preparation for these materials, and measurement of iodide by HPLC are described here. Solid samples require off-line, pre-column derivatization, as iodine is bound in organic compounds. Our motivation for developing these methods is in the geochemical interpretation of iodine concentrations in natural waters and sediments, and for the preparation of samples for ^{129}iodine/iodine ratio determination. The ^{129}I isotope system has recently come into use in hydrogeologic studies, in marine chemistry and in investigations of releases from nuclear facilities.

A variety of methods have been used for the detection of iodine in geologic samples. Notable examples are Ce–As reduction catalysis [1], colorimetry [2,3], X-ray fluorescence spectrometry [4], and neutron activation [5–7]. Analysis by HPLC has several advantages over these methods, principal among them the greater dynamic range and lower detection limit for the ion chromatography (IC) system described below. These features are essential for the measurement of a wide range in I concentrations in the variety of sample materials analyzed. The small sample volume required to make a concentration measurement is also advantageous, especially if the sample will be used for ratio determination. ^{129}Iodine/iodine ratios are measured by accelerator mass spectrometry, which requires a sample size of approximately 1 mg I. Low I concentrations in some materials make extraction of 1 mg a significant challenge. Depending on the sample matrix, interferences present and

* Corresponding author. Present address: Department of Oceanography, Texas A & M University, College Station, TX 77843, USA.

0021-9673/95/$09.50
SSDI 0021-9673(94)01247-4

concentration level, HPLC has greater accuracy and better reproducibility than neutron activation or colorimetric methods. Interfering elements or compounds in geologic materials often make detection of I by GC or neutron activation impractical [6,7]. Unlike X-ray spectrometry, inductively coupled plasma, GSC, or neutron activation analyses, HPLC requires iodide in dilute aqueous solutions for sample injection. Extraction and conversion of iodine from solid samples into this form are accomplished in various ways, as described below. Lastly, the speed, ease, and relatively low cost with which iodide measurements can be carried out using this HPLC set-up make possible large-scale investigations involving numerous samples.

General anion-exchange columns and conductivity detectors are capable of separating and detecting iodide at levels of a few ppm in matrices with similar levels of other anions. However, natural materials typically contain much lower levels of iodine, and levels of other constituents that are several orders of magnitude higher. An HPLC system that relies on pre-column derivatization of halides to organo-halogen compounds and UV detection [8] and a flow-through electrode system [9], used for detection of trace iodide in natural waters and biological samples have previously been reported. In addition, an HPLC detection method for iodinated halogens which incorporates post-column, on-line UV irradiation prior to oxidative electrochemical detection, was developed for determination of trace levels of organoiodides in pharmaceuticals [10]. Compared to the method used here, those systems require more extensive sample treatment and are less versatile in the types of starting materials that can be analyzed. The detection limits and accuracy levels are similar to those reported here. Despite its advantages, this HPLC method is limited by its ability to detect only iodide. Therefore, if precise determination of concentrations for each of the various iodine species in the original sample matrix is critical, one of the methods referred to above may be more appropriate than the HPLC method described here.

The IC system configuration described here has excellent selectivity for iodide in a variety of matrices and a working range of a few ppb to approximately 100 ppm, which are required for analysis of geologic materials. Naturally occurring interferences are quite rare, and are restricted to organic derivatives. Under ideal conditions, this system has a detection limit (method limit of detection = $3s$, s = standard deviation at zero level) of 0.45 ng (equating to 1.8 ppb) with a reproducibility of 3 ppb standards of 7%. Reproducibility of standards, prepared from reagent grade KI diluted with distilled deionized water (18 MΩ), in the range 50 ppb–3 ppm is 3%.

2. Experimental

The IC system set-up described here was modified from the version suggested by the manufacturer, Dionex (Sunnyvale, CA, USA) for a series 2000i Dionex BioLC. Development of the system parameters is described in [11]. The separation column used is the Dionex AG7 —this is the "guard" column which is normally used to protect the longer analytical column (AS7). The AG7 column (5 cm × 4 mm I.D.) consists of 10-μm packing material and 350-nm microbeads with 5% latex cross-linking. Separation is by adsorption rather than by ion exchange with the hydrophobic functional groups on this column. The guard column is used alone for two reasons: the typical lifetime of a column used for derivatives of geologic materials is about 6 months (using 0.45-μm and organic filters for samples when necessary, and with an average daily use of approximately 5 h), so the lower expense of the guard column is attractive, and the time for a single analysis is shortened from 16 to 8 min, without degradation of peak separation. Detection is by amperometry (at a fixed potential: +0.8 V) with a Pt working electrode and a Ag/AgCl reference electrode. Results are improved by soaking the working electrode in a saturated KI solution after approximately 40 h use. The mobile phase used is 45 mM HNO_3, made with Ultrex ultrapure reagents. Using the shorter column, with a flow-

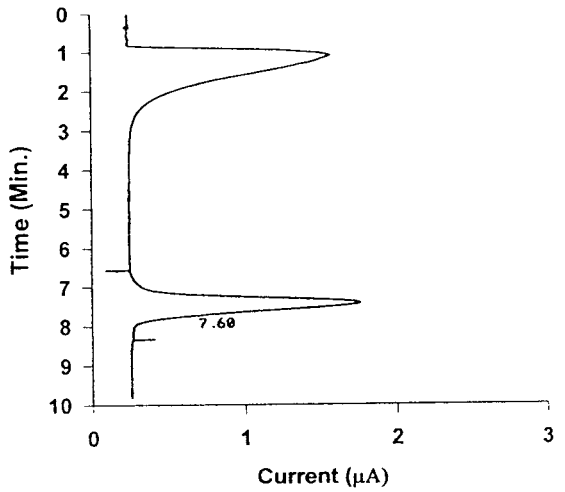

Fig. 1. Chromatogram from a sediment sample extract. Iodide concentration is 1.86 ppm; peak is labelled with a retention time of 7.60 min. The leading peak is 2 m*M* (sodium) hydrogensulfite —the collection solution and reducing agent. Injection volume is 250 μl; detection is by amperometry.

rate of 1.0 ml/min, the retention time for iodide is approximately 7 min. A SP 4400 Spectra-Physics integrator plots peak areas which are used for quantification. Good separation is achieved between iodide and other common anions, and between iodide and sodium hydrogensulfite, the reducing agent commonly used to convert any iodate present to iodide (Fig. 1). Sodium hydrogensulfite concentrations of up to 10 m*M* do not interfere with the iodide peak. For solutions with low I concentrations, a 250 μl sample is injected, however smaller sample loops can be used at concentrations above approximately 1 ppm. Organic pre-filters must be employed when organic compounds potentially exist in the sample matrix.

3. Off-line pre-column sample preparation

Table 1 shows the various types of materials from which iodine has been extracted, the preparation required for analysis by HPLC, and typical concentrations with associated accuracy. In general, our results for iodine concentrations in the original materials agree with concentrations determined by the other methods listed above. Direct comparisons were made with the colorimetric method for some saline water samples, and with the neutron activation method for two sediment samples. For the water samples, the absolute difference between the concentration values for the two methods was less than or equal to 5%, while results for the sediments agreed to within 12%.

For dilute waters from oxidizing environments including rainwater, snow, ice and some ground waters, iodine may exist primarily as iodate. Addition of a reducing agent, such as sodium hydrogensulfite is necessary to convert iodate to iodide. Experiments carried out on laboratory standards made from reagent grade KIO_3 and KI

Table 1
Summary of results for HPLC analysis of iodide in various sample matrices

Material	Preparation	Typical concentration range	Representative R.S.D. for HPLC method (%)
Meteoric waters	Conversion to I^-, concentration	<0.5 ppb–10 ppb	10
Hydrothermal and ground waters	Conversion to I^-	10 ppb–0.5 ppm	3
Saline water	Dilution	0.5 ppm–300 ppm	7
Sediment/soil extracts	Chemical breakdown and distillation	0.1 ppm–10 ppm	5
Plant/animal extracts	Single combustion or alkali leach and fusion	20 ppb–3 ppm	5
Crude oil extracts	Continuous combustion	0 ppb–50 ppb	10

salts indicate that 99.7% (R.S.D. of 0.4%) of IO_3^- is converted to I^- in the presence of excess sodium hydrogensulfite. While natural waters contain other species that will compete for reduction with iodate, the high sodium hydrogensulfite concentrations allowed by the system configuration (up to 10 m*M*; pH 5–6) are sufficient for most water compositions. For filtered natural water samples (in which only iodide and iodate are present and thermodynamically stable) iodate concentrations can be determined by the difference (iodide + iodate) − iodide. Preconcentration by vacuum distillation of extremely dilute samples such as continental rainwater may be required.

Oil field brines and other saline formation waters, which typically contain 100 g/l or more total dissolved solids, must be diluted by at least 10:1 for analysis by HPLC. Reproducibility is compromised and retention times are shifted for these solutions, because of extremely high anion (especially chloride) concentrations. Chloride/iodide ratios are generally in the range 500:1 to 1000:1. Although these fluids have naturally high levels of chloride, bromide, sulphate, nitrate, sodium, calcium, magnesium, ammonium and potassium, none of these was found to interfere with the iodide peak. Repeated measurements (at least 3) at various dilutions (at least 2) must be performed for each sample to achieve errors of $<10\%$. Dilutions of up to 500:1 (in which iodide concentrations would be ca. 0.5 ppm) may still be in a range well above the detection limit, in which the best results are achieved. In these waters, iodine should exist only as iodide given that the brines reside in a strongly reducing environment. Conversion to iodate may take place during sampling and/or storage, therefore treatment with a reducing agent may be necessary. If separation of inorganic and organic I species is desired, a solid-phase extraction filter such as Envirelut (Varian) can be used on fluid volumes of up to 2 l prior to sample preparation and concentration determination by HPLC.

Iodine is biophilic, and is bound to organic compounds in sediments and soils. Depending on the organic content of the sediment or soil, I levels may be <1 ppm to several hundred ppm. Although as yet untested, the method of extraction described here would also presumably work for ground or crushed rock material. Extraction of iodine from these materials is accomplished by chemical breakdown of organic molecules in an all-glass apparatus with nitric acid and 30% hydrogen peroxide. Iodine in the gaseous form (i.e., as I_2) is forced into a gas-washing bottle with nitrogen gas. The collection solution is 10–100 m*M* sodium hydrogensulfite, which reduces the iodine to iodide, and the concentration in the solution is then measured by HPLC. (See [12] for a more thorough description of the chemical procedure.) Depending on the sample size and the composition of the sample, extraction of the 1 mg of I necessary for ratio determination may take several days. Recovery rates for samples spiked with 1-iodooctadecane were 80–90%.

For samples with high iodine concentrations, or when removal of only a relatively small amount of iodine is necessary, extraction can be accomplished by a single combustion [13], or by alkali leach and fusion [14,15]. Combustion in oxygen of 10 g or less of material in a pressurized bomb is appropriate for samples consisting mainly of organic material. This includes plant and animal parts and hydrocarbons. Incomplete combustion due to the presence of inorganic compounds in the matrix results in poor reproducibility for soils and sediments. The alkali leach and fusion method involves heating a sample mixed with sodium hydroxide and sodium peroxide for 2 h at 600°C, and is likewise appropriate for relatively small sample sizes. Reported recovery rates for this method are approximately 80% for meteorite samples [14]. In these methods, the final collection solution contains a reducing agent and iodine as iodide. The collection solution can be injected for concentration determination after filtration through a 0.45-μm filter.

Once iodine concentrations have been measured, and 1 mg or more is collected in solution, the procedure for extraction of iodine into carbon tetrachloride and subsequent precipitation as silver iodide, as described in [16] is followed. Measurements of $^{129}I/I$ are made by accelerator mass spectrometry using a cesium sputter source

on solid AgI targets [17,18]. Ratios for pre-anthropogenic samples are in the range $20 \cdot 10^{-15}$–$1500 \cdot 10^{-15}$.

4. Applications

Iodine and its long-lived isotope ^{129}I have been used in a wide variety of applications in marine geochemistry and hydrogeochemistry. Iodine concentrations and pre-anthropogenic $^{129}I/I$ ratios have been used for identification of sources and tracing of migration pathways for hydrothermal waters [16] and sedimentary basin brines [12,19], and in other ground water studies [20–22]. For these applications, extraction of sufficient iodine for ratio measurement by accelerator mass spectrometry is straightforward, and the principal use of the IC system is in concentration determination. The advantages of the HPLC system described here are high selectivity, a high level of accuracy, and very little sample preparation at a low cost.

Natural $^{129}I/I$ ratios have also been used in the study of organic material dating and diagenesis in marine sediments [12]. HPLC is used for monitoring the extraction of iodine from the sediments, the course of which shows significant variation from sample to sample. This is due to variable sediment sample compositions, including organic contents ranging from 0.1 to 10% organic carbon and matrices consisting of, e.g., primarily silicates or primarily carbonates.

Investigations using anthropogenic ^{129}I have focused on tracking point source emissions from nuclear facilities [15,23,24], and using the anthropogenic input signal as a tracer for the marine carbon cycle and ocean circulation [25,26]. Because ^{129}I levels are quite high in most of these samples (which may be ground water, surface water, meteoric water, seawater, soil, seaweed or other plant or animal parts) the iodine extracted from them can be combined with carrier material of a known ratio to increase bulk material to form a suitably sized sample for measurement by accelerator mass spectrometry (AMS). Using this method, the overall accuracy of the ratio measurement depends on knowledge of the amount of I contributed from the sample and from the carrier material, so precise measurement of I concentration by HPLC is invaluable. I concentrations in the original material are determined from average recovery rates for the derivitization method chosen.

5. Conclusions

The HPLC method for detection of iodide described here has been applied to samples from a variety of geologic materials, including meteoric waters, ground waters, surface waters, saline formation waters, and derivatives of soils, sediments, crude oil and plant and animal parts. $^{129}I/I$ ratios were subsequently measured on AgI samples made from these materials. The HPLC method has the advantages of having a wider range and lower detection limit than other wet chemistry methods, and is more versatile with greater selectivity than GC or neutron activation methods. Under ideal conditions, this method has a detection limit of 0.45 ng and a reproducibility of standards of 3% in the optimum working range.

Acknowledgements

Funding for the purchase and maintenance of the IC system was provided by Texaco. Additional support came from the National Science Foundation grant EAR-9118879 and a grant from the American Chemical Society Petroleum Research Fund. Our appreciation for assistance in laboratory procedures goes to Bradley Ritts.

References

[1] V.W. Truesdale and C.P. Spencer, *Marine Chem.*, 2 (1974) 33.
[2] V.W. Truesdale and P.J. Smith, *Analyst*, 100 (1975) 111.
[3] S.D. Jones and V.W. Truesdale, *Limnol. Oceanogr.*, 29 (1984) 1016.
[4] R. Francois, *Geochim. Cosmochim. Acta*, 51 (1987) 2417.

[5] A.J. Bartel and H.T.J. Millard, in A.T. Miesch (Editor), *Geochemical Survey of Missouri; Methods of Sampling, Laboratory Analysis and Statistical Reduction of Data; Professional Paper 954-A*, US Geological Survey, Washington, DC, 1976, p. 15.
[6] M. Ebihara, N. Saito, H. Akaiwa and K. Tomura, *Anal. Sci.*, 8 (1992) 183.
[7] Y. Muramatsu and S. Yoshida, *J. Radioanal. Nucl. Chem.*, 169 (1993) 73.
[8] K.K. Verma, A. Jain and A. Verma, *Anal. Chem.*, 64 (1992) 1484.
[9] E. Nakayama, T. Kimoto and S. Okazaki, *Anal. Chem.*, 57 (1985) 1157.
[10] C.M. Selavka and I.S. Krull, *Anal. Chem.*, 59 (1987) 2699.
[11] K. Han, W.F. Koch and K.W. Pratt, *Anal. Chem.*, 59 (1987) 731.
[12] J.E. Moran, *Ph.D. Dissertation*, University of Rochester, Rochester, NY, 1994.
[13] S. Tullai, L.E. Tubbs and U. Fehn, *Nucl. Inst. Meth. Phys. Res.*, B29 (1987) 383.
[14] K. Nishiizumi, D. Elmore, M. Honda, J.R. Arnold and H.E. Gove, *Nature*, 305 (1983) 611.
[15] L.R. Kilius, J.C. Rucklidge and C. Soto, *Nucl. Inst. Meth. Phys. Res.*, B92 (1994) 393.
[16] U. Fehn, K.E. Peters, S. Tullai-Fitzpatrick, P.W. Kubik, P. Sharma, R.T.D. Teng, H.E. Gove and D. Elmore, *Geochim. Cosmochim. Acta*, 56 (1992) 2069.
[17] D. Elmore, H.E. Gove, R. Ferraro, L.R. Kilius, H.W. Lee, K.H. Chang, R.P. Beukens, A.E. Litherland, C.J. Russo, K.H. Purser, M.T. Murrell and R.C. Finkel, *Nature*, 286 (1980) 138.
[18] P.W. Kubik, D. Elmore, T.K. Hemmick, H.E. Gove, R.T.D. Teng, U. Fehn, S. Jiang and S. Tullai, *Nucl. Inst. Meth. Phys. Res.*, B29 (1987) 138.
[19] A.G. Collins, *Chem. Geol.*, 4 (1969) 169.
[20] J.T. Fabryka-Martin, D.O. Whittemore, S.N. Davis, P.W. Kubik and P. Sharma, *Applied Geochem.*, 6 (1991) 447.
[21] J.T. Fabryka-Martin, S.N. Davis and D. Elmore, *Nucl. Inst. Meth. Phys. Res.*, B29 (1987) 361.
[22] J.T. Fabryka-Martin, S.N. Davis, D. Elmore and P.W. Kubik, *Geochim. Cosmochim. Acta*, 53 (1989) 1817.
[23] M. Paul, D. Fink, G. Hollos, A. Kaufman, W. Kutschera and M. Magaritz, *Nucl. Inst. Meth. Phys. Res.*, B29 (1987) 341.
[24] U. Rao, U. Fehn and R.T.D. Teng, *Geol. Soc. Am. Abstracts with Programs*, 26, No. 7 (1994) 33.
[25] D.R. Schink, P.H. Santschi, O. Corapcioglu, P. Sharma and U. Fehn, *EOS, Trans. Am. Geophys. Union*, 75, No. 3 (1994) 113.
[26] F. Yiou, G.M. Raisbeck, Z.Q. Zhou and L.R. Kilius, *Nucl. Inst. Meth. Phys. Res.*, B92 (1994) 436.

ELSEVIER

Journal of Chromatography A, 706 (1995) 221–228

JOURNAL OF CHROMATOGRAPHY A

Determination of nitrite levels in refrigerated and frozen spinach by ion chromatography

N. Bosch Bosch[a], M. García Mata[a], M.J. Peñuela[a], T. Ruiz Galán[b], B. López Ruiz[b,*]

[a]*Departamento de Nutrición y Bromatología II, Facultad de Farmacia, Universidad Complutense, 28040 Madrid, Spain*
[b]*Sección Departamental de Química Analítica, Facultad de Farmacia, Universidad Complutense, 28040 Madrid, Spain*

Abstract

The determination of nitrites in samples of spinach after different times of refrigeration and freezing was studied. After cooking, the liquid and solid obtained were analysed. Ion chromatography with electrochemical detection, in which cell is composed of a single large porous graphite working electrode, was used as these solutions had, in many instances, concentrations of nitrites around 50 ng/ml; these levels are close to, or even below, the determination limits of other analytical methods usually employed. However, using this electrochemical detection, the determination of levels around 20 ng/ml was performed with good accuracy. The results obtained indicate that the freezing procedure does not modify the nitrite levels of the samples. In contrast, the refrigeration technique produces a considerable increase in their concentration 4–8 days later.

1. Introduction

In recent years there has been growing concern about the role of the nitrite ion in metahaemoglobin formation and as an important precursor in the formation of N-nitrosamines, many of which have been shown to be carcinogens. This gives rise to nitrite toxicosis, which may be a serious problem in babies and adults [1]. The occurrence of nitrite salts in the environment and accordingly in food and, in addition, their use as food preservatives is widespread [2–4].

It is therefore important that sensitive and accurate methods be available for the determination of nitrite ion. A large number of methods have been developed for the determination of this ion, based principally on spectrophotometric and fluorimetric techniques, but these have limited sensitivity and accuracy which depend on unstable colors [5–10]. More recently, several voltammetric and polarographic methods have been reported [11–18], some limited by poor sensitivity and others by long analysis times or the need to be adapted to flow systems. However, methods based on solid electrodes are more desirable for sensing, flow applications and short analysis times.

In the last decade, ion chromatography (IC) has undergone significant changes. Nowadays it has a much wider scope, which ranges from the determination of inorganic and organic cations to that of inorganic and organic anions [19,20]. Conductivity detection has been improved in several respects such as high suppression capacity, which not only represented a significant

* Corresponding author.

0021-9673/95/$09.50
SSDI 0021-9673(95)00153-0

increase in sensitivity but also opened the door to gradient elution in IC using suppressed conductivity detection with corresponding optimization of the time and resolution of the chromatogram [21]. In spite of these improvements, conductivity detection has insufficient sensitivity for our aim of designing a procedure for detecting lower levels of nitrite in spinach.

Recently, various studies have been reported with some modification over traditional IC, using organic modifiers in the eluents [22], electrostatic separation [23], column switching [24], etc., with the aim of improving both the sensitivity and resolution in anion chromatographic separations. Most of these modifications require a special column treatment or equipment that is not always compatible with these determinations.

In this paper, a simple method based on the use of a very sensitive coulometric detector combined with a traditional separation exchanger for the determination of low concentrations of nitrites is discussed. After optimization of the method, it was tested with spinach samples in order to study the possible influence of the storage procedure and time on the nitrite content of this kind of vegetable. Spinach was chosen because it is one of the vegetables in which nitrites can most frequently be found. All the measurements were made simultaneously by the IC method and a reference spectrophotometric method and the results were compared.

2. Experimental

2.1. Chemicals

All chemicals were of analytical-reagent grade or HPLC grade (Merck, Darmstadt, Germany). Working standard solutions were prepared by appropriate dilutions of stock standard solutions. The pH was adjusted with aqueous sodium hydroxide. The eluents, standards and all solutions were prepared using ultra-pure 18 MΩ cm water obtained by passing doubly distilled water through a Milli-Q system (Millipore).

2.2. Apparatus

The components of the IC equipment were the following: a Kontron Model 320 high-pressure pump system, a Rheodyne injector with a 20-μl loop, a IC anion PRP-X100 column (5 μm particle size, 125 mm × 4 mm I.D.) (Hamilton) and an ESA Coulochem II coulometric detector equipped with a Model 5020 analytical cell. This cell contains two chambers in series; each chamber includes a porous graphite coulometric electrode (two high-surface-area electrodes), a double counter electrode and a double reference electrode in a stainless-steel body that is capable of withstanding pressures up to 600 psi.

All chromatograms were processed using the KONTRON called PC Integration Pack program.

The conditions for analysis were as follows: eluent, 2 m*M* phthalic acid–10% acetone (pH 5.0); flow-rate, 1.0 mL/min; injection volume, 20 μl; and oxidation potential, 700 mV. All measurements were carried out at room temperature. Under these conditions, the net retention time was 3.65 ± 0.5 min.

2.3. Sample preparation

Eight packages of each of three brands of frozen spinach were bought and kept at −18°C until their study. These samples were analysed during 4 months. At the beginning of each month we proceeded as follows.

The total contents of two packages of each brand of spinach were defrosted and their nitrite content was measured (DF). The spinach was then boiled together with 1 l of tap water to minimize errors in analysis due to different amounts of nitrites in different packets. The tap water used in the sample pretreatment was previously analysed and found to be free from nitrite. The time of treatment was about 5 min from the time it started to boil; the spinach was then cooled immediately and drained. The nitrite level was determined in both the cooking liquid (CL) and the cooked spinach (CS) and the remainder was reserved for subsequent treat-

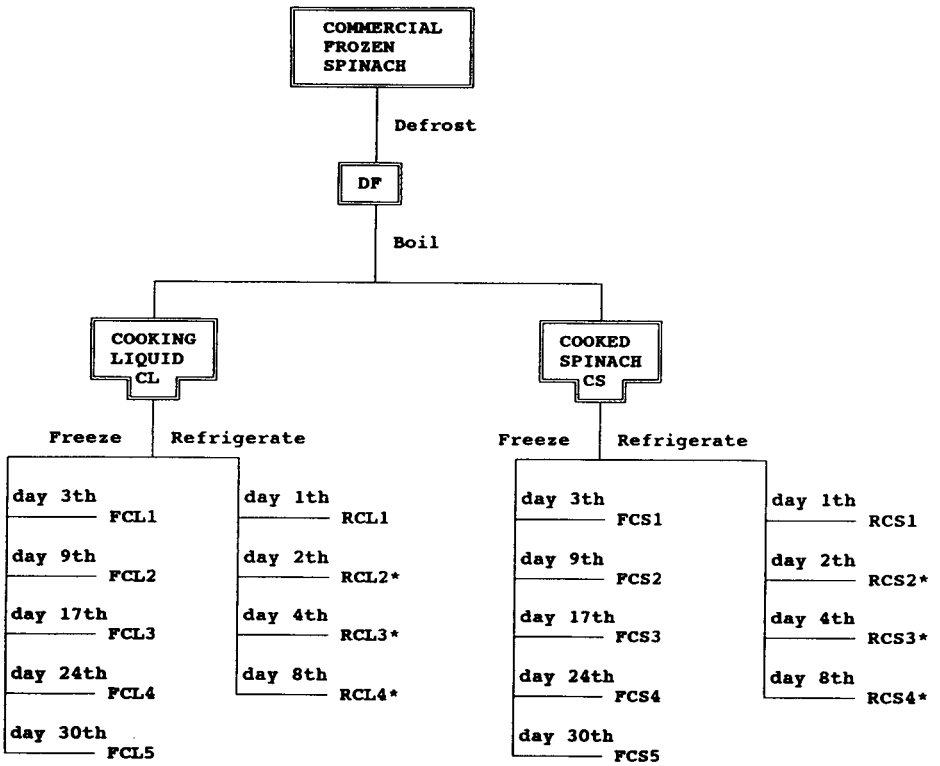

Fig. 1. Schematic diagram showing the treatment of the samples, the storage procedure and the day of analysis. * = sample whose nitrite level has been determined by spectrophotometric and ion chromatographic methods.

ment. One part, liquid and solids separated, was frozen (−18°C) and the other was refrigerated (2–5°C). Samples for measuring nitrite concentration were taken during 1 month as shown in Fig. 1.

In all instances, after trituration of the cooked spinach, three samples were taken from the homogenate for nitrite determination. Three aliquots of the cooking liquid were also analysed.

This procedure was applied in order to investigate the changes in nitrite content during storage. This study was another of the main objectives of this work.

The method used in nitrite extraction is described in the NORME AFNOR (FR-AFNOR-NF.V.04.409.1974) [25], which uses borax to reach a pH of about 8.6 to avoid nitrite destruction. Hot water extraction of this ion from samples was followed by cleaning, filtration and nitrite assay by the IC procedure.

3. Results and discussion

3.1. Spectrophotometric method

The most common procedure to determine nitrite ion is that in which, in the presence of acid buffer, nitrite is converted into nitrous acid, which diazotizes sulfanilamide. The diazotized product couples with N-(1-napthyl)ethylenediamine to produce a red-violet azo dye. The limit of detection for this method is 0.1 μg/ml in the final extract.

Only the nitrite level of the samples kept

under refrigeration for at least 4 days of storage could be determined by this method.

We observed a high dispersion of the nitrite content of these samples, which was in the range 12.18–177 mg $NaNO_2$/kg. As expected, the longer the storage time, the higher was the concentration of nitrites. In addition, higher levels of nitrites in the samples agree with a significant decrease in nitrate levels, which were also determined.

3.2. Chromatographic method

Preliminary experiments

We started this work with a traditional IC detection system, namely a conductimetric detector. The limit of determination for nitrites was found to be around 0.1 μg/ml with this kind of detector, but we expected to find lower concentrations in spinach samples, especially in those taken before storage. In addition, as the samples were boiled using the usual culinary procedure, we found a large peak corresponding to chlorides from sodium chloride whose retention time is lower than that of nitrites, making detection of the nitrite peak impossible. Because of these two problems we investigated other types of detection, and finally we chose electrochemical detection.

Factors affecting the detection system

In an electrochemical detector, for a given sample, the potentiostat applies a voltage to a working electrode. The potential is the driving force that causes an oxidation or reduction reaction to take place at the surface of the working electrode. Determination of sample concentration is based on the measurement of the current generated, which is proportional to sample concentration. Measurement of the current resulting from oxidation or reduction of a species at the surface of a working electrode is called amperometry. In the amperometric detector some fraction (usually 5–15%) of the species is oxidized (or reduced). In contrast, in a coulometric detector essentially 100% of the species is oxidized (or reduced). Since a coulometric detector has a very high conversion efficiency, it can provide an enhanced signal compared with an amperometric detector.

As the Coulochem II system contains two working electrodes, we first studied the influence of the working electrodes' potentials both on the oxidation current of the nitrites and on the elimination of possible interferences. After several experiments we found the optimum response when the potentials were +0.200 V for the first electrode and +0.700 V for the second whose current was measured and registered. Under these experimental conditions, Pearson's correlation coefficient for a concentration range of 20–100 ng/mL was 0.9968.

Results

In contrast with the reference methods, IC presents two advantages: a short analysis time, which was always around 5 min, and most important a suitable sensitivity and accuracy, as proof that the concentration of nitrites has been determined in all of the samples studied. Table 1 shows the results for the spinach just after defrosting, without cooking (DF) and just before cooking, liquid (CL) and cooked spinach (CS) before storage. The results are the means of three determinations. The relative standard deviations (R.S.D.s) were generally in the range

Table 1
Concentration of nitrites (mg $NaNO_2$/kg spinach) in spinach samples before starting the storage procedure during the 4 months after the purchase

Brand	Month	DF	CL	CS
A	1	1.82	N.D.[a]	1.32
	2	3.25	2.30	3.70
	3	N.D.	3.40	4.82
	4	2.67	1.80	4.30
B	1	2.20	1.44	1.53
	2	2.16	1.26	3.40
	3	1.83	4.80	1.84
	4	2.75	2.00	2.48
C	1	N.D.	1.40	1.80
	2	1.87	1.50	2.17
	3	1.64	1.50	2.20
	4	2.20	1.54	1.80

DF = defrosted sample; CL = cooking liquid; CS = cooked spinach.
[a] N.D. = not detected.

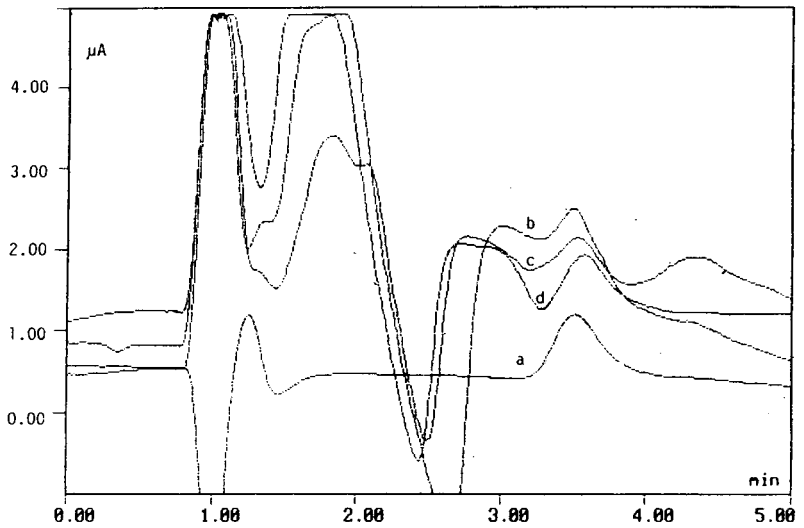

Fig. 2. Chromatograms of (a) standard solution of nitrite (80 ng/ml), (b) defrosted sample (DF), (c) cooked spinach (CS) and (d) cooking liquid (CL) of brand B analysed 4 months after purchase. Chromatographic conditions: IC anion PRP-X100 column, 5 μm particle size (125 mm × 4 mm I.D.); mobile phase, 2 m*M* phtalic acid–10% acetone (pH at 5.0); flow-rate, 1.0 ml/min; injection volume, 20 μl, electrochemical detection at +700 mV.

2–16%, being higher only in four instances. This study was carried out using three different brands and, as Table 1 shows, the levels of nitrites before storage were very similar, irrespective of the brand and the time for which they were stored before analysis. These levels were,

Table 2
Concentrations of nitrites (mg $NaNO_2$/kg spinach) during different times of both freezing and refrigeration storage procedures, expressed as the mean and relative standard deviation of twelve analyses from 4 months after the purchase

Brand	Freezing			Refrigeration		
	Day	Solid: FCS	Liquid: FCL	Day	Solid: RCS	Liquid: RCL
A	3	8.29 ± 5.02	5.13 ± 4.22			
	9	3.48 ± 1.05	2.34 ± 0.24	1	2.29 ± 0.77	2.14 ± 0.56
	17	3.23 ± 1.27	2.05 ± 0.70	2	3.77 ± 0.63	1.00 ± 0.11
	24	2.95 ± 0.90	1.52 ± 0.40	4	9.10 ± 10.2	7.16 ± 9.36
	30	5.60 ± 1.56	3.50 ± 0.44	8	[a]	[a]
B	3	3.94 ± 2.32	1.99 ± 0.92			
	9	3.90 ± 2.95	1.53 ± 1.19	1	3.71 ± 3.74	1.73 ± 0.97
	17	4.90 ± 2.98	2.71 ± 1.80	2	7.12 ± 7.36	2.00 ± 1.10
	24	4.36 ± 1.27	2.71 ± 1.55	4	15.5 ± 8.69	1.67 ± 0.53
	30	3.71 ± 2.36	1.82 ± 0.84	8	[a]	[a]
C	3	8.32 ± 6.32	4.50 ± 4.64			
	9	3.80 ± 1.28	3.20 ± 2.66	1	2.02 ± 0.36	1.82 ± 0.40
	17	3.40 ± 2.01	1.30 ± 0.30	2	4.77 ± 0.25	1.57 ± 0.27
	24	2.00 ± 0.75	1.49 ± 0.44	4	5.93 ± 3.49	6.35 ± 5.48
	30	2.80 ± 1.45	3.77 ± 3.20	8	[a]	[a]

[a] Samples also analysed by the spectrophotometric method.

fortunately and as expected, very low. The mean of all samples was 2.32 mg $NaNO_2$/kg spinach and the R.S.D. was 41%, but for brand C the mean was 1.78 mg $NaNO_2$/kg spinach and the R.S.D. was 16%.

The final concentration of nitrites is given in mg $NaNO_2$/kg spinach but the nitrite levels of the sample injected into the chromatograph were about 20–50 ng/ml. These results show that IC is a selective and accurate method even when the concentration of nitrite is very low.

The chromatograms in Fig. 2 correspond to a standard solution of 80 ng/ml of nitrite and to the defrosted (DF), cooking liquid (CL) and cooked spinach (CS) of brand B analysed 4 months after purchase.

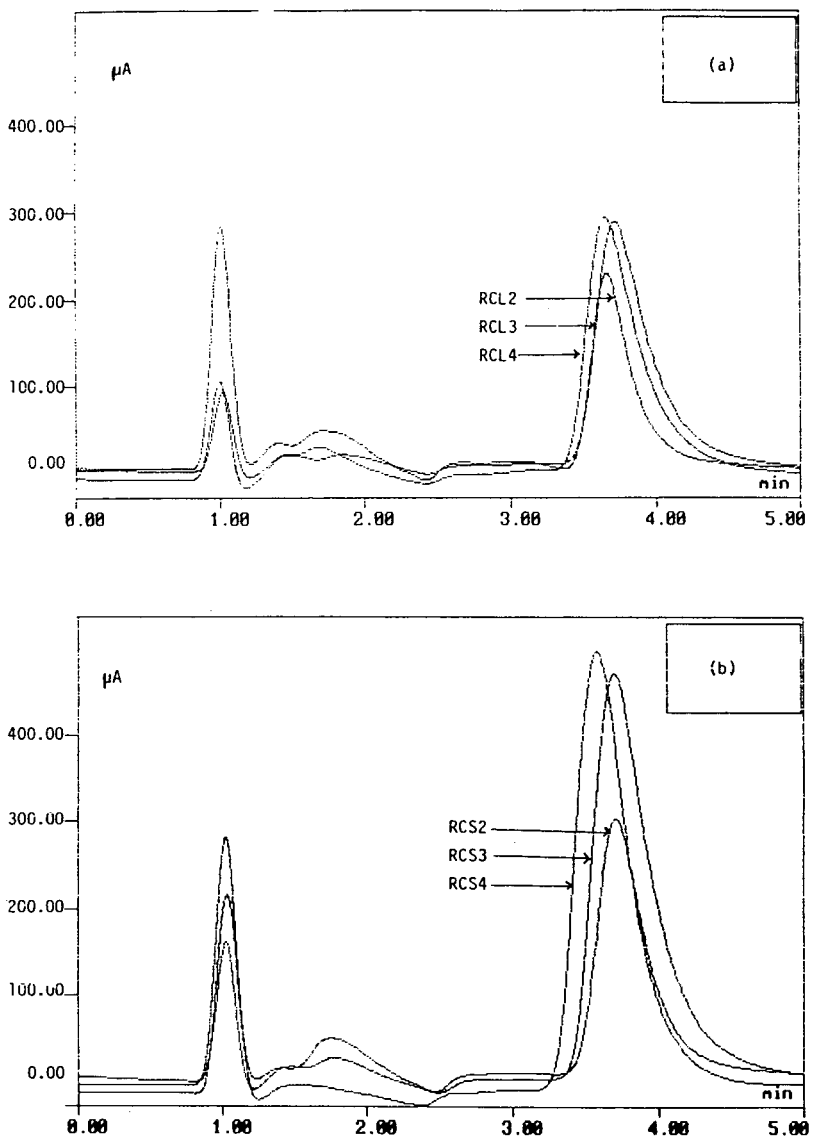

Fig. 3. Chromatograms of refrigerated samples for different times: (a) cooking liquid (RCL) of the samples and (b) cooked spinach (RCS). These determinations were started 4 months after purchase. Chromatographic conditions as in Fig. 2.

Table 2 gives the concentration of nitrites in the samples kept in storage, which could be determined only by IC because the limit of detection of the spectrophotometric method was above these levels. The dispersion of these results is due to the fact that the samples were analysed 4 months after purchase and the results, unlike those in Table 1, are assembled according to the days of storage but not to the months after purchase. However, these results show that the freezing procedure does not affect the nitrite levels. Storage for 2 days under refrigeration does affect the nitrite levels. These levels become significant after 4 days under refrigeration.

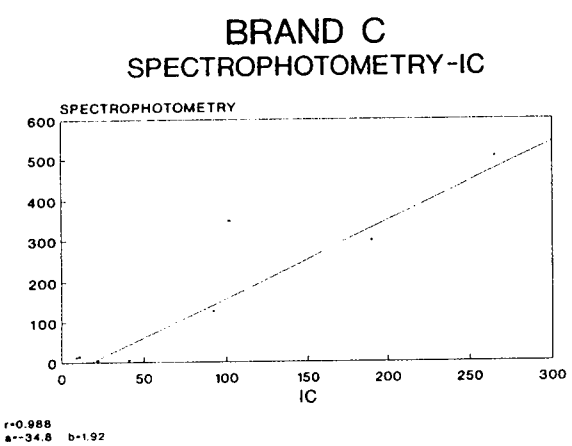

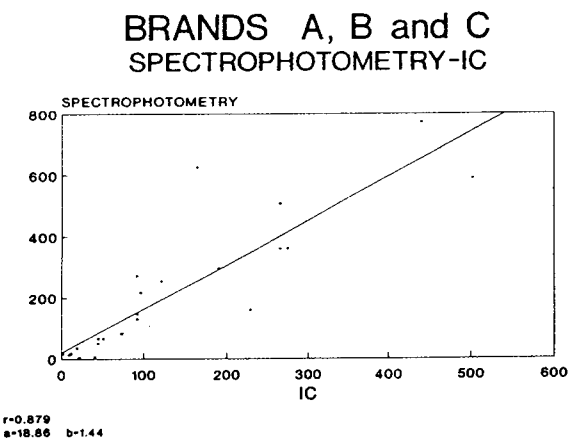

Fig. 4. Correlation graphs between the nitrite concentrations (mg $NaNO_2$/kg spinach) obtained by the spectrophotometric and chromatographic methods.

We were able to arrive at this conclusion because of the higher sensitivity of IC compared with the reference methods.

The remainder of the samples were analysed by both methods. Fig. 3 shows the chromatograms for the refrigerated samples. It is possible to see the evolution of the nitrite levels with the time of refrigeration, both in cooking liquid (RCL) and in cooked spinach (RCL). In these samples the concentration of nitrites increased significantly up to 700 mg $NaNO_2$/kg spinach.

Fig. 4 shows the correlation between the results obtained by the two methods studied when the concentration of nitrites was higher than the limit of detection of the spectrophotometric method. We can deduce that there is a good correlation between both methods except for brand B. Brands A and C show a good correlation coefficient but in both instances the slope was higher than unity, meaning that the results had the same tendency but the spectrophotometric values were always higher than chromatographic values. We can explain this as a result of the difference between the times of analysis: spectrophotometric analyses were made on the day of the extraction but the chromatographic analyses at least 2 days later. This time appears to be sufficient to cause oxidation of nitrite to nitrate.

4. Conclusion

Ion chromatography with electrochemical detection could be considered as a suitable method for the determination of nitrite in vegetable samples because of its detection limit, which is significantly lower than those of reference methods.

Concerning the other aim of our study, when the spinach is kept frozen, the nitrite levels remain unchanged, but the refrigeration procedure seriously affects the nitrite levels and these become dangerously high.

From these results we recommend that cooked vegetables should never be kept under refrigeration for more than 2 days.

References

[1] W. Lijinsky and S.S. Epstein, *Nature*, 223 (1970) 21.
[2] T. Shibamoto and L.F. Bjeldanes, *Introduction to Food Toxicology*, Academic Press, San Diego, 1993.
[3] J.M. Hill, *Nitrates and Nitrites in Food and Water*, Ellis Horwood, New York, 1991.
[4] J.M. Concon, *Food Toxicology. Principles and Concepts. Part A*, Marcel Dekker, New York, 1988.
[5] E. Szekely, *Talanta*, 15 (1968) 795.
[6] A. Chaube, A.K. Baveja and V.K. Gupta, *Talanta*, 110 (1984) 391.
[7] S. Flamerez and W.A. Bashir, *Analyst*, 110 (1985) 1513.
[8] J. Boussex, M. Junca and R. Lauret, *Ann. Technol. Agric.*, 29 (1980) 415.
[9] P. Brugel, *Ann. Technol. Agric.*, 34 (1980) 757.
[10] M. Cuzzoni and G. Gazzani, *Ind. Aliment.*, 18 (1979) 703.
[11] I.A. Cox and P.J. Kulesza, *Anal. Chim. Acta*, 158 (1984) 335.
[12] K. Kalcher, *Talanta*, 33 (1986) 489.
[13] A.P. Doherty, R.J. Forster, M.R. Smyth and J.G. Vos, *Anal. Chim. Acta*, 255 (1991) 45.
[14] C.M.G. Van der Berg and H. Li, *Anal. Chim. Acta*, 212 (1988) 31.
[15] Z. Gao, G. Wang and Z. Zhao, *Anal. Chim. Acta*, 230 (1990) 1.
[16] M. Lookabaugh and I.S. Krull, *J. Chromatogr.*, 452 (1988) 295.
[17] N. Gorbunov and E. Esposito, *J. Chromatogr.*, 619 (1993) 133.
[18] H.-J. Kim and Y.-K. Kim, *Anal. Chem.*, 61 (1989) 1485.
[19] H. Small, T.S. Stevens and W.C. Baumann, *Anal. Chem.*, 47 (1975) 1801.
[20] H. Small, *Ion Chromatography*, Plenum Press, New York, 1989.
[21] J. Weiss, *Ionenchromatographie*, VCH, Weinheim, 1991.
[22] J.D. Lamb and R.G. Smith, *J. Chromatogr.*, 640 (1993) 33.
[23] W. Hu and H. Haraguchi, *Anal. Chim. Acta*, 285 (1994) 335.
[24] C. Umile and J.F.K. Huber, *J. Chromatogr.*, 640 (1993) 27.
[25] *Determination de la Teneur en Nitrites (Méthode de référence). Viandes et Produits à Base de Viandes*, NORME AFNOR, NF.V.04.409, 1974.

ELSEVIER

Journal of Chromatography A, 706 (1995) 229–239

JOURNAL OF CHROMATOGRAPHY A

Control of errors in anion chromatography applied to environmental research

A.P. Rowland*, C. Woods, V.H. Kennedy

Institute of Terrestrial Ecology, Merlewood Research Station, Grange-over-Sands, Cumbria, LA11 6JU, UK

Abstract

Chemically suppressed ion chromatography has developed into a precise and reliable method for quantifying common anionic species. Equipment has improved, columns have been developed to offer faster analysis and three generations of chemical suppressors have evolved to provide easier care and improved performance. A range of sample types which include rainwater, soil solutions and canopy leachates have been analysed. A build-up of sample impurities gradually affects the performance of the column resulting in loss of separation and increase in mobile phase back-pressure over time. Approximately 8000 samples per annum have been analysed for chloride, nitrate and sulphate over a period of 11 years. A quality system describing calibration characteristics, measures of accuracy, precision and a model for quality control are presented.

1. Introduction

At Merlewood Research Station ion chromatography is employed routinely for the analysis of chloride, nitrate and sulphate in environmental samples. This technique is used in conjunction with inductively coupled plasma-optical emission spectrometry (ICP-OES) for cation analyses and continuous flow colorimetry for ammonium, phosphate, silicate and dissolved organic carbon to provide an analytical facility for ecological researchers. The laboratory has had 11 years experience in anion analysis using ion chromatography. During this period separator columns have improved and a new type of membrane suppressor has been developed. Ion chromatography provides a very reliable and robust analytical technique.

The Analytical Section routinely analyses rainfall, cloud water, throughfall/canopy leachates, soil solutions and stream/drainage water. Samples typically originate from projects studying nutrient cycling in forest or moorland ecosystems or monitoring pollutant movement. Throughput is in the region of 8000 aqueous samples per annum from sites and experimental plots distributed throughout the UK. Typically, samplings occur at fortnightly or monthly intervals, with researchers collecting and preparing samples for submission to the analytical laboratory. This experimental approach requires clear protocols in the field and the laboratory, as well as rigorous quality control (qc) procedures for analytical methods.

A variety of texts exist [1–3] providing general advice on types of quality control procedures with rare publications reporting the application of quality systems [4,5]. Mullins [3] proposed a working model for detecting bias from internal quality control. Within this model the fundamen-

* Corresponding author.

0021-9673/95/$09.50
SSDI 0021-9673(94)01151-6

tal problem is to establish a σ value for each determination which provides a realistic estimate of the spread of results. Miller's [6] statement that "the practical question is clear: should outlying results be rejected or not before the mean, standard deviation etc. of the data are calculated" focuses on the major issue facing laboratories who attempt to use "real" data-sets to establish working control limits.

The objective of this paper is to evaluate the components of the methodology needed to produce good quality data from chemically suppressed anion chromatography. It includes consideration of calibration procedures, column degradation and common interferences encountered in the analysis of mainly aqueous samples. The whole quality system is also reviewed. A method for quality control in water analysis using synthetic reference samples is proposed. Options for determining working limits for internal quality control, the use of control charts and the benefits of regular participation in a national proficiency testing scheme are discussed.

2. Experimental

2.1. Sample preparation

Samples are collected from the field site, filtered through GF/F filter within 24 h, stored at 4°C and analysed as soon as possible, usually within 4 weeks of collection. Immediately prior to ion chromatography, all samples are filtered through a glass fibre and a membrane filter (< 0.45 μm) and passed through a C_{18} cartridge to remove possible organic contaminants. To minimise sample processing cost, filters are used for a batch of (up to 25) samples or until difficulty is experienced in passing the solution through the filter. Filters are cleaned with 30 ml water between each sample to eliminate possible cross contamination of samples.

2.2. Equipment

Dionex 2010i ion chromatograph is used with a conductivity detector, auto sampler (ISCO) and sample load pump. A PC data system (AI450) is used to control automation through contact closures and to change ranges on the detector to optimise the performance for each ion (range settings $Cl^- = 300$ μS cm^{-1}, $NO_3^- = 10$ μS cm^{-1} and $SO_4^{2-} = 100$ μS cm^{-1}). A procedure has been established to wash each side of the 4-way injection valve between samples to prevent sample carry-over.

2.3. Column

The system is configured with AG4A guard and AS4A separator columns and operated with a mobile phase of $NaHCO_3$ (2.8 mM) and Na_2CO_3 (2.2 mM) at a flow-rate of 1.8 ml min^{-1}. k' Values are calculated from the relative separation of F^- (t_1) and SO_4^{2-} (t_2) [$k' = (t_2 - t_1)/t_1$]. A micro membrane chemical suppressor (0.0125 M H_2SO_4 flow-rate = 3 ml min^{-1}) reduces the background conductivity from the mobile phase.

2.4. Analytical run

The instrument is calibrated daily with 8 standards (prepared fresh each week) followed by an analytical run of 99 samples. There are drift check samples every 11 experimental samples and qc samples with each batch of samples (maximum of 25). Data is transferred from the chromatography software (.csv file) into the laboratory management system for report compilation.

2.5. Quality control samples

Synthetic solutions (Table 1) for use as quality control reference samples are analysed with each batch. Analytical data from these samples is used to verify that the analytical process is under control. It has been established that: each stock solution is stable for one year; separate synthetic reference solutions are needed for cation checks; working solutions are prepared on the day of analysis by accurate dilution of the stock solution (one hundred-fold); synthetic solutions are also

Table 1
Recipe for anion solution (stock reference 3)

Chemical	Weight (g)	Theoretical solution concentration (mg l^{-1})
NH_4Cl	0.382	15 Cl^-
NaCl	2.05	
$NaNO_3$	0.607	1.0 NO_3^--N
Na_2SO_4	1.059	2.5 SO_4^{2-}-S
Na_2SiF_6	0.671	1.0 Si
Na_2HPO_4	0.0687	0.15 PO_4^{3-}-P

Dissolve salts separately in water, combine and dilute to one litre.

stable at half concentration (Ref. [4]); a minimum of 2 qc samples need to be analysed with each batch of environmental samples to produce useful qc information.

2.6. Computation of standard deviation (σ) from quality control samples to derive warning and action limits for Shewhart charts

σ can be calculated by three alternative methods: (1) using the full data-set; (2) a computation based on the spread of the results within the inter-quartile range (IQR) i.e., sort data, determine median, divide data into quartiles, determine quartile range on quartiles adjacent to median (IQR); $\sigma_{(IQR)} = IQR/1.35$; (3) a computation of the median value of all the differences from the median; median of absolute deviation (MAD) = median $[|x_i - \text{median}(x_i)|]$; $\sigma_{(MAD)} = MAD/0.6745$.

2.7. Quality control model

Mullins [3] proposed the following model to evaluate quality control measurements: (1) one reading outside 3 standard deviations (σ); (2) nine points in a row on one side of the mean; (3) six points in succession increasing or decreasing; (4) fourteen points in a row alternating up and down; (5) two out of three points outside 2σ; (6) four out of five points in sequence greater than σ; (7) fifteen points in a row within plus or minus σ; (8) eight points in a row beyond σ (above or below).

In practice, we have found points 1, 2 and 5 the most useful indicators.

3. Results and discussion

3.1. Anion chromatography performance

Ions of interest

Ion chromatography is routinely used for the analysis of aqueous samples for Cl^-, NO_3^-, SO_4^{2-}. Sample phosphate-P concentrations in natural ecosystems tend to be low (0.005–0.2 mg l^{-1}), therefore they are more difficult to analyse under standard chromatographic conditions. In order to quantify low levels of P down to 0.005 mg l^{-1}, PO_4^{3-} analysis is more conveniently determined on a multi-channel continuous flow colorimetry system (molybdenum blue).

Calibration

Studies over a period of 10 years have repeatedly shown that there were significantly lower residuals when a 3rd order regression was applied to calibration data (Table 2). The same effect applied for the hollow fibre suppressor originally used and, more recently, to the replacement micro-membrane suppressor. The initial impression gained, on the evaluation of the correlation coefficient (r) (Table 2), is that the data fit is linear. Further examination of the correlation values (r^2) confirms that the relationship is best described by a 3rd order mathematical equation.

Duory-Berthod et al. [7] predicted deviation from linearity caused by the effect of the increasing hydrogen ion concentration during elution of the strong acid analytes as they suppressed the ionisation of carbonic acid. Polite et al. [8] investigated the chloride linearity of calibration with a micro-membrane suppressor over 5 orders of magnitude and reported linear calibration with a correlation coefficient of 0.9960. Chloride analysis over the calibration range 0.1 to 25 mg l^{-1} can yield a bias in the region of 5% (mid-

Table 2
Calibration data (May 1994)

Cl^- ($mg\,l^{-1}$)	Cl^{-1} area	NO_3^--N ($mg\,l^{-1}$)	NO_3^--N area	SO_4^{2-}-S ($mg\,l^{-1}$)	SO_4^{2-}-S area
0	4.4	0	0	0	82.4
2.5	147.0	0.3	403.4	1.0	360.9
5	326.6	0.6	734.5	2.0	687.5
7.5	427.7	0.9	1116	3.0	1036
10	602.4	1.2	1568	4.0	1449
15	904.9	1.8	2367	6.0	2235
20	1278	2.4	3220	8.0	3069
25	1671	3.0	4363	10	4072

Correlation coefficients from calibration data

Coefficient	Order of fit	Cl^-	NO_3^-	SO_4^{2-}
r		0.9979	0.9974	0.9973
r^2	1st	0.9957	0.9951	0.9946
r^2	2nd	0.9992	0.9991	0.9998
r^2	3rd	0.9994	0.9996	0.9998
Cl^-	$y = 6.32 + 59.6x - 0.281x^2 + 0.0225x^3$			
NO_3^-	$y = -4.39 + 1330x - 98.0x^2 + 46.4x^3$			
SO_4^{2-}	$y = 67.7 + 296x + 10.4x^2 - 0.00997x^3$			

range) for a linear calibration when compared to a 3rd order calibration prediction.

Care is required if laboratories adopt a policy of using computer 3rd order predictions for evaluating calibration response. False values may occur when samples exceed the value of the top calibration response by a factor of 2 (e.g., cloud water sometimes exceed concentrations of 50 mg l^{-1} Cl^-). Checking procedures need to be devised to monitor both the area and solution concentration in order to detect samples requiring dilution and re-analysis.

Contamination of columns by components from the sample matrix

The guard column, connected into the chromatography system, provides an effective and vital function in protecting the separator column. Soluble organic compounds or other soluble components of the sample, such as trace metals, present in samples collected for environmental studies gradually accumulate on the guard column. This deterioration in the column produces loss in separation efficiency in the system and poses a threat to the separator column. Soil solution from the organic horizon and stem flow from coniferous trees can have a significant impact (Table 3) on the guard column within a short period (e.g. 10 samples). In contrast, soil solution from mineral soil horizons, throughfall and rainfall do not contain sufficient contaminants to produce deterioration on the guard column.

Table 3
Effects of sample matrices on guard column efficiency ($n = 10$)

Solution matrix	k' Factor	Change detected
Rain	1.84	+0.03
Mineral soil solution	1.83	−0.01
Organic soil solution	1.68	**−0.15**
Throughfall	1.65	−0.03
Stem flow	1.48	**−0.18**

With use, the separation efficiency k' of the guard column is gradually reduced whilst there is also an associated increase in column back-pressure (Fig. 1). The manufacturers recommend columns should be cleaned or replaced when k' reaches half its original value. Leaks begin to occur, most notably in the load/inject valve, when the combined back-pressure of the guard and separator column exceeds 1400 p.s.i. (1 p.s.i. = $6.89 \cdot 10^3$ Pa). Guard columns are discarded when the combination of reduced separating efficiency and high back pressure results in unacceptable chromatographic performance which could lead to contamination of the analytical column. Sodium nitrate has been found to be the most effective salt for cleaning out contaminants from guard columns; note the improvements in performance at events 4, 10 and 17 (Fig. 1) after guard column clean-up.

Stationary phase cartridges provide a means of removing substances which contribute to deterioration in the guard column and in the performance of the chromatographic system. SEP-PAK C_{18} solid-phase extraction cartridges (Waters) absorb some of the organic content; 33 and 45% of the dissolved organic carbon, respectively, was removed from throughfall and from organic horizon soil solution. It is our policy to remove some of the contaminant loading from the sample before injection. However, in economic terms, it could be argued that the guard column itself gives effective protection and should therefore be regarded as disposable.

Chromatography interferences

Samples collected from upland areas or from forest ecosystems in the UK are typically from regions of higher than average rainfall. Under these circumstances, soluble organic compounds which co-elute, such as maleate or tartrate [9] are unlikely to be present in sufficient concentrations to significantly affect the quantification of chloride, nitrate and sulphate. Soluble low molecular mass organic acids, detected in cloud water samples and aqueous extracts of plant material, elute immediately following the solvent dip and are well separated from chloride. In contrast, extracts of soil or leaf material prepared in the laboratory may require sample clean-up, changes in chromatography or integration methodology in order to quantify components accurately. For example, in a study to investigate sulphate deposition onto *Pinus sylvestris*, a chloroform pre-extraction procedure was used to remove surface waxes prior to a water extraction. Residual amounts of chloroform eluted on the leading edge of the sulphate peak so that it was impossible to quantify the peak accurately. Chloroform contamination could not be removed from the sample matrix using solid-phase clean-up (C_{18}, CN or NH2); evaporation

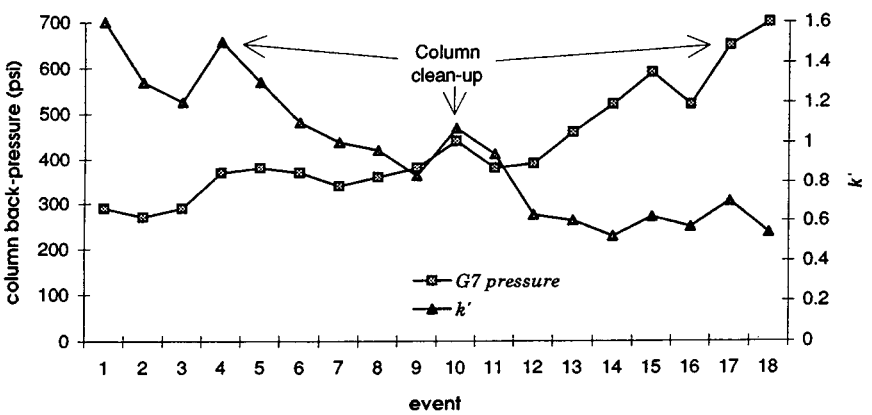

Fig. 1. Guard column back-pressure and k' over the period of analytical operation.

proved to be an effective method of contaminant removal.

3.2. Quality control for anion chromatography

Precision

Analytical laboratories gather data on the analytical performance over a period of time in order to understand the performance of the instrumental method and as a basis for establishing quality control data to validate each analysis.

Published values for within-batch precision are slightly lower than those achieved on a routine overnight analytical run (Table 4). Within-batch data is always superior to between-batch precision. Therefore, within batch qc sample data does not provide a realistic data-set from which to derive qc limits to detect bias. It would almost certainly be too strict and would result in large numbers of valid reference sample values being flagged as outliers.

Preparation of reference samples for quality control

There is a wealth of general information on the theory and framework for quality control systems in analytical laboratories. Unfortunately most of this information relates to laboratories specialising in a few specific methods for measuring concentrations well above the detection limit for the method. For environmental water samples, the main difficulty is in obtaining a quality control reference sample which is stable and suitable for measuring bias on multi-element analysers at concentration levels within the selected calibration range.

Internal reference samples are made up from salt solutions of known theoretical composition. They are prepared completely independently of calibration stock solutions (Table 1). To maintain reference solutions with solution concentrations typical of study samples, it was necessary to prepare separate qc reference sample solutions for cation and anion analysis. To ensure that stability of the reference samples is maintained, stock solutions are prepared at 100 times the required concentration, stored in the refrigerator and diluted daily for use. Sufficient reference solution is prepared for 1.5 years, with a policy to prepare fresh stock solutions annually. The preparation of new stock solutions for each of the two reference solutions is staggered by 0.5 years to ensure continuity is maintained. These solutions are reproducible in preparation and have provided analytical data for a stable qc system over the 2.5 year review period (Fig. 2).

Use of quality control reference solutions

Two qc samples, with different anion concentrations are analysed with each batch of study samples. This protocol has provided a suitable framework for collecting information on batch bias and as a means of validating analytical data for environmental samples over a period of 8 years.

Fig. 2 illustrates nitrate quality control data for qc reference solution 3. Sub-samples of reference 3 were analysed with each batch of samples to validate the analytical values obtained within that batch of determinations. Shewhart control charts, marking the means of the two reference solutions form a working basis for detecting gross error (e.g. points in the region of batch 150).

Table 4
Within batch precision data obtained on reference 3 solution (6-7-'94) ($n = 9$)

	Chloride	Nitrate-N	Sulphate-S
Mean (mg l^{-1})	15.9	1.16	2.90
Within batch σ	0.145	0.0101	0.0432
%R.S.D.	0.91	0.87	1.5
Within batch %R.S.D. [9]	0.7	0.7	0.5
Between batch %R.S.D. [9]	2.8	3.4	3.1

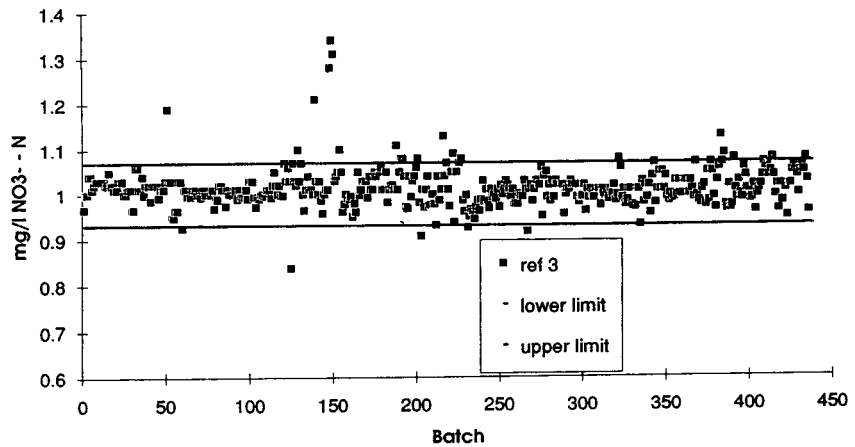

Fig. 2. Shewhart plot of NO_3^- qc reference sample 3 values obtained over a period of 2.5 years.

The plot of reference 3 NO_3^- data over a period of 2.5 years (Fig. 2) clearly shows that gross bias occurred around batch 150. Bias was confirmed by data obtained for the other qc solution analysed with those batches. It has been noted that such gross errors rarely occur and are detectable without recourse to sophisticated procedures. However, in addition to normal variation, it is evident that there are periods when the spread of data increases. This property influences the standard deviation of the data-set.

Interpretation and use of reference sample data

As discussed earlier, the main issue relates to whether any data points should be rejected from the data-set before computing standard deviation values [6].

Three general approaches are available for the treatment of outliers: parametric statistics —(Dixon or Gubbs tests) for normal distributions; non-parametric tests —inter-quartile range (IQR) and trimmed means; robust statistics —median absolute deviation (MAD).

In our experience, computation of warning and action limits at 2 and 3σ derived from the whole data-set is unlikely to provide a working system as the limits will be derived from data containing values obtained when the analytical system may have been out of control. Parametric methodology is a useful tool for rejection of one (or possibly two) outliers from a "normally distributed" population. However data-sets may be heavily tailed and skewed (Fig. 3). Non-parametric and robust statistics offer more acceptable approaches where outliers are accommodated rather than discarded and are applicable to data-sets which demonstrate non-normal distribution.

Over a short period, performance may be atypical and yield data for calculation of qc limits that are too narrow or too wide. For NO_3^- data, Table 5 shows that the analytical performance was far more precise during the first 30 determinations than during the 2.5 year period of the whole data-set, with performance over the most recent batches more typical of the whole review period. The spread of analytical data for the lower concentration reference 4 qc sample is slightly larger (0.5 mg l^{-1} NO_3^--N, 5.1% R.S.D.) compared toreference 3 (1.0 mg l NO_3^--N, 4.3% R.S.D.).

Practical significance of alternative computational methods for σ

In retrospect the qc data-set ($n = 436$) has been evaluated using a variety of basic statistical techniques and an assessment made of their application. The relative standard deviation (as %R.S.D.) computed from the median of absolute deviation (MAD) is similar to the %R.S.D. derived from the whole data-set. Ref. [4] (most recent data) is a heavily tailed distribution giving

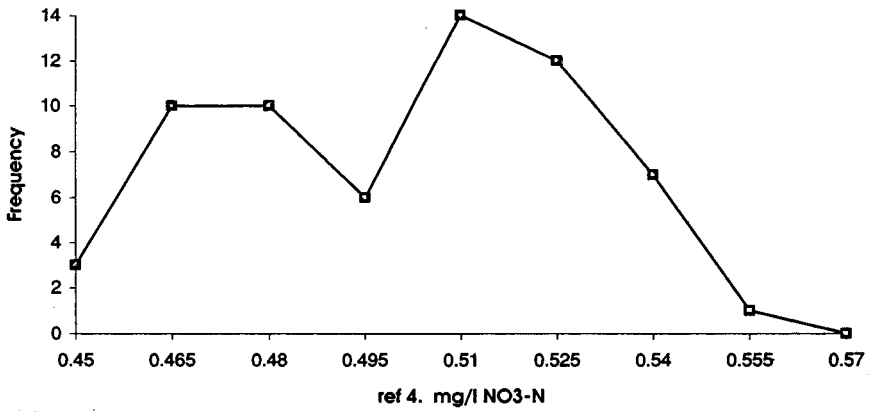

Fig. 3. Distribution histogram of recent NO_3^- qc reference sample 4 data ($n = 62$).

σ calculated from MAD slightly greater than σ calculated from the whole data-set [6]. Experience has shown that limits computed on this basis includes biased data and is therefore only useful for identifying gross error and does not detect analytical bias at an early stage.

The use of the inter quartile range to determine the standard deviation provides lower values for σ than the other calculation methods. The aim of any qc system is to detect small shifts in calibration at an early stage as well as gross bias in each batch, and the use of limits based on σ derived from IQR provides a basis for detecting change either by smaller amounts or at an earlier time than with wider limits. Statistically, this is a sound approach as the IQR σ is unaffected by extreme values. However in the practical application of 3σ limits based on a single qc analysis, 12% of nitrate reference 3 values are noted as outside analytical control. Analysis of two different control samples to confirm the presence of analytical error identifies only 3% of batches as biased. Further visual evaluation of the system retrospectively confirmed that this approach was practical and provided a working basis for detecting outliers and bias at an early stage.

Quality control charts and trouble shooting

Analysts use Shewhart charts to plot qc values which contain markings to indicate the mean or median, warning and action limits. We have found that this forms the basis of a good system to identify bias or gross error when used in conjunction with a protocol for identifying the occurrence of bias (Table 5). Examination of a plot of qc data for sulphate (Fig. 4) reveals a problem between batches 250 and 300. Graphically, a plot of the cumulative sum (CUSUM) of the difference from the mean (Fig. 5), provides an alternative charting tool. Whilst Shewhart charts provide instant recognition for one rogue

Table 5
NO_3^- reference 3 qc data for relative standard deviation derived by three alternative statistical treatments

% R.S.D. (Ref. [3])	$n = 436$	$n = 30$ (first 30 from 436)	$n = 62$ (most recent data)
Whole data-set	4.3	1.9	3.8
Inter-quartile range (IQR)	1.5	1.1	1.9
Median absolute deviation (MAD)	3.0	1.9	3.4

Table 6
Comparison of recent proficiency testing data with internal qc reference values

Chloride			Nitrate			Sulphate		
%qc bias	%AQ bias	z Score	%qc bias	%AQ bias	z Score	%qc bias	%AQ bias	z Score
−2	−6	−0.33	+5	−2	−0.13	−6	−2	−0.09
+5	−5	−0.23	−4	−2	−0.11	0	−4	−0.25
+3	−2	−0.03	+3	+3	+0.16	0	−5	−0.07
0	+2	+0.06	+1	+1	+0.09	+1	−9	−0.09
+3	−4	−0.15	−3	−3	−0.14	−2	−4	−0.18
0	−5	−0.28	0	−2	−0.11	−1	0	0

AQ = AQUACHECK, Water Research Centre.

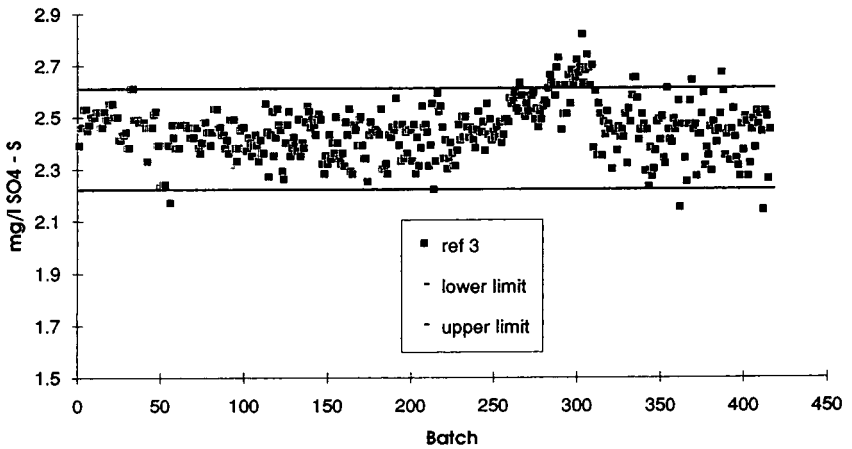

Fig. 4. Shewhart plot of SO_4^{2-} qc reference sample 3 values obtained over a period of 2.5 years.

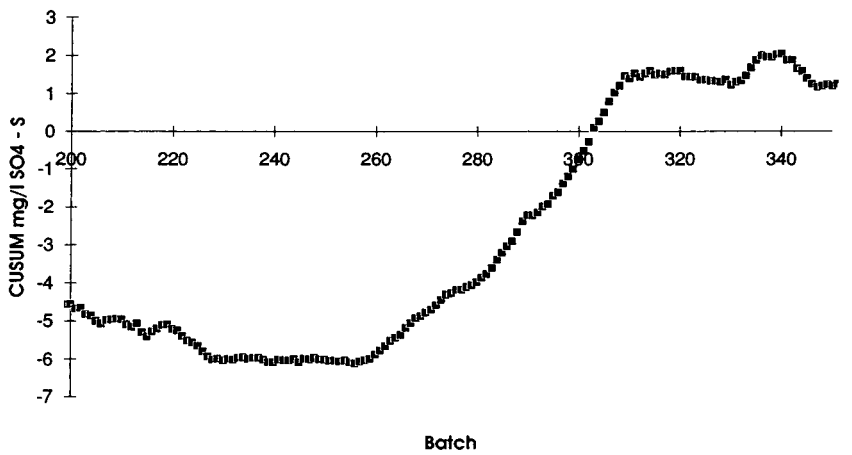

Fig. 5. CUSUM plot of SO_4^{2-} qc reference sample 3 values.

value, it is noticeably much easier to visualise the occurrence of a problem in the method with CUSUM charts, enabling the operator to detect the bias at a much earlier time than with Shewhart charts.

It proved to be particularly difficult to trace the source of the bias detected by the quality control system, especially as the bias seemed to be in all three anion components but with a much greater effect on sulphate results. Initially the chromatographer checked the most obvious causes of bias such as the stock solutions, the quality control samples, calibration equipment and injection modules. Eventually the source of the bias was traced to a faulty guard column.

Measures of accuracy

As part of the whole quality system, accrediting agencies insist on participation in proficiency testing schemes in order to assess proficiency against the wider analytical community. In the UK, the Water Research Centre (WRc) operate the AQUACHECK scheme to which nearly 400 laboratories from the water supply industry and research institutes subscribe.

Participation in a recognised proficiency testing scheme provides an external measure to link to internal quality control procedures, adds confidence to internal quality control procedures and provides a single point measure for detecting gross differences from the wider analytical community. It is important that samples received as part of a proficiency testing exercise are analysed using normal routine procedures in order that the data obtained provides an accurate picture of analytical bias.

z Scores represent an alternative way of displaying the relationship between the laboratory error and the maximum acceptable error for each determinand [z score = (result − reference value)/error threshold − z values > 1 indicate unacceptable results for monitoring drinking water]. Recent data collated from the ion chromatography tests (Table 5) show that the AQUACHECK z scores are very low for all three determinands and well below limits outlined in specifications. The bias values reported when the z score is low are not correlated with the data from the internal qc measure as all the data is within the experimental error of the method. Proficiency tests appear to provide a clear indication of significant bias from one single analysis when z scores approach unity. For smaller deviations it is possible to detect analytical differences from other laboratories over a longer period.

At a more detailed level: for Cl^-, the internal control samples indicates a different picture to the proficiency test results; NO_3^- —agree very closely with proficiency test results; SO_4^{2-} —one batch reported as 9% from proficiency test (z score very low), —in contrast within laboratory measure detected only 1% bias.

Participation in proficiency testing schemes is an important component of the overall quality system. It provides additional supporting information to validate instrumentation, methodology and internal quality control procedures. However results from inter-laboratory comparison tests should never be interpreted in isolation.

4. Conclusions

The most important aspects for controlling analytical error in anion chromatography are through establishing clear working protocols for the operation and calibration of the instrument, and through the application of robust quality control systems to validate analytical determinations.

Chemically suppressed ion chromatography of chloride, nitrate and sulphate produces non-linear calibration responses in the analytical ranges used in the analysis of environmental samples. It is recommended that multi-point calibration and a 2nd or 3rd order mathematical regression be applied to minimise calibration bias.

The integrity of the chromatography system may be maintained through routine use of sample clean-up to remove dissolved organic fractions before injection and through monitoring the guard column k' and back-pressure status. Experience has shown that interference from species which co-elute with Cl^-, NO_3^- and SO_4^{2-}

from aqueous solutions collected in ecological research are very uncommon and in low concentrations. Cross-ion interference is encountered in the analysis of extracts from soil or plant material for salt or mineral acid extractants.

A quality control system has been proposed to monitor for gross error or small shifts in bias: using two or more synthetic solutions of differing concentration; calculating mean, warning and action limits based on inter-quartile range values and reviewing the system periodically; constructing both Shewhart and CUSUM charts; rejecting data based on specified criteria (e.g. [3]) and on the basis of 2 or more qc sample values; participation in regular, well-organised inter laboratory proficiency testing schemes to validate internal qc procedures.

Acknowledgements

Thanks are expressed to Professor M. Hornung for comments on the script and to J.D. Roberts, A.L. Hodgson and J. Parrington for support in collecting and monitoring the data.

References

[1] O.L. Davies and P.L. Goldsmith (Editors), *Statistical Methods in Research and Production*, Longmans, 4th ed., 1984.
[2] Analytical Methods Committee, *Analyst*, 114 (1989) 1497–1503.
[3] E. Mullins, *Analyst*, 119 (1994) 369–375.
[4] J.A. Gardner, S. Coleman and S.G. Farrow, *Anal. Proc.*, 30 (1993) 292–295.
[5] V.H. Kennedy, A.P. Rowland and J. Parrington, *Commun. Soil Sci. Plant Anal.*, 25 (1994) 1695–1627.
[6] J.N. Miller, *Analyst*, 118 (1993) 455–461.
[7] M. Doury-Berthod, P. Giampaoli, H. Fitsh, C. Seila and C. Poitrenaud, *Anal. Chem.*, 57 (1985) 2257–2263.
[8] L.D. Polite, H.M. McNair and R.D. Rocklin, *J. Liq. Chromatogr.*, (1987) 829–838.
[9] Methods for the Examination of Waters and Associated Materials (MEWAM), *The Determination of Anions and Cations, Transitional Metals, Other Complex Ions and Organic Acids and Bases in Water by Chromatography 1990*, HMSO, London, 1990.

ELSEVIER

Journal of Chromatography A, 706 (1995) 241–247

JOURNAL OF CHROMATOGRAPHY A

Ion chromatographic determination of major ions in fog samples

M. Achilli[a,*] L. Romele[a], W. Martinotti[b], G. Sommariva[c]

[a]*CISE SpA, Via Reggio Emilia 39, 20090 Segrate (MI), Italy*
[b]*ENEL SpA CRAM, Via Rubattino 54, 20154 Milan, Italy*
[c]*DIONEX Srl, Via Grigna 9, 20155 Milan, Italy*

Abstract

An ion chromatographic configuration including column switching and gradient elution was used for the determination of major cations (Na^+, Ca^{2+}, Mg^{2+}, K^+, NH_4^+) and anions (Cl^-, NO_2^-, NO_3^-, SO_4^{2-}) in fog water samples. The results showed that ion-exchange chromatography compares very well with the more generally used spectroscopic techniques for cation determinations. Detection limits range from 6 μg/l (Na^+) to 40 μg/l (K^+). Precise and accurate analysis of natural fog water samples can be performed with cost and time savings in comparison with other techniques.

1. Introduction

Past observations on the chemical composition of fog water samples collected in Europe, Japan and USA have revealed high acidity [1–3] associated with high concentrations of NO_3^- and SO_4^{2-} [4,5]. These results have given rise to concern over potential damage to vegetation, materials, crops and public health, with growing evidence that the pollutant input in areas characterized by high fog occurrence can be relevant to terrestrial ecosystems. Lindberg et al. [6] and Saxena and Lin [7] suggested that the environmental impact of acidic fog can be as great as, if not greater than, that caused by acid rain.

The chemical composition of fog water as collected from different sites has been determined by several workers [1,8–12]. Spectroscopic techniques have widespread use in the determination of major cations in liquid samples especially, inductively coupled plasma atomic emission spectrometry (IC-AES) (Ca^{2+}, Mg^{2+}, Na^+) and flame atomic emission spectrometry (FAES) (K^+).

For NH_4^+ determination, the indophenol spectrophotometric method [13] is used normally in manual or automatic systems [flow-injection analysis (FIA)]. Ion chromatography (IC) is generally used for major anion determinations analysis (NO_3^-, SO_4^{2-}, Cl^-, NO_2^-, PO_4^{3-}) [14–18].

In this paper, an IC remote-controlled switching technique with two-column operation is described for both cation and anion determinations in fog water samples. A comparison was made between this and other generally used techniques in our laboratory for alkaline and alkaline-earth metals. The replacement of the potentially dangerous and expensive tetrabutylammonium hydroxide regenerant with a recently developed

* Corresponding author.

0021-9673/95/$09.50
SSDI 0021-9673(94)01289-X

self-regenerating suppressor reduces environmental problems caused by liquid waste discharge. The IC technique was applied to fog water samples collected in Po valley (Northern Italy) during the winter season 1993–1994.

Experimental

2.1. Reagents

All chemicals were of analytical-reagent grade and all reagents, eluents and standard solutions were prepared using water purified with a Milli-Q system (Millipore).

NaCl, $NaNO_3$, Na_2SO_4, KH_2PO_4 and $NaNO_2$ (Fluka) were used to prepare stock standard anion solutions (1000 mg/l). Orion 951007 1000 mg/l N–NH_4 standard solution was used as the NH_4^+ stock standard solution. Carlo Erba 1000 mg/l atomic absorption stock standard cation solutions were used.

Sodium carbonate and sodium hydrogencarbonate (Merck) were used for preparation of the eluent for IC anion determinations and methanesulphonic acid (Fluka) for that for cation determinations.

2.2. Instrumentation

A modified Dionex 2000i ion chromatograph with a Dionex gradient pump, eluent degassing module and conductivity detector was used. Anions were separated on an AS4A-SC ion-exchange column (4 mm I.D.), with an AG4A-SC guard column, and detected after suppression with an ASRS1 anion electrical self-regenerating suppressor. Cations were separated on a CS12 ion-exchange column (4 mm I.D.), with a CG-12 guard column, and detected after suppression with CSRS1 cation electrical self-regenerating suppressor. Switching from the anion to the cation column was effected using a PC remote-driven dual stack nitrogen-actuated Dionex valve. Acquisition of data and chromatograms and remote control of instrumentation were performed with Dionex AI450 software on a PC station.

For comparison, a Spectroflame ICP atomic emission spectrometer was used for Na^+, Ca^{2+} and Mg^{2+} determination, a Pye Unicam flame atomic emission spectrometer was used for K^+ determination and a Lachat flow-injection instrument for NH_4^+ determination by the indophenol spectrophotometric method.

2.3. Anion-exchange chromatographic analysis

The anions Cl^-, NO_3^-, NO_2^-, PO_4^{3-} and SO_4^{2-} were eluted using eluent 1 (4 m*M* $NaCO_3$ + 2.4 m*M* $NaHCO_3$) and eluent 2 (Milli-Q-purified water) with a linear gradient programme from eluent 1–eluent 2 = 40:60 initially to pure eluent 1 after 12 min, at a flow-rate of 1 ml/min.

The injection volume was 100 μl, the run time was set to 12 min, the cycle time was 15 min per analysis and the conductivity detector full-scale was 30 μS.

2.4. Cation-exchange chromatographic analysis

Isocratic elution was used for Na^+, Ca^{2+}, Mg^{2+}, K^+ and NH_4^+ determination with 20 m*M* methanesulphonic acid as eluent (1 ml/min). The injection volume was 100 μl, the run time was set to 12 min, the cycle time was 15 min per analysis and the conductivity detector full-scale was 3 μS.

3. Results and discussion

3.1. Anion determination

A typical chromatogram is reported in Fig. 1, showing retention times for the various anions. With the actual operating conditions a good correlation for the calibration graph was obtained for all anions ($r^2 \approx 0.99$) in the range 1–20 mg/l (1–5 mg/l for nitrite). A quadratic fit was employed because of the behavior of high-concentration standard solutions: a positive deviation was observed, probably due to ageing of the column. This effect (mostly evident for sulphate and phosphate) was not studied further.

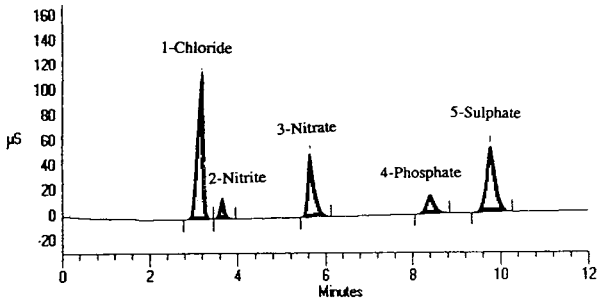

Fig. 1. Typical anion chromatogram for standard solution (4 mg/l NO_2^-, 10 mg/l other anions). Column, Dionex AS4A; injection volume, 100 μl; conductivity detector full-scale, 30 μS; gradient elution with carbonate eluent as described in the text.

The relative standard deviation was less than 1% at the 5 mg/l concentration level and between 0.7 and 3% at the 1 mg/l concentration level (Table 1).

A practical detection limit for the proposed method was calculated considering that during routine analysis a lower limit of integration is imposed corresponding to an area of 1500. Including also the effect of error in instrumental determination at low concentration, detection limits of 30 μg/l for chloride, 50 μg/l for nitrite, 60 μg/l for nitrite, 200 μg/l for phosphate and 40 μg/l for sulphate were obtained.

Table 1
Precision data for ion chromatographic determination of anions

Anion	R.S.D. (%)	
	1 mg/l[a]	5 mg/l[b]
Chloride	3.0	0.6
Nitrite	1.1	
Nitrate	0.7	0.6
Phosphate	2.0	0.8
Sulphate	1.2	0.6

Injection volume, 100 μl; detector full-scale, 30 μS.
[a] Sample size: 11.
[b] Sample size: 5.

3.2. Cation determination

Vial contamination

Two types of autosampler vials for standards and samples were tested for background contamination. Contamination from plastic and glass vials was checked before use. Whereas the contamination levels in glass vials for K^+, Mg^{2+} and NH_4^+ were below the detection limit, the levels for Na^+ and Ca^{2+} were higher (about 25 μg/l) and it was not possible to reduce them below the detection limit. Plastic autosampler vials showed a greater contamination problem. Even after repeated washings with nitric acid and Milli-Q-purified water in an ultrasonic bath the levels remained unchanged. The best results were obtained using new glass vials cleaned with Milli-Q-purified water in an ultrasonic bath six times for at least 10 min. Samples and standards were transferred directly to the vials, in order to avoid other sources of contamination. Glass vials not conditioned with acids are highly recommended, because the same vials can be used for anion analysis, thus saving time for complete analysis.

It must be remembered that cation concentrations in real fog water samples (see Table 5) are much higher than the contamination levels for Ca^{2+} and Na^+.

Linearity

Five standard solutions with increasing concentrations (0.2, 0.5, 1, 2 and 5 mg/l) were used for calibration for cation determinations (Ca^{2+}, Na^+, K^+, Mg^{2+} and NH_4^+). The calibration was linear for Ca^{2+} ($y = 85260x + 472.5$; $r^2 = 0.9998$), Na^+ ($y = 73670x = 680.5$; $r^2 = 0.9998$), K^+ ($y = 47220x - 1331$; $r^2 = 0.9998$) and Mg^{2+} ($y = 136800x - 1907$; $r^2 = 0.9998$), whereas the best fit for ammonium was a quadratic type ($x = 4.15^{-11}y^2 + 1.31^{-5}y - 0.09149$). For ammonium a negative deviation from linearity was observed, probably due to the decrease in mobility with increasing concentration. Interferences from the other cations were excluded because the same effect was observed for solutions containing NH_4^+ only at concentrations up to 20 mg N/l.

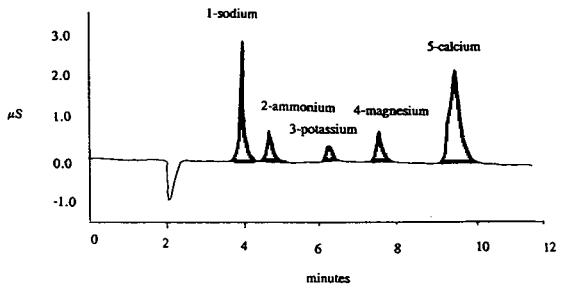

Fig. 2. Typical cation chromatogram for standard solution (2 mg/l all cations). Column, Dionex CS-12; injection volume, 100 μl; conductivity detector full-scale, 3 μS; elution with 20 m*M* methanesulphonic acid as described in the text.

Linearity was checked up to 20 mg/l using single-element standard solutions. From the practical point of view a quadratic fit must be used if ammonium is to be determined; if not, both types of fit can be used.

A typical chromatogram obtained for a standard solution is shown in Fig. 2.

Interferences

Possible interferences between alkali and alkaline earth metals were checked on single-element standard solutions by adding different concentrations of other alkali or alkaline earth metals and recording the value of the integrated areas. Preliminary results showed that some interferences between elements that elute close together are likely to exist, even if the data are sometimes contradictory; further studies are necessary.

Precision

The precision of the analysis of real samples was calculated at two concentration levels, as found into two fog water samples collected in the Po valley (Northern Italy). From Table 2 it can be seen that the relative standard deviation (R.S.D.) ranges from 0.67 to 5.03% for higher concentrations and from 1.57 to 3.32% for lower concentrations.

Accuracy

As internal reference materials for checking the accuracy of cation determinations, two artificial fog water samples were prepared and analysed with the proposed method. The results obtained were compared with the average data resulting from an intercomparison exercise on samples organized with other laboratories. As shown in Table 3, good accuracy can be obtained for all the parameters, recoveries ranging from 89.5 to 113%.

Detection limit

As for anion determinations, a practical detection limit for the proposed method was calculated considering a lower limit for area integration of 500. The calculated detection limits were

Table 2
Precision data for ion chromatographic determination of cations

Cation	Concentration (mg/l)	R.S.D. (%)	Concentration (mg/l)	R.S.D. (%)
Na^+	0.31	4.2 (1.0[a])	2.4	5 (0.5[a])
NH_4^+	2.73	1.6 (2.0[b])	27.02	2.4 (1.5[b])
K^+	0.21	4.8 (3.9[c])	1.77	4 (0.4[c])
Mg^{2+}	0.17	2.3 (0.4[a])	1.48	0.7 (0.3[a])
Ca^{2+}	0.52	3.3 (0.8[a])	4.26	0.9 (0.2[a])

Injection volume, 100 μl; detector full-scale, 3 μS; sample size, 10.
[a] By ICP-AES.
[b] By indophenol FIA spectrophotometric method.
[c] By FAES.

Table 3
Comparison between reference and found values for artificial fog water samples

Cation	Reference value[b] (mg/l)	Found (mg/l)	Difference (%)
Solution A[a]			
NH_4^+	200.9 ± 3.5	179	−11
Ca^{2+}	7.34 ± 0.15	7.27	−1
Mg^{2+}	4.27 ± 0.09	4.50	+5
Na^+	3.86 ± 0.10	4.02	+4
K^+	3.89 ± 0.03	4.02	+3
Solution B[a]			
NH_4^+	25.8 ± 0.3	24.7	−4
Ca^{2+}	0.97 ± 0.02	1.00	+3
Mg^{2+}	0.57 ± 0.01	0.62	+9
Na^+	0.48 ± 0.02	0.53	+10
K^+	0.51 ± 0.01	0.56	+10

[a] Solution A, high level; solution B, low level.
[b] Reference values ±95% confidence interval ($n = 9$).

6, 15, 40, 20, and 12 μg/l for Na^+, NH_4^+, K^+, Mg^{2+} and Ca^{2+}, respectively.

Comparison with other commonly used techniques

Comparison with spectroscopic techniques for Na^+, Ca^{2+}, Mg^{2+} and K^+ determination and the indophenol FIA spectrophotometric procedure for ammonium determination was carried out on the basis of precision, sensitivity and practical considerations on time and cost of analysis.

In our laboratory Na^+, Ca^{2+} and Mg^{2+} are normally determined using ICP-AES and K^+ by FAES. Detection limits for these elements are 10, 5, 2 and 10 μg/l for Na^+, Ca^{2+}, Mg^{2+} and K^+, respectively.

Except for Mg^{2+}, these limits are better than those previously reported for IC analysis; however, the latter are more than sufficient for cation determination in fog water samples. It must be remembered also that the calculated IC detection limits are practical limits for the method proposed in this work; the theoretical limits are lower.

The detection limit for ammonium is lower than that for the indophenol method (25 μg/l).

Precision data for cation determinations by spectroscopic and FIA techniques are reported in Table 3; the values range from 0.2 to 1.5% for higher concentration levels and from 0.4 to 3.9% for lower concentration levels. As shown, the results for ammonium are similar for both techniques, whereas for the other elements the spectroscopic precision is better than that for the IC technique, although in the latter case the R.S.D. is less than 5% and therefore suitable for fog water samples analysis.

The results show that for fog water analysis, the IC, spectroscopic and FIA methods have similar analytical performances and can be used for routine laboratory analysis. From the practical point of view it must be stressed, however, that with only the one IC instrumentation with the switching technique described in this work both cation and anion determinations can be performed in two successive runs in the same autosampler vials. Otherwise, three different analytical techniques must be used, with time and cost penalties.

In Table 4, data obtained from the IC analysis of real fog water samples are compared with results from spectroscopic techniques for calcium, sodium, potassium and magnesium. The agreement between the two series of data is acceptable for most of the samples; some of the differences can be explained by the fact that

Table 4
Comparison between ion chromatographic and atomic spectroscopic results for cation determination in fog water samples

Sample	ICP-AES			FAES	IC			
	Ca (mg/l)	Mg (mg/l)	Na (mg/l)	K (mg/l)	Ca (mg/l)	Mg (mg/l)	Na (mg/l)	K (mg/l)
MI14-93	4.09	0.49	1.81	1.61	3.82	0.49	1.61	1.87
MI15-93	4.26	0.34	1.36	1.79	4.11	0.40	1.03	1.86
MI16-93	2.03	0.34	0.76	1.21	1.85	0.35	0.72	1.36
MI17-93	4.87	0.48	1.09	1.57	4.61	0.50	0.98	1.59
MI19-93	4.32	0.44	1.39	1.57	4.05	0.46	1.24	1.76
MI21-93	2.89	0.31	1.20	1.60	2.69	0.34	1.11	1.97
MI01-94	4.29	0.62	3.02	2.14	4.39	0.71	3.13	2.54
MI02-94	2.37	0.19	1.32	0.65	2.67	0.33	1.44	1.03
MI03-94	3.28	0.36	2.34	1.61	3.33	0.48	2.27	2.29
MI04-94	N.D.	N.D.	N.D.	5.20	15.90	2.20	4.23	6.28
MI05-94	6.16	1.27	2.46	2.52	6.13	1.38	2.68	3.00
VE24-93	1.55	0.17	0.47	1.02	1.43	0.17	0.48	1.08
VE25-93	3.99	0.43	1.94	2.60	3.73	0.41	1.89	2.73
VE26-93	2.81	0.21	1.88	1.53	2.53	0.22	1.80	1.62
VE27-93	4.69	1.59	2.51	1.68	4.31	1.47	2.30	1.79
VE28-93	3.28	0.51	1.49	1.93	3.06	0.53	1.29	2.21
VE29-93	7.07	0.93	1.51	5.30	6.62	1.01	1.52	5.70
VE30-93	4.26	0.47	0.80	2.86	4.19	0.58	0.95	3.18
VE31-93	17.04	0.71	1.65	1.93	15.40	0.79	1.61	2.20
VE33-93	3.35	0.61	4.85	2.13	3.14	0.70	4.46	2.30
VE34-93	2.79	0.47	2.12	1.37	2.63	0.58	2.09	1.60
VE01-94	1.82	0.48	2.53	0.73	1.90	0.58	2.45	0.98
VE02-94	2.08	0.35	2.27	1.50	2.26	0.45	2.30	1.78
VE04-94	1.21	0.29	0.78	0.53	1.07	0.29	0.67	0.59

Samples were collected in the Po Valley (Northern Italy) during the winter season 1993–1994.

practical reasons led to a time delay between chromatographic and spectroscopic analyses.

Application to real samples

The proposed IC method was applied to the determination of major cations and anions in fog water samples collected in the Po valley (Northern Italy) during the winter season 1993–1994. Samples were collected by using an automatic sampler with a PTFE impactor; an automatic optical device allowed differentiation between fog and rain.

In Table 5, complete analytical results are reported. NO_3^- and SO_4^{2-} are the species that make the largest contribution to acidity, while NH_4^+ is the principal neutralizing compound, in particular in highly industrialized urban area [Milan (MI)].

4. Conclusions

The proposed IC two-columns switching technique is suitable for the rapid, precise and accurate determination of major cations and anions in fog water samples. Acceptable detection limits are obtained for all the ions. The time of analysis is significantly shortened as only one ion chromatograph is used, without the need for atomic spectroscopic and spectrophotometric (manual or automatic) instrumentation, thus lowering operational costs.

Environmental problems related to waste dis-

Table 5
Results of the analysis of fog water samples using the method described in this work

Sample	Cl (mg/l)	NO_2 (mg/l)	NO_3 (mg/l)	SO_4 (mg/l)	Ca (mg/l)	Mg (mg/l)	Na (mg/l)	K (mg/l)	NH_4 (mg/l)
MI14-93	9.92	<0.05	47	97	3.82	0.49	1.61	1.87	46.7
MI15-93	0.54	<0.05	<0.06	<0.04	4.11	0.40	1.03	1.86	155.1
MI16-93	6.52	<0.05	35	61	1.85	0.35	0.72	1.36	27
MI17-93	21.9	<0.05	83	149	4.61	0.50	0.98	1.59	88.1
MI19-93	14.9	<0.05	57	117	4.05	0.46	1.24	1.76	59.2
MI21-93	15.5	<0.05	71	115	2.69	0.34	1.11	1.97	67.7
MI01-94	28.3	<0.05	111	338	4.39	0.71	3.13	2.54	149.3
MI02-94	10.0	0.2	12	41	2.67	0.33	1.44	1.03	26.6
MI03-94	9.25	<0.05	103	95	3.33	0.48	2.27	2.29	57.1
MI04-94					15.90	2.20	4.23	6.28	141.1
MI05-94	12.6	33.5	370	200	6.13	1.38	2.68	3.00	163.7
VE24-93	2.60	3.4	28	36	1.43	0.17	0.48	1.08	21.8
VE25-93	12.4	1.3	20	28	3.73	0.41	1.89	2.73	15
VE26-93	2.78	4.8	46	31	2.53	0.22	1.80	1.62	23.9
VE27-93	10.4	3.5	50	37	4.31	1.47	2.30	1.79	26.7
VE28-93	11.8	3.0	44	130	3.06	0.53	1.29	2.21	66.1
VE29-93	13.4	5.5	77	141	6.62	1.01	1.52	5.70	73.4
VE30-93	5.33	7.7	44	42	4.19	0.58	0.95	3.18	37.3
VE31-93	8.51	6.8	68	123	15.40	0.79	1.61	2.20	59.2
VE33-93	9.34	3.6	38	110	3.14	0.70	4.46	2.30	47.2
VE34-93	9.02	<0.05	39	42	2.63	0.58	2.09	1.60	33.4
VE01-94	11.1	2.1	10	34	1.90	0.58	2.45	0.98	18.9
VE02-94	5.63	2.5	22	95	2.26	0.45	2.30	1.78	42.1
VE04-94	2.84	<0.05	155	34	1.07	0.29	0.67	0.59	45.7

Samples were collected in the Po Valley (Northern Italy) during winter season 1993–1994.

charge of potentially dangerous tetrabutylammonium hydroxide regenerant for suppression are avoided with the use of an electrical self-regenerating suppressor.

References

[1] D.J. Jacob, J.M. Waldman, J.W. Munger and M.R. Hoffmann, *Environ. Sci. Technol.*, 19 (1985) 730.
[2] J.W. Munger, J. Collett, Jr., B. Daube, Jr. and M.R. Hoffmann, *Atmos. Environ.*, 24B (1990) 185.
[3] J.M. Waldman, J.W. Munger, D.J. Jacob and M.R. Hoffmann, *Tellus*, 37B (1985) 91.
[4] J.W. Munger, D.J. Jacob, J.M. Waldman and M.R. Hoffmann, *J. Geophys. Res.*, 88 (1983) 5109.
[5] R.L. Brewer, E.C. Ellis, R.J. Gordon and L.S. Shepard, *Atmos. Environ.*, 17 (1983) 2267.
[6] S.E. Lindberg, G.M. Lowett, D.D. Richter and D.W. Johnson, *Science*, 231 (1986) 141.
[7] V.K. Saxena and H.H. Lin, *Atmos. Environ.*, 24A (1990) 329.
[8] J.M. Waldman, J.W. Munger, D.J. Jacob, J.J. Morgan and M.R. Hoffmann, *Science*, 218 (1982) 677.
[9] R.K. Kapoor, S. Tiwari, K. Ali and G. Singh, *Atmos. Environ.*, 27A (1993) 2455.
[10] E. Ganor, Z. Lebin and D. Pardess, *Atmos. Environ.*, 27A (1993) 1821.
[11] S. Fuzzi, G. Cesari, F. Evangelisti, M.C. Facchini and G. Orsi, *Atmos. Environ.*, 24A (1990) 2609.
[12] S.N. Pandis, J.H. Seinfeld and C. Pilinis, *Atmos. Environ.*, 24A (1990) 1957.
[13] *Standard Methods for the Examination of Water and Wastewater*, American Public Health Association, Washington, DC, 1985.
[14] C. Umile and J.F.K. Huber, *J. Chromatogr.*, 640 (1993) 27.
[15] H. Schumann and M. Enrst, *J. Chromatogr.*, 640 (1993) 241.
[16] V. Schwartz, *J. Chromatogr.*, 640 (1993) 299.
[17] W. Shotyk, *J. Chromatogr.*, 640 (1993) 309.
[18] R.A. Durst, W. Davison, K. Toth, J.E. Rothert, M.E. Oeden and B. Griepink, *Pure Appl. Chem.*, 63 (1991) 907.

ELSEVIER

Journal of Chromatography A, 706 (1995) 249–252

JOURNAL OF CHROMATOGRAPHY A

Cation trace analysis of snow and firn samples from high-alpine sites by ion chromatography

A. Döscher[a,*], M. Schwikowski[a], H.W. Gäggeler[a,b]

[a]*Paul Scherrer Institut, CH-5232 Villigen PSI, Switzerland*

[b]*Universität Bern, CH-3012 Bern, Switzerland*

Abstract

Ion chromatography with self-regenerating suppression and conductivity detection was used for the simultaneous determination of Na^+, NH_4^+, K^+, Mg^{2+} and Ca^{2+} in melted snow samples from high-alpine sites. Concentrations in the samples showed a high variability and were in the range of 0.3 to 800 μg/kg. Samples with concentrations higher than 2 μg/kg representing summer snow were analyzed using a 100-μl sample loop. In order to determine the low concentrations in winter snow samples (<2 μg/kg), preconcentration of 2-ml samples was applied resulting in improved detection limits of 0.1–0.4 μg/kg depending on the cation.

1. Introduction

Cold glaciers from high-alpine sites represent important archives to study the regional climate history. Firn and ice cores from such glaciers can be used to reconstruct the anthropogenic emissions in Europe [1]. Furthermore, they are the only archives allowing the reconstruction of the free tropospheric conditions. Free tropospheric conditions prevail during winter at high-alpine sites [2].

In the framework of the Swiss National Research Program NFP 31 "Climate Changes and Natural Disasters" an ice core drilling project was started at the Monte Rosa massif, Switzerland, in 1993. Test drillings of 5 to 7 m depth were performed to find a suitable site for a later deep core drilling. Snow samples from the test drilling of shallow cores were analyzed for Na^+, NH_4^+, K^+, Mg^{2+} and Ca^{2+}. These cations can be considered as tracers for different sources: Ca^{2+} and Mg^{2+} are components from the earth crust and indicate the amount of mineral dust; NH_4^+ is a tracer for anthropogenic activities while Na^+ is usually a mixture from two sources, seaspray and mineral dust [3].

As analytical method ion chromatography (IC) was applied, since only small sample volumes are available and the limits of detection are generally low. After the introduction of IC in the 1970s [4] a fast development of different techniques followed. However, the improvements were less pronounced for cation than for anion chromatography. For many years the analysis of samples with monovalent (Na^+, NH_4^+ and K^+) and divalent cations (Mg^{2+} and Ca^{2+}) was not possible by a single chromatographic run under fixed conditions [5]. Since then three different approaches for the determination of all cations in a single run were described: (a) using a gradient eluent [6], (b) eluent step change [6,7] and (c) column switching [6,8]. Quite recently the suc-

* Corresponding author.

0021-9673/95/$09.50
SSDI 0021-9673(95)00084-4

cessful separation of mono- and divalent cations by isocratic, single chromatography was introduced [9,10]. In order to decrease the detection limits to ultra-low ranges, preconcentration techniques using 5-ml samples were applied [9] or a larger sample loop of 500 μl was used requiring 5 ml of sample volume [8]. Both techniques consume relatively large sample volumes.

The concentrations of mono- and divalent cations in winter snow layers of high-alpine sites are very low and detection limits of about 0.1 μg/kg are needed. In order to achieve a good depth and corresponding time resolution, and to enable the determination of other parameters from the same core with comparable resolution, only small sample volumes are available for IC analysis. Therefore a preconcentration technique using a sample volume of 2 ml was developed, followed by separation in a single isocratic run. The concentrations of Na^+, K^+, Mg^{2+} and Ca^{2+} determined by ion chromatography were compared to analyses by inductively coupled plasma optical emission spectrometry (ICP-OES).

2. Experimental

2.1. Sampling

Firn core drilling was performed in June 1993 on Grenzgletscher (Monte Rosa massif) at an altitude of about 4200 m above sea level. The core was drilled with a 6 cm diameter electrical drill with an aluminum core barrel. Core sections with a length of 40 to 70 cm were recovered and packed in polyethylene tubes. During sample handling polyethylene gloves were worn to minimize contamination of the core surface. The packed core sections were transported in insulation boxes using dry ice to keep them frozen. Samples were stored in a deep-freeze and further sample preparation was performed in a cold room, maintained at −15°C. Core sections were cut into 5-cm pieces using a stainless steel knife on a PTFE plate. For each 5-cm sample a recoring technique was applied, by cutting out the inner part with a sampling vial (Sarstedt polypropylene, 2.8 cm I.D.). These decontaminated samples were melted prior to analysis using a microwave oven. The samples were not filtered before analyses to minimize contamination and sample consumption. The use of unfiltered samples did not influence the analytical performance of the column. More than thousand samples could be analyzed with the same column since only in very few samples a particle sedimentation was visible. All instruments and sample vials were firstly rinsed, secondly soaked for at least one week, and thirdly rinsed again with ultrapure water (18 MΩ cm quality).

2.2. Ion chromatography

Analyses were performed by a Sykam IC system consisting of a pump (S 8110), and a conductivity detector (S 3110, with a cell constant of 0.4), complemented by a Dionex precolumn (CG 12), a Dionex column (CS 12) and a cation self-regenerating suppressor [CSRS-I(4 mm)]. As eluent 6.5 m*M* methanesulfonic acid was used with a flow-rate of 1 ml/min. The obtained background conductivity was in the range of 0.62–0.88 μS. To inject samples without preconcentration an autosampler (Talbot ASI-5), equipped with a 100-μl sample loop, was used. In order to preconcentrate, the sample loop was replaced by a concentrator column (CG 12). The concentrator column was loaded by pumping 2 ml of the sample through it, using an infusion pump (Predicor 5003-1) equipped with a polyethylene syringe. After switching the injection valve the concentrator column was left in the eluent flow. Data were recorded with a Hewlett-Packard multichannel interface (HP 35900C) connected to a personal computer. Data evaluation was performed by ChemStation software (HP3365).

Standard solutions were prepared with the concentrations of NH_4^+ and Ca^{2+} being about five times higher than those of Na^+, K^+, Mg^{2+}, according to the usual composition of the snow samples. Stock standard solutions were prepared by diluting commercial standard solutions (Merck; 1000 mg/kg) every week, which were stored at 5°C in a refrigerator. Standard solu-

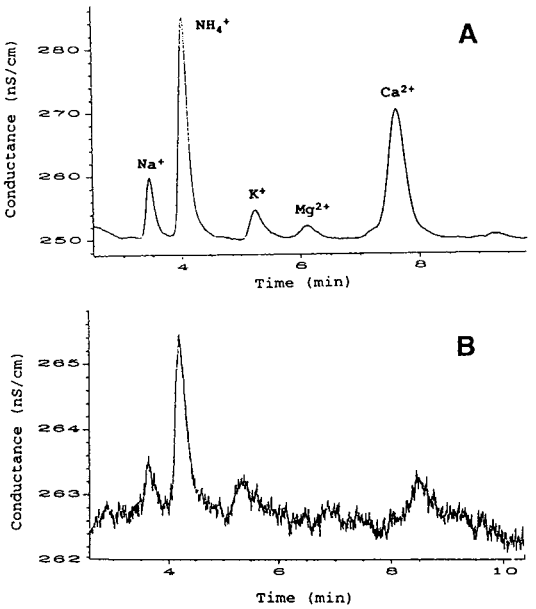

Fig. 1. Chromatograms of the same snow sample with (A) and without (B) preconcentration, with the following measured concentrations: 1.3 μg/kg Na^+, 4.5 μg/kg NH_4^+, 1.8 μg/kg K^+, 0.3 μg/kg Mg^{2+} and 5.7 μg/kg Ca^{2+}.

tions with concentrations <1 mg/kg were prepared just before calibration. All dilutions of standard solutions and all blank measurements were performed with ultrapure water (18 MΩ cm quality).

2.3. ICP-OES

The decontaminated samples were also analyzed by ICP-OES (ARL3410). For this analyses every sample (5 ml) was acidified with HNO_3 to about 0.1 *M*.

3. Results

Only with the preconcentration technique the very low cation concentrations in the winter snow samples could be determined, as shown in Fig. 1. The achieved limits of detection and the measuring ranges are listed in Table 1. To compare the achieved limits of detection with already published values, they were defined as the amount of solute producing a signal-to-noise ratio of 3. Previously reported values for Na^+ and Mg^{2+} [8,9] could be improved by a factor of about 2.5. The limit of detection for Ca^{2+} was lower by about a factor of 4 than that from Legrand et al. [9] and was similar to that from Buck et al. [8]. For K^+ similar values were obtained by our method and by Legrand et al. [9] and Buck et al. [8]. When the autosampler was used blank concentrations of about 8 μg/kg Ca^{2+} and about 4 μg/kg NH_4^+ were measured, resulting in relatively high limits of detection. With the preconcentration technique no Ca^{2+} peak above the background was observed, in-

Table 1
Measuring ranges and limits of detections with and without preconcentration

Cation	Without preconcentration		With preconcentration	
	Measuring range (μg/kg)	Detection limit (μg/kg)	Measuring range (μg/kg)	Detection limit (μg/kg)
Na^+	2–200	1.6	0.2–8.0	0.1
NH_4^+	15–200	7.5[a]	2.0–15.0	0.4[a]
K^+	4–200	3.2	0.2–8.0	0.2
Mg^{2+}	2–200	1.5	0.2–8.0	0.1
Ca^{2+}	20–300	10[a]	1.0–30.0	0.2

The limits of detection were defined as the amount of solute producing a signal-to-noise ratio of 3.
[a] The limits of detection were defined as the blank value plus 3 × the standard deviation of the blank value.

dicating that the autosampler caused some contamination. The blank concentration of NH_4^+ could also be reduced but not entirely eliminated. The blank value determined after preconcentration was in the range of 0.3 μg/kg, presumably caused by laboratory air. A dissolution of ammonia from laboratory air causing contamination was also observed by Legrand et al. [11] and Saigne et al. [12]. Our blank value could be kept stable by handling samples, standards, and blanks under identical conditions. The measuring ranges shown in Table 1 were suitable for most samples except for a few summer snow samples which were analyzed after diluting the sample. The relation between NH_4^+ concentration and conductivity was linear up to 200 μg/kg.

Ca^{2+} concentrations of the firn core samples analyzed by IC as well as by ICP-OES agreed well (Fig. 2). The same was true for Na^+, K^+ and Mg^{2+} (not shown). It is assumed that with IC only the dissolved part of the components is detected. However, the very good agreement with ICP-OES indicates that for this concentration range the undissolved mineral dust does not lead to an underestimation by the IC analyses. Limits of detection achieved by IC for K^+ and Na^+ were one order of magnitude lower than by ICP-OES and they were comparable for Ca^{2+} and Mg^{2+}.

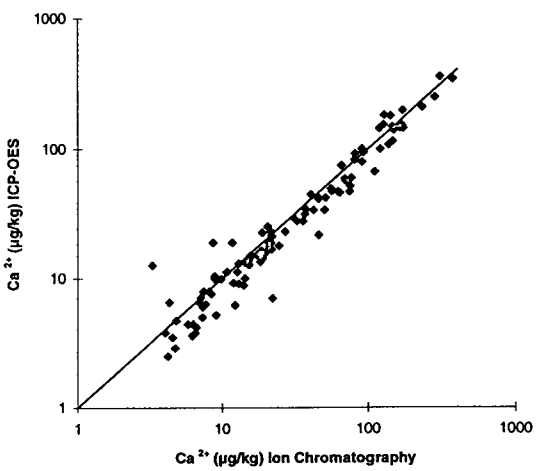

Fig. 2. Concentration of Ca^{2+} measured by ICP-OES as a function of the Ca^{2+} concentration measured by IC. The solid line represents the 1:1 relationship.

With the developed method concentrations of Na^+, NH_4^+, K^+, Mg^{2+}, Ca^{2+} in 2-ml samples of a firn core have been determined.

Acknowledgements

This work was supported by the Swiss National Science Foundation (NFP 31). We thank R. Keil for performing the ICP-OES analyses. Careful reading of the manuscript by Dr. U. Baltensperger is highly acknowledged.

References

[1] D. Wagenbach, K.O. Münnich, U. Schotterer and H. Oeschger, *Ann. Glaciol.*, 10 (1988) 183–187.
[2] U. Baltensperger, H.W. Gäggeler, D.T. Jost, M. Emmenegger and W. Nägeli, *Atmos. Environ.*, 25A (1991) 629–634.
[3] M. Schwikowski, P. Seibert, U. Baltensperger and H.W. Gäggeler, *Atmos. Environ.*, 29A (1995) in press.
[4] H. Small, T.S. Stevens and W.C. Baumann, *Anal. Chem.*, 47 (1975) 1801–1809.
[5] U. Baltensperger and S. Kern, *J. Chromatogr.*, 439 (1988) 121–127.
[6] R.D. Rocklin, M.A. Rey, J.R. Stillian and D.L. Campbell, *J. Chromatogr. Sci.*, 27 (1989) 474–479.
[7] R. Udisti, S. Bellandi and G. Piccardi, *Fresenius' J. Anal. Chem.*, 349 (1994) 289–293.
[8] C.F. Buck, P.M. Mayewski, M.J. Spencer, S. Whitlow, M.S. Twickler and D. Barrett, *J. Chromatogr.*, 594 (1992) 225–228.
[9] M. Legrand, M. De Angelis and F. Maupetit, *J. Chromatogr.*, 640 (1993) 251–258.
[10] U. Nickus and M. Kuhn, *J. Chromatogr. A*, 671 (1994) 225–229.
[11] M.R. Legrand, M. De Angelis and R. Delmas, *Anal. Chim. Acta*, 156 (1984) 181–192.
[12] C. Saigne, S. Kirchner and M. Legrand, *Anal. Chim. Acta*, 203 (1987) 11–21.

ELSEVIER

Journal of Chromatography A, 706 (1995) 253–258

JOURNAL OF CHROMATOGRAPHY A

Oxidative decomposition of organic water pollutants with UV-activated hydrogen peroxide Determination of anionic products by ion chromatography

Claudia Scheuer[a,*], Birgit Wimmer[a], Heidrun Bischof[a], Le Nguyen[a], Jürgen Maguhn[b], Peter Spitzauer[c], Antonius Kettrup[c], Dietrich Wabner[a]

[a]*Arbeitsgruppe Angewandte Elektrochemie und Chemische Umwelttechnik, TU München, Lichtenbergstrasse 4, 85748 Garching, Germany*

[b]*GSF-Institut für Ökologische Chemie, Schulstrasse 10, 85356 Freising, Germany*

[c]*Lehrstuhl für Ökologische Chemie, TU München, 85350 Freising, Germany*

Abstract

Organic water pollutants are decomposed by UV-activated hydrogen peroxide. Using ion chromatography, inorganic and organic anions formed by the oxidative treatment can simultaneously be determined at trace levels without any sample preparation. For identification of anionic metabolites of 2,4-dichlorophenoxyacetic acid (2,4-D), 2-nitrobenzoic acid and nitrobenzene, an ion chromatographic system with a combination of two detectors based on physically different principles, conductivity and UV absorption, is used. Hence the anionic water components can reliably be identified by two parameters: retention time and the concentration-independent specific ratio of conductivity and UV absorption response.

1. Introduction

The increasing pollution by pesticides and other organic compounds endangers drinking water supplies worldwide. In addition to removal by adsorption, methods for the oxidative degradation of persistent compounds are gaining more and more importance. Mainly combinations of ozone, hydrogen peroxide and UV radiation (O_3–H_2O_2, O_3–UV, H_2O_2–UV) have been tested for water treatment [1]. These methods are based on the formation of hydroxyl radicals, which are the strongest oxidants (+2.85 V) in aqueous media apart from fluorine. They are able to decompose and even mineralize organic components in water by oxidation. H_2O_2–UV has turned out to remove several pesticides effectively from water on laboratory and pilot-plant scales.

2,4-Dichlorophenoxyacetic acid (2,4-D), 2-nitrobenzoic acid and nitrobenzene were treated with UV-activated hydrogen peroxide. Carboxylic acids such as acetic, fumaric, formic, glycolic, maleic, malonic and oxalic acid and the inorganic ions chloride and nitrate were found to be formed during the oxidative treatment [2]. The organic decomposition products can be identified by GC–MS and HPLC, but by employing ion-exchange chromatography the inorganic and organic anions can be determined simultaneously without further sample preparation steps. As co-elution of organic and inorganic ions is pos-

* Corresponding author.

0021-9673/95/$09.50
SSDI 0021-9673(95)00005-4

sible, the retention time is not sufficient for reliable identification. For this purpose, a second indicator is obtained by installing two detectors (conductivity and UV absorption) in series. The response ratio for conductivity and UV detection is independent of concentration and is specific for each compound. The combination of the respective retention time with the corresponding response ratio allows reliable peak identification. Elucidation of the mechanisms and quantification of all products are required for the official approval of oxidative treatment to improve the quality of drinking water.

2. Experimental

2.1. Chemicals

All chemicals were of analytical-reagent grade and used without further purification. Deionized water was used for preparing the model solutions for the degradation experiments and ultra-pure water (conductivity <0.07 μS) for ion chromatography. Hydrogen peroxide (35% technical grade, non-stabilized) was purchased from Peroxidchemie (Höllriegelskreuth, Germany).

2.2. Procedures

All irradiation experiments were carried out in a stirred batch reactor at 20°C. To aqueous solutions containing 2,4-dichlorophenoxyacetic acid (0.186 m*M*), 2-nitrobenzoic acid (0.155 m*M*) or nitrobenzene (0.130 m*M*) hydrogen peroxide was added so that its initial concentration ranged from 1.45 to 5.88 m*M*. The mixture was irradiated for 1 h with a TNN 15/32 low-pressure mercury lamp (Heraeus, Hanau, Germany) with emission maxima at 185 and 254 nm.

The determination of anions was performed with a Dionex (Sunnyvale CA, USA) 4506i ion chromatographic system with Dionex AI 450 external PC control software. The injection volume was 50 μl. Separation was performed on an AS 5 A column (250 × 4 mm I.D., alkanol quaternary amine, 5 μm, 20°C) from Dionex. The eluents were prepared under a helium atmosphere. For eluent A (0.75 m*M* NaOH) 39 μl of 50% NaOH were added to 1000 ml of water and for eluent B (200 m*M* NaOH) 10.4 ml of 50% NaOH were added to 990 ml of water. The water was previously thoroughly degassed with helium to remove traces of dissolved CO_2. Gradient elution was applied as follows: 0.0–5.0 min, 100% A; 25.0 min, 85% A + 15% B; 35.0 min, 57% A + 43% B; 35.1 min, 100% A. The flow-rate was 1.0 ml/min. The regenerant for micromembrane suppression was 25 m*M* sulfuric acid. Two detectors in series (conductivity and UV absorption, 200 nm) were used for identification. Retention times and responses were determined by the analysis of external standards. The quantification limits for the identified anionic fragments ranged from 0.001 to 0.006 m*M*.

3. Results

3.1. Identification of anionic metabolites

Some inorganic and organic ions could not be separated under the chosen analytical conditions (e.g., glyoxylate–chloride, tartrate–sulfate, malonate–sulfite). For a reliable identification, the retention times and the specific ratio of conductivity and UV absorption response were determined for each compound of the external standard (see Table 1). The measurements demonstrated a deviation of the response ratio from 1 to 14% for the same compound, depending on the degree of overlapping by neighbouring peaks. A deviation of more than 15% indicates a wrong identification or co-elution with another substance. The procedure was applied to the anionic decomposition products of 2,4-D (Figs. 1 and 2), 2-nitrobenzoic acid and nitrobenzene. Thus the inorganic ions chloride and nitrate and also the organic ions acetate, glycolate, malonate and oxalate could be unequivocally identified. Owing to the constant distance of the two detectors, the retention time difference of pure substances has to be constant, here 0.11–0.14 min, deviations point to impurities. Concerning

Table 1
Identified substances, retention times and specific response ratios (conductivity/UV absorption)

No.	Substance	Retention time (min)	Response ratio		Deviation (%)
			Standard	Sample 2,4-D	
1	Acetate	4.88	16219	–	–
2	Glycolate	5.45	16671	18538	11
3	Formate	7.24	60256	63706	6
4	Chloride	13.82	42368	45059	6
5	Nitrate	20.77	668	677	1
6	Malonate	23.33	21524	22186	3
7	Maleate	24.25	543	1015	46
8	Oxalate	25.73	3671	3836	4
9	Fumarate	28.85	690	1117	61
10	2,4-D	33.27	–	–	–

fumarate, a difference of 0.21 min and the deviation of the response ratio indicated co-elution with another compound. Maleate also turned out to be overlapped. Further, an unknown UV-active substance was formed after 15-min irradiation of 2-nitrobenzoic acid and nitrobenzene, overlapping the formate peak.

3.2. Decomposition of 2,4-D

Ion chromatographic analysis shows that the degradation rate depends on the hydrogen peroxide concentration; the decomposition rate is enhanced by increasing the initial hydrogen peroxide concentration. Almost complete degradation was attained after 20-min irradiation with an initial H_2O_2 concentration of 1.45 m*M*, after 10 min with 2.96 m*M* H_2O_2 and after 5 min with 5.88 m*M* H_2O_2 (Fig. 3). Increasing the H_2O_2 concentration seems to accelerate the dechlorination. With 5.88 m*M* hydrogen peroxide, 0.366 m*M* chloride was formed. Fig. 4 shows the degradation of 2,4-D and the concentration course of the main fragments. In all experiments the formation of acetate, fumarate and maleate was observed. The concentration of acetate was always close to the quantification limit. Small amounts of fumarate and maleate were detected

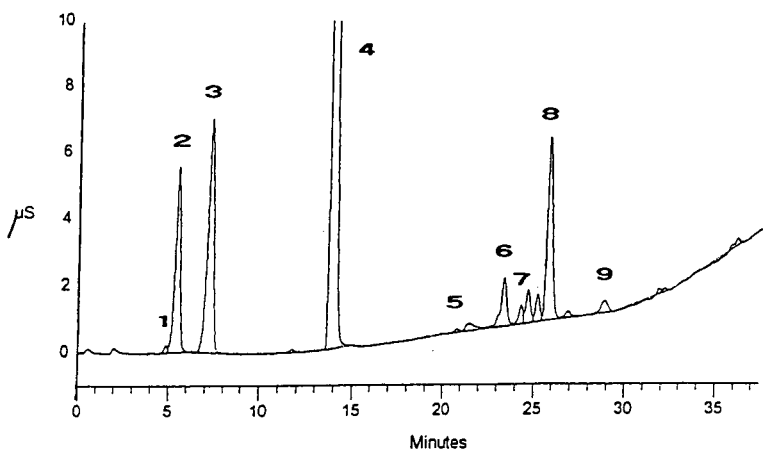

Fig. 1. Conductivity chromatogram: decomposition of 2,4-D, 2.96 m*M* H_2O_2, 10-min irradiation. For identification of peaks, see Table 1.

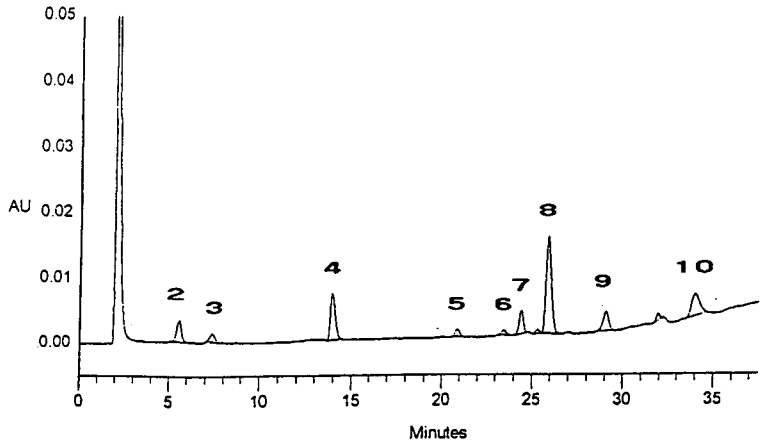

Fig. 2. UV absorption chromatogram: decomposition of 2,4-D, 2.96 m*M* H_2O_2, 10-min irradiation. For identification of peaks, see Table 1.

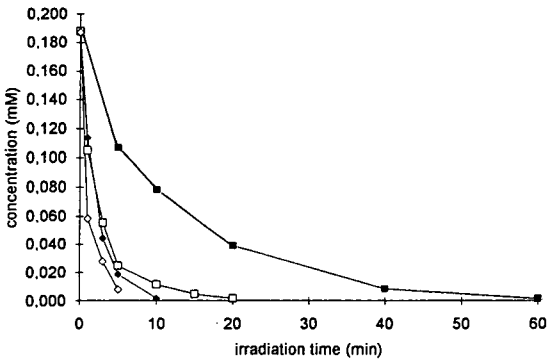

Fig. 3. Decomposition of 2,4-D with different initial H_2O_2 concentrations: ■ = 0.00 m*M*; □ = 1.45 m*M*; ◆ = 2.90 m*M*; ◇ = 5.88 m*M*.

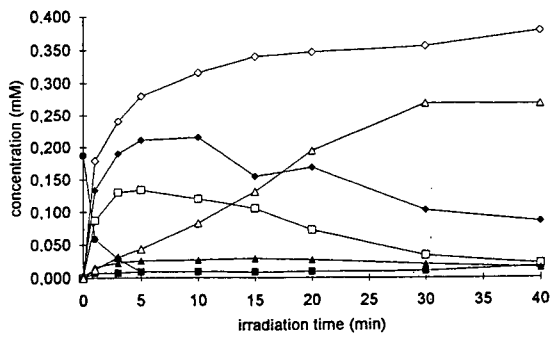

Fig. 4. Decomposition of 2,4-D with 5.88 m*M* H_2O_2. ■ = Acetate; □ = glycolate; ◆ = formate; ◇ = chloride; ▲ = malonate; △ = oxalate; ○ = 2,4-D.

during the first 15 min of irradiation. The concentration of malonate reached about 0.020–0.040 m*M* in the first 20 min. After 5 min of irradiation with an initial H_2O_2 concentration of 5.88 m*M* the concentrations of formate and glycolate reached maxima of 0.210 and 0.130 m*M*, respectively. Oxalate was detected with concentrations up to 0.270 m*M* after 30 min. The formation of formate, glycolate and oxalate increased with increasing H_2O_2 concentration. All of the detected carboxylic acids decomposed on further irradiation.

3.3. Decomposition of 2-nitrobenzoic acid and nitrobenzene

Fig. 5 shows the degradation of 2-nitrobenzoic acid and the concentration course of the main anionic metabolites. With an initial H_2O_2 concentration of 5.88 m*M* the concentration of 2-nitrobenzoic acid was reduced to 5% within 25 min of irradiation. Nitrobenzene was decomposed to 5% within 60 min with an initial H_2O_2 concentration of 4.00 m*M*. Its concentration was determined spectrophotometrically by measuring the absorbance of the solution at 266 nm.

Fig. 6 shows the concentration course of the main anionic degradation products of nitrobenzene. The nitro group was split off from both

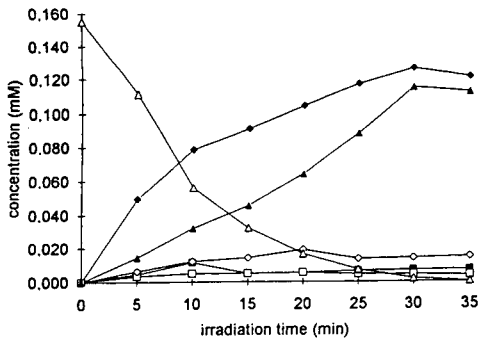

Fig. 5. Decomposition of 2-nitrobenzoic acid with 5.88 m*M* H_2O_2. ■ = Acetate; □ = glycolate; ◆ = nitrate; ◇ = malonate; ▲ = oxalate; △ = 2-nitrobenzoic acid.

compounds, yielding 0.126 and 0.095 m*M* nitrate, respectively. During the oxidative decomposition acetate and glycolate reached concentrations of 0.005–0.012 m*M*, close to their quantification limits. In both instances maleate was formed in concentrations up to 0.005 m*M*; fumarate was not detected. The formation of formate could only be quantified during the first 15 min of irradition because the formate peak was subsequently overlapped by another UV-active substance. The maximum concentration of malonate was 0.019 m*M* for 2-nitrobenzoic acid and 0.010 m*M* for nitrobenzene. Oxalate again turned out to be the main organic decomposition product, 0.115 m*M* being formed from 2-nitrobenzoic acid and 0.080 m*M* from nitrobenzene.

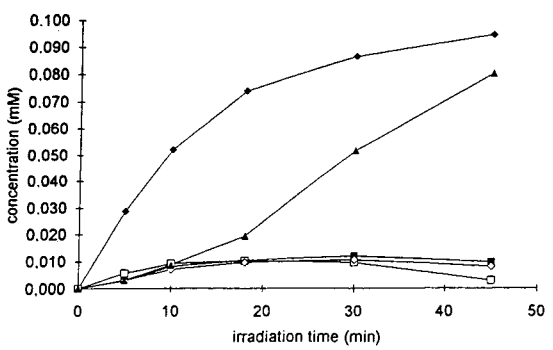

Fig. 6. Decomposition of nitrobenzene with 4.00 m*M* H_2O_2. ■ = Acetate; □ = glycolate; ◆ = nitrate; ◇ = malonate; ▲ = oxalate.

4. Discussion

The oxidative treatment of the investigated organic compounds in dilute aqueous solutions leads to a rapid decrease of the parent compound, yielding a variety of decomposition products. The analytical method applied allows the simultaneous observation of the degradation of the pollutant, except for nitrobenzene, and the formation of anionic products. 2,4-D was reduced to the detection limit within 10 min of irradiation and 2-nitrobenzoic acid to 5% within 25 min. Anionic C_3 and C_4 fragments such as malonate, maleate and fumarate were found to be formed by the oxidative treatment. The detection of malonate and maleate in all experiments, and in some instances of fumarate, confirms the destruction of the aromatic ring soon after the start of irradiation. The degradation of the aromatic ring proceeds either by direct ring opening or via quinoid intermediates [3,4]. Generally, the concentration of carboxylic acids increases with increasing the initial H_2O_2 concentration. Concerning the degradation of 2,4-D, however, the malonate concentration was lower when the initial concentration of H_2O_2 was 5.88 m*M* than it was with an initial H_2O_2 concentration of 2.96 m*M*. The reason may be a faster degradation to smaller fragments. In all experiments 10–20% of malonate were formed relative to the initial concentration of the substrate. The amounts of C_4 fragments were also very low compared with glycolate and oxalate. It is presumed that they are rapidly oxidated to C_2 and C_1 fragments (oxalate, formate) and finally CO_2. The experiments show that oxalate is one of the main products of the decomposition process and that the concentrations of acetate, glycolate, formate and oxalate were also reduced by further irradiation. This was additionally demonstrated by treating an acetate solution, yielding formate and oxalate. After 60 min of irradiation acetate was decomposed completely, and 30 min later the oxalate also. Formate seems to be a short-lived metabolite, being oxidized to CO_2. It is presumed that glycolate decomposes in a similar way [5]. The nitro group and the Cl atom are to a great extent rapidly split off from the

aromatic ring, forming nitrate and chloride; 73% and 81% of the nitro groups were detected as nitrate on decomposing nitrobenzene and 2-nitrobenzoic acid, respectively, and with 98.5% of chlorine split off from 2,4-D, almost complete dechlorination was observed.

5. Conclusions

In order to apply oxidative treatment to improve the quality of drinking water, investigations had to be made concerning the degradation rates and degradation products of organic pollutants. The results presented show an almost complete decomposition of the investigated compounds; even aromatic ring systems were decomposed and finally mineralized to CO_2. Hence oxidative treatment results in an effective detoxification of polluted water. Once approved officially, the technique can be installed in water works without further scaling up because units of pilot-plant scale can simply be run in parallel according to the output of water.

Ion chromatography is a suitable technique for determining inorganic and small organic anions at concentrations down to 0.001 to 0.006 m*M*. As the concentrations of these anions will be lower in real water samples compared with the model solutions, it has to be proved whether installing an on-line accumulation technique results in lower detection limits.

Acknowledgement

This work was supported by the Bayerische Forschungsstiftung.

References

[1] O. Legrini, E. Oliveros and A.M. Braun, *Chem. Rev.*, 93 (1993) 671–698.
[2] G. Reynolds, N. Graham, R. Perry and R.G. Rice, *Ozone Sci. Eng.*, 11 (1989) 339–382.
[3] P.C. Kearney, M.T. Muldoon and C.J. Somich, *Chemosphere*, 16 (1987) 2321–2330.
[4] D.G. Crosby and A.S. Wong, *J. Agric. Food Chem.*, 14 (1966) 596–599.
[5] Y. Ogata, K. Tomizawa and K. Takagi, *Can. J. Chem.*, 59 (1981) 14–18.

ELSEVIER

Journal of Chromatography A, 706 (1995) 259–269

JOURNAL OF CHROMATOGRAPHY A

Simultaneous determination of small organic and inorganic anions in environmental water samples by ion-exchange chromatography

Adrian A. Ammann*, Thomas B. Rüttimann

Biogeochemistry Department, Swiss Federal Institute for Environmental Science and Technology (EAWAG), CH-8600 Dübendorf, Switzerland

Abstract

Anion-exchange chromatography at elevated pH values is the method of choice for the simultaneous determination of weak and strong low-molecular-mass organic and inorganic acids. These are important species found in the environment where most of them are formed and further degraded, particularly if microbial activities are involved. A step gradient procedure with a weak eluent such as borate on a low-capacity column was developed for the simultaneous one-run one-column determination of most of these types of components in environmental water samples. High selectivity and detection limits below 1 μM were achieved. Other yet unknown coelutions of 3-hydroxybutyrate with fluoride and 2-hydroxybutyrate with propionate were found. The different retention characteristics of a high-capacity column was used to obtain additional evidence to identify interfering components. These separation procedures were used to investigate fog, lake sediment pore water and rain after roof run-offs.

1. Introduction

Research on distribution and transformations of chemical species in the environment has led to an increased demand for analytical methods that quantify most of the species of the same kind in one run. This is an ultimate condition in the case of low amounts of available samples.

High-performance liquid chromatography (HPLC) in the ion-suppression mode or ion-exclusion chromatography [1] has been applied to separate organic acids. Acidic eluents that keep weak organic acids protonated are used. In this neutral molecular form they can be separated by hydrophobic interaction chromatography. Stronger organic and inorganic acids that remain in the ionic form are excluded and discarded. In addition, because of a very weak chromophore, ultraviolet detection has to be performed at very short wavelengths where solvents absorb. This leads to high detection limits (ppm). After organic acids are extracted from water by an organic solvent they can be separated by gas chromatography (GC) with high selectivity. This extraction step allows the concentration of the acids and lowers the detection limits (ppb). However, these methods provide only a restricted section of the whole anion

* Corresponding author.

0021-9673/95/$09.50
SSDI 0021-9673(95)00003-8

profile of an environmental sample. A much broader insight is given by anion-exchange chromatography at elevated pH values, which is very suitable for the analysis of weak and strong organic and inorganic acids. It is often the preferred method for the analysis [2] of these compounds, which are involved in environmental transformation processes where most are formed and further degraded particularly in association with microbial activity [3]. Therefore simultaneous monitoring for organic and inorganic nutrients is essential [4].

For anionic species, anion-exchange chromatography became a powerful tool when high-capacity suppressors [5] and hydroxide-selective anion separator columns were introduced. This combination allows gradient elution which is the most efficient technique for selectivity management to be applied in conjunction with conductivity detection, the most common direct and sensitive technique for the detection of ionic species. Because of the dynamic range of the suppressor capacity, an increasing eluent concentration (e.g. hydroxide up to 150 m*M*) results in a minimal increase of background conductivity.

Singly charged low-molecular-mass aliphatic organic anions ($C_{n<6}$) exhibit a very low affinity (capacity factors, k') to the anion separator columns so that only a weak eluent strength can provide sufficient selectivity to separate those acids. However, weak eluents do not virtually elute doubly charged low-molecular-mass organic and inorganic anions. Usually, anion chromatographic procedures focus on the latter ones by applying a medium or high eluent strength such as hydroxide at the expense of selectivity of low-molecular-mass organic acids that can be expected to be present in environmental samples. Different strategies involving more than one column have been applied, e.g. samples were automatically injected several times for separation under isocratic (AS4A–carbonate [6]) and gradient (AS5A–OH^-) conditions [7]. An alternative for gradient separation is a column-switching procedure between two columns with different capacities that are isocratically eluted [8]. Gradient elution has been applied to quantify low-concentrated inorganic and organic anions in Greenland ice. The insufficient separation between acetate and glycolate and between sulphate and oxalate has not been improved significantly using a hydroxide gradient on a multiphase column [9]. A weak eluent such as borate (1.3 m*M*) on an AS4A column provided a better resolution in the isocratic mode for low-affinity anions [10] and in a gradient mode (7–21 m*M*) for higher-affinity anions [11]. However, none of these procedures have been shown to separate acetate from lactate, propionate and glycolate.

As we and others [11] have encountered these problems in environmental water samples, an investigation started, aimed to separate environmentally relevant low-molecular-mass aliphatic organic acids including some of their hydroxy analogues in the same run on one column that separates inorganic anions (see Table 1). A varying selection of these species can be found in environmental water samples depending on the emitting sources and the ongoing biological and chemical activity. For example, glycolate is formed by photosynthesis since the same enzyme that catalyses the fixation of CO_2 has also an oxygenase activity which produces glycolate [12]. Its formation and disappearance in algae blooming during day time has been monitored by GC [13]. Under anaerobic conditions biopolymers are degraded in water by fermentative processes to, e.g., acetate, lactate, propionate, butyrate and formate. Since low-molecular-mass organic acids are readily taken up by microorganism, these compounds serve as nutrients and are further oxidized [14]. In atmospheric waters such as fog water and aerosols these acids can be present. They are formed in the aquatic phase from photochemically induced gas-phase precursors [15].

A better separation of low-molecular-mass organic acids allows the identification of these chemical species. This is important in order to correctly diagnose a water body and assign the nature of degradation path (e.g., biological or photochemical) and its mechanism [16] as well as an accurate determination of carbonate by titration (alkalinity), often the main anion in environmental water samples.

Table 1
Retention times (t_R) of environmental relevant low-molecular-mass organic and inorganic components on two different columns

Component		AS11 gradient t_R (min)	AS10 borate isocratic	
Name (abbreviation)	Composition		7 m*M* t_R (min)	5 m*M* t_R (min)
3-Hydroxybutyrate (3-OHBu)	$H_3CHOHCH_2CCOO^-$	5.0	7.2	
Fluoride	F^-	5.1	6.5	8.1
Lactate (La)	$H_3CHOHCCOO^-$	5.6	7.9	10.1
Acetate (Ac)	H_3CCOO^-	5.8	7.9	10.1
Glycolate (Gl)	HOH_2CCOO^-	6.2	8.6	
Propionate (Pr)	$H_3CH_2CCOO^-$	7.0	8.6	
2-Hydroxybutyrate (2-OHBu)	$H_3CH_2CHOHCCOO^-$	7.0	8.8	
Formate (Fo)	$HCOO^-$	8.0	12.0	16
Butyrate (Bu)	$H_3CH_2CH_2CCOO^-$	8.6	9.6	12.5
Methanesulfonate (MSA)	$H_3C\,SO_3^-$	9.0	-	
Pyruvate (Pu)	$H_3COCCOO^-$	10.0	16.0	
Valerate (Va)	$H_3CH_2CH_2CH_2CCOO^-$	10.8	12.6	
Chloride	Cl^-	13.0	45	
Nitrite	NO_2^-	14.0		
Carbonate	CO_3^{2-}	14 ± 0.4		
Phosphate	PO_4^{3-}	16.2	∞	
Bromide	Br^-	16.6		
Nitrate	NO_3^-	17.1	∞	
Sulfite	SO_3^{2-}	17.8	∞	
Sulfate	SO_4^{2-}	19.0	∞	
Oxalate (Ox)	$^-OOCCOO^-$	21.0	∞	

2. Experimental

2.1. Instrumentation

A DX-300 chromatographic system (Dionex) was used with a standard AGP pump, a PED in the conductivity detection mode, and AI-450 software 3.31. The anion separator columns (200 × 4 mm) IonPac AS10 and AS11 and their corresponding guard columns (50 × 4 mm) AG10 and AG11 were used. The eluent (1 ml/min) conductivity was chemically suppressed by a micromembrane suppressor (AMMS II) regenerated by 25 m*M* H_2SO_4 (10 ml/min) or a self-regenerating suppressor (ASRS, current setting 3) that uses the column effluent to supply the proton generated by water electrolysis. An anion trap column (ATC-1, 9 × 24 mm) was installed in front of the injection valve to minimise interferences from anionic impurities in the eluent during gradient elution.

2.2. Chemicals

The chemicals used were of highest purity available from Fluka and Merck. Borate eluents were prepared from $Na_2B_4O_7 \cdot 10H_2O$ in 18-MΩ (Nanopure) water and kept under helium pressure.

Stock solutions (1000 ppm) of organic acids were prepared by dissolution of the sodium salts of the acids with freshly purified and 0.2-μm filtered, deionized water (18 MΩ) in carefully rinsed glass volumetric flasks. Stored at 4°C these stocks could be used for a few months. Calibration was obtained from freshly prepared standard solutions. Depending on concentration, storage and handling condition they could be used for a few days.

Turbid samples were filtered through prewashed (2 h at 80–100°, 18-MΩ deionized water) filters (0.45 μm). Depending on the concentration, 10-, 25- or 50-μl samples were injected.

3. Results and discussion

3.1. Chromatographic procedures

A preliminary comparison of borate and hydroxide as eluents for the separation of low-molecular-mass organic components in fog samples revealed that borate provides a better resolution on the more hydrophilic columns AS11 and AS10. Therefore, the separation was investigated with borate as eluent. Its background conductivity was chemically suppressed. For the low-capacity AS11–AG11 (55 μequiv.) and the high-capacity AS10–AG10 (210 μequiv.) columns a different procedure was established.

3.2. Step gradient procedure on a low-capacity separator (AS11)

The chemical suppression allows a gradient to be applied, and only a gradient provides the selectivity necessary to separate several low-affinity (F^-, organics) as well as high-affinity (doubly charged organics and inorganics) anions. In the same run for gradient elution the low-capacity column is preferred: it needs a lower eluent strength which gives shorter retention times and a smaller increase in background conductivity during the gradient allowing lower concentrations to be determined. A step gradient (see Table 2) with its almost flat baseline during the important sequence of the chromatogram turned out to be optimal for short retention times, consistent peak integration and low detection limits. The large affinity range of the anions we are interested in can be divided in three affinity classes. Each of them corresponds to a borate concentration level needed for elution. Low-affinity species (F^-, all single-charged organics) are best separated in the initial part (see Fig. 1) by a slightly linear gradient of 1–6 m*M* borate. The duration and concentration of this initial step can be adjusted to the number and types of low-molecular-mass organic acids. This, of course, affects the retention times of anions that elute later. A second medium-affinity group is envisaged by an increase to 20 m*M* borate for a short time to detect chloride and nitrite. Carbonate eluted at varying retention times around nitrite. Disturbed nitrite peaks have been observed for carbonate concentrations higher than 40 mg/l. All other anions (e.g. PO_4^{3-}, Br^-, NO_3^-, SO_3^{2-}, SO_4^{2-} and oxalate) are eluted during a third step of 45 m*M* borate. Detection limits were determined to be 0.5–1 μM depending on the species. In 25 min this procedure achieved the best selectivity so far known for low-molecular-mass organic acids as well as separation and quantification of common inorganic anions in the same run. For a similar purpose on the same column it was proposed [17] to use a hydroxide gradient that starts at a very low concentration (0.5 m*M*) containing 10% methanol. Every time we used hydroxide at

Table 2
Borate step gradient for the simultaneous separation of organic and inorganic anions on a low-capacity anion separator column

Time (min)	Flow (ml)	% E1 1 m*M* borate	% E2 50 m*M* borate	E_{mix} borate (m*M*)	Comment	
0	1	100	0	1	Injection	start gradient
8.0	1	90	10	6		end first step
8.1	1	40	60	30		start second step
10.6	1	40	60	30		end second step
10.7	1	10	90	45		start third step
19.7	1	10	90	45		end third step
19.8	1	100	0	1	Start initial condition	
23.8	2	100	0	1	Speed up reconditioning	
25.8	1	100	0	1	Release	
27.5	1	100	0	1	Initial conditions	

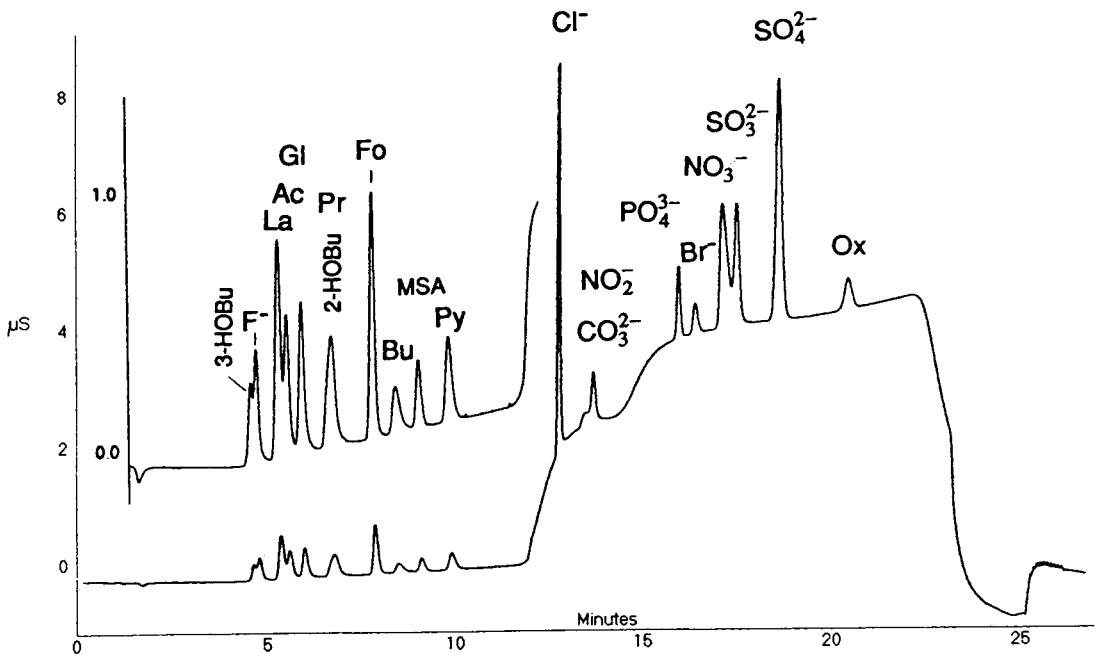

Fig. 1. Chromatogram obtained by the step gradient procedure (Table 2) from a standard solution (25 μl injected) containing F^- (0.25 mg/l), 3-OHBu, La, Ac, Gl, Pr, 2-OHBu, Fo, Bu, MSA, Py, Ox (all 1.0 mg/l), Cl^- (2.0 mg/l), NO_2^- (0.65 mg/l), CO_3^{2-} (40 mg/l), PO_4^{3-} (1.2 mg/l), Br^- (0.8 mg/l), NO_3^- (4.4 mg/l), SO_3^{2-} (4.0 mg/l), SO_4^{2-} (4.0 mg/l). For abbreviations, see Table 1. The inset has an expanded response for the same time scale.

the same concentration and methanol at varying percentages (5, 10, 20%) a decrease of selectivity compared to the borate eluent was observed for low-affinity species. There is evidence from the changes in the elution sequence between the two different anion separators (Table 1) and the increasing affinity with increasing carbon chain of unsubstituted aliphatic monocarboxylic acids that the separation mechanism involves hydrophobic attraction which is reduced by methanol. Such an eluent is the best choice to reduce the retention times of organic anions with a high hydrophobic attraction for which a borate eluent is not ideal.

We used this procedure to investigate separation problems associated with the low affinity of low-molecular-mass organic acids. As depicted in Fig. 1, several of these acids have been separated, which were up to now not or poorly resolved, such as acetate from lactate and glycolate from propionate. However, on this column other yet unknown interferences were found: 3-hydroxybutyrate (3-OHBu) almost coeluted (shoulder) with F^- and 2-OHBu perfectly coeluted with propionate. On an AS10 column 3-OHBu was perfectly baseline-separated whereas the occurrence of 2-OHBu was only indicated by a shoulder in the propionate and glycolate (coeluting) peak, respectively.

3.3. Isocratic separation on the high-capacity anion separator AS10

A high-capacity column is not recommended for the simultaneous separation of low- and high-affinity anions because of the previously mentioned reasons. Nevertheless, such a column can provide an excellent resolution for low-affinity species. Borate (7 m*M*, isocratic) was used to separate these species (Fig. 2). For example, fluoride and formate were separated by 6 min. This is twice the resolution compared to the step gradient procedure (Fig. 1) on the low-capacity column. The more polar species (3-OHBu, lac-

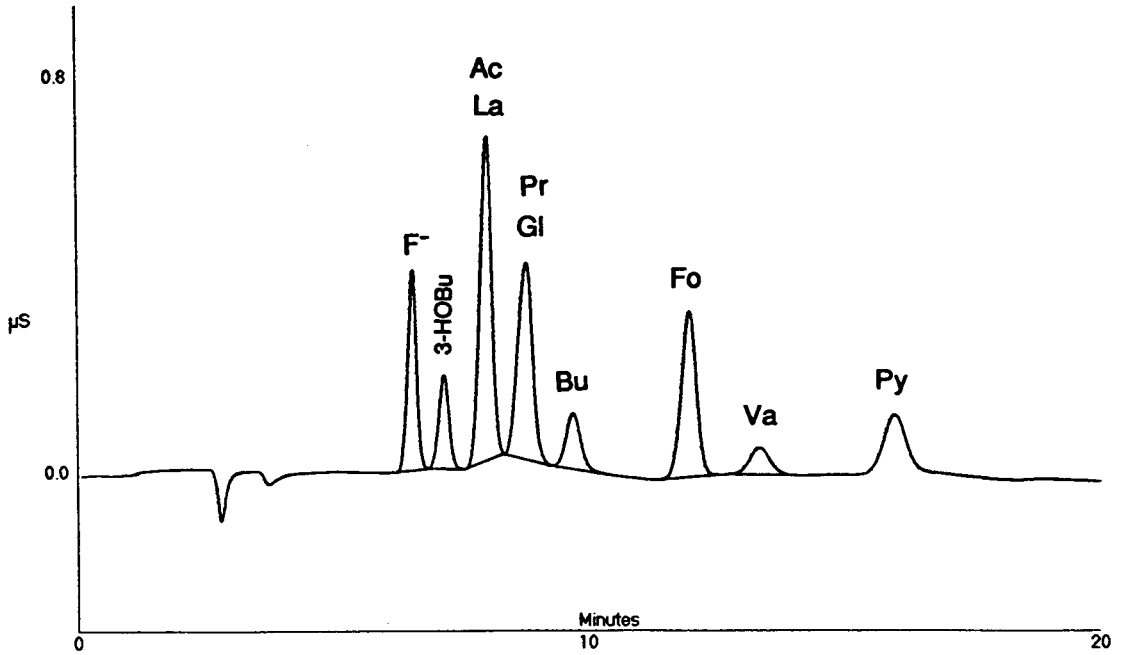

Fig. 2. Chromatogram obtained on the high-capacity column AS10 by isocratic (7 m*M* borate) elution of a standard solution (25 µl injected) containing F^- (0.25 mg/l), 3-OHBu, La, Ac, Gl, Pr, Fo, Bu, Va, Py (all 1 mg/l). For abbreviations, see Table 1.

tate, glycolate, 2-OHBu, formate and pyruvate) are better retained on this higher-capacity column. This different retention characteristic may help to identify some components in samples. Unfortunately two other α-hydroxy compounds, lactate and glycolate, coelute with acetate and propionate, respectively (Table 1). A linear borate gradient (5–15 m*M*) was applied instead of isocratic conditions but no indication was observed that the two compounds coeluted.

The combination of this weak eluent strength on a high-capacity column drastically increased the retention times of strong organic and inorganic acids. Chloride, for example, was eluted after 45 min and others were not eluted at all or at much longer retention times, probably as such broad peaks that they could no longer be detected. In this way the column acted on line as a sample preparation column as well as a separator for low-affinity anions. The long retention time of chloride allowed the ending of a run after the low-affinity anions had been separated (around 20 min) and the injection of another sample so that chloride from the previous run appeared at the end of the following chromatogram, keeping each analysis interference free of chloride from the former injected sample as shown in Fig. 3. The the column capacity for the accumulation of high-affinity species is sufficient to provide separations without a disturbed peak shape for up to fifteen to twenty fog sample injections (25 µl). Obviously this depends on the sample concentrations of the species accumulating on the column. After around thirty injections the loading of the column resulted in clearly disturbed peaks with a shoulder in the onset of the peak as shown in Fig. 4 and asymmetry factors < 0.7. After rinsing with 200 m*M* NaOH and reequilibration with 7 m*M* borate the column had the original performance.

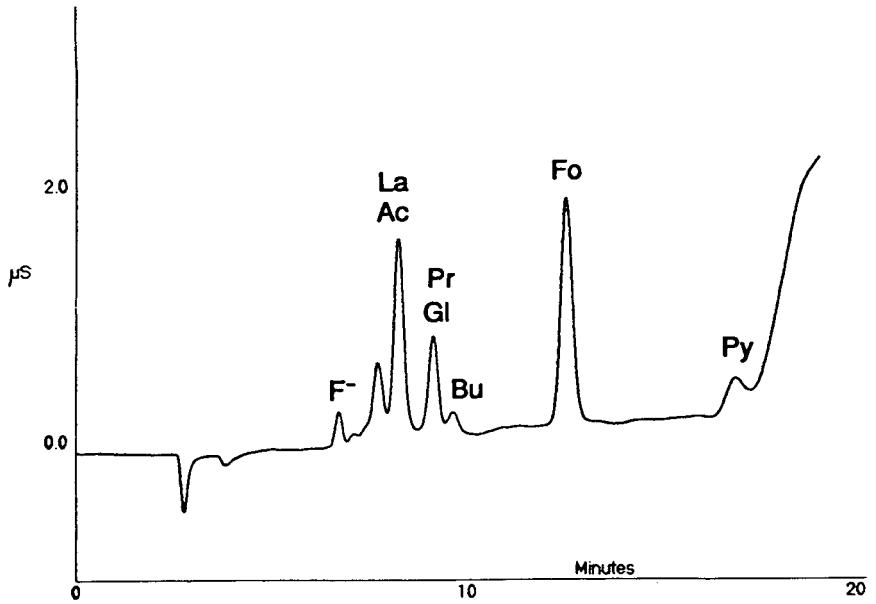

Fig. 3. Chromatogram of a fog sample (25 µl injected) on the high-capacity column AS10 by isocratic elution (7 m*M* borate).

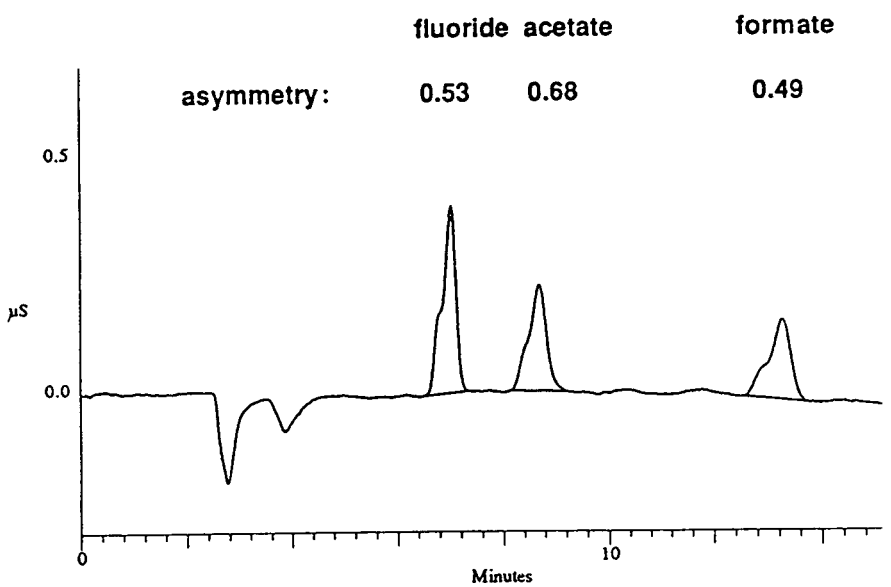

Fig. 4. Chromatogram of a standard solution containing fluoride, acetate and formate (0.1, 0.5 and 0.5 mg/l, respectively, 50 µl injected) obtained on the high-capacity column AS10 after more than twenty consecutive fog sample injections without column wash.

3.4. IC analysis of anions in environmental water samples

Fog water

The composition and concentrations found in fog water [18] strongly depend on emitting sources (e.g. traffic, heating, incinerators) and their variations and meteorological conditions. In our recent IC work we focused on low-molecular-mass organic acids because of their role as iron ligands in iron cycling [16,19]. Biological transformations are of less importance and, since combustion is the main source chemical [20] and photochemical [21] transformations take place in a oxidative environment, we can expect higher concentrations of oxidised forms of low-molecular-mass organic acids. Fog samples were collected as described [16] and subjected to IC analysis within hours. In separate aliquots of stored samples SO_3^{2-} was preserved with glycerol and organic acids with chloroform. As depicted in Fig. 3, fog can contain a variety of low-molecular-mass organic acids. Among them acetate (10–400 μM) and formate (10–150 μM) were always found in highest concentrations. Together they accounted for 3–10% of dissolved organic carbon. Propionate, butyrate, pyruvate and oxalate ranged from below detection limits (0.5–1 μM) to 10 μM. The identification of components eluting between F^- and acetate (see Fig. 3) and the separation of acetate from possibly present lactate as well as propionate from glycolate by the step gradient procedure remain to be done in an appropriate fog event.

Lake sediment pore water

Sediments are an important factor in the cycling of the elements in a lake. Biological and chemical reactions at the water sediment boundary decide whether elements are incorporated into the sediment or kept dissolved in the water. These processes occur in a layer of a few centimetre thick or less. The sampling device for sediment pore water, a dialysis chamber [22], delivers around 10-ml samples for one depth. Many or, if possible, all dissolved species have to be determined in such low-volume samples in order to investigate the complicated transformations. Usually, less then 4 ml are available for an analysis of the anion profile. Since these oxygen-free water samples contain dissolved Fe(II) and Mn(II) that are readily oxidised and precipitated in contact with oxygen at elevated pH we checked a possible coprecipitation of low-molecular-mass organic acids. A solution of 200 μM Mn(II) and 300 μM Fe(II) dissolved in a standard solution containing acetate (8.4 μM), propionate (2.7 μM) and formate (4.4 μM) was aired and brought to pH 12 by NaOH. An intense dark precipitation formed but no decrease of the organic acids compared to the untreated standard solution was found. From this we conclude that no coprecipitation under the chromatographic conditions occurred.

The sediment pore water sampled in lake Sempach during summer (June) and winter (January) contained very low amounts (usual < 2 μM, maximum 6 μM) of acetate. Since both the formation and degradation of low-molecular-mass organic acids are controlled by different communities of microorganisms only a low intermediate concentration during balanced rates can be observed. So far only once in the summer (June, lake Baldegg) high acetate concentrations up to 90 μM and elevated levels of other organic acids were detected (Fig. 5). This is considered as an exceptional case due to an increase in sedimentation of particulate organic matter that resulted probably during a short period in a overproduction of low-molecular-mass organic acids.

Rain water from roof run-offs

In extended dense populated areas ground water supply by direct infiltration of rain water became minimal. The water is collected on roofs and roads and drained to the sewage treatment plants. Ground water levels decrease and during storms sewage treatment plants are overloaded and lose their efficiency. Therefore rain from roof run-offs is under investigation for a direct infiltration into the ground. We determined anion profiles in rain water after passage over different roofs. The samples contain species characteristic of the dry deposition before rainfall and chemical and biological transformations

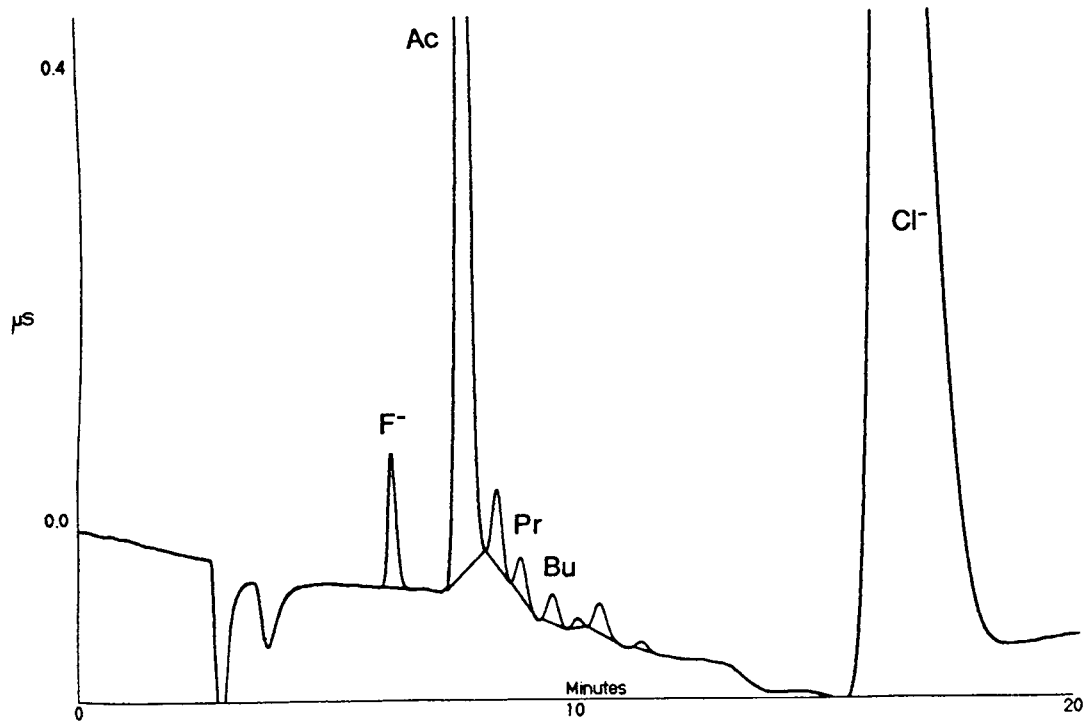

Fig. 5. Chromatogram of a sediment pore water sample (50 µl injected) on the high-capacity column AS10 using 7 m*M* borate isocratic as eluent. For abbreviations, see Table 1.

occurring in the microenvironment of the roof. An example is given in Fig. 6. The sample from a glass fibre plastic roof has a quite similar composition to fog water. In this case the degradation of plastic is suspected to be the main source of organic acids.

4. Conclusions

The step gradient procedure presented allows the determination of low-molecular-mass organic and inorganic acids in the same run on one column in a reasonably short time. This makes it a unique method to simultaneously obtain a large section of an anion profile in environmental samples. For complex mixtures of low-molecular-mass organic acids a second column with a different retention characteristic helps to identify the components. However, the final proof that no coelution occurred can only be provided by a detection that gives structural information, such as mass spectrometry.

The occurrence of low-molecular-mass organic acids in environmental samples points to the decisive role of microbial activities. Only when these are unimportant (in atmosphere) or temporarily imbalanced, low-molecular-mass organic acid concentrations higher than a few micromoles can be found.

Acknowledgements

The sampling of fog water by A. Kotronarou, sediment pore water by N. Urban, M. Mengis and B. Wehrli and rain from roof run-offs by J. Eugster and I. Brunner is gratefully acknowledged.

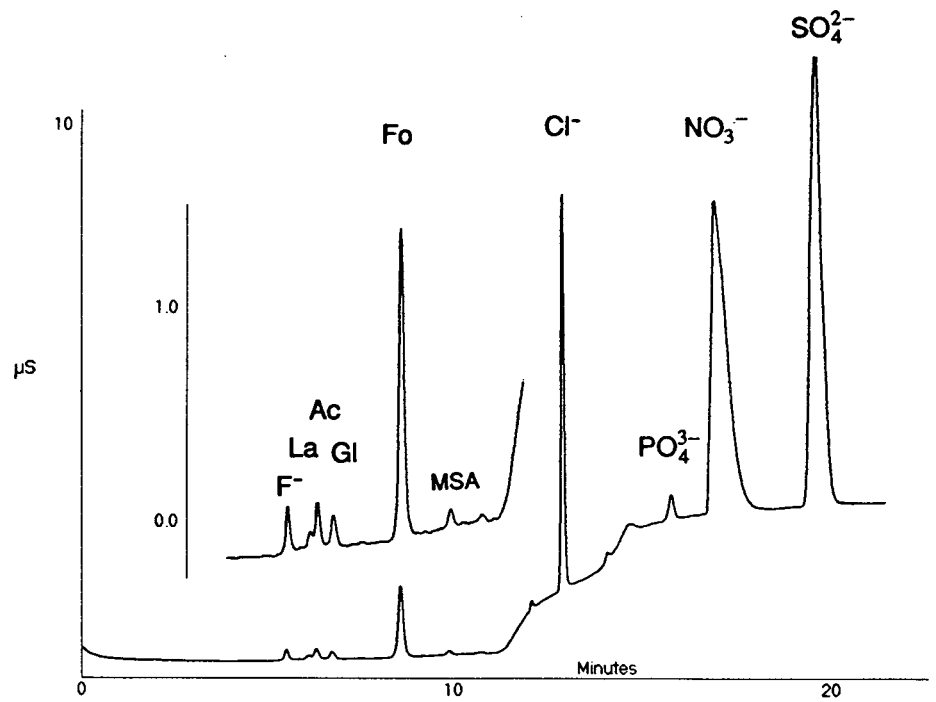

Fig. 6. Chromatogram of rain water sampled after running down a glass fibre plastic roof. Separation (25 μl injected) was performed by step gradient (see Table 2) on a low-capacity column AS11. For abbreviations, see Table 1. The inset has an expanded response for the same time scale.

References

[1] J. Morris and J.S. Fritz, *LC·GC Int.*, 7 (1994) 43.
[2] P.R. Haddad and P.E. Jackson, *Ion Chromatography. Principles and Applications* (*J. Chromatogr. Library*, Vol. 46), Elsevier, Amsterdam, 1990; J. Weiss, *Ionenchromatographie*, VCH, Weinheim, 1991.
[3] R. Mitchell (Editor), *Environmental Microbiology*, Wiley-Liss, New York, 1992; F.H. Chapelle, *Ground-Water Microbiology and Geochemistry*, Wiley, New York, 1993; M.J. Klug and C.A. Reddy (Editors), *Current Perspectives in Microbial Ecology*, American Society for Microbiology, Washington, DC, 1984.
[4] J.R. Bragg, R.C. Prince, J.E. Harner and R.E. Atlas, *Nature*, 368 (1994) 413.
[5] St. Rabin, J. Stillian, V. Barreto, K. Friedman and M. Toofan, *J. Chromatogr.*, 640 (1993) 97.
[6] U. Baltensperger and S. Kern, *J. Chromatogr.*, 439 (1988) 121.
[7] E. Dabek and J.F. Dlouh, *J. Chromatogr.*, 640 (1993) 217.
[8] C. Umile and J.F.K. Huber, *J. Chromatogr.*, 640 (1993) 27.
[9] M. Legrand, M. De Angelis and F. Maupetit, *J. Chromatogr.*, 640 (1993) 251.
[10] H. Westberg and P. Zimmerman, in L. Newman (Editor), *Measurement Challenges in Atmospheric Chemistry* (*Adv. Chem. Series*, Vol. 232), American Chemical Society, Washington DC 1993, Ch. 10, p. 284; J.A. Morales, H.L. de Medina, M.G. de Nava, H. Velasques and M. Santana, *J. Chromatogr. A*, 671 (1994) 193.
[11] W. Shotyk, *J. Chromatogr*, 640 (1993) 309.
[12] L. Stryer, *Biochemistry*, W.H. Freeman, New York, 1988, p. 535.
[13] U. Münster and R.J. Chrost, in J. Overbeck and R.J. Chrost (Editors), *Aquatic Microbial Ecology* (*Brock/Springer Series in Contemporary Bioscience*) Springer, New York, 1990, Ch. 2, p. 24.
[14] A.J.B. Zehnder and W. Stumm, in A.J.B. Zehnder (Editor), *Biology of Anaerobic Microorganisms*, Wiley, New York, 1988, Ch. 1.
[15] R. Atkinson, *Atmos. Environ.*, 24A (1990) 1.
[16] A. Kotronarou and L. Sigg, *Environ. Sci. Technol.*, 27 (1993) 2725.
[17] Dionex, *Installation and Troubelshooting Guide for the IONPAC AS11*, 1992.

[18] C.A. Johnson, L. Sigg, J. Zobrist, *Atmos. Environ.*, 21 (1987) 2365.
[19] Ph. Behra, L. Sigg, *Nature*, 344 (1990) 419.
[20] L. Sigg, W. Stumm, J. Zobrist and F. Zürcher, *Chimia*, 41 (1987) 159; Ph. Behra, L. Sigg and W. Stumm, *Atmos. Environ.*, 23 (1989) 2691.
[21] Y. Zuo, J. Hoigné, *Environ. Sci. Technol.*, 26 (1992) 1014.
[22] H. Brandel and K. Hanselmann, *Aquatic Sci.*, 53 (1991) 55.

ELSEVIER

Journal of Chromatography A, 706 (1995) 271–275

JOURNAL OF CHROMATOGRAPHY A

Matrix-elimination ion chromatography with post-column reaction detection for the determination of iodide in saline waters

Ana C.M. Brandão[a,*], Wolfgang W. Buchberger[b], Edward C.V. Butler[c], Peter A. Fagan[d], Paul R. Haddad[d]

[a]*Institute of Antarctic and Southern Ocean Studies, University of Tasmania, GPO Box 252C, Hobart, Tasmania 7001, Australia*

[b]*Department of Analytical Chemistry, Johannes Kepler University, A-4040 Linz, Austria*

[c]*CSIRO Division of Oceanography, Marine Laboratories, GPO Box 1538, Hobart, Tasmania 7001, Australia*

[d]*Department of Chemistry, University of Tasmania, GPO Box 252C, Hobart, Tasmania 7001, Australia*

Abstract

An ion chromatographic method has been developed for the determination of traces of iodide in saline waters. A Dionex IonPac AS11 anion-exchange column was used with a mobile phase containing sodium chloride in order to remove interferences of the sample matrix in both the chromatographic separation and detection. This matrix-elimination procedure was reinforced by a post-column reaction detection that was both selective and sensitive for iodide and was based on the reaction of iodide with 4,4′-bis(dimethylamino)diphenylmethane in the presence of N-chlorosuccinimide. Detection was carried out at 605 nm. The detection limit for iodide in seawater is at about 0.8 ppb for a 150-μl injection, and the relative standard deviation at 5 ppb is better than 4%. Bromide is a potential interference, but is well separated from iodide. No interferences from dissolved organic matter in natural samples have been observed.

1. Introduction

There are many reasons to measure trace levels of iodine. It is an essential micronutrient for many organisms —both terrestrial and marine. It is released as one of the by-products from the operation of nuclear reactors. Iodine is also a useful element to characterize soils, ground waters, saline formation waters and other brines [1], and in its different forms or species, it is a possible indicator of oceanic biological productivity [2], and is useful in studying the redox chemistry of natural waters [3].

In natural waters, iodine exists almost exclusively as the anions, iodate and iodide. The prevalence of one over the other depends on redox chemistry: iodate is dominant under oxidizing conditions, iodide under reducing conditions. Of the several methods that can be used to determine iodate in natural waters, automated

* Corresponding author.

0021-9673/95/$09.50
SSDI 0021-9673(94)01207-5

colorimetry [4] and polarography [5,6] operate well even in saline[1] waters. Very few methods allow trace iodide to be determined directly in natural waters, and only a couple in saline waters. The voltammetric method of Luther et al. [7] with a detection limit of 0.01–0.03 ppb (mass/volume, equivalent to μg I/l) is very sensitive. Its drawback is that it is not a very rapid method of analysis. Dissolved organic matter might also interfere in some natural waters. Nakayama et al. [8] have described another electrochemical procedure that is very sensitive, too, for iodide measurement in seawater. It uses a flow-through iodide-selective electrode, and is automated. However, the instrumentation appears quite complex and is not readily available. As far as we know the originators are the only ones to have used this procedure to determine iodide.

Ion chromatography (IC) seems to offer advantages for the determination of iodide. The halide elutes late both in anion-exchange chromatography and ion interaction chromatography, so that it is usually well separated from interferences. There have been two problems for saline water analysis: (i) deterioration of chromatographic efficiency with injection of the high-chloride matrix, and (ii) lack of sensitivity. The first has been solved by using the matrix-elimination technique, where chloride is added to the mobile phase [9–11]. Although various detectors have been tried including UV absorption [9,11], amperometry [9,12] and potentiometry [13], sensitivity remains an obstacle.

In this study, we have addressed both problems for determining iodide in saline water by IC by combining the matrix-elimination technique with a sensitive and selective post-column reaction for iodide. The post-column reaction is derived from an IC method described earlier [14,15] which uses the reaction of iodide with 4,4′-bis(dimethylamino)diphenylmethane ("tetrabase") in the presence of chloramine T. Several modifications of this reaction necessary in combination with the matrix-elimination technique are described in this paper, and results from an application to analysis of seawater samples are presented.

[1] By saline, we mean natural waters that are dominated by sodium chloride.

2. Experimental

2.1. Instrumentation

The IC instrumentation consisted of two 510 solvent-delivery systems (Waters, Milford, MA, USA), a 7010 injection valve (Rheodyne, Cotati, CA, USA), an AS 11 column (Dionex, Sunnyvale, CA, USA), a temperature-control module (Waters), a knitted reaction coil made from PTFE tubing (114 cm × 0.5 mm I.D.), a Model 450 variable-wavelength UV–visible absorbance detector (Waters) and a Maxima 820 chromatography data workstation (Waters). The second pump was fitted with pulse dampener (Waters).

2.2. Reagents and procedures

The mobile phase was prepared by dissolving 0.4 ml methanesulphonic acid (Fluka, Buchs, Switzerland) and 5.84 g sodium chloride in 700 ml water, adding a solution containing 0.8 g 4,4′-bis(dimethylamino)diphenylmethane (Merck, Darmstadt, Germany) in 200 ml of methanol, and making up to 1 l. The post-column reagent comprised 1.5 g/l N-chlorosuccinimide and 15 g/l succinimide (both obtained from Aldrich, Milwaukee, WI, USA) in a succinate buffer prepared from 11.8 g/l succinic acid adjusted to pH 4.0. All chemicals used were of analytical grade. Water was treated with a Milli-Q (Millipore, Bedford, MA, USA) water-purification system. The mobile phase and the post-column reagent were filtered through a 0.45-μm filter and degassed before use.

Seawater samples were injected directly without sample preparation apart from a filtration through a 0.2-μm filter. The flow-rate of the mobile phase was 0.9 ml/min and that of the post-column reagent 0.3 ml/min. The detection wavelength was 605 nm.

3. Results and discussion

3.1. Optimization of the post-column reaction

Originally discovered by Feigl and Jungreis [16], iodide catalyses the reaction between the tetrabase and hypochlorite (generated by the hydrolysis of chloramine T) yielding a quinoidal product of intense blue color which gradually turns into green. These reagents have been used successfully in IC and post-column reaction detection for iodide [14,15], though the stability of chloramine T solutions as a source of hypochlorite was not completely satisfactory. Therefore, substitution of chloramine T by other reagents with better stability was attempted. The use of N-chlorosuccinimide/succinimide seemed to be a promising alternative. Considerable experience with this reagent was already available from earlier work dealing with the post-column reaction detection of cyanide [17] which involved the oxidation of cyanide to cyanogen chloride. Although chloramine T was the usual oxidation reagent for cyanide, the alternative reagent N-chlorosuccinimide was found to be more suitable for application in a post-column reaction system. Therefore, this reagent suggested itself for employment in the detection of iodide.

As mentioned above, the blue color of the post-column reaction is not stable and careful optimization of the reaction conditions is necessary. The optimum of the reaction time is in the order of 14 s depending strongly on the temperature and other reaction conditions. We tried to keep the length of the mixing capillary as short as possible so that a high backpressure would be avoided. This was done with respect to an eventual use of alternative post-column reagent-delivery systems that are driven by pressure. These systems would allow a generally pulseless flow and therefore a minimum of baseline noise, but do not tolerate high backpressures.

It should be remembered that one of the reagents, namely the tetrabase, is a component of the mobile phase so that only one post-column reagent pump is necessary for the addition of the N-chlorosuccinimide/succinimide reagent (a post-column reaction solution consisting of a mixture of tetrabase and the oxidizing reagent would not be stable so that both reagents must be pumped individually; the incorporation of the tetrabase into the mobile phase does not interfere with the chromatographic separation and does not lead to side reactions with iodide during the separation process). The practicable pH for the reaction is limited to a range below 4.5 because the tetrabase is not soluble at higher pH values. Generally, sensitivity decreases with decreasing pH. In practice, a pH not higher than 4.0 was chosen in order to avoid precipitation in the reaction coil under all circumstances. Increasing the tetrabase concentration from 0.4 to 0.8 g/l results in a four-fold increase in sensitivity. Higher concentrations can lead to solubility problems and have not been investigated. The temperature effect was investigated in a range from 35 to 65°C. Up to 55°C, the sensitivity increased linearly and was roughly doubled for each 10°C. This increase in sensitivity leveled off at temperatures above 55°C. Unfortunately, the signal-to-noise ratio did not increase to the same extent because of increased background absorption (even without iodide, the reaction between hypochlorite and tetrabase does occur, although the reaction kinetics are slow). A temperature of 45°C yielded the best signal-to-noise ratio. Finally, the sensitivity depends on the concentration of the N-chlorosuccinimide. An increase in its concentration from 1 to 1.5 g/l yields an increase in sensitivity of approximately 50%. Higher concentrations pose problems with respect to solubility and have not been investigated further.

3.2. Analysis of seawater samples

Generally, samples of high ionic strength such as seawater cannot be injected directly onto the separation column due to severe peak broadening as a result of self-elution by the sample matrix itself and loss of band-compression effects. Special techniques such as on-column matrix elimination can overcome these problems. In this case, the matrix ion is used as component of the eluent in a concentration close to —or even higher than— the sample matrix. In reality, high eluent concentrations may lead to

retention times that are too short. Therefore, a compromise must be found and the optimum concentration will be low enough to achieve a reasonable retention time but high enough to avoid poor peak shapes. Fig. 1 shows the dependence of the number of theoretical plates for the iodide peak as a function of sodium chloride concentration of the matrix and injection volume (in all cases, the concentration of sodium chloride in the eluent was kept at 5.84 g/l, at which concentration a reasonable retention time of approximately 5.5 min can be achieved, while still providing effective matrix elimination). With respect to separation efficiency, a decrease in injection volume is preferable to a dilution of the sample matrix. An injection volume of 150 μl was chosen as a compromise between sensitivity and separation efficiency. One should be aware of the fact that the data in Fig. 1 indicate just a moderate separation efficiency achievable with this mobile phase. This is not a big obstacle as we are not dealing with a complicated separation problem. The only interfering peak (reacting in the tetrabase/N-chlorosuccinimide system) would be bromide, but it elutes near the void volume well separated from iodide. The pseudohalide, thiocyanate, might be expected to show some reaction with the reagent; nevertheless, the experiments indicated no interferences from thiocyanate up to 1.5 ppm.

The response of the post-column reaction detector was found to be linear in a range up to 100 ppb for an injection volume of 150 μl. The detection limit (given as signal-to-noise ratio of 3) was approximately 0.8 ppb (injection volume of 150 μl) corresponding to an absolute amount of 120 pg injected. This detection limit is approximately five times poorer than that obtained earlier with a mobile phase containing methanesulfonic acid without sodium chloride [14,15]. Obviously, the relatively high concentration of sodium chloride in the eluent decreases the sensitivity of the post-column reaction. Nevertheless, detection limits are still good enough for the application described in this paper. Most of the baseline noise could be attributed to small irregularities in the flow-rates of the pumps used for delivering the mobile phase and the post-column reagent. Therefore, efficient pulse dampeners are crucial. The use of syringe pumps instead of reciprocating piston pumps might have some potential for further reduction of baseline noise. Unfortunately, this sort of instrumentation has not been available for this study.

Fig. 2 shows a typical chromatogram for the determination of iodide in seawater. The reproducibility was checked by injecting a seawater sample six times which yielded a relative stan-

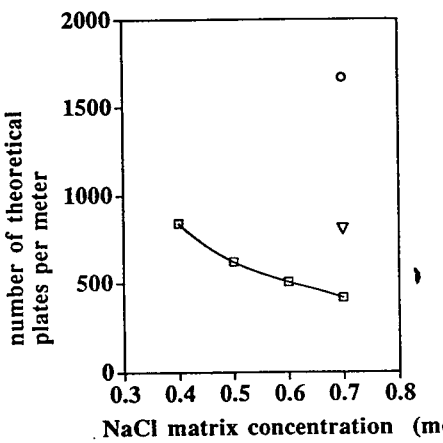

Fig. 1. Dependence of the number of theoretical plates for the iodide peak as a function of the sodium chloride concentration of the matrix and the injection volume. Injection volumes: □ = 200 μl; ▽ = 150 μl; ○ = 100 μl.

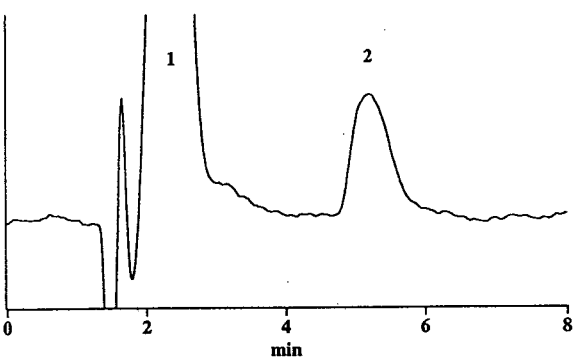

Fig. 2. Typical chromatogram for the determination of iodide in seawater. Injection volume: 150 μl; wavelength: 605 nm; 0.01 AUFS; other conditions as in Experimental section. Peaks: 1 = bromide; 2 = iodide (5 ppb).

dard deviation of 3.2% for 5 ppb iodide. Quantification was done by external standards. Generally, the range of iodide concentrations to be expected in seawater samples is relatively narrow. Therefore, it seemed justified to use only two external standards covering the lower and higher end of this range. The following injection sequence was observed: standard 1–sample 1–sample 1–standard 2–sample 2–sample 2–standard 1–sample 3– . . . . For each sample, the standards enclosing this sample were used for quantification.

Organic matter present in natural waters can interfere with voltammetric methods, but we have not observed any problems with our IC method in the analysis of several marine and estuarine water samples. Even if organic interference was subsequently noted in different samples, we believe that it could be removed by pre-treatment of the sample by passing it through a small cartridge containing a suitable reversed-phase substrate.

If other salts in addition to sodium chloride are present in a saltwater sample, then it is possible that the eluent recommended above will not be adequate for good chromatography. However, by appropriate adjustment of the eluent to include other major salts to restore effective matrix elimination [11], and then re-optimization of the post-column reaction, it should be possible to determine iodide in an even larger range of water samples.

We will be looking to apply this method to iodide determination in various marine and other natural waters as part of ongoing work in our laboratories.

4. Conclusions

Matrix-elimination IC in combination with selective post-column reaction detection shows a range of attractive features that should make this technique an interesting alternative to existing methods for trace determination of iodide in high-ionic-strength matrices. Ion chromatography can easily be automated and adapted to a high sample throughput. The instrumentation is robust and can be made compatible with the requirements of remote operation, such as shipboard analysis. In this way, problems associated with sample transport and sample preservation might be reduced considerably. The detection limit of this technique for iodide is low enough (and can still be improved to some extent by instrumental modifications as indicated above) to be a valuable tool for investigations of iodine speciation in diverse saline waters.

Acknowledgement

Technical support from Dionex Corporation is gratefully acknowledged.

References

[1] R. Fuge and C.C. Johnson, *Environ. Geochem. Health*, 8 (1986) 31; and references cited therein.
[2] T.D Jickells, S.S. Boyd and A.H. Knap, *Mar. Chem.*, 24 (1988) 61.
[3] J.D. Smith, E.C.V. Butler, D. Airey and G. Sandars, *Mar. Chem.*, 28 (1990) 353.
[4] V.W. Truesdale, *Mar. Chem.*, 6 (1978) 253.
[5] J.R. Herring and P.S. Liss, *Deep Sea Res.*, 21 (1974) 777.
[6] K. Takayanagi and G.T.F. Wong, *Talanta*, 33 (1986) 451.
[7] G.W. Luther, C. Branson-Swartz and W.J. Ullman, *Anal. Chem.*, 60 (1988) 1721.
[8] E. Nakayama, T. Kimoto and S. Okazaki, *Anal. Chem.*, 57 (1985) 1157.
[9] K. Ito and H. Sunahara, *J. Chromatogr.*, 502 (1990) 121.
[10] K. Ito, Y. Ariyoski, F. Tanabiki and H. Sunahara, *Anal. Chem.*, 63 (1991) 273.
[11] Marheni, P.R. Haddad and A. McTaggart, *J. Chromatogr.*, 546 (1991) 221.
[12] K. Han, W.F. Koch and K.W. Pratt, *Anal. Chem.*, 59 (1987) 731.
[13] E.C.V. Butler and R.M. Gershey, *Anal. Chim. Acta*, 164 (1984) 153.
[14] W. Buchberger and K. Winsauer, *Mikrochim. Acta Wien*, III (1985) 347.
[15] W. Buchberger, *J. Chromatogr.*, 439 (1988) 129.
[16] F. Feigl and E. Jungreis, *Fresenius' Z. Anal. Chem.*, 161 (1958) 87.
[17] P.A. Fagan and P.R. Haddad, *J. Chromatogr.*, 550 (1991) 559.

ELSEVIER

Journal of Chromatography A, 706 (1995) 277–280

JOURNAL OF CHROMATOGRAPHY A

Ion chromatographic determination of nutrients in sea water

S. Carrozzino*, F. Righini

SMP, USL 13, Via Marradi 114, 57125 Leghorn, Italy

Abstract

The application of ion chromatography, with eluent suppression and conductometric detection, to the determination of nitrate and phosphate concentrations in sea water was investigated. The aim was to evaluate the concentration of both species simultaneously and without the need to pretreat the sample, thus avoiding the disadvantages inherent in the usual analytical methods (molecular spectroscopy of suitable derivatives). The determination of nitrate was also accomplished using UV detection at 210 nm by means of a diode-array detector connected in series with the conductivity detector. In this way, by comparing the absorption spectra of nitrate in the standard solution and in the samples and by checking the purity index of the related peaks, the effectiveness of the chromatographic separation and the lack of interferences in the analysis were monitored. About 40 samples of sea water, taken over several months in four different locations, were analysed after filtration and dilution. In all the samples nitrate was detectable and the separation between the peaks of nitrate and bromide was complete, even when the bromide concentration was as high as 70 ppm. Only some of the samples, owing also to the nearly always necessity for dilution, showed a concentration of phosphate higher than the limit of detection.

1. Introduction

Some areas of the Italian coastline are affected by eutrophication. In such cases, Italian legislation requires that the regions activate plans for biological and chemical control. As nitrate and orthophosphate are among the chemical species to be evaluated, we directed our efforts towards the achievement of an analytical method that could be both reliable and rapid.

2. Experimental

2.1. Samples

Samples of sea water were taken in four resorts on the Tyrrhenian coast, Calambrone, Naval Academy, Tre Ponti and Chioma. Chioma lies about 7 km to the south of the town of Leghorn (Tuscany), while Calambrone lies about 4 km to the north of the town and about 9.5 km to the south of the mouth of the river Arno. Naval Academy and Tre Ponti are situated on the town coastline. The samples were taken in the period from January 1992 until May 1993, at a distance of about 0.5 m from land and at a depth of about 40 cm. They were put in polyethylene bottles and kept at 4°C until analysis. Aliquots of 5 ml were usually diluted five- or tenfold with analytical-reagent grade water (specific resistance >18 MΩ cm); they were then filtered through 0.45-μm filters and finally injected.

The samples taken at Calambrone always showed a lower salinity, owing to the proximity

* Corresponding author.

0021-9673/95/$09.50
SSDI 0021-9673(94)01246-6

of the mouth the river of Arno, and they were sometimes analysed undiluted.

2.2. Apparatus

A Dionex Model 4500i ion chromatograph equipped with an autosampler, Dionex conductivity detector II, Spectra-Physics Model 4270 integrator, Perkin-Elmer Model 235 diode-array detector and Epson AX2e PC with Perkin–Elmer Omega software was used. The chromatographic conditions were as follows: mobile phase, 180 m*M* sodium carbonate–170 m*M* sodium hydrogencarbonate, 4.5 ml diluted to 1 l (conductivity 10–11 μS cm), pumped at 2 ml/min; regenerant, 25 m*M* sulphuric acid; regenerant flow-rate, 5 ml/min; loop, 20 μl; and detection wavelength, 210 nm.

The ion chromatographic (IC) guard column and analytical column used were Dionex Ion Pac AG4A-SC (50 × 4 mm I.D.) and Ion Pac As4A-SC (250 × 4 mm I.D.), respectively.

Millipore Millex GS 0.45-μm syringe filters (25 mm) were used. A Millipore Milli-Q 50 water-purification system was utilized.

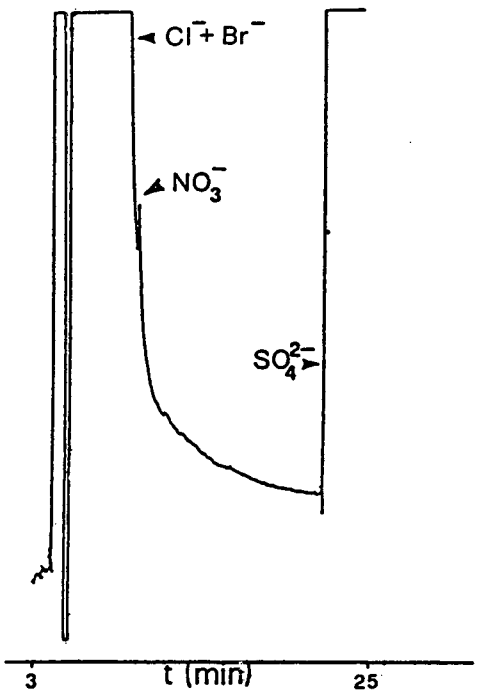

Fig. 1. Chromatogram obtained with conductimetric detection (range 0.3 μS cm) for a sample of sea water diluted tenfold.

3. Results and discussion

The difficulties to overcome in the IC determination of nutrients in sea water arise from the high salinity of the samples, due to the especially high content of chlorides and sulfates, and from the comparatively low concentrations of the species of interest. On the one hand, high salinity makes it almost always necessary to dilute the samples, but on the other hand, the dilution can lower the concentrations of the analytes below the limits of detection, thus restricting the usefulness of the dilution itself. The concentration of nitrate ion in the samples is about two and four orders of magnitude lower than those of bromide and chloride, respectively. For this reason, when using conductometric detection, the peak of chloride tends to cover the adjacent peaks of bromide and nitrate, as shown in Fig. 1.

In Fig. 2 is instead shown the UV chromatogram at 210 nm of the same sample as in Fig. 1. UV detection removes the disadvantage of the interference of chloride, as its absorptivity is very low at the selected wavelength and it is therefore more suitable for the determination of nitrates in sea water.

To achieve a good separation between the peaks of bromide and nitrate, we diluted the concentrated eluent solution (180 m*M* sodium carbonate–170 m*M* sodium hydrogencarbonate) to a conductivity of about 10–11 μS cm. The mobile phase usually used in the analysis of fresh water is more concentrated (15–20 μS cm). For all the samples analysed, the separation between the peaks of bromide and nitrate was complete under the chromatographic conditions adopted, as shown in Fig. 2. Further, the comparison between the absorption spectra of nitrate in the standard solutions and in the samples and the values of the purity index of the related peaks

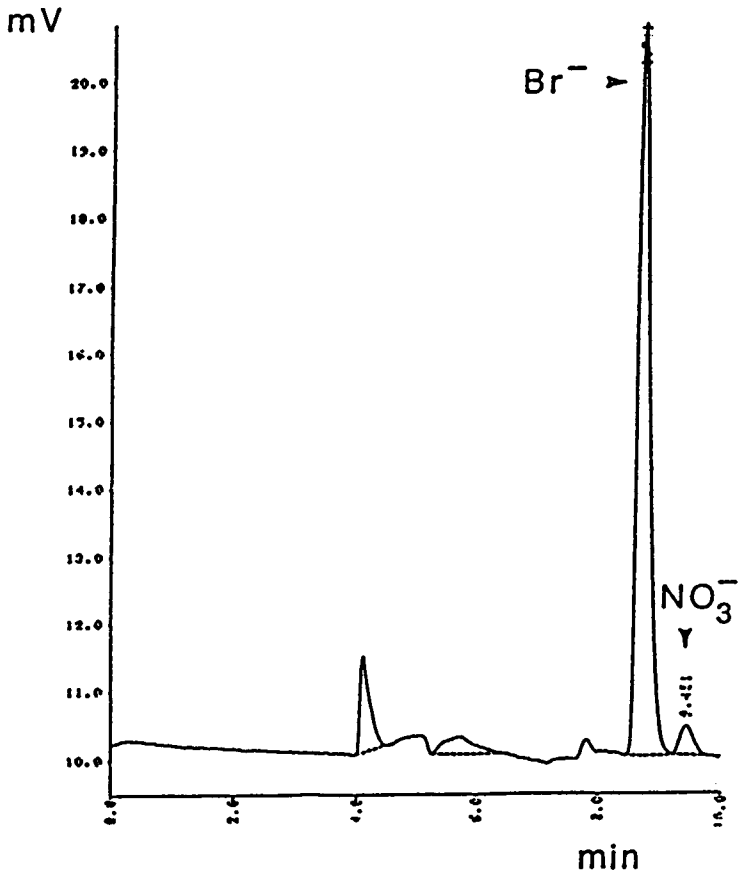

Fig. 2. Chromatogram obtained with UV detection for the same sample as in Fig. 1 ($\lambda = 210$ nm; nitrate concentration, 89 μg/l; bromide concentration, 3.6 μg/l).

indicated the lack of any interference in the analysis.

A good separation between the two peaks was also obtained with a more concentrated mobile phase, having a conductivity of about 20 μS cm, pumped at 1 ml/min, but the retention times became longer and the shape of the peaks broadened.

The concentration of nitrate ion in the samples examined ranged from 0.3 to 11.1 mg/l. The minimum nitrate detectable concentration in sea water was 0.04 mg/l.

The samples taken at Calambrone nearly always showed the highest concentrations of nitrate, owing to the proximity to the mouth of the river Arno, which receives civil and industrial wastes from a densely populated area and whose average flow is 99.3 m^3/s. The average value of the nitrate concentration (6.6 mg/l) is twenty times higher than that obtained for the same location in the period from August 1989 to September 1990 [1]. However, the period of that investigation was particularly dry and warm and the corresponding poor flow of the river could have reduced their supply of nutrients to the sea. The river supply, owing also to the morphology of the coast in this area, is a determinant factor. In fact, the trend of the values of salinity that were reported indicates that the slowly downward-sloping depth contour slackens the mixing between brackish and fresh water along the coast; the latter appears to slide over the former,

producing a poorly salty layer that is about 2 m deep and many miles long.

The concentrations of the soluble orthophosphate ion were evaluated by means of conductimetric detection. This kind of determination presented some difficulties. In fact, the limit of detection of orthophosphate by IC with conductimetric detection is 40 μg/l [2], which is 10–15 times higher than in the usual analytical methods based on molecular spectroscopy of suitable derivatives [3,4]. Moreover, from a previous investigation [1] in the area of Calambrone, the average concentration of phosphate, measured all the year round, was found to be about 26 μg/l, that is, lower than the limit of detection. Finally, the high salinity of the sample often prevented us from using adequate levels of sensitivity of the detector or made it essential to dilute the samples, with a further lowering of the concentration of this analyte. Therefore, the concentration of phosphate could be evaluated only in those samples which, despite the dilution, showed a concentration of phosphate higher than the limit of detection; the minimum phosphate concentration detectable in sea water was 0.1 mg/l.

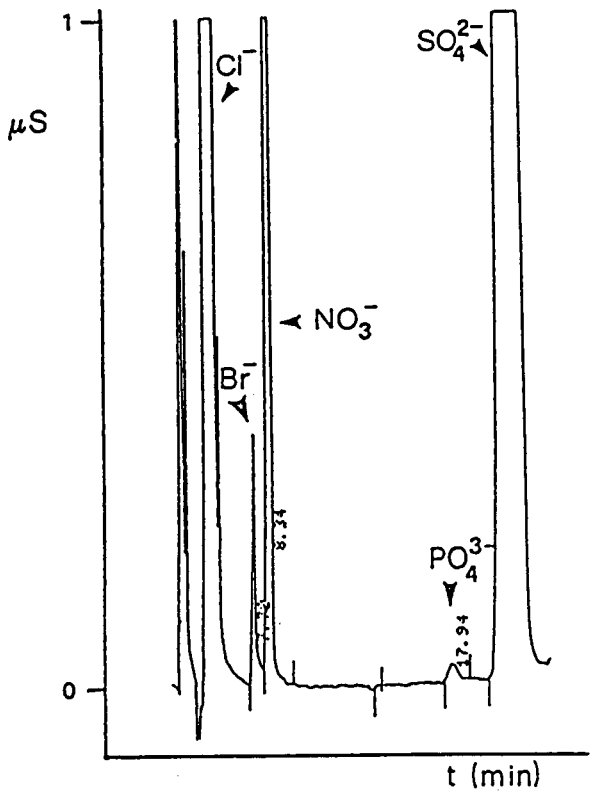

Fig. 3. Chromatogram obtained with conductimetric detection for undiluted sea water taken at Calambrone (range 1.0 μS cm).

Fig. 3 shows the peak of phosphate in the chromatogram of a sample characterized by a low level of salinity. The detectable values range from 0.3 to 1.6 mg/l of orthophosphate and are related to the Calambrone and Tre Ponti locations during the winter months, when the rainfall and the supply of nutrients by the streams are higher.

References

[1] S. Buzzichelli, S. Cavalieri and G. Ceccarelli, *Progetto Mare. Ricerca sullo Stato Biologico, Chimico e Fisico dell'Alto Tirreno*, Università di Firenze, Florence, 1993, p. 529.

[2] G. Valsecchi and G. Tartari, *Notiziario Metodi Analitici per le acque*, CNR, Leghorn, 1992, No. 12 (1), pp. 1–9.

[3] R. Mosello, R. Baudo, G. Tartari, M. Camusso, G. Margo, H. Muntau, A. Barbieri and G. Righetti, *Documenta dell'Istituto Italinao di Idrobiologia*, 1989, No. 18.

[4] J.D.H. Strickland and T.R. Parsons, *Fish. Res. Board Can. Bull.*, 1972, No. 167.

ELSEVIER

Journal of Chromatography A, 706 (1995) 281–286

JOURNAL OF CHROMATOGRAPHY A

Ion chromatography of organic-rich natural waters from peatlands
III. Improvements for measuring anions and cations

Philipp Steinmann, William Shotyk*

Geologisches Institut, Universität Bern, Baltzerstrasse 1, CH-3012 Bern, Switzerland

Abstract

Organic-rich, anaerobic pore waters from peatlands have been sampled using peepers which filter the waters in situ. Pore waters collected using these devices are neither oxidized nor degassed. Anions (F^-, acetate, formate, Cl^-, HCO_3^-, NO_2^-, Br^-, NO_3^-, PO_4^{3-}, SO_4^{2-} and $S_2O_3^{2-}$) and cations (Na^+, K^+, Mg^{2+} and Ca^{2+}) were analyzed using ion chromatography (IC). With a Na borate gradient increasing from 4.9 to 24.5 m*M*, F^-, acetate, formate, Cl^-, HCO_3^-, NO_3^-, PO_4^{3-} and SO_4^{2-} can be quantified in one run (12 min). The high concentrations of dissolved CO_2 in the pore waters are manifested as a broad HCO_3^- peak in the chromatograms. This allows HCO_3^- to be quantified (with a linear calibration curve from 40 to 800 μg/g), but interferes with the Br^- and NO_2^- peaks. Measurement of these two species requires sample degassing to remove dissolved CO_2. While $S_2O_3^{2-}$ can also be determined using a modified borate gradient (7 to 35 m*M*), its concentration in the pore water samples is below the detection limit of approximately 30 ng/g. In an earlier report, IC measurements of Na^+, K^+, Mg^{2+}, and Ca^{2+} in peat bog pore waters were found to yield significantly lower concentrations compared to inductively coupled plasma analyses of the same samples. Here, 20 m*M* methanesulfonic acid was used to acidify the pore waters to pH 2 prior to injection. Following this sample pretreatment, the measured concentrations of Na^+, K^+, Mg^{2+}, and Ca^{2+} obtained by IC were significantly higher than in the unacidified samples and were in good agreement with the concentrations determined independently using inductively coupled plasma mass spectrometry.

1. Introduction

Ion chromatography (IC) has been used to measure both anions (Cl^-, NO_2^-, Br^-, NO_3^-, HPO_4^{2-}, SO_4^{2-} and oxalate) and cations (Na^+, NH_4^+, K^+, Mg^{2+} and Ca^{2+}) in organic-rich natural waters from peatlands [1,2]. The pore waters in these previous studies had been squeezed from peat cores and vacuum-filtered through a 0.2-μm membrane filter. As a result, the samples were both degassed and partly oxidized. Unfortunately, HCO_3^- is completely removed from the pore waters when they are degassed, and the concentrations of other important ionic species (NO_2^-, NO_3^-, PO_4^{3-}, SO_4^{2-}, NH_4^+) may be greatly increased or decreased because of oxidation. Therefore, in these vacuum-filtered water samples, reliable measure-

* Corresponding author.

0021-9673/95/$09.50
SSDI 0021-9673(95)00103-4

ments could be obtained only for Cl^-, Na^+, K^+, Mg^{2+} and Ca^{2+}.

In the present study, IC methods are applied to peat bog pore waters sampled with peepers. Peepers are in situ diffusion-equilibrium pore water samplers and provide pore water samples which are neither oxidized nor degassed. The species determined, typical concentration ranges of these ions in bog pore waters and retention times are given in Table 1. Because the peeper samples are not degassed, they may contain high concentrations of dissolved carbon dioxide. Using a borate eluent, however, HCO_3^- can be quantified in these samples in addition to Cl^-, NO_3^-, PO_4^{3-} and SO_4^{2-}. The borate eluent may be modified so that $S_2O_3^{2-}$ also elutes.

In the previous study [2], IC measurements of Na^+, K^+, Mg^{2+} and Ca^{2+} in peat bog pore waters were found to yield significantly lower concentrations compared to inductively coupled plasma (ICP) analyses of the same samples. In the present investigation this discrepancy was resolved by acidifying the pore waters to pH 2 prior to injection.

Table 1
Typical range of solute concentrations found in organic-rich peat bog pore waters sampled with peepers

Species	Concentration range (μg/g)	Retention time (min)
Fluoride	<0.03	2.1
Acetate	<0.02–2 (17)	2.3
Formate	<0.02	2.8
Chloride	0.3–2	4.2
Nitrite	<0.02	5.1
Bicarbonate	100–350 (700)	5.5
Bromide	<0.02	6.7
Nitrate	<0.02	7.3
Phosphate	<0.02–1 (2)	9.5
Sulfate	<0.01–0.3	11
Thiosulfate	<0.05	40
Sodium	0.25–1.1	4.1
Potassium	0.02–0.8 (4)	6.2
Magnesium	0.03–0.3 (2.5)	7.6
Calcium	0.1–4 (35)	9.6

The pH range is typically 4–5, while DOC concentrations range from 30 to 80 mg/l. The exceptional values given in parentheses are mainly found in deeper peat layers where groundwater can infiltrate. Retention times refer to the elution conditions given in the text. Note that thiosulfate was determined with the special gradient described in the text.

2. Experimental

2.1. Location of sites

The pore waters studied were collected from two continental bogs in the Franches-Montagne region of the Jura Mountains, Switzerland. One of the bogs, Tourbière de Genevez (TGe), consists of 1.5 m of peat, while at the other site, Etang de la Gruyère (EGr), peat accumulation is more than 6 m. More detailed descriptions of the sites are given elsewhere [3].

2.2. Sampling of peat pore waters

The pore waters analyzed in this study were obtained using peepers [4]. Peepers were originally designed for studying pore waters in lake or sea sediments [5]. They consist of a single Plexiglas housing made up of individual 30-ml chambers that are filled with deionized, deaerated water and covered with a 0.2-μm membrane filter. The chambers are inserted into the bog at different depths and are allowed to equilibrate with the pore waters for about five weeks. To prevent oxidation during sample collection and handling, the peepers are pulled directly from the bog into N_2-filled glove bags. Individual chambers are then sampled through the glove bag using syringes. The samples are brought to the laboratory in the closed syringes, which are kept in a cold-storage bag, and then analyzed immediately. Because a 0.2-μm filter is built into the sampler, there is no need to vacuum-filter the pore waters prior to analysis and therefore there is no degassing.

2.3. Ion chromatography

The IC system used was a Dionex 4500i equipped with Dionex AG4A SC/AS4A-SC (anions) and CG12/CS12 (cations) analytical columns. Suppressed conductivity detection was

accomplished by using ASRS-I and CSRS-I suppressors, respectively. Injection volume was 100 μl.

Anions were analyzed using a gradient method with a sodium borate ($Na_2B_4O_7 \cdot 10H_2O$) eluent (flow-rate: 2 ml/min). With this method the column was equilibrated with the weaker eluent (4.9 m*M* sodium borate) for 5 min prior to injection; 0.5 min after injection the strength of the eluent was increased linearly to reach 24.5 m*M* sodium borate 7 min after injection. This eluent concentration was held to the end of analysis at 12 min.

The CS 12 column was eluted with 20 m*M* methanesulfonic acid (MSA) at a flow-rate of 1 ml/min. Eluents were degassed and pressurized with N_2 gas.

Carbonate standards were made by dissolving sodium bicarbonate in degassed, deionized water in a closed, completely filled bottle. Preparation of all other standards, resulting calibration curves and limits of detection, as well as the use of OnGuard-P cartridges were described previously [1,2].

Typical retention times for the ions are given in Table 1. The retention times of all peaks decreased continually in the course of a day, probably because the columns became progressively contaminated by humic acids which are abundant in the organic-rich samples. However, the columns were readily reconditioned by rinsing with 0.1 *M* NaOH for 30–60 min at the end of each day.

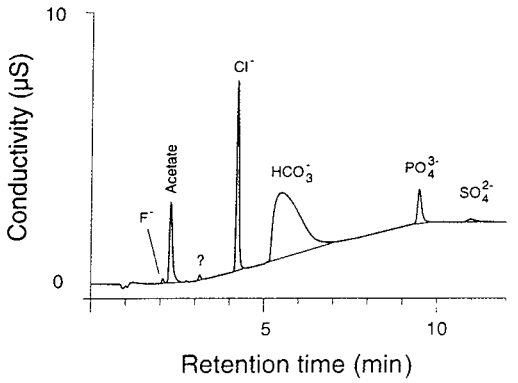

Fig. 1. Chromatogram of fresh pore water from a peat bog collected with a peeper. Gradient: 4.9 to 24.5 m*M* Na borate. The solute concentrations are: <25 ng/g fluoride, 1.6 μg/g acetate, 1.15 μg/g chloride, 227 μg/g bicarbonate, 1.31 μg/g phosphate, <25 ng/g sulfate. The peak labeled "?" is possibly due to acrylate.

3. Results

3.1. Chloride, nitrate, phosphate and sulfate

A typical anion chromatogram of a pore water sample (collected with peepers) obtained with the above borate gradient is shown in Fig. 1. The peaks attributed to Cl^-, PO_4^{3-} and SO_4^{2-} are well separated and the concentrations of these species (cf. Table 1) are readily quantified. A nitrate peak would also be separated from the other peaks, but nitrate concentrations were below the detection limit in most peeper samples (cf. Table 1).

The samples obtained using peepers showed PO_4^{3-} concentrations up to five times higher and SO_4^{2-} concentrations up to ten times lower than pore water samples squeezed from peat cores which were taken from the same bogs [1]. The lower PO_4^{3-} concentrations in the squeezed pore waters were probably the indirect result of sample oxidation; PO_4^{3-} was precipitated together with Fe^{3+} resulting from the oxidation of Fe^{2+} [6]. The higher SO_4^{2-} concentrations in the squeezed pore waters were probably also created during sample oxidation. Because only very low concentrations of inorganic reduced sulfur species have been measured in the pore waters from the peeper samples [7] the higher concentrations of SO_4^{2-} in the squeezed samples must have been due to the oxidation of organic sulfur compounds.

3.2. Bicarbonate

The large amount of dissolved CO_2 results in the broad bicarbonate peak seen in Fig. 1. Although the shape of the peak is not ideal, the calibration curve for bicarbonate was linear in

the range 40–800 μg/g bicarbonate. The equation of a typical calibration curve (obtained from standards at 50, 100, 200, 400 and 800 μg/g bicarbonate) is

$$\text{concentration} = -13.1 + 1.98 \cdot \text{area} \quad (r^2 = 0.9999)$$

where area is the peak area (μS s) and concentration is the bicarbonate concentration in μg/g. The ability of the method to measure simultaneously high bicarbonate concentrations and low concentrations of other anions meets ideally with the composition of peatland pore waters (see Table 1). Due to the irregular peak shape the method is not suitable for measuring bicarbonate concentrations below approximately 10 μg/g. Note that during IC analysis all of the dissolved CO_2 species ($CO_2 + H_2CO_3 + HCO_3^- + CO_3^{2-}$) are converted to HCO_3^-. The measured HCO_3^- concentration, therefore, corresponds to the concentration of total dissolved CO_2, $[CO_2]_T$, in the waters.

3.3. Organic anions and fluoride

Acetate and formate were found in the pore water samples. These peaks were identified by standard addition of acetate or formate to the samples (retention times are given in Table 1). Acetate may occasionally occur in high concentrations (up to 17 μg/g). High acetate concentrations are also sometimes observed in lake sediments [8]. The possible co-elution of other organic acids with formate and fluoride cannot be excluded. For formate and fluoride, therefore, only maximum concentrations can be given. Another organic anion spiked to samples was acrylate. The acrylate peak was separated from acetate and formate and only low concentrations of acrylate were found in the samples (Fig. 1). Acrylate was presumably leached from the sampling device, which consists of acrylic glass (Plexiglas).

3.4. Thiosulfate

Various inorganic sulfur species can be measured using IC (e.g. Ref. [9]). In an effort to measure thiosulfate, the borate gradient method was modified as follows: 7 m*M* Na borate for 10 min, increasing to 35 m*M* Na borate from 10 to 40 min and maintaining at 35 m*M* for 5 min. Thiosulfate eluted after 40 min with a detection limit of about 30 ng/g $S_2O_3^{2-}$. However, no thiosulfate peaks were recorded in the peat bog pore water samples.

3.5. Nitrite and bromide

At high HCO_3^- concentrations it is impossible to measure low concentrations of NO_2^- and Br^- because both peaks are overlapped by the huge HCO_3^- peak. However, nitrite and bromide can be measured using the isocratic method described previously [1]. Unfortunately, in CO_2-charged waters analyzed isocratically, the broad HCO_3^- peak overlaps the Cl^- and the NO_2^- peak. Accurate measurement of Cl^-, NO_2^- and Br^- in these samples requires degassing prior to injection.

3.6. Measurements of Na, K, Mg, and Ca by IC versus ICP mass spectrometry (MS)

As noted previously [2] concentrations of Na^+, K^+, Mg^{2+}, and Ca^{2+} in organic-rich pore waters measured by ICP were found to be 20–40% higher than those measured by IC. One possible explanation for these differences is that the OnGuard-P cartridges used to remove dissolved humic materials had also retained the fraction of these cations that were bound to the humic acids. To dissociate the metal–organic complexes the pore water samples studied here were acidified to approximately pH 2 with MSA. MSA was added to give a final concentration of 20 m*M* in the samples, the same concentration of MSA as in the eluent. Sodium, K, Mg and Ca were determined in a set of 21 pore water samples using both IC and ICP-MS methods. Good agreement was found between the two methods, with the regression curves having slopes close to 1 and high coefficients of correlation (Fig. 2). When the results shown in Fig. 2 are compared with those shown in Fig. 6 of Ref. [2], it is clear that organic-rich waters must be acidified before

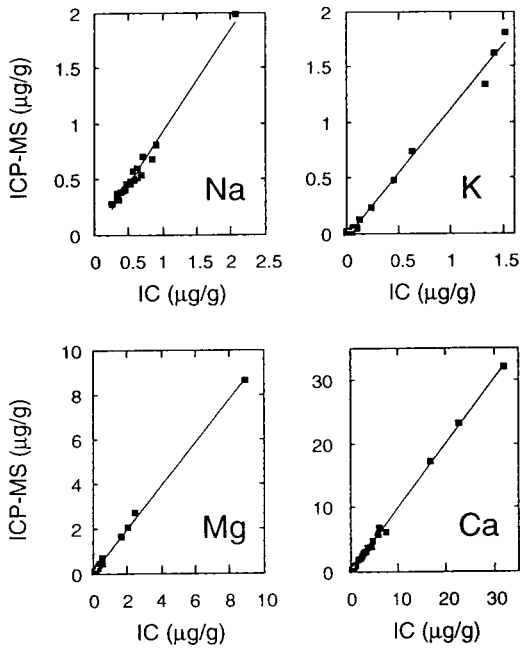

Fig. 2. Comparison of measured metal concentrations using ICP-MS versus IC. A set of 21 samples from the bogs at EGr and TGe was analyzed using both methods. The linear regression equations are as follows: Na, ICP-MS = 0.93 IC − 0.01 ($r^2 = 0.979$); K, ICP-MS = 1.14 IC − 0.02 ($r^2 = 0.993$); Mg, ICP-MS = 0.97 IC − 0.03 ($r^2 = 0.998$); Ca, ICP-MS = 1.01 IC − 0.07 ($r^2 = 0.998$).

analyzing cations by IC. Moreover, because humic substances are less soluble at low pH values, sample acidification should improve the efficiency of the organics-removal cartridges, thereby extending the life of the analytical columns.

4. Summary and conclusions

IC was used to analyze anions and cations in pore waters obtained using in situ diffusion-equilibrium samplers (peepers). These results were compared with those of an earlier IC study in which the pore waters were obtained from the same bogs by squeezing peat samples and vacuum-filtering the expressed solutions. Individual water samples were removed from the peeper chambers by syringe in a N_2-filled glove bag in the field. The samples were injected into the ion chromatograph using the same syringe, and this procedure guarantees minimal sample degassing and oxidation.

The isocratic separation of anions described previously [1] is inappropriate for these samples, because a broad HCO_3^- 'peak' interferes with the determination of Cl^- and NO_2^-. For quantitative measurement of anions with the isocratic method, the samples must be degassed prior to injection.

Alternatively, the borate gradient method described here allows the samples to be injected without degassing and allows the quantitative determination of HCO_3^-, in addition to F^-, acetate, formate, Cl^-, NO_3^-, PO_4^{3-} and SO_4^{2-} in a single run (12 min). Because HCO_3^-, Cl^-, SO_4^{2-}, NO_3^- and PO_4^{3-} are by far the dominant inorganic anions in peat bog pore waters collected in situ, this new method is ideally suited for the analysis of inorganic anions in these samples.

A second gradient method extends the analytical capability to include $S_2O_3^{2-}$, but this species was not detected in the pore waters.

To measure Na^+, K^+, Mg^{2+} and Ca^{2+} in organic-rich waters by IC, the samples must first be acidified to pH 2. This was accomplished by adding sufficient 20 m*M* MSA to each sample. Following this pretreatment, the measured cation concentrations were significantly higher than in the unacidified samples and were in good agreement with the concentrations determined independently using ICP-MS. Acidification of the samples appeared to liberate the organically bound fraction of each of these cations, an essential step in analyzing these waters by IC.

Acknowledgements

We are grateful to Professor Albert Matter of this Institute for providing laboratory facilities and equipment. Financial support from the Canton of Bern (SEVA Lottofonds) and the Swiss National Science Foundation (Grants 21-30207.90 and 30207.92) is sincerely appreciated. Many thanks are due to Dr. Peter Blaser and

Dr. Jörg Luster (at WSL) for providing ICP-MS and DOC analyses. Mr. Hanspeter Bärtschi and Mr. Anton Steinmann built the peeper chambers. Ms. Annatina Janett helped to collect the peepers in the field. Special thanks are due to colleagues from Dionex (Switzerland) (formerly at Henry A. Sarasin) for technical support.

References

[1] W. Shotyk, *J. Chromatogr.*, 640 (1993) 309–316.
[2] W. Shotyk, *J. Chromatogr.*, 640 (1993) 317–322.
[3] W. Shotyk and P. Steinmann, *Chem. Geol.*, 116 (1994) 137–146.
[4] P. Steinmann, *Ph.D. Thesis*, University of Bern, Bern, 1995.
[5] R.M. Hesslein, *Limnol. Oceanogr.*, 21 (1976) 912–914.
[6] W.B. Lyons, H.E. Gaudette and G.M. Smith, *Nature*, 277 (1979) 48–49.
[7] P. Steinmann and W. Shotyk, *J. Chromatogr. A*, 706 (1995) 287–292.
[8] A.A. Ammann and T.B. Rüttimann, *J. Chromatogr. A*, 706 (1995) 259–269.
[9] M. Weidenauer, P. Hoffmann and K.H. Lieser, *Fresenius Z. Anal. Chem.*, 331 (1988) 372–375.

ELSEVIER

Journal of Chromatography A, 706 (1995) 287–292

JOURNAL OF CHROMATOGRAPHY A

Ion chromatography of organic-rich natural waters from peatlands
IV. Dissolved free sulfide and acid-volatile sulfur

Philipp Steinmann, William Shotyk*

Geologisches Institut, Universität Bern, Baltzerstrasse 1, CH-3012 Bern, Switzerland

Abstract

Organic-rich, acidic, anaerobic pore waters from two peat bogs in Switzerland were analyzed for sulfide using ion chromatography (IC) with electrochemical detection. With one Dionex CarboPac PA1-Guard as separator column and another one in front of the 100-μl injection loop, it was possible to separate sulfide and cyanide with detection limits as low as 1 ng/g sulfide. Pore water samples were obtained using in situ diffusion–equilibrium pore water samplers (peepers). Samples were collected under N_2 to prevent sample oxidation. Instead of preserving the dissolved sulfide with zinc acetate, sulfide was preserved by collecting the samples into 5-ml syringes containing 1 ml of concentrated eluent. In this way, the pH of the sample increased to 12 and no volatile H_2S was lost. Measured sulfide concentrations in the pore waters were all below 20 ng/g. Some samples were spiked in the field to contain 5 ng/g sulfide. This amount could be detected using IC, whereas unspiked aliquots of the same samples yielded no sulfide peak. Based on the measurements of total dissolved sulfur, sulfate and sulfide, almost all of the sulfur in the pore waters is organically bound. The IC method presented here is well suited for the measurement of acid-volatile sulfur (AVS), and was applied to AVS measurements of some pore water samples. Trapping the volatilized H_2S in eluent gave low detection limits and allowed rapid analyses without further treatment of the solution. The measured concentrations of AVS were not significantly different from the concentrations of free dissolved sulfide, suggesting that metal–sulfide complexes are relatively unimportant sulfur species in these waters.

1. Introduction

A variety of analytical methods are available for measuring sulfide in natural waters, including colorimetry, ion-selective electrode potentiometry, polarography, gas chromatography, atomic absorption spectroscopy, titrimetry and fluorimetry [1]. Unfortunately, all these methods are either subject to possible interferences and/or lack adequate sensitivity. To avoid the interference of halogens, cyanide, thiocyanate and thiosulfate, Rocklin and Johnson [2] used ion chromatography (IC) with amperometric detection to separate sulfide (HS^-) from the other species and quantify HS^- to concentrations as low as 30 ng/g. At concentrations below approximately 20 ng/g, however, they reported irreproducible peaks which sometimes disappeared entirely.

The lack of success at very low HS^- concentrations (<20 ng/g) is a significant limitation of the method because dissolved sulfide is a trace

* Corresponding author.

0021-9673/95/$09.50
SSDI 0021-9673(95)00195-6

constituent in most natural waters. The reproducibility problem at these low concentrations was studied in detail by Han and Koch [3] who attributed this to impurities in the eluent and adsorption of sulfide on the separator column. By carefully cleaning the columns, using a second guard column to remove contaminants from the eluent before the injection loop, and minimizing the length of the separator column, Han and Koch [3] achieved detection limits as low as 0.1 ng/g.

Despite the progress which has been made with respect to the IC of HS^- measurements, sample collection and preservation remains a challenge. The usual practice is to preserve the dissolved sulfide by adding zinc acetate, but this leads to severe peak tailing when the sample is directly injected into the chromatograph [1]. Moreover, poor reproducibility, plugged columns and coated electrodes were observed. After only two or three injections, acid cleaning of the columns and detector became necessary [1]. As an alternative to direct injection, Goodwin et al. [1] developed a continuous-flow procedure to separate sulfide from the sample matrix by gas dialysis prior to IC analysis.

The purpose of the study presented here was to measure dissolved sulfide in organic-rich, anaerobic waters from peat bogs by IC using direct injection without adding zinc acetate to preserve the samples. To accomplish this, pore water samples were collected using diffusion–equilibrium pore water samplers (peepers) which filter the waters in situ. This avoids degassing the samples and maintains their existing redox condition [4]. After equilibration the peeper chambers were removed from the bog into plastic glove bags under N_2. The samples were collected from the individual sample chambers of the peepers into syringes containing concentrated eluent. The high pH of this eluent preserves dissolved sulfide and the samples can be injected directly into the ion chromatograph.

A secondary objective of the study was to measure acid-volatile sulfur (AVS) in these waters and to compare these results with the concentrations of free dissolved sulfide.

2. Experimental

2.1. Location of sites

The pore waters studied were collected from two continental bogs in the Franches-Montagne region of the Jura Mountains, Switzerland. One of the bogs, Tourbière de Genevez (TGe), consisted of 1.5 m of peat, while at the other site, Étang de la Gruyère (EGr), peat accumulation was more than 6 m. More detailed descriptions of the sites are given elsewhere [5].

2.2. Sampling of peat pore waters

The pore waters analyzed in this study were obtained using in situ diffusion–equilibrium pore water samplers (peepers) [6]. Peepers were originally designed for studying pore waters in lake or sea sediments [7]. They consist of a single housing made up of individual 30-ml Plexiglas chambers that are filled with deionized, deaerated water and are covered with a 0.2-μm membrane filter. The chambers were inserted into the bog at different depths and allowed to equilibrate with the pore waters for about five weeks. To prevent oxidation during sample collection and handling, the peepers were pulled directly from the bog into N_2-filled glove bags. Individual chambers were then sampled directly through the glove bag using syringes. Syringes were assembled with plastic tips instead of stainless-steel needles in order to avoid adsorption of sulfide on the needle. The syringes contained 1 ml of concentrated eluent (five times) to which 4 ml of sample were added. Each sample, therefore, consisted of a slightly diluted pore water aliquot with pH and ethylene diamine (EDA) concentration similar to those of the eluent (see below). This step was needed to prevent losses of volatile H_2S. The samples were brought to the laboratory in the closed syringes — which were kept in a cold-storage bag — and were then analyzed immediately. Because a 0.2-μm filter was built in the sampler, there was no need to vacuum-filter the pore waters prior to analysis.

2.3. Ion chromatography

IC was performed using a Dionex 4500i IC system. Cyanide and sulfide were separated on a Dionex PA1 guard column using 0.5 *M* sodium acetate–0.1 *M* NaOH–0.5% (v/v) EDA as an eluent [8]. Only clear EDA (stored cold) was used to make up the eluent. The eluent flow-rate was 1 ml/min.

All standards were prepared in deaerated 0.1 *M* NaOH solutions made with deionized water (18 MΩ) and 50% NaOH solution (8 g/l). The sulfide stock solution was prepared by dissolving 690 mg/l $Na_2S \cdot 9H_2O$. The cyanide stock solution was made up by dissolving 189 mg/l NaCN. The stock solutions were then diluted in the NaOH solution given above to obtain the working standards.

Metal accumulation on the column degrades its performance [3]. This made periodic rinsing of the columns necessary. Column clean-up was done by first rinsing the columns with deionized water, then for 30 min with 0.1 *M* HCl and again thoroughly with deionized water. Following this the columns were reconnected to the detector and equilibrated with the eluent. In order to trap metals from the eluent an additional guard column was placed between the pump and the injection loop, as suggested by Han and Koch [3]. The resulting back-pressure of the two guard columns used was approximately 700 p.s.i.

The Ag working electrode was polished with toothpaste and the reference electrode filled with eluent. The potential applied at the Ag electrode was 0.00 V. The volume of the injection loop was 100 μl.

In order to minimize column contamination the samples were injected through organics-removal cartridges (Dionex OnGuard-P) which remove humic material present in the sample.

When switching from this sulfide application to another application (e.g. anions or cations detected with suppressed conductivity) on the same ion chromatograph, the whole system must be thoroughly rinsed with deionized water (24 h or longer). Disassembly of the pump heads and rinsing all parts with deionized water helps to shorten the time needed to clean the system.

2.4. Acid-volatile sulfur

A 20-ml volume of pore water was acidified with 10 ml of 1 *M* HCl in a 100-ml three-neck distillation flask assembled with a Liebig condenser and gas tubes. The flask was continually flushed with N_2 gas. The evolved H_2S was collected in a gas trap consisting of a 25-ml glass cylinder filled with 20 ml of eluent. Sample and HCl were allowed to react for 10 min at room temperature and were then heated up and boiled for another 10 min. Similar set-ups (but with a different trap solution and some other analytical technique) have been used to determine AVS in sediments (e.g. Refs. [9] and [10]).

3. Results

3.1. Separation, calibration and precision

With retention times of approximately 1.2 and 2.0 min, sulfide and cyanide were clearly separated. Fig. 1 shows that on a PA-1 guard column the sulfide and cyanide peaks are also well separated from a system peak (occurring when sample matrix is 0.1 *M* NaOH). Other anions that can be detected using amperometry are SO_3^{2-}, $S_2O_3^{2-}$, I^- and Br^- [2]. With the method described here, these ions gave no peaks at concentrations of 1 μg/g. Because all of these species are present in concentrations far below 1 μg/g in the pore waters studied, they cannot interfere with the sulfide measurements.

The sensitivity of the method depends on the condition of the column and the Ag electrode used and can differ considerably between two measuring periods. For example, while it was sometimes possible to calibrate down to 1 ng/g sulfide, at other times concentrations below 10 ng/g could not be detected. One possible reason for the fluctuations of performance between measuring periods might be column contamination due to the build-up of humic substances and

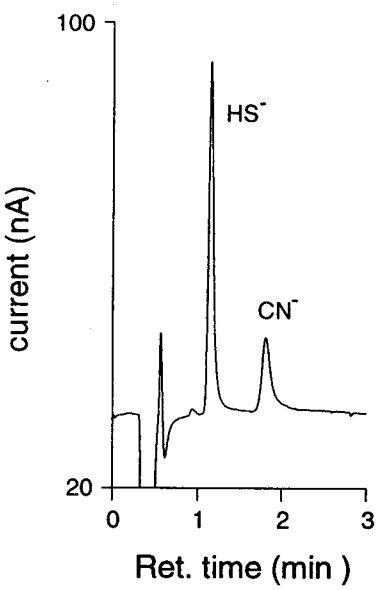

Fig. 1. Chromatogram of a standard (made up in 0.1 *M* NaOH) obtained using a Dionex PA1-Guard column and NaOH–EDA–acetate eluent. Sulfide and cyanide concentrations are 50 and 25 ng/g, respectively. The peak at 0.6 min was always observed when injecting 0.1 *M* NaOH.

metal sulfides [3]. After a column rinse as described earlier it was normally possible to detect 5 ng/g sulfide. During a single measuring period lasting several days, the system was stable. The response for cyanide is similar to that of sulfide but the cyanide peaks are broader. Nevertheless, the detection limit for cyanide is on the order of 5 ng/g or less.

Although Han and Koch [3] achieved good linearity down to concentrations of 1 ng/g HS^-, in this study calibration curves for sulfide typically were non-linear in the low ng/g range but linear at higher concentrations. A typical calibration curve at low concentrations (obtained with standards at 2, 5, 10 and 30 ng/g sulfide) is

$$\text{concentration} = 1.38 + 0.426 \cdot \text{area} - 0.0012 \cdot \text{area}^2 \quad (r^2 = 0.9997)$$

where concentration is the sulfide concentration (ng/g) and area is the peak area (nA s). The reproducibility of the method is good, with relative standard deviations (R.S.D.) for standards $< 5\%$ at the 10 ng/g level. The R.S.D. of pore water samples at this concentration can be as high as 10%. To reduce the R.S.D. for samples and to compensate for anomalous values occasionally recorded (outliers), measurements were usually done in triplicate. The R.S.D. for means of duplicate determinations of samples was 7%. Outliers may be caused by negative peaks occasionally superimposed on the analyte peak (compare baselines in Fig. 2).

As noted by others [2,3] the first few injections each day are used to condition the cell and give either a poor response or no response at all.

3.2. Effect of organics-removal cartridges

The organics-removal cartridges used showed no influence on the sulfide measurements. This is illustrated in Fig. 2 which compares a sample spiked to contain 10 ng/g sulfide and cyanide injected through an OnGuard-P cartridge with a 10 ng/g standard measured without a cartridge.

3.3. Preservation of sulfide in the pore water samples

To evaluate the effectiveness of the measures taken to prevent oxidation of sulfide and loss of

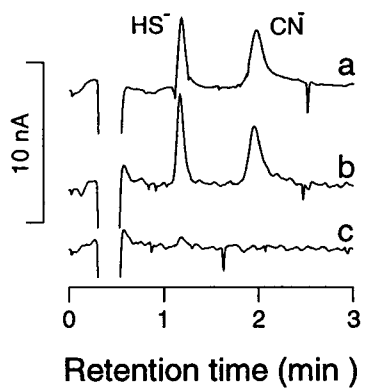

Fig. 2. (a) Chromatogram obtained from a standard containing 10 ng/g sulfide and cyanide. The standard was injected without an organics-removal cartridge. (b) Chromatogram of a pore water spiked with 10 ng/g sulfide and 10 ng/g cyanide. This sample was injected through an organics-removal cartridge. The unspiked pore waters contains only traces of sulfide (c).

volatile H_2S (described above), some samples were spiked in the field. A 4-ml pore water sample was sampled in a syringe containing 1 ml of a 25 ng/g sulfide standard made up in eluent. Therefore, upon mixing, these samples contained an additional 5 ng/g sulfide. On returning to the laboratory the added 5 ng/g sulfide could be measured, whereas no sulfide peak was detected in the unspiked samples of the same pore waters.

3.4. Acid-volatile sulfur

To determine the possible importance of sulfide complexed by metals, AVS was measured in the pore water samples as described above. The acid added during this procedure volatilizes sulfide as H_2S. The method has been shown to volatilize sulfur from (solid) FeS and ZnS but not from organic substances [10,11]. We obtained good recoveries (up to 85%) of standards containing only 1 μg of sodium sulfide using a simple trap (a 25-ml glass cylinder and a 2-ml glass pipette) to remove H_2S from the N_2 gas stream. The absolute detection limit is estimated to be approximately 0.1 μg sulfide. Trapping volatilized sulfide in eluent followed by IC analyses is a rapid and sensitive technique for AVS determinations.

3.5. Simultaneous measurement of sulfide and sulfate

Rocklin and Johnson [2] used a suppressor together with a conductivity detector after the electrochemical detector. This allowed the amperometric detection of sulfide and cyanide together with the conductometric detection of Cl^-, Br^-, NO_3^-, PO_4^{3-} and SO_4^{2-} in the same run. An experiment with a similar set-up using an AS4A-SC separator column yielded good results initially. However, after about one day the baseline started to increase and eventually became irregular. This is due to the EDA contained in the eluent. EDA is now known to damage the suppressor [12], and this combined set-up should not be used.

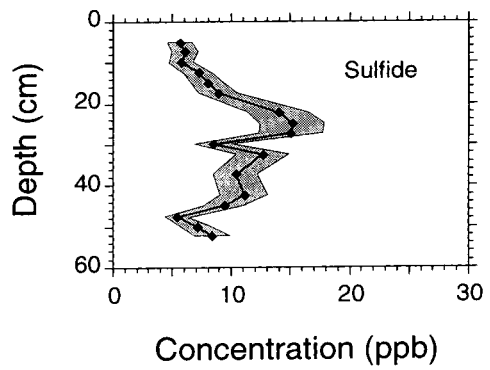

Fig. 3. Sulfide concentration profile measured at Tourbière de Genevez (TGe). The filled rhombs indicate means of duplicate measurements. The 99% confidence limits are indicated.

3.6. Sulfide in bog pore waters

Neither sulfide nor AVS was found in the pore waters of Étang de la Gruyère (EGr). In the other bog studied (Tourbière de Genevez, TGe) free sulfide levels were low (<20 ng/g) but measurable. A typical HS^- profile is given in Fig. 3.

Pore water samples from TGe contained 7–16 ng/g AVS, which is comparable to the concentrations of free sulfide measured by direct injection of the samples. This comparison shows that free, dissolved sulfide measured by direct injection of the samples represents the total sulfide in the bog pore waters.

At both bogs the concentrations of sulfate in the pore waters generally were found to be low (<20 ng/g sulfur in most samples), while total dissolved sulfur and dissolved organic carbon (DOC) were generally high (around 500 ng/g S and 30–70 μg/g DOC). It appears, therefore, that the bulk of the sulfur in these pore waters is organically bound.

No free or acid-volatile cyanide was recorded in any of the samples.

4. Conclusions

IC with amperometric detection allows the determination of sulfide and cyanide at low ng/g

concentrations in organic-rich peat bog pore waters. Samples of 4 ml (mixed with 1 ml of concentrated eluent to avoid loss of volatile H_2S) are sufficient to rinse the organics-removal cartridge and analyze the samples in triplicate; this entire procedure requires 10 min. No other pretreatment and no preservation with zinc acetate is needed when the pore water samples are handled as described above. The comparison with AVS shows that free dissolved sulfide measured by direct injection represents the total dissolved sulfide in those waters.

The combination of the H_2S trap containing eluent and IC to measure sulfide represents an effective, sensitive procedure for measuring AVS. This method is likely to find broad applications for measuring AVS in other kinds of sediments and pore water.

Acknowledgements

We are grateful to Professor Albert Matter of this Institute for helping to provide and maintain laboratory facilities and equipment. Financial support from the Canton of Berne (SEVA Lottofonds) and the Swiss National Science Foundation (Grants 21-30207.90 and 21-30207.92) is sincerely appreciated. Annatina Janett helped to collect the peepers in the field. Hanspeter Bärtschi and Anton Steinmann built the peeper chambers. Thanks are due to René Trost (Dionex (Switzerland) AG), Stefan Brand and Edgar Meder (Henry A. Sarasin AG) for technical support.

References

[1] L.R. Goodwin, D. Francom, A. Urso and F.P. Dieken, *Anal. Chem.*, 60 (1988) 216–219.
[2] R.D. Rocklin and E.L. Johnson, *Anal. Chem.*, 55 (1983).
[3] K. Han and W.F. Koch, *Anal. Chem.*, 59 (1987) 1016–1020.
[4] P. Steinmann and W. Shotyk, *J. Chromatogr.*, 706 (1995) 281–286.
[5] W. Shotyk and P. Steinmann, *Chem. Geol.*, 116 (1994) 137–146.
[6] P. Steinmann, *Ph.D. Thesis*, in preparation.
[7] R.M. Hesslein, *Limnol. Oceanogr.*, 21 (1976) 912–914.
[8] Dionex, *Application Update*, AU107, 1986.
[9] R.W. Howarth and B.B. Jorgensen, *Geochim. Cosmochim. Acta*, 48 (1984) 1807–1818.
[10] L.A. Baker, D.R. Engstrom and P.L. Brezonik, *Limnol. Oceanogr.*, 37 (1992) 689–702.
[11] R.K. Wieder, G.E. Lang and V.A. Granus, *Limnol. Oceanogr.*, 30 (1985) 1109–1115.
[12] J. Weiss, personal communication, 1992.

ELSEVIER

Journal of Chromatography A, 706 (1995) 293–299

JOURNAL OF CHROMATOGRAPHY A

Ion chromatography of organic-rich natural waters from peatlands V. Fe^{2+} and Fe^{3+}

Philipp Steinmann, William Shotyk*

Geologisches Institut, Universität Bern, Baltzerstrasse 1, CH-3012 Bern, Switzerland

Abstract

Pore waters from two peat bogs in the Jura mountains, Switzerland, were analyzed for Fe^{2+} and Fe^{3+} using ion chromatography (IC). In order to prevent oxidation, the samples were collected under N_2 using in situ diffusion-equilibrium pore water samplers (peepers). The metals were separated on a Dionex CS-5 analytical column and detected by visible absorbance at 520 nm after post-column mixing of the pyridine–2,6-dicarboxylic acid eluent with 4-(2-pyridylazo)resorcinol. The concentrations of total Fe determined by IC ranged from 0.1 to 2 μg/g and agreed well with total Fe measured in the same samples with inductively coupled plasma spectroscopy. However, a problem is caused by humic substances present in the samples because they gradually contaminate the column. Contaminated columns show reduced precision, peak tailings and reduction of Fe^{3+} to Fe^{2+} on the column. The relatively high Fe^{3+} concentrations measured in the pore waters are not an oxidation artefact, but instead reflect the stabilization of the trivalent oxidation state by complexation with humic substances.

1. Introduction

The usual approach to determine Fe^{2+} and Fe^{3+} in geological materials is to use a colorimetric method (e.g. Refs. [1] and [2]). Organic-rich natural waters from peatlands, however, may be intensely colored due to high concentrations of dissolved humic materials. For example, peat bog pore waters in the Jura mountains of Switzerland contain dissolved organic carbon (DOC) concentrations on the order of 50–120 mg/l [3]. Their color might interfere with a colorimetric determination of Fe^{2+}. Moreover, a few preliminary tests with bog waters using a colorimetric method showed unstable (drifting) readings upon the addition of the reducing agent.

In contrast to colorimetric methods which necessitate sample preparation and separate determination of Fe^{2+} and total Fe, ion chromatography (IC) offers the possibility to measure both Fe^{2+} and Fe^{3+} simultaneously with a single injection [4]. This approach has recently been used to successfully determine Fe^{2+} and Fe^{3+} in acid digests of rocks [5].

The principle objective of the study presented here is to evaluate the IC method for direct measurement of Fe^{2+} and Fe^{3+} in organic-rich, anaerobic waters from peatlands. The sampling procedure employed peepers and this approach

* Corresponding author.

0021-9673/95/$09.50
SSDI 0021-9673(95)00040-2

has been shown to involve minimal sample alteration [6].

2. Experimental

2.1. Location of sites

The pore waters studied were collected from two continental bogs in the Franches-Montagnes region of the Jura Mountains, Switzerland. The elevation is approximately 1000 m above sea level. One of the bogs, Tourbière de Genevez (TGe), consists of 1.5 m of peat, while at the other site, Étang de la Gruyère (EGr), peat accumulation is more than 6 m. More detailed descriptions of the sites are given elsewhere [3].

2.2. Sampling of peat pore waters

The pore waters analyzed in this study were obtained using peepers [7]. Peepers were originally designed for studying pore waters in lake or sea sediments [8]. They consist of a single housing made up of individual 30-ml Plexiglass chambers that are filled with deionized, deaerated water and covered with a 0.2-μm membrane filter. The chambers were inserted into the bog at different depths and allowed to equilibrate with the pore waters for about five weeks. To prevent oxidation during sample collection and handling, the peepers were pulled directly from the bog into N_2-filled glove bags. Individual chambers were then sampled through the glove bag using syringes. Syringes were assembled with plastic tips instead of stainless-steel needles to prevent sample contamination. The samples were brought to the laboratory in closed syringes which were kept in a cold storage bag and then analyzed immediately. Because a 0.2-μm filter was built into the sampler, there was no need to vacuum-filter the pore waters prior to analysis.

2.3. Ion chromatography

A CS-5 column with a CG-5 guard column was used for most measurements. In addition, a glass-lined column (from SGE, Weiterstadt, Germany) and a PEEK column filled with Nucleosil 5 SA and 10 SA resins (Macherey Nagel, Germany) were also tested.

The eluent used for the CS-5 column was 6 m*M* pyridine–2,6-dicarboxylic acid (PDCA)–90 m*M* acetic acid–40 m*M* NaOH. The eluent was adjusted to pH 4.8 with NH_4OH. Detection was accomplished by mixing the eluent with a 4-(2-pyridylazo)resorcinol (PAR) post-column reagent containing 0.5 m*M* PAR, 1.0 *M* 2-dimethylaminoethanol, 0.5 *M* NH_4^+OH and 0.3 *M* sodium bicarbonate. The flow-rate of the eluent was 1 ml/min, while the PAR reagent was added at 0.5 ml/min. In contrast to a report by Yan et al. [9] no increase in sensitivity was observed on heating the reaction coil.

The eluent used with the Nucleosil columns was 115 m*M* tartaric acid adjusted to pH 4 with NH_4OH (adapted from Ref. [10] with higher pH to reduce the retention time of Fe^{2+}). The size of the injection loop used was 100 μl.

2.4. Calibration

Iron(III) standards were prepared by diluting a 1000 mg/l Merck standard in dilute (pH 3) HCl solution (prepared with 1 *M* HCl, Merck p.a.). To prevent photoreduction of Fe^{3+} the standards were kept in the dark. Iron(II) standards were prepared by dissolving 702 mg ammonium–iron(II) sulfate in 1 l of deionized water acidified with HCl to pH 3. Ascorbic acid (1 mg/l) was added to reduce all the iron. When Fe^{3+} standards were analyzed after Fe^{2+} standards (containing ascorbic acid), considerable reduction of Fe^{3+} was observed. For this reason the instrument was calibrated for Fe^{2+} after the pore water samples had been measured.

3. Results

3.1. Detection limits, precision and accuracy

Using CS-5/CG-5 columns detection limits initially were 5 ng/g for Fe^{3+} and 10 ng/g for Fe^{2+}. However, due to the presence of humic acids in the samples the column performance

declined with time and did not meet normal IC standards with respect to precision and detection limit.

The following replicate measurements illustrate the precision of the method: The relative standard deviation (R.S.D.) of a 50 ng/g Fe^{3+} standard was 7.7% ($n = 11$). A mixed Fe(II)–Fe(III) standard ($n = 21$) measured alternately with pore water samples gave an R.S.D. of 6.8% for the total iron concentration (200 ng/g total Fe). A mixed standard with 400 ng/g total Fe measured with no samples injected between the standards gave an R.S.D. of 2.5% ($n = 9$). The precision for the samples is slightly poorer because the peaks seen in the sample chromatograms are generally broader.

Accuracy can be estimated by comparing the IC and inductively coupled plasma (ICP) spectroscopy data for these waters. The sum of Fe(II) and Fe(III) measured with the IC are comparable to the concentrations of total dissolved iron measured by ICP (Table 1).

Calibration curves were linear for both Fe^{3+} (50 ng/g to 1 μg/g) and Fe^{2+} (100 ng/g to 2 μg/g). Calibration curves for the low ng/g range are shown in Fig. 1.

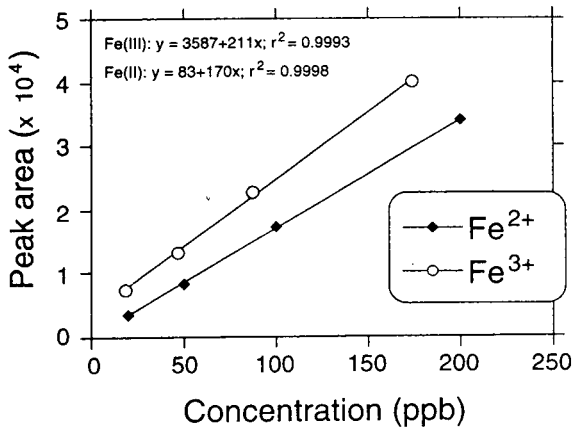

Fig. 1. Calibration curves for Fe(II) and Fe(III) obtained on a CS-5 column contaminated with humic materials. The corresponding Fe(III) peaks were shaped approximately as shown in Fig. 3.

3.2. Effects of organics-removal cartridges

Iron, like other cations, may be complexed by humic substances present in the pore water samples. When the humic substances are removed by using an organics-removal cartridge (Dionex OnGuard-P) this portion of iron may be lost. Ranging from 8 to 74% of total dissolved Fe, on average about 40% of the Fe was lost in this way. Both Fe^{2+} and Fe^{3+} were lost (see Table 1). The difference in the iron concentrations between measurements where humic acids were removed with an OnGuard-P cartridge and measurements without a cartridge might be taken as an estimate for the amount of iron complexed by humic acids. However, the results were variable and the distribution of complexed species (as determined in this way) in

Table 1
Iron(II), iron(III) and total iron concentrations of pore water samples from TGe as determined by IC compared to total dissolved iron measured by ICP

Depth (cm)	Fe^{2+} (IC) (ng/g)	Fe^{3+} (IC) (ng/g)	ΣFe (IC) (ng/g)	Fe total (ICP) (ng/g)	Fe^{2+} retained (%)	Fe^{3+} retained (%)
18	327	112	439	511	35.8	58.2
25	504	139	643	728	38.6	51.4
40	639	214	853	968	44.9	36.1
55	989	353	1342	1460	48.5	34.7
65	1400	509	1909	2005	22.4	34.0

The correlation between IC and ICP is excellent ($r^2 = 0.999$). Apparently, the sum of Fe^{2+} and Fe^{3+} (measured by IC) is less than total dissolved Fe (measured by ICP) by 5 to 14%. A part of this difference may be due to extremely stable organic complexes of Fe which were not measured by IC. The amount of iron retained on the organics-removal cartridges is variable and gives only a rough estimate for the degree of iron complexation by humic material.

a profile was often irregular. This suggests that the amount of iron lost when passing the sample by hand through an OnGuard-P cartridge is variable and gives only a very rough idea of the degree of complexation with humic acids.

In order to liberate iron from the complexes and therefore avoid its retention on the cartridge a few attempts were made to acidify the samples with HCl to pH 1. Those measurements also showed irregular results: sometimes more iron was measured in the treated than in the untreated samples, while at other times considerably less iron was measured in the treated sample. Slow kinetics of complexation reactions of iron and humic substances might be one reason for these findings. Because more humic substances are retained on the cartridges in the acidified samples more iron is also removed when replacement of complexed metals by protons is slow. In the end, it was decided not to use the cartridges despite the possible damage of humic acids to the columns.

3.3. Effects of humic substances present in the samples

On-column redox reactions are a general problem with IC determination of Fe^{3+} and Fe^{2+}. Some authors mention problems with the oxidation of Fe^{2+} on a CS-5 separator column even after the column had been rinsed with 0.1 *M* Na_2SO_3 [11], while other studies with the same column do not report such problems [5,12].

In the present study, a major problem was the reduction of Fe^{3+} due to the accumulation of humic substances on the column. After a number of injections the column was permanently in a slightly 'reducing state'. While iron(III) standards measured on an uncontaminated column yielded sharp Fe^{3+} peaks and showed no Fe^{2+} peak, a poisoned column showed tailing of the Fe^{3+} peak and a discrete Fe^{2+} peak. The Fe^{2+} peak reflects reduction of Fe(III) at the beginning of the column (guard column). Tailings show deterioration of the retention behavior for Fe(III). The decline of the iron(III) peak with time is illustrated in Fig. 2. Rinsing the columns with 0.1 *M* NaOH and exchanging the guard

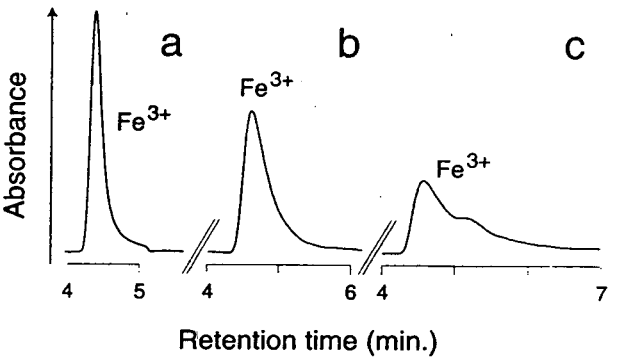

Fig. 2. Effect on the Fe(III) peak of contamination of a CS-5 column by humic materials. While an uncontaminated column gives sharp peaks (a), with increasing contamination peak tailing occurs (b), and finally the peaks become irregular (c). Moreover, some of the Fe^{3+} is reduced to Fe^{3+} on a contaminated column.

column were necessary to regenerate column performance. An example chromatogram of bog pore water obtained with an already contaminated column is shown in Fig. 3.

3.4. Monitoring of possible redox reaction on the column

The extent to which the Fe^{2+}/Fe^{3+} ratio was possibly changed on the column was determined by analyzing a mixed Fe^{2+}–Fe^{3+} standard subsequent to each sample. The appropriate Fe^{2+}–

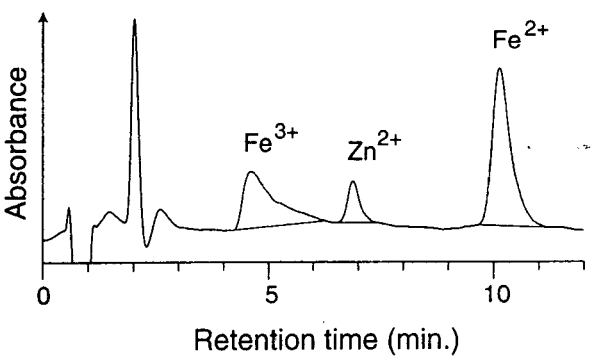

Fig. 3. Chromatogram of a bog pore water sample. Column: CS-5; eluent 6 m*M* PDCA. The column is considerably contaminated with humic material present in the samples as is seen from the tailing of the Fe^{3+} peak. In addition to iron it was possible to measure Zn^{2+}.

Fe^{3+} ratio of the standard had been measured with an uncontaminated column. Measurements on an uncontaminated column also showed that the Fe^{2+}/Fe^{3+} ratio of the mixed iron standard did not change in the course of a day (R.S.D. = 4%, $n = 9$).

Compared to the true Fe^{3+} concentration of the mixed standard, almost all measurements made subsequent to pore water samples showed less Fe^{3+} but more Fe^{2+}. Hence, during the measurements of the samples, the column was in a reducing state. The concentrations of total Fe in the mixed standards, however, was constant (see above). Maximum reduction observed in the control standards ranged from 15% to 20% of Fe^{3+} reduced. Normally it was less, often not more than 5%. However, no significant correlation was found between the extent of reduction in the control standards and the Fe^{2+} content, the total Fe concentration, or the Fe^{2+}/Fe^{3+} ratio of the preceding pore water sample. Due to this non-correlation and due to the conditioning effect of the intermittent mixed standards the samples are not likely to have affected each other.

Analysis of intermittent mixed standards (with Fe^{3+} and Fe^{2+} concentrations similar to the pore water samples) suggests that some of the trivalent iron in the pore waters may have been reduced to Fe^{2+}. The measured Fe^{3+} concentrations in these waters, therefore, represent minimum values. The true Fe^{3+} concentrations of these waters may be 5–15% higher. Samples were probably less affected by the column contaminants (humic acids) than the control standards because the latter conditioned the columns and because the samples had already been in contact with those contaminants previously. Without question, the Fe^{3+} measured in the bog pore waters is not an on-column oxidation artefact.

3.5. Performance of silica-based columns

Silica-based resins (Nucleosil 10 SA) packed in a glass-lined column were successfully used for Fe^{2+} and Fe^{3+} determinations in rainwater [11]. On the other hand, on-column reduction of Fe^{3+} was reported using columns filled with a similar resin (Nucleosil 5 SA) [13].

A few tests were done using silica-based columns. With the methods specified above a PEEK column packed with Nucleosil 5 SA resin showed a sensitivity that was comparable to that of the CS-5 column and higher than that of a glass-lined column filled with Nucleosil 10 SA. Both columns showed a slight reduction of Fe^{3+} after the injection of a Fe^{2+} standard. The main problem, however, was a system peak underlying the Fe^{3+} peak when the pH of the sample was below 4. This made measurements of low Fe^{3+} concentrations impossible.

3.6. Iron content and speciation in peatland pore waters

The concentrations of Fe^{2+} and Fe^{3+} in pore waters from Tourbière de Genevez (TGe) and Étang de la Gruyère (EGr) are given in Table 1 and Fig. 4, respectively. Total dissolved Fe concentrations are up to ten times higher at TGe compared with EGr. This difference may be explained as follows. The amount of mineral matter in the peats is higher at TGe than at EGr, and increases progressively with depth [3]. As a consequence, the Fe concentrations in the peats

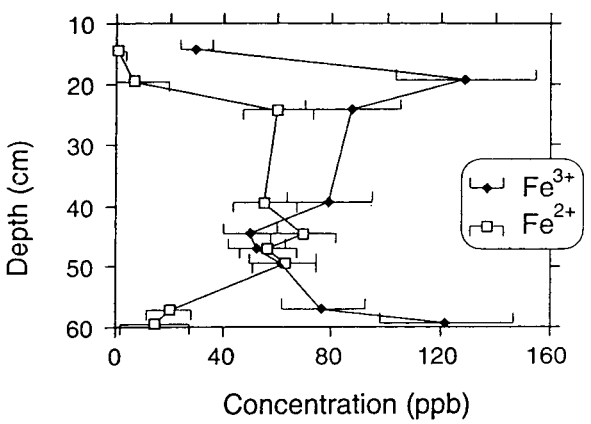

Fig. 4. Iron speciation in bog pore waters from Etang de la Gruyère (EGr). The estimated 95% confidence limits are indicated.

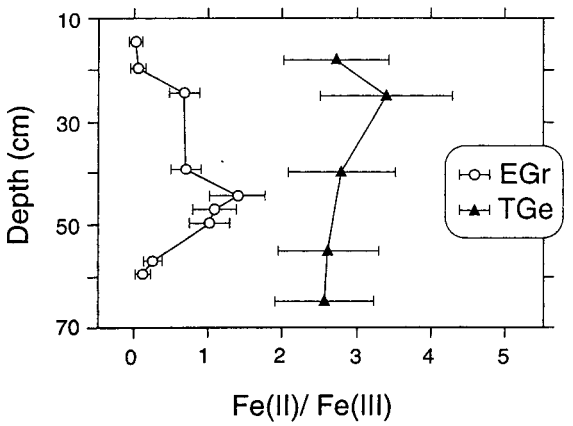

Fig. 5. Ratio of Fe^{2+}/Fe^{3+} measured in two peat bog profiles from the Jura Mountains, Switzerland. The 95% confidence limits are indicated.

at TGe are higher, and these too increase with depth.

A second difference between the two bogs is the Fe^{2+}/Fe^{3+} ratio which is higher at TGe than at EGr (Fig. 5). This may reflect a lower redox potential in the pore waters of TGe. This hypothesis is supported by the occurrence of sulfide at TGe, while at EGr no sulfide was detectable [14]. In both bogs, however, the Fe^{2+}/Fe^{3+} ratio is orders of magnitude lower than would be expected for pore waters which are anoxic and sulfidic. The high concentrations of DOC may have contributed to the relative abundance of Fe^{3+} in both bogs by forming stable Fe^{3+} complexes. For example, if the dissolved organic matter provides enough sites that stabilize Fe(III) relative to Fe(II), then a relatively low $Fe(II)_{total}/Fe(III)_{total}$ ratio may be in equilibrium with a high ratio of (free) Fe^{2+}/Fe^{3+} (see e.g. Ref. [15]).

4. Conclusions

IC can be used to measure Fe^{2+} and Fe^{3+} simultaneously in anaerobic water samples. Pore water samples which were filtered in situ using peepers installed in the bog required no pretreatment prior to injection. If the samples are maintained in an anoxic condition during sample collection and handling (as described in this paper), reliable measurements of Fe^{2+} and Fe^{3+} can be made with the following limitations. First, the abundance of humic acids in organic-rich natural waters —such as those from peatlands— leads to progressive contamination of the CS-5 separator column. This leads to broadening of the Fe^{3+} peak and diminished precision. Second, the humic materials adsorbed to the column also reduce part of the Fe^{3+} present in the samples to Fe^{2+}. Despite this, no more than 20% (and often much less) of the Fe^{3+} was reduced in any sample. The precision of the measurements is approximately ± 10% (R.S.D.) for both Fe^{2+} and Fe^{3+}.

In order to reduce the organic contamination problem the humic materials must be removed from the samples prior to analysis. One possible approach could be to incorporate dialysis membranes in the design of the peepers to allow in situ separation of free, dissolved inorganic anions and cations from large-molecular-weight humic acids. Once such a system had equilibrated, Fe^{2+} and Fe^{3+} could be measured in the dialyzed solutions by IC; this would provide the free metal ion concentrations while minimizing column contamination. Organically bound Fe^{2+} and Fe^{3+} could be measured (from undialyzed samples containing the humic fraction) by acidifying the samples to at least pH 1 and thus liberating metals from complexes. The humic material could then be adsorbed on a suitable resin.

Acknowledgements

We are grateful to Professor Albert Matter of this Institute for helping to provide and maintain laboratory facilities and equipment. Financial support from the Canton of Berne (SEVA Lottofonds) and the Swiss National Science Foundation (Grants 21-30207.90 and 30207.92) is sincerely appreciated. Many thanks are due to Dr. Peter Blaser and Dr. Jörg Luster (at WSL) for ICP and DOC analyses, René Trost (Dionex Switzerland), Stefan Brand and Edgar Mäder

(Henry A. Sarasin) for technical support, Ruth Mäder for some preliminary colorimetric measurements, Hanspeter Bärtschi and Anton Steinmann for constructing the peepers and Annatina Janett for field assistance.

References

[1] S.F. Fritz and R.K. Popp, *Am. Mineral.*, 70 (1985) 961–968.
[2] P. Komadel and J.W. Stucki, *Clays Clay Miner.*, 36 (1988) 379–381.
[3] W. Shotyk and P. Steinmann, *Chem. Geol.*, 116 (1994) 137–146.
[4] J. Weiss, *Handbook of Ion Chromatography*, Dionex, Sunnyvale, CA, 1986.
[5] Y. Kanai, *Analyst*, 115 (1990) 809–812.
[6] P. Steinmann and W. Shotyk, *J. Chromatogr.*, 706 (1995) 281–286.
[7] P. Steinmann, *Ph.D. Thesis*, University of Bern, Bern, 1995.
[8] R.M. Hesslein, *Limnol. Oceanogr.*, 21 (1976) 912–914.
[9] D. Yan, J. Zhang and G. Schwendt, *Fresenius Z. Anal. Chem.*, 331 (1988) 601–606.
[10] H. Hofmann, P. Hoffman and K.H. Lieser, *Fresenius J. Anal. Chem.*, 340 (1991) 591–597.
[11] T. Sinner, P. Hoffmann and H.M. Ortner, *Spectrochim. Acta*, 48B (1993) 255–261.
[12] C.O. Moses, A.T. Herlihy, J.S. Herman and A.L. Mills, *Talanta*, 35 (1988) 15–22.
[13] A. Seubert and G. Wünsch, *Anal. Chim. Acta*, 256 (1992) 331–348.
[14] P. Steinmann and W. Shotyk, *J. Chromatogr.*, 706 (1995) 287–292.
[15] W. Stumm and B. Sulzberger, *Geochim. Cosmochim. Acta*, 56 (1992) 3233–3257.

ELSEVIER

Journal of Chromatography A, 706 (1995) 301–305

JOURNAL OF CHROMATOGRAPHY A

Determination of anions in oilfield waters by ion chromatography

Rainer Kadnar*, Josef Rieder

ÖMV-AG, Laboratory for Exploration and Production, Gerasdorferstrasse 151, A-1210 Vienna, Austria

Abstract

For the characterization of oilfield waters (formation waters, injection waters, filtrates of drilling mud, etc.) the minor components bromide, iodide and sulfate are very important among the major components chloride and hydrogencarbonate. The chloride content of these water samples is mostly higher than 1% (10 000 ppm), whereas the concentration of the minor components is in the lower ppm range. The proposed method permits the determination of the above three minor components in one ion chromatographic (IC) run. For separation an IonPac AS9-SC analytical column is used with sodium carbonate as eluent. Detection is performed by suppressed conductivity. Chloride will be titrated because of its high concentration. In principle it is also possible to determine chloride by IC if the sample is diluted to an appropriate concentration.

1. Introduction

In exploration and production of crude oil and natural gas, the analysis of water samples is also very important. Oil and gas reservoirs are often accompanied by formation water. This is normally a highly saline brine of a composition typical for each geological formation. Formation waters in Austria differ widely in salinity and composition. The major component is sodium chloride, mostly at concentrations higher than 10 000 ppm (up to 70 000 ppm). Formation waters contain, compared with sea water, higher concentrations of the biogenic elements bromine, iodine and nitrogen and lower concentrations of sulfate and magnesium. For classification of water samples, the contents of bromide, sulfate and iodide are of interest in addition to the contents of chloride and hydrogencarbonate. In some instances a knowledge of the contents of nitrate, phosphate, fluoride, thiocyanate or organic acids is of interest.

Typical applications are the analyses of liquid samples taken from exploration wells (filtrates of drilling mud, water samples from tests) to see if there is any influx of formation water, analyses of water produced together with oil or gas to characterize the original formation water, quality check of injection water used for improved oil recovery projects and tracer studies to observe the influence of injection water or drilling mud on formation water.

In the past, various gravimetric, volumetric and photometric methods have been used to determine the mentioned anions [1, 2]. In the last few years, ion chromatography (IC) has been used as an alternative possibility for the determination of anions in aqueous solutions.

* Corresponding author.

0021-9673/95/$09.50
SSDI 0021-9673(95)00174-3

The main problem for the IC determination of anions in formation water is the large excess of chloride (from 100:1 up to 1000:1) compared with the minor components. Our aim was to find a method for the separation and determination of bromide, sulfate and iodide (concentrations mostly <100 ppm) in presence of chloride at concentrations of 10 000 ppm and higher. If possible, the determination should be performed in a single IC run with only one detector.

A Dionex Application Note [3] describes the determination of the relevant anions, but it is necessary to use two different columns (HPIC-AS2 and HPIC-AS5) for separation. Weiss [4] described some useful methods for the separation of bromide, nitrate and sulfate on IonPac AS1, AS2, AS3, AS4, AS4A, AS5, AS5A and AS9 analytical columns. Iodide and thiocyanate can be separated on an IonPac AS4, AS5 or CS5 column [4]. In this paper, a method for the separation of bromide, sulfate and iodide in brines using an IonPac AS9-SC analytical column with Na2CO_3 as eluent in a single run is described.

2. Experimental

The installation manual of the IonPac AS9-SC column [5] describes several different eluents for the separation of inorganic anions. For this work we tested various mixtures of Na_2CO_3 and $NaHCO_3$ as eluents to separate chloride, bromide, sulfate and iodide. Tests were performed on new and used ("aged") columns.

2.1. Instrumentation

The equipment used for this work was a DX-300 gradient ion chromatographic system (Dionex, Sunnyvale, CA, USA). The separated components were detected by a pulsed electrochemical detector (PED) in the conductivity mode (10 μS range). An AMMS-II micro membrane suppressor system was used for chemical suppression. The AMMS-II was continuously regenerated with 12.5 m*M* sulfuric acid at a flow-rate of 4–6 ml/min. Integration was performed by an HP 3396A integrator (Hewlett-Packard) and by CLAS/2000 (Chromatography Laboratory Automation Software, Perkin-Elmer). Columns used for separation were an AS9-SC analytical column (250 × 4 mm I.D.) and an AG9-SC guard column (50 × 4 mm I.D.). The AS9-SC analytical column has selectivity and performance identical with those of the AS9 but with added features to improve efficiency and solvent compatibility, and has an ion-exchange capacity of ca. 30 μequiv. per column [5].

2.2. Reagents

All reagents were of analytical-reagent grade (Merck, Darmstadt, Germany). Deionized water (18 MΩ) from a Milli-Q water-purification system (Millipore) was employed throughout.

2.3. Calibration standards

Stock standard solutions were prepared for each anion separately by dissolving salts in deionized water. Mixed anion working standard solutions for calibration were prepared every month from the stock standard solutions. Calibration graphs were constructed for analyte concentrations up to 10 ppm of bromide, sulfate and iodide. The ratio of chloride to bromide was 130:1 in all calibration standard solutions.

2.4. Ion chromatographic conditions

The injection volume was 25 μl. The eluent used for separation was 3 m*M* Na_2CO_3 at a flow-rate of 2 ml/min. The expected background conductivity was 13–15 μS and the system pressure was normally 1200–1400 p.s.i.

2.5. Sample preparation

All samples were filtered through a 0.45-μm filter and diluted with deionized water (18 MΩ) so that the expected analyte concentrations were within the calibration range. To prevent column contamination by liquid hydrocarbons, the di-

luted samples were filtered through OnGuard RP cartridges before injection.

3. Results and discussion

Experiments have shown that it is possible to achieve good separations of chloride–bromide and sulfate–iodide using new columns. As eluents we tested Na_2CO_3 and various combinations of Na_2CO_3 and $NaHCO_3$.

One of the weak points of the column is the rapid decrease in capacity of the AS9-SC (decrease in retention times with time). Maybe this is caused by components of the water samples, which cannot be removed by column clean-up procedures (the use of the AS9-SC column is possible only in the pH range 2–11, so strong acidic or basic clean-up solutions cannot be used).

With Na_2CO_3 as eluent it is possible to achieve a good separation of sulfate–iodide with "aged" columns and the separation of chloride–bromide is acceptable. Fig. 1 shows the chromatograms of an anion standard solution containing 1000 ppm chloride, 7.7 ppm bromide, 4.9 ppm sulfate and 9.1 ppm iodide, separated on a new and an "aged" column. Between the two runs shown in Fig. 1 ca. 300 analytical runs were carried out, representing the "ageing". As the decrease in retention times proceeds (when the retention time of iodide reaches <40% of the initial value), the determination of bromide is only possible when there is no large excess of chloride. Hence eventually the column becomes unusable for our application.

With Na_2CO_3–$NaHCO_3$ mixtures as eluent it is not always possible to separate sulfate–iodide satisfactorily, depending on the eluent and the column condition. In the worst case the two anions cannot be separated at all. Fig. 2 shows the separation of an anion standard solution on an "aged" AS9-SC column (after ca. 200 analytical runs) using different eluents (the concentrations of anions in the standard solution were the same as in Fig. 1).

Fig. 3 shows two chromatograms of liquid samples taken during an open hole test at an exploration well. The filtrate of the drilling mud contains organic acids and chloride as major anions and the concentration of bromide and iodide is <2 ppm. The water sample shows, compared with the analysed drilling mud filtrate, a lower content of organic acids and an enhanced chloride content; the concentrations of the analytes are 68.2 ppm bromide and 23.4 ppm iodide. The sample was diluted 1:20.

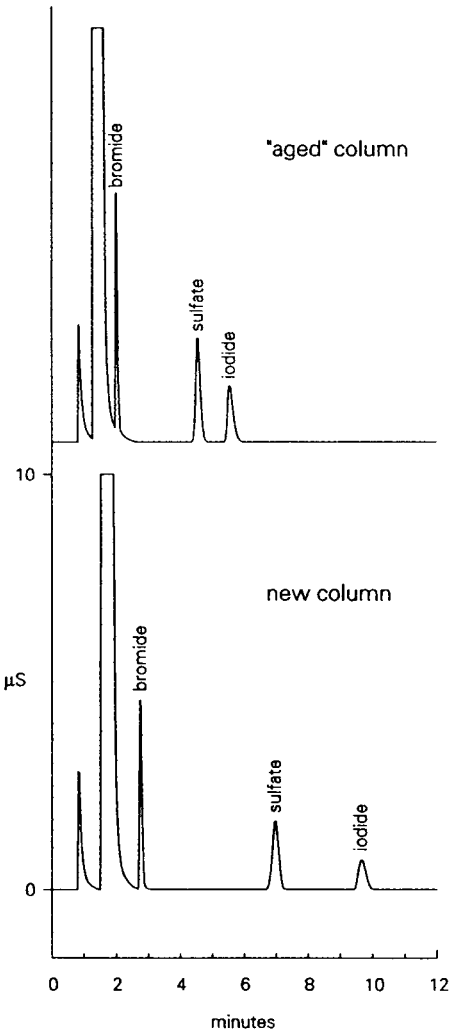

Fig. 1. Separation of anions in a standard solution (chloride to bromide ratio = 130:1) using the IonPac AS9-SC and AG9-SC columns with 3 m*M* Na_2CO_3 as eluent, with new and "aged" columns.

Fig. 4 shows the chromatogram of a water

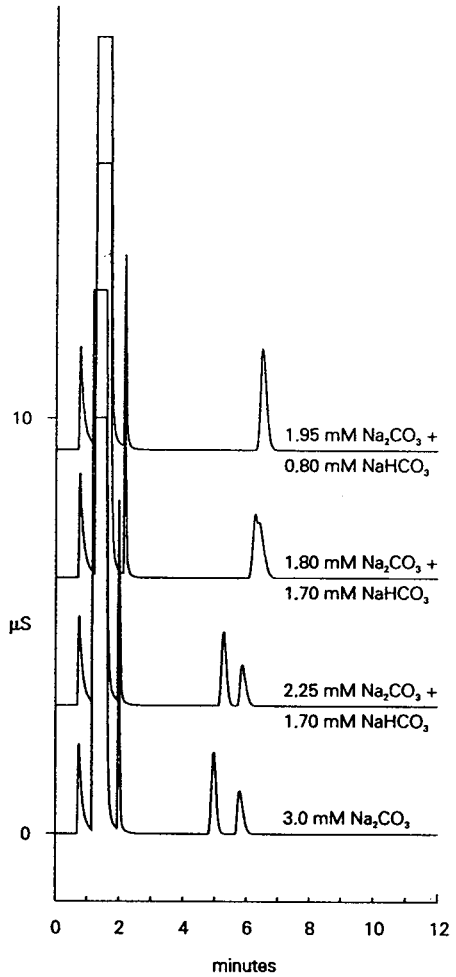

Fig. 2. Separation of anions in a standard solution (chloride to bromide ratio = 130:1) using "aged" IonPac AS9-SC and AG9-SC columns with various mixtures of Na_2CO_3 and $NaHCO_3$ as eluent.

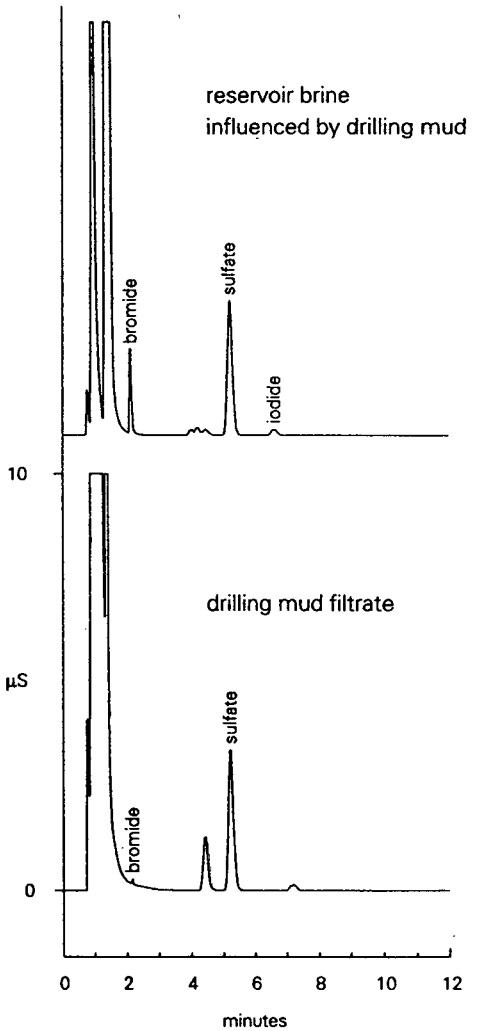

Fig. 3. Separation of anions in aqueous samples from an open hole test using the IonPac AS9-SC and AG9-SC columns with 3 m*M* Na_2CO_3 as eluent.

sample from a gas well containing 17 650 ppm chloride, 28.1 ppm bromide, 590 ppm sulfate and 15.1 ppm iodide. The sample was diluted 1:25. The ratio of chloride to bromide is ca. 630:1.

Generally it is also possible to determine other anions in various aqueous solutions with our separation method. Depending on the sample matrix, quantification is not always easy. Fig. 5 shows a chromatogram of an anion standard solution, obtained with 3 m*M* Na_2CO_3 as eluent. The analyte concentrations in this solution were 1.9 ppm fluoride, 3.2 ppm chloride, 3.5 ppm nitrite, 5.1 ppm bromide, 3.7 ppm nitrate, 3.5 ppm orthophosphate, 4.2 ppm sulfate, 10.0 ppm iodide, 6.6 ppm oxalate, 9.9 ppm thiocyanate and 5.2 ppm thiosulfate. For separation of phosphate–hydrogensulfide and sulfite–sulfate, a mixture of Na_2CO_3 and $NaHCO_3$ should be used as the result. The presence of tartrate in the water sample would enhance the sulfate content (co-elution of these two anions). Fluoride and

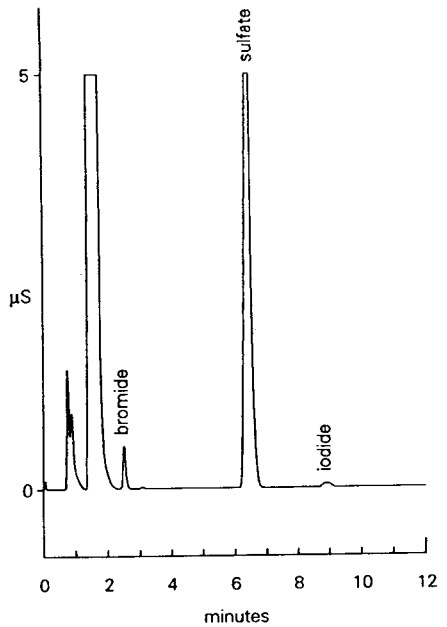

Fig. 4. Separation of anions in a water sample from a gas well (chloride to bromide ratio = 630:1) using the IonPac AS9-SC and AG9-SC columns with 3 m*M* Na_2CO_3 as eluent.

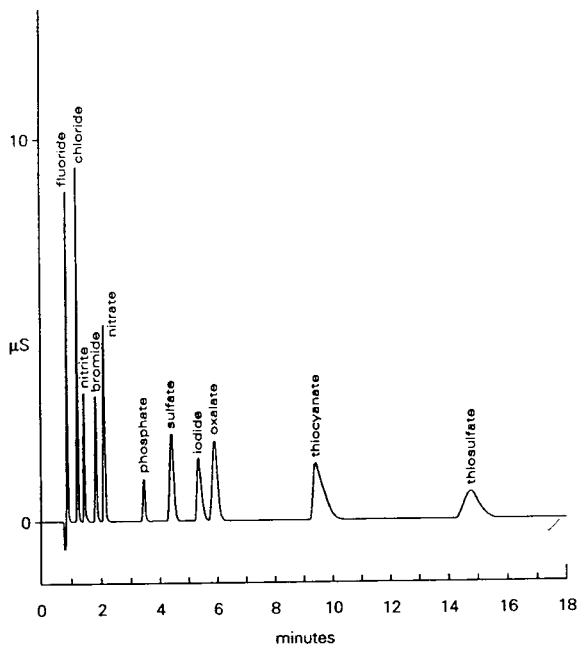

Fig. 5. Separation of anions in an anion standard solution using "aged" IonPac AS9-SC and AG9-SC columns with 3 m*M* Na_2CO_3 as eluent.

small carboxylic acids (formate, acetate, propionate, butyrate) elute near the front and should not be determined using the AS9-SC column. The separation of these anions should be performed on an IonPac AS10 column with $Na_2B_4O_7$ as eluent [6].

4. Conclusion

The described method for the separation of anions on an IonPac AS9-SC column with 3 m*M* $NaCO_3$ as eluent is useful for the determination of bromide, sulfate and iodide in oilfield waters and in other aqueous solutions. The detection limits are 0.1 ppm for bromide and sulfate and 0.2 ppm for iodide. With an optimized system the determination of bromide is possible even when the chloride to bromide ratio is up to 1000:1. The determination of sulfate and iodide is not dependent on the chloride excess and can be performed without analytical problems. Other anions, such as nitrate, oxalate, phthalate, thiocyanate and thiosulfate, can also be determined. Weak points of the method are the rapid loss of capacity, resulting in decreasing retention times and incomplete resolution of chloride–bromide, and the pH sensitivity of the AS9-SC column.

References

[1] *APHA, AWWA and WPCF, Standard Methods for the Examination of Water and Waste Water*, American Public Health Association, Washington, DC, 12th ed., 1965.
[2] *Deutsche Einheitsverfahren zur Wasser-, Abwasser- und Schlamm-Untersuchung*, Verlag Chemie, Weinheim, 1960.
[3] *Dionex Application Note 3: Determination of Tracer Ions in Oilfield Drilling Fluids and Geological Brines*, Dionex, Sunnyvale, CA, 1987.
[4] J. Weiss, *Ionenchromatographie*, VCH, Weinheim, 2nd ed., 1991.
[5] *Installation Instructions and Troubleshooting Guide for the IonPac AG9-SC Guard Column and the IonPac AS9-SC Analytical Column*, Dionex, Sunnyvale, CA, 1992.
[6] R. Kadnar and J. Rieder, *J. Chromatogr.*, in press.

ELSEVIER

Journal of Chromatography A, 706 (1995) 307–313

JOURNAL OF CHROMATOGRAPHY A

Determination of aluminium in natural waters by single-column ion chromatography with indirect UV detection

M.L. Litvina*, I.N. Voloschik, B.A. Rudenko

V.I. Vernadsky Institute of Geochemistry and Analytical Chemistry, Russian Academy of Sciences, 19 Kosygin Str., 117975 Moscow, Russian Federation

Abstract

The selective, sensitive and rapid determination of Al was achieved using ion-exchange separation and indirect UV detection. A solution of Ce salt was used as the eluent. The parameters influencing the shape of the Al peak, the selectivity of Al separation and sensitivity of its determination were studied. The separation of Al on chemically modified and on silica gel-based dynamically coated sorbents was achieved. With direction injection the detection limit under the optimum conditions was 50 ng/ml. The time of analysis was about 6 min. The use of a simple preconcentration procedure permitted the detection limit to be decreased. Preconcentration of Al was performed on a complexing sorbent with iminodiacetate functional groups. The technique presented was applied to the determination of Al in natural and tap waters. The technique also provides the determination of alkaline earth metals along with Al.

1. Introduction

The determination of Al and alkali and alkaline earth metal cations is an important part of water quality control during the process of tap water purification. Significant concentrations of Al in tap water can appear because of the contamination of water sources by the waste waters from industrial plants or as a result of water treatment with Al-containing reagents at waterworks. The concentration of Al in natural waters varies from 0.01 to about 250 μg/ml, while the concentration of Al in tap water should not exceed 500 ng/ml [1].

A spectrophotometric method is commonly used for the determination of Al in water, but is time consuming and does not provide sufficient selectivity and sensitivity of analysis [2].

Usually the chromatographic determination of Al involves separation on a cation-exchange column with an eluent containing a complexing agent. Spectrophotometric detection with or without a colour-forming postcolumn reaction is used [3–10].

In this work, Al was determined by ion chromatography (IC) with indirect UV detection. A solution of a non-complexing trivalent Ce salt was used as the eluent. We consider this method to be the simplest and the most rapid for the determination of the cations in question [11,12]. It can be also conventionally used for the determination of alkaline earth metal cations. We attempted to widen the possibilities of the above method, using it for the determination of Al.

* Corresponding author.

0021-9673/95/$09.50
SSDI 0021-9673(95)00254-5

2. Experimental

A Hewlett-Packard Model 1084A liquid chromatograph equipped with a UV detector with a fixed wavelength of 254 nm was used. The stainless-steel separation columns used were 50 × 3 mm I.D. with a surface-sulphonated cation exchanger and 150 × 3 mm I.D. with dynamically coated Separon C_{18} sorbent (both from Elsiko, Moscow, Russian Federation). The dynamically coated column was prepared by passing a 0.01 m*M* solution of dodecylbenzenesulphonic acid (flow-rate 1 ml/min) through it for 1 h. A cartridge (30 × 3 mm I.D.) packed with laboratory-made sorbent containing iminodiacetate (IDA) functional groups (exchange capacity 0.1–0.5 mequiv./g) was used for the preconcentration of metal ions. Analytical-reagent-grade Mg, Ca, Sr, Ba, Cr, Ce, Pb, Al and Fe salts and methoxylamine hydrochloride were used for the preparation of eluent and standard solutions. Purified water was obtained using a Milli-Q apparatus (Millipore). Samples of tap and river waters were filtered through a 0.45-μm filter before injection into the chromatograph.

3. Results and discussion

A sufficiently effective and rapid separation of alkaline earth metals was obtained on both columns with indirect UV detection. Fig. 1 shows the separation of four alkaline earth metal cations with a 1 m*M* solution of Ce(III) salt as eluent. The time of analysis did not exceed 5–7 min. It should be mentioned that a better selectivity of Ca and Sr separation was observed on the surface-sulphonated cation exchanger.

As the solution of Ce(III) does not possess any complexing ability, the order of elution of cations with this eluent is the same as with an acid-containing eluent. The singly charged cations are eluted first, then doubly charged and finally triply charged cations. This is why a more concentrated solution of Ce(III) is preferably used for the elution of Al, which is a strongly retained cation.

It was found that to obtain a well shaped peak of Al, the pH of eluent should be decreased to <3.

Fig. 2 shows the chromatogram obtained under the above conditions for alkaline earth

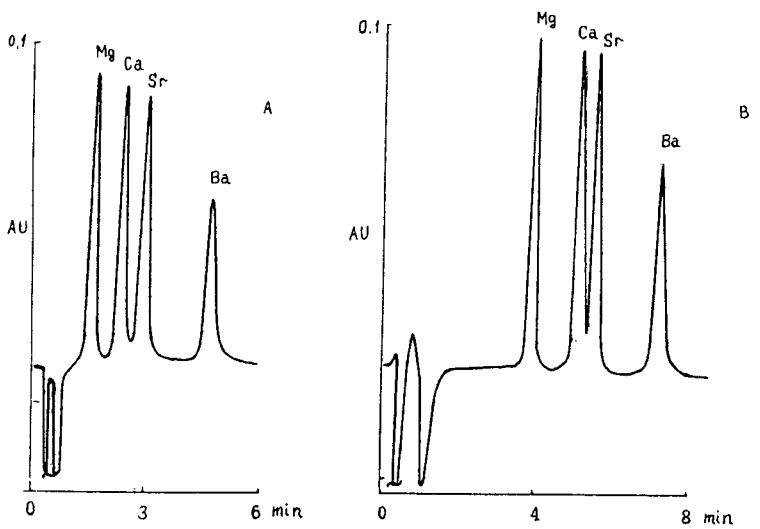

Fig. 1. Separation of alkaline earth metals with indirect UV detection. Column, (A) 50 × 3 mm I.D. with surface-sulphonated sorbent and (B) 150 × 3 mm I.D. with dynamically coated sorbent; eluent, 1 m*M* $Ce(NO_3)_3$ (pH 6.2); flow-rate, (A) 1 and (B) 0.8 ml/min; injection volume, 10 μl; indirect UV detection at 254 nm. Concentrations of cations: Mg = 1.25, Ca = 2, Sr = 3, Ba = 4 μg/ml.

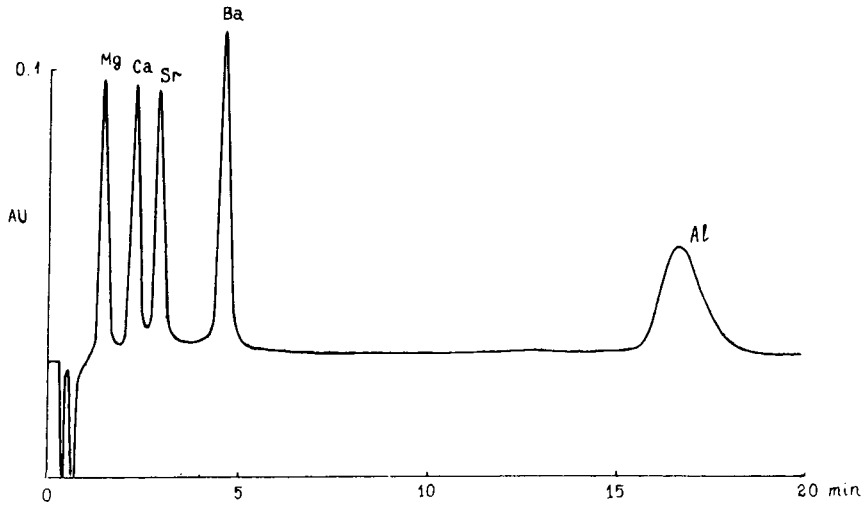

Fig. 2. Separation of alkaline earth metals and Al with indirect UV detection. Column, 50 × 3 mm I.D. with surface-sulphonated sorbent; eluent, 1 m*M* $Ce(NO_3)_3$–3 m*M* HNO_3 (pH 2.5); flow-rate, 1 ml/min. Concentrations of cations: Mg = 1.25, Ca = 2, Sr = 3, Ba = 4, Al = 5.4 μg/ml.

metal cations along with Al cation. To study the interference of other strongly retained cations on the determination of Al, we investigated the chromatographic behaviour of Ba, Pb, Cr(III) and Fe(III). Being eluted by a neutral eluent (pH 6.2), Al produces a wide peak, the area of which can hardly be calculated. Other strongly retained cations, such as Pb and Cr(III), demonstrate the same behaviour when a neutral eluent is used.

The separations of cations on the surface-sulphonated and the dynamically coated sorbents are presented in Fig. 3. The model mixture analysed contained Ba, Pb, Cr(III) and Fe(III). Fe(III) cation has a long retention time and does not appear on the chromatogram. It can be seen that Cr(III) cation interferes with the determination of Al under these conditions. For qualitative identification of Al and Cr cations when both are present in a sample, a 1 m*M* solution of methoxylamine hydrochloride and 1 m*M* nitric acid was added to the cerium(III) nitrate eluent (Fig. 4).

The addition of methoxylamine to the eluent results in a good resolution between Al and Cr. However, the efficiency of their separation is not sufficient. A decrease in the nitric acid concentration in the eluent leads to an improvement in peak shape. Also, the retention time of Al is strongly decreased. This is demonstrated by the chromatogram in Fig. 5, where Al is eluted earlier than Mg. Cr(III) cation is eluted as an individual peak.

Although not the direct purpose of this study, it should be mentioned that the above chromatographic conditions can be used for the determination of Cr(III) cation and for rapid determination of Mg and Ca in the presence of a large amount of Al. For example, Fig. 6 shows the chromatogram of a technological solution obtained after desorption of Mg and Ca from a natural zeolite ion exchanger. Separation was performed with two different eluents, namely a solution of cerium(III) nitrate with addition of either methoxylamine or nitric acid. It can be seen that when methoxylamine is added to the eluent, the analysis time is five times shorter.

An eluent containing methoxylamine can be used only for a limited number of Al-containing samples, because interference from alkali metal cation peaks and the system peak is possible. This is why for their determination we used

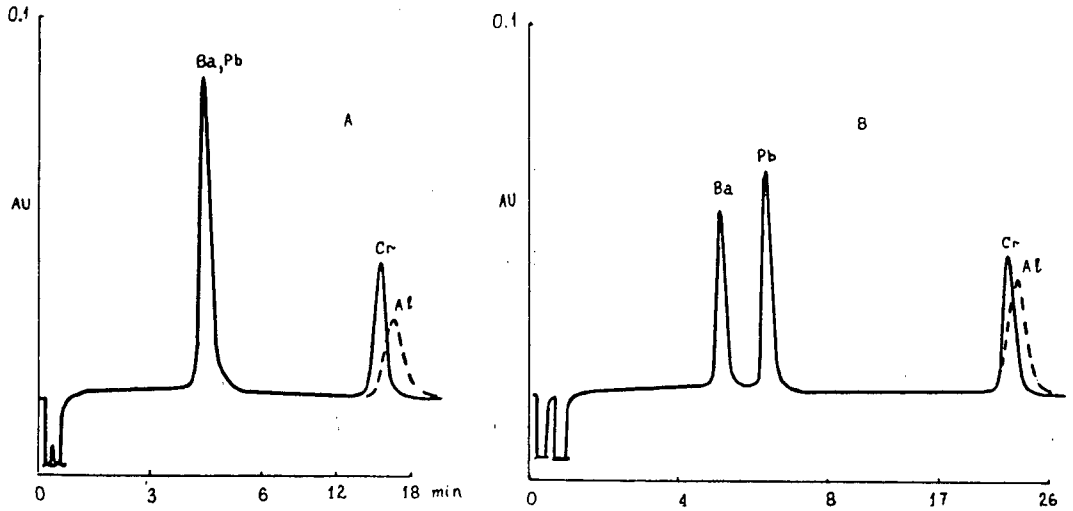

Fig. 3. Separation of Al and the strongly retained cations Ba, Pb and Cr(III). Column, (A) 50 × 3 mm I.D. with surface-sulphonated sorbent and (B) 150 × 3 mm I.D. with dynamically coated sorbent; eluent, 1 m*M* $Ce(NO_3)_3$–3 m*M* HNO_3 (pH 2.5); indirect UV detection at 254 nm; line recorder rate decreased threefold after (A) 6 and (B) 8 min.

conditions, under which alkali metal cation and system peaks do not interfere with the determination of Al. These chromatographic conditions are as in Fig. 2.

The retention time of Al depends linearly on the concentration of the eluent. More concentrated solutions of cerium(III) nitrate were used as eluent to shorten the analysis time. Thus, 3 m*M* cerium(III) nitrate solution with a low pH of 2.5 was used for the determination of Al in water. Under these conditions the retention time of Al does not exceed 6 min. As tap and natural water analyses were the object of this work, the presence of noticeable amounts of Cr(III) was not observed and hence its interference was excluded.

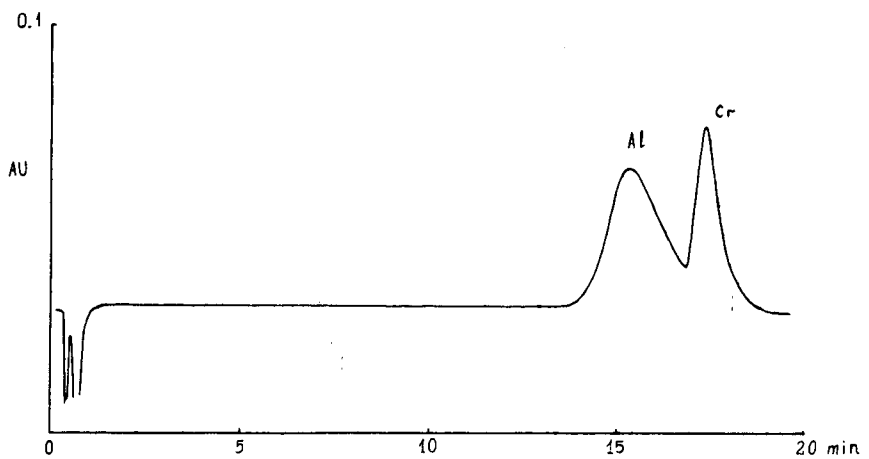

Fig. 4. Separation of Al and Cr(III) cations with a methoxylamine hydrochloride and nitric acid-containing eluent: 1 m*M* $Ce(NO_3)_3$–1 m*M* methoxylamine hydrochloride–1 m*M* HNO_3 (pH 2.9). Other conditions as in Fig. 2.

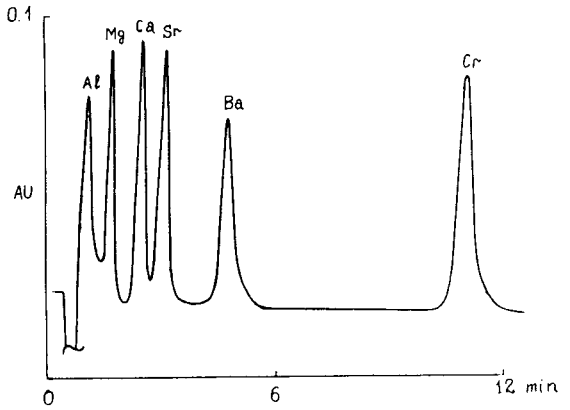

Fig. 5. Separation of cations with a methoxylamine hydrochloride-containing eluent: 1 m*M* $Ce(NO_3)_3$–1 m*M* methoxylamine hydrochloride (pH 5.8). Other conditions as in Fig. 2.

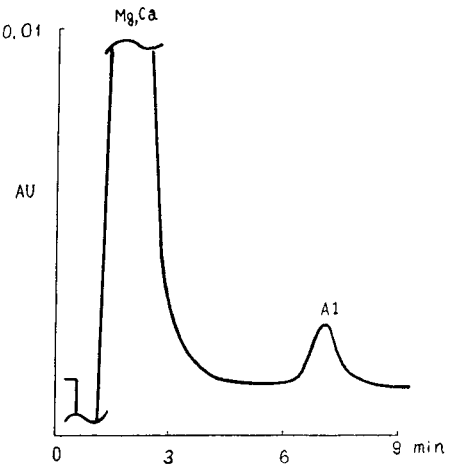

Fig. 7. Determination of Al in tap water by IC with direct sample injection. Column, 50 × 3 mm I.D. with surface-sulphonated sorbent; eluent, 3 m*M* $Ce(NO_3)_3$–3 m*M* HNO_3 (pH 2.5); flow-rate, 1 ml/min; indirect UV detection at 254 nm; attenuation, 2; injection volume, 100 μl.

A close linear dependence between this peak area and the concentration of Al was observed up to at least 100 μg/ml. The detection limit (calculated for $S/N = 3$) obtained for Al, based on a 200-μl injection volume, was 50 ng/ml.

Preliminary sample mineralization was not applied, because the Al cations are not bound into strong complexes in tap water. The water sample was injected directly into the chromatograph. Fig. 7 shows a chromatogram for Moscow tap water. After direct injection of 100 μl of sample this water was found to contain 270 ng/ml of Al.

The sensitivity of the determination under these conditions is not high enough for the analysis of waters with trace concentrations of Al. To increase the sensitivity of the method,

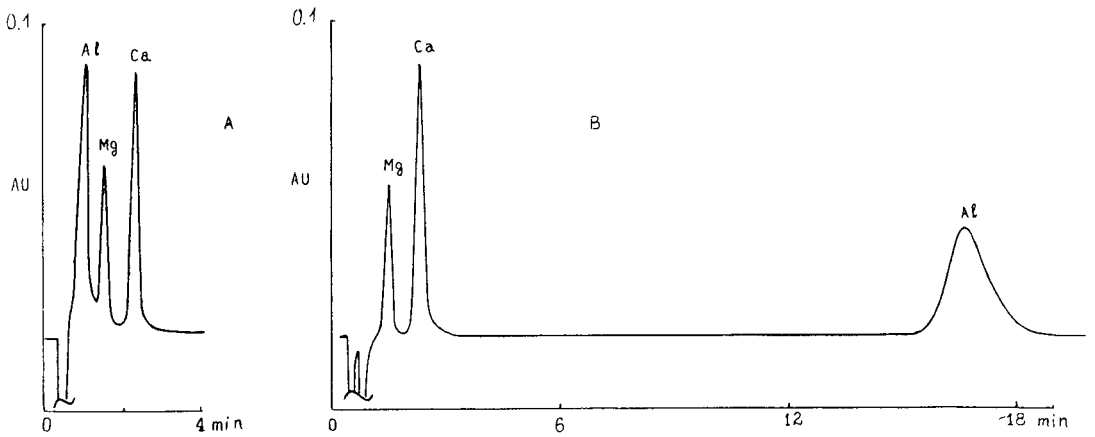

Fig. 6. Determination of Ca and Mg in the presence of Al. Column, 50 × 3 mm I.D. with surface-sulphonated sorbent; eluent, (A) 1 m*M* $Ce(NO_3)_3$–1 m*M* methoxylamine hydrochloride (pH 5.8) and (B) 1 m*M* $Ce(NO_3)_3$–3 m*M* HNO_3 (pH 2.5); flow-rate, 1 ml/min; indirect UV detection at 254 nm.

preconcentration was applied. Preconcentration of Al was performed on a 30 × 4 mm I.D. cartridge packed with IDA sorbent, through which 20 ml of sample were passed. Mg and Ca cations were selectively washed out from the sorbent with 1 *M* ammonium acetate solution, then Al was washed out with 1 ml of 2 *M* nitric acid. In this case, the injection volume was only 10 μl.

A chromatogram for Moskva river water obtained using preconcentration is shown in Fig. 8. The chromatogram shows that the preconcentration procedure permitted the same injection volume to be retained for the determination of Al as for the determination of Ca and Mg, although the concentration of Mg and Ca in river water was two orders of magnitude higher than the Al concentration. It is sufficient to change the attenuation in this case. Preconcentration also permits the concentration of the eluent to be increased and thus the time of analysis for Al to be shortened.

Table 1 gives the results for the determination of Al in Moscow tap water and in Moskva river water. It can be seen that the tap water is noticeably contaminated with Al after treatment at the waterworks.

To control the reliability of this technique, the same sample was analysed by an inductively coupled plasma (ICP) method. The comparison showed an adequate correlation between the results of the two methods (Table 1).

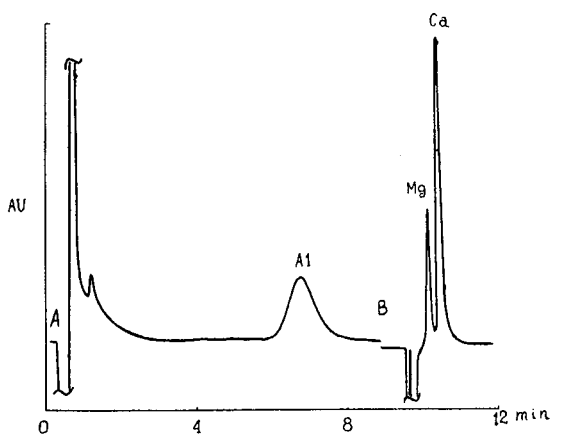

Fig. 8. Determination of Al, Mg and Ca in river water by IC. Eluent, 3 m*M* $Ce(NO_3)_3$–3 m*M* HNO_3 (pH 2.5); attenuation, (A) 2 and (B) 6; injection volume, 10 μl. Other conditions as in Fig. 7.

Table 1
Determination of Al, Mg and Ca in Moskva river water and in Moscow tap water by IC and ICP methods

Element	Concentration (mg/l)			
	River water		Drinking water	
	IC	ICP	IC	ICP
Al	0.08	0.07	0.27	0.28
Mg	15.5	15.1	14.7	15.0
Ca	62.4	61.7	60.2	59.8

The suggested technique for the determination of Al with indirect UV detection is characterized by good reproducibility. The efficiency of separation and the retention times of the cations are virtually unchanged even after 300 sample injections.

4. Conclusions

The proposed IC technique for the determination of Al along with alkaline earth metal cations in natural and tap waters, based on a cation-exchange separation with indirect UV detection, has a detection limit of about 50 ng/ml and the Al peak response is linear up to 100 μg/ml. The results correlate well with those obtained by an ICP method. The suggested method provides a rapid, selective and sensitive determination of Al in multi-component mixtures of cations.

References

[1] C.T. Priscoll, J.P. Baker, J.J. Bisogni and C.L. Schofield, *Nature*, 84 (1980) 161.
[2] Yu.V. Novikov, K.O. Lastochkina and Z.N. Boldina, *Metody Issledovanya Kachestva Vody Vodoiomov*, Nauka, Moscow, 1990.
[3] B.D. Karcher, I.S. Krull, R.G. Schleicher and S.B. Smith, Jr., *Chromatographia*, 24 (1987) 705.
[4] N.E. Fortiev and J.S. Fritz, *Talanta*, 32 (1985) 1047.

[5] *Wescan Application* No. 316, 1982.
[6] P.R. Haddad and R.C. Foley, *Anal. Chem.*, 61 (1989) 1435.
[7] M.P. Palmieri and J.S. Fritz, *Anal. Chem.*, 59 (1987) 2226.
[8] D. Yan and G. Schwedt, *Fresenius' Z. Anal. Chem.*, 320 (1985) 252.
[9] P. Jones, L. Ebdon and T. Williams, *Analyst*, 113 (1988) 641.
[10] J. Carnevale and P.E. Jackson, *J. Chromatogr.*, 671 (1994) 115.
[11] J.H. Sherman and N.D. Danielson, *Anal. Chem.*, 59 (1987) 490.
[12] J.H. Sherman and N.D. Danielson, *J. Agric. Food Chem.*, 36 (1988) 966.

ELSEVIER

Journal of Chromatography A, 706 (1995) 315–319

JOURNAL OF CHROMATOGRAPHY A

Ion chromatographic determination of beryllium in rock and waste waters with a chelating sorbent and conductimetric detection

I.N. Voloschik*, M.L. Litvina, B.A. Rudenko

V.I. Vernadsky Institute of Geochemistry and Analytical Chemistry, Russian Academy of Sciences, 19 Kosygin St., 117975 Moscow, Russian Federation

Abstract

The sensitive separation of Be and other alkaline earth metals on a complexing sorbent with iminodiacetate (IDA) functional groups using indirect conductimetric detection is described. The selectivities of the separation of Be and other alkaline earth metals on IDA and surface-sulphonated sorbents were compared. The influence of the nature of the mobile phase complexing agent on the selectivity of the separation between Be and other alkaline earth metals was studied. An eluent containing dipicolinic acid and nitric acid proved to be optimum for the elimination of interferences from transition metals. The detection limit for Be was 10 μg/l. Preconcentration of Be on the complexing IDA sorbent increases the sensitivity of determination. This technique was successfully applied to the analysis of rock and natural water samples.

1. Introduction

Beryllium metal and its compounds are widely involved in present day technologies. Beryllium-containing waste waters from industrial plants and power plants can contaminate natural waters, which may in turn lead to the pollution of tap water. The concentration of Be in natural waters varies from 0.1 to 500 ng/ml. High concentrations of Be are observed in regions with W and Mo deposits. In addition to the pollution of natural waters, there is another source of Be in potable water, namely wetted parts made of copper–nickel alloys. It should be stressed that Be ion is noted for its ecological toxicity. The mechanism of Be toxicity involves the destruction of cellular membranes and decrease in enzyme activity. Also, Be is carcinogenic [1]. All of the above emphasizes the need to develop simple, selective and sensitive techniques for the measurement of Be.

This paper describes a technique for the sensitive determination of Be by ion chromatography (IC).

2. Experimental

Analyses were carried out with a Hewlett-Packard Model 1084A liquid chromatograph using a conductimetric detector. The stainless-steel separation columns used were 50 × 3 mm I.D. packed with a laboratory-prepared surface-sulphonated sorbent and 250 × 3 mm I.D. packed with a laboratory-prepared chelating iminodiacetate (IDA) sorbent. The exchange

* Corresponding author.

0021-9673/95/$09.50
SSDI 0021-9673(95)00253-7

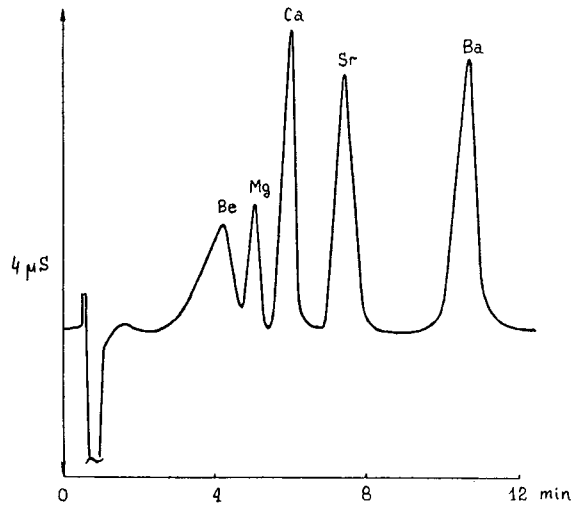

Fig. 1. Separation of alkaline earth metal cations on surface-sulphonated cation exchanger. Column, 50 × 3 mm I.D.; eluent, 2 m*M* ethylenediamine–2 m*M* citric acid–2 m*M* tartaric acid; flow-rate, 1 ml/min; indirect conductimetric detection.

capacity of both sorbents was 0.1–0.5 mequiv./g. An IDA sorbent-packed cartridge (30 × 3 mm I.D.) was used for the preconcentration of metal ions. Analytical-reagent grade chemicals were used for the preparation of eluent and standard solutions. Purified water was obtained from a Milli-Q apparatus (Millipore).

3. Results and discussion

Normally, a surface-sulphonated cation exchanger is used for the IC determination of Be. Detection is carried out with a conductimetric or a spectrophotometric detector after postcolumn reaction [2–5]. Fig. 1 shows an example of the separation of alkaline earth metal cations, including Be on a surface-sulphonated cation-exchanger using conductimetric detection. A mixture of ethylenediamine, tartaric acid and citric acid was used as the eluent. As can be seen, Be is eluted earlier than Mg and Ca on this sorbent. Some transition and heavy metal cations elute before Mg and interfere with the determination of Be. Also, the Be peak is wide and this technique is not sufficiently sensitive.

A more selective and sensitive determination of Be was achieved by using a complexing sorbent, such as a silica gel-based sorbent with IDA functional groups [6–8], for the separation. This sorbent is characterized by a higher selectivity for transition and heavy metal cations and for Be; the higher selectivity is due to the fact that in contrast to other alkaline earth metals, Be forms more stable complexes with the IDA functional groups. Fig. 2 shows the chromatogram of a model mixture of cations, including Be, separated on the IDA sorbent with an eluent

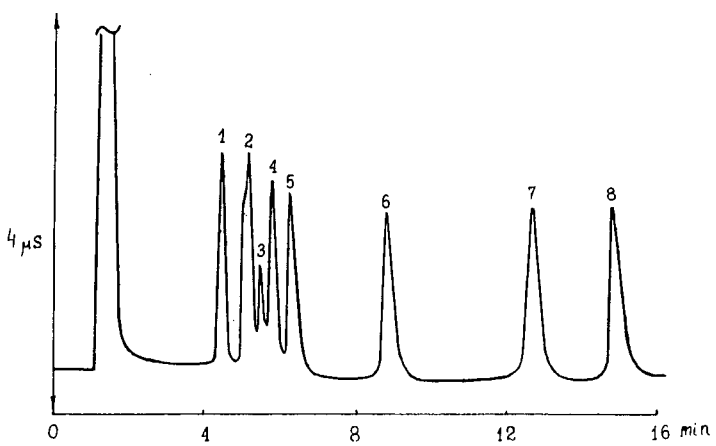

Fig. 2. Separation of alkaline earth, transition and heavy metals on IDA sorbent using non-complexing eluent. Column, 250 × 3 mm I.D.; eluent, 7 m*M* HNO_3; flow-rate, 1 ml/min; indirect conductimetric detection. Peaks: 1 = Mg; 2 = Ca, Sr; 3 = Mn; 4 = Ba; 5 = Be; 6 = Co; 7 = Cd; 8 = Zn.

containing nitric acid, using indirect conductimetric detection. It can be seen that Be is eluted after the other alkaline earth metals; this differs from the order of elution on the surface-sulphonated cation exchanger.

With the IDA stationary phase, Be is fully separated from Mg, Ca, Al and Fe(III), which are the main matrix components of rock and waste water samples.

Beryllium cation is more strongly retained than Mn and Ba cations on the IDA sorbent. Sr and Ca cations have similar retention times under these elution conditions.

The above conditions can be used for determination of Be along with some transition and heavy metals. The long retention times of transition and heavy metals significantly increase the time of analysis. Therefore, to shorten the time of analysis, to increase the separation of Be from other alkaline earth metal cations and to eliminate the interference of transition and heavy metal cations, we used a complexing eluent. A number of organic complexing acids were studied, e.g., citric, tartaric, oxalic and dipicolinic acid. All of these acids are capable of forming coordination complexes with divalent cations.

Dipicolinic acid was found to be the most suitable. This compound forms stable complexes with transition and heavy metal cations and these complexes are not retained on the IDA sorbent. As alkaline earth metals and Be do not form stable complexes with dipicolinic acid, their retention times do not vary significantly from those obtained with the non-complexing mobile phase.

Fig. 3 shows the chromatogram of a model mixture of cations obtained on the IDA sorbent with an eluent containing dipicolinic and nitric acid. Transition and heavy metal cations are eluted before Mg and do not increase the time of analysis. The selectivity for the separation of Be from Ba and transition metal cations is increased.

Under the above conditions, Ca and Sr are well separated on the IDA sorbent and Be is eluted as a narrow, well shaped peak. These chromatographic conditions were found to be the most selective for separating Be from other cations.

A close linear dependence between the peak area and the concentration of the analyte ions over a wide range of concentrations was observed with this technique. The detection limit (calculated for $S/N = 3$) obtained for Be, based on a 175-μl injection volume was 2 ng/ml.

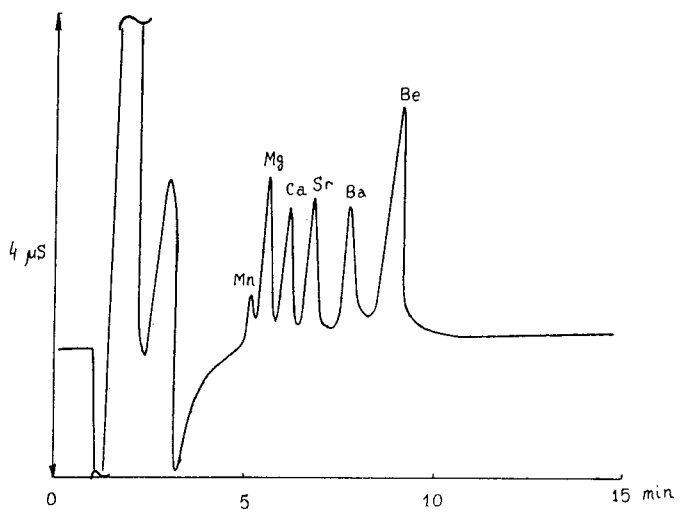

Fig. 3. Separation of cations including Be on IDA sorbent using complexing eluent. Column, 250 × 3 mm I.D.; eluent, 5 m*M* HNO_3–2 m*M* dipicolinic acid; flow-rate, 1 ml/min; indirect conductimetric detection.

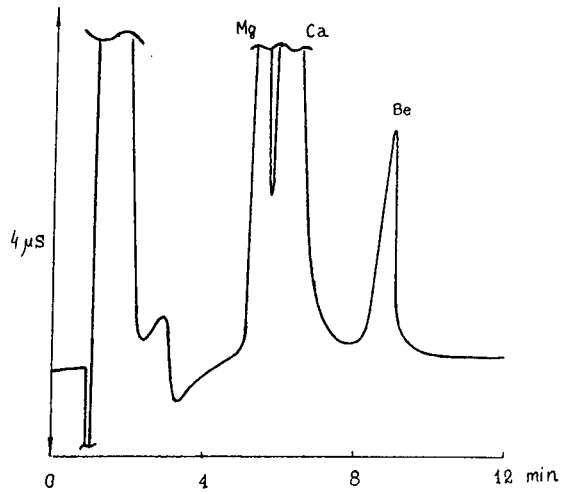

Fig. 4. Determination of Be in a geological sample by IC. Column, 250 × 3 mm I.D. with IDA sorbent; eluent, 5 m*M* HNO_3–2 m*M* dipicolinic acid; flow-rate, 1 ml/min; indirect conductimetric detection.

We analysed a number of rock samples containing Be, and a number of samples with preset contents of Be. Sample preparation involved the dissolution of 1 g of the sample in a mixture of concentrated hydrofluoric and hydrochloric acid, evaporation to dryness, dissolution of the residue in hydrochloric acid and dilution with water [9].

The chromatogram of a rock sample and the chromatographic conditions for the determination of Be are shown in Fig. 4.

The relative standard deviation of the results was <5%, as evidenced from a comparison of the results for model samples with preset Be contents (Table 1).

Table 1
Determination of Be in model samples by IC

Be concentration (μg/ml)	
Present in model sample	Found by IC
0	0
10	9.8
20	20.1
30	29.2

Two samples of the minerals Albit and Muskovit with unknown Be contents were analysed using the same technique. The results of IC and spectrometric analyses of these samples are given in Table 2. As can be seen, the results obtained by the two methods agree closely.

As already mentioned, Be is noted for its high ecological toxicity, and concentrations of Be exceeding 200 ng/l constitute an environmental hazard. The procedure for preconcentration on a cartridge packed with IDA sorbent was used for the determination of Be at this level. The conditions of sorption concentration of Be on this sorbent were studied.

With the help of the preconcentration procedure, the detection limit of Be in waters by the IC method was decreased to 50 ng/l. A 500-ml volume of the sample was preconcentrated for this value.

A number of waste water samples from the Ust'-Kamenogorsk metal plant were analysed using the preconcentration procedure. A 100-ml volume of the sample was passed through the cartridge packed with the IDA sorbent. The main part of the sorbed Mg and Ca was washed out from the cartridge with 20 ml of 0.01 *M* nitric acid. Concentrated Be with the remainder of the sorbed Ca was washed out with a further 2 ml of 1 *M* nitric acid. The pH of the samples was increased to 2.5 before injection into the chromatograph.

Fig. 5 shows the chromatogram of the Be-containing waste water. The concentration of Be in this sample was 1 μg/l. Five out of ten samples analysed contained high concentrations of Be. These data were verified by spectrometric analysis.

Table 2
Determination of Be in geological samples

Sample No.	Be concentration (μg/ml)	
	IC	Spectrometric method
1	13.3	12.1
2	75.1	73.9

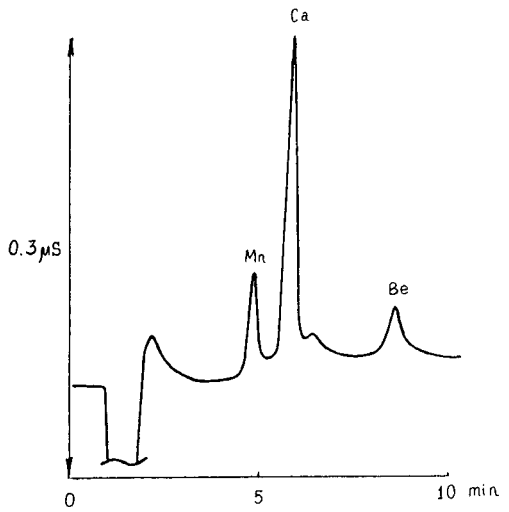

Fig. 5. Determination of Be in waste water by IC. Column, 250 × 3 mm I.D. with IDA sorbent; eluent, 7 m*M* HNO_3–2 m*M* dipicolinic acid; flow-rate, 1 ml/min; indirect conductimetric detection.

4. Conclusions

The feasibility of using IC for the trace determination of Be in rock and natural water samples, based on cation-exchange separation on a complexing sorbent and indirect conductimetric detection, was successfully demonstrated. The method had a detection limit of 2 μg/l and the Be peak response was linear up to at least 100 mg/l.

Satisfactory accuracy was shown. No interferences from alkaline earth, transition and heavy metals were found. The results of the chromatographic method agreed with those obtained by an independent spectrometric method.

The results demonstrate that the IC method using a complexing sorbent provides high selectivity and sensitivity of Be determination and may be employed for the routine determination of Be.

References

[1] H. Noda, K. Saitoh and N. Suzuki, *Chromatographia*, 14 (1981) 189.
[2] M. Betti and S. Cavalli, *J. Chromatogr.*, 538 (1991) 365.
[3] P.K. Dasgupta, *J. Chromatogr. Sci.*, 27 (1989) 422.
[4] B. Kondratjonok and G. Schwedt, *Fresenius' Z. Anal. Chem.*, 337 (1988) 332.
[5] M.L. Litvina, I.N. Voloschik and B.A. Rudenko, *J. Chromatogr.*, 671 (1994) 29.
[6] A. Bonn, S. Reiffenstuhl and J. Jandik, *J. Chromatogr.*, 499 (1990) 669.
[7] P.N. Nesterenko, T.I. Tihomirova, V.N. Fadeeva, I.B. Yuferova and Q.Y. Kukriavtsev, *Zh. Anal. Khim.*, 46 (1991) 1108.
[8] I.N. Voloschik, M.L. Litvina and B.A. Rudenko, *J. Chromatogr.*, 671 (1994) 205.
[9] H. Arginier, *Chim. Anal. (Paris)*, 12 (1960) 600.

ELSEVIER

Journal of Chromatography A, 706 (1995) 321–325

JOURNAL OF CHROMATOGRAPHY A

Determination of chloride in the leachates of stabilised waste by ion chromatography and by a volumetric method Analysis and comparison

L. Musmeci*, E. Beccaloni, M. Chirico

Istituto Superiore di Sanitá, Viale Regina Elena 299, 00161 Rome, Italy

Abstract

This study investigates the determination of the total chloride content in the leachates of samples of stabilised municipal solid waste incinerator fly ash (Portland cement), using two different leaching methods. The chloride content of the leachates obtained by two different methods was analysed by ion chromatography and by a volumetric method.

The results obtained with the two methods are very similar, although the results obtained by the volumetric method were generally lower.

1. Introduction

The potential environmental hazard of waste materials varies greatly with wastes from different sources. Although the minimisation of waste production, and its elimination where possible, is the first priority, it is clear that it will not be possible to eliminate a number of significant types of waste. These will, nonetheless, have to be dealt with in an environmentally acceptable manner. Several such types of waste will require treatment before disposal, to minimise adverse environmental effects [1,2]. In some cases, tested wastes, suitably stabilised with Portland cement, for instance, can be used in the construction industry [3]. The problem here is the development of a standard method to verify the leachability of hazardous substances from stabilised waste [4–6].

In view of the increased need for waste treatment, the methods evaluated in this paper will prove relevant to the Community Directive on Landfills of Waste Materials and to future regulations in the field of waste minimisation, treatment and use. A number of factors, such as the tortuosity factor and the retardation factor are considered in determining whether the stabilisation process has been correctly carried out. The retardation factor is a measure of the chemical retardation of a component of the product, and the chloride ion is useful in evaluating this factor [7,8].

In this paper the results of two different methods to determine chloride are compared. One is a very fast and easy to perform volumetric method and the other a more accurate chromatographic method.

* Corresponding author.

0021-9673/95/$09.50
SSDI 0021-9673(95)00007-0

Two different chloride release tests are also compared, one with liquid phase renewal [9] and the other based on a single extraction [10].

2. Materials and methods

The specimens were 4 cm cubes composed of very rapid-hardening Portland cement produced with fly ash from a municipal solid waste incinerator (MSWI), natural sand and water. Their composition was: Portland cement class C (540 kg/m^3), MSWI fly ash (210 kg/m^3), natural sand (0.5–1 mm, 560 kg/m^3), silver sand (125–500 μm, 560 kg/m^3) and water (300 kg/m^3).

Three separate, identically composed samples were analysed: T1, T2 and T3.

The leaching tests used were:

Test A [acetic acid extraction (AAT)]: extraction by 24-h immersion in an aqueous solution at pH 5.0 ± 0.2 of acetic acid (0.5 *M*) with continuous agitation at a controlled temperature with a sample/extracting solution mass ratio of 1:16. The pH was controlled throughout the test (initially every 30 min) and kept at 5.0 ± 0.2 by adding 0.5 *M* acetic acid solution. At the end of the test the leachate was filtered.

Test B [tank leaching test (TLT)]: extraction with water and replacement of the water after 2, 8, 24, 48, 72, 102, 168 and 384 h (8 steps), with a sample extracting solution mass ratio of 1:5, at a controlled temperature without agitation. The pH was not measured during the test, but at the end of each extraction step the leachate obtained was filtered and after measurement of the pH acidified to pH 2. Part of the sample was kept unacidified for the analysis of sulphates, bromides and chlorides.

The concentration of chloride ions was determined in the elution solutions after decanting and/or centrifugation to obtain a solution without suspended particles.

Two analytical techniques were used: ion chromatography and titration by a volumetric method.

The analysis was conducted using a Dionex 2000 i/SP ion chromatograph with a single pump for the eluent (isocratic), with an analytical column, a guard column and chemical suppression of the eluent's conductivity. The working parameters were: analytical column: Dionex Ion Pac A S4 A (250 × 4 mm) composed of a 16-μm polystyrene–divinylbenzene substrate agglomerated with anion-exchange latex which had been completely aminated; guard column: Ion Pac A G4 G (50 × 4 mm); column pressure: 970 p.s.i. (1 p.s.i. = 6894.76 Pa); eluent: 1.8 m*M* Na_2CO_3/1.7 m*M* $NaHCO_3$; flow-rate: 2.0 ml/min; detection: suppressed conductivity at 30 μS FS; standard: 50 μl chloride ions 2.0 mg/l; sample loop volume: 50 μl.

The Mohr method was adopted with 0.1 *M* silver nitrate as titrant by detecting the final point by using 5% potassium chlorate as the indicator (pH 7–9).

3. Results and discussion

To determine the detection limits of the two methods used to determine the chloride concentration, under the conditions described above, a series of ten tests were carried out at decreasing concentrations. For each series the standard deviation was not to exceed ± 0.70 for the chromatographic method and ± 1.7 for the volumetric method.

Table 1 shows data on the five determinations of the chloride ion content by the chromatographic method and Table 2 by the volumetric method, for both the extraction methods (A and B). The extraction data for method A are subdivided into sections numbered 1–8, since the method requires eight steps.

An extraction process using long stirring periods is clearly better for solid samples such as the ones used.

It was, however, decided to measure the quantity of chloride ions released from the samples using two tests. Test A and B were chosen for two reasons: A is used in an international intercalibration test to evaluate the stabilization process for hazardous waste to minimize heavy metal release and B is currently used in Italy for the same purpose.

Table 1
Results of the analysis with the chromatographic method for the two elution tests

Sample	Chloride ion concentration (mg/l)	Mean (mg/l)	S.D. (mg/l)
Test A			
Blank-1	≤1.00, ≤1.00, ≤1.00, ≤1.00, ≤1.00		
T1-1	68.60, 65.80, 72.90, 69.80, 72.30	69.88	±2.58
T2-1	67.20, 73.90, 67.20, 67.20, 68.60	68.82	±2.90
T3-1	68.70, 69.90, 70.40, 66.80, 67.10	68.52	±1.61
Blank-2	≤1.00, ≤1.00, ≤1.00, ≤1.00, ≤1.00		
T1-2	68.10, 68.40, 68.80, 69.70, 67.40	68.48	±0.85
T2-2	61.70, 60.10, 63.50, 64.10, 63.50	62.58	±1.65
T3-2	81.50, 81.50, 79.90, 66.40, 67.40	75.34	±7.74
Blank-3	≤1.00, ≤1.00, ≤1.00, ≤1.00, ≤1.00		
T1-3	101.70, 102.00, 103.20, 102.60, 106.60	103.22	±1.97
T2-3	101.70, 102.50, 106.60, 106.60, 109.40	105.36	±3.20
T3-3	102.50, 102.00, 97.70, 100.00, 97.40	100.12	±2.16
Blank-4	≤1.00, ≤1.00, ≤1.00, ≤1.00, ≤1.00		
T1-4	101.70, 102.00, 102.70, 106.60, 108.00	104.20	±2.89
T2-4	102.00, 102.50, 95.40, 95.40, 96.00	98.26	±3.65
T3-4	102.50, 101.70, 95.40, 99.40, 97.40	99.28	±2.95
Blank-5	≤1.00, ≤1.00, ≤1.00, ≤1.00, ≤1.00		
T1-5	75.00, 74.20, 83.40, 84.60, 84.60	80.36	±5.28
T2-5	79.20, 80.10, 81.80, 73.40, 72.00	77.30	±4.33
T3-5	84.20, 85.00, 74.70, 72.60, 75.40	78.30	±5.77
Blank-6	≤1.00, ≤1.00, ≤1.00, ≤1.00, ≤1.00		
T1-6	82.50, 83.70, 81.40, 81.40, 82.60	82.32	±0.96
T2-6	82.50, 81.70, 77.10, 75.80, 70.60	77.54	±4.83
T3-6	78.70, 79.20, 70.00, 68.60, 70.00	73.30	±5.19
Blank-7	≤1.00, ≤1.00, ≤1.00, ≤1.00, ≤1.00		
T1-7	132.80, 135.60, 141.60, 131.40, 132.80	134.84	±1.99
T2-7	146.00, 143.70, 141.60, 140.90, 143.60	143.16	±2.08
T3-7	146.10, 143.00, 141.50, 138.40, 138.00	141.40	±2.53
Blank-8	≤1.00, ≤1.00, ≤1.00, ≤1.00, ≤1.00		
T1-8	289.60, 290.00, 289.90, 284.00, 292.70	289.24	±3.22
T2-8	283.80, 279.20, 286.90, 284.70, 284.70	283.88	±2.92
T3-8	282.70, 282.70, 281.00, 281.70, 281.80	281.98	±0.89
Test B			
Blank	≤1.00, ≤1.00, ≤1.00, ≤1.00, ≤1.00		
T1	30.80, 30.80, 29.70, 28.60, 30.10	30.00	±0.91
T2	28.70, 28.70, 29.00, 28.30, 28.50	28.64	±0.26
T3	30.80, 30.10, 29.90, 31.00, 30.20	30.40	±0.47

Table 2
Results of the analysis with the volumetric method for the two elution tests

Sample	Chloride ion concentration (mg/l)	Mean (mg/l)	S.D. (mg/l)
Test A			
Blank-1	≤30.00, ≤30.00, ≤30.00, ≤30.00, ≤30.00		
T1-1	58.30, 62.45, 65.06, 64.99, 60.72	62.30	±2.89
T2-1	56.56, 56.70, 64.50, 64.36, 58.20	60.0	±4.04
T3-1	66.12, 67.96, 61.52, 60.25, 65.80	64.33	±3.28
Blank-2	≤30.00, ≤30.00, ≤30.00, ≤30.00, ≤30.00		
T1-2	54.57, 54.72, 60.53, 60.67, 58.65	57.83	±3.01
T2-2	56.56, 57.13, 54.43, 54.72, 60.21	56.61	±2.32
T3-2	57.76, 57.90, 54.29, 54.43, 59.76	56.83	±2.39
Blank-3	≤30.00, ≤30.00, ≤30.00, ≤30.00, ≤30.00		
T1-3	94.98, 94.13, 99.65, 100.65, 100.60	98.00	±3.18
T2-3	91.02, 90.87, 94.84, 94.27, 95.03	93.00	±2.37
T3-3	96.82, 96.68, 90.58, 90.44, 95.32	93.96	±3.21
Blank-4	≤30.00, ≤30.00, ≤30.00, ≤30.00, ≤30.00		
T1-4	107.17, 94.98, 86.61, 86.11, 102.61	95.50	±9.41
T2-4	94.41, 93.42, 86.19, 85.06, 96.01	91.02	±5.02
T3-4	94.13, 94.13, 85.95, 85.38, 86.70	89.26	±4.47
Blank-5	≤30.00, ≤30.00, ≤30.00, ≤30.00, ≤30.00		
T1-5	63.51, 63.65, 71.16, 69.19, 74.76	70.45	±6.89
T2-5	64.93, 63.51, 63.93, 64.07, 68.40	64.97	±1.99
T3-5	68.75, 75.00, 61.38, 62.23, 70.01	67.47	±5.69
Blank-6	≤30.00, ≤30.00, ≤30.00, ≤30.00, ≤30.00		
T1-6	73.86, 75.13, 65.49, 66.34, 69.40	70.04	±4.34
T2-6	74.56, 73.57, 66.34, 66.06, 70.20	70.15	±3.95
T3-6	73.15, 74.14, 63.79, 60.50, 60.50	66.56	±6.59
Blank-7	≤30.00, ≤30.00, ≤30.00, ≤30.00, ≤30.00		
T1-7	117.23, 117.23, 123.47, 123.47, 119.91	120.26	±3.13
T2-7	126.31, 125.74, 129.71, 129.00, 120.30	126.21	±3.71
T3-7	123.19, 124.04, 111.99, 111.56, 115.40	117.24	±6.59
Blank-8	≤30.00, ≤30.00, ≤30.00, ≤30.00, ≤30.00		
T1-8	236.17, 237.59, 243.68, 243.40, 240.40	240.25	±3.37
T2-8	235.32, 236.17, 227.38, 228.23, 229.55	231.33	±4.11
T3-8	241.56, 241.07, 215.47, 215.33, 228.38	228.36	±12.96
Test B			
Blank	≤30.00, ≤30.00, ≤30.00, ≤30.00, ≤30.00		
T1	31.60, 31.18, 31.76, 29.91, 30.30	30.95	±0.81
T2	30.46, 31.18, 30.46, 30.33, 29.91	30.47	±0.46
T3	30.90, 31.18, 30.46, 30.05, 29.80	30.49	±0.57

As can be seen from Tables 1 and 2, the chloride ion values obtained with test B were always lower than those obtained with test A, since the test B contact time was too short to reach maximum leaching. In fact the values of test A increased with extraction time and reached their maximum with step 8, where the total contact time was 384 h.

The chloride ion concentrations found by the chromatographic method and those found by the volumetric method were very similar, though the results obtained by the volumetric method were generally lower.

The results obtained by both methods were analysed using two statistical tests: the t test and the variance test:

The *variance test* for coupled data, applied to the results of elution tests A and B demonstrated that there is a significant difference between the two methods, with lower values obtained with the volumetric method ($F = 26.23$, $p < 0.0001$).

The *t test* for coupled data, applied to the results of elution tests A and B with the two analytical methods, confirmed the evaluation of the variance test ($t = 5.122$ with 23 liberty degrees, $p < 0.0001$).

4. Conclusions

The tank leaching test is a good method for characterizing the leaching behaviour of solids.

The volumetric method is one of extreme analytical simplicity, but its limitation is the subjective judgement required of the tester in determining the end point of titration. Also the volumetric method cannot be applied when high sensitivity is required or the amount of chloride is low (its optimal range is 1000–2500 ppm of chloride). For high concentrations and when a very rapid analysis is required, it is, however, a good solution, though the possibility of lower results must be kept in mind.

Acknowledgements

The authors wish to thank Dr. Leonello Attias and Dr. Maurizio Semproni for their assistance.

References

[1] J.R. Conner, *Chemical Fixation and Solidification of Hazardous Wastes*, Chemical Waste Management, Inc./ Van Nostrand Reinhold, New York, 1990.

[2] J.J.J.M. Goumans, H.A. van der Sloot, Th.G. Aalbers, *Waste Materials in Construction —Proceedings of the International Conference on Environmental Implications of Construction with Materials*, Elsevier, Amsterdam, 1991.

[3] E.F. Barth, *Stabilization and Solidification of Hazardous Wastes; Pollution Technology Review 186*, NDC, USA, 1990.

[4] *Test Methods for Evaluating Solid Waste; SW-846, 3rd Division*, US Environmental Protection Agency, Cincinnati, OH, 1986.

[5] W. Lowenbach, *Compilation and Evaluation of Leaching Test Methods; EPA 600/2-78-095*, US Environmental Protection Agency, Cincinnati, OH, 1978.

[6] *Toxicity Characterisic Leaching Procedure (TCLP), Fed. Reg.*, Vol. 51, No. 114, Friday, June 13 (1986) 21685–21693 (proposed rules); *Fed. Reg.*, No. 261, March 29 (1990) (final version); *EPA Toxicity Test Procedure (EP-tox), Appendix II, Fed. Reg.*, Vol. 45, No. 98 (1980) 33127–33128.

[7] H.A. van der Sloot, *Waste Management Res.*, 8 (1990) 215–228.

[8] *NEN 7345 (formely Draft NVN 5432): Determination of the Release of Inorganic Constituents from Construction Materials and Stabilized Waste Products*, Netherlands Normalisation Institute, Delft, 1993.

[9] H.A. van der Sloot, O. Hjelmar, Th.G. Aalbers, M. Wahlstrom and A.M. Fallman, *TN 292 Document: Proposed Leaching Test for Granular Solid Waste*, ECN, Petten, 1993.

[10] US Environmental Protection Agency, *Fed. Reg.*, Vol. 43, No. 243 (1978).

ELSEVIER

Journal of Chromatography A, 706 (1995) 327–337

JOURNAL OF CHROMATOGRAPHY A

Separation of anionic surfactants on anion exchangers

Ning Pan, Donald J. Pietrzyk*

Department of Chemistry, University of Iowa, Iowa City, IA 52242, USA

Abstract

Two anion-exchange columns, PRP-X100 and IonPac AS11, that differ in anion-exchange capacity and porous properties are evaluated for applications in the separation of anionic surfactants such as alkane sulfonates, alkyl sulfates, and linear alkylbenzene sulfonates. Retention of the anionic surfactants on the anion exchangers is due to both anion-exchange processes and interactions between the anionic surfactant and exchanger polymeric matrix. The effects of mobile phase solvent composition and counter-anion, counter-anion concentration, and mobile phase cation are evaluated. Isocratic baseline separation of alkane sulfonates and alkyl sulfates in the carbon number range of C_6 to C_{12} are possible on the IonPac AS11 anion-exchange column using a 40:60 acetonitrile–water, LiOH eluent with post-column suppression and conductivity detection. Typical detection limits for alkane sulfonates and alkyl sulfates are about 14 pmol. Linear alkylbenzene sulfonate (LAS) homologs can be separated and partial separation of LAS positional isomers is also possible.

1. Introduction

Over half of the surfactants consumed in commercial and industrial products and processes are anionic surfactants. Of the various available forms of anionic surfactants those most used as the acids or their salts are the linear alkylbenzene sulfonates (LAS), which are biodegraded in an aerobic condition, the alkane sulfonates (RSO_3^-), the alkyl sulfates ($ROSO_4^-$), and the alkyl ether sulfates. In most applications and formulations the anionic surfactants are a mixture of homologs. While the carbon number can range from C_6 to C_{18} most industrial mixtures are composed of a narrower range of homologs and their mixtures are often expressed in terms of average C number. For the LAS surfactants the mixtures can be even more complex because the position of the benzene sulfonate ring on the alkyl chain for a given alkylbenzene sulfonate can vary depending on the alkyl chain length and the manufacturing process.

Establishing a simple and reliable method for the analysis of anionic surfactants is essential for quality control in anionic surfactant manufacturing and in commercial applications or in the study of the environmental fate of the anionic surfactants since they are often discharged into the environment. Procedures that do not differentiate among the anionic surfactant homologs are limited in their application. For this reason and because detection limits are also favorable separation techniques such as thin-layer chromatography [1,2], gas chromatography (GC) [3–8], capillary electrophoresis (CE) [9–12], and liquid chromatography (LC) [13–32] are widely employed in anionic surfactant analysis. GC and LC are particularly valuable since each can be interfaced with mass spectrometry

* Corresponding author.

0021-9673/95/$09.50
SSDI 0021-9673(95)00075-5

[4,5,8,25] which allows sensitive identification of individual separated homologs.

LC anionic surfactant separations are based on one of three general approaches and each takes advantage of either the hydrophobic or the anionic property of the surfactant. In one LC strategy anionic surfactants are retained on reversed stationary phases because of the hydrophobic property of the surfactant and resolution of the anionic surfactant homologs comes about because of differences in hydrophobicity of the homologs [13–21]. A second LC strategy is based on retention of the anionic surfactants on anion exchangers. In this case separation occurs because of differential ionic interactions between the surfactant anionic group for each of the homologs and the ionogenic groups of opposite charge on the anion exchanger [22–24]. Both silica bonded phase and organic polymer-based anion exchangers are useful for these kinds of separations although the latter is usually preferred because of the pH limitations of the silica-based anion exchangers. In the third LC strategy a pairing ion or ion interaction reagent, such as a quaternary ammonium salt, is included in the mobile phase and retention and resolution are due to a differential interaction between the reversed stationary phase, the ion interaction reagent, and the anionic surfactant analyte [25–33].

The three LC separation strategies can be used to isolate and/or concentrate trace quantities of anionic surfactants in a precolumn or solid-phase extraction strategy. This kind of application is particularly beneficial with reversed stationary phases and anion exchangers and each of these has been successfully employed in the analysis of anionic surfactants in environmental samples [13,17,19,29].

Each of the LC anionic surfactant separation strategies is subject to specific factors which can be manipulated to enhance retention, resolution, and even detection. For example, in the reversed-phase LC separation of anionic surfactants retention of the surfactant is enhanced as eluent ionic strength is increased and the extent of the enhancement is cation-dependent when different electrolytes are used as the ionic strength electrolyte [14,21]. Column efficiency depending on the ionic strength and the cation is also increased which increases resolution significantly. These improved chromatographic characteristics were attributed to association between the mobile phase cation and the anionic surfactant. In the LC separation of the anionic surfactants in the presence of an ion interaction reagent resolution can be improved by employing a more hydrophobic ion interaction reagent, varying the mobile phase organic solvent content or ionic strength, and/or by selecting different types of ion interaction reagents [25–33]. The ion interaction reagent, if detector-active, can also provide the basis for the indirect detection of the anionic surfactants [30–33]. In the anion-exchange separation of anionic surfactants detection can be improved when RSO_3^-, $ROSO_3^-$, or alkyl ether sulfates are being separated by elution with an eluent chromophoric counter-anion, such as phthalate, sulfosalicylate, *m*-sulfobenzoate, or naphthalene disulfonate. This type of eluent also allows anionic surfactants to be detected by an indirect absorbance detection strategy at a wavelength where the eluent counter-anion absorbs [22,23].

This report focuses on our studies on the retention and separation of anionic surfactants on anion exchangers. The importance of anion-exchange capacity, the influence of the anion-exchange matrix on retention, and the effect of eluent cation on anionic surfactant retention on anion exchangers were evaluated. Optimum conditions for the separation of RSO_3^-, $ROSO_3^-$, and LAS analytes on anion exchangers are established.

2. Experimental

2.1. Reagents and instrumentation

Alkane sulfonates and alkyl sulfates were purchased from Chem Service and Eastman Kodak as the sodium salts or free acids. Benzene-, *p*-toluene-, and *p*-ethylbenzenesulfonic acids, *p*-hydroxybenzoic acid (PHBA), potassium acid phthalate (KHP), and trimesic acid

were purchased from Eastman Kodak, Sigma, EM Science, or Aldrich. Commercial mixtures of LAS surfactants and pure samples of sodium salts of 2-nonyl-, 2-decyl-, 2-tetradecyl-, and 2-pentadecylbenzenesulfonate were obtained from Procter and Gamble. The pure samples were shown to be free of other positional isomers by LC [21]. Acetonitrile and methanol (EM Science) were analytical-reagent grade. LC water was freshly prepared by passing in house distilled water through a Millipore Milli-Q Plus water treatment system.

Two commercially available prepacked anion-exchange columns were studied. A macroporous polystyrene–divinylbenzene copolymer-based anion exchanger, PRP-X100, was obtained from Hamilton as a 10-μm particle, 150 mm × 4.6 mm I.D. column with an exchange capacity of 190 μequiv. per column. A second pellicular-type polystyrene–divinylbenzene latex-modified anion exchanger, IonPac AS11, was obtained from Dionex as a 13- μm particle, 250 mm × 4.6 mm column with an anion-exchange capacity of 45 μequiv. per column.

Beckman Model 110A reciprocating pumps and a Beckman Model 332 gradient controller delivered the eluent while sample injection was by a Rheodyne 7125 injector with a 20-μl sample loop. Detection was by UV absorbance (LAS analytes) with a Spectra Physics SP 8450 or SP100 variable-wavelength detector at 220 or 225 nm or by a Waters M-430 conductivity detector (RSO_3^-, $ROSO_3^-$ analytes) following suppression with a Dionex AMMS-1 anion micromembrane suppresser. Chromatographic data were collected on a Spectra Physics 4270 integrator and handled by Spectra Physics WINner chromatographic software.

2.2. Procedures

Anion-exchange columns were evaluated periodically with a F^-, Cl^-, Br^-, NO_2^-, NO_3^- test sample where each anion was 0.1 mg/ml. An aqueous 4.0 m*M* *p*-hydroxybenzoic acid solution at 2.0 ml/min and a 21 m*M* NaOH solution at 1.0 ml/min were used for the PRP-X100 and IonPac AS11 columns, respectively, and analytes were detected by conductivity.

Mobile phase solutions were prepared by dilution of a known volume of aqueous salt, acid, or base solution of known concentration which had been determined by titration versus standards. Organic solvent–water eluents (v/v) were degassed for several minutes prior to their use. Analyte solutions of known concentration (0.030 to 0.30 mg/ml) were prepared in deionized water or 1:1 acetonitrile–water. Standard analyte solutions for the calibration curves were prepared by a series of dilutions of standard solutions of the analyte. Sample injection was by Hamilton syringe, eluent flow-rate was 1.00 ml/min with the IonPac AS11 column and 2.0 ml/min with the PRP-X100 column, temperature was 25°C, and inlet pressure and void volume, which depended on the column and the eluent, was 500 to 900 p.s.i. and 0.9–1.0 ml, respectively. Aqueous 25 m*M* H_2SO_4 at 1.0 ml/min was used to regenerate the anion micromembrane suppresser. Multiple measurements were averaged to establish capacity factors, column efficiency, and calibration curve data. Retention order and peak identity were confirmed by comparison to retention times for known standards except where noted.

3. Results and discussion

3.1. Anion exchangers

Analyte anion retention in typical anion-exchange processes is affected by eluent counter-anion, counter-anion concentration, solvent composition, and pH, particularly when the analyte anion has a weak base property. Retention is also influenced by anion-exchange capacity and increases as the capacity of the exchanger increases. Two types of anion exchangers, PRP-X100 and IonPac AS11, were investigated. Both are strong base-type anion exchangers containing the quaternary ammonium ionogenic group. The PRP-X100, however, has an anion-exchange capacity of about four times that of the IonPac AS11 and is macro-

porous while the IonPac AS11 is pellicular. Consequently, both anion exchangers have the potential for hydrophobic interactions between the analyte anion and the polymeric exchanger matrix when the analyte anion also contains a hydrophobic center in addition to ordinary anion exchange at the anion exchange ionogenic group. Since anionic surfactants contain both an anionic center and a hydrophobic property due to the hydrocarbon chain, these analytes are likely to participate in a mixed-mode type interaction with polymeric stationary phases that possess both anion-exchange ionogenic groups and a matrix that can participate in a reversed-phase type of interaction with the hydrophobic portion of the analyte. As anion-exchange capacity increases and the number of charged ionogenic groups increases the exchanger surface becomes more polar and the extent of the reversed-phase interaction at the exchanger polymeric matrix should decrease. Mixed mode-type interactions have been observed before with anionic surfactant analytes and an aminefluorocarbon silica bonded stationary phase column [23] as well as with other type of analytes and mixed stationary phase surfaces [34–36] and commercial columns have become available to take advantage of mixed-mode interactions.

The PRP-X100 and the IonPac AS11 are strong-base anion exchangers and participate in typical anion-exchange processes. Both are polystyrene–divinylbenzene copolymer-based, but the macroporous property of the PRP-X100 favors a greater hydrophobic interaction between the anionic surfactant and the exchanger matrix than for the IonPac AS11. However, the exchange capacity of the IonPac AS11 is about one fourth that of the PRP-X100 and the lower capacity suggests that the hydrophobic interaction would also be extensive on this anion exchanger.

As the carbon chain of an anionic surfactant increases, its ability to undergo a hydrophobic interaction with the anion-exchange matrix should also increase. The eluent conditions that will affect this type of interaction are: eluent solvent composition, type of organic modifier, eluent ionic strength, pH if the analyte has weak acid properties, and mobile phase cation. Eluent ionic strength and the cation dependency are especially important in anionic surfactant separations because these variables when optimized will improve chromatographic peak shape, column efficiency, and resolution and therefore improve both the quality of the separation and the detection limit [14,21].

3.2. Effect of eluent organic modifier

Figs. 1A and B show that as organic modifier increases in the eluent anionic surfactant retention on the PRP-X100 and IonPac AS11 decreases. The large change in retention for the C_4 to C_{10} RSO_3^- analytes used in Fig. 1 is much greater than what would be expected if only anion-exchange processes were involved in anionic surfactant retention and these processes were the only ones being affected. The major effect of the solvent is to influence the interaction between the RSO_3^- surfactant and the exchanger polymeric matrix. Furthermore, the interaction of the RSO_3^- surfactant with the matrix is significantly greater on the PRP-X100, which increases as the alkyl chain length of the RSO_3^- surfactant increases, since a much stronger eluent solvent, acetonitrile–water, is required to lower the retention of the RSO_3^- surfactants on the PRP-X100. For the IonPac AS11 an acetonitrile–water eluent solvent, which is much weaker in its eluent strength towards reversed-phase interactions, is sufficiently strong to lower the RSO_3^- surfactant anion exchanger matrix retention.

3.3. Effect of mobile phase counter-anion

Increasing eluent counter-anion concentration decreases anionic surfactant retention typical of an anion-exchange process. Fig. 2A and B illustrate how different eluent counter-anions at a fixed counter-anion concentration influence anion surfactant retention on the two anion exchangers. For both anion exchangers the eluent solvent is adjusted to an organic modifier

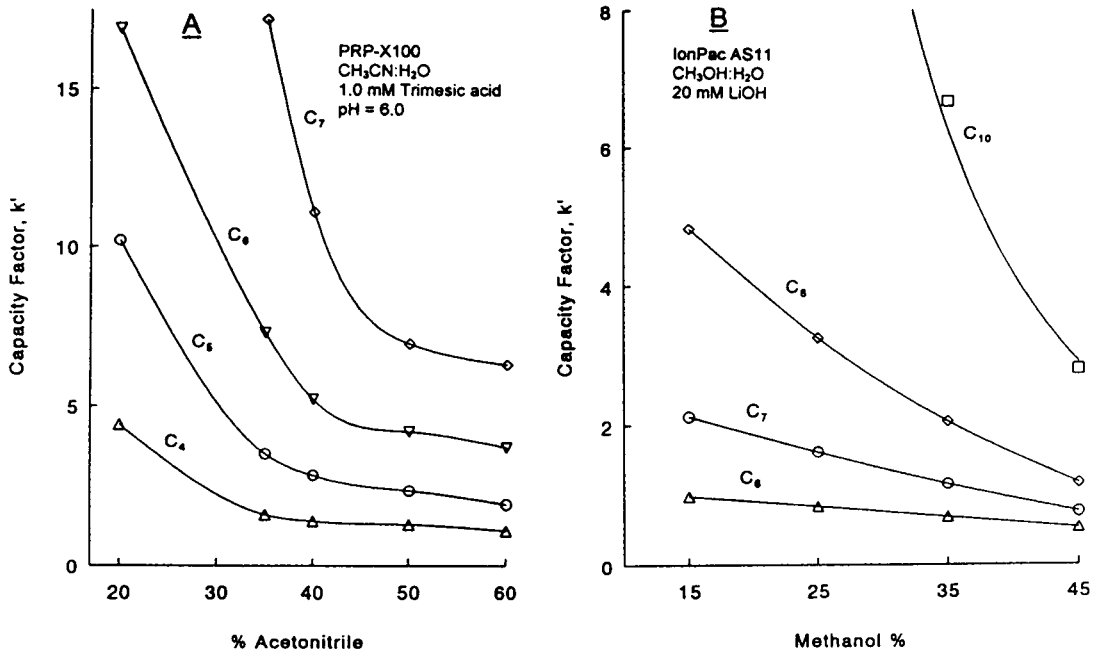

Fig. 1. Effect of mobile phase modifier on the retention of alkane sulfonates of differing alkyl chain lengths on (A) PRP-X100 and (B) IonPac AS11.

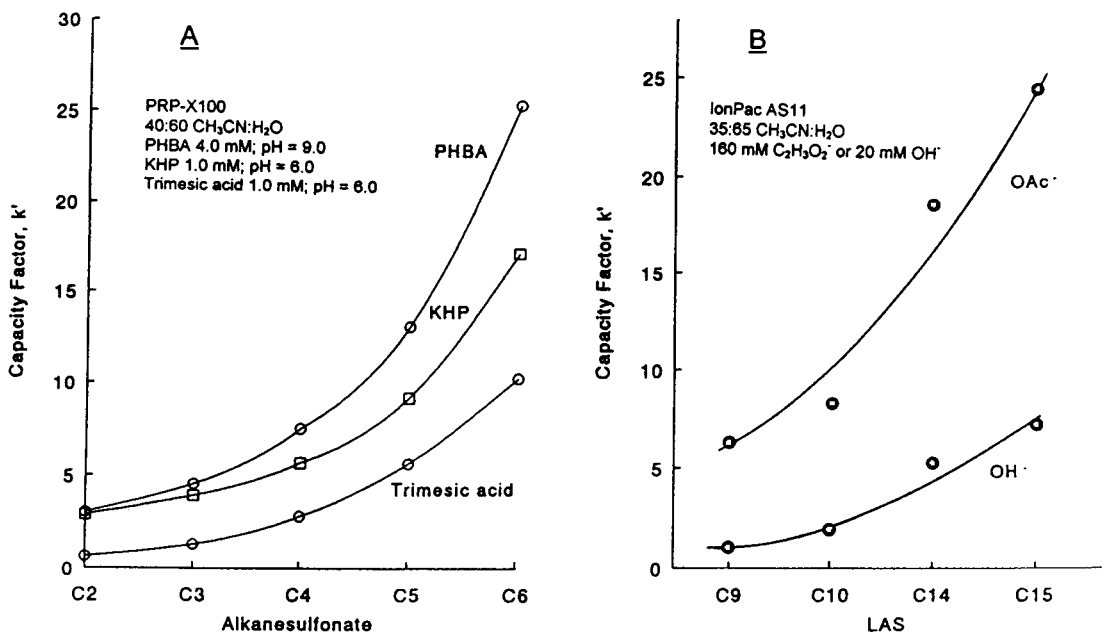

Fig. 2. Effect of mobile phase counter-anion on the retention of (A) alkane sulfonates on PRP-X100 and (B) LAS derivatives on IonPac AS11.

concentration that minimizes anionic surfactant–anion-exchange matrix interaction for the series of anion surfactants studied.

For the PRP-X100 anion exchanger (see Fig. 2A), which has the higher anion-exchange capacity, strong eluent counter-anions, such as PHBA, KHP, and trimesic acid that are appreciably multivalent at the pH used, are required to reduce the retention of the RSO_3^- analytes where the alkyl carbon chain ranges from C_2 to C_6. Favorable elution times are obtained only for the shorter-carbon-chain RSO_3^- analytes and when the eluent contains the stronger, multivalent counter-anions. If the counter-anion concentration is increased RSO_3^- retention decreases typical of an anion-exchange process. When the organic modifier in the eluent in Fig. 2A is decreased, RSO_3^- surfactant retention increases and the increase is consistent with a mixed-mode interaction [23]. For longer-carbon-chain RSO_3^- analytes than used in Fig. 2A retention on the PRP – X100 is even higher and elution, even with the stronger eluent counter-anion sodium trimesate, is not favorable in terms of elution time.

For the IonPac AS11 (see Fig. 2B), or the anion exchanger with the lower anion-exchange capacity and lower matrix interaction, elution of the RSO_3^- analytes is possible with weak eluent counter-anions, such as OH^- and $C_2H_3O_2^-$, both of which are also compatible with post-column suppression to enhance conductivity detection. Even the more hydrophobic LAS derivatives, which were the analytes in Fig. 2B, have low retention in the presence of the eluent OH^- and $C_2H_3O_2^-$ counter-anions and are eluted in reasonable elution times. When C_9 and C_{10} RSO_3^- analytes were used and eluent OH^- concentration was increased from 10 to 60 m*M*, log *k'* versus log OH^- concentration curves were linear up to 40 m*M* OH^-. Slopes were about 1 indicating that at the eluent solvent conditions in Fig. 2B retention is primarily due to anion exchange [23]. Furthermore, elution time for the anionic surfactants can be reduced even more by increasing the OH^- or $C_2H_3O_2^-$ eluent concentration.

3.4. Effect of mobile phase cation

In reversed-phase chromatography of anionic surfactants the retention, column efficiency, and resolution are enhanced depending on eluent cation and its concentration. Association between the anionic surfactant and the cation was suggested to be a major contributor to the enhanced chromatographic performance [14,21]. In anion exchange of anionic surfactants association between the eluent cation and the surfactant anion should reduce anion surfactant retention on the anion exchanger. When electrolytes providing different cations and the same counter-anion were used as eluent additives retention of the anionic surfactants is influenced by the cation but only to a small extent. This is illustrated in Fig. 3 where retention of benzene-, *p*-toluene-, and *p*-ethylbenzenesulfonic acid on the IonPac AS11 is plotted as a function of eluent acetoni-

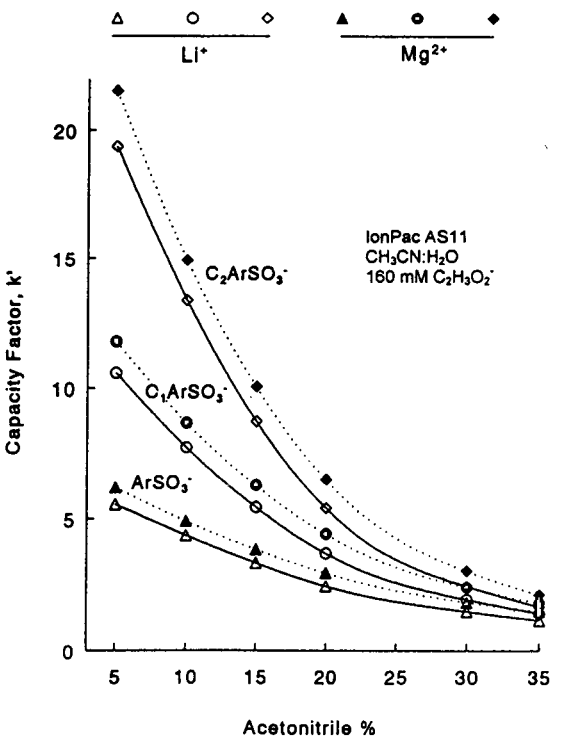

Fig. 3. Effect of eluent cation on the retention of short-alkyl-chain LAS derivatives on IonPac AS11.

trile/water ratio at a constant Li^+ and Mg^{2+} acetate concentration where the acetate concentration of the two eluents are equivalent. The Mg^{2+} consistently causes a small enhancement in the anionic surfactant retention compared to the Li^+ eluent. This enhancement was also observed when comparing the effects of Mg^{2+} and Li^+ in a 35:65 acetonitrile–water, 160 m*M* $C_2H_3O_2^-$ eluent on LAS retention for alkyl chain lengths of C_0 to C_{15} and for LAS retention where $LiC_2H_3O_2$ and $Mg(C_2H_3O_2)_2$ concentrations were increased in a 20:80 acetonitrile–water eluent. A similar Mg^{2+} over Li^+ enhancement in retention for the short-carbon-chain LAS analytes was determined for the PRP-X100 anion exchanger.

The cation, if it undergoes association with the anionic surfactant as suggested previously [14,21], can affect retention on the anion exchanger in two ways. First, the association can affect the interaction between the anionic surfactant and the exchanger matrix to increase retention. The associated cation anionic surfactant is less polar than the dissociated anionic surfactant and therefore is better able to undergo an interaction with the matrix. Or second, the association can cause retention of the anionic surfactant at the anion exchange site to be less since the cation anionic surfactant-associated species reduces the anionic character of the anionic surfactant. The fact that Mg^{2+} as the eluent cation has a greater affect over Na^+ or Li^+ as the eluent cation is consistent with the cation having a greater influence on the matrix interaction. The cation effect is not large, however, and manipulation of the eluent cation to alter anionic surfactant retention on the anion exchanger offers only a modest advantage in retention and separation of anionic surfactants on the polymer-based anion exchangers.

3.5. Separations

The low-capacity IonPac AS11 anion exchanger is more versatile than the PRP-X100 anion exchanger for the separation of anionic surfactants because on the former anion exchanger the matrix interactions are less, elution of the anionic surfactants is possible with weaker eluent counter-anions, column efficiency is better, and resolution is more favorable. For these reasons only separations using the IonPac AS11 anion exchanger are described here; data for anionic surfactant separations on the PRP-X100 are available elsewhere [37]. The low exchange capacity for the IonPac AS11 limits the sample size in order to avoid a sample overload of the column. A acetonitrile–water, LiOH solution, which provides a OH^- eluent counter-anion and an acetonitrile concentration that reduces matrix interaction with the anionic surfactants, was used. The OH^- counter-anion is readily handled by post-column suppression which permits an enhanced conductivity detection of the separated anionic surfactants. LAS or other anionic surfactants that contain a chromophore were detected by UV.

Fig. 4 illustrates the baseline separation of a

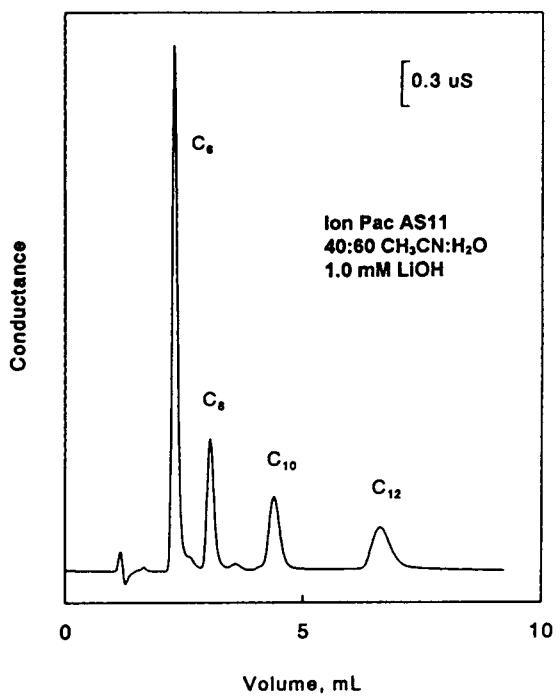

Fig. 4. Separation of C_6 to C_{12} alkane sulfonates on IonPac AS11.

mixture of even-carbon C_6 to C_{12} RSO_3^- analytes using an isocratic elution where the eluent is 40:60 acetonitrile–water, 1.0 m*M* LiOH. Under these eluent solvent conditions interaction of the RSO_3^- analytes with the matrix is low and resolution is primarily due to anion exchange. The RSO_3^- analytes were detected by conductivity following suppression by an anion micromembrane suppresser.

$ROSO_3^-$ analytes of even carbon number in the C_6 to C_{12} range are also baseline-resolved on the IonPac AS11 with the same eluent as used in Fig. 4. The $ROSO_3^-$ analyte of the same carbon number as the RSO_3^- analyte has a higher retention on both the IonPac AS11 and PRP-X100 anion exchangers. This same selectivity is also observed when reversed-phase columns are employed [14]. Because of the difference mixtures of $ROSO_3^-$ and RSO_3^- analytes are separable by isocratic elution on the IonPac AS11 column. This is illustrated in Fig. 5 where a mixture of even-carbon C_6 to C_{12} RSO_3^- and $ROSO_3^-$ analytes are baseline-resolved. In Fig. 5 the shoulder on the $C_6SO_3^-$ peak and the unidentified peak preceding the $C_8SO_3^-$ where shown to be introduced by the $ROSO_3^-$ analyte samples and the two unidentified peaks appear to be due to lower-carbon-number $ROSO_3^-$ analytes. When log k' values for the retention of the RSO_3^- and $ROSO_3^-$ analytes are plotted versus carbon number a linear relationship is obtained for each series of homologs. From the $ROSO_3^-$ graph the k' values for the two unknown peaks in Fig. 5 correspond to the C_4 and $C_5OSO_3^-$ analytes. No attempt was made to unequivocally identify the two unknown peaks. If the acetonitrile concentration in the eluents used in Figs. 4 and 5 is reduced, interaction between the RSO_3^- and $ROSO_3^-$ surfactants and the matrix increases, particularly as carbon chain length increases, and the eluent LiOH concentration must be increased to obtain elution times similar to those in Figs. 4 and 5.

Short-chain LAS analytes are baseline-resolved on the IonPac AS11 anion-exchange column. This is illustrated in Fig. 6 where benzene-,

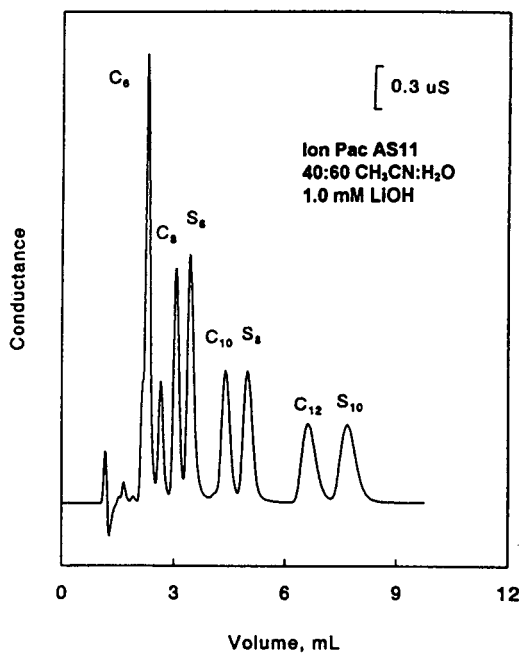

Fig. 5. Separation of C_6 to C_{12} alkane sulfonates (C) and alkyl sulfates (S) on IonPac AS11.

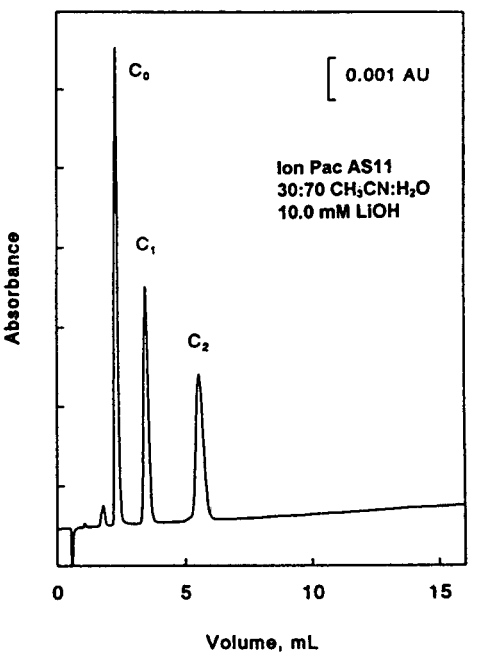

Fig. 6. Separation of short-alkyl-chain LAS derivatives on IonPac AS11.

p-toluene-, and *p*-ethylbenzenesulfonate are separated and detected by UV at 220 nm. In Fig. 6 the acetonitrile eluent concentration is high enough so that retention is primarily due to anion exchange.

Chromatograms for the separation of a commercial sample of long-chain LAS homologs and isomers in the C_{10} to C_{14} range are shown in Fig. 7A and B. In Fig. 7A the eluent was 30:70 acetonitrile–water, 50 m*M* $MgCl_2$. At this acetonitrile concentration matrix interaction between the IonPac AS11 and the C_{14} to C_{16} LAS homologs and isomers is significant. Thus, $MgCl_2$ was selected as the eluent electrolyte since it provides a counter-anion that increases elution strength and a cation that affects matrix retention. The LAS mixture was known to contain C_{10} to C_{14} homologs and for each homolog there are several positional isomers. As shown in Fig. 7A the LAS homologs are completely resolved and the positional isomers are only partially resolved. The resolution between adjacent homologs is about 1.1. Since the positional isomers have the same anionic character, the resolving power of the anion exchanger for these isomers is less favorable than what can be obtained by reversed-phase chromatography [21] and the partial resolution of the isomers is due to the matrix interaction and influence of the Mg^{2+} in the eluent. When an eluent containing 1.5 m*M* LiOH and 40:60 acetonitrile–water was used (see Fig. 7B), each LAS homolog was eluted as a single chromatographic peak. For such an eluent condition the resolving force that influences the interaction between the LAS analyte and the matrix which is necessary to resolve the positional isomers is diminished, thus, the separation is primarily a separation of homologs due to anion exchange. This separation condition would be preferred if an isomeric separation is not required.

The C_{10} and C_{14} LAS peaks in Fig. 7A and B were identified by comparison to pure 2-positional C_{10} and C_{14} LAS standards while the C_{11}, C_{12},

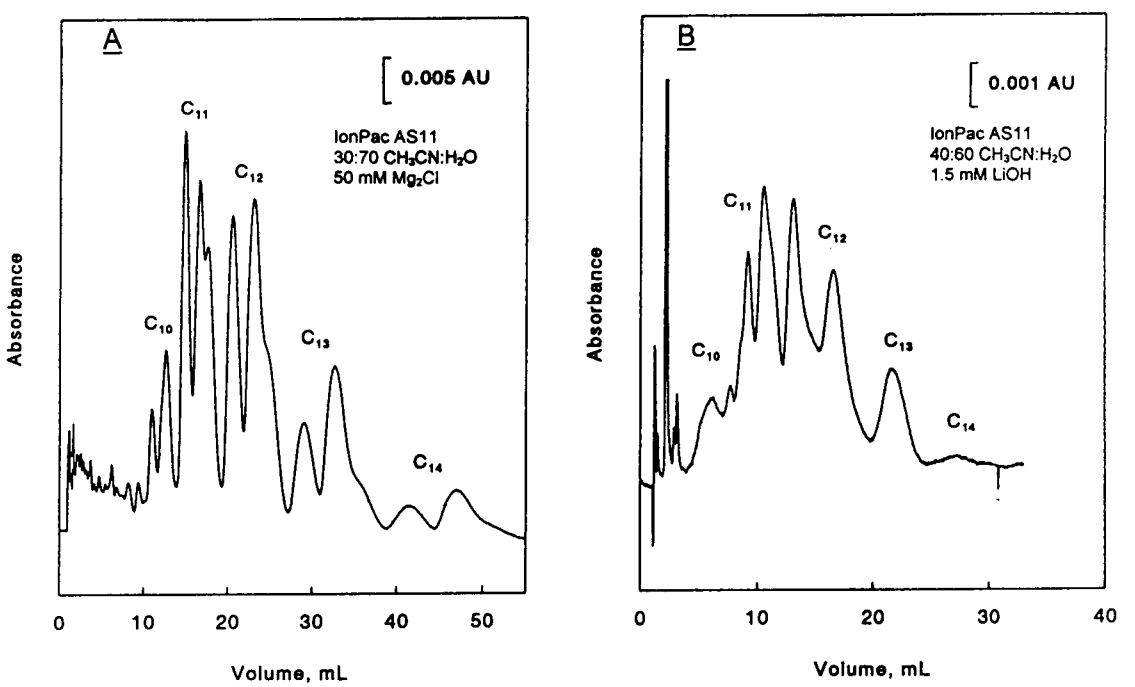

Fig. 7. Separation of a commercial mixture of C_{10} to C_{14} (A) LAS homologs and positional isomers and (B) LAS homologs on IonPac AS11.

and C_{13} LAS peaks were determined according to the elution order and previous work with the LAS sample by reversed-phase chromatography [21]. All other anionic surfactant analyte peaks in Figs. 4, 5, and 6 were confirmed by comparison to chromatographic data for individually injected standards and/or by peak spiking.

A calibration curve was prepared with the IonPac AS11 column and a standard solution of pure $C_8OSO_3^-$ as the test analyte. The eluent in Fig. 4 was used and detection was by conductivity following post-column suppression. The calibration curve, which was defined by the equation (peak area) = $(6.84 \cdot 10^4)$ (nmol of C_8 OSO_3^-) − 783 where $r = 0.9995$, was linear throughout the concentration range (0.050–1.0 nmol) studied. Background conductance following suppression was low (1–2 μS) and because of this a detection limit of 14 pmol was obtained for a 3:1 signal-to-noise ratio.

4. Conclusion

Anionic surfactants are retained on PRP-X100 and IonPac AS11 anion exchangers by a mixed-mode interaction. The analytes undergo anion exchange as well as an interaction with the exchanger polymeric matrix. The retention due to anion exchange and the matrix interaction is greater on the PRP-X100 which has a higher anion-exchange capacity and a porous polymeric structure. Increasing the eluent organic modifier decreases anionic surfactant retention because of the solvent effect on matrix anionic surfactant interaction. Increasing the eluent counter-anion concentration decreases the retention because of its effect on the anion-exchange process but because the IonPac AS11 has a low anion-exchange capacity weak-eluent counter-anions can be employed to reduce anionic surfactant retention on this exchanger. Eluent cation will affect the matrix interaction but the change in retention due to the cation is small. Isocratic baseline-resolved separations of C_6 to C_{12} RSO_3^- and $ROSO_3^-$ analytes are possible with a 40:60 acetonitrile–water, 1.0 m*M* LiOH eluent. Since the background conductivity is significantly reduced by post-column suppression detection is very sensitive. LAS homologs are separable while only partial resolution of LAS positional isomers is obtained.

Acknowledgements

The authors are grateful to Procter and Gamble for providing pure 2-positional LAS isomers. Special thanks also goes to Hamilton and Dionex for supplying the anion-exchange columns.

References

[1] D.W. Armstrong and G.Y. Stine, *J. Liq. Chromatogr.*, 6 (1983) 23–33.
[2] T. Takeuchi, T. Niwa and D. Ishri, *Chromatographia*, 23 (1987) 929–933.
[3] H. Hon-Nami and T. Hanya, *J. Chromatogr.*, 161 (1978) 205–212.
[4] Q.W. Osburn, *J. Am. Oil Chem. Soc.*, 63 (1986) 257–263.
[5] J. McEvoy and W. Giger, *Environ. Sci. Technol.*, 20 (1986) 376–378.
[6] R.E.A. Escott and D.W. Chandler, *J. Chromatogr. Sci.*, 27 (1989) 134–138.
[7] M.L. Trehy, W.E. Gledhill and R.G. Orth, *Anal. Chem.*, 62 (1990) 2581–2586.
[8] P. Sandra and F. David, *J. High Resolut. Chromatogr.*, 13 (1990) 414–417.
[9] W.C. Brumley, *J. Chromatogr.*, 603 (1992) 267–272.
[10] P.L. Desbène, C. Rony, B. Desmazières and J.C. Jacquier, *J Chromatogr.*, 608 (1992) 375–383.
[11] S. Chen and D.J. Pietrzyk, *Anal. Chem.*, 65 (1993) 2770–2775.
[12] S.A. Shamsi and N.D. Danielson, *Anal. Chem.*, 66 (1994) 3757–3764.
[13] M.A. Castles, B.L. Moore and S.R. Ward, *Anal. Chem.*, 61 (1989) 2534–2540.
[14] D. Zhou and D.J. Pietrzyk, *Anal. Chem.*, 64 (1992) 1003–1008.
[15] P. MacCarthy, R.W. Klusman, S.W. Cowling and J.A. Rice, *Anal. Chem.*, 65 (1993) 244R–292R.
[16] K. Inaba and K. Amano, *Int. J. Environ. Anal. Chem.*, 34 (1988) 203–213.
[17] Y. Yokayama and H. Sato, *J. Chromatogr.*, 555 (1991) 155–162.
[18] T. Bán, E. Papp and J. Inczédy, *J. Chromatogr.*, 593 (1992) 227–231.
[19] A. Marcomini, A. DiCorcia, R. Samperi and S. Capri, *J. Chromatogr.*, 644 (1993) 59–71.

[20] J.B. Li and P. Jandik, *J. Chromatogr.*, 546 (1991) 395–403.
[21] S. Chen and D.J. Pietrzyk, *J. Chromatogr. A*, 671 (1994) 73–82.
[22] J.R. Larson, *J. Chromatogr.*, 356 (1986) 379–381.
[23] S. Maki, J. Wangsa and N.D. Danielson, *Anal. Chem.*, 64 (1992) 583–589.
[24] Y. Yokoyama, M. Kondo and H. Sato, *J. Chromatogr.*, 643 (1993) 169–172.
[25] G.R. Bear, *J. Chromatogr.*, 371 (1986) 387–402.
[26] R.H. Schreuder and A. Martijn, *J. Chromatogr.*, 435 (1988) 73–82.
[27] J.J. Conboy, J.D. Henion, M.W. Martin and J.A. Zweigenbaum, *Anal. Chem.*, 62 (1990) 800–807.
[28] A. DeCorcia, M. Marchetti, R. Samperi and A. Marcomini, *Anal. Chem.*, 63 (1991) 1179–1182.
[29] O. Zerbinati, G. Ostacoli, D. Gastaldi and V. Zelano, *J. Chromatogr.*, 640 (1993) 231–240.
[30] B. Sachok, S.N. Deming and B.A. Bidlingmeyer, *J. Liq. Chromatogr.*, 5 (1982) 389–402.
[31] D.J. Pietrzyk, P. Rigas and D.J. Yuan, *J. Chromatogr. Sci.*, 27 (1989) 485–490.
[32] G. Eppert and G. Liebscher, *J. Chromatogr. Sci.*, 29 (1991) 21–25.
[33] J.A. Boiani, *Anal. Chem.*, 59 (1987) 2583–2586.
[34] T.R. Floyd, J.B. Crowder and R.A. Hartwick, *LC Mag.*, 3 (1985) 508–520.
[35] H.J. Issaq and J.J. Gutierrez, *J. Liq. Chromatogr.*, 11 (1988) 2851–2861.
[36] R. Saari-Nordhaus and J.M. Anderson, Jr., *Anal. Chem.*, 64 (1992) 2283–2287.
[37] N. Pan, *M.S. Thesis*, University of Iowa, Iowa City, IA, 1993.

ELSEVIER

Journal of Chromatography A, 706 (1995) 339–343

JOURNAL OF CHROMATOGRAPHY A

Determination of anions in amine solutions for sour gas treatment

Rainer Kadnar*, Josef Rieder

ÖMV-AG, Laboratory for Exploration and Production, Gerasdorferstrasse 151, A-1210 Vienna, Austria

Abstract

In sour gas treatment, various amine solutions are used to remove the acidic components H_2S and CO_2. These components are absorbed by the amine solution and stripped during amine regeneration. Other anions (contaminants) tie up the amine by forming heat-stable salts (HSS) which cannot be regenerated. HSS also can be formed from amine degradation by-products, i.e., organic acids. Hence the acid gas-carrying capacity of the amine will be reduced. HSS also can promote corrosion and cause foaming problems. Therefore, the determination of anions in amine solutions is very important. Using the analytical columns IonPac AS9-SC and AS10, it is possible to determine all anions of interest by ion chromatography.

1. Introduction

Natural gas often contains high concentrations of H_2S or/and CO_2 (the highest concentrations in natural gas from Austria are 2.2 vol.-% H_2S and 16 vol.-% CO_2). This gas is called "sour gas" and is very corrosive, so it is necessary to remove the acidic components before feeding the gas in pipelines.

One possibility is gas washing with amine solutions. Most plants use diethanolamine (DEA), monoethanolamine (MEA) or methyldiethanolamine (MDEA) for the absorption of the acidic gases. The amine solution is continuously regenerated by stripping H_2S and CO_2. Other anions which are either fed to the amine solution by contamination (e.g., chloride and nitrate) or formed in the treating units as amine degradation by-products (i.e., organic acids) tie up the amine by forming heat-stable salts (HSS) which cannot be regenerated. Anions observed in HSS originate from a variety of sources [1] and are listed in Table 1. To reduce problems during sour gas treatment, HSS should be minimized and should not exceed 10% of the total amine concentration [1,2]. When the concentration of any of these HSS exceeds 500 ppm, problems can be expected in the treatment unit [3]. They inactivate a portion of the basic amine and increase the rate of corrosion in the unit, resulting in higher levels of iron sulfide in the system, which subsequently causes foaming problems [3].

In our sour gas treatment plant, MDEA is used as a scrubbing solution for sour gas washing. For diagnosing corrosion and foaming problems it is useful to analyse the amine solution at several locations: the "rich" MDEA (fully charged with H_2S and CO_2) from the contactor, the "semi-lean" MDEA (partially regenerated) and the "lean" MDEA (regenerated amine, containing only small amounts of H_2S and CO_2)

* Corresponding author.

0021-9673/95/$09.50
SSDI 0021-9673(94)01210-5

Table 1
Common sources of the anions of HSS (heat-stable salts)

Anion	Source
Chloride	Make-up water Brine with inlet gas Well treatment chemicals with inlet gas
Nitrate, nitrite	Make-up water Corrosion inhibitors
Sulfate, sulfite, thiosulfate	Sulfur species oxidation products Component in gas
Formate, oxalate, acetate	Acid in the feed gas O_2 degradation Thermal degradation
Thiocyanate	Reaction product of H_2S and CN
Phosphate	Corrosion inhibitors Phosphoric acid activated carbon Cotton filters
Fluoride	Well treatment chemicals with inlet gas

before and after the carbon filter, and the amine before and after the mechanical filter [4].

Analytical procedures used for monitoring MDEA quality are based on different methods [5]. Recommended are, e.g., the determination of pH, MDEA concentration, foaming tendency, foam stability, liquid hydrocarbons, suspended solids, iron, chloride, HSS and acid gas loading [2]. For the determination of carboxylic acids no useful method was available in our laboratory. Ion chromatography seemed to be an appropriate method for the determination of inorganic and organic anions in amine solutions.

2. Experimental

Several different eluents were tested in combination with the IonPac AS9-SC (Na_2CO_3 and Na_2CO_3–$NaHCO_3$ mixtures) and AS10 (NaOH and $Na_2B_4O_7$) analytical columns for anion separation in amine solutions. These experiments resulted in three useful methods for the determination of all anions of interest.

2.1. Instrumentation

The equipment used was a DX-300 gradient ion chromatography system (Dionex, Sunnyvale, CA, USA). The separated components were detected by a pulsed electrochemical detector (PED) used in the conductivity mode (10 μS range). An AMMS-II micro-membrane suppressor system was used for chemical suppression. The AMMS II was continuously regenerated with 12.5 m*M* sulfuric acid at a flow rate of 4–6 ml/min. Integration was performed with an HP 3396A integrator (Hewlett-Packard) and CLAS/2000 (Chromatography Laboratory Automation Software; Perkin-Elmer). The columns used for separation were AS9-SC and AS10 (250 × 4 mm I.D.) separation columns and AG9-SC and AG10 (50 × 4 mm I.D.) guard columns.

2.2. Reagents

All reagents were of analytical-reagent grade (Merck, Darmstadt, Germany; sodium hydroxide, 50% solution from J.T. Baker, Deventer, Netherlands). Deionized water (18 MΩ) ob-

tained from a Milli-Q water purification system (Millipore) was employed throughout.

2.3. Calibration standards

Stock standard solutions were prepared for each anion separately by dissolving salts in deionized water. Anion standard mixtures for calibration were prepared every week from the stock standard solutions. Evaluation was done by constructing calibration graphs up to concentrations of 2 ppm for fluoride, 10 ppm for inorganic anions and oxalate and 40 ppm for small carboxylic acids.

2.4. Ion chromatographic conditions

The injection volume was 25 μl. Specific conditions for the three methods are given in Table 2.

2.5. Sample preparation

All samples were filtered and diluted with deionized water so that the analyte concentrations were within the calibration range. Before injection, the diluted samples were filtered through 0.45-μm nylon filters. For the determination of carboxylic acids and sulfur species, the samples were diluted as short as possible before injection to prevent increases in concentration of these analytes owing to oxidation processes.

3. Results and discussion

The determination of anions in amine solutions by IC cannot be performed without analytical problems. In particular, the analysis of "rich" amine samples is subject to interferences between carbonate and early-eluting anions (using method 2 or 3). In addition to the absorbed H_2S and CO_2, the amine solutions analysed contained chloride, nitrate, orthophosphate, sulfur oxidation products (sulfite, sulfate, thiosulfate), oxalate and small carboxylic acids (formate, acetate, propionate).

Method 1 was used for separation and determination of fluoride, acetate, propionate, butyrate and formate using the IonPac AS10 column with 3.5 m*M* $Na_2B_4O_7$ as eluent. The presence of other anions in the amine solutions that could not be eluted with this eluent (or very late) requires a column purge step after 20 min of elution (5 min of elution with 70 m*M* $Na_2B_4O_7$). Samples were diluted 1:20 with deionized water.

Fig. 1 shows the chromatograms of a "semi-lean" MDEA and the corresponding standard anion solution containing 1.9 ppm of fluoride, 10.5 ppm of acetate, 10.1 ppm of propionate, 9.5 ppm of butyrate and 7.8 ppm of formate.

Method 2 was used for determination of nitrate, phosphate, sulfate, oxalate, thiocyanate and thiosulfate. Separation was performed on an IonPac AS9-SC column with 1.8 m*M* Na_2CO_3–1.7 m*M* $NaHCO_3$ as eluent [6].

In "lean" MDEA samples, chloride and nitrite can also be determined. In "semi-lean" and

Table 2
Specific conditions for the three methods

Parameter	Method 1	Method 2	Method 3
Analytical column	AS10	AS9-SC	AS10
Guard column	AG10	AG9-SC	AG10
Anion trap column			ATC-1
Eluent	3.5 m*M* $Na_2B_4O_7$	1.8 m*M* Na_2CO_3–1.7 m*M* $NaHCO_3$	100 m*M* NaOH
Eluent flow-rate (ml/min)	1	2	1
Background conductivity (μS)	2–4	14–16	4–7
System pressure (p.s.i.)	2300–2500	1300–1400	2500–2600

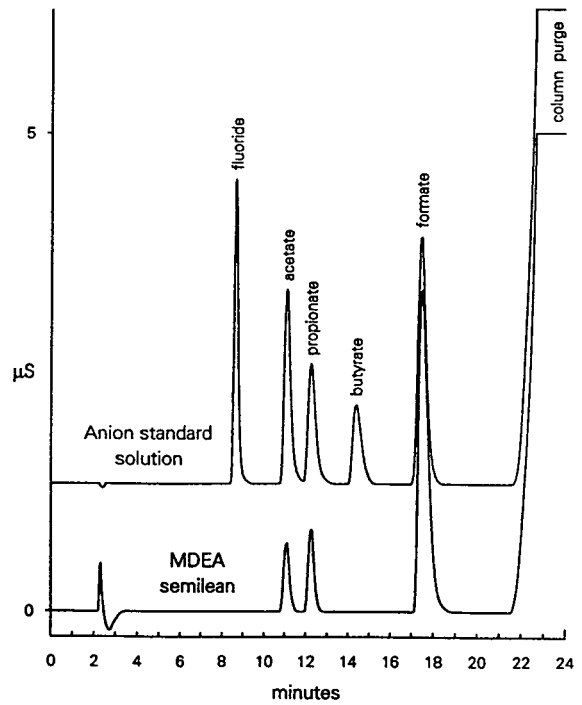

Fig. 1. Separation of anions in MDEA with IonPac AS10 + AG10 columns with 3.5 m*M* $Na_2B_4O_7$ as eluent (method 1).

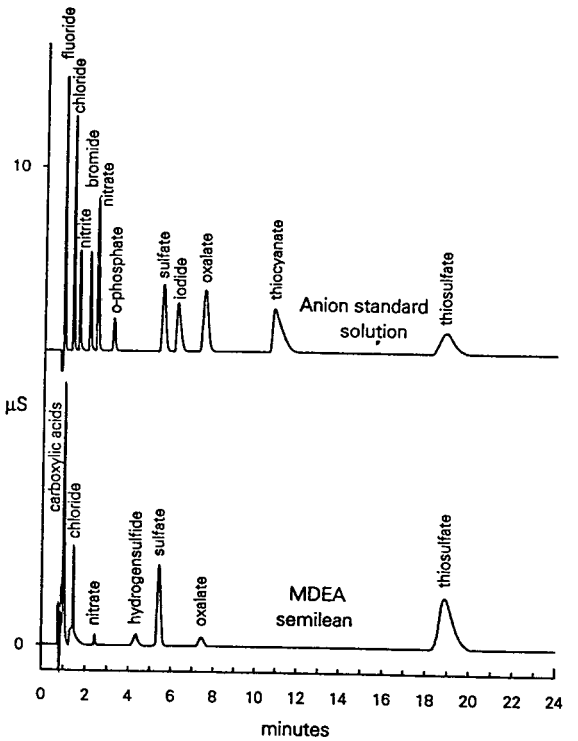

Fig. 2. Separation of anions in MDEA with IonPac AS9-SC + AG9-SC columns with 1.8 m*M* Na_2CO_3–1.7 m*M* $NaHCO_3$ as eluent (method 2).

"rich" MDEA, carbonate interferes with these early-eluting ions. Quantification is possible but time consuming. Samples were diluted 1:10 or 1:20 with deionized water; for the determination of phosphate it was necessary to dilute the sample 1:5 because of its small content. Weak points of the method are the rapid loss of capacity (decrease in retention times with time) and the pH sensitivity of the column (application in the pH range 2–11 only; the pH of amine solutions is up to 11.5).

Fig. 2 shows the chromatograms of a "semi-lean" MDEA and an anion standard solution containing 1.9 ppm of fluoride, 3.2 ppm of chloride, 3.5 ppm of nitrite, 5.1 ppm of bromide, 3.7 ppm of nitrate, 3.5 ppm of orthophosphate, 4.2 ppm of sulfate, 10.0 ppm of iodide, 6.6 ppm of oxalate, 9.9 ppm of thiocyanate and 5.2 ppm of thiosulfate.

Method 3 was used in our laboratory when the determination of chloride could not be performed with method 2 because of carbonate interferences (peak overlap). Other anions could also be determined, as shown in Fig. 3. Separation was performed with an IonPac AS10 column with 100 m*M* NaOH as eluent [7]. The eluent was purified with an anion trap column (ATC-1) for carbonate removal.

With new columns a good separation of hydrogensulfide–chloride and nitrite–sulfate ion pairs is possible. Using aged columns, incomplete resolution of these pairs of ions may occur. Determination of fluoride and small carboxylic acids is not useful because of incomplete resolution (fluoride–acetate) and co-elution (acetate–propionate). Hydrogensulfide should be eliminated by precipitation as cadmium sulfide or by oxidation with H_2O_2 to avoid problems in the determination of chloride. Another disadvantage of this method is the very late elution of thiosulfate (about 50 min). When the determination of chloride alone is necessary, a column purge step

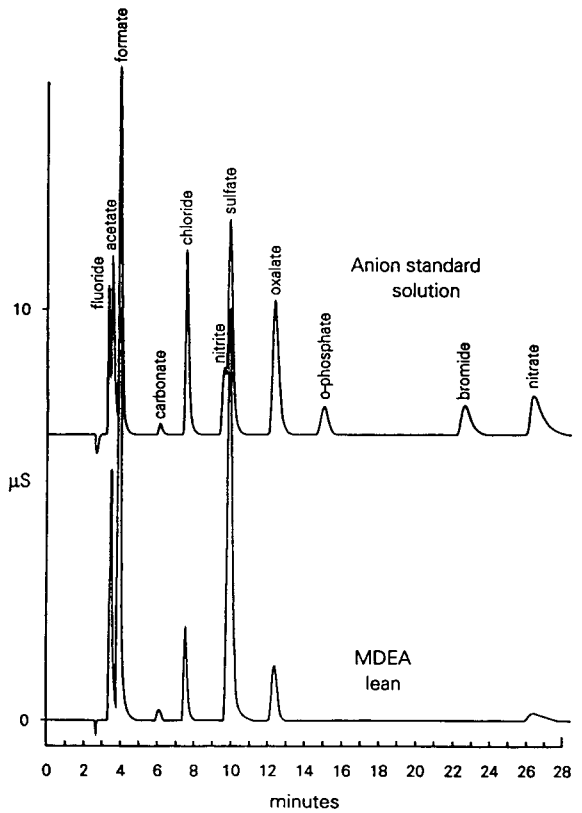

Fig. 3. Separation of anions in MDEA with IonPac AS10 + AG10 columns with 100 m*M* NaOH as eluent (method 3).

after 10 min would be efficient for shortening the analysis time.

4. Conclusions

Methods 1 and 2 are applicable for the determination of anions in MDEA with sufficient sensitivity. Method 3 must be further optimized (e.g., by incorporating a column purge step). For routine control it is not necessary to check all the anionic components in the amine solutions. The determination of the small carboxylic acids (method 1) and oxalate (method 2), as an indicator of the presence of HSS, of orthophosphate (method 2), which is eluted as a contaminant from filter materials, and chloride (method 3), which shows the influence of formation water, is useful.

References

[1] M.S. DuPart, T.R. Bacon and D.J. Edwards, *Hydrocarbon Process.*, May (1993), 89–94.
[2] S.A. von Phul and C.D. Houston, presented at the *72nd Annual GPA Convention, 15–17 March 1993, San Antonio, Texas.*
[3] D. Tunnell, *Petrochem. Gas Processing, HTI Q.*, Autumn (1994), 119–122.
[4] C.R. Pauley, *Chem. Eng. Prog.*, July (1991), 33–38.
[5] *Analysenvorschrift für das aktivierte MDEA-Verfahren der Fa. BASF*, 6th Revision, BASF, Ludwigshafen, 1990.
[6] *Installation Instructions and Troubleshooting Guide for the IonPac AG9-SC Guard Column and the IonPac AS9-SC Analytical Column*, Dionex, Sunnyvale, CA, 1992.
[7] *Installation Instructions and Troubleshooting Guide for the IonPac AG10 Guard Column and the IonPac AS10 Analytical Column*, Dionex, Sunnyvale, CA, 1991.

ELSEVIER

Journal of Chromatography A, 706 (1995) 345–351

JOURNAL OF CHROMATOGRAPHY A

Elucidation of the degradation mechanism of 2-chloroethanol by hydrogen peroxide under ultraviolet irradiation

G. Pace[a], A. Berton[a], L. Calligaro[b], A. Mantovani[b,*], P. Uguagliati[c]

[a]*Centro di Chimica Metallorganica del C.N.R., Via Marzolo 9, 35131 Padua, Italy*

[b]*Istituto di Chimica Industriale, Facoltà di Ingegneria, Università di Padova, Via Marzolo 9, 35131 Padua, Italy*

[c]*Dipartimento di Chimica, Facoltà di Scienze, Università di Venezia, Calle Larga S. Marta, 30100 Venice, Italy*

Abstract

Oxidation of 2-chloroethanol by H_2O_2 under UV irradiation has been studied. Analysis of reactants and products was performed by gas and ion chromatography. In this study we have compared the disappearance of 2-chloroethanol with the contemporaneous appearance of Cl^- ions and conductivity changes of the solution. It was found that the oxidation of 2-chloroethanol yields quantitative amounts of Cl^- ions. Moreover, the rate of change of the solution conductivity is comparable with the rate of formation of Cl^-. Acetic, glycolic and formic acids and acetaldehyde were formed in the reaction although at low concentrations.

1. Introduction

Although there are several chemical water purification methods for organic pollutants, involving diverse process techniques (hydrolysis, oxidation, etc.), none of these processes is devoid of secondary pollution effects. For example, to remove pollutants present in low concentrations, a high concentration of reagent is necessary. A real difficulty arises in the elimination of numerous substances by appropriate chemical agents, owing to the low toxicity levels displayed (even fractions of ppb), since the conversion rate of a substrate at very low concentrations may be extremely small. Oxidation of aqueous pollutants is a widely used method. The oxidizing ability of the reagent, albeit high, may not be sufficient to eliminate the trace pollutant, as dictated by the Nernst equation relating the potential of a redox couple to the concentration ratio of the species involved. This difficulty might be overcome by choosing an oxidant that will oxidize not only the initial reduced substrate but also its oxidized form resulting from the first oxidation stage. The ·OH radical potential ranks among the highest available, its value being only lower than that of fluorine. Moreover, its reaction rates with organic compounds are very high (of the order of $10^9\ M^{-1}\ s^{-1}$) [1–6]. Table 1 lists the standard redox potentials of some oxidants.

The reaction with ·OH radical appears to be the major route for the oxidative degradation of organic compounds in many processes (atmospheric or ozone-promoted degradation, etc.) [7–12]. The reaction products are, generally, small oxygenated compounds that are easily biodegradable.

For a hydrocarbon, a viable conversion would

* Corresponding author.

0021-9673/95/$09.50
SSDI 0021-9673(95)00156-5

Table 1
Standard redox potentials of some oxidants

Species	$E°$ (V)
Fluorine	3.03
Hydroxyl radical	2.80
Atomic oxygen	2.42
Ozone	2.07
Hydrogen peroxide	1.78
Perhydroxyl radical	1.70
Hypobromous acid	1.59
Chlorine dioxide	1.57
Hypochlorous acid	1.49
Chlorine	1.36
Bromine	1.09
Iodine	0.54

be its complete mineralization to CO_2 and H_2O. By oxidation with superoxide anion, O_2^-, polyhalogenated aromatic hydrocarbons and chlorinated organic compounds are completely transformed to CO_2, H_2O and HX [13–16].

Oxidation with the 'Advanced Oxidation Process', H_2O_2–UV irradiation, is an attractive method for the oxidation of organic pollutant compounds in aqueous media: photolysis of H_2O_2 is one of the simplest ways to produce hydroxyl radicals (reaction 1).

In the present work we have studied the interaction of the radical ·OH with 2-chloroethanol in water. The substrate chosen can be taken as a model for the study of simplified reaction mechanisms thanks to its simple structure and its high solubility in water.

The data we have gathered may be of help in dealing with more complex mechanisms such as the interaction of ·OH with aromatic polycyclics, pesticides, etc. Hydrogen peroxide in diluted aqueous solution is known to produce ·OH radicals by photolysis under UV irradiation ($\lambda < 370$ nm) [3,6,10,17,18]:

$$H_2O_{2(aq)} \xrightarrow{h\nu} 2 \cdot OH_{(aq)} \quad (1)$$

At high light intensities the photolysis rate is proportional to I_{abs} and, thus, to the concentration of H_2O_2 ($I_{abs} \propto I_0\,[H_2O_2]$ where I_0 is the incident light intensity). At low intensities the photolysis rate is proportional to $(I_{abs})^{1/2} \cdot [H_2O_2]$. Under these conditions the rate is proportional to $[H_2O_2]^{1.5}$ [17].

Several reports have appeared on the use of ·OH to remove organic pollutants from aqueous solutions [1–5,12], and numerous methods for the kinetic study of these reactions have been described, involving electron paramagnetic resonance spectrometry, chromatographic techniques, etc. [1–5,10–12,19]. In order to measure the degradation rate of an organic compound we have devised a procedure that will allow a correlation between the changes in the organic substrate concentration and H_2O_2, Cl^- and the conductivity, as will be described in the following sections.

2. Experimental

2.1. Irradiation apparatus

The photolysis reactions were carried out in a glass apparatus of the type shown in Fig. 1 with a volume of 1825 ml equipped with a Helios Italquartz 13F 125-W high-pressure mercury vapour lamp with inner water cooling (emission radiation in the range 280–380 nm). The entire equipment (shielded with aluminium foil) was immersed in a thermostat at 25.0 ± 0.1°C. Measurements were carried out in 10-ml solution aliquots in order not to cause significant changes in the total volume and, hence, in the irradiation conditions of the solution.

2.2. Materials

All reagents were of analytical grade and used as received. Hydrogen peroxide solutions (Prolabo, 30% with 0.0005% sodium stannate as stabilizer) were used as received without further treatment. Titration with cerium sulphate indicated a 32% titre. Water was obtained from a Millipore deionizer and filtered on 0.2-μm cellulose filters.

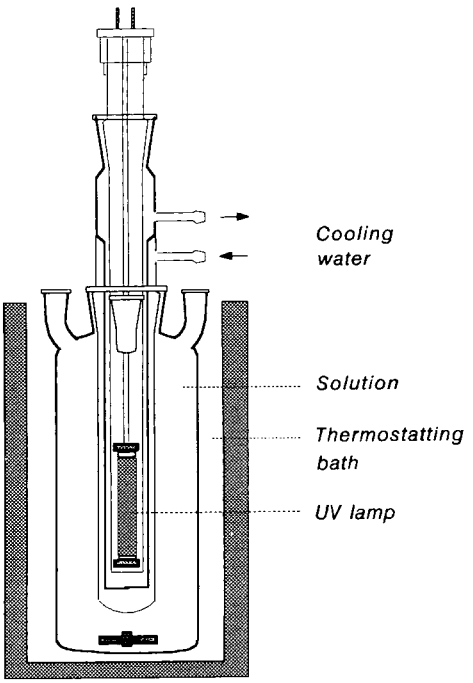

Fig. 1. Schematic drawing of the thermostatted photochemical reactor with magnetic stirrer.

2.3. Analyses

Hydrogen peroxide was determined photometrically by the neocuproine method [20]. 2-Chloroethanol was determined with a Hewlett-Packard 5890 gas chromatograph equipped with an HP-3392A integrator (FFAP-packed column; injection temperature, 200°C; flame ionization detector, 250°C; nitrogen gas carrier, 60 p.s.i.; oven temperature, 150°C).

Analysis of Cl^- and other reaction products was performed by ion chromatography (IC) with a Dionex DX 300 instrument (column, IonPac AS4A-SC, 250 × 4 mm; guard column, IonPac AG4A-SC, 50 × 4 mm; eluent, 5.0 m*M* $Na_2B_4O_7$; flow-rate, 2.0 ml/min; detection, conductivity). The aldehydes were analyzed by HPLC through conversion to their 2,4-dinitrophenylhydrazones (column, Erbasil S 5-C_{18}, 250 × 4 mm; eluent, acetonitrile–water; gradient: 35 to 85% acetonitrile in 12 min; detection, UV–visible (380 nm)). The conductivity of the solution during the irradiation was measured with a Radiometer CDM 83 conductimeter.

2.4. Procedure

In each run, 1825 ml of deaerated N_2-saturated aqueous solution of H_2O_2 and 2-chloroethanol at the appropriate concentrations were placed in the glass reactor. The water had been irradiated prior to the addition of the reactants. The solution was kept at 25.0 ± 0.1°C under a N_2 flux throughout the irradiation. Different H_2O_2–2-chloroethanol molar ratios (1:1, 1:2, etc.) were employed.

Kinetic runs were also carried out under the same experimental conditions with solutions containing H_2O_2 (10^{-3} *M*) or 2-chloroethanol (10^{-3} *M*) alone as reference blanks.

3. Results and discussion

When photolysis of H_2O_2 is carried out in the presence of 2-chloroethanol, the main chemical reactions of the organic compounds are:

organic compound + ·OH → products

organic compound + $h\nu$ → products

The extent of degradation of 2-chloroethanol by UV irradiation in the absence of H_2O_2 is about 6% after 1 h (Fig. 2).

Reaction of ·OH with chlorinated organic compounds affords mainly hydrogen abstraction. Halogen abstraction by ·OH is thermodynamically unfavoured [1,2]. Interaction of 2-chloroethanol with ·OH radicals is believed to yield mainly two different organic radicals:

$$ClCH_2CH_2OH \xrightarrow[-H_2O]{\cdot OH} \underset{\mathbf{a}}{ClC\dot{H}CH_2OH} + \underset{\mathbf{b}}{ClCH_2\dot{C}HOH} \quad (2)$$

Radicals **a** and **b** undergo fast conversion with formation of Cl^- ions and several degradation products. Globally:

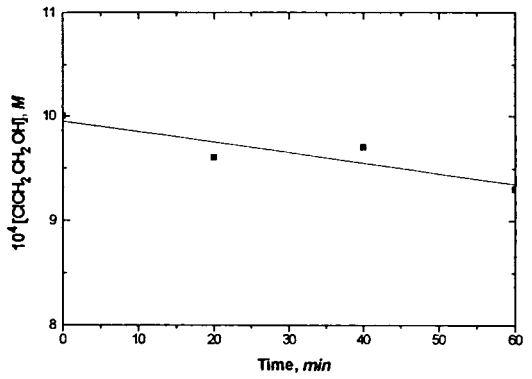

Fig. 2. Degradation of 10^{-3} M 2-chloroethanol by UV irradiation in the absence of H_2O_2.

$$H_2O_2 \xrightarrow[\text{slow, } k_1]{h\nu} 2 \cdot OH$$

$$\cdot OH + ClCH_2CH_2OH \xrightarrow{\text{fast}} \text{oxidation products} + Cl^-$$

Scheme 1

The oxidative degradation of 2-chloroethanol was followed by monitoring the disappearance rate of H_2O_2 and of the organic substrate along with the formation rate of chloride ion and the companion changes in electric conductivity of the solution. Fig. 3 shows the ion chromatogram versus time, indicating the steady increase of Cl^-.

Under our experimental conditions the rate of consumption of H_2O_2 has been found to be first order in H_2O_2:

$$-d[H_2O_2]/dt = k_1[H_2O_2]$$

which reveals in a monoexponential rate law

$$A_t = A_\infty + (A_0 - A)\exp(-k_1 t)$$

where A is a physicochemical property with a value proportional to the extent of reaction ([2-chloroethanol], $[Cl^-]$, $[H_2O_2]$ or conductivity). This corresponds to the monomolecular rate-determining splitting of H_2O_2 into $\cdot OH$ radicals under irradiation, followed by fast reaction of

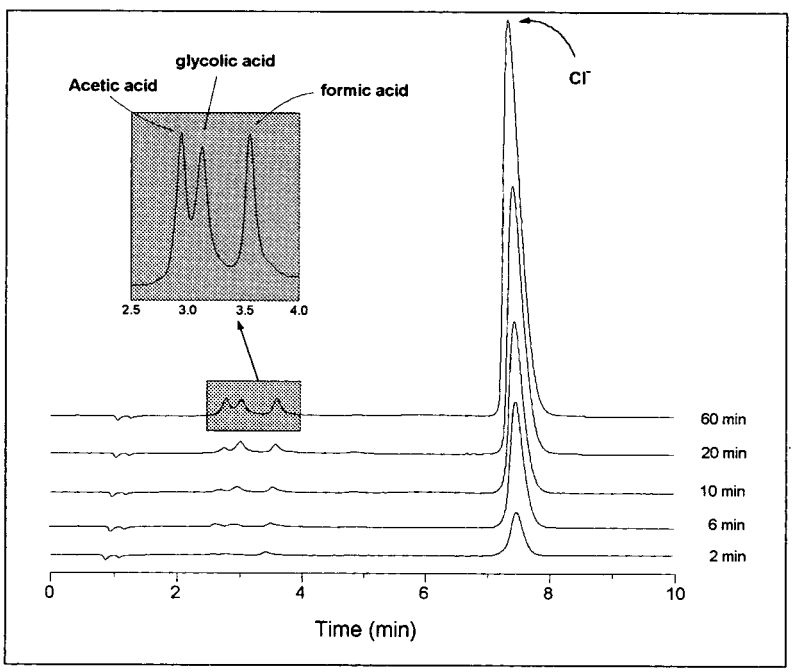

Fig. 3. Ion chromatogram versus time indicating the steady increase of Cl^-, and the appearance of traces of organic acids ($[ClCH_2CH_2OH]/[H_2O_2]$ molar ratio = 1).

Table 2
Rate parameters observed for the reaction between H_2O_2 and $ClCH_2CH_2OH$ under UV irradiation under N_2 at 25°C

$[ClCH_2CH_2OH]$ (10^3 M)	$[H_2O_2]$ (10^3 M)	$10^4 k^a_{(H_2O_2)}$ (s^{-1})	$10^4 k^b_{(ClCH_2CH_2OH)}$ (s^{-1})	$10^4 k^c_{(Cl^-)}$ (s^{-1})	$10^4 k^d_{(conductivity)}$ (s^{-1})
0	1	7.8 ± 0.5	–	–	–
1	1	4.0 ± 0.8	8.1 ± 0.5	8.0 ± 0.3	7.8 ± 0.2
1	0.5	3.5 ± 0.8	8.0 ± 0.8	7.3 ± 0.8	6.7 ± 0.1
5	1.0	3.0 ± 0.3	7.7 ± 0.8	4.7 ± 0.2	4.8 ± 0.2
50	1.0	2.8 ± 0.6	–[e]	3.2 ± 0.2	2.0 ± 0.3

[a] First-order rate constants for the consumption of H_2O_2.
[b] First-order rate constants for the disappearance of $ClCH_2CH_2OH$.
[c] First-order rate constants for the appearance of Cl^-.
[d] First-order rate constants for the increase in conductivity.
[e] Value omitted for the not significantly variation of $[ClCH_2CH_2OH]$.

radicals with the chlorinated substrate leading to its degradation products and Cl^- (Scheme 1).

Rate data in Table 2 indicate that with a $[ClCH_2CH_2OH]/[H_2O_2]$ molar ratio of 1, the disappearance rate of 2-chloroethanol, the formation rate of Cl^- and the conductivity increase rate are about twice the rate of H_2O_2 consumption. The experimental data for such molar ratios are reported in Fig. 4.

Fig. 4a shows the monoexponential decrease of organic substrate with time, the companion increase in $[Cl^-]$ and their sum.

Fig. 4b shows the relationship between increasing $[Cl^-]$ and increasing specific conductivity of the reaction solution. It appears that the latter arises virtually from Cl^- (as HCl), the contribution from other conducting species (such as weak, undissociated organic acids) being probably negligible. The data in Table 2 are in agreement with the simple mechanism in Scheme 1, in which the slow decomposition of H_2O_2 is followed by rapid degradation of the chlorinated substrate with formation of the conducting chloride ion. On increasing the 2-chloroethanol/hydrogen peroxide molar ratio, the rate of disappearance of 2-chloroethanol is virtually unchanged while that of appearance of chloride decreases. It is likely that other, more complex mechanisms become operative under these conditions, although we are not in a position to suggest any based on the presently available data.

The existence of radical **a** has been proved, whereas radical **b** could only hypothesized [19]. As a matter of fact, radical **b**, once formed, decomposes rapidly, leading to radical **c** and then Cl^- (Scheme 2).

Interaction of 2-chloroethanol with **c** would

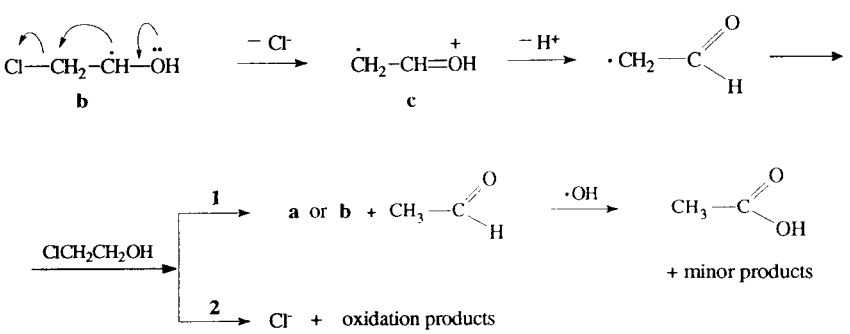

Scheme 2

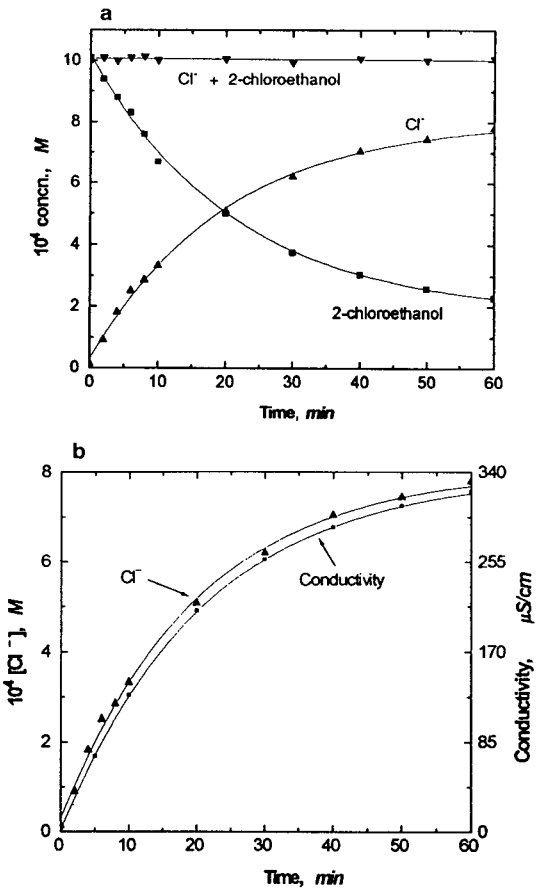

Fig. 4. Experimental data for $[ClCH_2CH_2OH]/[H_2O_2]$ molar ratio of 1. (a) Monoexponential changes with time of $[ClCH_2CH_2OH]$, $[Cl^-]$, and their sum. (b) Relationship between the increase of $[Cl^-]$ and the increase of conductivity of the reaction solution.

produce Cl^-, acetaldehyde and its oxidation products (acetic, formic, glycolic acids, etc.), according to paths 1 and 2 (Scheme 2). Path 1 appears to be less favoured. In fact the acetaldehyde intermediate is expected to be easily oxidized to acetic acid. As a matter of fact the concentration of C-2 carboxylic acids was found to be quite low. In a typical run, after 1 h only $2 \cdot 10^{-3}$ mmol/l CH_3CHO and $6 \cdot 10^{-2}$ mmol/l CH_3COOH corresponding to ca. 6% of total carbon were obtained. The following other oxidation products were detected, albeit at low concentrations: HCOOH ($7 \cdot 10^{-2}$ mmol/l), $HOCH_2COOH$ ($2 \cdot 10^{-2}$ mmol/l). To confirm the suggested mechanism, we studied the behaviour of acetaldehyde (10^{-3} *M*) under the same conditions (H_2O_2 10^{-3} *M*, UV irradiation). The acetaldehyde was easily oxidized; after 60 min, ca. $5 \cdot 10^{-4}$ mol/l of CH_3COOH were formed, corresponding to 50% of total carbon. Further Cl^- may arise from the intermediate **a** (Scheme 3).

Reactions of radicals **a** or **b** with $\cdot OH$ are ruled out. The rate constant for the decomposition of H_2O_2 (k_1) was measured at different H_2O_2 and initial substrate concentrations (Table 2). As can be seen, the presence of 2-chloroethanol causes a marked decrease in the rate of H_2O_2 consumption (k_1 for H_2O_2 alone $= 7.8 \cdot 10^{-4}$ s^{-1}). It appears that partial reformation of H_2O_2 may be due to reactions of the type suggested by Baxendale and Wilson [21].

4. Conclusions

As shown by Fig. 4a, there is a reverse relationship between the disappearance of 2-chloroethanol and the formation of Cl^-. In fact, the sum $[ClCH_2CH_2OH] + [Cl^-]$ remains constant throughout the irradiation. Accordingly,

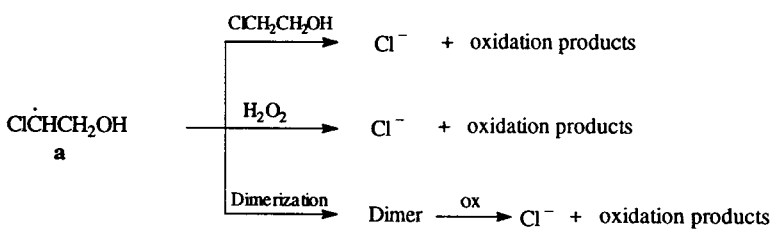

Scheme 3

two interesting observations are possible: (i) the degradation rate of 2-chloroethanol can be followed by monitoring the Cl^- ion; (ii) no significant concentrations of chlorinated compounds are formed.

In this work, simple techniques have been devised, involving both HPIC and electric conductivity, which allow the kinetics of a degradation reaction to be easily followed while monitoring at the same time the fate of the halogenated organic substrate.

References

[1] M. Anbar and P. Neta, *J. Chem. Soc. (A)*, (1967) 834.
[2] M. Anbar, D. Meyerstein and P. Neta, *J. Chem. Soc. (B)*, (1966) 742.
[3] T. Mill and C.W. Gould, *Environ. Sci. Technol.*, 13 (1979) 205.
[4] N. Getoff, *Appl. Radiat. Isot.*, 37 (1986) 1103.
[5] M.N. Schuchmann, H.-P. Schuchmann and C. von Sonntag, *J. Am. Chem. Soc.*, 112 (1990) 403.
[6] R.G. Zepp, B.C. Faust and J. Hoigné, *Environ. Sci. Technol.*, 26 (1992) 313.
[7] G.R. Peyton, F.Y. Huang, J.L. Burleson and H.W. Glaze, *Environ. Sci. Technol.*, 16 (1982) 448.
[8] J. Staehelin and J. Holiné, *Environ. Sci. Technol.*, 16 (1982) 676.
[9] L. Forni, D. Bahnemann and E. Hart, *J. Phys. Chem.*, 86 (1982) 255.
[10] W.L. Dilling, S.J. Gonslor, G.U. Boggs and C.G. Mendoza, *Environ. Sci. Technol.*, 22 (1988) 1447.
[11] J. Kochany and J.R. Bolton, *J. Phys. Chem.*, 95 (1991) 5116.
[12] J. Kochany and J.R. Bolton, *Environ. Sci. Technol.*, 26 (1992) 262.
[13] H. Sugimoto, S. Matsumoto and D.T. Sawyer, *Environ. Sci. Technol.*, 22 (1988) 1182.
[14] F.W. Karasek and L.C. Dickson, *Science*, 237 (1987) 754.
[15] H. Sugimoto, S. Matsumoto and D.T. Sawyer, *J. Am. Chem. Soc.*, 109 (1987) 8081.
[16] T. Nguyen and D.F. Ollis, *J. Phys. Chem.*, 88 (1984) 3386.
[17] D.E. Lea, *Trans. Faraday Soc.*, 45 (1949) 81.
[18] O. Legrini, E. Oliveros and A.M.Braun, *Chem. Rev.*, 93 (1993) 671.
[19] B.C. Gilbert, J.P. Larkin and R.O.C. Norman, *J. Chem. Soc. Perkin II*, (1972) 794.
[20] A.N. Baga, G.R. Alastair Johnson, N.B. Nazhat and R.A. Saadalla-Nazhat, *Anal. Chim. Acta*, 204 (1988) 349.
[21] J.H. Baxendale and J.A. Wilson, *Trans. Faraday Soc.*, 53 (1957) 344.

ELSEVIER

Journal of Chromatography A, 706 (1995) 353–359

JOURNAL OF CHROMATOGRAPHY A

Contribution of high-performance liquid chromatographic analysis of carbohydrates to authenticity testing of honey

I. Goodall[a,*,1], M.J. Dennis[b], I. Parker[b], M. Sharman[b]

[a]*University of East Anglia, School of Chemical Sciences, Norwich, NR4 7TJ, UK*

[b]*CSL Food Science Laboratory, Norwich Research Park, Colney Lane, Norwich, NR4 7UQ, UK*

Abstract

A high-performance anion-exchange liquid chromatography method with pulsed amperometric detection was developed to investigate the oligosaccharide composition of honey. Quantification was achieved by reference to a maltotetraose internal standard. The oligosaccharide profiles of 91 authentic UK honey samples were obtained and multivariate statistical techniques employed to investigate whether these profiles could be used as a basis for identification of flower source. Canonical Discriminant Analysis proved most successful. Results indicated that honey oligosaccharide profiles have a potentially valuable role to play in the assessment of floral origin of honey though it is unlikely that this procedure alone will allow unambiguous determination of all floral types.

1. Introduction

In the UK the regulatory provisions regarding the composition and labelling of honey are contained in the Honey Regulations 1976 (1976/1832) and the Food Labelling Regulations 1980 Amendment (1980/1849). Honey Regulations 1976 (1976/1832) implement Council Directive 74/409/EEC which sets honey composition criteria, defining a number of parameters including minimum reducing sugar content and maximum moisture, sucrose and water-insoluble solids content. The UK regulatory provisions also account for misrepresentative labelling of honey origin and state: (i) If a type of blossom or plant is indicated, the honey must be wholly or mainly from that source; (ii) If a name of a country, etc. is indicated, the honey must originate wholly from that place.

Hence, the blending of honeys from different floral or geographical origins is permitted in the UK, so long as the labelling does not claim that the honey is from a single source. Since single flower honeys or honeys from a specific geographical origin command premium prices there may be an economic incentive to misrepresent the source of a honey.

The detection of misrepresentative honey labelling has been carried out in the past using melissopalynology [1–4] (pollen analysis), but this technique requires a high level of expertise and is very time consuming. Other techniques have been applied. Determination of geographical origin has been attempted on the basis of free amino acid content [5–8] and chemical composition [9,10], with varying degrees of success. Determination of floral origin has received less attention, although identification on the basis of

* Corresponding author.

[1] Present address: CSL Food Science Laboratory, Norwich Research Park, Colney Lane, Norwich, NR4 7UQ, UK.

SSDI 0021-9673(94)01074-9

chemical composition [11,12] has shown potential.

In 1988, Swallow and Low [13] published a paper on the analysis and quantification of the carbohydrates in honey. This method employed high-performance anion-exchange liquid chromatography (HPAE) with pulsed amperometric detection (PAD) [14–19]. It was observed that oligosaccharide profiles appeared to be characteristic of floral source. Hence, they could potentially act as "fingerprints" for floral origin identification. This paper details the development of a new method, based on that employed by Swallow and Low, to determine the floral authenticity of honey.

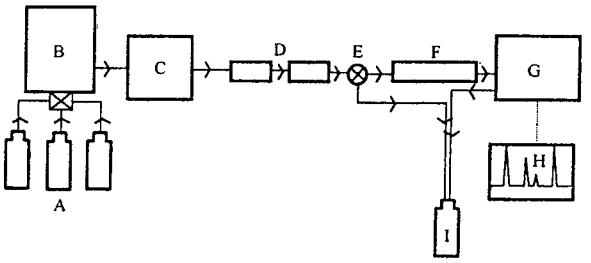

Fig. 1. HPAE–PAD schematic layout. The arrows represent the mobile phase flow path, (A) solvents leading to proportioning valve, (B) Waters 625 LC system and pump, (C) Gilson 231 XL autosampler fitted with a 20-μl injection loop, (D) two Dionex PA1 guard columns (50 × 4.6 mm), (E) Universal valve switching module fitted with a Tefzel rotor seal, (F) Dionex PA100 column (250 × 4.6 mm), (G) Waters 464 electrochemical detector, (H) Waters Millennium 2010 chromatography manager, (I) waste.

2. Experimental

2.1. Instrumentation

The HPAE apparatus comprised of a Waters 625 LC system (Milford, MA, USA), a Gilson 231 XL autosampler (Middleton, WI, USA) fitted with a 20-μl injection loop and a Universal Valve Switching Module (UVSM) fitted with a Tefzel (base resistant) rotor seal which was supplied by Anachem (Luton, Bedfordshire, UK). Separation of the oligosaccharides took place on two Dionex PA1 guard columns (50 × 4.6 mm) and a Dionex PA100 column (250 × 4.6 mm) (Sunnyvale, CA, USA). Detection was carried out by a Waters 464 electrochemical detector, operated in pulse mode, employing a stainless steel cell, a single gold working electrode, and a base resistant reference electrode. The data collection system was a Waters Millennium 2010 Chromatography Manager. Fig. 1 shows a schematic diagram of the apparatus layout.

2.2. Chemicals

Sodium hydroxide solution (46–48%), analytical reagent grade, was purchased from Fisons Scientific Equipment (Loughborough, Leicestershire, UK). Sodium acetate 3-hydrate, HPLC grade, was purchased from Merck (Lutterworth, Leicestershire, UK). Maltotetraose, HPLC grade, was from Sigma (Poole, Dorset, UK). Anion-exchange resin, AG 1-X8 100–200 mesh formate form, was from Bio-Rad (Richmond, CA, USA). Water was purified using a Milli-Q water purification system (Millipore, Milford, MA, USA). 0.22-μm filters were from Millipore.

2.3. Samples

Samples were obtained from various hive sites in the UK during 1992. Standard pollen analysis techniques were employed to determine the floral pollen percentages present in each honey sample. 600 Pollen grains per sample were analysed to obtain this data. The conversion from pollen percentages to floral nectar percentages was achieved by the use of pollen coefficients which take into account the over or under representation of pollen from a particular nectar source in the honey. The data referring to the floral nectar percentages was used to determine the description of the honey sample in terms of floral origin and purity. Unifloral samples were classified as those where one flower type constituted more than 50% of the nectar source.

The variety of unifloral samples was limited by the collection scheme. Six distinct unifloral types were provided by 91 samples. These were: bramble (70 samples), ling [heather] (5 samples), oil

seed rape (8 samples), white clover (5 samples), hawthorn (2 samples), willow-herb (1 sample).

2.4. Method

Sample preparation

Amounts of 0.80 (±0.15) g of each honey sample were dissolved in water. Then 400 μl of a 20 mg/ml aqueous maltotetraose (internal standard) solution was added before making up to 20 ml in a volumetric flask with water. The sample solution was cleaned-up by passing it through 8 ml of anion-exchange resin loaded as a water slurry into a disposable 10-ml plastic syringe plugged with glass wool. The sample solution was not collected until a viscosity change was observed as droplets from the syringe entered a container. Once this change had been observed ≈3 ml were allowed to pass through the resin into a measuring cylinder prior to the collection of the remaining eluent. Each solution was filtered (0.22 μm) before chromatographic analysis.

Enzymes in the honey sample solutions were shown to reduce the concentration of the added maltotetraose internal standard over a period of time. By keeping the time between the addition of internal standard to the honey sample solutions and the clean-up stage to below 15 min any enzyme effect was made negligible.

Preparation of eluents

Three solutions were employed in a gradient elution program, 0.1 *M* sodium hydroxide, 0.1 *M* sodium hydroxide–0.1 *M* sodium acetate 3-hydrate and 0.3 *M* sodium hydroxide. Sodium hydroxide solutions were prepared by diluting known weights of 46–48% sodium hydroxide. All weights were accurate to within 0.01 g. 46–48% sodium hydroxide solution is used for mobile phase preparation because it is low in sodium carbonate (<0.1%) which can cause variations in chromatographic retention times by competing with the carbohydrates for stationary phase sites. Mobile phase solutions were prepared as quickly as possible to minimise any absorption of carbon dioxide from the atmosphere and sparged for at least 20 min with helium (100 ml/min) before use.

Chromatographic conditions

The injection volume of sample solution was 20 μl. The composition and flow-rate of the mobile phase throughout each HPAE sample analysis is detailed in Table 1. For the first 3 min after sample injection the eluent flow passes through the guard columns and is diverted to waste by the switching valve. For the remainder of the run the eluent passes from the switching valve to the PA100 column. The two PA1 guards provided sufficient retention of the oligosaccha-

Table 1
HPAE gradient system for the separation of honey oligosaccharides

Line	Time after injection (min)	Flow (ml/min)	%A 0.1 *M* sodium hydroxide	%B 0.1 *M* sodium hydroxide and 0.1 *M* sodium acetate	%C 0.3 *M* sodium hydroxide
1	0.0	0.75	100	0	0
2	10.0	0.75	100	0	0
3	45.0	0.75	0	100	0
4	46.0	0.75	0	100	0
5	47.5	1.50	0	0	100
6	55.5	1.50	0	0	100
7	57.0	1.50	100	0	0
8	65.0	1.50	100	0	0
9	70.0	0.75	100	0	0
10	75.0	0.75	100	0	0

Mobile phase composition and flow-rate changes between adjacent lines were linear with respect to time.

Table 2
Pulsed amperometric detection program

Pulse potential (mV)	Duration (s)	Comments
E^a	0.2	Measurement pulse
$E + 650$	0.2	Cleaning pulse
$E - 650$	0.5	Conditioning pulse

[a] The definition of E is given in the text.

rides such that >95% of the high concentration monosaccharides (glucose and fructose) could be sent to waste whilst the oligosaccharides were retained. The remaining monosaccharides and oligosaccharides could then be separated on the PA100 column without any overloading. The column switching technique also reduced any column and detector deterioration. All oligosaccharides are eluted within 45 min. Column washing and re-equilibration extends the run time to 75 min.

Pulsed amperometric detection

The electrochemical detector was operated in pulsed mode, using the three pulse repeated cycle given in Table 2. E, the optimum measurement potential [20], was determined by use of a cyclic voltammogram (CV). When running a CV the pulsed electrochemical detector was operated in the scan mode and the current and electrode potential responses were monitored whilst eluent (0.1 M sodium hydroxide, 0.75 ml/min) was passed through the electrode cell. The electrode potential was cyclically varied from −700 mV to 700 mV and back to −700 mV at a rate of 10 mV/s. As the potential became more negative a peak in the current response was observed, corresponding to the reduction of gold oxide formed on the electrode. The potential corresponding to this peak was E.

Data analysis

Up to 40 characteristic oligosaccharide peaks (see Fig. 2) were identified in each of the honey samples according to retention time. The peak heights of these oligosaccharides were measured for each sample and ratioed to the peak height of the internal standard, maltotetraose, eluted at approximately 45 min. Peak height measurement was performed by the Millennium 2010 Chromatography Manager. SPSS 5.0 for Windows (SPSS, Chicago, IL, USA) was used to perform multivariate statistical analysis on the peak height ratios.

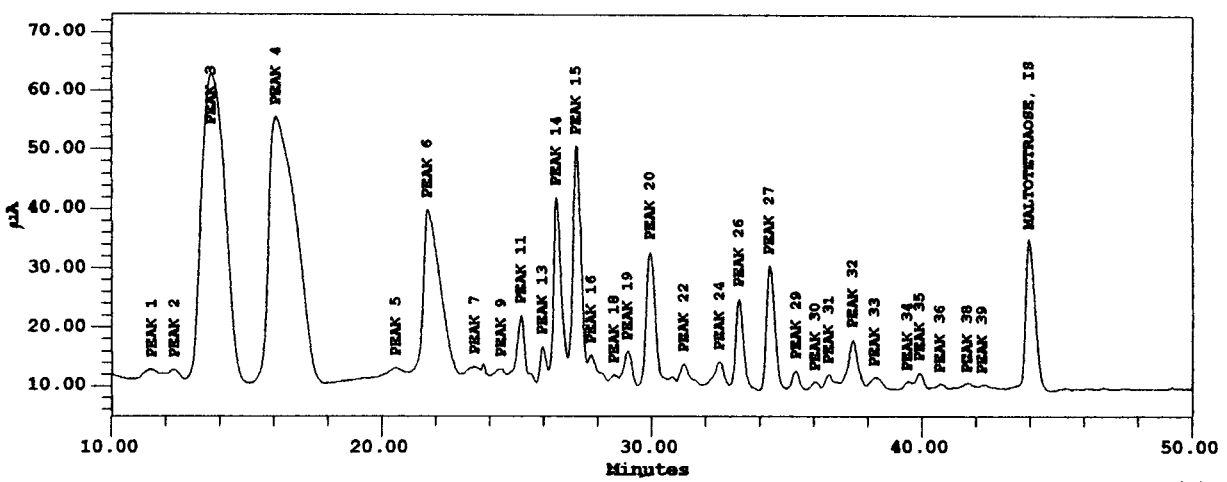

Fig. 2. A typical honey chromatogram with a number of labelled peaks. Standard compounds were not available for many of the oligosaccharides of interest so all peaks were quantified against a maltotetraose internal standard. Maltotetraose elutes in a clear area of the chromatogram at approximately 45 min.

3. Results

All 40 measured oligosaccharide peak height ratios for the honey samples were employed in the multivariate statistical analyses. Hierarchical Cluster Analysis (HCA), Principal Component Analysis (PCA) and Canonical Discriminant Analysis (CDA) were all evaluated for their ability to identify unifloral honeys. The success of the statistical analyses was judged against the floral classification by melissopalynology. PCA and HCA both identified an outlier bramble sample and this was removed from the data set. The use of CDA proved most valuable in differentiating the sample groups.

Canonical Discriminant Analysis (CDA) was used to find functions based on the peak height ratios which maximised separation between honey types. Fig. 3 shows how the analysis has split the six unifloral groups. The ling samples have been completely isolated from the remaining samples using CDA. Similarly the oil seed rape samples show a good separation from the rest of the honey samples. Whilst hawthorn and willow samples appear separated from the other samples, the number of determinations for these samples would have to be increased before any statistical conclusions are drawn. It appears that the white clover samples cannot be separated from bramble.

In CDA, sample classification into floral group can be performed by the software by application of Fisher's classification coefficients [21]. In order to test the discrimination functions, the analysis was repeated omitting one of the ling/oil seed rape/bramble/white clover samples at a time, then classifying this "unknown" with respect to floral origin. 100% of the ling samples were classified correctly. 62.5% of the oil seed rape samples were classified correctly. 70% of the bramble samples were classified correctly. None of the white clover samples were classified correctly.

The white clover samples were all misclassified as bramble. The three misclassified oil seed rape samples were all classified as bramble. In two cases (samples A and B, see Fig. 3) this can be explained by the quantity of bramble in the sample (sample A was 21% bramble; sample B was 25% bramble) and it can be concluded that a

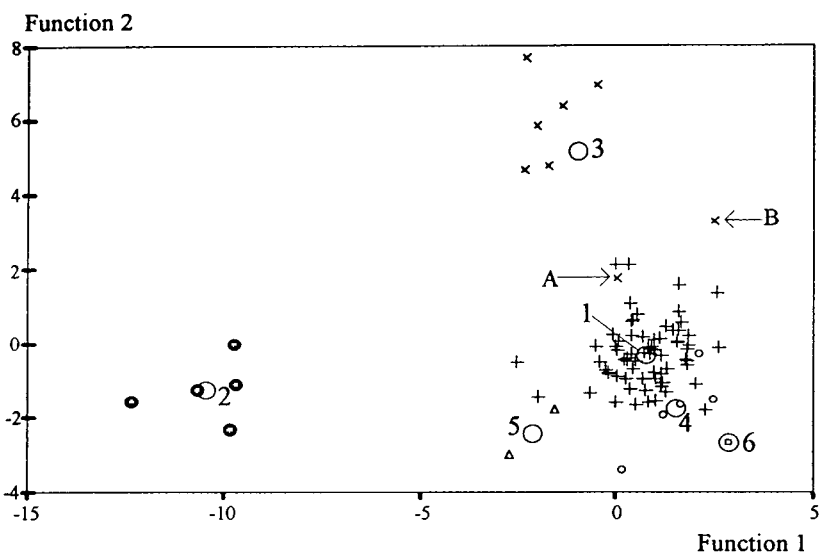

Fig. 3. Separation of the six unifloral honey groups using Canonical Discriminant Analysis. (Numbered ○) Group centroids; (+) Group 1: Bramble, 69 samples; (●) Group 2: Ling, 5 samples; (x) Group 3: Oil seed rape, 8 samples; (○) Group 4: White clover, 5 samples; (△) Group 5: Hawthorn, 2 samples; (□) Group 6: Willow-herb, 1 sample. Samples A and B are referred to in the text.

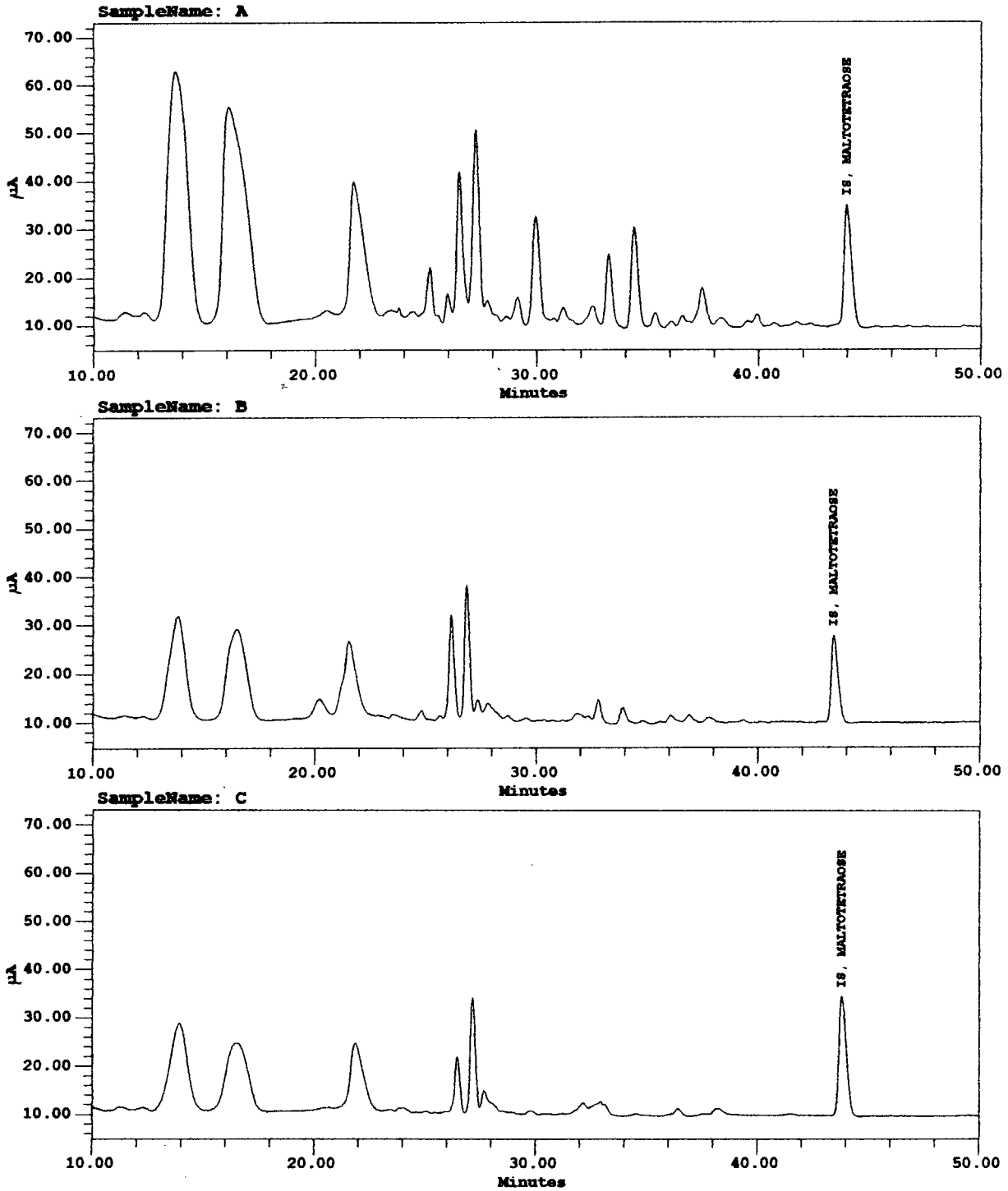

Fig. 4. Oligosaccharide profiles of three typical unifloral honeys: (A) bramble, (B) ling and (C) oil seed rape.

small bramble component has a significant effect on the oligosaccharide profile. For the third sample the reasons for the misclassification are unclear, but may be due to the small data set. The successful classification of five oil seed rape honeys demonstrates that there is a definite region within which a honey can be correctly classified as oil seed rape.

The 100% success rate in classifying the ling samples demonstrates the ability of the derived discriminant functions in differentiating between ling and other floral honeys. Fig. 4 consists of three chromatograms illustrating a typical bramble, a typical ling and a typical oil seed rape sample. These chromatographic patterns are highly repeatable for the ling and rape samples although more variable for the bramble.

4. Conclusions

The high classification rate for ling, bramble and rape samples shows that oligosaccharide profiles are a potentially valuable tool in floral identification. Analysis is quicker than melissopalynology (which can account for at least a day's work in the laboratory per sample) and requires less expertise. It may also be anticipated that the method will be unaffected by filtration during honey processing which can result in the loss of pollen. The misclassification of clover, however, shows the method is not applicable to all floral types.

While the floral species identification is limited at present, a more comprehensive database of unifloral samples may improve the statistical separations seen so far. A possible extension of the technique could be its application to the determination of geographical origin, which is difficult to ascertain by melissopalynology since some floral species which were once native to particular countries are now widespread throughout the world.

Acknowledgements

The authors thank Peter Roberts and the University of Aberystwyth for collecting the honey samples and performing the melissopalynology.

References

[1] R.W. Sawyer, *J. Assoc. Pub. Anal.*, 13 (1975) 64.
[2] J. Louveaux, A. Maurizio and G. Vorwohl, *Bee World*, 51(3) (1970) 125.
[3] J. Louveaux, A. Maurizio and G. Vorwohl, *Bee World*, 59(4) (1979) 139.
[4] N.H. Low, C. Schweger and P. Sporns, *J. Apic. Res.*, 28(1) (1989) 50.
[5] A.M.C. Davies, *J. Apic. Res.*, 14(1) (1975) 29.
[6] A.M.C. Davies, *J. Food Sci. Technol.*, 11 (1989) 515.
[7] J. Gilbert, M.J. Shephard, M.A. Wallwork and R.G. Harris, *J. Apic. Res.*, 20(2) (1981) 125.
[8] A.M.C. Davies and R.G. Harris, *J. Apic. Res.*, 21(3) (1982) 168.
[9] M.T. Sancho, S. Muniategui, J.F. Huidobro and J. Simal-Lozano, *J. Apic. Res.*, 30(3/4) (1991) 168.
[10] R.P. Crecente and C.H. Latorre, *J. Agric. Food Chem.*, 41 (1993) 560.
[11] A. Krauze and R.I. Zalewski, *Z. Lebensm. Unters. Forsch.*, 192 (1991) 19.
[12] R.I. Zalewski, *Food Qual. Pref.*, 3 (1991/2) 223.
[13] K.W. Swallow and N.H. Low, *J. Agric. Food Chem.*, 38 (1988) 1828.
[14] R.D. Rocklin and C.A. Pohl, *J. Liq. Chromatogr.*, 6(9) (1983) 1577.
[15] R.R. Townsend, M.R. Hardy, O. Hindsgaul and Y.C. Lee, *Anal. Biochem.*, 174 (1988) 459.
[16] M.R. Hardy and R.R. Townsend, *Proc. Natl. Acad. Sci.*, 85 (1988) 3289.
[17] K.W. Swallow, N.H. Low and D.R. Petrus, *J. Assoc. Off. Anal. Chem.*, 74(2) (1991) 341.
[18] N.H. Low and G.G. Wudrich, *J. Agric. Food Chem.*, 41 (1993) 902.
[19] K.W. Swallow and N.H. Low, *J. Assoc. Off. Anal. Chem.*, 77(3) (1994) 695.
[20] R.W. Andrews and R.M. King, *Anal. Chem.*, 62 (1990) 2130.
[21] R.A. Fisher, *Annals of Eugenics*, 7 (1936) 179.

ELSEVIER

Journal of Chromatography A, 706 (1995) 361–373

JOURNAL OF CHROMATOGRAPHY A

Determination of monomeric sugar and carboxylic acids by ion-exclusion chromatography

Klaus Fischer[b,*], Hans-Peter Bipp[a], Dieter Bieniek[a], Antonius Kettrup[b]

[a]*Institut für Ökologische Chemie, GSF-Forschungszentrum, Ingolstädter Landstrasse 1, D-85764 Oberschleißheim, Germany*

[b]*Lehrstuhl für Ökologische Chemie, TU München, D-85350 Freising-Weihenstephan, Germany*

Abstract

The influence of the temperature and the eluent (proton) concentration on the retention and separation of thirty organic compounds, including sugar acids, lactones, hydroxy acids, mono acids and dicarboxylic acids, on the Merck cation- exchange column Polyspher OA-HY was studied by applying ion-exchange chromatographic methods and HPLC instrumentation. The different responses of the various groups of compounds to changes of the chromatographic parameters were used to select the optimized separation conditions. A combination of two parameter sets (I: temperature of 45°C, sulphuric acid eluent concentration of 0.01 *N*, flow-rate of 0.5 ml min^{-1}; II: 10°C, 0.1 *N* H_2SO_4, same flow-rate) was found to enhance the chromatographic versatility and substance identification. Five-point linear calibrations were conducted under both conditions, and the respective relative standard deviations, mean percentage errors and detection limits were determined.

1. Introduction

Many scientific disciplines are in need of analytical methods for the accurate, sensitive and fast determination of sugar acids in various types of samples. Subject areas involved in sugar acid analysis are for instance phytochemistry, phytopathology, clinical chemistry, microbiology, and food and beverage engineering. New areas of application are coming up in the field of environmental technologies. Organic residues, derived from agriculture and food engineering, are under investigation for their potential to serve as sources of chelating agents able to remove heavy metals from polluted materials. Sugar acids are known to be effective chelators under alkaline pH conditions [1,2]. They are easily obtainable from the oxidation of carbohydrate-rich residues (molasses, potato peel sludge, wine yeast, whey powder) by nitric acid [3].

The different sample types reflect the various research topics leading to the analysis of sugar acids. For instance, under investigation are liquors from sugar processing [4–6], culture media of bacteria [7,8], fermentation broths [9], plant materials [10,11], beverages [11–13], degradation products of acidic polysaccharides [7,11], products of catalytic sugar oxidation [14,15] and alkaline sugar degradation [16].

Besides colorimetric analysis, enzymatic determination, thin-layer and gas–liquid chromatography, several techniques of liquid chromatography have gained importance in sugar acid analysis.

* Corresponding author.

0021-9673/95/$09.50
SSDI 0021-9673(94)01220-2

Whereas the application of anion-exchange resins under various pressure conditions was dominant in the sixties and seventies (a brief overview is given in Ref. [7]), an increasing preference for ion-exclusion techniques started with the availability of small-size, pressure-durable, pH-stable polymer-based materials. Frequently, the ion-exclusion chromatographic separation of organic acids is performed on strong cation exchangers such as sulphonated polystyrene–divinylbenzene (PSDVB) polymers. The Donnan exclusion effect, caused by the ionic repulsion between the negatively charged resin and the more or less negatively charged analytes, is the main separation principle. Under separation conditions allowing the analytes to deprotonate to a certain degree, the pK_a values of the acids and the proton concentration in the mobile phase are deciding factors for the separation process. Further influences on the partition behaviour of organic acids can be derived from size-exclusion effects, hydrophobic (reversed-phase) interactions and Van der Waals forces. In general, the influence of these secondary factors on the separation process increases with decreasing water solubilities, increasing pK_a values, molecular sizes and polarizabilities of the analytes and increasing proton concentration of the mobile phase. Because size-exclusion effects and Van der Waals forces contribute to the chromatographic behaviour of sugar acids, it can be expected that the exchange capacity of a certain resin and the physical (resin structure, degree of cross-linking) and chemical (presence of further polarizable functional groups) properties of the ion exchanger affect the chromatographic performance.

Ion-exclusion chromatographic separations of sugar acids have been conducted with Aminex or BioRad HPX-87H columns mainly, using sulphuric acid as eluent and UV or RI detection [4–7,9,10,17]. The HPX-87H column (300 × 7.8 mm I.D.) is packed with 9-μm spherical, sulphonated PSDVB beads with 8% cross-linking, providing an ion-exchange capacity of 1.7 mmol g^{-1}.

The Merck (Darmstadt, Germany) Polyspher OA-HY cation-exchange column, identical to the Interaction (Mountain View, CA, USA) ORH-801 column according to the information of the company, contains a similar bed material. The ion exchanger (Merck 46-67A resin, identical to the Interaction IC 8101-8) consists of 8-μm spherical, sulphonated PSDVB beads with 8% cross-linking. The ion-exchange capacity is not noted [18]. Although this column is widely used for organic acid analysis [19], no investigations have been published on the applicability and performance of the column in sugar acid determination. We have therefore made some efforts to close this information gap and to extend the already existing experience in sugar acid analysis. Besides questions of the retention behaviour of these compounds, aspects of obtainable determination sensitivity and accurate quantification are in the foreground of the study. Because the practical aspects of this study are orientated towards the analysis of products formed during the acidic oxidation of carbohydrate-rich residues, several aliphatic mono- and polyfunctional carboxylic acids were additionally included in the investigation.

2. Experimental

2.1. Materials

All materials were of puriss. or p.A. quality (purity >99%) unless stated otherwise. Some lactones were studied both in their original chemical forms and as acids after saponification with equivalent amounts of diluted sodium hydroxide (Merck, p.A.) solution (pH kept between 8.0 and 9.0 until complete saponification had occurred).

Glycolic acid, L-threonic acid (hemi-Ca salt, >97%), D-glyceric acid (hemi-Ca salt, monohydrate, >98%), D-erythrono-1,4-lactone, D-ribono-1,4-lactone, D-galactono-1,4-lactone (purum), malonic acid, glutaric acid (98%), L-lactic acid (40% solution in water, purum), *n*-propionic acid, 5-keto-D-gluconic acid (K salt, monohydrate), sorbic acid (>98%), D-quinic acid (<98%), 2-keto-glutaric acid and adipic

acid were purchased from Fluka (Buchs, Switzerland). Oxalic acid dihydrate, glyoxylic acid monohydrate (97%), D-gluconic acid (Na salt), D-galacturonic acid (monohydrate), succinic acid, formic acid, acetic acid and *n*-butyric acid were obtained from Merck. Other chemicals and their sources were D-glucaric (or -saccharic) acid, K salt; 2-keto-D-gluconic acid (hemi-Ca salt, monohydrate), L-mannono-1,4-lactone, D-mannurono-6,3-lactone and D-gulono-1,4-lactone from Sigma (St. Louis, MO, USA) and D-galactaric acid (>98%) and glucuronic acid (Na salt, monohydrate) from Roth (Karlsruhe, Germany).

All aqueous solutions and dilutions were prepared with ultrapure Milli-Q water (Millipore, Eschborn, Germany). Calibration standards were prepared by mixing aliquots of aqueous stock solutions and subsequent dilution to the desired concentration by addition of 0.01 *N* sulphuric acid (Merck, Titrisol).

2.2. Apparatus

The liquid chromatograph consisted of a Gynkotek (Germering, Germany) 600-200 dual piston high-pressure pump with a Gynkotek 250-B ternary gradient former and an Erma ERC-3520 eluent degasser unit, a Rheodyne (Cotati, CA, USA) 8125 injector for manual and automatic injection, fitted with a 20-μl sample loop, a Gynkotek Gina 50 autosampler and an SPD-10AV Shimadzu (Duisburg, Germany) dual-beam UV–VIS detector (detection wavelength set to 210 nm). Normal detection sensitivity was 0.01 a.u.f.s. except in the determination of substance detection limits (0.002 a.u.f.s.). The separations were carried out on a sulphonated polystyrene–divinylbenzene-based Merck Polyspher OA-HY cation-exchange column (300 × 6.5 mm I.D.), packed with Merck 46–67 Å resin (identical with Interaction IC 8101-8 resin, 8 μm particle size, 8% cross-linking) and combined with a guard column (20 × 3.0 mm I.D.) containing the same resin. The columns were enclosed in a thermostat (Industrial Electronics). Sulphuric acid in various concentrations served as eluent.

Data collection and processing was handled by the Gynkosoft (Gynkotek) chromatography data system.

3. Results

3.1. Determination of capacity factors

It is well known that temperature and proton (eluent) concentration are deciding factors in the retention behaviour of organic acids in ion-exclusion chromatography. Therefore, the influence of these factors on the retention times was studied extensively. Capacity factors related to the separation system (combination of guard and separation column) were calculated on the basis of the observed retention times and void times (eluent peak). The results are combined in Figs. 1–6.

The effect of temperature on the chromatographic behaviour of the organic acids is illustrated in Figs. 1–3.

In general, the retention of the sugar acids increases with increasing temperature (Fig. 1). Strong effects are provoked in the case of D-galactaric, D-gluconic and L-threonic acids, whereas only slight changes are recognizable in the case of D-glucaric and D-galacturonic acids. The retention of D-glucuronic and D-galacturonic acids increases almost regularly with increasing temperature. The retention of D-galactaric and L-threonic acids is particularly enhanced by a rise in temperature from 55 to 65°C.

In contrast to the retention of sugar acids, the retention of lactones decreases with increasing temperature (Figs. 1 and 2). This effect is the more pronounced as the molecular masses of the aldono-lactones decrease. Slight variations of the reaction of the hexono-lactones on changes of the separation temperature are noticeable: the difference between the k' values at 10 and 65°C is 0.01 for D-galactono-1,4-lactone and 0.08 for D-mannono-1,4-lactone. The response of the D-mannurono-6,3-lactone is stronger: the decrease of its capacity factor is 0.26 units within the same temperature range.

Short-chain hydroxy and keto acids do not

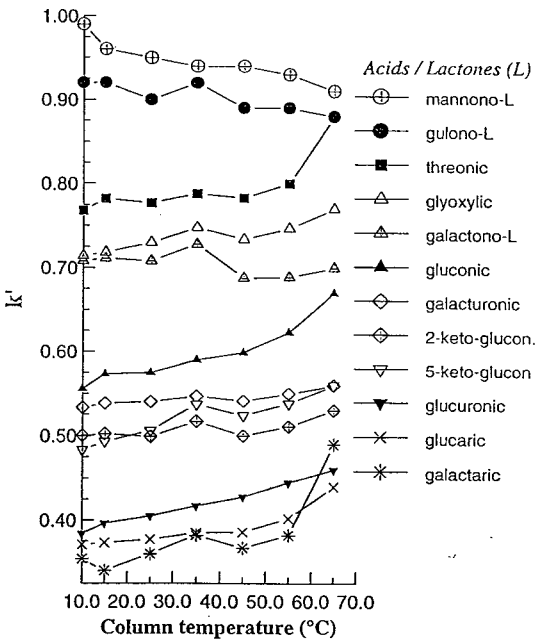

Fig. 1. Effect of temperature on capacity factors of sugar acids and hexono-1,4-lactones.

show a uniform retention behaviour (Figs. 1 and 2). The retention of D-glyceric and D-quinic acids seems to be independent of temperature within the range tested, whereas the retention times of L-lactic and glyoxylic acids increase with increasing temperature. The retention time of glycolic acid is slightly shortened.

The decline of the retention of mono- and dicarboxylic acids with increasing temperature is a function of the alkyl chain length generally (Fig. 3). Increasing carbon numbers of the compounds increase the difference between the capacity factors at low and high temperatures. The retention times of the dicarboxylic acids decrease almost linearly with increasing temperature within the observed value range. The retention of the monocarboxylic acids remains approximately constant between 10 and 35°C. The introduction of an α-keto group into glutaric acid eliminates the temperature influence totally.

The differences between the k'-values of the acids at 10 and 65°C are as follows: formic 0.09, acetic 0.11, n-propionic 0.19, n-butyric 0.40,

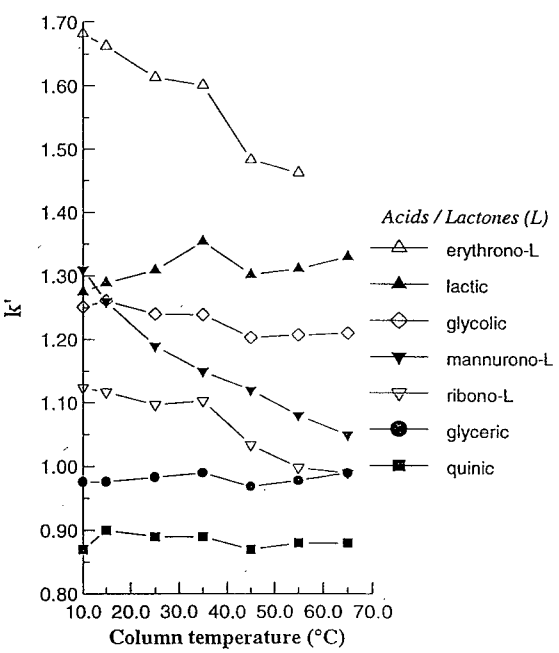

Fig. 2. Effect of temperature on capacity factors of lactones and hydroxy acids.

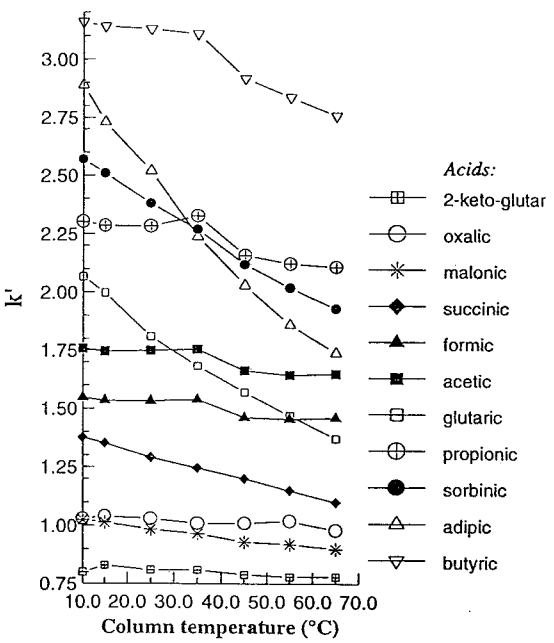

Fig. 3. Effect of temperature on capacity factors of mono- and dicarboxylic acids.

oxalic 0.05, malonic 0.12, succinic 0.28, glutaric 0.70 and adipic 1.15.

The influence of the eluent (i.e. proton) concentration on the separation process is depicted in Figs. 4–6.

According to the low pK_a values of oxalic, malonic, 2-keto-D-gluconic and 2-keto-glutaric acids, their capacity factors are shifted to greater values by increasing the proton concentration. For these compounds, the pH influence is more important for the definition of their retention times than the temperature conditions are. The effects of the two chromatographic parameters are roughly balanced in the case of sorbic acid. Practical consequences are inherent, for instance for the improvement of the resolution between 2-keto-D-gluconic acid and 5-keto-D-gluconic acid.

Except the keto acids, the sugar acids show slight or moderate responses on the variation of the sulphuric acid concentration (Fig. 4). The retention factors increase with increasing sulphuric acid concentration from 0.001 to 0.02 *N*

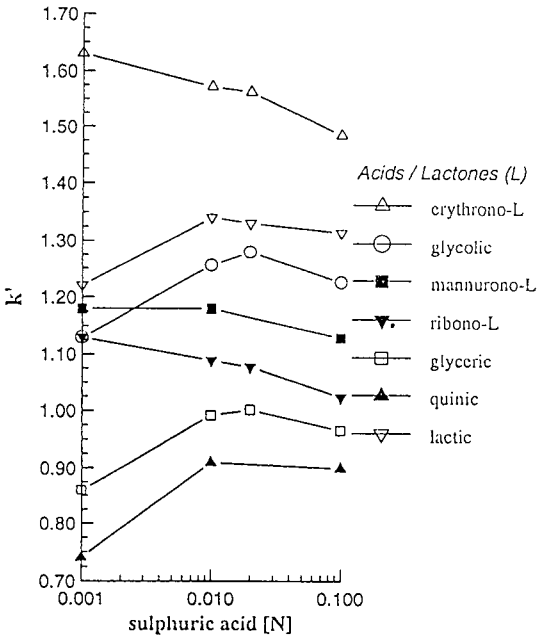

Fig. 5. Effect of sulphuric acid concentration on capacity factors of lactones and hydroxy acids.

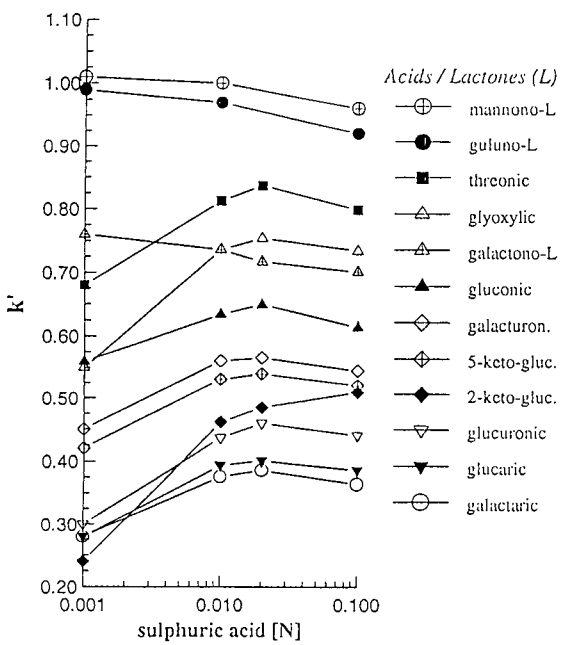

Fig. 4. Effect of sulphuric acid concentration on capacity factors of sugar acids and hexono-1,4-lactones.

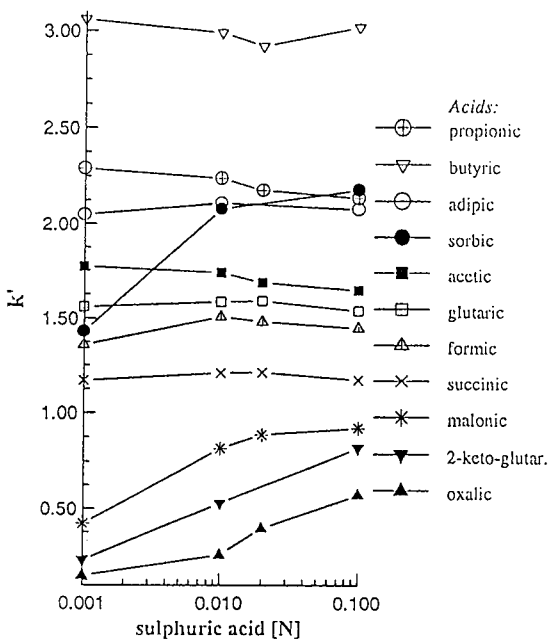

Fig. 6. Effect of sulphuric acid concentration on capacity factors of mono- and dicarboxylic acids.

and tend to decrease slightly with a further elevation of the H_2SO_4 concentration. The retention of the lactones decreases with increasing sulphuric acid concentration. The dimension of this effect is correlated with the molecular size of the lactones in the same way as it is described for the influence of the temperature on their chromatographic properties.

A change of the eluent flow-rate does not alter the capacity factors significantly. A certain influence is noticeable for glutaric acid. Nevertheless, in some cases the improvement of the peak separation obtainable by lowering the flow-rate surpasses the adverse effects of peak broadening and peak-height reduction. Examples are the separation of the substance combinations L-threonic acid–malonic acid and D-erythrono-1,4-lactone–glutaric acid.

3.2. Selection of chromatographic standard conditions

Reflecting the chromatographic behaviour of the compounds tested, it seemed favourable to select two distinct separation conditions, which differ in their separation performances for various groups of analytes. Further, the combination of the results received from different chromatographic conditions should improve the chemical identification of analytes. Separation condition I (45°C, 0.01 *N* H_2SO_4, 0.5 ml min^{-1} flow-rate) intends to achieve a relatively increased retention of sugar acids together with a shortage of the retention of dicarboxylic acids and 2-keto-D-gluconic acid. In contrast to that, separation condition II (10°C, 0.1 N H_2SO_4, 0.5 ml min^{-1} flow-rate) aims at characteristically altered (higher) retention of dicarboxylic acids, higher retention of 2-keto-D-gluconic acid and consequently increased resolution of 2-keto- and 5-keto-D-gluconic acid. Furthermore the chemical stabilities of sugar acids should be increased to prevent the formation of lactones during chromatographic analysis.

The separation performances of these analytical conditions are shown in Figs. 7 and 8. The substance combinations are chosen to demonstrate separation capabilities for complex mixtures. Although compromises regarding the resolution were accepted, the resolutions obtained are adequate for substance characterizations by their retention times and for quantification provided that the concentrations of the substance pairs 2-keto-D-gluconic acid–5-keto-D-gluconic

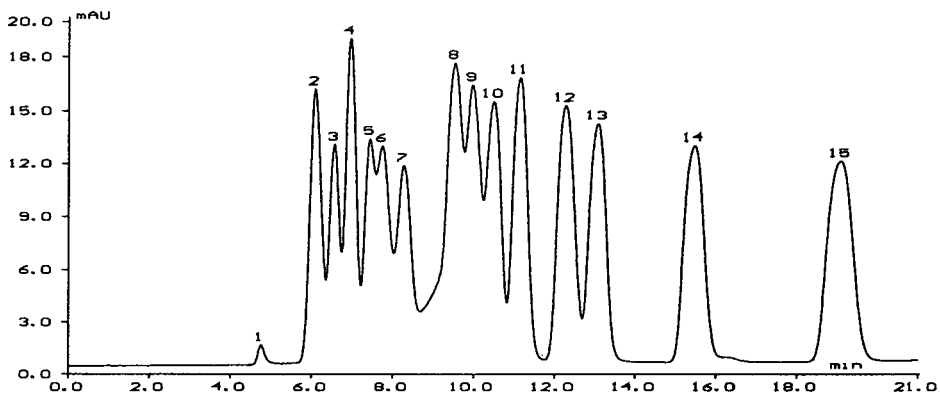

Fig. 7. Separation of sugar acids, lactones and aliphatic acids at high column temperature and low sulphuric acid concentration (conditions I). Conditions: Merck OA-HY column plus guard column; temperature, 45°C; flow-rate, 0.5 ml/min; eluent, 0.01 *N* H_2SO_4; UV detection at 210 nm and 0.01 a.u.f.s. Peaks (concentrations in mmol/l): 1 = void peak; 2 = oxalic acid (0.05); 3 = D-galactaric acid (0.2); 4 = glucuronic acid (0.5); 5 = D-galacturonic acid (0.5); 6 = gluconic acid (0.5); 7 = D-galactono-1,4-lactone (0.5); 8 = D-glyceric acid (0.5); 9 = D-ribono-1,4-lactone (2.0); 10-succinic acid (1.0); 11 = latic acid (1.0); 12 = glutaric acid (1.0); 13 = acetic acid (2.0); 14 = propionic acid (2.0); 15 = *n*-butyric acid (2.0).

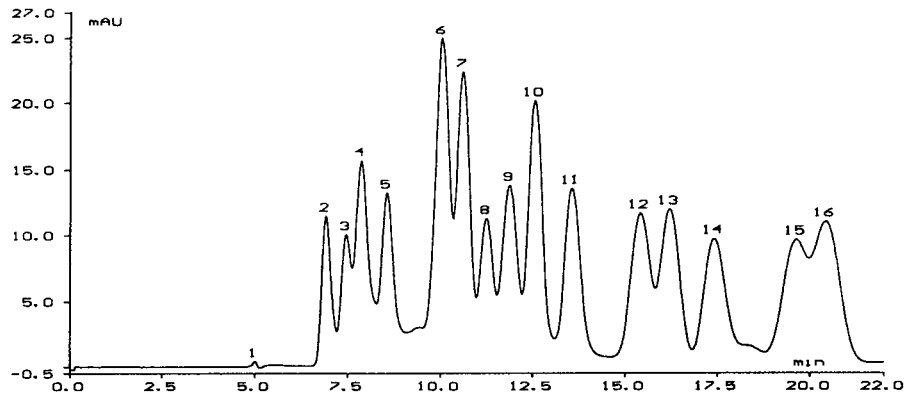

Fig. 8. Separation of sugar acids, lactones and aliphatic acids at low column temperature and high sulphuric acid concentration (conditions II). Conditions: Merck OA-HY column plus guard column; temperature, 10°C; flow-rate, 0.5 ml/min; eluent, 0.1 *N* H_2SO_4; UV detection at 210 nm and 0.01 a.u.f.s. Peaks (concentrations in mmol/l): 1 = void peak; 2 = D-glucaric acid (0.5); 3 = 5-keto-D-gluconic acid (0.5); 4 = D-galacturonic acid (0.5); 5 = glyoxylic acid (1.0); 6-malonic acid (1.0); 7 = D-ribono-1,4-lactone (2.0); 8 = glycolic acid (1.0); 9 = succinic acid (1.0); 10 = formic acid (2.0); 11 = acetic acid (2.0); 12 = glutaric acid (1.0); 13 = propionic acid (2.0); 14 = sorbic acid (not specified); 15 = adipic acid (1.0); 16 = butyric acid (2.0).

acid and D-glyceric acid–D-ribono-1,4-lactone (condition I) are of the same order of magnitude.

Hexaric, hexuronic and hexonic acids have capacity factors between 0.35 and 0.60 under chromatographic conditions I. The capacity factors of the corresponding lactones range from 0.70 to 1.10. The narrow retention ranges for sugar acids and lactones with identical carbon numbers have two consequences. First, the separation of compounds, which differ in their configuration only, is very difficult if not impossible at all. Second, the separation of mono- and dicarboxylic acids, having capacity factors greater than 1.2, can be achieved in one run together with sugar acids.

Oxalic acid, well separated from the void volume, has the shortest retention time and does not provide complications for the separation of dicarboxylic sugar acids.

Omitting the galactose-derived acids the chromatographic conditions I allow the separation of glucose-derived sugar acids together with further sugar acids and lactones (D-galactono-1,4-lactone, L-mannono-1,4-lactone, D-mannurono-6,3-lactone, D-erythrono-1,4-lactone) and other organic acids.

The chromatographic separation at conditions II delivers complementary informations, useful for the identification of dicarboxylic acids especially.

The chromatographic conditions II achieve better results for following substance combinations, which were not or poorly separated at 45°C and 0.01 *N* H_2SO_4: D-glucuronic–2(5)-keto-D-gluconic acid (absence of D-glucaric acid); separation of malonic acid from L-threonic acid, glyoxylic acid, D-galactono-1,4-lactone and D-quinic acid, separation between D-ribono-1,4-lactone, glycolic acid and succinic acid as well as between formic acid, D-erythrono-1,4-lactone and glutaric acid (absence of acetic acid). Additionally, separation of adipic and sorbic acid is possible.

3.3. Calibration

Specific calibration standards were prepared for both separation conditions. Standard I (condition I) contains oxalic, D-glucaric, 2-keto-D-gluconic, 5-keto-D-gluconic, D-gluconic, L-threonic, D-glyceric, succinic, L-lactic, glutaric, acetic, *n*-propionic and *n*-butyric acids together with D-ribono-1,4-lactone (fourteen compounds). Standard II (conditions II, eight compounds) comprises D-gluconic, malonic, succinic, glycolic,

formic, glutaric and adipic acids together with D-ribono-1,4-lactone. The calibrations were performed by analysis of five concentration levels of the standard mixture, each injected twice. The ratio of the maximum/minimum level of each substance was 50:1. With respect to the different detection sensitivities of the compounds, four concentration ranges were chosen to obtain approximately equal peak areas for each compound. Calibration functions were calculated using curve fitting by means of linear regression analysis. Moreover, relative standard deviations and percentage mean errors were determined for the highest and lowest calibration level on the database of five subsequent standard injections. Detection limits for single substances within given substance combinations were deduced from signal-to-noise ratios obtained by analysis of further dilutions of the minimum standard.

Calibration parameters and some statistical data are listed in Tables 1 and 2.

Despite the partially poor resolution, all compounds were calibrated resulting in coefficients of linear regression of the data points >0.999. The correspondence between the calibration functions of D-glucaric and D-gluconic acid at conditions I and the good agreement between the standardization of D-gluconic acid at both conditions demonstrate the consistency of the calibration procedures. The determination of the R.S.D. values (lowest level, conditions I) yielded a more homogeneous data set with values ranging typically from 4 to 8%. The mean R.S.D. of the six sugar acids and lactones (7.5%) is somewhat higher than that of the eight other acids (4.9%). Regarding the R.S.D. values, very precise results can be obtained for 5-keto-D-gluconic acid, propionic acid and butyric acid even at low concentrations.

The R.S.D. values deduced from the analysis of the concentrated standard I ranged from 0.2 to 2.57. Again the mean of the R.S.D. values of sugar acids and lactones (1.33) is slightly higher than that of the other acids (0.85%). The specific detector response for 50 μmol l^{-1} substance concentrations ranged from 5.05 to 0.2 detection units with typical response ranges of 0.5–0.7 units for C_6 sugar acids, 0.35–0.4 units for methyl group-containing dicarboxylic acids and 0.15–0.2 units for monocarboxylic acids. The low detection sensitivity for D-ribono-1,4-lactone is consistent with the evaluation of the peak areas of other lactones obtained during the determination of their capacity factors.

Limit concentrations for substance identification at given substance combinations were determined instead of the calculation of detection limits for single-compound injections. This procedure achieves data with higher practical use.

Fig. 9 shows a separation of the minimum calibration standard for conditions II. The maximum peak height is about 0.5 ma.u.f.s. The good signal-to-noise ratio is obvious.

4. Discussion

Reflecting the general behaviour of organic acids including sugar acids on ion-exclusion columns, the Polyspher OA-HY column shows almost the same separation properties as described earlier [20,21] for other ion-exclusion chromatography columns. Some of the main effects are as follows:

- Increase of the capacity factors of mono- and dicarboxylic acids with increasing carbon number due to an increase of the pK_1 values and increasing hydrophobic interactions, resulting in a favoured adsorption on the gel beads.

- Decrease of the capacity factors with increasing polarity of the functional molecular groups, expressed by the elution order oxalic < glyoxylic < glycolic < acetic acid. This order is valid even under strong acidic elution conditions. Therefore, the parallel increase of the pK_1 values cannot be the reason for this effect. The sugar acids fit in this rule, as it can be deduced from their k' factor sequence: glucaric < glucuronic < ketogluconic < gluconic acid.

- Higher retention times of the neutral lactones compared with the free acid forms [15].

- The increase of the retention times of lactones (D-galactono- < D-ribono- < D-erythrono-1,4-lactone) and aldonic acids, represented by the formula $CH_2OH\text{-}(CHOH)_n\text{-}COOH$ (i.e. D-gluconic < L-threonic < D-glyceric < glycolic

Table 1
Parameters of linear calibration at separation conditions I

Acid/ lactone	Retention time (min)	Concentration range (μmol l^{-1})	Intercept (μA.U. min)	Slope ($\times 10^{-3}$)	Detector response[a] (mA.U. min)	Relative molar response[b]	R.S.D., high level[c] (%)	R.S.D., low level[c] (%)	Detection limit[d] (μmol l^{-1})
Oxalic	6.14	1–50	−47	102	5.05	9.35	1.01	4.97	0.2
D-Glucaric	6.65	10–500	30	10	0.52	0.96	2.57	12.13	2.0
2-Keto-D-gluconic	6.95	10–500	16	12	0.60	1.11	0.22	6.86	1.0
5-Keto-D-gluconic	7.33	10–500	0	14	0.71	1.31	1.09	3.78	1.0
Gluconic	7.75	10–500	27	10	0.54	'1'	1.04	8.01	1.0
L-Threonic	8.62	10–500	67	16	0.87	1.64	1.53	6.83	0.5
D-Glyceric	9.54	10–500	36	20	1.02	1.89	0.95	2.43	2.0
Succinic	10.51	20–1000	16	6	0.35	0.65	1.49	6.07	4.0
L-Lactic	11.15	20–1000	15	7	0.37	0.69	1.22	6.82	1.5
Glutaric	12.28	20–1000	7	7	0.38	0.70	0.94	7.71	1.0
D-Ribono-1,4-lactone	9.97	40–2000	39	3	0.16	0.30	1.55	5.58	10.0
Acetic	13.08	40–2000	1	3	0.16	0.30	0.74	7.09	2.0
Propionic	15.47	40–2000	2	3	0.31	0.26	0.26	3,82	4.0
Butyric	19.07	40–2000	1	4	0.21	0.39	0.2	0,41	4.0

Merck OA-HY guard and separation column, column temperature 45°C, 0.01 *N* sulphuric acid/0.5 ml min^{-1} flow-rate, five injection levels, two injections per level.
[a] Calculated for 50 μM concentrations.
[b] Relative to gluconic acid.
[c] Five manual injections.
[d] Limit concentration for substance identification at given substance combination coefficient of linear regression >0.999 for all calibration functions.

Table 2
Parameters of linear calibration at separation conditions II

Acid/ lactone	Retention time (min)	Concentration range (μmol l^{-1})	Intercept (μA.U. min)	Slope ($\times 10^{-3}$)	Detector response[a] (mAU min)	Relative molar response[b]	R.S.D., high level[c] (%)	R.S.D., low level[c] (%)	Detection limit[d] (μmol l^{-1})
Gluconic	7.88	10–500	17	11	0.55	'1'	2.31	10.16	1.0
Malonic	10.09	20–1000	24	7	0.38	0.69	1.23	11.24	5.0
Glycolic	11.25	20–1000	8	4	0.21	0.38	0.79	12.01	5.0
Succinic	11.87	20–1000	6	6	0.30	0.55	1.22	6.06	4.0
Glutaric	15.41	20–1000	6	7	0.36	0.65	0.74	5.44	4.0
Adipic	19.61	20–1000	14	8	0.39	0.71	0.04	6.66	10.0
D-Ribono-1,4-lactone	10.60	40–2000	28	4	0.24	0.44	1.05	6.51	10.0
Formic	12.57	40–2000	7	4	0.20	0.36	1.23	3.94	6.0

Merck OA-HY guard and separation column, column temperature 10°C, 0.1 *N* sulphuric acid, 0.5 ml min^{-1} flow-rate, five calibration levels, two injections per level.
[a] Calculated for 50 μmol l^{-1} concentrations.
[b] Relative to gluconic acid.
[c] Five manual injections.
[d] Limit concentration for substance identification at given substance combination coefficient of linear regression >0.999 for all calibration functions.

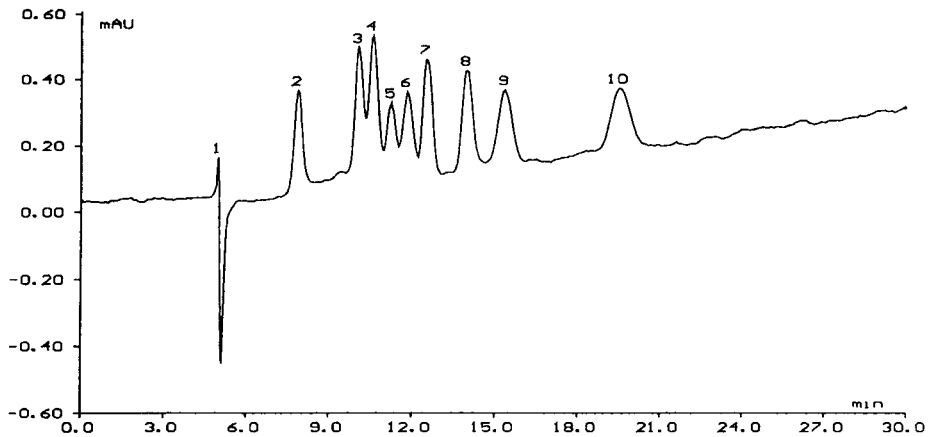

Fig. 9. Chromatogram of the minimum calibration level standard, obtained under conditions II. Conditions: Merck OA-HY column plus guard column; temperature, 10°C; flow-rate, 0.5 ml/min; eluent, 0.1 *N* H_2SO_4; UV detection at 210 nm and 0.01 a.u.f.s. Peaks (concentrations in μmol/l): 1 = void peak; 2 = gluconic acid (10.0); 3 = malonic acid (20.0); 4 = D-ribono-1,4-lactone (40.0); 5 = glycolic acid (20.0); 6 = succinic acid (20.0); 7 = formic acid (40.0); 8 = unknown; 9 = glutaric acid (20.0); 10 = adipic acid (20.0).

acid) with decreasing carbon numbers leads to the assumption that size-exclusion effects take part in the separation of the compounds. This hypothesis was formulated earlier [22] to explain the respective elution order obtained by ion-exchange chromatography of organic acids.

The differences in the effect of temperature on the retention behaviour of the compounds reflect differences in their chemical properties and retention mechanism. The increase of the capacity factors of sugar acids with increasing temperature is affected mainly by the partial formation of their lactones. A temperature-dependent increase of the retention times of some sugar acids following the order 2-keto-D-gluconic acid < 5-keto-D-gluconic < D-glucuronic acid < D-gluconic acid is also described by Hicks et al. [7]. They explain this with substance-specific degrees of lactonization under the chromatographic conditions provided. Dicarboxylic sugar acids seem to be more stable against lactonization than uronic and monocarboxylic acids.

The reduction of the capacity factors of most of the other compounds may be interpreted as follows:

- The balance of the lactone–acid equilibrium is favoured by an increase of the column temperature. The short retention times of the lactones are connected with the degree of their conversion into the acid form and the absolute retention time difference of the pure acid and lactone form under the given chromatographic conditions.

- The pK_a values decrease with increasing temperature causing an intensified repulsion by the Donnan membrane.

- As far as the adsorption of organic compounds onto the polymer material, caused by hydrophobic interactions, is an exothermic process (release of heat of adsorption), the free adsorption enthalpy is diminished by a rise of the temperature. Because the adsorption strength is a function of the number of active molecular units (i.e. methylene groups), which act in the adsorption process, the decline of the retention time depends on the carbon chain length. Based on the same reaction principles the increase of the substance retention with increasing carbon chain length of homologous aliphatic mono- and dicarboxylic acids at constant temperature and the decrease of their retention times with increasing molecular mass at increasing temperature are complementary effects.

- As a minor effect, the swelling of the column material under the influence of higher temperatures may reduce the pore volume and pore size,

resulting in a lower molecular size limit for entering the pores of the stationary phase.

Considering the influence of the proton concentration on the retention behaviour of the acids, the interpretations of Kihara et al. [20] were largely confirmed. For the dicarboxylic acids for instance, an important increase of the retention with an increase of the sulphuric acid concentration was found for those compounds only (oxalic, malonic and 2-keto-glutaric acid), which are partially dissociated at the lowest eluent concentration (pH of about 3). The achieved enhancements of the substance-specific retentions following the orders glyoxylic > glycolic >> acetic acid and D-glyceric > lactic >> *n*-propionic acid reflect the supporting influences of the additional functional groups on the dissociation of the carboxyl group. At pH 3, the pK_1 value may be the dominant factor for the separation of sugar acids with similar sizes and identical carbon numbers. This could be a reasonable explanation for the observed elution order of the glucose-derived acids at lowest sulphuric acid concentration: 2-keto-D-gluconic < D-glucaric acid < 5-keto-D-gluconic acid < D-gluconic acid. As a consequence of the repression of the acid dissociation at high eluent concentrations, the differences between the retention times of the sugar acids were reduced and size-exclusion effects seem to gain a higher importance for the separation process.

Due to the absence of an ionizable functional group, lactones do not respond to an increase of the proton concentration or respond with a small decrease of their retention times (D-ribono-1,4-lactone, D-erythrono-1,4-lactone and D-gulono-1,4-lactone). The latter effect may be attributed to a slightly diminished stability of the lactones against conversion into their acidic forms under these chromatographic conditions.

The systematic variation of main separation parameters confirmed that the capacity ranges are narrow for the detection of sugar acids and lactones, which are very similar in their molecular sizes and chemical properties. The capacity ranges for the tested sugar acids are 0.2–0.85 and 0.7–1.65 for lactones. These results are comparable with those of other authors. Hicks et al. [7] reported for the separation of sugar acids and lactones on BioRad-HPX-87-H (0.6 ml min^{-1} flow-rate, 35°C, 0.009 *N* sulphuric acid) approximately the same relative retention times (relative to D-glucuronic acid) as we found for 2-keto-D-gluconic acid, 5-keto-D-gluconic acid, D-galacturonic acid, D-gluconic acid, D-galactono-1,4-lactone, D-mannono-1,4-lactone, D-ribono-1,4-lactone and D-mannurono-6,3-lactone. It is assumed that the capacity factors are nearly identical as well. Further correspondences of the separation characteristics of the OA-HY column with the HPX-87-H column are noticeable for some mono and hydroxy acids. De Bruijn et al. [16] determined capacity factors for formic, acetic, glycolic, L-lactic and D-glyceric acids (conditions: 0.6 ml min^{-1} flow-rate, 0.01 *N* H_2SO_4, 60°C). We compared their values with our data, given in parentheses, for 0.5 ml min^{-1} flow-rate, 0.01 *N* H_2SO_4, 45°C: glyceric acid 1.01 (0.99), glycolic acid 1.19 (1.26), lactic acid 1.28 (1.34), formic acid 1.42 (1.51) and acetic acid 1.64 (1.74). Considering the differences of the chromatographic conditions, the correspondence of the data is substantial.

5. Conclusions

As a consequence of a detailed investigation of the chromatographic charateristics of the Merck HY-OA ion-exclusion column, two separation conditions were chosen, which use the different responses of sugar acids, lactones and dicarboxylic acids to changes of temperature and proton concentration for their separation and identification. Optimized separation conditions for some of those substance combinations, which can not be separated by one of the both methods, can be deduced from the plots of capacity factors. Sensible substance detection and linear calibration functions that are valid for greater concentration ranges as well as acceptable reproducibilities of single measurements were achieved with both methods. Furthermore, far-reaching similarities between the separation properties of Aminex/BioRad HPX-87H and

Merck OA-HY column were found by comparison of experimental with literature data.

Acknowledgements

We thank the ministries Bay. Staatsministerium für Landesentwicklung und Umweltfragen and Bay. Staatsministerium für Unterricht, Wissenschaft und Kunst for their generous support of the work which is integrated in a research association for waste research and exploitation of residues (BayFORREST).

References

[1] D.T. Sawyer, *Chem. Rev.*, 633 (1964).
[2] G.M. Escandar and L.F. Scala, *Can. J. Chem.*, 70 (1992) 2053.
[3] K. Fischer, H.-P. Bipp, P. Riemschneider, D. Bieniek and A. Kettrup, in P.A. Wilderer, U. Potzel and V. Rehbein (Editors), *Berichtsheft 2. Statusseminar*, BayFORREST-Forschungsverbund, Munich, 1994, p. 219.
[4] D.F. Charles, *Int. Sugar J.*, 83 (1981) 195.
[5] M.A. Clarke and W.S.C. Tsang, *Int. Sugar J.*, 86 (1984) 215.
[6] J.D. Blake, M.C. Clarke and G.N. Richards, *J. Chromatogr.*, 398 (1987) 265.
[7] K.B. Hicks, P.C. Lim and M.J. Haas, *J. Chromatogr.*, 319 (1985) 159.
[8] F. Gosselé, J. Swings and F. Deley, *Zbl. Bakt. Hyg. I Abt. Orig.*, C1 (1980) 178.
[9] E. Rajakylä, *J. Chromatogr.*, 218 (1981) 695.
[10] H. Ruffner and D. Rast, *Z. Pflanzenphysiol.*, 73 (1974) 45.
[11] W.-R. Sponholz, *GIT Fachz. Lab.*, (1990) 107.
[12] W.-R. Sponholz and H.H. Dittrich, *Vitis*, 23 (1984) 214.
[13] W.-R. Sponholz and H.H. Dittrich, *Vitis*, 24 (1985) 51.
[14] J.M.H. Dirkx, H.S. van der Baan and J.M.A.J.J. van der Broek, *Carbohydr. Res.*, 59 (1977) 63.
[15] J.M.H. Dirkx and L.A.Th. Verhaar, *Carbohydr. Res.*, 73 (1979) 287.
[16] J.M. de Bruijn, A.P.G. Kieboom, H. van Bekkum and P.W. van der Poel, *Int. Sugar J.*, 86 (1984) 195.
[17] K.B. Hicks, *Carbohydr. Res.*, 145 (1986) 312.
[18] D.J. Woo and J.R. Benson, Organic Acids Analysis Column ORH-801, *Interaction Product Bulletin*, (1982).
[19] P.R. Haddad and P.E. Jackson, *Ion Chromatography*, Elsevier, Amsterdam, 1990.
[20] K. Kihara, S. Rokushika and H. Hatano, *J. Chromatogr.*, 410 (1987) 103.
[21] R. Pecina, G. Bonn, E. Burtscher and O. Bobleter, *J. Chromatogr.*, 287 (1984) 245.
[22] O. Samuelson and L. Thede, *J. Chromatogr.*, 30 (1967) 556.

ELSEVIER

Journal of Chromatography A, 706 (1995) 375–383

JOURNAL OF CHROMATOGRAPHY A

Determination of some organic acids in sugar factory products

S. Lodi*, G. Rossin

Eridania Z.N. S.p.A., Laboratorio Chimico Centrale, Via Argine Ducale 397, Ferrara, Italy

Abstract

This work deals with the identification and quantitative evaluation of the following acids: citric, malic, lactic, formic, acetic, propionic, butyric, valeric, and pyroglutamic acid. The determination has been carried out using a Dionex ion chromatograph, and compared with standard high-performance liquid chromatographic methods and enzymatic analysis. Differences in products from sugar beet factories have been analyzed with the aim to control the fermentation process used. Satisfactory results have been obtained, despite the presence of the particularly complex matrix. With the exception of a few cases, it has been possible in this way to standardize an analytical method for the whole production process.

1. Introduction

For some time now the Laboratorio Chimico Centrale ERIDANIA, Ferrara, Italy, has been trying to determine which organic acids are present in various sugar industry products. This study has three main aims:

(1) To control undesired fermentation in sugar syrups, particularly the development of malic, acetic and lactic acids, the presence of which lowers the pH of the juices, thus facilitating sucrose inversion which leads to the formation of glucose and fructose with consequent sugar losses. These monosaccharides provide the substrate for the so-called Maillard reactions which take place between the monosaccharide C = O carbonyl groups and the NH_2 groups of amino acid compounds. These reactions lead to an undesired increase in juice colour.

(2) To control the type of fermentation occurring in the sugar beet pulp used as animal feed, because such use depends on the type of fermentation which takes place during storage in silos. Determination of the organic acid content of the pressed pulp is of particular importance for the sugar industry since this product is used as cattle feed. At the time of production, only traces of organic acids (lactic and acetic acids) are present in the pulp. However, during storage, uncontrolled fermentation increases the acid content to ca. 2–3% of the product. Of the greatest importance is the type of acid formed (i.e. lactic, acetic, iso, *n*-butyric, valeric) [1]. In the case of lactic fermentation, a good quality product is obtained with organoleptic properties making it suitable for use as cattle feed. On the other hand, the formation of acids such as propionic, butyric and valeric acids make the feed unpleasant; not only is it less appetizing, but it also causes environmental problems due to the intense, repelling odour.

(3) To control the formation of pyroglutamic acid, which is an indication of the presence of glutamine. As is shown in Fig. 1, the loss of

* Corresponding author.

0021-9673/95/$09.50
SSDI 0021-9673(94)01208-3

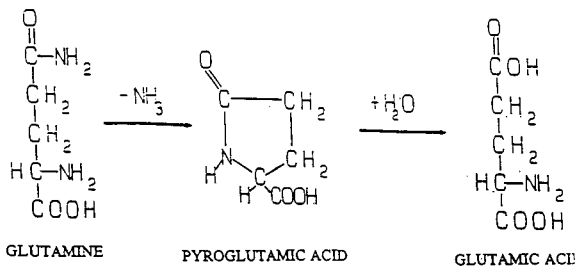

Fig. 1. Formation and hydrolysis of pyroglutamic acid.

ammonia during the calcocarbonic purification of glutamine leads to the formation of pyroglutamic acid which is partially hydrolyzed into glutamic acid. Given the fact that a poor sugar beet quality is also associated with a higher glutamine content and that the loss of NH_3 by the latter leads to increased air pollution and environmental damage, it can be inferred that the determination of pyroglutamic acid is of great importance.

2. Experimental

The analyses were performed using three methods: ion chromatography, high-performance liquid chromatography (HPLC) and enzymatic analysis.

2.1. Ion chromatography

The separation technique used in high-performance ion exclusion chromatography (HPIEC) is based on the Donnan effect. On the basis of this principle, the ionized compounds are more rapidly eluted than non-ionic ones which are held back by electrostatic partition forces such as the Van der Waals forces or the like. Weakly ionic compounds are then eluted more or less quickly, depending on their pK value and hydrophobicity.

The analyses were performed using a Dionex 4000i ion chromatograph with a 50-μl loop equipped with a conductometric detector of greater sensitivity than the UV detectors normally used in HPLC. As can be seen in the chromatogram of a standard mixture, peaks of a certain entity can be easily seen at 100 ppm (Fig. 2).

Separation was performed with an HPIEC-AS1 sulfonic column ($-SO_3H$) with approximately 9% styrene-divinyl benzene as the support, isocratic elution being performed at room temperature (column pressure 65 bar). In addi-

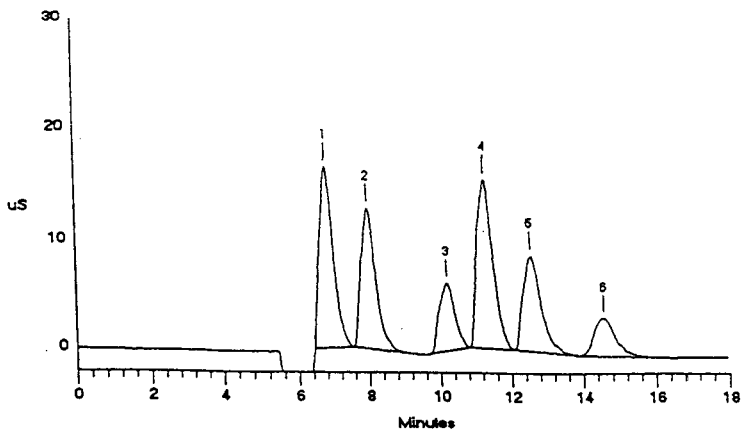

Fig. 2. Ion chromatogram. Column ICE AS1 Dionex. Eluent 2 mM HCl. Flow-rate 0.8 ml/min. Detector PED-conductivity. Standard solution of organic acids, 100 ppm. Peaks: 1 = citric; 2 = malic; 3 = lactic; 4 = formic; 5 = acetic; 6 = pyroglutamic.

tion, an AMMS-ICE membrane suppressor was set between the column and the detector to reduce the background conductivity and thus improve signal response [2]. A 2 m*M* HCl eluant was used at a flow-rate of 0.8 ml/min; regeneration of the cationic suppressor sites was achieved with 10 m*M* of the regenerant tetrabutyl ammonium hydroxide (TBAOH) at a flow-rate of 4 ml/min.

It must be pointed out that the method does not require any pretreatment of the sample solution. It was prepared dissolving the sample in the mobile phase at a concentration of about 1% of dry matter and subsequently filtrated on a 0.45-μm membrane, although any column contamination by proteins and the presence of interfering peaks caused by cations can be prevented by batch treatment with H^+ cation resins.

2.2. High-performance liquid chromatography

High-performance liquid chromatography was performed using a Varian 5000 chromatograph with a 10-μl loop equipped with a UV 100 detector. Separation was performed on a Biorad HPX-87H sulfonic column employing styrene-divinyl benzene as the support, isocratic elution taking place at 50°C (column pressure 50 bar). The eluant used was 5 m*M* H_2SO_4 at a flow-rate of 0.6 ml/min; detection was at a wavelength of

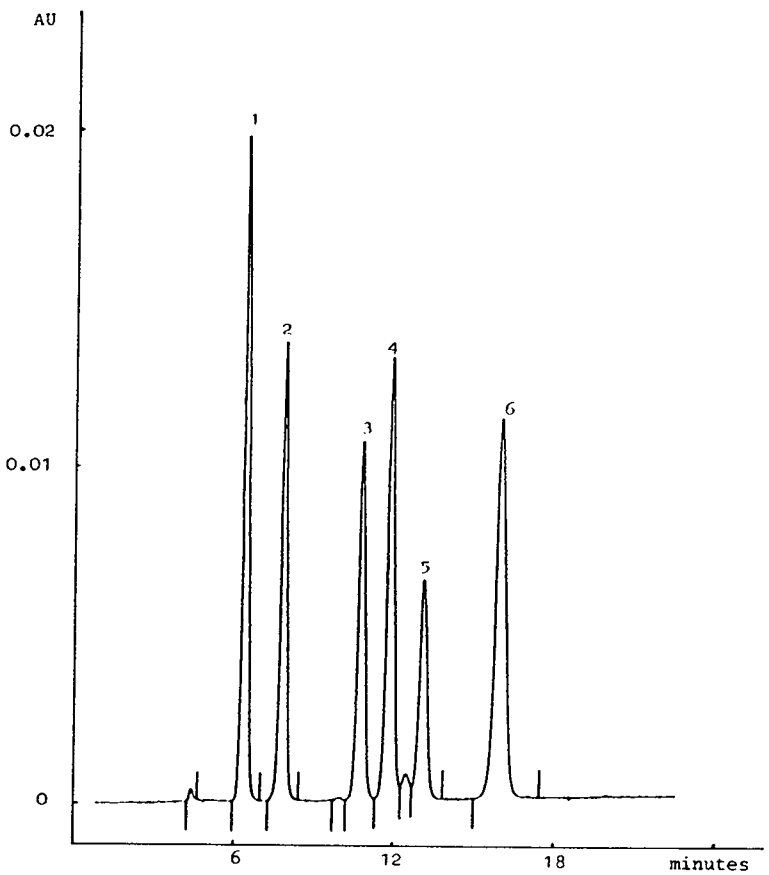

Fig. 3. High-performance liquid chromatogram. Column HPX-87H Biorad. Eluent 5 m*M* H_2SO_4. Flow-rate 0.6 ml/min. Detector UV 210 nm. Column temperature 50°C. Standard solution of organic acids, 500 ppm. Peaks: 1 = citric; 2 = malic; 3 = lactic; 4 = formic; 5 = acetic; 6 = pyroglutamic.

210 nm. The chromatogram in Fig. 3 shows the profile of a standard mixture.

2.3. Enzymatic analysis

For this technique the Boehringer Mannheim test was used containing predetermined quantities of selected, strictly controlled reagents. These were developed for the analysis of foodstuffs although they can be generally used for all types of matrices [3].

The NADH formed in the enzyme reaction is directly proportional to the amount of organic acid present and thus makes a precise, accurate determination possible. Tests were run at room temperature since the reactions caused by the enzymes proceed quite rapidly, even under these conditions [4].

Although this technique is not more difficult than the instrumental techniques described above, it gives greater accuracy since the enzyme only acts on the specific organic acid involved; in addition, it has the ability to distinguish between the various isomer forms. Thus, for example, for lactic acid we can determine both the L- and D-forms.

3. Results and discussion

Small amounts of some organic acids are present in sugar beets while others are present in beet processing products as a result of the breakdown of more complex organic structures or of transformation reactions taking place during production. In fact, when ion chromatograms of raw juice and molasses are compared (Figs. 4 and 5), one sees that marked amounts of lactic and pyroglutamic (PCA) acids are present in the latter. The former, derived from the chemical and biological destruction of sugar taking place during the production process, passes from an average of 0.2% of dry matter in raw juice to 2.5% in molasses, thus practically providing an index of sugar losses within the sugar factory. On the other hand, PCA is formed during the purification process as a result of a loss of ammonia by the glutamine (see Fig. 1).

Our methods of analysis do not allow the separation between propionic acid and PCA, because they are coeluted in the chromatogram; however, we have information from the literature on sugar beets that pyroglutamic acid (PCA) only is formed during the production process. Therefore, for the chromatograms con-

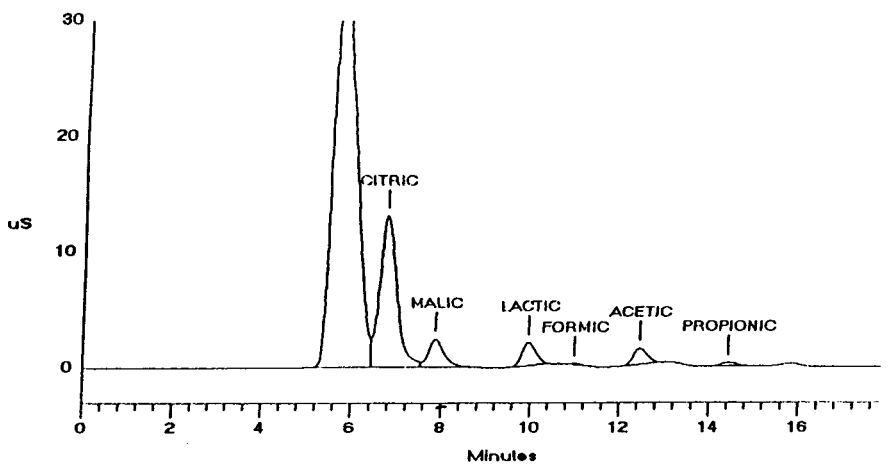

Fig. 4. Ion chromatogram. Sample solution of raw juice 10%.

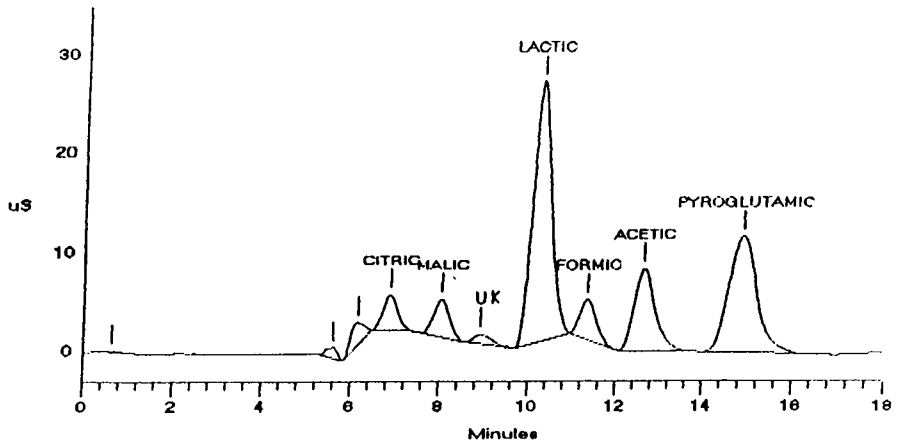

Fig. 5. Ion chromatogram. Sample solution of molasse 2%.

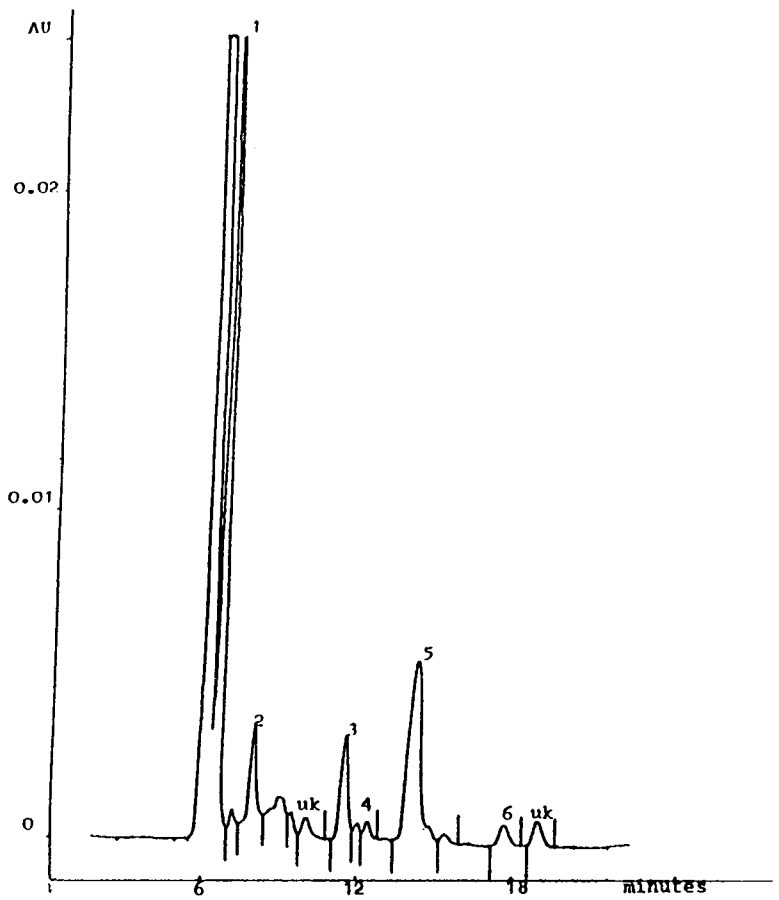

Fig. 6. High-performance liquid chromatogram. Sample solution of raw juice 10%. Peaks: 1 = citric; 2 = malic; 3 = lactic; 4 = formic; 5 = acetic; 6 = propionic; uk = unknown.

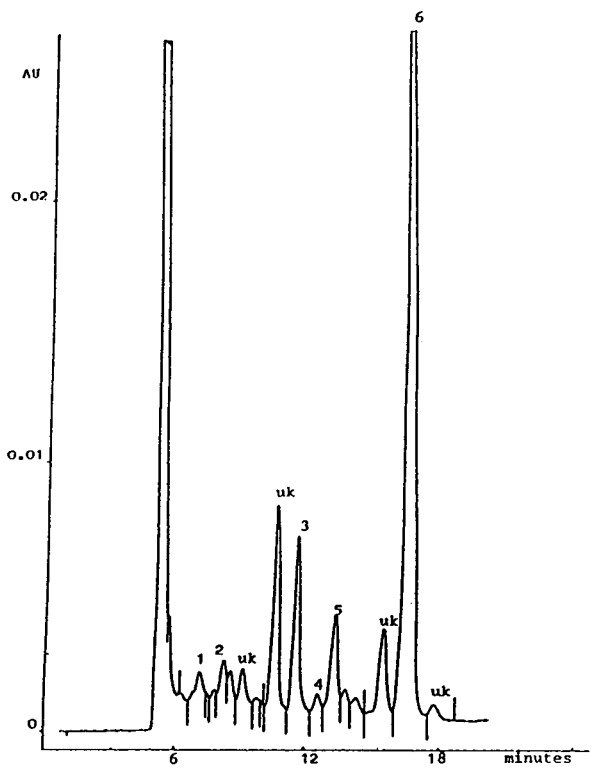

Fig. 7. High-performance liquid chromatogram. Sample solution of molasses 2%. Peaks: 1 = citric; 2 = malic; 3 = lactic; 4 = formic; 5 = acetic; 6 = pyroglutamic; uk = unknown.

cerning the raw juice (Figs. 4 and 6) the peak labelled 6 is identified as propionic acid, and for the chromatograms concerning the molasses (Figs. 5 and 7) the peak labelled 6 is identified as pyroglutamic acid.

In this regard it is worth noting that in the HPLC analysis the same samples showed different peaks, many of which are not identified (Figs. 6 and 7). This is due to the fact that, to be successful, HPLC analyses of organic acids in sugar production juices require isolation of the acid fraction through a difficult sample pretreatment process which is impractical for normal routine controls; therefore the samples for analysis were not submitted to any pretreatment [5–7].

With regard to the thick juices and factory-produced molasses, it has been found that L-lactic acid is predominant; in addition, the sum of the two isomers (D + L) is in good agreement with the total lactic acid determined by ion chromatography. This can be seen in Table 1, where the values are reported for a series of analyses performed on thick juices of eleven average samples from the 1993 sugar campaign.

The three methods were performed in parallel to determine the principal organic acids present. As an example, the results obtained in a series of molasse samples are given in Table 2. The values

Table 1
Comparison of enzymatic and ion-chromatography methods for lactic acid in thick juice

	Enzyme D-lactic (mg/g)	Enzyme L-lactic (mg/g)	Enzyme (D + L)-lactic (mg/g)	Total IC lactic (mg/g)
1	151	272	423	424
2	207	273	480	473
3	164	321	483	498
4	153	184	337	342
5	165	596	751	770
6	70	92	162	180
7	382	388	770	817
8	152	246	398	390
9	232	270	502	487
10	234	536	770	773
11	149	396	545	566

Table 2
Comparison of enzymatic analysis, HPLC and ion chromatography for organic acids in molasses

	Citric (mg/g)			Malic (mg/g)			Lactic (mg/g)			Formic (mg/g)			Acetic (mg/g)			PCA (mg/g)	
	Enz.	HPLC	IC	Enz.	HPLC	IC	Enz.	HPLC	IC	Enz.	HPLC	IC	Enz.	HPLC	IC	HPLC	IC
1	140	140	90	241	140	178	2111	1720	2256	277	225	264	594	1350	616	3320	2850
2	210	400	174	357	520	260	3058	2420	3254	305	240	268	411	375	520	2540	2194
3	205	180	138	255	60	190	2707	1920	2588	238	160	216	543	975	586	2740	2310
4	246	200	142	317	240	246	2076	1620	2324	345	180	324	647	612	670	3520	2954
5	163	400	80	305	540	244	2214	2720	2524	340	200	326	690	1488	732	3300	3014
6	98	480	36	163	80	118	1304	1000	1552	223	160	222	623	560	632	2420	2060
7	188	140	96	335	240	170	3444	3040	3980	309	180	282	673	1160	706	3320	3094
8	181	180	126	217	120	187	1601	1900	1931	264	220	266	642	1375	1374	3300	3055
9	159	140	105	217	80	168	2674	2320	3090	235	140	221	1078	1825	2228	2860	2753
10	244	380	53	364	700	284	2610	2620	2817	248	300	227	702	1450	1446	2840	2440
11	169	160	200	326	160	263	2220	1940	2686	307	180	299	434	788	910	2440	2321

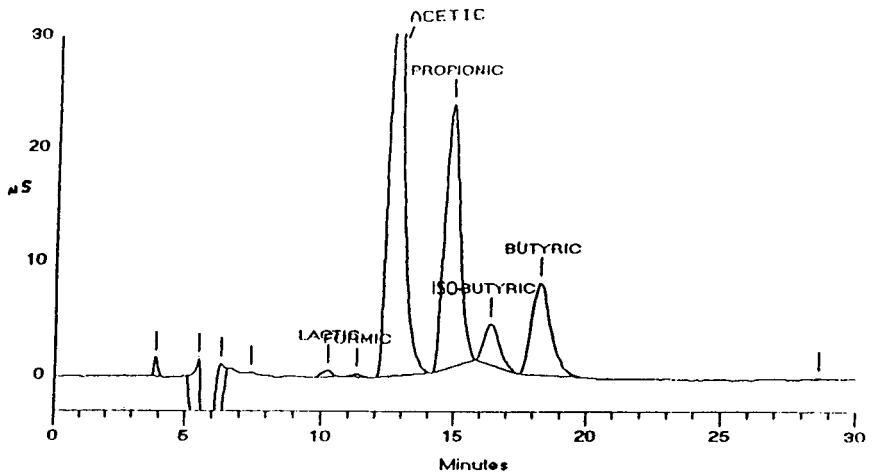

Fig. 8. Ion chromatogram. Sample solution of pressed pulps 5%.

clearly show that, except in a few isolated cases, the best agreement was always found between enzymatic analysis and ion chromatography [8]. Moreover, enzymatic analysis made it possible to show that, of the two isomers of malic acid (D and L), only L-malic acid is present in production juices.

The analyses of pressed pulp were performed in a similar manner as for the syrups and this study has shown that at the time the pressed pulp is placed in the silos the amount of organic acids present is quite low (about 5% of dry matter) and that controlled fermentation in an anoxic environment leads only to the formation of lactic and acetic acids. When fermentation takes place in an anoxic environment these acids are produced in such quantities as to lower the pH value to around 3.8–4.0. Since the low pH inhibits the onset of undesired fermentation, this makes it possible to maintain good organoleptic properties of the pulp, even during subsequent storage [9]. Hence, it can be noted that with decreasing anoxic conditions, the formation of undesired acids such as propionic and butyric acids will increase. The chromatogram (Fig. 8) of the analysis of a product of this type shows such a trend.

4. Conclusions

From the present study it can be concluded that a chromatographic analysis of the organic acids in our processed products does not allow a correct quantitative determination, and neither is it possible to distinguish between the D and L isomeric forms. In some cases enzymatic analysis was used to determine the amounts of D,L-lactic acid. The L-lactic acid content is an important parameter because it gives a measure of the fermentation activity in the different steps of the production process.

We also found that propionic acid and pyroglutamic acid cannot be separated by chromatography because they have the same retention time; enzymatic tests also do not allow their determination. Consequently we are now using a new ion chromatography column, IONPAC ICE AS6, with which their separation can be achieved if required.

References

[1] N. Kubadinow, P. Hollaus and W. Braunsteiner, *Zuckerindustrie*, 109 (1984) 38–45.

[2] C.A. Accorsi, *J. Chromatogr.*, 555 (1991) 65–71.
[3] *Enzymatic Analysis–Food Analysis*, Boehringer Mannheim.
[4] G. Henniger, *Z. Lebensm. Technol. Verfahrenstechn.*, 30 (1979) 137–144; 182–185.
[5] D.F. Charles, *Int. Sugar J.*, 83 (1981) 195.
[6] M.A. Clarke and W.S.C. Tsang, *Int. Sugar J.*, 86 (1984) 215.
[7] J.D. Blake and M.L. Clarke, *J. Chromatogr.*, 398 (1987) 265.
[8] P. Vratny, J. Mertova and D. Chadimova, *Listy Cukrov.*, 99 (1983) 55–63.
[9] N. Kubadinow, *Zuckerindustrie*, 107(12) (1982) 1107–1110.

ELSEVIER

Journal of Chromatography A, 706 (1995) 385–393

JOURNAL OF CHROMATOGRAPHY A

Ion-exclusion chromatography with conductimetric detection of aliphatic carboxylic acids on an H^+-form cation-exchange resin column by elution with polyols and sugars

Kazuhiko Tanaka[a,*], Kazutoku Ohta[a], James S. Fritz[b], Yo-Sang Lee[c], Soon-Bo Shim[c]

[a]*National Industrial Research Institute of Nagoya, 1-1, Hirate-cho, Kita-ku, Nagoya 462, Japan*
[b]*Ames Laboratory and Chemistry Department of Iowa State University, Ames, IA 50011-3020, USA*
[c]*Centre for Water Resources and Quality Management and Department of Civil Engineering of Chung Buk National University, Cheong Ju 360-763, South Korea*

Abstract

The Ion-exclusion chromatography (IEC) of normal aliphatic carboxylic acids of different acidity (pK_a) and hydrophobicity was investigated on a poly(styrene–divinylbenzene) (PS–DVB)-based strongly acidic cation-exchange resin column in the H^+ form and conductimetric detection. When water was used as the eluent, although the C_1–C_5 carboxylic acids were separated from strong acid (HCl) depending on the pK_a and the hydrophobicity, the resolution was low and the peaks were accompanied by leading depending on their hydrophobicities. To improve the peak shape and the peak resolution, aqueous eluents of polyols and sugars containing 1–8 alcoholic OH groups (methanol, ethylene glycol, glycerol, erythritol, xylitol, fructose, sorbitol, and sucrose) were tested for the IEC separation of the carboxylic acids. When aqueous eluents of polyols and sugars were used, the tendency for leading peaks was decreased drastically with increasing number of OH groups in the polyols and sugars. This is due mainly to the increase in the the hydrophilicity of the PS–DVB surface by the OH groups. An aqueous eluent of 10% methanol–0.15 *M* sucrose gave a reasonable resolution and highly sensitive detection for carboxylic acids. This eluent has a much lower background conductivity (ca. 4 μS cm^{-1}) and much higher detection sensitivity (ca. 170 times higher for valeric acid) than the 0.5 m*M* sulfuric acid (ca. 390 μS cm^{-1}) commonly used as an eluent in conventional IEC with conductimetric detection.

1. Introduction

Ion-exclusion chromatography (IEC) is a technique for the separation of organic and inorganic weak acids, especially those of a hydrophilic nature. Several reviews have been published on IEC [1–5]. Typically, a high-capacity cation-exchange resin in the H^+ form is used in IEC. When water is used as an eluent, peaks with a leading front edge (fronted peaks) are obtained for carboxylic acids such as butyric acid. This is a result of adsorption as a side-effect in IEC. Accordingly, an aqueous solution of a strong acid such as sulfuric acid is generally used as the eluent for the separation of weak acids [1]. This is done to suppress the ionization of the sample

* Corresponding author.

0021-9673/95/$09.50
SSDI 0021-9673(95)00041-0

acids and to ensure that they are entirely in their molecular forms. However, when conductivity detection is used, an acidic eluent causes a high background conductance and reduces the ability to detect sample acids.

In previous papers [6,7], we reported IEC using elution with a weak acid, such as benzoic or succinic acid, of low background conductivity. By using these weak acid eluents, highly sensitive conductimetric detection and high resolution for aliphatic carboxylic acids or F^- and PO_4^{3-} was accomplished.

A major aim of this research was to find an eluent that gives sharp chromatographic peaks for aliphatic carboxylic acids with some hydrophobicity, such as butyric and valeric acids, and highly sensitive detection for all aliphatic carboxylic acids without a high background conductance from the eluent itself. In this work, high-performance separation and highly sensitive conductimetric detection were achieved for aliphatic carboxylic acids by using a styrene–divinylbenzene copolymer (PS–DVB)-based strongly acidic cation-exchange resin in the H^+ form. The eluent was an aqueous solution containing a polyol or sugar with many OH groups. It is shown that excellent resolution and very sensitive conductimetric detection of aliphatic carboxylic acids are obtained using 0.15 *M* sucrose–10% methanol as the eluent.

2. Experimental

2.1. Apparatus

The ion chromatograph consisted of a Tosoh (Tokyo, Japan) CCPD metal-free eluent delivery pump with a flow-rate of 1 ml min^{-1}, equipped with a Rheodyne Model 7125 sample injector with a 100-μl PTFE loop.

Conductimetric detection was carried out with a Tosoh CM-8010 detector equipped with a constant-temperature controller maintained at 35°C.

The computing integrator was a System Instrument (Tokyo, Japan) Model 12 Chromatocorder.

2.2. Column

The separation column was a Tosoh glass column (300 mm × 8 mm I.D.). The column was packed by the slurry packing technique and equilibrated thoroughly with the eluent before the chromatographic run.

2.3. Resin

A Tosoh TSKgel SCX styrene–divinyl benzene copolymer-based strongly acidic cation-exchange resin in the H^+ form with a particle size of 5 μm and an exchange capacity of 4.2 mequiv. g^{-1} was used for all chromatographic runs.

2.4. Reagents and solutions

Standard solutions of aliphatic carboxylic acids and other inorganic acids were prepared as the acid or the salt from analytical-reagent grade chemicals without further purification.

Aqueous eluents containing polyols and sugars were prepared as 0.025–0.3 *M* solutions by dissolving the polyols (methanol, ethylene glycol, glycerol, erythritol, xylithol and sorbitol) and sugars (fructose and sucrose) in distilled, deionized water.

Methanol, ethylene glycol and glycerol were obtained from Wako (Osaka, Japan) and the other polyols, fructose and sucrose from Nikken Kasei (Tokyo, Japan).

3. Results and discussion

3.1. Effect of eluent composition on the separation and detection of carboxylic acids

As is well known, although carboxylic acids are separated from each other by elution with water, the resolution is very low and the peaks are fronted owing primarily to the hydrophobic adsorption effect as a side-effect in the IEC [6]. In an attempt to reduce peak fronting, polyols and sugars such as ethylene glycol, glycerol,

erythritol, xylitol, sorbitol, fructose and sucrose were tested and the elution performances were compared for the separation of various carboxylic acids. As shown in Table 1, these polyols and sugars have different numbers of alcoholic OH groups in the molecules.

Fig. 1a shows a complete IEC separation of strong acid (HCl) and C_1–C_5 aliphatic carboxylic acids with water as the eluent. As expected from the results in our previous papers on fundamental IEC research [4,6–9], the separation time was very long and the peaks were fronted, especially for the hydrophobic carboxylic acids such as propionic, butyric, and valeric acids. This is a consequence of an adsorption effect.

Fig. 1b shows a complete IEC separation of the strong acid (hydrochloric acid) and the carboxylic acids with 0.5 m*M* sulfuric acid as eluent. As expected from previous work [1,6], a high-resolution chromatogram was obtained by elution with 0.5 m*M* sulfuric acid, but the separation time was longer than with water as eluent and the conductimetric detection sensitivity was lower than with water as eluent. Additionally, the eluent background conductivity was extremely high and very noisy.

Fig. 1c–j show the IEC separation of the strong acid and the carboxylic acids by elution with polyols and sugars. As can be seen from the peak shape of valeric acid, fronting was dramatically decreased with increasing number of OH groups in the polyols and sugars. This means that the hydrophobicity of the PS–DVB cation-exchange resin surface was decreased by the adsorption of the polyols and sugars. Hence it is possible to modify the polarity of the cation-exchange resin surface by adsorption of polyols and sugars, especially using sucrose with eight alcoholic OH groups.

Table 1
Characteristics of polyols and sugars tested as eluents in ion-exclusion chromatography on a cation-exchange resin column for the separation of hydrochloric acid and some aliphatic acids

Polyol or sugar	Formula	No. of alcoholic OH groups
Methanol[a]	CH_3OH	1
Ethylene glycol[a]	$C_2H_6O_2$	2
Glycerol[a]	$C_3H_8O_3$	3
Erythritol[a]	$C_4H_{10}O_4$	4
Xylitol[a]	$C_5H_{12}O_5$	5
Fructose[b]	$C_6H_{12}O_6$	5
Sorbitol[a]	$C_6H_{14}O_6$	6
Sucrose[b]	$C_{12}H_{22}O_{11}$	8

[a] Alcohols (polyols).
[b] Sugars.

The retention volumes (V_R) of all carboxylic acids gradually increased with increasing number of OH groups in the polyols except methanol and sugars. The V_R of valeric acid increased from 41.1 mL for water as eluent to 47.1 ml for 0.2 *M* sucrose–water.

On the other hand, the V_Rs of carboxylic acids decreased with 0.2 *M* methanol–water as eluent compared with those with water and other polyol and sugar eluents. The V_R of valeric acid decreased from 41.1 ml with water to 34.5 ml with 0.2*M* methanol–water. This decrease might be due to the effect of the lipophilic property of the alkyl group in methanol rather than that of the hydrophilic property of the alcoholic OH group in methanol.

Although the mechanism of IEC is considered to involve partitioning of various analytes between the predominantly aqueous eluent and water inside the resin gel, several workers have proposed a mixed-mode mechanism in which there is also partitioning of the analytes due to the hydrophobic attraction of the analytes for the polymeric resin matrix [8,10,11].

The function of methanol in the eluent is to reduce this hydrophobic attraction by providing better solvation of the analytes in the mobile phase. However, sugar in the mobile phase is more effective in sharpening the sample peaks. The sugar additive coats the resin surface by a dynamic equilibrium between the liquid phase and the resin surface. The OH groups of the sugar make the resin surface more hydrophilic and decrease the attraction of the lipophilic parts of the analyte molecules.

Previous work has shown that sugars are indeed retained by ion-exchange resins [8]. Ali-

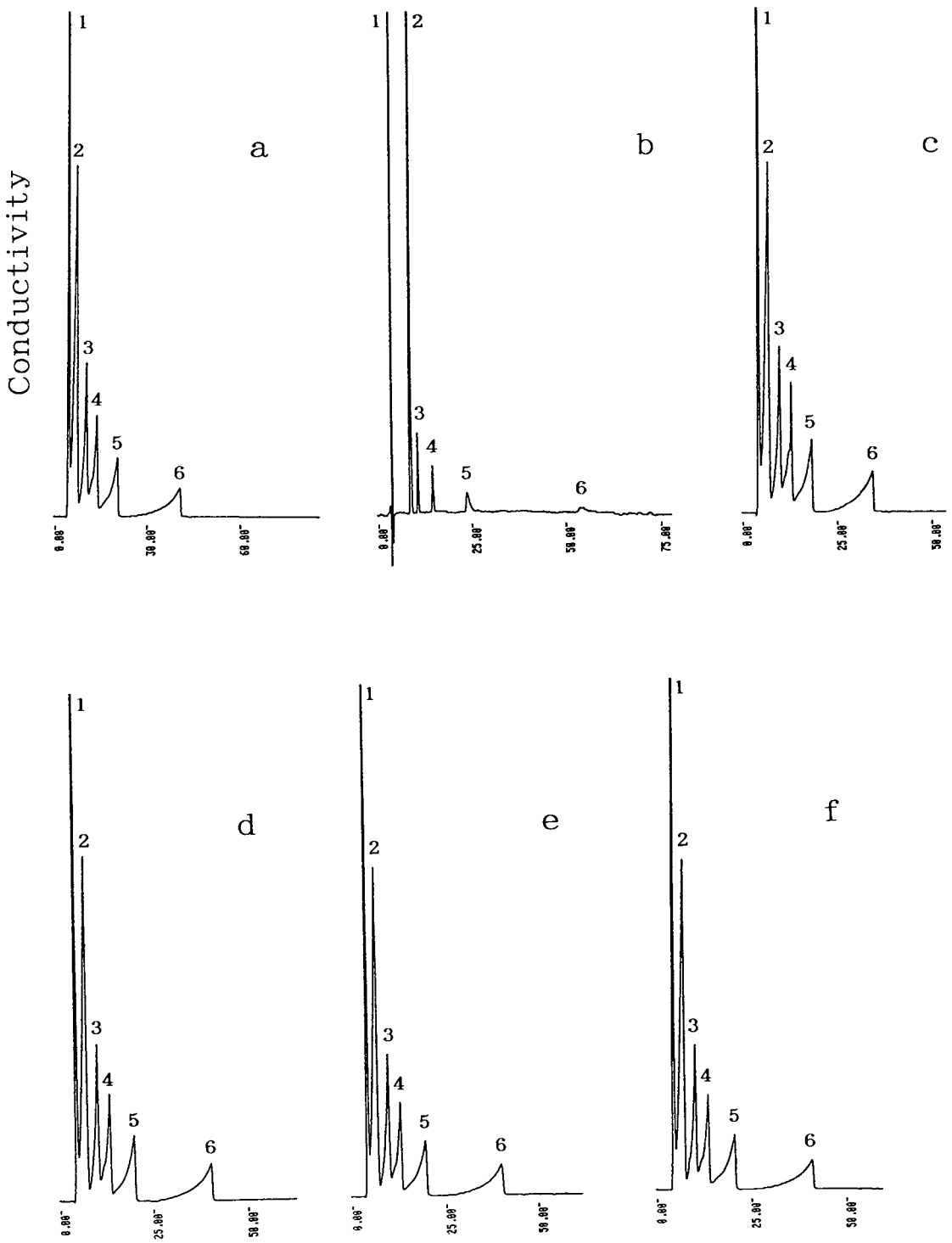

Fig. 1.

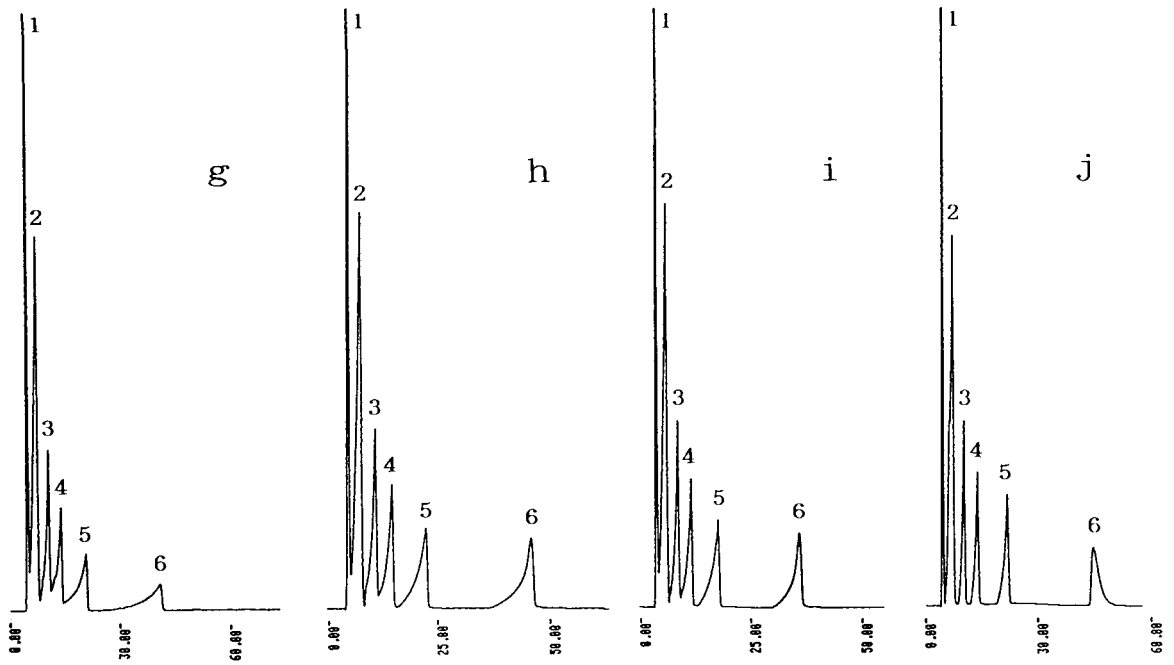

Fig. 1. Effect of eluent composition on IEC separation and conductimetric detection of a strong acid and some aliphatic carboxylic acids. Eluent: (a) water; (b) 0.5 m*M* sulfuric acid; (c) 0.2 *M* methanol–water; (d) 0.2 *M* ethylene glycol–water; (e) 0.2 *M* glycerol–water; (f) 0.2 *M* erythritol–water; (g) 0.2 *M* xylitol–water; (h) 0.2 *M* fructose–water; (i) 0.2 *M* sorbitol–water; (j) 0.2 *M* sucrose–water. Eluent flow-rate, 1 ml min^{-1}; column, Tosoh TSKgel SCX strongly acidic cation-exchange resin in the H^+ form (300 mm × 8 mm I.D.); column temperature, room temperature (20°C); sample concentration, 1 m*M* each; sample volume, 100 μl; detection sensitivity, 40 μS cm^{-1} full-scale (for sulfuric acid eluent, 16 μS cm^{-1} full-scale); unit of retention time, min. Peaks: 1 = strong acid (hydrochloric acid); 2 = formic acid; 3 = acetic acid; 4 = propionic acid; 5 = butyric acid; 6 = valeric acid. All figures time scale in min.

phatic alcohols such as *n*-butanol have also been found to sharpen carboxylic acid peaks by altering the resin surface [9].

It is well known that in conventional IEC with conductimetric detection using sulfuric acid as eluent, the detector responses of carboxylic acids decrease owing to ionization suppression by the H^+ ion of sulfuric acid [6,9]. To demonstrate the usefulness of polyols and sugars as eluents in IEC with conductimetric detection, the detector responses of carboxylic acids were compared.

As can be seen from the chromatograms of carboxylic acids with various polyols and sugars as eluents in Fig. 1, the detector responses of both formic and acetic acid were almost the same as those with water as eluent. The background conductivities of these polyol and sugar eluents were very low, viz., just ca. 6 μS cm^{-1} even with 0.3 *M* sucrose as eluent. Therefore, the noise level on the eluent background conductivity signal was extremely low.

From the above results, sucrose was judged to be the optimum eluent for the IEC separation and conductimetric detection of carboxylic acids.

3.2. Effect of sucrose concentration

In order to determine the optimum concentration of sucrose in the eluent, the effect of sucrose concentration on the IEC separation and conductimetric detection of some carboxylic acids was studied using 0.025–0.3 *M* sucrose. The V_Rs of carboxylic acids increased slightly

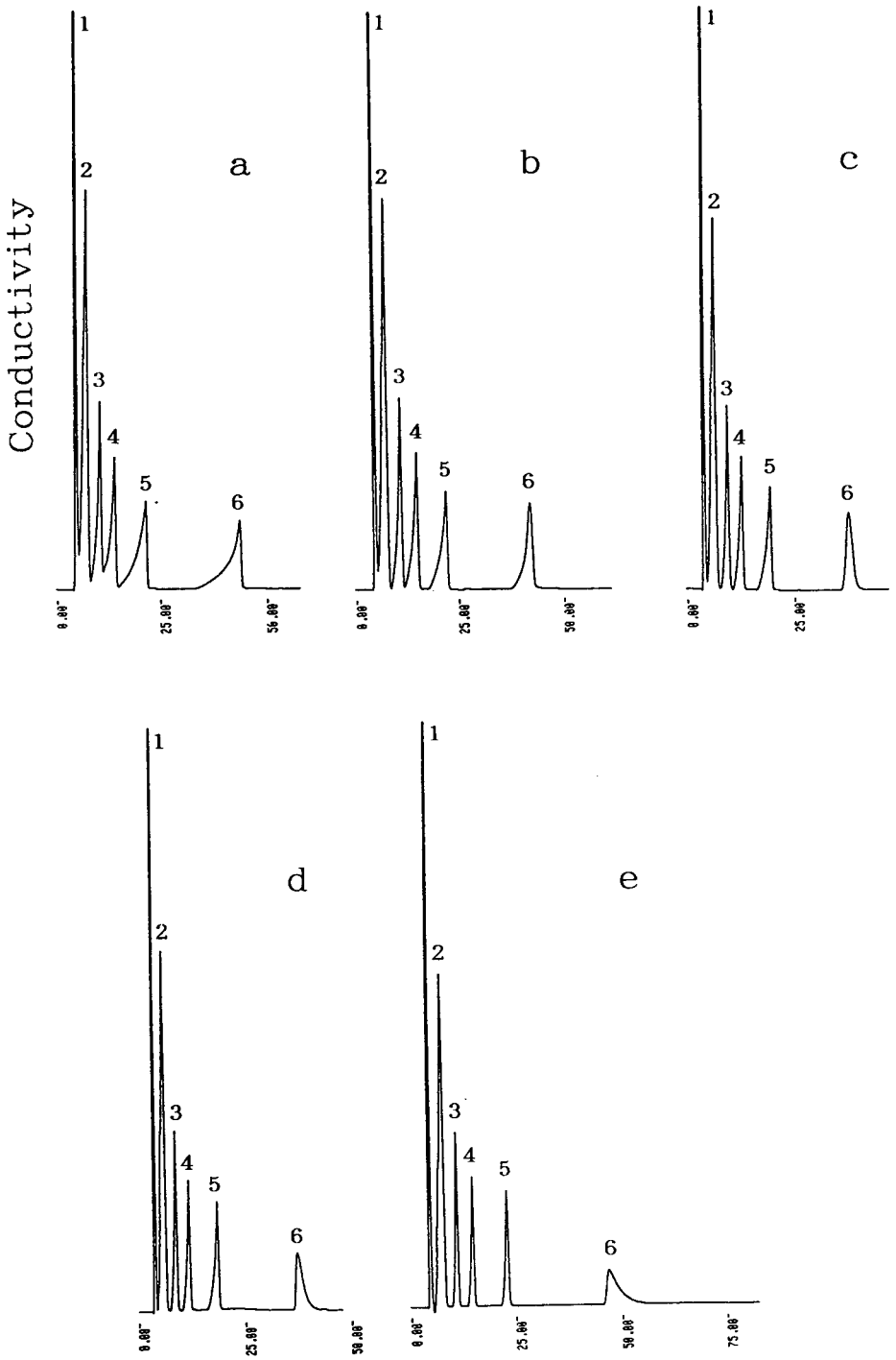

Fig. 2. Effect of sucrose concentration in eluent on IEC separation and conductimetric detection of hydrochloric acid and some carboxylic acids. Sucrose concentration: (a) 0.05; (b) 0.1; (c) 0.15; (d) 0.2; (e) 0.3 *M*. Other chromatographic conditions and peak identification as in Fig. 1.

with increasing concentration of sucrose in the eluent, as shown in Fig. 2. The background conductivity of the sucrose eluent ranged from ca. 0.5 μS cm^{-1} at 0.025 *M* to ca. 6 μS cm^{-1} at 0.3 *M*.

Although the detector responses(peak height) of carboxylic acids decreased with increasing concentration of sucrose in the eluent, there was no effect on the peak-area method, as shown in Fig. 2. A good chromatogram of carboxylic acids without fronting was obtained by elution with 0.15 *M* sucrose, as shown in Fig. 2d.

3.3. Effect of methanol concentration

As described previously [2], addition of an organic solvent to the eluent might be expected to reduce the adsorption of propionic, butyric and valeric acid on the cation-exchange resin surface and thus decrease their V_Rs. Additionally, the results described in the previous section (Fig. 1) indicated that the addition of methanol to an aqueous eluent decreases the V_Rs of hydrophobic aliphatic carboxylic acids such as propionic, butyric and valeric acid. Therefore, the effect of methanol concentration in the eluent on the V_Rs of carboxylic acids was examined. The results are shown in Fig. 3 for the addition of methanol to the 0.15 *M* sucrose eluent.

The decrease in the V_Rs of the hydrophobic carboxylic acids by addition of methanol to the sucrose eluent might be due to the effect of the lipophilic property of the alkyl group in methanol rather than that of the hydrophilic property of the alcoholic OH group in methanol.

The detector responses of carboxylic acids gradually decreased with increasing concentration of methanol in 0.15 *M* sucrose eluent, as shown in Fig. 3.

A reasonable separation and detection of carboxylic acids was accomplished by elution with 10% methanol in 0.15 *M* sucrose eluent, as shown in Fig. 3b. This eluent was chemically stable and there was no occurrence of fungi

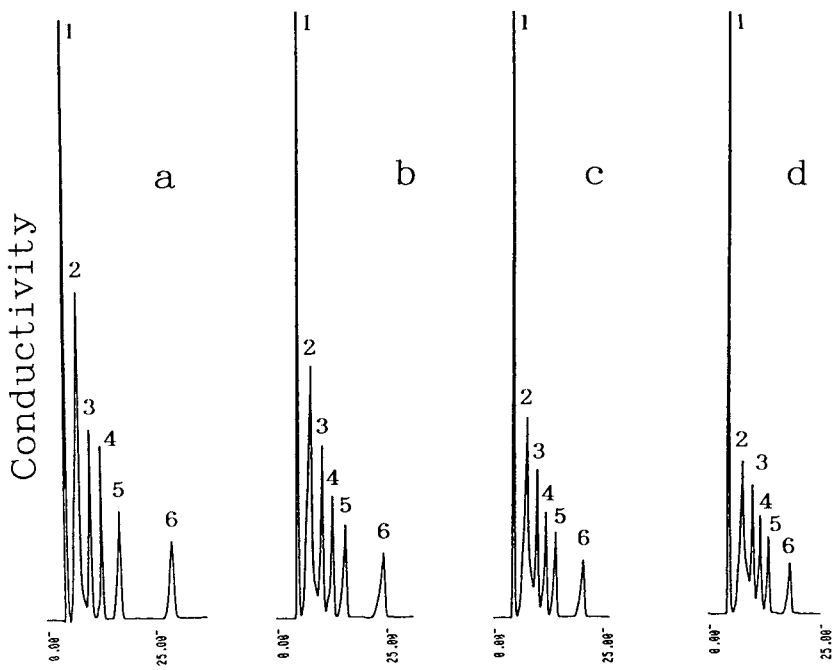

Fig. 3. Effect of methanol concentration in 0.15 *M* sucrose eluent on IEC separation and conductimetric detection of hydrochloric acid and some carboxylic acids. Methanol concentration: (a) 5; (b) 10; (c) 15; (d) 20%. Other chromatographic conditions and peak identification as in Fig. 1.

during chromatographic runs for several weeks, even at room temperature.

3.4. Retention volumes and distribution coefficients

The V_Rs and the distribution coefficients (K_d) of various carboxylic acids with 10% methanol–0.15 *M* sucrose as eluent are given in Table 1. The K_d values were calculated according to the following equation, which was given in previous papers [4,6]:

$$V_R = V_0 + K_d V_i$$

where V_R is retention volume, V_0 the column void volume and V_i the volume of liquid inside the resin in the column.

As can be seen from Table 2, the K_d values of carboxylic acids tend to increase with increasing pK_1 and hydrophobicity. Most of the K_d values are between 0 and 1, but those of propionic, butyric and valeric acid are greater >1. This means that adsorption by the resin matrix is a side-effect due to the greater hydrophobic nature of these acids.

Table 2
Retention volumes (V_R) and distribution coefficients (K_d) of a strong acid (hydrochloric acid), a very weak acid (carbonic acid) and weak acids (carboxylic acids) by elution with 10% methanol–0.15 *M* sucrose

Acid	pK_1	V_R (ml)[a]	K_d[a]
Hydrochloric acid	−7	4.98	0
Formic acid	3.8	8.02	0.34
Acetic acid	4.8	10.57	0.63
Propionic acid	4.9	12.58	0.86
Butyric acid	4.8	15.22	1.24
Valeric acid	4.8	25.22	2.28
Oxalic acid	1.3	5.00	0.00
Malic acid	1.9	6.45	0.17
Malonic acid	2.9	5.77	0.09
Tartaric acid	3.0	5.82	0.09
Citric acid	3.2	5.95	0.11
Succinic acid	4.2	8.54	0.40
Carbonic acid	6.4	13.85	1.00

Other chromatographic conditions as in Fig. 1.
[a] $V_R = V_0 + K_d V_i$; $V_0 = 4.98$ ml, $V_i = 8.87$ ml.

3.5. Calibration graph

A calibration graph was obtained by plotting peak height against carboxylic acid concentration in the range 0–3 m*M*. The calibration graph obtained was non-linear at concentrations >2 m*M*. This might be due to mainly to the decrease in the degree of dissociation of carboxylic acids at higher concentrations.

3.6. Reproducibility

The reproducibility of peak heights obtained by repeated injections of 1 m*M* standards is ca. 0.8% (relative standard deviation) for all the carboxylic acids.

3.7. Detection limits

The detection limits of carboxylic acids at a signal-to-noise ratio (S/N) of 3 on elution with 10% methanol–0.15 *M* sucrose are given in Table 3. As this method uses a non-acidic eluent, the eluent background conductivity was much lower (ca. 4 μS cm^{-1}) than that with 0.5 m*M* sulfuric acid as eluent (ca. 390 μS cm^{-1}). There-

Table 3
Comparison of detection limits of carboxylic acids by elution with (A) 0.5 m*M* sulfuric acid, (B) water and (C) 10% methanol–0.15 *M* sucrose

Acid	Detection limit (S/N = 3) (μM)		
	A[a]	B[b]	C[c]
Formic acid	8.4	0.12	1.40
Acetic acid	84	0.27	2.50
Propionic acid	150	0.40	3.44
Butyric acid	330	0.70	4.34
Valeric acid	1200	1.61	6.88

Other chromatographic conditions as in Fig. 1.
[a] Eluent background conductivity, 390 μS cm^{-1}; noise level, 0.21 μS cm^{-1}.
[b] Eluent background conductivity, ca. 390 μS cm^{-1}; noise level, 0.00321 μS cm^{-1}.
[c] Eluent background conductivity, ca. 4 μS cm^{-1}; noise level, 0.0236 μS cm^{-1}.

fore, the noise level on the eluent background conductivity was extremely low (0.0236 μS cm^{-1}). As there is no ionization suppression of carboxylic acids by H^+ ion in the acidic eluent, the detector response was as highly sensitive as the water eluent. The detection sensitivities of carboxylic acids (valeric acid) were ca. 6.5–174 times higher than those in conventional conductimetric IEC using sulfuric acid as the eluent, depending on their pK_a and V_R valves, as shown in Table 3.

Acknowledgements

We thank Mr. T. Uraji of Nikken Kasei for providing several polyols and sugars and for useful suggestions. This work was supported, in part, by the Agency of Industrial Science and Technology of the Ministry of International Trade and Industry in Japan, based on a Cooperative Agreement on Science and Technology for acid rain monitoring research by ion chromatography between the NIRIN and the AL/ISU, and also based on a Cooperative Agreement on Environmental Science and Technology for environmental water quality monitoring research by ion chromatography between the NIRIN and the CWRQM/CBNU.

References

[1] V.T. Turkelson and M. Richards, *Anal. Chem.*, 50 (1978) 1420.
[2] P.R. Haddad and P.E. Jackson, *Ion Chromatography*, Elsevier, Amsterdam, 1990.
[3] J.S. Fritz, *J. Chromatogr.*, 546 (1991) 111.
[4] K. Tanaka, T. Ishizuka and H. Sunahara, *J. Chromatogr.*, 174 (1979) 153.
[5] B.K. Glod and W. Kemula, *J. Chromatogr.*, 366 (1986) 39.
[6] K. Tanaka and J.S. Fritz, *J. Chromatogr.*, 361 (1986) 151.
[7] S. Nakajima, H. Harada, K. Tanaka, R. Kurokawa and R. Nakashima, *Suido Kyokai Zasshi*, 58, No. 6 (1989) 21.
[8] K. Tanaka and J.S. Fritz, *J. Chromatogr.*, 409 (1987) 271.
[9] J. Morris and J.S. Fritz, *Anal. Chem.*, 66 (1994) 2390.
[10] R.E. Smith, *Ion Chromatography Applications*, CRC Press, Boca Raton, FL, 1990.
[11] D.P. Lee and A.D. Lord, *LC · GC*, 4 (1987) 261.

ELSEVIER

Journal of Chromatography A, 706 (1995) 395–403

JOURNAL OF CHROMATOGRAPHY A

Use of ion chromatography for the measurement of organic acids in fruit juices

G. Saccani*, S. Gherardi, A. Trifirò, C. Soresi Bordini, M. Calza, C. Freddi

Stazione Sperimentale per l'Industria delle Conserve Alimentari, V.le F. Tanara 31/A, 43100 Parma, Italy

Abstract

A gradient ion chromatographic method to separate and determine main organic acids in fruit juices was developed. The method allows the separation of organic anions on Dionex OMNI PAC PAX-500 column by NaOH gradient elution and conductometric detection. The main organic acids of fruit juices (citric, malic, tartaric) were separated together with other less abundant acids. More than 500 samples of fruit juices were analysed, mainly orange juices from Brasil, Italy, Florida, California, as well as apple, cherry, grape and blackcurrant juices of different origin. The method has shown a high sensitivity and a satisfactory accuracy. The method also allows the simultaneous separation of lactic and acetic acids, produced by microbiological spoilage of juices, and of some important inorganic anions such as chlorides and nitrates.

1. Introduction

The identification and dosing of the various organic acids present in a fruit juice are of considerable importance, since they provide at the same time useful information regarding not only the authenticity of the product under examination but also regarding any processes of microbiological alteration it may have undergone previously.

At present, organic acids are measured [1–7] using enzymatic methods or liquid chromatographic techniques. Enzymatic analyses, however, require specific kits for each individual organic acid, they are rather time-consuming and use large amounts of reagents. The traditional HPLC techniques with refraction index or UV detection not always allow the separation of minor organic acids and often require preventive purification techniques to eliminate, for example, the interference of sugars or phenolic compounds, in particular the anthocyanines in red juices. This has a negative influence on the simplicity and rapidity of the method, especially evident in the case of routine quality control analysis. The introduction of conductivity detectors combined with ion chromatography with chemical suppression, has eliminated many of the above mentioned problems. Initially, this technique was applied above all to the analysis of inorganic ions [8–15], but recently methods suitable for the measurement of organic anions have also been developed [16,17].

The aim of the present work was thus to optimize the method proposed for wine samples by Kupina et al. [17] in order to develop a reliable and highly sensitive method allowing the

* Corresponding author.

0021-9673/95/$09.50
SSDI 0021-9673(95)00206-5

measurement not only of the main organic acids present in fruit juices (citric, malic and tartaric) but also of the minor acid compounds (galacturonic, isocitric, lactic and acetic) without the need for previous purification procedures.

2. Experimental

2.1. Instrumentation

The chromatographic system consisted of three Model 306 pumps with titanium head, a Model 805 electronic dumper, a Model 811C dynamic mixer, a Model 231 automated sample-injector (all from Gilson Medical Electronics, France), and a Model 431 conductivity detector (Waters, Milford, MA, USA).

The following columns and accessories were from Dionex Corp (Sunnivale, CA, USA): OmniPac Pax-500 Guard Column (P/N 42153) 50 × 4 mm I.D., OmniPac Pax-500 Column (P/N42152) 250 × 4 mm I.D., eluent purification column Ion pac ATC-1 (P/N 37151).

Chemical suppression was achieved by the Anion Micromembrane Suppressor AMMS-II (P/N 43074) with about 50 m*M* H_2SO_4 regenerant at a flow-rate of approximately 2 ml/min.

Acquisition and integration of chromatograms was performed with an AT 386 personal computer linked with a Gilson GSIOC 506 C system interface.

2.2. Chemicals

The eluents were prepared using redistilled water, anhydrous ethyl alcohol (J.T. Baker, Philipsburg, NJ, USA), methyl alcohol (HPLC grade, Carlo Erba, Milan, Italy) and 50% NaOH (J.T. Baker).

The samples were calibrated using solutions prepared with citric, malic, tartaric and acetic acids (Carlo Erba), D-isocitric, shikimic and lactic acids (Sigma, St. Louis, MO, USA), galacturonic acid (Merck, Darmstadt, Germany) and quinic acid (Fluka, Buchs, Switzerland).

The method under evaluation also allows the simultaneous separation of inorganic anions; for this purpose, standard mixtures were prepared containing chlorides (KCl), phosphates ($NaH_2PO4 \cdot H_2O$), nitrates ($NaNO_3$) and sulfates (Na_2SO_4) (Carlo Erba).

For all anions, stock solutions of 1000 mg/l were prepared weekly in redistilled water and, from these, mixtures were made with a concentration suitable to construct calibration curves over a linear range, depending on the amounts naturally occurring in the juices examined.

2.3. Mobile phases

Ternary gradient elution with a 1 ml/min flow-rate was used with the following mobile phases: Eluent A, 0.60 m*M* NaOH in water–ethanol–methanol (66.5:20:13.5, v/v); eluent B, 20 m*M* NaOH in water–ethanol (65:35, v/v); eluent C, 60 m*M* NaOH in water–ethanol (65:35, v/v). A linear gradient was used as shown in Table 1.

All solvents were filtered (0.45 μm) and degassed in an ultrasonic bath under vacuum for 5 min.

The operating conditions were: room temperature; injection volume, 20 μl; conductivity detector, 10 μS FS.

Table 1
Eluent gradient for ion chromatography

Time (min)	Eluent A (%)	Eluent B (%)	Eluent C (%)
0	100	0	0
4	100	0	0
15	0	100	0
19	0	100	0
27	0	0	100
39	0	0	100
40	100	0	0

Equilibration time between each injection: 15 min.

2.4. Sample preparation

Around 500 samples of orange, grapefruit, apple, grape, cherry and blackcurrant juices were taken into consideration. Particular attention was given to orange juices (ca. 60% of the samples), subdivided with respect to provenance area and extraction technology (first and second pressing juices). All samples were diluted with redistilled water to obtain organic acid concentrations falling within the linear range of the calibration curves, filtered with 0.45-μm filters and frozen at −18°C up to the time of analysis.

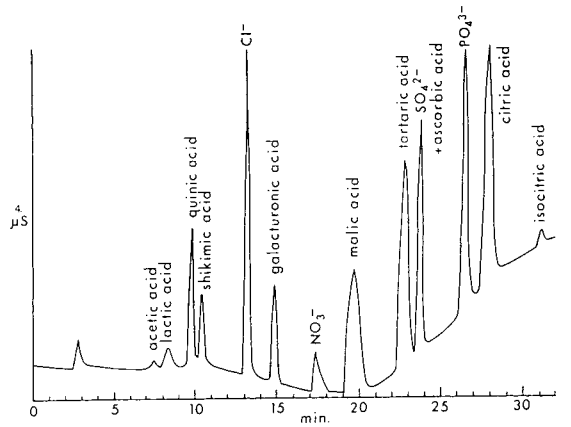

Fig. 1. Chromatogram of organic and inorganic anion standard solution.

3. Results and discussion

Reproducibility was tested by performing six analyses of a standard mixture containing the various organic acids. The data summarized in Table 2 show a good reproducibility.

Optimization of the analytical conditions resulted in the separation of a large number of organic and inorganic anions, as shown in Fig. 1; the concentrations of the various anions and their relative retention times are reported in Table 3 together with the determination limits.

The chromatograms presented in Figs. 2–4 show the profiles characteristic of the separation of organic and inorganic anions for orange, apple and grape juices; it can be seen that ion chromatography allows quantitation of the acids under study with acceptable sensitivity, despite the complexity of the matrices and the considerable quantitative imbalances between the various anions.

The differences in composition for the organic acids can be clearly seen in Tables 4–8, each of which refers to an individual organic acid.

As to the characterization of the examined orange juices, particular attention was paid not only to the data regarding citric, malic and isocitric acids, but also to the citric acid/malic acid and citric acid/isocitric acid ratios; these data were subsequently related to provenance area and extraction technology.

Table 2
Reproducibility tested on standard solutions ($n = 6$)

	Concentration (mg/l)	S.D.	R.S.D. (%).
Citric acid	750	22	2.88
Malic acid	200	3	1.55
Isocitric acid	10.0	0.2	2.04
Tartaric acid	750	15	1.94

S.D. = standard deviation; R.S.D. = relative standard deviation.

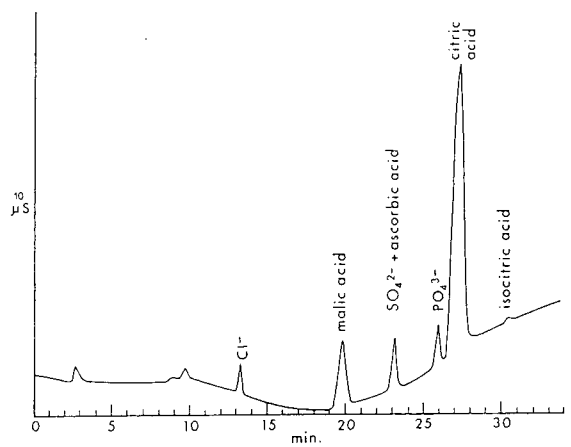

Fig. 2. Chromatogram of orange juice. Sample dilution 1:10.

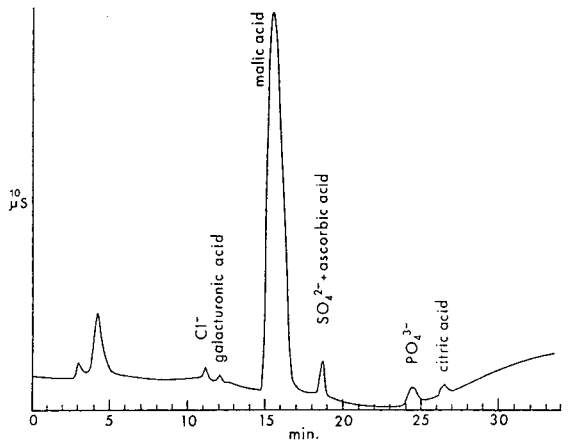

Fig. 3. Chromatogram of apple juice. Sample dilution 1:10.

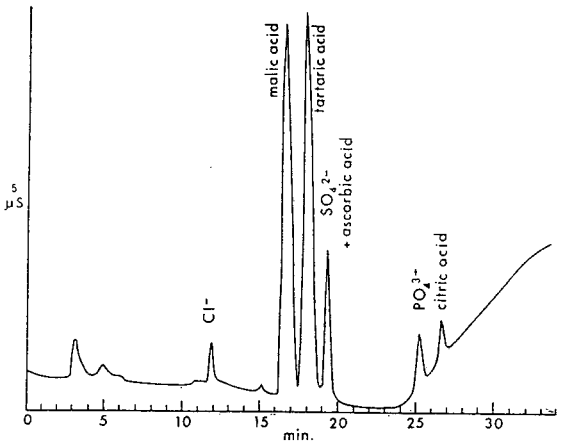

Fig. 4. Chromatogram of grape juice. Sample dilution 1:25.

The citric acid content (Table 4) shows considerable differences between samples based on provenance area, variety and extraction technology: juices coming from the Americas (Argentina, Brazil, Uruguay, Cuba, Florida and California) are characterized by a citric acid mean value substantially lower than that found in juices from the Mediterranean area (Morocco, Egypt, Israel) but above all in those of Italian provenance, which are characterized by high values. Extraction technology also influences the citric acid content, which is higher in first pressing juices; furthermore, juices of Italian origin obtained from pigmented orange varieties show lower values than those obtained from oranges of the "Biondo comune" variety.

For isocitric acid (Table 5), an analogous behaviour to that described for citric acid was observed, while for malic acid (Table 6) no significant differences between the various samples were found.

The citric acid/malic acid ratio (Table 8 and Fig. 5) reveals all the more significant differences: in particular, it can be seen that this ratio is always lower in second pressing juices than in first pressing juices, and that pigmented Italian

Table 3
Retention times and concentrations of standards in Fig. 1. For each anion the determination limit is also reported

	Retention time (min)	Concentration (mg/l)	Determination limit (mg/l)
Acetic acid	7.3	10	10
Lactic acid	8.3	10	10
Quinic acid	9.7	50	20
Shikimic acid	10.3	50	20
Chloride	13.0	10	2
Galacturonic acid	14.8	50	10
Nitrate	17.0	5	2
Malic acid	19.6	100	10
Tartaric acid	22.6	100	10
Sulfate + ascorbic acid	23.5	10 + 50	–
Phosphate	26.3	50	10
Citric acid	27.7	200	10
Isocitric acid	30.9	10	10

Table 4
Citric acid content (g/l) in different fruit juices

		Min.	Av.	Max.	*n*	S.D.
Orange juices (data referred to 11.2°Bx)	Italy Blond I pressing	10.42	20.05	26.62	15	4.68
	Italy Red I pressing	12.29	14.92	19.36	10	2.69
	Italy Mix I pressing	13.09	18.21	24.21	14	3.44
	Italy Blond II pressing	2.24	9.24	16.27	7	4.69
	Italy Red II pressing	5.12	8.28	12.99	7	2.59
	Italy Mix II pressing	8.04	10.01	14.03	7	1.98
	Mediterranean Basin	7.67	11.53	14.94	15	2.01
	Brasil-I pressing	6.32	9.01	17.24	58	1.80
	Brasil-II pressing	1.64	7.83	12.86	37	2.03
	Others South America	4.64	11.44	17.99	20	3.20
	USA and CUBA	3.57	8.36	19.40	34	3.70
Grapefruit juices (data referred to 10.0°Bx)		8.33	15.94	26.68	28	3.89
Apple juices (data referred to 11.2°Bx)	Germany	0.03	0.08	0.14	42	0.02
	Italy	0.02	0.06	0.13	28	0.02
	Others	0.03	0.06	0.11	14	0.02
Grape juices (data referred to 16.0°Bx)	France	0.15	0.24	0.41	21	0.06
	Italy	0.17	0.39	0.85	31	0.15
Cherry juices (data referred to 14.0°Bx)		0.05	0.23	0.62	40	0.14
Blackcurrant juices (data referred to 12.5°Bx)		21.15	29.63	65.44	67	5.37

S.D. = standard deviation.

juices show values lower than those obtained from oranges of the "Biondo comune" variety. In the latter, the citric acid/malic acid ratio of first pressing juices shows mean values clearly higher than those measured in the samples of American provenance.

Knowledge of the full profile of organic acids in a fruit juice has the undoubted advantage of enabling the immediate identification of the presence of acids not characteristic of the juice under examination and allows detection of the addition of a juice of different origin (of commercially lower value) and of previously occurring fermentation.

Thus Fig. 6 shows that the addition of a low percentage of pear juice (which usually has a citric acid mean value of 2.9 g/l) is detected by a considerable increase in the citric acid content. In cherry juice samples (Fig. 7) the addition of red beet juice is revealed by a rise in the chloride, nitrate and citric acid peaks. Fig. 8 shows the chromatogram of a red grape juice to which a low percentage of blackberry juice had been added, the addition being evident from the notable increase in isocitric acid, which is a characteristic of blackberry juice.

Examination of the acetic acid and lactic acid peaks leads to the detection of the onset of microbiological alteration the sample may have undergone; an example can be seen in the chromatogram in Fig. 9, referring to an altered orange juice sample.

The detection and dosing of galacturonic acid is an important reference index for judging the quality of a juice: galacturonic acid is the monomer constituting the pectin chain and thus its

Table 5
Isocitric acid content (mg/l) in different fruit juices

		Min.	Av.	Max.	*n*	S.D.
Orange juices (data referred to 11.2°Bx)	Italy Blond I pressing	154	201	232	11	25
	Italy Red I pressing	103	127	153	5	21
	Italy Mix I pressing	149	166	206	7	22
	Italy Blond II pressing	120	145	188	3	37
	Italy Red II pressing	83	97	114	4	13
	Italy Mix II pressing	–	–	–	–	–
	Mediterranean Basin	69	162	282	15	58
	Brasil-I pressing	51	83	185	58	21
	Brasil-II pressing	16	73	119	36	21
	Others South America	51	112	178	20	35
	USA and CUBA	28	94	228	31	42
Grapefruit juices (data referred to 10.0°Bx)		121	227	389	27	69
Cherry juices (data referred to 14.0°Bx)		traces	63	145	40	45
Blackcurrant juices (data referred to 12.5°Bx)		128	246	424	40	73

S.D. = standard deviation.

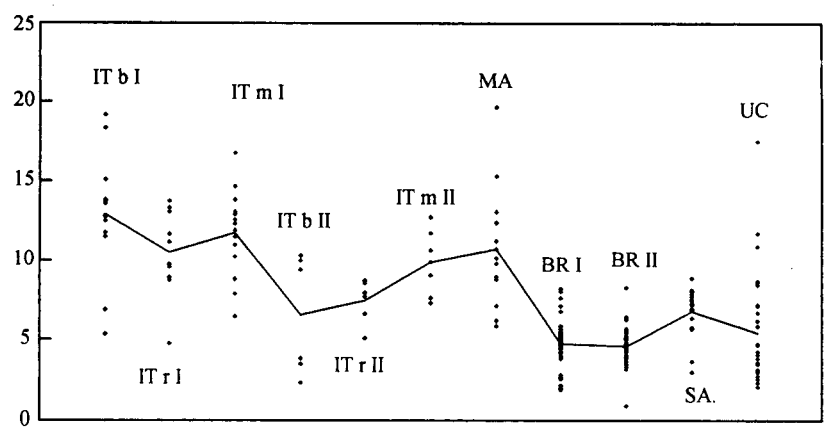

Fig. 5. Citric/malic ratio in different orange juices. IT bI = Italy Blond I pressing; IT rI = Italy Red I pressing; IT mI = Italy Mix I pressing; IT bII = Italy Blond II pressing; IT rII = Italy Red II pressing; IT mII = Italy Mix II pressing; MA = Mediterranean Basin; BR I = Brasil I pressing; BR II = Brasil II pressing; SA = other South America; UC = USA and Cuba.

Table 6
Malic acid content (g/l) in different fruit juices

		Min.	Av.	Max.	*n*	S.D.
Orange juices (data referred to 11.2°Bx)	Italy Blond I pressing	1.02	1.76	3.63	15	0.63
	Italy Red I pressing	0.92	1.53	2.70	10	0.51
	Italy Mix I pressing	1.07	1.61	2.12	14	0.36
	Italy Blond II pressing	0.94	1.36	1.98	7	0.34
	Italy Red II pressing	0.69	1.13	1.96	7	0.40
	Italy Mix II pressing	0.88	1.03	1.27	7	0.14
	Mediterranean Basin	0.19	1.16	2.12	15	0.48
	Brasil-I pressing	1.31	2.02	4.33	58	0.64
	Brasil-II pressing	1.11	1.72	2.53	37	0.34
	Others South America	1.22	1.68	2.22	20	0.27
	USA and CUBA	0.41	1.61	2.40	34	0.47
Grapefruit juices (data referred to 10.0°Bx)		0.18	0.52	1.00	28	0.19
Apple juices (data referred to 11.2°Bx)	Germany	4.18	7.14	11.48	43	1.43
	Italy	2.64	4.04	5.35	28	0.66
	Others	3.45	5.17	8.44	14	1.48
Grape juices (data referred to 16.0°Bx)	France	1.49	3.62	9.67	21	1.81
	Italy	1.99	4.48	9.62	31	1.87
Cherry juices (data referred to 14.0°Bx)		11.92	18.17	22.71	40	2.92
Blackcurrant juices (data referred to 12.5°Bx)		0.90	1.89	3.07	67	0.58

S.D. = standard deviation.

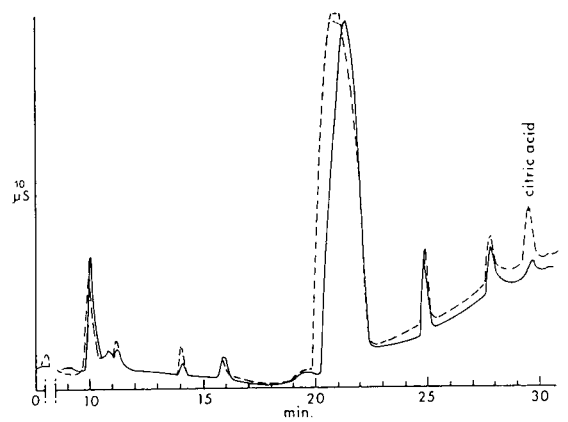

Fig. 6. Chromatograms of authentic apple juice (——) and apple juice with 10% of pear juice (– – –). Citric acid increase due to the addition of pear juice.

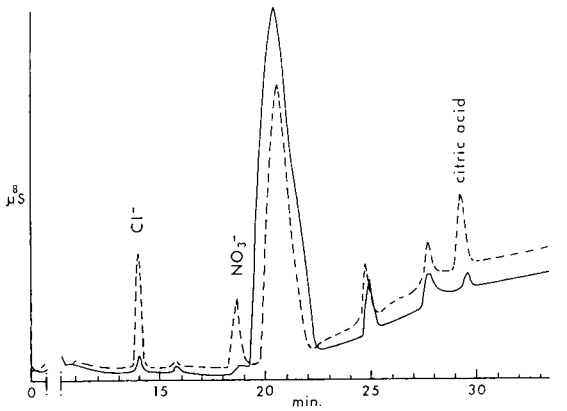

Fig. 7. Chromatograms of authentic cherry juice (——) and cherry juice with 10% of red beet juice (– – –). Chlorides, nitrates and citric acid increase due to the addition of red beet juice.

Table 7
Tartaric acid (g/l) content in grape juices

	Min.	Av.	Max.	*n*	S.D.
France	1.60	3.58	5.42	21	0.97
Italy	1.85	3.80	5.82	31	1.04

S.D. = standard deviation. Data referred to 16.0°Bx.

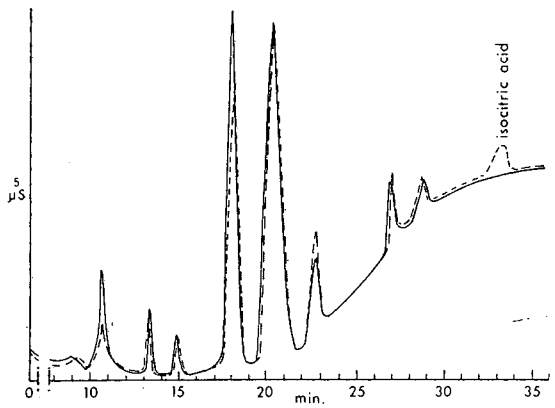

Fig. 8. Chromatograms of authentic red grape juice (——) and red grape juice with 5% of blackberry juice (– – –). Isocitric acid increase due to the addition of blackberry juice.

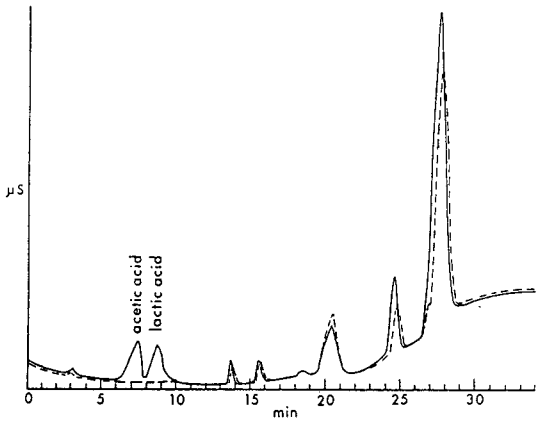

Fig. 9. Chromatograms of orange juices. The increase of acetic acid and lactic acid is indicative of microbial alteration.

presence in high quantities in a juice can be attributed to the spontaneous or induced enzymatic degradation of the pectins.

Therefore, while it is natural to find it in high quantities in clarified juices (Fig. 10), a high concentration of this compound in cloudy juices could indicate insufficient enzymatic inactivation.

Table 8
Citric acid/malic acid ratio in citrus juices

		Min.	Av.	Max.	*n*	S.D.
Orange juices	Italy Blond I pressing	4.81	12.40	19.18	15	4.09
	Italy Red I pressing	4.79	10.46	13.74	10	2.73
	Italy Mix I pressing	6.50	11.72	16.78	14	2.73
	Italy Blond II pressing	2.37	6.85	10.28	7	3.43
	Italy Red II pressing	5.11	7.49	8.76	7	1.26
	Italy Mix II pressing	7.27	9.86	12.76	7	2.04
	Mediterranean Basin	5.88	13.47	56.70	15	12.53
	Brasil-I pressing	1.90	4.76	8.19	58	1.30
	Brasil-II pressing	0.95	4.63	8.27	37	1.16
	Others South America	3.02	6.80	8.87	20	1.46
	USA and CUBA	2.14	5.92	17.52	34	3.65
Grapefruit juices		15.62	35.11	95.67	28	17.79

S.D. = standard deviation.

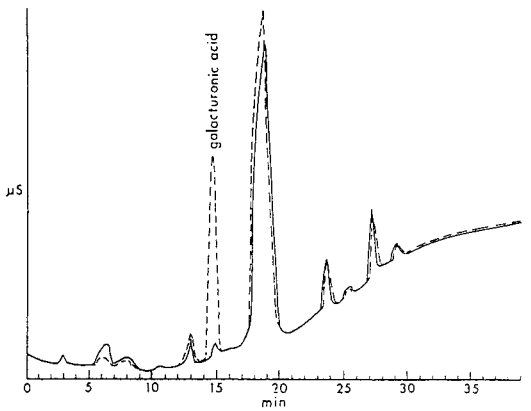

Fig. 10. Chromatograms of cloud apple juice (– – – – –) and clarified apple juice (———). Galacturonic acid increase due to the enzymatic degradation of pectins.

4. Conclusions

The analytical method proposed showed a high sensitivity and reproducibility and has the advantage of allowing quantitation of the main organic acids with a single analysis giving the complete profile of all the organic acids, including the minor ones, which characterize the juice.

Knowledge of the full organic acid profile is also very important in the control of the quality and genuineness of a juice.

Furthermore, ion chromatography also enabled the simultaneous separation of various inorganic anions of particular interest, such as chlorides and nitrates.

Finally, as for the characterization of orange juices, this study has shown the possibility of distinguishing Italian juices from those from other countries based on the organic acid content and their ratios; the extraction technique (first and second pressing juices) has also been found to have significant effects on the organic acid content.

Acknowledgement

This study was carried out within BCR-FLAIR program "Development of Advanced Analytical Methods for the Determination of the Authenticity of Fruit Juices" for the research "Determination of Organic Acids in Fruit Juices".

References

[1] J.D. Timpa and J.J. Burke, *J. Agric. Food Chem.*, 34 (1986) 910.
[2] M.C. Gancedo and B.S. Luh, *J. Food Sci.*, 51 (1986) 571.
[3] C.W. Wilson, P.E. Shaw and C.W. Campbell, *J. Sci. Food Agric.*, 33 (1982) 777.
[4] J.K. Palmer and D.M. List, *J. Agric. Food Chem.*, 21 (1973) 903.
[5] J.K. Palmer, The Connecticut Agricultural Experimental Station, New Haven, CT, *Bulletin 589* (1955).
[6] L. Bengtsson and O. Samuelson, *Anal. Chim. Acta*, 4 (1971) 93.
[7] L. Bengtsson, and O. Samuelson, *Chromatographia*, 4 (1971) 142.
[8] R.E. Barron and J. Fritz, *J. Chromatogr.*, 316 (1984) 201.
[9] D.T. Gjerde, J.S. Fritz and G. Schmuckler, *J. Chromatogr.*, 186 (1979) 509.
[10] D.T. Gjerde, G. Schmuckler and J.S. Fritz, *J. Chromatogr.*, 187 (1980) 35.
[11] H. Small, T.S. Stevens and W.C. Bauman, *Anal. Chem.*, 47 (1975) 1801.
[12] H.L. Heckenberg and P.R. Haddad, *J. Chromatogr.*, 299 (1984) 301.
[13] H.J. Cortes, *J. Chromatogr.*, 234 (1982) 517.
[14] P.R. Haddad and H.L. Heckenberg, *J. Chromatogr.*, 300 (1984) 357.
[15] A.A. Hafez, S.S. Goyal and D.W. Raines, *J. Chromatogr.*, 546 (1991) 387.
[16] *Dionex Application*, Dionex, Sunnyvale, CA, 1992.
[17] S.A. Kupina, C.A. Pohl and J.L. Ganotti, *Am. J. Enol. Vitic.*, 42 (1991) 1.

ELSEVIER

Journal of Chromatography A, 706 (1995) 405–419

JOURNAL OF CHROMATOGRAPHY A

Efficiency of chemical oligonucleotide synthesis evaluated by ion-exchange high-performance liquid chromatography

Zeno Földes-Papp[a,*], Eckhard Birch-Hirschfeld[b], Rudi Rösch[a], Manfred Hartmann[b], Albrecht K. Kleinschmidt[c], Hartmut Seliger[a]

[a]*Sektion Polymere, Universität Ulm, D-89069 Ulm, Germany*
[b]*Institut für Biotechnologie e.V., D-07745 Jena, Germany*
[c]*Universität Ulm, D-89069 Ulm, Germany*

Abstract

Ion-exchange high-performance liquid chromatography (HPIEC) is a method of choice for the separation of crude solid-phase synthesized oligonucleotides. It shows peaks for target and error sequences and it is used for quantification of oligonucleotide synthesis. This paper presents a homeodynamic model of polymer-supported oligonucleotide synthesis and a numerical solution, which accounts for elution profiles obtained by HPIEC. The elution profiles are consistent with the model. The chain-length distributions for 30mer syntheses on different support materials were also studied and the probability moment analysis was applied as a quantitative measure of the differential relationship of fractal dimension. The support systems for chemical synthesis of short oligonucleotides are classified according to this relationship.

1. Introduction

The preparation of high-purity oligonucleotides of extended length, large number or quantity is becoming increasingly important in genetic engineering [1–3], molecular biology and molecular medicine [4–6]. This is accomplished by chemical solid-phase synthesis on surface-reactive polymers as support systems [7].

Ion-exchange chromatography (IEC) is a method of choice for the purification and analysis of chemically synthesized oligonucleotides [8–11]. The separation of crude products of solid-phase synthesis is mainly based on the interaction of the negatively charged phosphate groups of the oligonucleotide backbone with the cations of the stationary phase. The elution profiles show peaks for target and error sequences. Error sequences are truncated or failure sequences formed in the course of oligonucleotide synthesis. No oligonucleotide synthesis provides 100% of the target sequence.

We are working on a theory for analysing chain-length distributions obtained in non-enzymatic and enzymatic nucleotide polymerization processes and at applying it to real systems. The modelling of HPIEC elution profiles is of practical relevance to oligonucleotide chemistry. The knowledge of the composition of the product provides information for various applications of synthetic nucleic acids fragments and their structurally modified analogues. Here we used the simulated HPIEC elution profiles to provide a basis for judging support systems of chemical

* Corresponding author.

0021-9673/95/$09.50
SSDI 0021-9673(94)01221-0

synthesis of short oligonucleotides by the fractal dimension, D_a.

2. Theory

Today, chemical oligonucleotide syntheses on solid supports are most frequently performed by phosphoramidite chemistry [12–14]. The synthesis is done by a cyclic repetition i of four reactions: detritylation, coupling (elongation), capping (termination) and oxidation in organic solvents. The chemical method of phosphoramidite synthesis used in this study exemplifies the general principle of multi-step condensation and capping reactions arranged in cyclic format. The same cyclic reaction principle of growth and termination of growth is put into practice in other chemical methods of oligonucleotide synthesis, e.g., when using H-phosphonate synthons.

In the condensation reaction the 3′ end of the incoming nucleotide building block binds covalently to the 5′ end of the immobilized chain. Chain propagation proceeds in the 3′ to 5′ direction (5′ to 3′ reactions are equally possible). In the capping reaction, the former unreacted chains are chemically capped, to some extent, to prevent them from reaction with the next incoming nucleotide building block. Nucleotide chains grow randomly with the coupling (elongation) probability d. The former unreacted chains (error sequences) stop growing with the capping (termination) probability p; d and p are independent of each other.

We have modelled analytically the dynamics of a non-enzymatic polymerization process by a new fractal formalism. Our fractal approach comes from fractal methods [15–22]. Here we elaborate on our theoretical concept in more details and compare it with experimental results obtained through IEC.

2.1. Growth model of chemical solid-supported oligonucleotide synthesis

We have recently formulated a model which generates variations of error sequences [23]. Error sequences l are truncated versions of a target sequence N. A sequence is based on entries of {0, 1, 2} [24]; 1 = nucleotide (arbitrary A, T, C, G); 0 = no nucleotide at position referring to the target sequence; 2 = stopping of growth. The sequence l of real numbers is a map $l: \mathbb{N} \rightarrow \mathbb{R}$ where the non-empty set of its members $L(\mathbb{N}) = \{l_j : j \in \mathbb{N}\}$. $\mathbb{N}$ and $\mathbb{R}$ denote the sets of positive integers and real numbers, respectively. The sum of all sequences might be generated by an iterative process (variation generator). The results of a probabilistic experiment such as chemical solid-supported oligonucleotide synthesis confirm this model. For the set L we assume that $N = \sup_{l \in L} l = \max\ L$ and $1 = \inf_{l \in L} l = \min\ L$. The model function

$$M(l, N) = M(l, N-1) + [M^{\cdot}(l-l, N-1) - M^{\cdot}(l, N-1)] \cdot d(N-1) \quad (1)$$

describes the relationships between these generated discrete sequences in the mathematical sequence space. Thus, M is the probability density of this homeodynamic system. $M^{\cdot}$ is the probability density of non-terminated error sequences:

$$M^{\cdot}(l, N) = M^{\cdot}(l, N-1) \cdot [1 - d(N-1) - p(N-1) + d(N-1) \cdot p(N-1)] + M^{\cdot}(l-1, N-1) \cdot d(N-1) \quad (2)$$

The probabilities d and p are explicit, real functions of the iteration step i satisfying $0 \leqslant d, p < 1$; d and p can be properly fitted in iteration steps i. Each particular solution is obtained from this general solution. This model depends on the nucleotide length N of a target sequence, the stepped-up probability of growth d and the stepped-up probability of termination of growth p. The experimental data are not sufficient to refine the model to highest resolution.

Theoretical analysis of properties of the model function (e.g., driving nucleotide polymerization) in the mathematical sequence space [25] shows, in principle, the validity of this function as applied to branched pseudorandom walks [26,27]. Operations of modelling were made for

arbitrary nucleotide sequences. We found that this kind of pseudo-random walks can be associated with frequency distributions M between the moments of probability of error sequences $M(l, N)$ and the moment of probability of the target sequence $M(N, N)$ with $l = \{N\}$.

2.2. Experimental validation of the growth model of chemical solid-supported oligonucleotide synthesis

For experimental validation of the model as described above, we consider here P as a probability which designates the relative frequency of the stochastic variable $\mathscr{L}(i)$. $\mathscr{L}(i)$ is completely characterized by the cumulative probability distribution $\Phi(l, N) = P(\mathscr{L} \leqslant l)$ with

$$\Phi(l, N) = \begin{cases} \sum_{l_j \leqslant 1} M(l_j, N) \text{ for discrete } \mathscr{L}: \\ \quad \begin{pmatrix} l_1 & l_2 & \cdots & l_n \\ M(l_1, N) & M(l_2, N) & \cdots & M(l_n, N) \end{pmatrix} \\ \quad \text{with} \begin{cases} M(l_j, N) = P(\mathscr{L} = l_j) \\ \sum_{l_j=1}^{N} M(l_j, N) = 1 \end{cases} \\ \int_1^l M(l, N)\, \mathrm{d}l \text{ for continuous } \mathscr{L}: \\ \quad \text{probability density } M(l, N) \\ \quad \text{with} \begin{cases} M(l, N) \geqslant 0 \\ \int_1^N M(l, N)\, \mathrm{d}l = 1 \end{cases} \end{cases} \tag{3}$$

The definition of a continuous stochastic variable $\mathscr{L}$ makes sense, because a suitable meaning for this property is, for example, the obtained resolution of the experimental technique used for separation of $\mathscr{L}$. Further, these formulations permit the quantitative evaluation of the synthesis parameters N, d and p from the HPLC experiments.

2.3. Fractal dimension D_a of a linear non-enzymatic nucleotide polymerization process

The dynamics of chemical solid-phase oligonucleotide synthesis is naturally expressed in terms of the exponent $D_a(N)$. The general solution of $D_a(N)$ for discrete $\mathscr{L}$ indicates that whenever N is scaling, $D_a(N)$ has also a geometric interpretation over a D_a-dimensional observing set. In this case, $D_a(N)$ is of geometric fractal dimensionality [22]. This is the content of Eq. (5) with "embedding" dimension 2.

If the generating function $M(l, N)$ satisfies the condition of Eq. 1 and also Eq. 2, and if

$$\Phi(l, N) = \sum_{l_j \leqslant l} M(l_j, N) \tag{4}$$

then

$$D_a(N) = 2 - N\left(\frac{\partial\{\ln[\Phi(N-1, N) - \Phi(1, N)]\}}{\partial N}\right) \tag{5}$$

With the additional restriction of $d(i) = d_0 =$ constant (or $\bar{d}$, average), our formalism implies that

$$D_a(N) = 2 - N \cdot \frac{d_0^{N-1}}{1 - d_0^{N-1}} \cdot \ln\left(\frac{1}{d_0}\right) \tag{6}$$

In practice, the additional restriction of $d(i) = d_0 = \bar{d} =$ constant often applies to short target oligonucleotides (in case of routine chemical oligonucleotide synthesis). We found here that for our models

$$\lim_{d_0 \to 0} D_a(N) = 2 \tag{7}$$

$$\lim_{d_0 \to 1} D_a(N) = 2 - \frac{N}{N-1} \tag{8}$$

$$\lim_{d_0 \to 1} \lim_{N \to \infty} D_a(N) = 1 \tag{9}$$

There is another interesting property of $D_a(N)$ that is of practical relevance. Let $I = \{i \in \mathbb{R}: 1 \leqslant i < N\}$, then the non-empty set I is obviously bound above and below. If $\mathscr{L}(i)$ is either a discrete or a continuous stochastic variable and there is a real function $d(i)$ so that for every $i \in I$

$$\prod_{i \in [1,N)} d(i) = M(N, N) \tag{10}$$

with $0 \leqslant d(i) < 1$, and if

$$1 - M(N, N) = P(1 \leqslant \mathscr{L} < N) \tag{11}$$

then

$$D_a(N) = 2 - N\left(\frac{\partial\{\ln[1 - M(N, N)]\}}{\partial N}\right) \quad (12)$$

Consequently, mappings for $\Sigma_{l_j \leq l} M(l_j, N)$, $\int_1^l M(l, N)\, dl$ and $\Pi_{i \in [1,N)} d(i)$ are equivalent in terms of their dynamics $D_a(N)$. For example, computing the analytical function for all truncated or failure sequences measured by a separation technique might be a hopeless task, but $D_a(N)$ guarantees that these sequences are considered and, moreover, $D_a(N)$ gives a measure of all error sequences. Eq. 12 shows the power of symbolic dynamics [24] used.

For constant values of d and p (d_0, p_0), the arguments for Eqs. 5 and 12 were given earlier. We show that if

$$\sum_{l=1}^{N-1} M(l, N) = 1 - M(N, N) = C\left(\frac{1}{N}\right)^{D_a(N)-2} \quad (13)$$

then, by changing the mathematical values of $N \rightarrow \infty$, we go to Eqs. 5 and 12. C is a constant of proportionality. The real, physical functions $d(i)$ and $p(i)$ are similar to those shown in Ref. [23], where for short oligonucleotides (e.g., $N \leq 50$) constant parameters are used.

3. Experimental

3.1. Reagents

5′-O-Dimethoxytrityldeoxynucleoside-3′-O-(2-cyanoethyl)-N,N-diisopropylaminophosphanes were purchased from Millipore, MWG Biotech, Roth and Applied Biosystems. The standard solutions for oligonucleotide synthesis (activation, capping, oxidation, detritylation) were also obtained from these companies. The phosphoramidites were dissolved in acetonitrile with water content ≤10 ppm (HPLC-grade acetonitrile was obtained from Merck) at final concentrations of 0.1 *M*. Acetonitrile (impurities ≤30 ppm) from Roth was used for routine syntheses. Other reagents were of analytical-reagent grade.

3.2. Chemical solid-phase oligonucleotide synthesis

Syntheses were performed on Applied Biosystems Model 380B and 394 DNA synthesizers, and on Pharmacia–LKB Gene Assembler Special/4 Primers with integrated software packages according to 0.2 μmol standard cycles (small scale cyanoethyl cycle 103a of version 2.0 or 2.01 for ABI 380B synthesizer or 0.2 μmol cyanoethyl cycle for ABI 394 synthesizer of Model 392/394T system software ROM version 2.0). Using the styrene-grafted polytetrafluoroethylene supports P_{29} and P_{19}, coupling and washing steps during the initial three elongations were run on the ABI Model 380B synthesizer for double the time (60 s) compared with the 0.2 μmol standard synthesis cycles. Polymer-supported oligonucleotides were cleaved from supports and deprotected by treatment with 28% aqueous ammonia solution for 5–12 h at 55°C. The following 30mer oligonucleotide sequences were synthesized: (i) dC_{30}; and (ii) 5′ d GAA CTG ACT GGT CAA CGT CTG CGT GAA GGT. The heterooligonucleotide target sequence is the initial part of the codogenous strand of the human γ-lipotropin gene [28].

3.3. Polymer supports

Polystyrene-grafted polytetrafluoroethylene

The procedures and results of the grafting reactions of styrene on to polytetrafluoroethylene are described elsewhere [29–31]. A coarse-grained polytetrafluoroethylene powder (Polychrom I) with an average particle diameter of 500–1000 nm was chosen as starting material. The grafting of styrene on to this material was accomplished by ^{60}Co irradiation in an eddy flow reactor in which a styrene-saturated nitrogen stream flowed through the polytetrafluoroethylene gravel. This procedure yielded products highly homogeneous in degree of grafting and avoided the formation of large amounts of styrene homopolymers. The degree of grafting (% styrene) was determined from the ratio of intensities of IR bands at 1560 and 1610 cm^{-1}, compared with a calibration graph or from

corrected values of carbon content in elemental analysis. The improved pathway of support functionalization with a long alkylamine spacer is briefly described in Ref. [32]. Characteristics of supports P_{19} and P_{29} are reported in Ref. [32]. P_{19} has a degree of grafting of 5–7% styrene, corresponding to 42–48 μmol nucleoside/g support, whereas the degree of grafting of P_{29} is 2–3%, corresponding to 11–18 μmol nucleoside/g support.

Polystyrene primer support

This support was obtained from Pharmacia–LKB Biotechnology (Uppsala, Sweden). Nucleoside loading was 20.8 μmol/g support material. Derivatized polystyrene particles were optimized for oligonucleotide synthesis up to 50 bases in length [33].

Controlled-pore glass (CPG)

In the case of CPG materials, the accessibility of the growing oligonucleotide chains is connected with the pore size. Small-pore CPG allows higher loading. Long chains can be made only with low-capacity supports [34]. For syntheses of 30mers, CPG 500 Å (small-pore CPG) was routinely used with 27 μmol nucleoside/g support or with 43 μmol nucleoside/g support. CPG 500 Å was purchased from Eppendorf-Biotronic and Roth. CPG 1000 Å was obtained from Millipore. PGL 1000 Å (pore glass) was purchased from Schuller in unmodified form and functionalized with a long alkylamine spacer in our laboratory. The nucleoside loading was 28 μmol/g support.

3.4. Estimation of repetitive trityl yields

Experimental estimates of relative average coupling yields were obtained by relating the 495-nm absorption of the solution of the individual detritylation steps to that of the detritylation of the support-bound nucleoside. In order to obtain correct yields, the solutions resulting from cleavage of the dimethoxytrityl protecting group were separately collected and absorptions at 495 nm were determined manually after acidification by addition of 0.1 *M* *p*-toluenesulfonic acid in acetonitrile [34].

3.5. Determination of oligonucleotide concentrations

Oligonucleotide concentrations in crude products were determined directly after cleavage from polymer support. Absorbance (*A*) was measured at 260 nm on a Pharmacia–LKB Ultrospec Plus spectrophotometer or on a Beckman DU 7500 spectrophotometer with integrated software.

3.6. HPIEC analysis

HPIEC analyses, as represented in Fig. 1, were carried out with an Applied Biosystems Model 152A system. The HPLC-column, Superformance 50–10 LiChrospher 4000 DMAE (5 μm), was a gift from Merck (Darmstadt, Germany). The following conditions were used: detection, UV at 254 nm; flow-rate, 1.5 ml/min; room temperature; eluent, buffer A, 20 m*M* sodium acetate (pH 6.5)–acetonitrile (80:20), buffer B, 20 m*M* sodium acetate (pH 6.5)–acetonitrile (80:20)–1 *M* LiCl. A linear gradient was applied as indicated in Fig. 1.

HPIEC analyses reported in Fig. 2 and Tables 1 and 2 were carried out on a Bio-Rad Model 2700 system (Software Series 800 HRLC System, Version 2.30.1a) equipped with a column oven and with an AS-100T HRLC automatic sampling system. A Bio-Rad UV-1806 UV–Vis detector was used. A Mono Q HR 5/5 anion-exchange column was obtained from Pharmacia–LKB Biotechnology. The following conditions were used: detection, UV at 260 nm; flow-rate, 1 ml/min; temperature, 60°C; eluent, buffer A, 10 m*M* NaOH–0.1 *M* NaCl (pH 11), buffer B, 10 m*M* NaOH–1 *M* NaCl (pH 11). Linear gradients from 0 to 100% buffer B were applied over 30 and 40 min, respectively. Water used for mobile phases was purified with a Milli-Q Plus water-purification system (Millipore, Bedford, MA, USA). Sample solutions were filtered through a Millipore filter (pore size 0.45 μm).

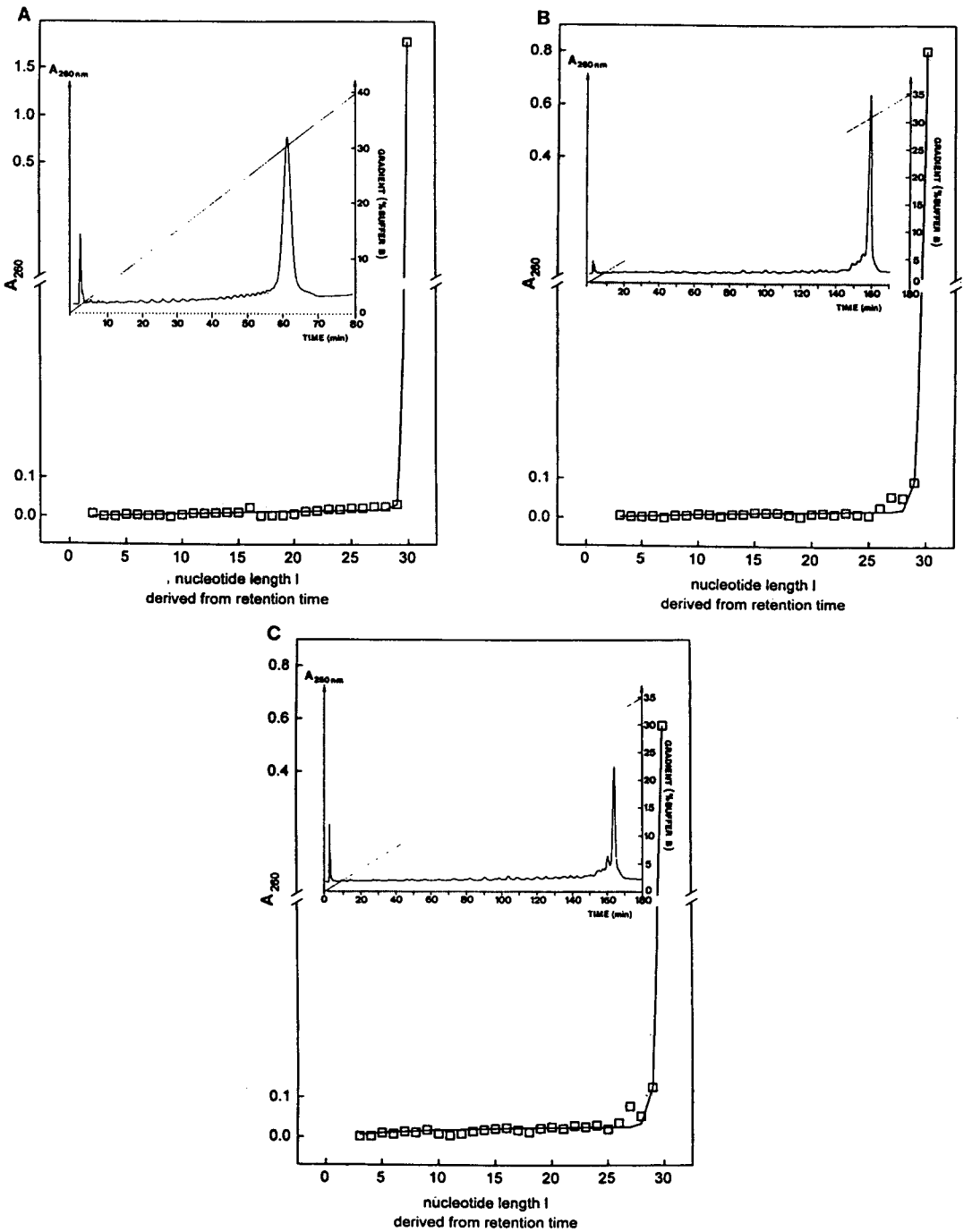

Fig. 1. Experimental anion-exchange HPLC elution profiles (insets) of crude products of (A) dC_{30} synthesis on CPG 500 Å support (Eppendorf-Biotronic), (B) 30mer heterooligonucleotide synthesis on P_{29} support and (C) 30mer heterooligonucleotide synthesis on P_{19} support. Experimental values (□) of chromatograms are compared with theoretical values (——) obtained by proper setting of synthesis parameters d_0 (constant coupling efficiency) and p_0 (constant capping efficiency). 1.25 AU of crude products were applied in (B) and (C).

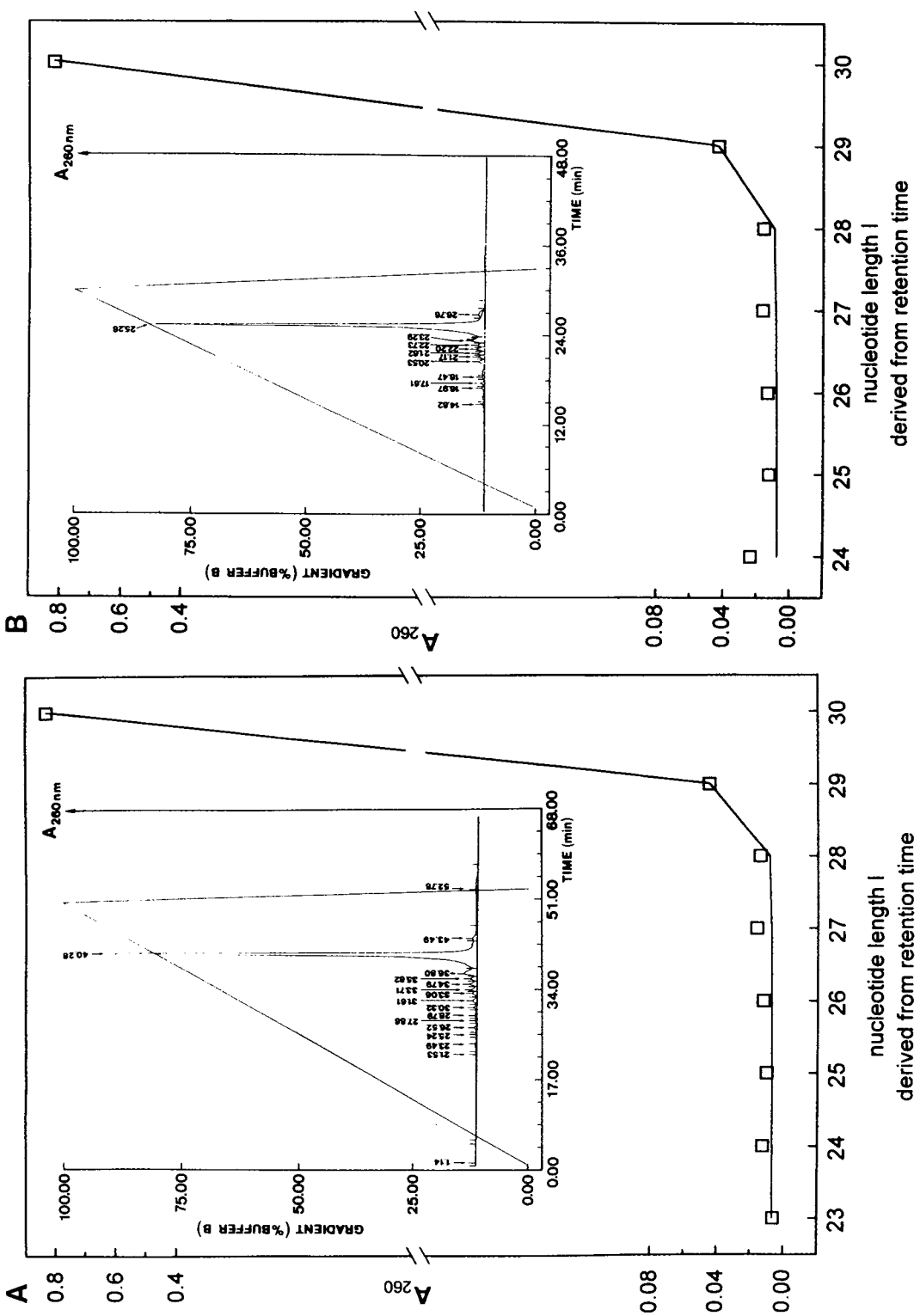

Fig. 2. (*Continued on page 412*)

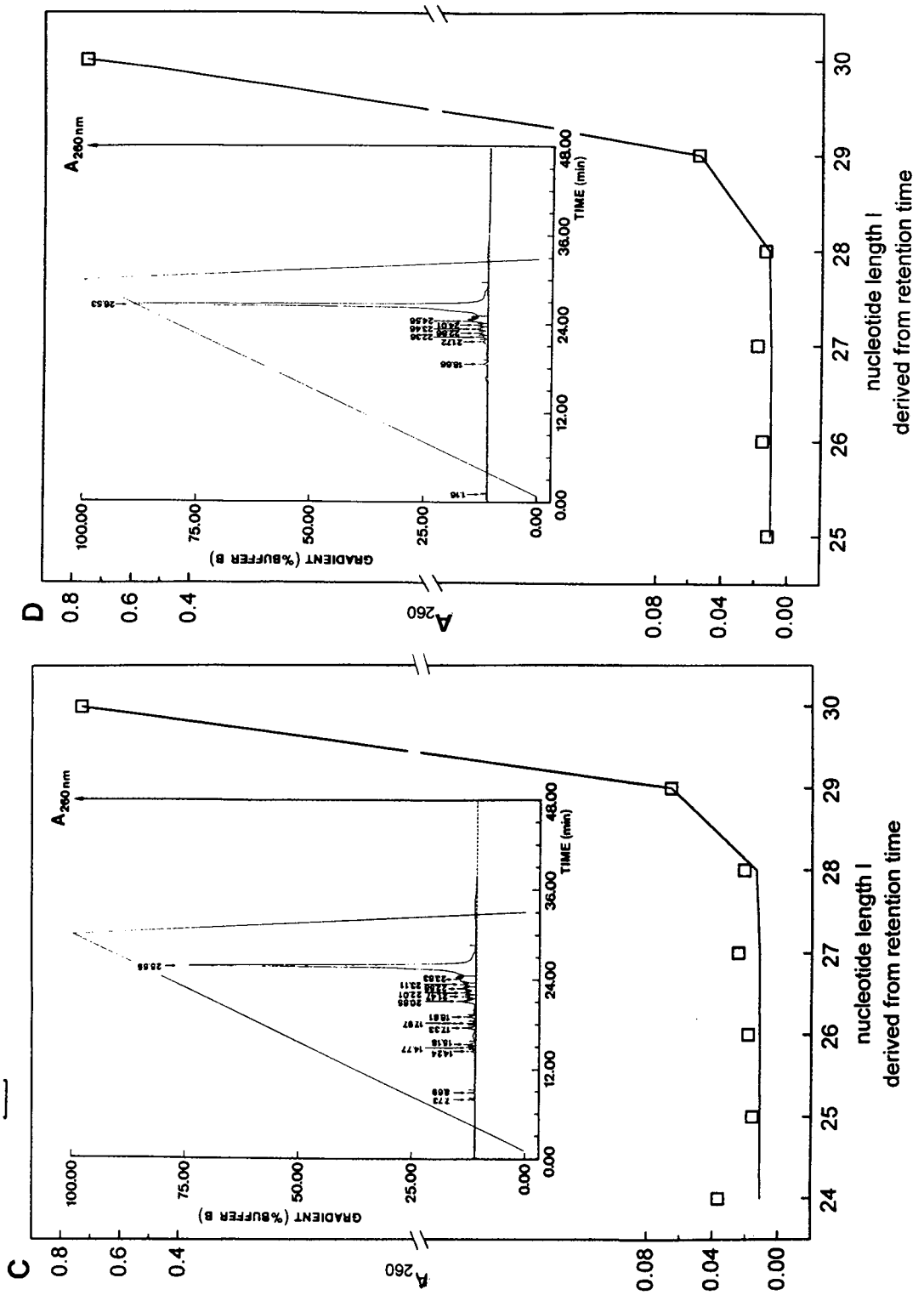
C
D
A260
A260nm
GRADIENT (%BUFFER B)
TIME (min)
nucleotide length l
derived from retention time

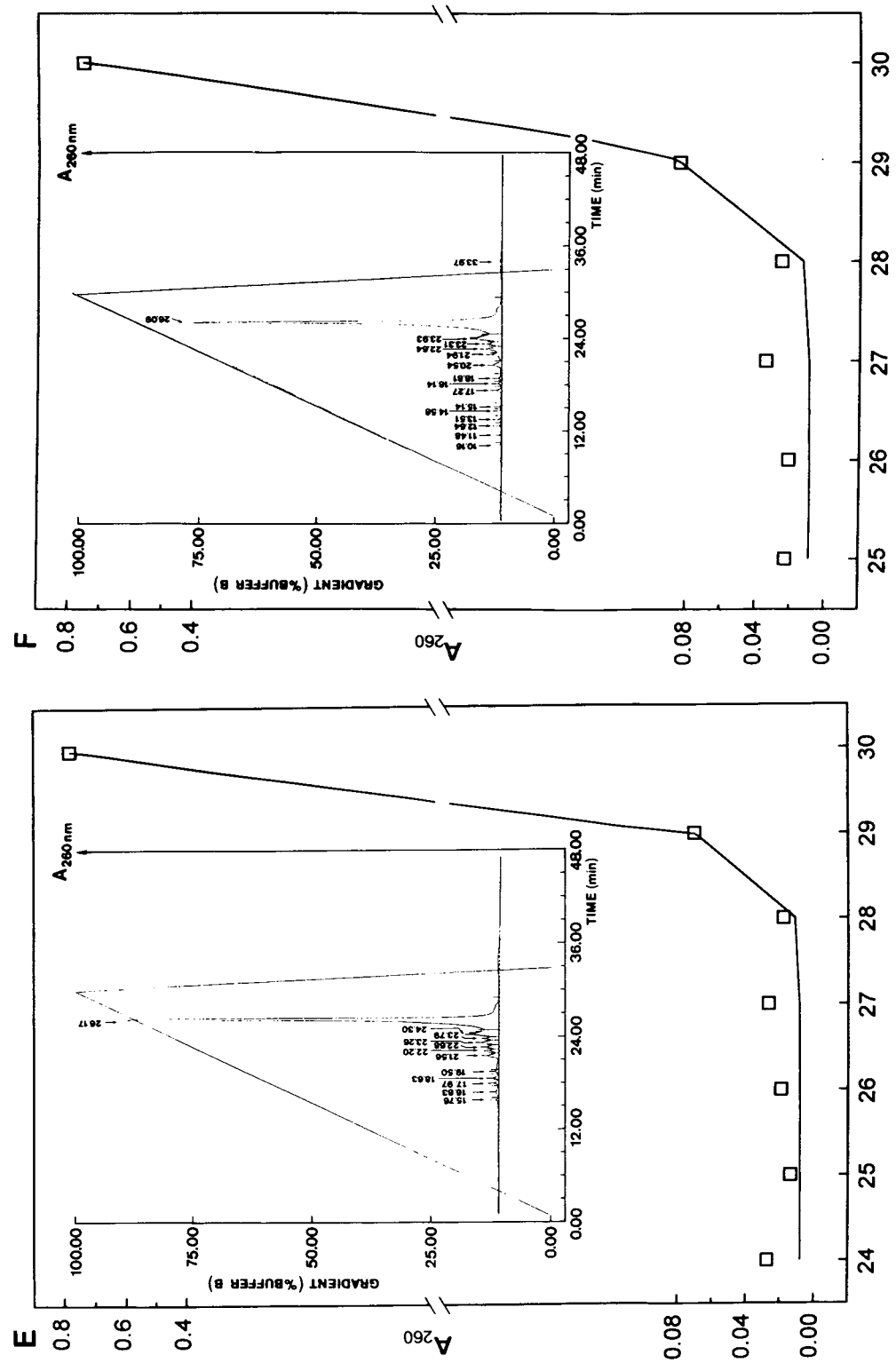

Fig. 2. Determination of parameters d_0 (constant coupling efficiency) and p_0 (constant capping efficiency) characterizing the course of chemical oligonucleotide synthesis. Theoretical curves (——) were fitted to experimental values (□) taken from anion-exchange HPLC elution profiles (insets) of crude products of 30mer heterooligonucleotide. 1 AU of crude products were analysed. (A) CPG 500 Å support obtained from Roth, $d_0 = 0.98897$, $p_0 = 0.85950$; (B) CPG 1000 Å support obtained from Millipore, $d_0 = 0.98789$, $p_0 = 0.87755$; (C) PGL 1000 Å support, $d_0 = 0.98149$, $p_0 = 0.85850$; (D) polystyrene primer support obtained from Pharmacia–LKB Biotechnology, $d_0 = 0.98373$, $p_0 = 0.87600$; (E) P_{29} support [32], $d_0 = 0.98613$, $p_0 = 0.80011$; (F) P_{19} support [32], $d_0 = 0.98455$, $p_0 = 0.77500$.

Table 1
Comparison of a typical result for solid-supported oligonucleotide syntheses performed on Applied Biosystems Model 380B and 394 DNA synthesizers in the optimum reaction mode

Synthesizer	N	DMTr[a] (%)	d_0	p_0	D_a	$\frac{2-\frac{N}{N-1}}{2-N\cdot\left(\frac{d_0^{N-1}}{1-d_0^{N-1}}\cdot\ln\frac{1}{d_0}\right)}$ [b]
Model 380B	30	66.92	0.98908 ±0.00090 ($n=3$)	0.86450 ±0.00999 ($n=3$)	1.12141 ±0.01215 ($n=3$)	0.86105 ±0.00935 ($n=3$)
Model 394	30	85.80	0.98846 ±0.00101 ($n=3$)	0.85471 ±0.01664 ($n=3$)	1.12983 ±0.01353 ($n=3$)	0.85465 ±0.01019 ($n=3$)

The support material was CPG 500 Å obtained from Roth. The 30mer heterooligonucleotide target was synthesized. 1 AU of crude products were analysed by anion-exchange HPLC.
Randomization of different syntheses and of different HPLC runs. Estimates were calculated from a sample using the following equations for the mean ($\bar{x}$) and for the standard deviation (s) of the mean from a normally distributed population: $\bar{x}=\frac{1}{n}\cdot\Sigma_{j=1}^{n}x_j$, $s=\sqrt{\frac{1}{n-1}\cdot\Sigma_{j=1}^{n}(x_j-\bar{x})^2}$.
[a] Total trityl yield after $N-1$ cycles (see Experimental).
[b] The relation $[2-N/(N-1)]/D_{a,measurable}$ is a universal measure for multi-cycle synthesis conditions (for explanation, see text).

4. Results and discussion

The crude product of synthesis of a dC_{30} obtained after cleavage from the support and deprotection was chosen as the sample species (Fig. 1A). We first studied a homooligonucleotide synthesis in order to avoid different elution behaviours of truncated or failure sequences with increasing chain length. The separation of the dC_{30} was examined using the Superformance 50–10 LiChrospher 4000 DMAE (5 μm) column. As shown in the inset in Fig. 1A, a component elution was obtained. The peaks of single nucleotides and of dinucleotides were checked by comparison with standards. The products of protecting group cleavage were also eluted with the first and second peaks. However, the retention time of the target was very close to that of error sequences of length $N-1$. The open squares are the data from the HPLC experiment. The solid line without symbols is the result obtained by our theory. It is worth noting that A values of a clean separation of N and $N-1$ sequences are most important for the computer simulation of anion-exchange HPLC profiles of crude products of short oligonucleotides.

The next series of experiments together with computer simulation results are shown in Fig. 1B and C. Samples of syntheses of a heterooligonucleotide target sequence (see Experimental) were used. Although selected from systematic investigations, the mobile phase for complete component elution was unable to give an adequate resolution of $N-1$ peaks. The slight discrepancies observed between the calculated parameters can be explained by this experimental factor.

The insets in Fig. 2A–F show HPLC analyses with the Mono Q HR 5/5 anion-exchange column. This system is optimized for separation of N and $N-1$ peaks. Further, we checked the "purity" of the N and $N-1$ peaks by re-chromatography. The occurrence of minor peaks which seem to correspond to products longer than the target sequence has been reported previously (see, for instance, the examples shown in Ref. [35]), but explanations are not at hand. These results indicated that, in each instance, the experimental values are within acceptable limits.

Table 2
Influence of different support materials on synthesis result

Support	N	DMTr[a] (%)	d_0	p_0	D_a	$\frac{2-\frac{N}{N-1}}{2-N\cdot\left(\frac{d_0^{N-1}}{1-d_0^{N-1}}\cdot\ln\frac{1}{d_0}\right)}$ [b]
CPG 500 Å (Roth)	30	77.36 (n = 2)	0.98877 ±0.00092 (n = 6)	0.85961 ±0.01339 (n = 6)	1.12562 ±0.01239 (n = 6)	0.85785 ±0.00942 (n = 6)
CPG 1000 Å (Millipore)	30	69.47 (n = 1)	0.98655 ±0.00122 (n = 3)	0.88653 ±0.00910 (n = 3)	1.15527 ±0.01621 (n = 3)	0.83586 ±0.01178 (n = 3)
PGL 1000 Å	30	58.90 (n = 1)	0.97989 ±0.00164 (n = 3)	0.87974 ±0.01878 (n = 3)	1.24033 ±0.02018 (n = 3)	0.77857 ±0.01265 (n = 3
Polystyrene primer support (Pharmacia)	30	86.33 (n = 3)	0.98699 ±0.00488 (n = 7)	0.83528 ±0.05336 (n = 7)	1.14820 ±0.06309 (n = 7)	0.84296 ±0.04387 (n = 7)
P_{29}	30	70.94 (n = 3)	0.98516 ±0.00421 (n = 9)	0.76151 ±0.07125 (n = 9)	1.17254 ±0.05550 (n = 9)	0.82514 ±0.04025 (n = 9)
P_{19}	30	61.40 (n = 2)	0.98591 ±0.00494 (n = 7)	0.75857 ±0.09647 (n = 7)	1.16242 ±0.06413 (n = 7)	0.83275 ±0.04525 (n = 7)

The 30mer heterooligonucleotide target was synthesized. 1 AU of crude products were analyzed by anion-exchange HPLC. Randomization of different syntheses and of different HPLC runs. Estimates were calculated from a sample using following equations for the mean ($\bar{x}$) and for the standard deviation (s) of the mean from a normally distributed population: $\bar{x} = \frac{1}{n}\cdot\sum_{j=1}^{n} x_j$, $s = \sqrt{\frac{1}{n-1}\cdot\sum_{j=1}^{n}(x_j-\bar{x})^2}$.

[a] Total trityl yield after $N-1$ cycles of different syntheses (see Experimental).

[b] See Table 1, footnote b.

By assuming given values of d_0 and p_0, theoretical curves were calculated and iterated to best fit the experimental data. By means of our theory we thus generated parameters d_0 *and* p_0 from the experimental HPLC elution profiles obtained; d_0 is the average (constant) coupling (elongation) probability of each synthesis cycle and p_0 is the average (constant) capping (termination) probability of each synthesis cycle. These parameters depend on the number of reaction cycles i and on internal or external conditions, which all are taken into account by proper scaling of d and p. The d_0 values obtained from experiments were used for calculating the fractal dimension D_a of the growth process.

The problem of comparison in growth patterns such as chemical oligonucleotide synthesis is, in essence, a matter of converting the experimentally accessible information into otherwise inaccessible information about the real process. By the differential relation D_a we produce a geometric image of error sequences formed by the course of chemical oligonucleotide synthesis. This physical growth pattern is directly related to the efficiency of error sequences dynamics. Different syntheses of oligonucleotides and single-stranded DNA sequences can now be directly compared. If their values of D_a are equal, they are of the same performance in all steps of oligonucleotide growth. Further, the local fractal

dimension D_a quantifies the influence on nucleotide length N of different target sequences. The measurable values of the exponent D_a can be normalized to an idealized synthesis of constant growth without error production. In the case of a synthesis of constant growth without error production, D_a becomes $D_a = 2 - N/(N-1)$ (Eq. 8). Hence the relation $[2 - N/(N-1)]/D_{a,measurable}$ is a universal quantitative measure for multi-cycle synthesis conditions. This measure is revealed by two-dimensional graphs of functions M. The function M specifies the growth process under study. For example, M expresses chemical solid-supported oligonucleotide synthesis. It is clear from Eq. 12 that the relation $[2 - N/(N-1)]/D_{a,measurable}$ can also be a quantitative measure for chemical oligonucleotide synthesis carried out in solution. Obviously, the coupling efficiency (d) or individual yields (e.g., repetitive trityl yields) do not allow the quantitative characterization of chemical oligonucleotide synthesis of different target length. They reflect the quantitative influence on any reaction step only.

The coupling efficiency d of chemical oligonucleotide synthesis is not a constant value in the proper sense. It is convenient to use constant values for solid-phase synthesis of short oligonucleotides. In this case, our universal quantitative measure becomes

$$\frac{2 - \dfrac{N}{N-1}}{2 - N \cdot \dfrac{d_0^{N-1}}{1 - d_0^{N-1}} \cdot \ln\left(\dfrac{1}{d_0}\right)} \qquad (14)$$

The parameters N and d_0 of the relationship can be combined with experiments. The relationship can be extended to average values of d ($\bar{d}$). Hence more complicated growth systems are described with the same simplicity.

In Table 1 we compare a typical result of chemical solid-phase oligonucleotide syntheses performed on the Applied Biosystems Model 380B and 394 DNA synthesizers in the optimum reaction mode. In our study the parameters d_0, p_0 and the measures D_a and $[2 - N/(N-1)]/D_{a,measurable}$ did not reveal any differences related to the apparatus used for these syntheses. One of the major interests has been to explore new polymer support systems, because the good accessibility of a reactive polymer support is responsible for the overall efficiency of a chemical oligonucleotide synthesis.

Table 2 shows the influence of different support materials on the synthesis results. First we considered the most widely used support materials such as controlled-pore glass and polystyrene support (Primer Support from Pharmacia). These materials show similar efficiencies for producing high yields of the target sequence {$[2 - N/(N-1)]/D_{a,measurable}$ values in column 7 of Table 2}. It is noteworthy that the capping probability p_0 is much lower for syntheses with styrene supports (polystyrene primer support) than for syntheses carried out with controlled-pore glass. The decrease in p_0 values may be due to free functional groups of styrene supports which did not react during the further functionalization of support materials or to a slight steric hindrance of chains resulting in decreased accessibility of some growing ends. Differences in capping efficiency may shift the composition of the truncated and failure sequences toward longer chains. A practical consequence of this finding might be that the isolation of the target sequence N from error sequences $N-1$, $N-2$, $N-3$, $N-4$ in crude products can be more easily handled in the case of CPG synthesis. Such differences of composition may be of importance for application of solid-phase synthesized oligonucleotides, especially in the biomedical field. A zero-capping step prior to synthesis is to be recommended to block unreacted COOH and NH_2 groups on styrene supports. Recently, we have described a versatile support material based on tetrafluoroethylene powder grafted with polystyrene. A feature of this support material is that the oligonucleotide reactions proceed only in the polystyrene surface coat, the thickness of which can be easily regulated by the grafting procedure [32]. We have measured the efficiency of this support material using the same criteria as applied above for CPG and polystyrene supports. The results summarized in Table 2 suggest that this new material is comparable in its performance to those supports which are established and most widely used in oligo-

nucleotide chemistry. In principle, the physical model applied to D_a is sensitive enough to distinguish various support materials. However, for short oligonucleotides the theoretical result is involved in an optimum experimental resolution between N and $N-1$ peaks obtained in the chromatogram.

A phenomenon observed in the experiments and proved by simulations of anion-exchange HPLC elution profiles is that A values of $N-1$ error sequences must decrease with the increase in d values. Similar considerations hold for the influence of p_0 values. Usually the yield of the target sequence is determined only by measured absorbance at 260 nm. For the calculation of d values in the literature this may lead to an overestimation. Monitoring the trityl yield (column 3 of Table 2) also provides some obstacles [36] which may result in an overestimation of d values. In our homoeodynamic model of solid-supported oligonucleotide synthesis, the yields of all truncated or failure sequences and the yield of the target are considered for obtaining d and p values in each reaction cycle.

Automation and optimization of chemical reactions on solid support materials allow syntheses of chains of extended nucleotide length and the preparation of oligonucleotides in large amounts [32,37–39]. As an example, we previously analysed experimentally and theoretically the attempted synthesis of an unusually long 238mer sequence. Neither HPLC, capillary electrophoresis nor polymerase chain reaction techniques in the crude product of chemical synthesis followed by sequencing led to the isolation of any amount of the 238mer target sequence. Nevertheless, the calculation of d and p could be done by simulation of the overall pattern of experimental nucleotide length distribution of error sequences obtained by quantitative agarose gel electrophoresis [25]. In a parallel approach, this sequence has been prepared in the meantime by splint ligation of two 119mer oligonucleotides with a 40 nucleotide splint. From the resulting 238 nucleotide single-stranded DNA, the double-stranded fragment was amplified via PCR using special primers carrying, in addition, unique restriction sites for subsequent cloning in the BamHI and HindIII region of the PTZ18/19 plasmid [3]. Sequencing of clones proved the success of the preparation.

5. Conclusions

In the literature there are no investigations dealing with non-enzymatic and enzymatic nucleotide growth processes under the dynamic aspect of error sequences production. Here we analysed the dynamics of chemical oligonucleotide synthesis by a new fractal formalism. We are currently elaborating on our theoretical concept in the direction of both non-enzymatic and enzymatic nucleotide polymerization processes. In this paper, theoretical results are compared with the experimental separation of the products of solid-supported oligonucleotide synthesis by HPIEC. Fig. 2 shows that there is a good correlation between the results of HPIEC and theoretical calculations by assuming given values of coupling and capping efficiencies. One of the novel aspects of this work is that the distribution of solid-phase products which is based on the efficiencies of coupling and capping is now accessible to calculation. On this basis, we have presented first data that allow the evaluation of support systems for chemical synthesis of short oligonucleotides by our differential relationship of fractal dimension. From these results slight differences can be seen between the performances of different support materials (Table 2, column 7). It is possible that with more experimental material at hand, quantitative differences concerning the performance of the support systems will more clearly emerge. Our approach has the advantage that model parameters and measures derived from the theory possess physical and chemical significance for the multi-step process which we see through HPIEC.

Acknowledgements

We thank Dr. Wei-Guo Peng of Softlab (Munich, Germany) for writing the computer program used. The computer code was written in C algorithmic language on PC under DOS/Windows and VAX under VMS, compiled with

Turbo C^{++} from Borland and VAX C from Digital Equipment, respectively. We thank Ms. Anita Willitzer for skilful technical assistance. This work was supported by the Deutsche Forschungsgemeinschaft and the Stiftung zur Förderung der molekularbiologischen Forschung Universität Ulm.

References

[1] J.W. Engels and E. Uhlmann, *Angew, Chem., Int. Ed. Engl.*, 28 (1989) 716–734.
[2] L.C. Klotz, R.W. Schatz, A.P. Kerr and C.R. Morris (Editors), *The Commercial Potential of Human Oligonucleotide Therapy*, Decision Resources, Burlington, 1992.
[3] Z. Földes-Papp, *Studies on Synthesis of Oligonucleotides and DNA Sequences: Dynamics of Error Sequences: Fractality and Experiments, Ph.D. Thesis*, University of Ulm, Ulm, 1994.
[4] E. Wickstrom (Editor), *Prospects for Antisense Nucleic Acid Therapy of Cancer and AIDS*, Wiley, New York, 1991.
[5] J.A.H. Murray (Editor), *Antisense RNA and DNA: a Comprehensive Guide to Successful Use of Antisense Nucleic Acids*, Wiley, New York, 1992.
[6] Z. Földes-Papp, *Gen. Physiol. Biophys.*, 11 (1992) 3–38.
[7] H. Seliger, R. Bader, E. Birch-Hirschfeld, Z. Földes-Papp, K.H. Gührs, M. Hinz, R. Rösch and C. Scharpf, *React. Polym.*, (1995) in press.
[8] H. Seliger, in S. Agrawal (Editor), *Methods in Molecular Biology, Vol. 20: Protocols for Oligonucleotides and Analogs: Synthesis and Properties*, Humana Press, Totowa, NJ, 1993, pp. 391–435.
[9] S. Agrawal (Editor), *Methods in Molecular Biology, Vol. 26: Protocols for Oligonucleotide Conjugates: Synthesis and Analytical Techniques*, Humana Press, Totawa, NJ, 1994.
[10] H. Kössel and H. Seliger, in W. Herz, H. Grisebach, G.W. Kirby (Editors), *Progress in the Chemistry of Organic Natural Products*, Vol. 32, Springer, Vienna, 1975, pp. 297–508.
[11] W.J. Warren and G. Vella, *BioTechniques*, 14 (1993) 598–606.
[12] R.L. Letsinger, J.L. Finnan, G.A. Heavner and W.B. Lunsford, *J. Am. Chem. Soc.*, 97 (1975) 3278–3279.
[13] S.L. Beaucage and M.H. Caruthers, *Tetrahedron Lett.*, 22 (1981) 1859–1862.
[14] M.H. Caruthers, G. Beaton, J.V. Wu and W. Wiesler, *Methods Enzymol.*, 211 (1992) 3–20.
[15] B. Mandelbrot, *Les Objets Fractals: Forme, Hasard et Dimension*, Flammarion, Paris, 1975.
[16] B.B. Mandelbrot, *The Fractal Geometry of Nature*, Freeman, New York, 1983.
[17] T.F. Nonnenmacher, in T.F. Nonnenmacher, G.A. Losa and E.R. Weibel (Editors), *Fractals in Biology and Medicine*, Birkhäuser, Basle, 1994, pp. 22–38.
[18] G. Baumann, A. Barth and T.F. Nonnenmacher, in T.F. Nonnenmacher, G.A. Losa and E.R. Weibel (Editors), *Fractals in Biology and Medicine*, Birkhäuser, Basle, 1994, pp. 182–189.
[19] A.B. Çambel, *Applied Chaos Theory: A Paradigm for Complexity*, Academic Press, Boston, 1993.
[20] A. Bunde and S. Havlin (Editors), *Fractals in Sciences*, Springer, Berlin, 1994.
[21] J.L. Casti, *Reality Rules: II, Picturing the World in Mathematics: The Frontier*, Wiley, New York, 1992.
[22] B.J. West, *Fractal Physiology and Chaos in Medicine*, World Scientific, Singapore, 1990.
[23] Z. Földes-Papp, A. Herold, H. Seliger and A.K. Kleinschmidt, in T.F. Nonnenmacher, G.A. Losa and E.R. Weibel (Editors), *Fractals in Biology and Medicine*, Birkhäuser, Basle, 1994, pp. 165–173.
[24] R.L. Devaney, *An Introduction to Chaotic Dynamical Systems*, Benjamin/Cummings, Menlo Mark, CA, 1986.
[25] Z. Földes-Papp, W.-G. Peng, H. Seliger and A.K. Kleinschmidt, *J. Theor. Biol.*, (1995) in press.
[26] S. Redner and F. Leyvraz, in A. Bunde and S. Havlin (Editors), *Fractals in Sciences*, Springer, Berlin, 1994, pp. 212–217.
[27] G.H. Weiss, in A. Bunde and S. Havlin (Editors), *Fractals in Sciences*, Springer, Berlin, 1994, pp. 119–161.
[28] A.S.Y. Chang, M. Cochet and S.N. Cohen, in R. Håkanson and J. Thorell (Editors), *Biogenetics of Neurohormonal Peptides*, Academic Press, London, 1985, pp. 15–28.
[29] R. Weiss, E. Birch-Hirschfeld, W. Wittkowski and K. Friese, *Z. Chem.*, 26 (1986) 127–130.
[30] W. Witkowski, E. Birch-Hirschfeld, R. Weiss, V.F. Zarytova and V.V. Gorn, *J. Pract. Chem.*, 326 (1984) 320–328.
[31] E. Birch-Hirschfeld, Z. Földes-Papp, K.-H. Gührs, R. Weiss and H. Seliger, presented at the *3rd Swedish–German Workshop on Nucleic Acid Synthesis, Structure and Function, Uppsala, 1992*, abstracts, p. 35.
[32] E. Birch-Hirschfeld, Z. Földes-Papp, K.-H. Gührs and H. Seliger, *Nucleic Acids Res.*, 22 (1994) 1760–1761.
[33] *Product Bulletin Primer Support*, 56-1142-52, edition AA, Pharmacia, Uppsala.
[34] H. Seliger, A. Herold, U. Kotschi, J. Lyons and G. Schmidt, in K.S. Bruzik and W.J. Stec (Editors), *Biophosphates and Their Analogues—Synthesis, Structure, Metabolism and Activity*, Elsevier, Amsterdam, 1987, pp. 43–58.
[35] W.J. Warren and G. Vella, in S. Agrawal (Editor), *Methods in Molecular Biology, Vol. 26: Protocols for Oligonucleotide Conjugates: Synthesis and Analytical Techniques*, Humana Press, Totowa, NJ, 1994, pp. 233–264.

[36] *Applied Biosystems User Bulletin, 40 nanomole Polystyrene: New Highly Efficient DNA Synthesis Columns, No. 61*, ABI, 1991.
[37] R.W. Barnett and H. Erfle, *Nucleic Acids Res.*, 18 (1990) 3098.
[38] R.B. Ciccarelli, P. Gunyuzlu, J. Huang, C. Scott and F.T. Oakes, *Nucleic Acids Res.*, 19 (1991) 6007–6013.
[39] Z. Földes-Papp, R. Rösch, F. Ramalho Ortigao, M. Hinz, S. Conrad, R. Weiss, E. Birch-Hirschfeld and H. Seliger, presented at the *3rd Swedish–German Workshop on Nucleic Acid Synthesis, Structure and Function, Uppsala, 1992*, abstracts, p. 60.

ELSEVIER

Journal of Chromatography A, 706 (1995) 421–428

JOURNAL OF CHROMATOGRAPHY A

Determination of amino acids in biomass and protein samples by microwave hydrolysis and ion-exchange chromatography

Lars Joergensen*, Helle N. Thestrup

DB Lab, Dansk Bioprotein A/S, Stenhuggervej 9, 5230 Odense M, Denmark

Abstract

A fast method for protein hydrolysis based on controlled heating in a microwave oven is described. The samples are heated to 150°C for 10–30 min where conventional methods use 110°C for 24 h. The method was tested with pure protein samples and "real" protein samples with carbohydrates, fats, nucleic acids and minerals. The microwave method showed similar or better results than the conventional method. The effect of degassing and stabilising agents was also tested. Degassing and thioglycolic acid stabilise methionine and partly tryptophan. Degassing and phenol stabilise tyrosine, phenylalanine and histidine in performic acid oxidised samples.

1. Introduction

Ion-exchange chromatography (IEC) combined with post-column derivatization with ninhydrin and detection at 570 nm is a sturdy method widely used for amino acid measurement. Determinations of amino acids bound in proteins require a hydrolysis of the peptide linkages before measurement. This is typically done by a 24 h acid (6 *M* HCl) hydrolysis at 110°C. Hydrolysis can be performed by (a) open reflux method under an atmosphere of nitrogen, (b) hydrolysis in evacuated sealed tubes, or (c) hydrolysis in screw cap tubes in an atmosphere of nitrogen [1]. Similar results were found for the screw cap method and for the reflux method, but the screw cap method gave an increased loss of methionine [1]. Cyst(e)ine and tryptophan are lost during a common acid hydrolysis, and asparagine and glutamine are converted to aspartic acid and glutamic acid, respectively [2,3].

A much faster hydrolysis of proteins can be obtained by microwave hydrolysis [4,5]. Samples are rapidly heated in closed vessels to 150°C and a total protein hydrolysis can be obtained in less than 30 min. Péter et al. [4] used a commercial household microwave oven for hydrolysis of small peptides. They found that the microwave hydrolysis gave reduced racemization and higher recovery of sensitive amino acids than hydrolysis by conventional heating. Grimm [5] used a pressure controlled microwave oven and gas phase hydrolysis of pure proteins and peptides. He found a slightly higher loss of serine and threonine than by common gas phase hydrolysis at 110°C.

It is well known that hydrolysis of pure polypeptides and protein samples can behave very differently from "real" protein samples. The presence of iron or copper in protein samples can cause serious difficulties in production of unusual artefacts and in the loss of certain amino

* Corresponding author.

0021-9673/95/$09.50
SSDI 0021-9673(94)01107-9

acids [2], and the recovery of methionine and tryptophan has been reported to depend on the carbohydrate level of the sample [1,6].

This paper compares fast microwave hydrolysis of proteins with the traditional hydrolysis. The effect of degassing and stabilising agents is also described. Two "pure" protein sources, casein and gelatine, and a "real" protein source, BioProtein, were used as test protein. BioProtein is biomass produced from natural gas by microorganisms as described previously [7]. It contains about 70% raw protein, 10% carbohydrates, 10% fat, 7% nucleic acids and 5% minerals. The copper content is about 100 mg/kg and the iron content is about 200 mg/kg. Thus, it represents a difficult mixture for protein hydrolysis.

2. Experimental

2.1. Chromatographic system

The amino acids were separated by the sodium-based Pickering system for protein and collagen hydrolysates, the Pickering 150 × 4 mm I.D., 7-μm column ("high-efficiency") and 20 × 3 mm guard column being used (Pickering Labs., Mountain View, CA, USA). The system was combined with an Dionex Model 4500i ion chromatographic gradient pump equipped with a Dionex UV–Vis variable-wavelength detector, a Dionex autosampler, a Rheodyne injector and an IBM AT compatible computer with the Dionex AI-450 Model II data system.

The column was placed in a CHX650 column heater from Pickering Labs. and maintained at 55°C. A Dionex reagent pump and autoion reagent controller was used for post-column ninhydrin addition. The ninhydrin-eluent mixture was heated to 130°C in a Pickering post-column reactor.

The eluent flow-rate was 0.4 ml/min, the ninhydrin flow-rate was ca. 0.66 ml/min and the post-column reaction temperature 130°C. Absorption was monitored at 570 nm. Trione ninhydrin was used as post-column reagent.

2.2. Eluents and gradient programme

Eluent A: sodium citrate, pH 3.15 (40 g trisodium citrate dihydrate, 30 ml 30% HCl plus water to 2000 ml). Eluent B: sodium acetate, pH 7.40 (16.4 g sodium acetate, 105.2 g sodium chloride, water to 2000 ml). Eluent C: sodium regenerant pH 12.4 [0.7445 g EDTA, Titraples, 4.0 g sodium chloride, 10.2 ml sodium hydroxide (50% w/w), water to 1000 ml].

Gradient programme: 0–6 min 100% A; 6–28 min 100 to 0% A, 0 to 100% B; 28–42 min 100% B; 42–54 min 100 to 85% B, 0 to 15% C; 54–72 min 0 to 100% A, 100 to 0% B; 72–75 min 100% A.

2.3. Microwave system

A CEM (Matthews, NC, USA) MDS-2000 microwave sample preparation system equipped with temperature and pressure measuring and control device was used for microwave hydrolysis of protein samples. The power output was 630 ± 50 W. Samples were hydrolysed in CEM single-wall PTFE vials with double port cap. A CEM capping station was used for capping of the vials (torque 16.3 Nm). One port cap in one of the vials was fitted with a glass thermowell for the fiber-optic temperature probe. One port cap in another vessel was connected to the pressure sensing tube. The head spaces of the vials were connected through PTFE tubes fitted to the port caps. Normally two vials were operated together, but the system could handle up to eight vials simultaneously. Parameters for microwave acid hydrolysis are shown in Table 1.

2.4. Pre-hydrolysis oxidation

Some samples were oxidized by performic acid before hydrolysis in order to determine cystine/cysteine [8,9]: 20–50 mg protein sample was accurately weighed into the CEM vial and 5 ml ice-cold freshly prepared performic acid (0.5 ml 30% H_2O_2 and 4.5 ml formic acid, mixed at room temperature, after 30 min placed on ice), 250 μl 200 m*M* norleucine and when added 250 μl 10% phenol solution was mixed into it. The

Table 1
Typical parameters for the microwave acid hydrolysis

Parameter	Stage		
	1	2	3
Power (%)	100	100	0
Pressure	90	90	90
Run time (min)	3	30	20
Time @P (min)	–	20	–
Temperature (°C)	150	150	150
Fans speed (%)	100	100	100

Stage 1: the frozen sample is thawed (the temperature control does not tolerate a negative temperature; this stage is not necessary for unfrozen samples). Stage 2: when the sample(s) reach the set point temperature (or the set point pressure, whatever comes first), the temperature is kept for the time given by "Time @P" or for the "Run time", whatever comes first. Stage 3: the cooling phase.

oxidation mixture was kept at 0°C for 18 h. Care was taken to ensure that protein particles were thoroughly wetted and immersed in the oxidising medium during incubation. Following oxidation, the contents of the vials were frozen and the reagents removed in vacuum using a freeze-dryer (Note: performic acid is very corrosive to vacuum pumps). After drying, 5 ml water and 10 ml 30% HCl were added to the sample and it was prepared for microwave hydrolysis as described below.

2.5. Sample preparation

A 20–50-mg protein sample, 2.5 ml water or 2.5 ml 60 μM thioglycolic acid, 2.5 ml 10 mM norleucine and 10 ml 30% HCl were added to CEM single-wall PTFE vials. The vials were capped with a double port cap. Samples for degassing were frozen (− 80°C) in order to avoid bumping during evacuation [2] and the gas phase was replaced by evacuating and filling with nitrogen (99.995%) to 15 p.s.i. (1 p.s.i. = 6894.76 Pa). The evacuating/filling process was repeated four times.

The samples were either heated in an oven at 110°C or in the microwave oven programmed as showed in Table 1. The "Time @P" at 150°C was varied from 10 min to 60 min.

Hydrolysed samples were "neutralised" to about pH 2.2 by adding 3.5 ml 50% NaOH, diluted to 50 ml with sodium citrate pH 2.2 solution (40 g trisodium citrate dihydrate, 30 ml 30% HCl plus water to 2000 ml) and filtered (0.45 μm) before IEC.

IEC of the samples was performed in a random order. Each sample was hydrolysed twice and each hydrolysate was analysed twice. Results given in tables and figures represent mean of four determinations.

2.6. Reagents and chemicals

Trione ninhydrin reagent was obtained from Pickering Labs. Chemicals for eluents were of Suprapur or "zur Aminosäureanalyse" grade from Merck. All other chemicals were of analytical-reagent grade. Ultra-pure water (18.2 MΩ), obtained by use of a Millipore Milli-Q water-purification system (Bedford, MA, USA), was used throughout.

3. Results and discussion

The microwave acid hydrolysis can be described by three phases: (1) a fast-heating phase, (2) a constant-temperature phase, and (3) a cooling phase. Fig. 1 shows typical temperature and pressure curves for a 30-min acid hydrolysis of a BioProtein sample. The set-point temperature was reached within 4 min from start. The pressure was not constant during the constant temperature period. It initially rose to about 65 p.s.i. (peak at about 7 min from start) and then fell down to about 45 p.s.i. This pressure pattern was observed for all the hydrolysis experiments, although the pressure level varied somewhat. The pattern is probably due to a reduction in the HCl concentration during the hydrolysis, as some HCl is used by the reaction. The absolute pressure level may well depend on the type and amount of sample. This observation indicates that temperature is a better control parameter than pressure for performing reproductive micro-

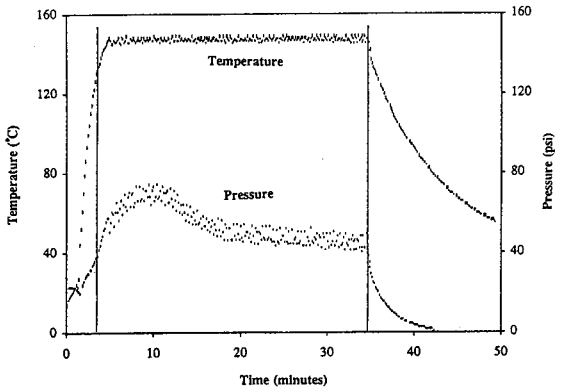

Fig. 1. Temperature and pressure curves for hydrolysis of a BioProtein sample in the microwave oven.

wave hydrolysis of protein samples; pressure control does not guarantee a constant hydrolysis temperature.

The effect of the hydrolysis time was initially tested in a series of experiments. The level of most amino acids increased when hydrolysis time was extended from 4 to 10 min and remained fairly constant when the hydrolysis time was further extended from 10 min and up to 60 min. Fig. 2 shows the measured amino acid level as a function of hydrolysis time for six selected amino acids. The amounts of serine and to a lesser extent threonine decreased when the hydrolysis time was extended. The level of isoleucine and valine increased when hydrolysis time was increased to 30 min. This is probably due to Leu–Leu, Ile–Leu, Ile–Val and Val–Gly peptide bindings in the protein that are difficult to hydrolyze [2,10]. A similar pattern was found for the same amino acids hydrolyzed at 110°C (Fig. 3).

Serine is known to be thermolabile under acid conditions and it has been suggested that serine is degraded due to first-order kinetics:

$$\ln A(t) = k_0 - k_1 t$$

where k_0 and k_1 are constants and $A(t)$ is the quantity of amino acid present after t h of hydrolysis; k_1 has been found to 0.0038–0.0043 h^{-1} [11]. We found that the serine degradation rate can be described by first-order kinetics with $k_1 = 0.84\ h^{-1}$ for hydrolysis times up to 20 min and $k_1 = 0.35\ h^{-1}$ for hydrolysis times between 20 and 60 min (Fig. 4). A similar biphasic behavior was not observed for hydrolysis at 110°C where k_1 was found to 0.0034 h^{-1} (results not shown).

Thioglycolic acid has been used to prevent the oxidation of methionine, tyrosine and carboxymethylcysteine during chromatography or acid hydrolysis of peptides and proteins [3,12]. Addition of thioglycolic acid has also been reported to improve tryptophan recovery [2]. Degassing can partly prevent the oxidation of methionine to methionine sulfoxide. We have tested the effect of degassing and thioglycolic acid on acid hydrolysis of BioProtein and two pure proteins, gelatine and casein, and compared traditional

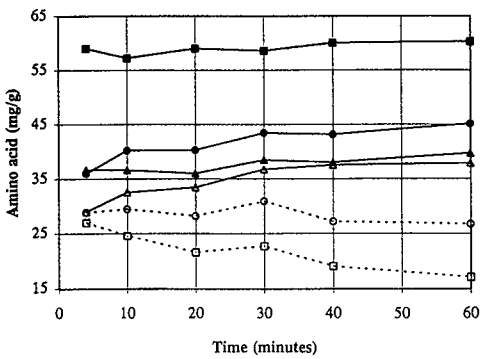

Fig. 2. Measured level of six different amino acids as a function of hydrolysis time. Hydrolyses were performed in a microwave oven at 150°C. ■ = Leucine; ● = valine; ▲ = glycine; △ = isoleucine; ○ = threonine; □ = serine.

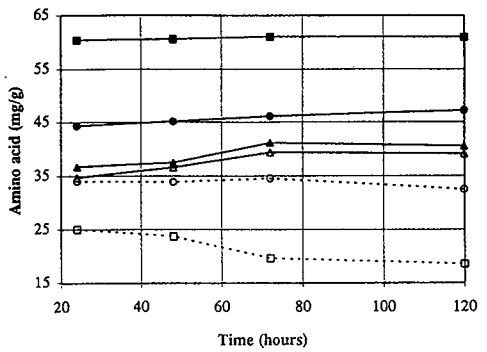

Fig. 3. Measured level of six different amino acids as a function of hydrolysis time. Hydrolyses were performed by heating to 110°C. ■ = Leucine; ● = valine; ▲ = glycine; △ = isoleucine; ○ = threonine; □ = serine.

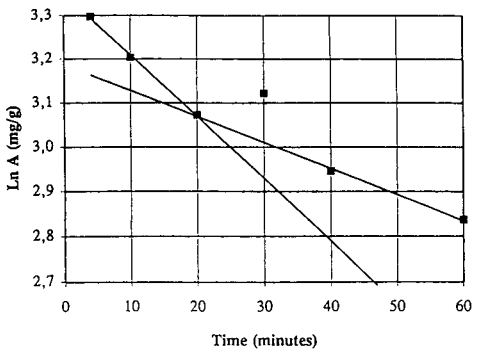

Fig. 4. Measured level of serine as a function of the hydrolysis time. Hydrolyses were performed in a microwave oven at 150°C. The lines represent the best fit for points at 4, 10 and 20 min [ln $A = 3.35 - 0.014t$ (min)] and at 20, 40 and 60 min [ln $A = 3.187 - 0.0059t$ (min)].

hydrolysis in closed vessels at 110°C for 24 h with hydrolysis in a microwave oven at 150°C for 10 and 30 min (Tables 2–5).

Methionine was found in the highest amount in degassed samples with thioglycolic acid (Table 2). However, the effect of degassing and addition of thioglycolic acid was small for the microwave hydrolyzed samples. In case of BioProtein the level increased from about 14 mg/g in the untreated sample to about 18.5 mg/g for the degassed and thioglycolic acid-treated sample. The effect was somewhat larger for gelatine whereas there was no effect at all for casein. This is in contrast to samples hydrolyzed at 110°C for 24 h. In that case there were some effect of degassing the samples and a large effect of adding thioglycolic acid to the samples. The observed differences between the microwave and the conventional method are probably due to the much longer treatment time for samples hydrolyzed at 110°C.

Tyrosine has been described to be seriously degraded during hydrolysis of certain proteins and hardly at all during others [2] and thioglycolic acid has been suggested as a stabilizing agent for tyrosine. We found that tyrosine was stable for all the sample types and conditions tested (Table 3).

Tryptophan is known to be acid labile and it is common to use basic hydrolysis to determine it. Thioglycolic acid has been reported to stabilize tryptophan during acid hydrolysis [6,12]. We found a higher level of tryptophan in the microwave-hydrolyzed samples but the level was much lower than expected from previous performed basic hydrolysis of the samples. The highest levels were found in degassed samples of casein with added thioglycolic acid. The low level found in BioProtein (expected level was 15.7 mg/g dry

Table 2
Measured level (mg/g) of methionine in samples hydrolyzed at 110°C for 24 h or at 150°C for 10 or 30 min

Sample	Treatment	No stabilisation	Degassed	Thioglycolic acid	Degassed + thioglycolic acid
BioProtein, dried	110°C, 24 h	0.1	6.7	14.0	16.3
	150°C, 10 min	14.5	15.8	16.5	18.3
	150°C, 30 min	13.5	16.0	18.2	18.5
BioProtein, fresh	110°C, 24 h	1.0	4.0	15.5	16.5
	150°C, 10 min	12.1	15.8	16.8	17.1
	150°C, 30 min	13.4	15.9	16.9	17.6
Gelatine	110°C, 24 h	2.0	2.5	8.6	9.0
	150°C, 10 min	2.9	4.4	8.8	9.6
	150°C, 30 min	1.9	4.6	9.0	9.6
Casein	110°C, 24 h	22.3	24.3	29.9	28.8
	150°C, 10 min	30.2	29.8	30.0	31.0
	150°C, 30 min	31.4	30.4	30.6	32.3

Table 3
Measured level (mg/g) of tyrosine in samples hydrolyzed at 110°C for 24 h or at 150°C for 10 or 30 min

Sample	Treatment	No stabilisation	Degassed	Thioglycolic acid	Degassed + thioglycolic acid
BioProtein, dried	110°C, 24 h	18.5	23.5	22.2	22.6
	150°C, 10 min	25.0	24.4	25.4	26.7
	150°C, 30 min	28.4	26.8	29.5	29.5
BioProtein, fresh	110°C, 24 h	20.9	22.3	23.4	23.5
	150°C, 10 min	25.2	25.6	24.4	24.7
	150°C, 30 min	24.3	27.7	27.2	27.3
Gelatine	110°C, 24 h	2.8	3.0	3.4	3.0
	150°C, 10 min	4.2	3.7	3.7	3.7
	150°C, 30 min	3.5	3.4	3.4	3.3
Casein	110°C, 24 h	55.5	52.7	57.3	54.9
	150°C, 10 min	52.5	55.8	54.8	56.3
	150°C, 30 min	56.3	57.1	56.1	56.8

matter) is probably due to its high content of carbohydrates as the recovery of tryptophan is negatively influenced by carbohydrates in the sample [6].

Cystine was unstable during acid hydrolysis, and the recovery was not increased by degassing (results not shown). The retention time of cysteine is similar to the retention time of proline and if the sample contains some cysteine it will not be measured correctly. Some of the cyst(e)ine was found as cysteic acid, especially in non-degassed samples. The cystine peak was absent in most samples where thioglycolic acid was added. Acid hydrolysis is known to cause very serious losses of cystine residues through severance of the disulfide bridges [2]. If oxygen

Table 4
Measured level (mg/g) of tryptophan in samples hydrolyzed at 110°C for 24 h or at 150°C for 10 or 30 min

Sample	Treatment	No stabilisation	Degassed	Thioglycolic acid	Degassed + thioglycolic acid
BioProtein, dried	110°C, 24 h	0.0	0.0	0.0	0.1
	150°C, 10 min	2.4	1.5	1.7	2.3
	150°C, 30 min	0.3	0.3	0.6	0.8
BioProtein, fresh	110°C, 24 h	0.2	0.3	0.6	0.3
	150°C, 10 min	1.8	1.5	2.8	2.9
	150°C, 30 min	1.2	0.4	0.8	1.1
Gelatine	110°C, 24 h	0.2	0.2	0	0.3
	150°C, 10 min	0.6	0.6	0.6	0.8
	150°C, 30 min	0.0	0.0	0.0	1.5
Casein	110°C, 24 h	0.1	0.1	3.4	4.2
	150°C, 10 min	7.5	6.4	5.6	11.8
	150°C, 30 min	7.4	3.6	10.9	7.9

Table 5
Measured level (mg/g) of tyrosine, phenylalanine, histidine, tryptophan and arginine in performic acid-oxidized samples of BioProtein

Amino acid	Hydrolysis time (min)	No stabilisation	Degassed	Phenol	Degassed + phenol	Non-oxidised sample
Tyrosine	10	0.7	1.0	2.0	6.8	27.0
	30	3.0	2.0	5.0	8.5	
Phenylalanine	10	2.1	1.9	24.0	31.6	32.4
	30	0.7	2.9	7.9	30.8	
Histidine	10	4.8	3.0	10.8	12.1	13.2
	30	1.6	5.5	13.5	12.7	
Tryptophan	10	7.7	8.1	0.9	5.3	15.7
	30	5.1	4.7	0.4	0.1	(basic hydrolysis)
Arginine	10	38.2	35.4	35.8	37.0	39.9
	30	39.8	39.4	39.6	40.1	

Samples were hydrolyzed in a microwave oven at 150°C for 10 or 30 min.

is present then the released thiol group will be oxidized, to a greater or lesser extent, to cysteic acid via cysteine and the sulfinic acid and sulfone. Cysteine suffers the same oxidative fate as cystine.

Cyst(e)ine can be quantitatively converted to cysteic acid by an oxidation with performic acid before the hydrolysis step [8,9]. However, performic acid oxidation is known to destroy tyrosine and tryptophan [10]. Loss of phenylalanine, histidine and arginine has also been reported [1,8]. Phenol can be added as a halogen scavenger to stabilize labile amino acids [8,13]. Table 5 shows the effect of degassing and adding of phenol on the detected level of tyrosine, phenylalanine, histidine, tryptophan and arginine. Degassing and phenol stabilize tyrosine, phenylalanine and histidine. The arginine level was not influenced by the peroxidation at all. The tryptophan level was highest in untreated samples, but the tryptophan quantitation was generally unreliable.

4. Conclusions

Microwave acid hydrolysis of protein samples is a fast method compared to conventional acid hydrolysis. A hydrolysis time of 10–30 min seems to be optimal as it cleaves most of the peptide linkages and shows no drastic loss of serine or threonine. Methionine was found to be fairly stable during microwave hydrolysis even when samples were degraded without degassing or addition of thioglycolic acid, although a higher level was found for degassed samples with thioglycolic acid added. Cyst(e)ine and tryptophan cannot be quantitatively determined after standard acid hydrolysis. Cyst(e)ine can be determined as cysteic acid after oxidation with performic acid. Phenol can be added to stabilise labile amino acid, but even then tyrosine and tryptophan cannot be determined correctly in oxidised samples. Thus, determination of all amino acids in a protein sample still requires three different hydrolyses: standard hydrolysis, peroxidation and hydrolysis and basic hydrolysis. However, the hydrolysis time can be reduced considerably by using the microwave technique.

References

[1] C.J. Rayner, *J. Agric Food Chem.*, 33 (1985) 722.
[2] S. Hunt, in G.C. Barrett (Editor), *Chemistry and Biochemistry of the Amino Acids*, Chapman & Hall, London, 1985, p. 376.
[3] M.V. Pickering, *LC·GC*, 8 (1990) 778.
[4] A. Péter, G. Laus, D. Tourwe, E. Gerlo and G. Van Binst, *Peptide Res.*, 6 (1993) 48.

[5] R. Grimm, *Application Note*, Hewlett Packard Bioscience, Publication No. 12-5091-4585, 1992.
[6] B. Penke, R. Ferenczi and K. Kovacs, *Anal. Biochem.*, 60 (1974) 45.
[7] L. Joergensen and H. Degn, *Biotechnol. Lett.*, 9 (1987) 71.
[8] V.C. Mason, M. Rudemo and S. Bech-Andersen, *Z. Tierphysiol., Tierernährg. Futtermittelkde.*, 43 (1980) 35.
[9] I.M. Moodie, D.L. Walsh and J.A. Burger, *J. Chromatogr.*, 261 (1983) 146.
[10] J. Ozols, *Methods Enzymol.*, 182 (1990) 587.
[11] M. Rudemo, S. Bech-Andersen and V.C. Mason, *Z. Tierphysiol., Tierernährg. Futtermittelkde.*, 43 (1980) 27.
[12] H. Matsubara and R.M. Sasaki, *Biochem. Biophys. Res. Commun.*, 35 (1969) 175.
[13] V.C. Mason, S. Bech-Andersen and M. Rudemo, *Z. Tierphysiol., Tierernährg. Futtermittelkde.*, 43 (1980) 146.

ELSEVIER

Journal of Chromatography A, 706 (1995) 429–436

JOURNAL OF CHROMATOGRAPHY A

Direct determination of seleno-amino acids in biological tissues by anion-exchange separation and electrochemical detection

S. Cavalli[a], N. Cardellicchio[b,*]

[a]*Dionex S.r.l., Laboratorio Applicazioni, via Tulipani 5, 20090 Pieve Emanuele MI, Italy*
[b]*CNR, Istituto Sperimentale Talassografico, via Roma 3, 74100 Taranto TA, Italy*

Abstract

Several studies have described the determination of selenium in protein extracts from tissues of marine or terrestrial animals, but have not identified the different chemical forms of selenium that are present. Selenium may be present as seleno-amino acids. Selenocysteine, for example, is a normal component of glutathione peroxidase, an antioxidant enzyme which may behave like other antioxidants, such as vitamin E, protecting the tissues against methylmercury toxicity.

The present study illustrates a method for the characterization of seleno-amino acids, such as selenocysteine and selenomethionine, in proteins extracted from the liver of marine mammals. The mechanism of detoxification of methylmercury, which involves seleno-compounds, is identified.

The analytical determination was carried out using high-performance anion-exchange chromatography coupled with integrated pulsed amperometric detection (HPAEC–IPAD). This method allows the direct determination of underivatized amino acids, eliminating the procedure of pre- or postcolumn derivatization.

The chromatographic separation was carried out on an anion-exchange column using a quaternary gradient elution. In order to optimize this method, interferences of amino acids and the influence of pH and ionic strength on the separation and electrochemical detection were studied. The IPAD response for the direct detection of amino acids is optimum at pH > 11. The detection limit ($S/N = 3$) for selenocysteine was found to be 450 μg/l.

The application of this method for the identification of seleno-amino acids in protein hydrolysates is also shown.

1. Introduction

1.1. Selenium metabolism in marine animals

Selenium has been recognized to be an essential nutrient element in certain species, but relatively high levels result in toxic effects. The biochemical cycle of this element is relatively complex because of the involvement of both inorganic and organometallic species, such as seleno-amino acids

Different studies on marine mammals showed that selenium is strictly correlated to the detoxification processes of methylmercury in the liver [1,2]. When the level of methylmercury increases above a certain threshold (i.e. 100 μg/g Hg wet weight) demethylation starts, which causes the formation of compounds with low toxicity, with a 1:1 Se/Hg molar ratio [3]. The structure of these compounds has not yet been completely determined.

Several studies have isolated selenium in protein extracts from muscle and liver tissues of marine animals [4–7], but have not identified the

* Corresponding author.

0021-9673/95/$09.50
SSDI 0021-9673(95)00233-2

chemical forms of selenium present. Selenium compounds in some marine fish have also been found to be associated with lipid material and have properties similar to lipoproteins.

Possible chemical transformations of selenium in marine animals have been reviewed by Maher et al. [4], but on this argument various interpretations still exist. Selenium-dependent glutathione peroxidase has been isolated in marine animals indicating that some selenium may be present as selenocysteine, as a normal component of glutathione peroxidase [8]. The identity of organoselenium compounds in the aquatic environment has not been fully established. In marine bacteria and plankton, selenium is predominantly found in protein as seleno-amino acids [9–11]. Selenomethionine has been isolated from the hydrophilic fulvate fraction of soil [12] and from protein of marine algae [13]

Alternatively, selenium may be in a non-protein moiety tightly held to protein, but not covalently bound. For example, it has been shown that selenium can readily form selenotrisulphides with thiols such as cysteine, glutathione, etc. [14]. These can then be incorporated and stabilized within protein structures. Chemical isolation of these types of compounds during extraction would prove difficult as destabilization results in the precipitation of elemental selenium. Many analytical procedures for selenium determination in different matrices exist. In recent years, in addition to the methods for the determination of the total selenium content, methods for the determination of different forms of selenium in water, soil, and biological matrices have been developed. Speciation of selenium is important in order to understand its biological cycle and to define the diffusion and the toxicity of this element in the ecosystem.

1.2. Chromatographic analysis

Progress in the determination of amino acids can be attributed to the technological advances in liquid chromatography and chromatographic detectors. Separations of amino acids in liquid chromatography are readily achieved by using reversed-phase stationary phases [15] or ion exchangers [16,17], and for the separation of complex mixtures, gradient elution is essential.

Sensitive photometric detection requires some kind of pre- or postcolumn derivatization. *o*-Phthalaldehyde (OPA) [18,19], a fluorescent derivatizing agent, offers excellent sensitivity, but the derivatives of OPA are not stable, OPA does not form adducts with secondary amino acids (e.g. proline and hydroxyproline), and the thiol group of amino acids may compete with the mercapto propionic acid used in the postcolumn reaction. Ninhydrin has been widely employed to enhance UV–Vis detection, but the reaction requires temperature control (135°C) and a postcolumn device is prone to plug. Furthermore, sensitivity for this reagent is lower than that for OPA. Recently HPLC analysis with the fluorescent reagent *N*-(iodoacetylaminoethyl)-5-naphthylamine-1-sulphonic acid has been utilized for the determination of selenocysteine in plasma at the μM level [20].

Detection methodology that does not require derivatization is preferred for ease and convenience, thus a selective detection, such as electrochemical detection has gained prominence in liquid chromatography as a sensitive and selective detection technique. Among the different electrochemical detection techniques, integrated pulsed amperometric detection (IPAD) has proven to be a selective and sensitive technique for the determination of amino acids without derivatization [21–23]. Amino acids can be detected directly at gold electrodes in an alkaline medium. The Au electrode is preferred over Pt in order to minimize the interference from dissolved oxygen [24].

IPAD, equipped with a Au electrode, is only selective for compounds containing oxidizable functional groups such as hydroxyl, amine and sulphide. IPAD is preferred over PAD in order to minimize baseline offset and drift during gradient pH elution.

A review has recently appeared on the different analytical methods used for speciation of selenium compounds [25]. Two different ana-

lytical approaches are reported in the literature for the determination of seleno-amino acids: gas chromatography and ion-exchange chromatography. The gas chromatographic methods require a precolumn preparation of volatile derivatives of seleno-amino acids [26–28], then the compounds are separated and identified by GC–MS. Various derivatizing reagents have been studied such as bis-(trimethylsilyl)acetamide, *N*-methyl - *N* - (*tert.* - butyldimethylsilyl)trifluoro - acetamide and cyanogen bromide. Ion-exchange chromatography separates seleno-amino acids from other amino acids [29–31], but one main problem is the oxidative destruction of these amino acids due to the protein hydrolysis procedure used in sample preparation [32]. Selenocysteine cannot be determined accurately under the classical hydrolysis conditions because of decomposition.

The most widely used hydrolysis procedure is gas-phase hydrolysis. Proteins are subjected to 6 *M* HCl vapour in the presence of 0.5% phenol for 24–72 h at 110°C. These conditions are known to destroy tryptophan and convert glutamine and asparagine to their acidic analogues. Furthermore, cysteine and cystine are at least partially converted to cysteic acid.

This paper shows the application of IPAD following gradient elution ion chromatography for the direct and simultaneous detection of selenocysteine and selenomethionine.

IPAD parameters, such as applied potentials and duration as well as the choice of reference electrode, were determined in order to optimize sensitivity for selenocysteine and selenomethionine detection. A gradient procedure, that incorporated a change in pH for the resolution of all the amino acids of interest, was developed. Furthermore, an innovative technique for protein hydrolysis, based on microwave irradiation [33,34], is shown. This technique overcomes the drawbacks of classical acidic hydrolysis of proteins, thus leading to a high recovery of seleno-amino acids.

This technique was used for the determination of the seleno-amino acid composition in protein hydrolysates of dolphin liver.

2. Experimental

2.1. Instrumentation

A metal-free modified Model 4000i quaternary gradient liquid chromatograph (Dionex, Sunnyvale, CA, USA) equipped with a PED-2 electrochemical detector (Dionex) was used to analyse amino acids. Data manipulation and the operation of all the components in the system were controlled by AI-450 chromatographic software (Dionex) interfaced via an advanced computer interface ACI-2 (Dionex) to a 80486-based computer (Olivetti, Ivrea, Italy). A modified MSD-81D microwave digester (CEM Co., Matthews, NC, USA) was used for protein hydrolysis. For mercury determination in dolphin liver, homogenized samples were digested under pressure in a Teflon vessel with a 1:1 (v/v) concentrated H_2SO_4–HNO_3 mixture for 4 h at 160°C. Mercury was determined by the cold vapour atomic absorption spectrophotometry using a modified 1100 B spectrophotometer (Perkin Elmer, Norwalk, CT, USA).

Total selenium was determined by graphite furnace atomic absorption spectrophotometry (GF-AAS) using a modified Model 3030 Zeeman spectrophotometer (Perkin Elmer). Before analysis, liver samples were digested under pressure in a Teflon vessel with concentrated HNO_3 for 4 h at 160°C. Methylmercury was determined by gas chromatography [35] using a modified Mega Model 5600 gas chromatograph (Carlo Erba, Rodano, Italy) equipped with a ^{63}Ni electron capture detector.

2.2. Reagents and standards

Sodium tetraborate, sodium acetate, sodium hydroxide, 50% solution low carbonate, hydrochloric acid, nitric acid, sulphuric acid, and phenol were of analytical reagent grade (Novachimica, Milano, Italy); amino acid standard solution, selenomethionine and selenocystine were obtained from Sigma (St. Louis, MO, USA). By reducing selenocystine with threo-1,4-dimercapto-2,3-butanediol (dithiothrei-

tol or DTT) (Aldrich, Milwaukee, WI, USA) selenocysteine was obtained. The reduction was carried out at pH 8.2–8.5 for 30 min at room temperature.

All reagents were prepared daily with ultra-pure deionized water (<0.1 μS at 25°C) obtained using a Milli-Q system (Millipore, Milford, MA, USA). Working standard solutions were prepared by serial dilution of stock solutions. In the case of seleno-amino acids the standard solution was prepared in 1 *M* HCl.

2.3. Microwave heating-gas phase hydrolysis of proteins

The biological tissue (dolphin liver) was homogenized; to 1 g of homogenate, 5.5 ml of water, 1 g of NaCl and 1.5 ml of concentrated HCl was added. The sample was sonicated for 30 min and centrifuged at 6000 *g* for 10 min.

The precipitate containing the protein fraction was then separated, washed with 0.1 *M* HCl and submitted to acidic digestion. Sample digest was cleaned up on a AG-50 resin and analysed by IC–IPAD. Atomic absorption analysis demonstrated that most of the selenium (>95%) was in the protein fraction.

For protein hydrolysis, 100 mg of purified liver proteins were placed in a reaction vessel with 10 ml 6 *M* HCl and 0.5% phenol solution, added in order to protect the easily oxidizable amino acids [36]. Teflon reaction vessels containing a sample, were then evacuated and purged with N_2. Pressure was set to 55 p.s.i. resulting in a temperature of 150°C. Hydrolysis was performed with microwave irradiation at 645 W for 25 min using a microwave digestion system. The resulting solution was then filtered through a 0.45-μm filter and diluted 1:1 with eluent A (see Table 1) prior to injection.

2.4. Chromatography of amino acids

Separation was carried out on a 250 × 4 mm I.D. AminoPac PA1 pellicular anion-exchange column (Dionex) at a flow-rate of 1 ml/min at room temperature. Injection loop was 50 μl.

Amino acids were separated with a sodium hydroxide, sodium borate and sodium acetate linear quaternary gradient system shown in Table 1. All eluents and the postcolumn reagent were prepared daily with ultra-pure deionized water. A 300 m*M* sodium hydroxide solution, used at 0.8 ml/min as a postcolumn addition, showed the tendency to reduce baseline shifts that occurred with sodium hydroxide gradient and to increase sensitivity. Fig. 1 shows a chromatogram of a standard solution of amino acids.

Table 1
Gradient conditions for separation of amino acids

Time (min)	A (%)	B (%)	C (%)	D (%)	Valve position
0.0	100	0	0	0	Load
4.0	100	0	0	0	Load
4.1	0	0	0	100	Load
13.9	0	0	0	100	Load
14.0	100	0	0	0	Load
25.8	100	0	0	0	Load
26.0	100	0	0	0	Inject
36.0	100	0	0	0	Inject
40.0	0	100	0	0	Inject
46.0	0	100	0	0	Inject
46.1	0	90	10	0	Inject
56.0	0	0	100	0	Load
60.0	0	0	100	0	Load
66.0	0	0	100	0	Load

Eluent A, 0.023 *M* sodium hydroxide–0.007 *M* sodium tetraborate. Eluent B, 0.08 *M* sodium hydroxide–0.023 *M* sodium tetraborate. Eluent C, 0.65 *M* sodium acetate. Eluent D, 1 *M* sodium hydroxide–0.3 m*M* sodium tetraborate. Flow-rate = 1 ml/min.

2.5. IPAD detection

Detection was effected by using integrated pulsed amperometry with a gold working electrode and a standard Ag/AgCl reference electrode: the pH electrode could better compensate the baseline drift, but it is prone to degradation in mid-term life. The working pulse potentials and duration, and the integration time, that were used throughout the detection of amino acids are shown in Table 2. The NH_3 groups were oxidized at +0.35 V; the reaction products are removed at +0.9 V, while the electrode is cleaned at a negative potential of −0.9 V.

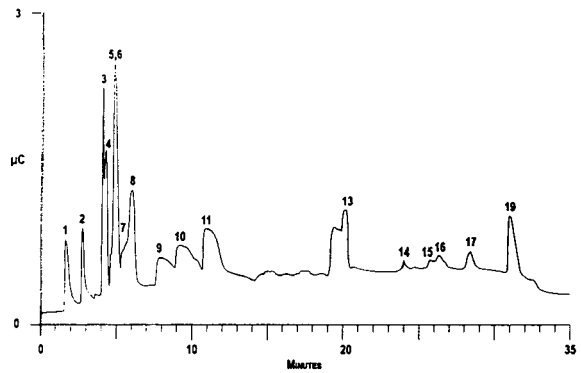

Fig. 1. Gradient elution of amino acids standard. Peaks: 1 = Arg; 2 = Lys; 3 = Thr; 4 = Ala; 5 = Gly; 6 = Ser; 7 = Val; 8 = Pro; 9 = Ileu; 10 = Leu; 11 = Met; 13 = His; 14 = Phe; 15 = Glu; 16 = Asp; 17 = Cys; 19 = Tyr. Chromatographic conditions as shown in Table 1. Column, AminoPac PA1. Detection, IPAD conditions as in Table 2.

3. Results and discussion

For the chromatographic determination of seleno-amino acids a separation on an anion-exchange column based on a quaternary gradient system, as shown in Table 1, was chosen. The separation on the AminoPac PA1 column is effectuated by the relative difference in the dissociation constants of the amino, carboxylic and R groups of each amino acid. Fig. 1 shows a typical example of chromatographic separation of a standard solution of amino acids. The detection protocol of the IPAD is shown in Table 2 and is relative to amino group detection. During the amperometric detection, the electrode current is continuously integrated during the cycle in which the electrode is oxidized and then reduced to its original state. Amines and sulphur compounds that have an unbalanced electron pair on their N and S atoms can be adsorbed at the oxide-free Au electrode surface when $E < 0.1$ V and anodically detected by oxide-catalysed reactions during the positive scan.

The advantage of using integrated amperometry compared to pulsed amperometry is the reduction in baseline drift due to the elimination of the charge caused by oxide formation and its reduction. The same gradient and detection system were also used for the seleno-amino acid determination. Experimental results show a good separation of the selenomethionine and selenocystine peaks from their corresponding sulphur analogues. As shown by the experimental results, the substitution of a sulphur atom with selenium increases the retention time of the corresponding amino acids, which can be easily identified because those zones of the chromatogram are relatively free from interfering peaks. Fig. 2 shows a chromatogram of a standard solution of methionine, selenomethionine,

Table 2
Time/potential used for IPAD detection of seleno-amino acids

Time (s)	Potential (V)
0.00	−0.10
0.20	−0.10
0.30	0.35
0.40	0.35
0.50	−0.10
0.70	−0.10
0.71	0.90
0.90	0.90
0.91	−0.90
1.00	−0.90

Integration time from 0.20 to 0.70 s. Reference electrode A–AgCl.

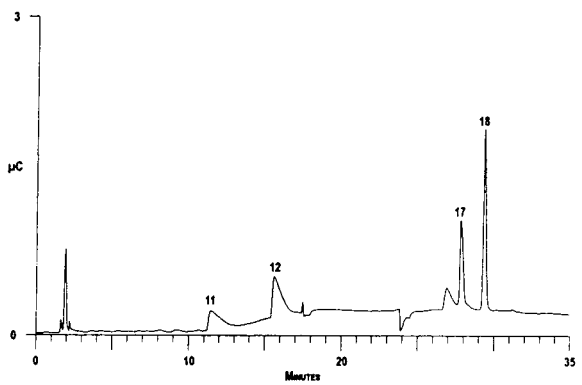

Fig. 2. Gradient elution of amino acids and seleno-amino acids standard. Peaks: 11 = Met; 12 = SeMet; 17 = Cys; 18 = SeCys. Chromatographic conditions as shown in Table 1. Column, AminoPac PA1. Detection, IPAD conditions as in Table 2.

cysteine, and selenocysteine (1 μg of each injected); because of the asymmetric peak shapes, peak areas were chosen for quantitation.

The anion exchange at alkaline pH is evidenced by the good separation of the seleno-amino acids from other amino acids. The baseline drift during the gradient results from changes in pH and ionic strength. In order to reduce the drift, a postcolumn addition of 300 m*M* NaOH at 0.5 ml/min was made. Detection limits for the determination of selenomethionine and selenocysteine were found to be 620 μg/l and 450 μg/l, respectively. The IPAD response shows good linearity for both selenomethionine and selenocysteine up to 10 mg/l. Quantitative analysis was carried out, using the standard addition method and measuring peak area. The reproducibilities of the peak areas were calculated by performing five replicate analyses of standard solutions of 1 mg/l of both selenomethionine and selenocysteine. The R.S.D.s for the peak areas were 4.7 and 8.1% for selenocysteine and selenomethionine, respectively.

This technique was used for the determination of seleno-amino acids in protein hydrolysate of dolphin liver.

Selenium, in fact, is considered to play a key role in reducing the toxic manifestations of mercury in rats [37,38]. Published studies suggest that mercury and selenium concentration may be correlated in man [39] and some marine organisms [40]. For instance, there is a significant correlation between selenium and mercury in black marlin liver [41], tuna tissues [42] and marine mammals [2,43].

Table 3 shows the mercury, methylmercury and selenium concentrations in the liver of 16 dolphin specimens (*Stenella coeruleoalba*) found beached along the coast of Apulia (southern Italy). Fig. 3 shows the behaviour of mercury and selenium concentration in liver. It is evident that a strict correlation exists between mercury and selenium accumulation. Because the presence of mercury in dolphin is mainly due to methylmercury intake in the diet, the low percentage of methylmercury in the liver demonstrates that a detoxification process exists which

Table 3
Mercury, methylmercury (HgMet), selenium and Se/Hg′ molar ratio in dolphin liver

Specimen	Hg (μg/g)[a]	HgMet		Se (μg/g)[a]	Se/Hg′
		(μg/g)[a]	(%)		
16	374.5	6.8	1.8	165.0	1.13
13	351.9	10.0	2.8	158.5	1.17
9	263.3	8.0	3.0	132.8	1.32
12	242.0	7.0	2.9	104.0	1.12
5	216.7	5.4	2.5	92.4	1.11
2	206.3	12.2	5.9	85.4	1.12
1	206.2	9.5	4.6	90.2	1.16
15	183.1	7.9	4.3	92.3	1.34
7	168.0	4.6	2.7	91.8	1.43
4	160.3	3.4	2.1	87.4	1.42
6	156.3	10.6	6.7	86.4	1.49
14	107.4	6.3	5.9	48.6	1.23
10	12.3	1.9	15.4	7.8	1.90
11	3.2	0.9	28.1	4.8	5.53
8	2.3	1.2	52.2	4.4	10.13
3	1.9	1.1	57.9	4.3	13.68

[a] μg/g wet weight.
$Hg' = Hg_{tot} - HgMet$.

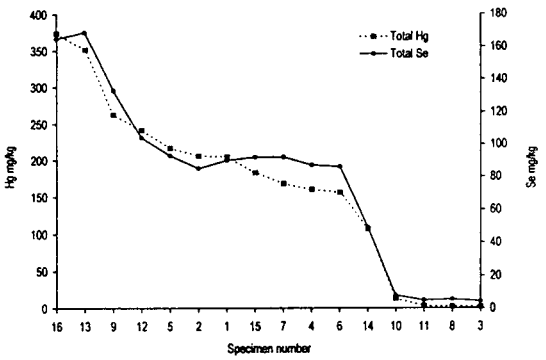

Fig. 3. Correlation between total mercury and total selenium concentration in liver of different dolphins (*Stenella coeruleoalba*).

involves the demethylation of methylmercury. Where concentrations of methylmercury are lower than 10%, the atomic ratio Se/Hg′, where $Hg' = Hg_{tot} - HgMet$, is approximately 1. This has also been observed by other researchers [1,2] and their conclusion was to consider the final product of methylmercury demethylation as a Hg–Se compound (tiemannite) which is insoluble and less toxic [1].

Recently, Palmisano et al. [3] suggested that very stable complexes such as Hg–selenoprotein could play an important role in mercury detoxification. The role of selenium in this process has not been completely explained. Demethylation is activated in the liver only when a threshold value of the methylmercury concentration is reached [3]. With these premises, the determination of seleno-amino acids in the protein fraction of dolphin liver is important in order to understand both the demethylation process of methylmercury and the selenium compound structure.

The analytical method proposed in the present work was applied to the determination of seleno-amino acids in hydrolysed samples of dolphin liver.

Hydrolysis was carried out in a microwave digester (the conditions have been described above) to reduce the risk of oxidative decomposition of sulphur-amino acids. In the same way, acidic hydrolysis tests on standard solutions of selenomethionine and selenocysteine showed a recovery better than 90%.

Fig. 4a shows a typical chromatogram of a hydrolysate (liver of dolphin No. 16) where a Ag–AgCl reference electrode was used. The gradient drift due to the change in pH and ionic strength of the eluent was partially compensated by the postcolumn addition of NaOH (300 m*M*). This sample contains a seleno-amino acid concentration close to the detection limit; the concentration of selenocysteine, calculated by the standard addition method, is 5 nmol/ml of hydrolysate. As shown in Fig. 4b, the selenocysteine peak was confirmed by the addition of selenocysteine standard solution (80 μg of SeCys was added to 100 mg of liver proteins). A substantial amount of the total selenium (>40% average value) was present in liver proteins such as selenocysteine.

This preliminary result seems to confirm the hypothesis that selenium is present in liver proteins such as seleno-amino acids. The main function of these proteins may be the binding of mercury, in Se–Hg bonds, in order to lower its toxicity.

Experimental work is progressing and we are also investigating hyphenated techniques such as IC–ICP or IC–ICP–MS in order to have a more

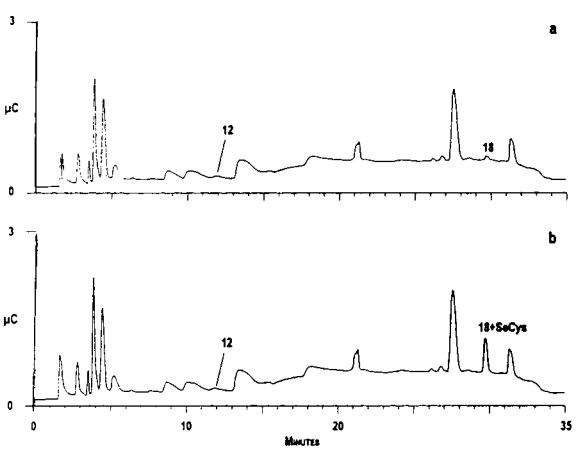

Fig. 4. (a) Gradient elution of protein hydrolysate of dolphin liver. Peaks: 12 = SeMet; 18 = SeCys. Chromatographic conditions as shown in Table 1. Column, AminoPac PA1. Detection, IPAD conditions as in Table 2. (b) Same sample as (a) spiked with selenocysteine standard solution (80 μg of SeCys was added to 100 mg of liver protein).

accurate detection system coupled with the chromatographic separation for reducing the number of peaks and to increase the selectivity of the method.

Acknowledgement

The authors acknowledge Pietro Ragone and Claudio Marra for their valuable assistance during this project and for helpful discussions.

References

[1] R. Martoya and J.P. Berry, *Vie Milieu*, 30 (1980) 7.
[2] J.H. Koeman, W.H.M. Peeters, C.H.M. Koudstaal-Hol, P.S. Tjioe and J.J.M. Degoeji, *Nature (London)*, 245 (1973) 385.
[3] F. Palmisano, N. Cardellicchio and P.G. Zambonin, *Mar. Environ. Res.*, 14 (1995) in press.
[4] W. Maher, S. Baldwin, M. Deaker and M. Irving, *Appl. Organomet. Chem.*, 6 (12) 103.
[5] J.J. Wrench and N.C. Campbell, *Chemosphere*, 10 (1981) 1115.
[6] S. Braddon-Galloway and J.E. Balthrop, *Comp. Biochem. Physiol.*, 82C (1985) 287.
[7] S. Braddon-Galloway and C.R. Sumpter, *Comp. Biochem. Physiol.*, 83C (1985) 13.
[8] T.C. Stadman, *FASEB*, 1 (1987) 375.
[9] A. Foda, H. Vandermeulens and J.J. Wrench, *Can. J. Aquat. Sci.*, 40 (1983) 215.
[10] J.J. Wrench, *Mar. Biol.*, 49 (1978) 231.
[11] J.J. Wrench and N. C Campbell, *Chemosphere*, 10 (1981) 1155.
[12] M. M Abrams and R.G. Burau, *Commun. Soil Sci. Plant Anal.*, 20 (1989) 221.
[13] N.R. Bottino, C.H. Banks, K.J. Irgolin, P. Micks, A.E. Wheeler and R.A. Zingaro, *Phytochemistry*, 23 (1984) 2445.
[14] H.E. Ganther, *Biochemistry*, 7 (1968) 2898.
[15] R.M. Waightman, E.C. Paik, S. Borman and H.A. Dayton, *Anal. Chem.*, 50 (1978) 1410.
[16] B. Kazee, D.E. Weisshaar and T. Kuwana, *Anal. Chem.*, 57 (1985) 2736.
[17] R.C. Engstrom, *Anal. Chem.*, 54 (1982) 2310.
[18] J.D.H. Cooper and D.C. Turnel, *J. Chromatogr.*, 227 (1982) 158.
[19] D.C. Turnel and J.D.H. Cooper, *Anal. Chem.*, 54 (1982) 527.
[20] W.C. Hawkes and M.A. Kutnink, *J. Chromatogr.*, 576 (1992) 263.
[21] L.R. Welch, W.R. LaCourse, D.A. Mead Jr., D.C. Johnson and T. Hu, *Anal. Chem.*, 61 (1989) 555.
[22] D.A. Mead, L.A. Larew, W.R. LaCourse and D.C. Johnson, in P. Jandik and R.M. Cassidy (Editors), *Advances in Ion Chromatography*, Century International, Franklin, MA, 1989, Vol. 1, p. 13.
[23] D.C. Johnson and W.R. LaCourse, *Anal. Chem.*, 62 (1990) 589.
[24] D.C. Johnson, *Nature*, 321 (1986) 451.
[25] X. Dauchy, M. Potin-Gautier, A. Astruc and H. Astruc, *Fresenius J. Anal. Chem.*, 348 (14) 792.
[26] K. Yasumoto, T. Suzuki and M. Yoshida, *J. Agric. Food Chem.*, 36 (1988) 463.
[27] M.M. Abrams and R.G. Burau, *Commun. Soil Sci. Plant Anal.*, 20 (1989) 221.
[28] K.A. Caldwell and A.L. Tappel, *J. Chromatogr.*, 32 (1968) 635.
[29] J.L. Martin and M.L. Gerlach, *Anal. Biochem.*, 29 (1969) 257.
[30] C.C.Q. Chin, *Methods Enzymol.*, 106 (1984) 17.
[31] R. Walter, D.H. Schlesinger and I.L. Schwartz, *Anal. Biochem.*, 27 (1969) 231.
[32] R.E. Huber and R.S. Criddle, *Biochim. Biophys. Acta*, 141 (1967) 587.
[33] H.M. Yu, S.T. Chem, S.H. Chiou and K.T. Wang, *J. Chromatogr.*, 456 (1988) 357.
[34] W.J. Kohr, R. Keck and R.N. Harkins, *Anal. Biochem.*, 122 (1982) 348.
[35] G. Westoo, *Acta Chem. Scand.*, 22 (1968) 2277
[36] C. Woodward, L.B. Gilman and W.G. Engelhart, *Int. Laboratory*, 9 (1990) 40.
[37] L.W. Chang and R. Suber, *Bull. Environ. Contam. Toxicol.*, 29 (1982) 285.
[38] A. Naganuma, Y. Kojima and N. Imura, *Res. Commun. Chem. Pathol. Pharmacol.*, 30 (1980) 301.
[39] L. Kosta, A.R. Byrne and V. Zelenko, *Nature*, 254 (1975) 238.
[40] E. Pellettier, *Mar. Environ. Res.*, 18 (1986) 111.
[41] N.J. Mackay, M.N. Kazacos, R.J. Williams and M.I. Leedow, *Mar. Pollut. Bull.*, 6 (1975) 57.
[42] H.E. Ganther and M.L. Sundle, *J. Food Sci.*, 1 (1974) 39.
[43] R. Wagerman, R.E.A. Stewart, P. Beland and C. Desjardins, in T.G. Smith, D.J. Aubin and J.R. Geraci (Editors), *Advances in Research on Beluga Whale Delphinapterus leucas*, Department of Fisheries and Oceans, Ottawa, Commun. Dir., 1990, pp. 191–206.

ELSEVIER

Journal of Chromatography A, 706 (1995) 437–442

JOURNAL OF CHROMATOGRAPHY A

Nitric oxide in biological fluids: analysis of nitrite and nitrate by high-performance ion chromatography

Steven A. Everett, Madeleine F. Dennis, Gillian M. Tozer, Vivien E. Prise, Peter Wardman, Michael R.L. Stratford*

Cancer Research Campaign Gray Laboratory, Mount Vernon Hospital, P.O. Box 100, Northwood, Middlesex HA6 2JR, UK

Abstract

The analysis of nitric oxide-derived nitrite and nitrate ions in biological fluids represents a proven strategy for determining nitric oxide participation in a diverse range of physiological and pathophysiological processes in vivo. In this article we describe a versatile method for the simultaneous measurement of NO_2^- and NO_3^- anions in both plasma and isolated tumour models based on anion-exchange chromatography with spectrophotometric detection (214 nm). This method compares well with the capillary electrophoresis technique, exhibiting an equivalent sensitivity for NO_2^-/NO_3^- anions and short run-times, i.e. not greater than 4 min. Comparisons are also made with two alternative but less satisfactory methods which employ ion-exchange or reversed-phase ion-pair chromatography with conductimetric as well as spectrophotometric detection. Technical problems associated with each method, particularly those arising from nitrate contamination, have been addressed.

1. Introduction

Since the identification of nitric oxide ($NO^\cdot$) as endothelium-derived relaxation factor (EDRF) [1] this free-radical species has been linked to multiple physiological and pathophysiological functions in vivo [2–4]. The signalling properties of EDRF–$NO^\cdot$ which modify vascular smooth muscle tone [5,6] and neurotransmission in peripheral and central nervous systems [7] contrast with the cytotoxic behaviour of $NO^\cdot$ when generated as part of the immune response [8,9].

A number of methods are capable of measuring the continuous release of $NO^\cdot$ [10] but those more commonly used include a chemiluminescence assay based on the reaction of $NO^\cdot$ with ozone [11] or luminol–H_2O_2 [12], spectrophotometric assays based on the oxidation of oxyhaemoglobin [13], electron paramagnetic resonance spectroscopy utilizing cheletropic traps [14] and $NO^\cdot$-selective electrode detectors [15]. However, these methods are not practical for clinical pharmacokinetic studies because of the short half-life (<5 s) of $NO^\cdot$ in vivo. In oxygenated aqueous solution $NO^\cdot$ is rapidly oxidized stoichiometrically to nitrite ions [16] according to Eq. 1:

$$4NO^\cdot + O_2 + 2H_2O \rightarrow 4NO_2^- + 4H^+ \quad (1)$$

Endogenous NO_2^- ion production in plasma cannot be assayed because of the nearly complete oxidation of NO_2^- to NO_3^- ions by, for example, oxyhaemoglobin [16] in Eq. 2:

* Corresponding author.

0021-9673/95/$09.50
SSDI 0021-9673(95)00078-X

$$4HbO_2 + 4NO_2^- + 4H^+ \rightarrow 4Hb^+ + 4NO_3^- + O_2 + 2H_2O \quad (2)$$

The traditional Griess method [17] and the more recent 2,3-diaminonaphthalene method [18] both require back-reduction of plasma NO_3^- ions to NO_2^- prior to analysis [19].

Cancer patients receiving interluekin-2 (IL-2) therapy produce a cytokine-inducible nitric oxide synthase (*i*NOS) which is responsible for increased plasma nitrate production. In patients receiving IL-2 and flavone-8-acetic acid cotherapy, there is a correlation between increased plasma nitrate and remission of advanced malignant melanoma [20]. Clinical trials and studies in tumour models of potential anticancer therapies (which mediate their effects by an increased expression or alternatively inhibition of *i*NOS in tumour-associated macrophages and vasculature [2,21,22]) would benefit from fast quantitation of $NO^{\cdot}$-derived products both systemically and in the tumour microenvironment.

For the determination of many inorganic anions high-performance ion chromatography (HPIC), capillary electrophoresis (HPCE) and liquid chromatography (HPLC) have become the methods of choice and offer a more direct approach to the determination of nitrite and nitrate ions in plasma. A recent HPCE method has been reported with the required sensitivity to measure basal levels of nitrite and nitrate ions in plasma with minimal sample preparation and short run times of no more than 3 min [23]. HPIC analysis of plasma nitrate and particularly nitrite have been hampered by the large amount of chloride ion (typically $[Cl^-] \sim 100$ mmol dm^{-3}) which results in insufficient peak resolution when utilizing conductimetric detection [24]. This problem has in part been circumvented by HPLC utilizing both UV [25] or alternatively electrochemical detection [26] neither of which require prior removal of Cl^- ions.

In this article we describe a versatile method for the rapid (≈4 min), simultaneous measurement of NO_2^-/NO_3^- anions in both plasma and tumour perfusate samples based on anion-exchange chromatography with spectrophotometric detection (214 nm). Comparisons are made with two alternative but less satisfactory methods which employ ion-exchange or reversed-phase ion-pair chromatography with conductimetric as well as spectrophotometric detection. Technical problems associated with each method, particularly those arising from nitrate ion contamination during sample work-up, have been tackled.

2. Experimental

2.1. Chemicals

Acetonitrile was from Rathburn (Walkerburn, UK) and tetrabutylammonium hydrogensulphate ($TBASO_4$) was from Fisons (Loughborough, UK). All other chemicals were from Merck (Poole, UK). The perfusate solution was Krebs-Henseleit buffer modified to contain 5% albumin.

2.2. Chromatography

Chromatography was performed using three different systems as follows.

System 1: DX100 chromatograph (Dionex, Camberley, UK) fitted with a WISP autosampler (Waters, Watford, UK). The column was an IonPac AS9-SC ion-exchange column, 250 mm × 4 mm (Dionex), and the eluent was 1.7 m*M* $NaHCO_3$, 1.8 m*M* Na_2CO_3, pumped at 1.5 ml/min. Detection was by conductivity (DX100) and absorbance at 214 nm using a 441 detector fitted with a zinc lamp (Waters). Data was acquired and processed using an 840 data system (Waters).

System 2: 820 chromatograph and data system, equipped with 510 pumps and a WISP autosampler. The separation was achieved by an ion-pairing technique using a Hypersil 5ODS reversed-phase column, 125 mm × 4.6 mm (Hichrom, Reading, UK), and the eluent was 4% acetonitrile, 5 m*M* $TBASO_4$, 20 m*M* KH_2PO_4, 20 m*M* H_3PO_4, with a flow-rate of 2 ml/min. Detection was by absorbance at 214 nm using a 486 detector (Waters).

System 3: Millennium chromatograph and data system, equipped with 616 pumps and a WISP autosampler. The column was an IonPac AS9-SC ion-exchange column, 250 mm × 4 mm (Dionex), and the eluent was 5 m*M* K_2HPO_4, 25 m*M* KH_2PO_4, with a flow-rate of 1.5 ml/min. Detection was by absorbance at 214 nm using a 486 detector. All water used to make up eluents and samples was freshly drawn from a Milli-Q system supplied from a Milli-RO unit (Millipore, Watford, UK).

2.3. Sample preparation

Perfusate samples were obtained from an isolated rat tumour or hind limb [27]. Plasma samples were obtained from the rat or mouse. All sample handling was carried out in a laminar flow hood. For use with Systems 1 and 3 (ion exchange), a 50-μl aliquot of sample was pipetted into a 300-μl glass tube (Sci-Vi, Chromacol, Welwyn, UK). Acetonitrile (50 μl) was added, and the tube with an autosampler limited-volume insert spring was put in a 4-ml WISP vial, capped, mixed and centrifuged at 2000 *g* for 2 min. The sample was then ready for injection. For use with System 2 (reversed-phase), samples (50 μl) were pipetted into 1.5-ml polypropylene tubes (Sarstedt, Leicester, UK), 400 μl acetonitrile were added, and the tube was capped, mixed and centrifuged (10 000 *g* 1 min). The supernatant was decanted into another 1.5-ml tube, the pellet washed with a further 400 μl of acetonitrile, the combined extracts were dried under nitrogen and the sample was reconstituted in 200 μl of water. Where ultrafiltration was used for sample preparation, the filters [microcentrifuge tube filters, cellulose triacetate, 12 000 molecular mass cut-off (Whatman, Maidstone, UK), Centricon-10, 10 000 cut-off (Amicon, Stonehouse, UK) or ultra-spin centrifuge filters, 30 000 cut off (Alltech Assoc. Carnforth, UK)] were washed with Milli-Q water, dried, and the sample was applied. After centrifugation [9500 *g*, 5 min (Whatman and Alltech), 5000 *g*, 30 min (Amicon)], the sample was transferred to an autosampler vial for injection.

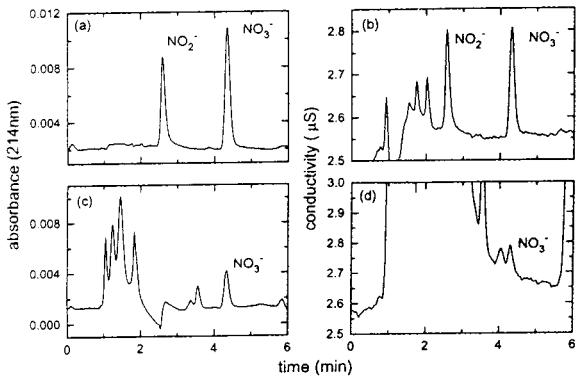

Fig. 1. Chromatograms of an acetonitrile-extracted aqueous standard containing 100 μ*M* nitrite and nitrate (a and b), and control mouse plasma (c and d). (a, c) Absorbance detection; (b, d) conductimetric detection. System 1 (anion-exchange, carbonate–bicarbonate eluent) was used.

3. Results

Figs. 1–3 show chromatograms of standards and plasma extracts using the three systems. In each case the separation of nitrate is acceptable, but quantification of nitrite is compromised in the first two systems by a large baseline disturbance when absorbance detection is used, or by the chloride peak with conductimetric detection. Only using the phosphate-based eluent was the nitrite sufficiently separated from the baseline dip. This is illustrated in Fig. 4 which shows chromatograms of perfusate buffer before and

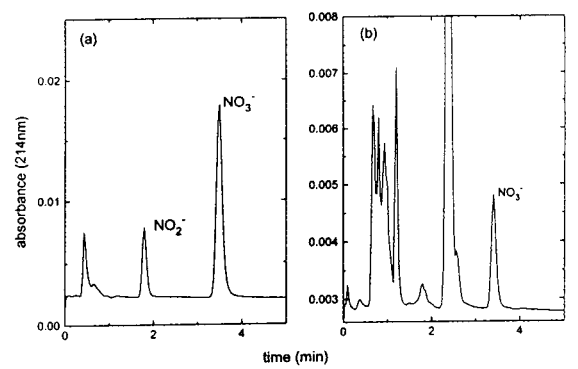

Fig. 2. Chromatograms of an acetonitrile-extracted aqueous standard containing 100 μ*M* nitrite and nitrate (a) and control mouse plasma (b) with absorbance detection at 214 nm. System 2 (reversed-phase chromatography) was used.

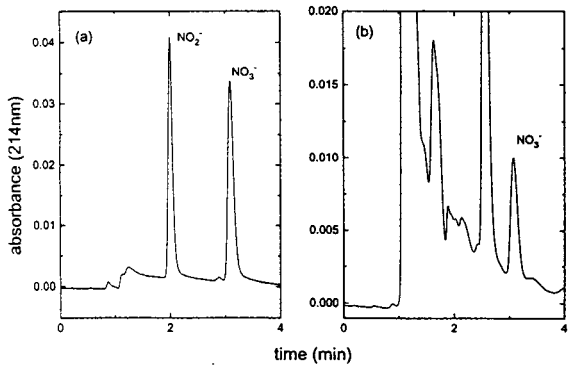

Fig. 3. Chromatograms of an acetonitrile-extracted aqueous standard containing 100 μM nitrite and nitrate (a) and control mouse plasma (b) with absorbance detection at 214 nm. System 3 (anion-exchange, phosphate eluent) was used.

after spiking with 5 μM nitrite and nitrate. Replicate extractions were also made of a perfusate sample using the three systems, and these are shown in Table 1. Because System 3 showed the lowest standard deviation, and permitted the measurement of nitrite, this system was selected for more detailed study.

The linearity of this method was assessed using extracted aqueous standards; calibration curves for both nitrite and nitrate were found to be linear over the range investigated (0.2–100 μM) (correlation coefficients, $r > 0.9993$ and >0.9997, respectively). The detection limit for nitrite was ~ 0.1 μM, governed by the shape of the baseline in this region. It was not possible to set a lower

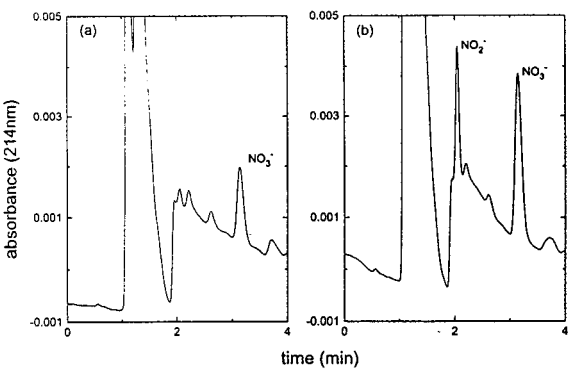

Fig. 4. Chromatograms of an acetonitrile-extracted perfusate buffer. (a) Control; (b) spiked with 5 μM nitrite and nitrate. System 3 (anion-exchange, phosphate eluent) was used.

Table 1
Repeat extractions of a perfusate using Systems 1, 2 and 3

	Nitrate concentration (μM)		
	System 1	System 2	System 3
	5.0	29.4	10.4
	10.5	32.6	8.6
	9.6	10.4	10.9
	6.5	11.1	11.4
		11.6	11.3
Mean ± S.D.	7.9 ± 2.6	19.0 ± 11.0	10.5 ± 1.1

detection limit for nitrate since all samples, including the Milli-Q water, contained detectable levels ≥ 0.5 μM. Recoveries of nitrite and nitrate from spiked plasma were 93.6 ± 2.9% and 94.6 ± 4.6% and from perfusates were 101.4 ± 3.1% and 99.4 ± 3.9%. Endogenous peak areas were subtracted prior to calculating these values. Intra- and inter-assay precision and accuracy and reproducibility were determined (Tables 2 and 3).

An alternative method of sample preparation was assessed using ultrafiltration to remove protein from the sample. However, all three filter types were heavily contaminated with nitrate which proved difficult to remove; the data are shown in Table 4.

4. Discussion

We have shown that nitrite and nitrate can be readily separated using several chromatographic and detection techniques as has already been demonstrated by a number of workers [24–26,28,29]. However, only one group [23] has addressed the question of sample contamination which we have found to be a major problem for nitrate determination. The contamination introduced by ultrafiltration, even after washing, did not encourage us to continue with the use of filters, although they have apparently been used successfully [23]; this may be a reflection of the larger sample volumes used.

We found that sample manipulations needed

Table 2
Intra- and inter-assay precision and accuracy of the HPIC procedure for nitrite and nitrate in perfusate buffer (System 3)

Component	Intra-assay		Inter-assay	
	R.S.D. (%)	Accuracy (%)	R.S.D. (%)	Accuracy (%)
Nitrite	1.58	99.35	1.27	100.20
Nitrate	5.21	100.80	3.35	100.80

Table 3
Mean and standard deviation ($n = 5$) of replicate analyses of mouse plasma (System 3)

Component	Mean concentration (μM)	S.D. (μM)
Nitrite	1.93[a]	0.24
Nitrate	15.60	0.72

[a] Peak co-elutes with nitrite.

to be kept to a minimum as illustrated by the standard deviation in Table 1. The reversed-phase method (System 2) would not tolerate injections of high concentrations of acetonitrile, and therefore the samples were dried down prior to injection. This involved two additional transfers, which resulted in large errors in the calculated concentrations. We attributed this contamination to nitrate-laden dust particles, and the situation was improved by carrying out the sample manipulations in a laminar flow hood where the air is filtered. By doing this, standard errors could be reduced, but were still much higher than using the single-step process. This was due in part to the fact that even new tubes were contaminated with 1–2 μM nitrate, occasionally much higher. Late-eluting peaks in plasma samples necessitated the use of a solvent gradient greatly extending the analysis time. This and the need to reduce sample manipulations to a minimum led us to discard the reversed-phase method (System 2). Also, in order to prevent a negative peak where nitrate eluted, it was necessary to prepare the eluent using freshly dispensed water; otherwise low concentrations of nitrate were not detected.

Measurement of low concentrations of nitrite are probably not relevant in plasma, but could be of importance in haemoglobin-free systems such as the perfused tumour. Both System 1 and

Table 4
Nitrate introduced by ultrafiltration treatments

Treatment	Nitrate concentration (μM)		
	Amicon	Whatman	Alltech
100 μl water[a]	19.4	–	–
50 μl water	–	10.4 ± 2.3	–
2×500 μl wash	–	1.9, 2.6[b]	–
50 μl water			
500 μl	–	4.1	17.9
2×500 μl wash	–	1.6, 2.9[b]	1.6, 2.3[b]
500 μl water			
2×500 μl wash	–	26.3 ± 1.8[c]	34.9 ± 2.3[c]
50 μl buffer + 450 μl water			

[a] Water contains up to 2 μM nitrate.
[b] Two observations.
[c] Perfusate buffer alone contains ~5 μM nitrate when analysed using the standard extraction method.

System 2 preclude the measurement of nitrite in either matrix. In System 2 there is a large interfering peak, while using System 1, the high concentration (~100 m*M*) of chloride gives a very large peak using conductimetric detection and is probably responsible for the dip using absorbance detection. Also, with conductimetric detection, there was an interference which would adversely affect the quantification of the nitrate (Fig. 1d). Although we did not assess the use of silver-based cation-exchange resins to remove chloride, we felt that the additional sample pretreatment steps involved were likely to exacerbate the contamination problem. Also, it is difficult to use such an approach with volumes of <0.5 ml, and sample amounts from biological systems are frequently rather limited. Absorbance detection for plasma nitrate appeared satisfactory, but we occasionally saw a distorted peak shape which suggested the presence of an interfering peak (not shown). Use of the phosphate-based eluent (System 3) has a number of advantages: it allows the determination of nitrite, while manipulation of the pH seemed to give more flexibility in altering the relative retention of potentially interfering peaks. However, it is not compatible with suppressed conductimetric detection.

Acknowledgements

This work is supported by The Cancer Research Campaign. Sponsorship from The Dionex Corporation is gratefully acknowledged. We thank Mr. Ralph Cochrane of Dionex (UK) for his many helpful discussions.

References

[1] R.M.J. Palmer, D.S. Ashton and S. Moncada, *Nature*, 333 (1988) 664.
[2] J.F. Kerwin, Jr. and M. Heller, *Med. Res. Rev.*, 14 (1994) 23.
[3] A.R. Butler and D.L.H. Williams, *Chem. Soc. Rev.*, (1993) 233.
[4] S. Moncada, M.A. Marletta, J.B. Hibbs, Jr. and E.A. Higgs (Editors), *The Biology of Nitric Oxide*, Vol. 2, Portland Press, London, 1992.
[5] R. Schulz and C.T. Triggle, *Trends Pharmacol. Sci.*, 15 (1994) 255.
[6] M. Feelisch, M. te Poel, R. Zamora, A. Deussen and S. Moncada, *Nature*, 368 (1994) 62.
[7] P. Klatt, K. Schmidt, G. Uray and B. Mayer, *J. Biol. Chem.*, 268 (1993) 14 781.
[8] J.B. Hibbs Jr., R.R. Taintor, Z. Vavrin and E.M. Rachlin, *Biochem. Biophys. Res. Commun.*, 157 (1988) 87.
[9] K. Isobe and I. Nakashima, *Biochem. Biophys. Res. Commun.*, 192 (1993) 499.
[10] S. Archer, *FASEB J.*, 7 (1993) 349.
[11] R.M.J. Palmer, A.G. Ferrige and S. Moncada, *Nature*, 327 (1987) 524.
[12] K. Kikuchi, T. Nagano, H. Hayakawa, Y. Hirata and M. Hirobe, *J. Biol. Chem.*, 268 (1993) 23106.
[13] M. Kelm, M. Feelisch, R. Spahr, H. Piper, E. Noack and J. Schrader, *Biochem. Biophys. Res. Commun.*, 154 (1988) 236.
[14] H. Korth, R. Sustmann, P. Lommes, T. Paul, A. Ernst, H. d. Groot, L. Hughes and K.U. Ingold, *J. Am. Chem. Soc.*, 116 (1994) 2767.
[15] H. Tsukahara, D.V. Gordienko, and M.S. Goligorsky, *Biochem. Biophys. Res. Commun.*, 193 (1993) 722.
[16] P.C. Ford, D.A. Wink and D.M. Stanbury, *FEBS Lett.*, 326 (1993) 1.
[17] L.C. Green, D.A. Wagner, J. Glogowski, P.L. Skipper, J.S. Wishnok and S.R. Tannenbaum, *Anal. Biochem.*, 126 (1982) 131.
[18] T.P. Misko, R.J. Schilling, D. Salvemini, W.M. Moore and M.G. Currie, *Anal. Biochem.*, 214 (1993) 11.
[19] J.B. Hibbs, C. Westenfelder, R. Taintor, Z. Vavrin, C. Kablitz, R.L. Baranowski, J.H. Ward, R.L. Menlove, M.P. McMurray, J.P. Kushner and W.E. Samlowski, *J. Clin. Invest.*, 89 (1992) 867.
[20] L.L. Thomsen, B.C. Baguley, G.J.S. Rustin and S.M. O'Reilly, *Br. J. Cancer*, 66 (1992) 723.
[21] E. Veszelovszky, L.L. Thomsen, Z. Li and B.C. Baguley, *Eur. J. Cancer*, 29A (1993) 404.
[22] G.D. Kennovin, D.G. Hirst, M.R.L. Stratford and F.W. Flitney, in S. Moncada, M. Feelisch, R. Busse and E.A. Higgs, (Editors), *The Biology of Nitric Oxide*, Vol. 4., Portland Press, London, 1994, p. 473.
[23] A.M. Leone, P.L. Francis, P. Rhodes and S. Moncada, *Biochem. Biophys. Res. Commun.*, 200 (1994) 951.
[24] B.C. Lippsmeyer, M.L. Tracy and G. Moeller, *J. Assoc. Off. Anal. Chem.*, 73 (1990) 457.
[25] Y. Michigami, Y. Yamamoto and K. Ueda, *Analyst*, 114 (1989) 1201.
[26] S. Kaku, M. Tanaka, M. Muramatsu and S. Otomo, *Biomed. Chromatogr.*, 8 (1994) 14.
[27] G.M. Tozer, K.M. Shaffi, V.E. Prise and V.J. Cunningham, *Br. J. Cancer*, 70 (1994) 1040.
[28] J. Osterloh and D. Goldfield, *J. Liq. Chromatogr.*, 7 (1984) 753.
[29] P. De Jong and M. Burggraaf, *Clin. Chim. Acta*, 132 (1983) 63.

ELSEVIER

Journal of Chromatography A, 706 (1995) 443–450

JOURNAL OF CHROMATOGRAPHY A

Ion chromatography as potential reference methodology for the determination of total sodium and potassium in human serum

Linda M. Thienpont[a,*], Jean E. Van Nuwenborg[a], Dietmar Stöckl[b,1]

[a]*Laboratorium voor Analytische Chemie, University of Ghent, Harelbekestraat 72, B-9000 Ghent, Belgium*

[b]*Institut für Standardisierung und Dokumentation im medizinischen Laboratorium e.V. (INSTAND e.V.), Johannes-Weyer Strasse 1, D-40225 Düsseldorf, Germany*

Abstract

The potential of ion chromatography to serve as a new reference method principle for the determination of total sodium and potassium in human serum was investigated. Sample pretreatment consisted of acidic dilution and filtration and detection was based on conductivity. Methods for the separate and simultaneous determination of both analytes were investigated. Further, the influence of calibration (using either a single-point calibration or a standard curve) on method imprecision, inaccuracy and analysis time was examined. The best method performance was achieved by separate analysis using single-point calibration with bracketing analysis scheme. For this variant, the mean total coefficient of variation for sodium and potassium was 1.0% and the mean method bias was −0.2% for sodium and +0.2% for potassium, as determined with three control materials from the National Institute of Standards and Technology. Our results are comparable to those of reference methods based on flame atomic emission spectrometry. Therefore, we consider ion chromatography as a valuable reference methodology for the determination of total sodium and potassium in human serum.

1. Introduction

Reference methods in laboratory medicine are used for accuracy assessment of routine methods, target-setting of internal and external quality control materials and certification of reference materials [1,2]. The currently accepted reference method principle for the determination of sodium and potassium in serum is flame atomic emission spectrometry (FAES) [3,4]. However, alternative methods are desirable since, for example, the use of two independent methods is advocated for the certification of reference materials [5]. A candidate method principle would be ion chromatography (IC), because it has been successfully applied to the determination of various serum electrolytes [6–9]. Recently, we indeed demonstrated the potential of IC to serve as a reference method principle by developing highly accurate methods for the determination of total calcium and magnesium in serum [10]. Here, we extend this application of IC to the determination of total sodium and potassium in serum. Emphasis was put on the use of standard reference materials (SRMs) from the National Institute of Standards and Technology (NIST) for calibration and ac-

* Corresponding author.

[1] Present address: Laboratorium voor Analytische Chemie, University of Ghent, Harelbekestraat 72, B-9000 Ghent, Belgium.

0021-9673/95/$09.50
SSDI 0021-9673(95)00152-2

curacy assessment. Sample pretreatment consisted of dilution with the methanesulfonic acid IC eluent and filtration. Methods for the separate and simultaneous determination of sodium and potassium were compared. In addition, the influence of single-point calibration (with adapting the dilution of serum) or calibration with a standard curve on method imprecision and inaccuracy was investigated. The first results of our studies are reported here.

2. Experimental

2.1. Instrumentation

Ion chromatography was carried out with a Model DX-100 ion chromatograph from Dionex (Sunnyvale, CA, USA) equipped with a 25-μl injection loop. For chromatographic separation an Ionpac CG12 guard column (50 mm × 4 mm I.D.) coupled to an Ionpac CS12 analytical column (250 mm × 4 mm I.D.) was used. Electronic suppression was achieved with a Cation Self-Regenerating Suppressor-I system (CSRS-I, 4 mm) used in the autosuppression recycle mode. Detection was based on conductivity. All the above-mentioned equipment was from Dionex. Integration of the chromatographic signals was performed with a C-R5A integrator from Shimadzu (Kyoto, Japan). An Elgastat Maxima Analytical water purification system from Elga (Bucks, UK) was used to produce water of ultrapure quality (18.2 MΩ). Weighings were done with an electronic 100-g balance (Mettler Toledo, Greifensee, Switzerland), Type AT261 Deltarange, with a readability of 10^{-5} g. The density of serum was determined with a Model DMA 35 densitometer (accuracy 1 mg/ml) from A. Paar (Graz, Austria).

2.2. Materials

Methanesulfonic acid (purissimum quality, i.e. purity >99%) was purchased from Fluka (Buchs, Switzerland). Filtrations were done with Millex-HV_{13} filters (0.45 μm pore size) from Millipore (Bedford, MA, USA). For filtration and injection, 1-ml Plastipak syringes from Becton Dickinson (Dublin, Ireland) were used. Pipetting was done using 1-ml and 200-μl pipet tips from Eppendorf (Hamburg, Germany). To exclude external contamination at any stage of the IC analysis, no glassware was used and hand contact of vials etc. was avoided. All vials and containers used were of polypropylene or polymethylpentene from Nalgene (Hereford, UK). They were rinsed with water and dried before use.

2.3. Standard materials

For calibration, standard materials of certified purity from the NIST (Gaithersburg, MD, USA) were used, i.e. sodium chloride (SRM 919a) and potassium chloride (SRM 918). For the single-point calibration approach, accurately weighed amounts of sodium chloride and potassium chloride were dissolved in water to give sodium concentrations of approximately 40 mmol/l (accurate to the second decimal) and potassium concentrations of 4.5 mmol/l (accurate to the third decimal). To the potassium chloride standard solution, pure sodium chloride was added to give a physiological concentration of approximately 130 mmol/l. Two stock solutions of each analyte were prepared and cross-checked for accuracy against each other. Deviations of less than 0.6% (on the basis of six measurements) were accepted. For the four-point calibration approach, stock solutions were prepared containing 100, 120, 140 and 160 mmol/l sodium and 2, 4, 6 and 8 mmol/l potassium, respectively. To the potassium chloride stock solutions, sodium chloride was added as described above. Solutions for the two-point calibration (used for the simultaneous determination of sodium and potassium) contained 100 (lowest calibration point) and 160 (highest calibration point) mmol/l sodium and 2 and 8 mmol/l potassium, respectively. These stock solutions were also cross-checked against each other before use. All standard solutions were stored in 500-μl portions in polypropylene vials at −20°C and discarded after two freeze–thaw cycles. The SRM 909, SRM 909a-1 and SRM 909a-2 lyophilized human

serum reference materials from NIST were reconstituted on a gravimetric basis according to the manufacturer's instructions (for SRM 909 procedure B was followed). The deviation of the volume of water used for reconstitution from the prescribed volume was taken into account and the maximum acceptable deviation was set to 0.5%. The certified concentrations of the NIST sera are listed in Tables 1 and 2. After reconstitution, the sera were aliquoted in 500-μl portions in polypropylene vials for storage at −20°C. Each aliquot was discarded after two freeze–thaw cycles.

2.4. Method

Sampling of serum and standards and further dilutions were carried out on a gravimetric basis. Volumes were chosen to give masses >25 mg to keep weighing errors below 0.1%. The pipetted volumes were calculated from the density of the solutions and the masses pipetted.

For the determination of sodium in serum using single-point calibration, a serum volume of 25 μl (containing approximately 3160–3700 nmol sodium) was sampled and diluted 200-fold with a 14 mmol/l aqueous methanesulfonic acid solution. After 1 h of equilibration, the acidified samples were filtered. The filter device was prerinsed with water three times and finally with the sample so that the first 500 μl of filtrate were discarded (care was taken to make the syringe air-free). In this way, any change in sample concentration by filtration was prevented. After filtration, a second dilution of the filtrates was done to give similar peak heights on injection of 25 μl of the diluted sample. Dependent on the serum sodium concentrations, the total dilution ranged from approximately 3500 to 4100. The final dilutions were injected without further treatment (25 μl containing approximately 0.90 nmol of sodium). The sodium standards were treated exactly in the same way as the serum samples: 25 μl of the stock solution (40 mmol/l) were diluted 1100-fold in two steps (before and after filtration) to give peak heights similar to those of the samples on injection of 25 μl of the dilution. For the determination of potassium in serum with single-point calibration, a similar approach was used: 35 μl of serum (containing approximately 125–217 nmol potassium) were sampled and further diluted 95- to 217-fold with a 14 mmol/l aqueous methanesulfonic acid solution to finally inject approximately 0.94 nmol of potassium in 25 μl of the dilution. For the standards, an aliquot of 34 μl (4.5 mmol/l) was diluted 120-fold and treated exactly in the same way as the samples.

For the quantification of sodium in serum using a four-point calibration curve, a fixed volume of 25 μl of serum was taken for analysis and diluted 6600-fold in two steps and filtered as described above (25 μl of the final dilution contained approximately 0.48–0.56 nmol sodium). Aliquots of 25 μl of each of the four sodium stock solutions (100, 120, 140 and 160 mmol/l) were treated in exactly the same way as the serum samples. For the quantification of potassium using a four-point calibration curve, 25 μl of serum were sampled and diluted 160-fold before filtration as described above (25 μl containing approximately 0.56–0.97 nmol potassium). For the standards, 25-μl aliquots of the different stock solutions (2, 4, 6 and 8 mmol/l) were treated in exactly the same way as described for the serum samples.

For the simultaneous quantification of sodium and potassium in serum using a two-point calibration curve, a fixed volume of 25 μl of serum was sampled, diluted 160-fold and filtered as described above (25 μl containing approximately 0.56–0.97 nmol of potassium and 19.77–23.20 nmol of sodium, respectively). The standards, containing 100–160 mmol/l sodium and 2–8 mmol/l potassium, again were treated in the same way as the samples.

The conditions for ion-exchange chromatography of sodium and potassium were elution at a flow-rate of 1 ml/min with an eluent of 14 mmol/l aqueous methanesulfonic acid [11]. In both methods, suppression was performed in the autosuppression recycle mode with the current setting at approximately 300 mA. Conductivity was measured with a detector range of 3 μS, except in the method for the simultaneous determination of sodium and potassium, in which

during the run (after elution of sodium and before elution of potassium) the range was switched from 100 to 3 μS.

2.5. Analysis and measurement protocol

For the quantification of total sodium and potassium in the lyophilized SRMs, three different vials were used to compensate for the variation in the dry-mass content in each vial. The concentration measured for each SRM serum was always calculated from twelve independent measurements performed on three different days. This means that every day four serum aliquots (A–D) from each SRM were analyzed. Measurements were done in the bracketing mode, i.e. injection of serum samples in between the standards. In the methods for the separate determination of sodium or potassium with single-point calibration, three independently weighed-in standards (I–III) were used. The bracketing injection protocol was as follows: standards I–III; samples 1A–D; second injection of standards I–III; samples 2A–D; etc. Calculation of the sodium or potassium concentrations in the serum samples was based on the results for the duplicate injections of the standards encompassing the samples.

In the methods for the separate determination of sodium or potassium using a four-point calibration curve, four different standards with increasing concentration (I–IV) were used. Injections of serum samples and standards were done according to the following scheme: standards I–IV; samples 1A–D; second injection of standards IV–I; samples 2A–D; etc. The concentrations of the serum samples were derived by interpolation on the linear regression curve of the standards encompassing the samples.

In the method for the simultaneous determination of sodium and potassium using a two-point calibration curve, a low-concentration (I), and a high-concentration (II) standard for both sodium and potassium were used. According to the bracketing measurement scheme, standards and serum samples were injected as follows: standards I, II; samples 1A–D; second injection of standards II, I; samples 2A–D; etc. Linear regression of the results for the standards encompassing a series of serum samples was applied for calculation of their concentrations.

2.6. Estimation of analytical performance

The precision and total error of the IC methods for the determination of total sodium and potassium in serum were estimated from replicate analyses of the three human serum SRMs from NIST according to the following measurement design: quadruplicate analysis of each serum in three independent series. The overall precision was estimated from the coefficient of variation (C.V., %) calculated for the twelve measurement results, the total error by the deviation of the mean of the twelve measurement results from the certified value.

2.7. Safety considerations

The method demands no specific safety precautions. Lyophilized control sera of human origin have to be handled as potentially infectious. General guidelines for work with acids have to be respected.

3. Results and discussions

The above described methods were intended for use as reference methods for target-setting in external quality assessment (EQA). We aimed at reaching the requirements for the German EQA scheme [12], imposing a maximum total error (T.E.) of 1.2% for sodium and 1.6% for potassium (T.E. includes method bias and 95% confidence interval). From these limits, specifications for maximum method bias, C.V., and number of measurements can be derived. For example, with a maximum method C.V. of 1.0% (1.5%) and twelve measurements, the 95% confidence interval is $\pm$ 0.64% ($\pm$0.95%), resulting in a bias limit of 0.56% for sodium and 0.65% for potassium [12]. To comply with this concept, every reference method value had to comprise twelve independent measurements and the limits for the C.V.s calculated from those twelve measurements

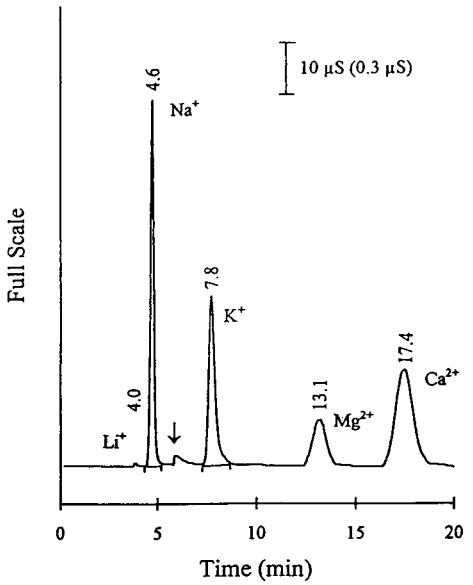

Fig. 1. Representative chromatogram of a serum sample processed for the simultaneous determination of sodium and potassium. The detector range was initially 100 μS and switched to 3 μS after the sodium peak (indicated by the arrow). For chromatographic conditions, see Experimental section.

were set to 1.0% for sodium and 1.5% for potassium. We investigated whether IC principally was able to achieve those specifications. We used the NIST SRMs 909, 909a-1 and 909a-2 for evaluation of method accuracy because, at the moment, they are the only available reference materials for serum total sodium and potassium. Chromatographic conditions were adopted from the recommendations for use of the CS12 column [11] and were identical for all methods. Before collecting data, the reliability of the chromatographic system (column head pressure, stability of baseline and background suppression) was verified. A representative chromatogram of a serum sample processed for the simultaneous determination of sodium and potassium is shown in Fig. 1. Good separation and high signal intensities were obtained for reliable quantification. For all methods, bracketing injection was chosen and similar sample preparation could be applied. The methods were different with respect to the mode of calibration (see Experimental).

For the separate determination of sodium and potassium two different calibration modes were used, i.e. single- and multiple-point calibration. In the single-point calibration mode, the same absolute amount of the analyte in both the standards and the serum samples was injected into the chromatographic system. For this reason, each serum sample had to be diluted as a function of its individual concentration which had to be roughly determined before IC analysis. Using this calibration mode, good method accuracy was achieved (see column A in Tables 1 and 2). The maximum deviation from the certified value was −0.4% for sodium and +0.4% for potassium. Method precision for potassium satisfied the preset requirement, but for sodium it was slightly higher than required. For sodium the maximum C.V. was 1.3% (required 1.0%). For potassium the maximum CV was 1.2% (required 1.5%). It should be noted that the

Table 1
Analytical performance of the proposed IC methods for the measurement of sodium according to different analytical approaches and derived from analysis of three certified human serum reference materials

Serum	A			B		C	
	Concentration (mmol/l)	Δ (%) Target	C.V. (%) (n = 12)	Δ (%) Target	C.V. (%) (n = 12)	Δ (%) Target	C.V. (%) (n = 12)
SRM 909	133.9	−0.4	0.7	+0.9	0.8	+0.2	1.3
SRM 909a-1	148.5	−0.2	1.3	+1.1	1.5	+1.8	1.4
SRM 909a-2	126.5	+0.1	0.9	+1.3	0.8	+1.2	0.9

A: Separate determination of sodium in serum using single-point calibration (bracketing). B: Separate determination of sodium using a four-point calibration curve. C: Simultaneous determination of sodium and potassium using a two-point calibration curve.

Table 2
Analytical performance of the proposed IC methods for the measurement of potassium according to different analytical approaches and derived from analysis of three certified human serum reference materials

Serum	A			B		C	
	Concentration (mmol/l)	Δ (%) Target	C.V. (%) ($n = 12$)	Δ (%) Target	C.V. (%) ($n = 12$)	Δ (%) Target	C.V. (%) ($n = 12$)
SRM 909	3.567	+0.4	1.0	−1.5	1.5	−1.3	1.5
SRM 909a-1	3.656	+0.3	0.7	−1.6	1.2	−1.3	1.4
SRM 909a-2	6.210	± 0.0	1.2	−1.5	0.7	−0.1	0.9

A: Separate determination of potassium in serum using single-point calibration (bracketing). B: Separate determination of potassium using a four-point calibration curve. C: Simultaneous determination of sodium and potassium using a two-point calibration curve.

precision data include the within- and between-day errors of weighing, variations introduced during sample pretreatment, errors during IC measurements and the variation in dry mass of the lyophilized controls.

In the four-point calibration mode, standard curves covering the whole pathophysiological concentration ranges were used, allowing a fixed dilution of all samples. The results were calculated by linear interpolation on the standard curves encompassing the sample measurements (see Experimental). According to the bracketing injection scheme, sixteen standards had to be analyzed in total for the analysis of the three NIST serum samples. The reason for injecting the first series of four standards in sequence of increasing concentration, and the second in reverse sequence was to outweigh eventual drifts in the system. Overall, this approach was more time-consuming than single-point calibration and gave less accurate results during our first experiments (see column B in Tables 1 and 2). For sodium a positive bias of approximately +1.0% was observed, while it was approximately −1.5% for potassium. Further studies (repeated measurement campaigns) have to be performed in order to clarify whether this bias was really due to the calibration mode or due to problems related to the actual measurement campaign. Method precision was not significantly different from the single-point calibration mode (see Tables 1 and 2).

For the simultaneous determination of sodium and potassium, a two-point calibration was performed, using the extremes of the four-point calibration curves. Again, all serum samples could equally be diluted. Results were calculated by linear interpolation on the standard curves. Because of the differences in absolute concentration between sodium and potassium (25–35-fold) and of fixed dilution, measurements had to be done at different detector ranges (100 μS for sodium and 3 μS for potassium, see Fig. 1). In order to increase the number of standards, double injection of the two standards encompassing a series of serum samples was performed, as shown in Fig. 2. This resulted in a total of eight standards for the analysis of the three NIST sera. Again, standards were injected in increasing and decreasing concentration sequence. Method accuracy and precision were similar to the four-point calibration approach (see column C in Tables 1 and 2). The same remark as above holds true for elucidating the source of increased inaccuracy as compared to single-point calibration. Nevertheless, because of time saving, simultaneous determination of sodium and potassium would be of particular interest for further method improvement.

The accuracy and precision reached for the IC methods for total sodium and potassium, in particular when using single-point calibration, are comparable to those of the proposed candidate reference methods based on FAES. For the FAES method of sodium, a mean C.V. of 0.5% and a maximum deviation of +0.7% from the

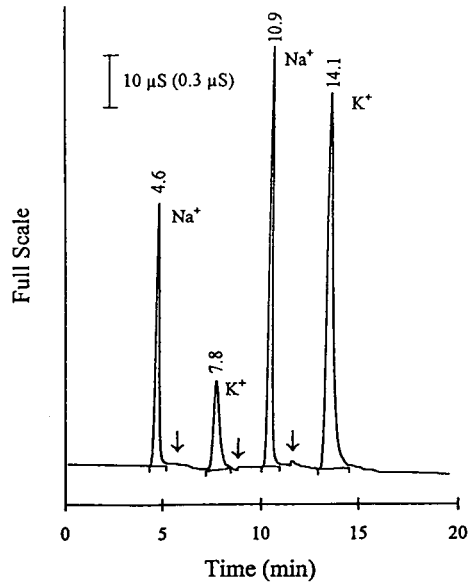

Fig. 2. Chromatogram for a double injection of standards for the simultaneous determination of sodium and potassium. The detector range was 100 μS for sodium and 3 μS for potassium (switching indicated by the three arrows). The second injection was done after elution of sodium as indicated by the first arrow.

certified target value was reported [3] (in our IC method, using single-point calibration, the mean C.V. was 1.0%; the maximum deviation was −0.4%). For the FAES method of potasssium, a mean C.V. of 1.3% and a deviation of +1.1% from the certified value was reported [4] (in our IC method, using single-point calibration, the mean C.V. was 1.0%; the maximum deviation was +0.4%).

4. Conclusion

We have developed IC methods which enable us to reliably determine total sodium and potassium in human serum. The sample pretreatment procedure is very simple, and the overall analysis time is reasonable. From the precision and accuracy obtained here, we suggest that IC principally may be considered as a valuable reference methodology, comparable to FAES. At this stage of the work, the results with single-point calibration fulfilled better the preset analytical requirements than those obtained with the calibration curve approach. However, further investigations should be performed to improve the precision and accuracy of the time-saving simultaneous determination of total sodium and potassium with the two-point calibration approach. The perspective of the use of IC as reference methodology is particularly attractive because of its great flexibility. Also clinically important divalent cations like calcium and magnesium or anions like chloride or phosphate can be analyzed with principally the same equipment. Further, IC might be an alternative to FAES when the latter is not available in laboratories relying predominantly on chromatographic techniques.

Acknowledgement

This research was supported by the Research Fund of the University of Ghent under Grant No. 01116692.

References

[1] J. Büttner, *J. Clin. Chem. Clin. Biochem.*, 29 (1991) 223.
[2] L.M. Thienpont and D. Stöckl, *Klin. Biochem. Metab.*, 2 (1994) 4.
[3] R.A. Velapoldi, R.C. Paule, R. Schaffer, J. Mandel and J.R. Moody, *National Bureau of Standards, NBS Special Publication 260-60*, U.S. Government Printing Office, Washington, DC, 1978.
[4] R.A. Velapoldi, R.C. Paule, R. Schaffer, J. Mandel, L.A. Machlan and J.W. Gramlich, *National Bureau of Standards, NBS Special Publication 260-63*, U.S. Government Printing Office, Washington, DC, 1979.
[5] N.M. Trahey, *NIST Standard Reference Materials Catalog 1992–93, National Institute of Standards and Technology Special Publication 260*, U.S. Government Printing Office, Washington, DC, 1992, p. 5.
[6] F.R. Nordmeyer, L.D. Hansen, D.J. Eatough, D.R. Rollins and J.D. Lamb, Anal. Chem., 52 (1980) 852.

[7] S.J. Rehfeld, H.F. Loken, F.R. Nordmeyer and J.D. Lamb, *Clin. Chem.*, 26 (1980) 1232.
[8] H. Shintani, *J. Chromatogr.*, 341 (1985) 53.
[9] S. Matsuhita, *Anal. Chim. Acta*, 172 (1985) 249.
[10] L.M. Thienpont, J.E. Van Nuwenborg and D. Stöckl, *Anal. Chem.*, 66 (1994) 2404.
[11] *Installation Instructions and Troubleshooting Guide for the IONPAC CS12 Analytical Column, Document No. 0.4657, Revision 01*, Dionex Corporation, Sunnyvale, CA, 1992.
[12] D. Stöckl and H. Reinauer, *Scand. J. Clin. Lab. Invest.*, 53 (Suppl. 212) (1993) 16.

ELSEVIER

Journal of Chromatography A, 706 (1995) 451–457

JOURNAL OF CHROMATOGRAPHY A

Plasma level determination of 1,4-butanedisulphonate by ion chromatography and conductimetric detection

E. Moro*, M. De Angelis, B. Fugazza

Department of Pharmacokinetics, Research and Development, BioResearch SpA, BASF Pharma, 20060 Liscate (MI), Italy

Abstract

A rapid, specific and reproducible liquid chromatographic method was developed for the determination of 1,4-butanedisulphonate in plasma. The method involves protein precipitation with perchloric acid, precipitation of perchlorate ions by addition of potassium carbonate followed by ion chromatography on an ion-exchange column connected with a conductimetric detector. Calibration graphs were linear over the concentration range 2.5–25 μg/ml; the intra-assay precision was $\leq$3.6% and the inter-assay precision was $\leq$5.8%. The analyte was stable in plasma and in perchloric acid at 37°C for 24 h. The assay procedure was applied to monitoring plasma levels in animals receiving chronic intravenous and oral administration of the analyte.

1. Introduction

1,4-Butanedisulphonic acid is the counter ion utilized for the preparation of a stable salt of S-adenosylmethionine, a drug with anticholestatic activity. As this acid is not commonly used for salt preparation, data on its pharmacokinetic properties in different animal species were required. For this purpose we had to develop a suitable assay method for this acid in biological fluids.

Although analytical procedures for determining inorganic anions such as sulphate in biological fluids [1] and in tissue [2] have been described, to date there is no method available for assaying butanedisulphonate and other linear alkylsulphonates in this kind of matrix. The main problems in developing such a method are related to the high polarity of the analyte, which makes both extraction with solvents and the subsequent chromatography and detection difficult.

In this paper, we describe a liquid chromatographic procedure that utilizes recent advances in separation and detection technology such as ion chromatography and conductimetric detection and allows the determination of concentrations of 1,4-butanedisulphonic acid in plasma of 2.5 μg/ml with no interference from endogenous components present in biological samples and good performance in terms of precision, accuracy and specificity.

2. Experimental

2.1. Chemicals and reagents

Standard 1,4-butanedisulphonic acid disodium salt [$NaO_3S(CH_2)_4SO_3Na$] was obtained from BioResearch (BASF-Pharma) with chemical purity $\geq$98%. 1,2-Ethanedisulphonic acid disodium salt, [$NaO_3S(CH_2)_2SO_3Na$], used as an

* Corresponding author.

0021-9673/95/$09.50
SSDI 0021-9673(94)01288-1

internal standard, was purchased from Fluka (Buchs, Switzerland).

Standard solutions of 1,4-butanedisulphonic acid disodium salt and of the internal standard in distilled water were stored at 4°C and used for 2 months; their detector response was checked daily. A 0.67 *M* perchloric acid solution was prepared by dilution with distilled water of 70% perchloric acid (Sp.gr. 1.67) of analytical-reagent grade (Merck, Darmstadt, Germany). Solutions of 5 m*M* sodium carbonate, 1.8 m*M* sodium hydrogencarbonate (used for mobile phase preparation), 3 *M* potassium carbonate and 0.014 *M* sulphuric acid were prepared diluting with distilled water of the Baker Analyzed Reagents (J.T. Baker, Deventer, Netherlands).

Water used for preparing all solutions was demineralized, distilled and filtered through a Type GTTP 0.2-μm filter (Millipore, Bedford, MA, USA).

2.2. Liquid chromatography

A DX-100 ion chromatograph (Dionex, Sunnyvale, CA, USA) equipped with a conductivity detector and an AMMS-II anion micro membrane suppressor (Dionex) was used.

The analytical column was a 25 cm × 4 mm I.D. Ion Pac AS9-SC (Dionex) packed with a 13-μm polyethylvinylbenzene–divinylbenzene substrate and an anion-exchange stationary phase protected by an AG9-SC guard column (Dionex).

The mobile phase contained 5 m*M* Na_2CO_3 and 1.8 m*M* $NaHCO_3$ pumped isocratically at room temperature at a flow-rate of 2.0 ml/min. The 0.014 *M* sulphuric acid for the suppression system was used at a flow-rate of 4.0 ml/min.

Samples were injected manually using a Model 7125 injector with a 100-μl loop (Rheodyne, Cotati, CA, USA) or a Model 231 XL automatic sample injector (Gilson, Villiers le Bel, France).

On-line data acquisition and subsequent calculations were performed with a Data Jet Integrator (Thermo Separation Products, Riviera Beach, FL, USA) and a Spectra 386 computer using Winner/386 Autolab software (Thermo Separation Products).

2.3. Sample preparation

Aliquots of 0.2–0.5 ml of plasma samples were mixed with suitable volumes (8–20 μl) of a 1 mg/ml solution of 1,2-ethanedisulphonic acid (internal standard) in water in order to obtain concentrations of 40 μg/ml plasma and with two volumes of 0.67 *M* perchloric acid. The mixture was vortex mixed and centrifuged at 6000 *g* at 0°C for 15 min.

A 0.5-ml volume of the clear, upper phase were measured into a test-tube and mixed with 0.1 ml of 3 *M* K_2CO_3 solution at 0°C in order to precipitate the main amount of ClO_4^- ions as the potassium salt. After centrifugation at 6000 *g* at 0–4°C for 15 min, 0.1 ml of the clear supernatant phase was transferred into another test-tube and diluted to 2.0 ml by addition of distilled water. Aliquots of 0.1 ml of this solution were injected into the chromatographic column.

2.4. Calibration graphs

Calibration graphs were constructed by transferring aliquots of the standard solutions of 1,4-butanedisulphonic acid (SD4) and internal standard into blank plasma to give final concentrations of 2.5, 5, 7.5, 12.5, 17.5 and 25 μg/ml of SD4 and a constant concentration of internal standard (40 μg/ml). These calibration standards were extracted as described above. The calibration graphs were obtained by plotting the peak-area ratio of SD4 to the internal standard versus the concentration of SD4 by least-squares analysis. For each calibration graph the correlation coefficient, *r*, the intercept and the slope were calculated. This procedure was repeated six times.

3. Results and discussion

3.1. Sample preparation and chromatographic system.

Owing to the high polarity characteristics of 1,4-butanedisulphonate, its extraction from biological matrices using organic solvents was not

practicable. We obtained good results by applying a method based on protein precipitation followed by direct injection into the chromatographic column of the clear supernatant obtained after centrifugation.

Addition of perchloric acid to plasma was optimum for protein precipitation and gave the clearest supernatant with the advantage of avoiding column contamination by plasma constituents and subsequent decrease in column efficiency. The amount and concentration of perchloric acid had to be optimized to minimize the dilution factor and the interference of the broad peak of perchlorate with a retention time of about 15 min that could overlap the internal standard peak.

The addition of K_2CO_3 solution to the clear supernatant phase precipitates the main amount of perchlorate but the aliquot remaining in solution (ca. 10%) represents a limiting factor of the analytical procedure in terms of sensitivity. By applying the method without addition of an internal standard it was possible to increase the sensitivity limit up to 1 μg/ml with minor consequences in terms of accuracy. The validation of this procedure is in progress.

By replacing the precolumn every 500 injections, the analytical column can be used for up to about 1500 analyses of biological samples. During routine analysis, the mobile phase could be slightly modified in relation to column efficiency: normally the concentration of $NaHCO_3$ solution was maintained constant with minor changes in Na_2CO_3 solution concentrations (between 5 and 7.5 m*M*).

In order to maintain good performance for a long time, the analytical column was washed with 200 ml of a CH_3CN–1 *M* NaCl (80:20, v/v) mixture after every 2 months of continuous use.

The retention times under the above chromatographic conditions for 1,4-butanedisulphonic acid and the internal standard were 5.0 and 10.0 min, respectively.

3.2. Limit of quantification

The limit of quantification of 1,4-butanedisulphonic acid in plasma samples was 2.5 μg/ml using a 0.2-ml specimen; this concentration represents the lowest level of the calibration graphs. The inter-assay relative standard deviation (R.S.D.) at this concentration was 5.8% ($n = 6$).

3.3. Linearity

The calibration graphs were linear over the concentration range 2.5–25 μg/ml with correlation coefficients $r > 0.998$ and minimal intercepts (0.0057; R.S.D. = 54.5%, $n = 6$). The mean value of the slope was 0.021 with a day-to-day R.S.D. of 2% ($n = 6$) (Table 1).

3.4. Reproducibility and accuracy

The precision (defined as the R.S.D. of replicate analyses) and the accuracy (defined as the deviation between the found and added concentrations) of the analytical procedure were evaluated on spiked samples at concentrations of 3.75 and 20 μg/ml. The intra-assay reproducibility was determined by analysing five specimens for each concentration of spiked plasma samples on the same day. The inter-assay reproducibility was obtained by analysing two specimens of spiked plasma samples for the two concentrations on six different days. The concentrations of SD4 in these spiked samples were determined by using the linear regression line of peak-area ratios versus concentration of calibration graphs constructed as described above. The results obtained are reported in Tables 2 and 3.

The R.S.D.s were 3.6% (3.75 μg/ml) and 2.9% (20 μg/ml) for the intra-day reproducibility ($n = 5$) and 2.28% (3.75 μg/ml) and 2.31% (20 μg/ml) for the inter-day reproducibility ($n = 12$). The accuracy, calculated for the same samples, was 99.9% and 102.3% for intra-day and 99.9% and 100.3% for inter-day assay, respectively.

3.5. Specificity

Fig. 1 shows typical chromatograms of (a) an extract of blank rat plasma, (b) a plasma standard spiked with SD4 at 5 μg/ml and internal standard and (c) a plasma sample of rat receiving

Table 1
Reproducibility of calibration graphs

Standard concentration (μg/ml)	Peak-area ratio (SD4 to internal standard)		
	Mean ($n = 6$)	Range	R.S.D. (%)
2.5	0.046	0.044–0.050	5.8
5.0	0.101	0.096–0.108	4.5
7.5	0.154	0.143–0.161	4.0
12.5	0.255	0.242–0.261	2.9
17.5	0.362	0.333–0.375	4.2
25.0	0.522	0.515–0.526	0.7
Calibration graph Parameter	Mean ($n = 6$)	Range	R.S.D. (%)
Slope	0.021	0.020–0.021	2.0
y-Intercept	−0.00574	−0.00085 to −0.0028	54.5
Correlation coefficient	0.9988	0.998–0.999	0.041

oral SD4 chronically at a dose of 225 mg/kg per day during a long-term toxicity study.

Blank plasma samples from humans, mouse and dog analysed by this method were found to be, as for rat plasma, free from endogenous contaminants at the retention times corresponding to SD4 and the internal standard. The chromatographic behaviour of the drug and possible impurities and metabolites was also evaluated to determine their potential for interference in the assay. The possible interference due to excipients administered with the drug were checked by analysing plasma samples from humans and animals treated with placebo preparations. The resulting chromatograms from these tests revealed no interfering peaks.

The high specificity of the method is enhanced through the use of a conductimetric detector, which is very sensitive for ionic substances, giving no signal for other constituents in the biological matrices.

3.6. Chromatographic system suitability test

Column efficiency

This was evaluated as the number of theoretical plates of the column calculated by using Labnet software (Thermo Separation Products)

Table 2
Intra-assay precision and accuracy

Nominal concentration (μg/ml)	Measured concentrations (μg/ml) and accuracy (%)						
	1	2	3	4	5	Mean	R.S.D. (%)
3.75	3.58	3.63	3.88	3.87	3.76	3.74	3.6
Accuracy (%)[a]	95.5	96.8	103.5	103.2	100.3	99.86	—
20.0	20.6	19.9	21.4	20.0	20.4	20.5	2.9
Accuracy (%)[a]	103.0	99.5	107.0	100.0	102.0	102.3	—

Rat plasma samples were prepared to contain SD4 at two concentrations and five replicates of each sample were analysed on the same day.

[a] Accuracy is expressed as (measured concentration/nominal concentration) · 100.

Table 3
Inter-assay precision and accuracy

Day	Nominal concentration (μg/ml)					
	3.75			20.0		
	Measured concentration (μg/ml)	Accuracy (%)[a]	R.S.D. (%)	Measured concentration (μg/ml)	Accuracy (%)[a]	R.S.D. (%)
1	3.72, 3.79	99.2, 101.1	1.3	21.2, 19.8	106.0, 99.0	4.8
2	3.55, 3.80	94.7, 101.3	4.8	20.2, 20.7	101.0, 103.5	1.7
3	3.75, 3.79	100.0, 101.1	0.7	20.0, 19.9	100.0, 99.5	0.3
4	3.76, 3.73	100.3, 99.5	0.6	20.1, 19.6	100.5, 98.0	1.8
5	3.64, 3.85	97.1, 102.7	4.0	19.8, 19.7	99.0, 98.5	0.3
6	3.72, 3.84	99.2, 102.7	2.2	19.7, 20.1	98.5, 100.5	1.4
Overall mean ($n = 12$)	3.74	99.9	2.28	20.1	100.3	2.31

Rat plasma samples were prepared to contain SD4 at two concentrations. Two aliquots of each concentration were analysed on six different days using a separate calibration graph for each day.
[a] Accuracy is expressed as (measured concentration/nominal concentration) · 100.

by the equation $N = 5.54\ (t_R/W)^2$, where t_R is the retention time of the SD4 peak and W its width at half-height. The calculated value of N was 2400.

Peak symmetry

Using the same software, the tailing factor of the SD4 peak was found to be 0.95. A similar value was obtained for the internal standard peak (0.96).

3.7. Stability

Rat plasma samples were spiked with two concentrations of 1,4-butanedisulphonic acid (2.5 and 8 μg/ml). Two samples for each concentration were immediately analysed as described above and used as reference samples ($t = 0$).

Two samples for each concentration were stored in a water-bath at 37°C for 24 h before analysis for testing the stability in plasma. To two samples for each concentration were added twice their volume of 0.67 *M* perchloric acid, then the mixture was centrifuged and 0.5 ml of the supernatant was stored in a water-bath at 37°C for 24 h before analysis for testing the stability in deproteinized samples by comparison with results obtained from two samples for each concentration analysed immediately after centrifugation.

The results obtained are reported in Table 4 and indicate that the analyte is stable for 24 h at 37°C both in rat plasma and in the dilute solution of perchloric acid used for the deproteinization procedure.

3.8. Application to biological samples

The method was successfully applied to the analysis of several plasma samples from humans and animals from pharmacokinetic and toxicology studies following oral and intravenous administration of SD4 alone and as the counter ion of S-adenosyl-L-methionine.

4. Conclusions

The described method is suitable for the determination of 1,4-butanedisulphonate ion in plasma samples deproteinized with perchloric acid. The results of the validation tests indicated that with this method it is possible to measure with good precision, accuracy and specificity up to 2.5 μg/ml of this analyte in plasma samples.

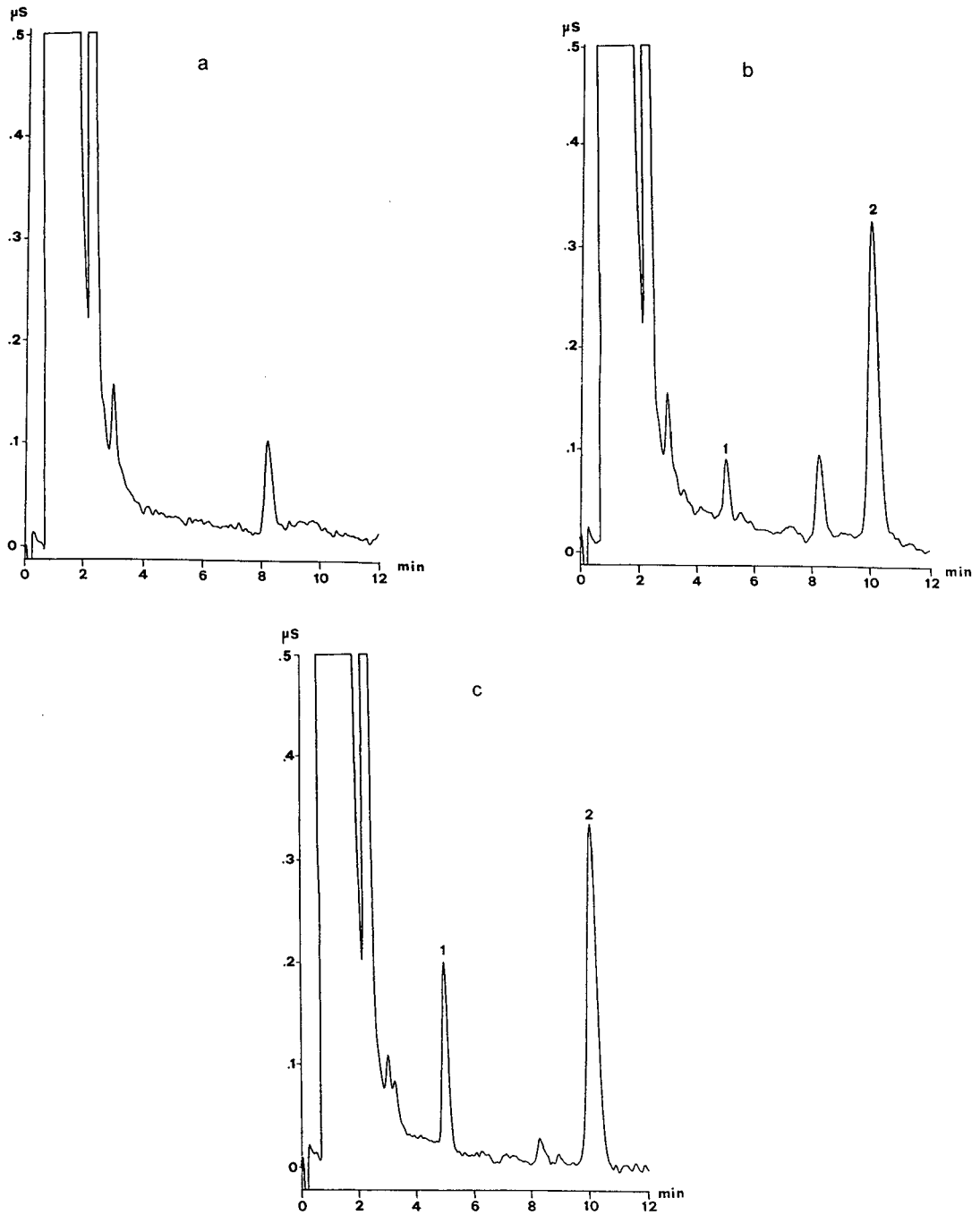

Fig. 1. Chromatograms of extracts from (a) blank rat plasma, (b) plasma spiked with 5μg/ml of 1,4-butanedisulphonic acid (SD4) and (c) plasma sample from a rat receiving oral SD4 chronically. Peaks: 1 = SD4; 2 = internal standard.

Table 4
Stability of SD4 in plasma and deproteinized samples

Concentration (μg/ml)	Sample and conditions	Mean recovery ($n = 2$) (%)	Sample and conditions	Mean recovery ($n = 2$) (%)
2.5	Rat plasma,	94.7	Rat plasma,	103.0
8.0	freshly prepared	95.1	24 h at 37°C	101.3
2.5	Rat plasma deproteinized with $HClO_4$,	100.4	Rat plasma deproteinized with $HClO_4$,	102.6
8.0	freshly prepared	105.0	24 h at 37°C	109.4

This procedure can be applied to the analysis of deproteinized plasma samples from rat, mouse, dog and man and in urine after the appropriate validation tests for each of the different biological matrices.

References

[1] D.E.C. Cole and C.R. Scriver, *J. Chromatogr.*, 225 (1981) 359–367.
[2] P. Rozman, H.J. Kim, C. Madhu and C.D. Klaassen, *J. Chromatogr.*, 574 (1992) 146–149.

ELSEVIER

Journal of Chromatography A, 706 (1995) 459–462

JOURNAL OF CHROMATOGRAPHY A

Analysis of the acidic microenvironment in murine tumours by high-performance ion chromatography

M.R.L. Stratford[a,*], C.S. Parkins[a], S.A. Everett[a], M.F. Dennis[a], M. Stubbs[b], S.A. Hill[a]

[a]*Cancer Research Campaign Gray Laboratory, P.O. Box 100, Mount Vernon Hospital, Northwood, Middlesex HA6 2JR, UK*
[b]*Magnetic Resonance Research Group, St. Georges Hospital Medical School, Tooting, London SW17 0RE UK*

Abstract

High-performance ion chromatography (HPIC) has been utilised to probe the biochemistry associated with changes in tumour pH following total vascular occlusion. Samples from the tumour extracellular compartment were obtained by insertion of a microdialysis probe and analysed by HPIC with conductivity detection. Separations were carried out by ion-exclusion chromatography using an IonPac ICE AS1 weak-acid column. The eluent (0.5 m*M* octanesulphonic acid) was chemically suppressed with 5 m*M* tetrabutylammonium hydroxide through a micromembrane suppressor. After complete vascular occlusion induced by a clamp, lactate levels increased in the extracellular compartment.

1. Introduction

Early reports suggested that tumours preferentially metabolise glucose by anaerobic glycolysis to lactic acid even if oxygen were available [1]. Because of the poor vascularity of tumours, lactic acid accumulates within the tumour and has often been proposed as a determinant of tumour acidity. The pH of the tumour microenvironment may be an important factor affecting the cellular uptake, distribution and activity of anticancer drugs [2–4]. The intra- to extracellular pH gradient (pH_i/pH_e) is in the opposite direction to, and of a larger magnitude than in normal tissues [3,5], and may be used to accumulate drugs with weak acidic functions within the relatively higher pH of the intracellular compartment, thereby enhancing tumour cell kill [6–8]. In this study, tumour acidity was altered by vascular occlusion in a murine tumour model [9] or using vinblastine, a vasoactive drug, which reduces tumour blood flow [10,11].

Microdialysis has previously been widely used to monitor changes in tissue metabolites during ischaemic periods, e.g. in heart or skeletal muscle [12,13]. We have investigated the relationship between tumour lactate concentrations and extracellular acidity using this technique, combined with ion-exclusion chromatography.

2. Experimental

2.1. Animals

Mice (CBA/Gy f TO males) were transplanted subcutaneously on the dorsum with the syngeneic adenocarcinoma CaNT. When the

* Corresponding author.

0021-9673/95/$09.50
SSDI 0021-9673(95)00016-X

tumours reached 7–9 mm in diameter, blood flow was occluded using a metal clamp and microdialysis was performed at various periods of time between 0 and 6 h of occlusion. Microdialysis was also performed up to 1 h after the clamp was removed. The cytotoxic agent vinblastine was administered intraperitoneally at 5 mg/kg (0.01 ml/g) body weight and microdialysis performed up to 6 h after injection. Immediately prior to the insertion of the microdialysis probe, animals were killed by cervical dislocation.

2.2. Sample preparation

Normal saline was pumped through the microdialysis probes (CMA/12, Biotech Instruments, Herts, UK) at 1 μl/min using a syringe infusion pump (Harvard Apparatus, MA, USA). The first 6 μl of the dialysate, which represent the dead volume of the probe and tubing, were discarded, and the next 16 μl collected directly into vials (limited-volume inserts, Waters, Watford, UK). The samples were then frozen at −20°C until analysis by HPIC.

2.3. Chromatography

Dialysates (5 μl) were injected using a WISP autosampler (Waters) onto a DX 100 system (Dionex, Camberley, UK). The column was a weak-acid IonPac ICE AS1 ion-exclusion column (Dionex), eluted with 0.5 m*M* octanesulphonic acid (Dionex) at a flow-rate of 1.2 ml/min. Detection was by conductivity following chemical suppression with 5 m*M* tetrabutylammonium hydroxide in counterflow through an AMMS ICE anion micromembrane suppressor at a flow-rate of 2 ml/min. Where spectrophotometric detection was used, a fixed-wavelength detector operating at 214 nm was inserted after the conductivity detector (Waters). Chromatograms were processed using an 840 data analysis system (Waters).

3. Results

Lactate recovery from stock solutions of lactate in saline was determined and found to be linear with respect to lactate concentrations up to 10 m*M* ($r > 0.999$). No significant differences were found between each probe, and the average recovery of 30% at 1 μl/min was used to calculate the tumour concentrations reported. Higher flow-rates resulted in a much reduced recovery (13% at 3 μl/min, 9% at 6 μl/min). The extent of carry-over from each consecutive sample was determined by allowing increasing volumes of dialysate to be discarded before collection of the next sample after transfer of the probe between saline and lactate solutions. If the first 6 μl of the dialysate were discarded, carry-over was minimal (Table 1). Intra-assay variability was assessed using replicate analyses of a control tumour dialysate ([lactate] = 1.95 ± 0.06 m*M*, mean ± S.D., $n = 5$). The intra-tumour heterogeneity was determined from the variation in lactate concentration obtained after inserting two probes into a number of tumours; the error was found to be 15.7 ± 12.3% (mean ± S.D., $n = 20$). Dialysates of standard lactate solutions were found to be stable; however, degradation of lactate was initially observed in dialysates obtained from some tumours if stored at room temperature overnight prior to analysis (Fig. 1). Also shown in Fig. 1 is the peak corresponding

Table 1
Carry-over of 45 m*M* lactate into saline during microdialysis at 1 μl/min

		[Lactate] (m*M*)
Lactate dialysed	Collect 15–30 min	13.9
Saline dialysed	Discard 0–6 min (6 μl), collect 6–18 min	0.18

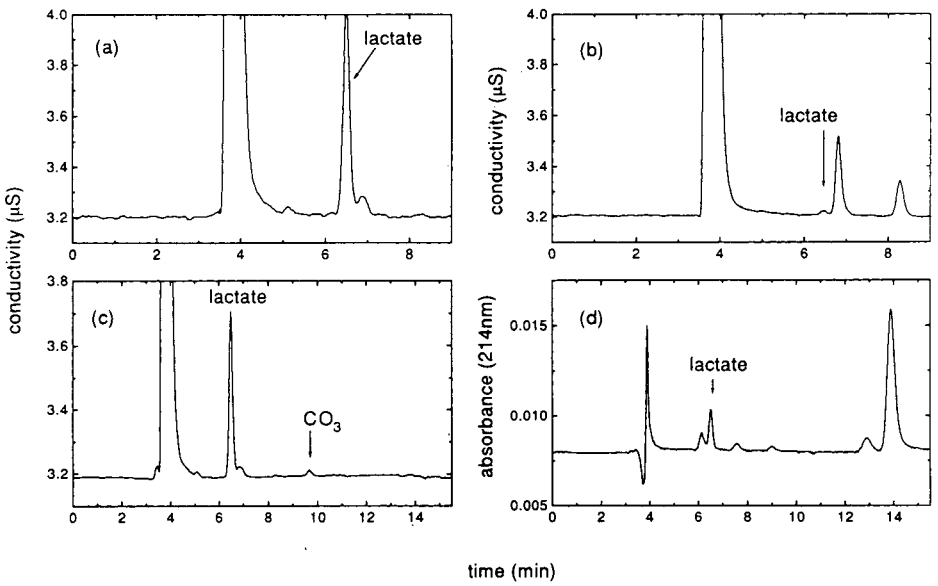

Fig. 1. HPLC profiles showing lactate in a tumour microdialysate analysed (a) immediately and (b) after 21 h at room temperature (sample diluted 1:3 with water); (c, d) extended analysis time showing carbonate (c) and unidentified UV-absorbing species (d). Chromatography was carried out on an IonPac-AS1 column, eluent 0.5 m*M* octanesulphonic acid.

to carbonate and a chromatogram showing the absorbance at 214 nm.

Lactate accumulation was determined in clamped or vinblastine-treated tumours as shown in Fig. 2. After vinblastine treatment there was no significant change in lactate concentration. In contrast, there was significant accumulation of lactate up to 6 h after vascular occlusion induced by clamping. It can be seen that the lactate accumulation appeared to correlate with the decrease in extracellular pH measured under identical treatment conditions. The open symbols indicate the reduction in tumour lactate concentration which occurs if the clamps were removed following a period of 6 h occlusion.

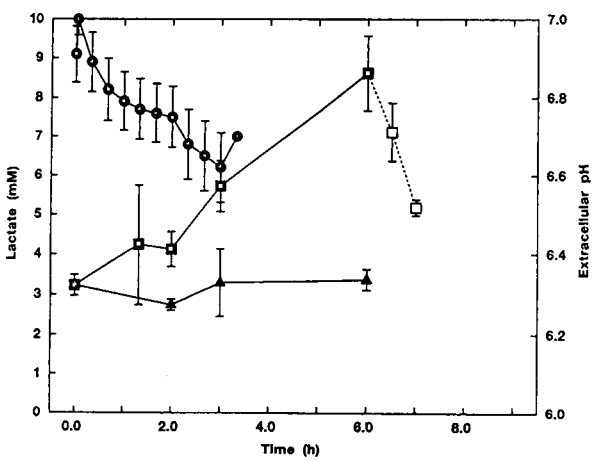

Fig. 2. Lactate accumulation and extracellular pH in CaNT tumours after clamping or vinblastine treatment. (▲) Lactate following vinblastine; (■) lactate following clamping; (□) lactate following clamp removal; (●) extracellular pH during clamp.

4. Discussion

The data presented here illustrates the use of ion-exclusion chromatography with conductimetric detection for analysis of lactate and other weak acids in the small volumes that are characteristically collected using microdialysis probes. The strong anions, particularly chloride which are present at high concentration in all biological samples, elute unretained under these conditions, allowing a rapid analysis. The peak shape

for lactate was good, and the error of replicate injections was ~3%. The sensitivity of the method is such that duplicate analyses can be made from as little as 16-μl collected volumes. Other anions such as carbonate were also detected although the quantification of this ion is complicated by its equilibration with atmospheric CO_2. The observation that lactate in tumour dialysates was sometimes degraded is unexplained, as dialysed lactate solutions are stable and degradative enzymes would not be expected to cross the dialysis membrane.

The increased capacity of tumour cells to metabolise glucose by glycolysis is a characteristic of solid tumours, and accumulated lactate has been shown using a variety of techniques, e.g. bioluminescence [2]. The present microdialysis data support these observations of high concentration in tumour relative to normal tissue (e.g. kidney, [lactate] = 0.1 m*M* [14]). The significant accumulation of lactate observed in response to ischaemia is not unexpected and not tissue-specific, although the magnitude in normal tissues are less than reported here in murine tumours. The reduction in tumour blood flow induced by the cytotoxic agent vinblastine is of the order of 50% at 6 h after the drug dose used here [10]. This partial vascular occlusion resulted in no significant accumulation of lactate over the time period studied, presumably because the residual blood flow was sufficient to remove any accumulated lactate. By comparison, the application of complete vascular occlusion, by clamping, resulted in a time-dependent increase in lactate. Because the pK_a of lactic acid is 3.7, the ion will be essentially fully dissociated under physiological conditions. The high extracellular proton concentration would be expected to result in the reduction in extracellular pH as shown, although the time course of the changes are slightly different. This may suggest that other factors, e.g. accumulation of other metabolites, may complicate the relationship. Preliminary observations were also made on the tumour lactate concentration during the period following clamp removal. The rapid decrease in tumour lactate observed suggests a reperfusion of the tumour allowing any accumulated lactate to be removed. Indeed, studies on tumour blood flow recovery after clamp removal would support this hypothesis [15].

In conclusion, we have used the combination of microdialysis with HPIC to investigate some of the biochemical changes occurring in the tumour microenvironment.

Acknowledgements

This work is supported by the Cancer Research Campaign. Sponsorship from Dionex is gratefully acknowledged.

References

[1] O. Warburg, in F. Dickens (Editor), *The Metabolism of Tumours*, Constable, London, 1930.
[2] P. Vaupel, *Nucl. Magn. Reson. Biomed.*, 5 (1992) 220.
[3] J.R. Griffiths, *Br. J. Cancer*, 64 (1991) 425.
[4] J.L. Wike-Hooley, J. Haveman and H.S. Reinhold, *Radiother. Oncol.*, 2 (1984) 343.
[5] M. Stubbs, Z.M. Bhujwalla, G.M. Tozer, L.M. Rodrigues, R.J. Maxwell, R. Morgan, F.A. Howe and J.R. Griffiths, *Nucl. Magn. Reson. Biomed.*, 5 (1992) 351.
[6] C.S. Parkins, J.A. Chadwick and D.J. Chaplin, *Anticancer Res.*, 14 (1994).
[7] R.B. Mikkelsen, C. Asher and T. Hicks, *Biochem. Pharmacol.*, 34 (1985) 2531.
[8] D.J. Chaplin, B. Acker and P.L. Olive, *Int. J. Radiat. Oncol. Biol. Phys.*, 16 (1989) 1131.
[9] C.S. Parkins, S.A. Hill, S.L. Lonergan, M.R. Horsman, J.A. Chadwick and D.J. Chaplin, *Int. J. Radiat. Oncol. Biol. Phys.*, 29 (1994) 499.
[10] S.A. Hill, S.J. Lonergan, J. Denekamp and D.J. Chaplin, *Eur. J. Cancer*, 29a (1993) 1320.
[11] B.C. Baguley, K.M. Holdaway, L.L. Thomsen, L. Zhuang and L.J. Zwi, *Eur. J. Cancer*, 27 (1991) 482.
[12] J.A. Delyani and D.G. Van Wylen, *Am. J. Physiol.*, 266 (1994) H1019.
[13] H. Rosdahl, U. Ungerstedt, L. Jorfeldt and J. Henriksson, *J. Physiol. (London)*, 471 (1993) 637.
[14] T. Eklund, J. Wahlberg, U. Ungerstedt and L. Hillered, *Acta Physiol. Scand.*, 143 (1991) 279.
[15] J. Denekamp, S.A. Hill and B. Hobson, *Eur. J. Cancer Clin. Oncol.*, 19 (1983) 271.

ELSEVIER

Journal of Chromatography A, 706 (1995) 463–468

JOURNAL OF CHROMATOGRAPHY A

CAG triplet analysis in families with androgen insensitivity syndrome by capillary electrophoresis in polymer networks

Cecilia Gelfi[a,b], Pier Giorgio Righetti[a,*], Fiorella Leoncini[a], Valeria Brunelli[c], Paola Carrera[d], Maurizio Ferrari[d]

[a]*Faculty of Pharmacy and Department of Biomedical Sciences and Technologies, University of Milan, Via Celoria 2 Milan 20133, Italy*

[b]*ITBA, CNR, Via Ampere 56, Milan, Italy*

[c]*Clinica Pediatrica III, University of Milan, Via Olgettina 60, Milan, Italy*

[d]*Istituto Scientifico H.S. Raffaele, Department of Laboratory Medicine, Via Olgettina 60, Milan, Italy*

Abstract

The potential use of capillary zone electrophoresis in polymer networks (linear polymers above the entanglement threshold, added to the background electrolyte for sieving purposes) for analysis of DNA fragments amplified by a polymerase chain reaction, is shown. In typical runs, the capillary is filled with Tris–borate–EDTA buffer, at pH 8.3, containing 6% linear polyacrylamide as a dynamic sieving matrix. Such formulations allow replenishing the capillary with fresh sieving solution when resolution decays after prolonged use (typically >30 injections per capillary are obtained). The DNA fragments are detected by their intrinsic absorbance at 254 nm. This system has been applied to the analysis of CAG triplet polymorphism in families carrying the androgen insensitivity syndrome. While easy separation is obtained for fragments 139 base pairs (bp) and 160 bp (in families carrying a difference of 7 CAG repeats) even more difficult cases (such as those of families exhibiting fragments of 136 and 139 bp, thus differing by only one CAG repeat) are resolved with precision and diagnostic value.

1. Introduction

The androgen receptor (AR) is a DNA-binding, transcription regulating protein. Mutations in the AR block the normal pathway of androgen action (testosterone and 5α-dihydrotestosterone) and result in a number of phenotypic abnormalities of male sexual development. A spectrum of different phenotypes is known: the complete androgen insensitivity syndrome (CAIS, also called Morris disease), the partial androgen insensitivity syndrome (PAIS), the infertile male syndrome, and the undervirilized fertile male, each of which is transmitted as an X-linked trait [1]. The androgen receptor abnormalities have been characterized in cultured genital skin fibroblasts from patients with androgen resistance. These defects span from normal binding, qualitative abnormalities to complete absence of androgen binding. Cloning of cDNA encoding the androgen receptor [2,3] has made possible to elucidate the molecular defects causing androgen resistance. In most patients mutations are single nucleotide substitutions within the coding region of the androgen re-

* Corresponding author.

0021-9673/95/$09.50
SSDI 0021-9673(95)00074-7

ceptor, indicating a heterogeneous mechanism causing androgen resistance [4].

The AR consists of different domains: a carboxyl terminus responsible for the hormone binding; a central region containing the DNA-binding domain with two Zinc-finger motifs and an amino terminus domain specific for transcriptional activation. The latter is characterized by the presence of three homopolymeric repeats of amino acids. In particular the CAG trinucleotide repeat in exon A was found to be polymorphic and ranging from 17 to 28 Gln residues [4]. The highly polymorphic CAG repeat in exon A represents a useful marker for determination of affected, unaffected and carrier members within pedigrees showing a recessive X-linked transmission of AIS. Inheritance of polymorphic fragments represents a marker for following transmission of the disease within a family, allowing the two maternal X chromosomes to be distinguished [5]. For this purpose, a nested polymerase chain reaction (PCR) has been developed for analysis of CAG repeats. The amplified fragments are usually resolved by conventional polyacrylamide gel electrophoresis (PAGE) either on 12% PAGE or on 6% T[1], 8 *M* urea sequencing gels.

In the present report, we demonstrate the applicability of capillary zone electrophoresis (CZE) to the resolution and detection of PCR-amplified DNA fragments in the AIS. Separation is achieved in novel sieving matrices, consisting of a flexible polymer network, rather than rigid gel structures, as proposed long ago by De Gennes [6]. Dynamic sieving matrices [7] are rapidly coming of age, and have been now successfully applied to the screening of cystic fibrosis [8,9] and of congenital adrenal hyperplasia [10].

2. Materials and methods

2.1. Subjects studied

Three generation families of patients diagnosed as suffering from complete or partial AIS

[1] T = (g acrylamide + g N,N′-methylenebisacrylamide)/100 ml solution.

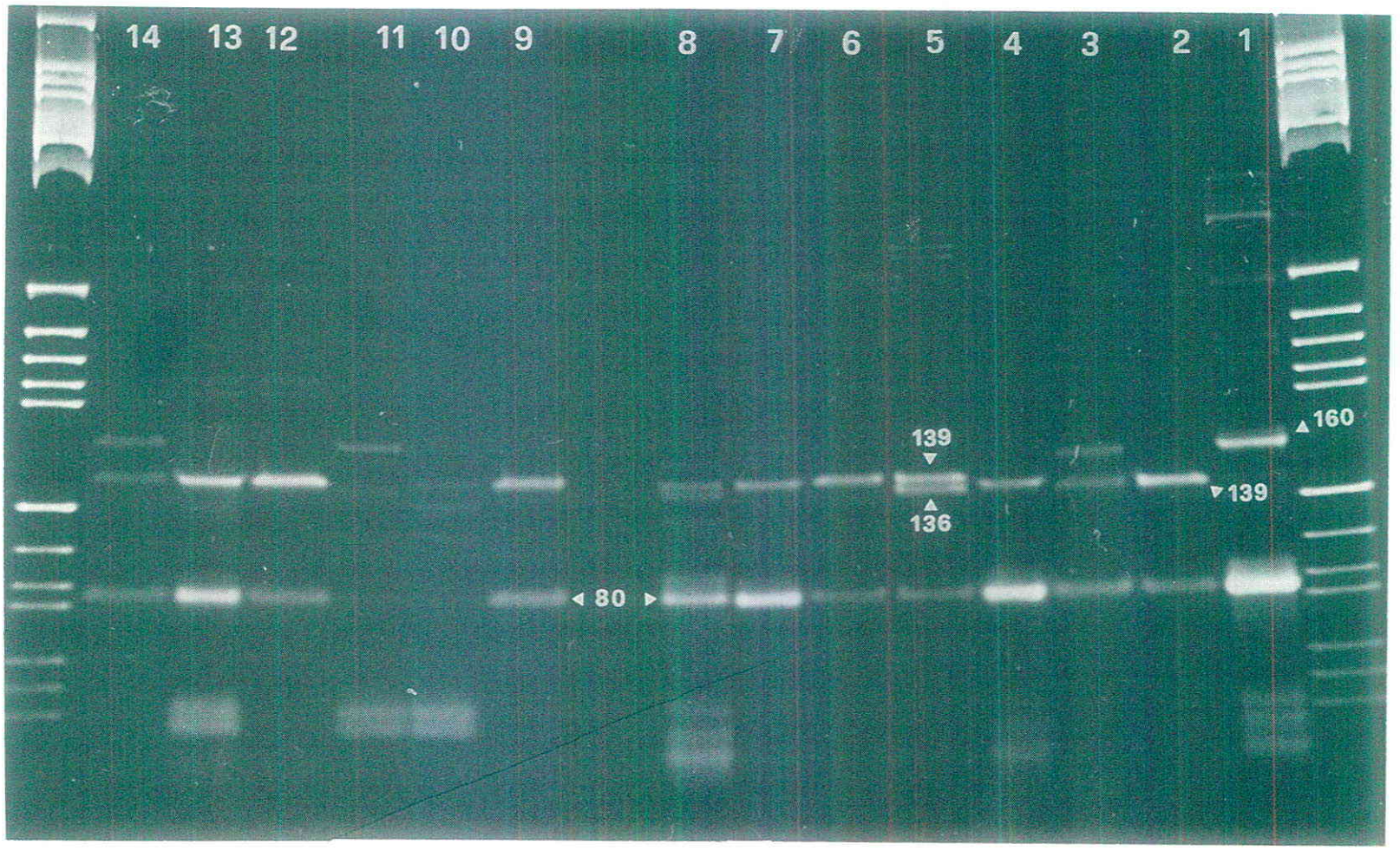

Fig. 1.

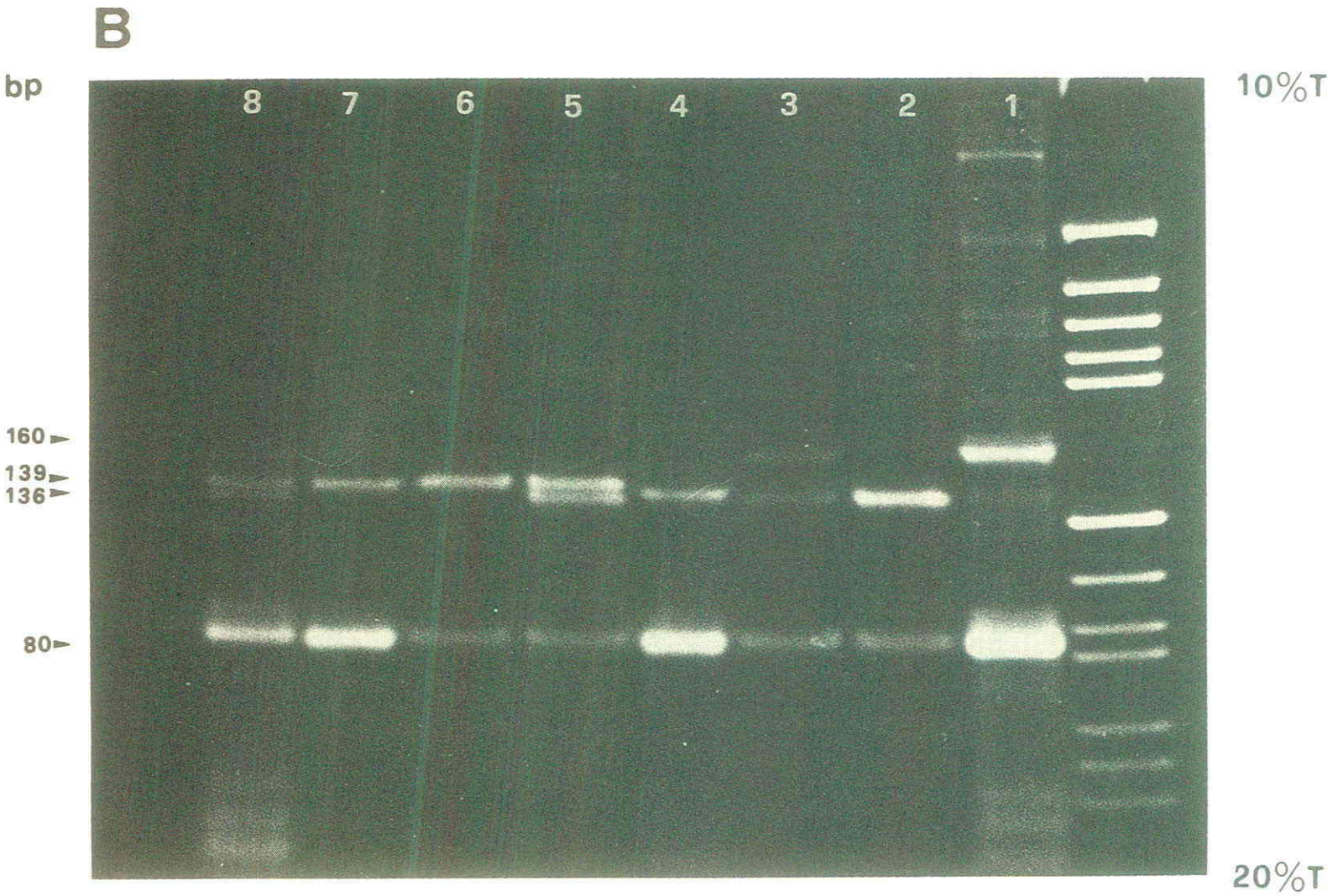

Fig. 1. Separation of nested PCR products in a 10–20% PAGE gradient gel in TBE buffer. The pBr 322/Hae III DNA was used as molecular mass standard. (A) Lanes: 1–3 = father, PAIS (affected child) and mother, respectively —the mother shows the presence of the two bands, the lower one being associated with the disease; 4–8 = father, mother, CAIS, CAIS (sister of the mother) and grandmother, respectively; 9–14: grandfather, grandmother, father, mother, CAIS and sister of the CAIS, respectively. In this last family the mother seems to be homozygous for the number of repeats and thus not informative. In order to obtain the exact size of the PCR fragments, electrophoresis of radiolabelled products was done in sequencing gradients, resulting in values of 136 bp for the smaller, 139 bp for the intermediate and 160 bp for the larger fragment (data not shown). (B) Close-up of a section of (A).

were studied. These patients are followed by the Department of Pediatrics, Endocrine Unit, S. Raffaele Hospital.

2.2. PCR amplification

Determination of CAG polymorphisms in the pedigrees of patients affected by AIS was carried out by two rounds of PCR. A first round of in vitro amplification was performed in the presence of primers A1 and A2, previously reported by La Spada et al. [11] for studying the CAG repeat expansion in spinobulbar muscular atrophy. A nested PCR was carried out by using primer 221 (5′-ACCTCCCGGCGCCAGTTTGCT-3′) and 360 (5′-AGAACCATCCTCACCCTGCT-3′) designed according to the sequence reported by Lubahn et al. [12]. The first round and nested PCR contained 250 ng of genomic DNA and 1 μl of first round PCR, respectively, with either 25 pmol of each primer or 3 pmol of the 5′ end ^{32}P-labelled 221 primer and 22 pmol of unlabelled, 400 μM each dNTP, 10 mM Tris · HCl, pH 8.3, 50 mM KCl, 1.5 mM $MgCl_2$, 5 units Taq polymerase (Taq = *Thermophilus aquaticus*) in a 100-μl final volume. Before addition of the enzyme, reactions were hot started for 3 min followed by 30 cycles (denaturation: 94°C for 1 min; annealing: 65°C for 1 min; extension: 72°C for 1 min) in a thermal cycler (Perkin-Elmer Cetus). The amplified fragments were analysed on 4% gels (3% agarose, 1% Nusieve), or on sequencing gels.

2.3. Capillary electrophoresis

CZE analyses were performed with the Waters Quanta 4000E capillary ion electrophoresis instrument from Millipore (Milford, MA, USA). We used 37 cm × 100 μm or 28 cm × 100 μm I.D. capillaries, coated by Hjertén's protocol [13], but with our novel monomer N-acryloylaminoethoxyethanol, offering extreme resistance to alkaline hydrolysis [14]. The capillary was then filled with a degassed solution of 6% acrylamide monomer (in the absence of cross-linker) in running buffer added with 1 μl of 40% persulphate and 1 μl of pure N,N,N′,N′-tetramethylethylenediamine (TEMED) per ml of gelling solution. After 90 min of polymerization, the capillaries were conditioned with separation buffer (TBE: 89 m*M* Tris, 89 m*M* boric acid, 2 m*M* EDTA, pH 8.3), for 30 min at 25°C and 100 V/cm in order to remove charged catalysts. The samples (desalted and concentrated with Centricon 30 membranes from Amicon, Beverly, MA, USA) were loaded electrophoretically by applying 140 V/cm for 30 s, a typical run lasting 35 min. The ultraviolet absorbance was monitored at 254 nm.

2.4. Polyacrylamide gel slab electrophoresis

The amplified products were analyzed by electrophoresis on a 10–20% polyacrylamide gradient gel in TBE buffer, pH 8.6. It should be noted that a constant-concentration gel (12% T), as routinely adopted in clinical practice, is unable to resolve fragments differing by only one CAG triplet. Thus, in those cases, one had to resort to sequence gels. In contrast, a 10–20% T gradient, as adopted here, has been found to solve the problem. The run was at 180 V for 4 h followed by 300 V for 1 h. Staining was by dye intercalation with ethidium bromide.

3. Results

Fig. 1 shows the screening of three different families in a 10–20% polyacrylamide gradient gel. As shown in the close-up of Fig. 1B, while in some individuals (see lane 3) heterozygous for two fragments, 139 base pairs (bp) vs. 160 bp in length, thus differing by 7 CAG repeats, the

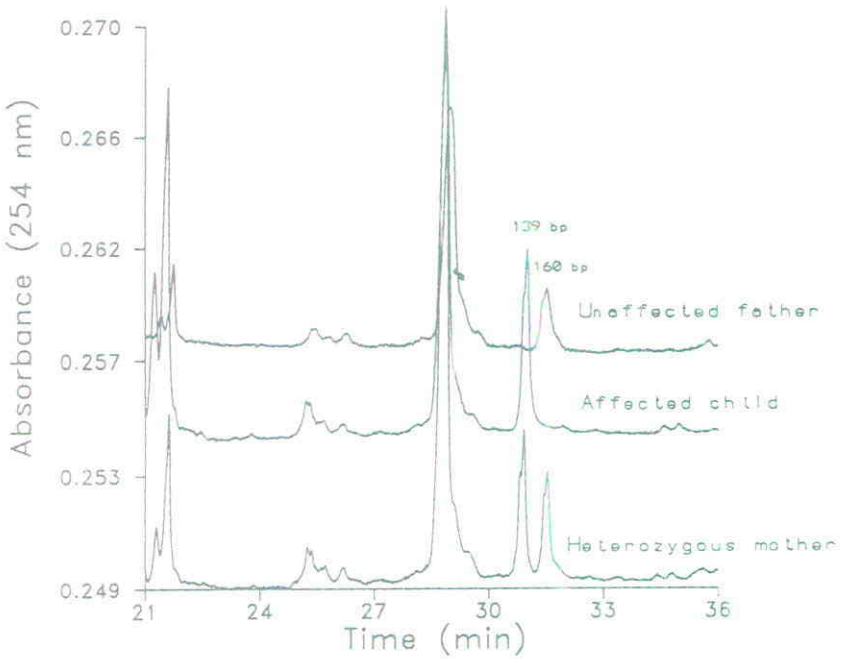

Fig. 2. Analysis of the samples in lanes 1–3 of Fig. 1 by CZE in polymer networks. Capillary length: 37 cm. Upper tracing: unaffected father, exhibiting the chain of 160 bp; intermediate tracing: affected child (chain of 139 bp); lower tracing: heterozygous mother, displaying both the 139 and 160 bp fragments (lane 3 in Fig. 1). In all cases the early peaks (ca. 21–23 min) correspond to the primers and the band located at ca. 29 min is a 80 bp constant amplification product.

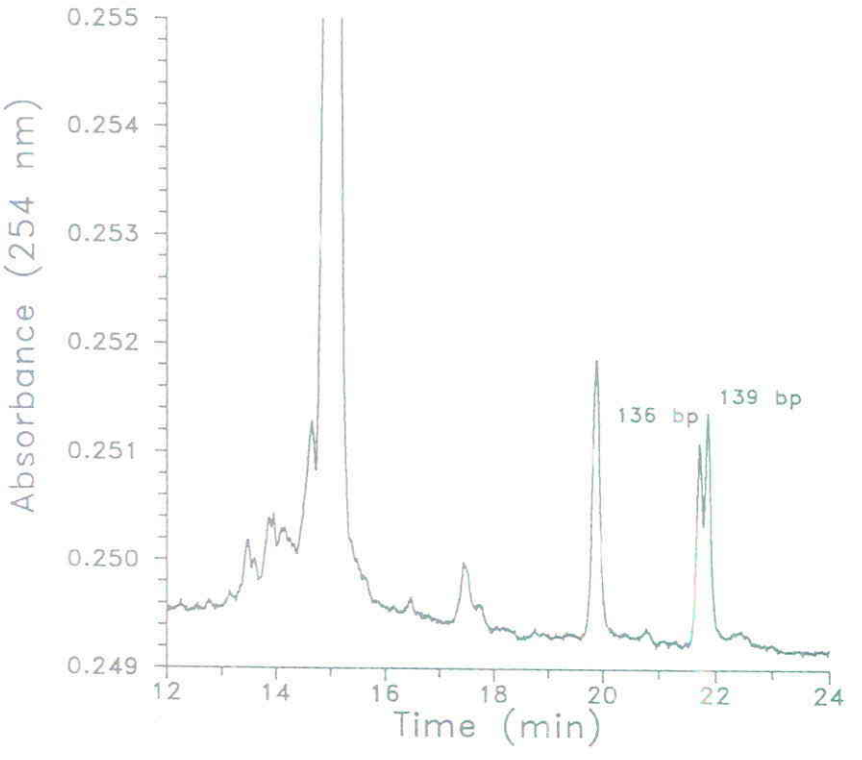

Fig. 3. CZE profile of the sample in lane 5 in Fig. 1 (heterozygous mother) displaying the two fragments sized 136 bp and 139 bp. Capillary length: 28 cm.

resolution of the two bands and diagnosis is quite easy, in other conditions, such as in lane 5, showing a carrier heterozygous for two bands differing by only one CAG triplet (136 vs. 139 bp), diagnosis is more difficult and could only be performed by using high-resolution, gradient gels and long running times.

As shown in Fig. 2, CZE could be a valid alternative for screening of PCR products from putative AIS patients. This figure represents the screening of the same family analyzed in lanes 1–3 in Fig. 1A. The upper tracing shows the pattern of the unaffected father, exhibiting only the 160 bp fragment. The intermediate tracing represents the affected child, carrying only the 139 bp DNA fragment. The lower tracing presents the electropherogram of the heterozygous carrier mother, with both 139 and 160 bp fragments. In all tracings, the early eluting peaks (ca. 21–23 min) represent primers, while the large peak at ca. 29 min represents an 80 bp constant fragment (primer dimers), visible in all sample tracks in Fig. 1A and B.

CZE in polymer networks can be utilized for resolution of more difficult cases, such as the sample in lane 5 of Fig. 1, where the two fragments are spaced only 3 bp apart. As shown in Fig. 3, also in this case the two 136 vs. 139 bp fragments can be separated, although not to baseline (note that, in this family, the 136 bp fragment represents the normal allele, whereas the 139 bp fragments represents the affected allele).

4. Discussion

CZE in polymer networks is rapidly emerging as a unique separation tool of extreme versatility. Dynamic sieving matrices are immune from the noxious problems of air-bubble formation (which would automatically open the electric circuit in such tiny channels) and from sample precipitation at the injection port. Due to the lack of a fixed-pore geometry, even large DNA fragments can open a pore in their wake, while they inevitably precipitate at the origin in cross-linked polyacrylamide gels. This allows repeated use of the same matrix (typically >30 runs). Even upon matrix fouling, the viscosity of a 6% polymer network still allows refilling of the capillary at the normal pressures utilized in CZE for, e.g., sample injection. As an extra bonus, the amount of sample required is truly minute (a few μl at the injection port, but only a few nl in the moving zone). Additionally, CZE does not require intercalating dyes (such as ethidium bromide, EtBr, mutagenic) for sample detection, as customary in slab-gel electrophoresis (although, occasionally, EtBr is added to the background electrolyte for modulating DNA velocities and thus increasing peak spacing). While at the moment CZE might not be so attractive for routine analyses, due to the availability of only a single channel, the novel generation of CZE equipment will provide batteries of channels (typically from 20 to 100), thus allowing for large sample handling abilities. This, coupled to the fully instrumental approach of CZE (with automatic storage of electropherograms on a magnetic support), might soon render this technique a challenge to conventional slab-gel electrophoresis.

5. Acknowledgements

Supported in part by a grant from the European Community (Human Genome Analysis, No. GENE-CT93-0018) and by grants from CNR, Comitati di Chimica (P.S. Tecnologie Chimiche Innovative) e di Biologia e Medicina to P.G.R.

References

[1] J.E. Griffin and J.D. Wilson, in C.R. Scriver, A.L. Beaudet, W.S. Sly and D. Valle (Editors), *The Metabolic Bases of Inherited Diseases*. McGraw-Hill, New York, 1989, pp. 100–120.

[2] C. Chang, J. Kokontis and S. Liao, *Science*, 240 (1988) 324-326.

[3] D.B. Lubahn, D.R. Joseph, P.M. Sullivan, H.F. Willard, F.S. French and E.M. Wilson, *Science*, 240 (1988) 327–330.

[4] M. Marcelli, W.D. Tilley, S. Zoppi, J.E. Griffin, J.D. Wilson and M.J. McPhaul, *J. Endocrinol. Invest.*, 15 (1992) 149–159.

[5] F. Mebarki, M.G. Forest, B. Lauras, A.M. Bertrand, P. Chatelain, M. David and Y. Morel, presented at the *75th Annual Meeting, Endocrine Society. Las Vegas, NV, 9–12 June 1993*, abstract No. 602.
[6] P.G. De Gennes, *Scaling Concepts in Polymer Chemistry*. Cornell University Press, Ithaca, NY, 1979.
[7] M. Chiari, M. Nesi and P.G. Righetti, *J. Chromatogr. A*, 652 (1993) 31–39.
[8] C. Gelfi, A. Orsi, P.G. Righetti, V. Brancolini, L. Cremonesi and M. Ferrari, *Electrophoresis*, 15 (1994) 640–643.
[9] C. Gelfi, P.G. Righetti, V. Brancolini, L. Cremonesi and M. Ferrari, *Clin. Chem.*, 40 (1994) 1603–1605.
[10] C. Gelfi, A. Orsi, P.G. Righetti, M. Zanüssi, P. Carrera and M. Ferrari, *J. Chromatogr. B*, 657 (1994) 201–205.
[11] A.R. La Spada, E.M. Wilson, D.B. Lubahn, A.E. Harding and K.H. Fischbeck, *Nature*, 352 (1991) 77–79.
[12] D.B. Lubahn, T.R. Brown, J.A. Simental, H.N. Higgs, C.J. Migeon, E.M. Wilson and F.S. French, *Proc. Natl. Acad. Sci. U.S.A.*, 86 (1989) 9534–9538.
[13] S. Hjertén, *J. Chromatogr.*, 347 (1985) 191–198.
[14] M. Chiari, C. Micheletti, M. Nesi, M. Fazio and P.G. Righetti, *Electrophoresis*, 15 (1994) 177–186.

ELSEVIER

Journal of Chromatography A, 706 (1995) 469–478

JOURNAL OF CHROMATOGRAPHY A

Comparison of capillary zone electrophoresis with ion chromatography and standard photometric methods for the determination of inorganic anions in atmospheric aerosols

Ewa Dabek-Zlotorzynska*, Joseph F. Dlouhy, Nicole Houle, Maria Piechowski, Scott Ritchie

Chemistry Division, Environmental Technology Centre, Environment Canada, 3439 River Road, Ottawa, Ontario K1A 0H3, Canada

Abstract

The capillary zone electrophoresis (CZE), ion chromatography and photometric techniques were compared for the analysis of nitrate and sulphate in high-volume sampled atmospheric aerosols. The CZE method with indirect UV detection utilizing a pyromellitate-based electrolyte was used. The comparative evaluation included response stability of instruments, detection limits, accuracy, precision, analysis time and other operational considerations. Statistical analysis of the results indicated that there was no evidence for systematic differences between the three techniques. The results suggest that CZE can be applied very advantageously in an anion analysis in atmospheric aerosols.

1. Introduction

The determination of inorganic acid species, in addition to other pollutants is a part of monitoring and assessing the ambient air quality in Canada under the National Air Pollution Surveillance (NAPS) network.

Sulphate and nitrate are the major anionic constituents of the atmospheric aerosols collected on filters with high-volume (Hi-Vol) samplers. Measurements of these species in atmospheric aerosols, provide information connected to acid rain. To date, the main method used in this laboratory for the determination of sulphate and nitrate in such samples is photometric analysis with an automated wet chemistry system (AWC) [1–3]. Photometric analysis of anions is being replaced by ion chromatography (IC), which offers advantages in terms of sensitivity and fully automated multiple analyte determination in a single assay. During the past decade IC, using chemically suppressed conductivity detection, has become established as a powerful analytical tool for determination of anions and cations in environmental samples including atmospheric aerosols [4–6].

IC is not the only method for separating ionic species. Capillary zone electrophoresis (CZE), a form of capillary electrophoresis (CE) where separation is mainly based on differences in solute size and charge at a given pH, has successfully been introduced as a new separation technique for the analysis of inorganic and organic ions [7,8]. Most published work is based on the

* Corresponding author.

0021-9673/95/$09.50
SSDI 0021-9673(94)01108-7

indirect photometric detection that can be used for the detection of compounds that have no optical absorbance. High efficiency, versatility, speed and economy of analysis are among the many attributes that promoted the application of CE in many real samples [9–18]. This technique also complements IC, and thus provides the confirmation of IC results [12,16]. The introduction of CE technique in an environmental analytical laboratory allows methods and results validation.

This paper presents the potential advantages of CE for the determination of sulphate and nitrate in atmospheric aerosols and compares this technique with photometric automated analysis and IC. The comparative evaluation includes detection limits, linearity, accuracy, precision, correlation between the results, analysis time and other operational considerations.

2. Experimental

2.1. Photometric automated wet chemistry (AWC)

The Technicon (Tarrytown, NY, USA) Auto-Analyzer II used in this study was a two flow path automated photometric system consisting of a 40 samples per tray sample changer, a peristaltic proportioning pump drawing up the reagents and samples through the system, a network of tubing, bubble injectors and mixing coils, two photometric detectors and a dual-pen chart recorder.

The following methods for photometric analysis with an AWC system were used: sulphate at 460 nm indirectly by releasing methylthymol blue (MTB) from a barium–MTB complex [1,2] and nitrate at 520 nm after reduction to nitrite as an azo dye [3].

The instrument was calibrated independently for each analyte with standard solutions at six different concentrations within the range 0.25–2.0 mg N/l for nitrate and 5–60 mg/l for sulphate. The standard solutions were prepared weekly. Calibration graphs were plotted based on the quadratic regression analysis of peak height measured manually.

2.2. Multi-dimensional IC

All IC equipment, columns and software used in this study were from Dionex (Sunnyvale, CA, USA). The multi-dimensional IC system [5,6] contained three ion chromatographs (Model 4500i) with gradient pumps (GPM), an ion chromatograph (Model DX-300) with an advanced gradient pump (AGP), an automated sample changer (ASM), one micromembrane chemical suppressor (AMMS-II 2 mm), three self-regenerating suppressors (ASRS-I 4 mm, CSRS-I 4 mm), four microconductivity detectors (CDM-2), one autoregeneration accessory (AutoRegen), trap, concentrator, guard and analytical columns. Two personal computers (IBM, PS 2/70) contained the operating and processing software (AutoIon 450) were connected to the equipment through interface modules (ACI).

Aqueous extracts of atmospheric aerosols were analyzed for 14 inorganic and organic anions and 11 inorganic cations using multi-dimensional IC. Four methods were applied: anion isocratic (IC-IA), anion gradient without (IC-GA) and with concentrator column (IC-GB) and cation gradient (IC-CAT). In this work, only isocratic and gradient anion IC methods were used for the comparative study. Separation of anions by isocratic elution was performed on an IonPac-AS4A column with an IonPac-AG4A guard column with CO_3^{2-}/HCO_3^- eluent, and by gradient elution on IonPac-AS10 column with an IonPac-AG10 guard column with NaOH eluent. Chromatograms of standard solutions are shown in Fig. 1.

Five standard calibrations were used for analysis of anions. Calibrations were performed over the range of concentrations expected in the samples (nitrate 0.4–16 mg/l, nitrite 0.1–4 mg/l and sulphate 0.4–80 mg/l).

Peak areas with linear least squares regression were used in anion gradient method, and with quadratic regression in anion isocratic elution.

Identification of individual ions was based on

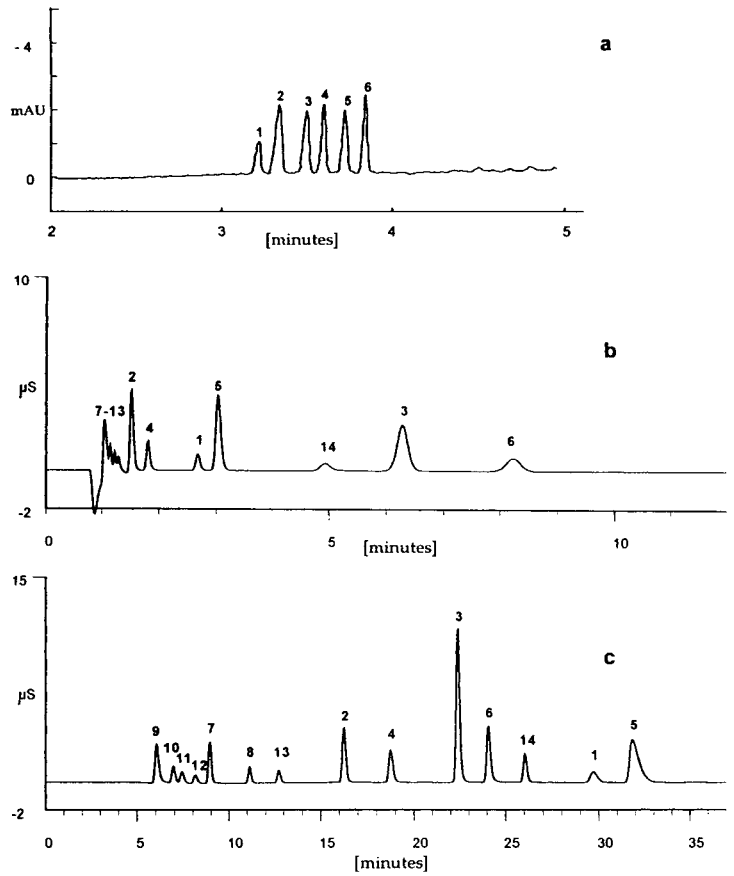

Fig. 1. Separation of an anion mixture standard by (a) CE, (b) isocratic IC and (c) gradient IC after baseline subtraction. Conditons: (a) electrolyte: 2.25 m*M* pyromellitic acid, 6.5 m*M* NaOH, 0.75 m*M* hexamethonium hydroxide, 1.6 m*M* triethanolamine, pH 7.7–7.9; capillary: 57 cm (50 cm to detector) × 75 μm I.D. fused silica; voltage: 30 kV, negative polarity, detector side anodic; detection: indirect UV at 254 nm; injection: pressure, 10 s; (b) columns: IonPac-AG4A and IonPac-AS4A (2 mm); eluent: 1.8 m*M* sodium carbonate–1.7 m*M* sodium hydrogencarbonate; flow-rate: 0.5 ml/min; suppressor: AMMS-II, 2 mm; regenerant: 25 m*M* sulphuric acid; regenerant flow-rate: ca. 5 ml/min; detector: conductivity; injection volume: 25 μl; (c) columns: IonPac-AG10 and IonPac-AS10 (4 mm); eluents: E1 = 20 m*M* NaOH, E2 = 200 m*M* NaOH; flow-rate: 1.0 ml/min; suppressor: ASRS-I, 4 mm, recycle mode; detector: conductivity; injection volume: 100 μl. Peaks: 1 = bromide; 2 = chloride; 3 = sulphate; 4 = nitrite; 5 = nitrate; 6 = oxalate; 7 = formate; 8 = methanesulphonate; 9 = fluoride; 10 = acetate; 11 = propionate; 12 = butyrate; 13 = chloroacetate; 14 = phosphate.

the comparison of elution times of analytes with those of standard solutions.

2.3. Capillary electrophoresis

A P/ACE 2100 CE system (Beckman Instruments, Fullerton, CA, USA) with a multi-wavelength UV detector, an automatic sample changer and a liquid thermostated capillary cartridge [capillary 57 cm (50 cm to detector) × 75 μm I.D.] and a personal computer (IBM PS/2 70) utilizing a Beckman Gold System (version 7.11) software for instrument control and for data collection and processing were used. Glass electrolyte vials (5 ml) and 30-sample carousel with 100-μl polyolefin microvials were used.

The running electrolyte consisted of 2.25 m*M* pyromellitic acid (PMA), 6.5 m*M* NaOH, 0.75 m*M* hexamethonium hydroxide (HMOH) and 1.6 m*M* triethanolamine (TEA) [8,16]. The pH

was between 7.7 and 7.9. Electrolyte was filtered by using a plastic syringe with a 0.22-μm syringe PTFE filter and degassed daily by creating a vacuum inside the syringe.

The capillary was reconditioned daily with 0.1 *M* NaOH (10 min), then rinsed with deionized water (5 min) and with the used electrolyte (5 min). Separation of anions presented in Fig. 1a was carried out using a method that consisted of a 1-min rinse of capillary with the running electrolyte prior to injection. The operating voltage of 30 kV with the reverse-polarity mode was applied. All injections were achieved using a 10 s pressure injection technique. Indirect UV detection at 254 nm was used.

Identification of individual ions was based on the comparison of migration times of analytes with those of standard solutions. All mixed standard solutions for the CE work were prepared every day that samples were analyzed. Calibrations were performed over the range of concentration expected in the samples. Six calibration standards were used at concentrations within the ranges 0.4–80, 0.4–16 and 0.1–4 mg/l for sulphate, nitrate and nitrite, respectively. Calibration graphs were plotted based on the linear regression analysis of the corrected peak area.

2.4. Reagents

All chemicals were purchased commercially from either Fisher Scientific (Ottawa, Canada), Technicon or Kodak (Rochester, NY, USA) in the highest purity available, and were used without further purification. Pyromellitate based electrolyte was obtained from Dionex.

All solutions were prepared with deionized water (18 MΩ cm) obtained by treating tap water using reverse osmosis and ion exchange (Millipore, Model RO 20 and Model SuperQ, Bedford, MA, USA).

2.5. Extraction procedure

Atmospheric aerosols, collected on PTFE-coated borosilicate glass fiber filters (Pallflex, TX40HI20WW, Putnam, CT, USA) using Hi-Vol samplers, were obtained from the Pollution Measurement Division, Environmental Technology Centre, Environment Canada.

Two discs, cut out from Hi-Vol filters, were placed in a 100-ml beaker. The filters were wetted with two drops of 30% Triton X-100 and then 25 ml of deionized water were added. The beakers were then covered with Parafilm 1"M" and extracted for 30 min in an ultrasonic bath (Branson and Smithkline, Shelton, CT, USA). Analysis was carried out as soon as possible after extraction (within less than 24 h).

2.6. Sample pretreatment

The only sample pretreatment was filtration by using a glass syringe with a 0.22-μm syringe PTFE filter connected.

2.7. Analysis of atmospheric aerosols

The number of Hi-Vol filter disc pairs that was analyzed for sulphate, nitrate and nitrite by CE, multi-dimensional IC and photometric AWC was 145. The parallel analysis of atmospheric aerosol extracts on each system was performed by different analysts.

2.8. Quality assurance

Each set (22) of atmospheric aerosol extracts was accompanied by two reagent blanks, an internal quality standard (a replicate of one of the standards used for calibration at the end of the daily run) and two external quality control samples [19] which were carried through the entire analytical scheme in a manner identical to samples.

3. Results and discussion

3.1. Performance characteristics

Response stability of instruments

Instrument response stability is a parameter which influences both accuracy and precision of the technique. Stability of instruments was ver-

ified by constructing calibration curves from standard solutions every day when samples were analyzed.

Within a seven working days during which some 150 samples were analyzed, very good stability of CE and IC systems was obtained. The relative standard deviations (R.S.D.s) of the linear coefficient were less than 5% for both the IC and CE systems (Table 1). Correlation coefficients of obtained calibration curves were in the range 0.9991–0.9999. Worse precision of calibration characteristic from run to run was obtained for the photometric analysis with the AWC system. The overall variability in the photometric AWC system within 7 days reflects mainly uncertainties in error due to manual measurement of peak heights.

Migration and retention time stability

With the exception of sulphate analyses by isocratic IC elution, the precision of retention times of anions in standard solutions was less than 1% within 7 running days (Table 1). The R.S.D.s of analyte migration times in standard solution by CE was found to be less then 3% between daily runs (Table 1). However, analyte migration times in CE are more strongly affected by the sample matrix than in IC. The high resolution of CE causes a slight change in migration time to be more significant with CE than IC. Because of the sample matrix effect on the analyte migration time, relative migration times with respect to a reference peak should be used with CE.

Detection limits

The method detection limits were calculated by analyzing dilute solutions. They were taken as three times the standard deviation of twenty replicate analyses of the sample containing analytes with the concentration about ten times higher than the estimated detection limit, the latter being the concentration giving a signal-to-noise ratio of 3.

The lowest detection limits were obtained by

Table 1
Performance of tested techniques

Parameter	Analytes	Photometric AWC	IC		CE
			Isocratic	Gradient	
Calibration range (mg/l)	NO_3^- (N)	0.25–2.00	0.09–4.00	0.09–4.00	0.09–4.00
	SO_4^{2-}	5–60	0.4–80	0.4–80	0.4–80
Linear coefficient (R.S.D., %)[a]	NO_3^- (N)	21.24	0.91	1.17	3.33
	SO_4^{2-}	14.99	1.30	0.66	4.20
Linearity R^2	NO_3^- (N)	0.9949	0.9999	0.9991	0.9997
	SO_4^{2-}	0.9972	0.9998	0.9999	0.9997
Retention time (R.S.D., %)	NO_3^- (N)	Not analyzed	0.85	0.39	2.65
	SO_4^{2-}	Not analyzed	1.78	0.26	2.46
Detection limit (mg/l)	NO_3^- (N)	0.056	0.003	0.011	0.035
	SO_4^{2-}	0.712	0.013	0.026	0.154
Number of samples per day		100	85	22	100
Number of analytes per day		200	595	550[b]	600

[a]Reported results are obtained from 7 measurements within 7 working days.
[b]For multi-dimensional IC.

IC followed by CE and photometric AWC (Table 1).

3.2. Accuracy and precision

To ensure the accuracy of the CE, IC and AWC results, external quality control samples (EQC) were used [19]. The data agree with the interlaboratory median values within 6% for reported anions at higher concentration and determined by the used analytical techniques (Table 2). Only sulphate results obtained by the photometric AWC method were higher. The accuracy and precision of the measurements becomes worse at concentration closer to quantitation limit, as expected. It can been seen that the photometric AWC methods are also less precise over-all than CE and IC methods. Specifically, the photometric AWC has inferior reproducibility for sulphate at lower concentration.

Correlation of CE, IC and photometric AWC results

The statistical analysis was performed to test the accuracy of the CE method when applied to the determination of nitrate and sulphate in atmospheric aerosols. Because the photometric AWC method measures total concentration of nitrate and nitrite (results are reported as nitrogen), nitrate and nitrite results obtained by IC and CE and expressed as nitrogen were added. The concentration of nitrite in all samples was always lower than nitrate concentration.

The relationship between concentrations (C) of analyzed anions obtained by the respective methods were evaluated by linear correlation [20] in the form:

$$C\ (\text{CE or IC}) = aC\ (\text{AWC}) + b\ (\text{mg/l})$$

or

$$C\ (\text{CE}) = aC\ (\text{IC}) + b\ (\text{mg/l})$$

as shown in Figs. 2 and 3 and Table 3. This statistical analysis showed no evidence of either relative or fixed bias between the three techniques, and the CE method is considered to be acceptable for the purpose of this type of measurement. The best correlation of results was obtained by both IC methods (Table 3).

The results were also expressed as median and

Table 2
Quality control sample

Analyte	Inter-laboratory median [19] (mg/l)	Method	Error (%)[a]	R.S.D. (%)[b]
Nitrate (N)	2.450	AWC	+0.7	4.57
		IC-IA	+0.79	1.18
		IC-GA	−4.05	0.63
		CE	+1.45	1.07
Sulphate	6.926	AWC	+9.47	4.01
		IC-IA	−5.85	0.5
		IC-GA	−0.79	0.71
		CE	+1.94	1.93

IC-IA, IC-GA = Isocratic and gradient IC elution, respectively.
[a]100 × (Mean concentration − inter-laboratory median concentration)/inter-laboratory median concentration.
[b]From 7 measurements obtained within 7 working days.

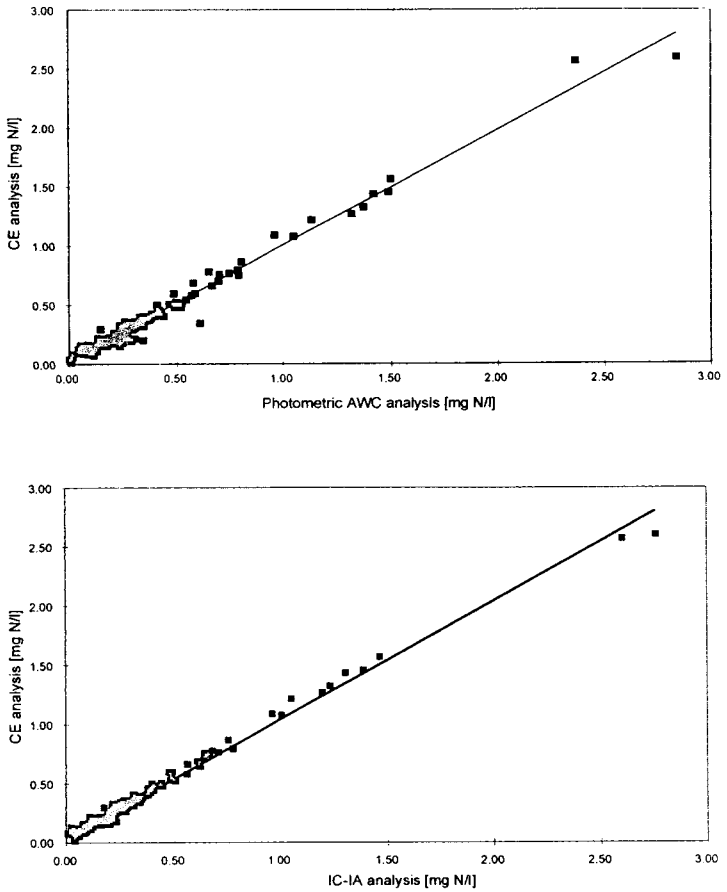

Fig. 2. Comparison of the results for the determination of nitrate plus nitrite in atmospheric aerosols using CE and photometric AWC or isocratic IC (the ± values are the confidence limits at the 95% level). Top: $n = 140$; slope = 0.975 ± 0.013; intercept = 0.031 ± 0.007; $R^2 = 0.9794$. Bottom: $n = 140$; slope = 0.999 ± 0.011; intercept = 0.040 ± 0.006; $R^2 = 0.9875$.

mean ratio of the individual results higher than quantitation limit of analyte obtained by the respective technique. Some outlier ratios were rejected. In all instances there was a close agreement between the tested techniques (Table 4). For the sulphate, mean ratios were within range 0.9393–1.0406 when compared to photometric AWC results. The lowest ratio was obtained by the evaluation of isocratic IC and AWC results. The excellent agreement between gradient IC and CE sulphate results was observed. The isocratic IC results were about 10% lower than gradient IC results. For total nitrate and nitrite as a nitrogen analysis, the better agreement was obtained by CE than IC when compared to AWC technique. Results obtained by gradient IC were about 10% lower.

3.3. Operational considerations

Analysis time

The number of analyte samples (an analyte is defined as an analysis of a constituent in a

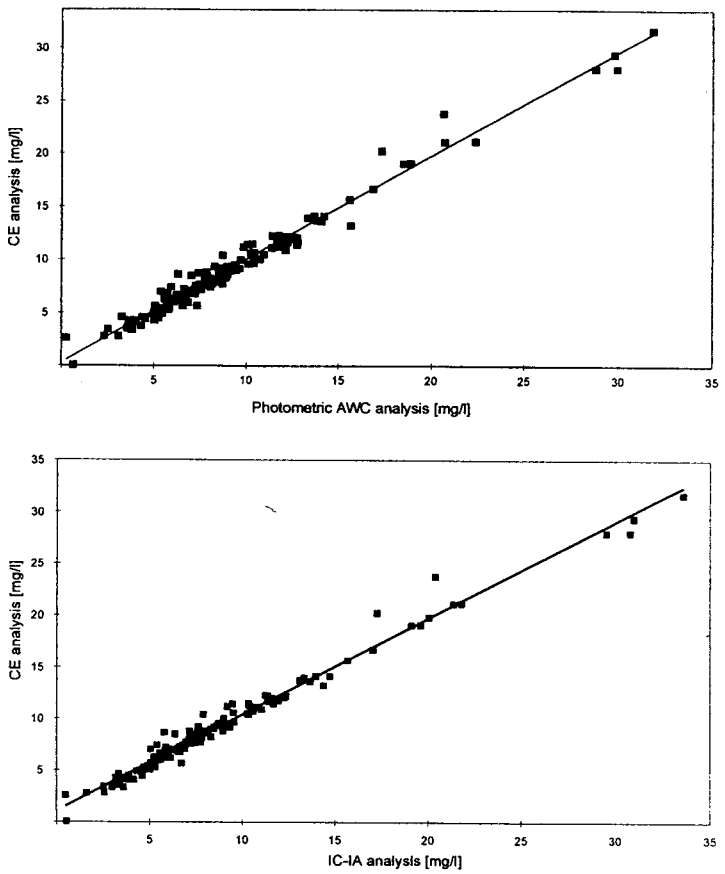

Fig. 3. Comparison of the results for the determination of sulphate in atmospheric aerosols using CE and photometric AWC or isocratic IC (the ± values are the confidence limits at the 95% level). Top: $n = 144$; slope = 0.979 ± 0.012; intercept = 0.273 ± 0.132; $R^2 = 0.9773$. Bottom: $n = 144$; slope = 0.936 ± 0.011; intercept = 1.040 ± 0.113; $R^2 = 0.9808$.

standard, a quality control sample or an actual sample) possible to analyze during the working day (AWC) and running overnight (IC and CE) is presented in Table 1. The slowest analysis is performed by the multi-dimensional IC system due to a long anion gradient method (Fig. 1). However, the ability of this system to make simultaneous determination of 14 anions and 11 cations on a single sample is highly advantageous. As a result of this, the number of analytes determined per day by both IC and CE is comparable and larger than the photometric AWC.

Cost of consumables

Estimation of operational costs due to consumables (chemicals, columns, autosampler vials etc.) based on 2400 samples being run per year was performed. The lowest analyte operational costs were estimated by the use of CE, followed by isocratic IC and photometric AWC.

Waste generation and disposal

CE wastes are generated in much smaller quantities than photometric AWC and IC wastes. Approximately 60 ml of electrolyte are gener-

Table 3
Statistical analysis results (± 95% confidence limit)

Method tested		Method compared	
		Photometric AWC	IC-IA
Nitrate + nitrite (N)			
CE[a]	R^2	0.9794	0.9875
	Slope	0.975 ± 0.013	0.999 ± 0.01111
	Intercept	0.031 ± 01.007	0.040 ± 0.006
IC-IA	R^2	0.9840	
	Slope	0.9711 ± 0.010	
	Intercept	− 0.007 ± 0.005	
IC-GA	R^2	0.9816	0.9977
	Slope	0.941 ± 0.010	0.970 ± 0.004
	Intercept	− 0.011 ± 0.006	− 0.005 ± 0.002
Sulphate			
CE[b]	R^2	0.9773	0.9808
	Slope	0.979 ± 0.012	0.936 ± 0.011
	Intercept	0.273 ± 0.132	1.040 ± 0.113
IC-IA	R^2	0.9918	
	Slope	1.043 ± 0.008	
	Intercept	− 0.810 ± 0.083	
IC-GA	R^2	0.9907	0.9974
	Slope	1.051 ± 0.008	1.007 ± 0.004
	Intercept	− 0.081 ± 0.089	− 0.742 ± 0.044

Total number of samples was 145. All results were blank corrected. IC-IA, IC-GA = Isocratic and gradient IC elution, respectively.
[a,b]5 and 1 outliers were rejected, respectively.

ated per day during which some 100 samples can be analyzed. This much is generated in 6, 120 and 30 min of photometric AWC, single isocratic IC or multi-dimensional IC system, respectively. Also, the photometric AWC wastes are more toxic.

4. Conclusions

When using the equipment and types of samples described in this paper the following were found: (i) sulphate and nitrate analysis by CE correlates well with automated photometric analysis and IC; (ii) both IC and CE offer advantages by performing sensitive simultaneous multi-ion analysis in one assay rather than two separate assays in photometric AWC; (iii) CE is less expensive to operate and less waste is generated than by IC. Both IC and CE produce less toxic waste than the photometric methods. Drawback of the CE method based on presented analysis is that CE is less sensitive than IC. However, the CE sensitivity is acceptable for the described application. Also CE analyte migration times are more strongly affected by the sample matrix. Because of this effect the use of an internal standard is recommended.

In conclusion, the results suggest that the CE can be applied very advantageously in a routine determination of sulphate, nitrate and other anions in atmospheric aerosols. The CE method may also be useful for comparison of the results when two independent methods are required for control of the quality of analytical work.

Table 4
Ratio of results

Methods	n_{tot} [a]	n_{out} [b]	Median	Mean	R.S.D. (%)
Nitrate + nitrite (N)					
CE vs. AWC	94	0	1.0420	1.0437	15.14
CE vs. IC-IA	124	5	1.1271	1.1639	17.06
CE vs. IC-GA	124	5	1.1692	1.2393	22.42
IC-IA vs. AWC	94	0	0.9490	0.9326	13.23
IC-GA vs. AWC	94	0	0.9164	0.8854	16.74
IC-GA vs. IC-IA	141	2	0.9580	0.9560	10.47
Sulphate					
CE vs. AWC	142	1	0.9969	1.0138	9.38
CE vs. IC-IA	145	3	1.0765	1.0862	10.42
CE vs. IC-GA	145	2	0.9563	0.9721	8.10
IC-IA vs. AWC	142	0	0.9367	0.9393	8.06
IC-GA vs. AWC	142	0	1.0427	1.0406	7.88
IC-GA vs. IC-IA	145	0	1.1233	1.1077	4.24

Total number of samples was 145. All results were blank corrected. IC-IA, IC-GA = Isocratic and gradient IC elution, respectively.
[a]Number of samples for which the individual result was higher than quantitation limit.
[b]Number of rejected outliers.

References

[1] A.L. Lazrus, K.C. Hill and J.P. Lodge, *Automation in Analytical Chemistry, Technicon Symposia, 1965*, Mediad, 1966, pp. 291–293.
[2] G. Colovos, M.R. Panesar and E.P. Parry, *Anal. Chem.*, 48 (1976) 1693–1696.
[3] *Industrial Methods AAII 100-70W*, Technicon, Tarrytown, NY, 1973.
[4] E. Sawicki, J.D. Mulik and E. Wittgenstein (Editors), *Ion Chromatographic Analysis of Environmental Pollutants*, Vol. I, Ann Arbor Publ., Ann Arbor, MI, 1978.
[5] E. Dabek-Zlotorzynska and J.F. Dlouhy, *J. Chromatogr.*, 640 (1993) 217–226.
[6] E. Dabek-Zlotorzynska and M. Piechowski, *Manual —Analysis of Ions in Atmospheric Aerosols by Multi-Dimensional Ion Chromatography*, Chemistry Division, ETC, Environment Canada, Ottawa, 1994.
[7] P. Jandik and G. Bonn, *Capillary Electrophoresis of Small Molecules and Ions*, VCH, New York, 1993.
[8] M.P. Harold, M. Jo Wojtusik, J. Riviello and P. Henson, *J. Chromatogr.*, 640 (1993) 463–471.
[9] B.F. Kenney, *J. Chromatogr.*, 546 (1991) 423–430.
[10] A. Nardi, M. Cristalli, C. Desiderio, L. Ossicini, S.K. Shukla and S. Fanali, *J. Microcol. Sep.*, 4 (1992) 9–11.
[11] W. Jones, *J. Chromatogr.*, 640 (1993) 387–395.
[12] K.A. Hargadon and B.R. McCord, *J. Chromatogr.*, 602 (1992) 241–247.
[13] D.L. Kelly and R.J. Nelson, *J. Liq. Chromatogr.*, 16 (1993) 2103–2112.
[14] J.P. Romano and J. Krol, *J. Chromatogr.*, 640 (1993) 403–412.
[15] J.B. Nair and C.G. Izzo, *J. Chromatogr.*, 640 (1993) 445–461.
[16] E. Dabek-Zlotorzynska and J.F. Dlouhy, *J. Chromatogr. A*, 671 (1994) 389–395.
[17] E. Dabek-Zlotorzynska and J.F. Dlouhy, *J. Chromatogr. A.*, 685 (1994) 145–153.
[18] E.L. Pretswell, A.R. Morrisson and J.S. Park, *Analyst*, 118 (1993) 1265–1267.
[19] N. Arafat and K. Aspila, *LRTAP Interlaboratory Study L-34 for Major Ions and Nutrients*, NWRI, Burlington, 1994.
[20] J.C. Miller and J.N. Miller, *Statistics for Analytical Chemistry*, Wiley, New York, 1984, pp. 82–94.

ELSEVIER

Journal of Chromatography A, 706 (1995) 479–492

JOURNAL OF CHROMATOGRAPHY A

Determination of nitrate and nitrite in vegetables by capillary electrophoresis with indirect detection

M. Jimidar, C. Hartmann, N. Cousement, D.L. Massart*

Pharmaceutical Institute, Vrije Universiteit Brussel, Laarbeeklaan 103, B-1090 Brussels, Belgium

Abstract

Nitrate and nitrite (and some other anions) were determined in vegetables by capillary electrophoresis (CE). The anions were extracted from the vegetables by mixing and diluting the samples with water at moderate temperature. The CE method is divided into two parts: a high-concentration-level method (for nitrate determination) and a low-concentration-level method (for nitrite determination). These CE methods were compared with a reference method (spectrophotometry after Jones reduction: official AOAC reference method for the determination of nitrates in foodstuffs). Parameters such as linearity, detection limit, quantification limit, precision and accuracy of the two techniques were investigated and compared. Both techniques resulted in acceptable linearity within their ranges. The detection limits of the CE methods were sufficiently low for the determination of the anions in vegetable samples. The precision and accuracy of the CE methods were comparable to those of the reference method. The precision was determined by evaluating the repeatability and the time-different intermediate precision, while the accuracy was investigated by comparing the slopes of the standard addition and external calibration lines and by evaluating the agreement between the results obtained with the CE and the reference spectrophotometric methods.

1. Introduction

Nitrate and nitrite are common and natural constituents of many foodstuffs. Their occurrence can also be the result of a deliberate addition during food processing. In the latter case they are considered as food additives. The presence of nitrate in foods is of concern because it can be reduced to nitrite, which is able to induce methaemoglobinaemia. Nitrates can also react with secondary and tertiary amines resulting in the formation of carcinogenic nitrosamines. The acceptable daily intake (ADI) recommended by the World Health Organization is 220 mg nitrate for an adult person of about 60 kg. For nitrite the recommended ADI is 8 mg [1].

The determination of nitrate and nitrite has already been performed by several techniques. Spectrophotometric [2–7], ion-selective electrode [8] and chromatographic [9–12] techniques have been reported. Recently, one can add capillary zone electrophoresis (CZE) to this list. The determination of nitrate and nitrite together with other anions by CZE was first reported by Jones and Jandik [13]. Their method is based on indirect detection of the anions. For this purpose one uses a background electrolyte, which in this

* Corresponding author.

0021-9673/95/$09.50
SSDI 0021-9673(94)01290-3

case is chromate [13–15]. At present CE is used for the determination of a wide variety of ions [13–21]. More recently, a direct UV detection method was described for the determination of nitrate and nitrite in water and urine samples [19].

The method for determining anions by CE has been further optimized by us [20,21]. Instead of using reagents with an unknown composition supplied by Waters (Milford, MA, USA), necessary for the determination of anions, we preferred to work with known substances. Therefore, in the optimization procedure cetyltrimethylammonium bromide (CTAB) was used instead of Anion-BT. The mobility of the anions as a function of the pH and the concentration of CTAB was described with a physical model [20,21]. By applying this model, a selectivity optimization was carried out [21], resulting in a good separation of ten inorganic anions.

The performance of the optimized method with complex sample matrices was studied in this work for the determination of nitrates and nitrites in vegetables. The aim was to compare the results of the CE method with that of a reference method. The AOAC describes several reference methods for the determination of different compounds in various matrices. For ions these are usually photometric methods. A specific reference method for the determination of nitrate and nitrite in vegetables has not been proposed by the AOAC. It does, however, provide a method for the determination of these anions in cheese [4]. Several workers have also applied this method or a slightly modified one to determinations in vegetables [2,3,5,6]. Nitrate is reduced to nitrite over a cadmium column (Jones reduction) and nitrite is then determined after diazotization of an aromatic amine followed by reaction of the diazonium compound with a coupling reagent. The colour intensity of the azo dye formed is proportional to the nitrate concentration [2–4,6].

Different extraction procedures have been described for nitrates and nitrites in the literature. Depending on the matrix, these procedures range from simple extraction with water followed by deproteinization for biological (food) samples [2–5,8,12], to ultracentrifugation or ultrafiltration for clinical samples [9,11]. The sample extraction procedure in the AOAC method [4] employs $ZnSO_4$, which would result in a large interfering peak for sulphate in the electropherogram. This makes the determination of anions with mobilities similar to sulphate impossible. An alternative extraction procedure was found in the literature [2,3] which was more compatible with the CE method. The method described by Lox and Okabe [2,3] closely resembles the AOAC procedure, but does not employ $ZnSO_4$ during the sample preparation. The sample preparation procedure consists in extraction of nitrates and nitrites with water at moderate temperature, followed by deproteinization with Carrez solutions. The deproteinization step is not necessary in the sample extraction procedure in the CE determinations, because proteins usually migrate much more slowly than small ions, and can therefore be flushed out of the capillary between the runs. The proteins might lead to fouling of the uncoated silica capillary, but with proper rinsing procedures one can avoid this problem.

2. Experimental

2.1. Reagents

All solutions were prepared using water purified with a Milli-Q system (Millipore, Bedford, MA, USA). Sodium chromate, sodium fluoride, sodium bromide, sodium chloride, sodium sulphate, sodium nitrite, sodium nitrate, sodium iodide, sodium thiosulphate, sodium molybdate, sodium tungstate, sodium monohydrogenphosphate, potassium hexacyanoferrate(II), sodium hydrogencarbonate, zinc acetate, sulphanilic acid, hydrochloric acid, (di)-sodium EDTA, ammonia, acetic acid, sodium oxalate, sodium citrate, sodium acetate, sodium propionate, sodium butyrate, sodium hydroxide, potassium hydroxide, cetyltrimethylammonium bromide and acetonitrile were purchased from Merck (Darmstadt, Germany) and sodium formate and 1-naphthylamine from UCB (Belgium).

2.2. Samples

Fifteen fresh vegetables were obtained at a local supermarket (winter season), namely spinach, lettuce, corn salad, celery, leek, watercress, endive, parsley, cauliflower, cucumber, white cabbage, red cabbage, broccoli, onion and tomato.

2.3. Preparation of solutions

Spectrophotometric method

Carrez I solution consisted of 53.00 g of potassium hexacyanoferrate(II) $[K_4Fe_2(CN)_6 \cdot 2H_2O]$ in 0.51 of water and Carrez II of 109.99 g of zinc acetate $[Zn(OAc)_2 \cdot 2H_2O]$ diluted to 0.51 with water. Griess solution A consisted of 1.4997 g of sulphanilic acid + 5 g of sodium chloride and 50 ml of acetic acid diluted to 250 ml with water, and Griess solution B of 0.0593 g of 1-naphthylamine + 50 ml of acetic acid diluted to 250 ml with water. Griess mixture was prepared daily by mixing equal amounts of Griess solutions A and B, and was kept in darkness.

Ammonium buffer consisted of 40 ml of hydrochloric acid + 100 ml of ammonia diluted to 1000 ml with water. This solution should have a pH between 9.6 and 9.7.

Sodium EDTA solution consisted of 20.8 g of Na_2EDTA + 30 ml of 15% NaOH diluted to 500 ml with water.

CE method

Sodium chromate was prepared as a 0.1 *M* stock standard solution. All buffers were prepared in 50-ml aliquots and filtered through a 0.45-mm Millex-HV syringe filter (Millipore, Molsheim, France). The buffers were adjusted to the final pH using 0.01 *M* sodium hydroxide.

The modifier was prepared as a 50 m*M* CTAB solution. The solubility was enhanced by the addition of 5% (v/v) of acetonitrile and stirring on a magnetic stirrer at moderate temperature. After dissolution, it was filtered through the same kind of syringe filter.

The buffer electrolyte was prepared as follows: 5 ml of 0.1 *M* sodium chromate solution and 2.3 ml of 50 m*M* CTAB solution were mixed, the pH was adjusted to 11.50 and the solution was diluted to 50.0 ml. Prior to analysis this solution was filtered through a Millex-HV filter.

Stock standard solutions of 1000 μg/ml of each anion were prepared in Milli-Q-purified water and stored in a refrigerator. Working standard solutions of each anion were prepared daily by dilution. The buffers were adjusted to the required pH using an Orion Model 520 A pH meter.

2.4. Apparatus

The equipment used included a Bamix mixer, a warm water-bath, S&S No. 598$\frac{1}{2}$ filters, Millex-HV 0.45-μm syringe filters (nitrate free) and a Shimadzu UV-2101PC UV–Vis Scanning spectrophotometer.

A Waters Quanta-4000 CE system equipped with a negative power supply was used. The capillaries were ordinary fused-silica capillaries (Waters AccuSep, 60-cm capillaries) of 75 μm I.D. and length 52 cm from the point of sample introduction to the point of detection. The electrophoretic zones were detected with a fixed-wavelength UV detector at 254 nm (mercury lamp). Depending on the concentration level in the samples, the hydrostatic injection mode (10 s) or the electromigration injection mode (10 s, −10 kV) was used for the injection of the samples. The electropherograms were recorded and integrated with a Waters Model 810 data workstation equipped with a W51-watchdog interface.

2.5. Preparation of the capillary

Each time before changing a buffer, the capillary was purged with 0.5 *M* potassium hydroxide solution (KOH) for 5 min, followed by Milli-Q-purified water for 5 min and the buffer electrolyte for 5 min. Between each run, the capillary was flushed with 0.1 *M* KOH for 1 min, followed by flushing with Milli-Q-purified water for 2 min and the running buffer for 2 min. Before shut-down, the capillary was flushed with 0.5 *M* KOH for 5-min and Milli-Q-purified water

for 5 min. The inlet and outlet of the capillary were kept in Milli-Q-purified water.

2.6. Preparation of the modified Jones reductor column

The cadmium column was prepared as described by Sen and Donaldson [5], with the minor difference that instead of generating the cadmium particles starting from cadmium sulphate, we used cadmium particles obtained from Merck. The efficiency of the column was also tested as described by Sen and Donaldson [5].

2.7. Sample preparation

The preparation of the samples consisted of weighing at least 10.0 to up to 50.0 g of fresh vegetable material (cut into small pieces) in a 250-ml beaker, adding 50 ml of Milli-Q-purified water, incubating for 30 min on a warm water-bath at about 50°C and homogenizing with the mixer for 1 min. After cooling, the slurry was transferred quantitatively into a 250-ml volumetric flask. For the spectrophotometric sample extract, 10 ml each of Carrez I and II solutions were added and diluted to volume with Milli-Q-purified water. For the CE sample extract, the addition of Carrez solutions is not needed. Finally, the samples were divided into small parts that were kept in a deep-freezer. Before injection into the CE system, the samples were first filtered through a Millex-HV 0.45-μm syringe filter.

No contamination from glass- and plasticware was observed. The use of Millex-HV filters is preferred as they are free from nitrate. Water (Milli-Q) blank samples, apart from a carbonate peak, did not give any indication of contamination.

2.8. Nitrate and nitrite determination

Spectrophotometry

Nitrate and nitrite were determined according to the method described by the AOAC [4] by direct interpolation of the absorbance of an unknown sample on a calibration line. A volume of each sample filtrate was pipetted into a 25-ml flask and after the addition of 5 ml of Na_2EDTA solution and 5 ml of ammonium buffer it was diluted to volume with water. These solutions were passed through the cadmium column. The eluate and rinsing solutions (ca. 40 ml of a solution prepared by mixing equal amounts of ammonium buffer and Na_2EDTA solutions) were collected in 50-ml volumetric flasks and diluted to volume with water. The calibration graph was prepared by sampling and treating different volumes of a 50 μg/ml standard nitrate solution similarly. Aliquots of 10 ml from each 50-ml flask were mixed with 10 ml of Griess mixture and kept in darkness for 20 min, then the intensity of the developed colour was measured at 526 nm. The procedure for nitrite determination was similar to that for nitrate, except that the samples were not passed through the cadmium column. The concentration of nitrate in the sample extract was obtained by subtracting the amount of nitrite from the original result of the nitrate determination.

Capillary electrophoresis

In CE of high-concentration-level samples, the extracts are injected for 10 s hydrostatically and run at 20 kV (negative potential). No further sample preparation, except sometimes dilution, is required. This procedure was applied to the determination of nitrate in vegetables, as it occurs in large amounts.

For the analysis of low concentration level samples, the injection was carried out by electromigration for 10 s at −10 kV. To reduce the baseline noise, the runs were also carried out at a lower voltage, namely −15 kV. This procedure was applied mainly to the determination of nitrite in the samples.

3. Results and discussion

With the CE method it is possible to separate several anions simultaneously within a short analysis time. In Fig. 1, an example of an electropherogram for a standard mixture of eighteen anions obtained with the low concen-

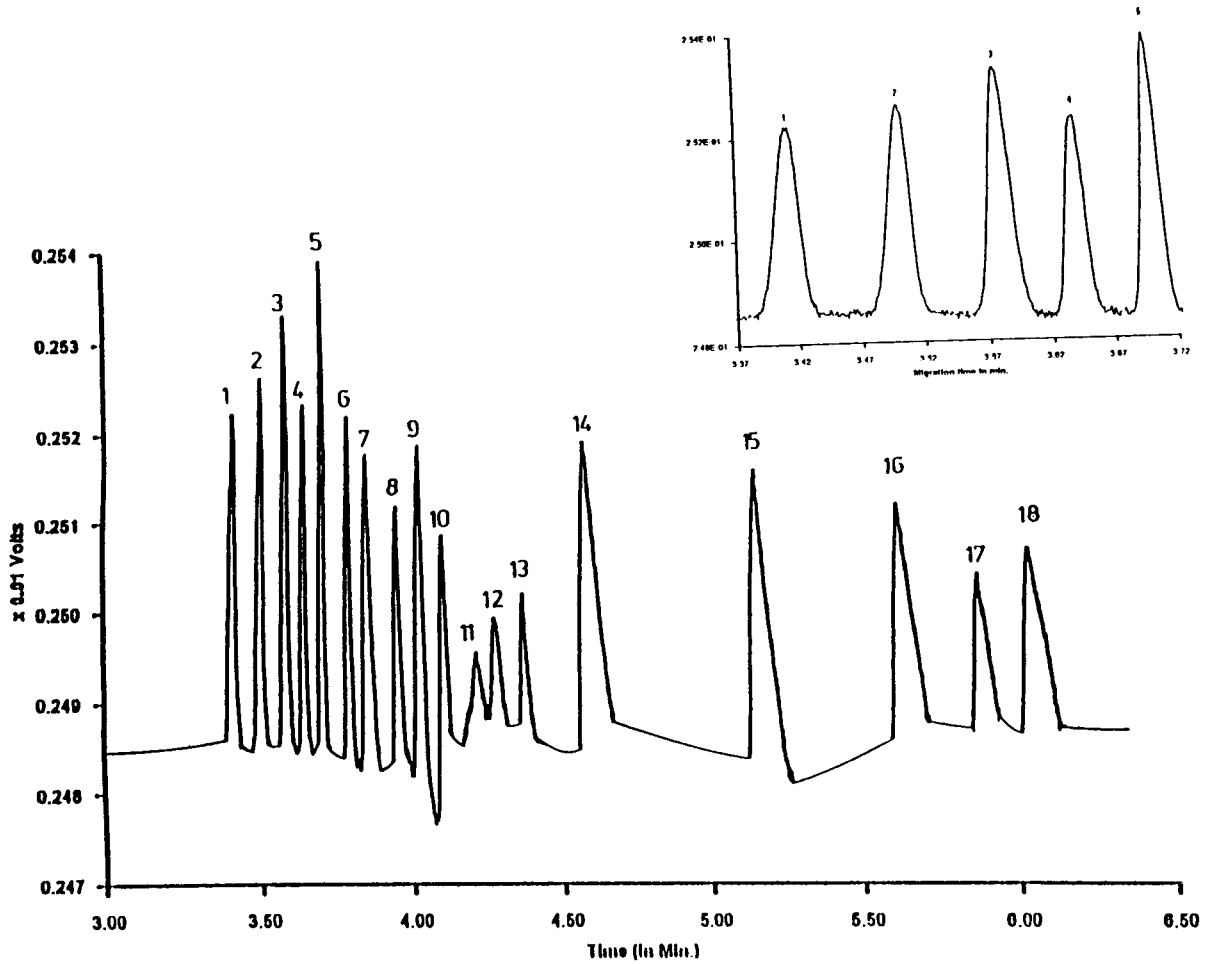

Fig. 1. Electropherogram of a standard mixture. Conditions: $[CrO_4^{2-}] = 10$ mM; pH = 11.50; [CTAB] = 2.30 mM. A mixture of the anions was injected for 10 s at −10 kV by electromigrative injection; the running voltage was −15 kV (with a current of ±30 μA). Peaks: 1 = Cl^-; 2 = Br^-; 3 = NO_2^-; 4 = SO_4^{2-}, 5 = $S_2O_3^{2-}$; 6 = oxalate; 7 = NO_3^-; 8 = MoO_4^{2-}; 9 = HCO_3^{2-}; 10 = WO_4^{2-}; 11 = F^-; 12 = formate; 13 = HPO_4^{2-}; 14 = citrate; 15 = acetate; 16 = propionate; 17 = BO_3^{2-}; 18 = butyrate. The concentration levels are given in the text.

tration level CE method is presented. As can be observed, all the anions, chloride (Cl^- 0.10 μg/ml), bromide (Br^- 0.50 μg/ml), nitrite (NO_2^- 0.10 μg/ml), sulphate (SO_4^{2-} 0.10 μg/ml), thiosulphate ($S_2O_3^{2-}$ 0.10 μg/ml), oxalate (0.10 μg/ml), nitrate (NO_3^- 0.10 μg/ml), molybdate (MoO_4^{2-} 0.10 μg/ml), hydrogencarbonate (HCO_3^- 0.10 μg/ml), tungstate (WO_4^{2-} 0.10 μg/ml), fluoride (F^- 0.05 μg/ml), formate (0.10 μg/ml), hydrogenphosphate (HPO_4^{2-} 0.10 μg/ml), citrate (1.0 μg/ml), acetate (1.0 μg/ml), propionate (1.0 μg/ml), borate (BO_3^{2-} 1.0 μg/ml) and butyrate (1.0 μg/ml), are separated completely in a separation window of about 3 min and with a run time of only 6.5 min. Most of the organic anions and borate are slow-moving anions compared with chromate. For this reason, they show significant peak tailing. Therefore, the concentration of these anions in Fig. 1 is ten times higher. For the high concentration level CE method these times are shorter as the runs are performed at higher voltage. This is the major advantage of the CE method over the spectrophotometric method. As can be observed

in the enlarged part of Fig. 1, the separation of the peak pairs chloride–nitrite and nitrite–sulphate shows high resolution. This is one of the advantages of the optimized method proposed by us [20,21] compared with the method of Jones and Jandik [13,15]. For this reason, the injection (e.g., by electromigration) of large amounts of chloride and sulphate ions does not interfere in the determination of nitrite.

As nitrate occurs in large amounts in most of the samples, the high concentration level CE method was applied to determine this anion in vegetables. The injection for this method was performed hydrostatically and resulted in an acceptable precision. Therefore, there was no need for an internal standard. In the low concentration level CE method the injection was performed by means of electromigration. As was expected, this injection procedure resulted in a poor precision. An internal standard was required to obtain low R.S.D. values. As can be observed in Fig. 1, thiosulphate, tungstate, molybdate and borate can be employed as possible internal standards. However, sodium thiosulphate was selected as it does not occur in the vegetable samples and it migrates just after sulphate and before oxalate (between the nitrite and the nitrate peak). If necessary one can always use one of the other possible internal standards. The low concentration level method was applied mainly for the determination of nitrite in the samples. Nitrites can occur in very low concentration levels in the samples. Owing to its toxicity, it is necessary to detect nitrite below the 0.1 μg/ml level [1].

Examples of the electropherograms obtained for real samples are shown in Fig. 2a, b, c and d for samples of spinach, spinach diluted 50-fold, endive and tomato, respectively. Some of the samples, e.g., spinach had to be diluted in order to obtain a signal in the linear range and to observe the separation between the oxalate and the nitrate peaks. As was stated before, several anions can be determined simultaneously with the CE method. However, this study was focused mainly on the determination of nitrate and nitrite in the vegetables. Since the method was not fully validated for the determination of the other anions, the concentrations obtained for these anions are shown only for indicative purposes (Table 1). As can be observed in the electropherograms in Fig. 2, several peaks are not identified. In general, peak identification in CE remains a difficult task until better detection systems become available for this purpose, e.g., CE–mass spectrometry. The unknown peaks are probably organic in nature. However, we were not able to identify them. In Fig. 2b, the height of the carbonate peak is not consistent with what is expected from the undiluted sample (Fig. 2a). Carbonate is known to show a strange quantitative behaviour in CE. Especially at low concentrations the reproducibility of the peak height is very poor. The determination of carbonate requires specific precautions in order to avoid contamination from the environment (CO_2) [15]. This anion is therefore usually not determined. The results for the determination of nitrate by the reference spectrophotometric (AOAC) and the high concentration level CE methods are shown in Table 2. Nitrite was not detected in the samples investigated in this study by either the spectrophotometric method or the low-concentration-level CE method. This means that the probable occurrence of nitrite in the vegetables lies below the limit of detection of these methods.

3.1. Linearity

High-concentration-level CE method

The linearity of the high-concentration-level method was judged from the residual plots. These plots indicated that the residual patterns were almost homogeneous, i.e., that there was no need for weighted regression. The quality coefficients [22] obtained for the regression lines were within the acceptable range. The linearity of the methods was also determined by an analysis of variance (ANOVA) test for lack of fit. At each concentration level (at least five), four runs were carried out for this purpose. In spectrophotometry no significant lack of fit was detected for either nitrite ($p > 0.1$) or nitrate ($p > 0.9$). In CE a significant lack of fit was detected for nitrite ($p < 0.025$), but not for nitrate ($p > 0.9$). In the regression procedure for nitrite in the CE and AOAC methods, a signifi-

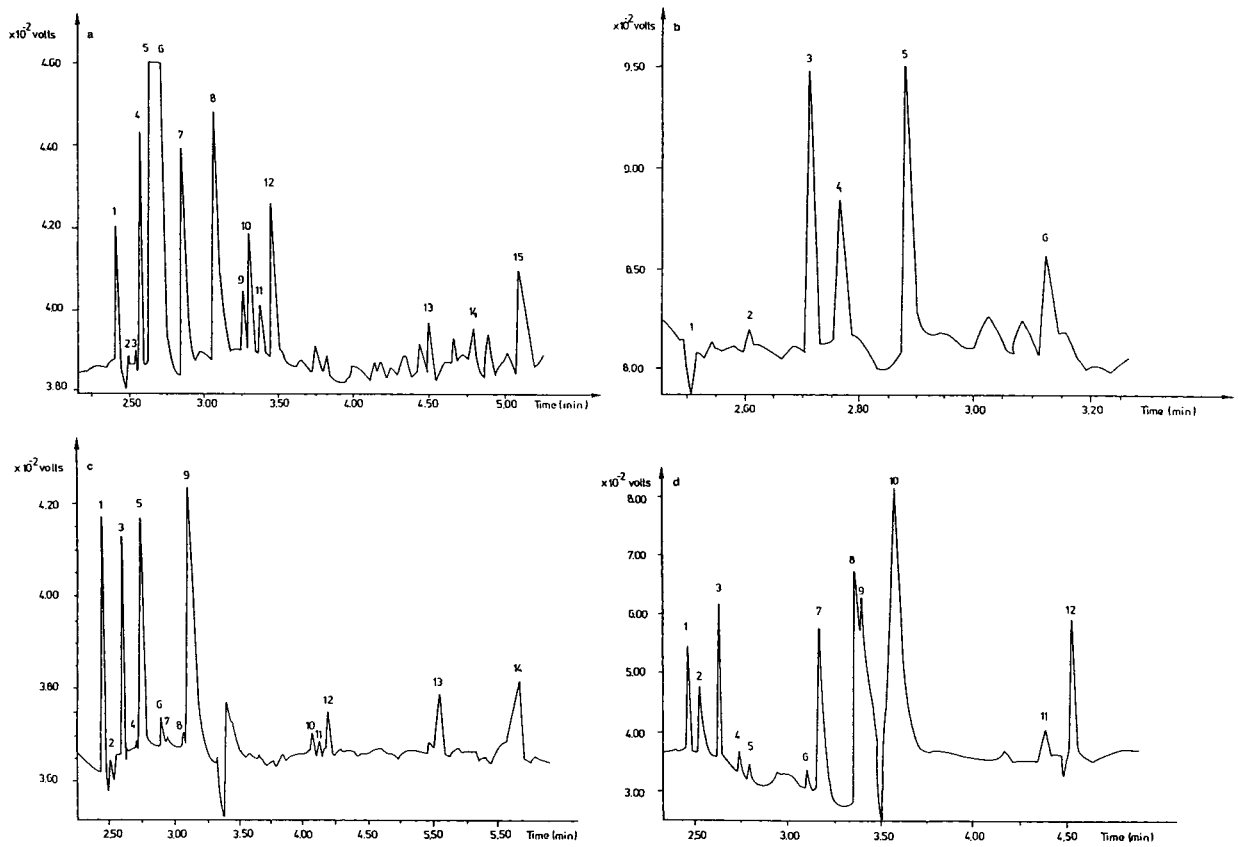

Fig. 2. Electropherograms of different samples. Conditions: $[CrO_4^{2-}] = 10$ mM; pH = 11.50; [CTAB] = 2.30 mM. The samples were injected hydrostatically for 10 s and the runs were performed at −20 kV (with a current of ±48 μA). (a) Spinach. Peaks: 1 = Cl^-; 2 = Br^-; 3 = unknown; 4 = SO_4^{2-}; 5 = oxalate; 6 = NO_3^-; 7 = CO_3^{2-}; 8 = HPO_4^{2-}; 9–11 = unknown; 12 = citrate; 13–15 = unknown. (b) Spinach diluted 50-fold. Peaks: 1 = Cl^-; 2 = SO_4^{2-}; 3 = oxalate; 4 = NO_3^-; 5 = CO_3^{2-}; 6 = HPO_4^{2-}. (c) Endive. Peaks: 1 = Cl^-; 2 = Br^-; 3 = SO_4^{2-}; 4 = oxalate; 5 = NO_3^-; 6 = CO_3^{2-}; 7 = unknown; 8 = formate; 9 = HPO_4^{2-}; 10 and 11 = unknown; 12 = propionate; 13 and 14 = unknown. (d) Tomato. Peaks: 1 = Cl^-; 2 = Br^-; 3 = SO_4^{2-}; 4 = oxalate; 5 = NO_3^-; 6 = formate; 7 = HPO_4^{2-}; 8, 9 = unknown; 10 = citrate; 11, 12 = unknown.

cant quadratic term in the linear model was detected. In the residual plots the lack of fit of the linear model for nitrite in the CE method was also observed. After reducing the range (up to 8 μg/ml), the lack of fit was found not to be significant. However, as nitrite occurs at very low levels in the samples, usually lower than the detection limit of the high concentration level CE method, one should apply the low concentration level CE method.

For nitrate both the high concentration level CE method and the spectrophotometric method gave fair linearity, only the ranges were different: The spectrophotometric method was found to be linear up to 2.5 μg/ml of nitrate, whereas the CE method was linear up to 10 μg/ml. Some statistics for the calibration lines are given in Table 3.

Low-concentration-level CE method

The low concentration level method was linear from 0.1 μg/ml up to 2.5 and 1.6 μg/ml for nitrite and nitrate, respectively. However, from the residual plots it was observed that the data were heteroscedastic. Therefore, weighted regression (weights: $1/s^2$) had to be applied which resulted in homogeneous residual patterns. These weighted calibration lines were used for quantitative purposes. Some statistics of these lines are also shown in Table 3.

Table 1
Results for the determination of anions in vegetables by CE

Sample	Concentration (mg/g)						
	Cl^-	Br^-	SO_4^{2-}	HPO_4^{2-}	Formate	Citrate	Oxalate
Spinach	0.239	0.001	0.457	1.815		1.088	9.015
Lettuce	0.446	0.001	0.242	6.75			0.047
Corn salad	2.241	0.031	0.363	3.583			
Celery	1.797	0.080	1.274	3.249			
Leek	0.431	0.110	0.103	3.185	0.099		
Watercress	0.364	0.097	0.942	3.408			
Endive	0.414	0.041	0.436	2.298			
Parsley	1.966	0.396	0.656	14.018	0.271		
Cauliflower	0.139	0.020	0.240	1.058			
Cucumber	0.230	0.130	0.246	2.329			0.009
White cabbage	0.187	0.001	1.025	1.454		1.777	
Red cabbage	0.142	0.089	0.688	0.642			0.002
Broccoli	0.108	0.105	0.827	1.109			0.009
Onion	0.217	0.638	0.157	1.284	0.179	6.865	
Tomato	0.238	0.761	0.379	0.637		25.083	0.054

3.2. Limits of detection (LOD) and quantification (LOQ)

The LOD was estimated as the concentration of nitrate or nitrite that would result in a signal three times higher than the background noise (blank). For the high-concentration-level CE method this resulted in a detection limit of 0.32 μg/ml for nitrate and 0.31 μg/ml for nitrite. The low-concentration-level CE method had an LOD

Table 2
Results for the determination of nitrate in vegetables

Sample	Points in Fig. 3	Concentration (mg/g)					
		Reference method			CE method		
		Run 1	Run 2	Mean	Run 1	Run 2	Mean
Spinach	1 and 12	3.34	3.33	3.335	3.395	3.405	3.4
Lettuce	2 and 13	2.33	2.46	2.395	2.422	2.563	2.493
Corn salad	3 and 14	3.04	2.93	2.985	2.905	2.887	2.896
Celery	4 and 15	3.818	4.029	3.924	3.431	3.717	3.574
Leek	5 and 16	0.14	0.11	0.125	0.113	0.112	0.113
Watercress	6 and 17	3.64	3.73	3.685	3.962	3.758	3.86
Endive	7 and 18	1.54	1.56	1.55	1.328	1.313	1.321
Parsley	8 and 19	0.299	0.252	0.276	0.293	0.274	0.284
Cauliflower[a]		0.009	0.009	0.009	0.009	0.011	0.010
Cucumber[a]		0.028	0.02	0.024	0.026	0.021	0.0235
White cabbage	9 and 20	0.046	0.039	0.043	0.043	0.046	0.045
Red cabbage	10 and 21	0.026	0.03	0.028	0.025	0.028	0.0265
Broccoli	11 and 22	0.171	0.175	0.173	0.243	0.261	0.252
Onion[a]		0.009	0.012	0.010	0.015	0.012	0.014
Tomato[a]		0.058	0.058	0.058	0.055	0.054	0.055

[a] Concentration of nitrate in the sample is below the limit of quantification.

Table 3
Regression statistics for the calibration and the standard addition lines

Parameter[a]	Nitrate		Nitrite	
	External	Addition	External	Addition
Spectrophotometric method				
Slope	0.331	0.332	0.505	0.540
CI slope	0.300–0.362	0.274–0.390	0.479–0.530	0.481–0.599
Intercept	−0.0045	0.2610	−0.0018	−0.0088
CI intercept	−0.055 to 0.046	0.166 to 0.356	−0.031 to 0.027	−0.076 to 0.059
Standard error	0.0286	0.0490	0.0131	0.0303
r	0.99662	0.99217	0.99962	0.99823
High-concentration-level CE method				
Slope	139.84	145.43	197.50	201.23
CI slope	128.19–151.49	136.24–154.61	192.03–202.96	173.61–228.85
Intercept	39.87	414.17	14.78	72.76
CI intercept	−31.67 to 111.42	361.67 to 466.67	−77.61 to 107.16	−305.90 to 451.42
Standard error	55.25	53.73	104.43	178.69
r	0.99221	0.99449	0.99884	0.99069
Low-concentration-level CE method				
Slope	2.181	2.271	2.459	2.499
CI slope	2.122–2.240	2.257–2.284	2.427–2.495	2.446–2.553
Intercept	−0.05312	0.54540	−0.3176	0.1890
CI intercept	−0.074 to −0.033	0.531 to 0.560	−0.049 to −0.014	0.169 to 0.209
Standard error	1.358	0.966	0.076	0.899
r	0.99926	0.99997	0.99929	0.99943

[a] CI = confidence interval; r = correlation coefficient.

of 0.037 and 0.034 μg/ml for nitrate and nitrite, respectively. For the reference method a detection limit of 0.040 and 0.020 μg/ml was obtained for nitrate and nitrite, respectively.

The LOQ is considered as the concentration at which the signal obtained is sufficiently precise and accurate for quantitative purposes. For the high-concentration-level CE method an LOQ of 1.05 μg/ml [R.S.D. ($n = 4$) = 3.83%] and 1.04 μg/ml [R.S.D. ($n = 4$) = 8.52%] was obtained for nitrate and nitrite, respectively. For the low-concentration-level CE method the LOQ was around 0.1 μg/ml for both nitrite [R.S.D. ($n = 6$) = 4.21%] and nitrate [R.S.D. ($n = 6$) = 7.37%]. An electropherogram obtained at this level for nitrite and nitrate is shown in Fig. 1. The accuracy data are discussed later. The spectrophotometric method had an LOQ of 0.10 μg/ml for both nitrate [R.S.D. ($n = 4$) = 12.15%] and nitrite [R.S.D. ($n = 4$) = 2.94%], respectively.

The low-concentration-level CE method is more sensitive than the high-concentration-level method because injection is performed by electromigration, which results in a sample stacking effect. This leads to a better detection limit and peak shape [23,24]. Additionally, the runs were performed at lower voltage, which decreased the generation of noise due to temperature effects. As mentioned earlier, the injection of samples containing large amounts of chloride and sulphate by this method did not adversely affect the separation.

3.3. Repeatability and time-different intermediate precision measure

High-concentration-level CE method

The repeatability (within-day precision) of the high-concentration-level CE method and the spectrophotometric method was determined by analysing a sample of spinach, endive and pars-

ley six times. These three vegetables represent high, medium and low concentration levels of nitrate, respectively. The residual standard deviations values of the methods are given in Table 4. As can be seen, both methods show adequate repeatability considering the concentration of nitrate in the samples. No significant difference could be detected, at a significance level of 5%, between the variances of the two methods (two-sided *F*-tests). This was the case for all the concentration levels. The results for the repeatability obtained for the CE method are

Table 4
Results for the precision of the high-concentration-level CE and the spectrophotometric method

Run	Repeatability					
	Spinach		Endive		Parsley	
	Ref.[a]	CE	Ref.[a]	CE	Ref.[a]	CE
1	2.986	3.500	1.770	1.448	0.214	0.276
2	3.265	3.350	1.659	1.388	0.224	0.291
3	3.014	3.475	1.734	1.440	0.230	0.298
4	3.207	3.575	1.727	1.490	0.232	0.286
5	3.340	3.375	1.735	1.558	0.220	0.272
6	3.168	3.550	1.632	1.570	0.216	0.268
Mean	3.163	3.471	1.709	1.482	0.223	0.282
S.D.	0.139	0.091	0.052	0.071	0.007	0.012
R.S.D. (%)	4.409	2.633	3.067	4.808	3.224	4.114
F-value	2.329		1.849		2.609	
F-crit. 5%[b]	7.15		7.15		7.15	
Day	Time-different intermediate precision measure[c]					
	Spinach		Endive		Parsley	
	Ref.[a]	CE	Ref.[a]	CE	Ref.[a]	CE
1	3.387	3.500	1.770	1.448	0.252	0.276
	3.231	3.350	1.659	1.388	0.299	0.291
2	3.173	3.395	1.539	1.328	0.214	0.293
	3.345	3.405	1.564	1.388	0.224	0.274
3	3.625	3.200	1.528	1.493	0.274	0.324
	3.078	3.125	1.479	1.305	0.243	0.278
4	3.331	3.525	1.628	1.520	0.320	0.295
	3.343	3.625	1.802	1.538	0.337	0.270
5	2.986	3.325	1.665	1.293	0.311	0.327
	3.265	3.300	1.463	1.353	0.316	0.302
Mean	3.276	3.375	1.626	1.405	0.275	0.293
S.D.	0.177	0.150	0.110	0.090	0.044	0.020
R.S.D. (%)	5.403	4.459	6.778	6.378	16.044	6.889
F-value	1.384		1.512		4.779	
F-crit. 5%[b]	4.03		4.03		4.03	

Concentrations in mg/g.
[a] Reference spectrophotometric method.
[b] Two-sided.
[c] For duplicate determinations.

comparable to those for the reference method, and are more or less in agreement with the results that had been obtained in previous studies [25].

The time-different intermediate precision (the term recommended by ISO for the between-day precision [26]) was assessed by analysing the samples of spinach, endive and parsley in duplicate during five days by both methods. The results are also shown in Table 4. As can be observed, the R.S.D. values of the CE method are generally lower, indicating a better time-different intermediate precision. When the variances were compared with F-tests, a significant difference was detected between the variances of the methods at low concentration level (parsley sample). A careful observation of the data in Table 4 reveals that the AOAC method results in higher nitrate levels for parsley starting from day 4. Therefore, the significant difference of the variances for the determination of nitrate in parsley is probably due to a measurement error.

Low-concentration-level CE method

The repeatability of the low-concentration-level CE method was investigated by determining three concentration levels of nitrate and nitrite six times. In Table 5 the results obtained with the weighted calibration procedure are given. As can be seen, this resulted in acceptable R.S.D. values. Considering the time-different intermediate precision, the weighted calibration procedure also resulted in an acceptable precision at the three concentration levels for both nitrite and nitrate. The results are given in Table 5. The R.S.D. values at the three concentration levels were also acceptable for quantitative purposes.

3.4. Accuracy

By comparing the slopes of an external and a standard addition calibration line, one can detect a possible influence of matrices. The slopes of both lines were compared by a t-test. There was no significant difference detected at the α-level of 5% between the slopes for either the reference method (nitrate, $0.05 < p < 0.10$; nitrite, $0.5 < p < 0.9$) or the CE method (nitrate, $0.05 < p < 0.10$; nitrite, $0.3 < p < 0.5$). This indicates that there were no relative systematic errors that influence the accuracy of the determination. In the comparison of the slopes of the weighted calibration lines from the low concentration level CE method by means of a t-test (α-level of 5%), no significant difference was detected (nitrite, $0.05 < p < 0.10$, nitrate, $0.5 < p < 0.9$). Some statistics for the calibration lines are given in Table 3. As no nitrite was detected by either the CE or the spectrophotometric method in any of the samples in this study, three concentration levels of nitrite were added to a (blank) sample. These samples were analysed six times and the results (weighted procedure) are presented in Table 6. As can be observed, the recovery of the spiked samples was within the range $100 \pm 10\%$. Therefore, one can conclude that the low-concentration-level CE method had an acceptable accuracy.

To investigate the accuracy further, the results obtained by the high-concentration-level CE method were compared with those of the reference method. When doing so it is sometimes not sufficient to look only at the numerical results, and a visual evaluation is recommended [27–29]. In addition to regression procedures, other visualization procedures have also been described [27,28] for method comparison. The percentage differences between the results of two methods are plotted against the mean of the two obtained values (Bland and Altman plot [29]). This was applied to evaluate the agreement between the results obtained for nitrate by the two techniques (Table 2). Good agreement was observed between the results of the two methods (orthogonal regression). The absence of a systematic proportional error was tested by a t-test ($\alpha = 5\%$), which confirmed that the slope of the orthogonal regression line was not significantly different from 1. Fig. 3 shows the Bland and Altman plot. The mean of the percentage differences in the experimental results between the two methods is slightly above the expected mean zero. However, this difference was not found to be signifi-

Table 5
Results for the precision of the low-concentration-level CE method with weighted regression

Repeatability at three concentration levels

Run	Nitrite			Nitrate		
	0.1 μg/ml	0.5 μg/ml	1.6 μg/ml	0.1 μg/ml	0.5 μg/ml	1.6 μg/ml
1	0.1045	0.4807	1.5606	0.0934	0.4541	1.6041
2	0.1181	0.4757	1.5805	0.0997	0.4976	1.5928
3	0.1125	0.4821	1.6010	0.1009	0.5046	1.5844
4	0.1128	0.4731	1.6318	0.1179	0.4750	1.6208
5	0.0993	0.4887	1.6670	0.1016	0.4932	1.6245
6	0.1070	0.5006	1.6262	0.1008	0.4868	1.6946
Mean	0.1090	0.4835	1.6112	0.1024	0.4852	1.6202
S.D.	0.0068	0.0100	0.0384	0.0082	0.0183	0.0396
R.S.D. (%)	6.20	2.07	2.38	7.98	3.76	2.45

Time-different intermediate precision

Day	Nitrite			Nitrate		
	0.1 μg/ml	0.5 μg/ml	1.6 μg/ml	0.1 μg/ml	0.5 μg/ml	1.6 μg/ml
1	0.1045	0.4807	1.5606	0.0934	0.4541	1.6041
	0.1181	0.4757	1.5805	0.0997	0.4976	1.5928
2	0.0755	0.4662	1.5568	0.1039	0.4597	1.5773
	0.0867	0.5018	1.5430	0.1109	0.4781	1.4916
3	0.0785	0.4679	1.5549	0.1038	0.4598	1.3620
	0.0897	0.5033	1.5411	0.1108	0.4782	1.4921
4	0.1183	0.4917	1.8212	0.1001	0.5137	1.7092
	0.0988	0.5301	1.5867	0.0999	0.4613	1.4793
5	0.1003	0.4933	1.5547	0.0713	0.5015	1.6657
	0.0998	0.4788	1.6435	0.1147	0.4934	1.5544
6	0.1026	0.5109	1.6664	0.1272	0.4909	1.7132
	0.1041	0.5452	1.7379	0.1127	0.5238	1.6357
Mean	0.0981	0.4955	1.6123	0.1040	0.4843	1.5731
S.D.	0.0135	0.0244	0.0891	0.0137	0.0229	0.1040
R.S.D. (%)	13.76	4.92	5.52	13.13	4.72	6.61

cant ($\alpha = 5\%$) by a t-test. The spread of the data points in Fig. 3 does not show a specific trend in the data, indicating also the absence of a systematic proportional error. Compared with the other samples, points 11 and 22, corresponding with the vegetable broccoli (Table 2), shows deviant behaviour when the evaluation is performed by the percentage difference. Nevertheless, globally one can conclude that the results for the determination of nitrate by the two methods are comparable.

4. Conclusions

The proposed CE methods are linear in the described ranges and have an acceptable precision and accuracy for the determination of ni-

Table 6
Results for the recovery of nitrite added to a blank vegetable sample

0.1 μg/ml added		0.5 μg/ml added		1.0 μg/ml added	
Found (μg/ml)	Recovery (%)	Found (μg/ml)	Recovery (%)	Found (μg/ml)	Recovery (%)
0.0867	86.70	0.4854	97.07	0.9512	95.12
0.0934	93.39	0.4879	97.57	1.0759	107.59
0.0946	94.56	0.5066	101.32	0.9601	96.01
0.0967	96.73	0.4863	97.25	1.0091	100.91
0.0926	92.64	0.4898	97.96	1.0417	104.17
0.0970	96.98	0.4879	97.59	0.9152	91.52
Mean	93.5016		98.1282		99.2210
S.D.	3.7587		1.5953		6.0642
R.S.D. (%)	4.02		1.63		6.11

trates and nitrites in vegetables. The LOD of the high-concentration-level CE method is too high for the determination of nitrite, but for the determination of nitrate in the vegetables this is not a problem. The concentration of nitrate in the samples is generally sufficiently high for accurate determinations. For nitrite, however, a lower LOD is achieved with the low-concentration-level CE method. An LOD of less than 50 μg/l is sufficiently low for determining dangerous amounts of nitrite considering the acceptable daily intake of nitrite. Therefore, the proposed CE methods appear to be acceptable for the determination of nitrates and nitrites in vegetables. The major advantage of the CE methods is that they are extremely fast, as a run requires only ca. 5 min, whereas in the spectrophotometric method up to 1 h can be required. This compensates for the disadvantage of having two methods in the CE technique for the determination of nitrate and nitrite. Another advantage is that one can determine several anions simultaneously.

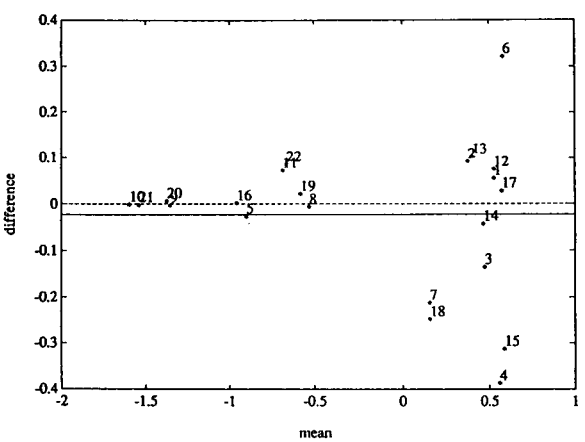

Fig. 3. Visual evaluation by the Bland and Altman plot for comparison of the results of nitrate determination obtained by the high-concentration-level CE method and the reference spectrophotometric method. The dashed and continuous lines represent the expected and the found means of the percentage difference in the experimental results, respectively. In order to observe the spread at low concentrations (around zero), the values of the mean concentration levels have been transformed to a logarithmic scale.

Acknowledgements

The authors thank ABOS, ChemoAC and the FGWO for financial support.

References

[1] D.L. Massart, H. Deelstra, P. Daenens and C. Van Peteghem, *Vreemde Stoffen in Onze Voeding; Soorten–Effecten–Normen (Monografiën Leefmilieu Nu)*, Pelckmans, Kapellen, Belgium, 2nd ed., 1986, pp. 185–196 and 262–264.

[2] F. Lox and A. Okabe, *J. Assoc. Off. Anal. Chem.*, 65 (1982) 157.

[3] F. Lox, *Forum Ware*, 8 (1980) 35.
[4] *Official methods of analysis of the Association of Official Analytical Chemists*, AOAC, Philadelphia, 15th ed., 1990, Section 973.31.
[5] N.P. Sen and B. Donaldson, *J. Assoc. Off. Anal. Chem.*, 61 (1978) 1389.
[6] R. Lees, *Food Analysis: Analytical and Quality Control Methods for the Food Manufacturer and Buyer (Laboratory Handbook of Methods of Food Analysis)*, Leonard Hill Books, London, 3rd ed., 1975, pp. 125–128.
[7] D.F. Boltz, *Colorimetric Determination of Non-Metals (Chemical Analysis, Vol. III)*, Interscience, New York, 1958, pp. 124–135.
[8] H.A. Mills, *J. Assoc. Off. Anal. Chem.*, 63 (1980) 797.
[9] Y. Michigami, Y. Yamamoto and K. Ueda, *Analyst*, 114 (1989) 1201.
[10] Z. Iskandarani and D.J. Pietrzyk, *Anal. Chem.*, 54 (1982) 2601.
[11] B.C. Lippsmeyer, M.L. Tracy and G. Möller, *J. Assoc. Off. Anal. Chem.*, 73 (1990) 457.
[12] J.P. de Kleijn and K. Hoven, *Analyst*, 109 (1984) 527.
[13] W.R. Jones and P. Jandik, *J. Chromatogr.*, 546 (1991) 445.
[14] M. Jimidar, M.S. Khots, T.P. Hamoir and D.L. Massart, *Quim. Anal.*, 12 (1993) 63.
[15] P. Jandik and W.R. Jones, *J. Chromatogr.*, 546 (1991) 431.
[16] M. Jimidar, T. Hamoir, W. Degezelle, D.L. Massart, S. Soykenç and P. Van de Winkel, *Anal. Chim. Acta*, 284 (1993) 217.
[17] Q. Yang, M. Jimidar, T.P. Hamoir, J. Smeyers-Verbeke and D.L. Massart, *J. Chromatogr. A*, 673 (1994) 275.
[18] A. Weston, P.R. Brown, P. Jandik, W.R. Jones and A.L. Heckenberg, *J. Chromatogr.*, 593 (1992) 289.
[19] G.M. Janini, K.C. Chan, G.M. Muschik and H.J. Issaq, *J. Chromatogr. B*, 657 (1994) 419.
[20] M. Jimidar and D.L. Massart, *Anal. Chim. Acta*, 294 (1994) 165.
[21] M. Jimidar, B. Bourguignon and D.L. Massart, *Anal. Chim. Acta.*, in press.
[22] P. Vankeerberghen and J. Smeyers-Verbeke, *Chemometr. Intell. Lab. Syst.*, 15 (1992) 195.
[23] J.L. Beckers and M.T. Ackermans, *J. Chromatogr.*, 629 (1993) 371.
[24] R. Chien and D.S. Burgi, *Anal. Chem.*, 64 (1992) 489A.
[25] M. Jimidar, T.P. Hamoir, A. Foriers and D.L. Massart, *J. Chromatogr.*, 636 (1993) 179.
[26] International Organization for Standardization, *Accuracy (Trueness and Precision) of Measurement Methods and Results*, ISO/DIS 5725-1 and 5725-3, Draft Versions, 1990–1991.
[27] C. Hartmann, J. Smeyers-Verbeke and D.L. Massart, *Analusis*, 21 (1993) 125.
[28] C. Hartmann and D.L. Massart, *J. Assoc. Off. Anal. Chem.*, 77 (1994) 1318.
[29] J.M. Bland and D.G. Altman, *Lancet*, 8 (1986) 307.

ELSEVIER

Journal of Chromatography A, 706 (1995) 493–501

JOURNAL OF CHROMATOGRAPHY A

Separation of some metallochromic ligands by capillary zone electrophoresis and micellar electrokinetic capillary chromatography

Miroslav Macka, Paul R. Haddad*, Wolfgang Buchberger[1]

Department of Chemistry, University of Tasmania, G.P.O. Box 252C, Hobart, Tasmania 7001, Australia

Abstract

Methods for the separation of several metallochromic ligands by capillary zone electrophoresis and micellar electrokinetic capillary chromatography were developed using an uncoated fused-silica capillary and an alkaline background electrolyte containing ethylenediaminetetraacetic acid (EDTA) and a zwitterionic additive. These additives were used to suppress sorption of the analytes on the capillary wall by interaction with sorbed metal ions present as impurities in the reagents used and also through polar interactions of the analytes. In model experiments it was shown that the addition of calcium or zinc ions to the background electrolyte reduces the electroosmotic flow, probably due to their sorption on silanol groups. They also have detrimental effects on the peak shape of most of the analytes. However, a separation of some metallochromic ligands could be achieved which involved complex equilibria with calcium or zinc added to the background electrolyte in an excess over the EDTA and with citrate added in an excess over the metals. Both methods yielded separation efficiencies up to approximately 500 000 theoretical plates but differed substantially in selectivity and ultraviolet–visible spectra of the separated ligands. Further, it was shown that analytes present as free ligands or as metal complexes that exhibit low effective mobilities and/or solubilities in the background electrolyte can be analysed after addition of sodium dodecylsulfate to the background electrolyte in a micellar separation mode.

1. Introduction

The uses of metallochromic ligands comprise a large area of analytical chemistry from complexometric titrations using metallochromic indicators [1,2] through photometric applications [1,2] to separation methods [3–13]. For many of these applications the purity of the ligand is not critical and some samples with a declared content of less than 50% may still function well, for example as indicators for complexometric titrations. Other analytical applications, such as photometric determination of metals or separation of metals using complexation with these ligands, may require the use of metallochromic ligands of higher quality [7]. In such cases, the reagents require thorough characterization and specification. The most widely used analytical methods [1,2] for the determination of the purity of metallochromic ligands are titration or photometry. However, these lack selectivity. Paper and thin layer chromatography may be used for

* Corresponding author.

[1] Present address: Department of Analytical Chemistry, Institute of Chemistry, Johannes-Kepler University, Altenbergerstrasse 69, A-4040 Linz, Austria.

0021-9673/95/$09.50
SSDI 0021-9673(95)01188-5

the determination of impurities but are limited in their efficiency and sensitivity.

Although capillary zone electrophoresis (CZE) and micellar electrokinetic capillary chromatography (MECC) are electromigration separation techniques with a rapidly growing number of applications [4–6], they have not been applied to the separation of metallochromic ligands. Several papers describe isotachophoretic [7] or CZE–MECC [8–13] separations of metal complexes of metallochromic ligands; however, the aim of those separations was the determination of the metals rather than the ligands.

In this paper we present methods for the separation of several azo and triphenylmethane metallochromic ligands (Fig. 1) by CZE and MECC. These metallochromic ligands are non-selective reagents forming coloured complexes with a wide range of metals [2]. Once adequate analytical methods have been established for the measurement and control of the purity of these ligands, they are intended for use in the CZE separation of metals with selective and sensitive detection in the visible (VIS) range.

2. Experimental

2.1. Instrumentation

The instrument used was a Quanta 4000 (Waters, Milford, MA, USA) interfaced to a Maxima 820 data station (Waters). Separations were carried out using an AccuSep (Waters) fused-

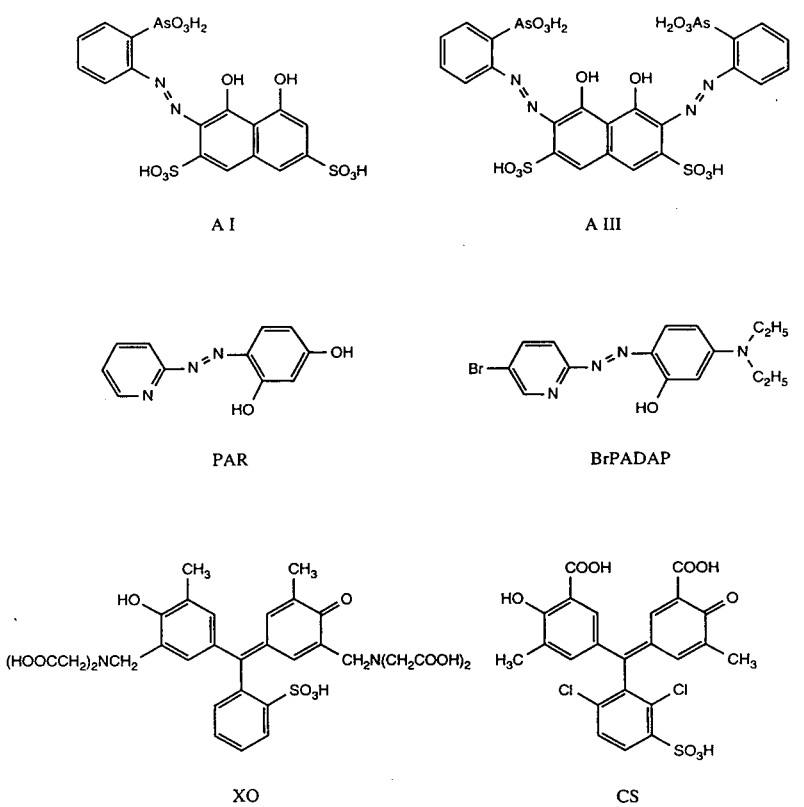

Fig. 1. Structures of metallochromic ligands: AI = arsenazo I, AIII = arsenazo III, PAR = 4-(2-pyridylazo)resorcinol, BrPADAP = 2-(5-bromo-2-pyridylazo)-5-(diethylamino)phenol, XO = xylenol Orange, CS = Chrome Azurol S (for synonyms, see Experimental).

silica capillary (60 cm × 75 mm I.D., length to detector 52 cm) initially washed with concentrated nitric acid (approximately ten capillary volumes) and then with 1 *M* sodium hydroxide overnight. An alkaline wash procedure consisting of 0.1 *M* sodium hydroxide containing 50% (v/v) methanol (solution A), followed by 1 *M* sodium hydroxide, solution A again, and finally water (at least ten capillary volumes of each) was performed whenever a background electrolyte (BGE) was changed (except for the experiments on the influence of increasing metal concentrations as given in Figs. 5 and 6). Injection was performed hydrostatically by elevating the sample at 98 mm for 10 s at the anodic side of the capillary. In order to reduce the consumption of BGE, the standard 20-ml buffer reservoir at the anodic side was modified to hold a plastic sample vial of approximately 0.6 ml, whilst at the cathodic (detector) side a buffer reservoir of 4 ml volume was used. The running voltage was + 25 kV. Direct photometric detection at 254 or 546 nm was used. Separation efficiency was calculated from the peak width at half height.

2.2. Reagents and procedures

The trisodium salt of arsenazo I [2-(4,5-dihydroxy-2,7-disulfo-3-naphthylazo)phenylarsenic acid, AI], the monosodiummonohydrate salt of 4-(2-pyridylazo)resorcinol (PAR), the sodium salt of xylenol orange {3,3′-bis[N,N-di-(carboxymethyl)aminomethyl)]-*o*-cresolsulfophthalein, XO} with a dye content of approximately 90% (XO sample A) and 2-(5-bromo-2-pyridylazo)-5-(diethylamino)phenol (BrPADAP) were obtained from Aldrich (Milwaukee, WI, USA). The monosodiumtrihydrate salt of arsenazo III [2,7-bis(2-arsonophenylazo)-1,8-dihydroxy-3,6-naphthalene disulfonic acid, AIII], approximately 60% content, was obtained from Sigma (St. Louis, MO, USA). The sodium salt of xylenol orange {3,3′-bis[N,N-di(carboxymethyl)aminomethyl)] - *o* - cresolsulfophthalein, XO}, purity approximately 96% (XO sample B), was obtained from BDH (Poole, UK). The trisodium salt of Chrome Azurol S (3″-sulfo-2″,6″-dichloro-3,3′-dimethyl-4-hydroxyfuchson-5,5′-dicarboxylic acid, CS) was obtained from Riedel de Haën (Hannover, Germany). Stock solutions (0.5 m*M*) of the metallochromic ligands were prepared in water (AI, AIII, PAR, XO and CS) or 50% aqueous acetonitrile (BrPADAP). Solutions of 0.1 m*M* were injected (5 s injection time) for the determination of mobilities (μ) and separation efficiencies (number of theoretical plates, *N*).

Ethylenediaminetetraacetic acid (EDTA), disodium salt, was obtained from Ajax (Sydney, Australia). Trisodium salt solutions of EDTA were prepared by titration with sodium hydroxide. Diethylenetriaminepentaacetic acid (DTPA) was obtained from Aldrich and *trans*-1,2-diaminocyclohexane - N, N, N′, N′ - tetraacetic acid (CyDTA) from BDH. Z1-Methyl (trimethylammonium propanesulfonate) was obtained from Waters. Water was treated with a Millipore (Bedford, MA, USA) Milli-Q water purification apparatus. All other chemicals were of analytical grade.

A formate–diethanolamine (DEOLA) buffer was prepared by appropriate dilution of formic acid and adjustment to pH 9.7 with DEOLA, to give final concentrations of 20 m*M* formate and approximately 50 m*M* DEOLA. The BGEs were prepared by adding to a 10-ml volumetric flask the desired volumes of 100 m*M* EDTA, calcium diformate (prepared as a 100 m*M* solution from appropriate amounts of calcium hydroxide and formic acid) or zinc sulfate (prepared as a 100 m*M* solution in 10 m*M* sulfuric acid), 100 m*M* citric acid and Z1-Methyl. The solution was then diluted to the mark with the formate–DEOLA buffer. Before use the BGE was degassed by vacuum and filtered with a Millex-HA 0.45-mm disc filter (Millipore).

The electroosmotic flow (EOF) was determined in the non-micellar BGEs by injections of mesityloxide (MSO) added in a 10 ppm concentration to the sample. With all BGEs containing the Z1-Methyl, a positive peak (probably due to refractive index change) was observed having exactly the same migration time as MSO. Therefore, the peak caused by Z1-Methyl was used as an EOF marker.

3. Results and discussion

3.1. Separation of metallochromic ligands using BGEs containing EDTA

Preliminary experiments using AI with BGEs comprising 10 m*M* phosphate at pH 7.0, 30 m*M* borate at pH 9.5 or formate–DEOLA at pH 9.7 yielded peaks which became broader and exhibited an increased migration time after each successive injection. The alkaline wash procedure (see Experimental) restored acceptable peak shapes ($N \approx 25\,000$) for the next one or two injections, after which the peak shape started to deteriorate again.

These preliminary experiments led to the hypothesis that metal ions present as impurities in the BGEs could influence separations by binding to silanol groups on the capillary wall [14–16,24]. To prevent this, 1 m*M* EDTA was added to the BGEs. A dramatic improvement in the reproducibility of migration times and in separation efficiency resulted for all BGEs. For comparison, we also tried DTPA and found the same effect as for EDTA, and CyDTA which yielded similar results for all analytes except AI which gave a very broad peak. For all further investigations, EDTA was incorporated into the BGE.

Z1-Methyl, a zwitterionic compound (trimethylammonium propanesulfonate), was also examined as an additive to the BGE. Generally, Z1-Methyl is used to suppress polar interactions of both macromolecules [17] and small anions [18] with the capillary wall. The addition of Z1-Methyl resulted in an increase in the EOF, an overall decrease in the effective mobilities of the analytes (probably due to changes in solvation) and an additional increase in separation efficiencies relative to EDTA electrolyte (see Table 1). The formate–DEOLA buffer gave the best results in terms of reproducibility and separation efficiency (compared to borate and carbonate at the same pH). The concentration of Z1-Methyl was optimized with respect to the separation of the unknown impurity close to the AI peak (see Fig. 2a). A concentration of 0.4 *M* Z1-Methyl gave satisfactory results. Examples of separations of metallochromic ligands using this electrolyte are given in Fig. 2 (AI, AIII and CS) and Fig. 3 (XO samples A and B).

Further manipulation of the composition of the BGE showed that analytes having effective mobilities which were too low for the above electrolyte system or which precipitated from this electrolyte could be analysed after addition of sodium dodecylsulfate to the BGE with subsequent use of the MECC separation mode. This is illustrated in Fig. 4 for BrPADAP which is analysed at a pH where the molecule is uncharged. The separation efficiency was approximately 26 000 theoretical plates.

Table 1
EOF, analyte mobility and separation efficiency in background electrolytes containing EDTA

Analyte	No Z1-Methyl in BGE		0.4 *M* Z1-Methyl in BGE	
	μ ($10^9\ m^2\ V^{-1}\ s^{-1}$)	N ($\times 10^3$)	μ ($10^9\ m^2\ V^{-1}\ s^{-1}$)	N ($\times 10^3$)
EOF	+58.6	–	+69.1	–
AI	−46.8	87	−41.7	234
AIII	−43.1	154	−39.9	387
XO	−42.7	146	−38.1	368
CS	−40.8	153	−34.3	373
PAR	−22.3	287	−18.3	473

Electrolyte: 1.0 m*M* EDTA, 20 m*M* formate–DEOLA pH 9.7; for other conditions, see Experimental. AI = arsenazo I, AIII = arsenazo III, XO = xylenol Orange, CS = Chrom Azurol S, PAR = pyridylazoresorcinol.

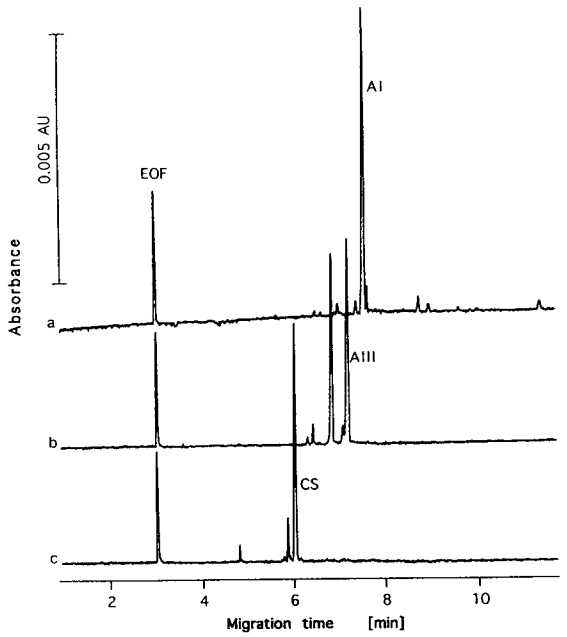

Fig. 2. Electropherograms of samples of (a) AI, (b) AIII and (c) CS in the presence of EDTA. BGE: 1.0 m*M* EDTA and 0.40 *M* Z1-Methyl in 20.0 m*M* formate–DEOLA pH 9.7. Detection wavelength: 254 nm. For other conditions, see Experimental.

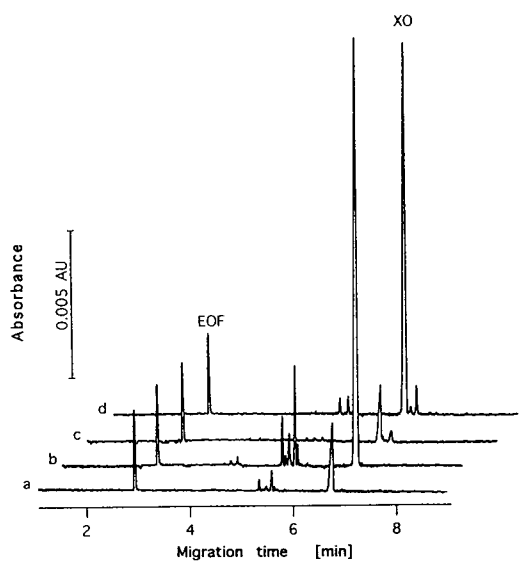

Fig. 3. Electropherograms of samples of (a, b) XO-A and (c, d) XO-B. Detection wavelength: 254 nm (a, c) or 546 nm (b, d). Other conditions as in Fig. 2.

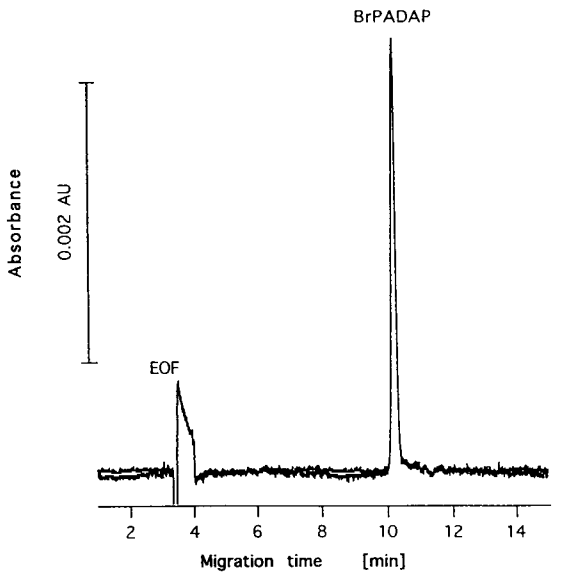

Fig. 4. Electropherogram of a sample of BrPADAP. BGE: 35 m*M* sodium dodecylsulfate, 1.0 m*M* EDTA and 0.40 *M* Z1-Methyl in 10 m*M* formate–DEOLA pH 9.7. Detection wavelength: 254 nm. For other conditions, see Experimental.

3.2. Addition of Ca(II) or Zn(II) to the BGE

The migration behaviour of the metallochromic ligands in BGEs containing metal ions was also studied. The presence of metal ions was considered to exert a possible influence on the separation efficiency and was also a potential means of manipulation of the separation selectivity of the metallochromic ligands through the involvement of these species in complexation equilibria with the metal ions added to the BGE. It has been demonstrated by Gebauer et al. [19] that a metal ion (Cd^{2+}) added to the BGE can influence effective mobilities of anions (chloride, sulfate and nitrate) through complexation and so change the selectivity of the separation. Other authors have added Zn^{2+} and Cu^{2+} to optimise the separations of oligonucleotides and peptides [20,21] or Ca^{2+} to avoid comigration of organic acids [22].

Preliminary experiments with added metal ions (Ca^{2+} as the diformate salt or Zn^{2+} as the sulfate salt) showed that without EDTA in the

BGE, added concentrations of 0.1 m*M* Ca^{2+} or Zn^{2+} ions caused the EOF to decrease and the peaks for the metallochromic ligands to exhibit severe broadening. When the BGE contained EDTA, the same effects were observed only when the metal ion concentrations in the BGE were in excess of the EDTA concentration (1.0 m*M*) (Fig. 5). Under such conditions, the observed decreased EOF was an indication of a decrease of the negative capillary wall charge, which is probably caused by sorption of the metal ions on the silanol groups of silica [14]. At the same time the effective mobilities of the ligands were decreasing and, furthermore, detrimental effects on peak shape and efficiency were observed for most analytes (except for XO and PAR in a BGE containing Ca^{2+}). In the case of PAR this latter behaviour can be explained by the fact that it does not form a complex with Ca^{2+}.

As suggested above, the results obtained in BGEs containing Ca^{2+} or Zn^{2+} ions are consistent with sorption of the metal ions on the silanol groups of the silica, causing a reduction in surface charge and hence a reduced EOF. At the same time, the free coordination sites of the sorbed metal could cause retardation of a ligand molecule through complexation effects [23]. Any such complexation–decomplexation of the solute with the metal sorbed on capillary wall would have a detrimental influence on the separation efficiency. Our results are in accordance with the recently reported [24] sorption of small aromatic acids caused by Fe^{3+} ions bound to the capillary wall as a result of Fe^{3+} ions present as trace (μg/l) impurities in the BGE.

Somewhat surprisingly, efficient separations of some metallochromic ligands could be carried out in BGEs containing Ca^{2+} or Zn^{2+} in excess over EDTA, provided that citric acid was also present at a concentration higher than the free metal concentration. Whilst such a BGE might appear unnecessarily complex, the EDTA (present as its Ca^{2+} or Zn^{2+} complex) is still a necessary component of the BGE because it can bind metal ions present as impurities that form stronger complexes than Ca^{2+} or Zn^{2+}, for example Fe^{3+}. Fig. 6 shows the dependence of

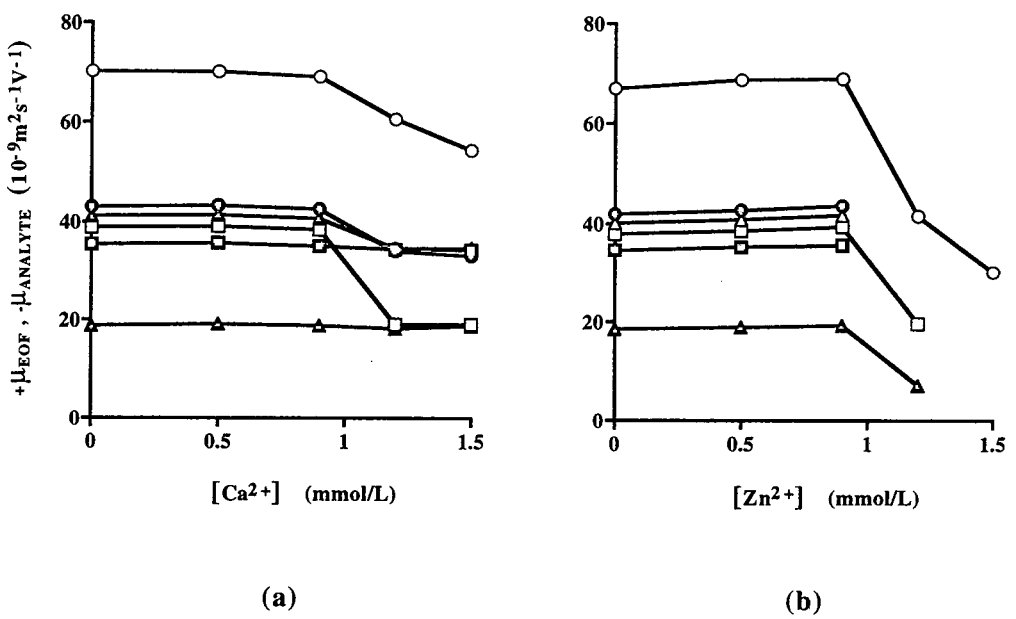

Fig. 5. Effect on EOF and analyte mobilities of (a) calcium or (b) zinc ions added to the BGE (0–1.5 m*M* Ca^{2+} or Zn^{2+}, 1.0 m*M* EDTA and 0.40 *M* Z1-Methyl in 20.0 m*M* formate–DEOLA pH 9.7): -○- = EOF, -●- = AI, -△- = AIII, -□- = XO, -■- = CS, -▲- = PAR. For other conditions, see Experimental.

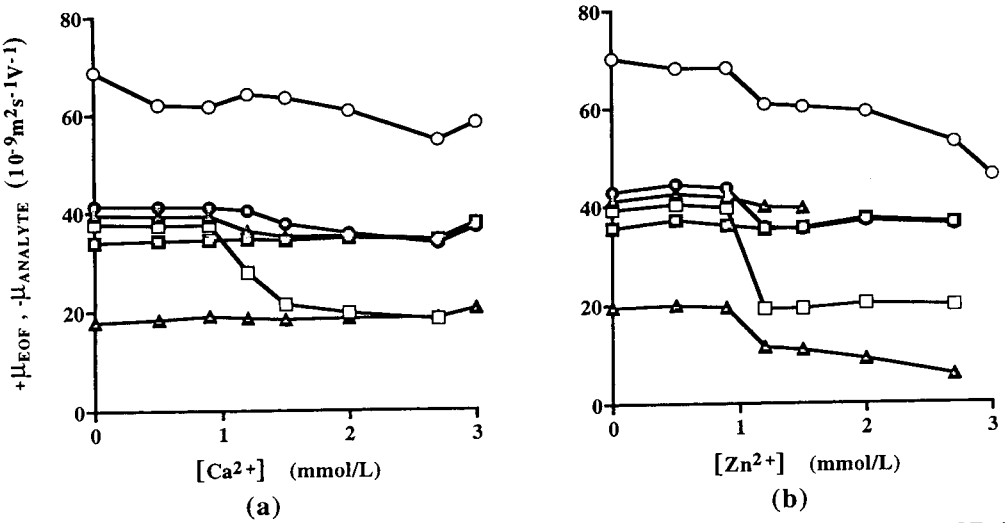

Fig. 6. Effect on EOF and analyte mobilities of (a) calcium or (b) zinc ions added to a BGE containing citrate. BGE: 0–3.0 m*M* Ca^{2+} or Zn^{2+}, 1.5 m*M* citric acid, 1.0 m*M* EDTA and 0.40 *M* Z1-Methyl in 20 m*M* formate–DEOLA at pH 9.7. Legend to curves as in Fig. 5. For other conditions, see Experimental.

the EOF and the mobilities of the metallochromic ligands on the concentration of Ca^{2+} or Zn^{2+} ions in BGEs containing citrate. Under the conditions used, the solute ligands will compete with citrate for the added metal ions, but since the citrate complexes are quite weak [25], it can be expected that the solute ligands will be the chief participators in complex formation. Visible absorption spectra of the ligands were recorded in the BGEs used in order to confirm that complex formation between the analytes and the Ca^{2+} or Zn^{2+} ions does occur. The spectra of the metallochromic ligands are known to change substantially upon complexation with metals [1,2]. The results given in Table 2 show clearly that complex formation has taken place, except for PAR with Ca^{2+} and for CS with both Ca^{2+} and Zn^{2+}.

Table 2
Wavelengths of maximum absorbance for metallochromic ligands in electrolytes without and with added metal ions

Electrolyte	Wavelengths of maximum absorbance (nm)					
	AI	AIII	XO	CS	PAR	BrPADAP
No added metal ion	500	559	579	425	414	444
1.5 m*M* Ca^{2+} added	525	597, 649	578[a]	425[b]	414[c]	525, 560[e]
1.5 m*M* Zn^{2+} added	518	587	573	425	492[d]	525, 558

Spectra measured in an electrolyte containing 1.0 m*M* EDTA, 1.5 m*M* citric acid and 0.1 *M* Z1-Methyl in 20 m*M* formate–DEOLA buffer pH 9.7. See Table 1 for solute identities.
[a] Band shape change.
[b] Increased absorbance.
[c] Decreased absorbance.
[d] Sideband ca. 520 nm.
[e] Partial complexation.

Electropherograms showing the separation of samples of XO and AI are given in Fig. 7. In addition to the good peak shapes evident from Fig. 7, a further advantage of the presence of citrate in the BGE is the fact that the decrease in the EOF at Ca^{2+} or Zn^{2+} concentrations exceeding 1.0 m*M* is considerably smaller (Fig. 6) than that without citrate (Fig. 5). Therefore, an explanation for the citrate influence on the separation may lie in the suppression of the sorption of Ca^{2+} and Zn^{2+} on the capillary wall as a result of their complexation with citrate. Alternatively, the effect might arise from saturation of the coordination sphere of the sorbed metal ions by citrate, thereby preventing sorption of the solute ligands, depending on the stability of such mixed complexes.

A 20 m*M* formate–DEOLA background electrolyte pH 9.7 containing 1.5 m*M* Zn^{2+}, 1.5 m*M* citric acid, 1.0 m*M* EDTA and 0.4 *M* Z1-Methyl could also be used for the separation of BrPADAP in a MECC mode after addition of 35 m*M* sodium dodecylsulfate. A separation efficiency of approximately 50 000 plates/m was achieved. It should be mentioned that in this MECC separation mode the citrate also prevented clouding of the BGE caused by precipitation of the Zn^{2+} salt of sodium dodecylsulfate.

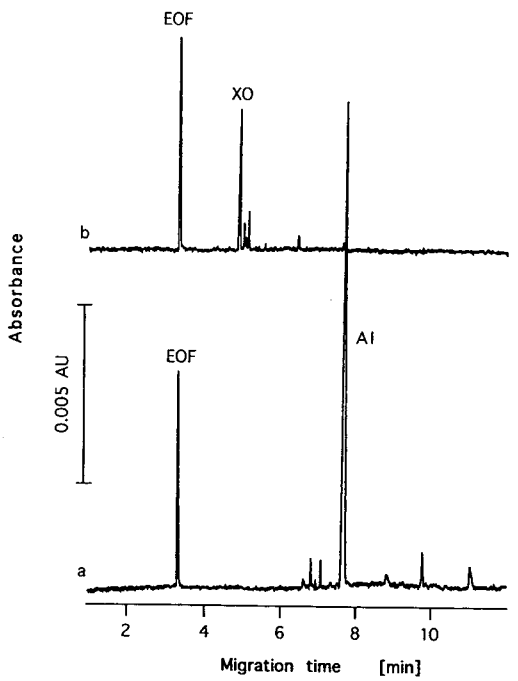

Fig. 7. Electropherograms of samples of (a) AI and (b) XO-A. BGE: 1.5 m*M* $Ca(formate)_2$, 1.5 m*M* citric acid, 1.0 m*M* EDTA and 0.40 *M* Z1-Methyl in 20 m*M* formate–DEOLA at pH 9.7. Detection wavelength: 254 nm. For other conditions, see Experimental.

4. Conclusions

CE and MECC can offer very efficient separations of metallochromic ligands if the BGE electrolyte contains a strong complexing agent to suppress the sorption of the analytes on the capillary walls via metal ions present as impurities, and Z1-Methyl to suppress other sorptions based on polar interactions. When metal ions (Ca^{2+} or Zn^{2+}) were added to the BGE in an excess over EDTA as a means of manipulating separation selectivity, decreases in the EOF and detrimental effects on the separation efficiency of most of the metallochromic ligands were observed, most probably as a result of sorptions of the metals on the capillary wall. With some ligands it was possible to retain an efficient separation even with Ca^{2+} or Zn^{2+} ions added when an excess of citrate was present in the BGE. In this way, separation selectivity could be varied if the analytes formed complexes having effective mobilities different from those of the free ligands. Furthermore, the spectra of metallochromic ligands also change substantially when complexed. This behaviour, together with the above-mentioned selectivity changes, can be used to elucidate if an unknown impurity is capable of complexation and if it has metallochromic properties.

Acknowledgement

We thank Waters Corporation for generous financial support for this project.

References

[1] F.J. Welcher, in P.W. West, A.M.G. MacDonald and T.S. West (Editors), *The Development of Organic Reagents in Inorganic Analysis, in Analytical Chemistry*, Elsevier, Amsterdam, 1963.

[2] K. Ueno, T. Imamura, and K.L. Cheng, *Handbook of Organic Analytical Reagents*, CRC Press, Boca Raton, FL, 2nd ed., 1992.

[3] P.R. Haddad and P.E. Jackson, *Ion Chromatography. Principles and Applications (J. Chromatogr. Library*, Vol. 46), Elsevier, Amsterdam, 1990.

[4] S.F.Y. Li, *Capillary Electrophoresis: Principles, Practice, and Applications (J. Chromatogr. Library*, Vol. 52), Elsevier, Amsterdam, 1992, Ch. 7, pp. 377–540.

[5] P. Jandik and G. Bonn, *Capillary Electrophoresis of Small Molecules and Ions*, VCH Verlagsgesellschaft, Weinheim, 1993, Ch. 4 and 5, pp. 211–290.

[6] F. Foret, L. Krivankova and P. Bocek, *Capillary Zone Electrophoresis*, VCH Verlagsgesellschaft, Weinheim, 1993, Ch. 10, pp. 211–334.

[7] I. Zelensky, D. Kaniansky, P. Havasi, Th.P.E.M. Verheggen and F.M. Everaerts, *J. Chromatogr.*, 470 (1989) 155.

[8] T. Saitoh, H. Hoshino and T. Yotsuyanagi, *J. Chromatogr.*, 469 (1989) 175.

[9] K. Saitoh, C. Kiyohara and N. Suzuki, *J. High Resol. Chromatogr.*, 14 (1991) 245.

[10] T. Saitoh, H. Hoshino and T. Yotsuyanagi, *Anal. Sci.*, 7 (1991) 495.

[11] N. Iki, H. Hoshino and T. Yotsuyanagi, *J. Chromatogr.*, 652 (1993) 539.

[12] A.R. Timerbaev, O.P. Semenova, P. Jandik and G.K. Bonn, *J. Chromatogr. A*, 671 (1994) 419.

[13] F.B. Regan, M.P. Meaney and S.M. Lunte, *J. Chromatogr. B*, 657 (1994) 409.

[14] R.K. Iler, *The Chemistry of Silica*, Wiley, New York, 1979, pp. 303 and 669.

[15] K. Salomon, D.S. Burgi and J.C. Helmer, *J. Chromatogr.*, 559 (1991) 69.

[16] J.E. Dickens, J. Gorse, J.A. Everhart and M. Ryan, *J. Chromatogr. B*, 657 (1994) 401.

[17] H.B. Hines and E.E. Brueggemann, *J. Chromatogr. A*, 670 (1994) 199.

[18] S.C. Grocott, L.P. Jefferies, T. Bowser, J. Carnevale and P.E. Jackson, *J. Chromatogr.*, 602 (1992) 257.

[19] P. Gebauer, M. Deml, P. Bocek and J. Janak, *J. Chromatogr.*, 455 (1989) 267.

[20] A.S. Cohen, S. Terabe, J.A. Smith and B.L. Karger, *Anal. Chem.*, 59 (1987) 1021.

[21] R.A. Mosher, *Electrophoresis*, 11 (1990) 765.

[22] S.P.D. Lalljie, J. Vindevogel and P. Sandra, *J. Chromatogr. A*, 652 (1993) 563.

[23] R.K. Iler, *The Chemistry of Silica*, Wiley, New York, 1979, pp. 410, 572 and 688.

[24] B. Gassner, W. Friedel and E. Kenndler, *J. Chromatogr. A*, 680 (1994) 25.

[25] R.M. Smith and A.E. Martell, *Critical Stability Constants*, Vol. 6, Plenum Press, New York, 1989, p. 356.

ELSEVIER

Journal of Chromatography A, 706 (1995) 503–515

JOURNAL OF CHROMATOGRAPHY A

Interpretation of migration behaviour of inorganic cations in capillary ion electrophoresis based on an equilibrium model

Q. Yang[a], Y. Zhuang[b], J. Smeyers-Verbeke[a], D.L. Massart[a,*]

[a]*Farmaceutisch Instituut, Vrije Universiteit Brussel, Laarbeeklaan 103, B-1090 Brussels, Belgium*

[b]*Université Libre Bruxelles, CP 243, Campus Plaine, B-1050 Brussels, Belgium*

Abstract

In capillary ion electrophoresis, the migration of inorganic cations in an aqueous–organic medium is influenced by complexation and interactions between the solutes and organic solvents. This can be accounted for by multiple chemical equilibria. Based on these equilibria, a migration model is proposed that describes the electrophoretic mobility of the cations in terms of absolute mobility, complex formation constants and the concentrations of complexing reagents and organic solvent. It was validated in a background electrolyte composed of imidazole, 2-hydroxyisobutyric acid (HIBA), 18-crown-6 and methanol. The parameters in this model were estimated experimentally and were in good agreement with the values in the literature. The model is useful for predicting the mobilities as a function of the concentrations of HIBA, 18-crown-6 and methanol, and consequently facilitates selectivity optimization.

1. Introduction

Capillary ion electrophoresis (CIE) has been widely studied for the determination of low-molecular-mass ions [1–4]. For inorganic ions, which generally have no optical absorption, indirect on-column detection is mostly applied [5]. By introducing an absorbing substance, so-called co-ion, into the electrolyte buffer, a constant background absorbance is obtained. The zones of non-absorbing ionic species are monitored because they lead to a decrease in light absorbance. The ideal co-ion should have a similar electrophoretic mobility to the analyte ions and have a higher absorption at a given detection wavelength to achieve the highest separation efficiency and detection sensitivity [6,7]. Imidazole, which has been found to be a suitable co-ion for the separation of alkali, alkaline earth and transition metal cations by CIE [8–10], was used in this work.

Separation in capillary electrophoresis is based on differences in electrophoretic mobilities. Ions with identical charge and size have identical electrophoretic mobilities, for instance, transition and rare earth metal cations, and the electrophoretic separation of these ions as such is impossible. However, their mobilities can be modified by introducing a chemical equilibrium in which the ions participate to form complexes. If the ions have different complex formation constants, their apparent electrophoretic mobilities should differ. The electrophoretic mobilities can also be affected by pH when the complexing reagent is a weak acid [11]. A second complexing reagent, such as a cyclic polyether, can be

* Corresponding author.

0021-9673/95/$09.50
SSDI 0021-9673(94)01242-3

applied if the simultaneous separation of all of the cations in question is not achieved. In addition, it has been found that the volume fraction of organic solvents in water can alter the magnitude of electrophoretic mobilities and consequently modify the separation selectivity [10, 12].

Up to now, the quantitative description of the electrophoretic mobilities of inorganic cations in capillary zone electrophoresis (CZE) has been little studied. Hirokawa et al. [13] studied the isotachophoretic electrophoresis separation of fourteen rare earth metal cations (Ln) using three different electrolyte systems, acetate acid (Ac), 2-hydroxyisobutyric acid (HIBA) and a mixture of Ac and HIBA. On the basis of multiple complex formation equilibria, they determined the absolute mobilities of Ln–Ac, Ln–HIBA and Ln–Ac–HIBA complexes and the formation constants of Ln–HIBA–Ac complexes from experimental data. It was concluded that the separation was due to the differences in the effective mobilities of the Ln cations caused by the different abundances of the complexes. Using a similar principle, Swaile and Sepaniak [14] described the electrophoretic mobilities of Ca^{2+} and Mg^{2+} in CZE as a function of the concentration of 8-hydroxyquinoline-5-sulfonic acid (HQS) and pH. Employing literature values for the formation constants of metal–HQS complexes and the acid dissociation constant of HQS, they calculated the mobilities of free Ca^{2+} and Mg^{2+} and their HQS complexes from experimental data. Quang and Khaledi [15] tried to describe the mobilities of metal cations as a function of the concentration of HIBA and pH using a phenomenological expression, but did not succeed because there were too many parameters involved in the expression. They were successful in doing so using an empirical expression. In the course of the preparation of this paper, we learned that Vogt and Conradi [16] have used a theoretical model to describe the mobility of rare earth metal cations with HIBA, lactate and acetate complexations. In their model, the effects of pH and ligand are considered simultaneously.

In a recent report Sahota and Khaledi [17], stressed the advantages of non-aqueous electrophoresis. They observed a lower current in a formamide medium. This allows an increase in ionic strength of the electrolyte buffer, and the application of a higher electric field and larger sample load in order to have a net positive effect on detection, efficiency and analysis time.

In this work, the migration behaviour of inorganic cations was studied in an organic–aqueous medium (methanol–water) with HIBA and 18-crown-6 ether as complexing agents. Based on multiple chemical equilibria, a migration model was developed, which was used to optimize the separation of twelve inorganic cations (NH_4^+, Li^+, Na^+, K^+, Mg^{2+}, Ca^{2+}, Sr^{2+}, Ba^{2+}, Mn^{2+}, Ni^{2+}, Zn^{2+} and Cu^{2+}).

2. Theory

In CIE, when an electrolyte buffer is composed of a complexing reagent HL (a weak acid), a cyclic polyether C and an organic solvent S, the following chemical equilibria take place:

(i) acid dissociation:

$$HL \rightleftharpoons H^+ + L^- \qquad K_a$$

(ii) complexation:

$$M^{2+} + L^- \rightleftharpoons ML^+ \qquad \beta_{ML}$$

$$ML^+ + L^- \rightleftharpoons ML_2^0 \qquad \beta_{ML2}$$

$$ML_2^0 + L^- \rightleftharpoons ML_3^- \qquad \beta_{ML3}$$

(iii) inclusion complexation:

$$M^{n+} + C \rightleftharpoons MC^{n+} \qquad \beta_{MC} \qquad (n = 1, 2)$$

(iv) solvation:

$$M^{n+} + S \rightleftharpoons MS^{n+} \qquad \beta_{MS}$$

where K_a, β_{ML}, β_{ML2}, β_{ML3}, β_{MC} and β_{MS} represent the equilibrium constants.

In (i), a weak-acid complexing reagent undergoes the acid dissociation in the electrolyte buffer.

In (ii), the divalent cations in question are complexed by HIBA. Mn^{2+}, Ni^{2+} and Cu^{2+} are known to form 1:1, 1:2 and 1:3 complexes, whereas the others form 1:1 and 1:2 complexes [18].

In (iii), a cyclic polyether C (i.e., 18-crown-6 and 15-crown-5 [19,20]) can host certain cations in its cavity by forming ion–dipole bonds with its

oxygen atoms carrying lone electron pairs [21]. The magnitude of the interaction depends on the match between the ionic radius of the cation M and that of the cavity. K^+, Sr^{2+} and Ba^{2+} are known to form 1:1 complexes with 18-crown-6 [21,22].

In (iv), an ion interacts with a group of polar solvent molecules through ion–dipole bonds and a solvation shell may be formed around the central ion [21]. For a given cation, the number of solvent molecules within the group is assumed to be the same and not to alter with the solvent concentration, which is of course an approximation. In principle, the solvent solvates all kinds of ions in solution, some to a greater extent than others, depending on the specific properties of the central ion regarding a certain solvent. However, solvation of the negatively charged complex ions has no direct influence on the mobilities of the cations under study. Moreover, as the free cations are smaller and have a higher electrical charge and density than the solvated ones, the solvation of the bare cations should have the most significant impact on the overall mobility of the cations. In light of the above considerations, only the solvation of the free cations is taken into account.

As a consequence of the simultaneous equilibria, the cations are present as the free cations and as various complexes in the electrolyte buffer. The concentrations of the various complexed species can be obtained by the following equations:

$$[ML^+] = \beta_{ML}[M][L^-] \quad (1)$$

$$[ML_2^0] = \beta_{ML2}[M][L^-]^2 \quad (2)$$

$$[ML_3^-] = \beta_{ML3}[M][L^-]^3 \quad (3)$$

$$[(MC)^{n+}] = \beta_{MC}[M][C] \quad (4)$$

$$[MS^{n+}] = \beta_{MS}[M][S] \quad (5)$$

L^- is the conjugated base of HL and its concentration depends on the pH of the electrolyte buffer:

$$[L^-] = \alpha_L\text{-}[HL] = \frac{K_a}{[H^+] + K_a}[HL] \quad (6)$$

where α_L- is the molar fraction of the complexing reagent capable of complexing with cation M and [HL] the concentration of the complexing reagent in the background electrolyte.

The total cation concentration of each of the analyte cations, C_M, is the sum of various chemical species present in the electrolyte buffer:

$$\begin{aligned} C_M &= [M] + [ML^+] + [ML_2^0] + [ML_3^-] + [MS^{n+}] \\ &\quad + [MC^{n+}] \\ &= [M] + \beta_{ML}\alpha_L\text{-}[HL][M] \\ &\quad + \beta_{ML_2}(\alpha_L\text{-}[HL])^2[M] \\ &\quad + \beta_{ML_3}(\alpha_L\text{-}[HL])^3[M] + \beta_{MC}[C][M] \\ &\quad + \beta_{MS}[S][M] \end{aligned} \quad (7)$$

Combining Eqs. 1, 2, 3, 4, 5 and 7, we obtain the expressions of molar fraction of the various ionic species α_M, α_{ML^+}, $\alpha_{ML^{-3}}$, $\alpha_{MS^{n+}}$ *and* $\alpha_{MC^{n+}}$:

$$\alpha_M = \frac{[M]}{C_M} = \frac{1}{(1 + \beta_{ML}\alpha_L\text{-}[HL] + \beta_{ML_2}(\alpha_L\text{-}[HL])^2 + \beta_{ML_3}(\alpha_L\text{-}[HL])^3 + \beta_{MC}[C] + \beta_{MS}[S])} \quad (8)$$

$$\alpha_{ML^+} = \frac{[ML^+]}{C_M} = \frac{\beta_{ML}\alpha_L\text{-}[HL]}{1 + \beta_{ML}\alpha_L\text{-}[HL] + \beta_{ML_2}(\alpha_L\text{-}[HL])^2 + \beta_{ML_3}(\alpha_L\text{-}[HL])^3 + \beta_{MC}[C] + \beta_{MS}[S]} \quad (9)$$

$$\alpha_{ML3^-} = \frac{[ML_3^-]}{C_M} = \frac{\beta_{ML_3}(\alpha_L\text{-}[HL])^3}{1 + \beta_{ML}\alpha_L\text{-}[HL] + \beta_{ML_2}(\alpha_L\text{-}[HL])^2 + \beta_{ML_3}(\alpha_L\text{-}[HL])^3 + \beta_{MC}[C] + \beta_{MS}[S]} \quad (10)$$

$$\alpha_{MS^{n+}} = \frac{[MS^{n+}]}{C_M} = \frac{\beta_{MS}[S]}{1 + \beta_{ML}(\alpha_L\text{-}[HL]) + \beta_{ML_2}[\alpha_L\text{-}[HL])^2 + \beta_{ML_3}(\alpha_L\text{-}[HL])^3 + \beta_{MC}[C] + \beta_{MS}[S]} \quad (11)$$

$$\alpha_{MC^{n+}} = \frac{[(MC)^{n+}]}{C_M} = \frac{\beta_{MC}[C]}{1 + \beta_{ML}\alpha_L\text{-}[HL] + \beta_{ML_2}(\alpha_L\text{-}[HL])^2 + \beta_{ML_3}(\alpha_L\text{-}[HL])^3 + \beta_{MC}[C] + \beta_{MS}[S]} \quad (12)$$

The effective electrophoretic mobility, μ_{eff}, of each resulting CZE zone is equal to the sum of the products of the mobilities of the free metal cations and the various ionic species:

$$\mu_{eff.} = \mu_0\alpha_M + \mu_{ML}\alpha_{ML^+} + \mu_{ML_3}\alpha_{ML_3} + \mu_{MS}\alpha_{MS^{n+}} + \mu_{MC}\alpha_{MC^{n+}} \quad (13)$$

The mobility of ML_2^0 is equal to zero and is therefore not taken into account in Eq. 13. Combining Eqs. 8–13, we obtain:

$$\mu_{eff.} = \frac{\mu_0 + \mu_{ML}\beta_{ML}\alpha_L\text{-}[HL] + \mu_{ML_3}\beta_{ML_3}(\alpha_L\text{-}[HL])^3 + \mu_{MC}\beta_{MC}[C] + \mu_{MS}\beta_{MS}[S]}{1 + \beta_{ML}\alpha_L\text{-}[HL] + \beta_{ML_2}(\alpha_L\text{-}[HL])^2 + \beta_{ML_3}(\alpha_L\text{-}[HL])^3 + \beta_{MC}[C] + \beta_{MS}[S]} \quad (14)$$

where μ_0, μ_{ML}, μ_{ML_3}, μ_{MS} and μ_{MC} are the electrophoretic mobilities of the various cationic species.

The electrophoretic mobilities of the cations depend on both solute-specific parameters and condition-dependent parameters. The former are β_{ML}, β_{ML_2}, β_{ML_3}, β_{MC}, β_{MS}, μ_0, μ_{ML}, μ_{ML_3}, μ_{MS} and μ_{MC} and the latter are the concentrations of complexing reagents [HL] and [C], the fraction of solvent in electrolyte buffer [S] and the pH of the buffer (see Eq. 6).

3. Experimental

3.1. Instrumentation

The CE instrument was a Waters Quanta 4000 capillary electrophoresis system with a twenty sample carousel and a zinc lamp detector (214 nm). Accusep fused-silica capillaries (60 cm × 75 μm I.D.) were used in all analyses. A positive voltage of 20 kV was applied. The detector time constant was 0.3 s. Samples were introduced by either hydrostatic or electromigration injection. The electropherograms were recorded and treated with a Waters Model 810 data workstation equipped with a W51-watch-dog interface. The temperature was kept at 23°C.

3.2. Capillary preparation and cleaning

Every morning, the capillary was washed for 1 min with 0.5 mol/l KOH, for 2 min with water purified with a Milli-Q system (Millipore) and for 3 min with the electrolyte buffer. Subsequently, it was conditioned for at least 15 min. Between each injection, the capillary was washed for 1 min with 0.1 mol/l KOH, for 1 min with Milli-Q-purified water and for 3 min with the electrolyte buffer. At the end of the day, the capillary was rinsed with Milli-Q-purified water for 5 min and left in the water.

3.3. Reagents and standards

Titrisol concentrates of 1000 μg/ml of Na^+, K^+, Mg^{2+}, Ca^{2+}, Mn^{2+}, Ba^{2+}, Sr^{2+}, Cr^{3+}, Zn^{2+} and Cu^{2+} (Merck, Darmstadt, Germany) were used. Stock standard solutions containing 1000 μg/ml of Ni^{2+}, NH_4^+ and Li^+ were prepared from their chloride salts (Merck). Working standard solutions containing different concentrations of the above elements were prepared by mixing the appropriate amounts of the stock standard solutions.

Imidazole (99%, w/w) was of analytical-reagent grade (Merck) and methanol was of chromatography grade (Merck). HCl was a commercial 0.1 mol/l solution (Merck). 2-Hydroxyisobutyric acid (99%, w/w) and 18-crown-6 (99%, w/w) were of analytical-reagent grade (Aldrich-Chemie, Steinheim, Germany).

3.4. Preparation of background electrolyte

First, three stock standard solutions containing 130.6 mmol/l of HIBA, 50.0 mmol/l of 18-crown-6 and 500.0 mmol/l of imidazole were

prepared. The background electrolytes were prepared by mixing appropriate amounts of the above stock standard solutions and corresponding volumes of methanol in a 100-ml plastic volumetric flask. The pH was then adjusted to ca. 4.5 (with a pH meter) by titration with 1 mol/l HCl or KOH. Just before use they were filtered through a 0.45-μm syringe filter (Millipore, Molsheim, France).

3.5. Calculation

The electrophoretic mobility of each cation, $\mu_{eff.}$, is calculated from the following equation:

$$\mu_{eff.} = \frac{L_t L_d}{V} \cdot \left(\frac{1}{t} - \frac{1}{t_0}\right) \quad (15)$$

where L_t (60 cm) is the total length of the capillary, L_d (52 cm) the distance from the injector to the detector, V the applied voltage (20 kV), t the migration time of the analyte cation and t_0 the migration time of water, which is used as the marker of electroosmotic flow (EOF).

The parameters in Eqs. 18–20 (see later) were estimated by non-linear regression using the Statistical Package for the Social Sciences (SPSS) [23]. The Levenberg–Marquardt algorithm was employed. Iteration was stopped when the relative decrease between successive residual sums of squares was $\leq 1.0 \times 10^{-8}$.

A computer program written with Matlab for Windows [24] is used for selectivity optimization.

4. Results and discussion

4.1. Effect of HIBA on migration

The effect of HIBA was studied by changing the concentration of HIBA from 0 to 10 mmol/l and in the absence of methanol and 18-crown-6 (pH 4.5). It was found that the mobilities of K^+, Na^+, Li^+ and NH_4^+ do not alter with increase in the concentration of HIBA (the results are not shown here), indicating that there is no complexation between these cations and HIBA. As shown in Fig. 1a, the mobilities of Sr^{2+}, Ba^{2+}, Mg^{2+}, Ca^{2+} and Mn^{2+} decrease slightly, whereas those of Ni^{2+}, Zn^{2+} and Cu^{2+} decrease rapidly as the concentration of HIBA increases. The steepness of the decline depends on the magnitude of the formation constants and Ni^{2+}, Zn^{2+} and Cu^{2+} are known to have larger formation constants with HIBA (see Table 2) [18].

As only small amounts of HIBA are added in the electrolyte buffer (up to 0.01 M) and because of the moderate complex formation ability of HIBA with the cations, the terms of the second and third order in Eq. 14 with respect to the concentration of HIBA may be neglected. Further, we assume that $\mu_{ML}\beta_{ML}\alpha_L\text{-}[HL] \ll \mu_0$, which means that μ_{ML} should be much smaller than μ_0. Swaile and Sepaniak [14] calculated that the mobility of 1:1 Ca–HQS complexes was ten times smaller than that of the free Ca^{2+}.

In the absence of an organic solvent and a polyether, Eq. 14 can be rearranged into a linear form as

$$\frac{1}{\mu_{eff.}} = \frac{1}{\mu_0} + \frac{\alpha_L\text{-}\beta_{ML}}{\mu_0} \cdot [HL] \quad (16)$$

This is verified in Fig. 1b, where the reciprocal of μ_{eff} is plotted against the concentration of HIBA and a straight-line relationship is obtained for all of the divalent cations. μ_0 and β_{ML} can then be estimated from the straight lines.

4.2. Effect of methanol on migration

The experiments were performed at a HIBA concentration of 6.5 mmol/l and in the absence of 18-crown-6 (pH 4.5), while the fraction of methanol was changed from 0 to 40% (v/v). The maximum concentration of methanol used in this work was 40% (v/v) based on the following considerations: first, methanol is a volatile solvent, and evaporation during measurements can cause irreproducibility in analytical performance; and second, increasing the concentration of organic solvent decreases the electrical current and can cause electrical breakdown [25,26]. In this work, the electrical current was as low as 4.8 μA at 40% methanol.

Fig. 2a shows a plot of $\mu_{eff.}$ as a function of

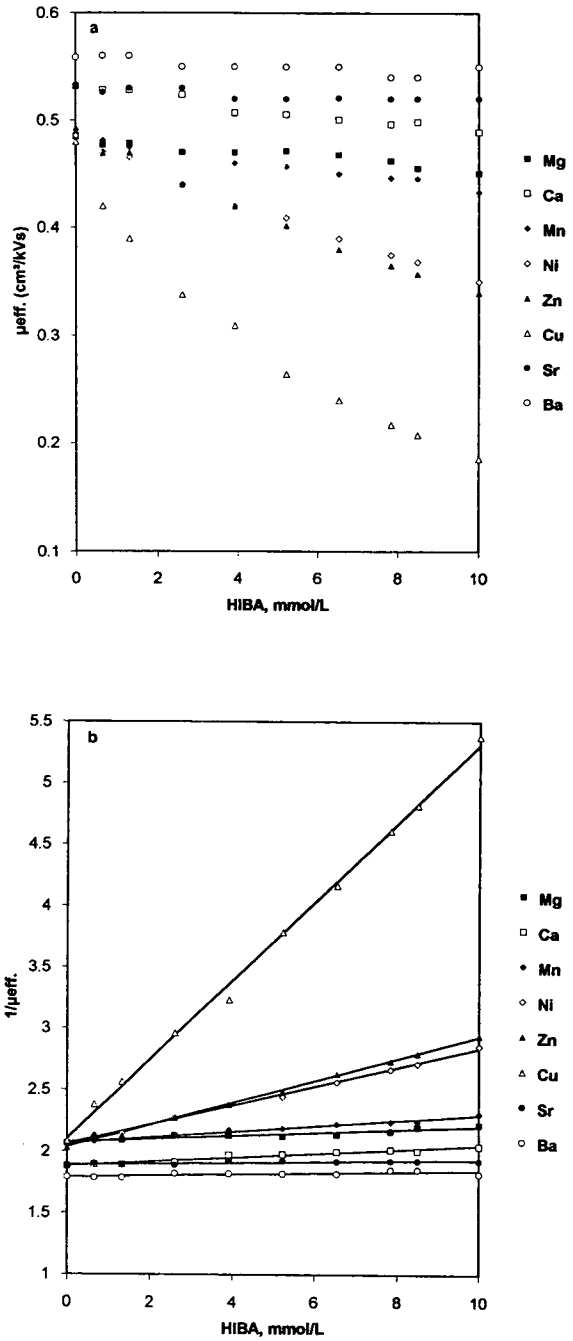

Fig. 1. (a) Electrophoretic mobility dependence of twelve inorganic cations on the concentration of HIBA. (b) Plot of reciprocal mobilities ($1/\mu_{eff.}$) against concentration of HIBA. Experimental conditions: applied voltage, +20 kV; hydrostatic injection from a 10-cm height for 30 s; background electrolyte, 5 mmol/l imidazole (pH 4.5).

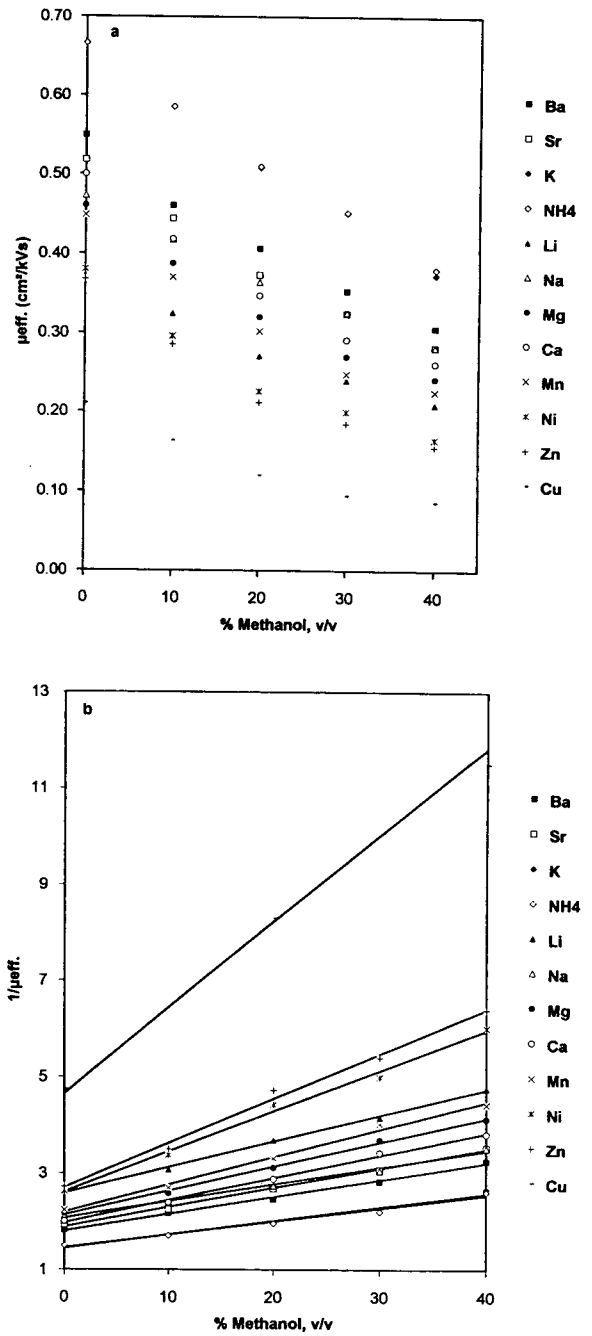

Fig. 2. (a) Electrophoretic mobility dependence of twelve inorganic cations on the fraction of methanol. (b) Plot of reciprocal mobilities ($1/\mu_{eff.}$) against fraction of methanol. Experimental conditions: applied voltage +20 kV; hydrostatic injection from a 10-cm height for 30 s; background electrolyte; 5 mmol/l imidazole–6.5 mmol/l HIBA (pH 4.5).

methanol concentration. The electrophoretic mobilities of all the inorganic cations decrease as the fraction of methanol in water increases. For some of the divalent cations such as Cu^{2+}, Zn^{2+}, Ni^{2+} and Mn^{2+}, non-linear relationships are obvious. A similar effect of organic solvents on retention times has been observed in RPLC [27].

β_{MS} is expected to be small because the interaction between the cations and methanol is of the ion–dipole type [19], which is very weak (the calculated interaction constants are less than 0.1; see later). The mobilities of the solvated cations are expected to be smaller than those of the bare cations. Therefore, $\mu_{MS}\beta_{MS}[S]$ may be much smaller than μ_0.

Accordingly, in the absence of a polyether, Eq. 14 can be rearranged in a linear form as

$$\frac{1}{\mu_{eff.}} = \frac{1 + \alpha_L \beta_{ML}[HL]}{\mu_0} + \frac{\beta_{MS}}{\mu_0} \cdot [S] \qquad (17)$$

The term $1 + \alpha_L \beta_{ML}[HL]$, is a constant as the pH and [HL] were not changed in this set of experiments. This is verified in Fig. 2b, where a linear relationship between the reciprocal of $\mu_{eff.}$ and methanol concentration is obtained for all of the cations. The values of β_{MS} can be estimated from the straight lines.

4.3. Effect of 18-crown-6 on migration

The experiments were conducted at a HIBA concentration of 6.5 mmol/l and at 20% (v/v) methanol (pH 4.5). As shown in Fig. 3a, the mobility of K^+ decreases continuously with an increase in the concentration of 18-crown-6, whereas the mobilities of Sr^{2+} and Ba^{2+} first decline rapidly and then level off when the concentration increases further, which must be due to saturation phenomena. The mobilities of the other cations are not significantly affected by the polyether. Na^+ is given as an example.

When plotting $1/\mu_{eff.}$ of K^+, Sr^{2+} and Ba^{2+} as a function of the 18-crown-6 concentration, curved lines are observed, suggesting that no simplification can be made (Fig. 3b).

From the above analysis, separately examining the migration dependence on HIBA, 18-crown-6

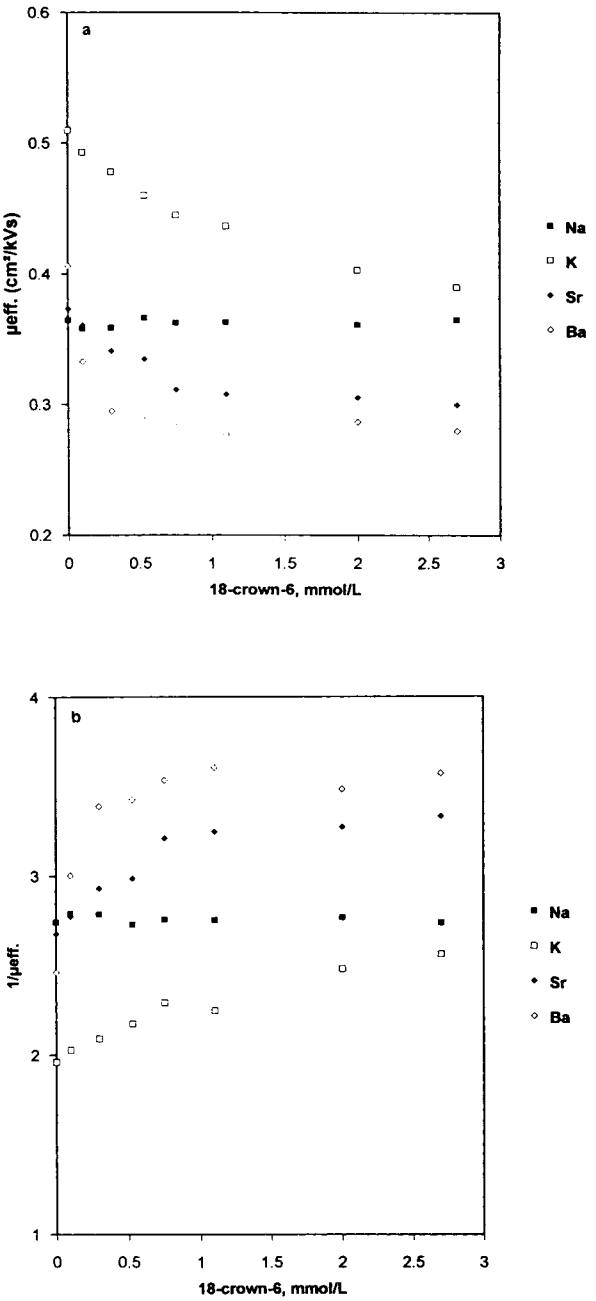

Fig. 3. (a) Electrophoretic mobility dependence of four inorganic cations on the concentration of 18-crown-6. (b) Plot of reciprocal mobilities ($1/\mu_{eff.}$) against concentration of 18-crown-6. Experimental conditions: applied voltage +20 kV; hydrostatic injection from a 10-cm height for 30 s; background electrolyte, 5 mmol/l imidazole–6.5 mmol/l HIBA–20% (v/v) methanol (pH 4.5).

and methanol, the twelve inorganic cations are classified into three groups according to their electrophoretic behaviour and for each of the groups a characteristic migration model is derived from Eq. 14:

(1) Na^+, NH_4^+ and Li^+:

$$\mu_{eff.} = \frac{\mu_0}{1 + \beta_{MS}[S]} \quad (18)$$

Only methanol affects their electrophoretic mobilities.

(2) Mg^{2+}, Mn^{2+}, Ca^{2+}, Ni^{2+}, Zn^{2+} and Cu^{2+}:

$$\mu_{eff.} = \frac{\mu_0}{1 + \beta_{ML}\alpha_L\text{-}[HL] + \beta_{MS}[S]} \quad (19)$$

Both HIBA and methanol influence their electrophoretic mobilities and manipulation of the concentration of the two reagents can subsequently modify the selectivity.

(3) Ba^{2+}, Sr^{2+} and K^+:

$$\mu_{eff.} = \frac{\mu_0 + \beta_{MC}\mu_{MC}[C]}{1 + \beta_{MC}[C] + \beta_{ML}\alpha_L\text{-}[HL] + \beta_{MS}[S]} \quad (20)$$

For K^+, $\beta_{ML} = 0$. The mobilities of Ba^{2+} and Sr^{2+} are mainly affected by the polyether and by methanol. The effect of HIBA is only minor, as shown in Fig. 1.

4.4. Estimation of the parameters in the migration equations

The parameters in Eqs. 18–20 were estimated by non-linear regression. The initial values of the parameters required by the regression were obtained from the straight-line plots in Figs. 1b and 2b. We did not find a significant effect of the initial values on the estimation of the parameters.

The parameters are listed in Tables 1–4. Some literature values are also presented for comparison.

The calculated μ_0 is in good agreement with the experimentally obtained value. These values are lower than the values in the literature [28], but the sequence is the same as for those reported values. This may be due to the fact that

Table 1
Calculated electrophoretic mobilities (Calc.) compared with experimentally obtained mobilities (Exp.) and literature values [8,28]

Ion	μ_0(cm²/kV·s)			
	Calc.[a]	Exp.	Ref. [28]	Ref. [8]
Li^+	0.382 ± 0.012	0.382	0.402	0.39
Na^+	0.481 ± 0.011	0.473	0.521	0.48
NH_4^+	0.689 ± 0.019	0.667	0.764	
K^+	0.677 ± 0.021	0.688	0.764	0.68
Mg^{2+}	0.482 ± 0.005	0.485	0.551	
Ca^{2+}	0.532 ± 0.005	0.532	0.618	
Sr^{2+}	0.530 ± 0.006	0.532	0.616	
Ba^{2+}	0.559 ± 0.006	0.559	0.661	
Mn^{2+}	0.484 ± 0.006	0.488		
Ni^{2+}	0.485 ± 0.006	0.486		
Zn^{2+}	0.491 ± 0.008	0.493		
Cu^{2+}	0.470 ± 0.020	0.480		

[a] In the calculation of the parameters, all the concentrations are in mol/l. Values given are means ± S.E. ($n = 23$).

Table 2
Calculated formation constants (log β_{ML}) of the inorganic cations with HIBA and literature values [18]

Ion	Calculated log β_{ML}[a]	Ref. [18]		
		Log β_{ML}	Log β_{ML2}	Log β_{ML3}
Mg^{2+}	0.89 ± 0.14	0.81	1.47	
Ca^{2+}	1.06 ± 0.09	0.92	1.42	
Sr^{2+}	0.46 ± 0.28	0.55	0.73	
Ba^{2+}	0.59 ± 0.21	0.36	0.51	
Mn^{2+}	1.17 ± 0.07	0.96	1.54	1.56
Ni^{2+}	1.69 ± 0.04	1.67	2.80	2.84
Zn^{2+}	1.76 ± 0.04	1.71	3.01	
Cu^{2+}	2.31 ± 0.06	2.74	4.34	4.38

[a] See Table 1.

Table 3
Calculated formation constants (log β_{MC}) of the inorganic cations with 18-crown-6 and literature values [31,32] and the mobilities of these ions bound to 18-crown-6 (μ_{MC})

Ion	Log β_{MC}[a]	Ref. [31]	Ref. [32]	μ_{MC}
K^+	2.86 ± 0.30	2.03	2.1	0.31
Sr^{2+}	3.35 ± 0.20	2.72	2.9	0.28
Ba^{2+}	4.27 ± 0.13	3.87	4.1	0.28

[a] See Table 1.

Table 4
Calculated interaction constants (β_{MS}) of the inorganic cations with methanol and ionic radii [28]

Ion	β_{MS}[a]	r(pm) [28]
NH_4^+	0.077 ± 0.007	
Li^+	0.079 ± 0.008	60
Na^+	0.067 ± 0.006	95
K^+	0.071 ± 0.009	133
Mg^{2+}	0.095 ± 0.005	65
Ca^{2+}	0.098 ± 0.004	99
Sr^{2+}	0.082 ± 0.004	113
Ba^{2+}	0.076 ± 0.004	135
Mn^{2+}	0.109 ± 0.006	91
Ni^{2+}	0.168 ± 0.009	70
Zn^{2+}	0.189 ± 0.015	74
Cu^{2+}	0.366 ± 0.091	72

[a] See Table 1.

μ_0 in our case was obtained in an electrolyte buffer with an organic compound (5 mmol/l imidazole). This buffer may have a higher viscosity than pure water. As the electrophoretic mobility is inversely proportional to the viscosity of the medium, a decreased mobility can result. A lower mobility was also observed by Vogt and Conradi [16] and ascribed to the adsorption of non-complexed cations on the negatively charged capillary wall. In fact, the electrophoretic mobility usually found in standard tables [28,29] is a physical constant determined for full solute charge and extrapolated to infinite dilution. The calculated mobilities for Li^+, Na^+ and K^+ are in good agreement with the values reported by Beck and Engelhardt [8]. They obtained the mobilities in a 5 mmol/l imidazole background electrolyte buffer at pH 4.5 in CIE.

The calculated formation constants of the cations with HIBA (from Eqs. 18–20) are given in Table 2, and are in good agreement with the literature values [18]. The larger deviation in the formation constants of Ba^{2+} and Sr^{2+} with HIBA may be due to the fact that their effective mobilities change very slightly on adding HIBA to the electrolyte buffer.

All the experiments were performed at pH 4.5, where sufficient protonation of imidazole and dissociation of HIBA are guaranteed. In addition, the formation of hydroxides of the metal cations studied is negligible at this pH. Moreover, adsorption on the capillary wall may not be significant. The mole fraction of the conjugated base of HIBA, α_{L^-}, is calculated according to Eq. 6 using a pK_a of 3.971 [10] and equals 0.772 at pH 4.5. One should be aware that the real pK_a value is expected to be higher in a binary medium than in pure water [30], so the real mole fraction of L^- may be lower than 0.772. However, it was not found to cause a significant deviation, probably because the effect of pH on the cation mobility is secondary.

The calculated formation constants of K^+, Sr^+ and Ba^{2+} with 18-crown-6 ether are given in Table 3. The calculated values are higher than those reported in the literature [31,32]. On comparing Tables 1 and 3, it is seen that the cations bound to 18-crown-6 move towards the cathode at a mobility lower than the bare ones; this accounts for the decrease in effective mobility. It is also seen in Table 3 that the bound Sr^{2+} and Ba^{2+} have the same mobilities.

In Table 4, the calculated interaction constants between methanol and the cations along with the ionic radius obtained from Ref. [28] are listed. It is seen that within the same column of the Periodic Table (IA and IIA), the constants tend to decrease with increasing ionic radius. For group B, the constants tend to increase with decreasing radius. To our knowledge, these constants have not been reported previously. Fig. 4 shows a good correlation for the divalent cations between their formation constants with HIBA and their interaction constants with methanol.

4.5. Description of migration behaviour and optimization of separation

The validity of the proposed model was confirmed by comparing the calculated electrophoretic mobilities of the twelve cations with the observed values shown in Fig. 5. The slope of the best fit of the data computed with linear regression is 0.9978 ± 0.0081, which is not significantly different from 1; the intercept is 0.0009 ± 0.0034, which is not significantly different from 0. The line in Fig. 5 represents the case

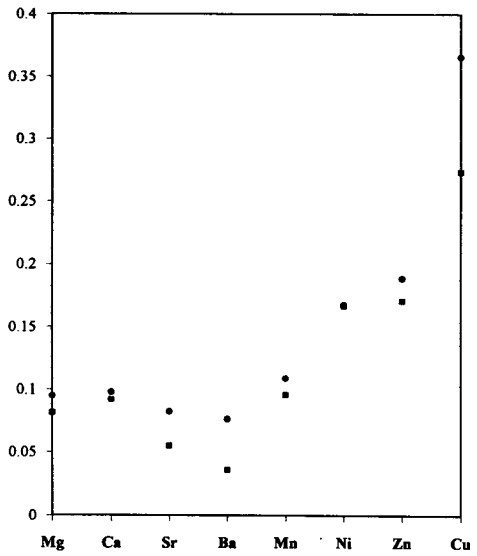

Fig. 4. Comparison for the divalent inorganic cations of the interaction constants with methanol and the formation constants with HIBA. ○ = β_{MS}; □ = 0.1 · log β_{ML}.

of perfect correlation. One concludes that the migration model represents the experimental data well.

Having obtained a migration model, one can try to predict the optimum separation in the whole experimental domain. To find the optimum experimental conditions, an optimization criterion is necessary. Different criteria have been used to find the optimum in capillary electrophoresis, such as the resolution between two adjacent peaks, R_s, the mobility ratio between two neighbouring solutes, α, and the mobility difference between two adjacent peaks, $\Delta\mu$, which is proportional to resolution. As peak cross-over is expected in this study, the absolute mobility difference is used. The optimization criterion is a mini-max criterion: one determines the absolute mobility difference of the worst separated pairs of ions, $|\Delta\mu_{min}|$, at each possible combination of the three variables and then determines the combination of the three variables for which a maximum $|\Delta\mu_{min}|$ is found.

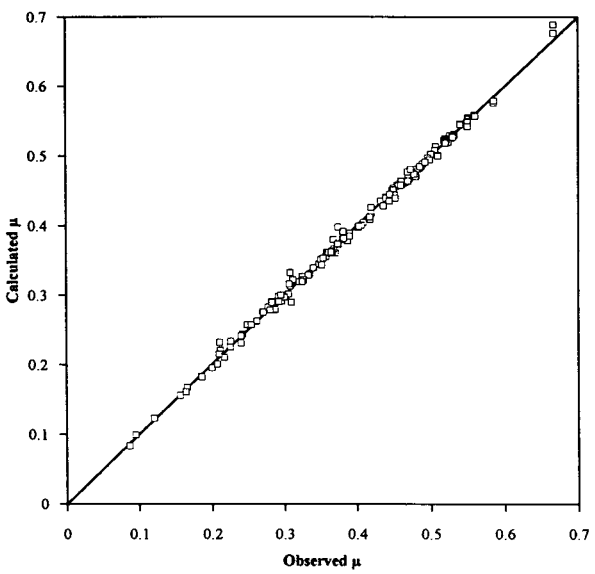

Fig. 5. Correlation plot of observed and predicted ionic mobilities of the cations (μ in $cm^2/kV \cdot s$).

Fig. 6a shows a contour plot of $|\Delta\mu_{min}|$ as a function of the concentration of HIBA and methanol concentration. It is seen that the higher $|\Delta\mu_{min}|$ values are located at higher concentrations of HIBA and medium methanol concentration. Fig. 6b shows a contour plot of $|\Delta\mu_{min}|$ as a function of the concentration of 18-crown-6 and methanol concentration at 6.5 mmol/l HIBA. In regions A and B, the best separations are predicted. Fig. 7 shows the separation of the twelve inorganic cations under the experimental conditions close to A, namely 6.5 mmol/l HIBA, 0.53 mmol/l 18-crown-6 and 20% (v/v) methanol. Baseline separation of the cations, including one additional ion (Cr^{3+}), is achieved.

As seen from Fig. 6b, when the methanol concentration is kept constant, $|\Delta\mu_{min}|$ does not change significantly if the concentration of 18-crown-6 increases over ca. 1 mmol/l. This is due to the mobilities of Sr^{2+} and Ba^{2+} having reached a more or less constant value in that the chemical equilibrium is saturated. Further increases in the concentration of 18-crown-6 only change the K^+ mobility, which does not influence the separation. On the other hand, on increasing the fraction of methanol while keeping the concentration of 18-crown-6 constant, $|\Delta\mu_{min}|$ changes in a non-continuous fashion. This is because the mobilities of Na^+, Ca^{2+},

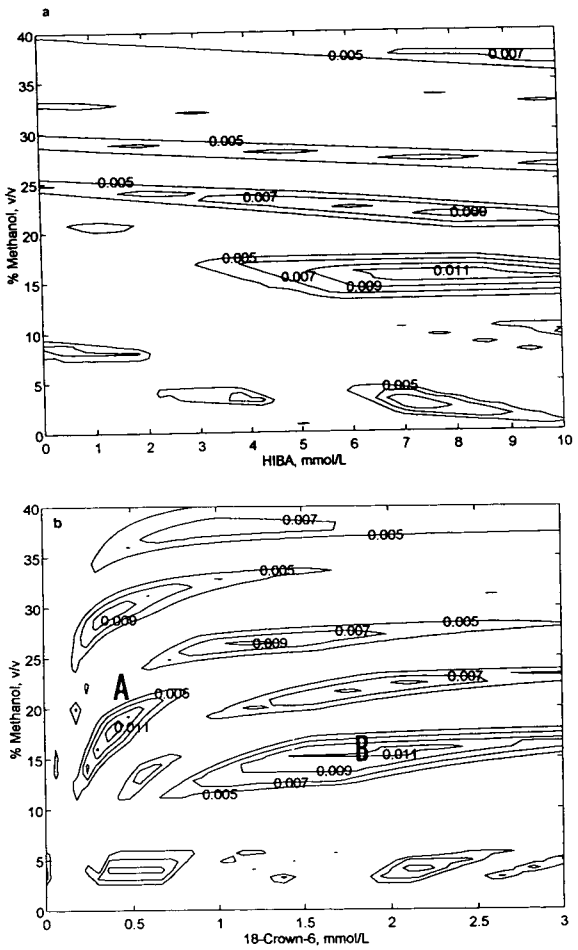

Fig. 6. (a) Plots presenting $|\Delta\mu_{min}|$ as a function of (a) methanol concentration and HIBA concentration and (b) methanol concentration and 18-crown-6 concentration. The lines delimit areas of equal $|\Delta\mu_{min}|$.

Mg^{2+}, Mn^{2+}, Li^+, Ni^{2+} and Zn^{2+} decrease with increasing fraction of methanol, so that these cations approach and cross over Sr^{2+} and Ba^{2+}, for which the mobilities are unchanged (see Fig. 8). Therefore, the concentration of methanol is critical for the separation and one should control this variable accurately to obtain a rugged separation.

Using the proposed model, the effect of methanol on the complexation of the inorganic cations with HIBA and 18-crown-6 can be simulated. As seen from Fig. 6, at high methanol concentrations (from 35 to 40%), $|\Delta\mu_{min}|$ hardly

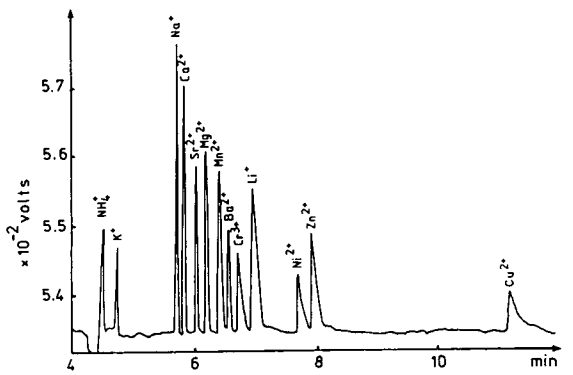

Fig. 7. Separation of a mixture containing NH_4^+, K^+, Na^+, Li^+, Mg^{2+}, Ca^{2+} and Cr^{3+} (2 μg/ml), Sr^{2+}, Ba^{2+}, Mn^{2+}, Ni^{2+} and Zn^{2+} (4 μg/ml) and Cu^{2+} (6 μg/ml). Experimental conditions: applied voltage +20 kV; hydrostatic injection from a 10-cm height for 20 s; $I \approx 6.0$ μA; $T \approx 23$°C; background electrolyte 5 mmol/l imidazole–6.5 mmol/l HIBA–20% (v/v)–methanol and 0.53 mmol/l 18-crown-6 (pH 4.5).

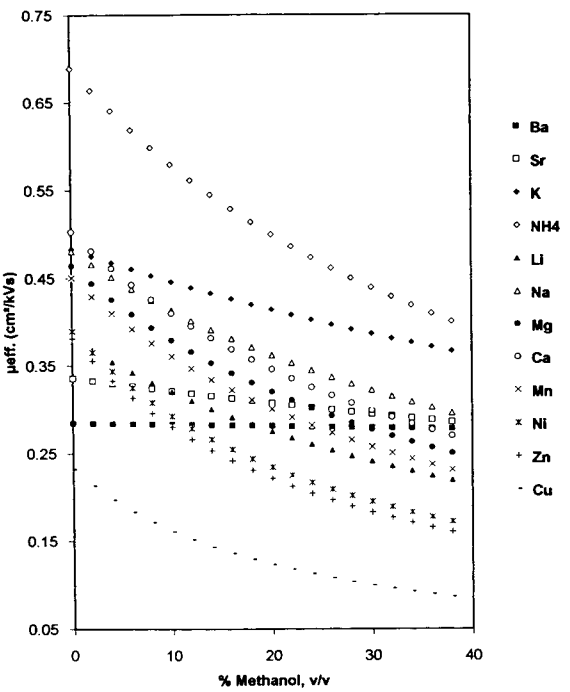

Fig. 8. Simulated change in electrophoretic mobilities of twelve inorganic cations as a function of methanol concentration at 6.5 mmol/l HIBA and 1.5 mmol/l 18-crown-6.

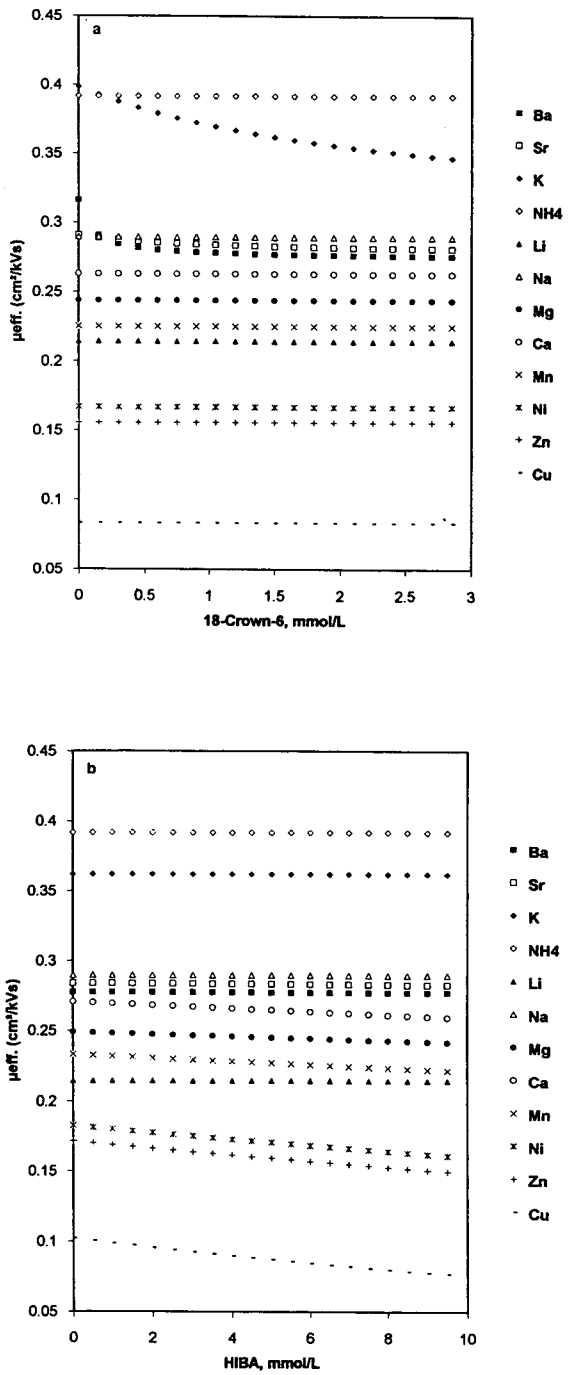

Fig. 9. Simulation of migration behaviour of twelve inorganic cations at a high fraction of methanol in water (40%, v/v) as a function of (a) 18-crown-6 concentration (6.5 mmol/l HIBA) and (b) HIBA concentration (1.5 mmol/l 18-crown-6).

changes. This is seen more clearly in Fig. 9a. At 40% methanol, the mobilities of Sr^{2+} and Ba^{2+} change slightly at concentrations of 18-crown-6 less than ca. 0.3 mmol/l, but they remain constant as the concentration of 18-crown-6 increases further. Sr^{2+} and Ba^{2+} are located between Na^{+} and Ca^{2+}. The Ba–Sr or Na–Sr distance determines $|\Delta\mu_{min}|$, which, however, does not vary any more in the presence of high concentrations of methanol. The selectivity gained from the inclusion complexation is therefore lost in this situation.

A similar effect was observed for HIBA, as shown in Fig. 9b, where the mobilities of the divalent cations do not change or change only slightly with increasing concentration of HIBA. Probably, methanol molecules interact with the cations in a direct way and most of the cations may have been solvated by the solvent molecules. The solvation competes for the cations with HIBA and 18-crown-6, resulting in a decrease in the apparent formation constants of the cations with HIBA and 18-crown-6. In this case, the selectivity is determined by methanol, which is insufficient, however, to separate all of the cations. We did observe this in a separate experiment, where there was no separation of Sr^{2+} and Na^{+} in the presence of 6.5 mmol/l HIBA and 40% methanol. Therefore, one should avoid too high a fraction of methanol when relatively weak complexing reagents are used.

5. Conclusions

Based on multiple chemical equilibria, a migration model was designed that describes the migration of inorganic cations in terms of absolute mobility, complex formation constants, the concentrations of complexing reagents and the fraction of organic solvent in the electrolyte buffer. This electrolyte buffer was composed of HIBA, 18-crown-6 and methanol together with a UV-absorbing substance, imidazole. Good agreement was achieved between theoretical predictions and experimental data. By applying this model, the separation of twelve inorganic cations was optimized. The selectivity of the separation

gained from complexation deteriorated when the ratio of methanol to water in the electrolyte buffer was too high (40%, v/v), as methanol decreases the apparent complex formation constants.

References

[1] P. Jandik, W.R. Jones, A. Weston and R.P. Brown, LC·GC, 5 (1991) 20.
[2] P.E. Jackson and P.R. Haddad, *Trends Anal. Chem.*, 12 (1993) 231.
[3] P. Jandik and G. Bonn, *Capillary Electrophoresis of Small Molecules and Ions*, VCH, New York, 1993.
[4] C.A. Monning and R.T. Kennedy, *Anal. Chem.*, 66 (1994) 280R.
[5] W.G. Kuhr and E.S. Yeung, *Anal. Chem.*, 63, (1991) 275A.
[6] F. Foret, S. Fanali, L. Ossicini and P. Bocek, *J. Chromatogr.*, 470 (1989) 299.
[7] V. Sustacek, F. Foret and P. Bocek, *J. Chromatogr.*, 545 (1991) 239.
[8] W. Beck and H. Engelhardt, *Chromatographia*, 33 (1992) 313.
[9] Q. Yang, M. Jimidar, T. Hamoir, J. Smeyers-Verbeke and D.L. Massart, *J. Chromatogr.*, *A*, 673 (1994) 275.
[10] Q. Yang, J. Smeyers-Verbeke, W. Wu, M.S. Koths and D.L. Massart, *J. Chromatogr.*, *A*, 688 (1994) 339.
[11] A. Weston, P.R. Brown, A.L. Heckenberg, P. Jandik and R. Jones, *J. Chromatogr.*, 602 (1992) 249.
[12] S. Motomizu, S. Nishimura, Y. Obata and H. Tanaka, *Anal. Sci.*, 7 (1991) 253.
[13] T. Hirokawa, N. Aoki and Y. Kiso, *J. Chromatogr.*, 312 (1984) 11.
[14] D.F. Swaile and M.J. Sepaniak, *Anal. Chem.*, 63 (1991) 179.
[15] C. Quang and M.G. Khaledi, *J. Chromatogr. A*, 659 (1994) 459.
[16] C. Vogt and S. Conradi, *Anal. Chim. Acta*, 294 (1994) 145.
[17] R.S. Sahota and M.G. Khaledi, *Anal. Chem.*, 66 (1994) 1141.
[18] J. Inczédy, in J. Tyson (Editor), *Analytical Application of Complex Equilibria*, Ellis Horwood, Chichester, 1976, p. 347.
[19] K. Bächmann, J. Boden and I. Haumann, *J. Chromatogr.*, 626 (1992) 259.
[20] K. Fukushi and K. Hiiro, *J. Chromatogr.*, 523 (1990) 281.
[21] R.T. Morrison and R.N. Boyd, *Organic Chemistry*, Allyn and Bacon, Boston, MA, 5th ed., 1987, ch. 6, p. 223.
[22] T. Okada and T. Usui, *Anal. Chem.*, 66 (1994) 1654.
[23] *SPSS/PC + Statistics 4.0*, SPSS, IL, 1990.
[24] *Matlab for Microsoft Windows*, MathWorks, 1992.
[25] I.M. Johansson, E.C. Huang, J.D. Henion and Z. Weigenbaum, *J. Chromatogr.*, 554 (1991) 331.
[26] G.M. Janini, K.C. Chan, J.A. Barnes, G.M. Muschik and H.J. Issak, *Chromatographia*, 35 (1993) 497.
[27] P.J. Schoenmakers and R. Tijssen, *J. Chromatogr. A*, 656 (1993) 577.
[28] R.C. Weast (Editor), *CRC Handbook of Chemistry and Physics*, CRC Press, Boca Raton, FL, 67th ed., 1986.
[29] D.N. Heiger, *High Performance Capillary Electrophoresis–An Introduction*, Hewlett-Packard, Waldbronn, 1992, ch. 2, p. 15.
[30] H. Freiser, *Concepts and Calculations in Analytical Chemistry. A Spreadsheet Approach*, CRC Press, Boca Raton, FL, 1992, ch. 2, p. 34.
[31] R.M. Smith and A.E. Martell, *Critical Stability Constants*, Plenum Press, New York, 1975.
[32] R.M. Izatt, K. Pawlak, J.S. Bradshaw and R.L. Bruening, *Chem. Rev.*, 91 (1991) 1721.

ELSEVIER

Journal of Chromatography A, 706 (1995) 517–526

JOURNAL OF CHROMATOGRAPHY A

Separation of metal cations by electrophoresis in a positively charged coated capillary

Kezhan Cheng, Zhongxi Zhao, Richard Garrick, Francis R. Nordmeyer, Milton L. Lee, John D. Lamb*

Department of Chemistry, Brigham Young University, Provo, UT 84602, USA

Abstract

In the expanding field of capillary electrophoresis, the use of coated capillaries is becoming more widespread. Application of a thin polymer coating on the surface of the silica capillary wall makes it possible to generate a capillary wall of positive or no charge when using a typical buffer of a pH of 5.0 to ca. 6.0, thereby altering the electroosmotic flow. Indeed, when a coating is used which carries a positive charge under appropriate buffer conditions, the electroosmotic flow is reversed from the normal direction. This reversal increases the migration times of metal cations and also improves separation efficiency. In this work, a positively charged coated capillary was used with a 2-aminopyridine buffer system for the separation of metal cations. Separations using this system compared favorably with other published results. The positively charged coated column yielded cation separations superior to those obtained with uncoated columns. This system proved effective for the separation of many cations, including lanthanides.

1. Introduction

Fused-silica capillaries are the most common columns used in capillary electrophoresis (CE) separations. Resolution is the function of the column efficiency, N, and relative migration velocity, $\Delta U/U_A$, expressed as $R_s = 1/4n^{1/2}(\Delta U/U_A)$ [1]. For biological samples, such as proteins or amino acids, there are two means by which higher resolution can be achieved. First, since the species of interest are often negatively charged, the electroosmotic flow (EOF) moves in a direction opposite that of the analytes, causing a large relative velocity difference. Second, biochemical analytes have large molecular masses and correspondingly small diffusion coefficients which contribute to a high theoretical plate number. By contrast, in metal cation separations, the EOF is codirectional with species migration, and band broadening results from the relatively high axial diffusion of the low-molecular-mass cations. If the EOF can be effectively decreased or reversed in direction so that it moves opposite the cations, then resolution can be increased due to the increase in $\Delta U/U_A$. Coating of the inner capillary wall is a technique commonly used to change the surface characteristic of such columns in order to bring out the desired change of EOF.

Capillary column technology for chromatography advanced significantly in the early 1980s. The chemistry involved in the production of

* Corresponding author.

0021-9673/95/$09.50
SSDI 0021-9673(94)01152-4

state-of-the art capillary columns for gas chromatography has been studied and reported in detail [2,3]. The fundamental physical and chemical properties of the capillary surface, the techniques of chemical modification of the capillary surface, and the production of uniform and stable stationary phase films have been described. Coated columns are commonly used in CE analysis of biological samples to increase separation efficiency and resolution [4,5]. Up to now, few cation separations by CE have adopted these column alteration techniques. C_1- and C_{18}-saturated hydrocarbon coatings were applied by Chen and Cassidy [6]. In their work with 75 μm I.D. C_{18}-coated capillaries, comparison of the heights equivalent to a theoretical plate (HETP values) suggested that the overall column efficiencies were smaller than those for an uncoated capillary. The interactions between the silica surface and the positively charged ions were reduced due to the hydrophobic coating. In their experiments, adsorption of the larger hydrophobic ions and associated peak tailing were observed. In this work we describe the use of coated capillaries in the separation of metal cations, and compare our results with other published metal cation separations by capillary electrophoresis.

2. Experimental

2.1. Apparatus

The following equipment was used in this research: Metrohm 654 pH Meter (Brinkmann, Metrohm, Switzerland); fused-silica capillaries (Polymicro Technologies, Phoenix, AZ, USA); CE system CES-1 (Dionex, Sunnyvale, CA, USA); Milli-Q water system (Millipore, Milford, MA, USA).

Metal cations were indirectly detected on-column by UV absorbance at 214 nm. Data were collected with Dionex AI400 and AI450 software together with a Model SP4270 integrator (Spectra-Physics, San Jose, CA, USA).

2.2. Materials

3-Aminopropyltrimethoxysilane (Aldrich) was used for the capillary coating The commercial 2-aminopyridine used to make the buffer was pale yellow. Therefore it was recrystallized in cyclohexane to yield white, flaky crystals. 2-Aminopyridine (0.941 g) was dissolved in water to produce 100 ml of buffer solution. To make the pH adjustment solution, acetic acid (99%) was diluted 10-fold. Buffer solutions of 15 m*M* 2-aminopyridine/acetate were prepared by diluting 2-aminopyridine stock solution and adjusting pH to 5.0 using the diluted acetic acid solution. In the separations of lanthanide samples, 2-hydroxyisobutyric acid (HIBA) (3.5 m*M*) was included in the buffer. The composition and pH of 2-aminopyridine/acetate buffer have been optimized for cation separations [7].

The 1.00 mg/ml metal cation standard solution was made by dissolving the appropriate weights of the nitrates of K^+, Na^+, Li^+, Mg^{2+}, Ca^{2+}, Ba^{2+}, Mn^{2+}, Zn^{2+}, Cd^{2+}, Cr^{3+} and lanthanides in 2% nitric acid.

All above solutions were prepared with deionized water (18 mΩ cm). Before use, all solutions were filtered through a 0.45-μm cellulose acetate membrane and degassed in an ultrasonic bath.

2.3. Preparation of coated columns

Several coated capillaries with different surface charges were prepared as previously described [8]. The coatings are listed in Table 1. In brief, the positively charged capillaries were prepared by the following steps: the capillaries were treated with deionized water (18 MΩ cm) before coating in order to ensure uniform distribution of silanol groups on the silica surface. The capillaries were filled with deionized water, then drained and sealed under nitrogen. They were then heated at 250°C for 2 h to increase the population of silanol groups on the surface. The capillaries were opened and purged with nitrogen for 1 h. The coating solutions consisted of varying amounts of 3-aminopropyltrimethoxysilane in methylene chloride. The capillaries

Table I
Capillary coatings

Name	Coating material	Description
Superox 4	Polyethylene glycol	Neutral
	Acryloyl-amido-2-2-methylpropanesulfonic acid	Negative charge
	3-Aminopropyltrimethoxysilane	Positive charge

were filled with coating solution and statically coated [9] at 40°C. The coated capillaries were purged with nitrogen for 1 h at 40°C and heated to 120°C under nitrogen pressure for 2 h to cross-link and bond the 3-aminopropyltrimethoxysilane on the surface. Before installing a coated capillary in the CE system, it underwent a rinsing process using 5-ml quantities each of methylene chloride, methanol and deionized water, in that order.

3. Results and Discussion

3.1. Selection of capillary coating

One method to modify the EOF in the capillary involves application of different coating materials to alter the surface charge on the capillary wall. A negatively charged capillary generates an EOF toward the cathode, while a positively charged capillary generates an electroosmotic flow toward the anode. The EOF, in turn, affects the separation. Fig. 1 shows electropherograms of the same metal cation standard using capillaries with coatings of different charge. The capillaries with charged coatings did not achieve good separations for biological samples [10]. However, we found that the column with the positive coating retained the cationic species much longer than the either the uncoated or neutral coated column. The uncoated column, on the other hand, unexpectedly retained the cations longer than the neutral coated column. No reasonable explanation for this anomaly has been found, and it will be the subject of future investigation.

The variation of separation efficiency determined from different cation peaks using different capillary coatings was measured in terms of theoretical plate numbers (Fig. 2). The positively charged coating (3-aminopropyltrimethoxysilane) gave higher efficiency than the uncoated column for most of the metal cations tested. The increase in plate number resulted from the repulsive force between the respective positive charges of the cations and of the capillary surface. The neutral polymer coating increased the plate number for the later peaks in the electro-

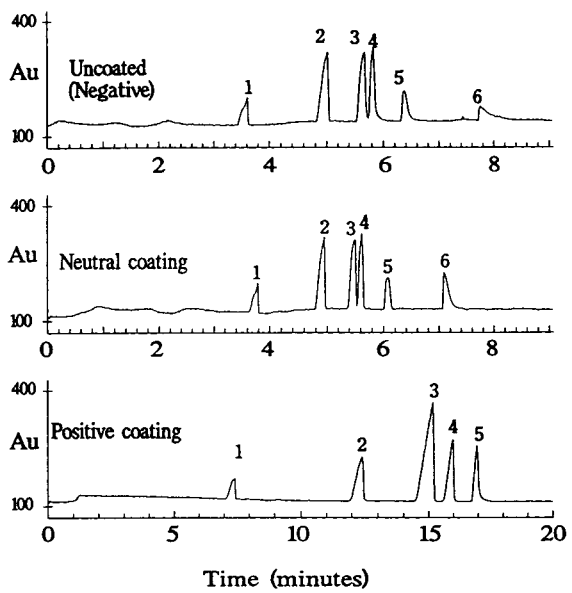

Fig. 1. Electropherograms of the separation of K^+, Ca^{2+}, Mn^{2+}, Zn^{2+}, Cd^{2+} and Cu^{2+} (which are labeled peaks 1, 2, 3, 4, 5 and 6, respectively) with different coated capillaries: neutral coating is polyethylene glycol; positive coating is 3-aminopropyltrimethoxysilane. Conditions: 15 m*M* 2-aminopyridine acetate buffer, pH 5.0, 25 000 V, 80 cm × 75 μm I.D. fused-silica capillary, 100 mm gravity injection for 30 s and indirect detection at 214 nm.

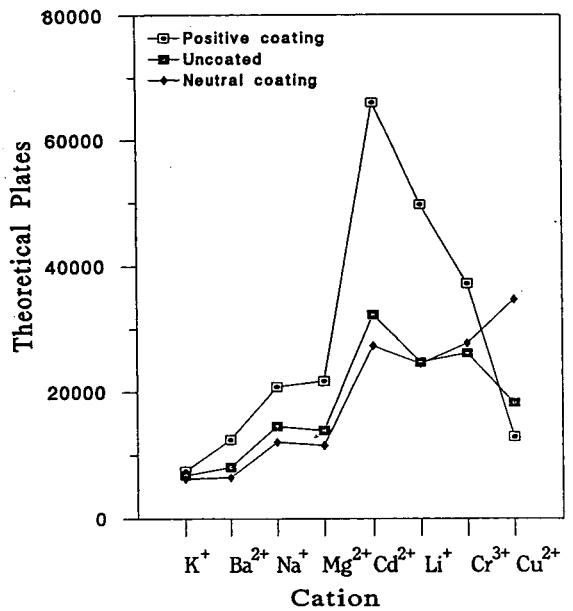

Fig. 2. Variation of separation efficiencies with different charged capillaries (the average of four determinations, standard deviation <3%). Neutral coating is polyethylene glycol; positive coating is 3-aminopropyltrimethoxysilane. Conditions as in Fig. 1.

pherogram because the interaction between the column wall and the cations was less than for a negatively charged wall surface. A negatively charged coating (sulfonic acid) was also evaluated. It yielded results similar to those of the uncoated capillary, as we expected. However, the later peaks in the electropherogram were more deformed than those using the uncoated capillary, so the corresponding results were not included in Fig. 2. Poor peak shapes were probably due to greater negative charge density which may have been present on the surface of the coated capillary. The positively charged capillary was selected for further experimentation, in part because of its superior separation efficiency.

Compared to uncoated capillaries, Chen and Cassidy's [6] C_{18}-coated capillaries yielded better peak resolution, although adsorption and peak tailing were observed for larger hydrophobic ions. In that work, the preparation of the C_{18}-coated capillary required two to three days. In contrast, the positively charged coating in our research is relatively simple and quick to prepare. Only 3 or 4 h were needed to apply a coating of 3-aminopropyltrimethoxysilane on the capillary wall. The resulting positively charged capillary provides improved separation efficiency and resolution in metal cation analysis over uncoated or C_{18}-coated columns. In contrast to the C_{18}-coated capillary, no adsorption of ions was observed in our experiments with the neutral coating, as indicated by the reproducibility of the cation migration times and by the peak shapes. In similar fashion, the statically coated capillaries did not display significant adsorption in protein separations reported in previous work [11]. Furthermore, using the 2-aminopyridine/acetate buffer and the positively charged capillary, we obtained a system which provided reproducible separation and high performance during hundreds of metal cation separation experiments.

3.2. The selection of coating solution concentration

A comparison was made of coated capillaries for which different 3-aminopropyltrimethoxysilane concentrations were used to prepare the columns. Fig. 3 shows that except in the case of Zn^{2+}, the separation efficiencies were similar for a given cation between different coating concentrations. The migration times of the cations changed with different capillary coating concentrations, but no variation was observed between 0.5 and 3.0 mg/ml (Fig. 4), which presents a reasonable working range. The variation of cation migration times is due to differences in EOF, as discussed in the next section. The cation bands broadened with increasing migration time, so the resolution of the peaks did not change significantly with coating concentration over the range 0.5–3.0 mg/ml.

The capillaries coated with the solution ranging from 0.5 to 3.0 mg/ml displayed similar metal cation separation behavior in terms of migration times and resolution. This behavior is due to similar EOFs, as will be discussed in more detail in the following section. Of these capillaries, the 2.0 mg/ml coated capillary was chosen

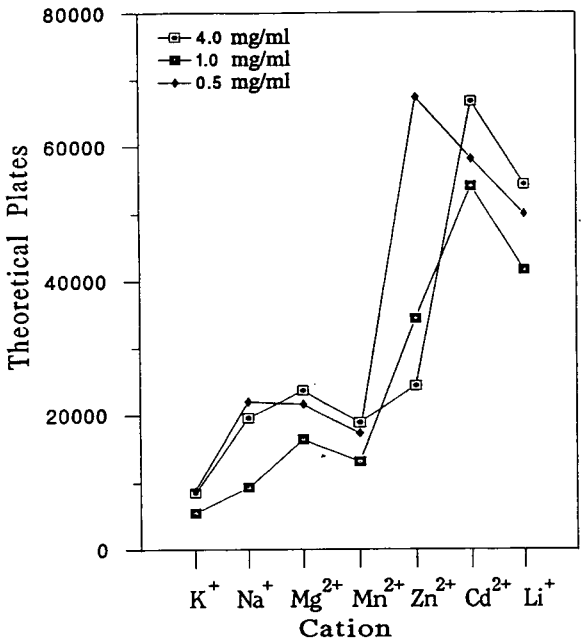

Fig. 3. Variation of separation efficiencies with capillaries coated by different concentrations of 3-aminopropyltrimethoxysilane (the average of four determinations, standard deviation <14%). Conditions as in Fig. 1.

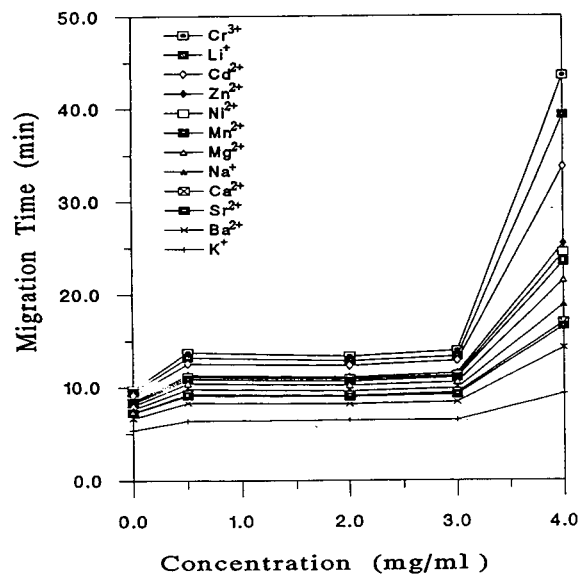

Fig. 4. Variation of cation migration times with capillaries coated with different concentrations of 3-aminopropyltrimethoxysilane. The standard deviation was <2.0%. Conditions as in Fig. 1.

for further investigation since it lies at the center of the acceptable working range.

3.3. Structure of the coating layer

The separation behavior of the coated column should be related to the properties of the coating surface. Generally in chromatography, coated columns are evaluated in terms of thickness, d_f, of the stationary phase, given by $d_f = cr/2000\rho$, where c is the concentration of the coating reagent, r is the column inside radius, and ρ is the density of the coating solution. However, this approach is not useful in CE because the capillary coating does not serve as a stationary phase. Specifically, only a portion of the coating solute was bound to the surface of the capillary as the solvent was evaporated because the bound portion is dependent on the reaction equilibrium. The remainder may have been washed away with the rinse. In CE, the separation behavior should be related to the percent of the capillary wall covered rather than to the coating thickness.

3.4. Electroosmotic flow

The concentration of coating solution should be related to the charge density on the column surface up to the point where the surface is completely covered. The charge density, in turn, can affect the direction and strength of the EOF. Using dimethylsulfoxide (DMSO) as the neutral marker, the EOF was observed to change direction when the capillary was coated with 3-aminopropyltrimethoxysilane. The rate of flow increased with the concentration of 3-aminopropyltrimethoxysilane coating solution, but not in a linear fashion (Fig. 5). This result accounts for the non-linearity in the change of cation migration times with coating (Fig. 4). The variation in cation migration times and in EOF could be caused by dynamic factors in the coating reaction or by technological factors in the column coating process. The dynamic factors could include the degree of activation of the original column surface, the evaporation rate of the solvent, and the temperature and flow-rate of the

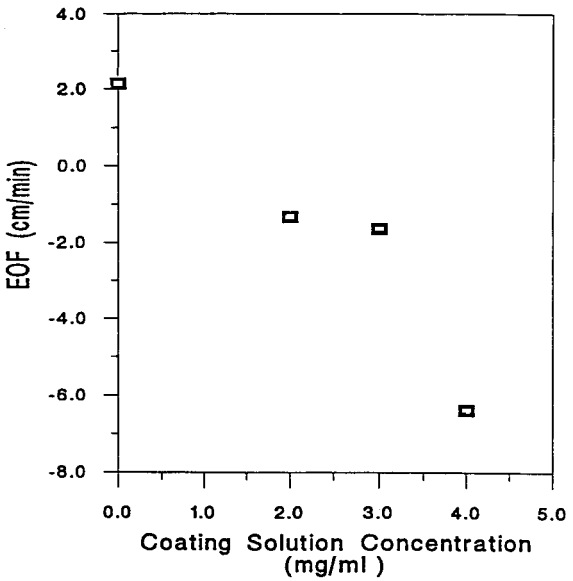

Fig. 5. Variation of electroosmotic flow (EOF) with capillaries coated using different concentrations of 3-aminopropyltrimethoxysilane (the average of six determinations, standard deviation <3%). Conditions: 15 m*M* 2-aminopyridine–acetate buffer, pH 5.0, 25 000 V, 80 cm × 75 μm I.D. fused-silica capillary, 100 mm gravity injection and indirect detection at 214 nm.

inert gas in the cross-linking reaction. The technological factors involve our ability to exactly reproduce the preparation of coating each time. Similar phenomena were observed in Chen and Cassidy's research [6], wherein the electroosmotic flow in a C_{18}-saturated hydrocarbon coated capillary varied with a relative standard deviation of 13%. This variation in coating efficiency has been noted in the reports of coated capillaries in gas chromatography [9] as well.

3.5. The selection of working voltage

The working voltage directly affects the migration of analytes and background electrolyte in the buffer, as well as the electroosmotic flow. Fig. 6 shows the effect of working voltage on the migration times of the metal cations using the 3-aminopropyltrimethoxysilane coated capillary. At working voltages of 18 000 and 22 000 V, a longer analysis time was needed than at higher

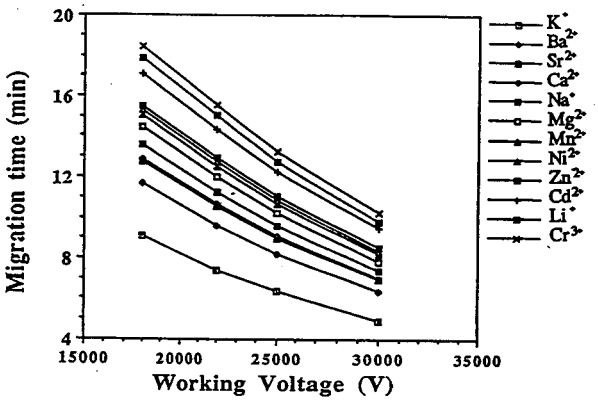

Fig. 6. Effect of working voltage on the migration times of the metal cations. Conditions as in Fig. 1.

voltage, with little variation in resolution between peaks. At 30 000 V working voltage, the resolution decreased between Sr^{2+} and Ca^{2+}, even though the analysis time shortened (Fig. 7). A similar situation was observed by Beck and Engelhardt [12]. A working voltage of 25 000 V was selected as optimal for our experiments to maintain good resolution and short analysis time.

In a CE system, the working voltage is one parameter to be optimized. However, it was observed that the signal-to-noise ratio was affected primarily by the working *current*. In contrast to voltage, the resolution between peaks was not altered by the working current. When the working current was lower than 15 μA, the electropherograms had broad peaks and longer migration times. When the current was between 18 and ca. 20 μA, the electropherogram had normal peak shapes and shorter migration times. If the current increased over 22 μA, the analysis time was further shortened, but more noise appeared because of Joule heating effects [13]. A typical working current of between 18 and ca. 20 μA was observed with the 2-aminopyridine/acetate buffer under our experimental conditions.

3.6. Metal cation separations

Twelve metal cations, Li^+, Na^+, K^+, Mg^{2+}, Ca^{2+}, Sr^{2+}, Ba^{2+}, Cr^{3+}, Mn^{2+}, Ni^{2+}, Zn^{2+} and

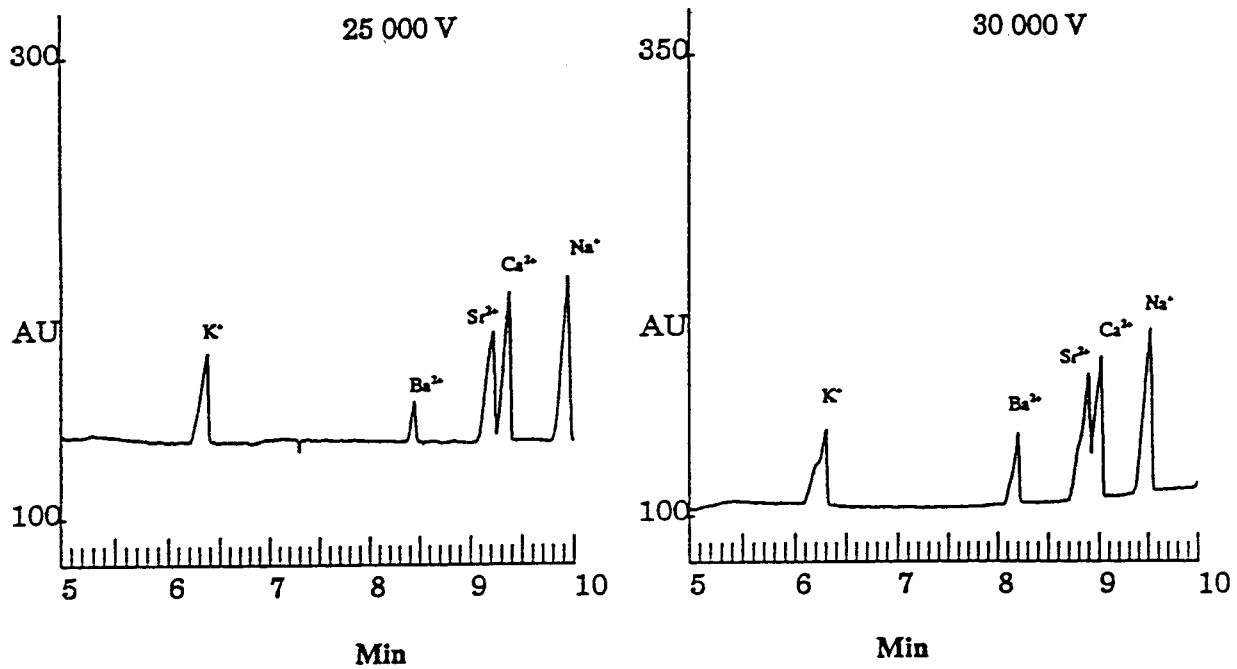

Fig. 7. Comparison of the resolution between the Sr^{2+} and Ca^{2+} peaks with different working voltages. Conditions as in Fig. 1.

Cd^{2+} were separated with baseline resolution using the 15 m*M* 2-aminopyridine/acetate buffer and the 2.0 mg/ml 3-aminopropyltrimethoxysilane coated capillary (Fig. 8, bottom). The concentrations of these cations were 5 μg/ml Na^+, K^+, Cr^{3+}, Mn^{2+}, Ni^{2+}, Zn^{2+} and Cd^{2+}; 8.5 μg/ml Ba^{2+}; 5.5 μg/ml Sr^{2+}; 2.5 μg/ml Ca^{2+}; 1.5 μg/ml Mg^{2+}; 1.0 μg/ml Li^+. This separation was achieved based on the effect of the positively charged coating on the EOF and on the mobility differences between the metal cations. Compared to uncoated capillaries, the positively charged capillary provided better resolution, although overall migration times increased. Fig. 8 compares the separation of a sample using an uncoated capillary (top) to that using a 2.0 mg/ml 3-aminopropyltrimethoxysilane coated capillary (bottom). A complete separation of twelve metal cations was achieved using the coated capillary with a longer total analysis time. Complete separation was not achieved by the uncoated capillary.

When we attempted to separate additional cations using the coated capillary, K^+ and NH_4^+ coeluted; however, when the concentrations of K^+ and NH_4^+ were diluted to lower than 0.1 μg/ml (close to the detection limit), K^+ and NH_4^+ were separated into two peaks. In the latter case, the difference in migration times was only 0.05 min (3 s). Other pairs of coeluted cations were Mn^{2+} and Fe^{2+}, Ni^{2+} and Co^{2+}, and Pb^{2+} and Cd^{2+}. Although a signal was obtained for Cu^{2+}, its migration time was so long (ca. 35–40 min) that axial diffusion produced a flat, large tailing peak.

Cation separations by the 3-aminopropyltrimethoxysilane coated capillary with the 2-aminopyridine/acetate buffer produced higher resolution but somewhat greater band broadening than with the uncoated capillary. As shown in Fig. 8, the twelve metal cations, Li^+, Na^+, K^+, Mg^{2+}, Ca^{2+}, Sr^{2+}, Ba^{2+}, Cr^{3+}, Mn^{2+}, Ni^{2+}, Zn^{2+} and Cd^{2+}, were separated in 14 mins. This separation has good resolution for all peaks, even though it requires a relatively longer analysis time due to the direction of the electroosmotic flow. This separation compares favorably to those reported elsewhere [14–17].

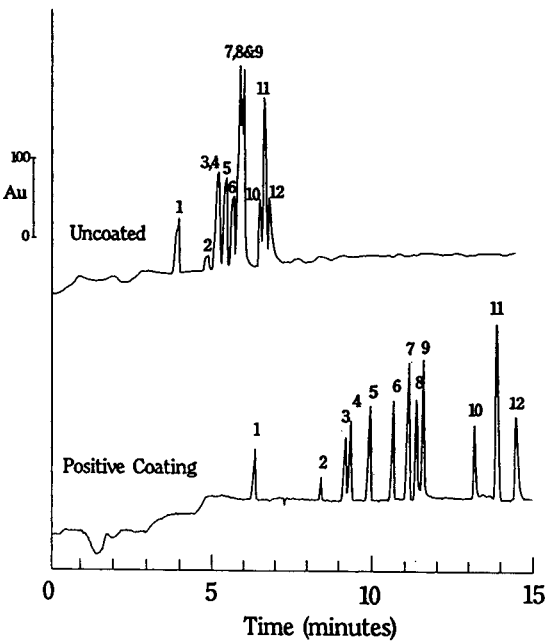

Fig. 8. Electropherogram comparing separations using an uncoated capillary (top) and a 2.0 mg/ml 3-aminopropyltrimethoxysilane coated capillary (80 cm × 75 μm I.D.) (bottom). Conditions as in Fig. 1. The peaks are K^+, Ba^{2+}, Sr^{2+}, Ca^{2+}, Na^+, Mg^{2+}, Mn^{2+}, Ni^{2+}, Zn^{2+}, Cd^{2+}, Li^+ and Cr^{3+} from 1 to 12 in order.

3.7. Quantitative analysis

Simultaneous, quantitative analysis of the twelve metal cations listed above was achieved by our method. The equations of the calibration curves, correlation coefficients, average standard deviations, and detection limits for these cations are listed in Table 2. Chen and Cassidy [6] observed that the signal-to-noise ratio obtained with a neutrally coated capillary was similar to that obtained with the uncoated capillary at pH 4.5 to ca. 5.0. In our experiments, the linear range of quantitative analysis and the detection limits of the positively charged capillary were superior to those of the uncoated capillary.

The sensitivity of our system was superior to that reported by others [12,15,16,18]. The principal reason for this result is that stacking efficiency, which focuses the sample zone into a narrow band, was more effective in the positively charged column than in the uncoated columns because the EOF was in the direction opposite to that of cation migration. Furthermore, baseline noise with the positively charged column was lower than with the uncoated column, resulting in a better signal-to-noise ratio. For the metal cations studied, the detection limits with the

Table 2
Parameters for quantitative analysis using 2 mg/ml 3-aminopropyltrimethoxysilane coated capillary

Ions	EC	r^2	R.S.D. (%)	DL (μg/ml)
Li^+	$y = 11.971 + 429.74x$	1.000	2.8	0.02
Na^+	$y = -10.971 + 52.054x$	1.000	1.4	0.08
K^+	$y = 13.069 + 27.265x$	1.000	2.0	0.03
Mg^{2+}	$y = -13.018 + 170.20x$	1.000	1.4	0.02
Ca^{2+}	$y = 7.8364 + 72.381x$	0.999	1.0	0.02
Sr^{2+}	$y = -9.3126 + 46.665x$	1.000	2.1	0.15
Ba^{2+}	$y = 16.400 + 4.1449x$	0.999	6.6	0.34
Cr^{3+}	$y = -17.566 + 61.992x$	1.000	2.4	0.15
Mn^{2+}	$y = -59.695 + 87.821x$	0.998	1.8	0.08
Ni^{2+}	$y = -51.144 + 67.331x$	0.999	1.2	0.35
Zn^{2+}	$y = 36.546 + 63.778x$	0.998	3.2	0.20
Cd^{2+}	$y = 5.2129 + 36.206x$	0.998	5.7	0.35

EC = Equations of calibration curves; y is absorbance and x is concentration (μg/ml); r^2 = correlation coefficient of the calibration curves; R.S.D. = relative standard deviation; DL = detection limit, signal-to-noise ratio 3.

coated capillary approached 0.1 to ca. 0.01 μg/ml. The linear ranges were from 0.5 to ca. 50 μg/ml for Na^+, K^+, Cr^{3+}, Mn^{2+}, Ni^{2+}, Zn^{2+} and Cd^{2+}, from 0.15 to ca. 15 μg/ml for Mg^{2+}, from 0.5 to ca. 5 μg/ml for Ca^{2+}, from 0.5 to ca. 55 μg/ml for Sr^{2+}, from 0.8 to ca. 20 μg/ml for Ba^{2+}, and from 0.1 to ca. 10 μg/ml for Li^+. In this simultaneous determination, the linear range of the calibration curves for alkaline earth metals were not as good as with the uncoated capillary. The linear range of Ca^{2+} was also smaller, because the peak of Sr^{2+} was superimposed on that of Ca^{2+} at higher concentrations. Also, a relatively large standard deviation of determination appeared at high concentrations of Sr^{2+}. For all others, the linear calibration range and the detection limits with the coated capillary were superior.

3.8. Use of a complexing agent to separate lanthanides

Two different buffer characteristics were varied to improve cation separations by our CE methods. First, by adjusting the pH of the buffer, we were able to change the EOF [9]. The second characteristic involved the addition of complexing agents to the buffer. The complexation equilibria enhanced the mobility differences between sample ions.

In the separation of metal cations, HIBA is commonly used as a complexing agent. In 1981, Nukatsuka *et al.* [19] described the use of HIBA as a complexing agent in the separation of lanthanides. In 1990 Foret *et al.* [16] reported its use in the separation of rare earth cations, alkali metal cations and Mg^{2+}. Researchers at Waters/Millipore have published comprehensive papers [14,18] describing the use of HIBA as a complexing agent. Differences in the mobilities of lanthanide ions were enhanced by the addition of HIBA to the buffer, but the elution order was not changed. For transition metals, on the other hand, the enhancement of mobility differences was accompanied by changes in elution order, for example, between Co^{2+} and Pb^{2+}.

In our experiments, 3.5 m*M* HIBA was added to the buffer. Efficient separation (Fig. 9) was achieved for almost all cations under the conditions: 60 cm × 75 μm I.D. capillary coated with 2.0 mg/ml 3-aminopropyltrimethoxysilane, 15 m*M* 2-aminopyridine/3.5 m*M* HIBA/acetate buffer (pH 5.0), 30 kV working voltage. The 24 cations were separated in 20 min. With HIBA added to the buffer, baseline noise was significantly increased.

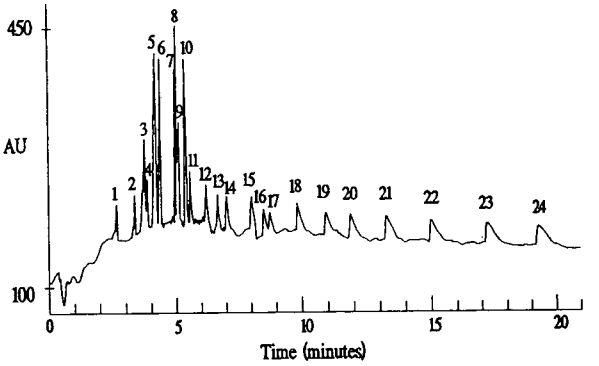

Fig. 9. Electropherogram showing the separation of 24 cations: K^+, Ba^{2+}, Ca^{2+}, Na^+, Mg^{2+}, Mn^{2+}, Zn^{2+}, Cd^{2+}, Li^+, Cr^{3+}, La^{3+}, Ce^{3+}, Pr^{3+}, Nd^{3+}, Sm^{3+}, Eu^{3+}, Gd^{3+}, Tb^{3+}, Dy^{3+}, Ho^{3+}, Er^{3+}, Tm^{3+}, Yb^{3+} and Lu^{3+} which are labeled from 1 to 24 in order. Concentrations: Li^+ was 1 μg/ml and others were 5 μg/ml. Conditions: 3-aminopropyltrimethoxysilane coated capillary (60 cm × 75 μm I.D.), 15 m*M* 2-aminopyridine–3.5 m*M* HIBA–acetate buffer, pH 5.0, 30 000 V, 100 mm gravity injection for 30 s, and detection at 214 nm.

4. Conclusions

Coated capillaries, commonly employing neutral coating materials, have been used in CE to separate biological samples [4,5,11]. The 3-aminopropyltrimethoxysilane coated capillary has been successfully used to separate 12 transition metal cations (Fig. 8). Both separation efficiency and resolution were superior to those obtained with uncoated capillaries. The lower limits of the linear range and the detection limits were improved ten fold over uncoated capillaries using the "UV-Cat 1" buffer [20] or the creatinine buffer [15]. Our method of capillary coating is easier and faster than the C_{18}-coated capillary [6]. No adsorption of analytes on the

bonded coating was observed in our experiments. The electroosmotic flow was stable for a long period of time, even after 50–ca. 60 runs. With the addition of complex-forming HIBA to the buffer, 24 metal cations were separated with the positively charged capillary in 20 min. With this capillary, the column efficiency and resolution achieved were higher than those obtained with the C_{18}-coated capillary.

References

[1] J.C. Giddings, *Sep. Sci.*, 4 (1969) 181.
[2] B. Tarbet, J. Bradshaw, K. Markides, B. Jones and M.L. Lee, *LC·GC*, 6 (1988) 232.
[3] B.W. Wright, P.A. Peaden and M.L. Lee, *Chromatographia*, 15 (1982) 584.
[4] M. Huang, W.P. Vorkink and M.L. Lee, *J. Microcol. Sep.*, 4 (1992) 135.
[5] M. Huang, W.P. Vorkink and M.L. Lee, *J. Microcol. Sep.*, 4 (1992) 233.
[6] M. Chen and R.M. Cassidy, *J. Chromatogr.*, 602 (1992) 227.
[7] K. Cheng, *Thesis*, Brigham Young University, Provo, UT, 1993.
[8] M. Huang, *Dissertation*, Brigham Young University, Provo, UT, 1992.
[9] J. Bouche and M. Verzele, *J. Gas Chromatogr.*, 6 (1968) 501.
[10] M. Huang and Z. Zhao, personal communication.
[11] Z. Zhao, *Dissertation*, Brigham Young University, Provo, UT, 1993.
[12] W. Beck and H. Engelhardt, *Chromatographia*, 33 (1992) 313.
[13] P.D. Grossman and J.C. Colburn, *Capillary Electrophoresis*, Academic Press, San Diego, CA, 1991.
[14] P. Jandik, W.R. Jones, A. Weston and P.R. Brown, *LC·GC*, 9 (1991) 634.
[15] A. Weston, P.R. Brown, P. Jadick, A.L. Heckenberg and R.J. William, *J. Chromatogr.*, 608 (1992) 395.
[16] F. Foret, S. Fanali, A. Nardi and P. Boček, *Electrophoresis*, 11 (1990) 780.
[17] J. Statler, *Dionex CE DataBase*, Dionex, Sunnyvale, CA, 22 February 1991.
[18] A. Weston, P.R. Brown, A.L. Hecbkenberg, P. Jandik and W.R. Jones, *J. Chromatogr.*, 602 (1992) 249.
[19] I. Nukatsuka, M. Taga and H. Yoshida, *J. Chromatogr.*, 205 (1981) 95.
[20] M. Koberdar, M. Konkowski, P. Younberg, W.R. Jones and A. Weston, *J. Chromatogr.*, 602 (1992) 235.

ELSEVIER

Journal of Chromatography A, 706 (1995) 527–534

JOURNAL OF CHROMATOGRAPHY A

Application of capillary electrophoresis in atmospheric aerosol analysis: determination of cations

Ewa Dabek-Zlotorzynska*, Joseph F. Dlouhy

Chemistry Division, Environmental Technology Centre, Environment Canada, 3439 River Road, Ottawa, Ontario K1A 0H3, Canada

Abstract

The feasibility of using capillary electrophoresis (CE) with a new electrolyte system for the analysis of alkali metal, alkaline-earth metal cations and ammonium in atmospheric aerosols has been demonstrated. 1,1′-Di-*n*-heptyl-4,4′-bipyridinium (DHPB) hydroxide was used as the UV-absorbing species, which allowed for the indirect UV detection of cations at 280 nm, while glycine, 18-crown-6 ether and methanol were employed to improve the separation of the studied cations. The precision of migration time and peak area was better than 0.2% and 5%, respectively. Separation efficiencies were between 90 000 and 600 000 theoretical plates per meter, and detection limits between 9 and 60 ng/ml. With the described electrolyte composition it is also possible to determine manganese and cadmium, and short-chain aliphatic amines. The comparison of CE results with ion chromatography obtained for cations in atmospheric aerosols is presented.

1. Introduction

Previous reported work [1] demonstrated the applicability of capillary electrophoresis (CE) with indirect UV detection to analyze inorganic and organic anions in atmospheric aerosols. The highly efficient separation of CE with high accuracy, precision, short analysis time and low reagent consumption makes it an excellent tool for such analysis. The introduction of CE in an environmental analytical laboratory allows also methods and results validation.

This work has been continued to investigate the usefulness of CE in the analysis of inorganic cations in atmospheric aerosols. At present, ion chromatography (IC) is extensively used by this laboratory in the analysis of alkali metal, alkaline-earth metal cations and ammonium in such samples [26,27]. Several reports have appeared recently describing the application of CE for the analysis of inorganic and organic cations with indirect UV detection [2–23]. Various electrolyte compositions using different UV absorbing carrier electrolytes and complexing agents have been employed. Because most inorganic cations have similar ionic mobilities, additional components in the electrolyte are required for the efficient separation. These components, typically negatively charged weak anionic complexing agents [2–7,9,10,12–23] or electroneutral crown ethers [8,11,14,17–23], selectively reduce

* Corresponding author.

0021-9673/95/$09.50
SSDI 0021-9673(95)00132-8

the mobility of inorganic cations and thus improve resolution of cationic analytes. In order to optimize cation CE separation and indirect UV detection efficiencies, it is important to choose a suitable combination of a UV-sensitive carrier electrolyte and complexing reagent [6,9,10, 12,14,16,23].

In this paper a new electrolyte composition will be described which permits separation of alkali metal, alkaline-earth metal cations and ammonium. 1,1′-Di-*n*-heptyl-4,4′-bipyridinium (DHPB) hydroxide was used as the UV-absorbing agent, which allowed the indirect UV detection of cations at 280 nm. Complexing agents such as glycolic acid, glycine and 18-crown-6 ether were tested in order to improve separation of the studied cations. The present work deals with the application of CE for the determination of cations of interest in atmospheric aerosols. This study was also performed to obtain independent complementary confirmation of the IC results.

2. Experimental

2.1. Capillary electrophoresis

A Beckman P/ACE 2100 instrument (Fullerton, CA, USA) with System Gold version 7.11 software was used for all CE measurements. The system features a UV detector, an autosampler and a liquid-cooled capillary cartridge. Capillaries from Polymicro Technologies (Phoenix, AZ, USA) with 57 cm (50 cm to detector) × 75 μm I.D. × 375 μm O.D. were used. Approximately 0.5 cm of the polyimide coating was burned off from the capillary to make a transparent window for the detector cell. Indirect UV detection was employed at 280 nm. All experiments were conducted at 25°C. A positive power supply of 25 kV was used and all injections were achieved by applying a 0.5-p.s.i. pressure for 10 s, unless otherwise noted.

A Beckman pH meter with a combination electrode was used to measure the pH of electrolytes.

2.2. Ion chromatography

A Dionex 4000i IC system (Dionex, Sunnyvale, CA, USA) equipped with a gradient pump (GPM), an advanced chromatography module (ACM) and a conductivity detector (CDM-2) was utilized for IC determination. A Dionex automated sampler (ASM) with 5-ml vials was used for sample loading. A 50-μl sample loop was used for the injection of samples.

The separations of alkali metal, alkaline-earth metal cations and ammonium were carried out on an IonPac CS12 column (250 mm × 4 mm I.D.) with an IonPac CG12 guard column (50 mm × 4 mm I.D.) at a flow-rate of 1.0 ml/min. A step gradient from 16 m*M* methanesulphonic acid (MSA) to 40 m*M* MSA at 8.0 min was used. Conductivity detection was carried out using a cation self-regenerating suppressor (CSRS-I) in the recycle mode.

The chromatograph was controlled and data were collected and processed on a personal computer using Dionex AI-450 software.

2.3. Reagents

MSA was obtained from Fluka (Ronkonkoma, NY, USA). All other chemicals were purchased from either Fisher Scientific (Ottawa, Canada) or Aldrich (Milwaukee, WI, USA) in the highest purity available, and were used without further purification. Deionized water obtained from a reversed-osmosis and an ion-exchange system (Millipore, Model RO 20 and Model SuperQ) was used for the preparation of all solutions, electrolytes and standards.

The ammonium standard solution was prepared from ammonium chloride. A stock solution of other used inorganic cations were prepared from National Institute of Standards and Technology (NIST, Gaithersburg, MD, USA) standards. All standard solutions were stored in polyethylene containers. Diluted working standard solutions were prepared daily.

2.4. Electrolytes and procedures

A 25 m*M* DHBP bromide, 100 m*M* 18-crown-

6 ether and 100 m*M* glycolic acid or 100 m*M* glycine were used for the preparation of the working electrolytes. OnGuard A cartridges (Dionex) in the hydroxide form were used to convert DHBP bromide to DHBP hydroxide. The electrolytes were adjusted to the final pH using acetic acid.

All electrolyte solutions were filtered through a 0.22-μm syringe PTFE membrane filter (Nalgene Brand Products, Rochester, NY, USA) and degassed by creating vacuum inside the syringe.

Each day before starting analysis, the capillary was rinsed with 0.1 *M* NaOH and water for 10 min, followed by the used electrolyte for 5 min. Between each run the capillary was flushed with the running electrolyte for 1 min.

Quantitation was based on multi-component calibration runs. Five mixed standards were employed to fit a calibration graph using the linear regression analysis of the corrected peak area.

Detection limits were defined as three times the standard deviation of eighteen replicate analyses of a standard with a concentration equal to about ten times the estimated detection limit, the latter being the concentration giving a signal-to-noise ratio of 3.

2.5. Extraction of atmospheric aerosols

Atmospheric aerosols, collected on PTFE-coated borosilicate glass fiber filters (Pallflex, TX40HI20WW) using Hi-Vol samplers and on thin PTFE filters using virtual dichotomous samplers, were obtained from the Pollution Measurement Division, Environmental Technology Centre, Canada.

Two 37-mm-diameter discs, cut out from Hi-Vol filters, were placed in a 100-ml beaker. The filters were wetted with two drops of 30% Triton TX-100 and then 25 ml of deionized water were added. The beakers were then covered with Parafilm 1"M" and extracted for 30 min in an ultrasonic bath (Branson and Smithkline, Shelton, CT, USA).

The extraction of water-soluble atmospheric aerosols collected on PTFE filters was performed with 15 ml of water by sonication in the ultrasonic bath. Before addition of water, the filters with collected aerosols were wetted with 100 μl of isopropanol.

Analysis was carried out as soon as possible after extraction (within less than 24 h). The unused extracts were preserved by storage at −20°C [32].

3. Results and discussion

3.1. Optimization of separation

The experimental parameters such as concentration of a carrier electrolyte, type and concentration of a complexing reagent, pH and effect of organic solvents were optimized to achieve suitable separation, the highest sensitivity and the shortest time of analysis. A mixture of cations of interest (NH_4^+, K^+, Na^+, Ca^{2+}, Mg^{2+}, Sr^{2+}, Ba^{2+}, 2 mg/l; Li^+, 0.5 mg/l) was pressure-injected for 5 s during these experiments.

In this study, DHBP hydroxide was selected as the UV-absorbing carrier electrolyte. DHBP absorbs strongly in the vicinity of 262 nm with a large molar absorptivity ($2.4 \cdot 10^4$ l mol^{-1} cm^{-1}) [28]. Because of the availability of a 280-nm filter in a used CE instrument, 280 nm was chosen as a representative detection wavelength throughout this work. DHBP is a quaternary ammonium ion, available commercially as the bromide, and it is in the form of a divalent ion over a wide pH range [28].

Glycolic acid and glycine were tested as the complexing reagents in order to obtain separation of the studied cations. Both reagents form weak complexes with alkali metal and alkaline-earth metal cations [29]. Transition metal cations are more strongly complexed by glycine [29]. 18-Crown-6 ether was added to the electrolyte containing a glycine or glycolic acid in order to separate NH_4^+ and K^+ cations. The crown ether complexes with potassium which permits the separation from ammonium. The migration times of barium and strontium are also increased due to complexation with the crown ether.

Preliminary experiments showed that separa-

tion of cations of interest could be obtained either with glycolic acid at pH 4 or glycine at pH 6.5 with incorporation of 18-crown-6 ether. However, strong drifts of the baseline due to the variation of Joule heating [17] in the electropherograms observed at a pH lower than 6 restricted the choice to glycine as a complexing agent.

On the basis of the performed experiments, the electrolyte containing the 5 m*M* DHBP, 6 m*M* glycine, 2 m*M* 18-crown-6 ether and 2% methanol at pH 6.5 was found to give the best compromise between peak separation, sensitivity and acceptable baseline noise. Methanol was added to the electrolyte in order to improve the resolution between sodium and magnesium. Organic solvents have successfully been used in adjusting the selectivity in CE [10,23,24]. Fig. 1 shows an electropherogram of a mixed cation standard under optimum conditions. Under these conditions cesium, rubidium, manganese and cadmium in addition to other cations of interest could be separated. Because glycine forms strong complexes with most transition metal cations, these cations could not be separated. However, glycine may be used to selectively mask cations to prevent their precipitation at higher pH and comigration of ions of similar mobilities.

The peak shape for most of the tested cations is symmetric although there is some peak fronting on the fast-migrating cations. The ionic mobility of DHBP measured with the 5 m*M* phosphate buffer at pH 6.5 was slightly lower ($2.8 \cdot 10^{-4}$ cm^2 V^{-1} s^{-1}) than the mobility of inorganic metal ions (around $4 \cdot 10^{-4}$ cm^2 V^{-1} s^{-1}). Separation efficiencies were between 90 000 and 600 0000 theoretical plates per meter at a concentration of 1 mg/l with a 10-s pressure injection.

Another example of the capability of the proposed method is the separation of alkyl amines. They are well separated from the inorganic cations, as can be seen in Fig. 2.

3.2. Analytical performance

Table 1 summarizes the migration time and peak-area precision (R.S.D.) for the tested cat-

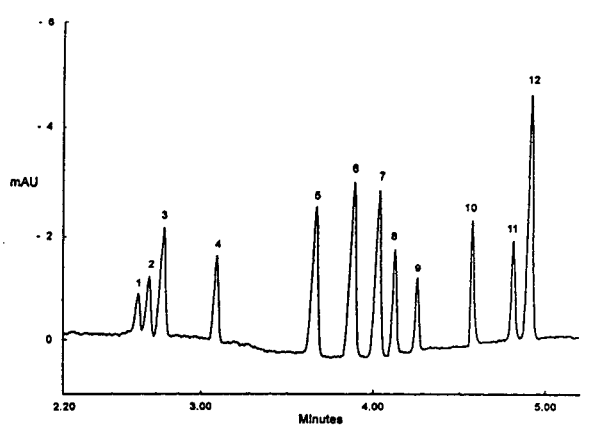

Fig. 1. Separation of inorganic cations under optimum conditions: electrolyte, 5 m*M* DHBP, 6 m*M* glycine, 2 m*M* 18-crown-6 ether, 2% methanol, pH 6.5; applied voltage, 25 kV; current, 12.5 μA; injection time, 5 s; indirect detection, 280 nm. Peaks: 1 = Cs^+ (4 mg/l); 2 = Rb^+ (4 mg/l); 3 = NH_4^+ (2 mg/l); 4 = K^+ (2 mg/l); 5 = Ca^{2+} (2 mg/l); 6 = Na^+(2 mg/l); 7 = Mg^{2+} (1 mg/l); 8 = Mn^{2+} (1 mg/l); 9 = Sr^{2+} (1 mg/l); 10 = Cd^{2+} (3 mg/l); 11 = Ba^{2+} (2 mg/l); 12 = Li^+ (0.5 mg/l).

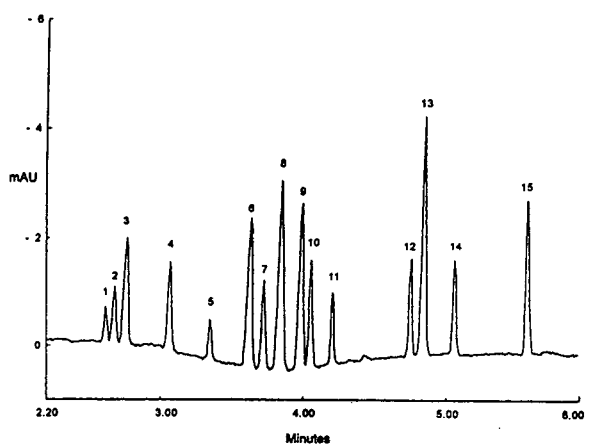

Fig. 2. Simultaneous separation of alkali metals, alkaline-earth metals, ammonium and amines. Conditions are the same as in Fig. 1. Peaks: 1 = Cs^+ (4 mg/l); 2 = Rb^+ (4 mg/l); 3 = NH_4^+ (2 mg/l); 4 = K^+ (2 mg/l); 5 = methylamine (2 mg/l); 6 = Ca^{2+} (2 mg/l); 7 = dimethylamine (2 mg/l) 8 = Na^+ (2 mg/l); 9 = Mg^{2+} (1 mg/l); 10 = trimethylamine (2 mg/l); 11 = Sr^{+2} (1 mg/l); 12 = Ba^{+2} (2 mg/l); 13 = Li^+ (0.5 mg/l), 14 = ethylamine (2 mg/l); 15 = triethylamine (4 mg/l).

Table 1
Precision and detection limits

Cation	R.S.D.[a] (%)		Detection limit (ng/ml)	
	Migration time	Peak area	CE[b]	IC[c]
Ammonium	0.13	1.92	42	12
Potassium	0.12	4.28	47	7
Calcium	0.12	2.81	42	9
Sodium	0.12	4.67	46	14
Magnesium	0.11	1.87	18	5
Manganese	0.18	3.17	39	10
Strontium	0.11	3.64	38	6
Barium	0.11	2.61	57	9
Lithium	0.11	2.65	9	2

[a] Relative standard deviations from eighteen replicates of a mixed standard solution at a concentration of 2 mg/l (Li^+ 0.5 mg/l) using the described method.
[b] Capillary electrophoresis utilizing the proposed electrolyte composition with a 10-s pressure injection.
[c] Ion chromatography with a 50-μl sample loop.

ions in a mixed standard under the conditions listed in Fig. 1. The precision of migration times and peak areas was better than 0.2% and 5%, respectively.

Table 2
Determination of major cations in water samples using capillary electrophoresis with the proposed electrolyte composition

	Interlaboratory median (μg/ml)	Found (μg/ml)	R.S.D.[c] (%)
Ammonium	0.900[a]	0.948	3.35
	–[b]	–	–
Potassium	0.101[a]	0.089	10.21
	0.500[b]	0.348	6.75
Calcium	3.200[a]	3.122	1.29
	13.500[b]	13.348	0.90
Sodium	0.334[a]	0.324	5.98
	1.340[b]	1.314	1.57
Magnesium	0.980[a]	1.025	0.97
	2.820[b]	2.684	0.44

[a] LRTAP 34/8 [30].
[b] LRTAP FP 64/3 [31].
[c] Reported results are the means and relative standard deviations from nine replicates with a 10-s pressure injection.

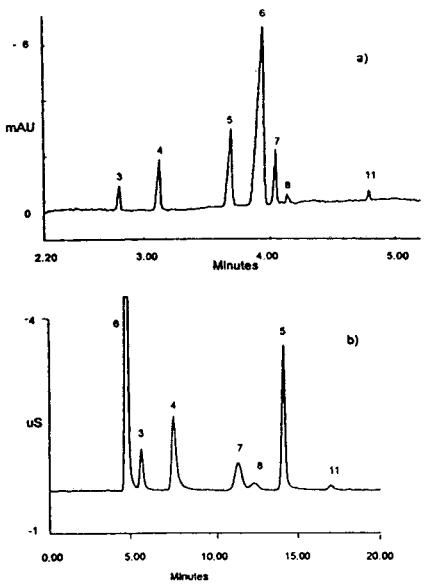

Fig. 3. Analysis of Hi-Vol-sampled atmospheric aerosol extract using (a) CE with a 10-s pressure injection and (b) IC methods. Peaks and other conditions are the same as in Fig. 1.

A linear relationship between corrected peak area and concentration was obtained in the 0.1–10 mg/l range for most tested cations. Correlation coefficients were ranged from 0.9990 to

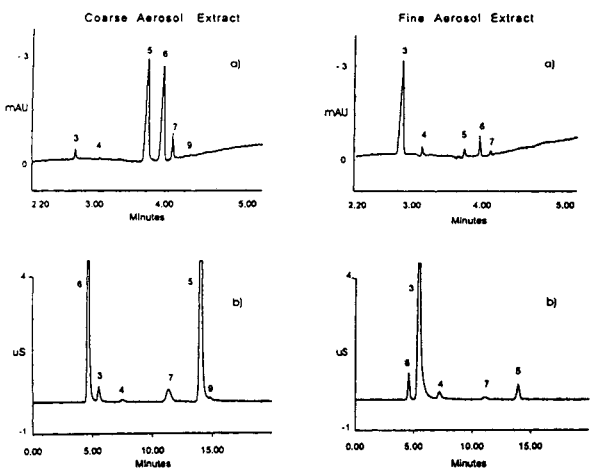

Fig. 4. Analysis of coarse and fine atmospheric aerosol extracts using (a) CE with a 10-s pressure injection and (b) IC methods. Peaks and other conditions are the same as in Fig. 1.

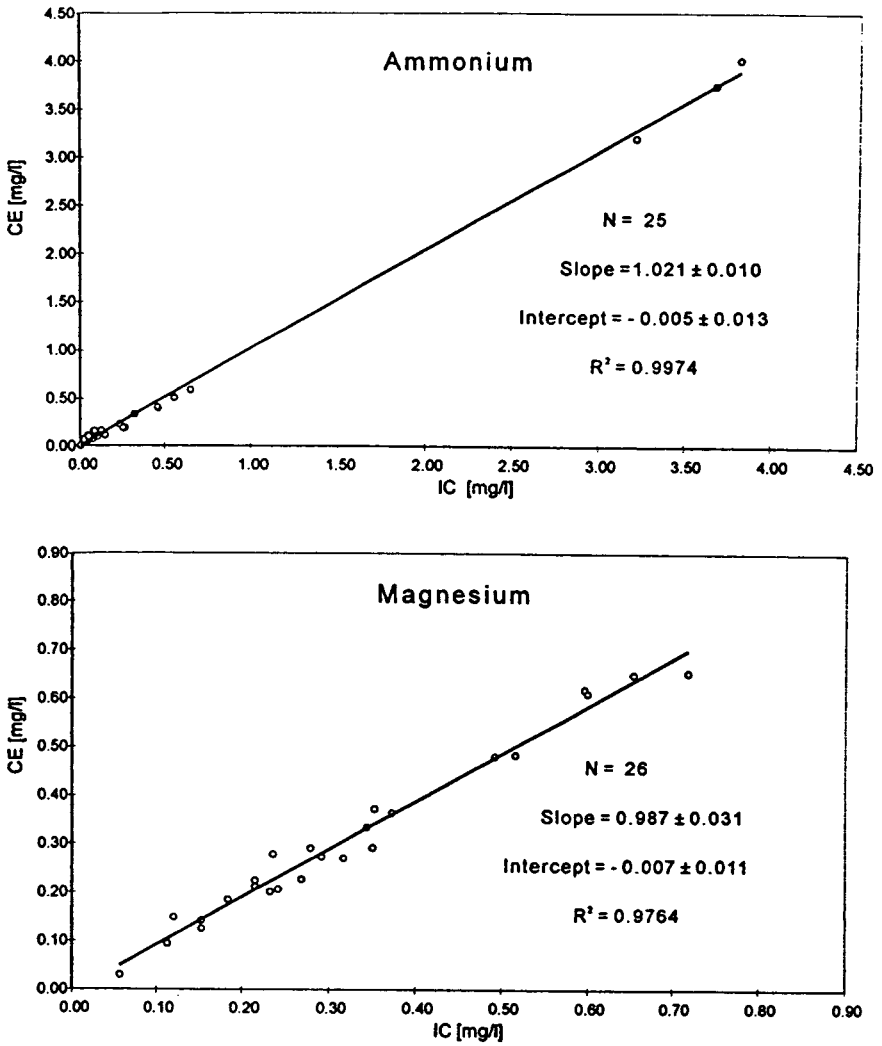

Fig. 5. Correlation plots for ammonium and magnesium determined by CE and IC methods in Hi-Vol-sampled atmospheric aerosols (±values are the confidence limits at 95% level).

0.9999 for all tested cations. Although the quantitation is possible at the 10 μg/ml level, the peaks become broader and the resolving power due to differences between the electrolytes and analyte mobilities [25] is diminished. The calibration linearity and sensitivity are much better in the lower concentration range when a 10-s pressure injection is used. When the analyte concentration is high, the injection time should be decreased or the DHBP concentration should be increased.

In order to evaluate the quantitative performance and accuracy of the method, two water samples used for round robin studies were analyzed. The results shown in Table 2 are in a good agreement with the interlaboratory median values [30,31]. The analytical results were also precise as shown by the standard deviation of nine replicates.

Detection limits of analytes (for a 10-s pressure injection) using the described method are listed in Table 1. It can been seen that most

Table 3
Statistical analysis results (±95% confidence limit) [33]

Cation	Concentration range (mg/l)	N	Slope[a] (A)	Intercept[a] (B)	r^2
Ammonium	0.04–3.82	25	1.021 ± 0.010	−0.005 ± 0.013	0.9974
Potassium	0.18–2	26	1.086 ± 0.043	0.007 ± 0.039	0.9649
Calcium	0.4–8	26	0.891 ± 0.021	0.055 ± 0.065	0.9864
Sodium	1.2–8	26	1.041 ± 0.025	−0.016 ± 0.107	0.9840
Magnesium	0.06–0.7	26	0.987 ± 0.031	−0.007 ± 0.011	0.9764

(CE) = A × concentration (IC) + B (mg/l).

cations have detection limits at the tens of ng/ml level. The results indicate that the proposed method gave better detection limits than obtained with other reported carrier electrolytes [4,7,11].

3.3. Analysis of cations in atmospheric aerosols

The proposed CE method was applied to the determination of inorganic cations in atmospheric aerosols. Fig. 3 shows the typical electropherogram and chromatogram of aqueous extract of atmospheric aerosols collected with Hi-Vol sampler. Ammonium, potassium, sodium, calcium and magnesium were the major cations in these samples. Barium was present at the mid-μg/ml level. Manganese and strontium were found only in a few samples. Some unidentified peaks were sometimes present in the electropherogram at a migration time close to 6 min.

Typical electropherograms of coarse and fine atmospheric aerosol extracts are presented in Fig. 4. Coarse atmospheric aerosol particles contain sodium, magnesium and calcium as the major cations. Ammonium is the major cation of fine atmospheric aerosols. Manganese was present at mid-μg/ml level in a few samples. The concentration of other cations was frequently under the detection limit.

The CE results were compared with those obtained by IC. A comparison of ammonium and magnesium results by CE with those obtained by IC for a series of Hi-Vol-sampled atmospheric aerosols is shown in Fig 5. Linear least-squares adjustment of each set of results yielded the equations (±95% confidence limits [33]) presented in Table 3. As can been seen the values determined from both techniques agree quite well. Some problems were encountered in the determination of calcium by IC. The calcium IC concentrations were significantly larger than the CE concentrations, also for quality control samples. These problems are not resolved yet. Attempts to do this are now in progress.

4. Conclusions

In conclusion, the results of this work show that CE utilizing the proposed electrolyte composition can be used for the detection and separation of alkali metal, alkaline-earth metal cations and ammonium in atmospheric aerosols. This method provides high separation efficiencies and a very good detectability at 280 nm. Results obtained are in a good agreement with those obtained by IC. CE offers a complementary method and allows easy peak confirmation.

References

[1] E. Dabek-Zlotorzynska and J.F. Dlouhy, *J. Chromatogr.*, 671 (1994) 389–395.
[2] F. Foret, S. Fanali, A. Nardi and P. Bocek, *Electrophoresis*, 11 (1990) 780–783.
[3] P. Jandik and G.K. Bonn, *Capillary Electrophoresis of Small Molecules and Ions*, VCH, New York, 1993.
[4] A. Weston, P.R. Brown, P. Jandik, W.R. Jones and A.L. Heckenberg, *J. Chromatogr.*, 593 (1992) 289–295.

[5] M. Koberda, M. Konkowski, P. Youngberg, W, R. Jones and A. Weston, *J. Chromatogr.*, 602 (1992) 235–240.
[6] A. Weston, P.R. Brown, A.L. Heckenberg, P. Jandik and W.R. Jones, *J. Chromatogr.*, 602 (1992) 249–256.
[7] W. Beck and H. Engelhardt, *Chromatographia*, 33 (1992) 313–316.
[8] K. Bachmann, J. Boden and J. Haumann, *J. Chromatogr.*, 626 (1992) 259–265.
[9] M. Chen and R.M. Cassidy, *J. Chromatogr.*, 640 (1993) 425–431.
[10] Y. Shi and J.S. Fritz, *J. Chromatogr.*, 640 (1993) 473–479.
[11] J.M. Riviello and M.P. Harrold, *J. Chromatogr.*, 652 (1993) 385–392.
[12] T.I. Lin, Y.H. Lee and Y.C. Chen, *J. Chromatogr.*, 654 (1993) 167–176.
[13] M. Jimidar, T. Hamoir, W. Degezelle, D.L. Massart, S. Soykenc and P. Van de Winkel, *Anal. Chim. Acta*, 284 (1993) 217–225.
[14] W. Beck and H. Engelhardt, *Fresenius J. Anal. Chem.*, 346 (1993) 618–621.
[15] R.A. Carpio, P. Jandik and E. Fallon, *J. Chromatogr.*, 657 (1993) 185–191.
[16] C. Quang and M.G. Khaledi, *J. Chromatogr.*, 659 (1994) 459–466.
[17] E. Simunicova, D. Kaniansky and K. Loksikova, *J. Chromatogr.*, 665 (1994) 203–209.
[18] *Determination of Inorganic Cations by Capillary Electrophoresis*, Dionex, Sunnyvale, CA, 1994, Application Note No. 91.
[19] *Analysis for Trace Level of Alkali Metals, Alkaline Earth Metals, and Ammonium by Capillary Electrophoresis*, Dionex, Sunnyvale, CA, 1994, Technical Note No. 35.
[20] W. Buchberger, K. Winna and M. Turner, *J. Chromatogr.*, 671 (1994) 375–382.
[21] R.R. Chadwick, J.C. Hsieh, K.S. Resham and R.B. Nelson, *J. Chromatogr.*, 671 (1994) 403–410.
[22] M. Jo Wojtusik and M.P. Harrold, *J. Chromatogr.*, 671 (1994) 411–417.
[23] Y. Shi and J.S. Fritz, *J. Chromatogr.*, 671 (1994) 429–435.
[24] M. Jimidar, T. Hamoir, A. Foriers and D.L. Massart, *J. Chromatogr.*, 636 (1993) 179–182.
[25] R.A. Wallingford and A.G. Ewing, *Adv. Chromatogr.*, 29 (1989) 1–76.
[26] E. Dabek-Zlotorzynska and J.F. Dlouhy, *J. Chromatogr.*, 640 (1993) 217–226.
[27] E. Dabek-Zlotorzynska and M. Piechowski, *Analysis of Ions in Atmospheric Aerosols by Multi-Dimensional Ion Chromatography* (Manual), Chemistry Division, ETC, Environment Canada, Ottawa, 1994.
[28] H. Sato, *J. Chromatogr.*, 465 (1989) 339–349.
[29] R.M. Smith and A.E. Martell, *NIST Critical Stability Constants of Metal Complexes Database*, NIST Standard Reference Database 46, 1993.
[30] N. Arafat and K. Aspila, *LRTAP Interlaboratory Study L-34 for Major Ions and Nutrients*, NWRI, Burlington, 1994.
[31] H. Alkema, *Ecosystem Interlaboratory QA Program, Study FP64 for Major Ions and Nutrients*, NWRI, Burlington, 1994.
[32] E. Dabek-Zlotorzynska, D.Mathieu and J.F. Dlouhy, *The Stability of Aqueous Extracts of Atmospheric Aerosols. Ion Chromatographic Determination of the Effects of Some Preservation Methods*, Environmental Technology Centre, Environment Canada, Ottawa, 1993.
[33] J.C. Miller and J.N. Miller, *Statistics for Analytical Chemistry*, Wiley, New York, 1984, pp. 96–100.

ELSEVIER

Journal of Chromatography A, 706 (1995) 535–553

JOURNAL OF CHROMATOGRAPHY A

Effect of the concentration of 18-crown-6 added to the electrolyte upon the separation of ammonium, alkali and alkaline-earth cations by capillary electrophoresis

C. Francois, Ph. Morin*, M. Dreux

Laboratoire de Chimie Bioorganique et Analytique (LCBA), URA CNRS 499, B.P. 6759, 45 067 Orleans Cedex 2, France

Abstract

Capillary zone electrophoresis with indirect ultraviolet absorption detection was carried out to determine ammonium, alkali and alkaline-earth cations using a background electrolyte buffer containing 10 m*M* imidazole (pH 4.5) and 18-crown-6 as complexing agent. The optimization of the experimental parameters (18-crown-6 concentration, pH, temperature, running voltage) was studied. The crown ether concentration appeared to be a very convenient parameter to monitor the selectivity of the cations during the analysis of complex matrix aqueous samples. Adding 2.5 m*M* 18-crown-6 to the 10 m*M* imidazole electrolyte system (pH 4.5) generally gave the maximum resolution of ammonium and potassium cations; nevertheless, it was possible to shift the potassium peak in the electropherogram by adding up to 300 m*M* 18-crown-6. The stability constant of 18-crown-6 complexes with four cations (K^+, NH_4^+, Ba^{2+}, Sr^{2+}) has also been experimentally determined by capillary electrophoresis; it was confirmed that K^+ has a stability complex constant with 18-crown-6 (log $K_s = 2.1$) higher than NH_4^+ (log $K_s = 1.01$). Simultaneous quantitation of sodium, calcium, potassium, ammonium, magnesium and lithium has been performed in such optimized separation conditions.

1. Introduction

Capillary electrophoresis (CE) is currently undergoing rapid development owing to its efficiency, high resolution, relative simplicity, UV detection at low wavelengths (190 nm), speed and automatization of separations, and low buffer consumption. Its drawbacks compared to liquid-phase chromatography are the rather weak reproducibility of the electroosmotic flow assuring the migration times, and a lower concentration sensitivity. However, this technique is available not only for the separation of inorganic and organic anions and cations, but also for the separation of ionizable and neutral organic molecules.

During the last five years, CE has been widely applied to the analysis of inorganic cations in various aqueous samples [1–16]; the analytical approach is based on the indirect detection mode because of the transparency of inorganic cations in the UV region, and separation using operating conditions such as the electroosmotic flow must be in the same direction as the electrophoretic

* Corresponding author.

0021-9673/95/$09.50
SSDI 0021-9673(95)00193-X

mobility of the ions analyzed in order to minimize their migration time.

Initially, Aguilar et al. [2] separated the cations Fe^{2+}, Cu^{2+} and Zn^{2+} in the form of their cyanide complexes in CE; a phosphate buffer (20 m*M*) was used at pH 7 and direct UV detection was carried out at 214 nm. Then, Swaile and Sepaniak [11] used a laser-based fluorimetric detector to detect cations Ca^{2+}, Mg^{2+} and Zn^{2+}, complexed by 8-hydroxyquinoline-5-sulfonic acid; this technique was applied to the detection of calcium(II) and magnesium(II) in blood serum.

Foret et al. [4] separated fourteen lanthanides by CE using an electrophoretic buffer consisting of an α-hydroxyisobutyric acid as complexing agent and creatinine as the indirect UV detector marker; in fact, the similarity between the electrophoretic mobilities of alkali, alkaline-earth, rare-earth and metal cations requires the addition of a water-soluble complexing reagent to the electrolyte. The electrophoretic mobility of each cation thus decreases following their complexation in situ by α-hydroxyisobutyric acid, and selectivity is greatly improved. The factors affecting the separation of such cations were studied by Weston and co-workers [5,6]; the complexing agent was also α-hydroxyisobutyric acid and the compound allowing indirect UV detection was called UV Cat 1, a proprietary reagent developed at Waters. Very recently, Beck and Engelhardt [8] firstly proposed a nice alternative way for the separation of several alkali and alkaline-earth cations by using an imidazole-based electrophoretic buffer and indirect UV detection at 214 nm; their results demonstrated the applicability of this running electrolyte in routine analysis. Riviello and Harrold [15] reported another electrolyte system based on copper(II) as the primary electrolyte constituent; the determination of alkali metals, alkaline-earth metals and ammonium was obtained in less than 5 min. Finally, CE has recently received a great deal of attention as a tool for the analysis of transition metal cation mixtures [17–22]. Thus, Shi and Fritz [17] reported the separation of sixteen common metal ions and ammonium at pH 4.3, using 4-methylbenzylamine as a reagent for indirect detection, and lactic acid and 18-crown-6 as complexing agents.

However, potassium and ammonium cations have nearly identical ionic mobilities and thus comigrate under acidic pH conditions; the most common alternative is to add 18-crown-6 to the electroyte in order to promote complex formation with these two cations. However, the concentration of 18-crown-6 added to the imidazole electrolyte also influences the separation performances (electrophoretic mobility, peak efficiency, asymmetry factor and resolution of the other analyte cations).

The UV-absorbing organic cation (imidazolium), which has a quite similar electrophoretic mobility to that of these inorganic cations, was selected as the main constituent of the buffer, and 18-crown-6 was added in the electrolyte as the complexing agent. So, we report the role of 18-crown-6 added to the imidazole electrolyte for analyzing K^+, Na^+, Ca^{2+}, Li^+, Mg^{2+}, NH_4^+ cation mixtures by CE. Then, a method is presented to determine the stability constant of 18-crown-6 complexes with these cations.

2. Experimental

2.1. Apparatus

Separations were carried out on a P/ACE 2100 and P/ACE 5000 apparatus (Beckman Instruments, Fullerton, CA, USA) equipped with a UV detector with wavelength filters of 190, 200, 214, 254, 260 and 280 nm. Fused-silica capillaries (Beckman Instruments) 57 cm (50 cm to the detector) × 75 μm I.D. × 375 μm O.D. were used. The part of the capillary where separation takes place was kept at a constant temperature (25°C) by immersion in a cooling liquid circulating in the cartridge with a detection aperture of 100 μm × 800 μm. The solutes were injected at the anode end of the capillary in the hydrodynamic mode by azote superpressure (0.5 p.s.i). Data were collected using a IWT data acquisition system. The detector time constant

was 0.1 s and the data acquisition rate was 20 Hz.

The pH of each solution was verified on a Model ϕ10 pH meter (Beckman, Fullerton, CA, USA). The capillary tubing of fused silica was conditioned daily by rinsing with a solution of 1 *M* sodium hydroxide (10 min), then water (10 min), and finally the electrophoretic buffer (15 min). Between two consecutive analyses, the capillary was rinsed with water (3 min) and then with the electrophoretic buffer (5 min) to improve the reproducibility of the electroosmotic flow and migration times of the solutions. Linear regression were made using Regrelis program (Logedic, Vesoul, France).

2.2. Chemicals

All chemical products used were of analytical quality. Imidazole (99% purity) was obtained from Sigma (St. Louis, MO, USA) and 18-crown-6 from Aldrich (Milwaukee, WI, USA). The water used in the preparation of buffers and the water necessary for dilutions was of HPLC quality (Fisons, Farmitalia, Milan, Italy). The running buffer contained 10 m*M* imidazole and the concentration of 18-crown-6 varied from 0.01 up to 300 m*M*; the electrophoretic buffer pH was adjusted to the desired value by adding a 1 *M* stock solution of acetic acid (Carlo Erba, Milan, Italy). Finally, each buffer or rinsing solution was filtered before use through a membrane filter having a diameter of 25 mm and porosity of 0.2 μm (Whatman, Maidstone, UK).

2.3. Electrophoretic mobility determination procedure

From experimental data, the electrophoretic mobility (m^+) of a cation C^+ can be determined by

$$m^+ = \frac{L_d L_t}{V}\left(\frac{1}{t_m} - \frac{1}{t_0}\right) \quad (1)$$

where L_d is the length of the capillary from the inlet to the detector, L_t is the total length of the capillary, V the applied voltage, t_m the migration time of the cation and t_0 the migration time of a neutral marker (water).

3. Results and discussion

The use of indirect UV absorption is required since alkali and alkaline-earth metals have no UV absorbance. Hence, the electrophoretic buffer used for the separation of inorganic cations must contain an organic cation whose electrophoretic mobility must closely match those of the analyte cations, in order to obtain highly symmetrical peak shapes, and which also has an intense chromophore group in the UV region. As initially proposed by Beck and Engelhardt [8] imidazole (or 1,3-diaza-2,4-cyclopentadienyl ring) is a heterocyclic azote ($pK_{a_1} = 6.9$ and $pK_{a_2} = 14.5$) whose UV absorption spectrum has a maximum at 211 nm (pH 4.5). Besides, the imidazolium cation appears to have an electrophoretic mobility ($45.8 \cdot 10^{-5}$ cm^2 V^{-1} s^{-1} determined in 10 m*M* sodium acetate at pH 4.5) close to those of magnesium ($46.3 \cdot 10^{-5}$ cm^2 V^{-1} s^{-1}) and sodium ($48.0 \cdot 10^{-5}$ cm^2 V^{-1} s^{-1}), both determined in 10 m*M* imidazole electrolyte (pH 4.5). The sample injection was thus carried out at the anodic end of the capillary and detection at the cathodic end; the electroosmotic flow was in the same direction as the electrophoretic mobility of the cation.

The simultaneous determination of potassium and ammonium is important in agricultural, food and water samples. As potassium and ammonium have nearly identical electrophoretic mobilities, they would comigrate in the 10 m*M* imidazole electrolyte (pH 4.5). Two alternatives may exist. (i) Using an alkaline solution of benzylamine (10 m*M*, pH 9.25) as carrier electrolyte which allows the separation of potassium and ammonium cations by decreasing the electrophoretic mobility of the ammonium cation [1,6,14]; thus, the potassium cation migrates faster than ammonium but the electroosmotic flow increases, bringing about a shorter analysis time. Consequently, we cannot resolve all inorganic cations in a single run [14]. (ii) Adding

18-crown-6 to the electrolyte in order to promote complex formation with these two cations. The addition of this weak complexing agent alters the electrophoretic mobilities of the cations and their relative selectivity would depend on 18-crown-6 concentration. An inorganic cation (C^+) interacts with the neutral 18-crown-6 (L) according to the following chemical equilibrium:

$$C^+ + L \overset{K_s}{\rightleftharpoons} CL^+ \quad (2)$$

where K_s is the stability complex constant of the complex CL^+ between C^+ and the ligand L. The electrophoretic mobility (m^+) of the cation C^+ was determined as the weighted average of the electrophoretic mobility of the free cation (m_{C^+}) and of the complexed cation (m_{CL^+}) with 18-crown-6, as expressed by the following relationship:

$$m^+ = \frac{[C^+]}{[C^+]+[CL^+]} m_{C^+} + \frac{[CL^+]}{[C^+]+[CL^+]} m_{CL^+} \quad (3)$$

where $[C^+]$ and $[CL^+]$ represent the concentration at equilibrium of the free and complexed cation C^+ and CL^+, respectively. At a given pH value, the stability constant K_s of the complex CL^+ can be expressed as:

$$K_s = \frac{[CL^+]}{[C^+][L]} \quad (4)$$

where [L] is the 18-crown-6 concentration at equilibrium.

Combining eqs. 3 and 4 gives the following expression for the calculation of m^+:

$$m^+ = \frac{1}{1+K_s[L]} m_{C^+} + \frac{K_s[L]}{1+K_s[L]} m_{CL^+} \quad (5)$$

According to Eq. 5, the variation of the electrophoretic mobility (m^+) versus the value of the negative logarithm of the 18-crown-6 concentration (pL = −log [L]) allows to determine the stability constant K_s; indeed, this curve has a shape similar to an acid–base titration curve, and the abscissa of the inflection point will be equal to log K_s.

3.1. Effect of 18-crown-6 concentration on separation performances

The effect of imidazole concentration on selectivity was studied in the 1–15 m*M* range, by maintaining a constant pH value of 4.5. A significant modification in selectivity was observed for sodium and magnesium cations when the imidazole concentration varied from 1 up to 15 m*M* (Fig. 1a). While calcium and sodium cations are always well resolved whatever the imidazole concentration, the background co-ion concentration needs to be carefully selected in order to avoid comigration of sodium and magnesium (3 m*M*). Thus, sodium migrates faster than magnesium at imidazole concentrations higher than 3 m*M*, while a reversed migration order occurs at lower concentrations, which may be explained by a possible complexation of these cations with imidazole. Migration times decrease with the equivalent conductance limit, according to the following decreasing migration time order for the cations: potassium ($\lambda_{K^+} = 73.5$ S cm^2), calcium ($\lambda_{Ca^{2+}} = 59.5$), magnesium ($\lambda_{Mg^{2+}} = 53.1$), sodium ($\lambda_{Na^+} = 50.1$) and finally lithium ($\lambda_{Li^+} = 38.7$). Our migration order is not identical to that reported by Beck and Engelhardt [8], but the running electrolyte has not exactly the same composition and it is well known that the co-ion buffer concentration may influence the migration of the analytes.

Thus, if alkali and alkaline-earth cations are resolved by using an imidazole running electrolyte, potassium and ammonium cations would comigate under non-complexing conditions. The addition of a complexing agent (18-crown-6) to the electrolyte is necessary for the total resolution of these two cations. The concentration of 18-crown-6 added to the imidazole electrolyte may influence the separation performances (electrophoretic mobility, peak efficiency, asymmetry factor and resolution of the other analyte cations). Besides, no complete study has been previously performed on the selectivity change due to a modification of this complexing agent concentration in the imidazole electrolyte. So, electroosmotic mobility and electrophoretic mobilities of six cations have been determined over

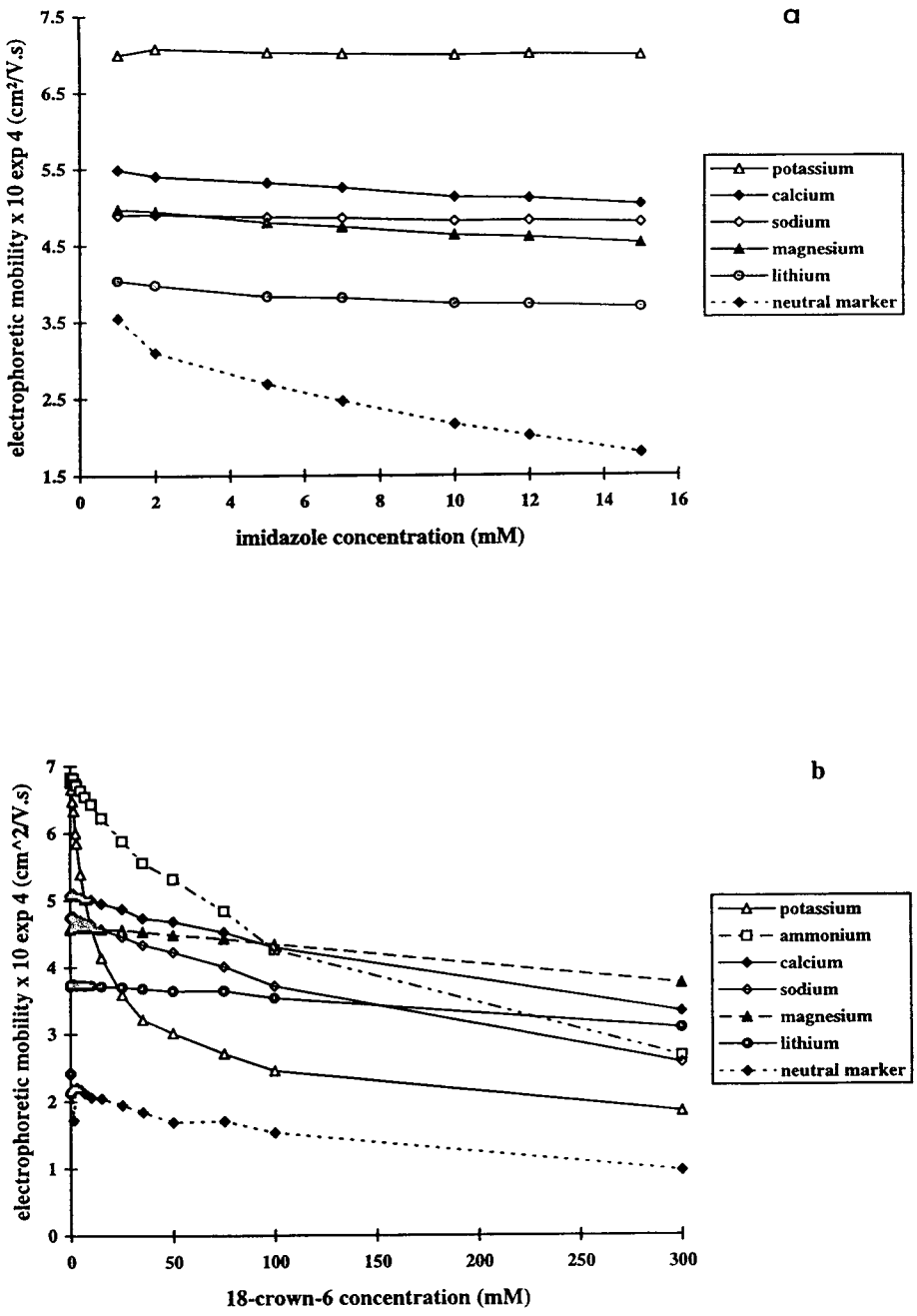

Fig. 1.

(Continued on p. 540)

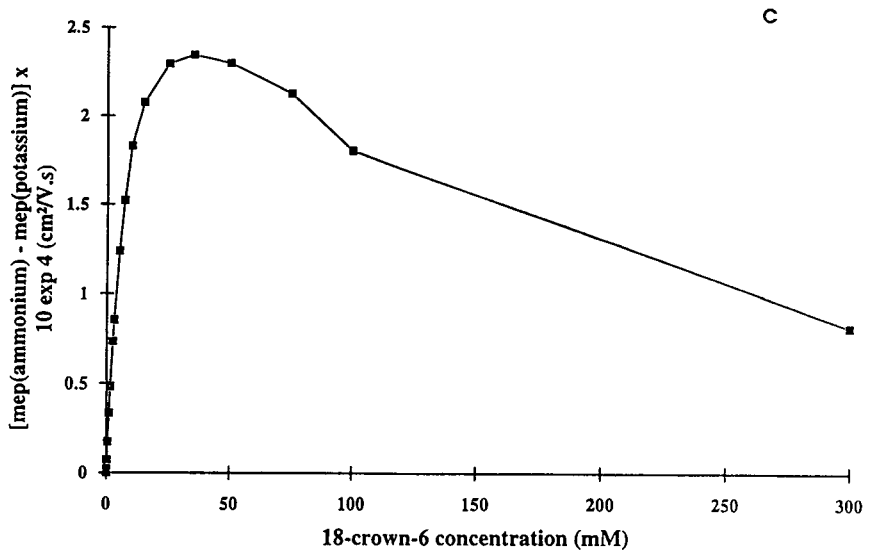

Fig. 1. (a) Influence of imidazole concentration on the electrophoretic mobility of several cations. Fused-silica capillary dimensions, 57 cm (50 cm to detector) × 75 μm I.D., 100 μm × 800 μm aperture; electrolyte, imidazole, pH 4.5; indirect UV detection, 214 nm; applied voltage, 15 kV (positive polarity); temperature, 25°C; hydrodynamic injection, 2 s; cation concentration, 5 ppm. (b) Influence of 18-crown-6 concentration added to the imidazole running electrolyte on the electrophoretic mobility of several cations. Experimental conditions as in (a) except electrolyte (10 m*M* imidazole, 18-crown-6, pH 4.5) and applied voltage (30 kV). (c) Difference in electrophoretic mobilities of ammonium and potassium versus the concentration of 18-crown-6. Experimental conditions as in (b).

the 10^{-5}–3.10^{-1} *M* 18-crown-6 concentration range using 10 m*M* imidazole buffer at pH 4.5 (Table 1). By increasing the 18-crown-6 concentration in the running electrolyte (10 m*M* imidazole, pH 4.5), the electrophoretic mobilities of potassium and ammonium decrease more rapidly than the electrophoretic mobilities of other cations (Fig. 1b); up to 7 m*M*, the migration order of these cations is not modified while a reversal of migration order of calcium and potassium is observed beyond this concentration. According to a previous study [16], the crown-complexed cations have lower ionic mobilities than the solvated cations. Besides, several migration order and selectivity changes are also observed for other cations at higher complexing agent concentration: for example, potassium migrates more slowly than magnesium beyond 10 m*M*, then more slowly than lithium beyond 25 m*M*. Fig. 2 illustrates the effect of 18-crown-6 concentration on the separation of a standard mixture of six cations. It is possible to shift the potassium peak in the electropherogram by adding a selected 18-crown-6 concentration to the 10 m*M* imidazole electrolyte (pH 4.5): so, potassium matrix samples will be resolved by using 35 m*M* 18-crown-6 in the electrolyte while ammonium matrix samples will be better resolved beyond 300 m*M* 18-crown-6. We have calculated the difference in electrophoretic mobilities of ammonium and potassium versus the concentration of 18-crown-6; the selectivity between these two cations does not remain constant and reaches a maximum at 35 m*M* (Fig. 1c), unlike previously reported results [12]. So, the crown ether concentration appears to be a very convenient parameter to monitor the selectivity of cations, particularly during the analysis of potassium and sodium matrix samples.

Finally, the variation of crown ether concentration also allows the determination of the stability complex constant of each cation by plotting the electrophoretic mobility versus the mathematical expression: -log[18-crown-6] (Fig. 3a). The abscissa of the inflection point is equal to log K_s, and the stability complex constants

Table 1
Influence of 18-crown-6 concentration on electrophoretic mobility (m_{ep}) of some inorganic cations

18-Crown-6 concentration (mM)	$m_{ep} \times 10^{-4}$ (cm^2/V s)					
	Potassium	Ammonium	Calcium	Sodium	Magnesium	Lithium
0.01	6.768	6.768	5.057	4.732	4.566	3.708
0.02	6.773	6.773	5.063	4.737	4.572	3.714
0.05	6.773	6.773	5.061	4.737	4.572	3.712
0.07	6.810	6.810	5.085	4.758	4.592	3.726
0.1	6.775	6.812	5.077	4.754	4.592	3.732
0.2	6.755	6.826	5.089	4.748	4.599	3.736
0.5	6.655	6.828	5.089	4.759	4.599	3.729
1	6.475	6.808	5.086	4.758	4.601	3.735
1.5	6.331	6.815	5.106	4.768	4.621	3.745
2.5	5.999	6.733	5.069	4.734	4.596	3.734
3	5.852	6.706	5.059	4.723	4.590	3.725
5	5.392	6.630	5.049	4.706	4.597	3.731
7	5.016	6.538	5.016	4.676	4.588	3.724
10	4.597	6.430	5.012	4.650	4.597	3.728
15	4.145	6.221	4.952	4.570	4.570	3.715
25	3.589	5.882	4.871	4.461	4.561	3.701
35	3.216	5.559	4.733	4.338	4.530	3.677
50	3.018	5.315	4.685	4.230	4.486	3.646
75	2.710	4.837	4.520	4.011	4.426	3.646
100	2.454	4.262	4.295	3.715	4.341	3.534
300	1.851	2.670	3.333	2.572	3.751	3.088

Experimental conditions as in Fig. 1b.

with 18-crown-6 have been determined at 25°C for potassium, ammonium, barium and strontium (Table 2); these values agree with those reported in the literature [23,24]. The high K_s value for potassium results in a migration speed that is reduced relative to ammonium, enabling the two cations to be separated. On the other hand, the weaker value of K_s for sodium, calcium, magnesium and lithium explain the flat shape of the curves (Fig. 1b).

However, the complexation process may be easily followed by the degree of complexation x of the cation C^+, defined as

$$x = \frac{[CL^+]}{[C^+] + [CL^+]} = \frac{m_{C^+} - m^+}{m_{C^+} - m_{CL^+}} \quad (6)$$

where m_{CL^+}, m_{C^+} and m^+ are the electrophoretic mobilities of the complexed cation, the free cation and the partially complexed cation by the 18-crown-6, respectively. The variation of complexation degree versus the expression $-\log$[18-crown-6] is shown in Fig. 3b.

In order to determine the best separation conditions, a series of 10 mM imidazole running electrolytes having different 18-crown-6 concentrations (0.1–8 mM) were tested. Fig. 4 reports the change in resolution between two consecutive peaks. In particular, the resolution between ammonium and potassium peaks and also between potassium and calcium peaks are very sensitive to complexing agent concentration. However, a modification of 18-crown-6 concentration does not improve the resolution between the other cations. Overall, running electrolyte with 2.5 mM 18-crown-6 seems to give the best total resolution.

3.2. Effect of running electrolyte pH

The influence of running electrolyte pH upon electrophoretic mobility and resolution of several

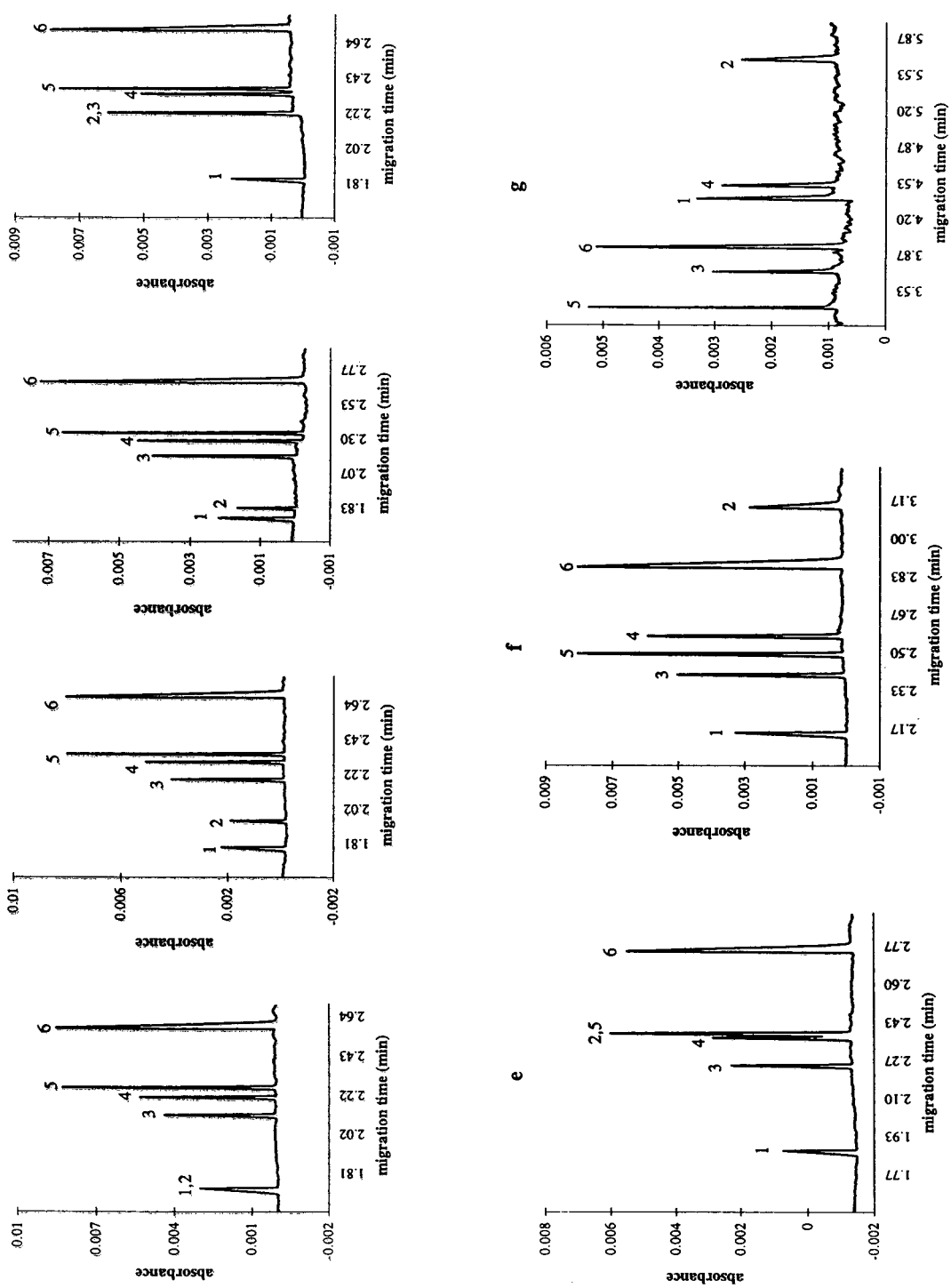

Fig. 2. Influence of 18-crown-6 concentration added to the imidazole running electrolyte on the migration order of an inorganic cation mixture. Experimental conditions as in Fig. 1b except 18-crown-6 concentration: (a) 0.01 m*M*; (b) 1.0 m*M*; (c) 2.5 m*M*; (d) 7.0 m*M*; (e) 10 m*M*; (f) 35 m*M*; (g) 300 m*M*. Cations (5 ppm): 1 = NH_4^+; 2 = K^+; 3 = Ca^{2+}; 4 = Na^+; 5 = Mg^{2+}; 6 = Li^+.

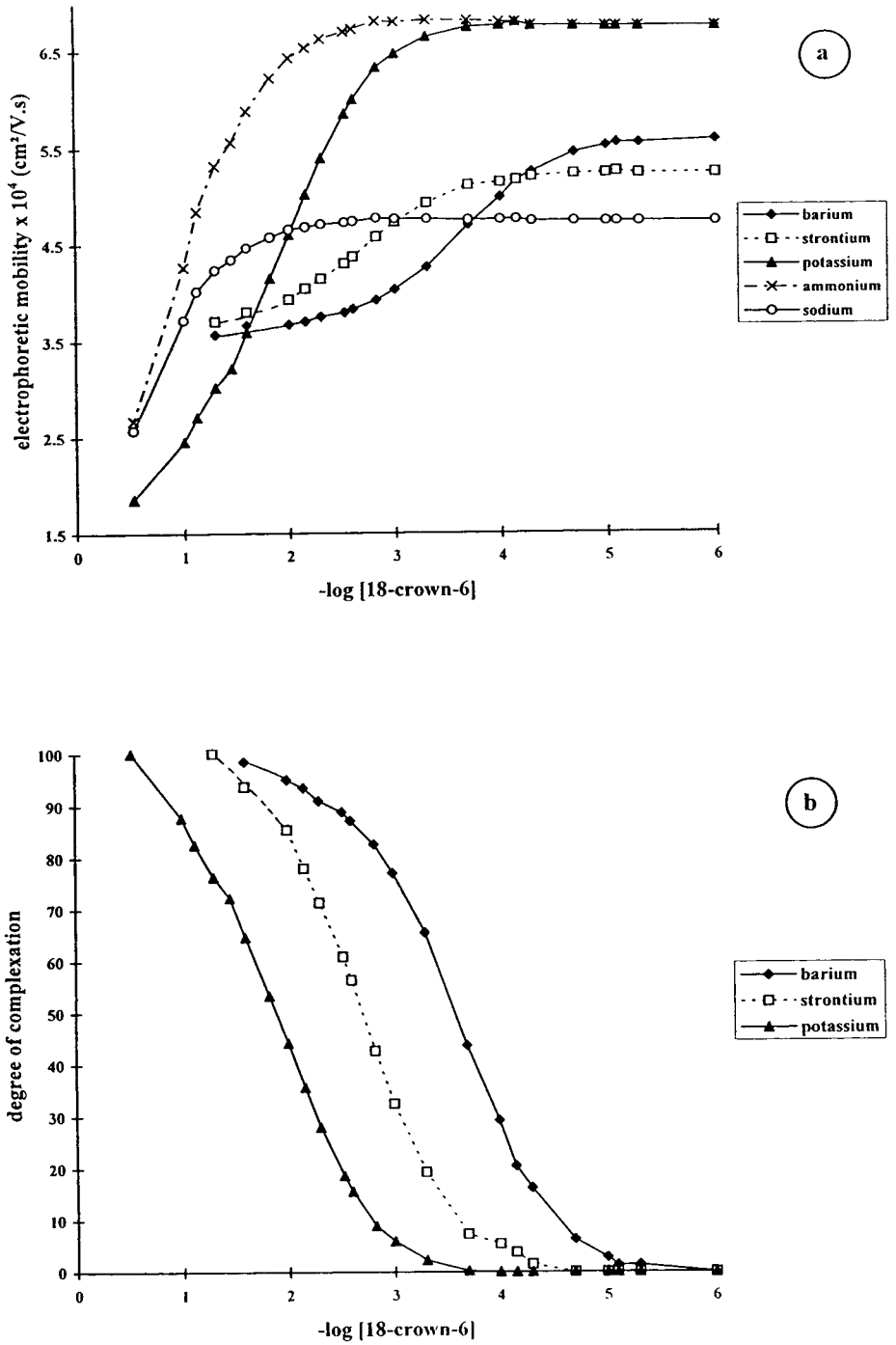

Fig. 3. Variation of the electrophoretic mobility and complexation degree of several inorganic cations versus the mathematical expression: −log [18-crown-6]. Experimental conditions as in Fig. 1b.

Table 2
Stability constant of 18-crown-6 complexes for several cations

Cation	log K_{exp}	log K^a	log K^b
Ammonium	1.01	0.9	1.23
Potassium	2.1	2.1	2.03
Barium	3.6	4.1	3.87
Strontium	2.7	2.9	2.72
Calcium	–	1.0	–
Sodium	–	1.0	0.8

Experimental conditions as in Fig. 1b.
[a] Literature data were taken from Ref. [24].
[b] Literature data were taken from Ref. [23].

cations has been performed on imidazole electrolyte without addition of 18-crown-6, then with addition of 2.5 m*M* 18-crown-6 (Fig. 5). The electroosmotic flow increased as the pH increased from 3.5 to 6.0, hence the CE separation time could be shortened at pH 6.0. The complex formation between 18-crown-6 and cations was obviously independent of the pH of the running electrolyte (Fig. 5a and c). We also found that the resolution was not very sensitive to pH using imidazole electrolyte (Fig. 5b) whereas the resolution between K^+ and Ca^{2+} or Ca^{2+} and Na^+ depended on the pH using this complexing electrolyte (Fig. 5d).

3.3. Effect of running voltage

The effect of voltage on separation resolution has been studied using imidazole- and 18-crown-6-based electrolyte. An increasing voltage between 5 and 30 kV induced a shorter analysis time but a constant electrophoretic mobility of cations (Fig. 6). Moreover, an increasing voltage induced an increase in peak efficiency and resolution (Table 3). Fig. 6 shows that the current linearly increases with applied voltage; therefore, the amount of heat generated is totally

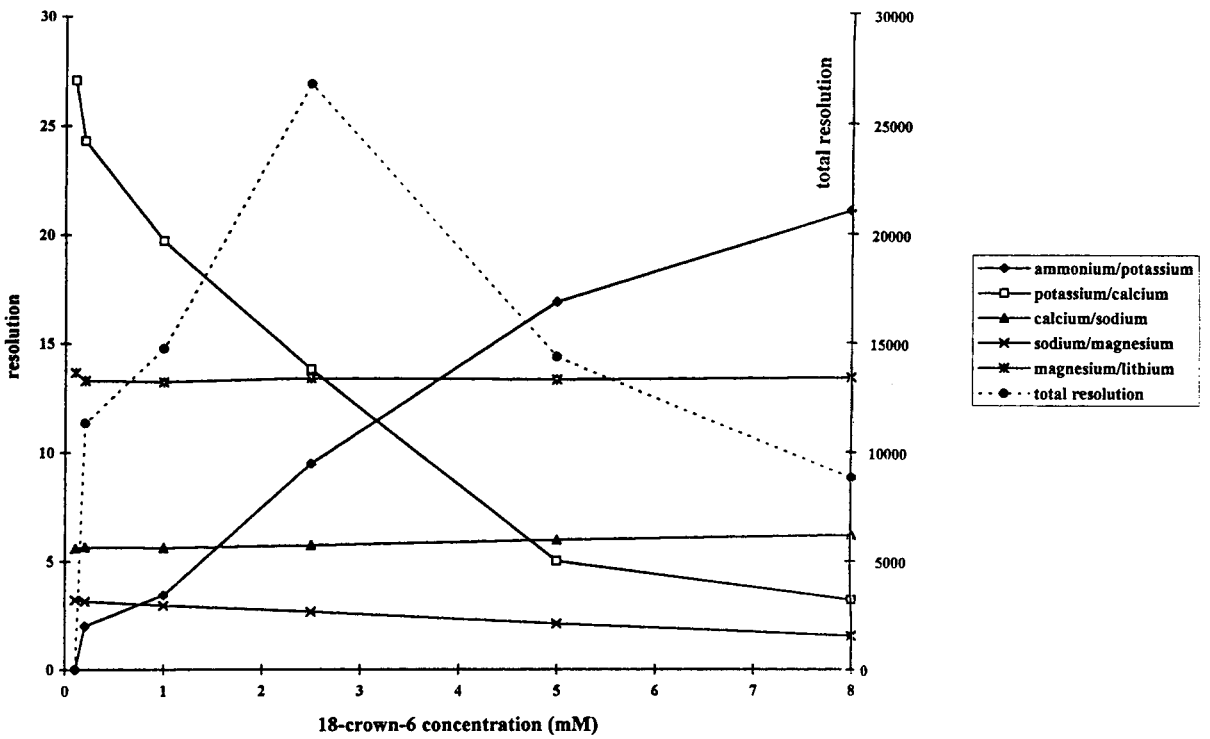

Fig. 4. Influence of 18-crown-6 concentration on the CE resolution of several cations. Experimental conditions as in Fig. 1b.

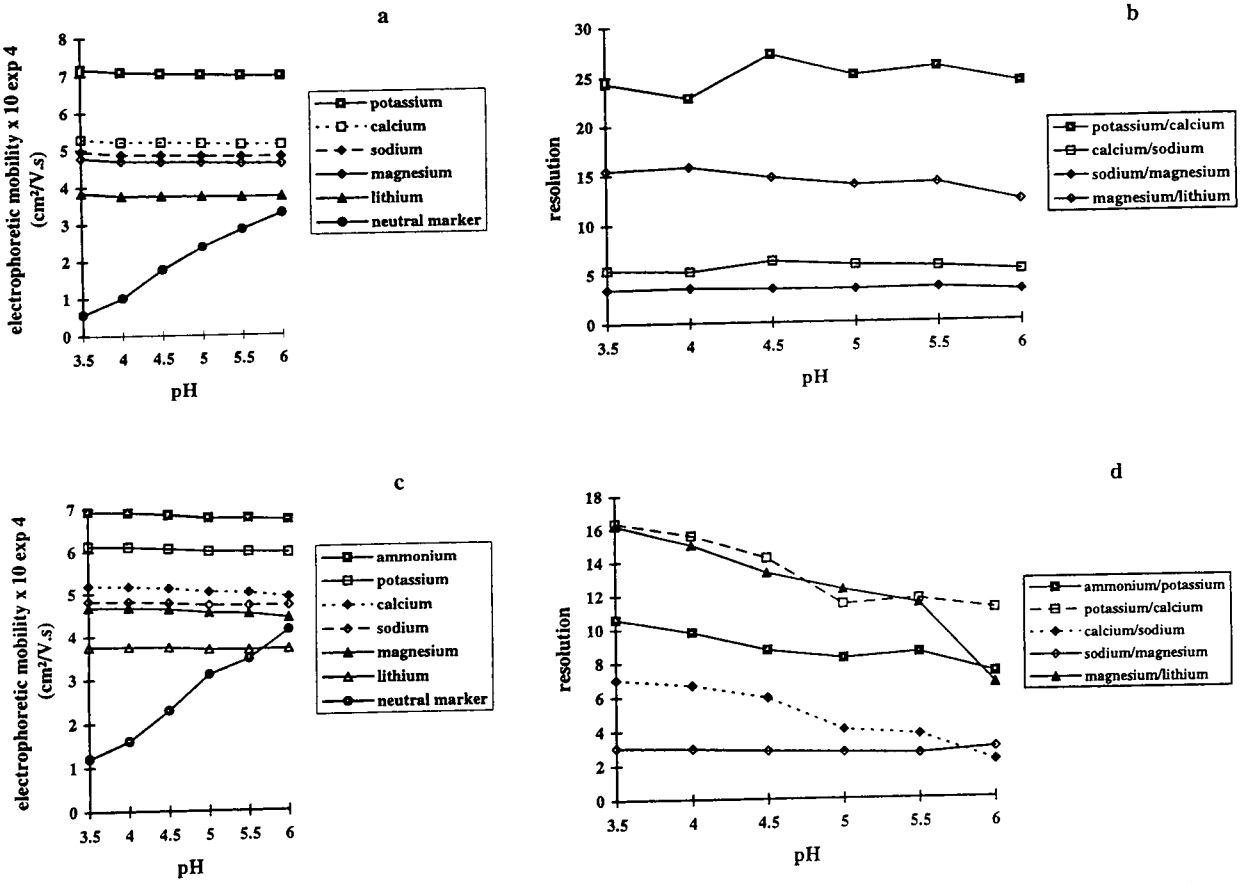

Fig. 5. Influence of buffer pH on the electrophoretic mobility and resolution of several cations. Fused-silica capillary dimensions, 57 cm (50 cm to detector) × 75 μm I.D., 100 μm × 800 μm aperture; electrolyte, 10 m*M* imidazole; indirect UV detection, 214 nm; applied voltage, 20 kV (positive polarity); hydrodynamic injection, 2 s; cation concentration, 5 ppm. (a, b) without 18-crown-6; (c, d) with 2.5 m*M* 18-crown-6.

dissipated. Thus, we can work equally well at 5 as at 30 kV. The 75 μm I.D. of the capillary tube allows a good thermal dispersion.

3.4. Effect of temperature

Temperature variations affect several physical parameters (viscosity, dielectric constant, pH) and consequently the electroosmotic flow-rate and the electrophoretic mobility of the analytes. This study was carried out at five different temperatures (20, 25, 30, 35, 40°C) with an imidazole- and 18-crown-6-based electrolyte. Temperature variations in the range 20–40°C did not significantly alter the selectivity of our separation at pH 4.5. When the temperature increased from 20 to 40°C, the migration times decreased and, thus, the electrophoretic mobilities of cations increased (Fig. 7). The peak efficiency was slightly better at low temperatures because the diffusion coefficient decreased at lower temperatures; thus, working at 25°C maintains a high peak efficiency and resolution without too long analysis times (Table 4).

3.5. Quantitative aspect

The influence of hydrodynamic injection time on the corrected peak area, peak area and peak height was studied with an imidazole and 18-

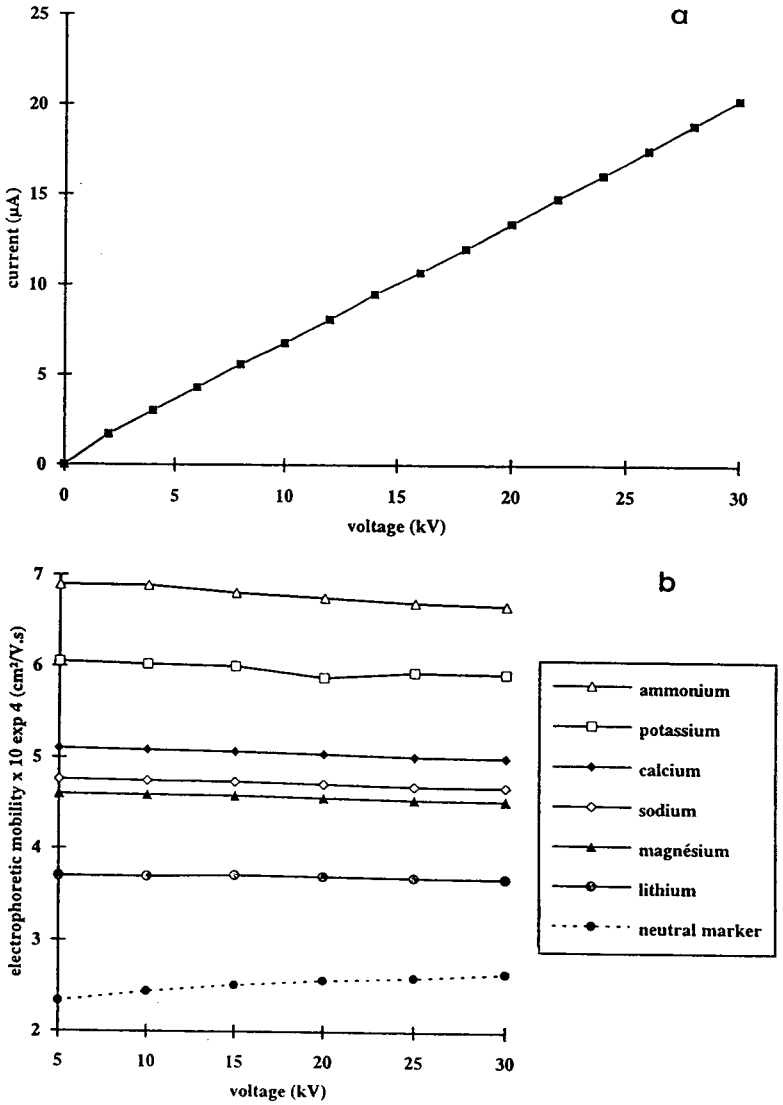

Fig. 6. Dependence of cation electrophoretic mobility and current versus running voltage. Experimental conditions as in Fig. 5 except electrolyte (10 m*M* imidazole, 2.5 m*M* 18-crown-6, pH 4.5). (a) Current; (b) electrophoretic mobility.

crown-6-based electrolyte at pH 4.5. Fig. 8a–c shows that it is preferable to work with corrected peak area, where the correlation coefficients are slightly higher than those obtained with peak area (Table 5). On the other hand, when the injection time increases from 1 to 10 s, peak height is not a linear function, except for sodium and magnesium. Indeed, these two cations have an electrophoretic mobility close to that of imidazole ($4.709 \cdot 10^{-4}$, $4.562 \cdot 10^{-4}$ cm^2 V^{-1} s^{-1} in an imidazole and 18-crown-6-based electrolyte and $4.583 \cdot 10^{-4}$ cm^2 V^{-1} s^{-1} in an acetate electrolyte, respectively). So, if the electrophoretic mobility of the cation is close to that of the co-ion and if the limited column capacity is not reached, it is possible to use the peak height for quantitation. In our case, the correlation coefficient for sodium and magnesium are 0.99932 and

Table 3
Influence of applied voltage on peak efficiency (N) and resolution (R_s)

Voltage (kV)	N (ammonium)	N (potassium)	N (calcium)	N (sodium)	N (magnesium)	N (lithium)
5	71 800	104 500	172 900	113 800	191 900	78 800
10	89 500	179 400	278 800	213 100	320 100	109 900
15	80 900	199 500	277 400	262 700	368 100	89 400
20	82 000	209 700	295 500	302 100	380 800	89 200
25	99 100	228 800	290 500	340 800	371 600	94 200
30	101 600	280 400	296 400	348 600	374 200	113 500

	R_s (ammonium–potassium)	R_s (potassium–calcium)	R_s (calcium–sodium)	R_s (sodium–magnesium)	R_s (magnesium–lithium)
5	7.07	11	4.36	2.18	11.73
10	8.2	13.89	5.66	2.82	13.96
15	7.9	14.07	5.84	2.97	12.85
20	7.82	14.31	6.05	3.05	12.71
25	8.19	14.47	6.14	3.06	12.76
30	8.37	15.17	6.12	3.04	13.54

Experimental conditions as in Fig. 6.

0.99955, respectively. The repeatability in terms of the migration times was less than 0.5% R.S.D. and, in terms of corrected peak area, was better than 5% R.S.D.

A notable decrease in efficiency was observed when the injection time increased from 1 to 10 s. For example, there was 81% decrease in peak efficiency for ammonium and 80% for lithium for a concentration of 2 ppm. This loss of peak efficiency was also less important for the cations having an electrophoretic mobility close to that of imidazole (15% decrease). This study confirms the limited column capacity in free capillary electrophoresis.

The influence of solute concentration on the three parameters was studied with an imidazole and 18-crown-6-based electrolyte at pH 4.5 Fig. 9a–c shows the influence of cation concentration in the 2.5–50 ppm range on the corrected peak area, peak area and peak height. The correlation

Table 4
Influence of temperature on peak efficiency (N) and resolution (R_s)

Temperature (°C)	N (ammonium)	N (potassium)	N (calcium)	N (sodium)	N (magnesium)	N (lithium)
20	124 600	350 500	436 900	469 700	557 800	146 300
25	110 510	305 700	362 700	463 800	561 800	107 900
30	93 100	218 200	316 500	378 800	439 100	93 900
35	104 300	231 600	332 000	393 300	410 700	124 600
40	92 700	196 300	322 100	341 600	381 900	107 400

	R_s (ammonium–potassium)	R_s (potassium–calcium)	R_s (calcium–sodium)	R_s (sodium–magnesium)	R_s (magnesium–lithium)
20	12.02	17.26	7.81	3.9	16.6
25	8.7	16.37	6.98	3.47	14.21
30	6.51	14.86	6.08	2.76	12.39
35	5.91	15.59	5.93	2.55	13.22
40	4.79	14.97	5.4	2.28	12.07

Experimental conditions as in Fig. 7.

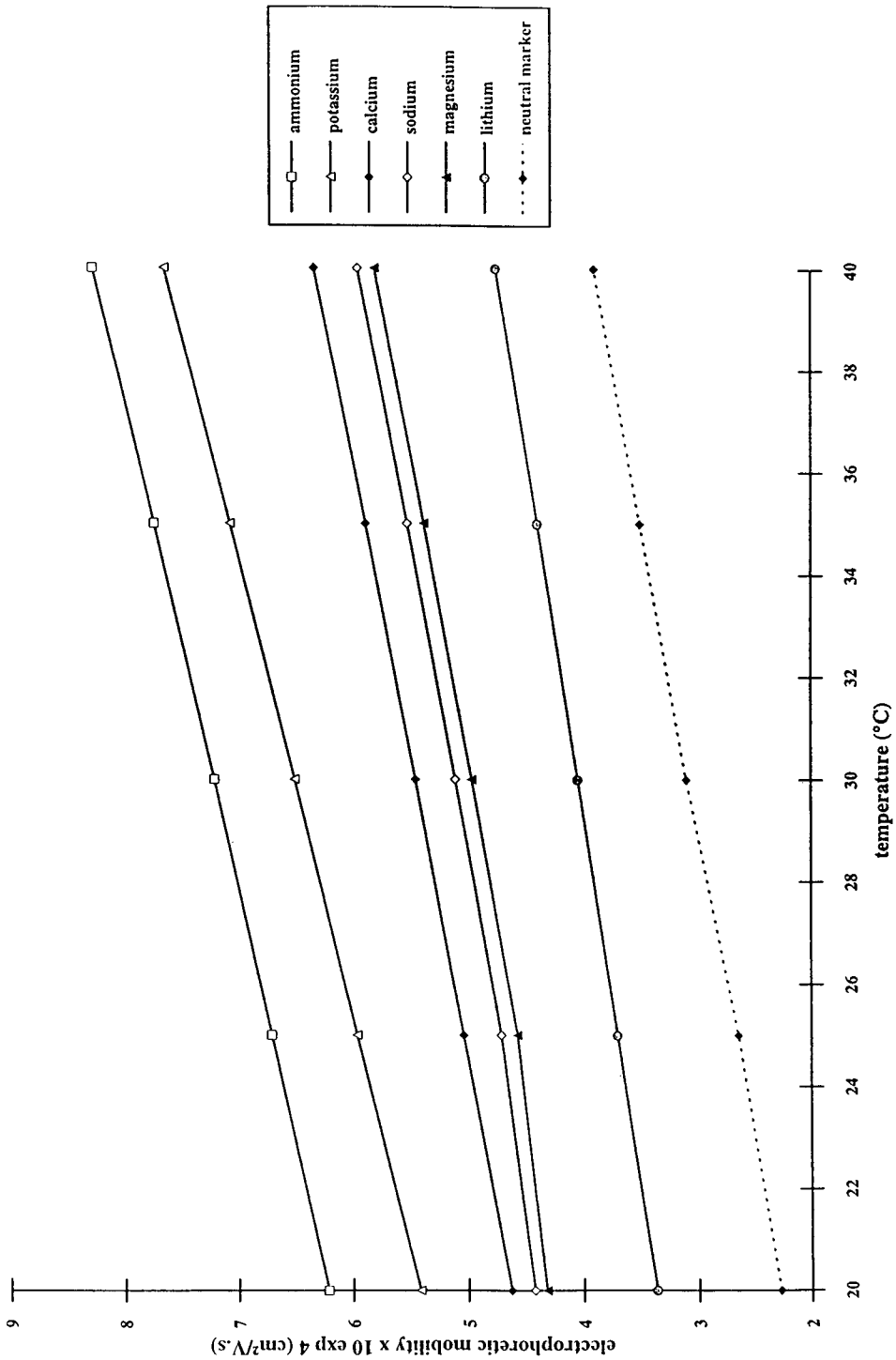

Fig. 7. Variation of electrophoretic mobility with temperature modification. Experimental conditions as in Fig. 6 except applied voltage (30 kV).

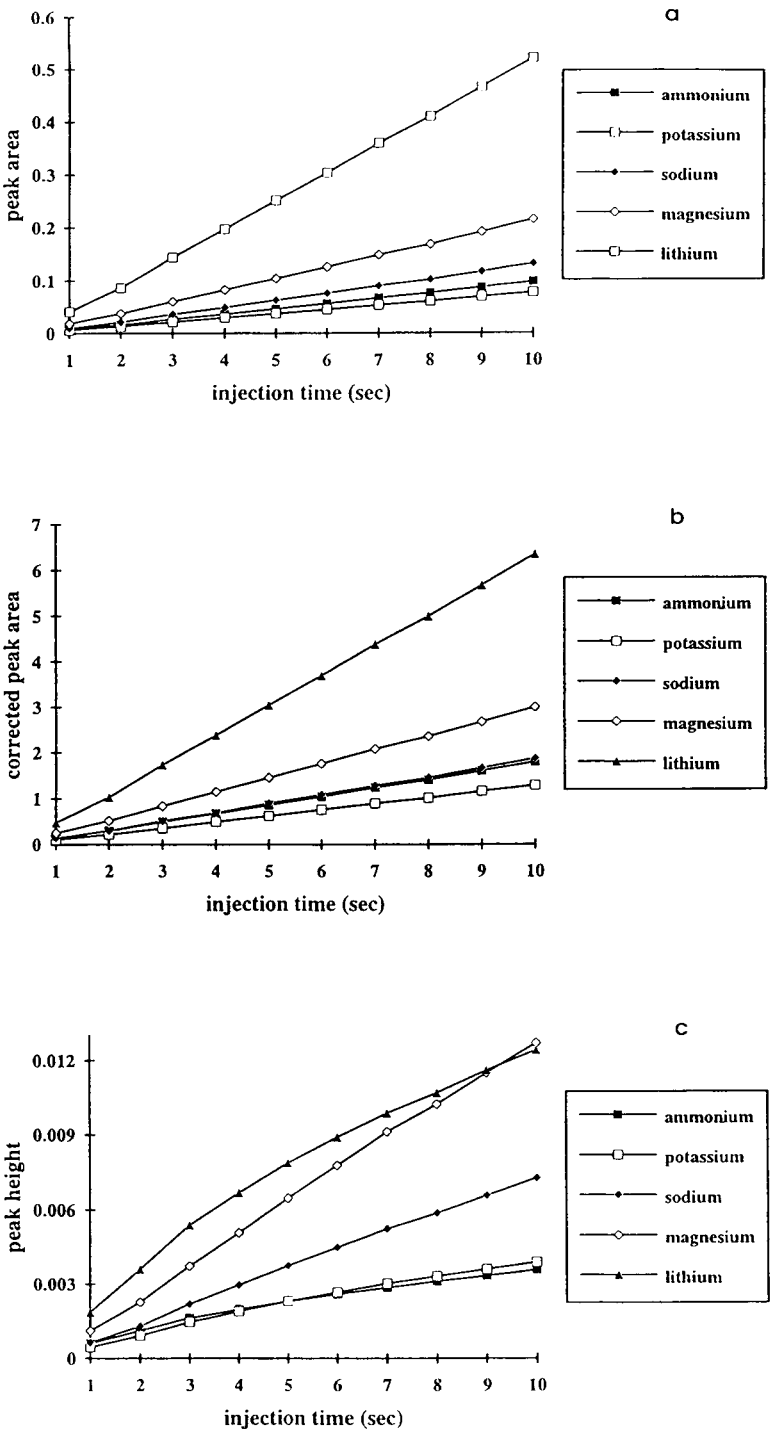

Fig. 8. Influence of injection time versus peak area, corrected peak area and peak height. Experimental conditions as in Fig. 6 except cation concentration (2 ppm). (a) Peak area; (b) corrected peak area; (c) peak height.

Table 5
Influence of hydrodynamic injection time on peak height, peak area and corrected peak area of several cations

Cation	Slope	Intercept	Correlation coefficient
Corrected peak area			
Ammonium	0.183	−0.054	0.99990
Potassium	0.132	−0.036	0.99987
Sodium	0.192	−0.066	0.99981
Magnesium	0.304	−0.069	0.99991
Lithium	0.654	−0.228	0.99989
Peak area			
Ammonium	0.010	-3.5×10^{-3}	0.99964
Potassium	0.008	-2.7×10^{-3}	0.99974
Sodium	0.013	-4.9×10^{-3}	0.99974
Magnesium	0.022	-5.3×10^{-3}	0.99984
Lithium	0.054	−0.018	0.99988
Peak height			
Ammonium	0.00032	5.6×10^{-4}	0.98852
Potassium	0.00038	2.6×10^{-4}	0.99374
Sodium	0.00074	-5.3×10^{-4}	0.99932
Magnesium	0.00013	-1.6×10^{-4}	0.99955
Lithium	0.00011	1.6×10^{-4}	0.98935

Experimental conditions as in Fig. 8.

Table 6
Slopes and correlation coefficients of calibration plot for quantitative analysis of several cations

Cation	Slope	Intercept	Correlation coefficient
Corrected peak area			
Ammonium	0.140	−0.095	0.99960
Potassium	0.080	−0.041	0.99978
Calcium	0.143	−0.071	0.99952
Sodium	0.132	−0.041	0.99950
Magnesium	0.244	−0.224	0.99977
Lithium	0.502	−0.510	0.99975
Peak area			
Ammonium	7.64×10^{-3}	-6.18×10^{-3}	0.99966
Potassium	4.77×10^{-3}	-2.81×10^{-3}	0.99981
Calcium	9.56×10^{-3}	-4.46×10^{-3}	0.99956
Sodium	9.42×10^{-3}	-7.02×10^{-3}	0.99982
Magnesium	17.51×10^{-3}	-16.59×10^{-3}	0.99977
Lithium	40.99×10^{-3}	-53.75×10^{-3}	0.99920
Peak height			
Ammonium	1.3×10^{-4}	1.28×10^{-3}	0.97537
Potassium	1.4×10^{-4}	9.2×10^{-4}	0.97841
Calcium	2.7×10^{-4}	1.81×10^{-3}	0.97656
Sodium	3.6×10^{-4}	1.11×10^{-3}	0.99060
magnesium	8.0×10^{-4}	1.24×10^{-3}	0.99438
Lithium	4.5×10^{-4}	4.18×10^{-3}	0.97609

Experimental conditions as in Fig. 9.

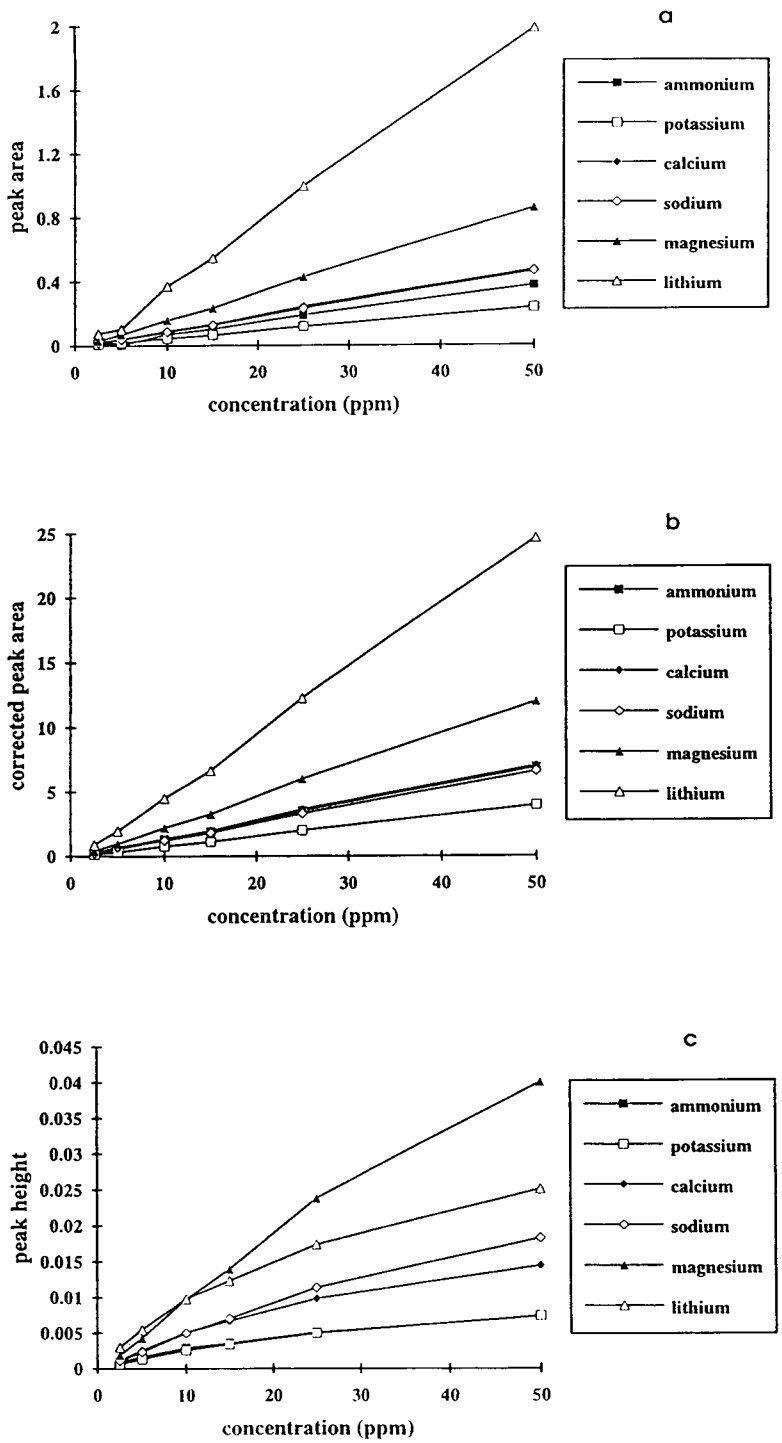

Fig. 9. Linear calibration plots for inorganic cations. Fused-silica capillary dimensions, 57 cm (50 cm to detector) × 75 μm I.D., 100 μm × 800 μm aperture; electrolyte, 10 m*M* imidazole, 2.5 m*M* 18-crown-6, pH 4.5; indirect UV detection, 214 nm; applied voltage, 25 kV; hydrodynamic injection, 2 s. (a) Peak area; (b) Corrected peak area; (c) Peak height.

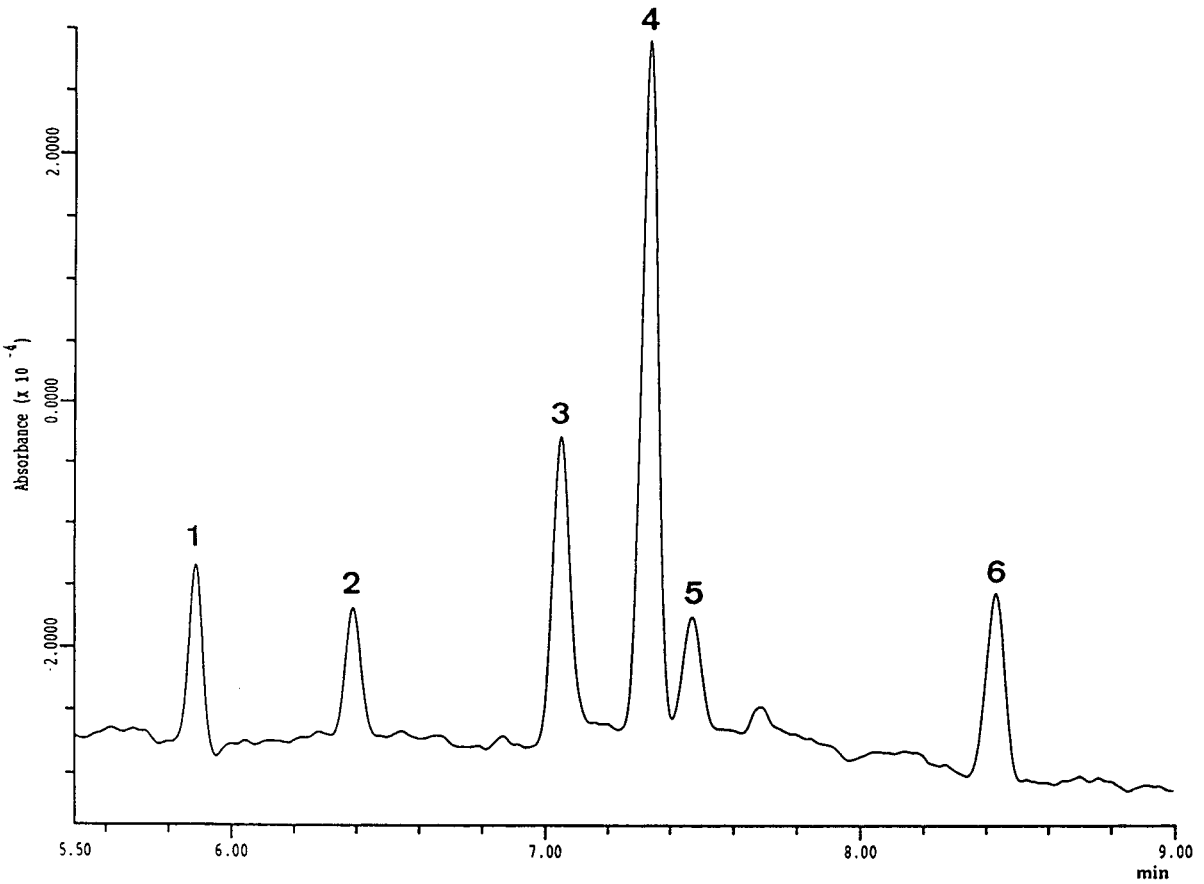

Fig. 10. Separation of an inorganic cation mixture at 10-ppb level. Experimental conditions as in Fig. 9 except hydrodynamic injection (2 s). Cations: 1 = NH_4^+; 2 = K^+; 3 = Ca^{2+}; 4 = Na^+; 5 = Mg^{2+}; 6 = Li^+.

coefficient always reaches 0.999 for all cations when corrected peak area and peak area were used (Table 6). As previously stated, for the cations that have an electrophoretic mobility close to that of imidazole (sodium and magnesium), their peak height versus concentration is a linear function up to 25 ppm. The correlation coefficients are equal to 0.999 in the 2.5–25 ppm concentration range. Beyond this value, we observed a loss of linearity due to the limited column capacity. Lastly, an important decrease in efficiency was also observed when the solute concentration was increased from 2.5 to 50 ppm. For example, a loss in peak efficiency of 94% for ammonium and 93% for lithium occurred. This loss in peak efficiency was less important for sodium and magnesium (54% and 64%, respectively).

Although the peak efficiency decreases with increasing injection time, the separation of an inorganic cation standard is possible at low concentrations (10 ppb) without loss of resolution, by increasing the hydrodynamic injection time up to 20 s (Fig. 10).

4. Conclusion

The separation of ammonium, alkali and alkaline-earth cations by CE is easily achieved

with an imidazole-based electrolyte to which 18-crown-6 has been added. The separation of potassium–ammonium or strontium–barium is favoured by complex formation with 18-crown-6. The determination of the stability complex constant with 18-crown-6 for several cations can be experimentally determined by CE from electrophoretic mobilities versus −log[18-crown-6] curves. The high stability constants for potassium, barium and strontium induce in a lower migration velocity than those of ammonium and other cations. So, during the analysis of complex matrix samples, the crown ether concentration appears to be a very convenient parameter to monitor the selectivity of cations.

Acknowledgements

The authors thank the Eurothermes Society (Dr. Drutel, La Bourboule, France) for support of this work and Mrs. Depernet for her technical assistance.

References

[1] Ph. Morin, C. François and M. Dreux, *Analusis*, 22 (1994) 178.
[2] M. Aguilar, X. Huang and R. Zare, *J. Chromatogr.*, 480 (1989) 427.
[3] N. Wu, W. Horvath, P. Sun and C. Huie, *J. Chromatogr.*, 635 (1993) 307.
[4] F. Foret, S. Fanali, A. Nardi and P. Bocek, *Electrophoresis*, 11 (1990) 780.
[5] A. Weston, P. Brown, A. Heckenberg, P. Jandik and W. Jones, *J. Chromatogr.*, 602 (1992) 249.
[6] A. Weston, P. Brown, P. Jandik, W. Jones and A. Heckenberg, *J. Chromatogr.*, 593 (1992) 289.
[7] M. Chen and R. Cassidy, *J. Chromatogr.*, 602 (1992) 227.
[8] W. Beck and H. Engelhardt, *Chromatographia*, 33 (1992) 313.
[9] M. Koberda and M. Konkowski, P. Younberg, W. Jones and A. Weston, *J. Chromatogr.*, 602 (1992) 235.
[10] L. Gross and E. Yeung, *Anal. Chem.*, 62 (1990) 427.
[11] D. Swaile and M. Sepaniak, *Anal. Chem.*, 63 (1991) 179.
[12] K. Bachmann, J. Boden and I. Haumann, *J. Chromatogr.*, 626 (1992) 259.
[13] X. Huang, T. Pang, M. Gordon and R. Zare, *Anal. Chem.*, 59 (1987) 2747.
[14] Ph. Morin, C. François and M. Dreux, *J. Liq. Chromatogr.*, 17 (1994), 3869.
[15] J. Riviello and M. Harrold, *J. Chromatogr.*, 652 (1993) 385.
[16] E. Simunicova, D. Kaniansky and K. Loksikova, *J. Chromatogr.*, 665 (1994) 203.
[17] Y. Shi and J. Fritz, *J. Chromatogr.*, 640 (1993) 473.
[18] Y. Shi and J. Fritz, *J. Chromatogr.*, 671 (1994) 429.
[19] Y. Lee and T. Lin, *J. Chromatogr.*, 675 (1994) 227.
[20] M. Chen and R. Cassidy, *J. Chromatogr.*, 640 (1993) 425.
[21] C. Quang and M. Khaledi, *J. Chromatogr.*, 659 (1994) 459.
[22] A. Timerbaev, O. Semenova and G. Bonn, *Chromatographia*, 37 (1993) 497.
[23] R.M. Smith and A.E. Martell, *Critical Stability Constants*, Plenum Press, New York, 1975.
[24] R.M. Izatt, K. Pawlak, J.S. Bradshaw and R.L. Bruening, *Chem. Rev.*, 91 (1991) 1721.

ELSEVIER

Journal of Chromatography A, 706 (1995) 555–562

JOURNAL OF CHROMATOGRAPHY A

Capillary electrophoretic analysis of the reactions of bifunctional reactive dyes under various conditions including a study of the analysis of the traditionally difficult to analyse phthalocyanine dyes

Kelvin N. Tapley

Department of Colour Chemistry and Dyeing, University of Leeds, Leeds LS2 9JT, UK

Abstract

Good analytical techniques for the separation and detection of reactive dyes are necessary not only to monitor residual liquors and effluents but also to aid in optimisation of dye synthesis, purification, formulation and application. HPLC, although generally widely employed, often has difficulty in analysing certain reactive dyes, especially the phthalocyanine-based dyes.

CE analysis of several bifunctional reactive dyes has been carried out with subsequent activation and hydrolysis reactions for a bis-sulfatoethyl sulfone dye, under different pH and temperature conditions, being monitored. A variety of buffers were investigated; the use of acetonitrile in a micellar buffer system proving to be particularly successful.

1. Introduction

In the early studies of dye analysis using capillary electrophoresis (CE) systems the buffers employed were basically just the conventional aqueous buffers such as phosphate, borate and citrate [1–3]. More recently, however, workers have employed micellar buffer systems to analyse a range of dyes and intermediates [4–6] including some selective reactive dyes [4,6].

The work reported on in this paper has been more directly concerned with monitoring the reactions of reactive dyes as they proceed. In the present study the introduction of acetonitrile into the micellar buffer system was found to be beneficial for the analysis of reactive dyes particularly the Procion Turquoise H-A (ICI) (a phthalocyanine-based) dye. This and the actual conditions employed will be discussed in more detail in the relevant sections later in this paper.

Reactive dyes are employed primarily in the coloration of cellulosic materials with which they form covalent bonds. The first commercial bifunctional reactive dye is generally accepted as being Remazol Black B (HOE) which is a bis-sulfatoethyl sulfone dye as illustrated in Fig. 1. The majority of the work reported on in this paper concerns the analysis of this dye and monitoring the activation and subsequent hydrolysis of this dye.

The main and most obvious advantage of bifunctional dyes is the possibility for higher fixation values than with monofunctional dyes. This is because hydrolysis of one of the reactive groups in a bifunctional dye still leaves a dye capable of reacting with the fibre, this is not the

0021-9673/95/$09.50
SSDI 0021-9673(94)01206-7

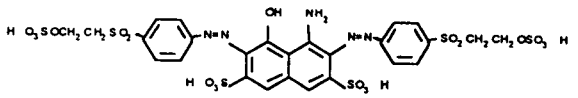

Fig. 1. Structure of Remazol Black B (HOE) dye.

case with monofunctional dyes. This may be demonstrated by looking at the following example where it is hypothetically assumed that the probability of a reactive group (R) being hydrolysed (H) by the end of a set time, such as a dyeing cycle, is 25% (i.e. one in four). Thus, the probability of a reactive group is 75% i.e. three in four. For a bifunctional dye, R–D–R′, there are four possible outcomes:

R–D–R′ (no hydrolysed groups), R–D–H and H–D–R′ (one hydrolysed and one reactive group) and H–D–H (both groups hydrolysed).

Statistically:

R–D–R′	R–D–H	H–D–R′	H–D–H
3/4 × 3/4	3/4 × 1/4	1/4 × 3/4	1/4 × 1/4
9/16	3/16	3/16	1/16

Therefore, there would only be one in sixteen molecules, i.e. 6.25% of dye molecules, which were totally hydrolysed and unable to react with the fibre. Thus instead of having 75% of the dye with a reactive group, as in the case of a monofunctional dye, you now have 93.75% of the dye with at least one reactive group for a bifunctional dye. In this example it is assumed that the hydrolysis of the two reactive groups in the bifunctional dye occurs independently of each other. This simplified example serves to highlight the potential of bifunctional dyes over monofunctional dyes, there are of course many factors which will influence the efficiency of the dye–fibre reaction.

The Remazol Black B dye may be represented as:

$$HO_3S–O–CH_2–CH_2–SO_2–D–SO_2–CH_2–CH_2–O–SO_3H \quad (A)$$

where D represents the dye chromophore (including the bridging groups between the chromophore and the sulfonyl groups).

The β-sulfatoethyl sulfone (SES) is in fact the precursor of the actual reactive group which is the vinyl sulfone (VS), this is generated under dyeing conditions (typically: pH 11, 50°C). Under these alkaline conditions, in addition to the reaction of the dye with ionised hydroxyl groups of cellulose, there is the potential for hydrolysis of the dye to the fibre-unreactive β-hydroxyethyl sulfone (HES) form of the dye to occur. The major products from the stepwise activation and then hydrolysis of Remazol Black B under alkaline conditions are represented below (structures B–E):

$$HO_3–S–O–CH_2–CH_2–SO_2–D–SO_2–CH=CH_2 \quad (B)$$

$$H_2C=CH–SO_2–D–SO_2–CH=CH_2 \quad (C)$$

$$HO–CH_2–CH_2–SO_2–D–SO_2–CH=CH_2 \quad (D)$$

$$HO–CH_2–CH_2–SO_2–D–SO_2–CH_2–CH_2–OH \quad (E)$$

Other products formed under alkaline conditions may include dialkyl ether derivatives where two dye molecules are linked through an ether bond. This type of compound, resulting from the reaction of a HES group from one dye molecule with a VS group of another dye molecule [7], is in equilibrium with the reactants. This means that as more of the VS groups are hydrolysed the concentration of these higher-molecular-mass compounds will start to decrease.

A range of bis-monochlorotriazinyl dyes was successfully introduced by ICI (now known as Zeneca) in the late 1960s and early 1970s under the trade name Procion H-E (ICI) dyes. These were developed to take advantage of the higher fixation values possible with bifunctional dyes. These dyes benefited from having a second triazinyl ring system which enhanced further the substantivity of these dyes, so that in an exhaust dyeing application very high levels of exhaustion, and hence fixation could be achieved [8].

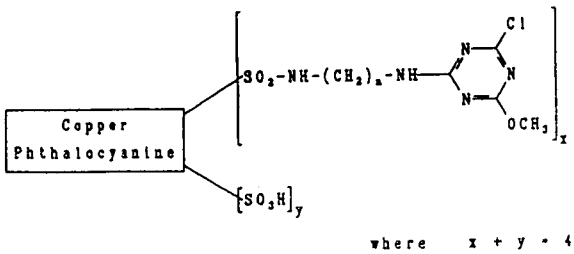

Fig. 2. Representation of the structure of Procion Turquoise H-A.

The second major dye studied as part of this current research was Procion Turquoise H-A (Zeneca) which is based on monochlorotriazinyl reactive groups attached to a copper phthalocyanine chromophore. Due to the complicated synthesis involved in its manufacture this dye is in fact a mixture of related compounds. The basic structure of this dye is outlined in Fig. 2. Analysis of phthalocyanine dyes by HPLC has been largely unsuccessful or unsatisfactory. In this present CE analysis study, by manipulation of buffer composition and pH, it has been possible to obtain some very good separations.

Mixed bifunctional dyes such as those in the Sumifix Supra (NSK) range offer several notable advantages over conventional mono- and bifunctional dyes. The reason for this lays in the difference in reactivity of the two reactive groups, with the VS (generated during dyeing from the SES) reacting typically at 50°C and the monochlorotriazine at 80°C. Thus the dyes are less sensitive to temperature variations during dyeing. Other advantages include minimal sensitivity to alkali and inorganic salts and they are affected less by changes in liquor ratios [9].

In this study the hydrolysis reactions of a selection of model dyes under various pH and temperature conditions were investigated with the aid of CE analysis.

2. Experimental

2.1. Chemicals

The original reactive dyes were of commercial grade (from the manufacturers) and were used without purification. The sodium dodecyl sulfate (SDS) was from Sigma (Poole, UK). The acetonitrile, HPLC grade, was supplied by Vickers Lab. (Burley-in-Wharfdale, UK). All other reagents were analytical grade supplied by BDH (Poole, UK).

2.2. Analysis

A Dionex CE system, CES1, (Dionex, Sunnyvale, CA, USA) was employed for all analyses. An uncoated fused-silica capillary of 59 cm total length × 75 μm I.D. was used. A variety of buffers were investigated with the following buffer composition being particularly good with the selection of dyes employed in this study: 10 m*M* SDS [$CH_3(CH_2)_{11}SO_3^-Na^+$], 10 m*M* sodium tetraborate ($Na_2B_4O_7 \cdot 10H_2O$) and 6 m*M* potassium dihydrogenphosphate (KH_2PO_4) which was made up in acetonitrile–deionised water (1:9, v/v), to give a final pH of pH 9.0. A hydrodynamic injection method was employed with the samples being raised to 50 mm for 10 s. The analyses were run in the constant current mode, generally set at 25 μA (requiring an average voltage of 11 kV). Detection was by an on-line UV–Vis detector positioned at the cathode. The detection wavelength was generally set at the λ_{max} for each dye (Remazol Black B = 597 nm and Procion Turquoise H-A = 666 nm). The AI 450 software (Dionex) was used for peak integration/analysis.

2.3. Remazol Black B activation/hydrolysis investigations

The pH of a fresh solution of Remazol Black B (1.0 g/l) was adjusted by addition of sodium hydroxide solution (concentration varied depending on the pH value required). The dye solution, in a sealed vessel was then placed in a water bath at the required temperature. Small samples were taken for analysis after various time intervals. The temperatures investigated were 32, 45, 61 and 75°C. The pH values investigated were 8, 9, 10 and 11.

3. Results

3.1. Bifunctional SES reactive dye

The main dye analysed in this section was Remazol Black B, a bifunctional reactive dye containing two SES groups per molecule. These results highlight how CE analysis has been utilised to study the reactions of compounds of this type. The selected electropherograms included give an indication of the type of results which were achieved.

Using a micellar buffer system, as previously described in the *Analysis* section, the five major components present/formed under alkaline conditions could be separated and identified. These are labelled (A–E) in the electropherogram displayed in Fig. 3.

The SES groups were converted into the VS form of the dye, the actual reactive form of the dye, by increasing the pH value and/or temperature of the dye solution. Fig. 4 shows a typical example of the CE analysis of a partially activated Remazol Black B dye solution. The actual sample in Fig. 4 was from a dye solution after 30 min at 61°C, pH 9. The conversion to the divinyl sulfone derivative occurring via the monosulfatoethyl sulfone monovinyl sulfone derivative. Under increasingly more severe conditions the divinyl sulfone derivative was hydrolysed to the dihydroxyethyl sulfone derivative via the monovinyl sulfone monohydroxyethyl sulfone derivative. Fig. 5 is of a largely hydrolysed Remazol Black B dye solution.

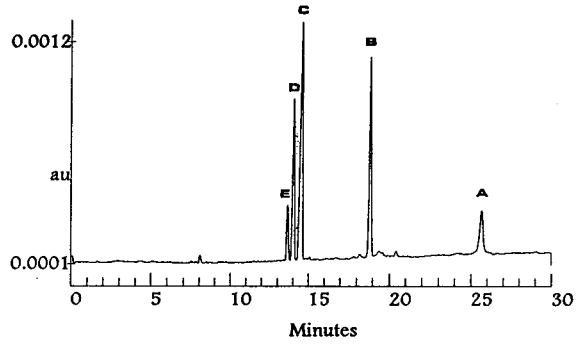

Fig. 3. Electropherogram of Remazol Black B and associated forms (from combined sample of dye solution after 300 min at 32°C, pH 8 with dye solution neutralised after 60 min at 75°C, pH 11). Analysis conditions as described in the *Analysis* section.

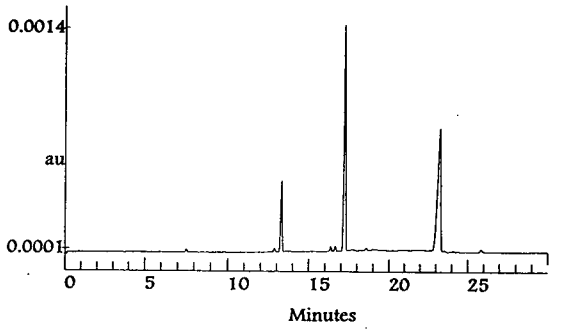

Fig. 4. Electropherogram of partially activated Remazol Black B (dye solution after 30 min at 61°C, pH 9). Analysis conditions as described in the *Analysis* section.

When dye solutions were kept under moderately mild alkaline conditions for prolonged periods of time some interesting CE results were obtained; for example Fig. 6 shows an electropherogram of a Remazol Black B dye solution after 116 h at 75°C, pH 9. Some of the various compounds eluted between 16 and 23 min were thought to be due to dialkyl ether derivatives formed from the reaction of a HES group of one dye molecule reacting with a VS grouping of another dye molecule.

The rates of activation and hydrolysis of Remazol Black B dye solutions under various pH and temperature conditions were successfully

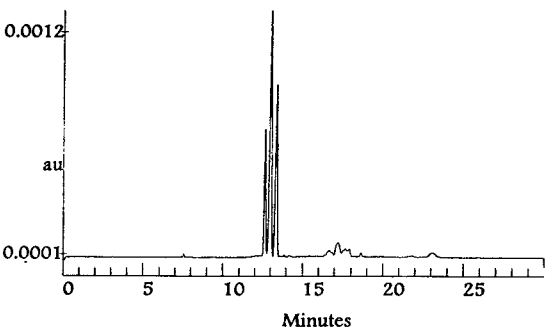

Fig. 5. Electropherogram of largely hydrolysed Remazol Black B (dye solution after 330 min at 61°C, pH 11). Analysis conditions as described in the *Analysis* section.

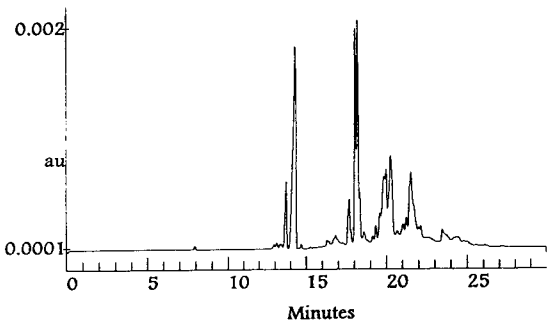

Fig. 6. Electropherogram of Remazol Black B dye solution after 116 h at 75°C, pH 9. Analysis conditions as described in the *Analysis* section.

investigated by CE analysis employing a micellar buffer system containing 10% (v/v) acetonitrile. The results were largely as expected. By plotting the % peak area (which was proportional to concentration) for each component against time of "reaction" then it was possible to graphically represent the rate of both activation and hydrolysis. A selection of the data obtained is presented in Tables 1–4. Tables 1–3 give an indication of how the speed of the conversion of the original dye to the divinyl sulfone form, via the monosulfatoethyl sulfone monovinyl sulfone, was dependent on both the pH of the solution and the temperature. From all the results obtained the pH value was of greater significance than the temperature employed during this study. Table 4 gives an indication of the speed of hydrolysis of the dye solution at 61°C, pH 11.

Table 1
Data illustrating the activation of Remazol Black B at 32°C, pH 8

Time (min)	Percentage composition based on peak area			
	SES–SES	VS–SES	VS–VS	VS–HES
0	92	6	0	0
90	75.6	19.6	2	0
195	70	23.7	2.2	0.4
1 230	43	43	10.5	0.8
1 545	39	44.6	12.1	0.8
10 080	7.1	39.7	50	1.2

Table 2
Data illustrating the activation of Remazol Black B at 61°C, pH 9

Time (min)	Percentage composition based on peak area			
	SES–SES	VS–SES	VS–VS	VS–HES
0	92	6	0	0
30	48.6	42.6	11.8	0.4
60	36.1	46	17.9	0.5
90	28.2	46.4	24.5	0.9
120	22.2	45.8	31	1
360	11	39.3	48.7	1.1

3.2. Phthalocyanine-based chlorotriazinyl reactive dye

An initial attempt to separate the different phthalocyanine-based dye components present in a commercial sample of Procion Turquoise H-A (ICI) by CE utilised a successful buffer from an entirely different project (by the author, at Leeds) and was as described in the method at the start of this section but with 20 m*M* SDS instead of 10 m*M* (current 30 μA). This analysis showed a number of coloured components to be present but they were not baseline resolved, instead all migrating and being detected as a spiked hump between about 13 min and 26 min. Greater resolution was achieved when the buffer contained 10 m*M* SDS. A further increase in resolution was obtained when acetonitrile was employed in the buffer as a co-solvent with water

Table 3
Data illustrating the activation of Remazol Black B at 32°C, pH 11

Time (min)	Percentage composition based on peak area			
	SES–SES	VS–SES	VS–VS	VS–HES
0	92	6	0	0
5	6.5	37	53	1
15	0	1.4	94.5	1.8
30	0	1.2	96.9	1.9
60	0	1.3	97	1.7
90	0	1.3	96.3	2.4

Table 4
Data illustrating the activation and hydrolysis of Remazol Black B at 61°C, pH 11

Time (min)	Percentage composition based on peak area				
	SES–SES	VS–SES	VS–VS	VS–HES	HES–HES
0	92	6	0	0	0
15	3	1.8	95	3.2	0
30	4.5	6	80	5.3	0
60	2	2.7	74.8	9.1	0.5
90	2	1	70.5	11.2	8
330	0	0	30.4	47.3	18.4
1230	0	0	2.3	22.6	58
1470	0	0	1.6	18.3	61.7
2760	0	0	0	10.4	73.2
3960	0	0	0	0	91.8
4080	0	0	0	0	93.4

(25/75) —an example of the results achieved, with a controlled current of 25 μA, is displayed as Fig. 7. This electropherogram clearly showed that the Procion Turquoise H-A was indeed a mixture containing a high number (>12) of coloured components (detection at 666 nm); unfortunately a rather long analysis run time was required for this separation.

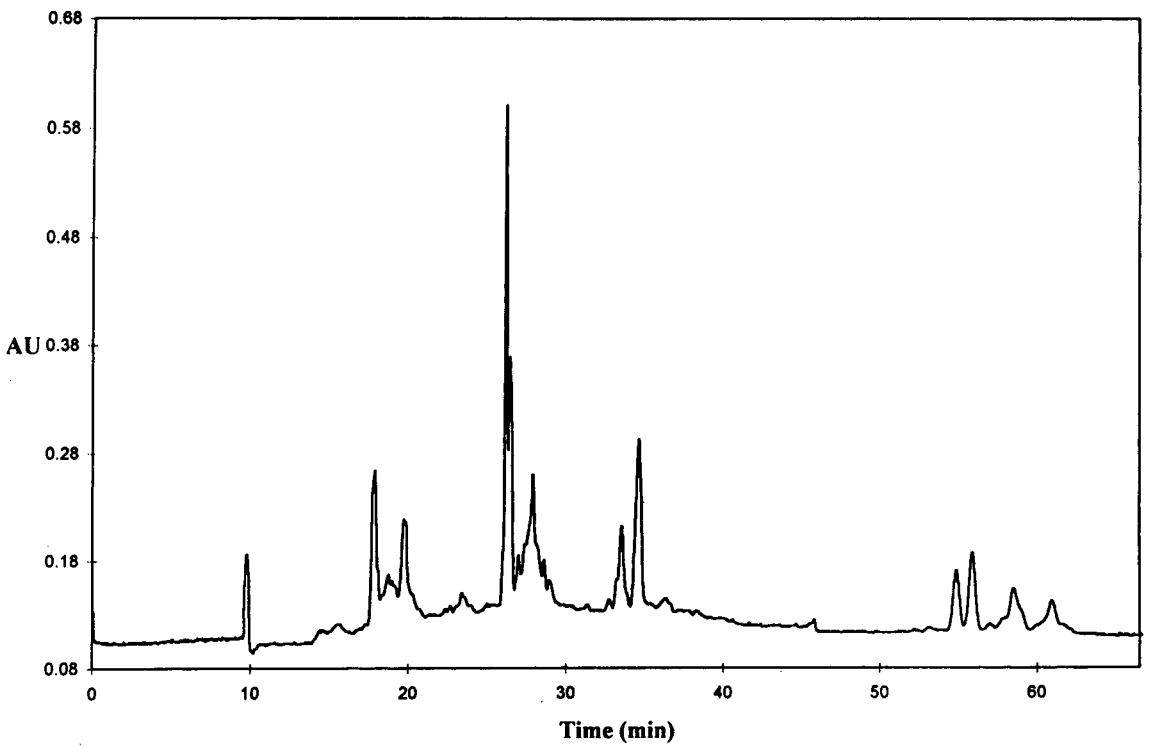

Fig. 7. Electropherogram of Procion Turquoise H-A. Buffer: acetonitrile–deionised water (25:75). Other additives and conditions as described in the *Analysis* section.

By decreasing the acetonitrile content of the buffer to 10% a much shorter analysis time was achieved but with a reduction in the resolution obtained. This buffer (as described in the Experimental section) was employed to obtain the results shown in Figs. 8 and 9.

The electropherogram for the dye solution at pH 7 was the same as that obtained when the dye solution was adjusted to pH 11 prior to analysis. Fig. 8 shows the result for the analysis of the fresh dye solution at pH 11. On heating the dye solution, at pH 11, to 80°C for 1 h a significantly different electropherogram (Fig. 9) was obtained with the loss and addition of a number of peaks. These results gave evidence for the hydrolysis of dyes containing reactive chlorotriazinyl groups (peaks not present in Fig. 9) to dyes with the fibre-unreactive hydroxytriazinyl analogues (new peaks in Fig. 9).

The electropherograms displayed in this subsection demonstrated the potential of CE to analyse and aid in the study of this dye and dyes of this type based on a phthalocyanine chromophore. A full study and interpretation of the results for phthalocyanine dyes has still to be undertaken.

3.3. Mixed bifunctional reactive dyes

A number of mixed bifunctional reactive dyes have been successfully analysed using buffer systems very similar to or the same as those already described in this paper. The Sumifix Supra dyes contain both a SES reactive moiety and a monochlorotriazine reactive grouping. Reactions, including hydrolysis, of these different groups were distinguished and monitored —this forming part of some continuing research work at the Colour Chemistry and Dyeing Department, University of Leeds.

4. Conclusions

A variety of bifunctional reactive dyes were successfully analysed by micellar electrokinetic

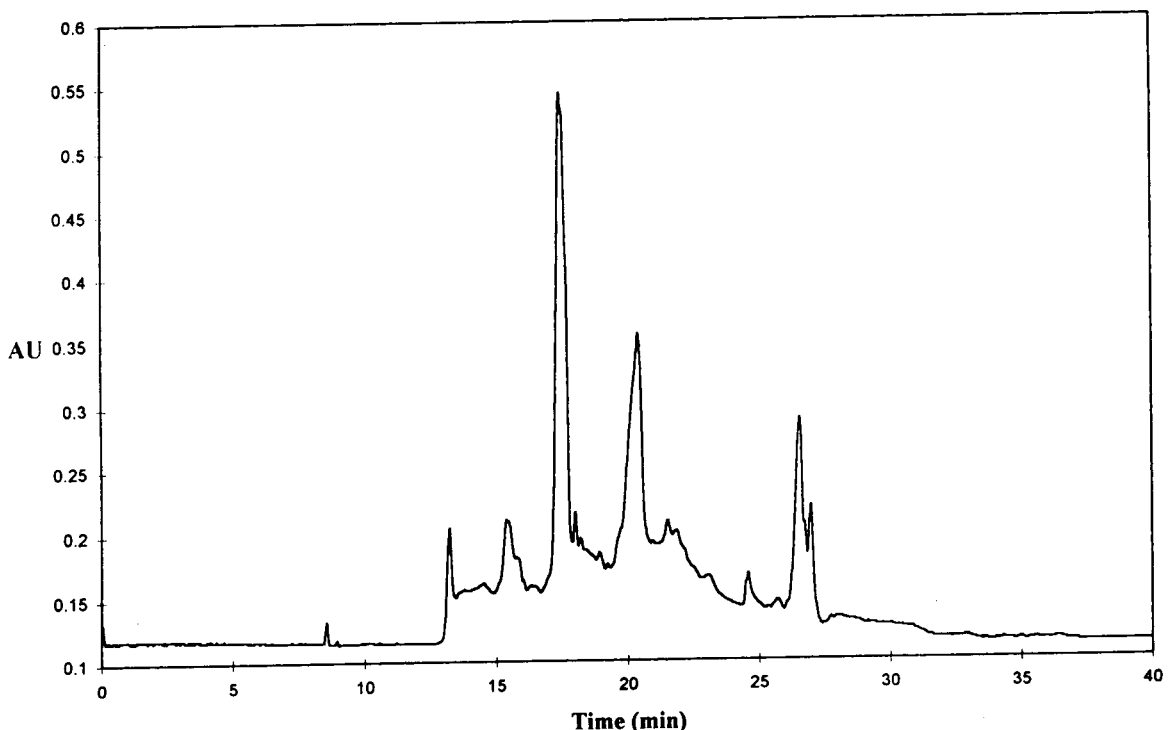

Fig. 8. Electropherogram of Procion Turquoise H-A at pH 11. Analysis conditions as described in the *Analysis* section.

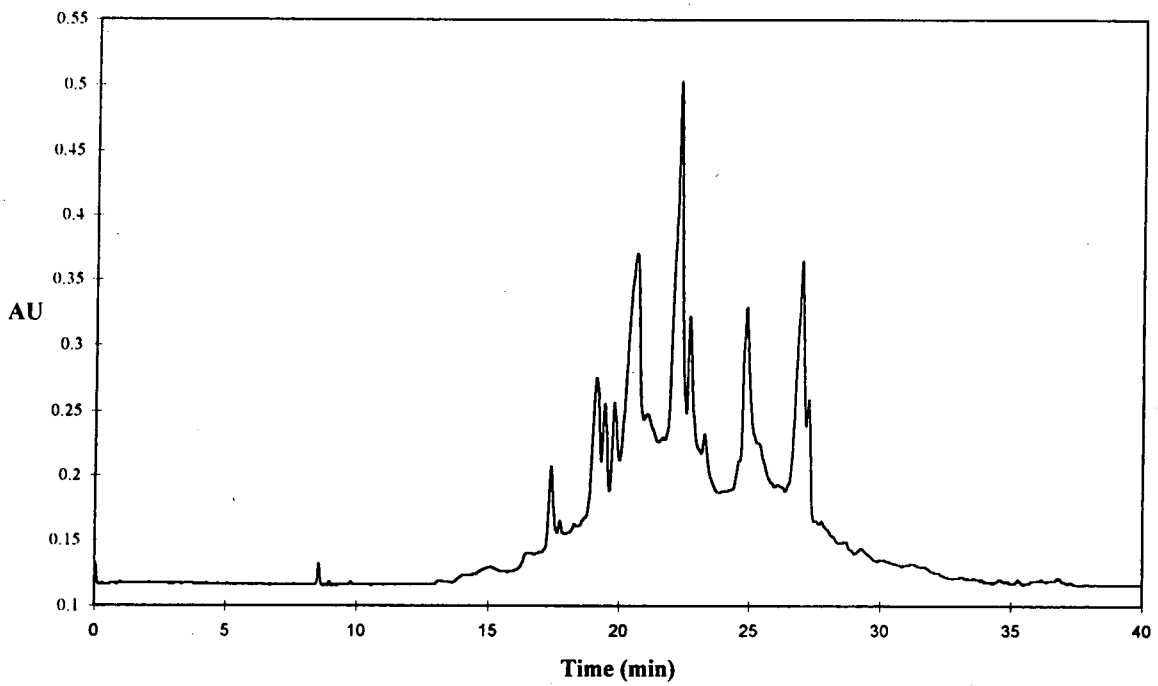

Fig. 9. Electropherogram of Procion Turquoise H-A dye solution at pH 11 after heating to 80°C for 1 h. Analysis conditions as described in the *Analysis* section.

capillary chromatography. The employment of acetonitrile at a ratio of 1:9 with the aqueous buffer generally improved the resolution of the different components in the samples. Examples of the potential applications of buffer systems of this type include: checking the purity of reactive dye samples; monitoring the reactions plus rate of reactions (kinetic studies) of reactive dyes with nucleophiles; analysing coloured effluents; investigating components in residual dye baths; investigating the breakdown of reactive dyes and the identity of breakdown species from effluent treatment processes.

Acknowledgement

I would like to thank Mohammed Asaf (Environmental Monitoring Unit, Colour Chemistry Department, University of Leeds) who was responsible for carrying out many of the stability tests and the associated analysis.

References

[1] E.D. Lee, W. MÜck, J.D. Henion and T.R. Covey, *Biomed. Environm. Mass Spec.*, 18 (1989) 209.
[2] S.N. Croft and D.M. Lewis, *Dyes Pigments*, 18 (1992) 309.
[3] S.N. Croft and D. Hinks, *J. Soc. Dyers Colourists*, 108 (1992) 546.
[4] K.P. Evans and G.L. Beaumont, *J. Chromatogr.*, 636 (1993) 153.
[5] S.M. Burkinshaw, D. Hinks and D.M. Lewis, *J. Chromatogr.*, 640 (1993) 413.
[6] K.N. Tapley, presented at the *Capillary Electrophoresis Symposium, University of Leeds, Leeds, June 1993.*
[7] H.-U. von der Eltz, *Melliand Textilber.*, (1965) 286.
[8] A.H.M. Renfrew and J.A. Taylor, *Rev. Prog. Coloration*, 20 (1990) 1.
[9] S. Abeta, T. Yoshida and K. Imada, *Am. Dye. Rep.*, 73, No. 7 (1984) 26.

ELSEVIER

Journal of Chromatography A, 706 (1995) 563–569

JOURNAL OF CHROMATOGRAPHY A

Membrane-based solid-phase extraction as a sample clean-up technique for anion analysis by capillary electrophoresis

Raaidah Saari-Nordhaus*, James M. Anderson, Jr.

Alltech Associates, Inc., 2051 Waukegan Road, Deerfield, IL 60015, USA

Abstract

The use of membrane-based solid-phase extraction disks as a sample clean-up technique for anion analysis by capillary electrophoresis is discussed. The polytetrafluoroethylene membrane is impregnated with high-purity polystyrene–divinylbenzene sulfonated cation-exchange resin beads. Three different chemistries are used to remove various interfering components from the sample. The applications of this technique for the analysis of various anions in difficult samples are demonstrated.

1. Introduction

Capillary electrophoresis (CE) is an emerging ion separation and analysis technique [1,2]. It is attractive because it offers speed, high theoretical plates, and small sample and solvent requirements. Consumable costs are insignificant since the separation is done in an open tubular capillary as compared to a packed column in ion chromatography (IC). In most cases, sample preparation in CE is minimal. There is no expensive column to protect. Cations migrate in the opposite direction and do not interfere in the anion separation. Organic acids and neutral compounds migrate much later than the inorganic anions and are removed from the inorganic anions migration band.

However, as in IC, the separation of certain components can be complicated by the presence of interfering components in the sample matrix. The complications becomes particularly severe when the sample is contaminated with a high level of ionic species. Although it may be possible to separate the ionic matrix components from the analytes of interest, this separation becomes difficult to achieve when the concentration of the matrix ion is high. The interfering components can mask, broaden (reduces the efficiency), or change the migration time of the peaks of interest. Therefore, some type of sample clean-up is usually necessary to remove the interfering components.

Solid-phase extraction (SPE) is a widely used sample preparation technique. It is easy to use, requires small sample volume, and a wide variety of chemistries are readily available. In recent years, membrane-based SPE has become a popular and growing technique for sample clean-up [3–5]. It offers several advantages over the traditional packed-bed SPE cartridges such as higher flow-rates (because of the wide and thin membrane), less plugging (due to its larger surface area), and elimination of channeling (due to its uniform and stable extraction matrix). SPE has been used widely for sample clean-up in IC.

* Corresponding author.

0021-9673/95/$09.50

Both traditional packed-bed cartridges [6,7] and the new membrane-based disk have been used [8]. This paper examines the use of SPE disks as a sample clean-up technique for the analysis of anions by CE.

2. Experimental

2.1. Instrumentation

The CE system employed was a Crystal 300 (ATI, Unicam, Madison, WI, USA) interfaced with a Linear (Thermo Separation Products, San Francisco, CA, USA) Model 204 UV–Vis detector. Indirect UV detection at 254 nm was used. Electropherograms were recorded on a SP 4400 Chromjet integrator (Thermo Separation Products, Santa Clara, CA, USA). The separations were carried out using polyimide-coated fused-silica capillaries obtained from Polymicro Technologies (Phoenix, AZ, USA). The dimension of the capillary used through out this work was 70 cm (effective length 60 cm) × 75 μm I.D. Sample introduction was by hydrodynamic injection (dynamic pressure injection) at 25 mbar, for 30 s.

Alltech's (Deerfield, IL, USA) Novo-Clean IC disks were used as the membrane-based SPE device. Fig. 1 shows the construction of the Novo-Clean IC disk. The 25-mm polytetrafluoroethylene (PTFE) membrane is impregnated with high-purity polystyrene–divinylbenzene sulfonated cation-exchange resin beads. The pore size of the disk is approximately 5 μm. It is housed in a high-purity polypropylene housing to eliminate ionic contaminations. The inlet and outlet of the housing accepts a luer-hub syringe and needle, respectively. As the sample passes through the membrane, specific ion-exchange interactions selectively retain matrix interferences while analytes pass through unchanged. Three chemistries in the hydrogen (Novo-Clean IC-H), silver (Novo-Clean IC-Ag) and barium (Novo-Clean IC-Ba) forms were used for the work discussed here. Table 1 summarizes the characteristics of each disk and its applications.

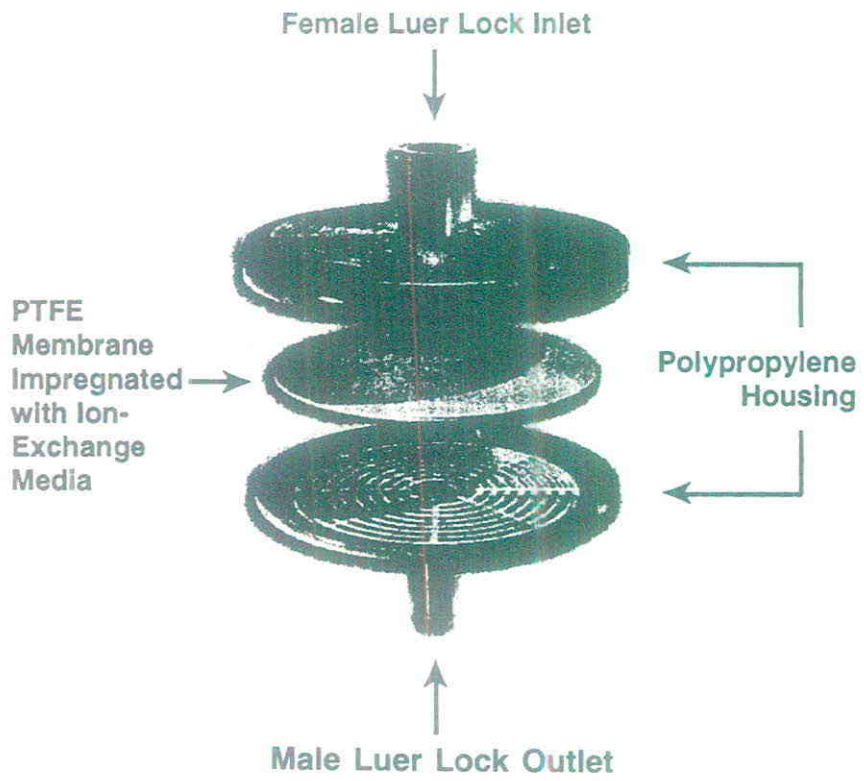

Fig. 1. The construction of the Novo-Clean IC disk.

2.2. Chemicals

The carrier electrolyte was prepared from sodium chromate (Aldrich, Milwaukee, WI, USA). Cetyltrimethylammonium bromide (CTAB) (Aldrich) was used as the electroosmotic flow (EOF) modifier. Sulfuric acid (5 *M*) was obtained from Fisher Scientific (Pittsburgh, PA, USA). Sodium hydroxide was obtained from Aldrich. Anion standards were prepared by diluting the 1000 ppm Certified IC Standard from Alltech. Deionized water was used for preparing all solutions.

2.3. Procedures

Before applying sample, the disk was preconditioned by passing 5–10 ml of deionized water using a luer-hub plastic syringe. The water was left in the device for 5 min to swell the membrane. Excess water was removed by pushing air through the disk. The sample was then passed through the disk at a flow-rate of 1.0 ml/min or less. The first 1 ml of the eluate was discarded to eliminate partial dilution of the analytes. The remaining eluate was collected for

Table 1
Characteristics of the Alltech Novo-Clean IC disks

Disk	Membrane	Retains	Applications
IC-H	Strong cation exchanger in the hydrogen form	Cations	Exchanges cations for hydrogen. Removes or concentrates sample cations or reduces pH of basic samples
IC-Ag	Strong cation exchanger in the silver form	Cations, chloride, iodide, bromide	Exchanges cations for silver. Removes excess halides through formation of silver halide salts
IC-Ba	Strong cation exchanger in the barium form	Cations, sulfate	Exchanges cations for barium. Removes excess sulfate through formation of barium sulfate

Capacity of all (25-mm) disks: 2.0 mequiv.

analysis. During removal of matrix interferences through precipitation reactions, the precipitates are retained on the disk while the soluble analytes passed through. No blockage of the extraction disk due to the precipitates was observed through out these experiments.

Each disk contains 2.0 mequiv. of either hydrogen (IC-H), barium (IC-Ba) or silver (IC-Ag). Under ideal conditions, it will remove an equal amount of hydroxide or carbonate (IC-H), sulfate (IC-Ba) or halides (IC-Ag) from the sample. In practice, the maximum capacity of the disk will be affected by the nature of the sample (concentration and ionic strength) and the rate at which the sample is loaded into the disk. The amount of contaminants that need to be removed from the sample must not exceed the total capacity of the disk. More than one disk can be used in series when the contaminant concentration is higher than the disk capacity. Also, it is possible to use the disk repeatedly as long as the contaminant concentration does not exceed the disk capacity. For best results, the sample size should not exceed 50% of the disk absolute capacity.

The electrolyte was 5 m*M* sodium chromate and 0.5 m*M* CTAB. The electrolyte was made from concentrated stock solutions containing 100 m*M* sodium chromate/0.69 m*M* sulfuric acid, and 20 m*M* CTAB. The pH of the electrolyte was adjusted with either 100 m*M* sodium hydroxide or 100 m*M* sulfuric acid.

3. Results and discussions

Unlike IC, very little information is available on sample clean-up for CE. Several approaches have been suggested to overcome simple problems. Optimizing the electrolyte conditions for a particular analysis by controlling the electrolyte pH, composition and ionic strength have been shown to solve a limited range of problems [9,10]. As an example, by increasing the concentration of the EOF modifier from 0.5 to 1.5 m*M*, 1 ppm chloride can be separated from 1000 ppm sulfate [10]. Adding organic solvents to the carrier electrolyte is another way to change the separation selectivity and is found useful for analyzing small amount of iodide in the present of large excess of sulfate [11]. The work described here uses a sample clean-up technique to remove the interfering components. Three

chemistries are used to solve a variety of interference problems.

The anions are separated using an electrolyte condition published elsewhere [12]. The electrolyte condition was not optimized for a specific matrix interference problem since the purpose of this work was to eliminate the interfering components using a sample pretreatment device, rather than changing the electrolyte condition.

3.1. Membrane-based SPE for removing hydroxide and carbonate

The Novo-Clean IC-H membrane contains sulfonic acid-functionalized resin in the hydrogen form. As sample passes through the disk, cations in the sample exchanges with hydrogen. The released hydrogen reacts with hydroxide or carbonate to form water or carbonic acid. The ion-exchange reaction that takes place in the disk is:

$$\text{Disk–H}^+ + \text{MOH,M}_2\text{CO}_3 \rightarrow \text{Disk–M} + \text{H}_2\text{O,H}_2\text{CO}_3$$

where M = cations. This SPE disk is ideal for removing hydroxide or carbonate from samples before the analysis of other anions. Strong-acid anions are not effected by this treatment. The recovery of strong acid anions after treatment with the Novo-Clean IC-H membrane was discussed in an earlier publication [8] using IC as the analytical technique. A similar result is expected in CE since the sample pretreatment is done prior to the analytical technique.

Fig. 2 shows electropherograms of technical-grade sodium carbonate. The sample contains 2 g sodium carbonate dissolved in 100 ml water. In the untreated sample, only the carbonate peak was observed. After treating the sample with a Novo-Clean IC-H, trace levels of chloride, sulfate, nitrite, nitrate and phosphate were found in the sample. Dilution is not suitable for this application since the concentration of the anions is very low compared to carbonate.

Fig. 3 shows another application of the Novo-Clean IC-H disk to remove excess hydroxide. Fig. 3a shows an electropherogram of a caustic solution. High hydroxide concentration masks the peaks of interest. The migration time for fluoride is also shortened by the highly conductive hydroxide ion. By treating the sample with

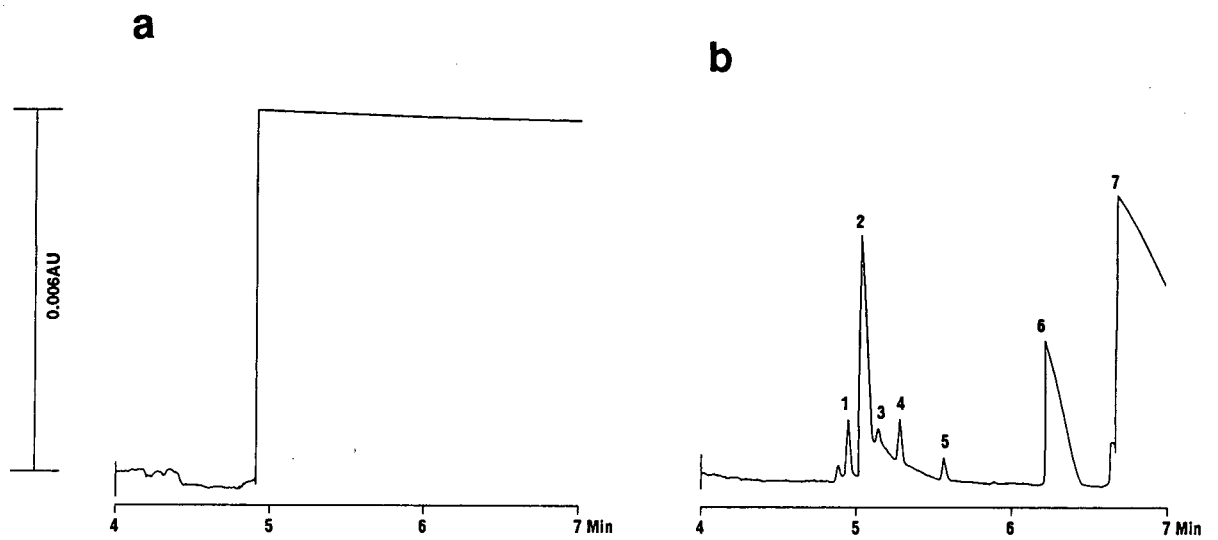

Fig. 2. Electropherograms of a technical-grade sodium carbonate. (a) Untreated; (b) treated with Novo-Clean IC-H. Conditions: fused silica 60 cm × 75 μm; 15 kV (negative); 5 m*M* sodium chromate with 0.5 m*M* CTAB, pH 8.0; indirect UV detection at 254 nm. Peaks: 1 = chloride (5 ppm); 2 = sulfate (32 ppm); 3 = nitrite (12 ppm); 4 = nitrate (10 ppm); 5 = unknown; 6 = phosphate (18 ppm); 7 = carbonate.

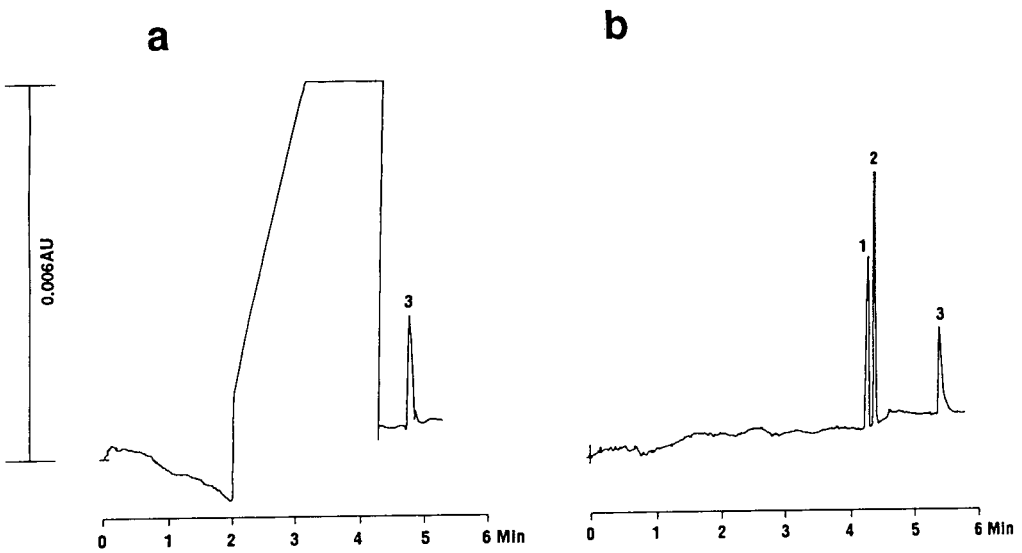

Fig. 3. Electropherograms of a caustic solution. (a) Untreated; (b) treated with Novo-Clean IC-H. Conditions: fused silica 60 cm × 75 μm; 15 kV (negative); 5 m*M* sodium chromate with 0.5 m*M* CTAB, pH 7.9; indirect UV detection at 254 nm. Peaks: 1 = chloride (18 ppm); 2 = sulfate (29 ppm); 3 = fluoride (9 ppm).

the Novo-Clean IC-H disk, the ions of interest are easily quantified as shown in Fig. 3b. The migration time returns to normal after hydroxide is removed.

3.2. Membrane-based SPE for removing halides

Novo-Clean IC-Ag membrane contains sulfonic acid-functionalized resin in the silver form. It is useful for removing excess halides from samples before the analysis of other anions. The Novo-Clean IC-Ag disk removes halides from the sample through the formation of insoluble silver halides. The ion-exchange reaction that take place in the IC-Ag disk is:

$$\text{Disk–Ag}^{+} + \text{MX} \rightarrow \text{Disk–M} + \text{AgX}$$

where M = cations and X = Cl, Br, I. When sample is passed through the disk, the sample cations exchange with silver. The released silver reacts with the anions in the sample. Anions that form insoluble or partially soluble silver salts will be removed completely or partially from the sample depending on their solubilities. Other anions that form soluble silver salts such as fluoride, nitrite, nitrate, phosphate and sulfate will pass through unchanged. The recovery of these other anions after sample pretreatment with the Novo-Clean IC-Ag membrane was discussed earlier [8].

Fig. 4 shows electropherograms of a hydrochloric acid digest paper coating. The sample (0.1 g) was dissolved in 1.0 ml concentrated HCl and diluted to 100 ml with water. In the untreated sample, the chloride peak masks the peaks of interest. After treating the sample with the Novo-Clean IC-Ag membrane, chloride is completely removed and nitrate, fluoride and phosphate peaks are easily quantified.

3.3. Membrane-based SPE for removing sulfate

Novo-Clean IC-Ba membrane contains sulfonic acid-functionalized resin in the barium form. It is useful for removing excess sulfate from samples before the analysis of other anions. The Novo-Clean IC-Ba disk removes sulfate from the sample through the formation of insoluble barium sulfate. The ion-exchange reaction that takes place in the IC-Ba disk is:

$$\text{Disk–Ba}^{2+} + \text{M}_2\text{SO}_4 \rightarrow \text{Disk–M} + \text{BaSO}_4$$

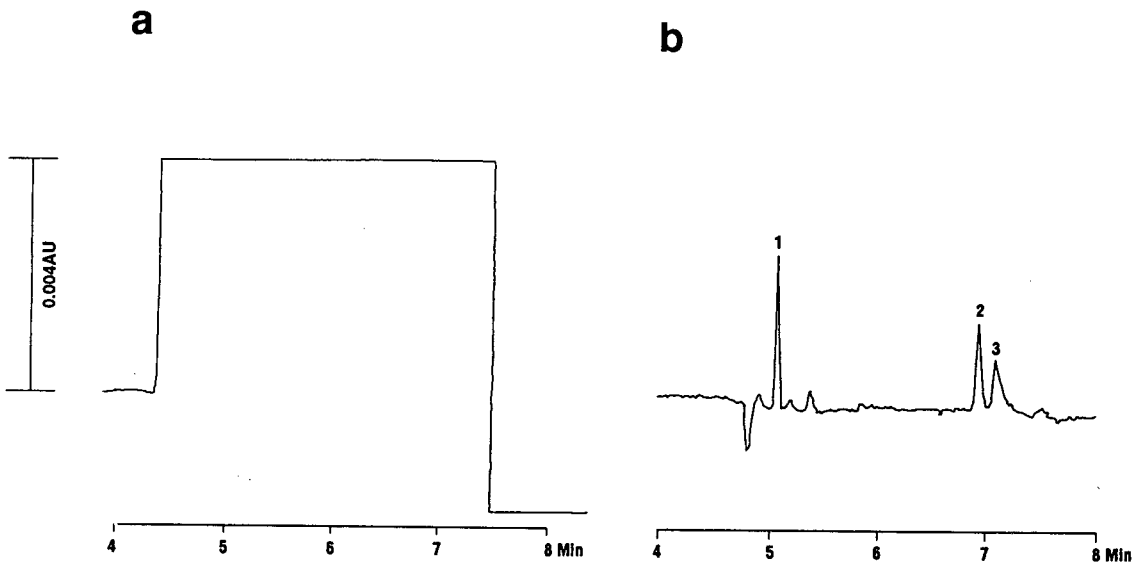

Fig. 4. Electropherograms of a hydrochloric acid digest paper coating. (a) Untreated; (b) treated with Novo-Clean IC-Ag. Conditions: fused silica 60 cm × 75 μm; 15 kV (negative); 5 m*M* sodium chromate with 0.5 m*M* CTAB, pH 7.9; indirect UV detection at 254 nm. Peaks: 1 = nitrate (6 ppm); 2 = fluoride (2 ppm); 3 = phosphate (5 ppm).

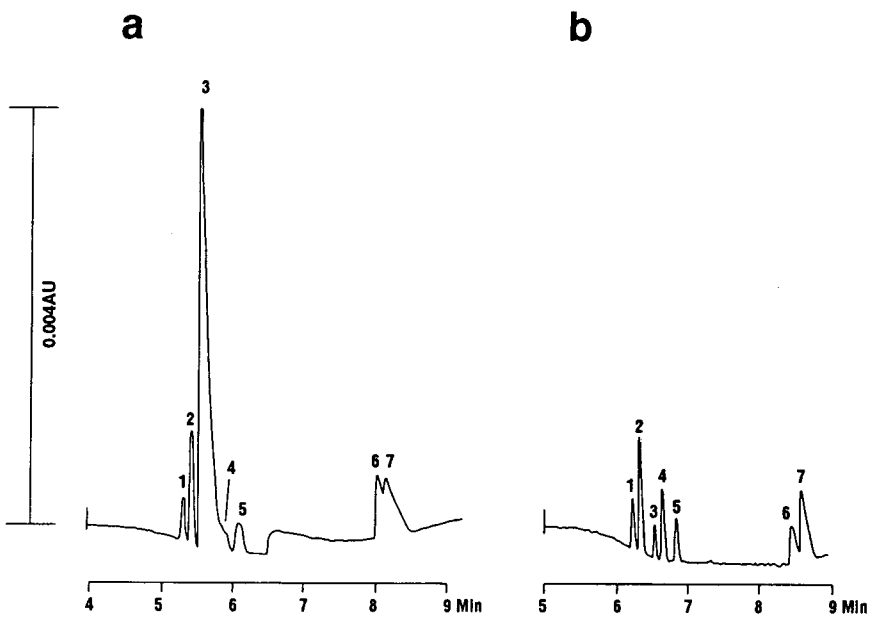

Fig. 5. Electropherograms of a standard of anions containing 500 ppm sulfate. (a) Untreated; (b) treated with Novo-Clean IC-Ba. Conditions: fused silica 60 cm × 75 μm; 15 kV (negative); 5 m*M* sodium chromate with 0.5 m*M* CTAB, pH 7.9; indirect UV detection at 254 nm. Peaks: 1 = bromide (10 ppm); 2 = chloride (10 ppm); 3 = sulfate; 4 = nitrite (10 ppm); 5 = nitrate (10 ppm); 6 = fluoride (5 ppm); 7 = phosphate (15 ppm).

where M = cations. When sample is passed through the disk, sample cations exchange with barium. The released barium reacts with sulfate in the sample to form insoluble barium sulfate. Since barium phosphate is partially soluble, some phosphate may be removed by this disk. Other anions that forms soluble barium salts such as fluoride, chloride, nitrite, bromide and nitrate will pass through unchanged. The recovery of these anions after sample pretreatment with the Novo-Clean IC-Ba membrane was discussed earlier [8].

Fig. 5 shows electropherograms of a standard of anions containing 500 ppm sulfate. In the untreated sample, the sulfate peak masks the chloride and nitrite peaks. Other anion peaks are broad and the resolution between fluoride and phosphate is poor. After treating the sample with the Novo-Clean IC-Ba disk, a large quantity of sulfate was removed and the separation efficiency and resolution are improved.

4. Conclusions

Membrane-based SPE is useful as a sample clean-up technique for removing high concentration of ionic contaminants before anion analysis by CE. The chemistries described here provide a selective method for removing hydroxide, carbonate, halides and sulfate. This technique provides a reliable method for eliminating matrix interferences in CE.

References

[1] W.R. Jones, P. Jandik and R. Pfeifer, *Am. Lab.*, May (1991) 40.
[2] P. Jandik, W.R. Jones, A. Weston and P.R. Brown, *LC·GC*, 9 (1991) 634.
[3] C. Markell, D.F. Hagen and V.A. Bunnelle, *LC·GC*, 9 (1991) 332.
[4] J. Horack and R.E. Majors, *LC·GC*, 11 (1993) 74.
[5] B. Bryan, *Today's Chemist at Work*, February (1994) 39.
[6] R. Saari-Nordhaus, J.M. Anderson, Jr. and I.K. Henderson, *Am. Lab.*, August (1990) 18.
[7] I.K. Henderson, R. Saari-Nordhaus and J.M. Anderson, Jr., *J. Chromatogr.*, 546 (1991) 61.
[8] R. Saari-Nordhaus, L.M. Nair and J.M. Anderson, Jr., *J. Chromatogr. A*, 671 (1994) 159.
[9] J. Romano, P. Jandik and W.R. Jones, *J. Chromatogr.*, 546 (1991) 411.
[10] W.R. Jones and P. Jandik, *J. Chromatogr.*, 608 (1992) 385.
[11] W. Buchberger and P.R. Haddad, *J. Chromatogr.*, 608 (1992) 59.
[12] W.R. Jones and P. Jandik, *J. Chromatogr.*, 546 (1991) 445.

ELSEVIER

Journal of Chromatography A, 706 (1995) 571–578

JOURNAL OF CHROMATOGRAPHY A

Separation of inorganic and organic anionic components of Bayer liquor by capillary zone electrophoresis I. Optimisation of resolution with electrolyte-containing surfactant mixtures

Paul R. Haddad*, Anthony H. Harakuwe, Wolfgang Buchberger[1]

Department of Chemistry, University of Tasmania, G.P.O. Box 252C, Hobart, Tasmania 7001, Australia

Abstract

The simultaneous separation of chloride, sulfate, oxalate, malonate, fluoride, formate, phosphate, carbonate and acetate in Bayer liquor using capillary zone electrophoresis with indirect detection is demonstrated using electrolytes comprising binary mixtures of the surfactants tetradecyltrimethylammonium bromide (TTAB) and dodecyltrimethylammonium bromide (DTAB). Two optimal electrolyte compositions were identified, namely 3 m*M* TTAB, 3 m*M* DTAB and 7.5 m*M* chromate at pH 9 (optimum 1) and 5 m*M* TTAB, 1 m*M* DTAB and 5.5 m*M* chromate at pH 9 (optimum 2). The separation selectivities of these electrolytes differ and the choice between them rests on consideration of the relative concentrations of the ionic species in the sample. Best results were obtained when the Bayer liquor sample was diluted by a factor of 500 before analysis. Linear calibrations were achieved in the working concentration range (1–10 μg/ml) and detection limits fell in the range 0.09–0.34 μg/ml for optimum 1 and 0.16–0.88 μg/ml for optimum 2. Recoveries of ions added to the diluted sample were close to quantitative, except for phosphate which showed low and variable recovery, and carbonate which was also variable due to absorption of carbon dioxide by the sample. Tartrate and succinate could not be resolved with either of the optimal electrolyte compositions.

1. Introduction

Pioneered by Jorgenson and co-workers in the 1980s [e.g. 1–3], capillary zone electrophoresis (CZE) is a differential migration separation technique that separates solutes according to their charge-to-mass ratios under an applied electric field. For the rapid separation of inorganic anions and low-molecular-mass organic acids, a suitable cationic surfactant (e.g. tetradecyltrimethylammonium bromide) is normally incorporated in the running electrolyte [4–6] to enable the electroosmotic flow (EOF) and the migrating anions to move in the same direction. Detection is usually performed in the indirect UV absorption mode since most inorganic anions show insufficient UV absorbance to permit sensitive direct detection. The high separation power, speed, quantitative reliability and unique selectivity of CZE make it attractive for the sepa-

* Corresponding author.

[1] Present address: Department of Analytical Chemistry, Institute of Chemistry, Johannes-Kepler University, Altenbergerstrasse 69, A-4040 Linz, Austria.

0021-9673/95/$09.50
SSDI 0021-9673(94)01049-8

ration of samples containing inorganic anions and short-chain carboxylic acid anions, such as Bayer liquors.

Bayer liquors are by-products of alumina (Al_2O_3) and aluminium metal production. Alumina is made from bauxite ore via the cyclic Bayer process, and in the production of aluminium metal, the alumina is reduced electrolytically using the Hall–Héroult process (see [7]). Liquors from these processes are typically of high pH and ionic strength and contain numerous anions such as chloride, sulfate, phosphate, fluoride, oxalate, silicate, succinate, malonate and formate [8,9].

The analysis of anions in Bayer liquor is vital for two main reasons, namely process monitoring (including quality control and optimisation of product yield and purity) and toxicology and environmental impact monitoring. On the process monitoring side, sodium ions associated with fluoride, chloride, sulfate and carbonate interfere with alumina precipitation in the Bayer process, increase liquor viscosity and reduce oxalate stability, making removal of the latter from process liquor difficult [8,10]. Low levels of gluconic and tartaric acids also inhibit precipitation [10]. The rapid determination of fluoride is important for the determination of cryolite ratio ($NaF:AlF_3$) [11], with a ratio of 2–3 needing to be maintained for optimal operation [12]. On the environmental monitoring side, fluoride is a universal toxin affecting humans, plants and animals. Free and complex cyanides are also present [11].

Ion chromatography (IC) is the only technique comparable to CZE for simultaneous separation of multiple anions. However, analysis of Bayer liquor using IC is not used routinely most probably due to co-elution of weakly retained species [6,7]. Furthermore, Bayer liquor is of high ionic strength and pH and is extremely difficult to separate by IC without clean-up or pre-treatment, for example by dialysis [13]. When injected directly, untreated samples reduce column life and performance [14], the latter being due primarily to severe disturbance of the acid–base equilibria in the system. The simultaneous and fully resolved separation of chloride, oxalate, malonate, fluoride, formate, carbonate, phosphate, acetate and citrate in Bayer liquor using IC is yet to be reported.

Separation by CZE of common anions in samples with simple matrices (e.g. tap water) poses few practical problems. However with complex and difficult matrices like Bayer liquor, anion separation can be problematic. Extreme pH is detrimental to bare capillaries [15] and the capillary surface may potentially be altered [16] with a resultant effect on EOF. Like IC, literature related to separation of anions in Bayer liquor using CZE is limited, but the separation of chloride, sulfate, oxalate [8] and fluoride [17] has been reported previously. However the optimised simultaneous separation of the above anions as well as malonate, formate, carbonate and acetate has not been reported to date. The main impediments appear to be inadequate resolution of a closely migrating cluster of anions comprising tartrate, succinate, fluoride, phosphate and formate; and deterioration of the baseline. Furthermore, resolution of fluoride and phosphate is acknowledged as being problematic [18].

In all of the above studies, a single cationic surfactant species has been used to reverse the EOF. In a previous paper, we have noted that certain selectivity effects in the separation of inorganic and organic anions arise when a binary mixture of surfactants is used [19]. The aim of the present work was to exploit these selectivity effects with a goal of achieving a fully resolved separation of the inorganic and organic ionic components of Bayer liquor using CZE.

2. Experimental

2.1. Instrumentation

A Waters Quanta 4000 automated CZE system coupled to a Maxima 820 data station (Dynamic Solutions, Ventura, CA, USA) was used to acquire all electropherograms. A polyimide-coated fused-silica capillary (Polymicro Technologies, Phoenix, AZ, USA) measuring 60 cm total length (52 cm effective length) × 75 μm I.D. was used throughout. A Model 8520 digital

pH meter (Hanna Instruments, Singapore) was used for all pH measurements.

2.2. Reagents and standards

Water from a Milli-Q (Millipore, Bedford, MA, USA) water-purification system was used throughout. Unless specified, all reagents were of analytical-reagent grade and sourced from Ajax Chemicals (Auburn, Australia). Tetradecyltrimethylammonium bromide (TTAB) and dodecyltrimethylammonium bromide (DTAB) were obtained from Aldrich (Milwaukee, WI, USA). Other reagents required were sodium chromate (laboratory-reagent grade, LR) for electrolyte preparation and potassium hydroxide (LR) for pH adjustment and capillary conditioning.

Standard stock solutions (1000 μg/ml) of each of the analytes were made from analytical-reagent grade sodium salts which had been dried at 100°C overnight (except where indicated). The salts used were *d*-gluconate (Fluka, Switzerland), malonate (undried; LR, BDH, Poole, UK), succinate (undried; LR, BDH), citrate (By-Products and Chemicals, Auburn, Australia), formate, acetate (anhydrous; Strem Chemicals, Newburyport, MA, USA), tartrate (Mallinckrodt, St. Louis, MO, USA), phosphate ($Na_3PO_4 \cdot 12H_2O$, undried), chloride (Rhône Poulenc, Victoria, Australia), nitrate, sulfate (May & Baker, Manchester, UK), fluoride (Rhône Poulenc, Manchester, UK) and carbonate (anhydrous). An oxalate standard solution was made by dissolving 0.3583 g undried $H_2C_2O_4 \cdot 2H_2O$ (Mallinckrodt) and titrating with NaOH to pH 6.1 and dilution to 200 ml. An adipate standard was made similarly by titrating 0.2535 g adipic acid (LR) to pH 8.6 and dilution to 200 ml. Working standards between 1 and 10 μg/ml were made by appropriate dilution of the stock solutions.

2.3. Procedures

Running electrolytes were prepared daily using accurately weighed amounts of TTAB and/or DTAB dried at 100°C for 1 h. After dissolution of the solid material and dilution to ca. 80% of final volume, the appropriate aliquot of 100 m*M* chromate was added and the pH adjusted to 9 ± 1 with HNO_3 or NaOH. Final dilution of the electrolyte was used to produce 5 m*M* chromate and the desired concentration(s) of surfactant(s).

Prior to use, the capillary was conditioned by vacuum flushing for 5 min each with water, absolute ethanol and then water; 8 min with 0.5 *M* KOH; 5 min with water; and finally for 10 min with the running electrolyte. All injections were performed in the hydrodynamic mode by gravity feed. Detection was at 254 nm in the indirect mode using chromate as the probe. The detector polarity was reversed so that detected peaks appeared in the positive direction. A voltage of 20 kV was applied from a negative power source for all separations and data acquisition was at 20 points/s. All measurements were made in replicates of ≥ 2 using fresh running electrolyte per analysis. Peak positions were confirmed by spiking with known standards.

3. Results and discussion

We have shown previously [19] that anion selectivity in CZE can be manipulated by using binary TTAB and DTAB mixtures in the running electrolyte. The work discussed here is an extension of this approach to achieve an optimised separation of inorganic anions and short-chain organic acid anions in Bayer liquor. Separation using single surfactants was performed first to provide a basis for comparison with the use of surfactant mixtures. Migration times were determined for the species anticipated to be present in the Bayer liquors (chloride, sulfate, fluoride, phosphate, carbonate, acetate, oxalate, malonate, formate, tartrate, succinate and citrate), as well as cyanide, adipate, gluconate and nitrate. The migration time of nitrate was important since nitric acid was to be used to adjust the electrolyte pH.

3.1. Use of DTAB and TTAB as single surfactants in the running electrolyte

Fig. 1 shows the separation of diluted Bayer liquor using 2.6 m*M* TTAB (Fig. 1a) and 2.6 m*M* DTAB (Fig. 1b) as single surfactants in the

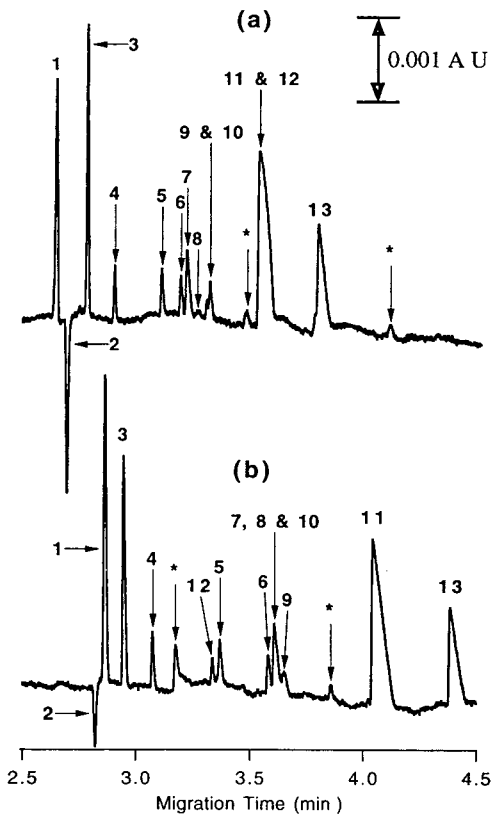

Fig. 1. Separation of 1:500 (v/v) diluted Bayer liquor using electrolytes comprising (a) 2.6 m*M* TTAB and (b) 2.6 m*M* DTAB, together with 5 m*M* chromate at pH 9.1. Injection was in the hydrostatic mode (raised 10 cm for 45 s) and detection was in the indirect spectrophotometric mode at 254 nm. A capillary of 60 cm total length (52 cm effective length) × 75 μm I.D. was used. Peaks: 1 = chloride; 2 = system (bromide); 3 = sulfate; 4 = oxalate; 5 = malonate; 6 = fluoride; 7 = formate; 8 = phosphate; 9 = tartrate; 10 = succinate; 11 = carbonate; 12 = citrate; 13 = acetate; * = unknown.

running electrolyte. The anions of interest were not fully resolved in either case, however separation using TTAB was generally superior to that obtained using DTAB. The system peak due to the presence of bromide in the electrolyte is a potential cause of interference and was observed to be larger with TTAB than for DTAB under identical conditions.

In the separation using DTAB as the single surfactant, nitrate migrates between sulfate and oxalate and the system peak may interfere with chloride, especially at lower dilution (higher ionic strength). Fluoride, formate, succinate and tartrate are unresolved, and phosphate co-migrates with formate and succinate. For the separation using TTAB as the single surfactant, fluoride was resolved from the usual interfering anions (formate, tartrate, phosphate and succinate) and the clean separation of chloride, sulfate and oxalate compares well with that achieved by Grocott et al. [8]. The disadvantages evident with this electrolyte are the possible non-resolution of closely migrating adjacent anions (e.g. fluoride and formate), especially where a large disparity in concentration exists, poor resolution of succinate and tartrate, and the likelihood that elevated levels of carbonate will interfere with the determination of citrate. In addition, nitrate co-migrates with oxalate, making any adjustment of electrolyte pH with nitric acid unsuitable, and there is a tendency for rapid crystal formation in the electrolyte.

3.2. Separation using TTAB and DTAB mixtures in the running electrolyte

Fig. 2 shows the effects on the relative migration times obtained for anions in a diluted Bayer

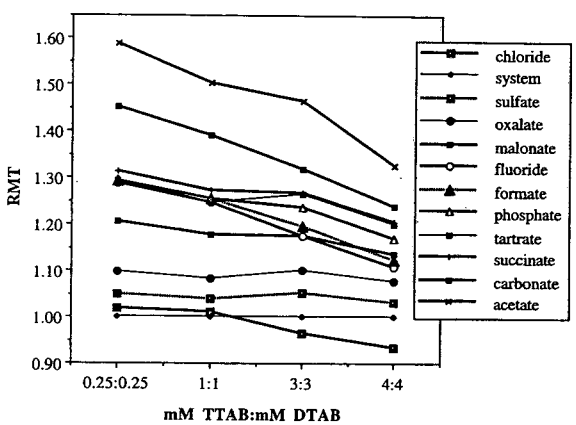

Fig. 2. Effect of electrolytes comprising equimolar surfactant mixtures on the relative migration times (RMT) for solutes in a 1:500 (v/v) diluted Bayer liquor. Conditions as in Fig. 1 except injection times and electrolyte pH were 30 s and 8.8, respectively. All migration times are normalised to the system peak.

liquor sample when various equimolar mixtures of TTAB and DTAB were used to modify the EOF. A number of selectivity effects are evident, but the general trend is that the relative migration times decrease as the total concentration of the surfactant mixture increases. The best separation occurs when both TTAB and DTAB are present at a concentration of 3 m*M*, although some species co-migrate (succinate and tartrate, fluoride and malonate). It can be noted that the migration order of the solutes using this mixture is different from that obtained with either of the two surfactants used singly (see Fig. 1). Further optimisation of the separation was investigated by changing the concentration of the chromate (present to permit the indirect UV absorbance detection of the analytes) in the electrolyte. Fig. 3 shows the results obtained when the chromate concentration was increased from 5 m*M* (as used in Fig. 2) to 7.5 m*M*. While the changes observed were only minor, the resolution of fluoride and malonate improved at the highest chromate concentration studied. It should be noted that increasing the concentration of chromate has a beneficial effect on the detection signal, as shown in Fig. 4 using chloride as the analyte anion. These studies suggested that an optimal separation could be

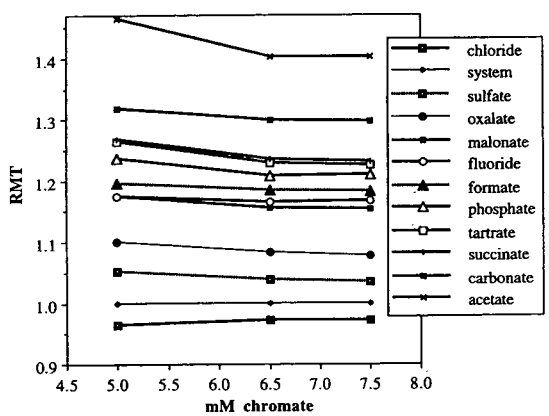

Fig. 3. Effect of chromate concentration in the running electrolyte on the relative migration times (RMT) for solutes in a 1:500 (v/v) diluted Bayer liquor. The electrolyte contained 3 m*M* TTAB and 3 m*M* DTAB. Other conditions as in Fig. 1. All migration times are normalised to the system peak.

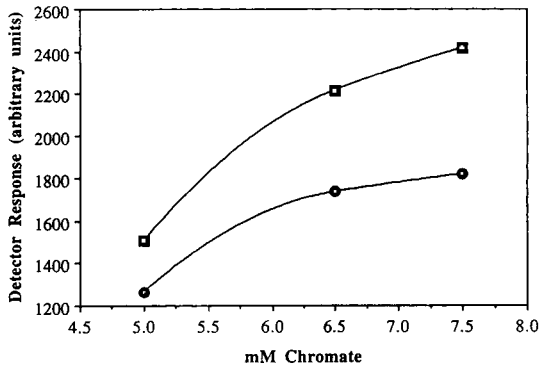

Fig. 4. Effect of chromate concentration variation on the detector response for chloride using electrolytes containing 3 m*M* TTAB and 3 m*M* DTAB. Other conditions as in Fig. 1. ○ = Peak area; □ = peak height.

achieved using an electrolyte containing 3 m*M* of both TTAB and DTAB and 7.5 m*M* chromate. An electropherogram obtained using this electrolyte (which will be designated as optimum 1) is shown in Fig. 5. A potential problem with this separation is the minimal separation of malonate, fluoride and formate which could lead to partial co-migration of these species if they were present at higher concentrations than shown in Fig. 5.

The empirical optimisation procedure described above was repeated for a wide range of mixtures of TTAB, DTAB and chromate. It was found that the separation selectivity could be manipulated to produce a desired electropherogram. For example, the resolution problem mentioned earlier for optimum 1 could be overcome using 5 m*M* TTAB, 1 m*M* DTAB and 5.5 m*M* chromate. The electropherogram obtained with this electrolyte, designated as optimum 2, appears in Fig. 6.

The two optima shown in Figs. 5 and 6 allow for some separation flexibility to be exercised, especially when there are large disparities in concentration between fluoride and adjacent anions. The two optima are also ideal for the separation of additional anions not shown in the two figures (e.g. nitrate, adipate, citrate and gluconate). Variations in the concentration of chromate in the electrolyte can be used to fine-tune the separation where necessary. The obvi-

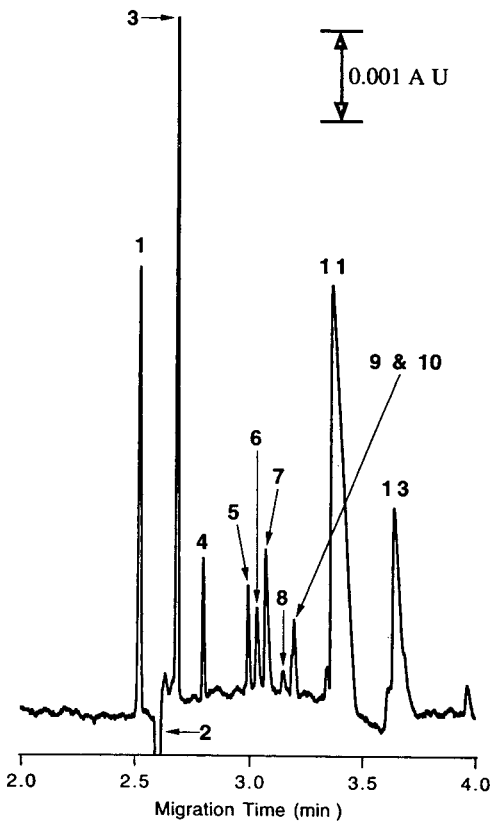

Fig. 5. Separation of 1:500 (v/v) diluted Bayer liquor using an electrolyte comprising 3 m*M* TTAB, 3 m*M* DTAB and 7.5 m*M* chromate (optimum 1). Other conditions as in Fig. 1.

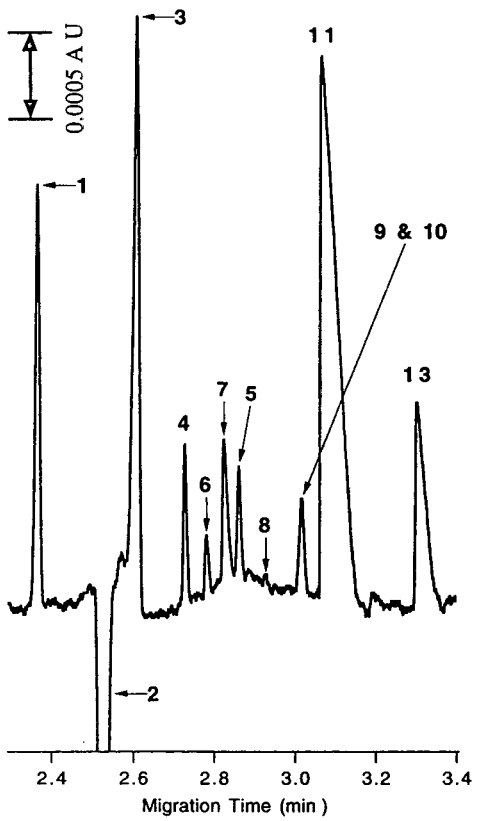

Fig. 6. Separation of 1:500 (v/v) diluted Bayer liquor using an electrolyte containing 5 m*M* TTAB, 1 m*M* DTAB and 5.5 m*M* chromate (optimum 2). Other conditions as in Fig. 1.

ous common disadvantage of both optima is the poor resolution of tartrate and succinate.

3.3. Analytical performance parameters

Using chloride as a model solute, Fig. 7 illustrates that detectability decreases with increasing (total) surfactant concentration. Whilst the responses obtained for optima 1 and 2 were less than for some of the other electrolyte compositions examined, a compromise between detectability and attainment of the desired resolution is necessary. For Bayer liquor, selectivity takes priority over detectability since the latter can easily be enhanced by using a lower sample dilution.

Table 1 summarises results related to quantification using the two optimal electrolyte compositions. For optimum 1, peak area precision was better than 6.6% R.S.D. for all solutes except carbonate, fluoride and phosphate. The high R.S.D. for the carbonate peak area is due to the absorption of carbon dioxide from air, whilst fluoride complexes strongly with iron and aluminium and low or variable values are often recorded in Bayer liquor analysis [17]. The determination of fluoride has been investigated in detail and will be reported in a subsequent publication. Phosphate was not detected at the 1:500 dilution used, so that a more concentrated sample was required. Phosphate response was noted to be very variable and this appeared to be a function of capillary conditioning regimes. All calibration plots had correlation coefficients

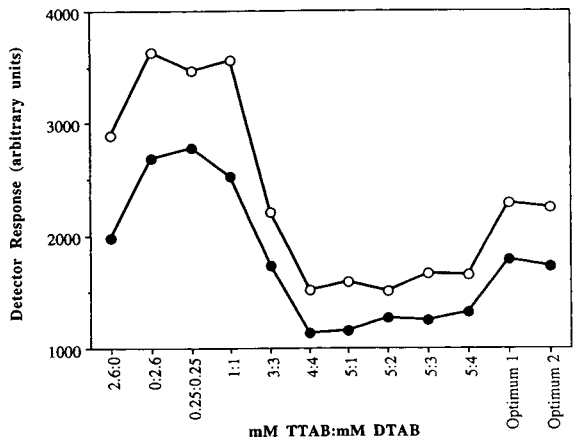

Fig. 7. Effect of surfactant combinations in the electrolyte on detector response for chloride. All electrolytes contained 5 m*M* chromate, except for optima 1 and 2. Conditions for optimum 1 and optimum 2 as in Figs. 5 and 6, respectively. Other conditions as in Fig. 1. ● = Peak area; ○ = peak height.

≥99.5%, except for phosphate and acetate, and recovery values were close to quantitative for all solutes except phosphate. For optimum 2, peak area precision was better than 7.8% R.S.D. (again except for carbonate, fluoride and phosphate). The low recovery observed for sulfate is a result of interference from the system peak; especially at low sample dilution. The detection limits (determined at 3 × baseline noise) of the solute anions are listed in Table 1, which shows that with the exception of phosphate, these detection limits are more than adequate for analysis of the 1:500 diluted Bayer liquor.

The two identified optima are limited by their inability to resolve tartrate and succinate. Furthermore, poor resolution of adjacent anions is a possibility at high and disparate solute concentrations. With optimum 1, acetate is prone to interference from citrate, whereas with optimum 2, the interference is likely to be from

Table 1
Summary of analytical performance parameters using optima 1 and 2

Anion	Peak area precision, % R.S.D. (*n*)		Correlation coefficient (r^2)		Concentration (μg/ml)		Recovery (%) (*n*)		Detection limit (μg/ml)	
	1	2	1	2	1	2	1	2	1	2
Chloride	1.5 (8)	1.7 (10)	99.8	99.6	4.1	4.3	107 (6)	109 (2)	0.14	0.16
Sulfate	2.7 (10)	1.7 (10)	100.0	99.8	4.4	5.1	108 (4)	71 (3)	0.11	0.22
Oxalate	3.4 (8)	2.0 (8)	99.9	99.9	0.8	0.9	100 (6)	104 (4)	0.11	0.16
Formate	4.8 (6)	4 (10)	99.6	99.5	1.4	1.5	99 (6)	98 (4)	0.15	0.29
Fluoride	8.6 (10)	6.4 (8)	99.9	100.0	0.4	0.4	106 (3)	109 (3)	0.09	0.17
Malonate	6.6 (10)	5.5 (5)	99.8	99.7	0.9	1.0	103 (6)	99 (4)	0.16	0.23
Phosphate[a]	n.d.	n.d.	99.6	98.5	0.1	0.4	87.8 (6)	95 (6)	0.07	0.88
Carbonate	21.7 (10)	20.6 (10)	–	–	–	–	–	–	–	–
Acetate	4.0 (8)	7.8 (8)	99.6	96.4	5.0	4.7	95 (6)	113 (2)	0.34	0.58

R.S.D. = Relative standard deviation; *n* = number of replicates; 1 = optimum 1; 2 = optimum 2; n.d. = not detected. Detection limit calculated at 3 × baseline noise.
[a]1:50 dilution used for quantification of phosphate.

adipate. There is a large disparity between the amount of phosphate detected using the two optima and this is again attributable to capillary conditioning regimes and capillary age and history. At the present time, the determination of phosphate using the methods reported in this paper is unreliable and will be examined further. The system peak is a potential source of interference for the determination of chloride and sulfate. However, the ionic strength and total surfactant concentration in the running electrolyte influence the behaviour and magnitude of the system peak. Interestingly, it has been noted that at equal concentration, DTAB yields a smaller system peak than TTAB. Where possible, maximum possible dilution of sample is advisable.

4. Conclusions

Two optimal running electrolytes able to fully resolve chloride, sulfate, oxalate, formate, fluoride, malonate, phosphate, carbonate and acetate in Bayer liquor were identified at (i) 3 m*M* TTAB, 3 m*M* DTAB and 7.5 m*M* chromate at pH 9 ± 1 and (ii) 5 m*M* TTAB, 1 m*M* DTAB and 5.5 m*M* chromate at pH 9 ± 1. Both optima employ binary surfactant mixtures in the running electrolyte and have different selectivities, allowing for some flexibility when separating samples with high and disparate anion concentrations.

Acknowledgements

Financial support from Waters is gratefully acknowledged. We thank Mr. Peter Fagan for valuable assistance and Dr. Peter E. Jackson for provision of the Bayer liquor samples.

References

[1] J.W. Jorgenson and K.D. Lukacs, *Science*, 222 (1983) 266.
[2] J.W. Jorgenson and K.D. Lukacs, *Anal. Chem.*, 53 (1981) 1298.
[3] J.W. Jorgenson, *Trends Anal. Chem.*, 3 (1984) 51.
[4] W.R. Jones and P. Jandik, *J. Chromatogr.*, 546 (1991) 445.
[5] W.R. Jones and P. Jandik, *Am. Lab.*, (1990) 51.
[6] J. Romano, P. Jandik, W.R. Jones and P.E. Jackson, *J. Chromatogr.*, 546 (1991) 411.
[7] N. Jarrett, in A.R. Burkin (Editor), *Production of Aluminium and Alumina*, Wiley, Chicester, 1987, p. 3.
[8] S.C. Grocott, L.P. Jeffries, T. Bowser, J. Carnevale and P.E. Jackson, *J. Chromatogr.*, 602 (1992) 257.
[9] T.J. Cardwell and W.R. Laughton, *J. Chromatogr. A*, 678 (1994) 364.
[10] L.K. Hudson, in A.R. Burkin (Editor), *Production of Aluminium and Alumina*, Wiley, Chicester, 1987, pp. 11–46.
[11] W.E. Haupin, in A.R. Burkin (Editor), *Production of Aluminium and Alumina*, Wiley, Chicester, 1987, pp. 168–175.
[12] W.E. Haupin, in A.R. Burkin (Editor), *Production of Aluminium and Alumina*, Wiley, Chicester, 1987, pp. 85–119.
[13] S. Laksana and P.R. Haddad, *J. Chromatogr.*, 602 (1992) 57.
[14] P.R. Haddad and P.E. Jackson, *Ion Chromatography —Principles and Applications (Journal of Chromatography Library*, Vol. 46), Elsevier, Amsterdam, 1990.
[15] C.L. Ng, H.K. Lee and S.F.Y. Li, *J. Chromatogr.*, 598 (1992) 133.
[16] M. Aguilar, X. Huang and R.N. Zare, *J. Chromatogr.*, 480 (1989) 427.
[17] P.R. Haddad and S. Vanderaa, presented at the *6th International Symposium on High Performance Capillary Electrophoresis, January 1994, San Diego, CA*, poster 509.
[18] N. Avdalovic, C.A. Pohl, R.D. Rocklin and J.R. Stillian, *Anal. Chem.*, 65 (1993) 1470.
[19] A.H. Harakuwe, P.R. Haddad and W. Buchberger, *J. Chromatogr.*, 685 (1994) 161.

Author Index Vol. 706

Vol. 706, Nos. 1 + 2

Journal of Chromatography A

NEWS SECTION

INTERNATIONAL ION CHROMATOGRAPHY SYMPOSIUM 1994, TURIN, 19–22 SEPTEMBER 1994

Fig. 1. The Scientific Committee: (from left to right), Peter Hajós, University of Veszprem; Paul Haddad, University of Tasmania; Hamish Small, HSR; Kazuhiko Tanaka, National Industrial Research Institute of Nagoya; Donald Pietrzyk, University of Iowa; John Stillian, Dionex Corporation; James Fritz, Iowa State University; Richard Cassidy, University of Saskatchewan; Corrado Sarzanini, University of Turin; John Lamb, Brigham Young University.

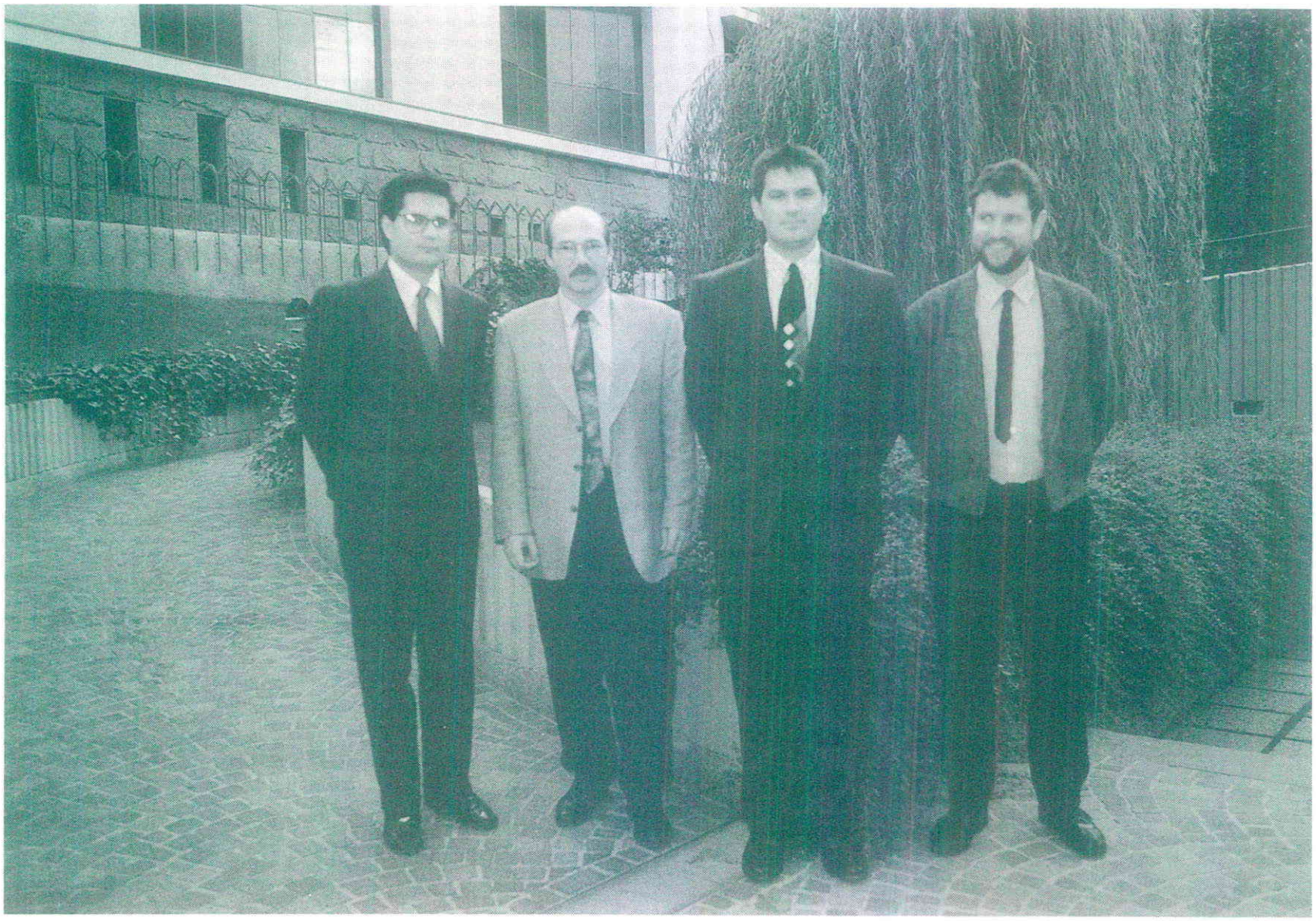

Fig. 2. The Student Award Winners: (from left to right), Brad Edwards, Brigham Young University; Ingo Haumann, Technische Hochschule Darmstadt; Philip Dumont, Iowa State University; Peter Fagan, University of Tasmania.

THE ELSEVIER SCIENCE COMPLETE CATALOGUE ON INTERNET

THE ELSEVIER SCIENCE COMPLETE CATALOGUE 1995 ON CD-ROM

These catalogues feature all journals, books and major reference works from Elsevier Science. Furthermore they allow you to access information about the electronic and CD-ROM products now published by Elsevier Science. Demonstration examples of some of these products are included.

Features include:

- All the journals, with complete information about journal editors and editorial boards
- Listings of special issues and volumes
- Listings of recently published papers for many journals
- Complete descriptions and contents lists of book titles
- Clippings of independent reviews of published books
- Book series, dictionaries, reference works
- Electronic and CD-ROM products
- Demonstration versions of electronic products
- Free text search facilities
- Ordering facilities
- Print options
- Hypertext features

ELSEVIER SCIENCE

Ci

Catalogue on **INTERNET**

ELSEVIER SCIENCE

Cd

Catalogue on **CD-ROM**

Extra features with the Catalogue on Internet

- Alerting facility for new & forthcoming publications
- Updated monthly

ELSEVIER SCIENCE COMPLETE CATALOGUE INTERNET: TRY IT TODAY!

gopher to: gopher.elsevier.nl
WWW: http://www.elsevier.nl/

CD-ROM (published yearly, free of charge)

Please contact:

Customer Service Department
Tel.: +31 (20) 485 3757
Fax: +31 (20) 485 3432
e-mail: nlinfo-f@elsevier.nl

ELSEVIER | PERGAMON | NORTH HOLLAND | EXCERPTA MEDICA

Carbohydrate Analysis

High Performance Liquid Chromatography and Capillary Electrophoresis

Edited by **Z. El Rassi**

Journal of Chromatography Library, Volume 58

The objective of the present book is to provide a comprehensive review of carbohydrate analysis by HPLC and HPCE by covering analytical and preparative separation techniques for all classes of carbohydrates including mono- and disaccharides; linear and cyclic oligosaccharides; branched heterooligosaccharides (e.g., glycans, plant-derived oligosaccharides); glycoconjugates (e.g., glycolipids, glycoproteins); carbohydrates in food and beverage; compositional carbohydrates of polysaccharides; carbohydrates in biomass degradation; etc.

The book will be of interest to a wide audience, including analytical chemists and biochemists, carbohydrate, glycoprotein and glycolipid chemists, molecular biologists, biotechnologists, etc. It will also be a useful reference work for both the experienced analyst and the newcomer as well as for users of HPLC and HPCE, graduates and postdoctoral students.

Contents: Part I. The Solute.
1. Preparation of carbohydrates for analysis by HPLC and HPCE (A.J. Mort, M.L. Pierce).
Part II. Analytical and Preparative Separations.
2. Reversed-phase and hydrophobic interaction chromatography of carbohydrates and glycoconjugates (Z. El Rassi).
3. High performance hydrophilic interaction chromatography of carbohydrates with polar solvents (S.C. Churms).
4. HPLC of carbohydrates with cation- and anion-exchange silica and resin-based stationary phases (C.G. Huber, G.K. Bonn). 5. Analysis of glycoconjugates using high-pH anion-exchange chromatography (R.R. Townsend). 6. Basic studies on carbohydrate - protein interaction by high performance affinity chromatography and high performance capillary affinity electrophoresis using lectins as protein models (S. Honda). 7. Modern size exclusion chromatography of carbohydrates and glycoconjugates (S.C. Churms). 8. High performance capillary electrophoresis of carbohydrates and glycoconjugates (Z. El Rassi, W. Nashabeh). 9. Preparative HPLC of carbohydrates (K.B. Hicks).
Part III. The Detection.
10. Pulsed electrochemical detection of carbohydrates at gold electrodes following liquid chromatographic separation (D.C. Johnson, W.R. LaCourse). 11. On-column refractive index detection of carbohydrates separated by HPLC and CE (A.E. Bruno, B. Krattiger). 12. Mass spectrometry of carbohydrates and glycoconjugates (C.A. Settineri, A.L. Burlingame). 13. Evaporative light scattering detection of carbohydrates in HPLC (M. Dreux, M. Lafosse). 14. Chiroptical detectors for HPLC of carbohydrates (N. Purdie). 15. Pre- and post-column detection-oriented derivatization techniques in HPLC of carbohydrates (S. Hase). 16. Post-column enzyme reactors for the HPLC determination of carbohydrates (L.J. Nagels, P.C. Maes). 17. Other direct and indirect detection methods of carbohydrates in HPLC and HPCE (Z. El Rassi, J.T. Smith). Subject index.

©1995 692 pages Hardbound
Price: Dfl. 425.00 (US$250.00)
ISBN 0-444-89981-2

ELSEVIER

ORDER INFORMATION

ELSEVIER SCIENCE B.V.
P.O. Box 330
1000 AH Amsterdam
The Netherlands
Fax: +31 (20) 485 2845

For USA and Canada:
P.O. Box 945, New York
NY 10159-0945
Fax: +1 (212) 633 3680

US$ prices are valid only for the USA & Canada and are subject to exchange rate fluctuations; in all other countries the Dutch guilder price (Dfl.) is definitive. Customers in the European Union should add the appropriate VAT rate applicable in their

Journal of Chromatography A and *Journal of Chromatography B: Biomedical Applications*

MONTH	1994	J	F	M	A	M[a]	J	J	
Journal of Chromatography A	Vols. 683–688	689/1 689/2 690/1 690/2	691/1 + 2 692/1 + 2 693/1 693/2	694/1 694/2 695/1 695/2	696/1 696/2 697/1 + 2 698/1 + 2	699/1 + 2 700/1 + 2 702/1 + 2 703/1 + 2	704/1 704/2 705/1 705/2	706/1 + 2 707/1 707/2 708/1	The publication schedule for further issues will be published later.
Bibliography Section				713/1			713/2		
Journal of Chromatography B: Biomedical Applications		663/1 663/2	664/1 664/2	665/1 665/2	666/1 666/2	667/1 667/2	668/1 668/2	669/1 669/2	

[a] Vol. 701 (Cumulative Indexes Vols. 652–700) expected in October.

INFORMATION FOR AUTHORS

(Detailed *Instructions to Authors* were published in *J. Chromatogr. A*, Vol. 657, pp. 463–469. A free reprint can be obtained by application to the publisher, Elsevier Science B.V., P.O. Box 330, 1000 AH Amsterdam, Netherlands.)

Types of Contributions. The following types of papers are published: Regular research papers (full-length papers), Review articles, Short Communications and Discussions. Short Communications are usually descriptions of short investigations, or they can report minor technical improvements of previously published procedures; they reflect the same quality of research as full-length papers, but should preferably not exceed five printed pages. Discussions (one or two pages) should explain, amplify, correct or otherwise comment substantively upon an article recently published in the journal. For Review articles, see inside front cover under Submission of Papers.

Submission. Every paper must be accompanied by a letter from the senior author, stating that he/she is submitting the paper for publication in the *Journal of Chromatography A* or *B.*

Manuscripts. Manuscripts should be typed in **double spacing** on consecutively numbered pages of uniform size. The manuscript should be preceded by a sheet of manuscript paper carrying the title of the paper and the name and full postal address of the person to whom the proofs are to be sent. As a rule, papers should be divided into sections, headed by a caption (*e.g.*, Abstract, Introduction, Experimental, Results, Discussion, etc.). All illustrations, photographs, tables, etc., should be on separate sheets.

Abstract. All articles should have an abstract of 50–100 words which clearly and briefly indicates what is new, different and significant. No references should be given.

Introduction. Every paper must have a concise introduction mentioning what has been done before on the topic described, and stating clearly what is new in the paper now submitted.

Experimental conditions should preferably be given on a *separate* sheet, headed "Conditions". These conditions will, if appropriate, be printed in a block, directly following the heading "Experimental".

Illustrations. The figures should be submitted in a form suitable for reproduction, drawn in Indian ink on drawing or tracing paper. Each illustration should have a caption, all the *captions* being typed (with double spacing) together on a *separate sheet.* If structures are given in the text, the original drawings should be provided. Coloured illustrations are reproduced at the author's expense, the cost being determined by the number of pages and by the number of colours needed. The written permission of the author and publisher must be obtained for the use of any figure already published. Its source must be indicated in the legend.

References. References should be numbered in the order in which they are cited in the text, and listed in numerical sequence on a separate sheet at the end of the article. Please check a recent issue for the layout of the reference list. Abbreviations for the titles of journals should follow the system used by *Chemical Abstracts.* Articles not yet published should be given as "in press" (journal should be specified), "submitted for publication" (journal should be specified), "in preparation" or "personal communication".

Vols. 1–651 of the *Journal of Chromatography*; *Journal of Chromatography, Biomedical Applications* and *Journal of Chromatography, Symposium Volumes* should be cited as *J. Chromatogr.* From Vol. 652 on, *Journal of Chromatography A* (incl. Symposium Volumes) should be cited as *J. Chromatogr. A* and *Journal of Chromatography B: Biomedical Applications* as *J. Chromatogr. B.*

Dispatch. Before sending the manuscript to the Editor please check that the envelope contains four copies of the paper complete with references, captions and figures. One of the sets of figures must be the originals suitable for direct reproduction. Please also ensure that permission to publish has been obtained from your institute.

Proofs. One set of proofs will be sent to the author to be carefully checked for printer's errors. Corrections must be restricted to instances in which the proof is at variance with the manuscript.

Reprints. Fifty reprints will be supplied free of charge. Additional reprints can be ordered by the authors. An order form containing price quotations will be sent to the authors together with the proofs of their article.

SIMPLY POWERFUL

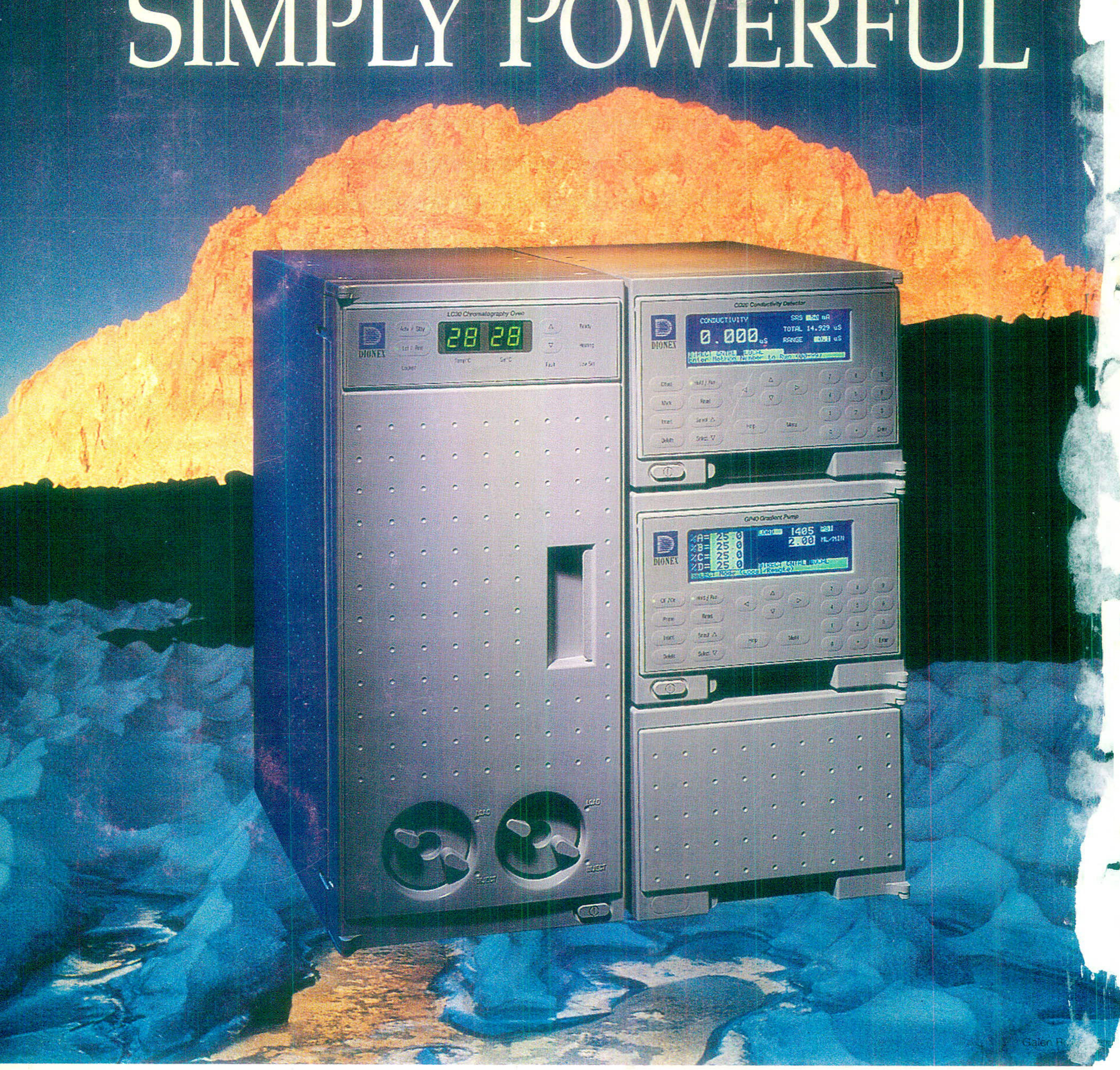

Introducing the New DX 500 Ion Chromatography Systems

Whether you're exploring new methods or facing a backlog of routine samples, the DX 500 meets all your IC application requirements.

It's that simple.

Compact, interlocking modules make it easy to configure exactly the DX 500 system you want. And whichever modules you select, uniform front panels put control at your fingertips for fast, accurate set-up and operation.

As for performance, no-compromise, precise, pulseless pumps help you achieve ideal gradient and isocratic flow. State-of-the-art conductivity, electrochemical, and optical detectors provide the ultimate in detection limits.

Even full PC-based system control is straightforward. Built-in PC-to-module communications create a unified environment for high-speed digital data transfer, real-time monitoring, and intuitive system control. Powerful PeakNet™ workstations simplify networking and automation with trouble-free software that has *true* Windows™ look, feel, and behavior.

And the entire DX 500 system—from sample injection to data management—comes with the Dionex Customer Satisfaction Guarantee, all of which makes choosing the right IC syste for your application much simpler.

For a free brochure on the DX 500 IC Sys call **1-800-723-1161** today. (Outside the U.S., tact your local Dionex sales representative.)

DIONEX

BETTER SEPARATIONS
THROUGH BETTER CHEMISTRY

ISO 9001 REGISTERED*

Dionex Corporation P.O. Box 3603, Sunnyvale, CA 94088-3603 (408) 737-0700 **Belgium** (015) 203800 **Canada** (905) 855-2551 **France** (1) 39 46 08 40
Germany (06126) 991-0 **Italy** (06) 30895454 **Japan** (06) 885-1213 **The Netherlands** (076) 714800 **Switzerland** (062) 33 99 66 **United Kingdom** (0276) 691722